Advances in Photosynthesis and Respiration 45
Including Bioenergy and Related Processes

Anthony W. D. Larkum
Arthur R. Grossman
John A. Raven *Editors*

Photosynthesis in Algae: Biochemical and Physiological Mechanisms

Springer

Photosynthesis in Algae: Biochemical and Physiological Mechanisms

Living stromatolites in intertidal region of Carbla in Hamelin Pool, Shark Bay, Western Australia. These biologically-generated structures are basically small limestone rocks with a superficial mat of many kinds of eubacteria including many cyanobacteria and several kinds of anoxygenic photosynthetic bacteria and sulfur bacteria. They are thought to be similar to fossil structures, which were the first known living structures on the Earth more than 3.5 billion years ago, and which were also the site of the precursors to cyanobacteria and anoxygenic photosynthetic bacteria. Photo by Warwick Hillier, Research School of Biological Sciences, Australian National University, Canberra, Australia

Advances in Photosynthesis and Respiration
Including Bioenergy and Related Processes

VOLUME 45

The book series Advances in Photosynthesis and Respiration – Including Bioenergy and Related Processes provides a comprehensive and state-of-the-art account of research in photosynthesis, respiration, bioenergy production and related processes. Virtually all life on our planet Earth ultimately depends on photosynthetic energy capture and conversion to energy-rich organic molecules. These are used for food, fuel, and fiber. Photosynthesis is the source of almost all Bioenergy on Earth. The fuel and energy uses of photosynthesized products and processes have become an important area of study and competition between food and fuel has led to resurgence in photosynthesis research. This series of books spans topics from physics to agronomy and medicine; from femtosecond processes through season-long production to evolutionary changes over the course of the history of the Earth; from the photophysics of light absorption, excitation energy transfer in the antenna to the reaction centers, where the highly-efficient primary conversion of light energy to charge separation occurs, through intermediate electron transfer reactions, to the physiology of whole organisms and ecosystems; and from X-ray crystallography of proteins to the morphology of organelles and intact organisms. In addition to photosynthesis in natural systems, genetic engineering of photosynthesis and artificial photosynthesis is included in this series. The goal of the series is to offer beginning researchers, advanced undergraduate students, graduate students, and even research specialists, a comprehensive, up-to-date picture of the remarkable advances across the full scope of research on photosynthesis and related energy processes. This series is designed to improve understanding of photosynthesis and bioenergy processes at many levels both to improve basic understanding of these important processes and to enhance our ability to use photosynthesis for the improvement of the human condition.

For more information, please contact the Series Editors Thomas D. Sharkey, Michigan State University, East Lansing, MI, U.S.A. E-mail: tsharkey@msu.edu; phone 1-517-353-0804 or Julian J. Eaton-Rye, Department of Biochemistry, University of Otago, New Zealand, E-mail: julian.eaton-rye@otago.ac.nz; phone 64-(0)3-479-7865. A complete list of references listed per volume can be found following this link: http://www.life.uiuc.edu/govindjee/Reference-Index.htm

More information about this series is available at: http://www.springer.com/series/5599

Photosynthesis in Algae: Biochemical and Physiological Mechanisms

Edited by

Anthony W. D. Larkum
Global Climate Custer, University of Technology Sydney, Ultimo, NSW, Australia

Arthur R. Grossman
Department of Plant Biology, Carnegie Institution for Science, Stanford University Stanford, CA, USA

and

John A. Raven
Division of Plant Sciences, University of Dundee at the JHI, Dundee, UK

Springer

Editors
Anthony W. D. Larkum
Global Climate Custer
University of Technology Sydney
Ultimo, NSW, Australia

John A. Raven
Division of Plant Sciences
University of Dundee at the JHI
Dundee, UK

Arthur R. Grossman
Department of Plant Biology, Carnegie
Institution for Science
Stanford University
Stanford, CA, USA

ISSN 1572-0233 ISSN 2215-0102 (electronic)
Advances in Photosynthesis and Respiration
ISBN 978-3-030-33396-6 ISBN 978-3-030-33397-3 (eBook)
https://doi.org/10.1007/978-3-030-33397-3

This Springer imprint is published by the registered company Springer Nature Switzerland AG.
The registered company address is: Gewerbestrasse 11, 6330 Cham, Switzerland

From the Series Editors

Advances in Photosynthesis and Respiration Including Bioenergy and Related Processes

Volume 45: Photosynthesis in Algae: Biochemical and Physiological Mechanisms

Collectively, algae are a diverse group of eukaryotes including large multicellular organisms such as kelps and many unicellular species. The number of algal species on the planet is not known, but estimates suggest tens of thousands. Their diversity ensures the algae are represented in many, if not all, ecosystems, and as such, they are of major importance as primary producers: they also represent an important group of organisms that benefit mankind. Many nations and cultures already utilize algae for food and fertilizer and a wide range of products such as agar and alginates. It is also recognized that algal cells have the potential to produce more biomass per unit area in a year than any other form of biomass: there is thus great potential for the production of biofuels and other high-value organic compounds.

In volume 45 of the Advances in Photosynthesis and Respiration (AIPH) series, Anthony Larkum, Arthur Grossman, and John Raven have assembled a team of experts on algal biochemistry, biophysics, and molecular biology to consider the diversity of algal photosynthesis, recognizing that these organisms (including the *Cyanobacteria*) can provide new knowledge for creative ways to apply algal photosynthesis to the many issues facing humanity today, from conservation biology to food and energy security. This volume joins volume 14 (*Photosynthesis in Algae*, edited by Anthony Larkum, Susan Douglas, and John Raven) in providing an extensive introduction to the molecular mechanisms utilized by the algae and the enormous potential that is stored in the gene pool of this vast group of organisms.

Authors of Volume 45

The current volume exemplifies the tradition of the AIPH book series in being an international book. It has authors from the following 12 countries: Australia (6), Canada (1), the Czech Republic (3), France (4), Germany (1), Italy (4), Hungary (2), Portugal (1), Sweden (1), Switzerland (1), the UK (4), and the USA (9). There are 37 authors (including the three editors) who, as noted above, are experts in the field of algal photosynthesis. Alphabetically (by last names), they are John **B**eardall, Erica Belgio, Debashish Bhattacharya, Claudia Büchel, Douglas **C**ampbell, Anna Paola Casazza, Paul M.G. Curmi, Geoffry A. **D**avis, Jeffery A. Davis, Nicholas **F**isher, Myriam M.M. **G**oudet, Howard Griffiths, Arthur R. Grossman, Parisa **H**eydarizadeh, Radek **K**aňa, Atsuko Kanazawa, Diana Kirilovsky, David Kramer, Anthony W.D. **L**arkum, Justine **M**archand, Moritz Meyer, Peter **N**eofotis, Ondřej **P**rášil, Dana C. Price, Antonietta **Q**uigg, Harry W. **R**athbone, John A. Raven, Jean-David Rochaix, Stefano

Santabarbara, Benoît Schoefs, João Serôdio, Cornelia Spetea, Milan Szabo, Imre Vass, and Robert Willows. We are grateful for their efforts in making this important volume.

Our Books

We list below information on the 44 volumes that have been published thus far (see http://www.springer.com/series/5599 for the series web site). Electronic access to individual chapters depends on subscription (ask your librarian), but Springer provides free downloadable front matter as well as indexes for all volumes. The available web sites of the books in the Series are listed below:

- **Volume 44 (2018)** ***The Leaf: A Platform for Performing Photosynthesis***, edited by William W. Adams III from the USA and Ichiro Terashima from Japan, with 14 chapters, 575 pp, hardcover ISBN 978-3-319-93592-8, eBook ISBN 978-3-319-93594-2 [http://www.springer.com/gp/book/9783319935928]
- **Volume 43 (2018)** ***Plant Respiration: Metabolic Fluxes and Carbon Balance***, edited by Guillaume Tcherkez from Australia and Jaleh Ghashghaie from France, with 18 chapters, 302 pp, hardcover ISBN 978-3-319-68701-8, eBook ISBN 978-3-319-68703-2 [http://www.springer.com/us/book/9783319687018]
- **Volume 42 (2016)** ***Canopy Photosynthesis: From Basics to Applications***, edited by Kouki Hikosaka from Japan, Ülo Niinemets from Estonia, and Neils P.R. Anten from the Netherlands, with 15 chapters, 423 pp, hardcover ISBN 978-94-017-7290-7, eBook ISBN 978-94-017-7291-4 [http://www.springer.com/book/9789401772907]
- **Volume 41 (2016)** ***Cytochrome Complexes: Evolution, Structures, Energy Transduction, and Signaling***, edited by William A. Cramer and Toivo Kallas from the USA, with 35 chapters, 734 pp, hardcover ISBN 978-94-017-7479-6, eBook ISBN 978-94-017-7481-9 [http://www.springer.com/book/9789401774796]
- **Volume 40 (2014)** ***Non-Photochemical Quenching and Energy Dissipation in Plants, Algae and Cyanobacteria***, edited by Barbara Demmig-Adams, Győző Garab, William W. Adams III, and Govindjee from the USA and Hungary, with 28 chapters, 649 pp, hardcover ISBN 978-94-017-9031-4, eBook ISBN 978-94-017-9032-1 [http://www.springer.com/life+sciences/plant+sciences/book/978-94-017-9031-4]
- **Volume 39 (2014)** ***The Structural Basis of Biological Energy Generation***, edited by Martin F. Hohmann-Marriott from Norway, with 24 chapters, 483 pp, hardcover ISBN 978-94-017-8741-3, eBook ISBN 978-94-017-8742-0 [http://www.springer.com/life+sciences/book/978-94-017-8741-3]
- **Volume 38 (2014)** ***Microbial BioEnergy: Hydrogen Production***, edited by Davide Zannoni and Roberto De Philippis from Italy, with 18 chapters, 366 pp, hardcover ISBN 978-94-017-8553-2, eBook ISBN 978- 94-017-8554-9 [http://www.springer.com/life+sciences/plant+sciences/book/978-94-017-8553-2]
- **Volume 37 (2014)** ***Photosynthesis in Bryophytes and Early Land Plants***, edited by David T. Hanson and Steven K. Rice from the USA, with 18 chapters, approximately 342 pp, hardcover ISBN 978-94-007-6987-8, eBook ISBN 978-94-007-6988-5 [http://www.springer.com/life+sciences/plant+sciences/book/978-94-007-6987-8]
- **Volume 36 (2013)** ***Plastid Development in Leaves During Growth and Senescence***, edited by Basanti Biswal, Karin Krupinska, and Udaya Biswal from India and Germany, with 28 chapters, 837 pp, hardcover ISBN 978-94-007-5723-33, eBook ISBN 978-94-007-5724-0 [http://www.springer.com/life+sciences/plant+sciences/book/978-94-007-5723-3]
- **Volume 35 (2012)** ***Genomics of Chloroplasts and Mitochondria***, edited by Ralph Bock and Volker Knoop from Germany, with 19

chapters, 475 pp, hardcover ISBN 978-94-007-2919-3 eBook ISBN 978-94-007-2920-9 [http://www.springer.com/life+sciences/plant+sciences/book/978-94-007-2919-3]

- **Volume 34 (2012)** ***Photosynthesis: Plastid Biology, Energy Conversion and Carbon Assimilation***, edited by Julian J. Eaton-Rye, Baishnab C. Tripathy, and Thomas D. Sharkey from New Zealand, India, and the USA, with 33 chapters, 854 pp, hardcover ISBN 978-94-007-1578-3, eBook ISBN 978-94-007-1579-0 [http://www.springer.com/life+sciences/plant+sciences/book/978-94-007-1578-3]
- **Volume 33 (2012)** ***Functional Genomics and Evolution of Photosynthetic Systems***, edited by Robert L. Burnap and Willem F.J. Vermaas from the USA, with 15 chapters, 428 pp, hardcover ISBN 978-94-007-1532-5, softcover ISBN 978-94-007-3832-4, eBook ISBN 978-94-007-1533-2 [http://www.springer.com/life+sciences/book/978-94-007-1532-5]
- **Volume 32 (2011)** ***C_4 Photosynthesis and Related CO_2 Concentrating Mechanisms***, edited by Agepati S. Raghavendra and Rowan Sage from India and Canada, with 19 chapters, 425 pp, hardcover ISBN 978-90-481-9406-3, softcover ISBN 978-94-007-3381-7, eBook ISBN 978-90-481-9407-0 [http://www.springer.com/life+sciences/plant+sciences/book/978-90-481-9406-3]
- **Volume 31 (2010)** ***The Chloroplast: Basics and Applications***, edited by Constantin Rebeiz, Christoph Benning, Hans J. Bohnert, Henry Daniell, J. Kenneth Hoober, Hartmut K. Lichtenthaler, Archie R. Portis, and Baishnab C. Tripathy from the USA, Germany, and India, with 25 chapters, 451 pp, hardcover ISBN 978-90-481-8530-6, softcover ISBN 978-94-007-3287-2, eBook ISBN 978-90-481-8531-3 [http://www.springer.com/life+sciences/plant+sciences/book/978-90-481-8530-6]
- **Volume 30 (2009)** ***Lipids in Photosynthesis: Essential and Regulatory Functions***, edited by Hajime Wada and Norio Murata both from Japan, with 20 chapters, 506 pp, hardcover ISBN 978-90-481-2862-4, softcover ISBN 978-94-007-3073-1, eBook ISBN 978-90-481-2863-1 [http://www.springer.com/life+sciences/plant+sciences/book/978-90-481-2862-4]
- **Volume 29 (2009)** ***Photosynthesis in Silico: Understanding Complexity from Molecules***, edited by Agu Laisk, Ladislav Nedbal, and Govindjee from Estonia, the Czech Republic, and the USA, with 20 chapters, 525 pp, hardcover ISBN 978-1-4020-9236-7, softcover ISBN 978-94-007-1533-2, eBook ISBN 978-1-4020-9237-4 [http://www.springer.com/life+sciences/plant+sciences/book/978-1-4020-9236-7]
- **Volume 28 (2009)** ***The Purple Phototrophic Bacteria***, edited by C. Neil Hunter, Fevzi Daldal, Marion C. Thurnauer, and J. Thomas Beatty from the UK, the USA, and Canada, with 48 chapters, 1053 pp, hardcover ISBN 978-1-4020-8814-8, eBook ISBN 978-1-4020-8815-5 [http://www.springer.com/life+sciences/plant+sciences/book/978-1-4020-8814-8]
- **Volume 27 (2008)** ***Sulfur Metabolism in Phototrophic Organisms***, edited by Christiane Dahl, Rüdiger Hell, David Knaff, and Thomas Leustek from Germany and the USA, with 24 chapters, 551 pp, hardcover ISBN 978-4020-6862-1, softcover ISBN 978-90-481-7742-4, eBook ISBN 978-1-4020-6863-8 [http://www.springer.com/life+sciences/plant+sciences/book/978-1-4020-6862-1]
- **Volume 26 (2008)** ***Biophysical Techniques in Photosynthesis***: *Volume II*, edited by Thijs Aartsma and Jörg Matysik both from the Netherlands, with 24 chapters, 548 pp, hardcover ISBN 978-1-4020-8249-8, softcover ISBN 978-90-481-7820-9, eBook ISBN 978-1-4020-8250-4 [http://www.springer.com/life+sciences/plant+sciences/book/978-1-4020-8249-8]
- **Volume 25 (2006)** ***Chlorophylls and Bacteriochlorophylls: Biochemistry, Biophysics, Functions and Applications***, edited by Bernhard Grimm, Robert J. Porra, Wolfhart Rüdiger, and Hugo Scheer from

Germany and Australia, with 37 chapters, 603 pp, hardcover ISBN 978-1-40204515-8, softcover ISBN 978-90-481-7140-8, eBook ISBN 978-1-4020-4516-5 [http://www.springer.com/life+sciences/plant+sciences/book/978-1-4020-4515-8]

- **Volume 24 (2006)** ***Photosystem I: The Light-Driven Plastocyanin:Ferredoxin Oxidoreductase***, edited by John H. Golbeck from the USA, with 40 chapters, 716 pp, hardcover ISBN 978-1-40204255-3, softcover ISBN 978-90-481-7088-3, eBook ISBN 978-1-4020-4256-0 [http://www.springer.com/life+sciences/plant+sciences/book/978-1-4020-4255-3]
- **Volume 23 (2006)** ***The Structure and Function of Plastids***, edited by Robert R. Wise and J. Kenneth Hoober from the USA, with 27 chapters, 575 pp, softcover ISBN: 978-1-4020-6570–6; hardcover ISBN 978-1-4020-4060-3, softcover ISBN 978-1-4020-6570-5, eBook ISBN 978-1-4020-4061-0 [http://www.springer.com/life+sciences/plant+sciences/book/978-1-4020-4060-3]
- **Volume 22 (2005)** ***Photosystem II: The Light-Driven Water:Plastoquinone Oxidoreductase***, edited by Thomas J. Wydrzynski and Kimiyuki Satoh from Australia and Japan, with 34 chapters, 786 pp, hardcover ISBN 978-1-4020-4249-2, eBook ISBN 978-1-4020-4254-6 [http://www.springer.com/life+sciences/plant+sciences/book/978-1-4020-4249-2]
- **Volume 21 (2006)** ***Photoprotection, Photoinhibition, Gene Regulation, and Environment***, edited by Barbara Demmig-Adams, William W. Adams III, and Autar K. Mattoo from the USA, with 21 chapters, 380 pp, hardcover ISBN 978-14020-3564-7, softcover ISBN 978-1-4020-9281-7, eBook ISBN 978-1-4020-3579-1 [http://www.springer.com/life+sciences/plant+sciences/book/978-1-4020-3564-7]
- **Volume 20 (2006)** ***Discoveries in Photosynthesis***, edited by Govindjee, J. Thomas Beatty, Howard Gest, and John F. Allen from the USA, Canada, and the UK, with 111 chapters, 1304 pp, hardcover ISBN 978-1-4020-3323-0, eBook ISBN 978-1-4020-3324-7 [http://www.springer.com/life+sciences/plant+sciences/book/978-1-4020-3323-0]
- **Volume 19 (2004)** ***Chlorophyll a Fluorescence: A Signature of Photosynthesis***, edited by George C. Papageorgiou and Govindjee from Greece and the USA, with 31 chapters, 820 pp, hardcover ISBN 978-1-4020-3217-2, softcover ISBN 978-90-481-3882-1, eBook ISBN 978-1-4020-3218-9 [http://www.springer.com/life+sciences/biochemistry+%26+biophysics/book/978-1-4020-3217-2]
- **Volume 18 (2005)** ***Plant Respiration: From Cell to Ecosystem***, edited by Hans Lambers and Miquel Ribas-Carbo from Australia and Spain, with 13 chapters, 250 pp, hardcover ISBN978-14020-3588-3, softcover ISBN 978-90-481-6903-0, eBook ISBN 978-1-4020-3589-0 [http://www.springer.com/life+sciences/plant+sciences/book/978-1-4020-3588-3]
- **Volume 17 (2004)** ***Plant Mitochondria: From Genome to Function***, edited by David Day, A. Harvey Millar, and James Whelan from Australia, with 14 chapters, 325 pp, hardcover ISBN: 978-1-4020-2399-6, softcover ISBN 978-90-481-6651-0, eBook ISBN 978-1-4020-2400-9 [http://www.springer.com/life+sciences/cell+biology/book/978-1-4020-2399-6]
- **Volume 16 (2004)** ***Respiration in Archaea and Bacteria: Diversity of Prokaryotic Respiratory Systems***, edited by Davide Zannoni from Italy, with 13 chapters, 310 pp, hardcover ISBN 978-14020-2002-5, softcover ISBN 978-90-481-6571-1, eBook ISBN 978-1-4020-3163-2 [http://www.springer.com/life+sciences/plant+sciences/book/978-1-4020-2002-5]
- **Volume 15 (2004)** ***Respiration in Archaea and Bacteria: Diversity of Prokaryotic Electron Transport Carriers***, edited by Davide Zannoni from Italy with 13 chapters,

350 pp, hardcover ISBN 978-1-4020-2001-8, softcover ISBN 978-90-481-6570-4, eBook ISBN 978-1-4020-3163-2 [http://www.springer.com/life+sciences/biochemistry+%26+biophysics/book/978-1-4020-2001-8]

- **Volume 14 (2004)** ***Photosynthesis in Algae***, edited by Anthony W.D. Larkum, Susan Douglas, and John A. Raven from Australia, Canada, and the UK, with 19 chapters, 500 pp, hardcover ISBN 978-0-7923-6333-0, softcover ISBN 978-94-010-3772-3, eBook ISBN 978-94-007-1038-2 [http://www.springer.com/life+sciences/plant+sciences/book/978-0-7923-6333-0]
- **Volume 13 (2003)** ***Light-Harvesting Antennas in Photosynthesis***, edited by Beverley R. Green and William W. Parson from Canada and the USA, with 17 chapters, 544 pp, hardcover ISBN 978-07923-6335-4, softcover ISBN 978-90-481-5468-5, eBook ISBN 978-94-017-2087-8 [http://www.springer.com/life+sciences/plant+sciences/book/978-0-7923-6335-4]
- **Volume 12 (2003)** ***Photosynthetic Nitrogen Assimilation and Associated Carbon and Respiratory Metabolism***, edited by Christine H. Foyer and Graham Noctor from the UK and France, with 16 chapters, 304 pp, hardcover ISBN 978-07923-6336-1, softcover ISBN 978-90-481-5469-2, eBook ISBN 978-0-306-48138-3 [http://www.springer.com/life+sciences/plant+sciences/book/978-0-7923-6336-1]
- **Volume 11 (2001)** ***Regulation of Photosynthesis***, edited by Eva-Mari Aro and Bertil Andersson from Finland and Sweden, with 32 chapters, 640 pp, hardcover ISBN 978-0-7923-6332-3, softcover ISBN 978-94-017-4146-0, eBook ISBN 978-0-306-48148-2 [http://www.springer.com/life+sciences/plant+sciences/book/978-0-7923-6332-3]
- **Volume 10 (2001)** ***Photosynthesis: Photobiochemistry and Photobiophysics***, edited by Bacon Ke from the USA, with 36 chapters, 792 pp, hardcover ISBN 978-0-7923-6334-7, softcover ISBN 978-0-7923-6791-8, eBook ISBN 978-0-306-48136-9 [http://www.springer.com/life+sciences/plant+sciences/book/978-0-7923-6334-7]
- **Volume 9 (2000)** ***Photosynthesis: Physiology and Metabolism***, edited by Richard C. Leegood, Thomas D. Sharkey, and Susanne von Caemmerer from the UK, the USA, and Australia, with 24 chapters, 644 pp, hardcover ISBN 978-07923-6143-5, softcover ISBN 978-90-481-5386-2, eBook ISBN 978-0-306-48137-6 [http://www.springer.com/life+sciences/plant+sciences/book/978-0-7923-6143-5]
- **Volume 8 (1999)** ***The Photochemistry of Carotenoids***, edited by Harry A. Frank, Andrew J. Young, George Britton, and Richard J. Cogdell from the USA and the UK, with 20 chapters, 420 pp, hardcover ISBN 978-0-7923-5942-5, softcover ISBN 978-90-481-5310-7, eBook ISBN 978-0-306-48209-0 [http://www.springer.com/life+sciences/plant+sciences/book/978-0-7923-5942-5]
- **Volume 7 (1998)** ***The Molecular Biology of Chloroplasts and Mitochondria in Chlamydomonas***, edited by Jean David Rochaix, Michel Goldschmidt-Clermont, and Sabeeha Merchant from Switzerland and the USA, with 36 chapters, 760 pp, hardcover ISBN 978-0-7923-5174-0, softcover ISBN 978-94-017-4187-3, eBook ISBN 978-0-306-48204-5 [http://www.springer.com/life+sciences/plant+sciences/book/978-0-7923-5174-0]
- **Volume 6 (1998)** ***Lipids in Photosynthesis: Structure, Function and Genetics***, edited by Paul-André Siegenthaler and Norio Murata from Switzerland and Japan, with 15 chapters, 332 pp, hardcover ISBN 978-0-7923-5173-3, softcover ISBN 978-90-481-5068-7, eBook ISBN 978-0-306-48087-4 [http://www.springer.com/life+sciences/plant+sciences/book/978-0-7923-5173-3]
- **Volume 5 (1997)** ***Photosynthesis and the Environment***, edited by Neil R. Baker from the UK, with 20 chapters, 508 pp, hardcover ISBN 978-07923-4316-5, softcover ISBN 978-90-481-4768-7, eBook ISBN 978-0-306-

48135-2 [http://www.springer.com/life+sciences/plant+sciences/book/978-0-7923-4316-5]

- **Volume 4 (1996)** ***Oxygenic Photosynthesis: The Light Reactions***, edited by Donald R. Ort and Charles F. Yocum from the USA, with 34 chapters, 696 pp, hardcover ISBN 978-0-7923-3683-9, softcover ISBN 978-0-7923-3684–6, eBook ISBN 978-0-306-48127-7 [http://www.springer.com/life+sciences/plant+sciences/book/978-0-7923-3683-9]
- **Volume 3 (1996)** ***Biophysical Techniques in Photosynthesis***, edited by Jan Amesz and Arnold J. Hoff from the Netherlands, with 24 chapters, 426 pp, hardcover ISBN 978-0-7923-3642-6, softcover ISBN 978-90-481-4596-6, eBook ISBN 978-0-306-47960-1 [http://www.springer.com/life+sciences/plant+sciences/book/978-0-7923-3642-6]
- **Volume 2 (1995)** ***Anoxygenic Photosynthetic Bacteria***, edited by Robert E. Blankenship, Michael T. Madigan, and Carl E. Bauer from the USA, with 62 chapters, 1331 pp, hardcover ISBN 978-0-7923-3682-8, softcover ISBN 978-0-7923-3682-2, eBook ISBN 978-0-306-47954-0 [http://www.springer.com/life+sciences/plant+sciences/book/978-0-7923-3681-5]
- **Volume 1 (1994)** ***The Molecular Biology of Cyanobacteria***, edited by Donald R. Bryant from the USA, with 28 chapters, 916 pp, hardcover ISBN 978-0-7923-3222-0, softcover ISBN 978-0-7923-3273-2, eBook ISBN 978-94-011-0227-8 [http://www.springer.com/life+sciences/plant+sciences/book/978-0-7923-3222-0]

Further information on these books and ordering instructions is available at http://www. springer.com/series/5599.

Special 25% discounts are available to members of the International Society of Photosynthesis Research (ISPR, http://www.photosynthesis-research.org/). See http://www.springer.com/ispr.

Future Advances in Photosynthesis and Respiration and Other Related Books

The readers of the current series are encouraged to watch for the publication of the forthcoming books (not necessarily arranged in the order of future appearance):

- *Photosynthesis and Climate Change* (working title) (Editors: Katie M. Becklin, Joy K. Ward, and Danielle A. Way)
- *Cyanobacteria* (Editor: Donald Bryant)
- *Photosynthesis in Algae: Biofuels and Value-Added Products* (Editors: Anthony Larkum and John Raven)
- *Our Photosynthetic Planet* (Editors: Mike Behrenfeld, Joe Berry, Lianhong Gu, Nancy Jiang, Anastasia Romanou, and Anthony Walker)
- *Modeling Photosynthesis and Growth* (Editors: Xin-Guang Zhu and Thomas D. Sharkey)

In addition to the above books, the following topics are under consideration:

Algae, *Cyanobacteria*: Biofuel and Bioenergy
Artificial Photosynthesis
ATP Synthase: Structure and Function
Bacterial Respiration II
Evolution of Photosynthesis
Green Bacteria and Heliobacteria
Interactions Between Photosynthesis and Other Metabolic Processes
Limits of Photosynthesis: Where Do We Go from Here?
Photosynthesis, Biomass and Bioenergy
Photosynthesis Under Abiotic and Biotic Stress

If you have any interest in editing/coediting any of the above listed books or being an author, please send an e-mail to Tom Sharkey (tsharkey@msu.edu) and/or to Julian Eaton-Rye (julian.eaton-rye@otago.ac.nz). Suggestions for additional topics are also welcome. Instructions for writing chapters in books in our series are available by sending e-mail requests to one or both of us.

We take this opportunity to thank and congratulate Anthony Larkum, Arthur Grossman, and John Raven for their outstanding editorial work; they have collectively done an excellent job not only in editing but also in organizing this book for all of us, and for their highly professional dealing with the reviewing process. We thank all 37 authors of this book (see the list given earlier and on the following pages); without their authoritative chapters, there would be no such volume. We give special thanks to Mr. Joseph Daniel of SPi Global, India, for directing the typesetting of this book. Once again, his expertise has been crucial in guiding the final steps that have brought this book to completion. We also thank Jacco Flipsen and Ineke Ravesloot (of Springer) for their friendly working relation with us that led to the production of this book and thank Zuzana Bernhart and her team at Springer for their ongoing organization and assistance with the AIPH series.

January 6, 2020

Thomas D. Sharkey
Biochemistry and
Molecular Biology
Michigan State University
East Lansing, MI, USA

Julian J. Eaton-Rye
Department of Biochemistry
University of Otago
Dunedin, New Zealand

Series Editors

A 2017 informal photograph of Govindjee (right) and his wife, Rajni (left), in Champaign-Urbana, Illinois (photograph by Dilip Chhajed)

Govindjee, who uses one name only, was born on October 24, 1932, in Allahabad, India. Since 1999, he has been Professor Emeritus of Biochemistry, Biophysics, and Plant Biology at the University of Illinois at Urbana-Champaign (UIUC), Urbana, IL, USA. He obtained his B.Sc. in Chemistry, Botany, and Zoology and his M.Sc. in Botany and Plant Physiology in 1952 and 1954, respectively, from the University of Allahabad. He learned his Plant Physiology from Shri Ranjan, who was a student of Frederick Frost Blackman (of Cambridge, UK). He then studied *Photosynthesis* at the UIUC, under two giants in the field, Robert Emerson (a student of Otto Warburg) and Eugene Rabinowitch (who had worked with James Franck), obtaining his Ph.D. in Biophysics in 1960.

Govindjee is best known for his research on excitation energy transfer, light emission (prompt and delayed fluorescence and thermoluminescence), primary photochemistry, and electron transfer in *Photosystem II* (PS II, water-plastoquinone oxidoreductase). His research, with many others, includes the discovery of a short-wavelength form of chlorophyll (Chl) *a* functioning in PS II, of the two-light effect in Chl *a* fluorescence, and, with his wife Rajni Govindjee, of the two-light effect (Emerson enhancement) in $NADP^+$ reduction in chloroplasts. His major achievements, together with several others, include an understanding of the basic relationship between Chl *a* fluorescence and photosynthetic reactions; a unique role of bicarbonate/carbonate on the electron acceptor side of PS II, particularly in the protonation events involving the Q_B binding region; the theory of thermoluminescence in plants; the first picosecond measurements on the primary photochemistry of PS II; and the use of fluorescence lifetime imaging microscopy (FLIM) of Chl *a* fluorescence in understanding photoprotection by plants against excess light. His current focus is on the *history of*

photosynthesis research and on *photosynthesis education*. He has served on the faculty of the UIUC for ~40 years.

Govindjee's honors include Fellow of the American Association for the Advancement of Science (AAAS); Distinguished Lecturer of the School of Life Sciences, UIUC; Fellow and Lifetime Member of the National Academy of Sciences (India); President of the American Society for Photobiology (1980–1981); Fulbright Scholar (1956), Fulbright Senior Lecturer (1997), and Fulbright Specialist (2012); Honorary President of the 2004 International Photosynthesis Congress (Montréal, Canada); First Recipient of the Lifetime Achievement Award of the Rebeiz Foundation for Basic Biology (2006); and Recipient of the Communication Award of the International Society of Photosynthesis Research (2007) and of the Liberal Arts and Sciences Lifetime Achievement Award of the UIUC (2008). Furthermore, he has been honored many times: (1) in 2007, through two special volumes of *Photosynthesis Research*, celebrating his 75th birthday and his 50-year dedicated research in photosynthesis (Julian J. Eaton-Rye, Guest Editor); (2) in 2008, through a special international symposium on "photosynthesis in a global perspective" held in November 2008 at the University of Indore, India, this was followed by a book *Photosynthesis: Basics and Applications* (edited by S. Itoh, P. Mohanty, and K.N. Guruprasad); (3) in 2012, through *Photosynthesis: Plastid Biology, Energy Conversion and Carbon Assimilation*, edited by Julian J. Eaton-Rye, Baishnab C. Tripathy, and Thomas D. Sharkey; (4) in 2013, through special issues of *Photosynthesis Research* (volumes 117 and 118), edited by Suleyman Allakhverdiev, Gerald Edwards, and Jian-Ren Shen celebrating his 80th (or rather 81st) birthday; (5) in 2014, through celebration of his 81st birthday in Třeboň, Czech Republic (O. Prasil [2014] *Photosynth Res* 122: 113–119); and (6) in 2016, through the award of the prestigious Prof. B.M. Johri Memorial Award of the Society of Plant Research, India. In 2018, *Photosynthetica* published a special issue to celebrate his 85th birthday (Julian J. Eaton-Rye, Editor).

Govindjee's unique teaching of the Z-scheme of photosynthesis, where students act as different intermediates, has been published in two papers: (1) P.K. Mohapatra and N.R. Singh [2015] *Photosynthesis Research* (123:105–114) and (2) S. Jaiswal, M. Bansal, S. Roy, A. Bharati, and B. Padhi [2017] *Photosynthesis Research* (131: 351—359). Govindjee is a Coauthor of a classic and highly popular book *Photosynthesis* (with E.I. Rabinowitch, 1969) and of the historical book *Maximum Quantum Yield of Photosynthesis: Otto Warburg and the Midwest Gang* (with K. Nickelsen, 2011). He is Editor (or Coeditor) of many books including *Bioenergetics of Photosynthesis* (1975); *Photosynthesis* (two volumes (1982)); *Light Emission by Plants and Bacteria* (1986); *Chlorophyll a Fluorescence: A Signature of Photosynthesis* (2004); *Discoveries in Photosynthesis* (2005); and *Non-Photochemical Quenching and Energy Dissipation in Plants, Algae and Cyanobacteria* (2015).

Since 2007, each year a **Govindjee and Rajni Govindjee Award** is given to graduate students by the Department of Plant Biology (odd years) and by the Department of Biochemistry (even years), at the UIUC, to recognize excellence in biological sciences. For further information on Govindjee, see his website at http://www.life.illinois.edu/govindjee.

Thomas D. (Tom) Sharkey obtained his bachelor's degree in Biology in 1974 from Lyman Briggs College, a residential science college at Michigan State University, East Lansing, Michigan, USA. After 2 years as a Research Technician, he entered a Ph.D. program in the Department of Energy Plant Research Laboratory at Michigan State University under the mentorship of Klaus Raschke and finished in 1979. His postdoctoral research was carried out with Graham Farquhar at the Australian National University, Canberra, where he coauthored a landmark review on photosynthesis and stomatal conductance. For 5 years, he worked in the Desert Research Institute, Reno, Nevada. After Reno, he spent 20 years as Professor of Botany at the University of Wisconsin in Madison. In 2008, he became Professor and Chair of the Department of Biochemistry and Molecular Biology at Michigan State University. In 2017, he stepped down as Department Chair and moved to the MSU-DOE Plant Research Laboratory completing a 38-year sojourn back to his beginnings. His research interests center on the exchange of gases between plants and the atmosphere and carbon metabolism of photosynthesis. The biochemistry and biophysics underlying carbon dioxide uptake and isoprene emission from plants form the two major research topics in his laboratory. Among his contributions are measurement of the carbon dioxide concentration inside leaves, an exhaustive study of short-term feedback effects in carbon metabolism, and a significant contribution to elucidation of the pathway by which leaf starch breaks down at night. In the isoprene research field, his laboratory has cloned many of the genes that underlie isoprene synthesis, and he has published many important papers on the biochemical regulation of isoprene synthesis. His work has been cited over 26,000 times according to Google Scholar in 2017. He has been named an Outstanding Faculty Member by Michigan State University and, in 2015, was named a University Distinguished Professor. He is a Fellow of the American Society of Plant Biologists and of the American Association for the Advancement of Science. He has coedited three books, the first on trace gas emissions from plants in 1991 (with Elizabeth Holland and Hal Mooney), volume 9 of this series (with Richard Leegood and Susanne von Caemmerer) on the physiology of carbon metabolism of photosynthesis in 2000, and volume 34 (with Julian J. Eaton-Rye and Baishnab C. Tripathy), *Photosynthesis*: *Plastid Biology*, *Energy Conversion and Carbon Assimilation*. He has been Coeditor of this series since volume 31.

Julian J. Eaton-Rye is a Professor in the Department of Biochemistry at the University of Otago, New Zealand. He received his undergraduate degree in Botany from the University of Manchester in the UK in 1981 and his Ph.D. from the University of Illinois in 1987, where he worked with Govindjee on the role of bicarbonate in the regulation of electron transfer through Photosystem II. Before joining the Biochemistry Department at Otago University in 1994, he was a Postdoctoral Researcher focusing on various aspects of Photosystem II protein biochemistry with Professor Norio Murata at the National Institute for Basic Biology in Okazaki, Japan, with Professor Wim Vermaas at Arizona State University and with Dr. Geoffrey Hind at Brookhaven National Laboratory. His current research interests include structure-function relationships of Photosystem II proteins in both biogenesis and electron transport as well as the role of additional protein factors in the assembly of Photosystem II. He has been a Consulting Editor for the Advances in Photosynthesis and Respiration series since 2005 and edited volume 34 (with Baishnab C. Tripathy and Thomas D. Sharkey), *Photosynthesis*: *Plastid Biology*, *Energy Conversion and Carbon Assimilation*. He is also an Associate Editor for the *New Zealand Journal of Botany* and for the Plant Cell Biology section *Frontiers in Plant Science*. He edited Frontiers Research Topic *Assembly of the Photosystem II Membrane-Protein Complex of Oxygenic Photosynthesis* (with Roman Sobotka) in 2016, which is available as an eBook [ISBN 978-2-88945-233-0]. He has served as the President of the New Zealand Society of Plant Biologists (2006–2008) and of the New Zealand Institute of Chemistry (2012) and has been a Member of the International Scientific Committee of the Triennial International Symposium on Phototrophic Prokaryotes (2009–2018). Currently, he is the Secretary of the International Society of Photosynthesis Research.

Contents

Part II Molecular Genetics of Algae

Part III Biochemistry and Physiology of Algae

Part IV Light-Harvesting Systems in Algae

Preface: A Brief Introduction to the Algae

This book covers the process and development of photosynthesis in algae. Photosynthesis is the process by which light energy, predominantly from the sun, is converted into the energy of organic compounds. These photosynthetic products underpin almost all life on Earth; previously, with geological processes, they produced petroleum and coal, and in the future, they can contribute to a wide range of ecological and societal needs. As the world is using up its reserves of petroleum and coal at increasing rates, it is becoming important to understand the replenishment processes, with both biological and geological systems involved. At the same time, the alarming increases in greenhouse gases and the harmful effects on global climate make the use of these fossil fuels less and less desirable. The alternative is to develop new technologies for solar energy conversion, and these will undoubtedly involve algal biofuel production on a massive scale. Much work has been done in this area over the last two decades. On the purely mechanical-physical level, it is possible to set up solar farms and convert sunlight into electrical energy. And from there, it is possible to generate hydrogen by splitting water or to drive chemical half cells involving algae or components of algae to generate hydrogen or useful organic products. Alternatively, it is possible to "farm" algae in a variety of ways to generate fuels or value-added products. However, before any of these futuristic developments can be envisaged, it is necessary to know much more about the photosynthetic processes that occur on the Earth today and the role that algae play in the ecosystems of the Earth. Algae are eukaryotic organisms that exist in a multiplicity of forms and carry out oxygenic photosynthesis. In this book, our definition also includes *Cyanobacteria* (bacteria which nevertheless possess a process of photosynthesis able to split water). About half a billion years ago (BYA), one branch of green algae (see below) finally colonized the land and gave rise to "land plants" (embryophytes), and all these plants inherit to a greater or lesser extent the photosynthetic mechanisms of their algal forebears. So algae can be used directly in the freshwater and marine systems of the world to generate fuels or value-added organic products, or they can be studied to understand how to enhance the photosynthetic systems that developed from a fraction of the gene pool available in algae.

The Evolution of Photosynthesis

Photosynthesis evolved on the Earth at a very early stage, maybe as early as 3.8 billion years ago (BYA). The earliest mechanisms would have used available sources of hydrogen including hydrogen gas itself, which was much more abundant on the early Earth. The organisms were anaerobic bacteria, but as available sources of reductant were depleted, a new form of photosynthesis was evolving by at least 3 BYA, and maybe much earlier in a primitive form, which could split water and use the hydrogen of water as its source. By 2.45 BYA, cyanobacteria had fully evolved and were liberating oxygen into the Earth's atmosphere. The oxygenation of the atmosphere in the Great Oxidation Event (GOE) was a revolutionary step, which made possible the endosymbiosis of aerobic proteobacteria and photosynthetic cyanobacteria in protists, which, with genetic integration, evolved into mitochondria and plastids.

The Evolution of Algae

Some dozen phyla of eukaryotic protist organisms, from a total of 60 odd phyla, were algae, i.e., they possessed plastids (photosynthetic organelles developed from cyanobacteria by endosymbiosis) and were oxygenically photosynthetic. After about 2 billion years of evolution and massive diversification, the scene was set for the colonization of the land. One phylum, the green algae, gave rise to a multicellular subgroup, the streptophytes. The streptophytes colonized the land, becoming embryophytes and giving rise to mosses, ferns, and cone-bearing and flowering plants. At the same time, a multicellular group of protists evolved which gave rise to the animals, which also colonized the land, leading to all the animal groups with which we are familiar and eventually leading just 2 million years ago, or so, to man.

The Evolution of Eukaryotic Algae

The oldest algae date to at least 1.5 BYA and are red algae. However, some of the algae appear to be much more recent. For example, the diatoms that have a characteristic outer "shell," the frustule, are only found in sediments which are from 135 MYA. Other algal groups do not have a characteristic skeleton and cannot be dated in this way. Their origins can only be estimated by phylogenetic means, that is, by comparing their DNA with known fossil ages. Such studies reveal a rich and diverse lineage to the algae, where a "primary endosymbiosis" that involved the transfer of all the modern algal pigments was followed by a secondary, and in some cases tertiary, endosymbiosis with interesting pigment combinations. On one of these lines, that leading to the Apicomplexans, of which the malarial parasite is an example, all photosynthetic pigments and most of the photosynthetic mechanisms were lost.

The Rainbow of Algal Photosynthetic Mechanisms

With this rich and diverse history, many different patterns of photosynthesis evolved to suit a rainbow of light climates and ecological niches. Today, it is instructive to understand the fundamental differences involved. However, it is just as important that our understanding reveals how to utilize these varying arrays of pigments and photosynthetic approaches in devising technological approaches to harvesting solar energy by algae.

This book is divided into 17 chapters. These deal with all the major aspects of algal photosynthesis. However, the use of algae to produce biofuels and value-added products has been left to a second volume.

Anthony W. D. Larkum
Ultimo, NSW, Australia

Arthur R. Grossman
Stanford, CA, USA

John A. Raven
Dundee, UK

About the Editors

Anthony (Tony) Larkum is Emeritus Professor at the University of Sydney, Australia, where he was a Staff Member in Plant Sciences for 25 years. He has had a distinguished career in plant physiology, marine biology and phylogenetics. In addition, he has published a book on Charles Darwin and his cousin, William Darwin Fox, entitled *A Natural Calling: Life, Letters and Diaries of Charles Darwin and William Darwin Fox* (Springer Verlag). One of the first scientists to apply underwater techniques, he has contributed over a wide range of fields to advancing the study of underwater organisms, including cyanobacteria, marine algae, seagrasses and corals. In addition to this, he has contributed extensively to the field of light-harvesting and photoinhibition in photosynthetic organisms, having published many papers, a number of reviews and several books on the subject. Overall, he has published 254 papers in scientific journals; and these have an h-index of 65 (35 since 2014). His most cited papers are on coral bleaching in corals (632) and the discovery of fluorescent pigments in corals (590). And his third most cited work is for coediting a book on seagrasses (*Seagrasses: Biology, Ecology and Conservation*, Springer) in 2006. The current book is the culmination of a lifetime of work in the many fields of photosynthesis in cyanobacteria, eukaryotic algae and seagrasses. His contribution to these fields has been acknowledged by awards and election to scientific committees and boards of scientific journals over the years. He is currently on the Editorial Committee of the *Journal of the Royal Society Interface*.

Arthur Robert Grossman has been a Staff Scientist at the Carnegie Institution for Science, Department of Plant Biology, since 1982 and holds a courtesy appointment as Professor in the Department of Biology at Stanford University. He has performed research across fields ranging from plant biology, microbiology, marine biology, ecology, genomics, engineering and photosynthesis and initiated large-scale algal genomics by leading the *Chlamydomonas* genome project. In 2002, he received the Darbaker Prize (Botanical Society of America) for work on microalgae and in 2009 received the Gilbert Morgan Smith Medal (National Academy of Sciences) for the quality of his publications on marine and freshwater algae. In 2017, he was Chair of the Gordon Research Conference on Photosynthesis and gave the Arnon endowed lecture on photosynthesis in Berkeley in March 2017. He has given numerous plenary lectures and received a number of fellowships throughout his career, including the Visiting Scientist Fellowship, Department of Life and Environmental Sciences (DiSVA), Università Politecnica delle Marche (UNIVPM) (Italy, 2014), the Lady Davis Fellowship (Israel, 2011) and most recently the Chaire Edmond de Rothschild (to work at the IBPC in Paris in 2017–2018). He has been Co-Editor-in-Chief of *Journal of Phycology* and has served on the editorial boards of many well-respected biological journals including the *Annual Review of Genetics*, *Plant Physiology*, *Eukaryotic Cell*, *Journal of Biological Chemistry*, *Molecular Plant* and *Current Genetics*. He has also served on scientific advisory boards for both nonprofit and for profit companies including Phoenix Bioinformatics, Exelixis, Martek Biosciences, Solazyme/TerraVia, Checkerspot and Phycoil.

John Raven, FRS, is an Emeritus Professor at the University of Dundee, UK; an Honorary Fellow of the James Hutton Institute, UK; a Visiting Professor at the University of Technology Sydney; and an Adjunct Professor at the University of Western Australia. He has wide research interests, including astrobiology, bioenergetics, biogeochemistry, ecophysiology, evolutionary biology and palaeobiology. The majority of his publications have involved studies on algae. He has published 482 scientific papers (Web of Science, 30 July 2019) and is a Clarivate Analytics Highly Cited Researcher in the Cross Field research area. Among his contributions to our knowledge of algal photosynthesis are studies of inorganic carbon acquisition mechanisms in the laboratory and in nature, photosynthetic electron flow pathways other than from water to carbon dioxide, interactions of photosynthetic and respiratory reactions in organismal bioenergetics, and the extremes of photon flux density at which algal photosynthesis and photolithotrophic growth can occur.

Contributors

Roberto Bassi
Department of Biotechnology, University of Verona, Verona, Italy

John Beardall
School of Biological Sciences, Monash University, Clayton, VIC, Australia

Erica Belgio
Centre Algatech, Institute of Microbiology, Academy of Sciences of the Czech Republic, Třeboň, Czech Republic

Debashish Bhattacharya
Department of Biochemistry and Microbiology, Rutgers University, New Brunswick, NJ, USA

Claudia Büchel
Institute of Molecular Sciences, Goethe University, Frankfurt am Main, Germany

Douglas A. Campbell
Department of Biology, Mount Allison University, Sackville, NB, Canada

Anna Paola Casazza
Istituto di Biologia e Biotecnologia Agraria, Consiglio Nazionale delle Ricerche, Milan, Italy

Paul M. G. Curmi
School of Physics, The University of New South Wales, Sydney, NSW, Australia

Geoffry A. Davis
DOE Plant Research Laboratory, Department of Chemistry and Department of Biochemistry and Molecular biology, Michigan State University, East Lansing, MI, USA

Jeffrey A. Davis
Centre for Quantum and Optical Science, Faculty of Science, Engineering and Technology, Swinburne University of Technology, Hawthorn, VIC, Australia

Nicholas Fisher
DOE Plant Research Laboratory, Department of Chemistry and Department of Biochemistry and Molecular biology, Michigan State University, East Lansing, MI, USA

Myriam M. M. Goudet
Department of Plant Sciences, University of Cambridge, Cambridge, UK

Howard Griffiths
Department of Plant Sciences, University of Cambridge, Cambridge, UK

Arthur R. Grossman
Department of Plant Biology, Carnegie Institution for Science, Stanford University, Stanford, CA, USA

Parisa Heydarizadeh
Metabolism, Bioengineering of Microalgal Molecules and Applications (MIMMA), Mer Molécules Santé, IUML – FR 3473 CNRS, Le Mans University, Le Mans, France

Radek Kaňa
Centre Algatech, Institute of Microbiology, Academy of Sciences of the Czech Republic, Třeboň, Czech Republic

Atsuko Kanazawa
DOE Plant Research Laboratory, Department of Chemistry and Department of Biochemistry and Molecular biology, Michigan State University, East Lansing, MI, USA

U.S. Department of Energy Plant Research Laboratory, Michigan State University, East Lansing, MI, USA

Diana Kirilovsky
Institute for Integrative Biology of the Cell (I2BC), CNRS, CEA, Université Paris-Sud, Université Paris-Saclay, Gif sur Yvette, France

David M. Kramer
DOE Plant Research Laboratory, Department of Chemistry and Department of Biochemistry and Molecular biology, Michigan State University, East Lansing, MI, USA

Anthony W. D. Larkum
Global Climate Custer, University of Technology Sydney, Ultimo, NSW, Australia

Justine Marchand
Metabolism, Bioengineering of Microalgal Molecules and Applications (MIMMA), Mer Molécules Santé, IUML – FR 3473 CNRS, Le Mans University, Le Mans, France

Moritz T. Meyer
Department of Plant Sciences, University of Cambridge, Cambridge, UK

Department of Molecular Biology, Princeton University, Princeton, NJ, USA

Peter Neofotis
DOE Plant Research Laboratory, Department of Chemistry and Department of Biochemistry and Molecular biology, Michigan State University, East Lansing, MI, USA

Ondřej Prášil
Centre Algatech, Institute of Microbiology, Academy of Sciences of the Czech Republic, Třeboň, Czech Republic

Faculty of Science, University of South Bohemia, České Budějovice, Czech Republic

Dana C. Price
Department of Plant Biology, Rutgers University, New Brunswick, NJ, USA

Antonietta Quigg
Texas A&M University at Galveston, Galveston, TX, USA

Harry W. Rathbone
School of Physics, The University of New South Wales, Sydney, NSW, Australia

John A. Raven
Division of Plant Sciences, University of Dundee at the James Hutton Institute, Dundee, UK

Climate Change Cluster, University of Technology Sydney, Ultimo, NSW, Australia

Jean-David Rochaix
Departments of Molecular Biology and Plant Biology, University of Geneva University, Geneva, Switzerland

Stefano Santabarbara
Centre for Fundamental Research in Photosynthesis, Vergiate, Varese, Italy

Photosynthesis Research Unit, Centro Studi sulla Biologia Cellulare e Molecolare delle Piante, Milano, Italy

Christo Schiphorst
Department of Biotechnology, University of Verona, Verona, Italy

Benoît Schoefs
Metabolism, Bioengineering of Microalgal Molecules and Applications (MIMMA), Mer Molécules Santé, IUML – FR 3473 CNRS, Le Mans University, Le Mans, France

João Serôdio
Department of Biology and CESAM – Centre for Environmental and Marine Studies, University of Aveiro, Aveiro, Portugal

Cornelia Spetea
Department of Biological and Environmental Sciences, University of Gothenburg, Gothenburg, Sweden

Milán Szabó
Institute of Plant Biology, Biological Research Centre, Hungarian Academy of Sciences, Szeged, Hungary

Climate Change Cluster, University of Technology Sydney, Ultimo, Australia

Imre Vass
Institute of Plant Biology, Biological Research Centre, Hungarian Academy of Sciences, Szeged, Hungary

Robert D. Willows
Department of Molecular Sciences, Macquarie University, Sydney, Australia

Author Index

The original version of this book was revised: This book was inadvertently published with a spell error in the name of the editor as Arthur R. Grossmann which has been corrected now. The correction to this book is available at https://doi.org/10.1007/978-3-030-33397-3_18

Part I

Introductory Chapters

Chapter 1

Recent Advances in the Photosynthesis of Cyanobacteria and Eukaryotic Algae

Anthony W. D. Larkum*
Climate Change Cluster, University of Technology Sydney, Ultimo, NSW, Australia

Arthur R. Grossman
Department of Plant Biology, Carnegie Institution for Science, Stanford University, Stanford, CA, USA

and

John A. Raven
Climate Change Cluster, University of Technology Sydney, Ultimo, NSW, Australia

Division of Plant Sciences, University of Dundee at the James Hutton Institute, Invergowrie, Dundee, UK

I. Algal Systematics

Since the publication of the 1st Edition, there have been very significant advances in a number of areas of algal classification and systematics. Within the Cyanobacteria several new Phyla have been added such as Malainabacteria (e.g. Thiel et al. 2018). In the eukaryotic algae there has been the addition in the Apicomplexa of *Chromera* (Chromerids) and *Vitrella* (Vitrellids), which have only Chl *a* (and seemingly have lost Chl *c*) (See Fig. 7, Chap. 10). In the other classes, much progress has been

*Author for correspondence, e-mail: a.larkum@sydney.edu.au

A. W. D. Larkum et al. (eds.), *Photosynthesis in Algae: Biochemical and Physiological Mechanisms*, Advances in Photosynthesis and Respiration 45, https://doi.org/10.1007/978-3-030-33397-3_1

made by the use of "-omics" approaches to tidying up the various families (see Chaps. 2, 10 and 16). Fortunately this has not altered our conception of how the algae evolved or when, as outlined in the first edition. It is still an open question as to how the primary plastids evolved (see Chaps. 2 and 10).

The presence of new chlorophylls (Chl *d* and Chl *f*), and their biosynthesis is described, alongside the better-known chlorophylls, in Chap. 10.

II. Cyanobacteria

Cyanobacteria have received many, many studies in the last years, not least because of their potential for bioenergy production and value-added products (Larkum et al. 2012; Ortiz-Marquez et al. 2013; Savakis and Hellingwerf 2015; Heimann 2016). The cyanobacteria are a very ancient and diverse group. They go back to at least the Great Oxidation Event, at ~2.4 billion years ago (Shih and Matzke 2013). However, the symbiotic event that led to plastids occurred much later. Shih and Matzke 2013 estimate 0.9 billion years ago, using molecular clock techniques calibrated by gene duplications. However the establishment of red algae to ~1.2 BYA, and possibly by ~1.6 BYA must suggest a much earlier date (Butterfield 2000, 2015; Bengtson et al. 2017) The monophyletic hypothesis of plastid phylogeny (and perhaps even the shopping-bag model – see Chap. 10) would suggest that a single taxon or closely related set of taxa gave rise to the primary plastids. However, it is not certain that such a taxon or set of taxa would have survived to the present time and attempts to locate this have not been successful so far (Ochoa de Alda et al. 2014; Archibald 2015; Sánchez-Baracaldo et al. 2017).

III. Crystal Structures

The past decade has seen a quantum jump in the available crystal structures of photosynthetic molecules and in the definition of these structures. Previously, rather low resolution structures of Photosystem I (PSII) and II (PSI) were available In the past decade we have seen a 1.9 A resolution of PSII (Umena et al. 2011) with avoidance of X-ray damage (Suga et al. 2015) and several high resolution structures of PSI (Jordan et al. 2001; Nelson 2018) including the novel approach of Nathan Nelson to use virus derived gene structures.

The new crystal structures have enriched our understanding of the basics of photosynthesis in many ways. The elucidation of the oxygen evolving centre of Photosystem II (the Mn_4CaO_5 centre – see Suga et al. 2015) has revealed the elegant workings of the O_2-forming cycle and opened up the way for biotechnological approaches to synthetic structures for oxygen evolution. More than that the insights into how the special pair of PSII operates in relation to its electron donors (Y_z and Cyt b_{559}) and acceptors (Phaeophytin, non-haem iron and Q_A and Q_B) have also opened up the way to biomimetic approaches.

Likewise the structures of Photosystem I have also elucidated the specific structure of this system and shown that both arms of PsaA and PsaB are functional in transporting electrons to the electron acceptor of P700 (Jordan et al. 2001).

Interestingly, however, in certain cyanobacteria it has been discovered that two special Chlorophylls (absorbing in the near infra-red, NIR) not only act as light-harvesting pigments but are specifically required for the equivalent of P680 and P700. In the case of Chl *d* in *Acaryochloris marina* this is P694 and P710 (Itoh et al. 2007) and in Chl *f* organisms it is P698 and P718 (Nuernberg et al. 2018).

Structures of anoxygenic photosynthetic bacteria are also providing new insights into the possible evolution of photosynthetic reaction centres. In the case of PS bacteria with Reaction Centre II type centres (Rhodobacter and Chlorobiaceae) large differences exist between these and RCII of PSII. And in the case of Type I RCs the recent structural model of *Heliobacterium* has revealed a Ca^{2+} site with remarkable site homologies to the Mn_4CaO_5 centre site. This has suggested that this site was blocked in the *Heliobacterium* line specifically to prevent the formation of oxygen (Cardona et al. 2018). Furthermore, the effects of the presence of oxygen have been looked for and found in both PSI and PSII and have been used, in conjunction with other evidence, to argue for an early evolution of oxygen evolution from manganese centres in forebears of cyanobacteria, possibly before 3.5 billion years ago (BYA) (Cardona et al. 2018).

IV. Light Harvesting

Cyanobacteria have continued to provide interesting new mechanisms and pigments. The phycobilisome, which is present in most cyanobacteria, has been shown to be under control in supplying energy to the reaction centres of thylakoids though the Orange Carotenoid Pigment. This is a mechanism of Non-photochemical Quenchin (NPQ) or Down Regulation and is described in Chap. 10 and 12. In terms of pigments the biggest breakthrough has been the discovery of Chl *f* (Chen et al. 2010) in cyanobacteria from stromatolites of the Hamelin Pool, Shark Bay and its subsequent finding in a range of other cyanobacteria (Ho et al. 2016); Nuernberg et al. 2018). Chl *f* may be the last chlorophyll to be discovered (Schliep et al. 2013); however, there has continued to be progress with all the other chlorophylls (Chap. 10) and in the case of near infra red (NIR) driven systems there has been surprising progress. In the first edition of this book in 2004 Chl *d* was a new chlorophyll (see Chap. 3 of that book) and the only other established absorber of NIR was the chlorophyll *a* of *Ostreobium* (Chap. 11). In the meanwhile Chl *d* organisms have been found extensively and many eukaryotic algae have been found with Chl *a* able to absorb in the NIR (see Chap. 11 and Wolf et al. 2018).

In Eukaryotic algae there have been continuous advances in terms of mechanisms and a general survey of these is given in Chap.10 with more detailed descriptions given in Chaps. 3, 11, 14, 15, 16 and 17. Perhaps the most exciting and controversial aspect of light harvesting is the role of coherent energy transfer in pigment beds and this is dealt with in detail in Chap. 15. There is now good evidence that coherent energy transfer occurs in certain members of the Cryptophyceae (Chap. 15) and also evidence that it plays a role in desert algae (Bar-Eyal et al. 2015, 2017).

In eukaryotic algae with primary plastids (i.e with two envelope membranes; viz. Chlorophyta, Rhodophyta and Glaucophyta) all have received intense investigation in term of their light harvesting. In the Chlorophyceae (a class in the Chlorophyta), *Chlamydomonas reinhardtii* has continued to be the favourite organism because it can be easily genetically transformed (Chap. 4). This has led to a much better understanding of how the supply of light energy is balanced between the two photosystems and how the reaction centres are protected from damagingly high levels of solar radiation, by non-photochemical quenching and other mechanisms (Chaps. 3, 10, 11, 12, 16 and 17). Like the vascular plant *Arabidopsis thaliana*, *C. reinhardtii* will continue to be a well-used organism into the future.

However, other algae are emerging for their use in microalgal biotechnology. Perhaps foremost here is *Nannochloropsis gaditana*, a member of the Eustigmatophyceae (with secondary plastids), which is transformable, possesses only Chl *a,* and which can be made to produce large amounts

of lipids (Radakovits et al. 2012). However there is a wide choice of microalgae, and even macroalgae, now available (Larkum et al. 2012; Borowitzka et al. 2016).

In particular, the red algae (Rhodophyta) are now receiving close attention, despite their complex phycobilisome structure (Ago et al. 2016; Zhang et al. 2017) (see Chap. 11).

In secondary plastids the structure of a four- (or three-) membrane envelope and complex thylakoid structure has not deterred significant advances in our understanding of the structure and light-harvesting mechanisms, especially in the diatoms (Wang et al. 2019) (see Chaps. 12 and 16).

V. Photoinhibition

Photoinhibition continues to be one of the most challenging topics in algal research. Clearly algae have evolved mechanisms to protect against photoinhibition of one photosystem or the other. And this involves down regulation of high energy supply to the photosytems by Non-photochemical quenching and other mechanisms (see Chap. 10). In this volume there is a welcome chapter devoted to this topic alone (Chap. 13).

Both Photosystem I (Tikkanen et al. 2014) and Photosystem II (Andersson and Aro 2001) are involved in photoinhibition. Generally PS I is more resistant to photoinhibition, although it has recently been shown that Flavodiiron is safety valve for PSI under fluctuating light and when the system is overstressed inhibition can occur and lead to serious inhibition of photosynthesis (Jokel et al. 2018). On the other hand it seems that photoinhibition of PSII is an unavoidable consequence of water splitting (i.e. the large E_m of $P_{680}/P_{680}+$) and the inability of placing carotenoids close to P680 (Chap. 10); the net result of this is the unavoidable production of singlet oxygen (see Chaps. 10 and 17) which constantly impairs D1 of PSII (Andersson and Aro 2001).

VI. Dinoflagellates and Coral Bleaching

Dinoflagellate single-celled algae are a curious example of algae with secondary plastids; in this instance with 3 envelope membranes and an enslaved nuclear fragment with affinities to red algae (Douglas et al. 2001). Few studies have focused on these interesting organisms since the publication of the first edition. The exception here is the great current interest in coral bleaching. Corals are a symbiosis between dinoflagellates (in the Symbiodiniaceae, generally called zooxanthellae) and the coral animal (in the Cnidaria). For unresolved reasons in many coral reefs around the world Symbiodiniaceae leave the coral host at seawater temperatures of 30–32 °C. In Chap. 17, it is suggested that reactive oxygen species (ROS – hydrogen peroxide and singlet oxygen) trigger the bleaching process. The reason why ROS should be produced is probably related to the fact that dinoflagellates have a Type II Rubisco, which is impaired at temperatures above 30 °C. ROS are implicated in many second messenger systems in higher plants, with much information recently obtained from *Arabidiopsis thaliana* for hydrogen peroxide signaling (Noctor et al. 2018). The hypothesis, which was proposed a long time ago and is still current, is that over-reduction of PSI as a result of inhibition of the Calvin-Benson Cycle generates hydrogen peroxide, which triggers the release of the zooxanthellae (Chap. 17).

VII. Carbon Uptake and Metabolism (See Chap. 7 & 8)

Carbon Metabolism

Photosynthetic carbon reduction cycle (PCRC) is the core of autotrophic carbon assimilation in cyanobacteria and algae. There is limited evidence of C_4 or C_3-C_4 metabolism as a precursor to C_3 biochemistry in algae, and no evidence of C_4 or C_3-C_4

metabolism in cyanobacteria (Raven et al. 2017). Regulation of the PCRC differs in (e.g.) diatoms from the canonical green algal and embryophyte mechanism (Jensen et al. 2017). The reactions of the PCRC that have the greatest control strength have been determined for a cyanobacterium, and are similar to those in embryophytes (Janasch et al. 2018. Although the phosphoglycolate synthesis by Rubisco is limited by CCMs in most algae, there is usually a significant flux through phosphoglycolate; not all of the resulting glycolate is excreted, and the pathway of glycolate metabolism is not clear in diatoms (it is not the photorespiratory carbon oxidation cycle nor the tartronic semialdehyde pathway) (Raven et al. 2017). Diatoms are further discussed in Chap. 16).

Inorganic Carbon Acquisition

Most algae, and all cyanobacteria, have CCMs (Raven et al. 2017). The structural, mechanism and control of the CCM in cyanobacteria is well understood with diffusive carbon dioxide entry, and active bicarbonate transporters, at the plasmalemma, energized carbon dioxide conversion to bicarbonate in the cytosol, and bicarbonate conversion to carbon dioxide in carboxysomes that contain all of cell's Rubisco in a liquid-like condensate (Wang et al. 2019). Among eukaryotic algae, the best understood organism is *Chlamydomonas reinhardtii*, where the Rubisco, contained in the pyrenoid, is in a liquid-like matrix (Freeman Rosenzweig et al. 2017), similar to that in carboxysomes. However, how the pyrenoid functions are performed in algae, including most macroalgae with CCMs, lacking pyrenoids needs further investigations.

VIII. Water-Water Cycles (See Chap. 8)

Recent advances in understanding how a fraction of the oxygen produced in photosystem II is reconverted to (ultimately) water downstream of photosystem II have focused on PTOX and flavodi-iron proteins, accepting electrons from, respectively, photosystem II (e.g. Houille-Vernes et al. 2011) and photosystem I (e.g. Shimakawa et al. 2015). These water-water cycles, and Asada-Halliwell-Foyer water-water cycle involving both photosystems and ascorbate peroxidase, have a number of potential roles, including providing additional ATP as an alternative to cyclic electron and transport and hence phosphorylation, or oxidative phosphophorylation, when the ATP:NADPH supplied by linear electron flow is lower than that required in metabolism. This function would conflict with a role of water-water cycles in dissipation of excess excitation energy unless there is facultative uncoupling, for which there is no evidence. Energy dissipation by photorespiration is subject to an analogous constraint in terms of the carboxylation:oxygenation ratio of Rubisco that is regulated solely by the CO_2:O_2 ratio at the active site, but energy dissipation can be increases by replacing the photorespiratory carbon oxidation cycle or tartronic semialdehyde pathway with conversion of glycolate, via glyoxalate, oxalate and formate, to CO_2 via a pathway not coupled to ATP synthesis, or, less likely, glycolate excretion (Eisenhut et al. 2008).

References

Ago H, Adachi H, Umena U, Tashiro T, Kawakami K et al (2016) Novel features of eukaryotic photosystem II revealed by its crystal structure analysis from a red alga. J Biol Chem 291:5676–5687

Andersson B, Aro EM (2001) Photodamage and D1 protein turnover in photosystem II. In: Aro EM, Andersson B (eds) Regulation of photosynthesis. Springer, Berlin, pp 377–393

Archibald JM (2015) Genomic perspectives on the birth and spread of plastids. Proc Natl Acad Sci U S A 112:10147–10153

Bar-Eyal L et al (2015) An easily reversible structural change underlies mechanisms enabling desert crust cyanobacteria to survive desiccation. Biochim Biophys Acta 1847(10):1267–1273.

ISSN 0005-2728. Disponível em: < <Go to ISI>://BIOSIS:PREV201500695204 >

Bar-Eyal L et al (2017) Changes in aggregation states of light-harvesting complexes as a mechanism for modulating energy transfer in desert crust cyanobacteria. Proc Natl Acad Sci U S A 114(35):9481–9486. ISSN 0027-8424. Disponível em: < <Go to ISI>://BIOSIS:PREV201700818255 >

Bengtson S, Sallstedt T, Bellanova V, Whitehouse M (2017) Three-dimensional preservationof cellular and subcellular structures suggests 1.6 billion-year-old crown group red algae. PLoS Biol 15:e2000735

Borowitzka MA, Beardall J, Raven JA (eds) (2016) The physiology of microalgae. pp. 681pp. Springer, Berlin

Butterfield NJ (2000) Bangiomorpha pubescens n. gen., n. sp.: implications for the evolution of sex, multicellularity, and the Mesoproterozoic/Neoproterozoic radiation of eukaryotes. Palaeobiology 26:386–404

Butterfield NJ (2015) Early evolution of Eukarota. Palaeontology 58:5–17

Cardona T et al (2018) Early Archean origin of photosystem II. Geobiology 17(2):127–150

Chen M et al (2010) A red shifted chlorophyll. Science 329:1318

Douglas S, Zauner S, Fraunholz M, Beaton M, Penny S et al (2001) The highly reduced genome of an enslaved algal nucleus. Nature 410:1091–1096

Eisenhut M, Ruth W, Haimovich M, Bauwe H, Kaplan A, Hagemann M (2008) The photorespiratory glycolate metabolism is essential for cyanobacteria and might have been conveyed endosymbiotically to plants. Proc Natl Acad Sci U S A 105:17189–17204

Freeman Rosenzweig ES, Xu B, Cuellae LK, Martinez-Sannchez A, Schaffer M, Strauss M, Cartwright HN, Ronceray P, Plitzko JM, Förster F, Wingreen NS, Engel BD, MacKinder LCM, Jonikas MC (2017) The eukaryotic CO_2-concentrating organelle is liquid-like and exhibits dynamic reorganization. Cell 171:148–162

Heimann K (2016) Novel approaches to microalgal and cyanobacterial cultivation for bioenergy and biofuel production. Curr Opin Biotechnol 38:183–189

Ho M et al (2016) Far-red light photoacclimation (FaRLiP) in Synechococcus sp. PCC 7335: I. regulation of FaRLiP gene expression. Photosynth Res 131(2):173–186PR

Houille-Vernes I, Rappoport F, Wollman FA, Alric J, Johnson X (2011) Plastid terminal oxidase 2 (PTOX2) is the major oxidase involved in chlororespiration in *Chlamydomonas*. Proc Natl Acad Sci U S A 110:4111–4116

Itoh S, Mino H, Itoh K, Shigenaga T, Uzumaki T, Iwaki M (2007) Function of chlorophyll d in reaction centers of photosysterns I and II of the oxygenic photosynthesis of *Acaryochloris marina*. Biochemistry 46:12473–12481

Janasch M, Aslund-Samulesson J, Steuer R, Hudson EP (2018) Kinetic modeling of the Calvin cycle identifies flux control and stable metabolomes in *Synechocystis* in carbon fixation. J Exp Bot 70:973–983

Jensen E, Clément R, Maberly SC, Gontero B (2017) Regulation of the Calvin-Benson-Bassham cycled in the enigmatic diatoms: biochemical and evolutionary variations on an original theme. Philos Trans R Soc B 372:20160401

Jokel M, Johnson X, Peltier G, Aro E-M, Allahverdiyeva Y (2018) Hunting the main player enabling Chlamydomonas reinhardtii growth under fluctuating light. Plant J 94:822–835

Jordan P, Fromme P, Witt HT, Klukas O, Saenger W, Krauss N (2001) Three-dimensional structure of cyanobacterial photosystem I at 2.5 A resolution. Nature 411:909–917

Larkum A, Ross I, Kruse O, Hankamer B (2012) Selection, breeding and engineering of microalgae for bioenergy and biofuel production. Trends Biotechnol 30:198–205

Nelson N (2018) A quest for the atomic resolution of plant photosystem I. In: Barber J, Ruban AV (eds) Photosynthesis and bioenergetics. World Scientific, London.

Noctor G, Reichheld J-P, Foyer CH (2018) ROS-related redox regulation and signaling in plants. Semin Cell Dev Biol 80:3–12

Nuernberg DJ et al (2018) Photochemistry beyond the red limit in chlorophyll f-containing photosystems. Science (Washington D C) 360(6394):1210–1213. ISSN 0036-8075. Disponível em: < <Go to ISI>://BIOSIS:PREV201800721231 >

Ochoa de Alda JAG, Esteban R, Diago ML, Houmard J (2014) The plastid ancestor originated among one of the major cyanobacterial lineages. Nat Commun 5:4937. https://doi.org/10.1038/ncomms5937

Ortiz-Marquez JCF, Do Nascimento M, Zehr JP, Curatti L (2013) Genetic engineering of multi-species microbial cell-factories as an alternative for bioenergy production. Trends Biotechnol 31:521–529

Radakovits R, Jinkerson RE, Fuerstenberg SI, Tae H, Settlage RE et al (2012) Draft genome sequence and genetic transformation of the oleaginous alga *Nannochloropsis gaditana*. Nature Commun 3:686

Raven JA, Beardall J, Sánchez-Baracaldo P (2017) The possible evolution, and future, of CO_2-concentrating mechanisms. J Exp Bot 68:3701–3716

Sánchez-Baracaldo P, Raven JA, Pisani D, Knoll AH (2017) Early photosynthetic eukaryotes inhabited

low-salinity habitats. Proc Natl Acad Sci U S A 114:E7737–E7745

Savakis P, Hellingwerf KJ (2015) Engineering cyanobacteria for direct biofuel production from CO2. Curr Opin Biotechnol 33:8–14

Schliep M, Cavigliasso G, Quinnell RG, Stranger R, Larkum AWD (2013) Formyl group modification of chlorophyll *a*: a major evolutionary mechanism in oxygenic photosynthesis. Plant, Cell Environ 36:521–527

Shih PM, Matzke NJ (2013) Primary endosymbiosis events date to the later Proterozoic with cross-calibrated phylogenetic dating of duplicated ATPase proteins. Proc Natl Acad Sci 110(30):12355–12360

Shimakawa G, Shaku K, Nishi A, Hayashi R, Yamamoto H, Sakamoto K, Makino A, Miyake C (2015) FLAVODIIRON2 and FLAVODIIRON4 proteins mediate an oxygen-dependent alternative electron flow in *Synecocystis* sp. PCC 6803 under CO_2-limited conditions. Plant Physiol 167:472–480

Suga S, Akita F, Hirata K, Ueno G, Murakami H et al (2015) Native structure of photosystem II at 1.95 Å resolution viewed by femtosecond X-ray pulses. Nature 517:99–103

Thiel V, Tank M, Bryant DA (2018) Diversity of chlorophototrophic bacteria revealed in the omics era. Ann Rev Plant Biol 69:21–29

Tikkanen M, Mekala NR, Aro E-M (2014) Photosystem II photoinhibition-repair cycle protects photosystem I from irreversible damage. Biochim Biophys Acta Bioenerg 1837:210–215

Umena Y, Keisuke Kawakami K, Shen JR, Kamiya N (2011) Crystal structure of oxygen-evolving photosystem II at 1. 9 Å resolution. Nature 473:55–60

Wang H, Yan X, Aigner H, Bracher A, Nguyen ND, Hee WY, Long BM, Price DG, Hartl EU, Hayer-Hartl M (2019) Rubisco condensate formation by CcmM in β-carboxysome biogenesis. Nature 566:131–135

Wolf BM, Niedzwiedzki DM, Magdaong NCM, Roth R, Goodenough U, Blankenship RE (2018) Characterization of a newly isolated freshwater Eustigmatophyte alga capable of utilizing far-red light as its sole light source. Photosynth Res 135:177–189

Zhang J, Ma J, Liu D, Qin S, Sun S et al (2017) Structure of phycobilisome from the red alga *Griffithsia pacifica*. Nature (London) 551:57–63

Chapter 2

The Algal Tree of Life from a Genomics Perspective

Debashish Bhattacharya*
Department of Biochemistry and Microbiology, Rutgers University, New Brunswick, NJ, USA

and

Dana C. Price
Department of Plant Biology, Rutgers University, New Brunswick, NJ, USA

I. Introduction

A large body of molecular, morphological, and fossil data demonstrates that primary plastids are derived from an ancient (≥1 Ga, up to 1.6 Ga; Butterfield 2000; Yoon et al. 2004; Parfrey et al. 2011; Blank 2013; Bengtson et al. 2017; Sánchez-Baracaldo et al. 2017) primary cyanobacterial endosymbiosis. This event occurred in the single common ancestor of three extant photosynthetic lineages collectively known as the Plantae, and more recently, the Archaeplastida (Cavalier-Smith 1981; Margulis 1981; Reyes-Prieto et al. 2007; Adl et al. 2005; Price et al. 2012; Cavalier-Smith 2017). These lineages include the Glaucophyta (glaucophyte algae), the Rhodophyta (red algae), and the Viridiplantae (green algae and land plants) that share a two-membrane bound photosynthetic plastid organelle. Once established in the Archaeplastida ancestor, the primary plastid spread to other lineages, including the SAR clade (stramenopiles [e.g. diatoms, kelps, plastid-lacking oomycetes] + Alveolata [dinoflagellates, ciliates, apicomplexans] + Rhizaria [e.g., chlorarachniophyte algae]), cryptophytes, haptophytes, and the

*Author for correspondence, e-mail: d.bhattacharya@rutgers.edu

A. W. D. Larkum et al. (eds.), *Photosynthesis in Algae: Biochemical and Physiological Mechanisms*, Advances in Photosynthesis and Respiration 45, https://doi.org/10.1007/978-3-030-33397-3_2

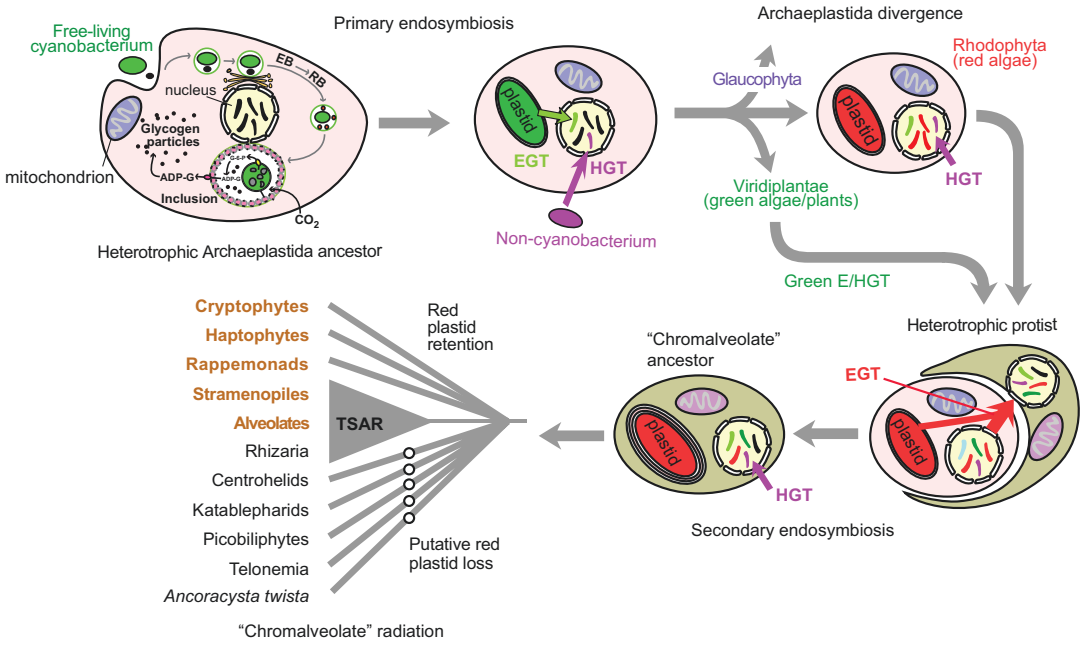

Fig. 2.1. The proposed history of plastid endosymbiosis in photosynthetic Archaeplastida and "chromalveolate" taxa. The primary cyanobacterial endosymbiosis, including contribution by chlamydial cells under the MATH is shown in the top left of this figure. Both EGT and HGT occurred throughout the history of Archaeplastida, prior to and after the split of its constituent phyla. A red alga was captured by the "chromalveolate" ancestor that may have been defined by the telonemid-SAR (TSAR) joint lineage (see Section III, below) and potentially including cryptophytes and haptophytes. There is evidence that this red algal secondary endosymbiosis was preceded by a cryptic green algal capture and subsequent loss of the organelle, leaving behind dozens to hundreds of green genes in the nucleus of diatoms and other chromalveolates (Moustafa et al. 2009; Dorrell et al. 2017). This complex series of gene transfer events was also added to by independent HGTs from external prokaryotes and eukaryotes. Given this scenario for origin of the plastid in most algal groups, it is not surprising that genomic data from these taxa provide reticulate phylogenetic signals when genes are analyzed individually or in groups, as described in the text. Image based on Qiu et al. (2013) and Brodie et al. (2017)

euglenids through multiple secondary and tertiary endosymbioses (Fig. 2.1). Many of these taxa that contain a red alga-derived plastid are colloquially referred to as "chromalveolates", a now defunct (i.e., polyphyletic) taxon that was hypothesized by Cavalier-Smith (1999) to share a single secondary endosymbiosis. Therefore, current data thus suggest that virtually all photosynthetic forms on our planet ultimately owe their photoautotrophic ability to a single cyanobacterial source. The sole exception to this rule is the clade of photosynthetic amoebae, *Paulinella*, to be described below that provides the only known case of an independent plastid primary endosymbiosis.

II. Why Inferring the Algal Tree of Life Is Non-trivial

Although of central importance to marine ecosystems and terrestrial life, the conversion of solar energy into carbohydrates and lipids through photosynthesis came at a high cost to photosynthetic cells. Light harvesting can capture excess energy that must be eliminated (mostly as heat), and photosynthetic electron flow is accompanied by the formation of reactive oxygen species (ROS) that can impair cellular functions (Peers et al. 2009; Knoefler et al. 2012). Therefore, the first algae, and every subsequent host of a serial plastid endosymbiosis depicted in Fig. 2.1 had to

cope with these challenges and integrate the flow of fixed carbon across cell compartments (Linka and Weber 2010; Karkar et al. 2015). These cells also needed to adapt to diurnal changes in light intensity, temperature, water and nutrient availability, and competition from other protists and predators to survive. These selective pressures necessitated major innovations, not only through mutation and gene duplication but also the acquisition of foreign genes from the endosymbiont *via* endosymbiotic gene transfer (EGT) as well as from external prokaryotic and eukaryotic sources through horizontal gene transfer (HGT) (Fig. 2.1). In addition, protein domains encoded by cyanobacterial (endosymbiont) genes were mixed and matched with domains from other genes to give rise to chimeric symbiogenetic (S)-genes with novel roles. Many of these S-gene functions evolved to deal with redox stress and light sensing to support the novel organelle (Méheust et al. 2016). An important, and unexpected perspective on how complex biotic interactions underlie plastid origin is offered by recent work done on the contribution of chlamydial genes to Archaeplastida.

The chlamydial connection is summarized under the ménage à trois hypothesis (MATH) that suggests a direct role for Chlamydiales obligate intracellular pathogens in plastid establishment. This idea is supported by the finding of 30–100 genes of chlamydial derivation in Archaeplastida that are involved in a range of key functions such as glycogen, tryptophan, and menaquinone metabolism (Ball et al. 2013, 2016; Qiu et al. 2013; Cenci et al. 2017, 2018). As shown in Fig. 2.1, under the MATH, the chlamydial infectious particle (EB: elementary body, black circle) entered the Archaeplastida host together with a free-living cyanobacterium (green circle). The EB remodeled the phagocytic membrane into a chlamydia-controlled inclusion and differentiated into reticulate bodies (RBs; pink circles) that attached to the inclusion and secreted chlamydial effector proteins corresponding to glycogen metabolism enzymes into both the inclusion and the host cytosol. Within the inclusion, the cyanobacterial endosymbiont is believed to have recruited chlamydial transporters via conjugation with the pathogen to facilitate export of glucose-6-phosphate (G-6-P) through the UhpC transporter of chlamydial origin (orange circle). This sugar phosphate was utilized for glycogen synthesis in the inclusion and excess ADP-G was released to the cytosol *via* a nucleotide sugar transporter (magenta circle) of eukaryotic origin. These processes led to the initial survival of the unprotected cyanobacterial endosymbiont in the chlamydial inclusion, precipitated gene transfers between compartments, and the integration of carbon flux that led to permanent plastid maintenance. Once the chlamydial cell was lost, the only "footprints" that remain of this hypothetical scenario are dozens of pathogen-derived HGTs with plastid-related functions. Consistent with the idea that EGTs, HGTs, and redirection of host-encoded proteins are critical to organellogenesis are the findings regarding evolution of the novel plastid in *Paulinella* spp. This plastidial organelle is a far younger version of the Archaeplastida organelle, having originated ca. 100 Ma (Kim et al. 2014).

Paulinella chromatophora and *P. micropora* are filose amoebae (Bhattacharya et al. 1995) with blue-green chromatophores (plastids). *P. chromatophora* was described in 1895 by Robert Lauterborn (Lauterborn 1895) and the photosynthetic *Paulinella* lineage is the only known case of an independent primary (alpha-cyanobacterial) plastid acquisition (Kies 1974; Marin et al. 2007; Yoon et al. 2009), making them models for understanding plastid establishment. The chromatophore genome is highly reduced in size and gene content (ca. 850 protein coding genes) relative to cyanobacterial genomes (Nowack et al. 2008; Yoon et al. 2009; Reyes-Prieto et al. 2010). Recent work shows that dozens of bacterial genes have been recruited to support lost organelle functions (due to Muller's ratchet acting on this non-

recombining DNA) (Nowack et al. 2016; DB and DCP unpublished data) as well as the retargeting of host proteins through a novel sorting pathway (Nowack and Grossman 2012; Singer et al. 2018). These results demonstrate that foreign gene transfer to the host nucleus is key in compensating for organelle genome reduction and suggests that phagotrophy (i.e., photosynthetic *Paulinella* are derived from a phagotrophic lineage; Bhattacharya et al. 2012) was retained early on in endosymbiosis to facilitate HGT, presumably via the ingestion of prey cells.

A final example of genetic complexity associated with endosymbiosis is provided by the work of Moustafa et al. (2009) who determined the phylogenetic origins of proteins encoded in the model diatoms *Thalassiosira pseudonana* and *Phaeodactylum tricornutum*, and found several hundred of green algal provenance shared by SAR and other "chromalveolates". These results suggested a cryptic (again, missing compartment) green algal endosymbiosis in the chromalveolate ancestor prior to the capture of the widespread red algal plastid in these taxa. This idea was tested and found wanting by some (e.g., Deschamps and Moreira 2012) but more recent work using a richer collection of genomes, with a focus on plastid proteomes (Dorrell et al. 2017), provided strong support for the original Moustafa et al. (2009) hypothesis. Therefore, accurately inferring algal relationships with the ETOL is not a trivial problem. Beyond testing Archaeplastida monophyly, the chromalveolate taxa have likely undergone serial plastid endosymbioses (e.g., Stiller et al. 2014) and sporadic HGTs over their >1 billion evolutionary history that will invariably muddy the waters (i.e., due to reticulate gene histories) when inferring phylogenetic relationships. Even in instances where Archaeplastida are found to be monophyletic, which is often the case in multigene trees (e.g., Rodríguez-Ezpeleta et al. 2005; Parfrey et al. 2011; Burki et al. 2016), and more robustly when using biochemical and metabolic pathway data (the MATH; Price et al. 2012), the spread of red and green genes in chromalveolates due to EGT and HGT will pull the Archaeplastida apart when included in multi-gene phylogenies. The issue of ancient algal gene transfer complicating ETOL inference was succinctly described by Hackett et al. (2007) when they first provided evidence of SAR monophyly, and has hounded reconstruction of the algal tree of life ever since.

III. Examples of Reticulate Behavior Among Algal Genes

In spite of the issues described above, many nodes in the broader ETOL have been solved, or at least well-supported using a "designer set" of 187 (Cavalier-Smith et al. 2015, 2016) to over 200 concatenated genes that have been manually checked to circumvent EGT/HGT and paralogy artifacts (e.g., 263 genes by Irwin et al. 2018; 248 genes by Strassert et al. 2019). Many of these studies have consolidated algal (and related non-photosynthetic [e.g., *Ancoracysta twista*]) groups (SAR; Burki et al. 2016; Janouškovec et al. 2017), and in others, brought them into question (Archaeplastida; Strassert et al. 2019). Of particular focus in these analyses are the cryptophytes and haptophytes that have been reported in several different positions in trees. Haptophytes were once identified as members of the novel clade 'Hacrobia' (Okamoto et al. 2009) that includes cryptophytes and other lineages such as telonemids and centrohelids (Burki et al. 2009), katablepharids and perhaps picobiliphytes (Okamoto et al. 2009; Yoon et al. 2011). However, the interrelationships of Hacrobia were unresolved (Okamoto et al. 2009), and later phylogenomic analyses refuted Hacrobia monophyly, placing haptophytes as sister to the SAR group (Baurain et al. 2010; Burki et al. 2012) together with telonemids and centrohelids (Burki et al. 2012) or in a later permutation as sister to centrohelids as

part of the 'Haptista' (Burki et al. 2016). The most recent work supports Archaeplastida paraphyly with cryptophytes sister to red algae (Adl et al. 2018), telonemids sister to SAR (the so-called "TSAR" lineage), and haptophytes sister to the Archaeplastida + Cryptophyta clade (Strassert et al. 2019). Based on these results, we can reasonably conclude that the phylogenetic position of SAR is likely to be well-established, yet despite a mountain of biochemical data, Archaeplastida monophyly is surprisingly ambiguous and the position of haptophytes (vis-à-vis cryptophytes and other protist lineages) within the ETOL remains unclear. These issues need to be resolved with the use of significantly more genome data from these taxa and perhaps novel approaches to the ETOL problem. Another obvious question to ask is whether, despite manual checking of designer gene sets, do these alignments contain sufficient phylogenetic power to resolve >1.6 billion-year-old divergences or alternatively, contain hidden signal of algal EGT/HGT (Hackett et al. 2007) that makes the resulting trees unstable?

The latter issue is real and can be shown using the "problematic" cryptophytes as an example of how single nuclear genes in algal genomes may contain highly complex phylogenetic signals. Figures 2.2 and 2.3 show maximum likelihood IQ-TREE analyses (Nguyen et al. 2015) with ultrafast bootstrap (UFB) approximations at nodes (2000 replicates; Minh et al. 2013) of 5 different genes encoded by cryptophytes and other ETOL lineages. The specific methods used to generate these alignments and trees are described in Price and Bhattacharya (2017) and incorporate the extensive MMETSP transcriptome data (Keeling et al. 2014) to expand taxonomic sampling, specifically among chromalveolates. Figure 2.2a presents the tree of a conserved 26S proteasome regulatory complex subunit that is involved in protein degradation. This analysis provides moderate support for the Hacrobia clade (UFB 78%) and most ETOL phyla are well supported in this robust phylogeny. Incidentally, a tree built using 88 concatenated plastid proteins also recovered Hacrobia monophyly with high RAxML bootstrap support (100%; Kim et al. 2017). In contrast, Fig. 2.2b shows the tree of a conserved SURF1 protein that is putatively involved in the biogenesis of cytochrome c oxidase and provides a very different view of cryptophyte evolution. In this tree, cryptophytes are weakly affiliated with red algae (UFB 67%) and haptophytes are sister to stramenopiles (UFB 77%), with several taxon misplacements likely due to cross-contamination in the EST data or mislabeling of MMETSP samples (e.g., *Madagascaria erythrocladiodes*). Regardless, the gene encoding SURF1 might provide an example of EGT from the red algal plastid endosymbiont in cryptophytes. In Fig. 2.2c, we find yet another phylogenetic scenario, whereby the U3 small nucleolar ribonucleoprotein IMP3 involved in 18S rRNA biogenesis splits the cryptophytes into two clades. One includes the aplastidial *Goniomonas pacifica* and green algae (UFB 77%), whereas the second photosynthetic clade is grouped with a red alga (UFB 64%) and other protists. Similar results are reported in Fig. 2.3a, in which a tree made from a hypothetical protein containing a domain of unknown function (DUF866) suggests cryptophyte polyphyly, showing the photosynthetic taxon grouping with red algae (UFB 90%) and haptophytes strongly affiliated with stramenopiles (UFB 97%). The final example tree (Fig. 2.3b) of a putative D123 protein involved in the cell division cycle supports the monophyly of photosynthetic cryptophytes and glaucophytes (UFB 82%) and the affiliation of haptophytes and stramenopiles (UFB 85%). It should be noted that these trees represent only a tiny fraction of the 1000s of phylogenies that we have generated. These examples provide evidence that single genes may each tell a unique story of algal evolution that merits attention, yet are clearly confounded by issues such as insuffi-

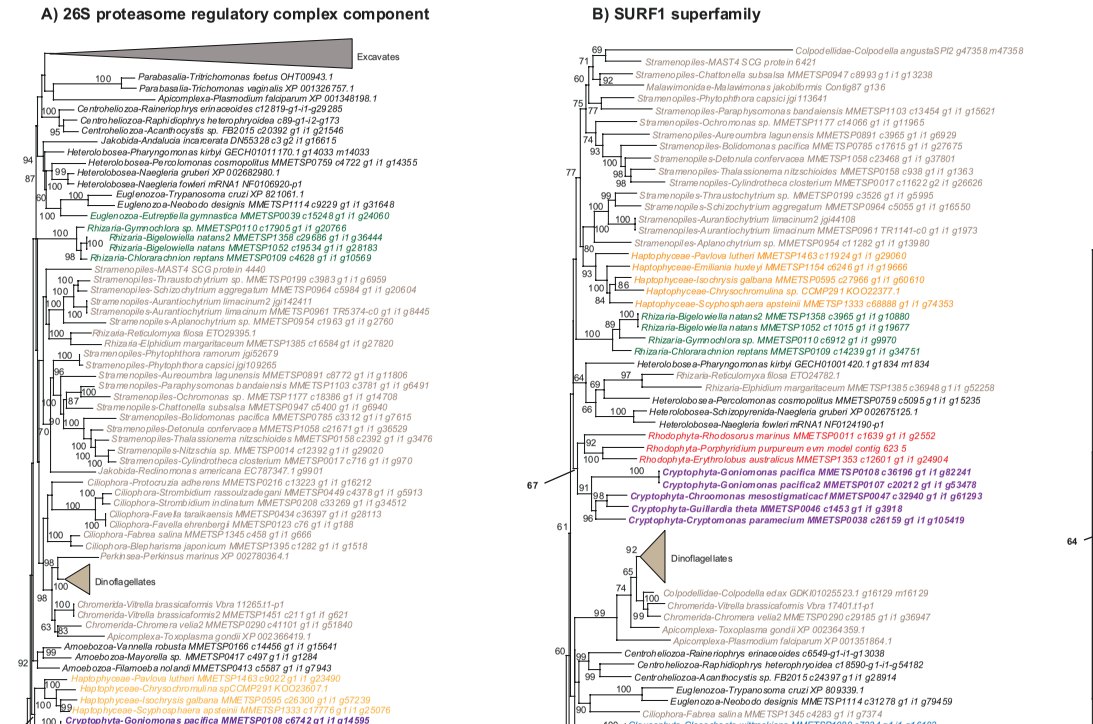

Fig. 2.2. Phylogenies of three proteins implicated in alga-derived EGT or HGT in "chromalveolates". (**a**) Phylogeny of a 26S proteasome regulatory complex component, (**b**) SURF1 superfamily protein, and (**c**) U3 small nucleolar ribonucleoprotein IMP3, inferred using IQ-TREE. The results of 1000 ultrafast bootstraps are shown at the branch nodes (when ≥60%), and the legends for substitution rates on branches are shown. Archaeplastida are shown in red (Rhodophyta), green (Viridiplantae), and light blue (Glaucophyta) text. SAR members are in brown text, cryptophytes in purple, haptophytes in orange, and photosynthetic chlororachniophytes in dark green. Dinoflagellates are summarized with the brown triangle. NCBI or MMETSP identifications are shown for each of the sequence entries

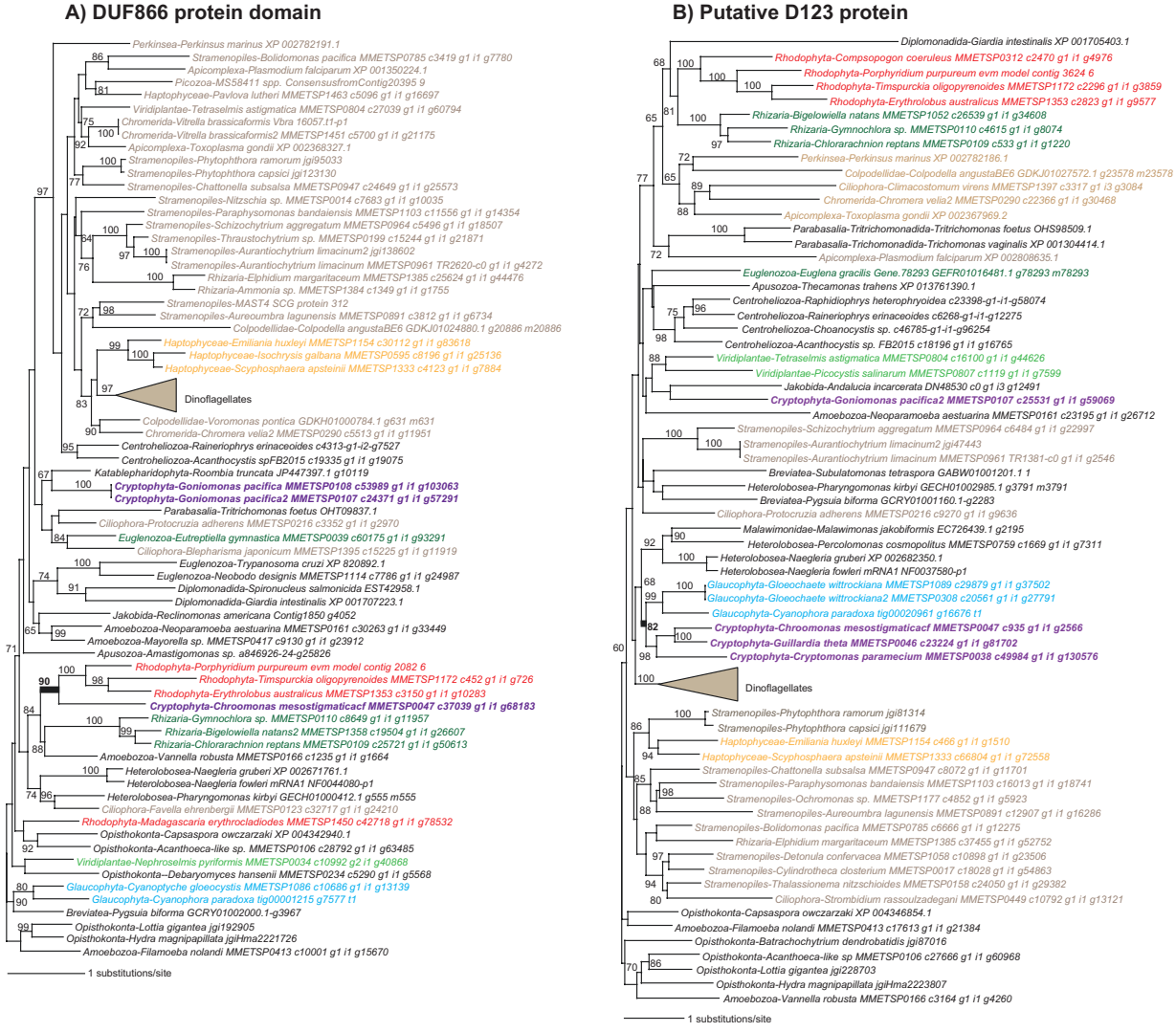

Fig. 2.3. Phylogenies of two proteins implicated in alga-derived EGT or HGT in "chromalveolates". (**a**) Phylogeny of a DUF866 protein domain containing sequence, and (**b**) putative D123 protein, inferred using IQ-TREE. The results of 1000 ultrafast bootstraps are shown at the branch nodes (when ≥60%), and the legends for substitution rates on branches are shown. Archaeplastida are shown in red (Rhodophyta), green (Viridiplantae), and light blue (Glaucophyta) text. SAR members are in brown text, cryptophytes in purple, haptophytes in orange, and photosynthetic chlororachniophytes in dark green. Dinoflagellates are summarized with the brown triangle. NCBI or MMETSP identifications are shown for each of the sequence entries

cient phylogenetic signal in single proteins, incomplete taxon sampling, paralog gains/losses, contamination, MMETSP taxon mislabeling (obvious cases are shown), or a combination of these factors. Nonetheless, single genes are the basis of phylogenetic inference and it is important to recognize their limitations prior to generating complex concatenated datasets to infer the ETOL.

IV. From Designer Datasets to Whole Genomes

Given the uncertainty associated with algal placements in the ETOL shown in Figs. 2.2 and 2.3 and previous studies, we chose to use another approach to this problem. Rather than trying to identify the "best set" of genes based on parameters such as length, conservation, paralogy, absolute distribution, evidence of EGT or HGT, we built a bioinformatic pipeline that follows a few simple rules and is fed predicted proteins from over a hundred genomic data sets from which a massive alignment is built, and an IQ-TREE inferred. The approach is described in Price and Bhattacharya (2017) and involves deriving de novo ortholog groups (OGs) to construct, in the example shown here, a 3000 OG dataset from 115 publicly available eukaryote proteomes. In brief, EST and/or predicted proteome data were retrieved for the target species and OrthoFinder (Emms and Kelly 2015) was used to construct OGs from the total data. Each group (or putative gene family) was parsed and we retained those that had low levels of paralogy (>80% of taxa were single-copy). Taxa with multi-copy representative proteins were removed from these groups, and the protein sequences corresponding to each individual group were aligned with MAFFT v. 7.3 (Katoh and Standley 2013). These alignments (summing to 2,458,432 aligned amino acids) were used to construct a maximum-likelihood phylogeny using IQ-TREE *via* a partitioned analysis in which each OG alignment represented a single partition with unlinked models of evolution chosen by IQ-TREE. Consensus tree branch support was determined by 2000 rapid bootstraps.

The phylogeny that resulted from this genome-wide approach is shown in Fig. 2.4. The position of telonemids (data not yet publicly available) is marked with an arrow based on Strassert et al. (2019). Several things relating to algae in the ETOL fall out. First, most phyla, including non-algal taxa receive strong UFB support. Archaeplastida monophyly is well-supported, with red algae as the earliest divergence. This latter result is consistent with the work of Lee et al. (2016) who studied the history of EGT among Archaeplastida and found 23 shared OGs in the plastid genomes of glaucophytes and Viridiplantae that were transferred to the nucleus from their putative common ancestor, versus only four such OGs being common to all three lineages, and only one shared OG being common to the Viridiplantae and rhodophytes. This pattern of intracellular gene movement supports the "red early" hypothesis, as depicted in Fig. 2.4. This tree also supports SAR monophyly and a common ancestry of cryptophytes, katablepharids, and picozoans with haptophytes sister to SAR. The broader story depicted in this genome-based perspective on the ETOL is that all algal groups and their non-photosynthetic sisters form a single clade in the tree (UFB 99%) that is distinct from opisthokonts, excavates, and their allies. The presence of plastid-lacking taxa at the base of cryptophytes suggests that this algal group may have undergone an independent algal secondary endosymbioses as suggested by Figs. 2.2b and 2.3a. This idea merits additional analysis given that some trees (both nuclear [Fig. 2.2a] and plastid based) favor Hacrobia monophyly. It is clear that the gene

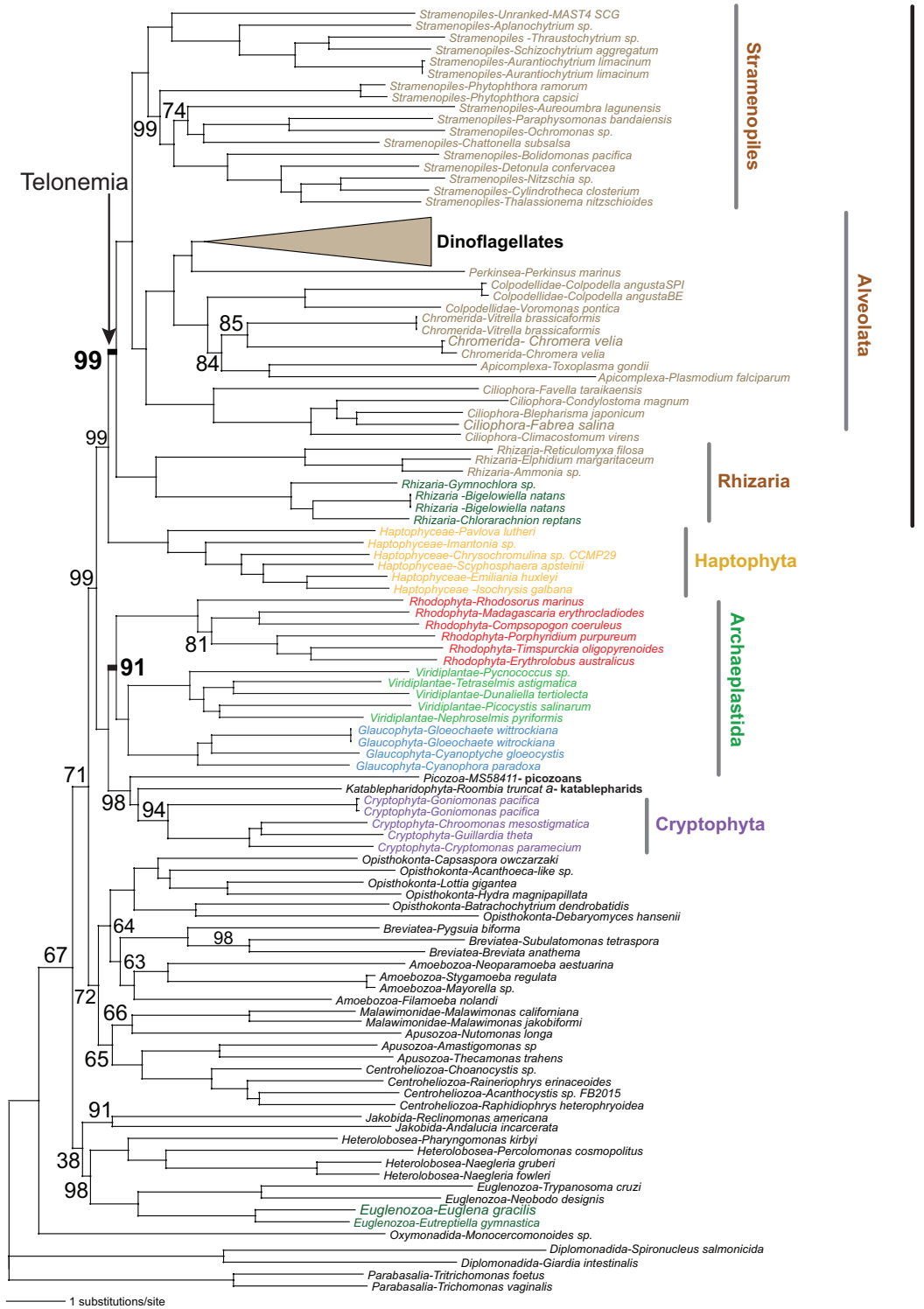

Fig. 2.4. Phylogeny built using IQ-TREE showing the positions of different algal groups in the ETOL. This tree was constructed using a partitioned 3000 OG dataset from 115 publicly available eukaryote proteomes. All nodes have 100% bootstrap support unless shown otherwise. Major algal groups are identified in the image. The putative position of telonemids is based on Strassert et al. (2019)

inventory of cryptophytes is highly chimeric in origin with *Goniomonas* species perhaps having the most complex pattern of algal EGT/HGT. This complexity notwithstanding, our current best estimate in this regard is that haptophytes are sister to SAR and telonemids.

To understand how this massive, genome-wide analysis compares to a tree inferred from a designer set of our making, we limited our dataset to OGs comprising the highly conserved odb9 (65 species; 303 OGs; 491,224 aligned amino acids) ortholog set implemented in BUSCO Eukaryota (Simão et al. 2015). The tree generated from this alignment is shown in Fig. 2.5. The topology is similar to Fig. 2.4, but appears to be more highly impacted by long-branch artifacts due to the high divergence rates among some excavates and ciliates, making these sister taxa to alveolates. Archaeplastida are again monophyletic but with glaucophytes as the earliest divergence in this clade. Hacrobia are paraphyletic with some plastid-lacking taxa being sister to haptophytes. In general, this tree receives 100% UFB support for most branches (as in Fig. 2.4) but appears to be more sensitive to divergence rate variation. This particular issue is not readily apparent in the genome-based tree.

V. Conclusions

Inferring algal phylogenetic relationships within the ETOL and generating a stable taxonomy is a vital but challenging frontier in photosynthesis research and more broadly in evolutionary biology. Once considered to be only a matter of time until all nodes are unequivocally established, the ETOL has only remained a significant problem for the fields of phylogenetics and genomics. This is because additional data have uncovered ever more complex behavior such as mixtures of photosynthetic and non-photosynthetic taxa suggesting massive plastid losses or multiple plastid gains that need to be accounted for before a "simple" framework of vertical evolution could be espoused. It is however clear that most algae are now securely placed within monophyletic groups and higher phyla such as Archaeplastida and SAR are well-established. Other orphan taxa such as cryptophytes and haptophytes continue to be difficult to place with confidence in the ETOL because of their history of endosymbioses and HGTs. This suggests that significantly more genomic data are needed to elucidate these processes and more robustly comprehend how photosynthetic ability and nuclear genomes have intersected over >1 billion years of eukaryotic history. From our perspective, the ETOL is best inferred using genome wide bioinformatic approaches that do not rely heavily on human intervention. Given the inherent biases associated with the field of phylogenetics, we surmise that allowing genomes to educate us is the more plausible approach to ETOL reconstruction and understanding how algae have evolved. Finally, a study was published after the submission of this manuscript that identified nonphotosynthetic, phagotrophic *Rhodelphis* species as sister organisms to the Rhodophyta within Archaeplastida (Gawryluk et al. 2019). These findings suggest that both phototrophy and predation were key components of the evolutionary history of this lineage.

Acknowledgments

We are grateful to the New Jersey Agricultural Experiment Station and the Rutgers University School of Environmental and Biological Sciences Genome Cooperative for supporting our genomics research. We also thank our many lab colleagues and collaborators for inspiring and nurturing our research in algal evolution.

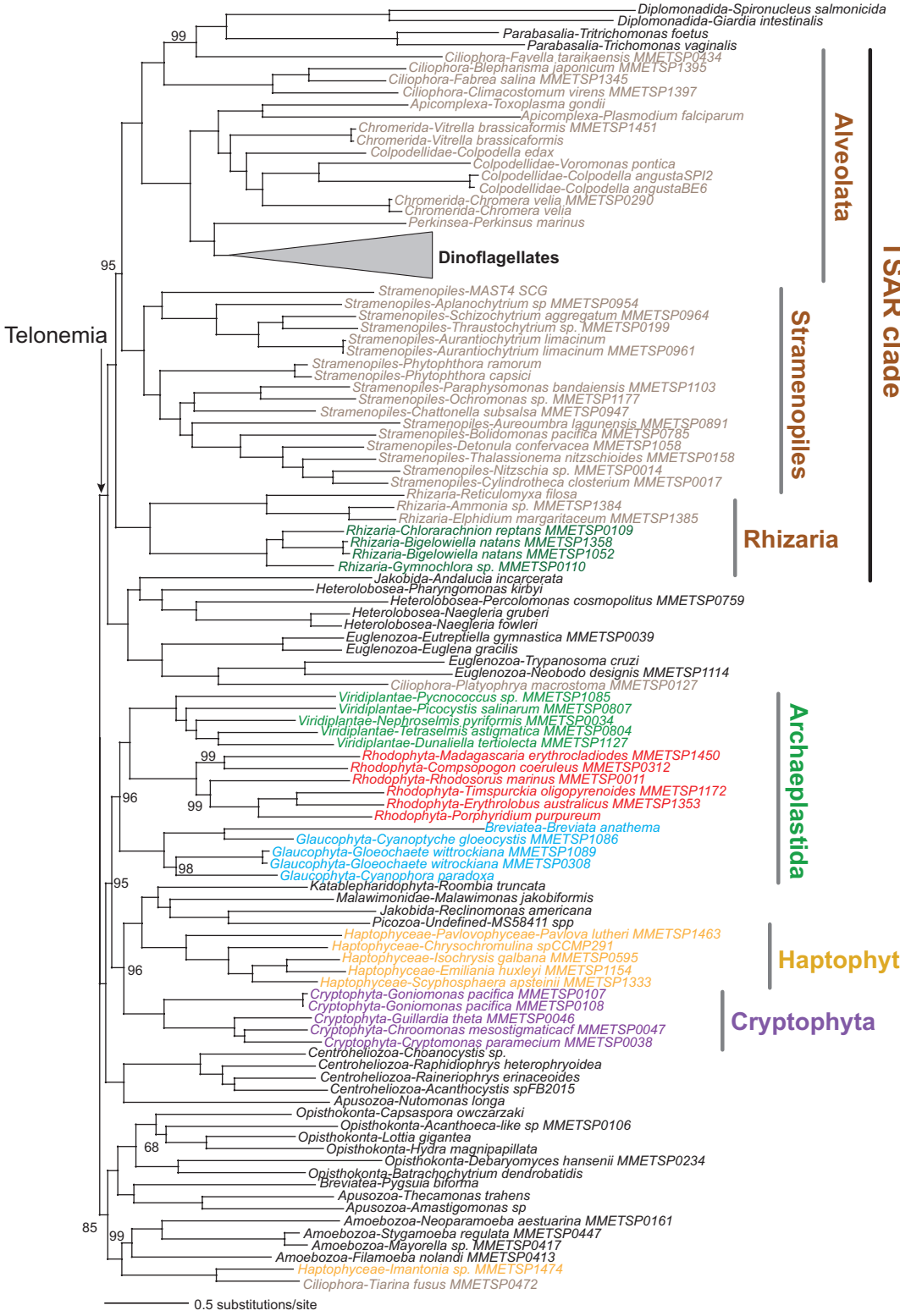

Fig. 2.5. Phylogeny built using IQ-TREE showing the positions of different algal groups in the ETOL. This tree was constructed using a partitioned 303 OG set based on the BUSCO Eukaryota dataset from 114 publicly available eukaryote proteomes. All nodes have 100% bootstrap support unless shown otherwise. Major algal groups are identified in the image. The putative position of telonemids is based on Strassert et al. (2019)

References

Adl SM, Simpson AG, Farmer MA, Andersen R, Anderson OR, Barta JR, Bowser SS, Brugerolle G, Fensome RA, Fredericq S, James TY, Karpov S, Kugrens P, Krug J, Lane CE, Lewis LA, Lodge J, Lynn DH, Mann DG, McCourt RM, Mendoza L, Moestrup O, Mozley-Standridge SE, Nerad TA, Shearer CA, Smirnov AV, Spiegel FW, Taylor MF (2005) The new higher level classification of eukaryotes with emphasis on the taxonomy of protists. J Eukaryot Microbiol 52:399–451

Adl SM, Bass D, Lane CE, Lukeš J, Schoch CL, Smirnov A, Agatha S, Berney C, Brown MW, Burki F, Cárdenas P, Čepička I, Chistyakova L, Del Campo J, Dunthorn M, Edvardsen B, Eglit Y, Guillou L, Hampl V, Heiss AA, Hoppenrath M, James TY, Karpov S, Kim E, Kolisko M, Kudryavtsev A, Lahr DJG, Lara E, Le Gall L, Lynn DH, Mann DG, Massana I Molera R, Mitchell EAD, Morrow C, Park JS, Pawlowski JW, Powell MJ, Richter DJ, Rueckert S, Shadwick L, Shimano S, Spiegel FW, Torruella I Cortes G, Youssef N, Zlatogursky V, Zhang Q (2018) Revisions to the classification, nomenclature, and diversity of eukaryotes. J Eukaryot Microbiol. https://doi.org/10.1111/jeu.12691

Ball SG, Subtil A, Bhattacharya D, Moustafa A, Weber AP, Gehre L, Colleoni C, Arias MC, Cenci U, Dauvillée D (2013) Metabolic effectors secreted by bacterial pathogens: essential facilitators of plastid endosymbiosis? Plant Cell 25:7–21

Ball SG, Bhattacharya D, Weber AP (2016) EVOLUTION. Pathogen to powerhouse. Science 351:659–660

Baurain D, Brinkmann H, Petersen J, Rodriguez-Ezpeleta N, Stechmann A, Demoulin V, Roger AJ, Burger G, Lang BF, Philippe H (2010) Phylogenomic evidence for separate acquisition of plastids in cryptophytes, haptophytes, and stramenopiles. Mol Biol Evol 27:1698–1709

Bengtson S, Sallstedt T, Belivanova V, Whitehouse M (2017) Three-dimensional preservation of cellular and subcellular structures suggests 1.6 billion-year-old crown-group red algae. PLoS Biol 15:e2000735

Bhattacharya D, Helmchen T, Melkonian M (1995) Molecular evolutionary analyses of nuclear-encoded small subunit ribosomal RNA identify an independent rhizopod lineage containing the Euglyphidae and the Chlorarachniophyta. J Eukaryot Microbiol 42:65–69

Bhattacharya D, Price DC, Yoon HS, Yang EC, Poulton NJ, Andersen RA, Das SP (2012) Single cell genome analysis supports a link between phagotrophy and primary plastid endosymbiosis. Sci Rep 2:356

Blank CE (2013) Origin and early evolution of photosynthetic eukaryotes in freshwater environments: reinterpreting proterozoic paleobiology and biogeochemical processes in light of trait evolution. J Phycol 49:1040–1055

Brodie J, Ball SG, Bouget FY, Chan CX, De Clerck O, Cock JM, Gachon C, Grossman AR, Mock T, Raven JA, Saha M, Smith AG, Vardi A, Yoon HS, Bhattacharya D (2017) Biotic interactions as drivers of algal origin and evolution. New Phytol 216:670–681

Burki F, Inagaki Y, Brate J, Archibald JM, Keeling PJ, Cavalier-Smith T, Sakaguchi M, Hashimoto T, Horak A, Kumar S, Klaveness D, Jakobsen KS, Pawlowski J, Shalchian-Tabrizi K (2009) Large-scale phylogenomic analyses reveal that two enigmatic protist lineages, telonemia and centroheliozoa, are related to photosynthetic chromalveolates. Genome Biol Evol 1:231–238

Burki F, Okamoto N, Pombert JF, Keeling PJ (2012) The evolutionary history of haptophytes and cryptophytes: phylogenomic evidence for separate origins. Proc Biol Sci 279:2246–2254

Burki F, Kaplan M, Tikhonenkov DV, Zlatogursky V, Minh BQ, Radaykina LV, Smirnov A, Mylnikov AP, Keeling PJ (2016) Untangling the early diversification of eukaryotes: a phylogenomic study of the evolutionary origins of Centrohelida, Haptophyta and Cryptista. Proc Biol Sci 283:1823

Butterfield NJ (2000) *Bangiomorpha pubescens* n. gen., n. sp.: implications for the evolution of sex, multicellularity, and the Mesoproterozoic/Neoproterozoic radiation of eukaryotes. Paleobiology 26:386–404

Cavalier-Smith T (1981) Eukaryote kingdoms: seven or nine? Biosystems 14:461–481

Cavalier-Smith T (1999) Principles of protein and lipid targeting in secondary symbiogenesis: euglenoid, dinoflagellate, and sporozoan plastid origins and the eukaryote family tree. J Eukaryot Microbiol 46:347–366

Cavalier-Smith T (2017) Kingdom Chromista and its eight phyla: a new synthesis emphasizing periplastid protein targeting, cytoskeletal and periplastid evolution, and ancient divergences. Protoplasma 255:297–357

Cavalier-Smith T, Fiore-Donno AM, Chao E, Kudryavtsev A, Berney C, Snell EA, Lewis R (2015) Multigene phylogeny resolves deep branching of Amoebozoa. Mol Phylogenet Evol 83:293–304

Cavalier-Smith T, Chao EE, Lewis R (2016) 187-gene phylogeny of protozoan phylum Amoebozoa reveals a new class (Cutosea) of deep-branching, ultrastructurally unique, enveloped marine Lobosa and clarifies amoeba evolution. Mol Phylogenet Evol 99:275–296

Cenci U, Bhattacharya D, Weber APM, Colleoni C, Subtil A, Ball SG (2017) Biotic host-pathogen interactions as major drivers of plastid endosymbiosis. Trends Plant Sci 22:316–328

Cenci U, Qiu H, Pillonel T, Cardol P, Remacle C, Colleoni C, Kadouche D, Chabi M, Greub G, Bhattacharya D, Ball SG (2018) Host-pathogen biotic interactions shaped vitamin K metabolism in Archaeplastida. Sci Rep 8:15243

Deschamps P, Moreira D (2012) Reevaluating the green contribution to diatom genomes. Genome Biol Evol 4:683–688

Dorrell RG, Gile G, McCallum G, Méheust R, Bapteste EP, Klinger CM, Brillet-Guéguen L, Freeman KD, Richter DJ, Bowler C (2017) Chimeric origins of ochrophytes and haptophytes revealed through an ancient plastid proteome. elife 6:e23717

Emms DM, Kelly S (2015) OrthoFinder: solving fundamental biases in whole genome comparisons dramatically improves orthogroup inference accuracy. Genome Biol 16:157

Gawryluk RMR, Tikhonenkov DV, Hehenberger E, Husnik F, Mylnikov AP, Keeling PJ (2019) Non-photosynthetic predators are sister to red algae. Nature 572(7768):240–243

Hackett JD, Yoon HS, Li S, Reyes-Prieto A, Rümmele SE, Bhattacharya D (2007) Phylogenomic analysis supports the monophyly of cryptophytes and haptophytes and the association of Rhizaria with chromalveolates. Mol Biol Evol 24:1702–1713

Irwin NAT, Tikhonenkov DV, Hehenberger E, Mylnikov AP, Burki F, Keeling PJ (2018) Phylogenomics supports the monophyly of the Cercozoa. Mol Phylogenet Evol 130:416–423.

Janouškovec J, Tikhonenkov DV, Burki F, Howe AT, Rohwer FL, Mylnikov AP, Keeling PJ (2017) A new lineage of eukaryotes illuminates early mitochondrial genome reduction. Curr Biol 27:3717–3724

Karkar S, Facchinelli F, Price DC, Weber AP, Bhattacharya D (2015) Metabolic connectivity as a driver of host and endosymbiont integration. Proc Natl Acad Sci U S A 112:10208–10215

Katoh K, Standley DM (2013) MAFFT multiple sequence alignment software version 7: improvements in performance and usability. Mol Biol Evol 30:772–780

Keeling PJ, Burki F, Wilcox HM, Allam B, Allen EE, Amaral-Zettler LA, Armbrust EV, Archibald JM, Bharti AK, Bell CJ, Beszteri B, Bidle KD, Cameron CT, Campbell L, Caron DA, Cattolico RA, Collier JL, Coyne K, Davy SK, Deschamps P, Dyhrman ST, Edvardsen B, Gates RD, Gobler CJ, Greenwood SJ, Guida SM, Jacobi JL, Jakobsen KS, James ER, Jenkins B, John U, Johnson MD, Juhl AR, Kamp A, Katz LA, Kiene R, Kudryavtsev A, Leander BS, Lin S, Lovejoy C, Lynn D, Marchetti A, McManus G, Nedelcu AM, Menden-Deuer S, Miceli C, Mock T, Montresor M, Moran MA, Murray S, Nadathur G, Nagai S, Ngam PB, Palenik B, Pawlowski J, Petroni G, Piganeau G, Posewitz MC, Rengefors K, Romano G, Rumpho ME, Rynearson T, Schilling KB, Schroeder DC, Simpson AG, Slamovits CH, Smith DR, Smith GJ, Smith SR, Sosik HM, Stief P, Theriot E, Twary SN, Umale PE, Vaulot D, Wawrik B, Wheeler GL, Wilson WH, Xu Y, Zingone A, Worden AZ (2014) The Marine Microbial Eukaryote Transcriptome Sequencing Project (MMETSP): illuminating the functional diversity of eukaryotic life in the oceans through transcriptome sequencing. PLoS Biol 12:e1001889

Kies L (1974) Electron microscopical investigations on *Paulinella chromatophora* Lauterborn, a thecamoeba containing blue-green endosymbionts (Cyanelles). Protoplasma 80:69–89

Kim KM, Park JH, Bhattacharya D, Yoon HS (2014) Applications of next-generation sequencing to unravelling the evolutionary history of algae. Int J Syst Evol Microbiol 64:333–345

Kim JI, Moore CE, Archibald JM, Bhattacharya D, Yi G, Yoon HS, Shin W (2017) Evolutionary dynamics of cryptophyte plastid genomes. Genome Biol Evol 9:1859–1872

Knoefler D, Thamsen M, Koniczek M, Niemuth NJ, Diederich AK, Jakob U (2012) Quantitative in vivo redox sensors uncover oxidative stress as an early event in life. Mol Cell 47:767–776

Lauterborn R (1895) Protozoenstudien II. *Paulinella chromatophora* nov. gen., nov. spec., ein beschalter Rhizopode des Sußwassers mit blaugrunen chromatophorenartigen Einschlussen. Z Wiss Zool 59:537–544

Lee J, Cho CH, Park SI, Choi JW, Song HS, West JA, Bhattacharya D, Yoon HS (2016) Parallel evolution of highly conserved plastid genome architecture in red seaweeds and seed plants. BMC Biol 14:75

Linka N, Weber APM (2010) Intracellular metabolite transporters in plants. Mol Plant 3:21–53

Margulis L (1981) Symbiosis in cell evolution. WH Freeman and Company, San Francisco

Marin B, Nowack EC, Glöckner G, Melkonian M (2007) The ancestor of the *Paulinella* chromatophore obtained a carboxysomal operon by horizontal gene transfer from a *Nitrococcus*-like γ-proteobacterium. BMC Evol Biol 7:85

Méheust R, Zelzion E, Bhattacharya D, Lopez P, Bapteste E (2016) Protein networks identify novel symbiogenetic genes resulting from plastid endosymbiosis. Proc Natl Acad Sci U S A 113:3579–3584

Minh BQ, Nguyen MA, von Haeseler A (2013) Ultrafast approximation for phylogenetic bootstrap. Mol Biol Evol 30:1188–1195

Moustafa A, Beszteri B, Maier UG, Bowler C, Valentin K, Bhattacharya D (2009) Genomic footprints of a cryptic plastid endosymbiosis in diatoms. Science 324:1724–1726

Nguyen LT, Schmidt HA, von Haeseler A, Minh BQ (2015) IQ-TREE: a fast and effective stochastic algorithm for estimating maximum likelihood phylogenies. Mol Biol Evol 32:268–274

Nowack ECM, Grossman AR (2012) Trafficking of protein into the recently established photosynthetic organelles of *Paulinella chromatophora*. Proc Natl Acad Sci U S A 109:5340–5345

Nowack ECM, Melkonian M, Glöckner G (2008) Chromatophore genome sequence of *Paulinella* sheds light on acquisition of photosynthesis by eukaryotes. Curr Biol 18:410–418

Nowack EC, Price DC, Bhattacharya D, Singer A, Melkonian M, Grossman AR (2016) Gene transfers from diverse bacteria compensate for reductive genome evolution in the chromatophore of *Paulinella chromatophora*. Proc Natl Acad Sci U S A 113:12214–12219

Okamoto N, Chantangsi C, Horak A, Leander BS, Keeling PJ (2009) Molecular phylogeny and description of the novel katablepharid *Roombia truncata* gen. et sp. nov., and establishment of the Hacrobia taxon nov. PLoS One 4:e7080

Parfrey LW, Lahr DJ, Knoll AH, Katz LA (2011) Estimating the timing of early eukaryotic diversification with multigene molecular clocks. Proc Natl Acad Sci U S A 108:13624–13629

Peers G, Truong TB, Ostendorf E, Busch A, Elrad D, Grossman AR, Hippler M, Niyogi KK (2009) An ancient light-harvesting protein is critical for the regulation of algal photosynthesis. Nature 462:518–521

Price DC, Bhattacharya D (2017) Robust Dinoflagellata phylogeny inferred from public transcriptome databases. J Phycol 53:725–729

Price DC, Chan CX, Yoon HS, Yang EC, Qiu H, Weber AP, Schwacke R, Gross J, Blouin NA, Lane C, Reyes-Prieto A, Durnford DG, Neilson JA, Lang BF, Burger G, Steiner JM, Löffelhardt W, Meuser JE, Posewitz MC, Ball S, Arias MC, Henrissat B, Coutinho PM, Rensing SA, Symeonidi A, Doddapaneni H, Green BR, Rajah VD, Boore J, Bhattacharya D (2012) *Cyanophora paradoxa* genome elucidates origin of photosynthesis in algae and plants. Science 335:843–847

Qiu H, Price DC, Weber AP, Facchinelli F, Yoon HS, Bhattacharya D (2013) Assessing the bacterial contribution to the plastid proteome. Trends Plant Sci 18:680–687

Reyes-Prieto A, Weber AP, Bhattacharya D (2007) The origin and establishment of the plastid in algae and plants. Annu Rev Genet 41:147–168

Reyes-Prieto A, Yoon HS, Moustafa A, Yang EC, Andersen RA, Boo SM, Nakayama T, Ishida K, Bhattacharya D (2010) Differential gene retention in plastids of common recent origin. Mol Biol Evol 27:1530–1537

Rodríguez-Ezpeleta N, Brinkmann H, Burey SC, Roure B, Burger G, Löffelhardt W, Bohnert HJ, Philippe H, Lang BF (2005) Monophyly of primary photosynthetic eukaryotes: green plants, red algae, and glaucophytes. Curr Biol 15:1325–1330

Sánchez-Baracaldo P, Raven JA, Pisani D, Knoll AH (2017) Early photosynthetic eukaryotes inhabited low-salinity habitats. Proc Natl Acad Sci U S A 114:E7737–E7745

Simão FA, Waterhouse RM, Ioannidis P, Kriventseva EV, Zdobnov EM (2015) BUSCO: assessing genome assembly and annotation completeness with single-copy orthologs. Bioinformatics 31:3210–3212

Singer A, Poschmann G, Mühlich C, Valadez-Cano C, Hänsch S, Hüren V, Rensing SA, Stühler K, Nowack ECM (2018) Massive protein import into the early-evolutionary-stage photosynthetic organelle of the amoeba *Paulinella chromatophora*. Curr Biol 27:2763–2773

Stiller JW, Schreiber J, Yue J, Guo H, Ding Q, Huang J (2014) The evolution of photosynthesis in chromist algae through serial endosymbioses. Nat Commun 5:5764

Strassert JFH, Jamy M, Mylnikov AP, Tikhonenkov DV, Burki F (2019) New phylogenomic analysis of the enigmatic phylum Telonemia further resolves the eukaryote tree of life. Mol Biol Evol 36:757–765.

Yoon HS, Hackett JD, Ciniglia C, Pinto G, Bhattacharya D (2004) A molecular timeline for the origin of photosynthetic eukaryotes. Mol Biol Evol 21:809–818

Yoon HS, Nakayama T, Reyes-Prieto A, Andersen RA, Boo SM, Ishida K, Bhattacharya D (2009) A single origin of the photosynthetic organelle in different *Paulinella* lineages. BMC Evol Biol 9:98

Yoon HS, Price DC, Stepanauskas R, Rajah VD, Sieracki ME, Wilson WH, Yang EC, Duffy S, Bhattacharya D (2011) Single-cell genomics reveals organismal interactions in uncultivated marine protists. Science 332:714–717

Part II

Molecular Genetics of Algae

Chapter 3

Chlorophyll-Xanthophyll Antenna Complexes: In Between Light Harvesting and Energy Dissipation

Christo Schiphorst and Roberto Bassi*
Department of Biotechnology, University of Verona, Verona, Italy

I. Introduction

In oxygenic photosynthesis light is captured and used to drive electrons from H_2O to NADPH, meanwhile building a proton gradient through the thylakoid membrane for ATP synthesis, and in the process water is split and oxygen is liberated to the environment. Photons are absorbed by proteins binding chlorophylls (Chls) and carotenoids (Cars) which, besides absorbing photons, also catalyse redox reactions to feed electron transport and a variety of photoprotective processes for coping with the highly variable nature of solar radiation (see Chap. 12).

Photosynthetic reaction centres (RCs) come in two sorts, depending on the type of electron acceptors: a quinone, in type II, and an Iron-Sulphur cluster in type I (Nitschke and William Rutherford 1991). These two RC-types, also referred to as Photosystem II (PSII) and Photosystem I (PSI), work in tandem and lead to oxygen production and linear electron transport, delivering electrons to carbon dioxide fixation and other mechanisms. In each RC the excitation of a chlorophyll pair, either P680 or

*Author for correspondence, e-mail: roberto.bassi@univr.it

A. W. D. Larkum et al. (eds.), *Photosynthesis in Algae: Biochemical and Physiological Mechanisms*, Advances in Photosynthesis and Respiration 45, https://doi.org/10.1007/978-3-030-33397-3_3

P700, leads to an oxidized special pair which is then neutralized by an electron from, respectively H_2O or plastocyanin. The electrons from the primary reductants enter the linear electron transport chain to reduce $NADP^+$.

The pigments for light harvesting and chromophores for electron transport are bound to transmembrane protein complexes called "Core Complexes", including the special pairs, which together form the RCs. Even though the RCs of the two photosystems are photosynthetically competent, as shown in core complex-only mutants, e.g. *ch1* in plants and Cao in algae (Dall'Osto et al. 2010; Polle et al. 2000) such plants show effective, yet reduced growth, because the light harvesting capacity is low, limiting the period of efficient electron transport rate to midday. In order to widen the photosynthetic efficient window, the RCs are endowed with antenna proteins: pigment-proteins which have a far higher density of chromophore per protein scaffold unit. Antenna proteins enhance the absorption cross section in two ways: (i) they harbour a greater variety of chromophores absorbing over different spectral intervals; and (ii) they increase the overall number of chromophores feeding the captured energy to each RC. Besides obvious advantages, antenna systems have downsides: building of pigment-protein arrays is energetically expensive while the daily variations in photon flux, not mentioning canopy movement, clouds passing before the sun, or waves in the sea, cannot be matched by a parallel dismantling and re-synthesis of antenna proteins. In addition, the subsequent reactions of linear electron transport chain occur in a wide kinetic range. Since plastoquinone is reduced to plastoquinol by PSII on a ns timescale, and its oxidation by Cyt b_6f occurs in ms, excess light therefore over-reduces plastoquinone leading to charge recombination, chlorophyll triplet state ($^3Chl*$) accumulation and reaction with O_2, causing reactive oxygen species (ROS), and especially in PSII, singlet oxygen ($^1O_2*$) production and photoinhibition. Similarly, superoxide is readily produced when the Calvin-Benson cycle is saturated and the flux of reductants from PSI exceeds the capacity of downstream metabolic reactions. Indeed, the high energy univalent reducing energy transfer (ET) intermediates obviously react with oxygen whenever they accumulate for lack of oxidized electron partners, creating ROS species, principally H_2O_2 and leading to photodamage. In this chapter we will review examples of how oxygenic photosynthetic organisms evolved a variety of different regulative, acclimative and ROS-scavenging mechanisms which are activated depending on light conditions. These prevent and/or reduce the damaging effects of excess light and the consequent oxidative stress while optimizing light harvesting.

II. Chromophores

Light harvesting is based on chromophores, i.e. pigments attached to proteins. These come in many different types depending on species. The key chromophore and most abundant in oxygenic photosynthesis is chlorophyll (Chl).

Chlorophylls absorb strongly in the blue (350–500 nm) and red regions (625–700 nm) of the visible light spectrum. The absorption peaks in the blue are named Soret-bands, or B-bands, while peaks in the red region are named Q-bands, see Fig. 3.1. Small differences in chromophore structure can have a drastic effect on the absorption spectrum (Chen and Blankenship 2011; Blankenship 2014). For example, the difference between Chl *a* and Chl *b*, consists of an aldehydic substituent of the tetrapyrrole ring structure *vs* a methyl group. This causes a strong red shift of the Soret bands and a blue shift of the Q bands, see Fig. 3.1. Besides the chemical structure, the environment greatly influences the Chl absorption spectrum by shifting or broadening the bands. This is an essential feature used by organisms to widen the spectral range of light harvesting towards wavelengths avail-

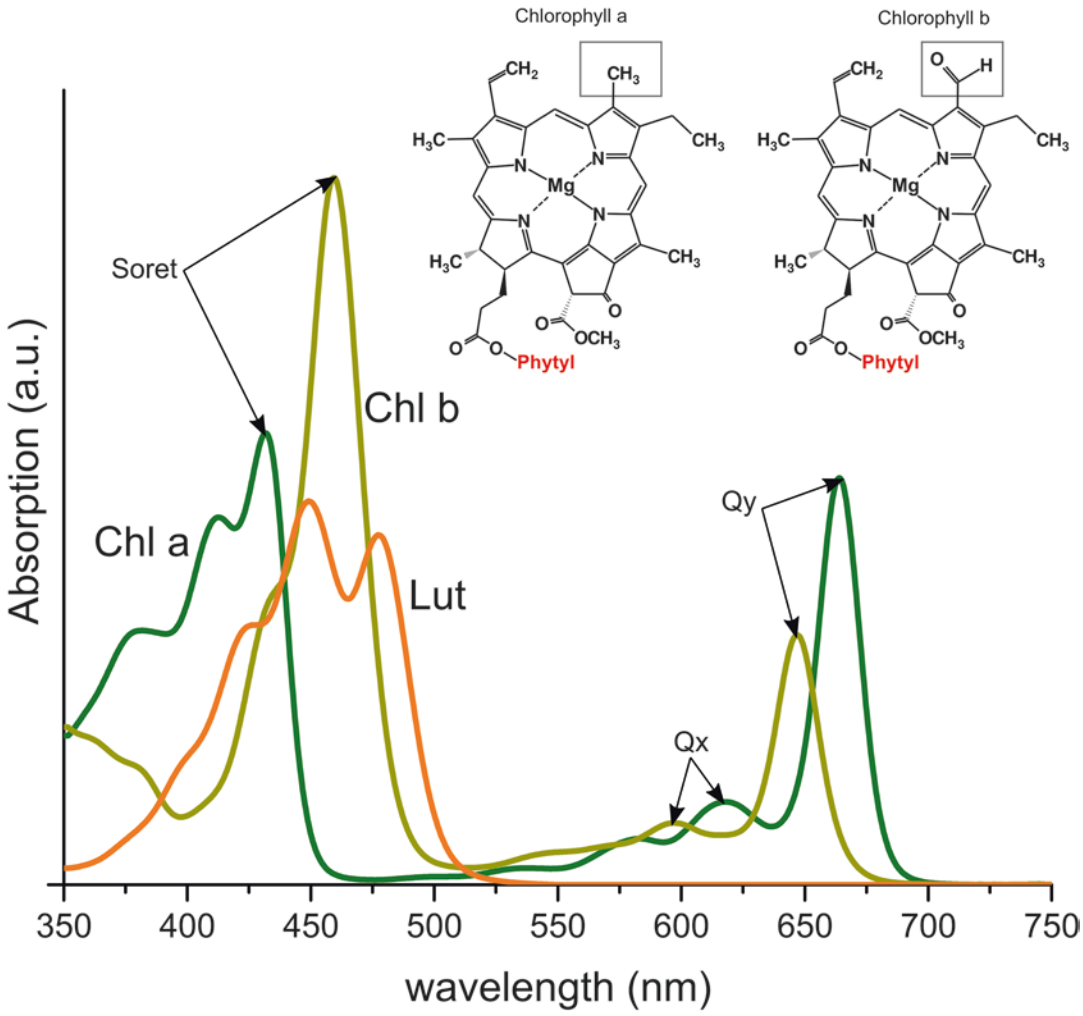

Fig. 3.1. Absorption spectra of Chl *a*, Chl *b* and the carotenoid lutein, together with the structures of Chl a and Chl b. The spectrum of lutein is shown as an example of the carotenoid absorption range. Spectra of additional carotenoids: β-carotene, violaxanthin and neoxanthin are similar and show small red or blue-shifts with respect to lutein

able in specific environmental niches (van Amerongen et al. 2000; Wientjes et al. 2012). Small changes in the binding of chromophore to a protein, i.e. the conformation of the pigment-protein, can drastically change the absorption and emission spectra of the chromophores, as shown for example by a shift of 35 nm in the emission spectrum in the LHCA4 protein, an antenna protein bound to PSI in plants and respective orthologues in algae (Morosinotto et al. 2003; Wientjes et al. 2012; Bassi et al. 1992). Moreover, coordination of chromophores in the protein scaffolds ensures optimal orientation and distance for efficient energy transfer.

Carotenoids (Cars) absorb strongly in the blue-green (420–570 nm) region of the light spectrum, but not in the Q region, therefore complementing the absorption spectrum in regions where Chl absorption is weak. The Cars include carotenes, composed by carbon and hydrogen, while xanthophylls, also contain oxygen (see Chap. 10). Carotenes (such as β-carotene) are located in the RCs, while

xanthophylls, including lutein (Lut), neoxanthin (Neo), violaxanthin (Vio) and zeaxanthin (Zea) are coordinated by antenna proteins. In most antenna proteins xanthophylls bind to four, conserved, binding sites called L1, L2, N1 and V1 in a ratio of 1:3 with Chlorophylls (Caffarri et al. 2001; Croce et al. 1999; Liu et al. 2004). Although xanthophylls have generally been assumed to play a minor role in light-harvesting, it is becoming evident that they are more important than previously assumed (Collini 2019). This is especially clear in diatoms, that contain Chl *c* instead of Chl *b* and complement their antennae complexes with huge amounts of Fucoxanthin (Fx) (Wang et al. 2019), see Chap. 16. Since Fx absorbs strongly in the blue-green light region, diatoms have a major advantage in aquatic environments where blue and green light penetrate much deeper than red light. Furthermore, the xanthophylls are especially important in photoprotection, as will be discussed later in this chapter.

Besides harvesting light, chromophores are essential for energy transfer of the absorbed photons. The excitons formed upon absorption by Chl or Cars are funnelled towards the RCs via an intricate organization of higher and lower energy absorbing chlorophylls (Cinque et al. 2000; Ramanan et al. 2015). Chlorophylls undergo transitions to several excited states: those promoted by blue light (Soret-band) are in general very short-lived (ps) and fall back in fs to the lower excited states (Q-bands), accompanied by the release of heat, the Q-bands have a longer lifetime (ns), see Fig. 3.2. The transition of Cars from the ground state to the first excited singlet state (S_1) is optically forbidden and does not occur; however, the transition to the S_2 state is allowed and absorbs strongly in the blue-green region, but excitons quickly fall back to the S_1 state. Carotenoid excitations can be transferred to the Soret bands of Chl *b* or to the Q bands of both Chl *a* and Chl *b* (Croce et al. 2001). Recently, an ultra-fast energy transfer from the Chl Soret bands or S_2 states of xanthophylls to the lower S_2 state of Lut2 in trimeric LHCII was detected. The energy in Lut2 can then be donated to an S_x-state (Son et al. 2019). A similar process was previously

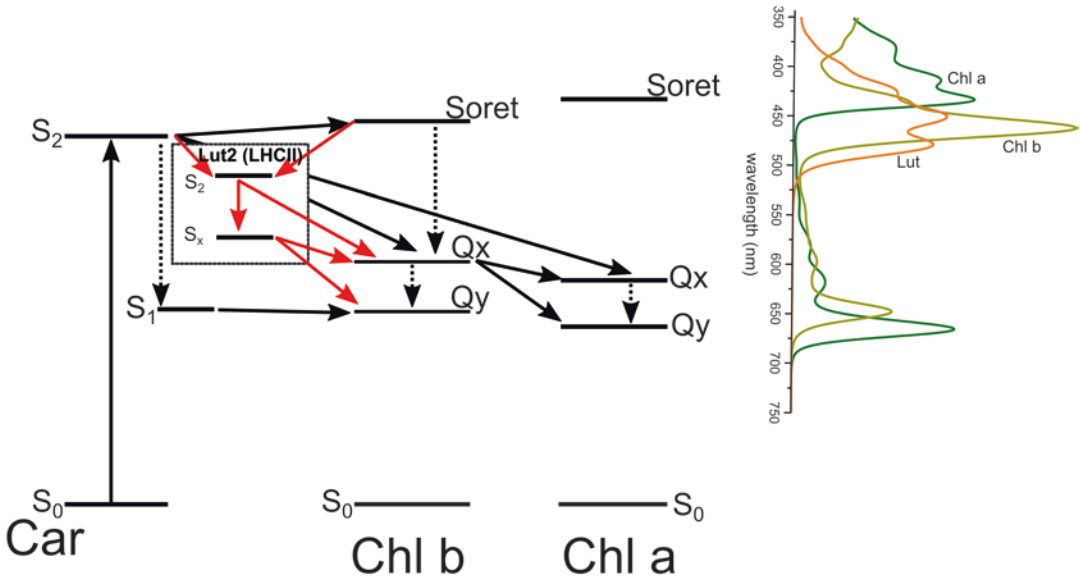

Fig. 3.2. Schematic of the energy levels of carotenoids and chlorophylls together with the absorption spectra of Chl *a*, Chl *b* and lutein. The black arrows indicate the original energy transfer found by Croce et al. 2001, while the red arrows depict the newly found energy transfer in LHCII trimers by Son et al. 2019

identified in the bacterial LH2 complex (Ostroumov et al. 2013). The S_x state in LHCII is unique to the Lutein binding site L2, due to the conformation imposed by the protein scaffold during trimerization (Liguori et al. 2017; Son et al. 2019). The S_x state serves as an efficient energy trap transferring to the lower Q_y and Q_x states of Chl (Son et al. 2019); see Fig. 3.2.

The core complexes, RCI and RCII are very 'expensive' pigment-protein machines, costing a lot of energy to produce. As mentioned above it is possible to produce mutants with only the core complexes; however, they do not have enough chromophores to function efficiently in dim light, and in nature the core complexes are surrounded by other chromophore-binding proteins: i.e. the second moiety of photosystems, the "antenna system", that funnel the excitations towards the RCs. The size of the antennae can easily be adjusted to the specific needs of the organism: in low light environments an organism will require more antenna complexes while high light conditions require smaller antennae complexes.

III. The Core Complexes of PSII and PSI

The PSII-core complex consists of least 20 subunits among which are the membrane intrinsic subunits D1 and D2 (binding the P680 special pair) and the two inner antenna proteins CP43 and CP47 (Umena et al. 2011; Wei et al. 2016; Su et al. 2017), see Fig. 3.3. In total the PSII-core contains approximately 35 Chl *a* and 11 β-carotenes (Umena et al. 2011), in-vivo it is always found as a dimer (Morris et al. 1997; Santini et al. 1994; Morosinotto et al. 2006).

On the luminal side of the thylakoid membranes, the core complex of PSII harbours the oxygen evolving complex (OEC) comprised of PsbQ, PsbP and PsbO subunits and the Mn cluster (Mn_4CaO_5) which splits water into protons and oxygen to obtain electrons for the electron transfer (Wei et al. 2016), see Fig. 3.3. The structure is very well conserved in all oxygenic photosynthetic organisms, from cyanobacteria to plants (Umena et al. 2011; Wei et al. 2016; Su et al. 2017).

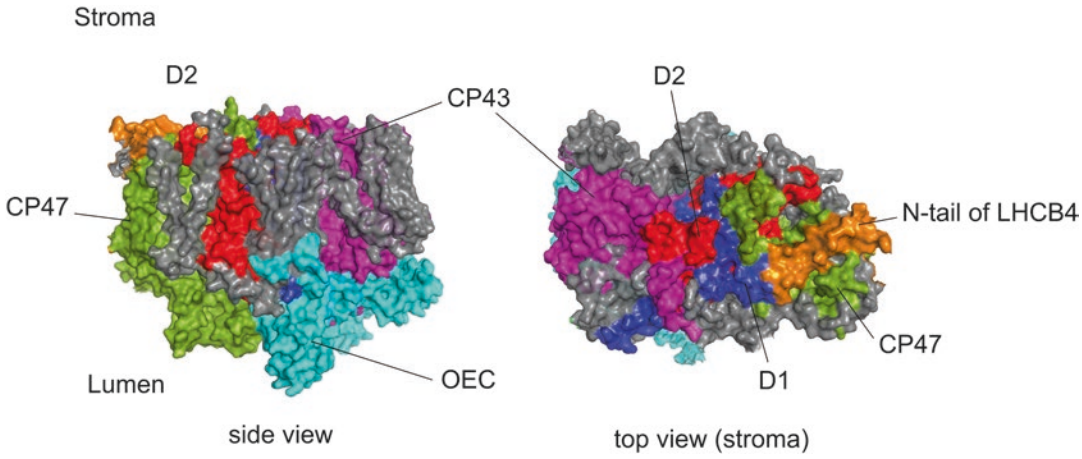

Fig. 3.3. Structure of the PSII-core complex; left shows the side view of the complex in the membranes and on the right is the top view from the stromal side. The Oxygen Evolving Complex as OEC (cyan), D1 (blue), D2 (red), CP43 (magenta), CP47 (green), the N-terminus tail of LHCB4 (orange). (Structure from Su et al. 2017, PDB-code 5XNM)

A critical feature of PSII core complex is the scarcity of carotenoids, considering that PSII is the major target site of charge recombination and photoinhibition (Rutherford and Mullet 1981) and carotenoids are antioxidants. Indeed, although carotenoids could, in principle, be photoprotective by quenching ^{3}Chl* issued from charge recombination, they cannot sit in the spot of their maximal efficiency, i.e. near P680. This is because of the highly positive redox intermediates of Mn created by successive oxidation of P680 (approx. +1 volt) which would oxidize carotenes, causing rapid turnover of carotenes (Telfer 2002). This makes PSII sensitive to photoinhibition from singlet oxygen and, at the same time, the trigger for the acclimative induction of photoprotective mechanisms. Even so carotenoids in PSII still conserve part of their photoprotective activity as singlet oxygen scavengers by a suicide mechanism, yielding carotenoid cleavage products among which is β-cyclocitral, a major signalling product (Carmody et al. 2016; D'Alessandro et al. 2018). Indeed, carotenoid biosynthesis has a peculiar flux regime with β-carotene being synthesized at high rate and rapidly turned over from binding sites, while the synthesis rate of downstream xanthophylls bound to LHC antenna proteins is more than 20 times lower despite their high abundance (Beisel et al. 2010). By contrast the antenna complexes of PSII have many carotenes, which are active and efficient in restricting the production of ROS species.

The core complex of PSI is also highly conserved throughout evolution, apart for small changes in subunit compositions and the formation of multimeric complexes. Cyanobacterial PSI contains approximately 12 protein subunits of which the two subunits, PsaA and PsaB, form the core of the reaction centre (Mühlenhoff et al. 1993; Jordan et al. 2001) as well as acting as inner antenna complexes, similar to CP43 and CP47 of PSII to which they show homology (Cardona 2017). Each PSI monomer contains a large inner antenna with 96 Chl *a* and 22 carotenoids besides the chromophores for electron transport, i.e. 3 Iron-Sulphur clusters and 2 phylloquinones (Jordan et al. 2001). PSI can be found as either a trimer or a tetramer, depending on the cyanobacterial species (Jordan et al. 2001; Watanabe et al. 2014; Li et al. 2014). The large chlorophyll complements of the PSI core complex imply it can function efficiently without external antenna complexes. Nevertheless, in higher plants and green algae PSI is only found as a monomer and is endowed with a multisubunit light harvesting complex called LHCI. The energy captured by LHCI is transferred to the RC in the core complex with an efficiency of almost 100% (Croce et al. 2000). The plant PSI-core complex is composed of 14 subunit, of which several are unique to plants and green algae, such as PsaG, PsaH, PsaN and PsaO, which have been shown to be involved in the binding of external antenna complexes (Scheller et al. 2001; Knoetzel et al. 2002; Amunts et al. 2010), see Fig. 3.7. PsaG and PsaN are essential for the binding of LHCI, while PsaH and PsaO are essential for the binding of LHCII which may migrate to PSI during state-transitions (Lunde et al. 2000; Jensen et al. 2002; Varotto et al. 2002; Amunts et al. 2010; Ben-Shem et al. 2003; Amunts et al. 2007; Pan et al. 2018), see Chap. 4.

The two photosystems differ slightly in their absorption maxima, the Chl dimer (P680) in PSII absorbs at 680 nm, while the Chl pair (P700) in PSI has a maximum at 700 nm. This difference in absorption peaks is important to decrease the overlap of their absorption bands and so to reduce competition for the same photons, allowing a balance of the energy absorption rate between the two PSs.

IV. Light Harvesting

If the core complexes of the two photosystems are very similar through many different organisms, the antenna complexes couldn't

be more diverse. To understand this diversity of the different antennae it is important to follow the evolutionary origin of the LHC complexes. The oxygenic photosynthesis that can be found in eukaryotes these day, e.g. plants and algae, actually arose from one or more endosymbiotic events, in which an eukaryote cell incorporated a cyanobacterial ancestor (Margulis 1981; Blankenship 2010; Jensen and Leister 2014; Keeling 2010). Integration of these prokaryotes with the host cell included transfer of genes to the nuclear genome, ultimately leading to plastids, such as cyanelles, rhodoplasts and chloroplasts, that we currently find in the glaucophytes, red algae and green algae respectively (Jensen and Leister 2014; Keeling 2010). The plastids have undergone a lot of changes from the initial cyanobacteria (Jensen and Leister 2014; Moreira et al. 2000). Differences among plastid types can be found in the antenna proteins: cyanobacteria use phycobilisomes for light harvesting and High-Light Inducible Proteins (HLIPs) for photoprotection, while green algae and plants rely on light harvesting complexes (LHCs) for both functions. Together with the development of different antenna systems a difference in chromophore composition emerged. Besides Chl *a*, which is found in all the algae species; different types of Chl can be found in different taxa.

In green algae and higher plants, LHCs are encoded by the multigenic *Lhc*-family (Jansson 1999). These antenna proteins connect to either the PSII-core (LHCB) or the PSI-core (LHCA). As mentioned above, these proteins bind Chl *a*, Chl *b* and carotenoids. The LHC-proteins have a similar structure that comprises three α-helices spanning the membrane (Liu et al. 2004; Ben-Shem et al. 2003). They most likely evolved from the HLIPs found in cyanobacteria (Dolganov et al. 1995), which bind Chl *a* and β-carotene but only contain one transmembrane helix (Knoppová et al. 2014; Staleva et al. 2015). HLIPs have been found to be involved in many different functions, such as light acclimation (Havaux et al. 2003), Singlet Oxygen Scavenging (Sinha et al. 2012), protection of assembly intermediated during biosynthesis of Chl-binding proteins (Chidgey et al. 2014) and the regulation and recycling of Chls (Xu et al. 2002; Vavilin and Vermaas 2002; Hernandez-Prieto et al. 2011; Vavilin et al. 2007). Light-harvesting, thus, doesn't seem to be one of the original functions of ancestral LHCs and yet modern LHCs are now the most abundant membrane proteins on Earth. Possibly because the changes, which made them light harvesters, are built over an ancestral photoprotection-efficient architecture which is crucial when colonizing a challenging environment such as land. Thus, light harvesting proteins of green algae and higher plants appear in a number of variants among which several have crucial photoprotective roles.

In green algae and higher plants each half of the dimeric PSII-core binds one copy of the monomeric antenna proteins LHCB4 (CP29) and LHCB5 (CP26), see Fig. 3.4. The double naming of these antenna proteins can be confusing since they are used interchangeably. The original names, from the '80s of last century are descriptive and made out of combining "CP" which stands for: Chlorophyll-Protein (CP) with the molecular weight of the respective holoprotein in green gels (Bassi et al. 2018). Later, when the complexity of genes encoding pigment-binding proteins was recognized, the fact that the green bands belonged to the common Light Harvesting Complex family was acknowledged by the "LHC" notation (*Lhc* for genes), followed by the letter 'a' or 'b' for their connection to either PSI or PSII respectively (Jansson et al. 1992). Even though this has worked well for most of the antenna proteins, LHCB4 and LHCB5 are often still indicated by CP29 and CP26 respectively, which ignores the fact that CP29 is encoded by three different genes with very similar properties (de Bianchi et al. 2008).

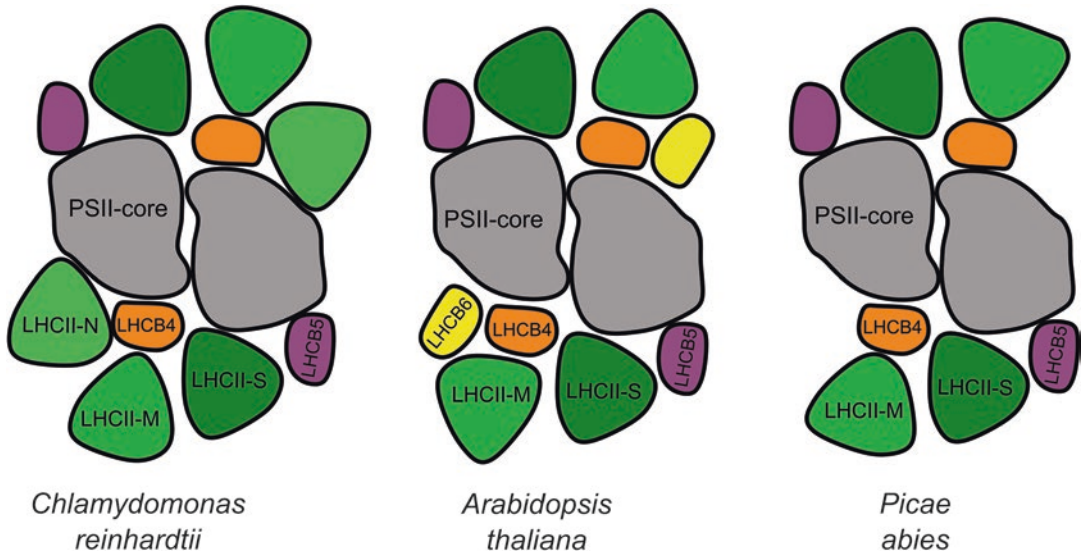

Fig. 3.4. Schematic overview of the PSII-supercomplexes in different organisms *Chlamydomonas reinhardtii*, *Arabidopsis thaliana* and *Picea abies*. PSII-core (grey), LHCB4 (orange), LHCB5 (purple), LHCB6 (yellow), LHCII trimers S, M and N (in green). (Schematic is based on the electron microscopy pictures of Kouřil et al. 2016)

LHCB4 (CP29) is located between LHCII-M (moderately bound) and the core of PSII with which it interacts at the internal antenna protein CP47 (Tokutsu et al. 2012; Drop et al. 2014; Yakushevska et al. 2003; Su et al. 2017; Egbert J. Boekema et al. 1999), see Fig. 3.5. LHCB4 couples excitation energy transfer between the PSII-core and the outer antenna complexes (Caffarri et al. 2011) and contains 13–14 chlorophylls (10 Chl *a* and 3–4 Chl *b*), a lutein, neoxanthin and violaxanthin (Pan et al. 2011; Wei et al. 2016). One additional interactor of LHCB4, in plants but not in algae, is LHCB6 (CP24) which coordinates additional LHCII-L (loosely bound) trimers accumulating in low light conditions (Ballottari et al. 2007). Finally, LHCB4 is an interacting partner of PSBS, the pH sensor protein essential for triggering Non-Photochemical Quenching (NPQ) (Dall'Osto et al. 2017).

LHCB5 (CP26) is bound to CP43, the other internal antenna protein of the PSII-core, together with the LHCII-S trimer (strongly bound) that is also interacting with LHCB4, see Fig. 3.5. Lhcb5 probably plays a role in the excitation energy transfer from LHCII to CP43, although less critical with respect to the energy transfer (ET) from LHCB4 to CP47 due to the presence of an alternative ET pathway directly from LHCII-S to CP43 (Caffarri et al. 2011; Wei et al. 2016). LHCB5 contains 13 chlorophylls (8–9 Chl *a* and 4–5 Chl *b*), 1–2 Lutein, 0–1 Violaxanthin and 1 Neoxanthin (Ballottari et al. 2009; Wei et al. 2016). LHCB5 bind Zeaxanthin upon high light exposure and this appears to be a major factor in the qZ component of NPQ (Dall'Osto et al. 2005), see below.

LHCII forms trimers in a homo- or heterotrimeric composition. Each LHCII monomer binds 8 chlorophylls *a* (Chl *a*), 6 chlorophylls *b* (Chl *b*) and 4 carotenoids; 2 Lutein, 1 Neoxanthin and 1 Violaxanthin or Zeaxanthin (Liu et al. 2004). The carotenoids are attached to binding sites named V1, L1, L2 and N1, respectively. While L1, L2 and N1 are active in ET to Chl *a*, V1 is not (Caffarri et al. 2001) and the violaxanthin ligand is exchanged to zeaxanthin in

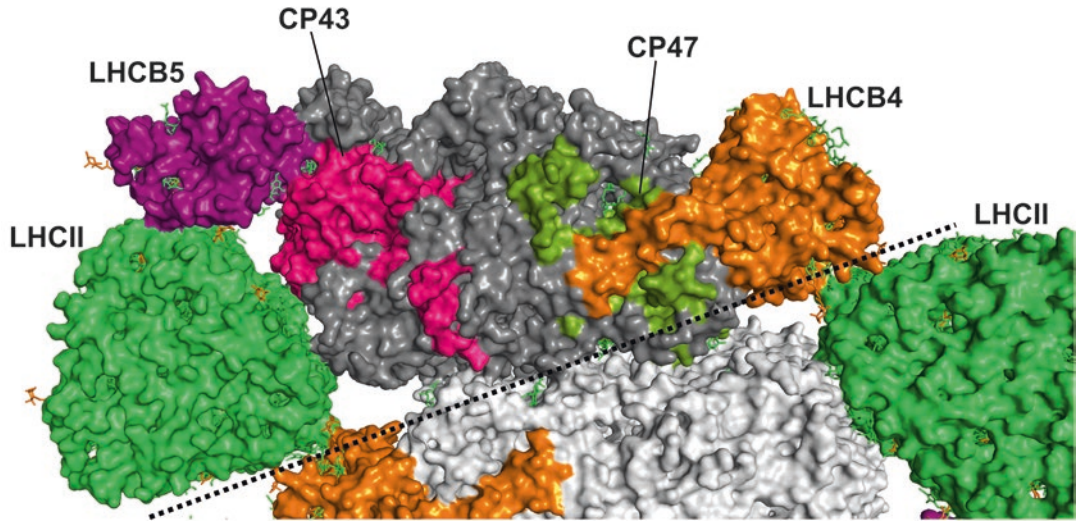

Fig. 3.5. Structure of the PSII-core complex (grey) with the major light harvesting complex LHCII (light green) and the minor complexes LHCB4 (orange) and LHCB5 (purple) attached to CP47 (dark green) and CP43 (violet), respectively. (Structure from Su et al. 2017, PDB code 5XNM)

HL. Although trimers are found in all the members of the green clade, they are more stable in higher plants. Trimerization confers special properties to LHCII by tuning its absorption spectrum: the Q_y transition of Chl *b* is enhanced and that of Chl *a* is red shifted (Peterman et al. 1997). Even more important is the twisting of lutein in binding site 2 causing a red-shift of the Lut2 S_1 state which makes it the hub for excitation delivery from cars to Chl *a* (Son et al. 2019). The ET from LHCII to the PSII-core occurs via the monomeric antennas (LHCB4 and LHCB5), while direct energy transfer from LHCII to PSII core is far less efficient as shown by the mutant lacking all monomeric antenna complexes (van Oort et al. 2010; Dall'Osto et al. 2017). Besides playing a major role in energy transfer to the core, both LHCB4 and LHCB5 are important in the proper organisation and stability of LHCII with the PSII-core (Yakushevska et al. 2003; de Bianchi et al. 2011).

In *Arabidopsis thaliana* LHCII is encoded by 9 genes, belonging to three groups (*Lhcb1–3*), LHCB1 and LHCB2 can form homotrimers or heterotrimers, while LHCB3 is only found in heterotrimeric complexes. Even though the sequences of the monomeric LHCIIs are very similar, they have different roles in regulation of energy transfer. LHCB1, the most abundant isoform, is necessary for NPQ (Pietrzykowska et al. 2014), while LHCB2 is essential for state 1–2 transitions (Leoni et al. 2013). A third type of LHCII protein, LHCB3 is even less abundant and its deletion has not shown a specific functional phenotype, so far (Damkjær et al. 2009).

In the green alga *C. reinhardtii* LHCII is also encoded by 9 genes but there is no correspondence with the *Lhcb1-3* genes in *A. thaliana* indicating these evolved after the divergence of *C. reinhardtii* from the green lineage (Ballottari et al. 2012). The genes found in *C. reinhardtii* were named (*Lhcbm1–9*) and can be divided into 4 different groups based on their sequence identity (Minagawa and Takahashi 2004; Teramoto et al. 2001).

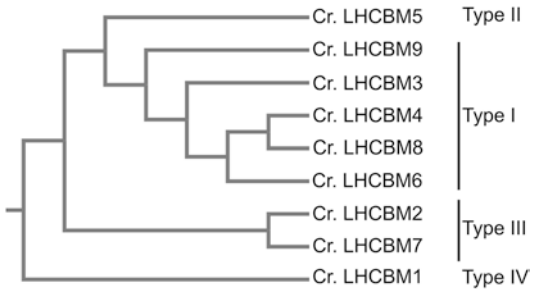

Fig. 3.6. Phylogenetic tree of the PSII antenna proteins found in *C. reinhardtii*

Table 3.1. Different PSII antenna proteins found in *C. reinhardtii* and their respective group. Based on Minagawa and Takahashi 2004 and Teramoto et al. 2001

Type I	LHCBM3, 4, 6, 8 and 9
Type II	LHCBM5
Type III	LHCBM2 and 7
Type IV	LHCBM1

The sequence identity in each group is high, while the averaged sequence identities between LHCBM6 (Type I) and Type II, Type III or Type IV is respectively 80%, 77% or 74% (Minagawa and Takahashi 2004), see Fig. 3.6. As is the case in plants, the different types of monomers in LHCII have different functions (Table 3.1).

A. *Type I (LHCBM3, 4, 6, 8 and 9)*

LHCBM4, 6 and 8 were primarily found as 'free' LHCIIs not connected to either photosystem (Girolomoni et al. 2016), suggesting them to be LHCII-only domains that are most likely involved in state-transitions (Girolomoni et al. 2016; Nagy et al. 2014; Ünlü et al. 2014). Knock-down of these subunits significantly reduced the capacity to perform state 1–2 transitions, the total LHCII content and the capacity to perform NPQ (Girolomoni et al. 2016).

LHCBM3, being one of the more abundant LHCII subunits, is mainly bound as heterotrimers to PSII (Drop et al. 2014). The precise role of LHCBM3, however, remains unclear, although it is possible that it has no other specific role besides light harvesting.

LHCBM9 is only found with very low abundance during normal growth conditions; however, it is strongly up-regulated during a variety of stress conditions, such as sulphur starvation or anaerobic growth (Nguyen et al. 2008; Grewe et al. 2014; González-Ballester et al. 2010; Sawyer et al. 2015). During up-regulation of LHCBM, other LHCBMs are replaced and the LHCII complexes reduce their fluorescence yield. Furthermore, PSII shows an increased dissipative state and an overall reduction of Reactive Oxygen Species (ROS) was observed, indicating that LHCBM9 is involved in photoprotection only during specific stress conditions (Grewe et al. 2014).

B. *Type II (LHCBM5)*

LHCBM5 is most likely involved in state transitions and is mainly found in the 'free' LHCIIs like LHCBM4, 6 and 8 (Drop et al. 2014); indicating that LHCBM5 is most likely involved in state-transitions, which is consistent with the fact that besides LHCBM5, LHCBM4, LHCBM6 and LHCBM8 can be phosphorylated by the Stt7 kinase, a protein essential for state 1–2 transitions (Takahashi et al. 2006; Lemeille et al. 2009).

C. *Type III (LHCBM2 and 7)*

LHCBM2 and LHCBM7, although slightly different in gene sequence, produce exactly the same mature amino acid sequence (Elrad and Grossman 2004; Stauber et al. 2003). Together with LHCBM3, LHCBM2 and LHCBM7, makes up most of the LHCII-trimers and silencing of the *Lhcbm2* and *Lhcbm7* genes in *C. reinhardtii,* therefore results in a decreased LHCII abundance (Ferrante et al. 2012). Furthermore, these mutants showed an increased sensitivity to superoxide anions, probably due to a lower level of neoxanthin in which LHCBM2/7 are

most likely enriched and which is involved in superoxide anion scavenging (Dall'Osto et al. 2007; Ferrante et al. 2012). Besides the sensitivity to superoxide anions, the ability to perform state transitions was decreased with the absence of LHCBM2 and LHCBM7 (Ferrante et al. 2012).

D. Type IV (LHCBM1)

LHCBM1 is the most highly abundant subunit in *C. reinhardtii* and it has been shown to be involved in NPQ. Absence of LHCBM1 leads to increased sensitivity to superoxide anions and singlet oxygen (Elrad et al. 2002; Ferrante et al. 2012). The sensitivity to superoxide anions is most likely related to a decreased level of neoxanthin, as observed in the *Lhcbm2/7* knock-downs. The reduced capacity of scavenging singlet oxygen is probably due to the location of LHCBM1, which is close to the reaction centre, where a lot of singlet oxygen is generally produced by charge recombination (Ferrante et al. 2012).

The PSII structure of flowering plants (angiosperms) is different in comparison to algae, because it contains a third monomeric protein named LHCB6 (CP24), which is unique to land plants and was found to be essential for the energy transfer to the core of PSII (Alboresi et al. 2008; van Oort et al. 2010). LHCB6 forms a stable dimer with LHCB4 (Su et al. 2017) and replaces the LHCII-N trimer, see Fig. 3.3. In the absence of LHCB4, LHCB6 is not expressed and a different supercomplex organisation was observed (de Bianchi et al. 2011). LHCB3 is another protein unique to land plants and belongs to the LHCII-M trimer (Alboresi et al. 2008; Dainese and Bassi 1991) and, together with LHCB6, is essential for the stable binding of the LHCII-M trimer to PSII (Caffarri et al. 2009; Kovács et al. 2006; Kouřil et al. 2013). It was generally believed that these proteins were crucial for the transition from the aquatic life to terrestrial; however, it was found that subgroups of gymnosperms lost functional LHCB6 and LHCB3 during their evolution, thus leading to a PSII supercomplex structure very similar to that found in algae (Kouřil et al. 2016). LHCB6 and LHCB3 are probably involved in long- and short-term light acclimation, since angiosperms adapted to high light conditions reduces the amount of these proteins, effectively decreasing the size of the PSII supercomplex (Kouřil et al. 2013).

V. Antenna Complexes of PSI

In the case of green algae and higher plants, the LHC-type antenna system is named Light Harvesting Complex I (LHCI). In higher plants the basic form of LHCI consists of two heterodimers, LHCA1/LHCA4 and LHCA2/LHCA3, which form a belt on one side of the PSI-core (Ben-Shem et al. 2003). These two heterodimers are very similar to the heterodimer of LHCB4/LHCB6 of PSII in plants (Su et al. 2017). Higher plant LHCA1-LHCA4 bind in total 45 Chl *a*, 12 Chl *b* and 13 carotenoids (Qin et al. 2015). Chl *b* is mainly bound to LHCA4 and LHCA2 which are located slightly further from the core of PSI (see Fig. 3.7) and most of the energy harvested by LHCI likely travels via LHCA1 and LHCA3 to PsaB and PsaA, respectively (Qin et al. 2015; Mazor et al. 2017). Despite the large size, this PSI-LHCI complex performs photochemistry with a quantum efficiency close to 1, meaning that it is able to produce an electron for almost every absorbed photon, thus making PSI the most efficient photochemical energy converter (Nelson 2009; Croce and van Amerongen 2013). Despite the well-defined location of LHCI-subunits, two additional *Lhca* genes are expressed in *A. thaliana*: the corresponding LHCA5 and LHCA6 proteins were located in large and rare PSI-NDH complexes catalysing cyclic electron transport (Peng et al. 2009).

The distribution of antenna subunit within the PSI-LHCI in green algae has been long

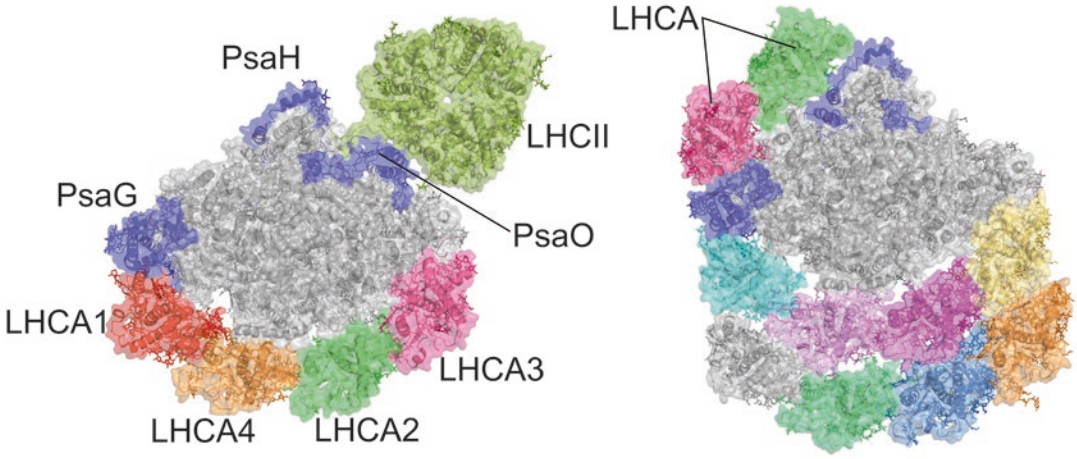

Fig. 3.7. Left: Crystal structure of maize PSI with LHCII attached. Structure from Pan et al. 2018, PDB code 5JZI. Right: Crystal structure of PSI-LHCI from *Bryopsis corticulans*. (Structure from Qin et al. 2019, PDB code 6IGZ)

debated, but a recent 3D structure seems to shed light on it (Qin et al. 2019). The 10 LHCI subunits (Bassi et al. 1992) are distributed into two different locations of the supercomplex. Eight form a double moon shaped arc with 4 LHCA proteins each while two additional LHCA subunits are bound opposite to the rest of LHCIs in between PsaH and PsaG, see Fig. 3.7. The PSI-LHCI supercomplex in *C. reinhardtii* contains less 'red forms' and more Chl *b* in comparison to plants, which leads to a blue-shift in the fluorescence emission spectrum 705 nm vs 730 nm (Drop et al. 2011; Bassi and Simpson 1987). This can be explained by the fact that algae live in water, where the blue light penetrates best. Water absorbs far red light and thus is a very poor energy medium for aquatic photosynthetic organisms.

Besides LHCI, LHCII is also known to bind to PSI in order to balance the energy distribution between the two photosystems, see Chap. 4. Beside LHCII binding to PSI upon transition to state 2, PSI complexes were found to bind LHCII-trimers in steady-state illumination conditions (Wientjes et al. 2013). The binding of LHCII to PSI, increases the total amount of chlorophylls by approximately 20% with a minimal quantum efficiency loss of 0.2% (Wientjes et al. 2013). Furthermore, it simplifies the acclimation to different light intensities, where the antenna size has to be increased or decreased, because only LHCB1 and LHCB2 have to be regulated (Wientjes et al. 2013; Ballottari et al. 2007).

In green algae, besides LHCII, the monomeric antenna complexes, LHCB4 and LHCB5, are also known to migrate from PSII to PSI during state 1–2 transitions, forming an even larger complex in comparison to the one found in plants (Kargul et al. 2005; Takahashi et al. 2006; Tokutsu et al. 2009; Drop et al. 2014).

VI. Fucoxanthin Chlorophyll Binding Proteins

The core complexes of diatoms are very similar to that found in green algae and form a monomer and dimer for PSI and PSII, respectively (Ikeda et al. 2013; Veith and Büchel 2007; Nagao et al. 2007; Chap. 16).

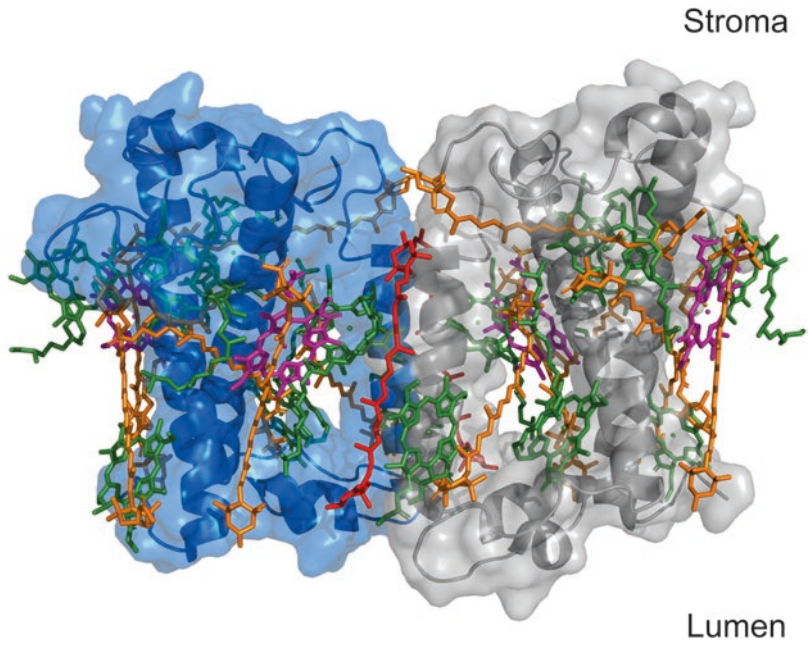

Fig. 3.8. Dimeric FCP in blue and grey. With Chl *a* (green), Chl *c* (magenta), Fx (orange) and diadinoxanthin (red). (Structure from Wang et al. 2019, PDB-code: 6a2w)

However, much remains unknown about the lateral distribution of the supercomplexes in the thylakoid membrane. The crystal structure of a dimeric Fucoxanthin Chlorophyll binding Protein (FCP) was reported to show that the LHC monomer binds 7 Chl *a*, 2 Chl *c*, 7 Fucoxanthin and 1 Diadinoxanthin (Wang et al. 2019), see Fig. 3.8. The FCP has a Car/Chl ratio close to 1, much higher than in green algae.

The backbone structure of the transmembrane helices of the FCP monomers is similar to that of the LHCs found in green algae and plants (Wang et al. 2019). Out of the four xanthophyll-binding sites of plant LHCII only two are conserved in FCP, which correspond to L1 and L2 sites, both hosting Fucoxanthin in FCP (Wang et al. 2019). The V1 and N1 binding sites of LHCII are not conserved in FCP, while 5 new Fucoxanthin binding sites are distributed at the periphery of the complex either in a transmembrane arrangement or parallel to the stromal surface. Finally, two Diadinoxanthin binding sites are located at the dimer interface (Wang et al. 2019). In total six of the nine Chls (four Chl *a* and two Chl *c*) are found in similar positions to LHCII, while the remaining three Chls *a* are bound in new positions. Each Fucoxanthin chromophore is closely associated to one or more Chls to allow for fast energy transfer from Fucoxanthin to Chl *a* (Papagiannakis et al. 2005; Akimoto et al. 2014; Gelzinis et al. 2015; Wang et al. 2019). Two Fucoxanthin molecules, Fx306 and Fx307, are not in close contact with any Chl *a* and likely transfer energy to neighbouring Chl *c*'s (Wang et al. 2019), which, in turn, efficiently transfer to Chl *a* (Gelzinis et al. 2015). Due to the high density of xanthophylls in the structure, it cannot be excluded that energy transfer occurs between the xanthophylls, like that observed from Lut1 to Lut2 in LHCII-trimers (Son et al. 2019). Besides an efficient energy transfer from Fucoxanthin to Chl *a*, the close proximity of the two species might allow a transfer

from Chl to Fucoxanthin in excess light conditions (Goss and Lepetit 2015).

VII. Photoprotection

Photosynthetic organisms must deal with an extreme variability of light: at sunrise light is limiting and fully used for photochemistry to fuel the electron transport. At midday, however, light can be too much, and the RCs are not able to quench all the singlet Chl excited states (^{1}Chl∗) generated by an oversupply of photon absorption. Thus, the excitations remain longer on the Chls, which gives the possibility to intersystem crossing and the production of Chl triplet states (^{3}Chl∗). ^{3}Chl∗ are dangerous because they can react with O_2 and create singlet oxygen ($^1O_2$∗), see Fig. 3.9.

The chlorophyll dimer in the RC of PSII is also prone to the production of $^1O_2$∗ due to the increased chance of creating ^{3}Chl∗ states upon charge recombination (Durrant et al. 1990). On the other hand, the presence of many carotenes on the LHCs provides for the quenching of high energy states without the harmful side reactions with oxygen. Protective strategies include scavenging of ROS (Asada 1999), prevention of the formation of ROS by quenching ^{3}Chl∗ (Dall'Osto et al. 2012) and quenching of the excess ^{1}Chl∗ through Non-Photochemical Quenching (NPQ). The half-life of singlet oxygen is 200 ns and it has been calculated to diffuse approximately 10 nm in physiological tissue (Gorman and Rodgers 1992; Sies and Menck 1992), meaning that the damage occurs in the place where the singlet oxygen is produced. While photosynthetic organisms have developed several strategies to counteract these negative by-products, the D1 subunit of PSII is still a prime target for ROS production and is the most turned-over protein in photosynthesis.

Nevertheless, photoprotective strategies have evolved to lessen damage to PSII. Of all the photoprotective strategies, the most dynamic process, NPQ, catalyses dissipation

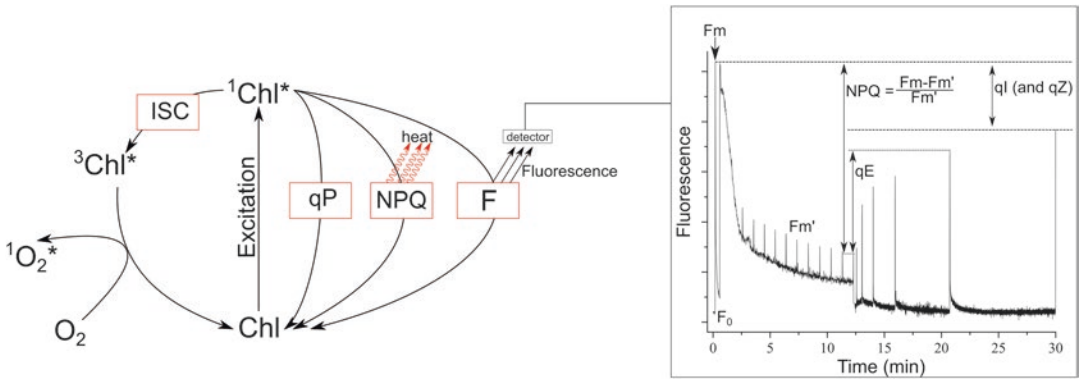

Fig. 3.9. Schematic of the different energy dissipation pathways of chlorophylls. Chlorophylls are excited by photons and transfer the excitation energy to the RCs where they are used for photochemistry (qP). In high light conditions the RCs are completely occupied, and the excited chlorophylls can follow two pathways, (i) the formation of chlorophyll triplets via Inter System Crossing (ISC) and reaction with oxygen leading to Reactive Oxygen Species (ROS) formation or (ii) excitations are dissipated has heat by Non-Photochemical Quenching (NPQ). A part of the excited states returns to the ground state by re-emitting a photon (fluorescence) which can be measured by chlorophyll fluorescence and gives information on the different aspects of NPQ such as energy dissipation (qE) and photoinhibition (qI). F_0 is the basal fluorescence, while Fm is the highest fluorescence after a saturating light pulse in dark adapted tissue. Saturating pulses are short enough not to activate NPQ, but ensure that PSII-RCs are closed. After measurement of Fm, actinic light is switched on and fluorescence drops due to the activation of NPQ mechanisms. Saturating light pulses give Fm′, with which NPQ can be calculated

of excess energy as heat, thereby introducing an alternative pathway to shorten the lifetime of the ^{1}Chl∗ and thus compete with ^{3}Chl∗ formation. NPQ rapidly (within seconds) reacts to the increased levels of the ^{1}Chl∗ and dissipates excess excitation energy as heat (Genty et al. 1989; Müller et al. 2001). NPQ is triggered by the low pH generated in the thylakoid lumen due to the inhibition of ATPase activity in excess light conditions. Indeed, when the rate of the CO_2 reducing Calvin-Benson cycle is saturated, ADP + Pi cannot regenerate thus inhibiting ATPase activity by lack of substrate and, consequently, the return of H^+, accumulated by water splitting and the Q-cycle in the stromal compartment. Also, NPQ requires special members of the LHC-protein family for its activation. Besides these light harvesting functions for PSII and PSI, LHCs also catalyse energy quenching through a reorganization of the interactions between chromophores either elicited by direct protonation of lumen-exposed acidic residues as in the case of LHCSR proteins (Ballottari et al. 2016) or caused by interactions with PSBS (Betterle et al. 2009), a proton sensitive protein itself. LHCSR (Light-Harvesting Complex Stress Related) and PSBS (Photosystem II subunit S), are indispensable for NPQ respectively in green algae (Peers et al. 2009) and vascular plants (Li et al. 2000) together with the xanthophylls Lut and/or Zea which are ligands for LHC proteins (Polle et al. 2001; Pogson et al. 1998; Niyogi et al. 2001). Interesting is the case of mosses, evolutionary intermediates between green algae and vascular plants occur, in which both PSBS and LHCSR proteins are active and both trigger NPQ (Alboresi et al. 2010).

The low lumenal pH also activates the protein violaxanthin de-epoxidase (VDE) which increases the length of the conjugated bonds of violaxanthin in two subsequent steps creating first antheraxanthin and then zeaxanthin (Demmig-Adams and Adams 1996). While violaxanthin is involved in light-harvesting and is able to transfer its excitation energy to Chl *a* (Arnoux et al. 2009; Owens et al. 1987; Peterman et al. 1997), the de-epoxidation increases the length of the conjugated bonds, thereby lowering the S_1 state below that of the Q_y band of the Chl and making zeaxanthin an excellent energy trap for Chl excitations (Frank et al. 1994), see Fig. 3.2.

Zeaxanthin induces photoprotection in two ways; i) it is effective in scavenging ROS because it is a very strong antioxidant (Havaux et al. 2007; Krinsky 1979; Edge et al. 1997) and ii) it enhances energy dissipation as heat (Niyogi et al. 1998).

The NPQ induced by the conversion of Vio into Zea, also referred to as the xanthophyll cycle (Fig. 3.10), is named qZ and conversion generally takes a few minutes. Relaxation of qZ, the conversion of Zea back into Vio by zeaxanthin epoxidase (ZEP), is

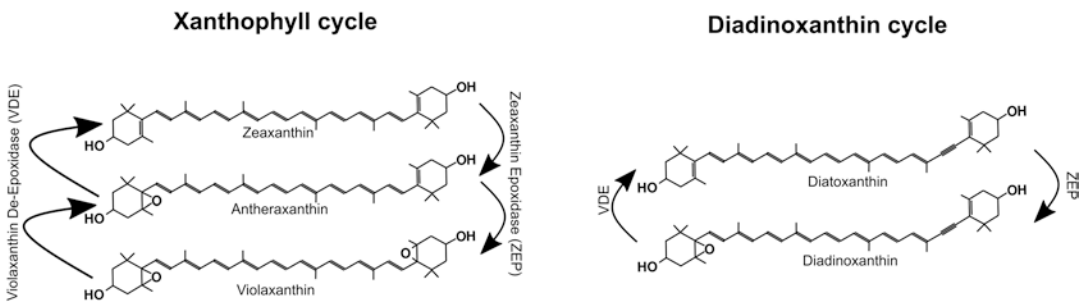

Fig. 3.10. The Violaxanthin cycle, generally referred to as the Xanthophyll cycle found in green algae and higher plants and the Diadinoxanthin cycle found in diatoms, dinoflagellates and haptophytes

far slower and can easily take up hours or even days if the organism experiences other stress factors. Similar to the xanthophyll cycle found in algae and plants, is the diadinoxanthin cycle found in diatoms, dinophytes (dinoflagellates) and haptophytes, where diadinoxanthin is directly converted into diatoxanthin (Hager and Stransky 1970), see Fig. 3.10. The proteins catalysing these reactions are very similar to VDE and ZEP, found in plants and green algae and some of these proteins are even able to convert both violaxanthin and diadinoxanthin into zeaxanthin and diatoxanthin respectively (Jakob et al. 2001). The main difference between VDEs of plants vs diatoms is the pH sensitivity. The de-epoxidases found in diatoms are already activated at a pH of 7.2, while the activity of VDE in higher plants requires a pH lower than 6.5 (Jakob et al. 2001) consistent with their reactivity to excess light. It is clear that in Chromealveolates (Chl *c*-containing algae - see Chap. 2) the equivalent of a Zeaxanthin Epoxidase (ZEP), forming diadinoxanthin from diatoxanthin, has been inherited from a red algal/green algal ancestor and that this has led not only to NPQ under high light by a Diadinoxanthin Epoxidase but also to the evolution of the special allenoic and acetylenic xanthophylls such as fucoxanthin, peridinin and vaucheriaxanthin, which are such a notable feature of diatoms and allied algae (Dautermann and Lohr 2017), see Chap. 16.

Due to the slow relaxation, qZ, is sometimes also confused with qI, the third component of NPQ which comprises photoinhibition and repair of damaged PSII. However, photoinhibition is damage caused by excess light and usually takes days before it relaxes, e.g. before all damaged proteins and chromophores have been repaired or replaced. It is not easy to distinguish qZ from qI without the use of inhibitors interfering either with the xanthophyll cycle (DTT) or D1 synthesis (chloramphenicol).

Another photoprotective mechanism of higher plants is (qM), i.e. the movement of chloroplasts to avoid excess light. Despite the fact that it induces a decrease in fluorescence, similar to qE or qZ, qM is not a genuine quenching process. Indeed, it relies on the decrease of the photon absorption when chloroplasts move away from direct light and align along the cell walls parallel to the incident light (Kasahara et al. 2002; Dall'Osto et al. 2014; Cazzaniga et al. 2013). Interestingly, qM is mediated by phot2, a blue light photoreceptor. Consistently, the phot mutation in unicellular algae makes them incapable of swimming away from excess light (Trippens et al. 2012).

qT, the quenching obtained when LHCII disconnects from long lifetime fluorescent PSII to connect with short lifetime fluorescent PSI, being quenched in the process, was found to be more pronounced in green algae, such as *C. reinhardtii*, than in plants (Kargul et al. 2005; Takahashi et al. 2006; Iwai et al. 2008). It is the re-distribution of antenna complexes, also known as State Transitions (Allorent et al. 2013), see Chaps. 4 & 10.

The biophysical mechanisms of energy dissipation have long been discussed and currently three main hypotheses are supported that all include the role of establishing new interactions between two or more chromophores within LHC proteins in response to thylakoid lumen acidification, binding of xanthophyll cycle pigments to allosteric sites or both. The first model was based on observations on isolated LHCII oligomers upon aggregation (Müller et al. 2010), where a charge transfer state was observed involving excitonic coupling between Chls. This model does not directly implicate carotenoids, like lutein and zeaxanthin in quenching reactions despite their crucial importance for NPQ *in-vivo* (Niyogi et al. 2001; Gilmore and Yamamoto 1993), thus considering these act as allosteric modulators of quenching proteins. Two other theories, instead, propose interactions between xanthophylls and Chls to be directly involved in quenching, but differ in the mode of these reactions: Holt et al. 2005 and Ahn

et al. 2008 proposed quenching is initiated by the formation of Chl dimers within LHCB4 yielding low lying states accepting electrons from excited zeaxanthin to form a transient Zea^{+}/Chl^{-} radical cation (Holt et al. 2005; Avenson et al. 2008). Charge recombination to the ground state then, produces heat dissipation of excited states. A third and simpler model involves LHCII aggregation within the thylakoid membrane as a consequence of a decreased pH in the lumen, which brings Chl and Lutein chromophores in closer contact to each other thus allowing energy transfer from Chl *a* to Lut1 followed by rapid decay to the ground of the short-lived S_1 state (Ruban et al. 2007). Similar to the case of model 1, zeaxanthin is not considered as a chromophore directly involved in the quenching reaction(s), but rather an allosteric modulator.

VIII. Triggers of Quenching Reactions

Genetic analysis identified two proteins, PSBS and LHCSR whose deletion completely impairs the triggering of qE in excess light, respectively in higher plants and algae (Li et al. 2000; Peers et al. 2009; Chap. 10).

PSBS, a four-helix protein, with homology to LHCs that does not bind pigments (Bonente et al. 2008; Fan et al. 2015; Peers et al. 2009). Thus, PSBS cannot be the actual site of quenching. However, PSBS carries two lumen-exposed acidic residues whose mutation fully impairs quenching (Li et al. 2004). Quenching reactions are therefore proposed to occur in interacting pigment-binding proteins among components of LHC antenna upon conformational changes consequent to interaction with PSBS. Two distinctive sites have been identified (Holzwarth et al. 2009): the monomeric antenna complexes (Ahn et al. 2008; de Bianchi et al. 2011) and LHCII (Ruban et al. 2007; Dall'Osto et al. 2017). Whether the PSBS-LHC interaction is direct (Ahn et al. 2008) or is a consequence of membrane reorganization (Betterle et al. 2009) is a matter of a lively debate.

In vivo measurements using WT mutants completely devoid of the monomeric antenna proteins LHCB4-6 (NoM) (Dall'Osto et al. 2017) showed that PSBS most likely interacts at two different sites, the first and fastest activated is the monomeric antenna complex LHCB4 where it induces a conformational change that not only increases the exchange rate of violaxanthin to zeaxanthin (Morosinotto et al. 2002) but also increases the interactions between Chl *a* and lutein (Li et al. 2009) or zeaxanthin (Avenson et al. 2008) and between two Chl *a* molecules (Ahn et al. 2008). The formation of a radical cation was detected in the WT plants, but not in the NoM mutant lacking the monomeric antenna LHCB4-6, suggesting that the quenching reaction is accompanied by the formation of either a zeaxanthin or lutein radical cation (Dall'Osto et al. 2017) and yet residual quenching is still active, involving PSBS and LHCII. Thus, it appears that quenching is a twofold process involving LHCB4 and PSBS to form the carotenoid cation ($Car^{\circ+}$) on one hand and LHCII and PSBS to form an ET from Chl to Zeaxanthin, followed by fast decay to the ground state (Dall'Osto et al. 2017).

LHCSR is strikingly different from PSBS by the fact that it binds Chl *a*, lutein and violaxanthin, the latter being replaced by zeaxanthin in HL (Bonente et al. 2011; Pinnola et al. 2015b). Also, LHCSR harbours lumen-exposed protonatable residues whose mutation (Ballottari et al. 2016) or truncation (Liguori et al. 2013) prevent quenching *in vivo*. Thus LHCSR, comprises both the functions, which are separated in PSBS: pH detection and catalysis of quenching (Bonente et al. 2011; Peers et al. 2009; Pinnola et al. 2015b).

The photophysical properties of LHCSR proteins have been studied on the pigment-complex reconstituted in vitro upon expression of the *C. reinhardtii* sequence in bacteria (Bonente et al. 2011; Liguori et al. 2013).

The protein showed, when compared to other LHCBs, a shorter lifetime (<100 ps vs 3.4–4.5 ns) which was further shortened at low pH (Bonente et al. 2011), suggesting that quenching *in vivo* might require the establishment of interaction(s) with antenna proteins for excitation energy being spilled over to LHCSR in its quenched state. Alternatively, it was suggested that the on-off switch between a quenched and unquenched state is loose, already causing activation at low light intensities (Niyogi and Truong 2013). A more "native" system was provided by the expression of LHCSR1 from *Physcomitrella patens* in tobacco and isolation of the tagged recombinant protein by affinity chromatography (Pinnola et al. 2015b). The major difference between the LHCSR proteins from *C. reinhardtii* and *P. patens* is the dependence on zeaxanthin for the moss protein (Pinnola et al. 2013) while the activity of LHCSR from *C. reinhardtii* is zeaxanthin-independent. The role of zeaxanthin in LHCSR appears to be, at least in part, allosteric since LHCSR dependence on de-epoxidation is very diverse among different species of unicellular algae (Quaas et al. 2015) while the radical cation identified in both *C. reinhardtii* and *P. patens* has the spectroscopic features of lutein (Bonente et al. 2011; Pinnola et al. 2016). Nevertheless, besides radical cation formation, an additional strong component, attributable to ET from Chl to zeaxanthin was reported (Pinnola et al. 2016). Thus, lutein can replace zeaxanthin in the $Car^{\circ+}$ dependent mechanisms (Li et al. 2009; Pinnola et al. 2016; Bonente et al. 2011) while quenching by excitation energy transfer to carotenoids appears to require zeaxanthin (Dall'Osto et al. 2017; Pinnola et al. 2016). It thus seems that the two mechanisms contributing to quenching in moss LHCSR are each localized in different antenna subunits in plants, namely $Car^{\circ+}$ in LHCB4 and excitation energy transfer to zeaxanthin followed by a decay to the ground state in LHCII (Dall'Osto et al. 2017), and that both are activated by PSBS.

The quenching process and contributions from Zea binding could be analysed in the PpLHCSR protein: the lifetime at neutral pH was 3.7 ns, very similar to that of the major antenna LHCII, while the fully quenched protein exhibited an 80 ps lifetime (Pinnola et al. 2017). Intermediate conditions yielded a mix of ns vs ps lifetimes in different ratios, suggesting LHCSR can switch between two conformations with the extent of quenching being determined by the abundance of the 80ps conformation. This was confirmed by single molecule spectroscopic studies (Kondo et al. 2017).

It is interesting to speculate on the evolution of LHCSR and PSBS. LHCSR is found in all algal systems except red algae and glaucophytes and it likely arose from 2-helix forebears in Cyanobacteria; see Chaps. 10 & 12. PSBS arose in the streptophyte line of green algae, which gave rise to liverworts and then to all land plants, see Chap. 2. It clearly evolved alongside (and possibly from LHCSR) and while LHCSR is present in green algae, streptophytes, liverworts, and mosses, but not in ferns, gymnosperms and flowering plants. Thus, in algae, energy quenching is largely accomplished by an LHCSR-dependent mechanism, while in land plants, from ferns on, PSBS is employed. Ferns and mosses, the first land colonizers, use PSBS and PSBS/LHCSR respectively, suggesting the transition from LHCSR to PSBS might be part of the adaptation from aquatic life to terrestrial life, or at least life in very shallow water (since PSBS is found in some green algae and certainly in streptophytes). Furthemore, LHCSR has been shown to be active when expressed in tobacco, implying that PSBS must have advantages over LHCSR, despite the fact that both are able to quench Chl fluorescence with similar efficiencies (as shown by the high level of quenching obtained in systems using each protein (Bonente et al. 2008; Sello et al. 2019)). Differences between the two systems include the site of interaction with core complex membranes which is

LHCB5 in algae and LHCB4 in plants (Semchonok et al. 2017; de Bianchi et al. 2008) and the localization in the thylakoid membranes: the grana membranes for PSBS and stroma membranes for LHCSR (Pinnola et al. 2015a; Girolomoni et al. 2019). Thus the interaction of LHCSR3 with the core complex of PSII (Xue et al. 2015) is restricted to PSII supercomplexes exposed to the interface with stroma membranes thus leaving a fraction of PSII units unprotected. Thus, it appears that the twofold process of quenching in PSBS (mentioned above) involving LHCB4 and PSBS to form the carotenoid cation ($Car^{\circ+}$) on one hand and LHCII and PSBS to form an ET from Chl to Zeaxanthin, followed by fast decay to the ground state (Dall'Osto et al. 2017) is a strong evolutionary trait.

IX. Conclusions

Although derived from photoprotective HLIPs proteins (Staleva et al. 2015), LHCs evolved into an extremely diversified superfamily, with members devoted to harvesting photons in specific narrow spectral bands such as LHCA4 to others which, at the opposite side of the functional range, do work in dissipating photon energy, just absorbed, by their interaction with partners in the antenna system like LHCII. While photosynthetic reaction centres remained essentially unmodified through evolution, LHC proteins have proved to be the critical and flexible factor in the evolution of photosynthetic organisms and their adaptation to the most diverse light regimes. It is clear that differences in the absorption range of LHCs are not only mediated by chromophore composition such as with FCP and LHCs, but are also driven by the protein environment. Besides light-harvesting, antenna complexes play essential roles in photoprotection. Since higher plants and algae generally seem to stay on the safe side and dissipate more energy than strictly necessary, improvements can be made to increase crop productivity for the production of food and fuel by engineering LHC proteins and/or their chromophores, as shown in tobacco (Kromdijk et al. 2016). Two proteins have been shown to be essential for the activation of the photoprotection mechanisms, LHCSR and PSBS found in algae and higher plants, respectively. The transition from LHCSR to PSBS upon land colonization, for Non-Photochemical Quenching, is a fascinating evolutionary development and one that, together with the elucidation of the quenching mechanism, still requires investigation.

Acknowledgements

We thank the Marie Curie Actions Initial Training Networks SE2B (675006-SE2B) and ENAC (Italian Civil Aviation Authority) for supporting the research on photosynthesis in plants and algae.

References

Ahn TK, Avenson TJ, Ballottari M, Cheng Y-C, Niyogi KK, Bassi R, Fleming GR (2008) Architecture of a charge-transfer state regulating light harvesting in a plant antenna protein. Science 320:794–797. Available at: http://www.ncbi.nlm.nih.gov/pubmed/18467588 [Accessed 13 Mar 2018]

Akimoto S, Teshigahara A, Yokono M, Mimuro M, Nagao R, Tomo T (2014) Excitation relaxation dynamics and energy transfer in fucoxanthin–chlorophyll a/c-protein complexes, probed by time-resolved fluorescence. Biochim Biophys Acta Bioenerg 1837:1514–1521. Available at: https://www.sciencedirect.com/science/article/pii/S0005272814000486 [Accessed 22 Mar 2019]

Alboresi A, Caffarri S, Nogue F, Bassi R, Morosinotto T (2008) In silico and biochemical analysis of Physcomitrella patens photosynthetic antenna: identification of subunits which evolved upon land adaptation S. D. Fugmann, ed. PLoS One 3:e2033. Available at: http://dx.plos.org/10.1371/journal.pone.0002033 [Accessed 15 Mar 2018]

Alboresi A, Gerotto C, Giacometti GM, Bassi R, Morosinotto T (2010) Physcomitrella patens mutants affected on heat dissipation clarify the evo-

lution of photoprotection mechanisms upon land colonization. Proc Natl Acad Sci U S A 107:11128–11133. Available at: http://www.pnas.org/content/pnas/107/24/11128.full.pdf [Accessed 29 Mar 2018]

Allorent G, Tokutsu R, Roach T et al (2013) A dual strategy to cope with high light in Chlamydomonas reinhardtii. Plant Cell 25:545–557. Available at: http://www.ncbi.nlm.nih.gov/pubmed/23424243 [Accessed 14 Mar 2018]

Amunts A, Drory O, Nelson N (2007) The structure of a plant photosystem I supercomplex at 3.4 Å resolution. Nature 447:58. https://doi.org/10.1038/nature05687

Amunts A, Toporik H, Borovikova A, Nelson N (2010) Structure determination and improved model of plant photosystem I. J Biol Chem 285:3478–3486. Available at: http://www.ncbi.nlm.nih.gov/pubmed/19923216 [Accessed 2 Jan 2019]

Arnoux P, Morosinotto T, Saga G, Bassi R, Pignol D (2009) A structural basis for the pH-dependent xanthophyll cycle in Arabidopsis thaliana. Plant Cell 21:2036–2044. Available at: http://www.plantcell.org/content/21/7/2036.abstract

Asada K (1999) The water-water cycle in chloroplasts: scavenging of active oxygens and dissipation of excess photons. Annual Reviews, Palo Alto. Available at: www.annualreviews.org [Accessed 15 Jan 2019]

Avenson TJ, Ahn TK, Zigmantas D, Niyogi KK, Li Z, Ballottari M, Bassi R, Fleming GR (2008) Zeaxanthin radical cation formation in minor light-harvesting complexes of higher plant antenna. J Biol Chem 283:3550–3558. Available at: http://www.ncbi.nlm.nih.gov/pubmed/17991753 [Accessed 22 Jan 2019]

Ballottari M, Dall'Osto L, Morosinotto T, Bassi R (2007) Contrasting behavior of higher plant photosystem I and II antenna systems during acclimation. J Biol Chem 282:8947–8958. Available at: http://www.jbc.org/cgi/content/short/282/12/8947 [Accessed 11 Jan 2019]

Ballottari M, Mozzo M, Croce R, Morosinotto T, Bassi R (2009) Occupancy and functional architecture of the pigment binding sites of photosystem II antenna complex Lhcb5. J Biol Chem 284:8103–8113. Available at: https://www.ncbi.nlm.nih.gov/pubmed/19129188

Ballottari M, Girardon J, Dall'Osto L, Bassi R (2012) Evolution and functional properties of photosystem II light harvesting complexes in eukaryotes. Biochim Biophys Acta Bioenerg 1817:143–157. Available at: http://www.sciencedirect.com/science/article/pii/S0005272811001460

Ballottari M, Truong TB, Re De E et al (2016) Identification of pH-sensing sites in the light harvesting complex stress-related 3 protein essential for triggering non-photochemical quenching in Chlamydomonas reinhardtii. J Biol Chem 291:7334–7346. Available at: http://www.ncbi.nlm.nih.gov/pubmed/26817847 [Accessed 14 Mar 2018]

Bassi R, Simpson D (1987) Chlorophyll-protein complexes of barley photosystem I. Eur J Biochem 163:221–230. Available at: http://doi.wiley.com/10.1111/j.1432-1033.1987.tb10791.x [Accessed 27 Mar 2019

Bassi R, Soen SY, Frank G, Zuber H, Rochaix JD (1992) Characterization of chlorophyll a/b proteins of photosystem I from Chlamydomonas reinhardtii. J Biol Chem 267:25714–25721

Bassi R, Rigoni F, Giacometti GM (2018) Chlorophyll binding proteins with antenna function in higher plants and green algae. Photochem Photobiol 52:1187–1206. https://doi.org/10.1111/j.1751-1097.1990.tb08457.x

Beisel KG, Jahnke S, Hofmann D, Köppchen S, Schurr U, Matsubara S (2010) Continuous turnover of carotenes and chlorophyll a in mature leaves of Arabidopsis revealed by 14CO2 pulse-chase labeling. Plant Physiol 152:2188–2199. Available at: http://www.ncbi.nlm.nih.gov/pubmed/20118270 [Accessed 23 Mar 2019]

Ben-Shem A, Frolow F, Nelson N (2003) Crystal structure of plant photosystem I. Nature 426:630. https://doi.org/10.1038/nature02200

Betterle N, Ballottari M, Zorzan S, De Bianchi S, Cazzaniga S, Dall'osto L, Morosinotto T, Bassi R (2009) Light induced dissociation of an antenna hetero-oligomer is needed for non-photochemical quenching induction. J Biol Chem. 284(22):15255–15266. Available at: http://www.jbc.org/cgi/doi/10.1074/jbc.M808625200 [Accessed 21 Jan 2019]

Blankenship RE (2010) Early evolution of photosynthesis. Plant Physiol 154:434–438. Available at: http://www.plantphysiol.org/content/154/2/434.abstract

Blankenship RE (2014) Molecular mechanisms of photosynthesis, 2nd edn. Washington University, St. Louis. Available at: http://www.amazon.com/Molecular-Mechanisms-Photosynthesis-Robert-Blankenship/dp/1405189754

Boekema EJ, van Roon H, Calkoen F, Bassi R, Dekker JP (1999) Multiple types of association of photosystem II and its light-harvesting antenna in partially solubilized photosystem II membranes. Biochemistry 38(8):2233–2239. Available at: https://pubs.acs.org/doi/abs/10.1021/bi9827161 [Accessed 25 Mar 2019]

Bonente G, Howes BD, Caffarri S, Smulevich G, Bassi R (2008) Interactions between the photosystem II

subunit PsbS and xanthophylls studied in vivo and in vitro. J Biol Chem 283:8434–8445. Available at: http://www.ncbi.nlm.nih.gov/pubmed/18070876 [Accessed 17 Jan 2019]

Bonente G, Ballottari M, Truong TB, Morosinotto T, Ahn TK, Fleming GR, Niyogi KK, Bassi R (2011) Analysis of LhcSR3, a protein essential for feedback de-excitation in the green alga Chlamydomonas reinhardtii. T. Shikanai, ed. PLoS Biol 9:e1000577. Available at: http://dx.plos.org/10.1371/journal.pbio.1000577 [Accessed 14 Mar 2018]

Caffarri S, Croce R, Breton J, Bassi R (2001) The major antenna complex of photosystem II has a xanthophyll binding site not involved in light harvesting. J Biol Chem 276:35924–35933. Available at: http://www.ncbi.nlm.nih.gov/pubmed/11454869 [Accessed 5 Mar 2019]

Caffarri S, Kouřil R, Kereïche S, Boekema EJ, Croce R (2009) Functional architecture of higher plant photosystem II supercomplexes. EMBO J 28:3052–3063. Available at: http://www.ncbi.nlm.nih.gov/pubmed/19696744 [Accessed 24 Jan 2019]

Caffarri S, Broess K, Croce R, van Amerongen H (2011) Excitation energy transfer and trapping in higher plant photosystem II complexes with different antenna sizes. Biophys J 100:2094–2103. Available at: https://www.sciencedirect.com/science/article/pii/S0006349511004073 [Accessed 12 Nov 2018]

Cardona T (2017) Photosystem II is a chimera of reaction centers. J Mol Evol 84:149–151. Available at: https://doi.org/10.1007/s00239-017-9784-x

Carmody M, Crisp PA, d'Alessandro S, Ganguly D, Gordon M, Havaux M, Albrecht-Borth V, Pogson BJ (2016) Uncoupling high light responses from singlet oxygen retrograde signaling and spatial-temporal systemic acquired acclimation. Plant Physiol 171:1734–1749. Available at: http://www.ncbi.nlm.nih.gov/pubmed/27288360 [Accessed 23 Mar 2019]

Cazzaniga S, Dall'Osto L, Kong S-G, Wada M, Bassi R (2013) Interaction between avoidance of photon absorption, excess energy dissipation and zeaxanthin synthesis against photooxidative stress in Arabidopsis. Plant J 76:568–579. Available at: http://doi.wiley.com/10.1111/tpj.12314 [Accessed 17 Jan 2019]

Chen M, Blankenship RE (2011) Expanding the solar spectrum used by photosynthesis. Trends Plant Sci 16:427–431. Available at: https://www.sciencedirect.com/science/article/pii/S1360138511000598?via%3Dihub [Accessed 4 May 2018]

Chidgey JW, Linhartová M, Komenda J et al (2014) A cyanobacterial chlorophyll synthase-HliD complex associates with the Ycf39 protein and the YidC/Alb3 insertase. Plant Cell 26:1267–1279. Available at: http://www.plantcell.org/content/26/3/1267.abstract

Cinque G, Croce R, Holzwarth A, Bassi R (2000) Energy transfer among CP29 chlorophylls: calculated Förster rates and experimental transient absorption at room temperature. Biophys J 79:1706–1717. Available at: https://www.sciencedirect.com/science/article/pii/S000634950076423X [Accessed 19 Apr 2018]

Collini E (2019) Carotenoids in photosynthesis: the revenge of the "accessory" pigments. Chem 5:494–495. Available at: https://www.sciencedirect.com/science/article/pii/S2451929419300701 [Accessed 26 Mar 2019]

Croce R, van Amerongen H (2013) Light-harvesting in photosystem I. Photosynth Res 116:153–166. Available at: http://link.springer.com/10.1007/s11120-013-9838-x [Accessed 2 Jan 2019]

Croce R, Weiss S, Bassi R (1999) Carotenoid-binding sites of the major light-harvesting complex II of higher plants. J Biol Chem 274:29613–29623. Available at: http://www.ncbi.nlm.nih.gov/pubmed/10514429 [Accessed 16 Mar 2018]

Croce R, Dorra D, Holzwarth AR, Jennings RC (2000) Fluorescence decay and spectral evolution in intact photosystem I of higher plants. Biochemistry 39:6341–6348. Available at: https://pubs.acs.org/doi/abs/10.1021/bi992659r [Accessed 23 Mar 2019]

Croce R, Müller MG, Bassi R, Holzwarth AR (2001) Carotenoid-to-chlorophyll energy transfer in recombinant major light-harvesting complex (LHCII) of higher plants. I femtosecond transient absorption measurements. Biophys J 80:901–915. Available at: https://www.sciencedirect.com/science/article/pii/S0006349501760699 [Accessed 24 Jan 2019]

D'Alessandro S, Ksas B, Havaux M (2018) Decoding β-cyclocitral-mediated retrograde signaling reveals the role of a detoxification response in plant tolerance to photooxidative stress. Plant Cell 30:2495–2511. Available at: http://www.ncbi.nlm.nih.gov/pubmed/30262551 [Accessed 23 Mar 2019]

Dainese P, Bassi R (1991) Subunit stoichiometry of the chloroplast photosystem 11 antenna system and aggregation state of the component chlorophyll a/b binding proteins. J Biol Chem 266(13):8136–8142. Available at: http://www.jbc.org/content/266/13/8136.full.pdf [Accessed 24 Jan 2019]

Dall'Osto L, Caffarri S, Bassi R (2005) A mechanism of nonphotochemical energy dissipation, independent from PsbS, revealed by a conformational change in the antenna protein CP26. Plant Cell 17:1217–1232. Available at: http://www.plantcell.org/content/17/4/1217.abstract [Accessed 29 Mar 2018]

Dall'Osto L, Cazzaniga S, North H, Marion-Poll A, Bassi R (2007) The Arabidopsis aba4-1 mutant reveals a specific function for neoxanthin in protection against photooxidative stress. Plant Cell 19:1048–1064. Available at: http://www.plantcell.org/content/19/3/1048.abstract

Dall'Osto L, Cazzaniga S, Havaux M, Bassi R (2010) Enhanced photoprotection by protein-bound vs free xanthophyll pools: a comparative analysis of chlorophyll b and xanthophyll biosynthesis mutants. Mol Plant 3:576–593. Available at: https://www.sciencedirect.com/science/article/pii/S1674205214607358 [Accessed 23 Mar 2019]

Dall'Osto L, Holt NE, Kaligotla S, Fuciman M, Cazzaniga S, Carbonera D, Frank HA, Alric J, Bassi R (2012) Zeaxanthin protects plant photosynthesis by modulating chlorophyll triplet yield in specific light-harvesting antenna subunits. J Biol Chem 287:41820–41834. Available at: http://www.ncbi.nlm.nih.gov/pubmed/23066020 [Accessed 24 Jan 2019]

Dall'Osto L, Cazzaniga S, Wada M, Bassi R (2014) On the origin of a slowly reversible fluorescence decay component in the Arabidopsis npq4 mutant. Philos Trans R Soc Lond B Biol Sci 369:20130221. Available at: http://www.ncbi.nlm.nih.gov/pubmed/24591708 [Accessed 15 Mar 2018]

Dall'Osto L, Cazzaniga S, Bressan M, Paleček D, Žídek K, Niyogi KK, Fleming GR, Zigmantas D, Bassi R (2017) Two mechanisms for dissipation of excess light in monomeric and trimeric light-harvesting complexes. Nat Plants 3:17033. Available at: http://www.nature.com/articles/nplants201733 [Accessed 14 Mar 2018]

Damkjær JT, Kereïche S, Johnson MP et al (2009) The photosystem II light-harvesting protein Lhcb3 affects the macrostructure of photosystem II and the rate of state transitions in *Arabidopsis*. Plant Cell 21:3245–3256. Available at: http://www.plantcell.org/content/21/10/3245.abstract [Accessed 12 Apr 2018]

Dautermann O, Lohr M (2017) A functional zeaxanthin epoxidase from red algae shedding light on the evolution of light-harvesting carotenoids and the xanthophyll cycle in photosynthetic eukaryotes. Plant J 92:879–891. Available at: https://doi.org/10.1111/tpj.13725

de Bianchi S, Dall'Osto L, Tognon G, Morosinotto T, Bassi R (2008) Minor Antenna Proteins CP24 and CP26 Affect the Interactions between Photosystem II Subunits and the Electron Transport Rate in Grana Membranes of *Arabidopsis*. Plant Cell 20:1012–1028. Available at: http://www.plantcell.org/content/20/4/1012.abstract

de Bianchi S, Betterle N, Kouril R, Cazzaniga S, Boekema E, Bassi R, Dall'Osto L (2011) Arabidopsis mutants deleted in the light-harvesting protein Lhcb4 have a disrupted photosystem II macrostructure and are defective in photoprotection. Plant Cell 23:2659–2679. Available at: http://www.ncbi.nlm.nih.gov/pubmed/21803939 [Accessed 13 Mar 2018]

Demmig-Adams B, Adams WW (1996) The role of xanthophyll cycle carotenoids in the protection of photosynthesis. Trends Plant Sci 1:21–26. Available at: https://www.sciencedirect.com/science/article/pii/S1360138596800197 [Accessed 16 Jan 2019]

Dolganov NA, Bhaya D, Grossman AR (1995) Cyanobacterial protein with similarity to the chlorophyll a/b binding proteins of higher plants: evolution and regulation. Proc Natl Acad Sci 92:636–640. Available at: http://www.pnas.org/content/92/2/636.abstract

Drop B, Webber-Birungi M, Fusetti F, Kouřil R, Redding KE, Boekema EJ, Croce R (2011) Photosystem I of Chlamydomonas reinhardtii contains nine light-harvesting complexes (Lhca) located on one side of the core. J Biol Chem 286:44878–44887. Available at: http://www.ncbi.nlm.nih.gov/pubmed/22049081 [Accessed 11 Jan 2019]

Drop B, Webber-Birungi M, Yadav SKN, Filipowicz-Szymanska A, Fusetti F, Boekema EJ, Croce R (2014) Light-harvesting complex II (LHCII) and its supramolecular organization in Chlamydomonas reinhardtii. Biochim Biophys Acta Bioenerg 1837:63–72. Available at: http://www.sciencedirect.com/science/article/pii/S0005272813001291

Durrant JR, Giorgi LB, Barber J, Klug DR, Porter G (1990) Characterisation of triplet states in isolated photosystem II reaction centres: oxygen quenching as a mechanism for photodamage. Biochim Biophys Acta Bioenerg 1017:167–175. Available at: https://www.sciencedirect.com/science/article/pii/000527289090148W [Accessed 21 Jan 2019]

Edge R, McGarvey DJ, Truscott TG (1997) The carotenoids as anti-oxidants — a review. J Photochem Photobiol B Biol 41:189–200. Available at: https://www.sciencedirect.com/science/article/pii/S1011134497000924 [Accessed 16 Jan 2019]

Elrad D, Grossman AR (2004) A genome's-eye view of the light-harvesting polypeptides of Chlamydomonas reinhardtii. Curr Genet 45:61–75. Available at: http://link.springer.com/10.1007/s00294-003-0460-x [Accessed 11 Jan 2019]

Elrad D, Niyogi KK, Grossman AR (2002) A major light-harvesting polypeptide of photosystem II functions in thermal dissipation. Plant Cell

14:1801–1816. Available at: http://www.plantcell.org/content/14/8/1801.abstract

Fan M, Li M, Liu Z, Cao P, Pan X, Zhang H, Zhao X, Zhang J, Chang W (2015) Crystal structures of the PsbS protein essential for photoprotection in plants. Nat Struct Mol Biol 22:729–735. Available at: http://www.nature.com/articles/nsmb.3068 [Accessed 13 Mar 2018]

Ferrante P, Ballottari M, Bonente G, Giuliano G, Bassi R (2012) LHCBM1 and LHCBM2/7 polypeptides, components of major LHCII complex, have distinct functional roles in photosynthetic antenna system of Chlamydomonas reinhardtii. J Biol Chem 287:16276–16288. Available at: http://www.ncbi.nlm.nih.gov/pubmed/22431727 [Accessed 15 Mar 2018]

Frank HA, Cua A, Chynwat V, Young A, Gosztola D, Wasielewski MR (1994) Photophysics of the carotenoids associated with the xanthophyll cycle in photosynthesis. Photosynth Res 41:389–395. Available at: http://link.springer.com/10.1007/BF02183041 [Accessed 17 Jan 2019]

Gelzinis A, Butkus V, Songaila E et al (2015) Mapping energy transfer channels in fucoxanthin–chlorophyll protein complex. Biochim Biophys Acta Bioenerg 1847:241–247. Available at: https://www.sciencedirect.com/science/article/pii/S0005272814006495 [Accessed 17 Jan 2019]

Genty B, Briantais JM, Baker NR (1989) The relationship between the quantum yield of photosynthetic electron transport and quenching of chlorophyll fluorescence. Biochim Biophys Acta 990:87–92

Gilmore AM, Yamamoto HY (1993) Linear models relating xanthophylls and lumen acidity to non-photochemical fluorescence quenching. Evidence that antheraxanthin explains zeaxanthin-independent quenching. Photosynth Res 35:67–78. Available at: http://link.springer.com/10.1007/BF02185412 [Accessed 21 Jan 2019]

Girolomoni L, Ferrante P, Berteotti S, Giuliano G, Bassi R, Ballottari M (2016) The function of LHCBM4 / 6 / 8 antenna proteins in Chlamydomonas reinhardtii. J Exp Bot 68(3):1–15

Girolomoni L, Cazzaniga S, Pinnola A, Perozeni F, Ballottari M, Bassi R (2019) LHCSR3 is a nonphotochemical quencher of both photosystems in Chlamydomonas reinhardtii. Proc Natl Acad Sci 116:4212–4217. Available at: http://www.pnas.org/content/116/10/4212.abstract

González-Ballester D, Casero D, Cokus S, Pellegrini M, Merchant SS, Grossman AR (2010) RNA-seq analysis of sulfur-deprived Chlamydomonas cells reveals aspects of acclimation critical for cell survival. Plant Cell 22:2058–2084. Available at: http://www.ncbi.nlm.nih.gov/pubmed/20587772 [Accessed 20 Dec 2018]

Gorman AA, Rodgers MA (1992) Current perspectives of singlet oxygen detection in biological environments. J Photochem Photobiol B 14:159–176. Available at: https://doi.org/10.1016/1011-1344(92)85095-C

Goss R, Lepetit B (2015) Biodiversity of NPQ. J Plant Physiol 172:13–32. Available at: https://www.sciencedirect.com/science/article/pii/S0176161714000686 [Accessed 17 Jan 2019]

Grewe S, Ballottari M, Alcocer M, D'Andrea C, Blifernez-Klassen O, Hankamer B, Mussgnug JH, Bassi R, Kruse O (2014) Light-harvesting complex protein LHCBM9 is critical for photosystem II activity and hydrogen production in Chlamydomonas reinhardtii. Plant Cell 26:1598–1611. Available at: http://www.ncbi.nlm.nih.gov/pubmed/24706511 [Accessed 20 Dec 2018]

Hager A, Stransky H (1970) Das Carotinoidmuster und die Verbreitung des lichtinduzierten Xanthophyllcyclus in verschiedenen Algenklassen. Arch Mikrobiol 73:77–89. Available at: http://link.springer.com/10.1007/BF00409954 [Accessed 17 Jan 2019]

Havaux M, Guedeney G, He Q, Grossman AR (2003) Elimination of high-light-inducible polypeptides related to eukaryotic chlorophyll a/b-binding proteins results in aberrant photoacclimation in Synechocystis PCC6803. Biochim Biophys Acta Bioenerg 1557:21–33. Available at: https://www.sciencedirect.com/science/article/pii/S0005272802003912 [Accessed 9 Jan 2019]

Havaux M, Dall'osto L, Bassi R, Rank B (2007) Zeaxanthin has enhanced antioxidant capacity with respect to all other xanthophylls in arabidopsis leaves and functions independent of binding to PSII antennae. Plant Physiol 145:1506–1520. Available at: http://www.ncbi.nlm.nih.gov/pubmed/12226199 [Accessed 15 Mar 2018]

Hernandez-Prieto MA, Tibiletti T, Abasova L, Kirilovsky D, Vass I, Funk C (2011) The small CAB-like proteins of the cyanobacterium synechocystis sp. PCC 6803: their involvement in chlorophyll biogenesis for Photosystem II. Biochim Biophys Acta – Bioenerg 1807:1143–1151. Available at: https://www.sciencedirect.com/science/article/pii/S0005272811001083 [Accessed 9 Jan 2019]

Holt NE, Zigmantas D, Valkunas L, Li X-P, Niyogi KK, Fleming GR (2005) Carotenoid cation formation and the regulation of photosynthetic light harvesting. Science 307:433–436. Available at: http://www.ncbi.nlm.nih.gov/pubmed/15662017 [Accessed 19 Apr 2018]

Holzwarth AR, Miloslavina Y, Nilkens M, Jahns P (2009) Identification of two quenching sites active in the regulation of photosynthetic light-harvesting studied by time-resolved fluorescence. Chem Phys Lett 483:262–267. Available at: https://www.sciencedirect.com/science/article/pii/S0009261409013803 [Accessed 22 Jan 2019]

Ikeda Y, Yamagishi A, Komura M, Suzuki T, Dohmae N, Shibata Y, Itoh S, Koike H, Satoh K (2013) Two types of fucoxanthin-chlorophyll-binding proteins I tightly bound to the photosystem I core complex in marine centric diatoms. Biochim Biophys Acta Bioenerg 1827:529–539. Available at: https://www.sciencedirect.com/science/article/pii/S0005272813000297 [Accessed 25 Mar 2019]

Iwai M, Takahashi Y, Minagawa J (2008) Molecular remodeling of photosystem II during state transitions in Chlamydomonas reinhardtii. Plant Cell 20:2177–2189. Available at: http://www.plantcell.org/content/20/8/2177.abstract

Jakob T, Goss R, Wilhelm C (2001) Unusual pH-dependence of diadinoxanthin de-epoxidase activation causes chlororespiratory induced accumulation of diatoxanthin in the diatom Phaeodactylum tricornutum. J Plant Physiol 158:383–390. Available at: https://www.sciencedirect.com/science/article/pii/S0176161704700474 [Accessed 17 Jan 2019]

Jansson S (1999) A guide to the Lhc genes and their relatives in Arabidopsis. Trends Plant Sci 4:236–240. Available at: http://www.sciencedirect.com/science/article/pii/S1360138599014193

Jansson S, Pichersky E, Bassi R et al (1992) A nomenclature for the genes encoding the chlorophylla/b--binding proteins of higher plants. Plant Mol Biol Rep 10:242–253. Available at: https://doi.org/10.1007/BF02668357

Jensen PE, Leister D (2014) Chloroplast evolution, structure and functions. F1000Prime Rep 6:40. Available at: http://www.ncbi.nlm.nih.gov/pubmed/24991417 [Accessed 3 Sept 2018]

Jensen PE, Rosgaard L, Knoetzel J, Scheller HV (2002) Photosystem I activity is increased in the absence of the PSI-G subunit. J Biol Chem 277:2798–2803. Available at: http://www.ncbi.nlm.nih.gov/pubmed/11707465 [Accessed 2 Jan 2019]

Jordan P, Fromme P, Witt HT, Klukas O, Saenger W, Krauß N (2001) Three-dimensional structure of cyanobacterial photosystem I at 2.5 Å resolution. Nature 411:909. Available at: https://doi.org/10.1038/35082000

Kargul J, Turkina MV, Nield J, Benson S, Vener AV, Barber J (2005) Light-harvesting complex II protein CP29 binds to photosystem I of Chlamydomonas reinhardtii under state 2 conditions. FEBS J 272:4797–4806. Available at: http://doi.wiley.com/10.1111/j.1742-4658.2005.04894.x [Accessed 12 Jan 2019]

Kasahara M, Kagawa T, Oikawa K, Suetsugu N, Miyao M, Wada M (2002) Chloroplast avoidance movement reduces photodamage in plants. Nature 420:829. https://doi.org/10.1038/nature01213

Keeling PJ (2010) The endosymbiotic origin, diversification and fate of plastids. Philos Trans R Soc B Biol Sci 365:729–748. Available at: http://rstb.royalsocietypublishing.org/content/365/1541/729.abstract

Knoetzel J, Mant A, Haldrup A, Jensen PE, Scheller HV (2002) PSI-O, a new 10-kDa subunit of eukaryotic photosystem I. FEBS Lett 510:145–148. Available at: http://doi.wiley.com/10.1016/S0014-5793%2801%2903253-7 [Accessed 11 Jan 2019]

Knoppová J, Sobotka R, Tichý M, Yu J, Konik P, Halada P, Nixon PJ, Komenda J (2014) Discovery of a chlorophyll binding protein complex involved in the early steps of photosystem II assembly in *Synechocystis*. Plant Cell 26:1200–1212. Available at: www.plantcell.org/cgi/doi/10.1105/tpc.114.123919 [Accessed 9 Jan 2019]

Kondo T, Pinnola A, Chen WJ, Dall'Osto L, Bassi R, Schlau-Cohen GS (2017) Single-molecule spectroscopy of LHCSR1 protein dynamics identifies two distinct states responsible for multi-timescale photosynthetic photoprotection. Nat Chem 9:772. Available at: https://doi.org/10.1038/nchem.2818

Kouřil R, Wientjes E, Bultema JB, Croce R, Boekema EJ (2013) High-light vs. low-light: Effect of light acclimation on photosystem II composition and organization in Arabidopsis thaliana. Biochim Biophys Acta – Bioenerg 1827:411–419. Available at: http://www.sciencedirect.com/science/article/pii/S0005272812011036 [Accessed 24 Jan 2019]

Kouřil R, Nosek L, Bartoš J, Boekema EJ, Ilík P (2016) Evolutionary loss of light-harvesting proteins Lhcb6 and Lhcb3 in major land plant groups – break-up of current dogma. New Phytol 210:808–814. Available at: http://doi.wiley.com/10.1111/nph.13947 [Accessed 12 Jan 2019]

Kovács L, Damkjær J, Kereïche S, Ilioaia C, Ruban AV, Boekema EJ, Jansson S, Horton P (2006) Lack of the light-harvesting complex CP24 affects the structure and function of the grana membranes of higher plant chloroplasts. Plant Cell 18:3106–3120. Available at: http://www.plantcell.org/content/18/11/3106.abstract

Krinsky NI (1979) Carotenoid protection against oxidation. Pure Appl Chem 51:649–660. Available at: http://www.degruyter.com/view/j/pac.1979.51.

issue-3/pac197951030649/pac197951030649.xml [Accessed 16 Jan 2019]

Kromdijk J, Głowacka K, Leonelli L, Gabilly ST, Iwai M, Niyogi KK, Long SP (2016) Improving photosynthesis and crop productivity by accelerating recovery from photoprotection. Science 354:857–861. Available at: http://www.ncbi.nlm.nih.gov/pubmed/27856901 [Accessed 9 Apr 2018]

Lemeille S, Willig A, Depège-Fargeix N, Delessert C, Bassi R, Rochaix J-D (2009) Analysis of the chloroplast protein kinase Stt7 during state Transitions A. R. Grossman, ed. PLoS Biol 7:e1000045. Available at: http://dx.plos.org/10.1371/journal.pbio.1000045 [Accessed 20 Dec 2018]

Leoni C, Pietrzykowska M, Kiss AZ, Suorsa M, Ceci LR, Aro E-M, Jansson S (2013) Very rapid phosphorylation kinetics suggest a unique role for Lhcb2 during state transitions in Arabidopsis. Plant J 76:n/a–n/a. Available at: http://doi.wiley.com/10.1111/tpj.12297 [Accessed 25 Mar 2019]

Li X-P, Björkman O, Shih C, Grossman AR, Rosenquist M, Jansson S, Niyogi KK (2000) A pigment-binding protein essential for regulation of photosynthetic light harvesting. Nature 403:391–395

Li X-P, Gilmore AM, Caffarri S, Bassi R, Golan T, Kramer D, Niyogi KK (2004) Regulation of photosynthetic light harvesting involves intrathylakoid lumen pH sensing by the PsbS protein. J Biol Chem 279:22866–22874. Available at: http://www.ncbi.nlm.nih.gov/pubmed/15033974 [Accessed 14 Mar 2018]

Li Z, Ahn TK, Avenson TJ et al (2009) Lutein accumulation in the absence of zeaxanthin restores nonphotochemical quenching in the Arabidopsis thaliana npq1 mutant. Plant Cell 21:1798–1812. Available at: http://www.ncbi.nlm.nih.gov/pubmed/19549928 [Accessed 21 Jan 2019]

Li M, Semchonok DA, Boekema EJ, Bruce BD (2014) Characterization and evolution of tetrameric photosystem I from the thermophilic cyanobacterium *Chroococcidiopsis* sp TS-821. Plant Cell 26:1230–1245. Available at: http://www.plantcell.org/content/26/3/1230.abstract

Liguori N, Roy LM, Opacic M, Durand G, Croce R (2013) Regulation of light harvesting in the green alga chlamydomonas reinhardtii: the c-terminus of lhcsr is the knob of a dimmer switch. J Am Chem Soc 135:18339–18342. Available at: http://pubs.acs.org/doi/10.1021/ja4107463 [Accessed 14 Mar 2018]

Liguori N, Xu P, van Stokkum IHM, van Oort B, Lu Y, Karcher D, Bock R, Croce R (2017) Different carotenoid conformations have distinct functions in light-harvesting regulation in plants. Nat Commun 8:1994. Available at: https://doi.org/10.1038/s41467-017-02239-z

Liu Z, Yan H, Wang K, Kuang T, Zhang J, Gui L, An X, Chang W (2004) Crystal structure of spinach major light-harvesting complex at 2.72 Å resolution. Nature 428:287. Available at: http://www.nature.com/articles/nature02373 [Accessed 9 Apr 2018]

Lunde C, Jensen PE, Haldrup A, Knoetzel J, Scheller HV (2000) The PSI-H subunit of photosystem I is essential for state transitions in plant photosynthesis. Nature 408:613–615. Available at: http://www.nature.com/articles/35046121 [Accessed 2 Jan 2019]

Margulis L (1981) Symbiosis in cell evolution. W. H. Freeman, New York. Available at: http://ci.nii.ac.jp/naid/10003011199/en/ [Accessed 3 Sept 2018]

Mazor Y, Borovikova A, Caspy I, Nelson N (2017) Structure of the plant photosystem I supercomplex at 2.6 Å resolution. Nat Plants 3:17014. Available at: http://www.nature.com/articles/nplants201714 [Accessed 10 Jan 2019]

Minagawa J, Takahashi Y (2004) Structure, function and assembly of photosystem II and its light-harvesting proteins. Photosynth Res 82:241–263. Available at: https://doi.org/10.1007/s11120-004-2079-2

Moreira D, Le Guyader H, Philippe H (2000) The origin of red algae and the evolution of chloroplasts. Nature 405:69–72. Available at: http://www.nature.com/articles/35011054 [Accessed 24 Sept 2018]

Morosinotto T, Baronio R, Bassi R (2002) Dynamics of chromophore binding to Lhc proteins in vivo and in vitro during operation of the xanthophyll cycle. J Biol Chem 277:36913–36920. Available at: http://www.ncbi.nlm.nih.gov/pubmed/12114527 [Accessed 4 May 2018]

Morosinotto T, Breton J, Bassi R, Croce R (2003) The nature of a chlorophyll ligand in Lhca proteins determines the far red fluorescence emission typical of photosystem I. J Biol Chem 278:49223–49229. Available at: http://www.jbc.org/cgi/content/short/278/49/49223 [Accessed 23 Mar 2019]

Morosinotto T, Bassi R, Frigerio S, Finazzi G, Morris E, Barber J (2006) Biochemical and structural analyses of a higher plant photosystem II supercomplex of a photosystem I-less mutant of barley. FEBS J 273:4616–4630. Available at: https://doi.org/10.1111/j.1742-4658.2006.05465.x

Morris EP, Hankamer B, Zheleva D, Friso G, Barber J (1997) The three-dimensional structure of a photosystem II core complex determined by electron crystallography. Structure 5:837–849. Available at: http://www.sciencedirect.com/science/article/pii/S0969212697002372

Mühlenhoff U, Haehnel W, Witt H, Herrmann RG (1993) Genes encoding eleven subunits of photosystem I from the thermophilic cyanobacterium Synechococcus sp. Gene 127:71–78. Available at: https://www.sciencedirect.com/science/article/pii/037811199390618D [Accessed 2 Jan 2019]

Müller P, Li XP, Niyogi KK (2001) Non-photochemical quenching. A response to excess light energy. Plant Physiol 125:1558–1566

Müller MG, Lambrev P, Reus M, Wientjes E, Croce R, Holzwarth AR (2010) Singlet energy dissipation in the photosystem II light-harvesting complex does not involve energy transfer to carotenoids. ChemPhysChem 11:1289–1296. Available at: http://doi.wiley.com/10.1002/cphc.200900852 [Accessed 21 Jan 2019]

Nagao R, Ishii A, Tada O et al (2007) Isolation and characterization of oxygen-evolving thylakoid membranes and photosystem II particles from a marine diatom Chaetoceros gracilis. Biochim Biophys Acta Bioenerg 1767:1353–1362. Available at: https://www.sciencedirect.com/science/article/pii/S0005272807002356 [Accessed 26 Mar 2019]

Nagy G, Ünnep R, Zsiros O et al (2014) Chloroplast remodeling during state transitions in Chlamydomonas reinhardtii as revealed by noninvasive techniques in vivo. Proc Natl Acad Sci U S A 111:5042–5047. Available at: http://www.ncbi.nlm.nih.gov/pubmed/24639515 [Accessed 3 Dec 2018]

Nelson N (2009) Plant photosystem I – the most efficient nano-photochemical machine. J Nanosci Nanotechnol 9:1709–1713. Available at: http://openurl.ingenta.com/content/xref?genre=article&issn=1533-4880&volume=9&issue=3&spage=1709 [Accessed 2 Jan 2019]

Nguyen AV, Thomas-Hall SR, Malnoë A, Timmins M, Mussgnug JH, Rupprecht J, Kruse O, Hankamer B, Schenk PM (2008) Transcriptome for photobiological hydrogen production induced by sulfur deprivation in the green alga Chlamydomonas reinhardtii. Eukaryot Cell 7:1965–1979. Available at: http://www.ncbi.nlm.nih.gov/pubmed/18708561 [Accessed 20 Dec 2018]

Nitschke W, William Rutherford A (1991) Photosynthetic reaction centres: variations on a common structural theme? Trends Biochem Sci 16:241–245. Available at: https://www.sciencedirect.com/science/article/pii/096800049190095D [Accessed 2 Jan 2019]

Niyogi KK, Truong TB (2013) Evolution of flexible non-photochemical quenching mechanisms that regulate light harvesting in oxygenic photosynthesis. Curr Opin Plant Biol 16:307–314. Available at: https://www.sciencedirect.com/science/article/pii/S1369526613000460?via%3Dihub [Accessed 29 Mar 2018]

Niyogi KK, Grossman AR, Björkman O (1998) Arabidopsis mutants define a central role for the xanthophyll cycle in the regulation of photosynthetic energy conversion. Plant Cell 10:1121–1134. Available at: http://www.plantcell.org/content/10/7/1121.abstract

Niyogi KK, Shih C, Soon Chow W, Pogson BJ, DellaPenna D, Björkman O (2001) Photoprotection in a zeaxanthin- and lutein-deficient double mutant of Arabidopsis. Photosynth Res 67:139–145. Available at: http://link.springer.com/10.1023/A:1010661102365 [Accessed 21 Jan 2019]

Ostroumov EE, Mulvaney RM, Cogdell RJ, Scholes GD (2013) Broadband 2D electronic spectroscopy reveals a carotenoid dark state in purple bacteria. Science (80-.) 340:52–56. Available at: http://science.sciencemag.org/content/340/6128/52.abstract

Owens TG, Gallagher JC, Alberte RS (1987) Photosynthetic light-harvesting function of violaxanthin in nannochloropsis spp. (eustigmatophyceae)1. J Phycol 23:79–85. Available at: https://onlinelibrary.wiley.com/doi/abs/10.1111/j.0022-3646.1987.00079.x

Pan X, Li M, Wan T, Wang L, Jia C, Hou Z, Zhao X, Zhang J, Chang W (2011) Structural insights into energy regulation of light-harvesting complex CP29 from spinach. Nat Struct Mol Biol 18:309. Available at: https://doi.org/10.1038/nsmb.2008

Pan X, Ma J, Su X, Cao P, Chang W, Liu Z, Zhang X, Li M (2018) Structure of the maize photosystem I supercomplex with light-harvesting complexes I and II. Science 360:1109–1113. Available at: http://www.ncbi.nlm.nih.gov/pubmed/29880686 [Accessed 11 Jan 2019]

Papagiannakis E, van Stokkum I, Fey H, Büchel C, van Grondelle R (2005) Spectroscopic characterization of the excitation energy transfer in the fucoxanthin-chlorophyll protein of diatoms. Photosynth Res 86:241–250. Available at: https://doi.org/10.1007/s11120-005-1003-8

Peers G, Truong TB, Ostendorf E, Busch A, Elrad D, Grossman AR, Hippler M, Niyogi KK (2009) An ancient light-harvesting protein is critical for the regulation of algal photosynthesis. Nature 462:518–521

Peng L, Fukao Y, Fujiwara M, Takami T, Shikanai T (2009) Efficient operation of NAD(P)H dehydrogenase requires supercomplex formation with photosystem I via minor LHCI in Arabidopsis. Plant Cell 21:3623–3640. Available at: http://www.ncbi.nlm.nih.gov/pubmed/19903870 [Accessed 11 Jan 2019]

Peterman EJG, Gradinaru CC, Calkoen F, Borst JC, van Grondelle R, van Amerongen H (1997) Xanthophylls in light-harvesting complex II of higher plants: light harvesting and triplet quenching. Biochemistry 36(40):12208–12215. Available at: https://pubs.acs.org/doi/abs/10.1021/bi9711689 [Accessed 16 Jan 2019]

Pietrzykowska M, Suorsa M, Semchonok DA, Tikkanen M, Boekema EJ, Aro E-M, Jansson S (2014) The light-harvesting chlorophyll a/b binding proteins Lhcb1 and Lhcb2 play complementary roles during state transitions in Arabidopsis. Plant Cell 26:3646–3660. Available at: http://www.ncbi.nlm.nih.gov/pubmed/25194026 [Accessed 15 Mar 2018]

Pinnola A, Dall'Osto L, Gerotto C et al (2013) Zeaxanthin binds to light-harvesting complex stress-related protein to enhance nonphotochemical quenching in Physcomitrella patens. Plant Cell 25:3519–3534. Available at: http://www.plantcell.org/content/plantcell/25/9/3519.full.pdf [Accessed 14 Mar 2018]

Pinnola A, Cazzaniga S, Alboresi A, Nevo R, Levin-Zaidman S, Reich Z, Bassi R (2015a) Light-harvesting complex stress-related proteins catalyze excess energy dissipation in both photosystems of Physcomitrella patens. Plant Cell 27:3213–3227. Available at: http://www.ncbi.nlm.nih.gov/pubmed/26508763 [Accessed 14 Mar 2018]

Pinnola A, Ghin L, Gecchele E et al (2015b) Heterologous expression of moss light-harvesting complex stress-related 1 (LHCSR1), the chlorophyll a-xanthophyll pigment-protein complex catalyzing non-photochemical quenching, in Nicotiana sp. J Biol Chem 290:24340–24354. Available at: http://www.ncbi.nlm.nih.gov/pubmed/26260788 [Accessed 14 Mar 2018]

Pinnola A, Staleva-Musto H, Capaldi S, Ballottari M, Bassi R, Polívka T (2016) Electron transfer between carotenoid and chlorophyll contributes to quenching in the LHCSR1 protein from Physcomitrella patens. Biochim Biophys Acta Bioenerg 1857:1870–1878

Pinnola A, Ballottari M, Bargigia I, Alcocer M, D'Andrea C, Cerullo G, Bassi R (2017) Functional modulation of LHCSR1 protein from Physcomitrella patens by zeaxanthin binding and low pH. Sci Rep 7:11158. Available at: http://www.nature.com/articles/s41598-017-11101-7 [Accessed 21 Mar 2018]

Pogson BJ, Niyogi KK, Björkman O, DellaPenna D (1998) Altered xanthophyll compositions adversely affect chlorophyll accumulation and nonphotochemical quenching in Arabidopsis mutants. Proc Natl Acad Sci U S A 95:13324–13329. Available at: http://www.ncbi.nlm.nih.gov/pubmed/9789087 [Accessed 16 Mar 2018]

Polle JEW, Benemann JR, Tanaka A, Melis A (2000) Photosynthetic apparatus organization and function in the wild type and a chlorophyll b -less mutant of *Chlamydomonas reinhardtii*. Dependence on carbon source. Planta 211:335–344. Available at: http://link.springer.com/10.1007/s004250000279 [Accessed 23 Mar 2019]

Polle JE, Niyogi KK, Melis A (2001) Absence of lutein, violaxanthin and neoxanthin affects the functional chlorophyll antenna size of photosystem-II but not that of photosystem-I in the green alga Chlamydomonas reinhardtii. Plant Cell Physiol 42:482–491

Qin X, Suga M, Kuang T, Shen J-R (2015) Structural basis for energy transfer pathways in the plant PSI-LHCI supercomplex. Science (80-.) 348:989–995. Available at: http://science.sciencemag.org/content/348/6238/989.abstract

Qin X, Pi X, Wang W, et al (2019) Structure of a green algal photosystem I in complex with a large number of light-harvesting complex I subunits. Nat Plants 5:263–272. https://doi.org/10.1038/s41477-019-0379-y

Quaas T, Berteotti S, Ballottari M, Flieger K, Bassi R, Wilhelm C, Goss R (2015) Non-photochemical quenching and xanthophyll cycle activities in six green algal species suggest mechanistic differences in the process of excess energy dissipation. J Plant Physiol 172:92–103. Available at: https://www.sciencedirect.com/science/article/pii/S0176161714002351 [Accessed 22 Jan 2019]

Ramanan C, Gruber JM, Malý P, Negretti M, Novoderezhkin V, Krüger TPJ, Mančal T, Croce R, van Grondelle R (2015) The role of exciton delocalization in the major photosynthetic light-harvesting antenna of plants. Biophys J 108:1047–1056. Available at: https://www.sciencedirect.com/science/article/pii/S0006349515001137 [Accessed 26 Mar 2019]

Ruban AV, Berera R, Ilioaia C et al (2007) Identification of a mechanism of photoprotective energy dissipation in higher plants. Nature 450:575–578. Available at: http://www.nature.com/articles/nature06262 [Accessed 14 Mar 2018]

Rutherford AW, Mullet JE (1981) Reaction center triplet states in photosystem I and photosystem II. Biochim Biophys Acta Bioenerg 635:225–235. Available at: https://www.sciencedirect.com/science/article/pii/0005272881900220 [Accessed 23 Mar 2019]

Santini C, Tidu V, Tognon G, Ghiretti Magaldi A, Bassi R (1994) Three-dimensional structure of the higher-

plant photosystem II reaction Centre and evidence for its dimeric organization in vivo. Eur J Biochem 221:307–315. Available at: https://febs.onlinelibrary.wiley.com/doi/abs/10.1111/j.1432-1033.1994.tb18742.x

Sawyer AL, Hankamer BD, Ross IL (2015) Sulphur responsiveness of the Chlamydomonas reinhardtii LHCBM9 promoter. Planta 241:1287–1302. Available at: https://doi.org/10.1007/s00425-015-2249-9

Scheller HV, Jensen PE, Haldrup A, Lunde C, Knoetzel J (2001) Role of subunits in eukaryotic photosystem I. Biochim Biophys Acta Bioenerg 1507:41–60. Available at: https://www.sciencedirect.com/science/article/pii/S0005272801001967 [Accessed 11 Jan 2019]

Sello S, Meneghesso A, Alboresi A, Baldan B, Morosinotto T (2019) Plant biodiversity and regulation of photosynthesis in the natural environment. Planta 249:1217–1228. Available at: https://doi.org/10.1007/s00425-018-03077-z

Semchonok DA, Sathish Yadav KN, Xu P, Drop B, Croce R, Boekema EJ (2017) Interaction between the photoprotective protein LHCSR3 and C2S2 photosystem II supercomplex in Chlamydomonas reinhardtii. Biochim Biophys Acta Bioenerg 1858:379–385. Available at: https://www.sciencedirect.com/science/article/pii/S0005272817300439?via%3Dihub [Accessed 15 Mar 2018]

Sies H, Menck CFM (1992) Singlet oxygen induced DNA damage. Mutat Res 275:367–375. Available at: https://www.sciencedirect.com/science/article/pii/092187349290039R [Accessed 21 Jan 2019]

Sinha RK, Komenda J, Knoppová J, SEDLÁŘOVÁ M, POSPÍŠIL P (2012) Small CAB-like proteins prevent formation of singlet oxygen in the damaged photosystem II complex of the cyanobacterium Synechocystis sp. PCC 6803. Plant Cell Environ 35:806–818. Available at: https://onlinelibrary.wiley.com/doi/abs/10.1111/j.1365-3040.2011.02454.x

Son M, Pinnola A, Bassi R, Schlau-Cohen GS (2019) The electronic structure of lutein 2 is optimized for light harvesting in plants. Chem 5:575–584. Available at: https://www.sciencedirect.com/science/article/pii/S2451929418305795 [Accessed 22 Mar 2019]

Staleva H, Komenda J, Shukla MK, Šlouf V, Kaňa R, Polívka T, Sobotka R (2015) Mechanism of photoprotection in the cyanobacterial ancestor of plant antenna proteins. Nat Chem Biol 11:287–291. Available at: http://www.nature.com/articles/nchembio.1755 [Accessed 9 Jan 2019]

Stauber EJ, Fink A, Markert C, Kruse O, Johanningmeier U, Hippler M (2003) Proteomics of Chlamydomonas reinhardtii light-harvesting proteins. Eukaryot Cell 2:978–994. Available at: http://ec.asm.org/content/2/5/978.abstract

Su X, Ma J, Wei X, Cao P, Zhu D, Chang W, Liu Z, Zhang X, Li M (2017) Structure and assembly mechanism of plant C2S2M2-type PSII-LHCII supercomplex. Science 357:815–820. Available at: http://www.ncbi.nlm.nih.gov/pubmed/28839073 [Accessed 18 Apr 2018]

Takahashi H, Iwai M, Takahashi Y, Minagawa J (2006) Identification of the mobile light-harvesting complex II polypeptides for state transitions in Chlamydomonas reinhardtii. Proc Natl Acad Sci U S A 103:477–482. Available at: http://www.pnas.org/content/103/2/477.abstract

Telfer A (2002) What is beta-carotene doing in the photosystem II reaction centre? Philos Trans R Soc Lond B Biol Sci 357:1431–1470. Available at: https://www.ncbi.nlm.nih.gov/pubmed/12437882

Teramoto H, Ono T, Minagawa J (2001) Identification of Lhcb gene family encoding the light-harvesting chlorophyll-a/b proteins of photosystem II in Chlamydomonas reinhardtii. Plant Cell Physiol 42:849–856. https://doi.org/10.1093/pcp/pce115

Tokutsu R, Iwai M, Minagawa J (2009) CP29, a monomeric light-harvesting complex II protein, is essential for state transitions in Chlamydomonas reinhardtii. J Biol Chem 284:7777–7782. Available at: http://www.ncbi.nlm.nih.gov/pubmed/19144643 [Accessed 12 Jan 2019]

Tokutsu R, Kato N, Bui KH, Ishikawa T, Minagawa J (2012) Revisiting the supramolecular organization of photosystem II in Chlamydomonas reinhardtii. J Biol Chem 287:31574–31581. Available at: http://www.jbc.org/content/287/37/31574.abstract

Trippens J, Greiner A, Schellwat J, Neukam M, Rottmann T, Lu Y, Kateriya S, Hegemann P, Kreimer G (2012) Phototropin influence on eyespot development and regulation of phototactic behavior in Chlamydomonas reinhardtii. Plant Cell 24:4687–4702. Available at: http://www.plantcell.org/content/24/11/4687.abstract

Umena Y, Kawakami K, Shen J-R, Kamiya N (2011) Crystal structure of oxygen-evolving photosystem II at a resolution of 1.9 Å. Nature 473:55. Available at: https://doi.org/10.1038/nature09913

Ünlü C, Drop B, Croce R, van Amerongen H (2014) State transitions in Chlamydomonas reinhardtii strongly modulate the functional size of photosystem II but not of photosystem I. Proc Natl Acad Sci U S A 111:3460–3465. Available at: http://www.ncbi.nlm.nih.gov/pubmed/24550508 [Accessed 3 Dec 2018]

van Amerongen H, van Grondelle R, Valkunas L (2000) Photosynthetic excitons. World Scientific, Singapore. https://doi.org/10.1142/3609

van Oort B, Alberts M, de Bianchi S, Dall'Osto L, Bassi R, Trinkunas G, Croce R, van Amerongen H (2010) Effect of antenna-depletion in photosystem II on excitation energy transfer in Arabidopsis thaliana. Biophys J 98:922–931. Available at: https://www.sciencedirect.com/science/article/pii/S0006349509017391 [Accessed 24 Jan 2019]

Varotto C, Pesaresi P, Jahns P, Lessnick A, Tizzano M, Schiavon F, Salamini F, Leister D (2002) Single and double knockouts of the genes for photosystem I subunits G, K, and H of Arabidopsis. Effects on photosystem I composition, photosynthetic electron flow, and state transitions. Plant Physiol 129:616–624. Available at: http://www.ncbi.nlm.nih.gov/pubmed/12223884 [Accessed 2 Jan 2019]

Vavilin DV, Vermaas WFJ (2002) Regulation of the tetrapyrrole biosynthetic pathway leading to heme and chlorophyll in plants and cyanobacteria. Physiol Plant 115:9–24. Available at: https://onlinelibrary.wiley.com/doi/abs/10.1034/j.1399-3054.2002.1150102.x

Vavilin D, Yao D, Vermaas W (2007) Small cab-like proteins retard degradation of photosystem II-associated chlorophyll in Synechocystis sp. PCC 6803: kinetic analysis of pigment labeling with 15N and 13C. J Biol Chem 282:37660–37668. Available at: http://www.ncbi.nlm.nih.gov/pubmed/17971445 [Accessed 9 Jan 2019]

Veith T, Büchel C (2007) The monomeric photosystem I-complex of the diatom Phaeodactylum tricornutum binds specific fucoxanthin chlorophyll proteins (FCPs) as light-harvesting complexes. Biochim Biophys Acta Bioenerg 1767:1428–1435. Available at: https://www.sciencedirect.com/science/article/pii/S000527280700206X [Accessed 25 Mar 2019]

Wang W, Yu L-J, Xu C et al (2019) Structural basis for blue-green light harvesting and energy dissipation in diatoms. Science (80–.) 363:eaav0365. Available at: http://science.sciencemag.org/content/363/6427/eaav0365.abstract

Watanabe M, Semchonok DA, Webber-Birungi MT, Ehira S, Kondo K, Narikawa R, Ohmori M, Boekema EJ, Ikeuchi M (2014) Attachment of phycobilisomes in an antenna–photosystem I supercomplex of cyanobacteria. Proc Natl Acad Sci 111:2512–2517. Available at: http://www.pnas.org/content/111/7/2512.abstract

Wei X, Su X, Cao P, Liu X, Chang W, Li M, Zhang X, Liu Z (2016) Structure of spinach photosystem II–LHCII supercomplex at 3.2 Å resolution. Nature 534:69. Available at: https://doi.org/10.1038/nature18020

Wientjes E, Roest G, Croce R (2012) From red to blue to far-red in Lhca4: how does the protein modulate the spectral properties of the pigments? Biochim Biophys Acta Bioenerg 1817:711–717. Available at: https://www.sciencedirect.com/science/article/pii/S0005272812000667#bb0025 [Accessed 24 Jan 2019]

Wientjes E, van Amerongen H, Croce R (2013) LHCII is an antenna of both photosystems after long-term acclimation. Biochim Biophys Acta Bioenerg 1827:420–426. Available at: https://www.sciencedirect.com/science/article/pii/S0005272813000029 [Accessed 11 Jan 2019]

Xu H, Vavilin D, Funk C, Vermaas W (2002) Small cab-like proteins regulating tetrapyrrole biosynthesis in the cyanobacterium Synechocystis sp. PCC 6803. Plant Mol Biol 49:149–160. Available at: https://doi.org/10.1023/A:1014900806905

Xue H, Tokutsu R, Bergner SV, Scholz M, Minagawa J, Hippler M (2015) Photosystem II subunit R is required for efficient binding of light-harvesting complex stress-related protein3 to photosystem II-light-harvesting supercomplexes in Chlamydomonas reinhardtii. Plant Physiol 167:1566–1578. Available at: http://www.ncbi.nlm.nih.gov/pubmed/25699588 [Accessed 24 Jan 2019]

Yakushevska AE, Keegstra W, Boekema EJ, Dekker JP, Andersson J, Jansson S, Ruban AV, Horton P (2003) The structure of photosystem II in Arabidopsis: localization of the CP26 and CP29 antenna complexes. Biochemistry 42:608–613. Available at: https://doi.org/10.1021/bi027109z

Chapter 4

The Dynamics of the Photosynthetic Apparatus in Algae

Jean-David Rochaix*
Departments of Molecular Biology and Plant Biology, University of Geneva University, Geneva, Switzerland

I. Introduction

Oxygenic photosynthetic organisms are constantly subjected to changes in light quality and quantity and have to adapt to this changing environment. On the one hand they need light energy and have to collect it efficiently especially when light is limiting, on the other, they have to be able to dissipate the excess absorbed light energy when the capacity of the photosynthetic apparatus is exceeded. The primary events of photosynthesis occur in the thylakoids, a complex network of membranes localized within chloroplasts. These primary reactions are mediated by three major protein-pigment complexes, photosystem II (PSII), the cytochrome b_6f complex (Cytb_6f) and photosystem I (PSI) embedded in the thylakoid membrane and which act in series. Both PSII and PSI are associated with their light-harvesting systems LHCII and LHCI, respectively, which collect and transfer the light excitation energy to the reaction centers of the two photosystems. In both cases a chlorophyll dimer is oxidized and a charge transfer occurs across the thylakoid membrane. PSII creates thereby a strong oxidant capable of splitting water on its donor side with concomitant evolution of molecular

*Author for correspondence, e-mail: Jean-David.Rochaix@unige.ch

A. W. D. Larkum et al. (eds.), *Photosynthesis in Algae: Biochemical and Physiological Mechanisms*, Advances in Photosynthesis and Respiration 45, https://doi.org/10.1007/978-3-030-33397-3_4

oxygen and the release of protons in the lumen while electrons are transferred along the photosynthetic electron transport chain through PSII to the plastoquinone pool and Cytb_6f. This complex pumps protons from the stromal to the lumen side of the thylakoid membrane while transferring electrons to plastocyanin and PSI. Ultimately the electrons are transferred to ferredoxin and NADP(H), the final acceptor. As a result of this photosynthetic electron flow, a protonmotive force is generated across the thylakoid membrane consisting of a proton gradient and membrane potential. A fourth complex, the ATP synthase complex, is functionally linked to the other three by using the proton gradient to produce ATP (Fig. 4.1). Both ATP and NADPH fuel the Calvin-Benson-Bassham cycle for CO_2 assimilation. Besides linear electron flow (LEF), cyclic electron flow (CEF) occurs in which electrons are transferred from the PSI acceptor ferredoxin to the plastoquinone pool either through a typeI/II thylakoid-bound NADH dehydrogenase (Burrows et al. 1998) or the antimycin-sensitive pathway involving Pgr5 and Pgrl1 (Munekage et al. 2002; Hertle et al. 2013). Analysis of a *pgr5* mutant of *Chlamydomonas* revealed that the loss of Pgr5 leads to a reduced proton gradient across the thylakoid membrane and to diminished CEF activity (Johnson et al. 2014). Pgrl1 has been proposed to act as a ferredoxin-plastoquinone reductase (Hertle et al. 2013). In contrast to linear electron flow which generates both reducing power and ATP, CEF produces exclusively ATP. The NADPH/ATP ratio can thus be modulated through regulation of CEF versus LEF. It should be noted however that *pgr5* and *pgrl1* mutants are still able to perform CEF under specific conditions such as high light or CO_2

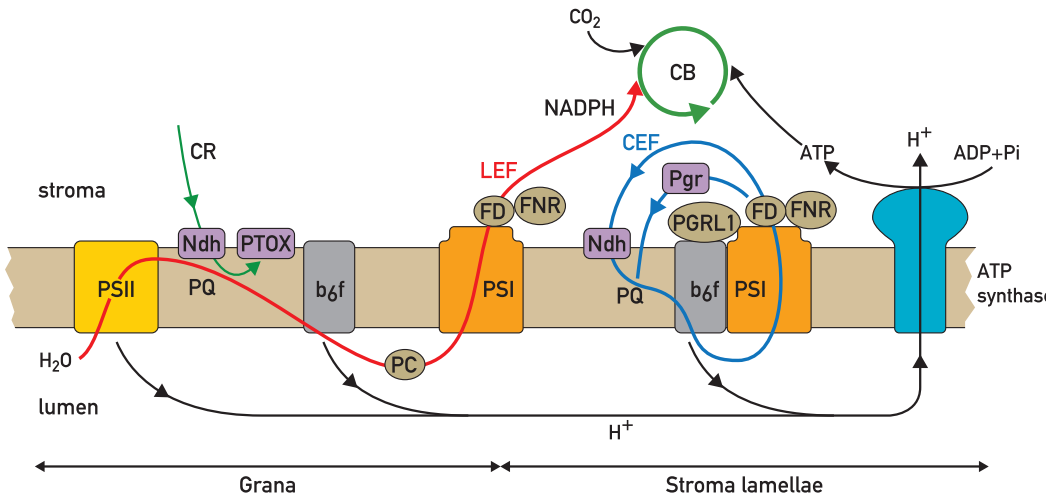

Fig. 4.1. Scheme of the photosynthetic electron transport chain with PSII, Cytb_6f, PSI and ATP synthase. Linear electron flow (LEF) and cyclic electron flow (CEF) are shown in red and blue, respectively with arrows indicating the direction of electron flow. The LEF pathway is driven by the two photochemical reactions of PSII and PSI: electrons are extracted by PSII from water and transferred subsequently to the PQ pool, Cytb_6f, plastocyanin (PC), PSI and ferredoxin (Fd). Ferredoxin-NADPH reductase (FNR) catalyzes the formation of NADPH at the expense of reduced Fd. The CEF pathway is driven by PSI in the stroma lamellae. In *Chlamydomonas reinhardtii* PSI forms a supercomplex with Cytb_6f, FNR, PGRL1, PGR5 and additional factors. Upon reduction of Fd, electrons are returned to the PQ pool either through the NADH complex (NdH) or via PGRL1 which acts as a Fd-PQ oxidoreductase. Both LEF and CEF are associated with proton pumping into the lumen. The resulting proton gradient is used by ATP synthase to produce ATP which together with NADPH drives CO_2 assimilation by the Calvin-Benson-Bassham cycle (CBB). G, grana; SL, stroma lamellae. Reproduced from (Rochaix 2014) with permission

limitation (Joliot and Johnson 2011; Nandha et al. 2007; DalCorso et al. 2008; Kono et al. 2014). This suggests that PGR5 and PGRL1 are not essential for CEF but are important for its regulation and control.

In addition to LEF and CEF, alternative electron transport occurs within the thylakoid membrane in which O_2 is used as electron sink. These pseudo-cyclic electron transport paths involve the plastoquinone terminal oxidase which can oxidize the plastoquinone pool and, on the acceptor side of PSI, flavodiiron proteins which can reduce O_2 directly to water (Allahverdiyeva et al. 2015; Shikanai and Yamamoto 2017). Alternatively reduction of O_2 gives rise to reactive oxygen species (ROS) which are scavenged by superoxide dismutase and ascorbate peroxidase to produce water through the water-water cycle (see Chap. 8). These alternative pathways are important for maintaining a proper redox balance of the electron transfer chain and, in the case of the flavoproteins, for photoprotection of PSII and PSI especially under fluctuating light (Zhang et al. 2012; Shimakawa et al. 2015). Together with CEF they contribute to the formation of the proton-motive force and hence to ATP synthesis without any net accumulation of NADPH (Allen 2003).

A striking feature of the thylakoid membrane is its lateral heterogeneity with two distinct domains consisting of appressed membranes, called grana, and stromal lamellae which connect the grana regions with each other (Andersson and Andersson 1980; Albertsson 2001). Whereas PSII is mainly localized in the grana regions, PSI and the ATP synthase are found in the stromal lamellae and in the margins of the grana (Dekker and Boekema 2005). This is because these two complexes have large domains protruding in the stromal phase which do not fit into the narrow membrane space between the grana lamellae. The organization of thylakoid membranes in grana and stromal regions is determined to a large extent by the resident photosystem complexes. As an example, mutants deficient in PSI contain mostly grana with few stroma lamellae (Amann et al. 2004; Barneche et al. 2006). In contrast to the photosystems, the Cytb_6f complex is equally distributed between the grana and stromal thylakoid regions. Grana formation appears to be mediated by van der Waals attractive forces and electrostatic interactions in which LHCII plays an important role (Kirchhoff et al. 2008).

The LHCII genes form a large family with each member encoding a protein with three transmembrane domains and up to eight chlorophyll *a*, six chlorophyll *b* and four xanthophyll molecules. In *Chlamydomonas* there are nine major and two minor LHCII and nine LHCI genes (Minagawa and Takahashi 2004). The LHCII antenna comprises LHCII trimers connected to the PSII core through the CP26 and CP29 LHCII monomers. The LHCII trimers bind PSII at three sites named S (strong), M (medium) and L (loose). In vivo, PSII assembles as dimers associated with two S and M LHCII trimers to form the $C_2S_2M_2$ PSII-LHCII supercomplex in land plants (Dekker and Boekema 2005). Supercomplexes with one to three LHCII trimers per monomeric PSII core have also been detected in *Chlamydomonas* (Drop et al. 2014; Nield et al. 2000; Tokutsu et al. 2012). In eukaryotic algae the PSI complex is monomeric with a core consisting of the PsaA/PsaB heterodimer and additional subunits as well as up to 10 LHCI proteins in Chlamydomonas based on biochemical studies and single-particle electron microscopy (Ozawa et al. 2018; Steinbeck et al. 2018). It is noticeable that in contrast to the conserved core photosynthetic complexes, the antenna systems are considerably more diverse with hydrophobic membrane-embedded LHCs in plants, green and red algae, and extrinsic hydrophilic phycobilisomes in red algae and cyanobacteria. Moreover in most green algae thylakoid membranes are not differentiated in grana and stroma regions (Gunning and Schwartz 1999).

The aim of this chapter is to provide a description of the remarkable dynamics and flexibility of the photosynthetic apparatus of algae in response to changes in environmental conditions, and to compare these responses with those of land plants. They include changes in light quality and quantity and in nutrient availability. These responses involve a reorganization of some of the photosynthetic complexes often mediated by post-translational modifications of their subunits through an extensive signalling network in chloroplasts and between chloroplasts and nucleus which modulates nuclear and plastid gene expression.

II. Adaptation to Changes in Light Conditions

A distinctive feature of photosynthetic organisms is the presence of light-harvesting systems that funnel the absorbed light energy to the corresponding reaction centers and thereby considerably increase their absorption cross-section. Several regulatory mechanisms operate on these antenna systems for controlling the energy flux to the reaction centers. This is particularly important under changing environmental conditions when the photosynthetic apparatus needs to adapt quickly. Under limiting light it optimizes its light absorption efficiency by adjusting the relative size of its antenna systems through the reversible allocation of a portion of LHCII between PSII and PSI, a process referred to as state transitions which occurs in algae, plants and cyanobacteria (for reviews see (Lemeille and Rochaix 2010; Wollman 2001)). In contrast when the absorbed light energy exceeds the capacity of the photosynthetic apparatus, it dissipates the excess excitation energy through non-photochemical quenching as heat thereby avoiding photodamage (for reviews see (Niyogi 1999; Niyogi and Truong 2013)).

A. State Transitions

Because the antenna systems of PSII and PSI have a different pigment composition, their relative light absorption properties change when the light quality varies. This is especially important for aquatic algae because the penetration of light in water changes depending on its wavelength; in particular, red light is more absorbed than blue light. Another example is provided by photosynthetic organisms growing under a canopy where far red light is enriched. These changes in light quality can result in an unequal excitation of PSII and PSI and thereby perturb the redox poise of the plastoquinone pool. Over-excitation of PSII relative to PSI leads to increased reduction of the plastoquinone pool and favours thereby docking of plastoquinol to the Qo site of the Cytb_6f complex (Vener et al. 1997; Zito et al. 1999). This process leads to activation of the chloroplast protein kinase Stt7/STN7 and to the phosphorylation of several proteins from LHCII (Depège et al. 2003; Bellafiore et al. 2005). Although the direct phosphorylation of LHCII by the Stt7/STN7 kinase has not yet been demonstrated, this kinase is the best candidate for the LHCII kinase because it is firmly associated with the Cytb_6f complex and in its absence state transitions do no longer occur (Lemeille et al. 2009). Furthermore it is widely conserved in land plants, mosses and algae. As a result of this phosphorylation, part of the LHCII antenna is detached from PSII and moves and binds to PSI thereby rebalancing the light excitation of PSII and PSI and enhancing photosynthetic yield. This process is reversible as overexcitation of PSI leads to the inactivation of the kinase and to dephosphorylation of LHCII by the PPH1/TAP38 protein phosphatase and its return to PSII (Pribil et al. 2010; Shapiguzov et al. 2010). Thus two different states can be defined, state 1 and state 2 corresponding to the association of the mobile

LHCII antenna to PSII and PSI, respectively. However, a strict causal link between LHCII phosphorylation and its migration from PSII to PSI has been questioned recently by the finding that some phosphorylated LHCII remains associated with PSII supercomplexes and that LHCII serves as antenna for both photosystems under most natural light conditions (Drop et al. 2014; Wientjes et al. 2013a, b). In plants, the LHCII S trimers comprise Lhcb1 and Lhcb2 whereas the M trimers contain Lhcb1 and Lhcb3 (Galka et al. 2012). Both the S and M trimers are most likely not involved in state transitions because the PSII-LHCII supercomplex is unchanged upon phosphorylation (Wientjes et al. 2013a) and PSI does not bind Lhcb3 in state 2 (Galka et al. 2012). Thus LHCII phosphorylation is not sufficient to dissociate all LHCII trimers from PSII. It has therefore been proposed that peripherally bound L trimers associate with PSI in state 2 (Galka et al. 2012). Moreover although Lhcb1 and Lhcb2 display similar phosphorylation kinetics during a state1 to state 2 transition, only phosphorylated Lhcb2 but not Lhcb1 is part of the PSI-LHCII supercomplex (Longoni et al. 2015). In this regard, it was shown recently by cryo-electron microscopy that the first three conserved residues of Lhcb2 including phosphorylated Thr3, interact with specific residues from PsaL, PsaO and PsaH (Pan et al. 2018). A PSI supercomplex has been isolated and characterized in *Chlamydomonas* (Steinbeck et al. 2018; Iwai et al. 2010). It consists of PSI, Cyt b_6f, LHCII, FNR (ferredoxin-NADPH reductase), PGRL1, a protein involved in CEF (Hertle et al. 2013) and additional factors (Fig. 4.1). The correlation between the occurrence of state transitions and CEF raised the possibility that state transitions may act as a switch between LEF and CEF in *Chlamydomonas* (Finazzi et al. 2002). This interpretation is however not compatible with recent studies which indicate that CEF is activated in the *stt7* mutant when the metabolic demand for ATP increases during the induction of the carbon concentrating mechanism when CO_2 is limiting (Lucker and Kramer 2013). Also, analysis of the *stt7* and *ptox2* mutants, locked in state 1 and 2, respectively, independent of the redox conditions led to similar conclusions (Takahashi et al. 2013). The *ptox2* mutant is deficient in the plastid terminal oxidase which controls the redox state of the PQ pool in the dark (Houille-Vernes et al. 2011). Whereas the accumulation of reducing power and transition to state 2 correlated well with the enhancement of CEF in the wild type, this was not the case for *ptox2*. In this mutant, CEF was not enhanced under aerobic conditions in the dark even though it is locked in state 2 with phosphorylated LHCII. Moreover, CEF enhancement and formation of the PSI-Cytb_6f supercomplex were still observed in the *stt7* mutant when the PQ pool was reduced. It can be concluded that both of these processes occur under reducing conditions with no correlation with state transitions and their associated LHCII reorganization and that it is the redox state of the photosynthetic electron transport rather than state transitions that controls CEF (Takahashi et al. 2013).

State transitions do not occur under high light because the LHCII kinase is inactivated (Schuster et al. 1986). The current view is that inactivation of the kinase is mediated by the ferredoxin-thioredoxin system and that a disulfide bond in the kinase rather than in the substrate may be the target site of thioredoxin (Rintamaki et al. 1997, 2000). In this respect the N-terminal region of the kinase contains indeed two Cys residues which are conserved in all species examined (Depège et al. 2003; Bellafiore et al. 2005). Both of these Cys are essential for the kinase activity because changes of either Cys through site-directed mutagenesis abolishes the kinase activity (Lemeille et al. 2009). It is noticeable that these Cys are located on the lumen side of the thylakoid membrane whereas the kinase catalytic domain is on the stromal side where the substrate sites of the LHCII

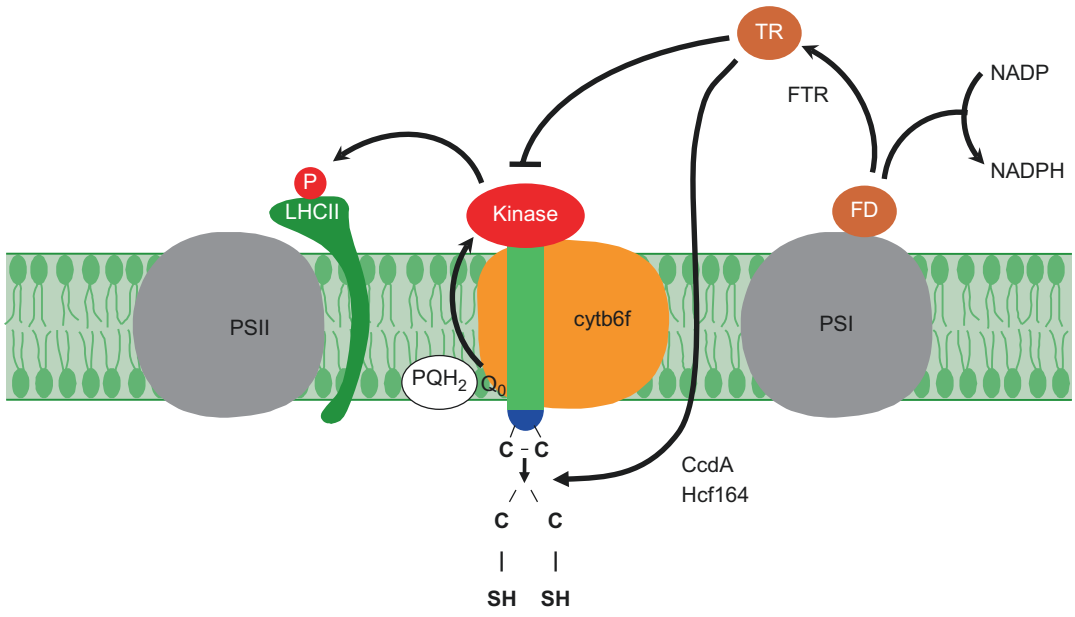

Fig. 4.2. Regulation of the Stt7/STN7 kinase

proteins are located (Depège et al. 2003; Lemeille et al. 2009) (Fig. 4.2). Although the conserved Cys residues in the lumen are on the opposite side of the stromal thioredoxin according to this model, one possibility is that thiol reducing equivalents are transferred across the thylakoid membrane through the CcdA and Hcf164 proteins which operate in this way during heme and Cyt b_6f assembly (Page et al. 2004; Lennartz et al. 2001). Alternatively, transfer of thiol reducing equivalents across the thylakoid membrane could also be mediated by Lto1 (Lumen Thiol Oxidoreductase 1) which catalyzes the formation of disulfide bonds in the thylakoid lumen and is required for PSII assembly (Karamoko et al. 2011; Du et al. 2015) (Fig. 4.2). Its sulfhydryl oxidizing activity is linked to the reduction of phylloquinone, a redox component of PSI. It is not clear whether phylloquinone is involved in other electron transfer processes besides those in PSI. Although the two lumenal Cys are prime candidates for the redox control of the activity of the Stt7/STN7 kinase, high light treatment did not change the redox state of these Cys (Shapiguzov et al. 2016). Another possibility is that high light affects the folding of the kinase in the thylakoid membrane, in particular through reactive oxygen species generated by the high light treatment.

The Stt7/STN7 kinase is associated with the Cytb_6f complex. This kinase contains a transmembrane domain connecting its N-terminus on the lumen side with two conserved Cys residues to the catalytic domain on the stromal side of the thylakoid membrane. The major substrates of this kinase are the LHCII proteins of the PSII antenna. The LHCII kinase is known to be inactivated by high light through the Fd/Trx system. This system could modulate the redox state of the two lumenal Cys through CcdA and Hcf164, two proteins known to mediate the transfer of thiol reducing equivalents across the thylakoid membrane. Another possibility is that this process is catalyzed by Lto1, the lumenal thiol oxidoreductase 1.

It is known that the activation of the kinase is intimately connected to the docking of plastoquinone to the Qo site of the Cyt b_6f complex (Vener et al. 1997; Zito et al. 1999) (Fig. 4.2). Electron transfer from plasto-

quinol to Cyt *f* is mediated by the Rieske protein and involves the movement of this protein from the proximal to distal position within the Cyt b_6f complex (Darrouzet et al. 2001; Breyton 2000). Recent studies have revealed that the two conserved Cys residues of the Stt7/STN7 kinase form an intramolecular disulfide bridge which appears to be essential for kinase activity (Shapiguzov et al. 2016). However no change in the redox state of these Cys could be detected during state transitions. It is only under prolonged anaerobic conditions that this disulfide bridge was reduced but at a significantly slower pace than transition from state 1 to state 2 which occurs under anaerobiosis in *Chlamydomonas* (Bulté et al. 1990). In wild-type *Arabidopsis* plants the STN7 kinase is only observed as a monomer both under state 1 and state 2 conditions although the dimer could be detected in plants overexpressing STN7 or in mutants with changes in either of the two luminal Cys of STN7 (Wunder et al. 2013). However these results do not exclude the possibility of rapid and transient changes in the redox state of these two Cys. In fact such changes were proposed to occur to accommodate all the known features of the Stt7/STN7 kinase (Shapiguzov et al. 2016). A transient change from an intra- to intermolecular disulfide bond may occur which would activate the kinase and be coupled to the movement of the Rieske protein during electron transfer from plastoquinol to Cyt *f*. Moreover it is interesting to note that an interaction site between the kinase and the Cytb_6f complex has been located close to the flexible glycine-rich hinge connecting the membrane anchor to the large head of the Rieske protein in the lumen (Shapiguzov et al. 2016). Given that a single chlorophyll *a* molecule with its phytyl tail close to the Qo site exists in Cytb_6f (Stroebel et al. 2003), it is also possible that the kinase senses PQH_2 binding to the Qo site through this chlorophyll *a* molecule of the Cytb_6f complex (Stroebel et al. 2003; Kurisu et al. 2003). It was proposed that this molecule may play a role in the activation of the Stt7/STN7 kinase based on site-directed mutagenesis of the chlorophyll *a* binding site (de Lacroix de Lavalette et al. 2008). The activation of the kinase would be triggered through the transient formation of a STN7 dimer with two intermolecular disulfide bridges which would transduce the signal to the catalytic domain on the stromal side of the thylakoid membrane (Shapiguzov et al. 2016).

Besides the lumenal side of the Cyt b_6f complex, its stromal side also appears to be involved in the activation of the Stt7/STN7 kinase. Analysis of mutants affected in the chloroplast *petD* gene encoding subunitIV of Cyt b_6f revealed that several residues of the stromal loop connecting helices F and G interact directly with the Stt/STN7 kinase and are critical for state transitions (Dumas et al. 2017).

Another proposal for the mechanism of activation of the Stt7/STN7 kinase is that hydrogen peroxide may be involved by oxidizing the luminal C1 and C2 to form intra and/or intermolecular disulfide bridges. It is based on the observation that singlet oxygen generated by PSII can oxidize plastoquinol with concomitant production of hydrogen peroxide in the thylakoid membranes (Khorobrykh et al. 2015). However this proposal is difficult to reconcile with the observation that these Cys exist mostly in the oxidized form and the conversion from intra- to inter-molecular disulfide bridges appears to be only transient (Shapiguzov et al. 2016).

State transitions involve remodeling of the antenna system of PSII within the thylakoid membranes. This poses a challenging problem especially considering the fact that amongst biological membranes, the thylakoid membrane is very crowded with 70% of the surface area of grana membranes occupied by proteins and 30% by lipids (Kirchhoff et al. 2008). Light-induced architectural changes in the folding of the thylakoid membrane are induced at least partly by changes in phosphorylation of thylakoid proteins catalyzed by the protein kinases Stt7/STN7 and

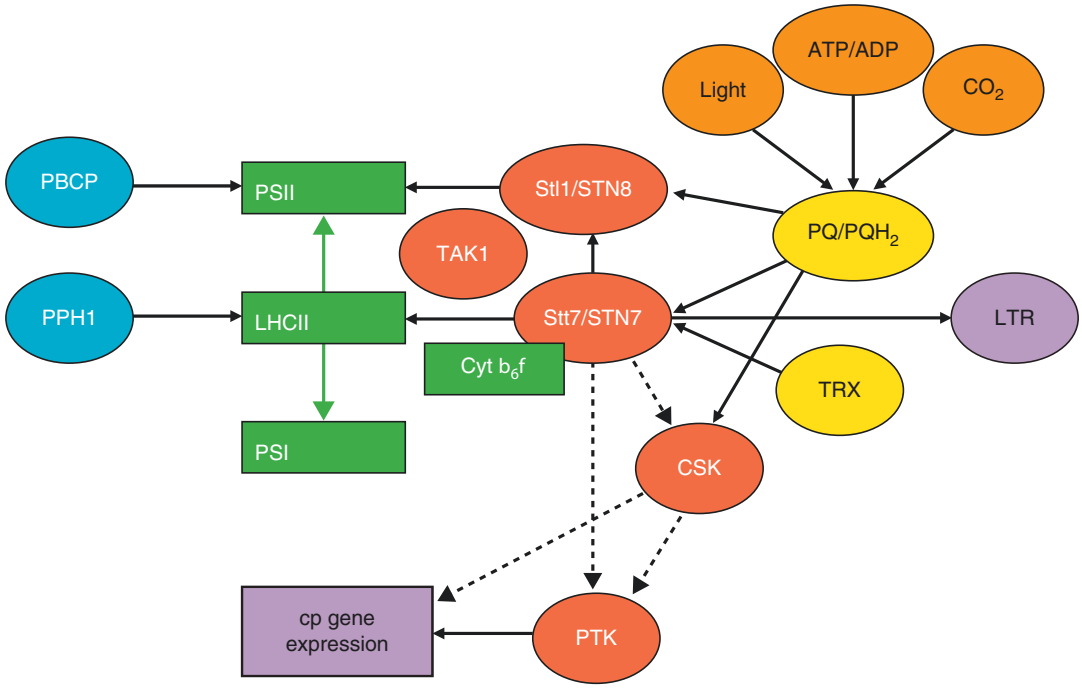

Fig. 4.3. Chloroplast signaling

Stl1/STN8 which most likely facilitate mobility of proteins in these membranes (Fristedt et al. 2009; Samol et al. 2012). These two kinases appear to play an important role in chloroplast signaling in response to changing environmental conditions (Fig. 4.3). Light irradiance, ambient CO_2 level and the cellular ATP/ADP ratio modulate the redox state of the plastoquinone pool of the electron transport chain which is sensed by the Stt7/STN7 kinase. Together with the Stl1/STN8 kinase and the two corresponding protein phosphatases PPH1/TAP38 and PBCP, Stt7/STN7 forms a central quartet which orchestrates the phosphorylation of the LHCII and the PSII core proteins (Fig. 4.3). PTK is another chloroplast Ser/Thr kinase of the casein kinase II family which is associated with the plastid RNA polymerase and acts as a global regulator of chloroplast transcription (Link 2003; Ogrzewalla et al. 2002). The CSK kinase shares structural features with cyanobacterial sensor histidine kinases and is conserved in all major plant and algal lineages except *C. reinhardtii* (Puthiyaveetil et al. 2008). Upon oxidation of the PQ pool, autophosphorylation of CSK occurs, an event which correlates with phosphorylation of the chloroplast σ factor Sig1 and the decrease of *psaAB* gene expression. Furthermore, CSK interacts with PTK and SIG1 in yeast two hybrid assays. Based on these results it was proposed that CSK is regulated by the redox state of the PQ pool through the STN7 kinase (Fig. 4.3) (Puthiyaveetil et al. 2008). However how the different kinases are linked within this chloroplast signaling network shown in Fig. 4.3 is still unclear.

The redox state of the PQ pool is modulated by the light irradiance, ATP/ADP ratio and ambient CO2 level. The protein kinases Stl1/STN8, Stt7/STN7, CSK, PTK and TAK1 (Snyders and Kohorn 1999, 2001) are shown with their targets indicated by arrows. *Broken arrows* indicate putative targets. *LTR* long term response involving retrograde signaling is mediated through Stt7/STN7.

Reproduced from (Rochaix 2013) with permission.

B. Non Photochemical Quenching (NPQ)

While state transitions are mainly involved in low light responses through an extensive reorganization of the antenna systems, other mechanisms for the regulation of light-harvesting operate when oxygenic photosynthetic organisms are suddenly exposed to large and sudden changes in light intensity in their natural habitat. In the case of aquatic algae even moderate water mixing can bring algae from full darkness to high light within minutes (MacIntyre et al. 2000; Schubert and Forster 1997). Under these conditions increased electron flow along the electron transport chain generates a large proton gradient. The resulting acidification of the thylakoid lumen leads to the de-excitation of singlet excited light-harvesting pigments and is measured as non-photochemical quenching of chlorophyll fluorescence (NPQ). NPQ comprises several components; the major one is the high energy state quenching qE which leads to the harmless heat dissipation of the absorbed excess light energy (Niyogi and Truong 2013; Ruban et al. 2012; Chap. 12). The other components which also contribute to fluorescence quenching are the photoinhibitory quenching qI and state transitions qT although qT is not associated with thermal dissipation of excitation energy. The qE mechanism occurs in all major algal taxa and land plants. However the underlying molecular mechanisms of heat dissipation of excess excitation energy differ. The qE process involves both the xanthophyll cycle and the PsbS protein in plants. Another protein, LhcsR, has been shown to mediate qE in algae (Niyogi 1999; Peers et al. 2009; Chaps. 3 & 12).

The proton gradient acts as a sensor of the state of the photosynthetic electron transport chain. The magnitude of this gradient is low under low light illumination and high under illumination with high light especially when it exceeds the capacity of the photosynthetic apparatus. The resulting acidification of the thylakoid lumen activates the xanthophyll cycle in which violaxanthin is de-epoxdized to zeaxanthin, a reaction catalyzed by violaxanthin de-epoxidase (VDE) which has an acidic pH optimum (Demmig-Adams and Adams 1992). The reverse reaction is catalyzed by zeaxanthin epoxidase with a broad pH optimum and which in contrast to VDE is active both in the dark and in the light. Because the turnover of this enzyme is considerably lower than that of VDE, zeaxanthin accumulates rapidly during high light illumination. The zeaxanthin-dependent NPQ depends greatly on the grana structure as unstacking of the membranes abolishes qE. It was proposed that the organization of LHCII in an aggregated state within the stacked grana region is essential for efficient qE (Horton et al. 2008). Both high proton concentration in the lumen and accumulation of zeaxanthin promote not only aggregation of LHCII but also that of the minor PSII antenna proteins CP29, CP26 and CP24 (Phillip et al. 1996; Wentworth et al. 2001). In plants qE occurs in the LHC proteins at multiple sites of the antenna system (Holwarth et al. 2009). These proteins have the ability to switch from an efficient light-harvesting mode to a light energy dissipating state (Kruger et al. 2012). Several mechanisms have been proposed including excitonic coupling, charge transfer and energy transfer between carotenoids and chlorophylls as well as chlorophyll-chlorophyll charge transfer states (for review see (Niyogi and Truong 2013)).

Another important player involved in NPQ is PsbS, a four-helix member of the LHC protein family (Li et al. 2000; Chaps. 3 & 10). However this protein does not bind pigments although a chlorophyll molecule was detected at the dimer interface in the PsbS crystals (Fan et al. 2015). This protein appears to act as a sensor of the lumen pH most likely through protonation of its acidic lumen residues which in turn induces a rearrangement of the light-harvesting system

required for induction of NPQ (Li et al. 2004; Betterle et al. 2009; Goral et al. 2012). In this sense PsbS would act as an antenna organizer, a view which is further supported by the fact that it is mobile in the thylakoid membrane (Teardo et al. 2007), and it is able to associate with both the PSII core complex and LHCII (Bergantino et al. 2003). Moreover, qE can be switched on without PsbS protein if the lumen pH is very low (Johnson and Ruban 2011). It thus appears that protonated PsbS allows for a fast and efficient rearrangement of the PSII antenna which is still possible in its absence but requires a longer time.

In *Chlamydomonas reinhardtii* and *Phaeodactylum tricornatum*, two representatives of green algae and diatoms, respectively, qE is mediated by Lhcsr, another three helix member of the LHC protein family (Peers et al. 2009; Chaps. 3 & 16). In high light, most Lhcsr genes are up-regulated in contrast to the light-harvesting genes which are down-regulated. Recent studies reveal that Lhcsr binds chlorophylls and xanthophylls *in vitro* and that it has a basal quenching activity associated with chlorophyll-xanthophyll charge transfer (Bonente et al. 2011). Its chlorophyll fluorescence lifetime is remarkably short and even shorter at low pH suggesting that this protein has some quenching activity even in low light which is enhanced at low pH. It was proposed that these properties could explain the low expression of Lhcsr under low light when constitutive quenching would be wasteful (Niyogi and Truong 2013). The *Chlamydomonas* Lhcsr is bound to PSII where it may interact with the LHC proteins, especially Lhcbm1 which is known to be involved in thermal dissipation (Allorent et al. 2013; Elrad et al. 2002; Ferrante et al. 2012). Interestingly, as several other LHC proteins, Lhcsr is phosphorylated by the Stt7 kinase and moves from PSII to PSI during a state 1 to state 2 transition (Allorent et al. 2013). This observation is particularly interesting with regard to chlorophyll fluorescence lifetime measurements which reveal two different kinetic components suggesting the existence of two underlying mechanisms (Amarnath et al. 2012).

It is noteworthy that although PsbS is also present in green algae, there is no evidence that it is involved in qE in these organisms under increased illumination. This is in contrast to the moss *Physcomitrella patens* that has both Lhcsr- and PsbS-dependent NPQ which operate independently and additively (Alboresi et al. 2010; Gerotto et al. 2012). The maintenance of these two mechanisms in mosses may be linked to a greater need for inducible NPQ in these organisms (Gerotto et al. 2011).

Two PsbS genes are present in the nuclear genome of the green alga *Chlamydomonas reinhardtii* that are expressed under specific conditions such as nitrogen deprivation (Miller et al. 2010), during a dark to light shift (Zones et al. 2015) and upon light stress (Correa-Galvis et al. 2016). PsbS is also strongly induced by UV-B light together with Lhcsr1 both of which contribute to qE under these conditions. UV irradiation leads to the monomerization of the cytoplasmic dimeric UVR8 receptor which then interacts with the E3 ubiquitin ligase COP1 (Constitutively Photomorphogenic 1), moves to the nucleus and induces changes in gene expression (Rizzini et al. 2011; Christie et al. 2012; Favory et al. 2009; Kaiserli and Jenkins 2007). Amongst the proteins upregulated in this response, PsbS and Lhcsr1 are prominent (Tilbrook et al. 2016) and they provide a direct mechanistic link between UVR8 receptor signaling and acclimation and photoprotection of the photosynthetic machinery of Chlamydomonas (Allorent et al. 2016; Allorent and Petroutsos 2017).

NPQ has also been investigated in diatoms, an ubiquitous group of unicellular marine algae which make an important contribution to the global carbon assimilation (Geider et al. 2001). Diatoms acquired their chloroplast through secondary endosymbiosis from a red algal ancestor (Keeling 2013). In these organisms, similar to plants and green algae, qE relies on three interacting

components, the light-induced proton gradient across the thylakoid membrane, the conversion of the xanthophyll diadinoxanthin (Dd) to diatoxanthin (Dt) catalyzed by the enzyme Dd-de-epoxidase which depends on a trans-thylakoid proton gradient and the Lhcx antenna proteins (for review see (Goss and Lepetit 2015). Amongst these, Lhcx1 appears to play a major role in qE as changes in its level are directly related to the quenching of light energy (Bailleul et al. 2010). Lhcx1 also plays an important general role in light responses in diatoms as it accumulates in different amounts in ecotypes originating from different latitudes. In contrast to land plants the proton gradient is unable to induce NPQ on its own in diatoms. It is only required to activate the de-epoxidation of Dd. The qE process represents an important photoprotective mechanism and involves a reorganization of the antenna complexes of diatoms (Goss and Lepetit 2015). However the quenching sites within the antenna systems of these organisms have not yet been precisely determined.

Another original feature of diatoms is the way they adjust the ATP/NADPH ratio which is important for proper carbon assimilation by the Calvin-Benson-Bassam cycle and for optimal growth. In plants and green algae this ratio is mainly set by the relative contributions of LEF and CEF and by the water-to-water cycles (Allen 2003) whereas in diatoms this ratio relies principally on energetic exchanges between plastids and mitochondria (Bailleul et al. 2015). These bidirectional organellar interactions involve the re-routing of reducing power generated by photosynthesis in the plastids to mitochondria and the import of ATP produced in the mitochondria to the plastids.

An additional remarkable feature of microalgae is the presence of flavodiiron (Flv) proteins which are involved in light-dependent electron flow. They catalyze O_2 reduction and thereby prevent oxidative damage when the photosynthetic electron transport chain is over-reduced. These proteins are also found in cyanobacteria and mosses but not in angiosperms. Analysis of *Chlamydomonas* mutants with deficiencies in Flv proteins by chlorophyll fluorescence and oxygen exchange measurement using [^{18}O]-labeled O_2 and mass spectrometry revealed that these proteins indeed participate in the photoreduction of oxygen during the induction phase of photosynthesis following a transition from the dark to the light when the Calvin-Benson-Bassham cycle is not yet activated (Chaux et al. 2017).

C. PSII Repair Cycle

Water splitting by PSII is one of the strongest oxidizing reactions which occurs in living organisms. As a result, photodamage to PSII is unavoidable. A remarkable feature of this system is that it is efficiently repaired (Nixon et al. 2010). PSII exists as a dimer in which each monomer consists of 28 subunits generally associated with two LHCII trimers in a supercomplex (Dekker and Boekema 2005). The PSII core consists of the two reaction center polypeptides D1 and D2 which form a central heterodimer which acts as ligand for the chlorophyll dimer P680 and the other redox components including the quinones Q_A and Q_B, the primary and secondary electron acceptors. Amongst all PSII subunits, D1 is the major target of photodamage and needs to be specifically replaced. This process, called PSII repair cycle, involves the partial disassembly of the PSII supercomplex, the removal and degradation of the damaged D1 protein, its replacement by a newly synthesized copy and the reassembly of the PSII complex (Fig. 4.4) (Aro et al. 1993). An important feature of this repair cycle is that it is compartmentalized within the crowded thylakoid membrane (Puthiyaveetil et al. 2014). Whereas damage of D1 occurs in the stacked grana region where most of PSII is located, the replacement of this protein takes place in the stroma lamellae. Although the exact role of phosphorylation

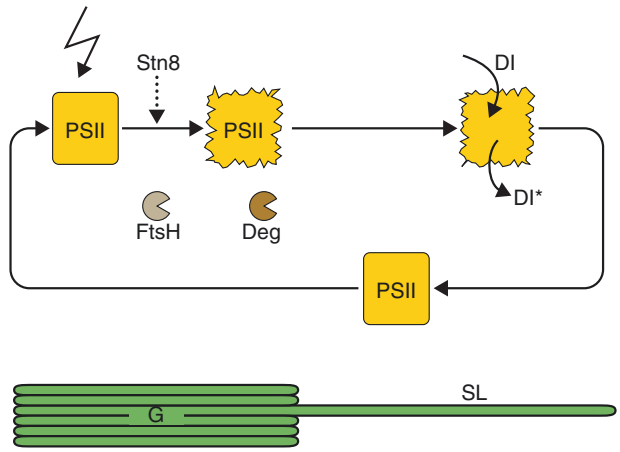

Fig. 4.4. PSII repair cycle

is not fully understood, the current view is that the PSII repair cycle starts with phosphorylation of the PSII core subunits D1, D2, CP43 and PsbH mediated by the STN8 kinase (Vainonen et al. 2005; Bonardi et al. 2005) which leads to the disassembly of the PSII-LHCII supercomplex thereby allowing PSII to move to the grana margins and stroma lamellae (Tikkanen et al. 2008; Herbstova et al. 2012). Dephosphorylation by the PSII core phosphatase Pbcp (Samol et al. 2012) and by other unknown phosphatases is followed by the degradation of D1 by the FtsH and Deg proteases and a newly synthesized D1 is co-translationally inserted into the PSII complex (Nixon et al. 2005). Finally the reassembled PSII complex moves back to the grana and reforms a supercomplex with LHCII. To make this cycle efficient, it is essential that the enzymes involved are confined to distinct thylakoid membrane subcompartments. Thus, the protein degradation occurs on the grana margins and protein synthesis on the stroma lamellae. In addition partial conversion of grana stacks to grana margins allows the proteases to access PSII (Puthiyaveetil et al. 2014).

High light illumination leads to photooxidative damage of the PSII reaction center, especially the D1 protein. The PSII core proteins are phosphorylated and the damaged complex migrates from the grana (G) to the stromal lamellae (SL). The D1 protein is degraded by the FtsH and Deg proteases and upon its removal from the PSII reaction center a newly synthesized D1 protein is inserted co-translationally into the complex which moves back to the grana and thereby completes the repair cycle. Reproduced from (Rochaix 2014) with permission.

D1 degradation is significantly retarded in *stn8* and *stn7 stn8* mutants of *Arabidopsis* in which the thylakoid membrane architecture is affected (Fristedt et al. 2009). In the absence of STN8, grana diameter is increased and there are fewer grana stacks. This observation is particularly intriguing as it suggests that PSII core phosphorylation is important for maintaining grana size, a parameter which is highly conserved in land plants and algae (Kirchhoff et al. 2008). Loss of STN8 also affects partitioning of FtsH between grana and stromal membranes and limits its access to the grana, and migration of D1 from the grana to the stroma lamellae is slowed down during the PSII repair cycle (Fristedt et al. 2009). These observations are thus compatible with the view that PSII core phosphorylation has a strong impact on thylakoid membrane folding and architecture mediated most likely by electrostatic repulsion between membrane layers as proposed earlier (Barber 1982).

Chlamydomonas is able to acclimate specifically to singlet oxygen stress which occurs inevitably as a result of PSII activity. Genetic analysis identified a key regulator of the gene expression response of this acclimation process (Wakao et al. 2014). This protein, Sak1 (singlet oxygen acclimation knocked-out 1) encodes an protein of unknown function with a domain conserved in some bZIP transcription factors of chlorophytes. It is located in the cytosol, and induced and phosphorylated after exposure to singlet oxygen. It could thus represent an important intermediate component of the retrograde signal transduction pathway underlying singlet oxygen acclimation.

III. Response of the Photosynthetic Apparatus to Micronutrient Depletion

The photosynthetic machinery comprises several protein-pigment complexes with specific cofactors including iron, copper, manganese and iron-sulfur centers. Under conditions of limitation of one of these micronutrients, the photosynthetic machinery displays a remarkable plasticity and ability to adapt to its new environment.

A. Copper Deficiency

When *Chlamydomonas* cells face copper deficiency, the copper-binding protein plastocyanin which acts as an essential electron carrier between the Cytb_6f complex and PSI, is degraded and replaced with Cyt *c6* (Merchant and Bogorad 1987). In this way the cells can maintain photosynthetic electron flow. Besides Cyt *c6,* Cpx (coproporphyrinogen oxidase) is also induced by copper deficiency at the transcriptional level (Moseley et al. 2002). The increase of Cpx1 expression may meet the demand for heme, the cofactor of Cyt *c6.* Crd1, another target besides Cyt *c6* and Cpx1 of this signal transduction pathway responsive to copper depletion, was identified through a genetic screen for a copper-conditional phenotype. Crd1 is a thylakoid diiron membrane protein which is required for the maintenance of PSI and LHCI in copper-deficient cells. It has an isoform, Cth1, which accumulates in copper-sufficient oxygenated cells whereas Crd1 accumulates in a reciprocal manner in copper- deficient cells or under anaerobiosis (Moseley et al. 2002). Crd1 and Cth1 are two isoforms of a subunit of the aerobic cyclase in chlorophyll biosynthesis with overlapping functions in the biosynthesis of Chl proteins (Tottey et al. 2003).

B. Iron Deficiency

Iron deficiency occurs often in nature and poses a challenge for photosynthetic organisms because of the abundance and importance of iron in the primary photosynthetic reactions. With its three 4Fe-4S centers PSI is a prime target under these conditions. Under conditions of iron limitation the level of PSI decreases when *Chlamydomonas* cells are gown in the presence of a carbon source such as acetate. Eventually, these Fe-deficient cells become chlorotic because of proteolytically-induced loss of both photosystems and Cyt b_6f (Moseley et al. 2000). Before chlorosis occurs, a graded response is induced in which the LHCI antenna is dissociated from PSI. This dissociation appears to be caused by the decrease of the amount of the peripheral chlorophyll-binding PsaK subunit of PSI which is required for the functional connection of LHCI to PSI. Interestingly loss of Crd1, the Fe-requiring aerobic oxidative cyclase in copper-sufficient cells, also leads to a lower accumulation of PsaK and to uncoupling of LHCI from PSI. It was proposed that a change in plastid iron content is sensed by the diiron enzyme Crd1 through the occupancy of its Fe-containing active site which determines its activity (Moseley et al. 2000). In turn this would affect the flux through the chlorophyll biosynthetic pathway and PsaK

stability. This response to Fe deficiency and also to light quantity and quality further involves a remodeling of the antenna complexes with the degradation of specific subunits and the synthesis of new ones leading to a new state of the photosynthetic apparatus which allows for optimal photosynthetic function and minimal photooxidative damage. The protective value of this antenna remodelling is further confirmed by the observation that the light sensitivity of a PsaF-deficient mutant (Farah et al. 1995) is alleviated in a *psaF-crd1* double mutant (Moseley et al. 2002). The proposed mechanism can be placed within a general framework for explaining the causal link between chlorosis induced by iron deficiency and loss of photosynthetic function.

Marine organisms can face iron limitation in the oceans. A deep-sea/low light strain of the marine green alga *Ostreococcus* has lower photosynthetic activity due to the limited accumulation of PSI (Cardol et al. 2008). Interestingly in this strain electron flow from PSII is shuttled to a plastid plastoquinol terminal oxidase thereby bypassing electron transfer through the Cytb_6f complex. This water-to-water cycle allows for the pumping of additional protons to the lumen thylakoid space and thus facilitates ATP production and enhances qE in the case of absorption of excess light excitation energy.

Micronutrient limitation can also act at the level of the biosynthesis of the photosynthetic apparatus which is mediated by the concerted action of the nuclear and chloroplast genetic systems. It is well established that subunits of the photosynthetic complexes originate from these two systems. In addition a large number of nucleus-encoded factors are required for chloroplast gene expression that act at various plastid post-transcriptional steps comprising RNA processing and stability, translation and assembly of the photosynthetic complexes. Many of these factors have unique gene targets in the plastid and often interact directly or indirectly with specific 5′-untranslated RNA sequences (Eberhard et al. 2008). One of these factors, Taa1 is specifically required for the translation of the PsaA PSI reaction center subunit in *C. reinhardtii* (Lefebvre-Legendre et al. 2015). Under iron limitation, this protein is down-regulated through a post-transcriptional process and it re-accumulates upon restoration of iron. Another recently identified factor is Mac1 which is necessary for stabilization of the *psaC* mRNA (Douchi et al. 2016). Under iron limitation both Mac1 protein and *psaC* mRNA are reduced two-fold and PsaC and PSI are destabilized. Thus PSI abundance appears to be regulated by iron availability through at least two of these nucleus-encoded plastid factors specifically involved in PSI biosynthesis. Another intriguing observation is that Mac1 is differentially phosphorylated in response to changes in the redox state of the electron transport chain raising questions to what extent post-translational protein changes modulate the assembly of photosynthetic complexes.

Similar findings have been reported for Mca1 and Tca1, two nucleus-encoded proteins that are required for the stability and translation of the *petA* mRNA encoding the Cyt *f* subunit in *C. reinhardtii*. Nitrogen deprivation leads to the proteolytic degradation of these factors and in turn to the loss of the Cyt b_6f complex (Boulouis et al. 2011; Raynaud et al. 2007). The response to nitrogen starvation also involves other factors required for the assembly of the Cyt b_6f complex and its hemes (Wei et al. 2014).

C. *Sulfur Deprivation and Hydrogen Production*

Many soil-dwelling algae like *Chlamydomonas* experience anoxic conditions especially during the night and are able to rapidly acclimate to anaerobiosis by shifting from aerobic to fermentative metabolism and can thus sustain energy production in the absence of photosynthesis (Gfeller and Gibbs 1984, 1985; Grossman et al. 2010). These anaero-

bic conditions lead to the expression of the oxygen-sensitive hydrogenase which catalyzes the production of hydrogen from protons and electrons derived from the photosynthetic electron transport chain. Sulfur deprivation of *Chlamydomonas* cells leads to a significant decline in photosynthetic activity within 24 h although there is no proportional concomitant decline in the levels of the major photosynthetic complexes (Yildiz et al. 1994; Davies et al. 1994). This decline in electron transport activity is due to the conversion of PSII centers from the Q_B-reducing to a Q_B non-reducing center (Wykoff et al. 1998). This system has been used for improving hydrogen production in *Chlamydomonas* cells (Melis et al. 2000). These cells as well other microalgal species possess a chloroplast (FeFe)-hydrogenase which acts as an additional sink when the photosynthetic electron transport chain is over-reduced under anaerobic conditions. Upon sulfur deprivation photosynthetic oxygen evolution decreases whereas respiration is maintained resulting in an anaerobic environment in a closed culture system. Although the exact physiological role of algal hydrogenases is not known, they are likely to play a significant role in redox poise, photoprotection and fermentative energy production (Grossman et al. 2010).

D. Nitrogen Deprivation

In contrast to sulphur deprivation which results in PSII deficiency in *Chlamydomonas* (Wykoff et al. 1998), nitrogen deprivation under heterotrophic growth conditions leads to the specific depletion of Rubisco and the Cytb_6f complex due to active proteolysis of this complexes by the Clp and FtsH proteases (Bulte and Wollman 1992; Majeran et al. 2000). These conditions lead to a significant increase in photorespiratory enzymes and to the conversion of thylakoid membranes into a matrix for oxidative catabolism of reductants. Besides Cytb_6f several factors involved in its biogenesis are also degraded under nitrogen deprivation. These protein degradations were proposed to be triggered by the intracellular production of nitric oxide (NO) generated by rerouting of nitrite during nitrogen starvation (Wei et al. 2014). Indeed, addition of NO donors or of nitrite, the most likely donor of NO, during nitrogen starvation enhanced Cytb_6f degradation whereas NO scavengers had the opposite effect (Wei et al. 2014). These proteolytic processes only occur in the presence of a reduced carbon source such as acetate, but not when respiration is impaired or under phototrophic growth conditions which require a functional photosynthetic apparatus. An important future task will be to elucidate the underlying signalling pathway especially as the overall process has implications for biofuel production in microalgae.

IV. Long Term Response: Changes in Nuclear and Chloroplast Gene Expression

While short term responses of the photosynthetic apparatus involve mostly post-translational mechanisms such as phosphorylation or changes in pH and ion levels, long term responses are mediated through changes in the expression of specific chloroplast and nuclear genes and their products. Environmental changes such as changes in light quantity and quality lead to changes in the state of the chloroplast which are perceived by the nucleus through a signalling chain referred to as retrograde signalling. The components of this signalling chain are still largely unknown although a few potential retrograde signals have been identified (Woodson and Chory 2012). Amongst these, tetrapyrroles appear to play a significant role. These compounds are involved in the chlorophyll biosynthetic pathway which needs to be tightly regulated to avoid photo-oxidative damage. Mg-protoporphyrin IX (Mg-Proto) was first shown to be involved in the repression of the LHCII genes in retrograde signal-

ling in *Chlamydomonas* (Johanningmeier and Howell 1984). However such a role for this tetrapyrrole in land plants gave rise to contradictory results and has been questioned (Strand et al. 2003; Mochizuki et al. 2008; Moulin et al. 2008). In contrast feeding experiments with Mg-Proto and hemin in *Chlamydomonas* induce expression of the gene of HemA (glutamyl-tRNA reductase) and of the heat shock proteins Hsp70A, Hsp70B and Hsp70E (Kropat et al. 1997, 2000; von Gromoff et al. 2008). In this alga both Mg-Proto and hemin are exclusively synthesized in the chloroplast. Genome-wide transcriptional profiling revealed that their exogenous addition to *Chlamydomonas* cells elicit transient changes in the expression of almost 1000 genes (Voss et al. 2011). They include only few genes of photosynthetic proteins but several genes of enzymes of the tricarboxylic acid cycle, heme- binding proteins, stress-responsive proteins and proteins involved in protein folding and degradation. Because these tetrapyrroles are not present in the natural environment of the algae, it is likely that these two tetrapyrroles act as secondary messengers for adaptive responses affecting not only organellar proteins but the entire cell. It is noticeable that these large changes in mRNA levels are not matched by similar changes in protein amount (Voss et al. 2011).

The synthesis of tetrapyrroles needs to be tightly controlled because some of these chlorophyll or heme precursors are very photodynamic and can cause serious photo-oxidative damage. In land plants the conversion of protochlorophyllide (PChlide) to chlorophyllide (Chlide) is light-dependent. In the dark, overaccumulation of PChlide is prevented through a negative feedback mediated by the Flu protein which inhibits glutamyl-tRNA reductase at an early step of the tetrapyrrole pathway (Fig. 4.5) (Meskauskiene et al. 2001). Although *Chlamydomonas* is able to synthesize chlorophyll in the dark, it also contains a Flu-like gene called Flp which gives rise to two transcripts by alternative splicing (Falciatore et al. 2005). The relative levels of the two corresponding Flp proteins correlates with the accumulation of specific porphyrin intermediates some of which have been implicated in a signalling chain from the chloroplast to the nucleus. Moreover, decreased levels of the Flp proteins lead to the accumulation of several porphyrin intermediates and to photobleaching when *Chlamydomonas* cells are transferred from the dark to the light. These Flp proteins therefore appear to act as regulators of chlorophyll synthesis and their expression is controlled both by light and plastid signals.

The heme and chlorophyll biosynthetic pathway branch at protoporphyrin IX (Prot IX). GTR, glutamyl tRNA reductase, is subjected to feedback inhibition by heme and FLU. In most land plants conversion of PChlide (protochlorophyllide) to Chlide is light-dependent (in *Chlamydomonas* this conversion also occurs in the dark (*D*)). Through its negative feedback on GTR, FLU prevents overaccumulation of PChlide in the dark. The steps affected by the *gun* and *hy* mutations which affect retrograde signaling, are indicated. *GSA,* glutamate 1-semialdehyde; *ALA,* 5-aminolevulinic acid; *Chl,* chlorophyll; *FC,* ferrochelatase, *HMOX1,* heme oxygenase; *BV,* biliverdin; *PCY,* bilin reductase; *PCB,* phytocyanobilin. Reproduced from (Rochaix 2013) with permission.

Additional evidence for the involvement of the tetrapyrrole biosynthetic pathway in retrograde signalling comes from the identification of a functional bilin biosynthesis pathway in *Chlamydomonas* (Duanmu et al. 2013). In this pathway protoporphyrin IX is converted to protoheme and Mg-Proto by Fe- and Mg-chelatase, respectively. While heme is used as prosthetic group for many hemoproteins, a portion of heme is converted to bilverdin IXa by heme oxygenase (Hmox1) and in the next step by a ferredoxin-dependent phytochromobilin synthase (PcyA) to phytochromobilin, which serves as chromophore of phytochromes (Fig. 4.5). However,

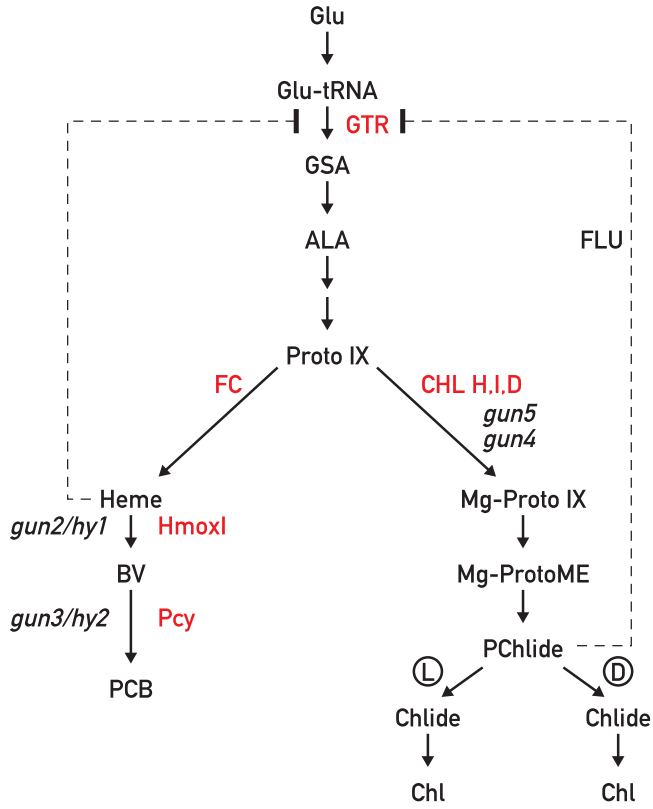

Fig. 4.5. Tetrapyrrole pathway

since *Chlamydomonas* as well as other chlorophytes do not produce phytochromes, the question arises about the role of this pathway in these algae. Some clues came from the analysis of a mutant of *Chlamydomonas* deficient in Hmox1 whose phototrophic growth is compromised and photoacclimates poorly upon a dark to light transition (Duanmu et al. 2013). Comparative transcriptomic studies of wild-type and *hmox1* cells revealed a set of nuclear genes that are up-regulated by bilins and that comprise members of the SOUL heme binding protein family and stress-activated genes, but not genes involved in the biosynthesis of the photosynthetic system or of tetrapyrroles. Further analysis revealed that the poor photoacclimation of the *hmox*1 mutant is due to the decreased light-dependent accumulation of PSI reaction center and of the light-harvesting antennae of PSII and PSI (Wittkopp et al. 2017). Moreover the *hmox1* mutant could be rescued by exogenous biliverdin IXa, the bilin generated by Hmox1 through a blue light-dependent process that is independent of photosynthesis (Wittkopp et al. 2017). These results point to the existence of a bilin-based blue light-sensing system including a still unknown regulatory chromoprotein that operates together with a retrograde signaling pathway. This system appears to have evolved in chlorophytes for the detoxification of reactive oxygen species and conveys robustness to the photosynthetic apparatus during photoacclimation. It remains to be seen whether bilins assume additional roles in chlorophytes besides ensuring smooth daily transitions from dark to light with minimal photo-oxidative damage.

A further striking example of the action of tetrapyrroles as mediators for plastid-to-

nucleus-communication is the identification of a tetrapyrrole-regulated ubiquitin ligase for cell cycle coordination from organelle to nuclear DNA replication in the red alga *Cyanidioschyzoan merolae* (Kobayashi et al. 2011, 2009; Tanaka and Hanaoka 2012).

Redox changes within the photosynthetic electron transport chain occur upon changes in light quality and quantity, CO_2 levels, nutrient availability and elevated temperature. As a result of unequal excitation of PSI and PSII or of insufficient electron acceptor capacity on the PSI acceptor side, the redox state of the plastoquinone pool is altered. In this case chloroplast gene expression is affected in land plants (Pfannschmidt et al. 1999) although the evidence is less convincing in algae. However in these organisms there is unambiguous evidence that nuclear gene expression is affected (Escoubas et al. 1995). A possible candidate for sensing the redox state of the plastoquinone pool is the chloroplast protein kinase Stt7/STN7 which is known to be activated when plastoquinol occupies the Qo site of the Cytb6f complex (Vener et al. 1997; Zito et al. 1999). During experiments in which plants were shifted from light preferentially absorbed by PSI to light preferentially absorbed by PSII, the expression levels of 937 genes changed significantly in *Arabidopsis* (Brautigam et al. 2009). 800 of these changes were dependent on Stn7 indicating that most of these genes are under redox control.

In all situations in which the redox poise of the plastoquinone pool is affected, the relative sizes of the PSII and PSI antennae play an important role. Several factors involved in antenna size were identified through a genetic screen in *Chlamydomonas* (Mitra et al. 2012). One of these factors Tla1 functions as a regulator of chlorophyll content and antenna size and is localized in the chloroplast envelope. In the *tla1* mutant, thylakoid membranes were disorganized, appressed grana membranes were lost and accumulation of the PSII core proteins was reduced (Mitra et al. 2012). The second identified factor Tla2 corresponds to FtsY required for insertion of proteins into thylakoid membranes (Kirst et al. 2012) and the third, Tla3 corresponds to SRP43, a component of chloroplast SRP, known to be essential for the integration of LHCII proteins into the thylakoid membrane (Mitra et al. 2012).

Another protein regulating antenna size in *Chlamydomonas* is Nab1, a cytoplasmic repressor of translation of specific Lcbm isoforms (Wobbe et al. 2009). By binding selectively to the mRNAs of these proteins with Lhcm6 mRNA as its principal target, it sequesters the RNA in translationally silent nucleoprotein complexes. The activity of Nab1 is regulated through a cysteine-based redox control and also by arginine methylation (Wobbe et al. 2009; Blifernez et al. 2011). This protein apparently senses the increased or decreased demand for LHCII protein synthesis through changes in the cytosolic redox state although the underlying molecular mechanisms are still unknown.

V. Conclusions and Perspectives

The photosynthetic apparatus is a complex machinery consisting of several large protein-pigment complexes whose components are encoded by both nuclear and chloroplast genes. Thus, the biosynthesis of this system involves two distinct genetic systems which act in a coordinate manner. In nature photosynthetic organisms are subjected to continuous environmental changes and need to adapt so as to maintain optimal photosynthetic activity and to protect themselves from photo-oxidative damage. These processes can be grouped in short term and long-term responses. The first occur in the second to minute range and involve light-induced protein conformational changes, post-translational protein modifications, cell compartment-specific pH changes and ion fluxes across the chloroplast and thylakoid membranes. The second occur in the minute to hour range and involve changes in gene expression and protein accu-

mulation which depend on an intricate bilateral communication system between chloroplasts and nucleus. Many nuclear genes encoding chloroplast proteins have been identified which are required for chloroplast gene expression and act mainly at post-transcriptional steps. Some of these factors appear to act constitutively while others assume a regulatory role because they have short half-lifes and their level varies greatly upon changes in environmental cues including light, temperature and nutrient availability. However the molecular mechanisms underlying the intercompartmental communication between chloroplast, mitochondria and nucleus are still largely unknown although several retrograde signals have been identified. They involve specific compounds such as tetrapyrroles and isoprenoids as well as plastid protein synthesis, the redox state of the photosynthetic electron transport chain and ROS generated under specific stress conditions. Moreover, a complex signalling network is operating within chloroplasts comprising several protein kinases and phosphatases, ion channels, and specific metabolites which act as signals and for the communication between chloroplast and nucleus. However the signalling chains connecting these different components are still largely unknown and their identification remains an important challenge for future research.

The flexibility of the thylakoid membrane is truly remarkable. Although it is crowded with proteins, it still allows for efficient remodeling of the photosynthetic complexes especially in response to changes in the quality and quantity of light. Among these responses state transitions and non-photochemical quenching have been studied extensively and some of the underlying molecular mechanisms have been elucidated. However many questions remain open. We still do not fully understand how the Stt7/STN7 kinase which plays a central role in state transitions and chloroplast signaling is activated and inactivated as a result of perturbations of the chloroplast redox poise. From an evolutionary point of view, it is particularly interesting to compare these adaptive responses in different photosynthetic organisms such as plants, fresh water and marine algae and cyanobacteria. In this respect NPQ, the dissipation of excess excitation energy as heat in the ligt-harvesting systems of the photosystems is of great importance and it is widely used in the plant kingdom. Recent studies on NPQ in different photosynthetic organisms raise several questions regarding the evolution of this essential photoprotective mechanism. For example it is not clear why the Lhcsr proteins were lost during the transition from aquatic to land plants. Moreover the qE process in most algae derived by secondary endosymbiosis from a red algal ancestor differs from that in extant red algae. All of these derived algae possess a xanthophyll cycle and Lhcsr-related proteins which are apparently absent in red algae (Goss and Lepetit 2015) and which have been suggested to be derived from green algae (Frommolt et al. 2008; Moustafa et al. 2009). It will clearly be important and challenging to elucidate these evolutionary puzzles.

Acknowledgements

Work in the author's laboratory was supported by grants from the Swiss National Science Foundation.

References

Albertsson P (2001) A quantitative model of the domain structure of the photosynthetic membrane. Trends Plant Sci 6(8):349–358

Alboresi A, Gerotto C, Giacometti GM, Bassi R, Morosinotto T (2010) Physcomitrella patens mutants affected on heat dissipation clarify the evolution of photoprotection mechanisms upon land colonization. Proc Natl Acad Sci U S A 107(24):11128–11133

Allahverdiyeva Y, Isojarvi J, Zhang P, Aro EM (2015) Cyanobacterial oxygenic photosynthesis is protected by flavodiiron proteins. Life (Basel) 5(1):716–743

Allen JF (2003) Cyclic, pseudocyclic and noncyclic photophosphoryaltion: new links in the chain. Trends Plant Sci 8:15–19

Allorent G, Petroutsos D (2017) Photoreceptor-dependent regulation of photoprotection. Curr Opin Plant Biol 37:102–108

Allorent G, Tokutsu R, Roach T, Peers G, Cardol P, Girard-Bascou J et al (2013) A dual strategy to cope with high light in Chlamydomonas reinhardtii. Plant Cell 25(2):545–557

Allorent G, Lefebvre-Legendre L, Chappuis R, Kuntz M, Truong TB, Niyogi KK et al (2016) UV-B photoreceptor-mediated protection of the photosynthetic machinery in Chlamydomonas reinhardtii. Proc Natl Acad Sci U S A 113(51):14864–14869

Amann K, Lezhneva L, Wanner G, Herrmann RG, Meurer J (2004) Accumulation of photosystem one1, a member of a novel gene family, is required for accumulation of [4Fe-4S] cluster-containing chloroplast complexes and antenna proteins. Plant Cell 16(11):3084–3097

Amarnath K, Zaks J, Park SD, Niyogi KK, Fleming GR (2012) Fluorescence lifetime snapshots reveal two rapidly reversible mechanisms of photoprotection in live cells of Chlamydomonas reinhardtii. Proc Natl Acad Sci U S A 109(22):8405–8410

Andersson B, Andersson J (1980) Lateral heterogeneity in the distribution of chlorophyll-protein complexes of the thylakoid membranes of spinach chloroplasts. Biochim Biophys Acta 593(2):427–440

Aro EM, Virgin I, Andersson B (1993) Photoinhibition of photosystem II. Inactivation, protein damage and turnover. Biochim Biophys Acta 1143(2):113–134

Bailleul B, Rogato A, de Martino A, Coesel S, Cardol P, Bowler C et al (2010) An atypical member of the light-harvesting complex stress-related protein family modulates diatom responses to light. Proc Natl Acad Sci U S A 107(42):18214–18219

Bailleul B, Berne N, Murik O, Petroutsos D, Prihoda J, Tanaka A et al (2015) Energetic coupling between plastids and mitochondria drives CO2 assimilation in diatoms. Nature 524(7565):366–369

Barber J (1982) The control of membrane organization by electrostatic forces. Biosci Rep 2(1):1–13

Barneche F, Winter V, Crevecoeur M, Rochaix JD (2006) ATAB2 is a novel factor in the signalling pathway of light-controlled synthesis of photosystem proteins. EMBO J 25(24):5907–5918. Epub 2006 Nov 30

Bellafiore S, Barneche F, Peltier G, Rochaix JD (2005) State transitions and light adaptation require chloroplast thylakoid protein kinase STN7. Nature 433:892–895

Bergantino E, Segalla A, Brunetta A, Teardo E, Rigoni F, Giacometti GM et al (2003) Light- and pH-dependent structural changes in the PsbS subunit of photosystem II. Proc Natl Acad Sci U S A 100(25):15265–15270

Betterle N, Ballottari M, Zorzan S, de Bianchi S, Cazzaniga S, Dall'osto L et al (2009) Light-induced dissociation of an antenna hetero-oligomer is needed for non-photochemical quenching induction. J Biol Chem 284(22):15255–15266

Blifernez O, Wobbe L, Niehaus K, Kruse O (2011) Protein arginine methylation modulates light-harvesting antenna translation in Chlamydomonas reinhardtii. Plant J 65(1):119–130

Bonardi V, Pesaresi P, Becker T, Schleiff E, Wagner R, Pfannschmidt T et al (2005) Photosystem II core phosphorylation and photosynthetic acclimation require two different protein kinases. Nature 437(7062):1179–1182

Bonente G, Ballottari M, Truong TB, Morosinotto T, Ahn TK, Fleming GR et al (2011) Analysis of LhcSR3, a protein essential for feedback de-excitation in the green alga Chlamydomonas reinhardtii. PLoS Biol 9(1):e1000577

Boulouis A, Raynaud C, Bujaldon S, Aznar A, Wollman FA, Choquet Y (2011) The nucleus-encoded trans-acting factor MCA1 plays a critical role in the regulation of cytochrome f synthesis in Chlamydomonas chloroplasts. Plant Cell 23(1):333–349

Brautigam K, Dietzel L, Kleine T, Stroher E, Wormuth D, Dietz KJ et al (2009) Dynamic plastid redox signals integrate gene expression and metabolism to induce distinct metabolic states in photosynthetic acclimation in Arabidopsis. Plant Cell 21(9):2715–2732

Breyton C (2000) Conformational changes in the cytochrome b6f complex induced by inhibitor binding. J Biol Chem 275(18):13195–13201

Bulte L, Wollman FA (1992) Evidence for a selective destabilization of an integral membrane protein, the cytochrome b6/f complex, during gametogenesis in Chlamydomonas reinhardtii. Eur J Biochem 204(1):327–336

Bulté L, Gans P, Rebeille F, Wollman FA (1990) ATP control on state transitions in Chlamydomonas. Biochim Biophys Acta 1020:72–80

Burrows PA, Sazanov LA, Svab Z, Maliga P, Nixon PJ (1998) Identification of a functional respiratory complex in chloroplasts through analysis of tobacco mutants containing disrupted plastid ndh genes. EMBO J 17(4):868–876

Cardol P, Bailleul B, Rappaport F, Derelle E, Beal D, Breyton C et al (2008) An original adaptation of photosynthesis in the marine green alga Ostreococcus. Proc Natl Acad Sci U S A 105(22):7881–7886

Chaux F, Burlacot A, Mekhalfi M, Auroy P, Blangy S, Richaud P et al (2017) Flavodiiron proteins promote fast and transient O2 photoreduction in Chlamydomonas. Plant Physiol 174(3):1825–1836

Christie JM, Arvai AS, Baxter KJ, Heilmann M, Pratt AJ, O'Hara A et al (2012) Plant UVR8 photoreceptor senses UV-B by tryptophan-mediated disruption of cross-dimer salt bridges. Science 335(6075):1492–1496

Correa-Galvis V, Poschmann G, Melzer M, Stuhler K, Jahns P (2016) PsbS interactions involved in the activation of energy dissipation in Arabidopsis. Nat Plants 2:15225

DalCorso G, Pesaresi P, Masiero S, Aseeva E, Schunemann D, Finazzi G et al (2008) A complex containing PGRL1 and PGR5 is involved in the switch between linear and cyclic electron flow in Arabidopsis. Cell 132(2):273–285

Darrouzet E, Moser CC, Dutton PL, Daldal F (2001) Large scale domain movement in cytochrome bc(1): a new device for electron transfer in proteins. Trends Biochem Sci 26(7):445–451

Davies JP, Yildiz F, Grossman AR (1994) Mutants of Chlamydomonas with aberrant responses to sulfur deprivation. Plant Cell 6(1):53–63

de Lacroix de Lavalette A, Finazzi G, Zito F (2008) b6f-Associated chlorophyll: structural and dynamic contribution to the different cytochrome functions. Biochemistry 47:5259–5265

Dekker JP, Boekema EJ (2005) Supramolecular organization of thylakoid membrane proteins in green plants. Biochim Biophys Acta 1706(1–2):12–39

Demmig-Adams B, Adams W-W (1992) Photoprotection and other responses of plants to high light stress. Annu Rev Plant Physiol Plant Mol Biol 43:599–626

Depège N, Bellafiore S, Rochaix JD (2003) Role of chloroplast protein kinase Stt7 in LHCII phosphorylation and state transition in Chlamydomonas. Science 299:1572–1575

Douchi D, Qu Y, Longoni P, Legendre-Lefebvre L, Johnson X, Schmitz-Linneweber C et al (2016) A nucleus-encoded chloroplast phosphoprotein governs expression of the photosystem I subunit PsaC in Chlamydomonas reinhardtii. Plant Cell 28(5):1182–1199

Drop B, Webber-Birungi M, Yadav SK, Filipowicz-Szymanska A, Fusetti F, Boekema EJ et al (2014) Light-harvesting complex II (LHCII) and its supramolecular organization in Chlamydomonas reinhardtii. Biochim Biophys Acta 1837(1):63–72

Du JJ, Zhan CY, Lu Y, Cui HR, Wang XY (2015) The conservative cysteines in transmembrane domain of AtVKOR/LTO1 are critical for photosynthetic growth and photosystem II activity in Arabidopsis. Front Plant Sci 6:238

Duanmu D, Rockwell NC, Casero D, Dent RM, Gallaher S, Yang W et al (2013) Retrograde bilin signaling enables Chlamydomonas greening and phototrophic survival. Proc Natl Acad Sci U S A 110(9):3621–3626

Dumas L, Zito F, Blangy S, Auroy P, Johnson X, Peltier G et al (2017) A stromal region of cytochrome b6f subunit IV is involved in the activation of the Stt7 kinase in Chlamydomonas. Proc Natl Acad Sci U S A 114(45):12063–12068

Eberhard S, Finazzi G, Wollman FA (2008) The dynamics of photosynthesis. Annu Rev Genet 42:463–515

Elrad D, Niyogi KK, Grossman AR (2002) A major light-harvesting polypeptide of photosystem II functions in thermal dissipation. Plant Cell 14(8):1801–1816

Escoubas JM, Lomas M, LaRoche J, Falkowski PG (1995) Light intensity regulation of cab gene transcription is signaled by the redox state of the plastoquinone pool. Proc Natl Acad Sci U S A 92(22):10237–10241

Falciatore A, Merendino L, Barneche F, Ceol M, Meskauskiene R, Apel K et al (2005) The FLP proteins act as regulators of chlorophyll synthesis in response to light and plastid signals in Chlamydomonas. Genes Dev 19(1):176–187

Fan M, Li M, Liu Z, Cao P, Pan X, Zhang H et al (2015) Crystal structures of the PsbS protein essential for photoprotection in plants. Nat Struct Mol Biol 22(9):729–735

Farah J, Rappaport F, Choquet Y, Joliot P, Rochaix JD (1995) Isolation of a psaF-deficient mutant of Chlamydomonas reinhardtii: efficient interaction of plastocyanin with the photosystem I reaction center is mediated by the PsaF subunit. EMBO J 14(20):4976–4984

Favory JJ, Stec A, Gruber H, Rizzini L, Oravecz A, Funk M et al (2009) Interaction of COP1 and UVR8 regulates UV-B-induced photomorphogenesis and stress acclimation in Arabidopsis. EMBO J 28(5):591–601

Ferrante P, Ballottari M, Bonente G, Giuliano G, Bassi R (2012) LHCBM1 and LHCBM2/7 polypeptides, components of major LHCII complex, have distinct functional roles in photosynthetic antenna system of Chlamydomonas reinhardtii. J Biol Chem 287(20):16276–16288

Finazzi G, Rappaport F, Furia A, Fleischmann M, Rochaix JD, Zito F et al (2002) Involvement of state transitions in the switch between linear and cyclic electron flow in Chlamydomonas reinhardtii. EMBO Rep 3(3):280–285. Epub 2002 Feb 15

Fristedt R, Willig A, Granath P, Crèvecoeur M, Rochaix JD, Vener A (2009) Phosphorylation of photosystem II controls functional macroscopic folding of plant photosynthetic membranes. Plant Cell

Frommolt R, Werner S, Paulsen H, Goss R, Wilhelm C, Zauner S et al (2008) Ancient recruitment by chromists of green algal genes encoding enzymes for carotenoid biosynthesis. Mol Biol Evol 25(12):2653–2667

Galka P, Santabarbara S, Khuong TT, Degand H, Morsomme P, Jennings RC et al (2012) Functional analyses of the plant photosystem I-light-harvesting complex II supercomplex reveal that light-harvesting complex II loosely bound to photosystem II is a very efficient antenna for photosystem I in state II. Plant Cell 24(7):2963–2978

Geider RJ, Delucia EH, Falkowski PG, Finzi J (2001) Primary productivity of planet earth: biological determinants and physical constraints in terrestrial and aquatic habitats. Glob Chang Biol 7:849–882

Gerotto C, Alboresi A, Giacometti GM, Bassi R, Morosinotto T (2011) Role of PSBS and LHCSR in Physcomitrella patens acclimation to high light and low temperature. Plant Cell Environ 34(6):922–932

Gerotto C, Alboresi A, Giacometti GM, Bassi R, Morosinotto T (2012) Coexistence of plant and algal energy dissipation mechanisms in the moss Physcomitrella patens. New Phytol 196(3):763–773

Gfeller RP, Gibbs M (1984) Fermentative metabolism of Chlamydomonas reinhardtii: I. Analysis of fermentative products from starch in dark and light. Plant Physiol 75(1):212–218

Gfeller RP, Gibbs M (1985) Fermentative metabolism of Chlamydomonas reinhardtii: II. Role of plastoquinone. Plant Physiol 77(2):509–511

Goral TK, Johnson MP, Duffy CD, Brain AP, Ruban AV, Mullineaux CW (2012) Light-harvesting antenna composition controls the macrostructure and dynamics of thylakoid membranes in Arabidopsis. Plant J 69(2):289–301

Goss R, Lepetit B (2015) Biodiversity of NPQ. J Plant Physiol 172:13–32

Grossman AR, Catalanotti C, Yang W, Dubini A, Magneschi L, Subramanian V (2010) Multilple facets of anoxic metabolism and hyrogen production in the unicellular green alga Chlamydomonas reinhardtii. New Phytol. https://doi.org/10.1111/j.1469-8137.2010.03534.x

Gunning EBS, Schwartz OM (1999) Confocal microscopy of thylakoid autofluorescence in relation to origin of grana and phylogeny in the green algae. Aust J Plant Physiol 26:695–708

Herbstova M, Tietz S, Kinzel C, Turkina MV, Kirchhoff H (2012) Architectural switch in plant photosynthetic membranes induced by light stress. Proc Natl Acad Sci U S A 109(49):20130–20135

Hertle AP, Blunder T, Wunder T, Pesaresi P, Pribil M, Armbruster U et al (2013) PGRL1 is the elusive ferredoxin-plastoquinone reductase in photosynthetic cyclic electron flow. Mol Cell 49(3):511–523

Holwarth AR, Miloslavina Y, Nilkens M, Jahns P (2009) Identification of two quenching sites active in the regulation of photosynthetic light-harvesting studies by time-resolved fluorescence. Chem Phys Lett 483:262–267

Horton P, Johnson MP, Perez-Bueno ML, Kiss AZ, Ruban AV (2008) Photosynthetic acclimation: does the dynamic structure and macro-organisation of photosystem II in higher plant grana membranes regulate light harvesting states? FEBS J 275(6):1069–1079

Houille-Vernes L, Rappaport F, Wollman FA, Alric J, Johnson X (2011) Plastid terminal oxidase 2 (PTOX2) is the major oxidase involved in chlororespiration in Chlamydomonas. Proc Natl Acad Sci U S A 108(51):20820–20825

Iwai M, Takizawa K, Tokutsu R, Okamuro A, Takahashi Y, Minagawa J (2010) Isolation of the elusive supercomplex that drives cyclic electron flow in photosynthesis. Nature 464(7292):1210–1213

Johanningmeier U, Howell SH (1984) Regulation of light-harvesting chlorophyll-binding protein mRNA accumulation in Chlamydomonas reinhardi. Possible involvement of chlorophyll synthesis precursors. J Biol Chem 259(21):13541–13549

Johnson MP, Ruban AV (2011) Restoration of rapidly reversible photoprotective energy dissipation in the absence of PsbS protein by enhanced DeltapH. J Biol Chem 286(22):19973–19981

Johnson X, Steinbeck J, Dent RM, Takahashi H, Richaud P, Ozawa S et al (2014) Proton gradient regulation 5-mediated cyclic electron flow under ATP- or redox-limited conditions: a study of DeltaATpase pgr5 and DeltarbcL pgr5 mutants in the green alga Chlamydomonas reinhardtii. Plant Physiol 165(1):438–452

Joliot P, Johnson GN (2011) Regulation of cyclic and linear electron flow in higher plants. Proc Natl Acad Sci U S A 108(32):13317–13322

Kaiserli E, Jenkins GI (2007) UV-B promotes rapid nuclear translocation of the Arabidopsis UV-B spe-

cific signaling component UVR8 and activates its function in the nucleus. Plant Cell 19(8):2662–2673

Karamoko M, Cline S, Redding K, Ruiz N, Hamel PP (2011) Lumen Thiol Oxidoreductase1, a disulfide bond-forming catalyst, is required for the assembly of photosystem II in Arabidopsis. Plant Cell 23(12):4462–4475

Keeling PJ (2013) The number, speed, and impact of plastid endosymbioses in eukaryotic evolution. Annu Rev Plant Biol 64:583–607

Khorobrykh SA, Karonen M, Tyystjarvi E (2015) Experimental evidence suggesting that H2O2 is produced within the thylakoid membrane in a reaction between plastoquinol and singlet oxygen. FEBS Lett 589(6):779–786

Kirchhoff H, Haferkamp S, Allen JF, Epstein DB, Mullineaux CW (2008) Protein diffusion and macromolecular crowding in thylakoid membranes. Plant Physiol 146(4):1571–1578

Kirst H, Garcia-Cerdan JG, Zurbriggen A, Melis A (2012) Assembly of the light-harvesting chlorophyll antenna in the green alga Chlamydomonas reinhardtii requires expression of the TLA2-CpFTSY gene. Plant Physiol 158(2):930–945

Kobayashi Y, Kanesaki Y, Tanaka A, Kuroiwa H, Kuroiwa T, Tanaka K (2009) Tetrapyrrole signal as a cell-cycle coordinator from organelle to nuclear DNA replication in plant cells. Proc Natl Acad Sci U S A 106(3):803–807

Kobayashi Y, Imamura S, Hanaoka M, Tanaka K (2011) A tetrapyrrole-regulated ubiquitin ligase controls algal nuclear DNA replication. Nat Cell Biol 13(4):483–487

Kono M, Noguchi K, Terashima I (2014) Roles of the cyclic electron flow around PSI (CEF-PSI) and O(2)-dependent alternative pathways in regulation of the photosynthetic electron flow in short-term fluctuating light in Arabidopsis thaliana. Plant Cell Physiol 55(5):990–1004

Kropat J, Oster U, Rudiger W, Beck CF (1997) Chlorophyll precursors are signals of chloroplast origin involved in light induction of nuclear heat-shock genes. Proc Natl Acad Sci U S A 94(25):14168–14172

Kropat J, Oster U, Rudiger W, Beck CF (2000) Chloroplast signalling in the light induction of nuclear HSP70 genes requires the accumulation of chlorophyll precursors and their accessibility to cytoplasm/nucleus. Plant J 24(4):523–531

Kruger TP, Ilioaia C, Johnson MP, Ruban AV, Papagiannakis E, Horton P et al (2012) Controlled disorder in plant light-harvesting complex II explains its photoprotective role. Biophys J 102(11):2669–2676

Kurisu G, Zhang H, Smith JL, Cramer WA (2003) Structure of the cytochrome b6f complex of oxygenic photosynthesis: tuning the cavity. Science 302(5647):1009–1014. Epub 2003 Oct 2

Lefebvre-Legendre L, Choquet Y, Kuras R, Loubery S, Douchi D, Goldschmidt-Clermont M (2015) A nucleus-encoded chloroplast protein regulated by iron availability governs expression of the photosystem I subunit PsaA in Chlamydomonas reinhardtii. Plant Physiol 167(4):1527–1540

Lemeille S, Rochaix JD (2010) State transitions at the crossroad of thylakoid signalling pathways. Photosynth Res 106:33–46

Lemeille S, Willig A, Depège-Fargeix N, Delessert C, Bassi R, Rochaix JD (2009) Analysis of the chloroplast protein kinase Stt7 during state transitions. PLoS Biol 7(3):e45

Lennartz K, Plucken H, Seidler A, Westhoff P, Bechtold N, Meierhoff K (2001) HCF164 encodes a thioredoxin-like protein involved in the biogenesis of the cytochrome b(6)f complex in Arabidopsis. Plant Cell 13(11):2539–2551

Li XP, Bjorkman O, Shih C, Grossman AR, Rosenquist M, Jansson S et al (2000) A pigment-binding protein essential for regulation of photosynthetic light harvesting. Nature 403(6768):391–395

Li XP, Gilmore AM, Caffarri S, Bassi R, Golan T, Kramer D et al (2004) Regulation of photosynthetic light harvesting involves intrathylakoid lumen pH sensing by the PsbS protein. J Biol Chem 279(22):22866–22874

Link G (2003) Redox regulation of chloroplast transcription. Antioxid Redox Signal 5:79–87

Longoni P, Douchi D, Cariti F, Fucile G, Goldschmidt-Clermont M (2015) Phosphorylation of the light-harvesting complex II isoform Lhcb2 is central to state transitions. Plant Physiol 169(4):2874–2883

Lucker B, Kramer DM (2013) Regulation of cyclic electron flow in Chlamydomonas reinhardtii under fluctuating carbon availability. Photosynth Res 117(1–3):449–459

MacIntyre HL, Kana TM, Geider RJ (2000) The effect of water motion on short-term rates of photosynthesis by marine phytoplankton. Trends Plant Sci 5(1):12–17

Majeran W, Wollman FA, Vallon O (2000) Evidence for a role of ClpP in the degradation of the chloroplast cytochrome b(6)f complex. Plant Cell 12(1):137–150

Melis A, Zhang L, Forestier M, Ghirardi ML, Seibert M (2000) Sustained photobiological hydrogen gas production upon reversible inactivation of oxygen evolution in the green alga Chlamydomonas reinhardtii. Plant Physiol 122(1):127–136

Merchant S, Bogorad L (1987) Metal ion regulated gene expression: use of a plastocyanin-less mutant of Chlamydomonas reinhardtii to study the Cu(II)-dependent expression of cytochrome c-552. EMBO J 6(9):2531–2535

Meskauskiene R, Nater M, Goslings D, Kessler F, op den Camp R, Apel K (2001) FLU: a negative regulator of chlorophyll biosynthesis in Arabidopsis thaliana. Proc Natl Acad Sci U S A 98(22):12826–12831

Miller R, Wu G, Deshpande RR, Vieler A, Gartner K, Li X et al (2010) Changes in transcript abundance in Chlamydomonas reinhardtii following nitrogen deprivation predict diversion of metabolism. Plant Physiol 154(4):1737–1752

Minagawa J, Takahashi Y (2004) Structure, function and assembly of Photosystem II and its light-harvesting proteins. Photosynth Res 82(3):241–263

Mitra M, Kirst H, Dewez D, Melis A (2012) Modulation of the light-harvesting chlorophyll antenna size in Chlamydomonas reinhardtii by TLA1 gene over-expression and RNA interference. Philos Trans R Soc Lond Ser B Biol Sci 367(1608):3430–3443

Mochizuki N, Tanaka R, Tanaka A, Masuda T, Nagatani A (2008) The steady-state level of Mg-protoporphyrin IX is not a determinant of plastid-to-nucleus signaling in Arabidopsis. Proc Natl Acad Sci U S A 105(39):15184–15189

Moseley J, Quinn J, Eriksson M, Merchant S (2000) The Crd1 gene encodes a putative di-iron enzyme required for photosystem I accumulation in copper deficiency and hypoxia in Chlamydomonas reinhardtii. EMBO J 19(10):2139–2151

Moseley JL, Allinger T, Herzog S, Hoerth P, Wehinger E, Merchant S et al (2002) Adaptation to Fe-deficiency requires remodeling of the photosynthetic apparatus. EMBO J 21(24):6709–6720

Moulin M, McCormac AC, Terry MJ, Smith AG (2008) Tetrapyrrole profiling in Arabidopsis seedlings reveals that retrograde plastid nuclear signaling is not due to Mg-protoporphyrin IX accumulation. Proc Natl Acad Sci U S A 105(39):15178–15183

Moustafa A, Beszteri B, Maier UG, Bowler C, Valentin K, Bhattacharya D (2009) Genomic footprints of a cryptic plastid endosymbiosis in diatoms. Science 324(5935):1724–1726

Munekage Y, Hojo M, Meurer J, Endo T, Tasaka M, Shikanai T (2002) PGR5 is involved in cyclic electron flow around photosystem I and is essential for photoprotection in Arabidopsis. Cell 110(3):361–371

Nandha B, Finazzi G, Joliot P, Hald S, Johnson GN (2007) The role of PGR5 in the redox poising of photosynthetic electron transport. Biochim Biophys Acta 1767(10):1252–1259

Nield J, Kruse O, Ruprecht J, da Fonseca P, Buchel C, Barber J (2000) Three-dimensional structure of Chlamydomonas reinhardtii and Synechococcus elongatus photosystem II complexes allows for comparison of their oxygen-evolving complex organization. J Biol Chem 275(36):27940–27946

Nixon PJ, Barker M, Boehm M, de Vries R, Komenda J (2005) FtsH-mediated repair of the photosystem II complex in response to light stress. J Exp Bot 56(411):357–363

Nixon PJ, Michoux F, Yu J, Boehm M, Komenda J (2010) Recent advances in understanding the assembly and repair of photosystem II. Ann Bot 106(1):1–16

Niyogi KK (1999) PHOTOPROTECTION REVISITED: genetic and molecular approaches. Annu Rev Plant Physiol Plant Mol Biol 50:333–359

Niyogi KK, Truong TB (2013) Evolution of flexible non-photochemical quenching mechanisms that regulate light harvesting in oxygenic photosynthesis. Curr Opin Plant Biol 16(3):307–314

Ogrzewalla K, Piotrowski M, Reinbothe S, Link G (2002) The plastid transcription kinase from mustard (Sinapis alba L.). A nuclear-encoded CK2-type chloroplast enzyme with redox-sensitive function. Eur J Biochem 269(13):3329–3337

Ozawa SI, Bald T, Onishi T, Xue H, Matsumura T, Kubo R et al (2018) Configuration of ten light-harvesting chlorophyll a/b complex I subunits in Chlamydomonas reinhardtii photosystem I. Plant Physiol 178(2):583–595

Page ML, Hamel PP, Gabilly ST, Zegzouti H, Perea JV, Alonso JM et al (2004) A homolog of prokaryotic thiol disulfide transporter CcdA is required for the assembly of the cytochrome b6f complex in Arabidopsis chloroplasts. J Biol Chem 279(31):32474–32482

Pan X, Ma J, Su X, Cao P, Chang W, Liu Z et al (2018) Structure of the maize photosystem I supercomplex with light-harvesting complexes I and II. Science 360(6393):1109–1113

Peers G, Truong TB, Ostendorf E, Busch A, Elrad D, Grossman AR et al (2009) An ancient light-harvesting protein is critical for the regulation of algal photosynthesis. Nature 462(7272):518–521

Pfannschmidt T, Nilsson A, Tullberg A, Link G, Allen JF (1999) Direct transcriptional control of the chloroplast genes psbA and psaAB adjusts photosynthesis to light energy distribution in plants. IUBMB Life 48:271–276

Phillip D, Ruban AV, Horton P, Asato A, Young AJ (1996) Quenching of chlorophyll fluorescence in the major light-harvesting complex of photosystem II:

a systematic study of the effect of carotenoid structure. Proc Natl Acad Sci U S A 93(4):1492–1497

Pribil M, Pesaresi P, Hertle A, Barbato R, Leister D (2010) Role of plastid protein phosphatase TAP38 in LHCII dephosphorylation and thylakoid electron flow. PLoS Biol 8(1):e1000288

Puthiyaveetil S, Kavanagh TA, Cain P, Sullivan JA, Newell CA, Gray JC et al (2008) The ancestral symbiont sensor kinase CSK links photosynthesis with gene expression in chloroplasts. Proc Natl Acad Sci U S A 105(29):10061–10066

Puthiyaveetil S, Tsabari O, Lowry T, Lenhert S, Lewis RR, Reich Z et al (2014) Compartmentalization of the protein repair machinery in photosynthetic membranes. Proc Natl Acad Sci U S A 111(44):15839–15844

Raynaud C, Loiselay C, Wostrikoff K, Kuras R, Girard-Bascou J, Wollman FA et al (2007) Evidence for regulatory function of nucleus-encoded factors on mRNA stabilization and translation in the chloroplast. Proc Natl Acad Sci U S A 104(21):9093–9098

Rintamaki E, Salonen M, Suoranta UM, Carlberg I, Andersson B, Aro EM (1997) Phosphorylation of light-harvesting complex II and photosystem II core proteins shows different irradiance-dependent regulation in vivo. Application of phosphothreonine antibodies to analysis of thylakoid phosphoproteins. J Biol Chem 272(48):30476–30482

Rintamaki E, Martinsuo P, Pursiheimo S, Aro EM (2000) Cooperative regulation of light-harvesting complex II phosphorylation via the plastoquinol and ferredoxin-thioredoxin system in chloroplasts. Proc Natl Acad Sci U S A 97(21):11644–11649

Rizzini L, Favory JJ, Cloix C, Faggionato D, O'Hara A, Kaiserli E et al (2011) Perception of UV-B by the Arabidopsis UVR8 protein. Science 332(6025):103–106

Rochaix JD (2013) Redox regulation of thylakoid protein kinases and photosynthetic gene expression. Antioxid Redox Signal 18(16):2184–2201

Rochaix JD (2014) Regulation and dynamics of the light-harvesting system. Annu Rev Plant Biol 65:287–309

Ruban AV, Johnson MP, Duffy CD (2012) The photoprotective molecular switch in the photosystem II antenna. Biochim Biophys Acta 1817(1):167–181

Samol I, Shapiguzov A, Ingelsson B, Fucile G, Crevecoeur M, Vener AV et al (2012) Identification of a photosystem II phosphatase involved in light acclimation in Arabidopsis. Plant Cell 24(6):2596–2609

Schubert H, Forster RM (1997) Sources of variability in the factors used for modellingprimary productivityin eutrophic waters. Hydrobiologia 349:75–85

Schuster G, Dewit M, Staehelin LA, Ohad I (1986) Transient inactivation of the thylakoid photosystem II light-harvesting protein kinase system and concomitant changes in intramembrane particle size during photoinhibition of Chlamydomonas reinhardtii. J Cell Biol 103(1):71–80

Shapiguzov A, Ingelsson B, Samol I, Andres C, Kessler F, Rochaix JD et al (2010) The PPH1 phosphatase is specifically involved in LHCII dephosphorylation and state transitions in Arabidopsis. Proc Natl Acad Sci U S A 107(10):4782–4787

Shapiguzov A, Chai X, Fucile G, Longoni P, Zhang L, Rochaix JD (2016) Activation of the Stt7/STN7 kinase through dynamic interactions with the cytochrome b6f complex. Plant Physiol 171(1):82–92

Shikanai T, Yamamoto H (2017) Contribution of cyclic and pseudo-cyclic electron transport to the formation of proton motive force in chloroplasts. Mol Plant 10(1):20–29

Shimakawa G, Shaku K, Nishi A, Hayashi R, Yamamoto H, Sakamoto K et al (2015) FLAVODIIRON2 and FLAVODIIRON4 proteins mediate an oxygen-dependent alternative electron flow in Synechocystis sp. PCC 6803 under CO2-limited conditions. Plant Physiol 167(2):472–480

Snyders S, Kohorn BD (1999) TAKs, thylakoid membrane protein kinases associated with energy transduction. J Biol Chem 274(14):9137–9140

Snyders S, Kohorn BD (2001) Disruption of thylakoid-associated kinase 1 leads to alteration of light harvesting in Arabidopsis. J Biol Chem 276(34):32169–32176

Steinbeck J, Ross IL, Rothnagel R, Gabelein P, Schulze S, Giles N et al (2018) Structure of a PSI-LHCI-cyt b6f supercomplex in Chlamydomonas reinhardtii promoting cyclic electron flow under anaerobic conditions. Proc Natl Acad Sci U S A 115(41):10517–10522

Strand A, Asami T, Alonso J, Ecker JR, Chory J (2003) Chloroplast to nucleus communication triggered by accumulation of Mg-protoporphyrinIX. Nature 421(6918):79–83

Stroebel D, Choquet Y, Popot JL, Picot D (2003) An atypical haem in the cytochrome b(6)f complex. Nature 426(6965):413–418

Takahashi H, Clowez S, Wollman FA, Vallon O, Rappaport F (2013) Cyclic electron flow is redox-controlled but independent of state transition. Nat Commun 4:1954–1961

Tanaka K, Hanaoka M (2012) The early days of plastid retrograde signaling with respect to replication and transcription. Front Plant Sci 3:301

Teardo E, de Laureto PP, Bergantino E, Dalla Vecchia F, Rigoni F, Szabo I et al (2007) Evidences for

interaction of PsbS with photosynthetic complexes in maize thylakoids. Biochim Biophys Acta 1767(6):703–711

Tikkanen M, Nurmi M, Suorsa M, Danielsson R, Mamedov F, Styring S et al (2008) Phosphorylation-dependent regulation of excitation energy distribution between the two photosystems in higher plants. Biochim Biophys Acta 1777(5):425–432

Tilbrook K, Dubois M, Crocco CD, Yin R, Chappuis R, Allorent G et al (2016) UV-B perception and acclimation in Chlamydomonas reinhardtii. Plant Cell 28(4):966–983

Tokutsu R, Kato N, Bui KH, Ishikawa T, Minagawa J (2012) Revisiting the supramolecular organization of photosystem II in Chlamydomonas reinhardtii. J Biol Chem 287(37):31574–31581

Tottey S, Block MA, Allen M, Westergren T, Albrieux C, Scheller HV et al (2003) Arabidopsis CHL27, located in both envelope and thylakoid membranes, is required for the synthesis of protochlorophyllide. Proc Natl Acad Sci U S A 100(26):16119–16124

Vainonen JP, Hansson M, Vener AV (2005) STN8 protein kinase in Arabidopsis thaliana is specific in phosphorylation of photosystem II core proteins. J Biol Chem 280(39):33679–33686

Vener AV, van Kan PJ, Rich PR, Ohad II, Andersson B (1997) Plastoquinol at the quinol oxidation site of reduced cytochrome bf mediates signal transduction between light and protein phosphorylation: thylakoid protein kinase deactivation by a single-turnover flash. Proc Natl Acad Sci U S A 94(4):1585–1590

von Gromoff ED, Alawady A, Meinecke L, Grimm B, Beck CF (2008) Heme, a plastid-derived regulator of nuclear gene expression in Chlamydomonas. Plant Cell 20(3):552–567

Voss B, Meinecke L, Kurz T, Al-Babili S, Beck CF, Hess WR (2011) Hemin and magnesium-protoporphyrin IX induce global changes in gene expression in Chlamydomonas reinhardtii. Plant Physiol 155(2):892–905

Wakao S, Chin BL, Ledford HK, Dent RM, Casero D, Pellegrini M et al (2014) Phosphoprotein SAK1 is a regulator of acclimation to singlet oxygen in Chlamydomonas reinhardtii. elife 3:e02286

Wei L, Derrien B, Gautier A, Houille-Vernes L, Boulouis A, Saint-Marcoux D et al (2014) Nitric oxide-triggered remodeling of chloroplast bioenergetics and thylakoid proteins upon nitrogen starvation in Chlamydomonas reinhardtii. Plant Cell 26(1):353–372

Wentworth M, Ruban AV, Horton P (2001) Kinetic analysis of nonphotochemical quenching of chlorophyll fluorescence. 2. Isolated light-harvesting complexes. Biochemistry 40(33):9902–9908

Wientjes E, van Amerongen H, Croce R (2013a) LHCII is an antenna of both photosystems after long-term acclimation. Biochim Biophys Acta 1827(3):420–426

Wientjes E, Drop B, Kouril R, Boekema EJ, Croce R (2013b) During state 1 to state 2 transition in Arabidopsis thaliana, the photosystem II supercomplex gets phosphorylated but does not disassemble. J Biol Chem 288(46):32821–32826

Wittkopp TM, Schmollinger S, Saroussi S, Hu W, Zhang W, Fan Q et al (2017) Bilin-dependent photoacclimation in Chlamydomonas reinhardtii. Plant Cell 29(11):2711–2726

Wobbe L, Blifernez O, Schwarz C, Mussgnug JH, Nickelsen J, Kruse O (2009) Cysteine modification of a specific repressor protein controls the translational status of nucleus-encoded LHCII mRNAs in Chlamydomonas. Proc Natl Acad Sci U S A 106(32):13290–13295

Wollman FA (2001) State transitions reveal the dynamics and flexibility of the photosynthetic apparatus. EMBO J 20(14):3623–3630

Woodson JD, Chory J (2012) Organelle signaling: how stressed chloroplasts communicate with the nucleus. Curr Biol 22(17):R690–R692

Wunder T, Liu Q, Aseeva E, Bonardi V, Leister D, Pribil M (2013) Control of STN7 transcript abundance and transient STN7 dimerisation are involved in the regulation of STN7 activity. Planta 237(2):541–558

Wykoff DD, Davies JP, Melis A, Grossman AR (1998) The regulation of photosynthetic electron transport during nutrient deprivation in Chlamydomonas reinhardtii. Plant Physiol 117(1):129–139

Yildiz FH, Davies JP, Grossman AR (1994) Characterization of sulfate transport in Chlamydomonas reinhardtii during sulfur-limited and sulfur-sufficient growth. Plant Physiol 104(3):981–987

Zhang P, Eisenhut M, Brandt AM, Carmel D, Silen HM, Vass I et al (2012) Operon flv4-flv2 provides cyanobacterial photosystem II with flexibility of electron transfer. Plant Cell 24(5):1952–1971

Zito F, Finazzi G, Delosme R, Nitschke W, Picot D, Wollman FA (1999) The Qo site of cytochrome b6f complexes controls the activation of the LHCII kinase. EMBO J 18(11):2961–2969

Zones JM, Blaby IK, Merchant SS, Umen JG (2015) High-resolution profiling of a synchronized diurnal transcriptome from Chlamydomonas reinhardtii reveals continuous cell and metabolic differentiation. Plant Cell 27(10):2743–2769

Chapter 5

Biosynthesis of Chlorophyll and Bilins in Algae

Robert D. Willows*
Department of Molecular Sciences, Macquarie University, Sydney, Australia

I. Introduction

Chlorophylls and bilins are tetrapyrrole pigments that are synthesized from the universal five carbon precursor aminolevulinic acid (ALA). Chlorophylls are used as light harvesting pigments but are also essential components for energy transduction within the reaction centres of photosystem I (PSI) and photosystem II (PSII), with chlorophyll a (Fig. 5.1) being the main chlorophyll found in algae and cyanobacteria. Like the chlorophylls, bilins are also used as light harvesting pigments for photosynthesis and they are also used in light sensing. As light harvesting pigments, bilins are usually covalently attached to proteins, known generally as phycobiliproteins, with phycocyanobilin (Fig. 5.1) being one of the most common bilins covalently attached through the $C3^2$ to the protein. These phycobiliproteins are subunits of a large light harvesting protein complex called a phycobilisome (PB) that is associated with PSII. In contrast light sensing bilins are covalently attached to proteins known generally as phytochromes that are used to sense light and produce chemical signals in response to both light quality and light intensity. The spectral properties of both phycobiliproteins and phytochromes are dependent both on the protein environment as well as the type of bilin pigment bound.

All algae and cyanobacteria make chlorophylls, but they don't all make phycobilisomes. Phycobilisomes appear to be restricted to the cyanobacteria, glaucophytes, red algae and the secondary endo-

*Author for correspondence, e-mail: robert.willows@mq.edu.au

A. W. D. Larkum et al. (eds.), *Photosynthesis in Algae: Biochemical and Physiological Mechanisms*, Advances in Photosynthesis and Respiration 45, https://doi.org/10.1007/978-3-030-33397-3_5

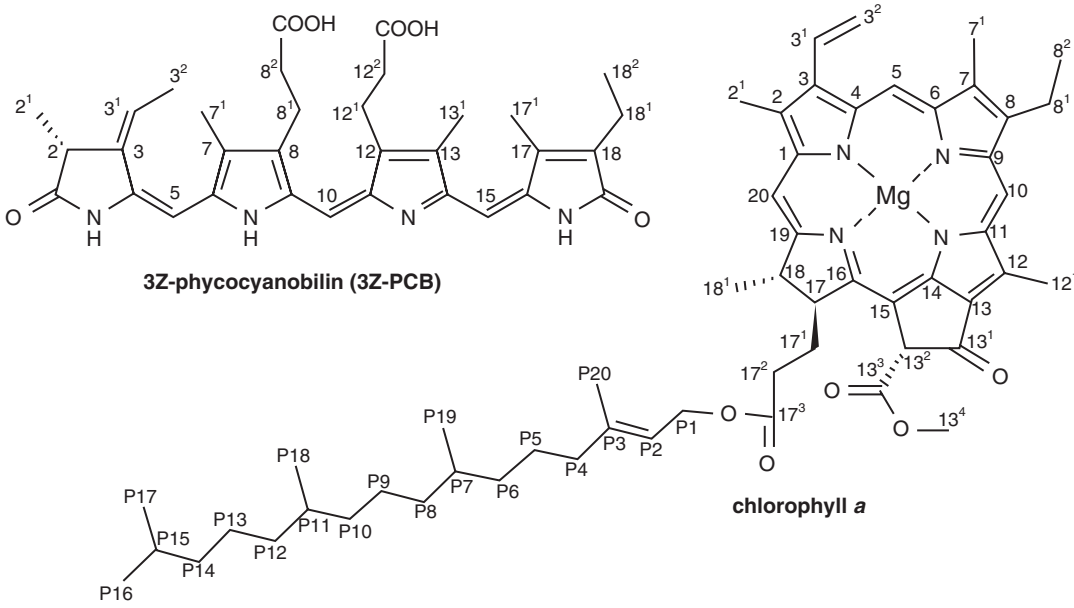

Fig. 5.1. Structure and numbering of a representative bilin and chlorophyll. 3Z-phycocyanobilin and chlorophyll *a*

symbiotic ancestors of the red algae such as the cryptophytes (Bernstein and Miller 1989; Stiller et al. 2014). While most cyanobacteria make phycobilisomes, the well known exceptions are the "Prochlorophytes" *Prochloron*, *Prochlorothrix*, and *Prochlorococcus* (Hess et al. 2001). These organisms have a small genome and are the most abundant primary producers on the planet. One of the possible reasons for the lack of phycobilisomes in these organisms is related to evolutionary pressure on nitrogen utilisation. In terms of pigment content chlorophyll dependent light harvesting complexes (LHCs) are more efficient in per pigment molecule in terms of nitrogen usage than PB's as LHCs utilise 1/3rd of the N per pigment molecule bound. The prochlorophytes are thought to be the ancestors of the green algal lineage, which also do not contain PB's, although they do make bilins and in some cases they have the genes to make certain phycobiliproteins and the corresponding bilin (Hess et al. 2001).

This chapter will concentrate on examining the diversity and biosynthesis of both bilins and chlorophylls which are used in light harvesting for photosynthesis and will not discuss in any detail the use of bilins in light sensing or signalling.

II. Diversity of Chlorophylls in Algae

The most common chlorophyll found in algae is chlorophyll *a*. Chlorophyll *a* is found in the reaction centres of photosystem I (PSI) and photosytem II (PSII) as well as a major component of the light harvesting complexes of both PSI and PSII. All algae make chlorophyll *a* except for a number of *Prochlorococcus* species which do not reduce the 8-vinyl group and so make and utilise DV-chlorophyll *a*.

Chlorophyll *a'* where the stereoisomer is inverted at position 13^2 in ring V (Fig. 5.2), is found in the PSI reaction centre complex

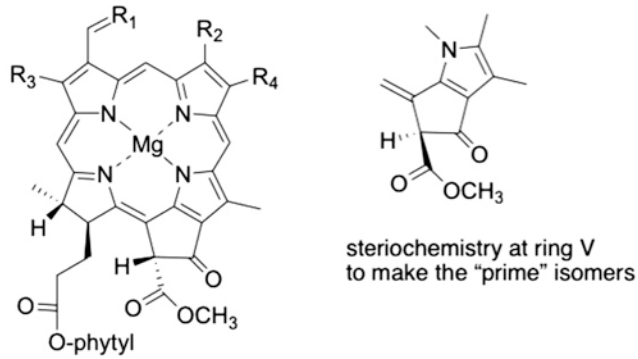

	R_1	R_2	R_3	R_4
chlorophyll *a*	CH_2	CH_3	CH_3	ethyl
chlorophyll *b*	CH_2	CHO	CH_3	ethyl
chlorophyll *d*	O	CH_3	CH_3	ethyl
chlorophyll *f*	CH_3	CH_3	CHO	ethyl
DV-chlorophyll *a*	CH_2	CH_3	CH_3	vinyl
DV-chlorophyll *b*	CH_2	CHO	CH_3	vinyl

	R_4	R_2
chlorophyll c_1	ethyl	CH_3
chlorophyll c_2	vinyl	CH_3
chlorophyll c_3	vinyl	CO_2CH_3

Fig. 5.2. Structure of chlorophylls found in algae

(Kobayashi et al. 1988; Jordan et al. 2001) as the chlorophyll responsible for the P700 absorbance. However, the mechanism of synthesis of chlorophyll *a'* presumably from chlorophyll a has not been determined. Chlorophyll *b* is the next most common chlorophyll in algae and is found in the LHC's and as accessory pigments of PSII of land plants, green algae as well as some of the prochlorophyta cyanobacteria. Other cyanobacteria as well as Rhodophyta and Glaucocystophyta algae in which chlorophyll *a* is the dominant pigment do not contain any chlorophyll *b* but instead contain phycobilins as accessory pigments (Tomitani et al. 1999).

Brown seaweeds, diatoms, chrysomonads, dinoflagellates, and cryptomonads contain one or more chlorophyll *c* pigments (Fig. 5.2) (Jeffrey 1968, 1969) in addition to chlorophyll *a*. Chlorophyll *c* pigments are accessory light harvesting pigments and have not been reported in the reaction centre. The general structure of chlorophyll *c* pigments was first deduced by Granick in 1949 as being similar to protochlorophyllide (Granick 1949). The complete structures of chlorophylls *c1* and *c2* shown in Fig. 5.2 with an acrylate at position C17 and a double bond between C17 and C18, were determined in 1971 (Budzikiewicz and Taraz 1971). A third member of the family, chlorophyll *c3*, was determined in 1989 (Fookes and Jeffrey 1989). Chlorophyll *c* pigments are usually found with the 17-acrylic acid unesterified, but isoprenylate esterified forms have been reported (Nelson and Wakeham 1989; Zapata and Garrido 1997). Chlorophylls *c* are porphyrins rather than chlorins and are thus more similar to protochlorophyllides than chlorophylls. Surprisingly, although chlorophyll *c* pigments are widely utilized by photosynthetic algae and appear to be important in chromatic adaptation (Garrido et al. 2016) almost nothing is known about how they are synthesized.

The far-red absorbing chlorophyll *d* was first discovered in small amounts in extracts in several red macroalgae (Manning and Strain 1943). More recently it has been found that chlorophyll *d* can be produced chemically from chlorophyll *a* under mild condi-

tions in the presence of thiols (Loughlin et al. 2014, 2015; Fukusumi et al. 2012; Oba et al. 2011). Thus it is possible that these first reports of chlorophyll *d* may have arisen due to the extraction method employed. However, in 1996, a novel cyanobacterium was isolated from colonial ascidians which contained chlorophyll *d* as the major chlorophyll constituting >95% of the total chlorophyll with most of the remainder being chlorophyll *a* (Miyashita et al. 1997). This organism, *Acaryochloris marina*, has chlorophyll *d′* in its PSI reaction centre complex that has a 740 nm absorbance maxima (Akiyama et al. 2001). It is worth noting that the primary electron acceptors in *A. marina* are chlorophyll *a* in PS I and the magnesium free chlorophyll *a* derivative, pheophytin *a*, in PS II, respectively (Akiyama et al. 2001, 2002a, b), which is true of all algal PSI and PSII reaction centres described so far except for the DV containing *Prochlorococcus* species.

In 2010 a new chlorophyll, chlorophyll *f* was discovered which has a formyl group at C2 (Chen et al. 2010) as shown in Fig. 5.2. The organism which made this chlorophyll *f*, *Halamicronema hongdechloris* is a filamentous cyanobacteria isolated from stomatolites from Shark Bay in Western Australia (Chen et al. 2010, 2012; Li et al. 2012) and has up to 20% of its content as chlorophyll *f* when grown under far red light. Subsequently, other organisms have been identified which make chlorophyll *f* under what has been termed FarLiP chromatic adaptation (Gan et al. 2014a, b; Akutsu et al. 2011). Most of these organisms also make some chlorophyll *d* although no chlorophyll *d* is made by *H. hongdechloris*.

III. Diversity of Bilins in Algae

Bilin diversity in algae is slightly more complicated than chlorophyll diversity as the bilins are usually, although not always, covalently attached as prosthetic groups to protein. In addition they are utilised in both light harvesting when bound to phycobiliproteins and associated with PBs, as well as in signalling when attached to phytochromes or more recently as freely diffusible signalling molecules (Wittkopp et al. 2017). In addition a number of the bilin reductions and isomerisations occur after or during covalent attachment of the pigments to the phycobiliproteins. Given this complexity, I will concentrate on the main types of bilins involved in light harvesting attached to phycobiliproteins, which are usually subunits of a functional PBs.

PBs are found mainly in cyanobacteria, red algae and the glaucophytes and are made up of large numbers of different phycobiliproteins to which bilins are attached. The variation of the spectral property of phycobiliproteins are mainly dictated by their prosthetic groups, which are linear tetrapyrroles known as phycobilins. The free phycobilins including phycocyanobilin, phycoerythrobilin and occasionally dihydrobiliverdin, shown in Fig. 5.3 (Frankenberg and Lagarias 2003; Glazer 1989), are covalently attached to the phycobiliproteins through cysteine residues on the proteins as shown in Fig. 5.4.

The core of the phycobilisome is made from allophycocyanin subunits, each containing the bilin phycocyanobilin covalently attached. From the core there are several outwardly oriented rods which are made from stacked disks of the phycobiliprotein, phycocyanin, that primarily has the pigment phycocyanobilin covalently bound. These disks may also contain other types of phycobiliproteins, such as phycoerythrin or phycoerythrocyanin. Phycoerythrin contains the pigments, phycoerythrobilin or sometimes phycourobilin, while phycoerythrocyanin contains a mixture of phycoviolobilin and phycocyanobilin. These pigments can be bound through one or two cysteine residues on the proteins as shown in Fig. 5.4.

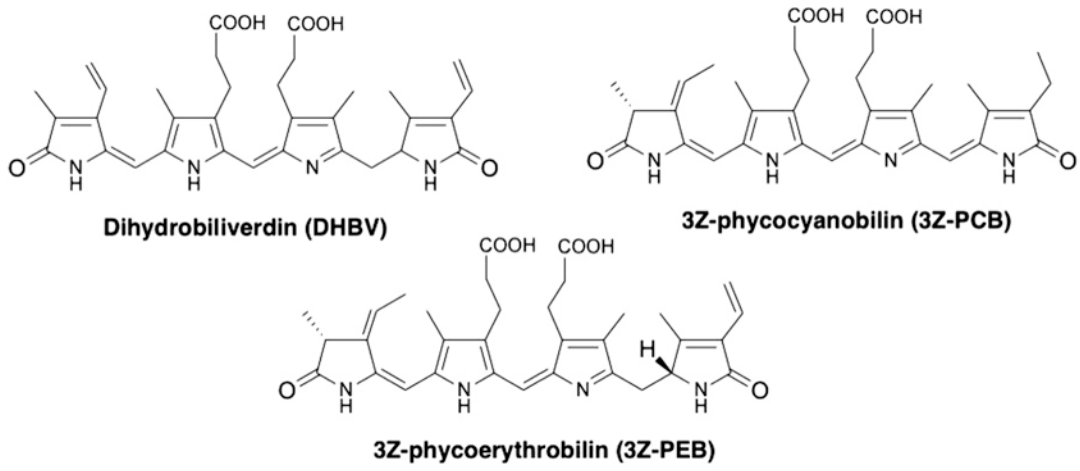

Fig. 5.3. Structures of free bilin pigments DHBV, PEB and PCB

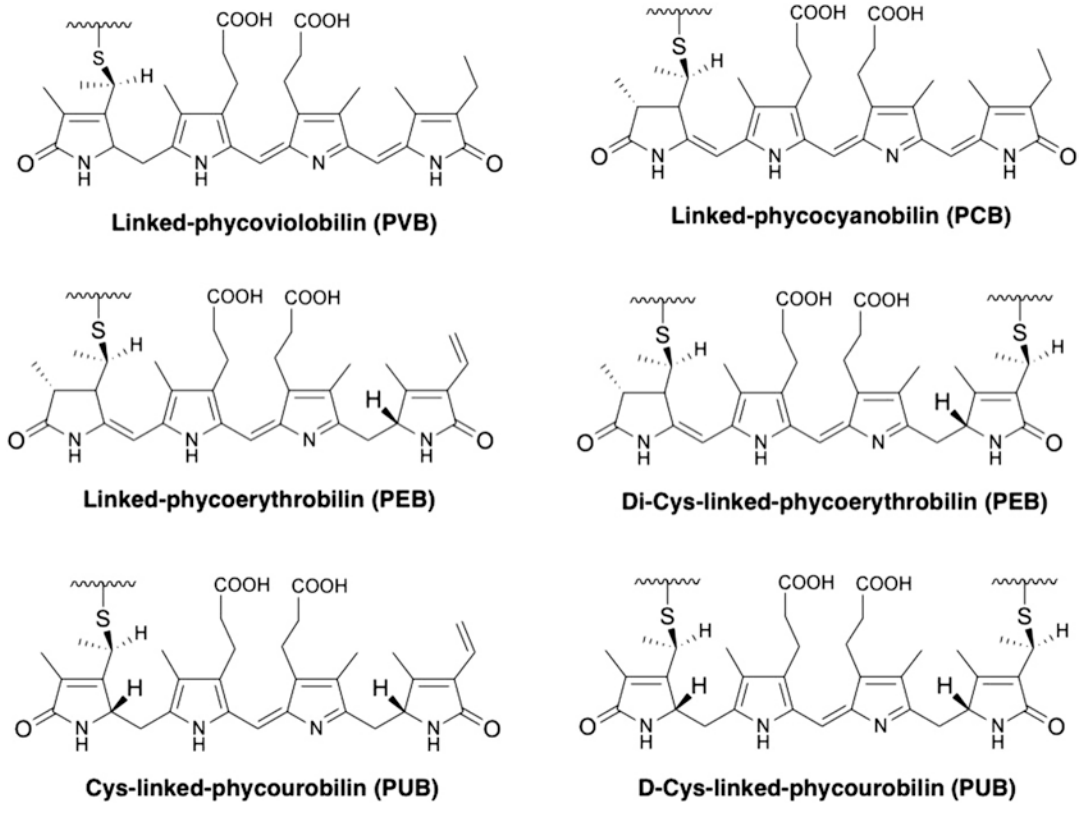

Fig. 5.4. Structures and attachments of bilins commonly found in phycobiliproteins. Cys-PVB, Cys-PCB, Cys-PEB, diCys-PEB, Cys PUB, diCys-PUB

As shown in Fig. 5.4 these bilins are attached through a cysteine residue to ring A and also sometimes attached to two cysteine residues through both ring A and ring D. The isomerisation to produce alternative bilins with different spectral properties occurs during pigment attachment using bilin lyases as discussed later.

IV. Overview of Biosynthesis of Bilins and Chlorophylls

Chlorophylls and bilins have common biosynthetic intermediates from aminolevulinate (ALA) up to and including the intermediate protoporphyrin IX (Fig. 5.5), which is the first coloured intermediate in

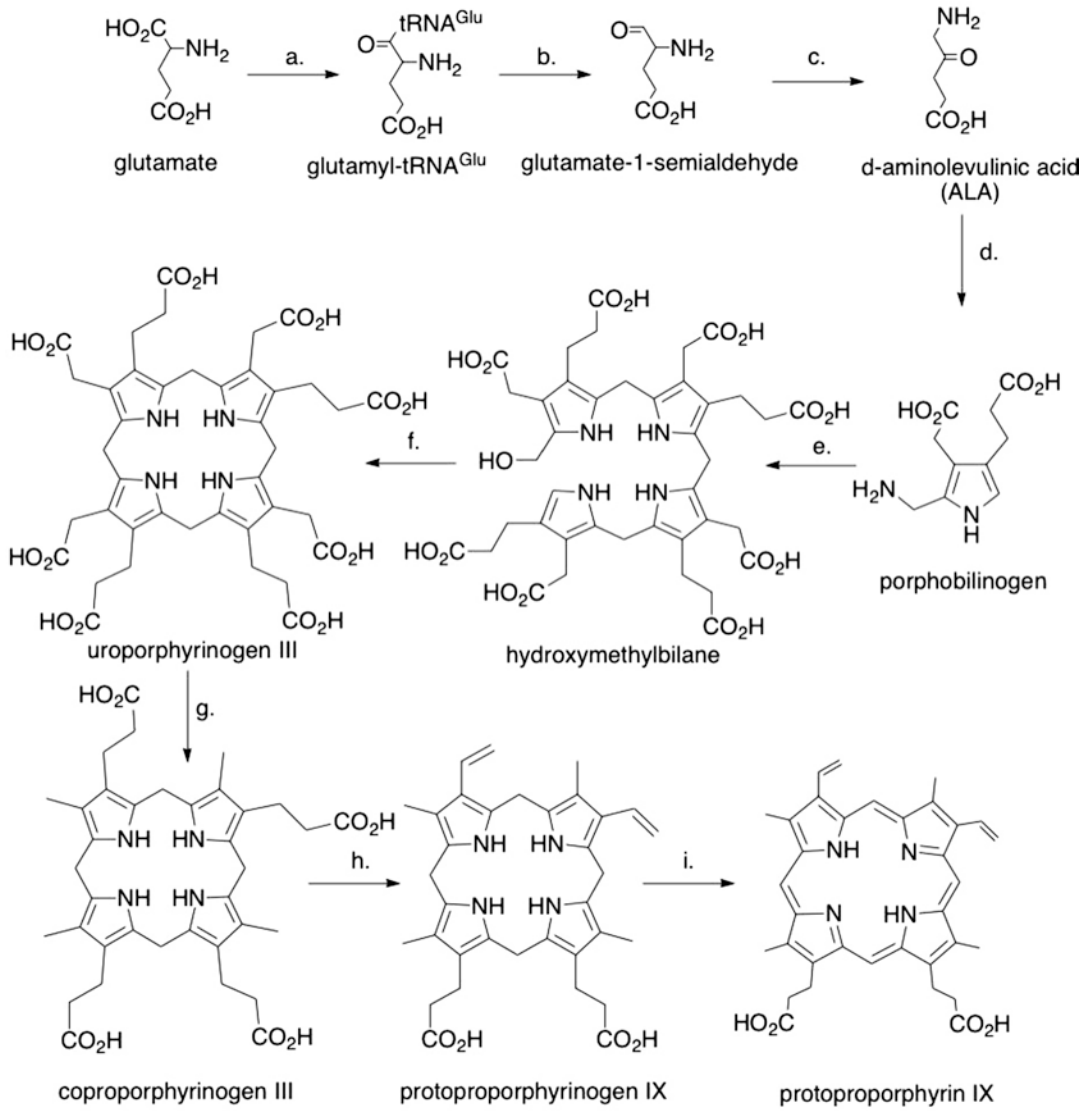

Fig. 5.5. Enzymatic steps and encoding genes from glutamate to protoporphyrin IX: (**a**) Glutamyl tRNA-synthetase, *gluRS*; (**b**) Glutamyl-tRNA reductase, *gluTR* or *hemA*; (**c**) glutamate-1-semialdehyde aminotransferase, *GSAT* or *hemL*; (**d**) porphobilinogen synthase or ALA-dehydratase, *PBGS* or *ALAD* or *hemB*; (**e**) Porphobilinogen deaminase or hydroxymethbilane synthase, *PBGD* or *HMBS* or *hemC*; (**f**) uroporphyrinogen III synthase, *UROS* or *hemD*; (**g**) uroporphyrinogen decarboxylase, *UROD* or *hemE;* (**h**) coproporphyrinogen III oxidase, Oxygen independent encoded by *hemN* and oxygen dependent enzyme encoded by *hemF* or *CPO*; (**i**) protoporphyrinogen IX oxidase, *PPO* or *hemG*

the synthesis of these pigments. From protoporphyrin IX the pathways branch (Figs. 5.6 and 5.7) with either magnesium inserted in the chlorophyll branch to make magnesium protoporphyrin or iron inserted to make heme on the pathway for bilin synthesis.

While the spectroscopic and physicochemical properties of chlorophylls, in particular, make them ideal for light harvesting and energy transduction, these properties also makes them reactive in the presence of oxygen and light. Thus when chlorophylls and their coloured intermediates are not positioned to allow dissipation of absorbed light energy either by Förster energy transfer to another pigment or transduction within the reaction centre, the excited state may react with molecular oxygen to form singlet oxygen. This makes chlorophyll synthesis a challenge in the presence of light as accumulation of non-protein bound chlorophyll or its coloured intermediates can cause oxidative stress and potentially cell death. In contrast to the chlorophylls, the bilins are not as photoreactive in their non-protein bound state and are even suggested to be antioxidants.

Thus regulation of chlorophyll biosynthesis in particular is essential in order to prevent accumulation of free pigment molecules that could result in cell death. The regulatory mechanisms involve both transcriptional and post-transcriptional controls with the key regulatory steps being: (1) aminolevulinate biosynthesis from glutamate; (2) The branch point for metal insertion to make either heme or Mg-protoporphyrin; (3) The reduction of protochlorophyllide to chlorophyllide. As discussed in more detail later, the primary regulatory factors involved in regulating one or more of these steps include: light, oxygen or reactive oxygen species, heme, and protochlorophyllide.

V. Biosynthesis of Protoporphyrin IX

The primary control point for both chlorophyll and heme/bilin synthesis is at the level of ALA synthesis. The enzymes involved in this regulatory process are glutamyl-tRNA reductase, GluTR or HemA, and glutamate-1-semialdehyde aminotransferase, GSAT or HemL (Fig. 5.5 reactions b and c). GluTR catalyses the NADPH dependent reduction of glutamyl-tRNA^{glu} while GSAT catalyses the isomerisation of glutamate-1-semialdehyde, produced by GluTR, to ALA. The x-ray crystal structure of GSAT from *Synechococcus* has been determined (Hennig et al. 1994, 1997) and it was suggested, based on the structure of an archeal GluTR (Moser et al. 2001), that the two enzymes form a stable complex *in vivo* to allow channeling of the unstable glutamate-1-semialdehyde directly from GluTR to GSAT. This interaction has been confirmed using the enzymes from *Chlamydomonas* by co-immunoprecipitation and kinetic analysis (Nogaj and Beale 2005). In addition the GluTR from *Chlamydomonas* was shown to form a stable complex with the glutamyl-tRNA synthetase (Jahn 1992) suggesting substrate channeling from glutamate through to ALA occurs without release of intermediates. Blue light is a transcriptional regulator of GSAT in *Chlamydomonas reinhardtii* (Im et al. 1996) and this regulation is modulated by nitrogen and carbon availability. Similarly GluTR transcription is regulated by light with both transcripts increasing significantly in the light, however, the quantity of GluTR and GSAT proteins and activity levels remain constant despite changes in transcript levels of up to sixfold, indicating that transcription does not regulate the activity (Nogaj et al. 2005; Srivastava et al. 2005).

When organisms are fed ALA they accumulate various tetrapyrroles depending on the relative activities of the enzymes in the pathway and when feeding occurs in the dark both protoporphyrin IX and protochlorophyllide often accumulate, suggesting some regulation of these steps which will be discussed later. This also indicates that ALA synthesis is a key control point and regulation of ALA synthesis by end products such as heme and intermediates such as protochlorophyllide have been reported for plants

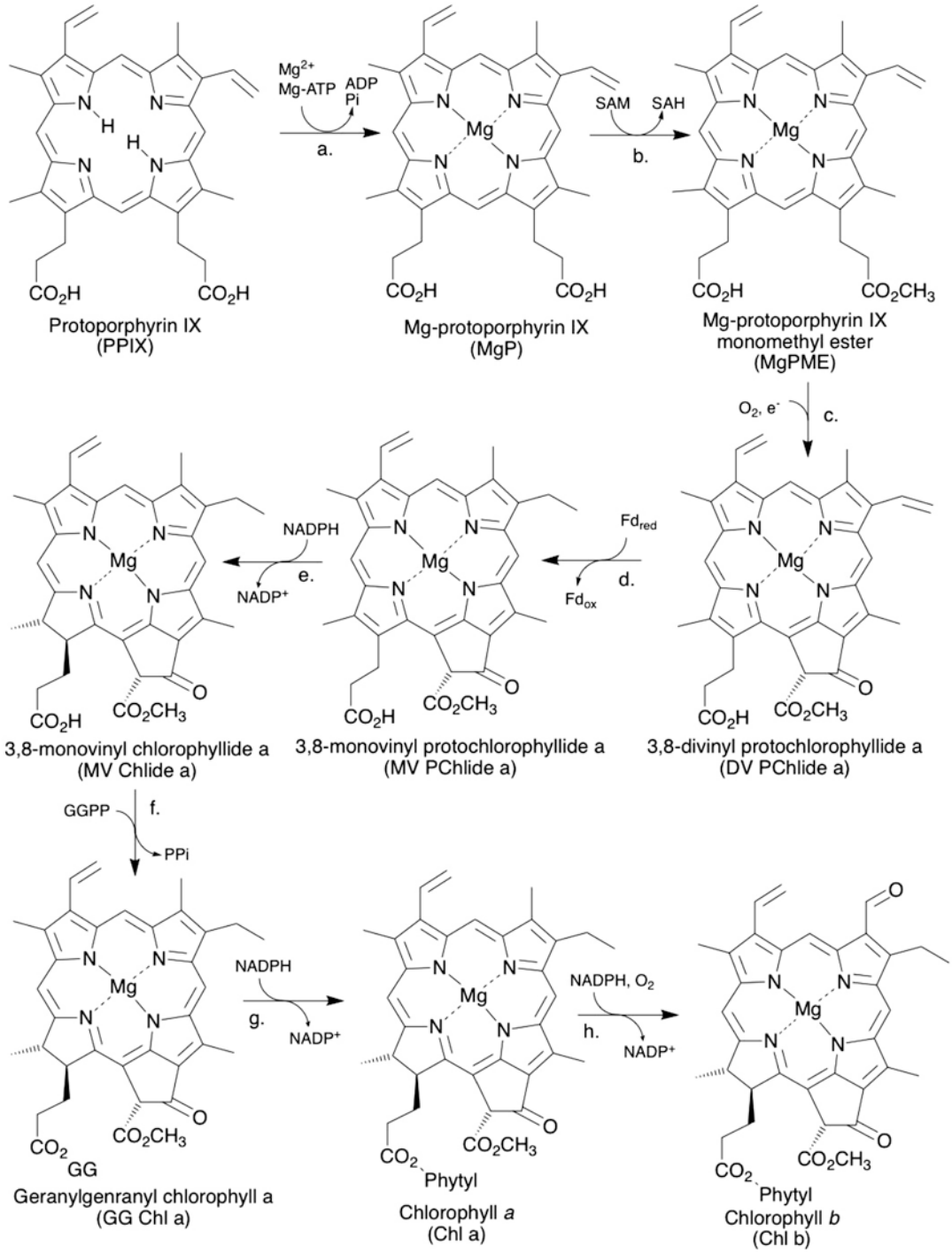

Fig. 5.6. Enzymatic steps and encoding genes from protoporphyrin IX to chlorophyll *b*: (**a**) Magnesium chelatase, *bchH/chlH, bchD/chlD, bchI/chlI* and *gun4*; (**b**) S-adenosylmethionone Mg- protoporphyrin IX monomethylester transferase, *chlM*; (**c**) MgPME oxidative cyclase, *acsF, bchE,* or *CTH1/ycf54*; (**d**) protochlorophyllide oxido-reductase. Light dependent enzyme encoded by *por* and light independent enzyme encoded by *bchB/chlB, bchN/chlN,* and *bchL/chlL*; (**e**) Divinyl reductase, *DVR*; (**f**) Chlorophyll synthase, *chlG*; (**g**) Geranylgeranyl reductase/Phytyl synthase, *chlP*; (**h**) Chlorophyll *a* oxygenase, *COA*

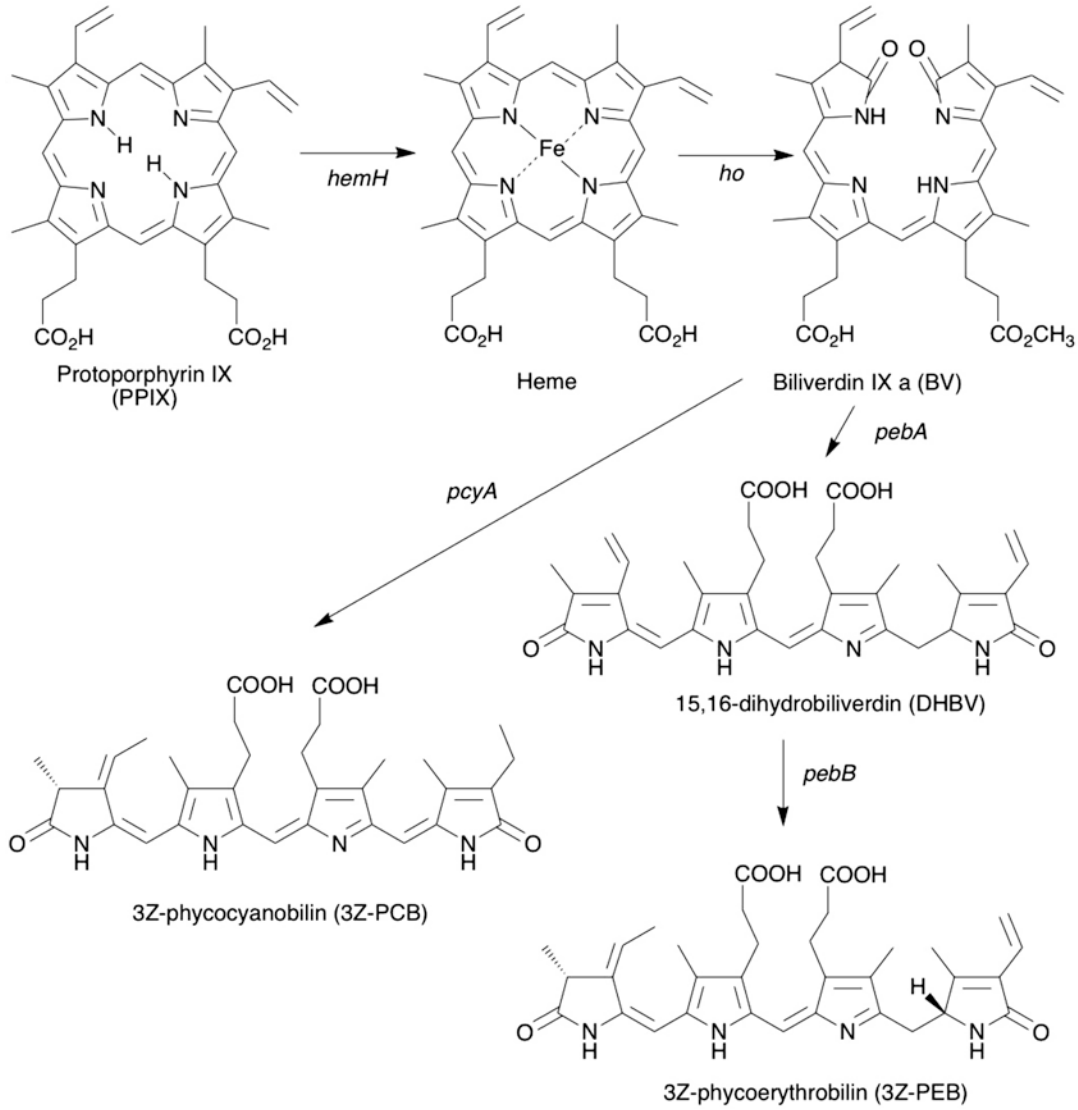

Fig. 5.7. Enzymatic steps and encoding genes from protoporphyrin to free bilins

and algae. Although heme has been reported to regulate barley GluTR activity through an N-terminal extension (Vothknecht et al. 1998), this may not occur in algae as heme and protoporphyrin IX have not been reported to regulate algal GluTR although they have been reported to regulate transcription of the GluTR (Vasileuskaya et al. 2005). Feedback regulation of ALA synthesis by protochlorophyllide or later intermediates has been long suspected due to the occurrence of brown mutants of *Chlamydomonas* which are unable to make chlorophyll but accumulate MgPPIX or PPIX. These mutants suggest the presence of a feedback regulatory mechanism on ALA synthesis involving intermediates after these enzymatic steps (Wang et al. 1974; Meinecke et al. 2010; Chekounova et al. 2001). In contrast plants that are mutated at the same biosynthetic steps as the brown *Chlamydomonas* mutants are yellow with no significant accumulation

of MgPPIX or PPIX, unless they are fed ALA (Henningsen et al. 1993). This suggests that heme may be a key regulator of ALA synthesis in plants but not in *Chlamydomonas* or perhaps in other algae.

Protochlorophyllide dependent feedback regulation of ALA synthesis is mediated by a protein called FLU which was first identified in *Arabidopsis thaliana* (Meskauskiene et al. 2001; Meskauskiene and Apel 2002). Unicellular algae such as *Chlamydomonas* also contain FLU, also called FLP, and this protein is alternatively spliced and was found to also be important in regulating ALA synthesis (Falciatore et al. 2005), presumably by interacting with protochlorophyllide.

All of the genes for steps from ALA to protoporphyrin IX have been identified in *Chlamydomonas* and in many cyanobacteria, including *Synechocystis* (Lohr et al. 2005; Merchant et al. 2007; Kaneko et al. 1996). One key difference between eukaryotic algae like *Chlamydomonas* and cyanobacteria is in in the later steps in protoporphyrin IX synthesis. Most cyanobacteria have oxygen-independent as well as an oxygen-dependent enzyme for coproporphyrinogen oxidase CPO and possibly protoporphyrinogen oxidase PPO, while eukaryotic algae, like *Chlamydomonas,* appear to only contain genes for the oxygen dependent enzymes (Lohr et al. 2005).

VI. Biosynthesis of Bilins from Protoporphyrin and Function of Bilin Lyases

Bilins are biosynthesized from protoporphyrin IX via heme as shown in Fig. 5.7. Fe^{2+} is inserted into protoporphyrin IX by ferrochelatase to make heme. Ferrochelatase is encoded by the *hemH* gene and is a single subunit enzyme with no cofactor requirement apart from the two substrates. The ferrochelatase of *Chlamydomonas* is located in the chloroplast and the heme and is associated with the chloroplast membranes (van Lis et al. 2005). The cellular needs for heme in *Chlamydomonas* are supplied by heme derived from the chloroplast, including heme required in the cytosol and mitochondria (van Lis et al. 2005), suggesting a transport mechanism must exist to supply heme to these compartments.

The initial committed step of bilin biosynthesis is the cleavage of heme by heme oxygenases to afford the first linear tetrapyrrole, biliverdin. The mammalian heme oxygenases are microsomal NADPH-cytochrome P450 dependent enzymes while the heme oxygenases from red algae and cyanobacteria are soluble ferredoxin dependent enzymes. The first ferredoxin dependent heme oxygenase was identified and cloned and expressed in *E.coli* from *Synechocystis* (Willows and Beale 1998). *Synechocystis* has two heme oxygenase genes *ho1* and *ho2*, the *ho1* is required under oxygen sufficient conditions, while *ho2* is required under low oxygen tension conditions and is located next to the oxygen independent coproporphyringen oxidase, *hemN* gene.

Biliverdin produced by heme oxygenase is further reduced by site specific reductases such as PebA, PebB and PcyA, to make, DHBV, 3Z-PEB and 3Z-PCB respectively as shown in Fig. 5.7. Like heme oxygenase these oxidoreductases are ferredoxin-dependent and belong to the interesting family of radical oxidoreductases known as of ferredoxin dependent bilin reductases (FDBRs). In recent years the family of FDBRs has expanded revealing novel activities (Kronfel et al. 2013; Biswas et al. 2011; Schluchter et al. 2010).

Most cyanobacteria make bilins such as 3Z-PCB in order to make PB's but eukaryotic green algae such as *Chlamydomonas* don't have PB's or indeed phytochromes yet they contain *ho* and *pcyA* type genes (Rockwell and Lagarias 2017). Recently it has been shown that these bilins are required in chloroplast nuclear signalling processes and are specifically required for photoacclimation in *Chlamydomonas* and this may also

be important in other algae which lack phytochromes or PB's (Wittkopp et al. 2017; Rockwell and Lagarias 2017; Duanmu et al. 2017; Formighieri et al. 2012).

The DHBV, 3Z-PEB and 3Z-PCB bilins are covalently attached to phycobiliproteins by bilin lyases. During the attachment the bilins can also undergo further isomerisation to bilins such as PUB and PVB shown in Fig. 5.4 (Arciero et al. 1988a; b, c; Fairchild et al. 1992; Swanson et al. 1992; Fairchild and Glazer 1994a, b). The bilin lyases fall into 3 main classes: The E/F-type such as CpcE/CpcF heterodimeric bilin lyase, the T-type including CpcT bilin lyase, and the S/U-type that includes CpcS/CpcU heterodimeric and homodimeric bilin lyases (Zhao et al. 2017).

The CpcE/F bilin lyase was the first bilin lyase characterized (Zhou et al. 1992) and catalyses the attachment of 3Z-PCB to Cys-84 of α-phycocyanin. Other members of this family include PecE/PecF and CpeY/CpeZ (Kronfel et al. 2013; Biswas et al. 2011; Zhao et al. 2000, 2007; Jung et al. 1995; Saunee et al. 2008; Shen et al. 2008; Overkamp et al. 2014). This family of lyases appears to have some members which can isomerize the bilin during attachment to the biliprotein whereas other members are capable of removing the bilin and transferring to a different biliprotein (Schluchter et al. 2010).

The T-type bilin lyases were first identified in *Synechococcus* PCC7002 where CpcT was shown to be involved in PCB attachment to Cys-153 of β-phycocyanin and unlike the other classes it appears to function by itself, probably as a homodimer (Shen et al. 2006; Zhou et al. 2014). The distribution of sequences similar to CpcT among other cyanobacteria suggests that this protein subgroup plays a role in cyanobacterial-type phycoerythrin biosynthesis, probably by attaching 3Z-PEB at the Cys-153 equivalent position of β-phycoerythrin (Schluchter et al. 2010).

The S/U family of lyases includes members such as CpcS, CpcU, CpcV (function unknown) and CpeS and CpeU bilin lyases (Bretaudeau et al. 2013; Six et al. 2007). This family has members which usually form homodimers (CpcS, CpeS) or heterodimers such as CpcS/U but does not appear to perform the transfer or removal of bilins like the other families. However some of these enzymes can recognise many different PBPs and attach bilins at their Cys-82 equivalent positions, and thus have a broader substrate specificity than the other types of lyases (Schluchter et al. 2010; Scheer and Zhao 2008).

Although, bilins have been reported to attach to the phycobiliproteins autocatalytically this is unlikely to occur to any extent *in vivo* as mutants lacking the bilin lyases are unable to assemble functional PBs (Shen et al. 2008).

VII. Biosynthesis of Chlorophylls from Protoporphyrin IX

Magnesium chelatase catalyses the first committed step to chlorophyll synthesis. The first high activity *in vitro* assay was with stromal and membrane extracts from pea chloroplasts (Walker and Weinstein 1991; Walker et al. 1992). This assay system was important as it identified that the enzyme assembly was protein concentration dependent. Subsequently the minimum requirements for magnesium chelatase activity were identified by expressing the three genes *bchH*, *bchD* and *bchI* from the anoxygenic photosynthetic bacteria *Rhodobacter sphaeroides* in *E. coli* and reconstituting the ATP dependent activity (Gibson et al. 1995). The orthologous genes from *Synechocystis*, *chlI, chlD* and *chlH (*Jensen et al. 1996a*)*, and barley, *xantha-H*, *xantha-G* and *xantha-F* (Jensen et al. 1996b) were also identified as magnesium chelatase components corresponding to the *bchI, bchD and bchH* genes of *Rhodobacter* respectively. In organisms that synthesize chlorophyll the genes are generally now called *chlI, chlD* and *chlH*. In plants

and algae these genes are regulated by light with higher expression in the light, particularly of the *chlH* gene, and they are often under circadian clock regulation (Chekounova et al. 2001; Jensen et al. 1996b; Lake and Willows 2003; Stephenson and Terry 2008).

One common feature of the magnesium chelatase from all sources is that it requires an ATP dependent assembly of the ChlI and ChlD subunits to form an activation complex (Willows and Beale 1998; Willows et al. 1996; Walker and Willows 1997; Guo et al. 1998; Petersen et al. 1998; Gibson et al. 1999; Reid and Hunter 2002; Sawicki and Willows 2008; Lake et al. 2004). This ChlI/ChlD complex acts like the "enzyme" to insert Mg^{2+} into protoporphyrin IX bound to the ChlH subunit with this large 132–155 kDa subunit behaving like a substrate in the reaction with a K_m in the 0.1–1 μM range (Willows and Beale 1998; Petersen et al. 1998; Sawicki and Willows 2008; Viney et al. 2007).

GUN4 is a fourth magnesium chelatase accessory subunit which was first identified in *A. thaliana* as being involved in the retrograde signalling system from the chloroplast to the nucleus (Larkin et al. 2003). The ChlH subunit of the *A. thaliana* is also known as GUN5 and is also involved in this signalling process (Mochizuki et al. 2001) suggesting an involvement of the magnesium chelatase in chloroplast to nuclear signalling. GUN4 binds protoporphyrin IX and magnesium protoporphyrin IX and is able to stimulate magnesium chelatase activity (Larkin et al. 2003) through interaction with ChlH (Wilde et al. 2004; Sobotka et al. 2008; Adhikari et al. 2009, 2011; Davison and Hunter 2011). This stimulation of magnesium chelatase activity is required for optimal chlorophyll synthesis (Wilde et al. 2004; Sobotka et al. 2008; Adhikari et al. 2009, 2011; Davison and Hunter 2011). It has been suggested that this porphyrin binding of both ChlH and GUN4 together with light is important in retrograde signalling by producing singlet oxygen (Stephenson and Terry 2008; Brusslan and Peterson 2002; Surpin et al. 2002; Muller et al. 2014; Tarahi Tabrizi et al. 2016).

The interaction of GUN4 with ChlH in plants requires a C-terminal extension of GUN4 that is absent in cyanobacteria (Tarahi Tabrizi et al. 2016; Zhou et al. 2012; Adams et al. 2014; Huang et al. 2014; Richter et al. 2016). In plants the phosphorylation or removal of this C-terminal extension prevents the interaction with ChlH and hence regulates magnesium chelatase activity (Zhou et al. 2012; Huang et al. 2014; Richter et al. 2016) *Chlamydomonas* and other eukaryotic algae also possess a C-terminal extension compared to cyanobacterial GUN4 proteins but it is unclear if this extension serves a similar function to the plant GUN4 in regulating magnesium chelatase activity.

The x-ray and electron-microscopy (EM) structures of magnesium chelatase subunits and complexes have been determined including; GUN4 from cyanobacteria and *Chlamydomonas* (Davison et al. 2005; Verdecia et al. 2005; Chen et al. 2015a; Tarahi Tabrizi et al. 2015); the x-ray and EM structures of BchI and the BchI/BchD complex from *Rhodobacter capsulatus* (Willows et al. 1999; Fodje et al. 2001; Lundqvist et al. 2010, 2013); and the x-ray structure of the cyanobacterial ChlH (Chen et al. 2015b). These crystal structures have informed catalytic models for magnesium chelatase activity which suggest that the ChlI/ChlD subunits form a AAA+ type molecular motor which drives an ATP dependent conformational change in the substrate ChlH-protoporphyrin IX-GUN4 complex to possibly bend the tetrapyrrole and expose and deprotonate the pyrrole nitrogens and allow Mg^{2+} insertion. The GUN4 then is involved in removing the Mg-protoporphyrin IX for trafficking to the next enzyme. One curious finding is that the ChlI subunits appear to be disassembled from the ChlD complex and recycled in each catalytic cycle which may explain a number of the kinetic properties of the enzyme and

the requirement for higher concentrations of ChlI or BchI *in vitro* assays (Lundqvist et al. 2013; Hansson et al. 2002; Zhang et al. 2015; Adams et al. 2016; Adams and Reid 2013; Brindley et al. 2015). To further complicate the regulatory landscape surrounding this enzyme, more than one *chlI* and *chlH* gene is sometimes found in plants and eukaryotic algae. The ChlI2 of *A. thaliana* has been shown to substitute for the ChlI1 protein (Rissler et al. 2002). In contrast, the *Chlamydomonas* ChlI2 has a C-terminal extension and is not able to substitute for the ChlI1 (Brzezowski et al. 2016). However, the *Chlamydomonas* ChlI2 has histidine kinase activity and is involved in activation of the magnesium chelatase by phosphorylation of a histidine on the C-terminal domain of ChlD (Sawicki et al. 2017).

The description of *Chlorella* mutants by Granick were pivotal in the characterisation of the next two steps in the pathway, catalysed by the S-adenosyl methionine-Mg-protoporphyrin IX monomethyl ester transferase and the magnesium protoporphyrin oxidative cyclase (Granick and Kett 1948; Granick 1961). The S-adenosyl methionine-Mg-protoporphyrin IX monomethyl ester transferase catalyses the methylation of the C-17 propanoate as shown in Fig. 5.6. The *chlM* gene encodes the single subunit enzyme catalysing this step and the cyanobacterial enzyme has been heterologously expressed in *E.coli* and the enzyme characterised (Shepherd and Hunter 2004; Shepherd et al. 2005; Dorgan et al. 2006; McLean and Hunter 2009). A brown *Chlamydomonas* has been characterised which has a defective *chlM* (Meinecke et al. 2010) and accumulates magnesium protoporphyrin IX. The *chlM* knockout of *Chlamydomonas* has also been performed using CRISPR based gene targeting and the brown phenotype is a useful visual screen to enable selection of mutants (Shin et al. 2016).

The oxidative cyclase has been partially characterised from plant and algal chloroplasts and requires molecular oxygen and NADPH. The enzyme activity can be separated into soluble and membrane components (Wong and Castelfranco 1984; Nasrulhaq-Boyce et al. 1987; Walker et al. 1988, 1991; Vijayan et al. 1992; Whyte et al. 1992; Whyte and Castelfranco 1993; Bollivar and Beale 1995, 1996) and is inhibited by lipid soluble Fe^{2+} chelators like dipyrridyl. Anaerobic photosynthetic bacteria have an oxygen independent cyclase encoded by *bchE* and many cyanobacteria have a *bchE* orthologue called *chlE*, which is not absolutely required for chlorophyll synthesis (Yamanashi et al. 2015). Cyanobacteria also have an aerobic oxygen dependent cyclase encoded by *acsF* or *chlA* (Ouchane et al. 2004; Minamizaki et al. 2008). Homologues of *acsF* were identified in *Chlamydomonas* as *crd1* or *chl27A* and *cth1* or *chl27B,* which are required for chlorophyll synthesis and are differentially regulated under low and high oxygen conditions respectively (Moseley et al. 2000, 2002; Allen et al. 2008). The *Chlamydomonas* CRD1 and CTH1 are di-iron membrane bound proteins and are part of the membrane component required for enzymatic activity of the cyclase. In addition, another part of the membrane component called Ycf54 has been identified (Hollingshead et al. 2012; Bollivar et al. 2014; Chen et al. 2017), while the soluble component of the cyclase activity appears to be ferredoxin reductase (Herbst et al. 2018).

The conversion of divinyl protochlorophyllide to chlorophyllide can be catalysed by two different types of protochlorophyllide reductases. These are known as LPOR and DPOR which stand for light-dependent- and dark- protochlorophyllide reductase respectively. These systems have been very well characterised and have been the subject of a number of extensive reviews (Fujita and Bauer 2003; Gabruk and Mysliwa-Kurdziel 2015; Layer et al. 2017; Rüdiger 2003; Nascimento et al. 2016). The LPOR enzyme requires light as a substrate in the enzymatic reaction and is a single polypeptide encoded

by *por* with many plants and algae having multiple *por* isoforms. The DPOR enzyme is a complex enzyme with three subunits called ChlL, ChlB and ChlN. The sequences of the subunits and structure of the DPOR is similar to nitrogenase (Moser et al. 2013) and like the nitrogenase its activity is oxygen sensitive. Algae and cyanobacteria generally have both types of enzymes so they are able to make chlorophyll in the dark utilizing DPOR or in the light utilising LPOR. In eukaryotes the genes for DPOR are located on the chloroplast genome while the *por* genes are located on the nuclear genome. The DPOR genes in cryptophytes have undergone recent gene loss (Kim et al. 2017) and yellow in the dark mutants of *Chlamydomonas* are the result of nuclear mutations which effect the accumulation of the chloroplast encoded ChlL subunit (Cahoon and Timko 2000).

With a few exceptions, such as *Prochloron*, chlorophylls in the photosystems of most chlorophyll containing organisms have an 8-ethyl group. This 8-ethyl group is formed by reduction of the divinyl-chlorophyllide *a* to monovinyl chlorophyllide *a* by an divinyl reductase. The 8-vinyl-reduction is catalysed by an NADPH dependent or ferredoxin dependent divinyl reductases. The enzyme is called DVR in eukaryotes such as *Chlamydomonas* and is NADPH dependent. Cyanobacteria have two types of enzyme with the BciA, homologous to DVR, being NADPH dependent while the second type known as BciB being ferredoxin dependent (Nagata et al. 2005; Liu and Bryant 2011; Wang et al. 2013; Canniffe et al. 2014; Chen et al. 2016). The BciA and BciB are unrelated to each other but both proteins have been found in cyanobacteria such as *A. marina*, where the genes had been misannotated as *nmrA* and *frhB* respectively, but both were shown to have divinyl reductase activity (Chen et al. 2016).

The final steps of chlorophyll *a* synthesis are catalysed by geranylgeranyl-pyrophosphate reductase and chlorophyll synthase, abbreviated ChlP and ChlG respectively (Addlesee et al. 1996; Oster et al. 1997). The ChlP catalyses an NADPH reduction of geranylgeranyl-pyrophosphate to phytyl-pyrophosphate and in plants this reductase is also required for tocopherol biosynthesis (Grasses et al. 2001). The plants with reduced levels of ChlP have chlorophyll *a* with geranylgeraniol esterified instead of phytol indicating chlorophyll synthase can use either geranylgeranyl-pyrophosphate or phytyl-pyrophosphate as a substrate (Grasses et al. 2001). The ChlG of plants, cyanobacteria and algae form a complex with the protein insertase, YidC/Alb3 and an assembly factor Ycf39, suggesting that chlorophyll *a* formed from ChlG is delivered directly to the photosystem proteins as they are inserted into the membrane (Proctor et al. 2018).

VIII. Synthesis of Chlorophyll *b*, *d* and *f*

The formyl oxygens present in all of these modified chlorophylls are derived from molecular oxygen (Schliep et al. 2010; Garg et al. 2017; Porra et al. 1993, 1994; Porra and Scheer 2001). The gene encoding chlorophyll *a* oxidase (CAO) was first identified using *Chlamydomonas* mutants (Tanaka et al. 1998) and the *Arabidopsis* gene was expressed in *E. coli* and the product shown to have CAO activity *in vitro* but it has not been completely characterised (Oster et al. 2000). The activity of the CAO from various organisms has been confirmed by mutation and/or overexpression with resulting changes in the chlorophyll *a* to chlorophyll *b* ratios (Tanaka et al. 2001). More recently the CAO from *Micromonas* was shown to consist of two homologous subunits CAO1 and CAO2 with both subunits required for chlorophyll *b* formation in an *Arabidopsis* chlorophyll *b*-less mutant (Kunugi et al. 2013).

The chlorophyll *f* synthase is a light dependent enzyme with a structure like the PSII reaction centre (Ho et al. 2016) but the

enzyme system which makes chlorophyll *d* is unknown. The enzymes that incorporate a formyl group into chlorophyll *a* require further investigation, especially in regard to their enzymatic mechanisms.

IX. Concluding Remarks

Future work on bilin and chlorophyll synthesis in algae will be to fill the obvious gaps in our knowledge of the structure and mechanism of various enzymes involved in their synthesis. In addition one of the more interesting aspects to bilin and chlorophyll synthesis in algae is the observation that chlorophyll *b* containing algae do not contain PB's and vice versa. The recent discovery that bilins are still synthesized by chlorophyte algae and appear to have a regulatory role suggests the pathways for bilin and chlorophyll synthesis are intertwined after they branch, at least in a regulatory sense. Future work on how this regulation occurs would advance our understanding of how pigment synthesis is regulated and coordinated with the pigment binding proteins.

Bibliography

Adams NB, Reid JD (2013) The allosteric role of the AAA+ domain of ChlD protein from the magnesium chelatase of synechocystis species PCC 6803. J Biol Chem 288(40):28727–28732

Adams NBP et al (2014) Structural and functional consequences of removing the N-terminal domain from the magnesium chelatase ChlH subunit of Thermosynechococcus elongatus. Biochem J 464(3):315–322

Adams NB et al (2016) Nanomechanical and thermophoretic analyses of the nucleotide-dependent interactions between the AAA(+) subunits of magnesium chelatase. J Am Chem Soc 138(20):6591–6597

Addlesee HA et al (1996) Cloning, sequencing and functional assignment of the chlorophyll biosynthesis gene, chlP, of Synechocystis sp. PCC 6803. FEBS Lett 389(2):126–130

Adhikari ND et al (2009) Porphyrins promote the association of genomes uncoupled 4 and a Mg-chelatase subunit with chloroplast membranes. J Biol Chem 284(37):24783–24796

Adhikari ND et al (2011) GUN4-porphyrin complexes bind the ChlH/GUN5 subunit of Mg-chelatase and promote chlorophyll biosynthesis in arabidopsis. Plant Cell 23(4):1449–1467

Akiyama M et al (2001) Detection of chlorophyll d' and pheophytin a in a chlorophyll d-dominating oxygenic photosynthetic prokaryote Acaryochloris marina. Anal Sci 17(1):205–208

Akiyama M et al (2002a) Quest for minor but key chlorophyll molecules in photosynthetic reaction centers – unusual pigment composition in the reaction centers of the chlorophyll d-dominated cyanobacterium Acaryochloris marina. Photosynth Res 74(2):97–107

Akiyama M et al (2002b) Detection of chlorophyll d' and pheophytin a in a chlorophyll d-dominating oxygenic photosynthetic prokaryote Acaryochloris marina. Plant Cell Physiol 43:S170–S170

Akutsu S et al (2011) Pigment analysis of a chlorophyll f-containing cyanobacterium strain KC1isolated from Lake Biwa. Photomed Photobiol 33:35–40

Allen MD, Kropat J, Merchant SS (2008) Regulation and localization of isoforms of the aerobic oxidative cyclase in Chlamydomonas reinhardtii. Photochem Photobiol 84(6):1336–1342

Arciero DM, Bryant DA, Glazer AN (1988a) In vitro attachment of bilins to apophycocyanin. I. Specific covalent adduct formation at cysteinyl residues involved in phycocyanobilin binding in C-phycocyanin. J Biol Chem 263(34):18343–18349

Arciero DM, Dallas JL, Glazer AN (1988b) In vitro attachment of bilins to apophycocyanin. III. Properties of the phycoerythrobilin adduct. J Biol Chem 263(34):18358–18363

Arciero DM, Dallas JL, Glazer AN (1988c) In vitro attachment of bilins to apophycocyanin. II. Determination of the structures of tryptic bilin peptides derived from the phycocyanobilin adduct. J Biol Chem 263(34):18350–18357

Bernstein LS, Miller KR (1989) Unique location of the phycobiliprotein light-harvesting pigment in the Cryptophyceae. J Phycol 25(3):412–419

Biswas A et al (2011) Characterization of the activities of the CpeY, CpeZ, and CpeS bilin lyases in phycoerythrin biosynthesis in Fremyella diplosiphonStrain UTEX 481. J Biol Chem 286(41):35509–35521

Bollivar D, Beale S (1995) Formation of the isocyclic ring of chlorophyll by isolated Chlamydomonas reinhardtii chloroplasts. Photosynth Res 43(2):113–124

Bollivar D, Beale S (1996) The chlorophyll biosynthetic enzyme Mg-protoporphyrin IX monomethyl ester (oxidative) cyclase. Characterization and par-

tial purification from Chlamydomonas reinhardtii and Synechocystis sp. PCC 6803. Plant Physiol 112(1):105–114

Bollivar D et al (2014) The Ycf54 protein is part of the membrane component of Mg-protoporphyrin IX monomethyl ester cyclase from barley (Hordeum vulgare L.). FEBS J 281(10):2377–2386

Bretaudeau A et al (2013) CyanoLyase: a database of phycobilin lyase sequences, motifs and functions. Nucleic Acids Res 41(Database issue):D396–D401

Brindley AA et al (2015) Five glutamic acid residues in the C-terminal domain of the ChlD subunit play a major role in conferring Mg(2+) cooperativity upon magnesium chelatase. Biochemistry 54(44):6659–6662

Brusslan J, Peterson M (2002) Tetrapyrrole regulation of nuclear gene expression. Photosynth Res 71(3):185–194

Brzezowski P et al (2016) Mg chelatase in chlorophyll synthesis and retrograde signaling in Chlamydomonas reinhardtii: CHLI2 cannot substitute for CHLI1. J Exp Bot 67(13):3925–3938

Budzikiewicz H, Taraz K (1971) Chlorophyll c. Tetrahedron 27(7):1447–1460

Cahoon A, Timko M (2000) Yellow-in-the-dark mutants of Chlamydomonas lack the CHLL subunit of light-independent protochlorophyllide reductase. Plant Cell 12(4):559–568

Canniffe DP, Chidgey JW, Hunter CN (2014) Elucidation of the preferred routes of C8-vinyl reduction in chlorophyll and bacteriochlorophyll biosynthesis. Biochem J 462(3):433–440

Chekounova E et al (2001) Characterization of Chlamydomonas mutants defective in the H subunit of Mg-chelatase. Mol Gen Genomics 266(3):363–373

Chen M et al (2010) A red-shifted chlorophyll. Science 329(5997):1318–1319

Chen M et al (2012) A cyanobacterium that contains chlorophyll f--a red-absorbing photopigment. FEBS Lett 586(19):3249–3254

Chen X et al (2015a) Crystal structures of GUN4 in complex with porphyrins. Mol Plant 8(7):1125–1127

Chen X et al (2015b) Crystal structure of the catalytic subunit of magnesium chelatase. Nat Plant 1:15125

Chen GE et al (2016) Two unrelated 8-vinyl reductases ensure production of mature chlorophylls in Acaryochloris marina. J Bacteriol 198(9):1393–1400

Chen GE, Canniffe DP, Hunter CN (2017) Three classes of oxygen-dependent cyclase involved in chlorophyll and bacteriochlorophyll biosynthesis. Proc Natl Acad Sci U S A 114(24):6280–6285

Davison PA, Hunter CN (2011) Abolition of magnesium chelatase activity by the gun5 mutation and reversal by Gun4. FEBS Lett 585(1):183–186

Davison PA et al (2005) Structural and biochemical characterization of Gun4 suggests a mechanism for its role in chlorophyll biosynthesis. Biochemistry 44(21):7603–7612

Dorgan KM et al (2006) An enzyme-coupled continuous spectrophotometric assay for S-adenosylmethionine-dependent methyltransferases. Anal Biochem 350(2):249–255

Duanmu D, Rockwell NC, Lagarias JC (2017) Algal light sensing and photoacclimation in aquatic environments. Plant Cell Environ 40(11):2558–2570

Fairchild CD, Glazer AN (1994a) Nonenzymatic bilin addition to the alpha subunit of an apophycoerythrin. J Biol Chem 269(46):28988–28996

Fairchild CD, Glazer AN (1994b) Oligomeric structure, enzyme kinetics, and substrate specificity of the phycocyanin alpha subunit phycocyanobilin lyase. J Biol Chem 269(12):8686–8694

Fairchild CD et al (1992) Phycocyanin alpha-subunit phycocyanobilin lyase. Proc Natl Acad Sci U S A 89(15):7017–7021

Falciatore A et al (2005) The FLP proteins act as regulators of chlorophyll synthesis in response to light and plastid signals in Chlamydomonas. Genes Dev 19(1):176–187

Fodje MN et al (2001) Interplay between an AAA module and an integrin I domain may regulate the function of magnesium chelatase. J Mol Biol 311(1):111–122

Fookes C, Jeffrey S (1989) The structure of chlorophyll c3, a novel marine photosynthetic pigment. J Chem Soc Chem Commun 23:1827–1828

Formighieri C et al (2012) Retrograde signaling and photoprotection in a gun4 mutant of Chlamydomonas reinhardtii. Mol Plant 5(6):1242–1262

Frankenberg N, Lagarias JC (2003) Biosynthesis and biological functions of bilins. In: Kadish KM, Smith KM, Guilard R (eds) The porphyrin handbook. Academic, Amsterdam, pp 211–235

Fujita Y, Bauer CE (2003) The light-independent protochlorophyllide reductase: a nitrogenase-like enzyme catalysing a key reaction for greening in the dark. In: Kadish KM, Smith KM, Guilard R (eds) The porphyrin handbook. Academic, Amsterdam, pp 109–156

Fukusumi T et al (2012) Non-enzymatic conversion of chlorophyll-a into chlorophyll-d in vitro: a model oxidation pathway for chlorophyll-d biosynthesis. FEBS Lett 586(16):2338–2341

Gabruk M, Mysliwa-Kurdziel B (2015) Light-dependent protochlorophyllide oxidoreductase: phylogeny, regulation, and catalytic properties. Biochemistry 54(34):5255–5262

Gan F, Shen G, Bryant DA (2014a) Occurrence of far-red light photoacclimation (FaRLiP) in diverse cyanobacteria. Life (Basel, Switz) 5(1):4–24

Gan F et al (2014b) Extensive remodeling of a cyanobacterial photosynthetic apparatus in far-red light. Science 345(6202):1312–1317

Garg H et al (2017) The C2(1)-formyl group in chlorophyll f originates from molecular oxygen. J Biol Chem 292(47):19279–19289

Garrido JL, Brunet C, Rodríguez F (2016) Pigment variations in Emiliania huxleyi (CCMP370) as a response to changes in light intensity or quality. Environ Microbiol 18(12):4412–4425

Gibson LCD et al (1995) Magnesium-protoporphyrin chelatase of Rhodobacter sphaeroides: reconstitution of activity by combining the products of the bchH, -I, and -D genes expressed in Escherichia coli. Proc Natl Acad Sci U S A 92(6):1941–1944

Gibson LC, Jensen PE, Hunter CN (1999) Magnesium chelatase from Rhodobacter sphaeroides: initial characterization of the enzyme using purified subunits and evidence for a BchI-BchD complex. Biochem J 337(Pt 2):243–251

Glazer AN (1989) Light guides. Directional energy transfer in a photosynthetic antenna. J Biol Chem 264(1):1–4

Granick S (1949) The pheoporphyrin nature of chlorophyll c. J Biol Chem 179(1):505

Granick S (1961) Magnesium protoporphyrin monoester and protoporphyrin monomethyl ester in chlorophyll biosynthesis. J Biol Chem 236:1168–1172

Granick S, Kett R (1948) Magnesium protoporphyrin as a precursor of chlorophyll in Chlorella. J Biol Chem 175:333–342

Grasses T et al (2001) Loss of alpha-tocopherol in tobacco plants with decreased geranylgeranyl reductase activity does not modify photosynthesis in optimal growth conditions but increases sensitivity to high-light stress. Planta 213(4):620–628

Guo R, Luo M, Weinstein JD (1998) Magnesium chelatase from developing pea leaves. Plant Physiol 116:605–615

Hansson A et al (2002) Three semidominant barley mutants with single amino acid substitutions in the smallest magnesium chelatase subunit form defective AAA+ hexamers. Proc Natl Acad Sci U S A 99(21):13944–13949

Hennig M et al (1994) Crystallization and preliminary X-ray analysis of wild-type and K272A mutant glutamate 1-semialdehyde aminotransferase from Synechococcus. J Mol Biol 242(4):591–594

Hennig M et al (1997) Crystal structure of glutamate-1-semialdehyde aminomutase: an alpha2-dimeric vitamin B6-dependent enzyme with asymmetry in structure and active site reactivity. Proc Natl Acad Sci U S A 94(10):4866–4871

Henningsen K, Boynton J, Wettstein D (1993) Mutants at xantha and albina loci in relation to chloroplast biogenesis in barley (Hordeum vulgare L.). Biologiske Skrifter 42:1–349

Herbst J et al (2018) Potential roles of YCF54 and ferredoxin-NADPH reductase for magnesium protoporphyrin monomethylester cyclase. Plant J 94:485–496

Hess WR et al (2001) The photosynthetic apparatus of Prochlorococcus: insights through comparative genomics. Photosynth Res 70(1):53–71

Ho MY et al (2016) Light-dependent chlorophyll f synthase is a highly divergent paralog of PsbA of photosystem II. Science 353(6302):886

Hollingshead S et al (2012) Conserved chloroplast open-reading frame ycf54 is required for activity of the magnesium protoporphyrin monomethylester oxidative cyclase in Synechocystis PCC 6803. J Biol Chem 287(33):27823–27833

Huang P et al (2014) Functional analysis of carboxyl-terminal of Oryza sativa Gun4, a regulatory protein of magnesium chelatase. Zhongguo Shengwu Huaxue Yu Fenzi Shengwu Xuebao 30(10):1017–1024

Im C, Matters G, Beale S (1996) Calcium and calmodulin are involved in blue light induction of the Gsa gene for an early chlorophyll biosynthetic step in Chlamydomonas. Plant Cell 8(12):2245–2253

Jahn D (1992) Complex formation between glutamyl-tRNA synthetase and glutamyl-tRNA reductase during the tRNA-dependent synthesis of 5-aminolevulinic acid in Chlamydomonas reinhardtii. FEBS Lett 314(1):77–80

Jeffrey SW (1968) Two spectrally distinct components in preparations of chlorophyll c. Nature 220(5171):1032–1033

Jeffrey SW (1969) Properties of two spectrally different components in chlorophyll c preparations. Biochim Biophys Acta 177(3):456–467

Jensen PE et al (1996a) Expression of the chlI, chlD, and chlH genes from the Cyanobacterium synechocystis PCC6803 in Escherichia coli and demonstration that the three cognate proteins are required for magnesium-protoporphyrin chelatase activity. J Biol Chem 271(28):16662–16667

Jensen PE et al (1996b) Structural genes for Mg-chelatase subunits in barley: Xantha-f, -g and -h. Mol Gen Genet 250(4):383–394

Jordan P et al (2001) Three-dimensional structure of cyanobacterial photosystem I at 2.5Å resolution. Nature 411(6840):909–917

Jung LJ, Chan CF, Glazer AN (1995) Candidate genes for the phycoerythrocyanin alpha subunit lyase.

Biochemical analysis of pecE and pecF interposon mutants. J Biol Chem 270(21):12877–12884

Kaneko T et al (1996) Sequence analysis of the genome of the unicellular cyanobacterium Synechocystis sp. PCC6803. DNA Res 3(3):109–136

Kim JI et al (2017) Evolutionary dynamics of cryptophyte plastid genomes. Genome Biol Evol 9(7):1859–1872

Kobayashi M et al (1988) Chlorophyll a′/P-700 and pheophytin a/P-680 stoichiometries in higher plants and cyanobacteria determined by HPLC analysis. Biochim Biophys Acta Biomembr 936(1):81–89

Kronfel CM et al (2013) Structural and biochemical characterization of the bilin lyase CpcS from Thermosynechococcus elongatus. Biochemistry 52(48):8663–8676

Kunugi M, Takabayashi A, Tanaka A (2013) Evolutionary changes in chlorophyllide a oxygenase (CAO) structure contribute to the acquisition of a new light-harvesting complex in micromonas. J Biol Chem 288(27):19330–19341

Lake V, Willows R (2003) Rapid extraction of RNA and analysis of transcript levels in Chlamydomonas reinhardtii using real-time RT-PCR: magnesium chelatase chlH, chlD and chlI gene expression. Photosynth Res 77(1):69–76

Lake V et al (2004) ATPase activity of magnesium chelatase subunit I is required to maintain subunit D in vivo. Eur J Biochem 271(11):2182–2188

Larkin RM et al (2003) GUN4, a regulator of chlorophyll synthesis and intracellular signaling. Science 299(5608):902–906

Layer G, Krausze J, Moser J (2017) Reduction of chemically stable multibonds: nitrogenase-like biosynthesis of tetrapyrroles. Adv Exp Med Biol 925:147–161

Li Y et al (2012) Extinction coefficient for red-shifted chlorophylls: chlorophyll d and chlorophyll f. Biochim Biophys Acta 1817(8):1292–1298

Liu Z, Bryant DA (2011) Multiple types of 8-vinyl reductases for (bacterio)chlorophyll biosynthesis occur in many green sulfur bacteria. J Bacteriol 193(18):4996–4998

Lohr M, Im CS, Grossman AR (2005) Genome-based examination of chlorophyll and carotenoid biosynthesis in Chlamydomonas reinhardtii. Plant Physiol 138(1):490–515

Loughlin PC, Willows RD, Chen M (2014) In vitro conversion of vinyl to formyl groups in naturally occurring chlorophylls. Sci Rep 4:6069

Loughlin PC, Willows RD, Chen M (2015) Hydroxylation of the C132 and C18 carbons of chlorophylls by heme and molecular oxygen. J Porphyrins Phthalocyanines 19(9):1007–1013

Lundqvist J et al (2010) ATP-induced conformational dynamics in the AAA+ motor unit of magnesium chelatase. Structure 18:354–365

Lundqvist J et al (2013) Catalytic turnover triggers exchange of subunits of the magnesium chelatase AAA+ motor unit. J Biol Chem 288(33):24012–24019

Manning WM, Strain HH (1943) Chlorophyll d, a green pigment of red algae. J Biol Chem 151:1–19

McLean S, Hunter CN (2009) An enzyme-coupled continuous spectrophotometric assay for magnesium protoporphyrin IX methyltransferases. Anal Biochem 394(2):223–228

Meinecke L et al (2010) Chlorophyll-deficient mutants of Chlamydomonas reinhardtii that accumulate magnesium protoporphyrin IX. Plant Mol Biol 72:643–658

Merchant S et al (2007) The Chlamydomonas genome reveals the evolution of key animal and plant functions. Science 318(5848):245–250

Meskauskiene R, Apel K (2002) Interaction of FLU, a negative regulator of tetrapyrrole biosynthesis, with the glutamyl-tRNA reductase requires the tetratricopeptide repeat domain of FLU. FEBS Lett 532(1–2):27–30

Meskauskiene R et al (2001) FLU: a negative regulator of chlorophyll biosynthesis in Arabidopsis thaliana. Proc Natl Acad Sci U S A 98(22):12826–12831

Minamizaki K et al (2008) Identification of two homologous genes, chlAI and chlAII, that are differentially involved in isocyclic ring formation of chlorophyll a in the cyanobacterium Synechocystis sp. PCC 6803. J Biol Chem 283(5):2684–2692

Miyashita H et al (1997) Pigment composition of a novel oxygenic photosynthetic prokaryote containing chlorophyll d as the major chlorophyll. Plant Cell Physiol 38(3):274–281

Mochizuki N et al (2001) Arabidopsis genomes uncoupled 5 (GUN5) mutant reveals the involvement of Mg-chelatase H subunit in plastid-to-nucleus signal transduction. Proc Natl Acad Sci U S A 98(4):2053–2058

Moseley J et al (2000) The Crd1 gene encodes a putative di-iron enzyme required for photosystem I accumulation in copper deficiency and hypoxia in Chlamydomonas reinhardtii. EMBO J 19(10):2139–2151

Moseley J et al (2002) Reciprocal expression of two candidate di-iron enzymes affecting photosystem I and light-harvesting complex accumulation. Plant Cell 14(3):673–688

Moser J et al (2001) V-shaped structure of glutamyl-tRNA reductase, the first enzyme of tRNA-dependent tetrapyrrole biosynthesis. EMBO J 20(23):6583–6590

Moser J et al (2013) Structure of ADP-aluminium fluoride-stabilized protochlorophyllide oxidoreductase complex. Proc Natl Acad Sci U S A 110(6):2094–2098

Muller AH et al (2014) Inducing the oxidative stress response in Escherichia coli improves the quality of a recombinant protein: magnesium chelatase ChlH. Protein Expr Purif 101:61–67

Nagata N et al (2005) Identification of a vinyl reductase gene for chlorophyll synthesis in Arabidopsis thaliana and implications for the evolution of Prochlorococcus species. Plant Cell 17(1):233–240

Nascimento SMD, Zou Y, Cheng Q (2016) Review of studies on the last enzymes in bacteriochlorophyll (Bchl) and chlorophyll (Chl) biosynthesis. Am J Plant Sci 7(12):1639–1651

Nasrulhaq-Boyce A, Griffiths W, Jones O (1987) The use of continuous assays to characterize the oxidative cyclase that synthesizes the chlorophyll isocyclic ring. Biochem J 243(1):23–29

Nelson JR, Wakeham SG (1989) A phytol-substituted chlorophyll c from Emiliania huxleyi (Prymnesiophyceae). J Phycol 25(4):761–766

Nogaj L, Beale S (2005) Physical and kinetic interactions between glutamyl-tRNA reductase and glutamate-1-semialdehyde aminotransferase of Chlamydomonas reinhardtii. J Biol Chem 280(26):24301–24307

Nogaj L et al (2005) Cellular levels of glutamyl-tRNA reductase and glutamate-1-semialdehyde aminotransferase do not control chlorophyll synthesis in Chlamydomonas reinhardtii. Plant Physiol 139(1):389–396

Oba T et al (2011) A mild conversion from 3-vinyl- to 3-formyl-chlorophyll derivatives. Bioorg Med Chem Lett 21(8):2489–2491

Oster U, Bauer CE, Rudiger W (1997) Characterization of chlorophyll a and bacteriochlorophyll a synthases by heterologous expression in Escherichia coli. J Biol Chem 272(15):9671–9676

Oster U et al (2000) Cloning and functional expression of the gene encoding the key enzyme for chlorophyll b biosynthesis (CAO) from Arabidopsis thaliana. Plant J 21(3):305–310

Ouchane S et al (2004) Aerobic and anaerobic Mg-protoporphyrin monomethyl ester cyclases in purple bacteria: a strategy adopted to bypass the repressive oxygen control system. J Biol Chem 279(8):6385–6394

Overkamp KE et al (2014) Insights into the biosynthesis and assembly of cryptophycean phycobiliproteins. J Biol Chem 289(39):26691–26707

Petersen BL et al (1998) Reconstitution of an active magnesium chelatase enzyme complex from the bchI, -D, and -H gene products of the green sulfur bacterium Chlorobium vibrioforme expressed in Escherichia coli. J Bacteriol 180(3):699–704

Porra R, Scheer H (2001) 18O and mass spectrometry in chlorophyll research: derivation and loss of oxygen atoms at the periphery of the chlorophyll macrocycle during biosynthesis, degradation and adaptation. Photosynth Res 66(3):159–175

Porra R et al (1993) Derivation of the formyl-group oxygen of chlorophyll b from molecular oxygen in greening leaves of a higher plant (Zea mays). FEBS Lett 323(1–2):31–34

Porra RJ et al (1994) The derivation of the formyl-group oxygen of chlorophyll b in higher plants from molecular oxygen. Achievement of high enrichment of the 7-formyl-group oxygen from 18O2 in greening maize leaves. Eur J Biochem 219(1–2):671–679

Proctor MS et al (2018) Plant and algal chlorophyll synthases function in Synechocystis and interact with the YidC/Alb3 membrane insertase. FEBS Lett 592(18):3062–3073

Reid JD, Hunter CN (2002) Current understanding of the function of magnesium chelatase. Biochem Soc Trans 30(4):643–645

Richter AS et al (2016) Phosphorylation of genomes uncoupled 4 alters stimulation of Mg chelatase activity in angiosperms. Plant Physiol 172(3):1578–1595

Rissler H et al (2002) Chlorophyll biosynthesis. Expression of a second chl I gene of magnesium chelatase in Arabidopsis supports only limited chlorophyll synthesis. Plant Physiol 128(2):770–779

Rockwell NC, Lagarias JC (2017) Ferredoxin-dependent bilin reductases in eukaryotic algae: ubiquity and diversity. J Plant Physiol 217:57–67

Rüdiger W (2003) The last steps in chlorophyll synthesis. In: Kadish KM, Smith KM, Guilard R (eds) The porphyrin handbook. Academic, Amsterdam, pp 71–108

Saunee NA et al (2008) Biogenesis of phycobiliproteins: II. CpcS-I and CpcU comprise the heterodimeric bilin lyase that attaches phycocyanobilin to CYS-82 OF beta-phycocyanin and CYS-81 of allophycocyanin subunits in Synechococcus sp. PCC 7002. J Biol Chem 283(12):7513–7522

Sawicki A, Willows RD (2008) Kinetic analyses of the magnesium chelatase provide insights into the mechanism, structure, and formation of the complex. J Biol Chem 283(46):31294–31302

Sawicki A et al (2017) 1-N-histidine phosphorylation of ChlD by the AAA(+) ChlI2 stimulates magnesium chelatase activity in chlorophyll synthesis. Biochem J 474(12):2095–2105

Scheer H, Zhao KH (2008) Biliprotein maturation: the chromophore attachment. Mol Microbiol 68(2):263–276

Schliep M et al (2010) 18O labeling of chlorophyll d in Acaryochloris marina reveals that chlorophyll a and molecular oxygen are precursors. J Biol Chem 285(37):28450–28456

Schluchter WM et al (2010) Phycobiliprotein biosynthesis in cyanobacteria: structure and function of enzymes involved in post-translational modification. In: Protein reviews. Springer Singapore, Springer New York, New York, pp 211–228

Shen G et al (2006) Identification and characterization of a new class of bilin lyase: the cpcT gene encodes a bilin lyase responsible for attachment of phycocyanobilin to Cys-153 on the beta-subunit of phycocyanin in Synechococcus sp. PCC 7002. J Biol Chem 281(26):17768–17778

Shen G, Schluchter WM, Bryant DA (2008) Biogenesis of phycobiliproteins – I. cpcS-I and cpcU mutants of the cyanobacterium Synechococcus sp PCC 7002 define a heterodimeric phyococyanobilin lyase specific for beta-phycocyanin and allophycocyanin subunits. J Biol Chem 283(12):7503–7512

Shepherd M, Hunter CN (2004) Transient kinetics of the reaction catalysed by magnesium protoporphyrin IX methyltransferase. Biochem J 382(Pt 3):1009–1013

Shepherd M, McLean S, Hunter C (2005) Kinetic basis for linking the first two enzymes of chlorophyll biosynthesis. FEBS J 272(17):4532–4539

Shin SE et al (2016) CRISPR/Cas9-induced knockout and knock-in mutations in Chlamydomonas reinhardtii. Sci Rep 6:27810

Six C et al (2007) Diversity and evolution of phycobilisomes in marine Synechococcus spp.: a comparative genomics study. Genome Biol 8(12):R259

Sobotka R et al (2008) Importance of the cyanobacterial Gun4 protein for chlorophyll metabolism and assembly of photosynthetic complexes. J Biol Chem 283(38):25794–25802

Srivastava A et al (2005) The Chlamydomonas reinhardtii gtr gene encoding the tetrapyrrole biosynthetic enzyme glutamyl-tRNA reductase: structure of the gene and properties of the expressed enzyme. Plant Mol Biol 58(5):643–658

Stephenson PG, Terry MJ (2008) Light signalling pathways regulating the Mg-chelatase branchpoint of chlorophyll synthesis during de-etiolation in Arabidopsis thaliana. Photochem Photobiol Sci 7(10):1243–1252

Stiller JW et al (2014) The evolution of photosynthesis in chromist algae through serial endosymbioses. Nat Commun 5(1):5764

Surpin M, Larkin R, Chory J (2002) Signal transduction between the chloroplast and the nucleus. Plant Cell 14:S327–S338

Swanson RV et al (1992) Characterization of phycocyanin produced by cpcE and cpcF mutants and identification of an intergenic suppressor of the defect in bilin attachment. J Biol Chem 267(23):16146–16154

Tanaka A, Ito H, Okada K (1998) Chlorophyll a oxygenase (CAO) is involved in chlorophyll b formaiton from chlorophyll a. Proc Natl Acad Sci U S A 95(21):12719

Tanaka R et al (2001) Overexpression of chlorophyllide a oxygenase (CAO) enlarges the antenna size of photosystem II in Arabidopsis thaliana. Plant J 26(4):365–373

Tarahi Tabrizi S et al (2015) Structure of GUN4 from Chlamydomonas reinhardtii. Acta Crystallogr Sect F 71:1094–1099

Tarahi Tabrizi S et al (2016) GUN4-protoporphyrin IX is a singlet oxygen generator with consequences for plastid retrograde signalling. J Biol Chem 291:8978–8984

Tomitani A et al (1999) Chlorophyll b and phycobilins in the common ancestor of cyanobacteria and chloroplasts. Nature 400(6740):159–162

van Lis R et al (2005) Subcellular localization and light-regulated expression of protoporphyrinogen IX oxidase and ferrochelatase in Chlamydomonas reinhardtii. Plant Physiol 139(4):1946–1958

Vasileuskaya Z, Oster U, Beck C (2005) Mg-protoporphyrin IX and heme control HEMA, the gene encoding the first specific step of tetrapyrrole biosynthesis, in Chlamydomonas reinhardtii. Eukaryot Cell 4(10):1620–1628

Verdecia MA et al (2005) Structure of the Mg-chelatase cofactor GUN4 reveals a novel hand-shaped fold for porphyrin binding. PLoS Biol 3(5):12

Vijayan P, Whyte B, Castelfranco P (1992) A spectrophotometric analysis of the magnesium protoporphyrin IX monomethyl ester (oxidative) cyclase. Plant Physiol Biochem (Paris) 30(3):271–278

Viney J et al (2007) Direct measurement of metal-ion chelation in the active site of the AAA+ ATPase magnesium chelatase. Biochemistry 46(44):12788–12794

Vothknecht U, Kannangara C, von Wettstein D (1998) Barley glutamyl tRNAGlu reductase: mutations affecting haem inhibition and enzyme activity. Phytochemistry 47(4):513–519

Walker CJ, Weinstein JD (1991) In vitro assay of the chlorophyll biosynthetic enzyme magnesium chelatase: resolution of the activity into soluble and membrane bound fractions. Proc Natl Acad Sci U S A 88(13):5789–5793

Walker CJ, Willows RD (1997) Mechanism and regulation of Mg-chelatase. Biochem J 327(Pt 2):321–333

Walker CJ et al (1988) The magnesium-protoporphyrin IX (oxidative) cyclase system. Studies on the mechanism and specificity of the reaction sequence. Biochem J 255(2):685–692

Walker CJ, Castelfranco PA, Whyte BJ (1991) Synthesis of divinyl protochlorophyllide. Enzymological properties of the Mg-protoporphyrin IX monomethyl ester oxidative cyclase system. Biochem J 276(Pt 3):691–697

Walker CJ, Hupp LR, Weinstein JD (1992) Activation and stabilization of Mg-chelatase activity by ATP as revealed by a novel in vitro continuous assay. Plant Physiol Biochem 30(3):263–269

Wang W-Y et al (1974) Genetic control of chlorophyll biosynthesis in chlamydomonas: analysis of mutants at two loci mediating the conversion of protoporphyrin-IX to magnesium protoporphyrin. J Cell Biol 63:806–823

Wang P et al (2013) One divinyl reductase reduces the 8-vinyl groups in various intermediates of chlorophyll biosynthesis in a given higher plant species, but the isozyme differs between species. Plant Physiol 161(1):521–534

Whyte B, Castelfranco P (1993) Further observations on the Mg-protoporphyrin IX monomethyl ester (oxidative) cyclase system. Biochem J 290(Pt 2):355–359

Whyte B, Fijayan P, Castelfranco P (1992) In vitro synthesis of protochlorophyllide: effects of magnesium and other cations on the reconstituted (oxidative) cyclase. Plant Physiol Biochem (Paris) 30(3):279–284

Wilde A et al (2004) The gun4 gene is essential for cyanobacterial porphyrin metabolism. FEBS Lett 571(1–3):119–123

Willows R, Beale S (1998) Heterologous expression of the Rhodobacter capsulatus BchI, -D, and -H genes that encode magnesium chelatase subunits and characterization of the reconstituted enzyme. J Biol Chem 273(51):34206–34213

Willows RD et al (1996) Three separate proteins constitute the magnesium chelatase of Rhodobacter sphaeroides. Eur J Biochem 235(1/2):438–443

Willows RD et al (1999) Crystallization and preliminary X-ray analysis of the Rhodobacter capsulatus magnesium chelatase BchI subunit. Acta Crystallogr D Biol Crystallogr 55(Pt 3):689–690

Wittkopp TM et al (2017) Bilin-dependent photoacclimation in Chlamydomonas reinhardtii. Plant Cell 29(11):2711–2726

Wong Y-S, Castelfranco PA (1984) Resolution and reconstitution of Mg-protoporphyrin IX monomethyl ester (oxidative) cyclase, the enzyme system responsible for the formation of the chlorophyll isocyclic ring. Plant Physiol 75:658–661

Yamanashi K, Minamizaki K, Fujita Y (2015) Identification of the chlE gene encoding oxygen-independent Mg-protoporphyrin IX monomethyl ester cyclase in cyanobacteria. Biochem Biophys Res Commun 463(4):1328–1333

Zapata M, Garrido JL (1997) Occurance of phytylated chlorophyll c in Isochrysis galbana and Isocrysis sp (clone T-ISO) (Prymnesiophyceae). J Phycol 33:209–214

Zhang H et al (2015) A point mutation of magnesium chelatase OsCHLI gene dampens the interaction between CHLI and CHLD subunits in rice. Plant Mol Biol Report 33(6):1975–1987

Zhao KH et al (2000) Novel activity of a phycobiliprotein lyase: both the attachment of phycocyanobilin and the isomerization to phycoviolobilin are catalyzed by the proteins PecE and PecF encoded by the phycoerythrocyanin operon. FEBS Lett 469(1):9–13

Zhao KH et al (2007) Lyase activities of CpcS- and CpcT-like proteins from Nostoc PCC7120 and sequential reconstitution of binding sites of phycoerythrocyanin and phycocyanin beta-subunits. J Biol Chem 282(47):34093–34103

Zhao C et al (2017) Structures and enzymatic mechanisms of phycobiliprotein lyases CpcE/F and PecE/F. Proc Natl Acad Sci U S A 114(50):13170–13175

Zhou J et al (1992) The cpcE and cpcF genes of Synechococcus sp. PCC 7002. Construction and phenotypic characterization of interposon mutants. J Biol Chem 267(23):16138–16145

Zhou S et al (2012) C-terminal residues of Oryza sativa GUN4 are required for the activation of the ChlH subunit of magnesium chelatase in chlorophyll synthesis. FEBS Lett 586(3):205–210

Zhou W et al (2014) Structure and mechanism of the phycobiliprotein Lyase CpcT. J Biol Chem 289(39):26677–26689

Part III

Biochemistry and Physiology of Algae

Chapter 6

Chloroplast Ion and Metabolite Transport in Algae

Justine Marchand, Parisa Heydarizadeh, and Benoît Schoefs*
Metabolism, Bioengineering of Microalgal Molecules and Applications (MIMMA), Mer Molécules Santé, IUML – FR 3473 CNRS, Le Mans University, Le Mans, France

and

Cornelia Spetea*
Department of Biological and Environmental Sciences, University of Gothenburg, Gothenburg, Sweden

I. Introduction

The chloroplast is an organelle specific for eukaryotic oxygenic photosynthetic organisms, namely algae and land plants. It is mostly known for being the host of a fundamental process called oxygenic photosynthesis, which has generated molecular oxygen and organic molecules in the Earth's biosphere for billion years. In addition, the plas-

*Author for correspondence, e-mail: benoit.schoefs@univ-lemans.fr; cornelia.spetea.wiklund@bioenv.gu.se

A. W. D. Larkum et al. (eds.), *Photosynthesis in Algae: Biochemical and Physiological Mechanisms*, Advances in Photosynthesis and Respiration 45, https://doi.org/10.1007/978-3-030-33397-3_6

tid is the most prominent member of the family of eukaryotic organelles, involved in many biosynthetic pathways such as those for production of carotenoids, lipids, amino acids, phytohormones, etc. (Solymosi 2012; Solymosi and Keresztes 2012; Heydarizadeh et al. 2013). The chloroplast is a heavily compartmented organelle: being composed of the outer and the inner envelope surrounding the organelle, the soluble stroma, the thylakoid membrane, and the enclosed (lumenal) space.

How chloroplasts appeared during evolution remains a tremendously exciting question. Several hypotheses have been proposed. The strongest, and so far adopted one, is that proposed by Margulis (Margulis 1970), according to which ancestral anaerobic eukaryotes became able to ingest solid particles such as photosynthetic prokaryotes related to cyanobacteria. In some cases, the ingested cyanobacteria continued to live and eventually evolved into chloroplasts surrounded by two membranes (primary plastids). The fact that algal and land plant cells take benefits from the energy-rich carbohydrates produced by the chloroplast led Mereschkowsky in 1905 to postulate that the exchange of carbohydrates might have been crucial for the stability of the host-endosymbiont relationship (Martin and Kowallik 1999). However, a membrane potentially represents an insurmountable barrier for hydrophilic compounds such as carbohydrates. The crossing is even more difficult when the chloroplast is surrounded by three or four membranes (secondary plastids) (Solymosi 2012). Therefore, to gain access to the molecules produced by the endosymbiont, crossing of membranes must be facilitated (McFadden 2014). The facilitators are membrane-spanning transport proteins. Today, the chloroplast membranes (envelope and thylakoid) can be seen as selective filters across which different types of compounds such as small ions, metabolites and nucleotides are transported through channels, secondary transporters and primary transporters/pumps, classified according to the Transport Classification System (Saier Jr. et al. 2009).

It is clearly established that the optimal function of a photosynthetic cell relies on chloroplast activity. Chloroplasts are sensitive to changes in the intensity of the environmental constraints (Spetea et al. 2014) and have developed strategies to survive the stress. Many of these strategies require changes in the nuclear gene expression, that are mediated by chloroplast signals sent to the nucleus (retrograde signalling, Gollan et al. 2015). According to the current knowledge in land plants, retrograde signalling would involve the transport out of the chloroplast of signal transduction components such as Ca^{2+} ions (Kmiecik et al. 2016), reactive oxygen species (ROS) (Galvez-Valdivieso and Mullineaux 2010), isoprenoid precursors: (Xiao et al. 2012), chlorophyll-precursors (Mochizuki et al. 2001; Strand et al. 2003; Woodson et al. 2011), nucleotide derivatives (Estavillo et al. 2011), carotenoid-derivatives (Ramel et al. 2012; Avendano-Vazquez et al. 2014) and various small metabolites (Schmitz et al. 2014).

It is evident that gene loss and lateral gene transfer have played an important role in the evolution of unicellular eukaryotic algae, as witnessed by comparative genomic studies of diatoms and red algae (Yoon et al. 2004; Chap. 2). These have resulted in modification of the transporter repertoire and/or their activity to satisfy the cell metabolic demands. A deeper knowledge in transporters of algae is required for the reconstruction of genome-scale metabolic networks and prediction of metabolic fluxes in 'control' environment as well as for studying the impact of mutations or changes in the environmental constraints on metabolic fluxes (Heydarizadeh et al. 2014; Weisse et al. 2015; Kim et al. 2016).

Extensive reviews and a Research Topic have been recently dedicated to ion and metabolite transport in the chloroplast of land plants (Spetea et al. 2016; Spetea et al. 2017; Szabo and Spetea 2017). In this chapter, we review the current knowledge about

Table 6.1. Characterized and predicted transport proteins in the chloroplast of algae. Yes, gene present; No, gene absent; n.d. not determined. The source of the data is indicated in the last column

			Algae						
		Land plant	Green algae	Diatoms	Red algae	Glaucophytes	Cryptophytes		
Type of transport protein	Substrate	*Arabidopsis thaliana*	*Chlamydomonas reinhardtii, Volvox carteri*	*Thalassiosira pseudonana, Phaeodactylum tricornutum*	*Galdiera sulphuraria, Cyanidioschyzon merolae*	*Cyanophora paradoxa*	*Guillardia theta*	Chloroplast localization	References
Voltage-dependent Cl^- channels (VCCN)	Cl^-	AtVCCN1, AtVCCN2	Yes	Yes	Yes	No	No	Thylakoid	Duan et al. (2016) and Herdean et al. (2016b)
Cl^- channels (CLC)	Cl^-	AtCLCe	CLV1, CLV4	Yes	No	No	Yes	Thylakoid	Marmagne et al. (2007), Pfeil et al. (2014), Herdean et al. (2016a) and Li et al. (2019a)
Mechanosensitive channels (MSL)	Cl^-	AtMSL2, AtMSL3	MSC1	Yes	Yes	Yes	Yes	Envelope	Haswell and Meyerowitz (2006), Nakayama et al. (2007), Verret et al. (2010) and Hamilton et al. (2015)
Two-pore K^+ channels (TPK)	K^+	AtTPK3	No	Yes	No	No	No	Thylakoid	Carraretto et al. (2013) and Pfeil et al. (2014)
Glutamate receptor (GLR)	Ca^{2+}	AtGLR3.4, AtGLR3.5	GLR3.4	Yes	No	No	No	Envelope	Teardo et al. (2011), Teardo et al. (2015), De Bortoli et al. (2016) and Li et al. (2019a)
Phosphate transporters (PHT)	Pi, H^+, Na^+	AtPHT4;1	PHT3	No	Yes	No	No	Thylakoids	Guo et al. (2008), Pavon et al. (2008), Pfeil et al. (2014) and Li et al. (2019a)
	Pi, H^+, ascorbate	AtPHT4;4	Yes	No	Yes	No	No	Envelope	Guo et al. (2008), Pfeil et al. (2014) and Miyaji et al. (2015)
	Pi, H^+	AtPHT2;1	Only charophytes	No	No	No	No	Envelope	Versaw and Harrison (2002) and Bonnot et al. (2017)
Nitrite transporters	NO_2^-	CsNrt1-L	NAR1.1	Yes	n.d.	n.d.	n.d.	Envelope	Rexach et al. (2000), Mariscal et al. (2006) and Pearson et al. (2015)

(continued)

Table 6.1. (continued)

			Algae						
		Land plant	Green algae	Diatoms	Red algae	Glaucophytes	Cryptophytes		
Type of transport protein	Substrate	*Arabidopsis thaliana*	*Chlamydomonas reinhardtii, Volvox carteri*	*Thalassiosira pseudonana, Phaeodactylum tricornutum*	*Galdiera sulphuraria, Cyanidioschyzon merolae*	*Cyanophora paradoxa*	*Guillardia theta*	Chloroplast localization	References
K^+/H^+ exchanger (KEA)	K^+, H^+	AtKEA1, AtKEA2, AtKEA3	Yes	No	Yes	No	Yes	Envelope (KEA1/2), thylakoid (KEA3)	Chanroj et al. (2012), Armbruster et al. (2014), Kunz et al. (2014) and Pfeil et al. (2014)
H^+/Cation exchagers (CAX)	Mn^{2+}	AtPAM71/ BICAT2 AtCMT1/ BICAT1	CGLD1, CMT1	No	Yes	No	No	Thylakoid (PAM71) Envelope (CMT1)	Schneider et al. (2016), Wang et al. (2016), Xing et al. (2017), Eisenhut et al. (2018) and Frank et al. (2019)
Magnesium transproters (MRS)	Mg^{2+}	AtMGT10	MGT10	n.d.	n.d.	n.d.	Yes	Envelope	Drummond et al. (2006), Saito et al. (2013), Liang et al. (2017) and Li et al. (2019a)
Iron transporters (PIC1/NicO)	Fe^{2+}	AtPIC1 AtNicO	Yes	n.d.	n.d.	n.d.	n.d.	Envelope/ thylakoid	Duy et al. (2011), Blaby-Haas and Merchant (2012) and Lopez-Millan et al. (2016)
Fe-deficiency-related proteins (FDR)	Fe^{2+}	ZmFDR3,4	Yes	n.d.	n.d.	n.d.	n.d.	Envelope/ thylakoid	Han et al. (2009) and Zhang et al. (2017)
Heavy metal associated proteins (HMA)	Cu^+	AtHMA8/ PAA2	CrHMA2–5	Yes, no cTP	No	No	n.d.	Thylakoids	Abdel-Ghany et al. (2005), Hanikenne and Baurain (2013), Pfeil et al. (2014), Guo et al. (2015) and Sautron et al. (2015)
	Cu^+, Ca^{2+}, Zn^{2+}, Cd^{2+}, Co^{2+}	AtHMA1	CrHMA1	Yes	Yes	Yes	n.d.	Envelope	Hanikenne and Baurain (2013), Boutigny et al. (2014) and Karkar et al. (2015)
	Cu^{2+}	AtHMA6	Yes	Yes, no cTP	No	No	n.d.	Envelope	Abdel-Ghany et al. (2005), Hanikenne and Baurain (2013), Pfeil et al. (2014) and Guo et al. (2015)

ABC cassette transporters (ABC)	Fe-S	AtNAP7 AtSufABSE	SufBCD	No	Yes	Yes	No	Envelope	Xu and Moller (2004), Hirabayashi et al. (2015) and Lane et al. (2016)
	SO_4^{2-}	AtSULTR3;1	SulP, SulP2, Sbp, Sabc	No	Yes	No	No	Envelope	Lindberg and Melis (2008)
Plastidic nucleotide translocators (NTT)	ATP, ADP	AtNTT1, AtNTT2	No	No	GsNTT	CpNTT	No	Envelope	Linka et al. (2003), Reiser et al. (2004) and Weber and Linka (2011)
	H^+, ATP	No	No	PtNTT1, TpNTT1	No	No	No	n.d.	Ast et al. (2009)
	ATP, dNTP	No	No	PtNTT2, TpNTT2	No	No	No	n.d.	Ast et al. (2009)
Thylakoid ATP/ ADP carrier (TAAC)	ATP, ADP, PAPS	AtTAAC/ PAPST	Yes	No	No	No	No	Envelope, thylakoids	Thuswaldner et al. (2007), Spetea et al. (2011) and Gigolashvili et al. (2012)
Triose-phosphate translocators (TPT)	G3P, DHAP, 3-PGA, Pi	AtTPT	Yes	n.d.	GsTPT	No	n.d.	Envelope	Flugge (1999), Linka et al. (2008), Weber and Linka (2011) and Johnson and Alric (2013)
	DHAP, PEP, Pi	No	No	PtTPT1, PtTPT2, PtTPT4a and PtTPT4b	No	No	GtTP1, GtTPT2	Envelope	Haferkamp et al. (2006) and Moog et al. (2015)
Phospho*enol* pyruvate translocators (PPT)	PEP, Pi	AtPPT	Yes	n.d.	GsPPT	n.d.	n.d.	Envelope	Flugge (1999), Weber et al. (2006), Linka et al. (2008) and Weber and Linka (2011)
Glucose 6-phosphate translocators (GPT)	Glc6P, G3P, 3-PGA, Pi	AtGPT	Yes	No	Yes, distinct substrate	No	No	Envelope	Linka et al. (2008) and Weber and Linka (2011)
Xylulose 5-phosphate translocators (XPT)	Xul5P, G3P, 3-PGA, Pi	AtXPT	Yes	Yes	Yes, distinct substrate	No	No	Envelope	Eicks et al. (2002), Flugge and Gao (2005), Linka et al. (2008) and Weber and Linka (2011)
UhpC transporter	Glc6P?	No	Yes	No	GsUhpC, CmUhpC	CpUhpC1, CpUhpC2	No	Envelope	Price et al. (2012) and Karkar et al. (2015)

(continued)

Table 6.1. (continued)

		Land plant	Algae						
			Green algae	Diatoms	Red algae	Glaucophytes	Cryptophytes		
Type of transport protein	Substrate	*Arabidopsis thaliana*	*Chlamydomonas reinhardtii, Volvox carteri*	*Thalassiosira pseudonana, Phaeodactylum tricornutum*	*Galdiera sulphuraria, Cyanidioschyzon merolae*	*Cyanophora paradoxa*	*Guillardia theta*	Chloroplast localization	References
Bicarbonate transporters	HCO_3^-, NO_2^-	n.d.	LCIA (NAR1;2)	Yes	n.d.	n.d.	n.d.	Envelope	Mukherjee (2013), Yamano et al. (2015) and Mackinder et al. (2017)
	HCO_3^-	AtBASS4	CIA8	Yes	n.d.	n.d.	n.d.	Thylakoid	Machingura et al. (2017)
	HCO_3^-?	No	CCP1, CCP2	n.d.	n.d.	n.d.	n.d.	Envelope	Spalding (2008) and Yamano and Fukuzawa (2009)
	HCO_3^-	n.d.	MITC11	Yes	n.d.	n.d.	n.d.	Chloroplast predicted	Brueggeman et al. (2012), Jungnick et al. (2014) and Kustka et al. (2014)
	HCO_3^-	n.d.	LCI11	TpBest1, TpBest2	n.d.	n.d.	n.d.	Thylakoid?	Qu and Hartzell (2008), Brueggeman et al. (2012), Kustka et al. (2014) and Mackinder et al. (2017)
	H^+,?	Cem	YCF10	n.d.	n.d.	n.d.	n.d.	Envelope	Spalding (2008) and Li et al. (2019a)
Organic acid transporters	OAA, Malate	At DiT1	LCI20	n.d.	n.d.	n.d.	n.d.	Envelope	Terashima et al. (2011) and Johnson and Alric (2013)
	Glycolate, glycerate	AtPLGG1	Yes	Yes	Yes	n.d.	n.d.	Chloroplast-prediction	Eisenhut et al. (2015)
	Glu, Asp	AtDiT2;1	Yes	n.d.	No	n.d.	n.d.	Envelope	Werner-Washburne and Keegstra (1985) and Eisenhut et al. (2015)
Amino acid transporters (PRAT)	Amino acids	AtPRAT	Yes	n.d.	n.d.	n.d.	n.d.	Envelope	Murcha et al. (2007), Pudelski et al. (2010) and Rossig et al. (2013)
Fatty acid transporters (FAX)	Fatty acids	AtFAX1–4	CrFAX1, CrFAX2	No	No	No	No	Envelope	Valenzuela et al. (2012), Li et al. (2015), Li et al. (2016) and Li et al. (2019b)
Lipid ABC transporters	PC, PG, DAG	AtTGD1–3	CrTGD2	n.d.	n.d.	n.d.	n.d.	Envelope	Lu et al. (2007) and Warakanont et al. (2015)

transport of ions and metabolites in algal chloroplasts. Table 6.1 includes information about transport proteins which were either characterized or predicted as land plant homologues in algal models for green algae: *Chlamydomonas reinhardtii* (*C. reinhardtii*) and *Volvox carteri* (*V. carteri*), red algae: *Galdiera sulphuraria* (*G. sulphuraria*) and *Cyanidioschyzon merolae* (*C. merolae*), diatoms: *Thalassiosira pseudonana* (*T. pseudonana*) and *Phaeodactylum tricornutum* (*P. tricornutum*), glaucophytes: *Cyanophora paradoxa* (*C. paradoxa*) and cryptophytes: *Guillardia theta* (*G. theta*). Figures 6.1 and 6.2 provide an overview of transport proteins in green algae, red algae and diatoms for ions and metabolites, respectively.

II. Chloroplast Ion Transport

Ions are involved in many biosynthetic pathways and physiological processes in all types of organisms and cells. Ions are critical for the pH, volume and osmoregulation of intracellular compartments as well as for intercellular communication. When present in non-adequate amounts, ions may cause stress-related symptoms (e.g., Masmoudi et al. 2013). Ions have to be imported from the cytosol to reach the various plastid sub-

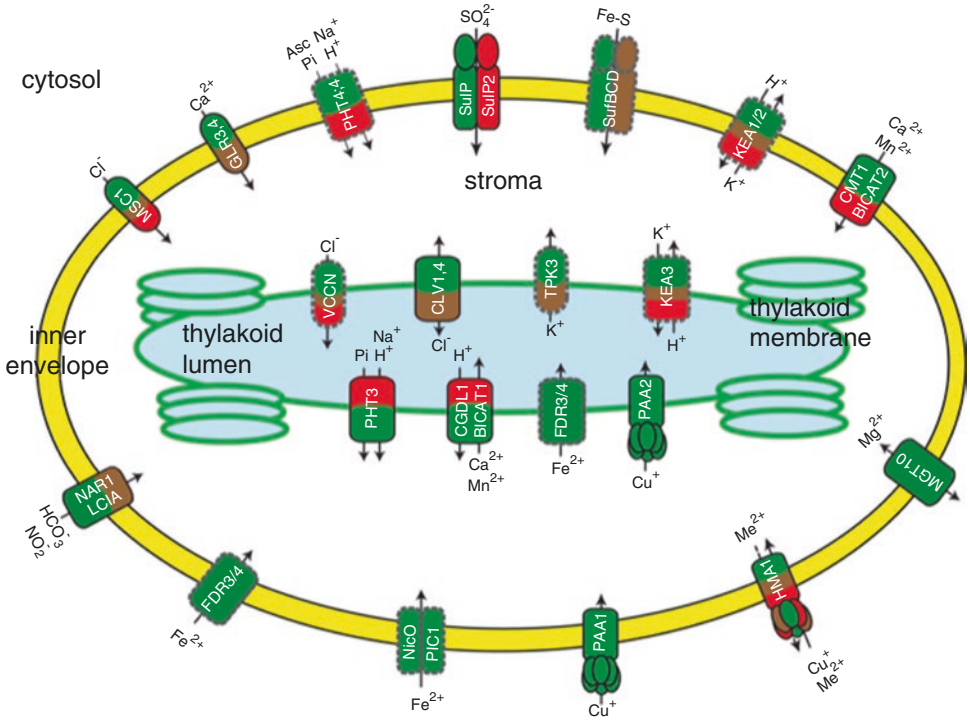

Fig. 6.1. **Current picture of ion transport proteins in chloroplast envelope and thylakoid membranes from algae**. Proteins identified or characterized in at least one algal model are framed with continuous black line. Plant homologues genes coding for putative transporters in algae are framed with broken grey line. Green algae, red algae and diatoms are represented in green, red and brown, respectively

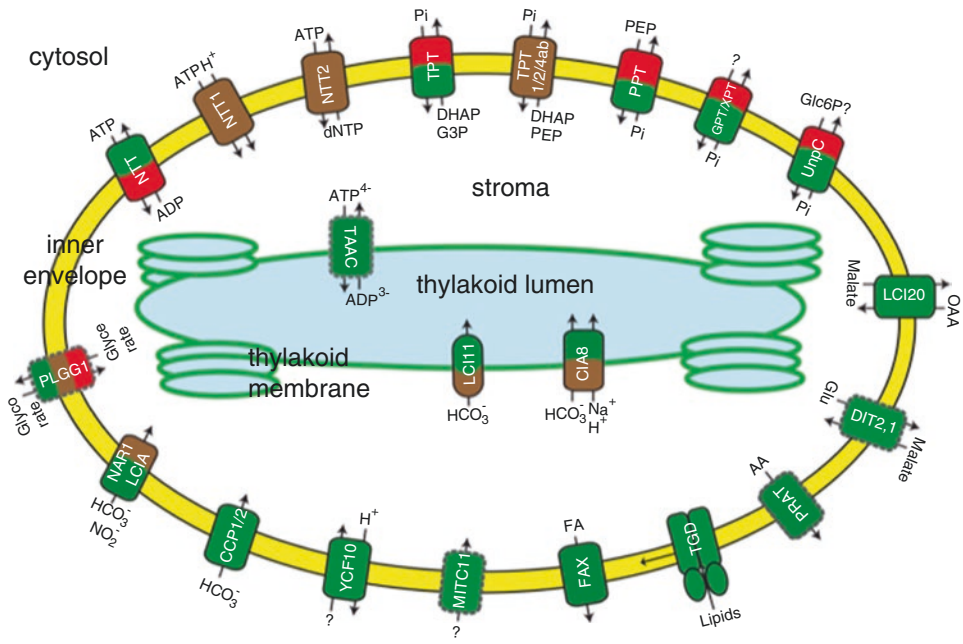

Fig. 6.2. **Current picture of metabolite transport proteins in chloroplast envelope and thylakoid membranes from algae**. Proteins identified or characterized in at least one algal model are framed with continuous black line. Plant homologues genes coding for putative transporters found in algae are framed with broken grey line. Green algae, red algae and diatoms are represented in green, red and brown, respectively

compartments of algae. Because of the charged nature of ions, they cannot spontaneously cross membranes and need to be translocated by ion channels, secondary transporters and pumps. Channels transport ions down their free energy gradient without consuming ATP. Pumps need ATP to transport ions across membranes, whereas secondary transporters (symporters and antiporters) use the concentration gradient of a co-transported ion.

Main anions used in the chloroplast are chloride (Cl^-: regulation of proton-motive force, osmosis, oxygen evolution), phosphate (Pi: ATP formation), sulfate (SO_4^{2-}: formation of cysteine and methionine), nitrite (NO_2^-: nitrogen assimilation) and bicarbonate (HCO_3^-: carbon assimilation) (Spetea and Schoefs 2010). The most abundant cation in the chloroplast is potassium (K^+), used in osmosis and regulation of proton-motive force, but divalent cations such as calcium, magnesium, manganese and iron (Ca^{2+}, Mg^{2+}, Mn^{2+} and Fe^{2+}) are also present since they are required as cofactors for enzymes, signaling, water oxidation, electron transport and thylakoid organization (Spetea and Schoefs 2010). Despite multiple evidence for ion–dependent activities in the chloroplast, the identity of the dedicated transport proteins is in most cases lacking in algae and even in land systems (Finazzi et al. 2014; Pfeil et al. 2014; Marchand et al. 2018).

A. Ion Channels

Within this superfamily, voltage-gated ion channels regulate ion conductance in response to changes in the voltage across the membrane. This family of ion channels shares a common structural and functional domain called the voltage sensor domain, which is able to detect fluctuations in the voltage across the membrane. The electrical energy generated in this domain during voltage activation is then transduced to the pore domain, leading to the opening of the chan-

nel. The pore domain contains a selectivity filter that determines which ions can permeate through the channel (Gouaux and Mackinnon 2005).

1. Voltage-Dependent Chloride Channels

Evidence for the existence of voltage-dependent anion channel activities has been reported for thylakoid membranes from the giant-celled charophyte alga *Nitellopsis obtusa* (Pottosin and Schönknecht 1995) and also from land plants (Schönknecht et al. 1988; Enz et al. 1993). It was only in the recent years that genes have been annotated with functions for such activities. In *Arabidopsis thaliana* thylakoids, two types of Cl^- channels have been characterized, namely the CLCe member of the CLC family (Marmagne et al. 2007; Herdean et al. 2016a), and the VCCN member of a new family of voltage-dependent chloride channels (VCCN1 and VCCN2; Duan et al. 2016, Herdean et al. 2016b). Phylogenetic analyses revealed candidates for CLCe-like genes in green algae, diatoms and cryptophytes (Pfeil et al. 2014), whereas candidates for *VCCN*-like genes were found in green algae, red algae, diatoms and cryptophytes (Herdean et al. 2016b). Mutants of two CLCe homologues in *Chlamydomonas reinhardtii* (CLV1 and CLV4) were found deficient in photosynthetic growth (Li et al. 2019a). The low-CO_2-inducible 11 protein (LCI11) from the same green alga is a weak homologue of VCCN1 and is discussed in Sect. III.C. It remains to be determined whether VCCN1- and CLCe-like proteins transport Cl^- or other anions in algae, and if they are involved in regulation of photosynthesis or other processes in the chloroplast.

2. Mechanosensitive Ion Channels

Acclimation to osmotic shock in living organisms relies on the presence of mechanosensitive ion channels (MscS; Martinac 2004). All analysed photosynthetic eukaryotes have at least one MscS-like (MSL) sequence (Verret et al. 2010). The chloroplast envelope of *A. thaliana* harbors two envelope-located MSL proteins (MSL2 and MSL3), which are hypothesized as Ca^{2+}-permeable channels affecting chloroplast shape and size (Haswell and Meyerowitz 2006). They are activated by increased membrane tension, which can happen during normal growth and development as well as under osmotic stress. One mechanosensitive ion channel named MSC1 was identified in *C. reinhardtii* as a homologue of *Escherichia coli* (*E. coli*) MscS and was localized to the chloroplast (Nakayama et al. 2007). The MSC1 channel displayed a strong preference for anions over cations. The Cl^- ion is proposed as the most likely substrate, and to be important for chloroplast morphology in *C. reinhardtii* (Nakayama et al. 2007).

3. K^+ Channels

Although K^+ is the major cation in the chloroplast and transport activities have been reported and hypothesized to affect photosynthesis (Pottosin and Dobrovinskaya 2015), no algal genes for K^+ channels have been thus far identified. Neverthless, identification of TPK3 in thylakoids from *A. thaliana* has confirmed this hypothesis (Carraretto et al. 2013). No algal homologues of TPK3 have been characterized thus far although putative sequences in green algae and diatoms have been revealed by phylogenetic analyses (Pfeil et al. 2014).

4. Ca^{2+} Channels

Ionotropic glutamate receptors (iGLRs) have a non-selective cation channel activity regulated by a broad range of amino acids. GLR3.4 and GLR3.5 have been localized to the chloroplast envelope in *A. thaliana* and function in Ca^{2+} influx, as indicated by electophysiological experiments in heterologous system (Teardo et al. 2011; Teardo et al. 2015). GLR-like sequences were found among the algal sequences (cryptophytes, diatoms, brown and green algae), but it appears that GLRs of land plants are not

closely related to the GLRs of green algae (De Bortoli et al. 2016). This would suggest that they play different physiological roles. Indeed, mutants of a GLR3.4 homologue in *C. reinhardtii* were found deficient of photosynthetic growth (Li et al. 2019a), whereas *A. thaliana* knock-out plants showed only a slight decrease in photosynthetic yield (Teardo et al. 2011).

B. Ion Transporters

Photosynthetic organisms also employ ion exchange proteins in addition to channels. In contrast to channels, they can drive transport against an electrochemical gradient and for this require co-transport of another ion usually H^+.

1. Phosphate Transporters

In land plants, transporters driving the net flow of Pi into the chloroplast belong to the PHT2 and PHT4 families. They have been intensively studied in *A. thaliana,* and include members localized to either the envelope: PHT2;1 (Versaw and Harrison 2002), PHT4;2, PHT4;4 and PHT4;5 (Guo et al. 2008) or the thylakoid membrane: PHT4;1 (Pavon et al. 2008). Phylogenetic analyses of PHT4 revealed homologues sequences in green algae and red algae but not in other groups (Pfeil et al. 2014). The thylakoid PHT4;1 was shown to regulate the function of the ATP synthase in *A. thaliana* (Karlsson et al. 2015), and mutants of the homologues protein in *C. reinhardtii* (PHT3) were found deficient in photosynthetic growth (Li et al. 2019a). Most algae harbor plastidic Pi transporters that work in exchange with phosphorylated organic compounds (see Sect. III.B.).

2. Sulfate Transporters

Sulfate is transported into the chloroplast stroma of *A. thaliana* via an envelope SO_4^{2-} H^+ symporter named SULTR3;1 (Cao et al. 2013). In addition, three other members of the same family are candidates for such activity (Buchner et al. 2004), but their chloroplast localization awaits validation. Phylogenetic analyses indicated homologous sequences of the SULTR family in major algae groups (Takahashi et al. 2011), but they are not predicted to localize in the chloroplast. In fact, distinct evolutionary paths of sulfate transport systems are proposed for green algae, since in *C. reinhardtii* a cyanobacterial-like ABC transport system was reported (see Sect. III.D.).

3. Nitrite Transporters

Since the nitrite reduction step in nitrate assimilation takes place in the chloroplast, transporters are required to supply it into the stroma. The molecular players involved differ completely in land plants from those found so far in algae. The CsNrt1-L is an envelope-located member of the H^+-dependent oligopeptide transporter family in *A. thaliana*, and was shown to function in nitrite uptake in yeast and chloroplast assays (Sugiura et al. 2007). CLCe was also suggested to play a role in nitrite assimilation in *A. thaliana* (Monachello et al. 2009), but other reports found it to be important for Cl^- homeostasis and photosynthesis (Marmagne et al. 2007; Herdean et al. 2016a). In the green alga *C. reinhardtii,* the NAR1.1 member of the bacterial formate/nitrite transporter family was shown to mediate nitrite transport into the chloroplast, and to improve nitrate use efficiency for cell growth under low CO_2 environments (Rexach et al. 2000). The NAR1.1 has two other chloroplast homologues, NAR1.2 and NAR1.5, where NAR1.2 is a bispecific nitrite and bicarbonate transporter strongly regulated by CO_2 availability ((Mariscal et al. 2006); see also Sect. III.C.). NAR1 homologues have been found in diatoms (Pearson et al. 2015), but have not yet been investigated in other algal groups.

4. Potassium Proton Exchangers

In *Arabidopsis* chloroplasts, three members of the K^+/H^+ exchange family (KEA) have been described to play role in K^+ and pH homeostasis, chloroplast integrity and maximal photosynthesis under changing conditions such as acclimation in transition from high to low light (Armbruster et al. 2014; Kunz et al. 2014). Transport mechanisms to regulate K^+ and pH homeostasis must also exist in algae to respond to developmental and environmental signals. Homologues of chloroplast KEAs were found in the available sequenced genomes of green algae, red algae and diatoms but not in glaucophytes (Chanroj et al. 2012; Pfeil et al. 2014). KEAs were also found in secondary endosymbionts such as cryptophytes, implying a function in K^+ transport across one or more of the four envelope membranes (Chanroj et al. 2012).

5. Manganese and Calcium Transporters

Photosynthetic water oxidation is performed by a Mn_4CaO_5 cluster associated with PSII on the lumenal side of the thylakoid membrane (Shen 2015). Ca^{2+} is also a universal signaling molecule (Verret et al. 2010), and Ca^{2+}-sensing proteins (CAS) have been identified in the thylakoid of both *A. thaliana* and *C. reinhardtii* (Allmer et al. 2006; Vainonen et al. 2008; Terashima et al. 2010). This implies that Mn^{2+} and Ca^{2+} ions are imported into the thylakoid lumen, and indeed, experimental evidence for a biochemical activity of a Ca^{2+}/H^+ exchanger has been reported in pea thylakoids (Ettinger et al. 1999).

A member of the H^+/cation exchanger (CAX) family in *A. thaliana* named PHOTOSYNTHESIS AFFECTED MUTANT71 (PAM71) was localized to the thylakoid membrane, and was shown to function in Mn^{2+} uptake into the thylakoid lumen (Schneider et al. 2016). Loss of a PAM71 homologue named Conserved in Green Lineage and Diatom 1 (CGLD1) in *C. reinhardtii* mutants resulted in both minimal growth and PSII activity, but supplementation of Mn^{2+} restored photosynthesis and growth (Schneider et al. 2016; Xing et al. 2017). Exposure of wild type cells to high light or peroxide-oxidative stress induced upregulation of the *CGLD1* gene expression, whereas the mutants displayed enhanced sensitivity to these conditions (Xing et al. 2017). Remarkably, the mutants are more resistant to singlet oxygen stress, which is attributed to an upregulated expression of several stress-responsive genes (Xing et al. 2017) and to an increased NPQ (Dent et al. 2015) by a mechanism that remains to be clarified.

A paralogue of PAM71, named CMT1, was localized to the inner envelope in *A. thaliana,* where it mediates Mn^{2+} uptake into the chloroplast stroma, thus working sequentially with PAM71 in manganese delivery to PSII (Eisenhut et al. 2018; Zhang et al. 2018). PAM71 and CMT1 also share homology with yeast and human Ca^{2+}/H^+ antiporters from the CaCA superfamily (Demaegd et al. 2013; Demaegd et al. 2014). Indeed, using a Ca^{2+}-reporter based approach, the same *A. thaliana* proteins were characterized as chloroplast Ca^{2+} transporters, named BICAT1 and BICAT2 (Frank et al. 2019). PAM71/BICATs are conserved in green algae such as *C. reinhardtii* and *V. carteri,* and red algae such as *G. sulphuraria*. Since they participate in Ca^{2+} homeostasis, important roles can be hypothesized in algal physiology, including the activation/deactivation of photoprotective mechanisms (Petroutsos et al. 2011), high-light response (Maruyama et al. 2014), regulation of the ATP availability for CO_2 fixation (Terashima et al. 2012), and in CCMs (Wang et al. 2014). The possibility of a broad divalent cation specificity of PAM71/BICAT algal homologues requires detailed electrophysiological investigations in heterologous system.

6. Magnesium Transporters

Mg^{2+} is the most abundant divalent cation, is a component of chlorophyll and thus essential for photosynthesis; it is cofactor of enzymes; and is important for osmoregulation and membrane organization (Schoefs 2005). In *A. thaliana*, one member of the MGT bacterial CorA Mg^{2+} transporter family (also known as MRS2 based on similarity to yeast MRS2) named MRS2–11/MGT10, was localized to the chloroplast envelope (Drummond et al. 2006; Liang et al. 2017; Sun et al. 2017), and plays a role in Mg^{2+} uptake (Drummond et al. 2006). MRS2-like sequences are also recognized in the genome of *C. reinhardtii* (Merchant et al. 2007; Liang et al. 2017). Mutants of the MGT10 homologue were found deficient in photosynthetic growth (Li et al. 2019a), and detailed studies are awaiting investigation of its role in algal chloroplasts.

7. Iron Transporters

The chloroplast contains up to 80% of the iron found in the leaf cell, since it is an essential cofactor for the electron transfer chain and catalytic processes such as chlorophyll biosynthesis and protein import (Balk and Schaedler 2014). Indeed, iron deficiency has multiple effects on photosynthesis in land plants and algae (Geider and La Roche 1994; Moseley et al. 2002; Lopez-Millan et al. 2016; Falkowski et al. 2017). For its transport into the plant chloroplast, there are several envelope Fe^{2+}/H^{+} exchange systems, namely the permease 1 in chloroplasts (PIC1) that interacts with the putative metal transport protein NicO, the multiple antibiotic resistance 1, also known as iron regulated 3 (MAR1/IREG3), and the non-intrinsic ABC transporter NAP14/ABCI11 (Lopez-Millan et al. 2016). The mechanism by which iron is transported into the chloroplast of algae is largely unknown, but homologues of NicO do exist in green algae (Blaby-Haas and Merchant 2012). In *C. reinhardtii*, expression of NicO increases with decreasing iron concentration but not in zinc- or copper-deficiency, making NicO a candidate for plastid iron transport in green algae.

Two envelope/thylakoid iron transporters have been characterized in maize and are known as Fe-deficiency-related FDR3 and FDR4 (Han et al. 2009; Zhang et al. 2017). They are missing in *A. thaliana,* but ZmFDR4 has homologues in green algae and is induced by iron deficiency in yeast (Zhang et al. 2017). Despite the essential roles of Fe^{2+} in the chloroplast and the large number of iron transport genes identified in plants, no homologues in other than green algae have been found. Such genes must also exist in, for example, red and brown algae, where iron deficiency was found to reduce chlorophyll content and increase the aggregation of light harvesting I complexes (Doan et al. 2003), effects that are also documented in land plants (Moseley et al. 2002).

C. Ion Pumps (P-ATPases)

P-type ATPases are primary transporters energized by hydrolysis of ATP with a wide range of specificities for small cations and also phospholipids (Moller et al. 1996; Palmgren and Harper 1999). This family of proteins can be divided into five major evolutionarily-related subfamilies, denoted P1–P5, grouping in phylogenetic trees according to the transported ion (Axelsen and Palmgren 1998). PIB-type ATPases specifically transport metal cations and can be further divided into monovalent (Cu^{+}/Ag^{+}) (subgroup IB-1) and divalent ($Zn^{2+}/Cd^{2+}/Pb^{2+}/Hg^{2+}/Cu^{2+}$) metal ATPases (IB-2 and IB-4 subgroups). Among the Cu^{+} ATPases in *Arabidopsis*, PAA1 and PAA2 (also known as HMA6 and HMA8, respectively) are chloroplast proteins transporting copper across the inner membrane and thylakoid membranes, respectively (Abdel-Ghany et al. 2005; Sautron et al. 2015). The envelope-localized HMA1 provides an additional route for import of Cu into the chloroplast, essential

under excess light conditions (Boutigny et al. 2014). HMA1 differs from PAA1 in that it can also import other metals/divalent cations (Zn^{2+}, Ca^{2+}, $Cd^{2+}$and Co^{2+}; Moreno et al. 2008). There is some disagreement between studies whether HMA1 can also export divalent cations (Boutigny et al. (2014) and references therein).

HMA1 homologues were found in all major algal groups, whereas PAA1 and PAA2 were present in green algae but not in glaucophytes, red algae and diatoms, suggesting secondary loss in these taxa (Hanikenne and Baurain 2013; Pfeil et al. 2014; Karkar et al. 2015). Such a loss may be linked to the absence of PC since transfer of photosynthetic electrons from the cytochrome b_6f to PSI is carried out by the iron-containing cytochrome c_6 in glaucophytes, red algae and diatoms (Fromme et al. 2003; Masmoudi et al. 2013). Interestingly, when copper is limiting in the environment, many green algae replace PC with cytochrome c_{6A}, which in turn is replaced back by PC under copper-replete conditions (Wood 1978); and is consistent with the knowledge that PC, which normally transports electrons from the cytochrome b_6f complex to PSI is substituted by cytochrome c_{6A} under copper-restriction (Howe et al. 2006). Homologues of PAA1 and PAA2 were identified in the diatom *T. pseudonana*, but since they do not possess signal peptides, they are probably involved in export of Cu^{+} to the Golgi compartment (Guo et al. 2015).

D. ABC Transporters

ATP-binding cassette (ABC) transporters represent the largest known family of proteins and are present in all eukaryotes and prokaryotes. Most members use the energy of ATP hydrolysis for driving translocation of various substrates. They participate in excretion of toxic compounds, lipid and heavy metal translocation, and could be classified as half-size or full-size depending on the number of nucleotide-binding and transmembrane domains (Rea 2007). Plant ABCs fall into eight subfamilies, ABCA to ABCI, with homologues in algae (green algae, red algae, glaucophytes), and have few unique sequences, reflecting the relatively simple life of a unicellular organism able to take up nutrients directly from the environment (Lane et al. 2016).

A cyanobacterial-like ABC transport system was reported in *C. reinhardtii*, whose subunits are coded by the *SulP, SulP2, Sbp* and *Sabc* genes (Lindberg and Melis 2008). This is a 380-kDa holocomplex localized to the envelope membranes and proposed to transport sulfate into the chloroplast. This ABC system has homologues in other green algae as well as in the red alga *C. merolae.* Remarkably, the cyanobacterial BicA transporter, which was initially annotated as a sulfate transporter, was shown to transport bicarbonate, implying diverse functions for the members of SulP family (Price et al. 2008).

Iron-sulfur (Fe-S) clusters participate in photosynthesis and other metabolic pathways, but it is not known how they are transported into the chloroplast. SufBCD (sulfur mobilization) is an ABC transporter that was first characterized in *E. coli* and proposed to function in Fe-S cluster biogenesis also in chloroplasts of land plants and algae (Hirabayashi et al. 2015). Noteworthy, the ABC-type dominates among *A. thaliana* transporters (Sanchez-Fernandez et al. 2001), but only a few homologues are present in the genomes of major algal groups (Lane et al. 2016), reflecting the relatively simple life of a unicellular organism able to take up nutrients directly from the environment.

III. Chloroplast Metabolite Transport

To supply the cell and the organism with primary metabolites, a large number of precursors, end products, and intermediates have to be transported in and out of the chloroplast.

In addition, chloroplasts cannot make ATP at night and must import it from the cytosol. Therefore, they are extensively connected to the cytosol by metabolite transporters that reside in the envelope membranes (Weber et al. 2005; Weber and Linka 2011). Below, we will review the current knowledge about transport in chloroplasts of ATP, carbohydrates, bicarbonate, organic acids, amino acids, fatty acids and lipids. Such knowledge is of vital importance since these metabolites participate in photosynthetic carbon fixation, photorespiration, biosynthesis of sugars, lipids and proteins, and must cross two-to-four envelope membranes to make a link between the cytosol and the chloroplast stroma; and must be responsive to light, shade and dark transitions. Extensive reviews have been published on metabolite transporters from the plant chloroplasts (Weber et al. 2004; Weber and Linka 2011; Eisenhut et al. 2015), but none so far have been dedicated to algal counterparts.

A. ATP Transporters

There are two structurally and phylogenetically different types of ATP transporters represented in chloroplast membranes, namely the plastidic nucleotide translocators (NTT1 and NTT2) (Reiser et al. 2004), and the thylakoid ATP/ADP carrier (TAAC) (Thuswaldner et al. 2007).

1. Plastidic Nucleotide Translocators

NTTs from photosynthetic organisms originate from the obligate intracellular bacteria *Rickettsia* and *Chlamydia*, which obtain their ATP by importing it from their eukaryotic host using NTTs (Reiser et al. 2004). NTT homologues have been found in the glaucophyte *C. paradoxa*, and the red alga *G. sulphuraria*, indicating an ancient origin for the NTT family (Weber and Linka 2011). The red alga NTT transports ATP into the stroma in exchange for ADP, i.e. like the plant homologues (Linka et al. 2003). Putative NTTs have been identified in the diatoms *T. pseudonana* and *P. tricornutum,* and were named NTT1 and NTT2 (Ast et al. 2009). Both proteins were localized to the envelope and shown to participate in nucleotide supply to plastids, but by distinct mechanisms from each other and from the ATP/ADP exchangers in primary plastids. NTT1 is a H^+ ATP symporter, whereas NTT2 facilitates the counter exchange of ATP for (deoxy-) nucleoside triphosphates (ATP/dNTP), thus resembling more those in obligate intracellular bacteria.

As compared to land plants and green algae, diatoms do not generate as much ATP during photosynthesis in the chloroplast to maintain the required ATP/NADPH ratio for optimal CO_2 fixation into biomass (Allen 2002; Cardol et al. 2009). The mechanism behind this paradox was recently unraveled in *P. tricornutum* (Bailleul et al. 2015) and involves extensive import of mitochondrial ATP (in exchange for chloroplast NADPH), that must take place across four envelope membranes. Whether NTT1/2 could play a role in the import of mitochondrial ATP into the chloroplast to supply the necessary energy for photosynthesis and growth of diatoms remains to be demonstrated. However, it should be noted that diatoms are among the most important contributors to the primary production in the ocean (Falkowski et al. 2004).

2. The Thylakoid ATP/ADP Carrier

TAAC belongs to the mitochondrial carrier family and transports ATP in exchange for ADP across the thylakoid membrane (Thuswaldner et al. 2007). ATP supplied by TAAC is required in the multistep repair of PSII during light stress in *A. thaliana* (Yin et al. 2010; Spetea and Lundin 2012). TAAC was also localized to the envelope and found to use additional substrates such as phosphoadenosine 5'phosphosulfate, PAPS (Gigolashvili et al. 2012). The envelope-localized protein is known as PAPST1, and is

proposed to play role in sulfur metabolism, including the biosynthesis of thiols, glucosinolates, and phytosulfokines. A close homologue of PAPST1, named PAPS2, is localized to the chloroplast envelope and exports to the cytosol phosphoadenosine 5′-phosphate (PAP) used in chloroplast-to-nucleus retrograde signalling (Ashykhmina et al. 2019). Phylogenetic analyses revealed TAAC/PAPST1 homologues in green algae, but not in red algae, brown algae, and diatoms (Spetea et al. 2011). This indicates that the gene arose on the line to green algae and land plants to fulfil functions specific to these photosynthetic eukaryotes.

B. Plastidic Phosphate Transporters

Carbohydrate transport across the chloroplast envelope is performed in exchange for Pi by plastidic phosphate translocators (pPTs), namely triose-phosphate translocators (TPTs), phosphoenolpyruvate translocators (PPTs), glucose-6-phosphate translocators (GPTs) and xylulose-5-phosphate translocators (XPTs) (Weber et al. 2005). The exchange of Pi with phosphorylated compounds guarantees a balance in the Pi content between the stroma and the cytosol and ensures a constant provision of Pi to sustain ATP synthesis (Weber et al. 2005; Weber and Linka 2011).

Phylogenetic analyses suggest that pPTs of green algae and red algae evolved from a nucleotide-sugar translocator that resided in the host endomembrane system before the cyanobacterium ancestor was captured (Weber et al. 2006). The nucleotide-sugar translocator gene of host origin was duplicated, and after having received the relevant targeting signals evolved into a gene coding for a pPT, providing the host cell with access to the energy produced by the endosymbiont's photosynthetic machinery. The monophyletic origin of the pPT family reflects its establishment early in plastid evolution, likely at the stage of the 'proto-alga' (Tyra et al. 2007). All three types of pPTs were found in green algae, while only TPTs and PPTs have been identified in red algae (Weber and Linka 2011). Chromalveolates, where secondary plastids occur, contain several pPTs that originated monophyletically from the TPT clade, whereas PPTs, GPTs and XPTs were apparently lost during secondary endosymbiosis (Weber et al. 2006). To date, no typical pPTs have been identified in glaucophytes, but Price et al. (2012) identified in the genome of *C. paradoxa* potential hexose-phosphate transporter genes closely related to the UhpC transporters of *Chlamydia*-like bacteria (see Chap. 2), such genes being also present in red and green algae genomes.

1. Triose-Phosphate Transporters

TPT was the first plant pPT characterized at the molecular level to mediate the exchange of G3P and 3-phosphoglycerate (3-PGA) produced in the chloroplast for cytosolic Pi (Flugge 1999). In *C. reinhardtii* as in most algae, the upper half of glycolysis (from hexose-phosphate to 3-PGA) is localized inside the chloroplast, while the lower half (from triose-phosphates to pyruvate) takes place in the cytosol (Johnson and Alric 2013). Therefore, TPTs of green algae are expected to accept as substrates G3P, 3-PGA and dihydroxyacetone phosphate (DHAP) with a reversible action, the directionality being determined by the concentrations of NAD(P)H and ATP in the chloroplast and cytosol. Active transport of the metabolites described above was proven in experiments using labelled CO_2 by several laboratories (Klock and Kreuzberg 1991; Ball 1998; Boschetti and Schmid 1998). Although the genes coding for TPTs have been found in the *C. reinhardtii* genome (Merchant et al. 2007), the proteins have not yet been characterized.

In red algae such as *G. sulphuraria*, phylogenetic analysis revealed a candidate orthologue (GsTPT) to the chloroplastic TPT (Weber et al. 2006). The GsTPT is able to transport DHAP and G3P but not 3-PGA, most likely representing an adaptation of car-

bon metabolism in red algae (Linka et al. 2008). In contrast to land plants and green algae, red algae do not store starch in the chloroplast. Instead, they produce storage carbohydrates such as floridean starch and floridoside (α-D-galactopyranosyl-1-2′-glycerol) in the cytosol (Patron and Keeling 2005). Therefore, the GsTPT exports G3P from the chloroplast even when present at low stromal concentrations, to fuel the massive demand of carbon in the cytosol (Linka et al. 2008). Since GsTPT is unable to transport 3-PGA, its role in the NADPH/ATP shuttle as mentioned for green algae can be excluded (Facchinelli and Weber 2011). In red algae growing heterotrophically, the GsTPT imports G3P into the plastid and sustain the carbon metabolism and NADPH production, thus bypassing the requirement for a GPT that is functional in plant heterotrophic (non-photosynthetic) plastids (Linka et al. 2008).

Metabolite exchange across four envelope membranes into secondary plastids becomes more complicated. In the cryptophyte *G. theta*, two TPTs (TPT1 and TPT2) have been reported (Haferkamp et al. 2006). As highlighted by assays using isolated complex plastidial membranes, these TPTs are able to catalyze the exchange of Pi with DHAP and phosphoenolpyruvate (PEP), but not with 3-PGA. This feature is reminiscent of the biochemical characteristics of the TPT from the red alga *G. sulfuraria* (Linka et al. 2008). Considering that cryptophytes likely acquired photosynthesis through secondary endosymbiosis of a red alga, the biochemical properties of their TPTs have derived through this earlier event. The localization of starch granules in the PPC is also consistent with the plastid having originated from a red alga storing floridean starch in the cytosol (Deschamps et al. 2006). Haferkamp et al. (Haferkamp et al. 2006) showed that night and day paths of sugar metabolism are regulated by differential expression of the two *TPT* genes in *G. theta*. *TPT1* is highly expressed during the night, whereas *TPT2* is mainly expressed in the light. The authors of this study proposed that TPT1 could be localized to the third and/or fourth membrane separating the PPC from the host cell cytoplasm (cER/PPM), where it could export starch degradation products to the cytosol. TPT2 probably resides in the IEM, where it exports triose-phosphates to the PPC to drive starch synthesis in the cytosol.

In the diatom *P. tricornutum*, four putative TPTs were identified in three out of the four plastid membranes (Moog et al. 2015). TPT1 was localized in the outer-most membrane (chloroplast endoplasmic reticulum), TPT2 in the periplastidial membrane, and TPT4a and TPT4b in the inner envelope membrane, all of them being most likely the product of gene duplications of the red algal endosymbiont transporter gene (Moog et al. 2015). These translocators have similar characteristics to their homologues in cryptophytes and apicomplexans, and thus are believed to connect ‘symbiont’ and ‘host’ metabolism by exchange of DHAP and PEP with Pi (Moog et al. 2015). The authors of this study also proposed that two TPTs are required in the IEM due to distinct substrate specificities (DHAP and/or PEP) or to separate the activities for export and import of C3-compounds. Five additional putative *TPT* genes were identified in the genome of *P. tricornutum,* but protein localization and characterization have still to be performed (Moog et al. 2015). Four genes coding for TPTs were identified in the eustigmatophyte *Nannochloropsis gaditana* (at least one with a plastid-targeting peptide: Alboresi et al. (2016)). Based on transcriptomic, lipidomic and metabolomic analyses, the authors proposed that TPTs in this alga control carbon partitioning between organelles, favouring cytoplasm, mitochondria and ER at the expense of the chloroplast, thus promoting lipid accumulation in the cytosol.

2. Phosphoenolpyruvate Transporters

In plastids of plants performing C3 photosynthesis such as *A. thaliana*, PPTs mediate

the uptake of PEP from the cytosol in exchange with Pi (Flugge 1999; Weber and Linka 2011). This is required to drive fatty acid biosynthesis, the shikimate pathway for synthesis of aromatic amino acids and of secondary metabolites such as flavonoids and anthocyanins (Flugge 1999). In plants performing C4 photosynthesis, PEP is exported by PPT to the cytosol where it serves as a CO_2 acceptor of the PEP-carboxylase reaction (Weber and von Caemmerer 2010). Shikimate and phenylalanine biosynthetic pathways have evolutionary origins in the endosymbiotic ancestors (Eicks et al. 2002; Richards et al. 2006; Tohge et al. 2013). Therefore, PPTs are expected to be present and function in similar processes in algae as well. In the red alga *G. sulphuraria*, a candidate PPT was identified (GsPPT), and the recombinant protein was found to have similar properties as the plant orthologue since it catalyzes the strict counter-exchange of PEP with Pi (Weber et al. 2006; Linka et al. 2008). The GsPPT is likely required to supply PEP into the stroma for fatty acid biosynthesis and shikimate pathway as in land plants.

3. *Glucose-6-Phosphate and Xylulose-5-Phosphate Translocators*

In land plants, GPTs are restricted to heterotrophic plastids, where they import glucose-6-phosphate (Glc6P), G3P and 3-PGA (in counter-exchange with Pi) for starch biosynthesis, fatty acids synthesis and for the oxidative pentose-P pathways (OPPPs) (Flugge et al. 2011). XPTs are closely related to GPTs and probably derived from the latter by retrotranscription and genome insertion, as suggested by the lack of introns in *XPT* genes (Knappe et al. 2003). XPTs accept xylulose-5-phosphate (Xul5P), ribulose 5-phosphate, erythose 4-phosphate, and also G3P and 3-PGA in counter-exchange with Pi (Eicks et al. 2002; Flugge and Gao 2005). The function of XPTs is mainly to provide Xul5P for the OPPPs inside the plastid, especially under conditions of high demand for intermediates of the cycles (Eicks et al. 2002; Knappe et al. 2003). Phylogenetic analysis indicated the monophyletic origin of GPTs and XPTs that likely reflects a recent gene duplication event specific to the green lineage (Knappe et al. 2003). Candidate genes for GPT/XPT orthologues are however present in the genome of the red alga *G. sulphuraria* (Linka et al. 2008), indicating an origin in early plastid endosymbiosis. Remarkably, these proteins have distinct biochemical characteristics from those of green algae, since in experiments using reconstituted membranes they only used 3-PGA and Glc6P inefficiently as substrates, and instead mediated a Pi/Pi exchange (Linka et al. 2008). The physiological substrates of these potential red algal proteins remain unknown, and it appears that GPT/XPT-type of transporters may have been lost during secondary endosymbiosis (Weber and Linka 2011).

The genomes of green and red algae but not of Chromalveolata, where secondary plastids occur, also possess sequences homologous to the bacterial UhpC hexose transporter (Price et al. 2012; Karkar et al. 2015; Hirakawa et al. 2017). The UhpC protein from *E. coli* was characterized as a Glc6P/Pi transporter that also acts as a receptor for expression of the sugar-P uptake system (Vastermark and Saier Jr. 2014). Some of the UhpC homologs of green and red algae have an N-terminal extension that was predicted to contain a chloroplast transit peptide (Hirakawa et al. 2017). In fact, Karkar et al. (2015) has localized two putative UhpC transporters from *G. sulphuraria* and *C. merolae* to the chloroplast envelope; however, their function in carbohydrate transport remains to be validated.

C. *Bicarbonate Transporters*

A biochemical carbon concentrating mechanism (CCM) uses energy-dependent active Ci transport to increase intracellular CO_2 concentration close to the RuBisCO active

site (Jungnick et al. 2014; Wang et al. 2015; Matsuda et al. 2017). Cyanobacteria possess a highly effective CCM that involves plasma membrane-located BicA transporters (Price et al. 2008). In algae, Ci species must cross the plasma membrane and the chloroplast envelope to reach the chloroplast stroma, which is believed to be the primary location for the accumulated Ci pool. The chloroplast of the green alga *C. reinhardtii* is able to take up both CO_2 and HCO_3^- (Amoroso et al. 1998). The expression of several genes for HCO_3^- transporters and CO_2 gas channels from the plasma membrane and the chloroplast envelope was found modulated in response to changes in external CO_2 concentration (Brueggeman et al. 2012; Fang et al. 2012). Bicarbonate transport in plastids and pyrenoids is also dealt with in Chaps. 7 & 9.

The transport of Ci into the chloroplast is performed by proteins belonging to the formate-nitrite transporter family, namely the low-CO_2-inducible A (LCIA, also known as NAR1.2), and of the mitochondrial carrier family, namely the low-CO_2-inducible chloroplast envelope proteins 1 and 2 (CCP1 and CCP2; Spalding 2008; Yamano and Fukuzawa 2009). To date, members of the LCIA protein family have been identified in the genome of prokaryotes, yeast, green algae such as *C. reinhardtii, V. carterii* and *Chlorella*, diatoms such as *T. pseudonana* and *T. oceanica* and eustigmatophytes such as *Nannochloropsis gaditana* (Mukherjee 2013). LCIA function as a NO_2^- or HCO_3^- transporter (Mariscal et al. 2006), and localizes to the chloroplast envelope (Yamano et al. 2015; Mackinder et al. 2017). Yamano et al. (2015) also demonstrated a cooperative uptake of HCO_3^- by LCIA and by the plasma membrane-localized high-light activated 3 (HLA3) transporter, and that the stability of HLA3 is dependent on the presence of LCIA. A Ca^{2+}-binding protein (CAS) is located in the thylakoid membrane in *C. reinhardtii* (Yamano et al. 2018), and regulates the expression of nuclear-encoded genes related to CCM such as LCIA and HLA3 (Wang et al. 2016). The CAS-mediated retrograde signalling from the chloroplast to the nucleus to regulate stress-responsive genes appear to be conserved during the evolution of the primary plastid lineages and possibly in the secondary plastid lineages.

There is experimental evidence in *C. reinhardtii* for a CCM mechanism involving HCO_3^- transport across the thylakoid membrane into the lumen. Here CAH3 converts HCO_3^- to CO_2, which due to the acidic pH in the light, becomes the abundant form in the lumen staying above the environmental levels (Moroney and Ynalvez 2007). Based on localization studies, LCIA/NAR1.2 was initially proposed as a possible thylakoid HCO_3^- transporter (Moroney and Ynalvez 2007; Mukherjee 2013); however, another report could not find evidence for such activity (Hunnik and Sultemeyer 2002). Most recently, the protein encoded by the *Cia8* gene in *C. reinhardtii* and belonging to the Na^+ bile acid symporter subfamily was localized to the thylakoid membrane (Machingura et al. 2017). The authors of this study propose that CIA8 could be the Ci transporter supplying HCO_3^- into the thylakoid lumen with the help of the H^+ gradient generated in the light. The *cia8* knockout mutant displayed reduced Ci uptake and photosynthetic rates in low CO_2 conditions, resulting in reduced growth. Such strong phenotype was not observed for *nar1.2* mutants, indicating that CIA8 makes a significant contribution to the CCM in *C. reinhardtii.* CIA8 has a close chloroplast-predicted homologue in *A. thaliana (BASS4),* and similar Na^+/bile acid transporters genes are also present in the marine diatom *P. tricornutum* (Machingura et al. 2017).

The *C. reinhardtii* CCP1 and CCP2 are chloroplast envelope-localized proteins and belong to a family of carriers with broad substrate specificity (Spalding 2008, Yamano and Fukuzawa 2009). CCP1 and CCP2 are both strongly up-regulated in low CO_2 conditions (Ramazanov et al. 1993). However, results brought by RNAi knockdown experiments raised doubts about their role in Ci transport since the mutants exhibited Ci

uptake and photosynthesis similar to wild-type cells (Pollock et al. 2004). The authors suggested that these proteins could be involved in the transport of metabolic intermediates important in acclimation to low CO_2. The existence of Ci transport systems that would compensate this loss may also explain the obtained results.

YCF10 has also been identified as a Ci transport candidate in *C. reinhardtii* (Spalding 2008). It displays a sequence homology with the plastid-encoded CemA protein from land plants and the cyanobacterial PxcA protein (Sasaki et al. 1993). To date, it is still not clear how YCF10 functions in *C. reinhardtii* chloroplast Ci transport, but a role close to that of PxcA is likely, namely in the light-induced H^+ extrusion from the chloroplast stroma (Spalding 2008). This may be required to maintain the alkaline stromal pH for functional CCM in chloroplasts. Most recently, mutants of YCF10 were found deficient in photosynthetic growth in *C. reinhardtii* (Li et al. 2019a), and will require more detailed analyses.

The LCI11 and MITC11 proteins have also been suggested to be involved in the CCM since their transcripts were found strongly up-regulated during growth under low CO_2 conditions in the green alga *C. reinhardtii* (Brueggeman et al. 2012) and the diatom *T. pseudonana* (Kustka et al. 2014). LCI11 is a chloroplast-predicted member of the bestrophin (Best) family, which can transport organic and inorganic anions including Cl^- and HCO_3^- (Qu and Hartzell 2008). The expression of LCI11 is upregulated by limiting CO_2 and it interacts with LCIB/LCIC (Mackinder et al. 2017), a stromal soluble complex converting CO_2 to HCO_3^- (Yamano et al. 2010). Therefore, LCI11 could be located in the thylakoid membrane where it transports HCO_3^- supplied by LCIB/LCIC into the lumen. In fact, LCI11 shares weak similarity to the *A. thaliana* thylakoid-located Cl^- channel VCCN1, which is also a member of the bestrophin family (Herdean et al. 2016b), suggesting that they may have a common origin but diverged to fulfill different functions in algae and land plants. MITC11 shows homology to mitochondrial carriers, and localization predictions place it as a chloroplast protein (Jungnick et al. 2014). Localization and functional studies for these two transporters have not yet been performed in algae.

D. Organic Acid Transporters

Another biochemical CCM in algae depends on exchange of OAA and malate between the chloroplast and the cytosol (Reinfelder 2011). In *C. reinhardtii*, chloroplasts and mitochondria exchange OAA and malate via the envelope LCI20 protein and the mitochondrial OMT (Johnson and Alric 2013). The *C. reinhardtii* LCI20 protein is orthologous to the *A. thaliana* envelope 2-oxoglutarate/malate translocator (DiT1), and was found in the chloroplast proteome (Terashima et al. 2011).

As mentioned earlier, the presence of an elevated concentration of oxygen in the proximity of RuBisCO results in oxygenase activity and photorespiration at the expense of carbon fixation. The occurrence of such a possibility is obviously higher in the absence of CCM. The photorespiratory metabolism is distributed in several specialized compartments (mitochondria, chloroplasts and peroxisomes), and translocators facilitate the metabolite flux through the photorespiratory cycle. Eisenhut et al. (2015) performed a phylogenetic analysis of known dicarboxylate transporters, DiT1, DiT2.1 and the plastidial glycolate/glycerate transporter PLGG1 from *A. thaliana*. Homologues PLGG1 sequences could be found in all algal groups and cyanobacteria, indicating that it had a cyanobiont origin. Green microalgae differ from land plants (and their predecessors, the charophytes) in that they do not have peroxisomes and perform the glycolate oxidation using a glycolate dehydrogenase in mitochondria (Igamberdiev and Lea 2002). This difference implies that the mitochondrion

needs a transporter comparable to the plastidic PLGG1, facilitating glycolate import and glycerate export. Indeed, homologues PLGG1 sequences found in *C. reinhardtii* and *V. carteri* had a dually-predicted location to mitochondria and chloroplasts; DiT1 and DiT2.1 have homologues in green algae but not in red algae or glaucophytes, implying that they have been acquired via horizontal transfer from *Chlamydia* or that they have been lost in the former (Eisenhut et al. 2015).

E. Amino Acid Transporters

Amino acids are the building blocks of proteins, and in land plants and algae they are synthesized in plastids. They can be used within plastids or are exported to the cytosol and mitochondria. Very little is known about the transport of amino acids into or out of chloroplasts. DiT2.1 is the only characterized chloroplast amino acid transporter in *A. thaliana* (Werner-Washburne and Keegstra 1985). It mediates the exchange of glutamate for malate and can also use the amino acid aspartate as a substrate. Members of the preprotein and amino acid transporter family in *A. thaliana*, PRAT1 and PRAT2, were localized to the chloroplast envelope and proposed to mediate export of amino acids to the cytosol (Murcha et al. 2007; Pudelski et al. 2010). Experimental evidence is available for the function of PRATs in protein import in plants, and homologues were found in three green algae, namely *C. reinhardtii*, *V. carteri*, and *Ostreococcus lucimarinus* (Rossig et al. 2013).

F. Fatty Acid Transporters

Fatty acids (FA) and lipids are not only used for membrane building but also for development and growth of cells. Indeed, some FA and lipids cannot be produced by human cells - the so-called essential lipids, and must be acquired through diet (Ulmann et al. 2014). In land plants and algae, FA are synthesized in plastids, exported to the ER for chain elongation for modifications and lipid assembly, and ultimately distributed within the cell (Heydarizadeh et al. 2013; Hurlock et al. 2014; LaBrant et al. 2018). Some lipids are reimported for plastid-specific lipid assembly (Browse et al. 1986; Heydarizadeh et al. 2013). Green algae such as *C. reinhardtii* have a similar lipid composition of chloroplast membranes to land plants (Boudiere et al. 2014).

Because lipophilic molecules such as FA cannot freely move in an aqueous environment, several modes of transport have been identified. These include membrane contact sites, diffusion, flip transfer, vesicular trafficking and protein-mediated transport. In the land plant *A. thaliana,* several ABC FA/lipid transporters have been described, but none of them were from the chloroplast (Do et al. 2017). Fatty Acid Export 1 (FAX1) was localized to the chloroplast envelope and proposed to transport free FA from the stroma to the inter-envelope space (Li et al. 2015). From there, FA could move to the cytosol thanks to the vectorial acylation transport mediated by Long-chain acyl-CoA synthetase 9 (LACS9). Phylogenetic analyses indicated that plastid FAX homologues are restricted to land plants and green algae (Li et al. 2015). Most recently, two homologues from *C. reinhardtii* (FAX1 and FAX2) have been found to export mainly C16 and C18 fatty acids for lipid biosynthesis (Li et al. 2019b). Overexpression of both FAXs increased the intracellular lipid content, especially triacylglycerol, which is important for the production of biofuels using microalgae.

G. Lipid ABC Transporters

For the assembly of plastid-specific lipids, they should be reimported into chloroplasts (Heydarizadeh et al. 2013; LaBrant et al. 2018). TRIGALACTOSYLDIACYLGLYCEROL1–3 (TGD1–3) is a multisubunit ABC transporter complex mediating lipid transfer from the endoplasmic reticulum

(ER) via the inter-envelope space to the chloroplast stroma of *A. thaliana* (Awai et al. 2006; Lu et al. 2007). The exact nature of the lipid species transported by the TGD complex is not fully elucidated, but obvious candidates are phosphatidic acid, phosphatidylcoline and diacylglycerol as central intermediates in lipid synthesis (LaBrant et al. 2018). The *C. reinhardtii* genome encodes putative plant orthologues of the chloroplast TGD1–3 complex required for the ER-to-chloroplast lipid trafficking (Warakanont et al. 2015). The same study localized the CrTGD2 to the inner envelope and reported on the reduced viability of a *tgd2* mutant due to altered galactoglycerolipid metabolism.

IV. Strategies for Identification of Missing Algal Transporters

Although the chloroplast hosts photosynthesis and multiple biosynthetic pathways vital for higher plant and algal cells, the transporters mediating the exchange of ions and metabolites are mostly unknown even in *A. thaliana* (Pick and Weber 2014; Szabo and Spetea 2017). The summary presented in Table 6.1 and illustrated in Figs. 6.1 and 6.2 clearly indicate the overwhelming number of missing algal transporters for both ions and metabolites, whose identification would greatly impact our understanding of the chloroplast homeostasis and metabolism. Bioinformatic analyses combined with experimental strategies have been used for identification and characterization of many chloroplast transporters from *A. thaliana* (Barbier-Brygoo et al. 2001; Spetea and Schoefs 2010). Heterologous expression provided insights into the type of substrate, whereas analyses of mutants revealed their physiological roles. Mass spectrometry-based proteomics revealed initial information about localization (Zybailov et al. 2008; Ferro et al. 2010; Yin et al. 2015) and were followed in many cases by more targeted approaches using fluorescent markers (for reviews, see Weber et al. 2004; Weber and Linka 2011; Eisenhut et al. 2015; Spetea et al. 2016; Spetea et al. 2017; Szabo and Spetea 2017). Similar strategies could be used to identify and characterize missing chloroplast transport proteins encoded by genes in the various algal models (Table 6.1). In addition, co-expression analyses of the known transporters in algae could aid to unravel new genes for transporters involved in common processes in the chloroplast (Weber and Bauwe 2013). Prediction tools for transmembrane topology, localization and phylogeny similar to those available for plants at ARAMEMNON (Schwacke and Flugge 2018) could be employed to mine the information in their sequences. A systematic localization of algal proteins could be done as in the study by Mackinder et al. (2017) using fluorescent protein tagging and mass spectrometry in *C. reinhardtii*.

A phylogenomic and network analysis approach was used to identify homologues in algae of validated metabolite transporters from the chloroplast envelope of *A. thaliana* (Karkar et al. 2015). Bioinformatic and protein localization in tobacco chloroplasts could show plastid targeting for two red algal putative UhpC transporters. This study also showed that more than half of the envelope transporter genes are of eukaryotic origin and that the captured cyanobacterium made a relatively minor contribution to the process. Similar analyses could also be performed using transporter gene sequences from cyanobacteria and non-photosynthetic bacteria. For instance, a novel and specific pyruvate/H^+ symporter has been reported in *E. coli* (Kristoficova et al. 2017). Such a transporter could have been acquired through horizontal gene transfer, enabling the use of pyruvate as a carbon source for the growth and survival of *E. coli*.

Some collections of algal mutants are available (Chlamydomonas Resource Center: http://chlamycollection.org/ and *Chlamydomonas* library project: https://

www.chlamylibrary.org/), and in addition, the new technique of genome editing with the help of CRISP/CAS9 system could be employed to generate knockout and knockdown mutants for algal genes absent in collections (Shin et al. 2016). Using algal mutants defective in the activity of putative transport proteins could allow to validate their function and physiological role as it has been done successfully for plant counterparts from the chloroplast envelope (Weber et al. 2004) and thylakoids (Spetea and Schoefs 2010). Indeed, many mutants of chloroplast transporters displayed altered photosynthesis in *A. thaliana* and *C. reinhardtii*, since they occupy key positions in the pathway exchanging ions and metabolites across chloroplast membranes (for reviews, see Brautigam and Weber (2011), Derks et al. (2015), Erickson et al. (2015), Szabo and Spetea et al. (2017), Marchand et al. (2018)). Most recently, the *Chlamydomonas* library was screened for mutants deficient in photosynthetic growth, and allowed identification of over 300 genes including transporters, whose characterization will facilitate understanding of chloroplast function in algae (Li et al. 2019a).

V. Conclusions and Perspectives

In this chapter, we have provided an overview of the current knowledge about ion and metabolite transport in the chloroplast of algae. Most of the reviewed studies predicted the existence of transport genes from genomic evidence, while only few reported on the localization and transport function of predicted genes. Most transporter genes were identified in the green alga *C. reinhardtii*, but some were found in models for red algae, diatoms, glaucophytes or cryptophytes. Most identified chloroplast transporters reside in the envelope and participate in carbon acquisition and metabolism. Only a few are located in the thylakoid membrane and play role in ion transport. The strategies used to characterize chloroplast transporters from plants could inspire future work in algae.

Algae represent a potentially non-expensive, scalable, CO_2-fixing, solar-powered source of diverse natural products such as lipids, pigments and proteins, that are synthesized mainly in the chloroplast (e.g., Mimouni et al. 2012; Heydarizadeh et al. 2013). One recent research development is synthetic biology, i.e. '*the deliberate (re) design and construction of novel biological and biologically-based systems to perform new functions for useful purpose, that draws on principles elucidated from biology and engineering'* (Jensen and Leister 2014). Through genetic engineering, synthetic biology can transform algae and their chloroplasts in cell factories for the production of exotic compounds such as vaccines and antibiotics (Scaife and Smith 2016). In this respect, the fact that the chloroplast genome is of prokaryotic origin offers many advantages because it is easily amenable. Despite of this enormous potential, the development of algal biotechnologies remains fragile, especially because of lack of a deep knowledge of the biochemistry, physiology, and stress responses of the algal cell activity (Heydarizadeh et al. 2014) and that also impacts on the economic viability of these technologies (Vinayak et al. 2015).

A better knowledge about ion and metabolite chloroplast transporters would help in the recovery of compounds from algal cells within downstream processing. Such processing aims to disrupt the physical and mechanical cell barriers preventing the recovery of interesting compounds. Several chemical and physical methods have been proposed to help the recovery process (Coustets et al. 2015; Vinayak et al. 2015), but they have been thus far only applied to small-scale tests (Coustets et al. 2015). The manipulation of intracellular compound circuits in intact algae using chloroplast transporters would certainly enable new opportunities in algal research and in the use

of algae as photoautotrophic tools for biotechnological applications. At the same time, such studies would serve to advance our understanding of biological barriers, a goal of central significance in the life sciences and agricultural and medical research.

References

Abdel-Ghany SE, Muller-Moule P, Niyogi KK, Pilon M, Shikanai T (2005) Two P-type ATPases are required for copper delivery in Arabidopsis thaliana chloroplasts. Plant Cell 17:1233–1251. https://doi.org/10.1105/tpc.104.030452

Alboresi A, Perin G, Vitulo N, Diretto G, Block M, Jouhet J, Meneghesso A, Valle G, Giuliano G, Marechal E, Morosinotto T (2016) Light remodels lipid biosynthesis in Nannochloropsis gaditana by modulating carbon partitioning between organelles. Plant Physiol 171:2468–2482. https://doi.org/10.1104/pp.16.00599

Allen JF (2002) Photosynthesis of ATP—electrons, proton pumps, rotors, and poise. Cell 110:273–276

Allmer J, Naumann B, Markert C, Zhang M, Hippler M (2006) Mass spectrometric genomic data mining: novel insights into bioenergetic pathways in Chlamydomonas reinhardtii. Proteomics 6:6207–6220. https://doi.org/10.1002/pmic.200600208

Amoroso G, Sultemeyer D, Thyssen C, Fock HP (1998) Uptake of HCO3- and CO2 in cells and chloroplasts from the microalgae Chlamydomonas reinhardtii and Dunaliella tertiolecta. Plant Physiol 116:193–201. https://doi.org/10.1104/pp.116.1.193

Armbruster U, Carrillo LR, Venema K, Pavlovic L, Schmidtmann E, Kornfeld A, Jahns P, Berry JA, Kramer DM, Jonikas MC (2014) Ion antiport accelerates photosynthetic acclimation in fluctuating light environments. Nat Commun 5:5439. https://doi.org/10.1038/ncomms6439

Ashykhmina N, Lorenz M, Frerigmann H, Koprivova A, Hofsetz E, Stuhrwohldt N, Flugge UI, Haferkamp I, Kopriva S, Gigolashvili T (2019) PAPST2 plays a critical role for PAP removal from the cytosol and subsequent degradation in plastids and mitochondria. Plant Cell 31: 231–249 https://doi.org/10.1105/tpc.18.00512

Ast M, Gruber A, Schmitz-Esser S, Neuhaus HE, Kroth PG, Horn M, Haferkamp I (2009) Diatom plastids depend on nucleotide import from the cytosol. Proc Natl Acad Sci U S A 106:3621–3626. https://doi.org/10.1073/pnas.0808862106

Avendano-Vazquez AO, Cordoba E, Llamas E, San Roman C, Nisar N, De la Torre S, Ramos-Vega M, Gutierrez-Nava MD, Cazzonelli CI, Pogson BJ, Leon P (2014) An uncharacterized apocarotenoid-derived signal generated in zeta-carotene desaturase mutants regulates leaf development and the xxpression of chloroplast and nuclear genes in Arabidopsis. Plant Cell 26:2524–2537. https://doi.org/10.1105/tpc.114.123349

Awai K, Xu C, Tamot B, Benning C (2006) A phosphatidic acid-binding protein of the chloroplast inner envelope membrane involved in lipid trafficking. Proc Natl Acad Sci U S A 103:10817–10822. https://doi.org/10.1073/pnas.0602754103

Axelsen KB, Palmgren MG (1998) Evolution of substrate specificities in the P-type ATPase superfamily. J Mol Evol 46:84–101

Bailleul B, Berne N, Murik O, Petroutsos D, Prihoda J, Tanaka A, Villanova V, Bligny R, Flori S, Falconet D, Krieger-Liszkay A, Santabarbara S, Rappaport F, Joliot P, Tirichine L, Falkowski PG, Cardol P, Bowler C, Finazzi G (2015) Energetic coupling between plastids and mitochondria drives CO2 assimilation in diatoms. Nature 524:366–369. https://doi.org/10.1038/nature14599

Balk J, Schaedler TA (2014) Iron cofactor assembly in plants. Annu Rev Plant Biol 65:125–153. https://doi.org/10.1146/annurev-arplant-050213-035759

Ball SG (1998) The molecular biology of chloroplasts and mitochondria in Chlamydomonas In: JD Rochaix, Goldschmidt-Clermont, M., Merchant, S. (ed) Advances in photosynthesis. Kluwer, Dordrecht, pp 550–567

Barbier-Brygoo H, Gaymard F, Rolland N, Joyard J (2001) Strategies to identify transport systems in plants. Trends Plant Sci 6:577–585

Blaby-Haas CE, Merchant SS (2012) The ins and outs of algal metal transport. Biochim Biophys Acta 1823:1531–1552. https://doi.org/10.1016/j.bbamcr.2012.04.010

Bonnot C, Proust H, Pinson B, Colbalchini FP, Lesly-Veillard A, Breuninger H, Champion C, Hetherington AJ, Kelly S, Dolan L (2017) Functional PTB phosphate transporters are present in streptophyte algae and early diverging land plants. New Phytol 214:1158–1171. https://doi.org/10.1111/nph.14431

Boschetti A, Schmid K (1998) Energy supply for ATP-synthase deficient chloroplasts of Chlamydomonas reinhardii. Plant Cell Physiol 39:160–168. https://doi.org/10.1093/oxfordjournals.pcp.a029353

Boudiere L, Michaud M, Petroutsos D, Rebeille F, Falconet D, Bastien O, Roy S, Finazzi G, Rolland N, Jouhet J, Block MA, Marechal E

(2014) Glycerolipids in photosynthesis: composition, synthesis and trafficking. Biochim Biophys Acta 1837:470–480. https://doi.org/10.1016/j.bbabio.2013.09.007

Boutigny S, Sautron E, Finazzi G, Rivasseau C, Frelet-Barrand A, Pilon M, Rolland N, Seigneurin-Berny D (2014) HMA1 and PAA1, two chloroplast-envelope PIB-ATPases, play distinct roles in chloroplast copper homeostasis. J Exp Bot 65:1529–1540. https://doi.org/10.1093/jxb/eru020

Brautigam A, Weber AP (2011) Do metabolite transport processes limit photosynthesis? Plant Physiol 155:43–48. https://doi.org/10.1104/pp.110.164970

Browse J, Warwick N, Somerville CR, Slack CR (1986) Fluxes through the prokaryotic and eukaryotic pathways of lipid synthesis in the '16:3′ plant Arabidopsis thaliana. Biochem J 235:25–31

Brueggeman AJ, Gangadharaiah DS, Cserhati MF, Casero D, Weeks DP, Ladunga I (2012) Activation of the carbon concentrating mechanism by CO2 deprivation coincides with massive transcriptional restructuring in Chlamydomonas reinhardtii. Plant Cell 24:3483–3483. https://doi.org/10.1105/tpc.112.240861

Buchner P, Stuiver CE, Westerman S, Wirtz M, Hell R, Hawkesford MJ, De Kok LJ (2004) Regulation of sulfate uptake and expression of sulfate transporter genes in Brassica oleracea as affected by atmospheric H(2)S and pedospheric sulfate nutrition. Plant Physiol 136:3396–3408. https://doi.org/10.1104/pp.104.046441

Cao MJ, Wang Z, Wirtz M, Hell R, Oliver DJ, Xiang CB (2013) SULTR3;1 is a chloroplast-localized sulfate transporter in Arabidopsis thaliana. Plant J 73:607–616. https://doi.org/10.1111/tpj.12059

Cardol P, Alric J, Girard-Bascou J, Franck F, Wollman FA, Finazzi G (2009) Impaired respiration discloses the physiological significance of state transitions in Chlamydomonas. Proc Natl Acad Sci U S A 106:15979–15984. https://doi.org/10.1073/pnas.0908111106

Carraretto L, Formentin E, Teardo E, Checchetto V, Tomizioli M, Morosinotto T, Giacometti GM, Finazzi G, Szabo I (2013) A thylakoid-located two-pore K(+) channel controls photosynthetic light utilization in plants. Science 342:114–118. https://doi.org/10.1126/science.1242113

Chanroj S, Wang G, Venema K, Zhang MW, Delwiche CF, Sze H (2012) Conserved and diversified gene families of monovalent cation/H(+) antiporters from algae to flowering plants. Front Plant Sci 3:25. https://doi.org/10.3389/fpls.2012.00025

Coustets M, Joubert-Durigneux V, Herault J, Schoefs B, Blanckaert V, Garnier JP, Teissie J (2015) Optimization of protein electroextraction from microalgae by a flow process. Bioelectrochemistry 103:74–81. https://doi.org/10.1016/j.bioelechem.2014.08.022

De Bortoli S, Teardo E, Szabo I, Morosinotto T, Alboresi A (2016) Evolutionary insight into the ionotropic glutamate receptor superfamily of photosynthetic organisms. Biophys Chem 218:14–26. https://doi.org/10.1016/j.bpc.2016.07.004

Demaegd D, Foulquier F, Colinet AS, Gremillon L, Legrand D, Mariot P, Peiter E, Van Schaftingen E, Matthijs G, Morsomme P (2013) Newly characterized Golgi-localized family of proteins is involved in calcium and pH homeostasis in yeast and human cells. Proc Natl Acad Sci U S A 110:6859–6864. https://doi.org/10.1073/pnas.1219871110

Demaegd D, Colinet AS, Deschamps A, Morsomme P (2014) Molecular evolution of a novel family of putative calcium transporters. PLoS One 9:e100851. https://doi.org/10.1371/journal.pone.0100851

Dent RM, Sharifi MN, Malnoe A, Haglund C, Calderon RH, Wakao S, Niyogi KK (2015) Large-scale insertional mutagenesis of Chlamydomonas supports phylogenomic functional prediction of photosynthetic genes and analysis of classical acetate-requiring mutants. Plant J 82:337–351. https://doi.org/10.1111/tpj.12806

Derks A, Schaven K, Bruce D (2015) Diverse mechanisms for photoprotection in photosynthesis. Dynamic regulation of photosystem II excitation in response to rapid environmental change. Biochim Biophys Acta 1847:468–485. https://doi.org/10.1016/j.bbabio.2015.02.008

Deschamps P, Haferkamp I, Dauvillee D, Haebel S, Steup M, Buleon A, Putaux JL, Colleoni C, d'Hulst C, Plancke C, Gould S, Maier U, Neuhaus HE, Ball S (2006) Nature of the periplastidial pathway of starch synthesis in the cryptophyte Guillardia theta. Eukaryot Cell 5:954–963. https://doi.org/10.1128/EC.00380-05

Do THT, Martinoia E, Lee Y (2017) Functions of ABC transporters in plant growth and development. Curr Opin Plant Biol 41:32–38. https://doi.org/10.1016/j.pbi.2017.08.003

Doan JM, Schoefs B, Ruban AV, Etienne AL (2003) Changes in the LHCI aggregation state during iron repletion in the unicellular red alga Rhodella violacea. FEBS Lett 533:59–62

Drummond RSM, Tutone A, Li YC, Gardner RC (2006) A putative magnesium transporter AtMRS2-11 is localized to the plant chloroplast envelope membrane system. Plant Sci 170:78–89. https://doi.org/10.1016/j.plantsci.2005.08.018

Duan Z, Kong F, Zhang L, Li W, Zhang J, Peng L (2016) A bestrophin-like protein modulates the proton motive force across the thylakoid membrane in

Arabidopsis. J Integr Plant Biol 58:848–858. https://doi.org/10.1111/jipb.12475

Duy D, Stube R, Wanner G, Philippar K (2011) The chloroplast permease PIC1 regulates plant growth and development by directing homeostasis and transport of iron. Plant Physiol 155:1709–1722. https://doi.org/10.1104/pp.110.170233

Eicks M, Maurino V, Knappe S, Flugge UI, Fischer K (2002) The plastidic pentose phosphate translocator represents a link between the cytosolic and the plastidic pentose phosphate pathways in plants. Plant Physiol 128:512–522. https://doi.org/10.1104/pp.010576

Eisenhut M, Hocken N, Weber AP (2015) Plastidial metabolite transporters integrate photorespiration with carbon, nitrogen, and sulfur metabolism. Cell Calcium 58:98–104. https://doi.org/10.1016/j.ceca.2014.10.007

Eisenhut M, Hoecker N, Schmidt SB, Basgaran RM, Flachbart S, Jahns P, Eser T, Geimer S, Husted S, Weber APM, Leister D, Schneider A (2018) The plastid envelope CHLOROPLAST MANGANESE TRANSPORTER1 is essential for manganese homeostasis in Arabidopsis. Mol Plant 11:955–969. https://doi.org/10.1016/j.molp.2018.04.008

Enz C, Steinkamp T, Wagner R (1993) Ion channels in the thylakoid membrane (a patch-clamp study). Biochim Biophys Acta 1143:67–76. https://doi.org/10.1016/0005-2728(93)90217-4

Erickson E, Wakao S, Niyogi KK (2015) Light stress and photoprotection in Chlamydomonas reinhardtii. Plant J 82:449–465. https://doi.org/10.1111/tpj.12825

Estavillo GM, Crisp PA, Pornsiriwong W, Wirtz M, Collinge D, Carrie C, Giraud E, Whelan J, David P, Javot H, Brearley C, Hell R, Marin E, Pogson BJ (2011) Evidence for a SAL1-PAP chloroplast retrograde pathway that functions in drought and high light signaling in Arabidopsis. Plant Cell 23:3992–4012. https://doi.org/10.1105/tpc.111.091033

Ettinger WF, Clear AM, Fanning KJ, Peck ML (1999) Identification of a Ca2+/H+ antiport in the plant chloroplast thylakoid membrane. Plant Physiol 119:1379–1386

Facchinelli F, Weber AP (2011) The metabolite transporters of the plastid envelope: an update. Front Plant Sci 2:50. https://doi.org/10.3389/fpls.2011.00050

Falkowski PG, Katz ME, Knoll AH, Quigg A, Raven JA, Schofield O, Taylor FJ (2004) The evolution of modern eukaryotic phytoplankton. Science 305:354–360. https://doi.org/10.1126/science.1095964

Falkowski PG, Lin H, Gorbunov MY (2017) What limits photosynthetic energy conversion efficiency in nature? Lessons from the oceans. Philos Trans R Soc Lond Ser B Biol Sci 372: 20160376. https://doi.org/10.1098/rstb.2016.0376

Fang W, Si YQ, Douglass S, Casero D, Merchant SS, Pellegrini M, Ladunga I, Liu P, Spalding MH (2012) Transcriptome-wide changes in Chlamydomonas reinhardtii gene expression regulated by carbon dioxide and the CO2-concentrating mechanism regulator CIA5/CCM1. Plant Cell 24:1876–1893. https://doi.org/10.1105/tpc.112.097949

Ferro M, Brugiere S, Salvi D, Seigneurin-Berny D, Court M, Moyet L, Ramus C, Miras S, Mellal M, Le Gall S, Kieffer-Jaquinod S, Bruley C, Garin J, Joyard J, Masselon C, Rolland N (2010) AT_CHLORO, a comprehensive chloroplast proteome database with subplastidial localization and curated information on envelope proteins. Mol Cell Proteomics 9:1063–1084. https://doi.org/10.1074/mcp.M900325-MCP200

Finazzi G, Petroutsos D, Tomizioli M, Flori S, Sautron E, Villanova V, Rolland N, Seigneurin-Berny D (2014) Ions channels/transporters and chloroplast regulation. Cell Calcium 58:86–97

Flugge UI (1999) Phosphate translocators in plastids. Annu Rev Plant Physiol Plant Mol Biol 50:27–45. https://doi.org/10.1146/annurev.arplant.50.1.27

Flugge UI, Gao W (2005) Transport of isoprenoid intermediates across chloroplast envelope membranes. Plant Biol (Stuttg) 7:91–97. https://doi.org/10.1055/s-2004-830446

Flugge UI, Hausler RE, Ludewig F, Gierth M (2011) The role of transporters in supplying energy to plant plastids. J Exp Bot 62:2381–2392. https://doi.org/10.1093/jxb/erq361

Frank J, Happeck R, Meier B, Hoang MTT, Stribny J, Hause G, Ding HD, Morsomme P, Baginsky S, Peiter E (2019) Chloroplast-localized BICAT proteins shape stromal calcium signals and are required for efficient photosynthesis. New Phytol 221:866–880. https://doi.org/10.1111/nph.15407

Fromme P, Melkozernov A, Jordan P, Krauss N (2003) Structure and function of photosystem I: interaction with its soluble electron carriers and external antenna systems. FEBS Lett 555:40–44

Galvez-Valdivieso G, Mullineaux PM (2010) The role of reactive oxygen species in signalling from chloroplasts to the nucleus. Physiol Plant 138:430–439. https://doi.org/10.1111/j.1399-3054.2009.01331.x

Geider RJ, La Roche J (1994) The role of iron in phytoplankton photosynthesis, and the potential for iron-limitation of primary productivity in the sea. Photosynth Res 39:275–301. https://doi.org/10.1007/BF00014588

Gigolashvili T, Geier M, Ashykhmina N, Frerigmann H, Wulfert S, Krueger S, Mugford SG, Kopriva S,

Haferkamp I, Flugge UI (2012) The Arabidopsis thylakoid ADP/ATP carrier TAAC has an additional role in supplying plastidic phosphoadenosine 5′-phosphosulfate to the cytosol. Plant Cell 24:4187–4204. https://doi.org/10.1105/tpc.112.101964

Gollan PJ, Tikkanen M, Aro EM (2015) Photosynthetic light reactions: integral to chloroplast retrograde signalling. Curr Opin Plant Biol 27:180–191. https://doi.org/10.1016/j.pbi.2015.07.006

Gouaux E, Mackinnon R (2005) Principles of selective ion transport in channels and pumps. Science 310:1461–1465. https://doi.org/10.1126/science.1113666

Guo B, Jin Y, Wussler C, Blancaflor EB, Motes CM, Versaw WK (2008) Functional analysis of the Arabidopsis PHT4 family of intracellular phosphate transporters. New Phytol 177:889–898. https://doi.org/10.1111/j.1469-8137.2007.02331.x

Guo J, Green BR, Maldonado MT (2015) Sequence analysis and gene expression of potential components of copper transport and homeostasis in Thalassiosira pseudonana. Protist 166:58–77. https://doi.org/10.1016/j.protis.2014.11.006

Haferkamp I, Deschamps P, Ast M, Jeblick W, Maier U, Ball S, Neuhaus HE (2006) Molecular and biochemical analysis of periplastidial starch metabolism in the cryptophyte Guillardia theta. Eukaryot Cell 5:964–971. https://doi.org/10.1128/Ec.00381-05

Hamilton ES, Schlegel AM, Haswell ES (2015) United in diversity: mechanosensitive ion channels in plants. Annu Rev Plant Biol 66:113–137. https://doi.org/10.1146/annurev-arplant-043014-114700

Han J, Song X, Li P, Yang H, Yin L (2009) Maize ZmFDR3 localized in chloroplasts is involved in iron transport. Sci China C Life Sci 52:864–871. https://doi.org/10.1007/s11427-009-0108-2

Hanikenne M, Baurain D (2013) Origin and evolution of metal P-type ATPases in Plantae (Archaeplastida). Front Plant Sci 4:544. https://doi.org/10.3389/fpls.2013.00544

Haswell ES, Meyerowitz EM (2006) MscS-like proteins control plastid size and shape in Arabidopsis thaliana. Curr Biol 16:1–11. https://doi.org/10.1016/j.cub.2005.11.044

Herdean A, Nziengui H, Zsiros O, Solymosi K, Garab G, Lundin B, Spetea C (2016a) The Arabidopsis thylakoid chloride channel AtCLCe functions in chloride homeostasis and regulation of photosynthetic electron transport. Front Plant Sci 7:115. https://doi.org/10.3389/fpls.2016.00115

Herdean A, Teardo E, Nilsson AK, Pfeil BE, Johansson ON, Unnep R, Nagy G, Zsiros O, Dana S, Solymosi K, Garab G, Szabo I, Spetea C, Lundin B (2016b) A voltage-dependent chloride channel fine-tunes photosynthesis in plants. Nat Commun 7:11654. https://doi.org/10.1038/ncomms11654

Heydarizadeh P, Poirier I, Loizeau D, Ulmann L, Mimouni V, Schoefs B, Bertrand M (2013) Plastids of marine phytoplankton produce bioactive pigments and lipids. Mar Drugs 11:3425–3471. https://doi.org/10.3390/md11093425

Heydarizadeh P, Marchand J, Chenais B, Sabzalian MR, Zahedi M, Moreau B, Schoefs B (2014) Functional investigations in diatoms need more than a transcriptomic approach. Diatom Res 29:75–89

Hirabayashi K, Yuda E, Tanaka N, Katayama S, Iwasaki K, Matsumoto T, Kurisu G, Outten FW, Fukuyama K, Takahashi Y, Wada K (2015) Functional dynamics revealed by the structure of the SufBCD complex, a movel ATP-binding cassette (ABC) protein that serves as a scaffold for iron-sulfur cluster biogenesis. J Biol Chem 290:29717–29731. https://doi.org/10.1074/jbc.M115.680934

Hirakawa Y, Nakayama T, Keilert N, Ki I (2017) Evolution of UhpC-type hexose-phosphate transporters in dinoflagellates. Phycol Res 65:166–170. https://doi.org/10.1111/pre.12164

Howe CJ, Schlarb-Ridley BG, Wastl J, Purton S, Bendall DS (2006) The novel cytochrome c6 of chloroplasts: a case of evolutionary bricolage? J Exp Bot 57:13–22. https://doi.org/10.1093/jxb/erj023

Hunnik EV, Sultemeyer D (2002) A possible role for carbonic anhydrase in the lumen of chloroplast thylakoids in green algae. Funct Plant 29:243–249

Hurlock AK, Roston RL, Wang K, Benning C (2014) Lipid trafficking in plant cells. Traffic 15:915–932. https://doi.org/10.1111/tra.12187

Igamberdiev AU, Lea PJ (2002) The role of peroxisomes in the integration of metabolism and evolutionary diversity of photosynthetic organisms. Phytochemistry 60:651–674

Jensen PE, Leister D (2014) Cyanobacteria as an experimental platform for modifying bacterial and plant photosynthesis. Front Bioeng Biotechnol 2(7). https://doi.org/10.3389/fbioe.2014.00007

Johnson X, Alric J (2013) Central carbon metabolism and electron transport in Chlamydomonas reinhardtii: metabolic constraints for carbon partitioning between oil and starch. Eukaryot Cell 12:776–793. https://doi.org/10.1128/EC.00318-12

Jungnick N, Ma YB, Mukherjee B, Cronan JC, Speed DJ, Laborde SM, Longstreth DJ, Moroney JV (2014) The carbon concentrating mechanism in Chlamydomonas reinhardtii: finding the missing pieces. Photosynth Res 121:159–173. https://doi.org/10.1007/s11120-014-0004-x

Karkar S, Facchinelli F, Price DC, Weber AP, Bhattacharya D (2015) Metabolic connectivity as a

driver of host and endosymbiont integration. Proc Natl Acad Sci U S A 112:10208–10215. https://doi.org/10.1073/pnas.1421375112

Karlsson PM, Herdean A, Adolfsson L, Beebo A, Nziengui H, Irigoyen S, Unnep R, Zsiros O, Nagy G, Garab G, Aronsson H, Versaw WK, Spetea C (2015) The Arabidopsis thylakoid transporter PHT4;1 influences phosphate availability for ATP synthesis and plant growth. Plant J 84:99–110. https://doi.org/10.1111/tpj.12962

Kim J, Fabris M, Baart G, Kim MK, Goossens A, Vyverman W, Falkowski PG, Lun DS (2016) Flux balance analysis of primary metabolism in the diatom Phaeodactylum tricornutum. Plant J 85:161–176. https://doi.org/10.1111/tpj.13081

Klock G, Kreuzberg K (1991) Compartmented metabolite pools in protoplasts from the green alga Chlamydomonas reinhardtii: changes after transition from aerobiosis to anaerobiosis in the dark. Biochim Biophys Acta 1073:410–415

Kmiecik P, Leonardelli M, Teige M (2016) Novel connections in plant organellar signalling link different stress responses and signalling pathways. J Exp Bot 67:3793–3807. https://doi.org/10.1093/jxb/erw136

Knappe S, Flugge UI, Fischer K (2003) Analysis of the plastidic phosphate translocator gene family in Arabidopsis and identification of new phosphate translocator-homologous transporters, classified by their putative substrate-binding site. Plant Physiol 131:1178–1190. https://doi.org/10.1104/pp.016519

Kristoficova I, Vilhena C, Behr S, Jung K (2017) BtsT - a novel and specific pyruvate/H(+) symporter in Escherichia coli. J Bacteriol 200(2):e00599–17 https://doi.org/10.1128/JB.00599-17

Kunz HH, Gierth M, Herdean A, Satoh-Cruz M, Kramer DM, Spetea C, Schroeder JI (2014) Plastidial transporters KEA1, −2, and −3 are essential for chloroplast osmoregulation, integrity, and pH regulation in Arabidopsis. Proc Natl Acad Sci U S A 111:7480–7485. https://doi.org/10.1073/pnas.1323899111

Kustka AB, Milligan AJ, Zheng H, New AM, Gates C, Bidle KD, Reinfelder JR (2014) Low CO2 results in a rearrangement of carbon metabolism to support C4 photosynthetic carbon assimilation in Thalassiosira pseudonana. New Phytol 204:507–520. https://doi.org/10.1111/nph.12926

LaBrant E, Barnes AC, Roston RL (2018) Lipid transport required to make lipids of photosynthetic membranes. Photosynth Res 138:345–360. https://doi.org/10.1007/s11120-018-0545-5

Lane TS, Rempe CS, Davitt J, Staton ME, Peng Y, Soltis DE, Melkonian M, Deyholos M, Leebens-Mack JH, Chase M, Rothfels CJ, Stevenson D, Graham SW, Yu J, Liu T, Pires JC, Edger PP, Zhang Y, Xie Y, Zhu Y, Carpenter E, Wong GK, Stewart CN Jr (2016) Diversity of ABC transporter genes across the plant kingdom and their potential utility in biotechnology. BMC Biotechnol 16(47). https://doi.org/10.1186/s12896-016-0277-6

Li N, Gugel IL, Giavalisco P, Zeisler V, Schreiber L, Soll J, Philippar K (2015) FAX1, a novel membrane protein mediating plastid fatty acid export. PLoS Biol 13:e1002053. https://doi.org/10.1371/journal.pbio.1002053

Li N, Xu C, Li-Beisson Y, Philippar K (2016) Fatty acid and lipid transport in plant cells. Trends Plant Sci 21:145–158. https://doi.org/10.1016/j.tplants.2015.10.011

Li X, Patena W, Fauser F, Jinkerson RE, Saroussi S, Meyer MT, Ivanova N, Robertson JM, Yue R, Zhang R, Vilarrasa-Blasi J, Wittkopp TM, Ramundo S, Blum SR, Goh A, Laudon M, Srikumar T, Lefebvre PA, Grossman AR, Jonikas MC (2019a) A genome-wide algal mutant library and functional screen identifies genes required for eukaryotic photosynthesis. Nat Genet 51:627–635. https://doi.org/10.1038/s41588-019-0370-6

Li N, Zhang Y, Meng H, Li S, Wang S, Xiao Z, Chang P, Zhang X, Li Q, Guo L, Igarashi Y, Luo F (2019b) Characterization of fatty acid exporters involved in fatty acid transport for oil accumulation in the green alga Chlamydomonas reinhardtii. Biotechnol Biofuels 12(14). https://doi.org/10.1186/s13068-018-1332-4

Liang S, Qi Y, Zhao J, Li Y, Wang R, Shao J, Liu X, An L, Yu F (2017) Mutations in the Arabidopsis AtMRS2-11/AtMGT10/VAR5 gene cause leaf reticulation. Front Plant Sci 8:2007. https://doi.org/10.3389/fpls.2017.02007

Lindberg P, Melis A (2008) The chloroplast sulfate transport system in the green alga Chlamydomonas reinhardtii. Planta 228:951–961. https://doi.org/10.1007/s00425-008-0795-0

Linka N, Hurka H, Lang BF, Burger G, Winkler HH, Stamme C, Urbany C, Seil I, Kusch J, Neuhaus HE (2003) Phylogenetic relationships of non-mitochondrial nucleotide transport proteins in bacteria and eukaryotes. Gene 306:27–35

Linka M, Jamai A, Weber AP (2008) Functional characterization of the plastidic phosphate translocator gene family from the thermo-acidophilic red alga Galdieria sulphuraria reveals specific adaptations of primary carbon partitioning in green plants and red algae. Plant Physiol 148:1487–1496. https://doi.org/10.1104/pp.108.129478

Lopez-Millan AF, Duy D, Philippar K (2016) Chloroplast iron transport proteins - function and impact on plant physiology. Front Plant Sci 7:178. https://doi.org/10.3389/fpls.2016.00178

Lu BB, Xu CC, Awai K, Jones AD, Benning C (2007) A small ATPase protein of Arabidopsis, TGD3, involved in chloroplast lipid import. J Biol Chem 282:35945–35953. https://doi.org/10.1074/jbc.M704063200

Machingura MC, Bajsa-Hirschel J, Laborde SM, Schwartzenburg JB, Mukherjee B, Mukherjee A, Pollock SV, Forster B, Price GD, Moroney JV (2017) Identification and characterization of a solute carrier, CIA8, involved in inorganic carbon acclimation in Chlamydomonas reinhardtii. J Exp Bot 68:3879–3890. https://doi.org/10.1093/jxb/erx189

Mackinder LCM, Chen C, Leib RD, Patena W, Blum SR, Rodman M, Ramundo S, Adams CM, Jonikas MC (2017) A spatial interactome reveals the protein organization of the algal CO2-concentrating mechanism. Cell 171(133–147):e14. https://doi.org/10.1016/j.cell.2017.08.044

Marchand J, Heydarizadeh P, Schoefs B, Spetea C (2018) Ion and metabolite transport in the chloroplast of algae: lessons from land plants. Cell Mol Life Sci 75:2153–2176. https://doi.org/10.1007/s00018-018-2793-0

Margulis L (1970) Origin of eukaryotic cells. Yale University Press, New Haven

Mariscal V, Moulin P, Orsel M, Miller AJ, Fernandez E, Galvan A (2006) Differential regulation of the Chlamydomonas Nar1 gene family by carbon and nitrogen. Protist 157:421–433. https://doi.org/10.1016/j.protis.2006.06.003

Marmagne A, Vinauger-Douard M, Monachello D, de Longevialle AF, Charon C, Allot M, Rappaport F, Wollman FA, Barbier-Brygoo H, Ephritikhine G (2007) Two members of the Arabidopsis CLC (chloride channel) family, AtCLCe and AtCLCf, are associated with thylakoid and Golgi membranes, respectively. J Exp Bot 58:3385–3393. https://doi.org/10.1093/jxb/erm187

Martin W, Kowallik KV (1999) Annotated English translation of Mereschkowsky's 1905 paper 'Uber natur und ursprung der chromatophoren im pflanzenreiche. Eur J Phycol 34:287–295. https://doi.org/10.1017/S0967026299002231

Martinac B (2004) Mechanosensitive ion channels: molecules of mechanotransduction. J Cell Sci 117:2449–2460. https://doi.org/10.1242/jcs.01232

Maruyama S, Tokutsu R, Minagawa J (2014) Transcriptional regulation of the stress-responsive light harvesting complex genes in Chlamydomonas reinhardtii. Plant Cell Physiol 55:1304–1310. https://doi.org/10.1093/pcp/pcu068

Masmoudi S, Nguyen-Deroche N, Caruso A, Ayadi H, Morant-Manceau A, Tremblin G, Bertrand M, Schoefs B (2013) Metals in diatoms: from heaven to hell – a review. Cryptogamie-Algologie 34:185–225

Matsuda Y, Hopkinson BM, Nakajima K, Dupont CL, Tsuji Y (2017) Mechanisms of carbon dioxide acquisition and CO2 sensing in marine diatoms: a gateway to carbon metabolism. Philos Trans R Soc Lond Ser B Biol Sci 372. https://doi.org/10.1098/rstb.2016.0403

McFadden GI (2014) Origin and evolution of plastids and photosynthesis in eukaryotes. Cold Spring Harb Perspect Biol 6:a016105. https://doi.org/10.1101/cshperspect.a016105

Merchant SS, Prochnik SE, Vallon O, Harris EH, Karpowicz SJ, Witman GB, Terry A, Salamov A, Fritz-Laylin LK, Marechal-Drouard L, Marshall WF, Qu LH, Nelson DR, Sanderfoot AA, Spalding MH, Kapitonov VV, Ren QH, Ferris P, Lindquist E, Shapiro H, Lucas SM, Grimwood J, Schmutz J, Cardol P, Cerutti H, Chanfreau G, Chen CL, Cognat V, Croft MT, Dent R, Dutcher S, Fernandez E, Fukuzawa H, Gonzalez-Ballester D, Gonzalez-Halphen D, Hallmann A, Hanikenne M, Hippler M, Inwood W, Jabbari K, Kalanon M, Kuras R, Lefebvre PA, Lemaire SD, Lobanov AV, Lohr M, Manuell A, Meir I, Mets L, Mittag M, Mittelmeier T, Moroney JV, Moseley J, Napoli C, Nedelcu AM, Niyogi K, Novoselov SV, Paulsen IT, Pazour G, Purton S, Ral JP, Riano-Pachon DM, Riekhof W, Rymarquis L, Schroda M, Stern D, Umen J, Willows R, Wilson N, Zimmer SL, Allmer J, Balk J, Bisova K, Chen CJ, Elias M, Gendler K, Hauser C, Lamb MR, Ledford H, Long JC, Minagawa J, Page MD, Pan JM, Pootakham W, Roje S, Rose A, Stahlberg E, Terauchi AM, Yang PF, Ball S, Bowler C, Dieckmann CL, Gladyshev VN, Green P, Jorgensen R, Mayfield S, Mueller-Roeber B, Rajamani S, Sayre RT, Brokstein P, Dubchak I, Goodstein D, Hornick L, Huang YW, Jhaveri J, Luo YG, Martinez D, Ngau WCA, Otillar B, Poliakov A, Porter A, Szajkowski L, Werner G, Zhou KM, Grigoriev IV, Rokhsar DS, Grossman AR, Annotation C, Team JA (2007) The Chlamydomonas genome reveals the evolution of key animal and plant functions. Science 318:245–251. https://doi.org/10.1126/science.1143609

Mimouni V, Ulmann L, Pasquet V, Mathieu M, Picot L, Bougaran G, Cadoret JP (2012) A. M-M and Schoefs B. The potential of microalgae for the production of bioactive molecules of pharmaceutical interest Curr Pharmaceutical Biotechnol 13:2733–2750

Miyaji T, Kuromori T, Takeuchi Y, Yamaji N, Yokosho K, Shimazawa A, Sugimoto E, Omote H, Ma JF, Shinozaki K, Moriyama Y (2015) AtPHT4;4 is a chloroplast-localized ascorbate transporter in

Arabidopsis. Nat Commun 6:5928. https://doi.org/10.1038/ncomms6928

Mochizuki N, Brusslan JA, Larkin R, Nagatani A, Chory J (2001) Arabidopsis genomes uncoupled 5 (GUN5) mutant reveals the involvement of mg-chelatase H subunit in plastid-to-nucleus signal transduction. Proc Natl Acad Sci U S A 98:2053–2058. https://doi.org/10.1073/pnas.98.4.2053

Moller JV, Juul B, le Maire M (1996) Structural organization, ion transport, and energy transduction of P-type ATPases. Biochim Biophys Acta 1286:1–51

Monachello D, Allot M, Oliva S, Krapp A, Daniel-Vedele F, Barbier-Brygoo H, Ephritikhine G (2009) Two anion transporters AtClCa and AtClCe fulfil interconnecting but not redundant roles in nitrate assimilation pathways. New Phytol 183:88–94. https://doi.org/10.1111/j.1469-8137.2009.02837.x

Moog D, Rensing SA, Archibald JM, Maier UG, Ullrich KK (2015) Localization and evolution of putative triose phosphate translocators in the diatom Phaeodactylum tricornutum. Genome Biol Evol 7:2955–2969. https://doi.org/10.1093/gbe/evv190

Moreno I, Norambuena L, Maturana D, Toro M, Vergara C, Orellana A, Zurita-Silva A, Ordenes VR (2008) AtHMA1 is a thapsigargin-sensitive Ca2+/heavy metal pump. J Biol Chem 283:9633–9641. https://doi.org/10.1074/jbc.M800736200

Moroney JV, Ynalvez RA (2007) Proposed carbon dioxide concentrating mechanism in Chlamydomonas reinhardtii. Eukaryot Cell 6:1251–1259. https://doi.org/10.1128/EC.00064-07

Moseley JL, Allinger T, Herzog S, Hoerth P, Wehinger E, Merchant S, Hippler M (2002) Adaptation to Fe-deficiency requires remodeling of the photosynthetic apparatus. EMBO J 21:6709–6720

Mukherjee B (2013) Investigation of the role of putative inorganic carbon transporters in the carbon dioxide concentrating mechanisms of Chlamydomonas reinhardtii. Dissertation etd-07062013-211518. Louisiana State University

Murcha MW, Elhafez D, Lister R, Tonti-Filippini J, Baumgartner M, Philippar K, Carrie C, Mokranjac D, Soll J, Whelan J (2007) Characterization of the preprotein and amino acid transporter gene family in Arabidopsis. Plant Physiol 143:199–212. https://doi.org/10.1104/pp.106.090688

Nakayama Y, Fujiu K, Sokabe M, Yoshimura K (2007) Molecular and electrophysiological characterization of a mechanosensitive channel expressed in the chloroplasts of Chlamydomonas. Proc Natl Acad Sci U S A 104:5883–5888. https://doi.org/10.1073/pnas.0609996104

Palmgren MG, Harper JF (1999) Pumping with plant P-type ATPases. J Exp Bot 50(SI) Conference: 11th International Workshop on Plant Membrane Biology Location):883–893

Patron NJ, Keeling PJ (2005) Common evolutionary origin of starch biosynthetic enzymes in green and red algae. J Phycol 41:1131–1141. https://doi.org/10.1111/j.1529-8817.2005.00135.x

Pavon LR, Lundh F, Lundin B, Mishra A, Persson BL, Spetea C (2008) Arabidopsis ANTR1 is a thylakoid Na+−dependent phosphate transporter: functional characterization in Escherichia coli. J Biol Chem 283:13520–13527. https://doi.org/10.1074/jbc.M709371200

Pearson GA, Lago-Leston A, Canovas F, Cox CJ, Verret F, Lasternas S, Duarte CM, Agusti S, Serrao EA (2015) Metatranscriptomes reveal functional variation in diatom communities from the Antarctic peninsula. ISME J 9:2275–2289. https://doi.org/10.1038/ismej.2015.40

Petroutsos D, Busch A, Janssen I, Trompelt K, Bergner SV, Weinl S, Holtkamp M, Karst U, Kudla J, Hippler M (2011) The chloroplast calcium sensor CAS is required for photoacclimation in Chlamydomonas reinhardtii. Plant Cell 23:2950–2963. https://doi.org/10.1105/tpc.111.087973

Pfeil BE, Schoefs B, Spetea C (2014) Function and evolution of channels and transporters in photosynthetic membranes. Cell Mol Life Sci 71:979–998. https://doi.org/10.1007/s00018-013-1412-3

Pick TR, Weber AP (2014) Unknown components of the plastidial permeome. Front Plant Sci 5:410. https://doi.org/10.3389/fpls.2014.00410

Pollock SV, Prout DL, Godfrey AC, Lemaire SD, Moroney JV (2004) The Chlamydomonas reinhardtii proteins CCP1 and CCP2 are required for long-term growth, but are not necessary for efficient photosynthesis, in a low-CO2 environment. Plant Mol Biol 56:125–132. https://doi.org/10.1007/s11103-004-2650-4

Pottosin I, Dobrovinskaya O (2015) Ion channels in native chloroplast membranes: challenges and potential for direct patch-clamp studies. Front Physiol 6(396). https://doi.org/10.3389/fphys.2015.00396

Pottosin I, Schönknecht G (1995) Patch clamp study of the voltage-dependent anion channel in the thylakoid membrane. J Membr Biol 148:143–156

Price GD, Badger MR, Woodger FJ, Long BM (2008) Advances in understanding the cyanobacterial CO2-concentrating-mechanism (CCM): functional components, ci transporters, diversity, genetic regulation and prospects for engineering into plants. J Exp Bot 59:1441–1461. https://doi.org/10.1093/jxb/erm112

Price DC, Chan CX, Yoon HS, Yang EC, Qiu H, Weber AP, Schwacke R, Gross J, Blouin NA, Lane C, Reyes-Prieto A, Durnford DG, Neilson JA, Lang BF, Burger G, Steiner JM, Loffelhardt W, Meuser JE, Posewitz MC, Ball S, Arias MC, Henrissat B, Coutinho PM, Rensing SA, Symeonidi A, Doddapaneni H, Green BR, Rajah VD, Boore J, Bhattacharya D (2012) Cyanophora paradoxa genome elucidates origin of photosynthesis in algae and plants. Science 335:843–847. https://doi.org/10.1126/science.1213561

Pudelski B, Kraus S, Soll J, Philippar K (2010) The plant PRAT proteins - preprotein and amino acid transport in mitochondria and chloroplasts. Plant Biol (Stuttg) 12 Suppl 1:42–55. https://doi.org/10.1111/j.1438-8677.2010.00357.x

Qu Z, Hartzell HC (2008) Bestrophin cl- channels are highly permeable to HCO3. Am J Physiol Cell Physiol 294:C1371–C1377. https://doi.org/10.1152/ajpcell.00398.2007

Ramazanov Z, Mason CB, Geraghty AM, Spalding MH, Moroney JV (1993) The low CO2-inducible 36-kilodalton protein is localized to the chloroplast envelope of Chlamydomonas reinhardtii. Plant Physiol 101:1195–1199

Ramel F, Birtic S, Ginies C, Soubigou-Taconnat L, Triantaphylides C, Havaux M (2012) Carotenoid oxidation products are stress signals that mediate gene responses to singlet oxygen in plants. Proc Natl Acad Sci U S A 109:5535–5540. https://doi.org/10.1073/pnas.1115982109

Rea PA (2007) Plant ATP-binding cassette transporters. Annu Rev Plant Biol 58:347–375. https://doi.org/10.1146/annurev.arplant.57.032905.105406

Reinfelder JR (2011) Carbon concentrating mechanisms in eukaryotic marine phytoplankton. Annu Rev Mar Sci 3:291–315. https://doi.org/10.1146/annurev-marine-120709-142720

Reiser J, Linka N, Lemke L, Jeblick W, Neuhaus HE (2004) Molecular physiological analysis of the two plastidic ATP/ADP transporters from Arabidopsis. Plant Physiol 136:3524–3536. https://doi.org/10.1104/pp.104.049502

Rexach J, Fernandez E, Galvan A (2000) The Chlamydomonas reinhardtii Nar1 gene encodes a chloroplast membrane protein involved in nitrite transport. Plant Cell 12:1441–1453

Richards TA, Dacks JB, Campbell SA, Blanchard JL, Foster PG, McLeod R, Roberts CW (2006) Evolutionary origins of the eukaryotic shikimate pathway: gene fusions, horizontal gene transfer, and endosymbiotic replacements. Eukaryot Cell 5:1517–1531. https://doi.org/10.1128/EC.00106-06

Rossig C, Reinbothe C, Gray J, Valdes O, von Wettstein D, Reinbothe S (2013) Three proteins mediate import of transit sequence-less precursors into the inner envelope of chloroplasts in Arabidopsis thaliana. Proc Natl Acad Sci U S A 110:19962–19967. https://doi.org/10.1073/pnas.1319648110

Saier MH Jr, Yen MR, Noto K, Tamang DG, Elkan C (2009) The transporter classification database: recent advances. Nucleic Acids Res 37:D274–D278. https://doi.org/10.1093/nar/gkn862

Saito T, Kobayashi NI, Tanoi K, Iwata N, Suzuki H, Iwata R, Nakanishi TM (2013) Expression and functional analysis of the CorA-MRS2-ALR-type magnesium transporter family in rice. Plant Cell Physiol 54:1673–1683. https://doi.org/10.1093/pcp/pct112

Sanchez-Fernandez R, Davies TG, Coleman JO, Rea PA (2001) The Arabidopsis thaliana ABC protein superfamily, a complete inventory. J Biol Chem 276:30231–30244. https://doi.org/10.1074/jbc.M103104200

Sasaki Y, Hakamada K, Suama Y, Nagano Y, Furusawa I, Matsuno R (1993) Chloroplast-encoded protein as a subunit of acetyl-CoA carboxylase in pea plant. J Biol Chem 268:25118–25123

Sautron E, Mayerhofer H, Giustini C, Pro D, Crouzy S, Ravaud S, Pebay-Peyroula E, Rolland N, Catty P, Seigneurin-Berny D (2015) HMA6 and HMA8 are two chloroplast cu+-ATPases with different enzymatic properties. Biosci Rep 35. https://doi.org/10.1042/BSR20150065

Scaife MA, Smith AG (2016) Towards developing algal synthetic biology. Biochem Soc Trans 44:716–722. https://doi.org/10.1042/BST20160061

Schmitz J, Heinrichs L, Scossa F, Fernie AR, Oelze ML, Dietz KJ, Rothbart M, Grimm B, Flugge UI, Hausler RE (2014) The essential role of sugar metabolism in the acclimation response of Arabidopsis thaliana to high light intensities. J Exp Bot 65:1619–1636. https://doi.org/10.1093/jxb/eru027

Schneider A, Steinberger I, Herdean A, Gandini C, Eisenhut M, Kurz S, Morper A, Hoecker N, Ruhle T, Labs M, Flugge UI, Geimer S, Schmidt SB, Husted S, Weber AP, Spetea C, Leister D (2016) The evolutionarily conserved protein PHOTOSYNTHESIS AFFECTED MUTANT71 is required for efficient manganese uptake at the thylakoid membrane in Arabidopsis. Plant Cell 28:892–910. https://doi.org/10.1105/tpc.15.00812

Schoefs B (2005) Protochlorophyllide reduction - what is new in 2005? Photosynthetica 43:329–343. https://doi.org/10.1007/s11099-005-0056-4

Schönknecht G, Hedrich R, Junge W, Raschke K (1988) A voltage-dependent chloride channel in the photosynthetic membrane of a higher-plant. Nature 336:589–592. https://doi.org/10.1038/336589a0

Schwacke R, Flugge UI (2018) Identification and characterization of plant membrane proteins using

ARAMEMNON. Methods Mol Biol 1696:249–259. https://doi.org/10.1007/978-1-4939-7411-5_17

Shen JR (2015) The structure of photosystem II and the mechanism of water oxidation in photosynthesis. Annu Rev Plant Biol 66:23–48. https://doi.org/10.1146/annurev-arplant-050312-120129

Shin SE, Lim JM, Koh HG, Kim EK, Kang NK, Jeon S, Kwon S, Shin WS, Lee B, Hwangbo K, Kim J, Ye SH, Yun JY, Seo H, Oh HM, Kim KJ, Kim JS, Jeong WJ, Chang YK, Jeong BR (2016) CRISPR/Cas9-induced knockout and knock-in mutations in Chlamydomonas reinhardtii. Sci Rep 6(27810). https://doi.org/10.1038/srep27810

Solymosi K (2012) Plastid structure, diversification and interconversions I. algae. Curr Chem Biol 6:167–186

Solymosi K, Keresztes A (2012) Plastid structure, diversification and interconversions II. Land plants. Curr Chem Biol 6:187–204

Spalding MH (2008) Microalgal carbon-dioxide-concentrating mechanisms: Chlamydomonas inorganic carbon transporters. J Exp Bot 59:1463–1473. https://doi.org/10.1093/jxb/erm128

Spetea C, Lundin B (2012) Evidence for nucleotide-dependent processes in the thylakoid lumen of plant chloroplasts--an update. FEBS Lett 586:2946–2954. https://doi.org/10.1016/j.febslet.2012.07.005

Spetea C, Schoefs B (2010) Solute transporters in plant thylakoid membranes: key players during photosynthesis and light stress. Commun Integr Biol 3:122–129

Spetea C, Pfeil BE, Schoefs B (2011) Phylogenetic analysis of the thylakoid ATP/ADP carrier reveals new insights into its function restricted to green plants. Front Plant Sci 2:110. https://doi.org/10.3389/fpls.2011.00110

Spetea C, Rintamaki E, Schoefs B (2014) Changing the light environment: chloroplast signalling and response mechanisms. Philos Trans R Soc Lond Ser B Biol Sci 369:20130220. https://doi.org/10.1098/rstb.2013.0220

Spetea C, Szabo I, Kunz HH (2016) Editorial: ion transport in chloroplast and mitochondria physiology in green organisms. Front Plant Sci 7:2003. https://doi.org/10.3389/fpls.2016.02003

Spetea C, Herdean A, Allorent G, Carraretto L, Finazzi G, Szabo I (2017) An update on the regulation of photosynthesis by thylakoid ion channels and transporters in Arabidopsis. Physiol Plant 161:16–27. https://doi.org/10.1111/ppl.12568

Strand A, Asami T, Alonso J, Ecker JR, Chory J (2003) Chloroplast to nucleus communication triggered by accumulation of mg-protoporphyrinIX. Nature 421:79–83. https://doi.org/10.1038/nature01204

Sugiura M, Georgescu MN, Takahashi M (2007) A nitrite transporter associated with nitrite uptake by higher plant chloroplasts. Plant Cell Physiol 48:1022–1035. https://doi.org/10.1093/pcp/pcm073

Sun Y, Yang R, Huang J (2017) The magnesium transporter MGT10 is essential for chloroplast development and photosynthesis in Arabidopsis thaliana. Mol Plant 10:1584–1587

Szabo I, Spetea C (2017) Impact of the ion transportome of chloroplasts on the optimization of photosynthesis. J Exp Bot 68:3115–3128. https://doi.org/10.1093/jxb/erx063

Takahashi H, Buchner P, Yoshimoto N, Hawkesford MJ, Shiu SH (2011) Evolutionary relationships and functional diversity of plant sulfate transporters. Front Plant Sci 2:119. https://doi.org/10.3389/fpls.2011.00119

Teardo E, Formentin E, Segalla A, Giacometti GM, Marin O, Zanetti M, Lo Schiavo F, Zoratti M, Szabo I (2011) Dual localization of plant glutamate receptor AtGLR3.4 to plastids and plasmamembrane. Biochim Biophys Acta 1807:359–367. https://doi.org/10.1016/j.bbabio.2010.11.008

Teardo E, Carraretto L, De Bortoli S, Costa A, Behera S, Wagner R, Lo Schiavo F, Formentin E, Szabo I (2015) Alternative splicing-mediated targeting of the Arabidopsis GLUTAMATE RECEPTOR3.5 to mitochondria affects organelle morphology. Plant Physiol 167:216–227. https://doi.org/10.1104/pp.114.242602

Terashima M, Specht M, Naumann B, Hippler M (2010) Characterizing the anaerobic response of Chlamydomonas reinhardtii by quantitative proteomics. Mol Cell Proteomics 9:1514–1532. https://doi.org/10.1074/mcp.M900421-MCP200

Terashima M, Specht M, Hippler M (2011) The chloroplast proteome: a survey from the Chlamydomonas reinhardtii perspective with a focus on distinctive features. Curr Genet 57:151–168. https://doi.org/10.1007/s00294-011-0339-1

Terashima M, Petroutsos D, Hudig M, Tolstygina I, Trompelt K, Gabelein P, Fufezan C, Kudla J, Weinl S, Finazzi G, Hippler M (2012) Calcium-dependent regulation of cyclic photosynthetic electron transfer by a CAS, ANR1, and PGRL1 complex. Proc Natl Acad Sci U S A 109:17717–17722. https://doi.org/10.1073/pnas.1207118109

Thuswaldner S, Lagerstedt JO, Rojas-Stutz M, Bouhidel K, Der C, Leborgne-Castel N, Mishra A, Marty F, Schoefs B, Adamska I, Persson BL, Spetea C (2007) Identification, expression, and functional analyses of a thylakoid ATP/ADP carrier from Arabidopsis. J Biol Chem 282:8848–8859. https://doi.org/10.1074/jbc.M609130200

Tohge T, Watanabe M, Hoefgen R, Fernie AR (2013) Shikimate and phenylalanine biosynthesis in the green lineage. Front Plant Sci 4:62. https://doi.org/10.3389/fpls.2013.00062

Tyra HM, Linka M, Weber AP, Bhattacharya D (2007) Host origin of plastid solute transporters in the first photosynthetic eukaryotes. Genome Biol 8:R212. https://doi.org/10.1186/gb-2007-8-10-r212

Ulmann L, Mimouni V, Blanckaert V, Pasquet V, Schoefs B, Chénais B (2014) The polyunsaturated fatty acids from microalgae as potential sources for health and disease. In: A angel Catalá (ed) polyunsaturated fatty acids: sources, antioxidant properties, and health benefits. Nova Publishers, New York, pp 23–44

Vainonen JP, Sakuragi Y, Stael S, Tikkanen M, Allahverdiyeva Y, Paakkarinen V, Aro E, Suorsa M, Scheller HV, Vener AV, Aro EM (2008) Light regulation of CaS, a novel phosphoprotein in the thylakoid membrane of Arabidopsis thaliana. FEBS J 275:1767–1777. https://doi.org/10.1111/j.1742-4658.2008.06335.x

Valenzuela J, Mazurie A, Carlson RP, Gerlach R, Cooksey KE, Peyton BM, Fields MW (2012) Potential role of multiple carbon fixation pathways during lipid accumulation in Phaeodactylum tricornutum. Biotechnol Biofuels 5:40. https://doi.org/10.1186/1754-6834-5-40

Vastermark A, Saier MH Jr (2014) The involvement of transport proteins in transcriptional and metabolic regulation. Curr Opin Microbiol 18:8–15. https://doi.org/10.1016/j.mib.2014.01.002

Verret F, Wheeler G, Taylor AR, Farnham G, Brownlee C (2010) Calcium channels in photosynthetic eukaryotes: implications for evolution of calcium-based signalling. New Phytol 187:23–43. https://doi.org/10.1111/j.1469-8137.2010.03271.x

Versaw WK, Harrison MJ (2002) A chloroplast phosphate transporter, PHT2;1, influences allocation of phosphate within the plant and phosphate-starvation responses. Plant Cell 14:1751–1766

Vinayak V, Manoylov KM, Gateau H, Blanckaert V, Herault J, Pencreac'h G, Marchand J, Gordon R, Schoefs B (2015) Diatom milking: a review and new approaches. Mar Drugs 13:2629–2665. https://doi.org/10.3390/md13052629

Wang L, Yamano T, Kajikawa M, Hirono M, Fukuzawa H (2014) Isolation and characterization of novel high-CO2-requiring mutants of Chlamydomonas reinhardtii. Photosynth Res 121:175–184. https://doi.org/10.1007/s11120-014-9983-x

Wang Y, Stessman DJ, Spalding MH (2015) The CO2 concentrating mechanism and photosynthetic carbon assimilation in limiting CO2: how Chlamydomonas works against the gradient. Plant J 82:429–448. https://doi.org/10.1111/tpj.12829

Wang C, Xu W, Jin H, Zhang T, Lai J, Zhou X, Zhang S, Liu S, Duan X, Wang H, Peng C, Yang C (2016) A putative chloroplast-localized Ca(2+)/H(+) antiporter CCHA1 is involved in calcium and pH homeostasis and required for PSII function in Arabidopsis. Mol Plant 9:1183–1196. https://doi.org/10.1016/j.molp.2016.05.015

Warakanont J, Tsai CH, Michel EJ, Murphy GR 3rd, Hsueh PY, Roston RL, Sears BB, Benning C (2015) Chloroplast lipid transfer processes in Chlamydomonas reinhardtii involving a TRIGALACTOSYLDIACYLGLYCEROL 2 (TGD2) orthologue. Plant J 84:1005–1020. https://doi.org/10.1111/tpj.13060

Weber AP, Bauwe H (2013) Photorespiration--a driver for evolutionary innovations and key to better crops. Plant Biol (Stuttg) 15:621–623. https://doi.org/10.1111/plb.12036

Weber AP, Linka N (2011) Connecting the plastid: transporters of the plastid envelope and their role in linking plastidial with cytosolic metabolism. Annu Rev Plant Biol 62:53–77. https://doi.org/10.1146/annurev-arplant-042110-103903

Weber AP, von Caemmerer S (2010) Plastid transport and metabolism of C3 and C4 plants--comparative analysis and possible biotechnological exploitation. Curr Opin Plant Biol 13:257–265. https://doi.org/10.1016/j.pbi.2010.01.007

Weber AP, Schneidereit J, Voll LM (2004) Using mutants to probe the in vivo function of plastid envelope membrane metabolite transporters. J Exp Bot 55:1231–1244. https://doi.org/10.1093/jxb/erh091

Weber AP, Schwacke R, Flugge UI (2005) Solute transporters of the plastid envelope membrane. Annu Rev Plant Biol 56:133–164. https://doi.org/10.1146/annurev.arplant.56.032604.144228

Weber AP, Linka M, Bhattacharya D (2006) Single, ancient origin of a plastid metabolite translocator family in Plantae from an endomembrane-derived ancestor. Eukaryot Cell 5:609–612. https://doi.org/10.1128/EC.5.3.609-612.2006

Weisse AY, Oyarzun DA, Danos V, Swain PS (2015) Mechanistic links between cellular trade-offs, gene expression, and growth. Proc Natl Acad Sci U S A 112:E1038–E1047. https://doi.org/10.1073/pnas.1416533112

Werner-Washburne M, Keegstra K (1985) L-aspartate transport into pea chloroplasts: kinetic and inhibitor evidence for multiple transport systems. Plant Physiol 78:221–227

Wood PM (1978) Interchangeable copper and iron proteins in algal photosynthesis. Studies on plastocyanin and cytochrome c-552 in Chlamydomonas. Eur J Biochem 87:9–19

Woodson JD, Perez-Ruiz JM, Chory J (2011) Heme synthesis by plastid ferrochelatase I regulates nuclear gene expression in plants. Curr Biol 21:897–903. https://doi.org/10.1016/j.cub.2011.04.004

Xiao Y, Savchenko T, Baidoo EE, Chehab WE, Hayden DM, Tolstikov V, Corwin JA, Kliebenstein DJ, Keasling JD, Dehesh K (2012) Retrograde signaling by the plastidial metabolite MEcPP regulates expression of nuclear stress-response genes. Cell 149:1525–1535. https://doi.org/10.1016/j.cell.2012.04.038

Xing J, Liu P, Zhao L, Huang F (2017) Deletion of CGLD1 impairs PSII and increases singlet oxygen tolerance of green alga Chlamydomonas reinhardtii. Front Plant Sci 8:2154. https://doi.org/10.3389/fpls.2017.02154

Xu XM, Moller SG (2004) AtNAP7 is a plastidic SufC-like ATP-binding cassette/ATPase essential for Arabidopsis embryogenesis. Proc Natl Acad Sci U S A 101:9143–9148. https://doi.org/10.1073/pnas.0400799101

Yamano T, Fukuzawa H (2009) Carbon-concentrating mechanism in a green alga, Chlamydomonas reinhardtii, revealed by transcriptome analyses. J Basic Microbiol 49:42–51. https://doi.org/10.1002/jobm.200800352

Yamano T, Tsujikawa T, Hatano K, Ozawa S, Takahashi Y, Fukuzawa H (2010) Light and low-CO2-dependent LCIB-LCIC complex localization in the chloroplast supports the carbon-concentrating mechanism in Chlamydomonas reinhardtii. Plant Cell Physiol 51:1453–1468. https://doi.org/10.1093/pcp/pcq105

Yamano T, Sato E, Iguchi H, Fukuda Y, Fukuzawa H (2015) Characterization of cooperative bicarbonate uptake into chloroplast stroma in the green alga Chlamydomonas reinhardtii. Proc Natl Acad Sci U S A 112:7315–7320. https://doi.org/10.1073/pnas.1501659112

Yamano T, Toyokawa C, Fukuzawa H (2018) High-resolution suborganellar localization of ca(2+)-binding protein CAS, a novel regulator of CO2-concentrating mechanism. Protoplasma 255:1015–1022. https://doi.org/10.1007/s00709-018-1208-2

Yin L, Lundin B, Bertrand M, Nurmi M, Solymosi K, Kangasjarvi S, Aro EM, Schoefs B, Spetea C (2010) Role of thylakoid ATP/ADP carrier in photoinhibition and photoprotection of photosystem II in Arabidopsis. Plant Physiol 153:666–677. https://doi.org/10.1104/pp.110.155804

Yin L, Vener AV, Spetea C (2015) The membrane proteome of stroma thylakoids from Arabidopsis thaliana studied by successive in-solution and in-gel digestion. Physiol Plant 154:433–446. https://doi.org/10.1111/ppl.12308

Yoon HS, Hackett JD, Ciniglia C, Pinto G, Bhattacharya D (2004) A molecular timeline for the origin of photosynthetic eukaryotes. Mol Biol Evol 21:809–818. https://doi.org/10.1093/molbev/msh075

Zhang XY, Zhang X, Zhang Q, Pan XX, Yan LC, Ma XJ, Zhao WZ, Qi XT, Yin LP (2017) Zea mays Fe deficiency-related 4 (ZmFDR4) functions as an iron transporter in the plastids of monocots. Plant J 90:147–163. https://doi.org/10.1111/tpj.13482

Zhang B, Zhang C, Liu C, Jing Y, Wang Y, Jin L, Yang L, Fu A, Shi J, Zhao F, Lan W, Luan S (2018) Inner envelope CHLOROPLAST MANGANESE TRANSPORTER 1 supports manganese homeostasis and phototrophic growth in Arabidopsis. Mol Plant 11:943–954. https://doi.org/10.1016/j.molp.2018.04.007

Zybailov B, Rutschow H, Friso G, Rudella A, Emanuelsson O, Sun Q, van Wijk KJ (2008) Sorting signals, N-terminal modifications and abundance of the chloroplast proteome. PLoS One 3:e1994. https://doi.org/10.1371/journal.pone.0001994

Chapter 7

Structural and Biochemical Features of Carbon Acquisition in Algae

John Beardall*
School of Biological Sciences, Monash University, Clayton, VIC, Australia

and

John A. Raven
Division of Plant Sciences, University of Dundee at the James Hutton Institute, Dundee, UK

Climate Change Cluster, University of Technology Sydney, Ultimo, NSW, Australia

School of Biological Science, University of Western Australia, Crawley, WA, Australia

I. Introduction

Cyanobacteria, eukaryotic algae and vascular plants ultimately depend on the enzyme ribulose-1,5-bisphosphate carboxylase oxygenase (Rubisco) for assimilation of CO_2 into organic matter, initially, via a 6C carboxyketone intermediate, in the form of 3-phosphoglycerate (Eq. 7.1).

*Author for correspondence, e-mail: john.beardall@monash.edu

A. W. D. Larkum et al. (eds.), *Photosynthesis in Algae: Biochemical and Physiological Mechanisms*, Advances in Photosynthesis and Respiration 45, https://doi.org/10.1007/978-3-030-33397-3_7

$$CO_2 + H_2O + D - \text{ribulose} - 1,5 - \text{bisphosphate} \rightarrow 2 \times 3 - \text{phosphoglycerate} \quad (7.1)$$

The 3-phosphoglycerate so formed undergoes a series of reactions, leading to the net production of one molecule of triose phosphate for every 3 CO_2 assimilated, in the Calvin-Benson-Bassham Cycle (Photosynthetic Carbon Reduction Cycle; PCRC) and the regeneration of one ribulose-1,5-bisphosphate. Each turn of the PCRC uses 2 NADPH plus 3 ATP per CO_2 assimilated, involving at least 9 mol photons absorbed per mol CO_2 assimilated (Raven et al. 2014) although, as will be described below, the precise energetic costs involved in net incorporation of CO_2 into carbohydrate usually exceed this.

There are a number of alternative pathways leading to net CO_2 assimilation in autotrophs (Raven et al. 2011, 2012) but, as discussed later in this chapter, cyanobacteria and algae appear to use only the PCRC (Beardall and Raven 2016). Indeed, 99% of primary productivity on the planet is carried out by processes that involve Rubisco and the PCRC (Raven 2009; Beardall and Raven 2016).

In this chapter, we examine the biochemical and structural constraints on carbon assimilation in cyanobacteria and eukaryotic algae and discuss the need for CO_2 concentrating mechanisms (CCMs) if these photoautotrophs are to achieve significant rates of net photosynthesis. In order to determine whether cells possess a capacity for CCMs, a number of criteria need to be satisfied, but there are currently misconceptions in the literature about what comprises proof of CCM activity. Accordingly, we discuss the mechanisms of biochemical and biophysical CCMs and the strengths and weaknesses of the various criteria that have been employed as yardsticks for CCM determination.

II. Carbon Assimilation

A. *The Characteristics of Most Rubiscos Necessitate Operation of a CCM*

In addition to the, relatively low catalytic rate, carboxylase activity shown in Eq. 7.1, Rubisco also possesses an oxygenase activity, leading, via a 5C peroxyketone intermediate, to the formation of one molecule of phosphoglycerate and one molecule of phosphoglycolate (Eq. 7.2).

$$O_2 + D - \text{ribulose} - 1,5 - \text{bisphosphate} \rightarrow 3 - \text{phosphoglycerate} + 2 - \text{phosphoglycolate} \quad (7.2)$$

The phosphoglycolate so formed can be acted upon by 2-phosphoglycolate phosphatase, leading to formation of glycolate. The latter can be excreted from cyanobacteria or plastids, leading to a net loss of 2 organic C. Alternatively 2 molecules of glycolate can enter the sequence of reactions known as the photorespiratory carbon oxidation cycle (PCOC, photorespiration) leading to formation of one molecule of 3-phosphoglycerate and the net loss of 1 C (Beardall and Raven 2016; Raven et al. 2011; Beardall et al. 2003). Eisenhut et al. (2008) showed that a cyanobacterium has two alternative pathways of glycolate metabolism in addition to the PCOC; deletion of all three of the pathways is lethal, so in this organism glycolate excretion alone is not an adequate sink for glycolate. The role of photorespiration as well as alternative pathways of electron flow and oxygen consumption in algae and cyanobacteria are discussed in a separate chapter in this volume (Raven et al. 2019).

CO_2 and O_2 compete for the same active site on Rubisco, and the achieved rates of the two carboxylase and oxygenase activities depends on the O_2:CO_2 ratio at the active site of the enzyme, according to the Selectivity Factor S_{rel} shown in Eq. 7.3.

$$S_{rel} = \left(K_{0.5}O_2 \times k_{cat}CO_2\right) / \left(K_{0.5}CO_2 \times k_{cat}O_2\right) \quad (7.3)$$

where $k_{cat}(CO_2)$ is the CO_2-saturated specific rate of carboxylase activity of Rubisco (mol CO_2 mol^{-1} active sites s^{-1}), $K_{1/2}$ (CO_2) is the concentration of CO_2 at which the CO_2 fixation rate by Rubisco is half of $k_{cat}(CO_2)$, $k_{cat}(O_2)$ is the O_2-saturated specific rate of oxygenase activity of Rubisco (mol O_2 mol^{-1} active sites s^{-1}) and $K_{1/2}$ (O_2) is the concentration of O_2 at which the O_2 fixation rate by Rubisco is half of $k_{cat}(O_2)$.

Autotrophs contain a broad range of different forms of Rubisco. These have been discussed extensively in the literature (Badger et al. 1998; Raven and Beardall 2003; Beardall and Raven 2016; Tcherkez et al. 2006; Whitney et al. 2011; Raven et al. 2011, 2012; Studer et al. 2014; Griffiths et al. 2017; Bathellier et al. 2018), so their characteristics are only summarised briefly here. There are 3 known main forms of Rubisco, referred to as Forms I, II and III. A fourth group Form IV) consists of Rubisco-like proteins which lack carboxylase activity and which may instead function in S metabolism (Hanson and Tabita 2001). Cyanobacteria and many algae have Form I Rubisco with 8 large and 8 small subunits (L_8S_8). Form I Rubiscos can be further categorised into Form IA and Form IB. *Prochlorococcus* and many marine *Synechococcus* species produce Form IA Rubisco, obtained by lateral gene transfer from an autotrophic proteobacterium (Raven et al. 2012). The vast majority of marine and freshwater cyanobacteria however possess the ancestral Form IB Rubisco, which was transferred in primary endosymbiosis to glaucocystophyte and thence chlorophyte algae and then by secondary endosymbiosis to chlorarachniophyte and euglenophyte algae (Raven et al. 2012). All red algae on the other hand possess Form ID RUBISCO, obtained by lateral gene transfer from an autotrophic proteobacterium (displacing the Form IB Rubisco transferred in primary endosymbiosis). Through secondary endosymbiosis this form of Rubisco appears, at least in those species that have been examined, to have been passed on to cryptophytes, haptophytes (e.g. cocolithophores) and heterokonts (= stramenopiles or ochristans, e.g. diatoms). Some Form IB Rubiscos have the very high selectivity for CO_2 over O_2 (Raven et al. 2012), though Tcherkez et al. (2006) suggest that Form 1D has the highest affinity for carbon dioxide and the highest carbon dioxide:oxygen selectivity.

On the other hand, the ancestral dinoflagellates and *Chromera veria*, both alveolates, possess Form II Rubisco, believed to have been obtained by lateral gene transfer from an autotrophic proteobacterium; Form II Rubisco comprises only 2 large subunits (L_2). Form III Rubiscos also lack small subunits (but can have more complex structures based on the L_2 basal structure ($(L_2)_4$, $(L_2)_5$), but are found only in Archaea so will not be considered further here.

These various forms of Rubisco have differing kinetic properties and in particular differing selectivity factors. Form IBc Rubiscos, found in most marine and freshwater β-cyanobacteria, have high $K_{1/2}(CO_2)$ values of 105–290 (with most values falling in the range of 200–260 μM). Selectivity factors vary from 38 to 56 mol mol^{-1} and CO_2-saturated specific reaction rates (k_{cat}) values range from 2.6 to 11.4 mol CO_2 mol^{-1} active sites s^{-1}. In contrast, the Form IAc Rubisco of the marine α-cyanobacterium *Prochlorococcus* MIT9313 has the highest known $K_{1/2}(CO_2)$ of a Form I Rubisco of 750 μM, combined with a moderate CO_2-saturated specific reaction rate of 4.7 mol CO_2 mol^{-1} active sites s^{-1} (Scott et al. 2007). On the other hand, green algae have Form 1B Rubiscos with higher affinity with $K_{0.5}(CO_2)$ values of 29–38 μM and higher S_{rel} of 61–83 mol mol^{-1} being reported, but with lower k_{cat} values (Raven and Beardall 2003).

The Form 1D Rubiscos found in heterokont and haptophyte algae (see Chap. 2) show values that are very variable. This can even be the case for the same organism; values of $K_{0.5}(CO_2)$ for partially purified Rubisco of the coccolithophore *Emiliana huxleyi* have been

reported as 72 μM (Boller et al. 2011), or 200 μM (Shiraiwa et al. 2004). Diatom Form ID Rubiscos are also variable (Boller et al. 2015; Young et al. 2016) with $K_{0.5}(CO_2)$ values varying from 23 to 68 μM, CO_2 selectivity from 57 to 116 mol mol^{-1} and specific reaction rates of 2.1 to 3.7 $site^{-1}$ s^{-1}. Form 1D Rubiscos in the Synurophyceae have reported $K_{0.5}(CO_2)$ values in vitro of 18.2 μM (*Mallomonas papulosa*), 28.4 μM (*Synura petersenii*) and 41.8 μM (*Synura uvella*) (Bhatti and Colman 2008; Raven and Giordano 2017). These $K_{0.5}(CO_2)$ should be taken in context of typical air-equilibrium CO_2 concentrations of 10–25 μM, depending on temperature, salinity etc.

Dinoflagellates (see Chap. 2) are unusual in being the only eukaryotic organisms possessing Form II Rubiscos. These enzymes are unstable *in vitro* and are thus poorly characterized, but appear to have very low selectivity factors (~37). Some idea of their kinetic properties can be obtained from work on Form II Rubiscos from photosynthetic proteobacteria, from which it is believed the dinoflagellate Form II Rubiscos originated by lateral gene transfer (Badger et al. 1998; Whitney et al. 1995). These have very low S_{rel} values (Whitney and Andrews 1998; Leggat et al. 1999; Raven and Beardall 2003) and dinoflagellates would thus struggle to perform net CO_2 assimilation at air-equilibrium CO_2 levels (Tortell 2000).

The general trend across all autotrophs is that a low $K_{½}(CO_2)$, and a high S_{rel} are correlated with a low $k_{cat}(CO_2)$, and *vice versa* (Tcherkez et al. 2006; Raven et al. 2012). Given the relatively low affinities and selectivity factors of most of the algae and cyanobacteria as discussed above, achievement of significant rates of net photosynthesis necessitates the operation of a CO_2 concentrating mechanism (CCM) to elevate CO_2 concentrations, and increase CO_2:O_2 ratios at the active site of Rubisco. The various forms which these mechanisms can take are discussed in more detail below.

It is worth noting in the context of enhancement of photosynthetic rates that, in contrast to terrestrial C_3 vascular plants, Rubisco in algae and cyanobacteria represents a relatively small proportion (~2–6%) of the total protein pool and hence investment in N (Losh et al. 2013; Raven 2013a; Flynn and Raven 2017), a resource which is frequently in limiting supply in aquatic, especially marine, systems. This may be related to CCM activity as terrestrial plants possessing a C4 biochemical CCM have lower Rubisco N:Total leaf N than C3 plants lacking CCMs (see Raven 2013a and references within). Furthermore N-limitation has been shown to cause upregulation of CCMs in some algae (Beardall et al. 1982, 1991; Young and Beardall 2005; Hu and Zhou 2010), improving N-use efficiency, though this is apparently not so in *Chlamydomonas reinhardtii* (Giordano et al. 2003; Chap. 4) or the diatom *Phaeodactylum tricornutum* (Li et al. 2012; Chap. 16).

B. The PCRC and Other Pathways for C Assimilation

Six pathways for the assimilation of CO_2 into organic matter have been identified in autotrophs, including those (C_4 photosynthesis among them) relying on activity of Rubisco in the PCRC. However, of those pathways found in nature, the only example that is not inhibited by oxygen, while exhibiting carboxylase activity with an ecologically relevant (at least in terms of the photic zone in marine and freshwater systems) affinity for CO_2 and has a lower energy (absorbed photon) cost than the PCRC, is the 3-hydroxypropionate bi-cycle (Bar-Even et al. 2010, 2011, 2012; Raven et al. 2012; Raven and Beardall 2016). However, fixation of CO_2 via the PCRC acting alone is the dominant pathway for carbon assimilation in cyanobacteria and algae. There is some evidence for C_4 photosynthesis in the marine ulvophycean alga *Udotea flabellum* (Reiskind et al. 1988; Reiskind and Bowes

1991) and, controversially, there are also reports of C_3-C_4 single cell intermediate photosynthesis in one species of a marine diatom (*Thalassiosira weisflogii*) (Reinfelder et al. 2000; Morel et al. 2002; Roberts et al. 2007a, b; Reinfelder 2011; Haimovich-Dayan et al. 2013), and although there is better evidence for C_4 photosynthesis in freshwater macrophytes and in seagrasses (Holaday and Bowes 1980; Salvucci and Bowes 1983; Magnin et al. 1997; Reiskind et al. 1997; Bowes et al. 1978; Bowes et al. 2002; Maberly and Madsen 2002; Bowes 2011; Koch et al. 2013; Larkum et al. 2017; Raven and Giordano 2017), the five alternative pathways for C assimilation described in Raven et al. (2012) are not represented in algal photosynthetic C assimilation.

Although the basic reactions of the PCRC are similar across the range of cyanobacteria and algae examined, recent work is indicating that there is considerable phylogenetic variation in the way the cycle is regulated. In terrestrial vascular plants, enzymes of the PCRC such as phosphoribulokinase (PRK), glyceraldehyde-3-phosphate dehydrogenase (GAPDH), fructose-1,6-bisphosphatase, and sedoheptulose-1,7-bisphosphatase are inactivated in the dark and activated in the light, while the key enzyme of the oxidative pentose phosphate (OPP) pathway, glucose-6-phosphate dehydrogenase shows the reverse. Of these, the two key enzymes in PCRC regulation are PRK and GAPDH. In green algae regulation of these 2 enzymes is under redox control, but PRK is not redox-regulated in the marine centric diatom *Odontella sinensis* (Michels et al. 2005) or the freshwater pennate diatom *Asterionella formosa* (Boggetto et al. 2007). In contrast *A. formosa* does show redox-activation of NADPH-dependent GAPDH (Boggetto et al. 2007), but this is lacking in *O. sinensis* GAPDH (Michels et al. 2005). Maberly et al. (2010) investigated the redox regulation of PRK and GAPDH in more detail, including the role of the protein CP12, and have been able to show considerable variation across different algal groups with the cryptophytes and haptophytes studied showing differing regulatory properties to another clade containing chromalveolates and a third with a mix of vascular plants, a diatom, a xanthophycean and an eustigmatophycean. Though the phylogenetic trends in regulation of the PCRC across photoautotrophs as discussed by Maberly et al. (2010) and more recently by Jensen et al. (2017) are not clear cut, the significance to the evolutionary history of algae is worthy of further investigation.

III. Occurrence of CCMs

It is apparent from the discussion above that the kinetics of Rubisco in most cyanobacteria and algae operating at, or below, air-equilibrium levels of CO_2 require operation of a CO_2 concentrating mechanism (CCM) to improve the supply of CO_2 to the active site, minimise photorespiration and improve net rates of carbon assimilation. Notable exceptions appear to be species that occur where CO_2 levels are high, such as in the Chrysophyceae and Synurophyceae (Maberly et al. 2009; Raven and Giordano 2017), freshwater red algae belonging to the Batrachospermales (Raven et al. 1982; Raven et al. 2005), as well as some marine algae where low light levels constrain photosynthesis so that CO_2 diffusion is sufficient to satisfy demand (Kübler and Raven 1994, 1995). In this regard it is interesting to note that the florideophycean red alga *Heminura frondosa*, thought to lack CCM activity on the basis of work on fresh material isolated from low light environments, expressed a CCM capacity when exposed to high light (Catriona Hurd, personal communication). Other exceptions are the coccoid symbiotic trebouxiophycean green alga *Coccomyxa*, using CO_2 from soil or host cell respiration (Raven and Colmer 2016), though this is apparently not the case for the Antarctic species *Coccomyxa subellipsoiea* (Blanc et al. 2012), and the aerophytic, terrestrial trebouxiophycean spe-

cies *Stichococcus minor* (Munoz and Merrett 1989). All other species examined, admittedly a small fraction of the conservative estimate of >70, 000 extant algal species (Guiry 2012), appear to have CCMs. Reports of a lack of CCM activity in the coccolithophore *Emiliania huxleyi* are now believed to be unfounded (Rost et al. 2007; Reinfelder 2011; Stojkovic et al. 2013). It could be expected that size might play a role in whether a CCM is expressed or not, as decreasing size would decrease diffusion resistance of CO_2 potentially diminishing the need for CCMs in smaller species (Raven 1986; Raven 1999). However, *Micromonas pusilla* (cell volume 2.1×10^{-18} m^3) has an active CCM (Iglesias-Rodriguez et al. 1998) and contains pyrenoids (Meyer and Griffiths 2013), and although *Ostreococcus* (cell volume ~ 0.48×10^{-18} m^3) lacks pyrenoids (Meyer and Griffiths 2013) and has an unclear CCM status (Schaum and Collins 2014); as discussed below an absence of pyrenoids does not equate with absence of CCM activity (see Chap. 9).

However, the expression of CCM activity varies greatly. Cyanobacteria with the low CO_2 affinity Form IA or Form IB Rubisco show highly expressed CCMs, while diatoms with Form ID Rubiscos with higher CO_2 affinity (Young et al. 2016) show lower CCM activity and green algae with relatively high affinity (see above) show relatively low capacity for CCM expression. Tortell (2000) and Griffiths et al. (2017) showed a broad inverse relationship between carbon concentration factor and Rubisco specificity factor, and a positive relationship between specificity factor and paleo CO_2 levels, though the data need to be interpreted carefully and expression of CCM activity is modulated by a range of environmental factors including CO_2 concentration, light level, temperature and nutrient availability (Beardall and Giordano 2002). The role of CCM activity in controlling competition between species is complex and involves interactions between Rubisco characteristics, dissolved inorganic carbon concentrations, CO_2 concentrating capacity and other environmental factors such as light (Ji et al. 2017; Beardall and Raven 2017). As stated above, members of the Chrysophyceae and Synurophyceae, lacking CCMs, became dominant when aqueous CO_2 concentrations were significantly above air equilibrium (Maberly 1996; Maberly et al. 2009). Van de Waal et al. (2011) showed that two strains of *Microcystis aeruginosa,* with differing affinities for DIC, were shown to sequentially dominate a culture based on the available CO_2 and Lines and Beardall (2018) attributed the success of the cyanobacterium *Cylindrospermopsis raciborskii* (= *Raphidiopsis raciborskii*: Aguilera et al. 2018) in a reservoir in Queensland Australia to its high CCM activity and affinity for CO_2 at low environmental concentrations. Shapiro (1990, 1997) and Low-Décarie et al. (2011, 2015) have shown from ecological observations and competition experiments that cyanobacteria have the capacity to outcompete other groups of photoautotrophs in freshwater phytoplankton communities. However, Ji et al. (2017) have shown that this is not always the case (see also Beardall and Raven 2017).

IV. Mechanisms of CCMs Versus Diffusive CO_2 Fluxes

A. Definition of CCMs and What Do We Need in Order to Demonstrate Operation of CCMs?

Unfortunately, despite many years of CCM-related research, there is still a good deal of misunderstanding about what comprises reliable and robust evidence for CCM activity. In general, irrespective of the mechanisms discussed below, CCM activity is characterised by several cellular physiological properties. (i) By definition, there needs to be a net positive gradient of $CO_{2\ in} > CO_{2\ out}$ Simple measurements showing intercellular [DIC] is higher than extracellular [DIC] are

insufficient as gradients in DIC could simply be a consequence of CO_2 equilibration between inside and outside the cell with higher pH internally than externally. Thus proof of CCM activity requires it to be demonstrated that dissolved CO_2 in the cells is higher than outside. Such measurements were originally done using radioisotopes measuring $[DIC]_{in}$, $[DIC]_{out}$ and internal (and external) pH (see e.g. Badger et al. 1980; Kaplan et al. 1980), but more recent approaches involve measurements using mass spectroscopy (see e.g. Sültemeyer et al. 1991) and are the preferred approach for laboratories with access to such instrumentation. (ii) Characteristically cells with active CCMs have $K_{0.5}CO_2$ values for DIC-dependent photosynthesis less than that for their Rubiscos and measurements of $K_{0.5}CO_2$ are useful and relatively simple approaches to measuring CCM capacity of cells. This approach requires that the CO_2-saturated *in vivo* Rubisco activity is not so high as to account for the ratio of *in vivo* to *in vitro* $K_{0.5}CO_2$. (iii) Diffusive supply of CO_2 followed by assimilation by Rubisco leads to a discrimination against heavier isotopes of C by about 30‰. Consequently, measuring carbon isotope discrimination $\delta^{13}C$ (or more accurately $\Delta^{13}C$ if measurements of source discrimination are made) in the organic component of algae can give an indication of possible CCM activity. Thus cells using CO_2 diffusion alone show $\Delta^{13}C$ values ~ −30‰ and discrimination values become less negative as CCM activity increases (Raven et al. 2005; Stepien 2015). However, this method depends on a known and constant discrimination between $^{13}CO_2$ and $^{12}CO_2$ in fixation by Rubisco, and it is known that there is significant variation in this discrimination in cyanobacteria and algae (Tcherkez et al. 2006; Scott et al. 2007; Boller et al. 2011; Boller et al. 2015). Furthermore, the ability of cells to express the full RubisCO fractionation factor also depends on the extent to which diffusive CO_2 supply exceeds cellular demand. As demand approaches the supply rates the effective fractionation factor is reduced (Laws et al. 1995).

Other parameters, more specific to particular mechanisms involved in CCMs, have often been mis-interpreted. These include using the presence of sequences for enzymes such as PEP carboxylase in genomes of algae as *prima facie* evidence for C_4 metabolism and the misconception that possession of external carbonic anhydrase can alone result in CO_2 accumulation. 'C_4 genes' are widespread in organisms lacking CCMs, or even photosynthesis (Aubry et al. 2011; Chi et al. 2014), so more than genomics is needed to show that C_4 photosynthesis occurs. The use of transcriptomics in combination with physiological measurements and pulse-chase labelling can, however, be informative (Roberts et al. 2007a).

Thus, in order of increasing importance, genomic information, transcriptomics and proteomics, enzyme activity measurements and short-term labelling experiments are required in order to distinguish between biochemical C_4 CCMs and biophysical CCMs based on active transport of inorganic carbon species (Fig. 7.1).

B. CCMs Based on Active Transport of Inorganic C Species

There are five variants of inorganic carbon transport in cyanobacteria, each with different physiological characteristics (Table 7.1). CO_2 can diffuse across the plasma membrane of cyanobacteria, probably with a least some CO_2 uptake effected by aquaporins (Kaldenhoff et al. 2014; Raven and Beardall 2016). However, on either the cytosolic face of the plasma membrane or on the thylakoid membrane there is an energized conversion of CO_2 to HCO_3^- via a NAD(P)H dehydrogenase, which effectively acts like a Ci-pump, even though direct active transport of CO_2 has not occurred. There are two NAD(P)H dehydrogenase systems: an inducible, high-CO_2 affinity, system (NDH-I_3) at the thyla-

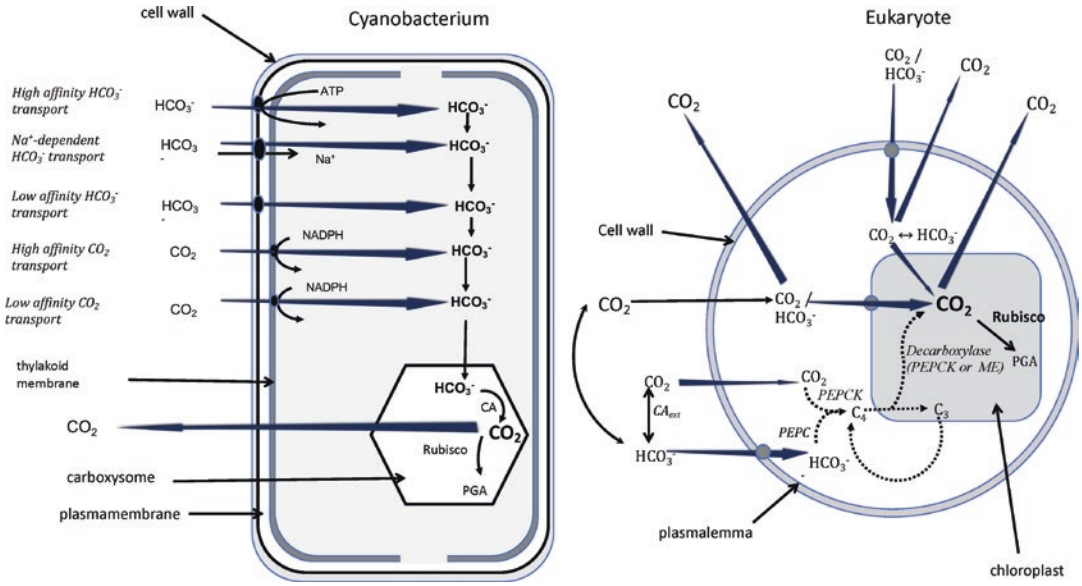

Fig. 7.1. Basic mechanisms of CCMs in a cyanobacterium (left) and a eukaryotic alga (right). No attempt has been made to represent the role of the pyrenoid in those algae that possess them (see Chap. 9). (See the text for details. Redrawn after Giordano et al. 2005)

Table 7.1. Inorganic carbon transporters in cyanobacteria

Transporter	Substrate	Affinity	Flux	Comments
BCT1	HCO_3^-	High	Low	ABC-type transporter found exclusively in freshwater β-cyanobacteria; low-CO_2 inducible
SbtA	HCO_3^-	High	Low	Sodium-dependent transporter
BicA	HCO_3^-	Low	High	Sodium-dependent transporter
NDH-13	CO_2	High	Low	Energized conversion of CO_2 to HCO_3^-
NDH-14	CO_2	Low	High	Energized conversion of CO_2 to HCO_3^-

koid membrane and a constitutive, low affinity, one (NDH-I_4, located probably at the plasma membrane) (Price et al. 2008). Cyanobacteria can also actively take up HCO_3^- from the medium using a number of different HCO_3^- pumps. In freshwater β-cyanobacteria only, the genes for a low-CO_2 inducible, high affinity HCO_3^- transporter, BCT1, are encoded by the *cmpABCD* operon which belongs to the traffic ATPase family (Omata et al. 1999). These genes are absent from the genomes of all marine α- and β-cyanobacteria so far sequenced. In *Synechocystis* 6803 and various other β-cyanobacteria, a high affinity, inducible, Na^+-dependent, HCO_3^- transporter (SbtA) is present (Shibata et al. 2002). BicA is another Na^+-dependent HCO_3^- transporter, and this is aligned with the SulP family of transporters (Price et al. 2004). Unlike SbtA though, this is a low affinity system. BicA and SbtA may both be forms of Na^+/HCO_3^- symporters, although to date this there is no conclusive evidence for this. Whatever the form of inorganic carbon transported, the outcome is for HCO_3^- delivered, directly or indirectly, to the cytosol. The HCO_3^- then diffuses into the polyhedral protein-walled bodies termed carboxysomes, which contain all the cell quota of Rubisco and show the only carbonic

anhydrase (CA) activity in the cell. CO_2 generated within the carboxysomes by this CA leads to the build-up to a higher steady state concentration than in the bulk medium, thus strongly favouring the carboxylase over the oxygenase activity of Rubisco (Smith and Ferry 2000; Price et al. 2002).

The mechanisms of CCMs in eukaryotic algae are not as well defined as they are in cyanobacteria and are more complicated because of the additional membranes the DIC needs to traverse. Inorganic carbon needs to be transported across the plasmalemma, then across the membranes of the chloroplast envelope and CO_2 then needs to be provided at a higher than ambient concentration to the active site of Rubisco, which is within the pyrenoids in those cells that possess them and in the stroma in cells without pyrenoids. Although all pyrenoid-containing algae have CCMs (Badger et al. 1998; Raven 1997a, b; Raven and Beardall 2003), not all algae with CCMs have pyrenoids (Badger et al. 1998; Morita et al. 1998, 1999; Raven 1997b, c; Raven and Beardall 2003; Kevekordes et al. 2006; Raven and Giordano 2017). Active transport mechanisms for DIC could thus be based on the plasma membrane, or the inner plastid envelope membrane, or both.

More recent molecular evidence has begun to characterise the various bicarbonate transporters in algal cells and a large number of candidate proteins have been identified. In diatom genomes there are genes for a number of solute carrier (SLC)-type transporters, also found in mammalian systems (Bonar and Casey 2008). Several of these have been implicated in bicarbonate transport in diatoms with, in *Phaeodactylum tricornutum*, the plasmalemma associated PtSLC4-2 being low-CO_2 inducible and having a high requirement for Na^+ (Nakajima et al. 2013). Similar transporters (PtSLC4-1, and PtSLC4-4) are also plasmalemma-located in *P. tricornutum* and likewise appear to be involved with HCO_3^- influx from low-CO_2 environments. Nakajima et al. (2013) also showed the existence of orthologous SLC4 genes in another diatom species, *Thalassiosira pseudonana*. Recent evidence (Tsuji et al. 2017a) suggests that in these diatoms plasmalemma HCO_3^- transport is driven, directly or indirectly, by energy generated by linear electron flow from photosystem II to photosystem I, contrasting with previous work suggesting a role for ATP from cyclic photophosphorylation (Ogawa and Ogren 1985; Ogawa et al. 1985; Palmqvist et al. 1990; Spalding et al. 1984), with some eustigmatophycean algae appearing to be unusual in having a CCM driven by respiratory ATP (Huertas et al. 2002). Plasmalemma-based bicarbonate transporters have also been demonstrated in the green alga *Chlamydomonas reinhardtii* (Ohnishi et al. 2010; Yamano et al. 2015) though the genes for these transporters (HLA3 and LCI1) do not appear to share homology with the SLC systems in diatoms (Tsuji et al. 2017a, b).

Physiological investigations have shown that algae can also take up CO_2 and this, in the absence of hard evidence for an active CO_2 transporter, is assumed to take place by passive diffusion (Patel and Merrett 1986; Colman and Rotatore 1995; Mitchell and Beardall 1996; Johnston and Raven 1996; Korb et al. 1997; Burkhardt et al. 2001; Rost et al. 2003; Trimborn et al. 2008; Kaldenhoff et al. 2014; Raven and Beardall 2016), possibly assisted by aquaporin channels, though a high permeability of cell membranes to CO_2, can have consequences for leakage (Tchernov et al. 2003; Raven and Beardall 2016).

Though there are some species in which CCM activity appears to be based solely at the plasmalemma (Rotatore and Colman 1990, 1991), there is also evidence for a role of the plastid envelope in CCMs in a range of other species, based on a demonstrable capacity for active transport of DIC. Thus, photosynthetically active chloroplasts from high- and low-CO_2 grown cells of two species of the Chlorophyceae have been shown

to possess low- and high-affinity DIC uptake systems respectively, as do the corresponding intact cells (Amoroso et al. 1998). Active uptake of both CO_2 and HCO_3^-, and CO_2 accumulation, have been demonstrated in isolated chloroplasts of *Chlamydomonas reinhardtii* and *Dunaliella tertiolecta* (Amoroso et al. 1998) and *Tetraedon minimum* and *Chlamydomonas noctigama* (van Hunnik et al. 2002). Molecular studies have identified genes for SLC4- type transporters associated with the chloroplast envelope membranes in diatoms (Nakajima et al. 2013; Tsuji et al. 2017b) and a number of putative transporters (LCIA, CCP1 and CCP2) have been suggested for the chloroplast envelope of *Chlamydomonas* (Wang et al. 2015; Yamano et al. 2015; Machingura et al. 2017), though the work of Mackinder et al. (2017) suggests CCP1 and CCP2 are less important. Matsuda et al. (2017) have also postulated a range of transporters for inorganic carbon transport across all 4 of the diatom chloroplast envelope membranes and the pyrenoid-penetrating thylakoids, though such transport systems remain uncharacterised and speculative at present.

CCMs also involve a range of CAs that maintain equilibrium between CO_2 and bicarbonate in the various cellular compartments (see De Mario et al. 2017 for a recent review). Importantly, in many algae an extracellular carbonic anhydrase (CA_{ext}) associated with the cell wall converts bicarbonate to CO_2, assisting the diffusion of the latter across the cell wall. Within the cell, internal CAs facilitate the interconversion of bicarbonate and CO_2 with active inorganic transport across the chloroplast envelope then occurring as described above. In green algae such as *Chlamydomonas*, the external CA is an α-CA, while in some diatoms this role is carried out by a β-CA. In other diatoms a ζ-CA is involved (Hopkinson et al. 2013) and δ-CA_{ext} has been reported in a dinoflagellate (Lapointe et al. 2008). The full range of carbonic anhydrases found in algae and cyanobacteria is discussed in DiMario et al. (2017). CA_{ext} activity is inducible by low CO_2 levels and in some cases is only found when rates of CO_2 consumption exceed the rate of uncatalysed supply from bicarbonate (Smith-Harding et al. 2018), which may explain in part at least the contradictory reports of external CA presence/absence in some species (John-McKay and Colman 1997).

As well as being involved in the supply of inorganic carbon across the plasmalemma, CAs may also be involved in CCMs based on acidification in the thylakoid. An α-CA (Cah3) is based on the inner side of the thylakoid membrane and is involved in the conversion of bicarbonate to CO_2 following transport of bicarbonate to the thylakoid lumen, the CO_2 thus produced could then leak out of the lumen to the site of Rubisco in the stroma or pyrenoid. However, direct evidence for such a mechanism is not yet available, though in *Chlamydomonas* there is CA compartmentalization evidence that is at least consistent with such a process (Pronina and Semenenko 1992; Pronina and Borodin 1993; Raven 1997c; Sinetova et al. 2012).

Acidification can also play a role in enhancing inorganic carbon supply in macroalgae and aquatic vascular plants where localised low pH and external carbonic anhydrase(s) at the cell surface shifts the bicarbonate:CO_2 ratio in favour of CO_2, increasing its concentration and enhancing its diffusion (or in some cases active transport) into the cell (Raven and Hurd 2012; Raven 2013a, b; Raven et al. 2014; Raven and Beardall 2016). Similar mechanisms are unlikely in microalgae due to the thinner diffusive boundary layer and enhanced CO_2 and proton leakage in small cells (Flynn et al. 2012; Raven and Beardall 2016).

C. C4 Photosynthesis as a CCM in Algae?

In some vascular plants photosynthetic carbon assimilation is based on an initial assimilation of bicarbonate, catalysed by the enzyme PEP carboxylase, which has a high affinity for its inorganic carbon substrate. The initial stable resulting products are the C_4 dicarboxylic acids malate or aspartate (depending on species) and these compounds are then transported from mesophyll cells to another type of cell, the bundle sheath cells, where their decarboxylation leads to enhanced supply of CO_2 at the active site of Rubisco, located therein (Sage 2004; Sage et al. 2011). This process thus acts as a biochemical CO_2 pump improving CO_2 supply. Studies in the late 1970's by Beardall and coworkers proposed the existence of single-cell C_4-like photosynthetic metabolism in diatoms (Beardall et al. 1976), though later work (Morris et al. 1978) ascribed their labelling patterns and other data to high rates of anaplerotic β-carboxylation through PEPCase. Such reactions are necessary to top up the intermediates of the TCA cycle as these are used to support biosynthetic processes such as protein synthesis (Aubry et al. 2011; Chi et al. 2014). Subsequently, Reinfelder et al. (2000) and Morel et al. (2002) revisited the topic and proposed that the marine diatom *Thalassiosira weisflogii* was also capable of C_4 photosynthesis. Subsequent work (Morel et al. 2002; Reinfelder et al. 2004; Roberts et al. 2007a, b) has provided better evidence for some form of C_4 (or more likely C_3-C_4 intermediate) mechanism in *Thalassiosira weisflogii*, though operation of a similar mechanism in other diatoms (*T. pseudonana* and *Phaeodactylum tricornutum*) has not been substantiated (Haimovich-Dayan et al. 2013; Clement et al. 2017; Ewe et al. 2018). Similarly, high levels of enzymes putatively involved in C_4 photosynthesis in the haptophyte *Emiliania huxleyi* were shown by pulse chase labeling experiments to instead be associated with anaplerotic β-carboxylation (Tsuji et al. 2009). Thus *T. weisflogii* remains the only microalga to date for which C_4 photosynthesis is a possibility, though it is more likely better aligned with C_3-C_4 intermediate metabolism (Roberts et al. 2007a). Nonetheless, C_4 metabolism in the macroalga *Udotea flabellum,* using PEP carboxykinase as the carboxylase, is well established (Reiskind et al. 1988; Reiskind and Bowes 1991).

V. Structural Aspects of CO_2 Acquisition

The role of carboxysomes in cyanobacterial inorganic carbon acquisition has been dealt with in detail recently by Kerfeld and Melnicki (2016) so will only be mentioned briefly here.

The polyhedral bodies known as carboxysomes are present in all cyanobacteria and contain most of the cyanobacterial cell's Rubisco and carbonic anhydrase, enclosed within a semi-permeable proteinaceous shell (Kinney et al. 2011; Espie and Kimber 2011). Details of carboxysomal structure and function can be found in Kerfeld and Melnicki (2016), but in brief HCO_3^- is transported into the carboxysome lumen and converted to CO_2 via carbonic anhydrase, thereby elevating CO_2 concentrations at the active site of Rubisco. The protein shell is thought to act in minimising CO_2 leakage, though as discussed by Raven and Beardall (2016) leakage is still likely to be significant given the large accumulation factor for CO_2 found in cyanobacteria. Indeed, Hopkinson et al. (2014) showed that approximately 50% of the inorganic carbon transported into cells of a species of *Prochloroccus* that lacks CO_2 recovery capacity was lost as CO_2 efflux.

In eukaryotic algae, the analogous structure to the carboxysome is the pyrenoid, a microcompartment within the chloroplast (see Chap. 9). Clearly, in algae that possess pyrenoids, the majority of the Rubisco is found there, with only a small portion of cel-

lular Rubisco in the stroma (McKay and Gibbs 1991). Green algal pyrenoids also contain Rubisco activase, supporting the notion that Rubisco in pyrenoids is catalytically active (McKay and Gibbs 1991). Non-green algal species do not express Rubisco activase, but utilise another protein, CbbX, which has activase-like properties (see Kroth 2015).

In contrast, in species without pyrenoids Rubisco is found throughout the stroma (McKay and Gibbs 1991 and references therein). Interestingly, if *Chlamydomonas reinhardtii* is grown at elevated CO_2 in order to down-regulate CCM expression, increased levels of Rubisco (and a three fold higher proportion of cellular Rubisco) appear in the stroma, though pyrenoid Rubisco levels remain high and similar to those in low-CO_2 grown cells (Borkhsenious et al. 1998). It is clear however, that possession of a pyrenoid is not a prerequisite of a CCM. While all algae with pyrenoids have CCMs, not all algal species with CCMs have pyrenoids (Giordano et al. 2005; Kevekordes et al. 2006), though pyrenoid loss from *Chlamydomonas* results in loss of CCM function (Meyer et al. 2012; Mitchell et al. 2017).

The fine structure, development and composition of pyrenoids in *Chlamydomonas reinhardtii* have been dealt with recently in the excellent reviews by Meyer et al. (2017), Meyer and Griffiths (2013), Mackinder (2018) and Mackinder et al. (2017) and so are not dealt with here in detail. The pyrenoid is surrounded by a starch sheath (although mutant studies suggest that this is not essential for the CCM: Villarejo et al. 1996) and, important for CCM activity, is traversed by membrane tubules, sometimes termed pyrenoid lamellae, or transpyrenoid thylakoids, that are contiguous with the photosynthetic thylakoid membranes (Engel et al. 2015). However, these tubules are distinct from stromal thylakoids in lacking O_2-evolving PSII centres and light harvesting antenna, and this is the case in red algae and diatoms as well as in the green algae (McKay and Gibbs 1991; Mustardy et al. 1990; Pyszniak and Gibbs 1992; Tsekos et al. 1996). The pyrenoid tubules do however, contain the α-CA (Cah3) described above, and this could be responsible for conversion of bicarbonate to CO_2 within the lumen of the pyrenoid tubules, which would then diffuse out of the lumen to the Rubisco in the bulk of the pyrenoid. A similar protein, Pt43233, is found in the diatom *Phaeodactylum tricornutum* (Kikutani et al. 2016), suggesting this could be a widespread mechanism in pyrenoid-containing algae.

Such a mechanism would also require transport of bicarbonate into the transpyrenoid thylakoid lumen; this could be downhill (passive) transport driven by the proton-motive force across the thylakoid (Raven 1997c), but no such transporter has been identified to date. It is important to note that many pyrenoids lack thylakoid tubules or lamellae (Dodge 1973; Badger et al. 1998).

In addition to the pyrenoid tubules as discussed above, for green and red algae with CCMs, the plasma membrane, or the inner plastid envelope membrane, or both, could be the location of the active transport mechanism(s) (Amoroso et al. 1998; Moroney and Chen 1998; Kaplan and Reinhold 1999; Villarejo et al. 2001; Young et al. 2001; Giordano et al. 2005). Other algae have one (dinophytes, euglenoids) or two (chlorarachniophytes, cryptophytes, haptophytes and heterokonts) additional chloroplast envelope membranes which are frequently, but incorrectly, termed the chloroplast endoplasmic reticulum (Cavalier-Smith 2000). The involvement of these additional envelope membranes in a CCM based on active transport processes as discussed above has not yet been examined. Hopkinson et al. (2011) and Matsuda et al. (2017) have suggested that, with 4 bounding membranes, diatoms might require a HCO_3^- transporter at each membrane, which would be a large energetic constraint

both in terms of running costs and capital investment. Gee and Niyogi (2017) showed that the carbonic anhydrase CAH1, expressed in the space between the outer and next innermost of the membranes round the plastids of *Nannochloropsis oceanica*, is essential for operation of the CCM in this alga with active HCO_3^- influx at the plasmalemma.

Acknowledgements

The University of Dundee is a registered Scottish charity No 015096. We are very grateful to Brian Hopkinson and Howard Griffiths for their useful comments.

References

Aguilera A, Berrendero Gómez E, Kastovsky J, Echenique RO, Salerno GL (2018) The polyphasic analysis of two native *Raphidiopsis* isolates supports the unification of the genera *Raphidiopsis* and *Cylindrospermopsis* (Nostocales, Cyanobacteria). Phycologia 57:130–146

Amoroso G, Sültemeyer DF, Thyssen C, Fock HP (1998) Uptake of HCO_3^- and CO_2 in cells and chloroplasts from the microalgae *Chlamydomonas reinhardtii* and *Dunaliella tertiolecta*. Plant Physiol 116:193–201

Aubry S, Brown NJ, Hibberd JM (2011) The role of proteins in C_3 plants prior to their recruitment into the C_4 pathway. J Exp Bot 62:3049–3059

Badger MR, Kaplan A, Berry JA (1980) The internal inorganic carbon pool of *Chlamydomonas reinhardtii*: evidence for a CO_2 concentrating mechanism. Plant Physiol 66:407–413

Badger MR, Andrews TJ, Whitney SM, Ludwig M, Yellowlees DC, Leggat W, Price GD (1998) The diversity and coevolution of Rubiscos, plastids, pyrenoids and chloroplast-based CO_2-concentrating mechanisms in algae. Can J Bot 76:1052–1071

Bar-Even A, Noor E, Lewis NE, Milo R (2010) Design and analysis of synthetic carbon fixation pathways. Proc Natl Acad Sci USA 107:8888–8894

Bar-Even A, Noor E, Savir Y, Liebermeister W, Davidi D, Tawfik DS, Milo R (2011) The moderately efficient enzyme: evolutionary and physicochemical trends shaping enzyme parameters. Biochemistry 50:4402–4404

Bar-Even A, Noor E, Milo R (2012) A survey of carbon fixation pathways through a quantitative lens. J Exp Bot 63:2325–2342

Bathellier C, Tcherkez G, Lorimer GH, Farquhar GD (2018) Rubisco is not really so bad. Plant Cell Environ 41:705–716

Beardall J, Giordano M (2002) Ecological implications of microalgal and cyanobacterial CCMs and their regulation. Funct Plant Biol 29:335–347

Beardall J, Raven JA (2016) Carbon acquisition by microalgae. In: Borowitzka M, Beardall J, Raven JA (eds) The physiology of microalgae. Springer Verlag, Berlin, pp 89–100

Beardall J, Raven JA (2017) Cyanobacteria vs green algae, which group has the edge? J Exp Bot 68:3697–3699

Beardall J, Mukerji D, Glover HE, Morris I (1976) The path of carbon in photosynthesis by marine phytoplankton. J Phycol 12:409–417

Beardall J, Griffiths H, Raven JA (1982) Carbon isotope discrimination and the CO_2 accumulating mechanism in *Chlorella emersonii*. J Exp Bot 33:729–737

Beardall J, Roberts S, Millhouse J (1991) Effects of nitrogen limitation on inorganic carbon uptake and specific activity of ribulose-1,5-P_2 carboxylase in green microalgae. Can J Bot 69:1146–1150

Beardall J, Quigg AS, Raven JA (2003) Oxygen consumption: photorespiration and chlororespiration. In: Larkum AWD, Douglas SE, Raven JA (eds) Photosynthesis in the Algae. Kluwer Academic Publishers, Dordrecht, pp 157–181

Bhatti S, Colman B (2008) Inorganic carbon acquisition in some synurophyte algae. Physiol Plant 133:33–40

Blanc G, Agarkova I, Grimwood J, Kuo A, Brueggeman A, Dunigan DD, Gurnon J, Ladunga I, Lindquist E, Lucas S, Pangilinan J, Pröschold T, Salamov A, Schmutz J, Weeks D, Yamada T, Lomsadze A, Borodovsky M, Claverie JM, Grigoriev IV, Van Etten JL (2012) The genome of the polar eukaryotic microalga *Coccomyxa subellipsoidea* reveals traits of cold adaptation. Genome Biol 13:R39. https://doi.org/10.1186/gb-2012-13-5-r39

Boggetto N, Gontero B, Maberly SC (2007) Regulation of phosphoribulokinase and glyceraldehyde 3-phosphate dehydrogenase in a freshwater diatom, *Asterionella formosa*. J Phycol 43:1227–1235

Boller AJ, Thomas PJ, Cavenaugh CM, Scott KM (2011) Low stable isotope fractionation by coccolithophore RuBISCO. Geochim Cosmochim Acta 75:7200–7207

Boller AJ, Thomas PJ, Cavenaugh CM, Scott KM (2015) Isotopic discrimination and kinetic param-

eters of RUBISCO from the marine bloom-forming diatom, *Skeletonema costatum*. Geobiology 13:33–43

Bonar PT, Casey JR (2008) Plasma membrane Cl^-/HCO_3^- exchangers: structure, mechanism and physiology. Channels 2:337–345

Borkhsenious ON, Mason CB, Moroney JV (1998) The intracellular localization of ribulose-1,5-bisphosphate carboxylase/oxygenase in *Chlamydomonas reinhardtii*. Plant Physiol 116:1585–1591

Bowes G (2011) Single-cell C4 photosynthesis in aquatic plants. In: Raghevendra AS, Sage R (eds) C4 photosynthesis and related CO_2 concentrating mechanisms. Springer, Berlin, pp 63–80

Bowes G, Holaday AS, Van TK, Haler W (1978) Photosynthetic and photorespiratory carbon metabolism in aquatic plants. In: Hall DO, Coombs J, Goodwin TW (eds) Photosynthesis 77, proceedings of the Fourth International Congress on Photosynthesis. The Biochemical Society, London, pp 289–298

Bowes G, Rao SK, Estavillo GM, Reiskind JB (2002) C4 mechanisms in aquatic angiosperms: a comparison with terrestrial C4 systems. Funct Plant Biol 29:379–392

Burkhardt S, Amoroso G, Riebesell U, Sültemeyer D (2001) CO_2 and HCO_3^- uptake in marine diatoms acclimated to different CO_2 concentrations. Limnol Oceanogr 46:1378–1391

Cavalier-Smith T (2000) Membrane heredity and early chloroplast evolution. Trends Plant Sci 5:174–182

Chi S, Wu S, Yu J, Wang X, Tang X, Liu T (2014) Phylogeny of C_4-photosynthesis genes based on algal and genomic data supports an archaeal/proteobacterial origin and multiple duplications for most C_4-related genes. PLoS One 9:e110154

Clement R, Lignon S, Mansuelle P, Jensen E, Pophillat M, Lebrun R, Denis Y, Pupo C, Maberly SC, Gontero B (2017) Responses of the marine diatom *Thalassiosira pseudonana* to changes in CO_2 concentration: a proteomic approach. Sci Rep 7:42333

Colman B, Rotatore C (1995) Photosynthetic inorganic carbon uptake and accumulation in two marine diatoms. Plant Cell Environ 18:919–924

Di Mario RJ, Machingura MC, Waldrop GL, Moroney JV (2017) The many types of carbonic anhydrases in photosynthetic organisms. Plant Sci 268:11–17

Dodge JD (1973) The fine structure of Algal cells. Academic, London, p 261

Eisenhut M, Ruth W, Haimovich M, Bauwe H, Kaplan A, Hagemann M (2008) The photorespiratory glycolate metabolism is essential for cyanobacteria and might have been conveyed endosymbiotically to plants. Proc Natl Sci USA 105:17199–17204

Engel BD, Schaffer M, Kuhn Cuellar L, Villa E, Plitzko JM, Baumeister W (2015) Native architecture of the *Chlamydomonas* chloroplast revealed by in situ cryo-electron tomography. elife 4:e04889

Espie GS, Kimber MS (2011) Carboxysomes: cyanobacterial RubisCO comes in small packages. Photosynth Res 109:7–20

Ewe D, Tachibana M, Kikutani S, Gruber A, Rio Bártulos S, Konert G, Kaplan A, Matsuda Y, Kroth PG (2018) The intracellular distribution of inorganic carbon fixing enzymes does not support the presence of a C4 pathway in the diatom *Phaeodactylum tricornutum*. Photosynth Res 137:263–283

Flynn KJ, Raven JA (2017) What is the limit for photoautotrophic growth rates? J Plankton Res 39:13–22

Flynn KJ, Blackford JC, Baird ME, Raven JA, Clark DR, Beardall J, Brownlee C, Fabian H, Wheeler GL (2012) Changes in pH at the exterior surface of plankton with ocean acidification. Nat Clim Chang 2:510–513

Gee CW, Niyogi KK (2017) The carbonic anhydrase CAH1 is an essential component of the carbon-concentrating mechanism of *Nannochloropsis oceanica*. Proc Natl Acad Sci USA 114:4537–4547

Giordano M, Norici A, Forssen M, Eriksson M, Raven JA (2003) An anaplerotic role for mitochondrial carbonic anhydrase in *Chlamydomonas reinhardtii*. Plant Physiol 132:2126–2134

Giordano M, Beardall J, Raven JA (2005) CO_2 concentrating mechanisms in algae: mechanisms, environmental modulation, and evolution. Annu Rev Plant Biol 6:99–131

Griffiths H, Meyer MT, Rickaby REM (2017) Overcoming adversity through diversity: aquatic carbon concentrating mechanisms. J Exp Bot 68:3689–3695

Guiry M (2012) How many species of algae are there? J Phycol 48:1057–1063

Haimovich-Dayan M, Garfinkel N, Ewe D, Marcus Y, Gruber A, Wagner H, Kroth PG, Kaplan A (2013) The role of C4 metabolism in the marine diatom *Phaeodactylum tricornutum*. New Phytol 197:177–185

Hanson TE, Tabita FR (2001) A ribulose 1,5- bisphosphate carboxylase/oxygenase (RubisCO)–like protein from *Chlorobium tepidum* that is involved with sulfur metabolism and the response to oxidative stress. Proc Natl Acad Sci U S A 98:4397–4402

Holaday AS, Bowes G (1980) C4 acid metabolism and dark CO_2 fixation in a submersed aquatic

macrophyte (*Hydrilla verticillata*). Plant Physiol 65:331–335

Hopkinson BM, Meile C, Shen C (2013) Quantification of extracellular carbonic anhydrase in two marine diatoms and investigation of its role. Plant Physiol 162:1142–1152

Hopkinson BM, Young JN, Tansik AL, Binder BJ (2014) The minimal CO_2-concentrating mechanism of *Prochlorococcus* spp. MED4 is effective and efficient. Plant Physiol 166:2205–2217

Hopkinson BM, Dupont CL, Allen AE, Morel FMM (2011) Efficiency of the CO_2-concentrating mechanism of diatoms. Proc Natl Acad Sci USA 108:3830–3837

Hu HH, Zhou QB (2010) Regulation of inorganic carbon acquisition by nitrogen and phosphorus levels in the *Nannnochloropsis* sp. World J Microbiol Biotechnol 26:957–961

Huertas IE, Colman B, Espie GS (2002) Inorganic carbon acquisition and its energization in eustigmatophyte algae. Funct Plant Biol 29:271–277

Iglesias-Rodriguez MD, Nimer NA, Merrett MJ (1998) Carbon dioxide-concentrating mechanism and the development of extracellular carbonic anhydrase in the marine picoeukaryote *Micromonas pusilla*. New Phytol 140:685–690

Jensen E, Clement R, Maberly S, Gontero B (2017) Regulation of the Calvin–Benson–Bassham cycle in the enigmatic diatoms: biochemical and evolutionary variations on an original theme. Philos Trans R Soc Lond B 372:20160401

Ji X, Verspagen JMH, Stomp M, Huisman J (2017) Competition between cyanobacteria and green algae at low versus elevated CO_2: who will win, and why? J Exp Bot 68:3815–3828

John-McKay M, Colman B (1997) Variation in the occurrence of external carbonic anhydrase among strains of the marine diatom *Phaeodactylum tricornutum* (Bacillariophyceae). J Phycol 33:988–990

Johnston AM, Raven JA (1996) Inorganic carbon accumulation by the marine diatom *Phaeodactylum tricornutum*. Eur J Phycol 31:285–290

Kaldenhoff R, Kai L, Uehlein N (2014) Aquaporins and membrane diffusion of CO_2 in living organisms. Biochim Biophys Acta 1840:1592–1595

Kaplan A, Reinhold L (1999) CO_2 concentrating mechanisms in photosynthetic microor ganisms. Annu Rev Plant Physiol Plant Mol Biol 50:539–559

Kaplan A, Badger MR, Berry JA (1980) Photosynthesis and intracellular inorganic carbon pool in the bluegreen algae *Anabaena variabilis*: response to external CO_2 concentration. Planta 149:219–226

Kerfeld C, Melnicki MR (2016) Assembly, function and evolution of cyanobacterial carboxysomes. Curr Opin Plant Biol 31:66–75

Kevekordes K, Holland D, Jenkins S, Koss R, Roberts S, Raven JA, Scrimgeour CM, Shelly K, Stojkovic S, Beardall J (2006) Inorganic carbon acquisition by eight species of *Caulerpa*. Phycologia 45:442–449

Kikutani S, Nakajima K, Nagasato C, Tsuji Y, Miyatake A, Matsuda Y (2016) Thylakoid luminal θ-carbonic anhydrase critical for growth and photosynthesis in the marine diatom *Phaeodactylum tricornutum*. Proc Natl Acad Sci USA 113:9828–9833

Kinney JM, Axen SD, Kerfeld CA (2011) Comparative analysis of carboxysome shell proteins. Photosynth Res 109:21–32

Koch M, Bowes G, Ross C, Zhang X-H (2013) Climate change and ocean acidification effects on seagrasses and marine macroalgae. Glob Chang Biol 19:103–132

Korb RE, Saville PJ, Johnston AM, Raven JA (1997) Sources of inorganic carbon for photosynthesis by three species of marine diatoms. J Phycol 33:433–440

Kroth PG (2015) The biodiversity of carbon assimilation. J Plant Physiol 172:76–81

Kübler JE, Raven JA (1994) Consequences of light limitation for carbon acquisition in three rhodophytes. Mar Ecol Prog Ser 110:203–209

Kübler JE, Raven JA (1995) The interaction between inorganic carbon supply and light supply in *Palmaria palmata* (Rhodophyta). J Phycol 31:369–375

Lapointe M, MacKenzie TDB, Morse D (2008) An external δ-carbonic anhydrase in a free-living marine dinoflagellate may circumvent diffusion-limited carbon acquisition. Plant Physiol 147:1427–1436

Larkum AWD, Davey PA, Kuo J, Ralph PJ, Raven JA (2017) Carbon-concentrating mechanisms in seagrasses. J Exp Bot 68:3773–3784

Laws EA, Popp BN, Bidigare RR, Kennicutt MC, Macko SA (1995) Dependence of phytoplankton carbon isotopic composition on growth rate and $[CO_2)_{aq}$: theoretical considerations and experimental results. Geochim Cosmochim Acta 59: 1131–1138

Leggat W, Badger MR, Yellowlees DC (1999) Evidence for an inorganic carbon-concentrating mechanism in the symbiotic dinoflagellate *Symbiodinium* sp. Plant Physiol 121:1247–1255

Li W, Gao K, Beardall J (2012) Interactive effects of ocean acidification and nitrogen-limitation on the diatom *Phaeodactylum tricornutum*. PLoS One 7(12):e51590. https://doi.org/10.1371/journal.pone.0051590

Lines T, Beardall J (2018) Carbon acquisition characteristics of six microalgal species isolated from a

subtropical reservoir: potential implications for species succession. J Phycol 54:599–607

Losh JL, Young JI, Morel FMM (2013) Rubisco is a small fraction of total protein in marine phytoplankton. New Phytol 198:52–58

Low-Décarie E, Fussmann GF, Bell G (2011) The effect of elevated CO_2 on growth and competition in experimental phytoplankton communities. Glob Chang Biol 17:2525–2535

Low-Décarie E, Bell G, Fussmann GF (2015) CO_2 alters community composition and response to nutrient enrichment of freshwater phytoplankton. Oecologia 177:875–883

Maberly SC (1996) Diel, episodic and seasonal changes in pH and concentrations of inorganic carbon in a productive English lake, Esthwaite Water. Cumbria Freshw Biol 35:609–622

Maberly SC, Madsen TV (2002) Freshwater angiosperms carbon concentrating mechanisms: processes and patterns. Funct Plant Biol 29:393–405

Maberly SC, Ball LA, Raven JA, Sültemeyer D (2009) Inorganic carbon acquisition by chrysophytes. J Phycol 45:1057–1061

Maberly SC, Courcelle C, Grobden R, Gontero B (2010) Phylogenetically-based variation in the regulation of the Calvin cycle enzymes, phosphoribulokinase and glyceraldehyde-3-phosphate dehydrogenase, in algae. J Exp Bot 61:735–745

Machingura MC, Bajsa-Hirschel J, Laborde SM, Schwartzenburg JB, Mukherjee B, Mukherjee A, Pollock SV, Förster B, Price GD, Moroney JV (2017) Identification and characterization of a solute carrier, CIA8, involved in inorganic carbon acclimation in *Chlamydomonas reinhardtii*. J Exp Bot 68:3879–3890

Mackinder LCM (2018) The *Chlamydomonas* CO_2-concentrating mechanism and its potential for engineering photosynthesis in plants. New Phytol 217:54–61

Mackinder L, Chen C, Leib R, Patena W, Blum SR, Rodman M, Ramundo S, Adams CM, Jonikas MC (2017) A spatial interactome reveals the protein organization of the algal CO_2 concentrating mechanism. Cell 171:133–147

Magnin NC, Cooley BA, Reiskind JB, Bowes G (1997) Regulation and localization of key enzymes during the induction of Kranz-less, C4-type photosynthesis in *Hydrilla verticillata*. Plant Physiol 115:1681–1689

Matsuda Y, Hopkinson BM, Nakajima K, Dupont CL, Tsuji Y (2017) Mechanisms of carbon dioxide acquisition and CO_2 sensing in marine diatoms: a gateway to carbon metabolism. Philos Trans R Soc B 372:20160403

McKay RML, Gibbs SP (1991) Composition and function of pyrenoids: cytochemical and immunocytochemical approaches. Can J Bot 69:1040–1052

Meyer M, Griffiths H (2013) Origins and diversity of eukaryotic CO_2-concentrating mechanisms: lessons for the future. J Exp Bot 64:769–786

Meyer MT, Genkov T, Skepper JN, Jouhet J, Mitchell MC, Spreitzer RJ, Griffiths H (2012) Rubisco small-subunit α-helices control pyrenoid formation in *Chlamydomonas*. Proc Natl Acad Sci USA 109:19474–19479

Meyer MT, Whittaker C, Griffiths H (2017) The algal pyrenoid: key unanswered questions. J Exp Bot 68:3739–3749

Michels AK, Wedel N, Kroth PG (2005) Diatom plastids possess a phosphoribulokinase with an altered regulation and no oxidative pentose phosphate pathway. Plant Physiol 137:911–920

Mitchell C, Beardall J (1996) Inorganic carbon uptake by an Antarctic sea-ice diatom, *Nitzschia frigida*. Polar Biol 21:310–315

Mitchell MC, Metodieva G, Metodiev MV, Griffiths H, Meyer M (2017) Pyrenoid loss impairs carbon-concentrating mechanism induction and alters primary metabolism in *Chlamydomonas reinhardtii*. J Exp Bot 68:3891–3902

Morel FMM, Cox EH, Kraepiel AML, Lane TW, Milligan AJ, Schaperdoth I, Reinfelder JR, Tortell PD (2002) Acquisition of inorganic carbon by the marine diatom *Thalassiosira weissflogii*. Funct Plant Biol 29:301–308

Morita E, Abe T, Tsuzuki M, Fujiwara S, Sato N, Hirata A, Sonoike K, Nozaki H (1998) Presence of the CO_2-concentrating mechanism in some species of the pyrenoid-less free-living algal genus *Chloromonas* (Volvocales, Chlorophyta). Planta 204:269–276

Morita E, Abe T, Tsuzuki M, Fujiwara S, Sato N, Hirata A, Sonoike K, Nozaki H (1999) Role of pyrenoids in the CO_2- concentrating mechanism: comparative morphology, physiology and molecular phylogenetic analysis of closely related strains of *Chlamydomonas* and *Chloromonas* (Volvocales). Planta 208:365–372

Moroney JV, Chen ZY (1998) The role of the chloroplast in inorganic carbon uptake by eukaryotic algae. Can J Bot 76:1025–1034

Morris I, Beardall J, Mukerji D (1978) The mechanisms of carbon fixation in phytoplankton. Mitt Internat Verein Limnol 21:174–183

Munoz J, Merrett MJ (1989) Inorganic carbon transport in some marine eukaryotic microalgae. Planta 178:450–455

Mustardy L, Cunningham FX, Gantt E (1990) Localization and quantitation of chloroplast enzymes and light-harvesting components using immunocytochemical methods. Plant Physiol 94:334–340

Nakajima K, Tanaka A, Matsuda Y (2013) SLC4 family transporters in a marine diatom directly pump bicarbonate from seawater. Proc Natl Acad Sci USA 110:1767–1772

Ogawa T, Ogren WL (1985) Action spectra for accumulation of inorganic carbon in the cyanobacterium, *Anabaena variabilis*. Photochem Photobiol 41:583–587

Ogawa T, Miyano A, Inoue Y (1985) Photosystem-I-driven inorganic carbon transport in the cyanobacterium, *Anacystis nidulans*. Biochim Biophys Acta 808:74–75

Ohnishi N, Mukherjee B, Tsujikawa T, Yanase M, Nakano H, Moroney JV, Fukuzawa H (2010) Expression of a low CO_2-inducible protein, LCI1, increases inorganic carbon uptake in the green alga *Chlamydomonas reinhardtii*. Plant Cell 22:3105–3311

Omata T, Price GD, Badger MR, Okamura M, Gohta S, Ogawa T (1999) Identification of an ATP-binding cassette transporter involved in bicarbonate uptake in the cyanobacterium *Synechococcus* sp. strain PCC 7942. Proc Natl Acad Sci U S A 96:13571–13576

Palmqvist K, Sundblad L-G, Wingsle G, Samuelsson G (1990) Acclimation of photosynthetic light reactions during induction of inorganic carbon accumulation in the green alga *Chlamydomonas reinhardtii*. Plant Physiol 94:357–366

Patel BN, Merrett MJ (1986) Regulation of carbonic anhydrase activity, inorganic carbon uptake and photosynthetic biomass yield in *Chlamydomonas reinhardtii*. Planta 169:81–86

Price GD, Maeda S, Omata T, Badger M (2002) Modes of active inorganic carbon uptake in the cyanobacterium *Synechococcus* sp. PCC7942. Funct Plant Bio 29:131–149

Price GD, Woodger FJ, Badger MR, Howitt SM, Tucker L (2004) Identification of a SulP-type bicarbonate transporter in marine cyanobacteria. Proc Natl Acad Sci U S A 101:18228–18233

Price GD, Badger MR, Woodger FJ, Long BJ (2008) Advances in understanding the cyanobacterial CO_2- concentrating-mechanism (CCM): functional components, Ci transporters, diversity, genetic regulation and prospects for engineering into plants. J Exp Bot 59:1441–1461

Pronina NA, Borodin VV (1993) CO_2-stress and CO_2 concentrating mechanism: investigation by means of photosystem-deficient and carbonic anhydrase-deficient mutants of *Chlamydomonas reinhardtii*. Photosynthetica 28:515–522

Pronina NA, Semenenko VE (1992) Pyrenoid role in CO_2 concentration and fixation in microalga chloroplasts. Russ J Plant Physiol 73:723–730

Pyszniak AM, Gibbs SP (1992) Immunocytochemical localization of photosystem I and the fucoxanthin–chlorophyll *a/c* light-harvesting complex in the diatom *Phaeodactylum tricornutum*. Protoplasma 166:208–217

Raven JA (1986) Physiological consequences of extremely small size for autotrophic organisms in the sea. In: Platt T, WKW L (eds) Photosynthetic picophytoplankton, Canadian bulletin of fisheries and aquatic sciences 214. Department of Fisheries and Oceans, Ottawa, pp 1–70

Raven JA (1997a) Inorganic carbon acquisition by marine autotrophs. Adv Bot Res 27:85–209

Raven JA (1997b) Putting the C in Phycology. Eur J Phycol 32:319–333

Raven JA (1997c) CO_2 concentrating mechanisms: a role for thylakoid lumen acidification. Plant Cell Environ 20:147–154

Raven JA (1999) Picophytoplankton. In: Round FE, Chapman DJ (eds) Progress in phycological research, volume 13. Biopress Ltd., Bristol, pp 33–106

Raven JA (2009) Contributions of anoxygenic and oxygenic phototrophy and chemolithotrophy to carbon and oxygen fluxes in aquatic environments. Aquat Microb Ecol 56:177–192

Raven JA (2013a) Rubisco: still the most abundant protein of Earth? New Phytol 198:1–3

Raven JA (2013b) Half a century of pursuing the pervasive proton. Progr Bot 74:3–34

Raven JA, Beardall J (2003) CO_2 acquisition mechanisms in algae: Carbon dioxide diffusion and carbon dioxide concentrating mechanisms. In: Larkum AWD, Douglas SE, Raven JA (eds) Photosynthesis in the Algae. Kluwer Academic Publishers, Dordrecht, pp 225–244

Raven JA, Beardall J (2016) The ins and outs of CO_2. J Exp Bot 67:1–13

Raven JA, Colmer TD (2016) Life at the boundary: photosynthesis at the soil-liquid interface. A synthesis focusing on mosses. J Exp Bot 67:1613–1623

Raven JA, Giordano M (2017) Acquisition and metabolism of carbon in the Ochrophyta other than diatoms. Philos Trans R Soc London B 372:20160400

Raven JA, Hurd CJ (2012) Ecophysiology of photosynthesis in macroalgae. Photosynth Res 113:105–125

Raven JA, Beardall J, Griffiths H (1982) Inorganic C sources for *Lemanea*, *Cladophora* and *Ranunculus* in a fast flowing stream: measurements of gas

exchange and of carbon isotope ratio and their ecological significance. Oecologia 53:68–78

Raven JA, Ball L, Beardall J, Giordano M, Maberly SC (2005) Algae lacking CCMs. Can J Bot 83:879–890

Raven JA, Giordano M, Beardall J, Maberly S (2011) Algal and aquatic plant carbon concentrating mechanisms in relation to environmental change. Photosynth Res 109:281–296

Raven JA, Giordano M, Beardall J, Maberly SC (2012) Algal evolution in relation to atmospheric CO_2: carboxylases, carbon concentrating mechanisms and carbon oxidation cycles. Philos Trans R Soc B 367:493–507

Raven JA, Beardall J, Giordano M (2014) Energy costs of carbon dioxide concentrating mechanisms. Photosynth Res 121:111–124

Raven JA, Beardall J, Quigg A (2019) Light-driven oxygen consumption in the water-water cycles and photorespiration, and light stimulated mitochondrial respiration (this volume)

Reinfelder JR (2011) Carbon concentrating mechanisms in eukaryotic marine phytoplankton. Annu Rev Mar Sci 3:291–315

Reinfelder JR, Kraepiel AML, Morel FMM (2000) Unicellular C_4 photosynthesis in a marine diatom. Nature 407:996–999

Reinfelder JR, Milligan AJ, Morel FMM (2004) The role of C_4 photosynthesis in carbon accumulation and fixation in a marine diatom. Plant Physiol 135:2106–2111

Reiskind JB, Bowes G (1991) The role of phosphoenol pyruvate carboxykinase in a marine macroalga with C_4-like photosynthetic characteristics. Proc Natl Acad Sci USA 88:2883–2887

Reiskind JB, Seaman PT, Bowes G (1988) Alternative methods of photosynthetic carbon assimilation in marine macroalgae. Plant Physiol 87:686–692

Reiskind JB, Madsen TV, Van Ginke LC, Bowes G (1997) Evidence that inducible C_4-like photosynthesis is a chloroplastic CO_2-concentrating mechanism in *Hydrilla*, a submersed monocot. Plant Cell Environ 20:211–220

Roberts K, Granum E, Leegood RC, Raven JA (2007a) C3 and C4 pathways of photosynthetic carbon assimilation in marine diatoms are under genetic, not environmental, control. Plant Physiol 145:230–235

Roberts K, Granum E, Leegood RC, Raven JA (2007b) Carbon acquisition by diatoms. Photosynth Res 93:79–88

Rost B, Riebesell U, Burkhardt S, Sültemeyer D (2003) Carbon acquisition of bloom- forming marine phytoplankton. Limnol Oceanogr 48:55–67

Rost B, Kranz SA, Richter K-U, Tortell PD (2007) Isotope disequilibrium and mass spectrometric studies of inorganic carbon acquisition by phytoplankton. Limnol Oceanogr Methods 5:328–337

Rotatore C, Colman B (1990) Uptake of inorganic carbon by isolated chloroplasts of the unicellular green alga *Chlorella ellipsoidea*. Plant Physiol 93:1597–1600

Rotatore C, Colman B (1991) The localization of active carbon transport at the plasma membrane in *Chlorella ellipsoidea*. Can J Bot 69:1025–1031

Sage RF (2004) The evolution of C_4 photosynthesis. New Phytol 161:341–370

Sage RF, Christin P-A, Edwards EJ (2011) The C_4 plant lineages of planet earth. J Exp Bot 62:3155–3169

Salvucci ME, Bowes G (1983) Two photosynthetic mechanisms mediating the low photorespiratory state in submersed aquatic angiosperms. Plant Physiol 73:488–496

Schaum CE, Collins S (2014) Plasticity predicts evolution in a marine alga. Proc R Soc Lond B 281:20141486

Scott KM, Henn-Sax M, Harmer TL, Longo DL, Frome CH, Cavenaugh CM (2007) Kinetic isotope effect and biochemical characterisation of Form IA Rubisco from the marine cyanobacterium *Prochlorococcus marinus* MIT9313. Limnol Oceanogr 55:2199–2204

Shapiro J (1990) Current beliefs regarding dominance of bluegreens: the case for the importance of CO_2 and pH. Verh Int Ver Theor Angew Limnol 24:38–54

Shapiro J (1997) The role of carbon dioxide in the initiation and maintenance of blue-green dominance in lakes. Freshw Biol 37:307–323

Shibata M, Katoh H, Sonoda M, Ohkawa H, Shimoyama M, Fukuzawa H, Kaplan A, Ogawa T (2002) Genes essential to sodium-dependent bicarbonate transport in cyanobacteria: function and phylogenetic analysis. J Biol Chem 277:18658–18664

Shiraiwa Y, Danbara A, Yoke K (2004) Characterization of highly oxygen-sensitive photosynthesis in coccolithophorids. Jpn J Phycol 52(Supplement):87–94

Sinetova MA, Kupiyanova EV, Mankelova AG, Allakhverdiev SI, Pronina NA (2012) Identification and functional role of the carbonic anhydrase Cah3 in thylakoid membranes of pyrenoid of *Chlamydomonas reinhardtii*. Biochim Biophys Acta 1817:1248–1255

Smith KS, Ferry JG (2000) Prokaryotic carbonic anhydrases. FEMS Microbiol Rev 24:335–366

Smith-Harding TJ, Mitchell JG, Beardall J (2018) The role of external carbonic anhydrase in photosynthesis during growth of the marine diatom *Chaetoceros muelleri*. J Phycol 53:1159–1170

Spalding MH, Critchley C, Govindjee, Ogren WL (1984) Influence of carbon dioxide concentration during growth on fluorescence induction characteristics of the green alga *Chlamydomonas reinhardtii*. Photosynth Res 5:169–176

Stepien CC (2015) Impacts of geography, taxonomy and functional group on inorganic carbon use patterns in marine macrophytes. J Ecol 103:1372–1383

Stojkovic S, Beardall J, Matear R (2013) CO_2 concentrating mechanisms in three Southern Hemisphere strains of *Emiliania huxleyi*. J Phycol 49:670–679

Studer RA, Christin P-A, Williams MA, Orengo CA (2014) Stability-activity trade-offs constrain the adaptive evolution of RubisCO. Proc Natl Acad Sci USA 111:2223–2228

Sültemeyer DF, Fock HP, Canvin DT (1991) Active uptake of inorganic carbon by *Chlamydomonas reinhardtii*: evidence for simultaneous transport of HCO_3^- and CO_2 and characterization of active transport. Can J Bot 69:995–1002

Tcherkez GGB, Farqhar GD, Andrews TJ (2006) Despite slow catalysis and confused substrate specificity, all ribulose bisphosphate carboxylases may be nearly perfectly optimized. Proc Natl Acad Sci USA 103:7246–7725

Tchernov D, Silverman J, Luz B, Reinhold L, Kaplan A (2003) Massive light-dependent cycling of inorganic carbon between oxygenic photosynthetic microorganisms and their surroundings. Photosynth Res 77:95–103

Tortell P (2000) Evolutionary and ecological perspectives on carbon acquisition in phytoplankton. Limnol Oceanogr 45:744–750

Trimborn S, Lundholm N, Thoms S, Richter KU, Krock B, Hansen PJ, Rost B (2008) Inorganic carbon acquisition in potentially toxic and non-toxic diatoms: the effect of pH-induced changes in seawater carbonate chemistry. Physiol Plant 133:92–105

Tsekos I, Reiss HD, Orfanidid S, Orologas N (1996) Ultrastructure and supramolecular organization of photosynthetic membranes of some marine red algae. New Phytol 133:543–551

Tsuji Y, Suzuki I, Shiraiwa Y (2009) Photosynthetic carbon assimilation in the coccolithophorid *Emiliania huxleyi* (Haptophyta): evidence for the predominant operation of the C_3 cycle and the contribution of β-carboxylases to the active anaplerotic reaction. Plant Cell Physiol 50:318–329

Tsuji Y, Mahardika A, Matsuda Y (2017a) Evolutionarily distinct strategies for the acquisition of inorganic carbon from seawater in marine diatoms. J Exp Bot 68:3949–3958

Tsuji Y, Nakajima K, Matsuda Y (2017b) Molecular aspects of the biophysical CO_2-concentrating mechanism and its regulation in marine diatoms. J Exp Bot 68:3763–3772

Van de Waal DB, Verspagen JMH, Finke JF, Vournazou V, Immers AK, Kardinaal WEA, Tonk L, Becker S, Van Donk E, Visser PM, Huisman J (2011) Reversal in competitive dominance of a toxic versus non-toxic cyanobacterium in response to rising CO_2. ISME J 5:1438–1450

van Hunnik E, Amoroso G, Sültemeyer D (2002) Uptake of CO_2 and bicarbonate by intact cells and chloroplasts of *Tetraedon minimum* and *Chlamydomonas noctigama*. Planta 215:763–769

Villarejo A, Martinez F, del Pino Plumed M, Ramazanov Z (1996) The induction of the CO_2 concentrating mechanism in a starch-less mutant of *Chlamydomonas reinhardtii*. Physiol Plant 98:798–802

Villarejo A, Rolland N, Flor M, Sültemeyer D (2001) A new chloroplast envelope carbonic anhydrase activity is induced during acclimation to low inorganic carbon concentrations in *Chlamydomonas reinhardtii*. Planta 213:286–295

Wang Y, Stessman DJ, Spalding MH (2015) The CO_2 concentrating mechanism and photosynthetic carbon assimilation in limiting CO_2: how *Chlamydomonas* works against the gradient. Plant J 82:429–448

Whitney SM, Andrews TJ (1998) The CO_2/O_2 specificity of single-subunit ribulose-bisphosphate carboxylase from the dinoflagellate, *Amphidinium carterae*. Aust J Plant Physiol 25:131–138

Whitney S, Shaw D, Yellowlees D (1995) Evidence that some dinoflagellates contain a ribulose-1,5-bisphosphate carboxylase/oxygenase related to that of the α-proteobacteria. Proc R Soc Lond B 259:271–275

Whitney S, Houtz RL, Alonso H (2011) Advancing our understanding and capacity to engineer Nature's CO_2-sequestering enzyme, Rubisco. Plant Physiol 155:27–35

Yamano T, Sato E, Iguchi H, Fukuda Y, Fukuzawa H (2015) Characterization of cooperative bicarbonate uptake into chloroplast stroma in the green alga *Chlamydomonas reinhardtii*. Proc Natl Acad Sci USA 112:7315–7320

Young EB, Beardall J (2005) Modulation of photosynthesis and inorganic carbon acquisition in a marine microalga by nitrogen, iron and light availability. Can J Bot 83:917–928

Young E, Beardall J, Giordano M (2001) Inorganic carbon acquisition by *Dunaliella tertiolecta* (Chlorophyta) involves external carbonic anhydrase and direct HCO_3^- utilization insensitive to the anion exchange inhibitor DIDS. Eur J Phycol 36:81–88

Young JN, Heureux AM, Sharwood RE, Rickaby RE, Morel FM, Whitney SM (2016) Large variation in the Rubisco kinetics of diatoms reveals diversity among their carbon-concentrating mechanisms. J Exp Bot 67:3445–3456

Chapter 8

Light-Driven Oxygen Consumption in the Water-Water Cycles and Photorespiration, and Light Stimulated Mitochondrial Respiration

John A. Raven*
Division of Plant Science, University of Dundee at the James Hutton Institute, Dundee, UK

Climate Change Cluster, University of Technology Sydney, Ultimo, NSW, Australia

School of Biology, University of Western Australia, Crawley, WA, Australia

John Beardall
School of Biological Sciences, Monash University, Clayton, VIC, Australia

and

Antonietta Quigg
Texas A&M University at Galveston, Galveston, TX, USA

*Author for correspondence, e-mail: j.a.raven@dundee.ac.uk

A. W. D. Larkum et al. (eds.), *Photosynthesis in Algae: Biochemical and Physiological Mechanisms*, Advances in Photosynthesis and Respiration 45, https://doi.org/10.1007/978-3-030-33397-3_8

I. Introduction

In addition to linear electron flow to the oxidised sources of elements essential for growth of photolithotrophic algae (CO_2, $NO_3^-$and SO_4^{2-}), there are a number of alternative electron transport pathways in algae that are dependent on, or stimulated by, light. Significant advances have been made in our understanding of those alternative electron transport pathways that involve O_2 uptake since the reviews by Beardall et al. (2003) and Miyake and Asada (2003) in the original edition of 'Photosynthesis of Algae'. Here we deal with the water-water cycles involving flavodiiron proteins, the Mehler Ascorbate Peroxidase (MAP) pathway or the Plastid Terminal Oxidase (PTOX), Rubisco (D-ribulose bisphosphate carboxylase-oxygenase) oxygenase and photorespiration, and mitochondrial electron transport. These topics have been discussed separately since 2003 in a number of reviews and primary research articles (e.g. Cardol et al. 2011; Oroszi et al. 2011; Nawrocki et al. 2015; Bailleul et al. 2015; Curien et al. 2016; Alric and Johnson 2017; Griffiths et al. 2017; Raven et al. 2017; Shikanai and Yamamoto 2017). Here we consider all of these possible processes, including the evidence of their occurrence, and their mechanisms, distribution, functions and interactions.

II. The Evidence of Light-Dependent O_2 Uptake

$^{18}O_2$ uptake is stimulated by light in photosynthetic organisms. The $^{18}O_2$ uptake in the light includes mitochondrial respiration as well as photorespiration and the various water-water cycles, but not cyclic electron flow round photosystem II (PSII) (Prasil et al. 1996; Feikema et al. 2006; Shinopoulos and Brudwig 2012; Ananyev et al. 2017). Badger et al. (2000); Brechignac and Andre (1984) and Franklin and Badger (2001) present new data and review earlier literature for, respectively, microalgae and macroalgae (Table 8.1). This method is only applicable to natural communities of phytoplankton when sampled in microcosms (Bailleul et al. 2017).

An alternative approach to estimating light-dependent O_2 uptake uses PSII fluorescence measured with fast repetition rate (FRRi) and/or pulse amplitude modulation (PAM) techniques (Kolber et al. 1998; Schreiber 1994). Giving absolute values of electron flow through PSII requires measurements of incident photosynthetically active radiation, and of its absorption as the absorption cross-section of PSII, or absorptance by the organism and an assumed allocation of absorbed photons between photosystem I (PSI) and PSII (Genty et al. 1989; Suggett et al. 2004, 2009; Fujiki et al. 2007). The results of these measurements of net electron flow rate through PSII (i.e. corrected for any cyclic flow electron: Prasil et al. 1996) can be converted to the gross rate of O_2 production. Converting these fluorescent estimates of gross O_2 production rate to the O_2 uptake rate requires measurement, or estimation, of electron flow to the reductive assimilation of CO_2, NO_3^- and SO_4^{2-} (Feikema et al. 2006; Shinopoulos and Brudwig 2012; Ananyev et al. 2017; Hughes et al. 2018). The fluorescence method has been used on laboratory cultures in parallel with ^{14}C-inorganic C assimilation measurements (Suggett et al. 2009; Alderkamp et al. 2012; Morelle and Claquin 2018), and has the advantage that it can be used on natural communities (Gilbert et al. 2000; Perkins et al. 2002; Kromkamp et al. 2008; Napoléon and Claquin 2012; Hancke et al. 2015; Schuback et al. 2016; Morelle et al. 2018). This method does not have a component from mitochondrial respiration in the calculated O_2 uptake in the light, contrasting with measurements of $^{18}O_2$ uptake. This chlorophyll fluorescence method has been used in parallel with the $^{18}O_2$ technique by Franklin and Badger (2001), Suggett et al. (2003, 2008, 2009), Claquin et al. (2004), Beardall et al. (2009), Waring et al. (2010) and Brading et al. (2011).

Table 8.1. Micro- and macro-algal taxa in which light dependent oxygen consumption has been demonstrated using $^{18}O_2$

Phylum	Class	References
Cyanobacteria		Hoch et al. (1963), Miller et al. (1988), Kana (1992, 1993), Li and Canvin (1997), Ermakova et al. (2016) and Boatman et al. (2018)
Rhodophyta	Bangiophyceae	Badger et al. (2000) and Franklin and Badger (2001)
Rhodophyta	Floridiophyceae	Brechignac and Andre (1984)
Chlorophyta	Chlorophyceae	Hoch et al. (1963), Bunt and Heeb (1971), Glidewell and Raven (1975), Sültemeyer et al. (1993, 1986), Xue et al. (1996), Suggett et al. (2003) and Dang et al. (2014)
Chlorophyta	Prasinophyceae	Suggett et al. (2009)
Chlorophyta	Trebouxiophyceae	Bunt and Heeb (1971) and Suggett et al. (2003)
Chlorophyta	Ulvophyceae	Franklin and Badger (2001)
Streptophyta	Charophyceae[a]	Lewitus and Kana (1995)
Cryptophyta	Cryptophyceae	Lewitus and Kana (1995)
Dinophyta	Dinophyceae	Badger et al. (2000), Suggett et al. (2003, 2008, 2009) and Brading et al. (2011)
Haptophyta	Pavlovophyceae[b]	Lewitus and Kana (1995)
Haptophyta	Prymnesiophyceae	Badger et al. (2000), Suggett et al. (2003) and McKew et al. (2013)
Ochrophyta	Bacillariophyceae	Bunt (1965), Bunt et al. (1966), Weger et al. (1989), Badger et al. (2000), Suggett et al. (2003), Claquin et al. (2004) and Waring et al. (2010)
Ochrophyta	Dichtyochophyceae[c]	Lewitus and Kana (1995)
Ochrophyta	Pelagophyceae	Suggett et al. (2009)
Ochrophyta	Phaeophyceae	Franklin and Badger (2001)

Updated from the earlier reviews by Badger et al. (2000), Brechignac and Andre (1984) and Franklin and Badger (2001)
[a]*Closterium* was assigned to the Conjugatophycae in Lewitus and Kana (1995); a broad definition of Charophyceae (=all alga members of the Streptophyta) is used here
[b]*Pavlova* was assigned to the Prymnesiophyceae in Lewitus and Kana (1995); *Pavlova* is now the type genus of the class Pavlovophyceae
[c]*Pseudondeinella* was assigned to the Chrysophyceae in the Lewitus and Kana (1995); this genus is now assigned to the Dichtyochophyceae

A further comparison with fluorescence estimates of PSII ETR is with the net O_2 production rate (Beer et al. 2000; Masojíder et al. 2001; Longstaff et al. 2002; Carr and Björk 2003; Figueroa et al. 2003; Gordillo et al. 2003; Rech et al. 2003; Colombo-Pallotta et al. 2006; Gloag et al. 2007; Wu et al. 2006; Lefebvre et al. 2007; Nielsen and Nielsen 2008; Bañares-España et al. 2012; Duarte et al. 2013; Torres et al. 2014) and ^{14}C-inorganic C incorporation (Morelle and Claquin 2018). While most of these measurements were made in the laboratory, Masojíder et al. (2001) worked on a freshwater cyanobacterial bloom through a diel cycle, while Longstaff et al. (2002) used O_2 and ETR measurements on *Ulva* in a photorespirometer at the depth from which the alga was collected, with re-equilibration of the water in the photorespirometer with ambient seawater every 15 min.

III. Possible Mechanisms of Light-Driven O_2 Uptake

A. *Water-Water Cycles*

The photoreduction of O_2 to H_2O in PS I by the electrons generated in PS II in chloroplasts is also referred to as the water-water cycle (Asada 2000) or, for the Mehler Ascorbate Peroxidase variant, the Foyer-Asada-Halliwell cycle (Foyer et al. 1991; Foyer and Noctor 2011). Photoreduction rates of O_2 in PS I are several orders of mag-

nitude lower than those of superoxide conversion to hydrogen peroxide catalysed by superoxide dismutase, hydrogen peroxide conversion to water catalysed by ascorbate peroxidase, and ascorbate reduction by reduced ferredoxin or catalysed by either dehydroascorbate reductase or monodehydroascorbate reductase (Asada 2000). Under photoinhibitory conditions when these intersystem electron carriers are over-reduced, the water-water cycle can scavenge active oxygen species to dissipate excess photon energy and electrons. In doing so, the water-water cycle acts as an alternative electron flux and can down-regulate PSII quantum yield using the proton gradient across the thylakoid membranes and the associated de-epoxidation of violaxanthin (Horton et al. 2000) and photorespiration (see below). The operation of the water–water cycle *in vivo* is thus a mechanism for the protection of the photosynthetic apparatus from photo-inactivation and damage under environmental stress conditions in microalgae and plants (Rizhsky et al. 2003; Driever and Baker 2011 and references therein). In vascular plant leaves, the water-water cycle initiates gene expression associated with light-induced reactive oxygen species involved in acclimation (Apel and Hirt 2004) or triggering of cell death (Mullineaux and Baker 2010). If the water–water cycle has a role in energy balance, that is, it regulates the supply of reductants relative to ATP to meet cellular metabolic needs (Kramer and Evans 2011; Driever and Baker 2011), then definitive evidence is still lacking.

In the following descriptions, photon costs assume 1 photon absorbed by the relevant light-absorbing complex per electron moved through PS I and1.25 photons absorbed by the relevant light-absorbing complex per electron moved through PS II (Raven et al. 2014). The value of 1.25 for PS II is based on the photon yield of not more than 0.8 electrons per photon absorbed by photosystem II based on chlorophyll *a* fluorescence (Raven et al. 2014).

B. The Mehler Ascorbate Peroxidase (MAP) Reactions Involving PSI and PSII

2.25 photons move 1 electron from H_2O to O_2, and 3 H^+ from the cytosol/stroma into the thylakoid lumen. Electrons from the reducing end of PSI carry out the 1 electron reduction of O_2 to produce the superoxide radical anion, $O_2^{-\cdot}$. Two $O_2^{-\cdot}$ are converted to 1 O_2 and 1 H_2O_2 (Roberty et al. 2014; Curien et al. 2016) (Fig. 8.1). The H_2O_2 is processed in a reaction catalysed by ascorbate peroxidase, which oxidises 2 ascorbate, producing H_2O and 2 monodehydroascorbate (MDA). The 2 MDA are reduced by two further electrons from PSI, either directly or via NADPH (Roberty et al. 2014; Curien et al. 2016; see also Margis et al. 2009). MDA is extremely reactive and can be reduced by photogenerated electrons from PSI at a rate comparable with that of $NADP^+$ reduction (Forti and Ehrenheim 1993). This is referred to as the "Mehler–ascorbate reaction". Alternatively, MDA can be reduced by photosynthesis through the MDA reductase enzyme, as these two pathways share the same electron transfer carriers which uses NADPH as a substrate (Forti and Elli 1995).

Miyake et al. (1991; see also Berntroitner et al. 2009) found relatively low activity of ascorbate peroxidase in 8 of the 10 β-cyanobacteria examined, and of MDA reductase in all 10 species. However, Helman et al. (2003); Gest et al. (2013) and Maruta et al. (2016) point out that there is no genetic evidence for ascorbate peroxidases in cyanobacteria, and that there is limited evidence supporting the occurrence of ascorbate in cyanobacteria. The phylogenetic analyses of Wheeler et al. (2015) and Maruta et al. (2016) failed to find ascorbate peroxidase genes in the Glaucocystophyta, porphyridialean red algae, Haptophyta and Chlorarachniophyta. Ascorbate peroxidase genes were found in the other eukaryotic algae examined, with the thylakoid-localised ascorbate peroxi-

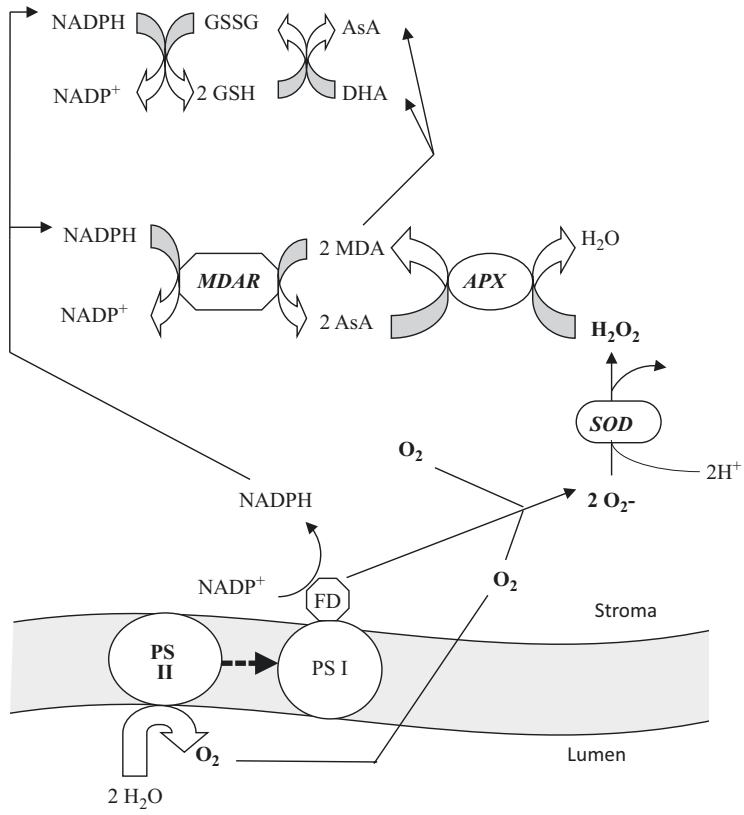

Fig. 8.1. Electrons flow from ferredoxin (Fd) to oxygen produced by PSII, generating superoxide O_{2-}. Superoxide can be acted upon by superoxide dismutase (SOD), producing hydrogen peroxide, which in turn is acted upon by ascorbate peroxidase, oxidizing ascorbic acid AsA which is dehydrogenated to monodehydroascorbate (MDA). MDA can be reduced back to AsA by monodehydroascorbate reductase (MDAR) using NADPH generated by the thylakoid photochemical apparatus. Alternatively, the MDA can disproportionate to AsA and dehydroascorbate (DHA). The DHA is reduced to (another) AsA by reduced glutathione (GSH)–DHA oxidoreductase and the oxidized glutathione (GSSG) is reduced back to GSH by NADPH generated by the thylakoid photochemical apparatus. For simplicity only a stromal based APX system is shown, though an APX has been demonstrated to be located on the stromal side of the thylakoid membrane. (Redrawn after Raven and Beardall 2005)

dase limited to the Streptophyta, i.e. charophycean algae and embryophytes. The dinoflagellate *Symbiodinium* has the MAP pathway (Krueger et al. 2014; Roberty et al. 2014), and the closely related chromerids (photosynthetic apicomplexans) have one (*Vitrella*) or two (*Chromera*) copies of a FeSOD (superoxide dismutase) as subunits of PSI (Sobotka et al. 2017). No parallel phylogenetic analyses seem to have been performed on the other enzymes of the MAP pathway. Further work is needed to determine if the selenocysteine-containing glutathione peroxidase found in *Chlamydomonas reinhardtii* (Fischer et al. 2009) could substitute for ascorbate peroxidase in the MAP pathway.

C. *Flavodiiron Protein Involving PSI and PSII*

2.25 photons move 1 electron from H_2O to O_2, and 3 H^+ from the cytosol/stroma to the thylakoid lumen (Fig. 8.2). The reduction of 1 O_2 by flavodiiron is by a 4 electron process producing 2 H_2O and is suggested to not produce reactive O species (Frazão et al. 2000; Roberty et al. 2014). Flavodiiron proteins in

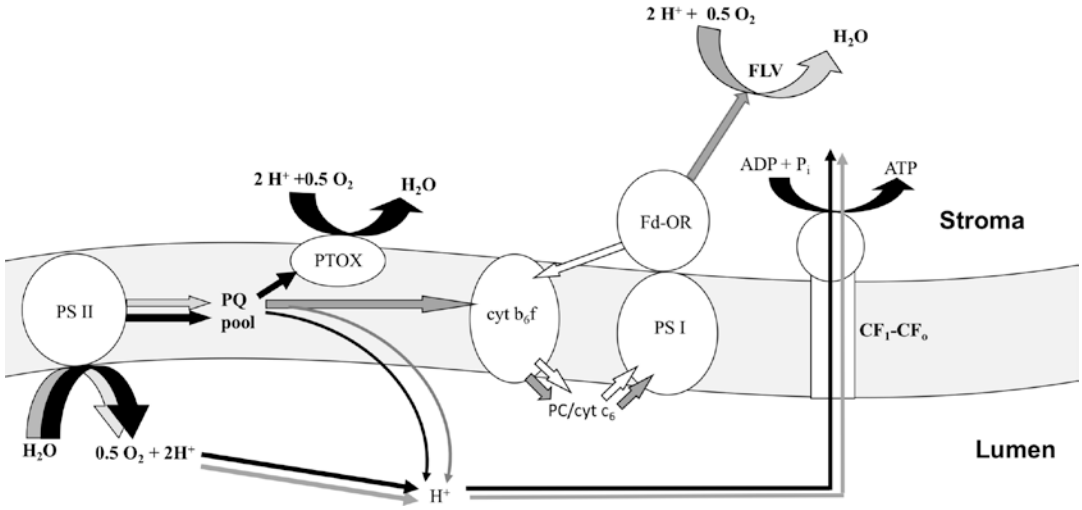

Fig. 8.2. Electron transport associated with electron flow to PTOX (plastid (plastoquinol) terminal oxidase) (black arrows) and to flavodiiron (FLV) proteins (grey arrows). Protons can cross the thylakoid membrane through the CF1–CF0 ATP synthetase. Cyclic electron transport is shown by the white arrows. Cyt b_6f = Cytochrome b_6f-Fe_{nh} complex; Cyt c_6 = Cytochrome c_6; Fd-OR = ferredoxin oxidoreductase; PC = Plastocyanin; PQ = Plastoquinone

oxygenic photosynthetic organisms occur in cyanobacteria and the eukaryotic algae that have been examined, as well as embryophytes other than flowering plants (Vicente et al. 2002; Zhang et al. 2009; Peltier et al. 2010; Jokel et al. 2015; Roberty et al. 2014; Shimakawa et al. 2015; Chaux et al. 2017; Illik et al. 2017; Shimakawa et al. 2017a, b). In cyanobacteria, as well as the (overall) 4 electron reduction of O_2 by PSI involving Flv 1 and Flv3 (Helman et al. 2003; Allahverdiyeva et al. 2011, 2013, 2015a, b), Flv2 and Flv4 are involved in protection of PSII from photodamage (Zhang et al. 2009; Bersanini et al. 2014; Allahverdiyeva et al. 2015a), and a heterocyst-expressed Flv3B is required for diazotrophic growth in oxic, but not in microoxic conditions (Ermakova et al. 2014). Flavodiiron protein is probably involved in photoprotection of cyanobacteria (Allahverdiyeva et al. 2013) and *Chlamydomonas* (Allahverdiyeva et al. 2015b) in fluctuating light. Rapid O_2 cycling is involved in O_2 protection of nitrogenase in the non-heterocystous diazotrophic cyanobacterium *Trichodesmium thiebaaultii* (Kana 1993), though it is not clear if this involves Flv2 and Flv4.

D. Plastid (Plastoquinol) Terminal Oxidase (PTOX) Involving PSII but not PSI

1.25 photons move 1 electron from H_2O to O_2, and 1 H^+ from the cytosol/stroma to the thylakoid lumen (Fig. 8.2; Cardol et al. 2008; Rochaix 2011; Nawrocki et al. 2015; Lea-Smith et al. 2016). The PTOX reaction involves, as is apparently the case for flavodiiron protein, a 4 electron process producing H_2O rather than reactive oxygen species (Yu et al. 2014). PTOX is apparently universal in oxygenic photosynthetic organisms: PTOX gene sequences are found in the Glaucocystophyta, Rhodophyta, Chlorophyta, Streptophyta (Archaeplastida), Chlorarachniophyta, Cryptophyta, Euglenophyta, Haptophyta and Ochrophyta (Cardol et al. 2003; Zehr and Kudela 2009; Cruz et al. 2011; Houille-Vernes et al. 2011; Nawrocki et al. 2015); see also Schuback et al. 2015; Misumi and Sonoike (2017), and in vascular plants (Streb et al. 2005). Bailey

et al. (2008) found that PTOX, or another pyrogallol-sensitive oxidase, functions in marine cyanobacteria (*Synechococcus* WH8102) to maintain PSII in a highly oxidized state. During fluctuating light conditions, oxidase activity works to maintain a highly oxidized pool of PSII when the cells experience high irradiances and prevents electron transport limitation by PSI activity during periods of low light.

In the open ocean, particularly the high-nutrient-low-chlorophyll corridors which are home to Fe-limited microalgae (Martin and Fitzwater 1988), PSI content is likely to be decreased (Strzeprek and Harrison 2004; Allen et al. 2008; Schuback et al. 2015). This in turn will lead to an over-reduction of PSII acceptors, increasing their susceptibility to photoinhibition (Barber and Andersson 1992). The cyanobacterium *Synechococcus* and the green alga *Ostreococcus* use the water-to-water cycle, catalyzed by the plastoquinone terminal oxidase, to redirect PSII-generated electrons into PTOX (Kuntz 2004; Bailey et al. 2008; Cardol et al. 2008). This alternate electron flow pathway can sustain a ΔpH to fuel ATP synthesis (solving the "ATP shortage" issue) and to trigger photoprotective responses in Fe-limited cells (Cardol et al. 2011).

As well as involvement in a water-water cycle, PTOX is involved in chlororespiration in the dark (*Thalassiosira pseudonana*: Cruz et al. 2011; *Chlamydomonas reinhardtii* (Houille-Vernes et al. 2011), and also in carotenoid synthesis (Nawrocki et al. 2015). Chlororespiration involves electron transfer from stromal NAD(P)H to plastoquinone (PQ) forming PQH_2, and oxidation by PTOX (Bennoun 1982) (Fig. 8.2). In cyanobacteria, and streptophyte (charophycean) and some chlorophyte (prasinophycean) algae, PQ reduction in the dark by a H^+-pumping multisubunit Type 1 Ndh1 complex (Strand et al. 2017; Laughlin et al. 2019) makes chlororespiration as a whole a H^+-pumping process. Other eukaryotic algae use a single subunit Type 2 Ndh2 (or PGRL1) that does not pump H^+, so the overall process does not pump H^+ (Nawrocki et al. 2015). Recently Li et al. (2016) concluded that cyclic electron flow around PSI might primarily function in photoprotection while the chlororespiratory pathway might play a more important role in the dark; together these two process coordinate to alleviate photoinhibition during heat stress.

E. Photorespiration

Rubisco is the core autotrophic carboxylase in oxygenic photosynthetic organisms (Bathellier et al. 2018). All Rubiscos have oxygenase activity, according to the equation:

$$\text{D} - \text{ribulose 1,5 bisphosphate} + \text{O}_2 \rightarrow$$
$$3 - \text{phospho} - \text{D} - \textit{glycerate} + 2 - \text{phosphoglycolate}$$

The oxygenase activity of Rubisco is competitive with the carboxylase activity. There is significant diversity in the selectivity for CO_2 relative to O_2, the affinities for CO_2 and O_2, and the substrate-saturated specific activities of carboxylase and oxygenase, among cyanobacteria, algae and embryophytes (Bathellier et al. 2018; Beardall and Raven (2018, this volume). Rubisco oxygenase activity occurs increasingly as the CO_2:O_2 at the Rubisco active site decreases (Hagemann et al. 2016; Griffiths et al. 2017; Bathellier et al. 2018). Although many cyanobacteria and algae excrete some of the glycolate produced by the action of 2-phosphoglycolate phosphatase on 2-phosphoglycolate, metabolism of glycolate is essential since knocking out all three pathways of glycolate metabolism has been shown to be lethal in a cyanobacterium (Eisenhut et al. 2008; see Eisenhut et al. 2017 for essentiality in a flowering plant).

Further metabolism (complete oxidation, or conversion to triose phosphate) of the 2-phosphoglycolate product of Rubisco oxygenase involves further O_2 uptake and CO_2 loss (Eisenhut et al. 2008; Hagemann et al. 2016). O_2 uptake occurs directly when the glycolate produced by phosphatase action on 2-phosphoglycolate is oxidised by glycolate oxidase in embryophytes and some eukaryotic algae, with H_2O_2 as the reduced product (Beardall et al. 2003). The H_2O_2 produced by superoxide dismutase is converted back into O_2 and H_2O by a catalase in the peroxisome (when present) during photorespiration. O_2 uptake is indirect when glycolate is oxidised to glyoxylate by mitochondrial glycolate dehydrogenase reducing Complex II of the respiratory electron transport chain (Beardall et al. 2003), and then, via PQ (plastoquinone: cyanobacteria) or UQ (ubiquinone: eukaryotes), Complex III and Complex IV (cytochrome oxidase) to O_2 (Raven and Beardall 2017). Alternatively, direct oxidation of PQH_2 (cyanobacteria) or via the mitochondrial alternative oxidase (AOX, a distant relative of PTOX: McDonald et al. 2003; McDonald and Vanleberghe 2006) in eukaryotic algae (McDonald et al. 2011) can occur. In all three cases (mitochondrial ETC, direct PQH_2 oxidation or AOX) the 4 electron reduction of O_2 produces H_2O.

Two of the pathways of glyoxylate metabolism, the photorespiratory carbon oxidation cycle and the tartronic semialdehyde pathway converting 2 glyoxylate to 1 triose phosphate and 1 CO_2, are overall reductive (Beardall et al. 2003; Eisenhut et al. 2008). The third pathway of glyoxylate metabolism, i.e. oxidation to oxalate, then decarboxylation to formate, and finally oxidation of formate to CO_2, involves a glyoxylate dehydrogenase (e.g. with glyoxylate as an alternative substrate for pyruvate dehydrogenase) and formate dehydrogenase, both with $NAD(P)^+$ as the electron acceptor (Bisswanger 1981; Alekeeva et al. 2011). Oxidation of NAD(P)H by the respiratory electron transport chain (see above) involves O_2 reduction to 2 H_2O by a 4 electron reaction. The default assumption as to the pathway of glyoxylate produced from 2-phosphoglycolate metabolism in eukaryotic algae is that it closely resembles the flowering plant photorespiratory carbon oxidation cycle (Beardall et al. 2003; Kern et al. 2013). However, this is not the case for those diatoms that have been investigated, where the pathway is incompletely resolved (Raven et al. 2000; Davis et al. 2017)

Photorespiration reduces acceptor limitation and generation of harmful reactive oxygen species (ROS) under high light conditions (Takahashi and Badger 2011). Interestingly, Eishenhut et al. (2017) found that photorespiration in *Arabidopsis thaliana* was not controlled at the transcriptional level despite physiological changes -rather regulation occurs at the level of post-translational modifications such as phosphorylation of enzymes, though whether this also occurs in algae and cyanobacteria is not known.

F. Mitochondrial Respiration

In addition to the relationship to photorespiration, light stimulation of O_2 uptake in mitochondrial respiration can also be related to the production of C skeletons for biosynthesis and for the energization of other processes that might otherwise be powered by a water to water cycle or cyclic electron flow (Larkum et al. 2017). For C skeleton synthesis, there is the possibility that the CO_2 production in the light exceeds that in the dark if the C skeleton synthesis related to protein and nucleic acid synthesis is largely confined to the light period, with mitochondrial respiration in the dark period used almost entirely in maintenance rather than growth processes (Raven 1976, 2013). Huertas et al. (2002a, b) showed that active HCO_3^- influx in the eustigmatophycean alga *Nannochloropsis* is powered by mitochondrial respiration. Bailleul et al. (2015; see also Weger et al.

1989) showed that mitochondrial respiration is essential for photosynthesis in the diatom *Phaeodactylum tricornutum* and that mitochondrial O_2 uptake is light stimulated.

The ratio of moles ADP phosphorylated per mole NAD(P)H oxidised depends on the occurrence of a H^+-pumping Complex I or a non-pumping alternative pathway to UQ, and the use of H^+-pumping complexes III and IV or the non-pumping alternate oxidase pathway to O_2 (Raven and Beardall 2017). The ATP: NAD(P)H ratio also depends on the H^+:ATP ratio of the F_OF_1 ATP synthase of mitochondria for eukaryotic algae, and the CF_OCF_1 of cyanobacteria. The H^+:ATP ratio from structural biology (the number of c-subunits per ATP synthase phosphorylating 3 ADP per rotation) is 3.33 for the *Chlamydomonas* mitochondrial ATP synthase (van Lis et al. 2007; Guo and Rubinstein 2018) and 4.33, 4.67 or 5.0 for different species of cyanobacteria (Pogoryelov et al. 2007; Guo and Rubinstein 2018). However, direct measurements of the H^+:ATP ratio give lower values, i.e. three for yeast mitochondria (structural biology prediction 3.3) and four for a flowering plant chloroplast (structural biology prediction 4.67) (Petersen et al. 2012; Turina et al. 2016).

G. Allocation of O_2 Uptake Among the Five Pathways

Allocation of O_2 uptake in the light among the five pathways listed above is complicated. There are problems with the specificity of inhibitors, and inhibitors, mutants, down-regulations and knock-outs can result in compensatory increases in the remaining processes that yield the same product(s). Methods that do not rely on inhibiting one pathway are transcriptomics (Levin et al. 2016) or proteomics (McKew et al. 2013), but have their own problems of not being directly related to biochemical or biophysical functions.

IV. Functions of the Light-Driven O_2 Uptake Processes

Although light-driven O_2 uptake processes described above serve to remove oxygen, with its attendant problem of toxicity as free radicals, the major function of the light-driven O_2 uptake processes described above is the relief of 'excitation pressure'. This relates to dissipation of the excitation of (especially) PSII in excess of use of energized electrons in 'useful' reduction processes, e.g. CO_2, NO_3^- and SO_4^{2-}. This is possible for any of the water-water cycles, provided they are not constrained by the rate at which ATP is consumed and hence the return ADP and inorganic phosphate for resynthesis of ATP, thus returning to the stroma/cytosol the H^+ that was pumped into thylakoid lumen by redox reactions of the water-water cycles. This also applies to the dissipation of energy transformed by photosynthetic processes by increased photorespiratory reactions; such an increase in Rubisco oxygenase (and downstream reactions) involves a corresponding increase in Rubisco carboxylase activity if there is no decrease in CO_2:O_2. When photorespiration is suppressed by high CO_2:O_2 at the active site of Rubisco by operation of a CO_2 concentrating mechanism, energy dissipation can occur by leakage from the carbon concentrating mechanism (CCM) (Sukenik et al. 1997; Tchernov et al. 1997).

An alternative means of preventing photodamage to PSII by excess excitation energy input is by non-photochemical quenching (NPQ). This loss of excess energy as heat is triggered by an increased proton motive force (pmf) across the thylakoid membrane resulting from an excess of light-driven H^+ movement into the thylakoid lumen greater than ATP consumption that allows additional H^+ flux out of the thylakoid lumen (Shikanai and Yamamoto 2017). Specifically, it is the pH difference component of the pmf rather than the electrical potential difference com-

ponent that leads to an increase in NPQ (Shikanai and Yamamoto 2017). Cyclic electron flow round PSI generates a pmf with a larger fraction of the electrical potential component than does linear electron flow through PSII (PTOX) or PSII and PSI where there is a larger pH difference component (Shikanai and Yamamoto 2017). This difference means that linear electron flow is more effective in producing NPQ than is a comparable H^+ flux driven by cyclic electron flow (Shikanai and Yamamoto 2017).

In the cyanobacterium *Synechocystis* PCC 6803 there are four flavodiiron proteins, Flv1 – Flv4 (Bersanini et al. 2014). Flv1 and Flv3 function in the manner mentioned above in accepting electrons from PSI and reducing O_2 to 2 H_2O in a 4 electron reaction (Bersanini et al. 2014). The Flv2/Flv4 dimer dissipates excitation pressure on PSII directly (Bersanini et al. 2014).

The MAP, flavodiiron and PTOX pathways can generate ATP in response to ATP:NADPH requirements of metabolism greater than are be supplied by linear electron flow from H_2O to CO_2, NO_3^- and SO_4^{2-}. Whether this requirement for additional ATP applies to CO_2 fixation depends on the CO_2 concentration, the occurrence or not of a CCM, and the H^+:ATP ratio of the CF_oCF_1 ATP synthetase (Raven et al. 2014). With saturating CO_2 the required ATP:NADPH:CO_2 of 3:2:1 for photosynthesis can be met by the ATP synthesised during electron flow from H^+ to $NADP^+$ during CO_2 assimilation by the Benson-Calvin cycle if the H^+:ATP ratio of the CF_oCF_1 ATP synthetase is 4.0 (Raven et al. 2014; see above under Mitochondrial respiration). However, with the H^+:ATP ratio of the CF_oCF_1 ATP synthetase of 4.67, as suggested by the structure of the synthase in flowering plants, CO_2-saturated photosynthesis requires additional ATP (Allen 2003). With sub-saturating CO_2 concentrations, an increased ATP:NADPH is needed for the CO_2 concentrating mechanism (CCM) and, generally, for the larger photorespiratory C flux when diffusive CO_2 entry occurs (Raven et al. 2014). The allocation of sources on ATP among the various possible sources by inhibitors, mutants and knock-outs is complicated by compensatory processes. With this proviso, none of the energy-requiring processes examined in the charophycean *Chara corallina* involve PSI (Smith and Raven 1974; Kiefer and Spanswick 1978) and, where investigated, are O_2-dependent (Smith and Raven 1974; Brechignac and Lucas 1987). These findings are consistent with energization of the processes from pseudocyclic photophosphorylation, i.e. ATP production linked to electron flow and H^+ pumping in a water-water cycle.

Miller et al. (1988) showed that inorganic C pumping in the CCM, presumably the HCO_3^- influx component, of *Synechococcus* UTEX 626 is paralleled by increased light-dependent $^{18}O_2$ uptake, consistent with energization by pseudocyclic photophosphorylation. However, Li and Canvin (1997) found that the parallel of the CCM and light-dependent $^{18}O_2$ uptake can be broken. Sültemeyer et al. (1993) showed that inorganic C pumping in the CCM of *Chlamydomonas reinhardtii* is paralleled by increased light-dependent $^{18}O_2$ uptake, again consistent with energization by pseudocyclic photophophosphorylation. Dang et al. (2014) also found an increase in light-dependent $^{18}O_2$ uptake in cells growing in low CO_2 (CCM) relative to high CO_2 (diffusive CO_2 entry) in wild-type *Chlamydomonas reinhardtii*. However, deficiency in the PGRL1 protein involved in cyclic electron flow and hence cyclic photophosphorylation increases not only light-dependent $^{18}O_2$ uptake, but also mitochondrial electron flow, so the ATP sources for the CCM are clearly subject to compensatory changes. Thus, for both the cyanobacterium and the chlorophycean alga, energization by pseudocyclic photophosphorylation is not obligatory.

Even in the presence of high CO_2:O_2 at the site of Rubisco there is some flux through P-glycolate, and subsequent metabolism of

some of the glycolate resulting from P-glycolate phosphatase (as opposed to excretion of all of the glycolate) is essential (Eisenhut et al. 2008). Elimination of all three pathways of glycolate metabolism in a cyanobacterium is, as mentioned earlier, lethal (Eisenhut et al. 2008). It must be re-emphasised that the dissipation of energy transformed by photosynthetic processes by increased photorespiratory reactions by increased Rubisco oxygenase (and downstream reactions) involves a corresponding increase in Rubisco carboxylase activity if there is no decrease in CO_2:O_2 at the active site of Rubisco.

V. Conclusions

Allocating the light-stimulated $^{18}O_2$-uptake among the possible alternative pathways by the use of inhibitors, mutants or knock-outs is undermined by the possibility, or even likelihood, of compensatory reactions. There is evidence from algae of water-water cycles involving the Mehler-Peroxidase Reaction, and the flavodiiron protein, using photosystems I and II, and involving the plastid (plastoquinol) terminal oxidase and only photosystem II, in many of the cyanobacteria and algae in which they have been sought. These pathways all pump H^+ into the lumen and so are coupled to ATP synthesis; this limits the extent to which the water-water cycles can function in photochemical quenching to the extent to which there are sinks for the ATP produced. The Rubisco oxygenase reaction, and photorespiratory enzymes that metabolise the resulting 2-phosphoglycolate, are universal in cyanobacteria and algae; their expression in air-equilibrium solutions is restricted in algae lacking CCMs. Also universal in algae are mitochondrial respiratory reactions, and their equivalents in cyanobacteria, although evidence on whether mitochondrial electron transport is light-stimulated is very limited.

Acknowledgements

We thank Pierre Cardol and David Suggett for their very helpful comments on the manuscript. The University of Dundee is a registered Scottish charity, No 015096. AQ acknowledges the support of the Texas Institute of Oceanography.

References

Alderkamp AC, Kulk BAGJ, Visser RJW, van Dijken GL, Mills MM, Arrigo KR (2012) The effects of iron limitation on the photophysiology of *Phaeocystis subarctica* (Prymnesiophyceae) and *Fragilariopsis cylindrus* (Bacillariophyceae) under dynamic irradiance. J Phycol 48:45–59

Alekeeva AA, Savim SS, Tishkov VI (2011) NAD^+-dependent formate dehydrogenase from plants. Acta Nat 3:38–54

Allahverdiyeva Y, Ermakova L, Eisenhut M, Zhang P, Richaud P, Aljani G, Hagemann M, Cournac L, Aro E-M (2011) Interplay between flavodiiron proteins and photorespiration in *Synechocystis* sp. PCC 6803. J Biol Chem 286:24007–24014

Allahverdiyeva Y, Mustila H, Ermakova L, Bersanini L, Richaud P, Aljani G, Battchikova M, Cournac L, Aro E-M (2013) Flavodiiron proteins Flv1 and Flv3 enable cyanobacterial growth and photosynthesis under fluctuating light. Proc Natl Acad Sci USA 110:4111–4116

Allahverdiyeva Y, Isojärvi J, Zhang P, Aro E-M (2015a) Cyanobacterial oxygenic photosynthesis is protected by flavodiiron proteins. Life 5:716–743

Allahverdiyeva Y, Suors M, Tikkanan M, Aro E-M (2015b) Photoprotection of photosynthesis in fluctuating light intensities. J Exp Bot 66:2427–2436

Allen JF (2003) Cyclic, pseudocyclic and noncyclic photophosphorylation: new links in the chain. Trends Plant Sci 8:15–19

Allen AE, La Roche J, Maheswari U, Lommer M, Schauer N, Lopez PJ, Finazzi G, Fernie AR, Bowler C (2008) Whole-cell response of the pennate diatom *Phaeodactylum tricornutum* to iron starvation. Proc Natl Acad Sci USA 105:10438–10443

Alric J, Johnson X (2017) Alternative electron transport pathways in photosynthesis: a confluence of regulation. Curr Opin Plant Biol 37:78–86

Ananyev G, Gates C, Kaplan A, Dismukes GC (2017) Photosystem II-cyclic electron flow powers exceptional photoprotection and record growth in the

microalgae *Chlorella ohadii*. Biochim Biophys Acta 1858:873–883

Apel K, Hirt H (2004) Reactive oxygen species: metabolism, oxidative stress, and signal transduction. Annu Rev Plant Biol 55:373–399

Asada K (2000) The water-water cycle as alternative photon and electron sinks. Philos Trans R Soc B Biol Sci 355:1419–1431

Badger MR, von Caemmerer S, Ruuska S, Nakano H (2000) Electron flow to oxygen in higher plants and algae: rates and control of direct photoreduction (Mehler reaction) and rubisco oxygenase. Philos Trans R Soc B 355:1433–1446

Bailey S, Melis A, Mackey KRM, Cardol P, Finazzi G, van Dijken G, Mine Berg G, Arrigo K, Schrager J, Grossman A (2008) Alternative photosynthetic electron flow to oxygen in marine *Synechococcus*. Biochim Biophys Acta 1777:269–276

Bailleul B, Berne N, Muik O, Petropsos D, Prihoda J, Tanaka A, Villanova V, Bligny R, Flori S, Falconet D, Krieger-Liszkay A, Santabarbara S, Rappoport F, Joliot P, Trichine L, Falkowski P, Cardol P, Bowler C, Finazzi G (2015) Energetic coupling between plastids and mitochondria drives CO_2 assimilation in diatoms. Nature 524:366–369

Bailleul B, Park J, Brown CM, Bidle KD, Lee SH, Falkowski PG (2017) Direct measurements of the light dependence of gross photosynthesis and oxygen consumption in the ocean. Limnol Oceanogr 62:1066–1079

Bañares-España J, Kromkamp JC, López-Roda V, Costas E, Flores-Moya A (2012) Photoacclimation of cultured strains of the cyanobacterium *Microcystis aeruginosa* to high-light conditions. FEMS Microbial Ecol 83:700–710

Barber J, Andersson B (1992) Too much of a good thing: light can be a bad thing for photosynthesis. Trends Biochem Sci 17:61–66

Bathellier C, Tcherkez G, Lorimer GH, Farquhar GD (2018) Rubisco is not really so bad. Plant Cell Environ 41:705–716

Beardall J, Raven JA (2018) Structural and biochemical features of carbon acquisition in algae. In: Larkum AWD, Grossman AR, Raven JA (eds) Photosynthesis in Algae. Springer, Berlin, in press

Beardall J, Quigg A, Raven JA (2003). Oxygen consumption: photorespiration and chlororespiration. In: Larkum, AWD, Douglas SE, Raven JA (eds) Photosynthesis in Algae. Springer, Berlin. pp 157–181. Volume 14 of Advances in photosynthesis and respiration. Kluwer, Dordrecht

Beardall J, Ihnken S, Quigg A (2009) Gross and primary production: closing the gap between concepts and measurements. Aquat Microb Ecol 56:113–122

Beer S, Larsson C, Poryan O, Axelsson L (2000) Photosynthetic rates of *Ulva* (Chlorophyta)_ measured by pulse amplitude modulated (PAM) fluorometry. Eur J Phycol 35:69–74

Bennoun P (1982) Evidence for a respiratory chain in the chloroplast. Proc Natl Acad Sci USA 79:4352–4356

Berntroitner M, Zamocky M, Furtmüller PG, Peschek GA, Obinger C (2009) Occurrence, phyologeny, structure, and function of catalases and peroxidases in cyanobacteria. J Exp Bot 60:423–440

Bersanini L, Battchikova N, Jokel M, Rehman A, Vass I, Allahverdiyeva Y, Aro E-M (2014) Flavodiiron protein Flv2/Flv4-related photoprotective mechanism dissipates excitation pressure of PSII in cooperation with phycobilisomes in cyanobacteria. Plant Physiol 164:805–818

Bisswange H (1981) Substrate specificity of the pyruvate dehydrogenase complex from *Escherichia coli*. J Biol Chem 256:815–822

Boatman TG, Davey PA, Lawson T, Geider BJ (2018) The physiological cost of diazotrophy for *Trichodesmium erythreanum* IMS101. PLoS One 13:e0195638

Brading P, Warner ME, Davey P, Smith DJ, Achterberg P, Suggett J (2011) Differential effects of ocean acidification on growth and photosynthesis among phylotypes of *Symbiodinium* (Dinophyceae). Limnol Oceanogr 56:927–938

Brechignac F, Andre M (1984) Oxygen uptake and photosynthesis of the red macroalga, *Chondrus crispus*, in seawater: effects of light and CO_2 concentration. Plant Physiol 75:914–923

Brechignac F, Lucas WJ (1987) Photorespiration and internal CO_2 accumulation in *Chara corallina* as inferred from the influence of DIC and O_2 on photosynthesis. Plant Physiol 83:163–169

Bunt J (1965) Measurements of photosynthesis and respiration in a marine diatom with the mass spectrometer and with carbon-14. Nature 75:293–300

Bunt JS, Heeb MA (1971) Consumption of O_2 in the light by *Chlorella pyrenoidosa* and *Chlamydomonas reinhardii*. Biochim Biophys Acta Bioenerg 226:354–359

Bunt JS, Owens OH, Hoch G (1966) Exploratory studies on the physiology and ecology of a psychrophilic marine diatom. J Phycol 2:96–100

Cardol P, Gloire G, Havaux M, Remacle C, Matagne R, Frank F (2003) Photosynthesis and state transitions in mitochondrial mutants of *Chlamydomonas reinhardtii* affected in respiration. Plant Physiol 133:2010–2020

Cardol P, Bailleul B, Rappaport F, Derelle E, Béal D, Breyton C, Bailey S, Wollman FA, Grossman A, Moreau H, Finazzi G (2008) An original adap-

tation of photosynthesis in the marine green alga *Ostreococcus*. Proc Natl Acad Sci U S A 105:7881–7788

Cardol P, Forti G, Finazzi G (2011) Regulation of electron transport in microalgae. Biochim Biophys Acta Bioenerg 1807:912–918

Carr K, Björk M (2003) A methodological comparison of photosynthetic oxygen evolution and estimated electron transport rate in tropical *Ulva* (Chlorophyceae) species under different light and inorganic carbon conditions. J Phycol 39:1125–1151

Chaux F, Burlacot A, Mekhalfi M, Auroy P, Blangy S, Richaud P, Peltier G (2017) Flavodiiron proteins promote fast and transient O_2 photoreduction in *Chlamydomonas*. Plant Physiol 167:472–480

Claquin P, Kromkamp JC, Martin-Jezequel V (2004) Relationship between photosynthetic metabolism and cell cycle of the marine alga *Cylindrotheca fusiformis* (Bacillariophyceae). Eur J Phycol 39:33–41

Colombo-Pallotta MF, García-Merndoza E, Ladah LB (2006) Photosynthetic performance, light absorption, and pigment composition of *Macrocystis pyrifera* (Laminariales. Phaeophyceae) blades from different depths. J Phycol 42:1225–1234

Cruz S, Goss R, Wilhelm C, Leegood R, Horton R, Jakob T (2011) Impact of chlorespiration on non-photochemical quenching of chlorophyll fluorescence and the regulation of the diadinoxanthin cycle in *Thalassiosira pseudonana*. J Exp Bot 62:509–519

Curien G, Flori S, Villova V, Magneschi L, Giustini C, Forti G, Matringe M, Petroutsos D, Kuintz M, Finazzi G (2016) The water to water cycles in microalgae. Plant Cell Physiol 57:1354–1363

Dang K-V, Plet J, Tolleter D, Jokel M, Cuiné S, Carrier P, Auray P, Richaud P, Johnson X, Alric J, Allahverdiyera Y, Peltier G (2014) Combined increase in mitochondrial cooperation and oxygen photoreduction compensate for deficiency in cyclic electron flow in *Chlamydomonas reinhardtii*. Plant Cell 26:3036–3050

Davis A, Abbriano R, Smith SR, Hildbrand M (2017) Clarification of photorespiratory processes and the role of malic enzyme in diatoms. Protist 168:134–153

Driever SM, Baker NR (2011) The water-water cycle in leaves is not a major alternative electron sink for dissipation of excess excitation energy when CO_2 assimilation is restricted. Plant Cell Environ 34:837–846

Duarte P, Ramos M, Galado G, Jesus B (2013) *Laminaria hyperborea* photosynthesis-irradiance relationships measured by oxygen production and pule-amplitude-modulated chlorophyll fluorometry. Aquat Biol 19:29–44

Eisenhut M, Ruth W, Haimovich M, Bauew H, Kaplan A, Hagemann M (2008) The photorespiratory glycolate metabolism is essential for cyanobacteria and may have been conveyed endosymbiotically to plants. Proc Natl Acad Sci USA 105:17199–17204

Eisenhut M, Brautigam A, Timm S, Florian A, Tohge T, Fernie AR, Bauwe H, Weber APM (2017) Photorespiration is crucial for dynamic response of photosynthetic metabolism and stomatal movement to altered CO_2 availability. Mol Plant 10:47–61

Ermakova M, Battchikova N, Richaud P, Leino H, Kosourov S, Isojärvi J, Peltier G, Flores E, Cournac L, Allahverdiyeva Y, Aro E-M (2014) Heterocyst-specific flavodiiron protein Flv3B enables oxic diazotrophic growth of the filamentous *Anabaena* sp. PCC 7120. Proc Natl Acad Sci USA 111:11205–11210

Ermakova M, Huokko T, Richaud P, Bersanini L, Howe CJ, Lea-Smith DJ, Peltier G, Allahverdiyeva Y (2016) Distinguishing the roles of thylakoid respiratory terminal oxidases in the cyanobacterium *Synechocystis* sp. PCC 6803. Plant Physiol 171:1307–1319

Feikema WO, Marsvölgyi MA, Lavud J, van Gorkum HJ (2006) Cyclic electron transfer in photosystem II in the marine diatom *Phaeodactylum tricornutum*. Biochim Biophys Acta 1757:829–834

Figueroa FL, Conde-Alvarez R, Gómez I (2003) Relation between electron transport rates determined pulse amplitude modulated fluorescence and oxygen evolution in macroalgae under different light conditions. Photosynth Res 75:259–275

Fischer BB, Dayer R, Schwarzenberg Y, Lemaine SD, Behra R, Liedtke A, Eggen RIL (2009) Function and regulation of the glutathione peroxidase homologous gene GPXH/GPXS in *Chlamydomonas reinhardtii*. Plant Mol Biol 71:569–583

Forti G, Ehrenheim AM (1993) The role of ascorbic acid in photosynthetic electron transport. Biochim Biophys Acta 1183:408–412

Forti G, Elli G (1995) The function of ascorbic acid in photosynthetic phosphorylation. Plant Physiol 109:1207–1211

Foyer CH, Noctor G (2011) Ascorbate and glutathions: the heart of the redox hub. Plant Physiol 155:2–18

Foyer CH, Lelandais M, Edwards EA, Mullineaux, PM (1991) The role of ascorbate in plants, interactions with photosynthesis and regulatory significance. In: Pell E, Steffen K (eds) Active oxygen/oxidative stress and plant metabolism. Current topics in plant physiology, vol 6. American Society of Plant Physiologists, pp 131–144

Franklin LA, Badger MR (2001) A comparison of photosynthetic electron transport rates in macroal-

gae measured by pulse amplitude modulated chlorophyll fluorescence and mass spectrometry. J Phycol 37:756–767

Frazão C, Silva G, Gomes CM, Matia P, Coelho R, Sicker L, Macedo S, Liu MY, Oliviera S, Teixeira M, Xavier AV, Rodrigues-Posada C, Carrondo MA, Le Gall J (2000) Structure of a dioxygen reduction enzyme from *Desulfovibrio gigas*. Nat Struct Mol Biol 7:1041–1045

Fujiki T, Suzue T, Kimoto H, Saino T (2007) Photosynthetic electron transport in *Dunaliella tertiolecta* (Chlorophyceae) measured by fast repetition rate fluorometry: relation of carbon assimilation. J Plankton Res 29:199–208

Genty B, Briantais J-M, Baker NR (1989) The relationship between yield of photosynthetic electron transport and quenching of fluorescence. Biochim Biophys Acta Bioenerg 990:87–92

Gest N, Gautier H, Stevens R (2013) Ascorbate as seen through plant evolution: the rise of a successful molecule? J Exp Bot 64:33–53

Gilbert M, Domin A, Becker A, Wilhelm C (2000) Estimation of primary productivity by chlorophyll *a in vivo* fluorescence in freshwater phytoplankton. Photosynthetica 38:111–126

Glidewell SM, Raven JA (1975) Measurements of simultaneous oxygen uptake and evolution in *Hydrodictyon africanum*. J Exp Bot 26:479–488

Gloag RS, Ritchie RJ, Chen M, Larkum AWD, Quinnell RG (2007) Chromatic photoacclimation, photosynthetic electron transport and oxygen evolution in the chlorophyll *d*-containing oxyphotobacterium *Acaryochloris marina*. Biochim Biophys Acta 1767:127–135

Gordillo FJL, Figueroa FL, Niell FX (2003) Photon- and carbon-use efficiency in *Ulva rigida* at different CO_2 and N levels. Planta 218:318–322

Griffiths H, Meyer MT, Rickaby REM (2017) Overcoming adversity through diversity: aquatic carbon concentrating mechanisms. J Exp Bot 68:2689–2695

Guo H, Rubinstein JL (2018) Cryo-EM of ATP synthases. Curr Opin Struct Biol 52:71–79

Hagemann M, Kern R, Maurino VG, Hanson DT, Weber APM, Sage RF, Bauwe M (2016) Evolution of photorespiration from cyanobacteria to land plants, considering protein phylogenies and acquisition of carbon concentrating mechanisms. J Exp Bot 67:2963–2976

Hancke K, Dais-Gaard T, Sejt MK, Markager S, Glud RN (2015) Phytoplankton productivity in an Arctic fjord (West Greenland): estimating electron requirements for carbon fixation and oxygen production. PLoS One 10:e0133275

Helman T, Tchernov D, Reinhold L, Shibata M, Ogawa T, Schwarz R, Ohad I, Kaplan A (2003) Genes encoding A-type flavoproteins are essential from photoreduction of O_2 in cyanobacteria. Curr Biol 13:230–235

Hoch G, Owens O van H, Kok B (1963) Photosynthesis and respiration. Arch Biochem Biophys 101:171–181

Horton P, Ruban AV, Wentworth M (2000) Allosteric regulation of the light-harvesting system of photosystem II. Philos Trans R Soc B: Biol Sci 355(1402):1361–1370

Houille-Vernes I, Rappaport F, Wollman FA, Alric J, Johnson X (2011) Plastid terminal oxidase 2 (PTOX2) is the major oxidase involved in chlororespiration in *Chlamydomonas*. Proc Nat Acad Sci USA 108:20820–20925

Huertas I, Colman B, Espie GS (2002a) Inorganic carbon acquisition and its energization in eustigmatophyte algae. Funct Plant Biol 29:271–272

Huertas IE, Colman B, Espie GS (2002b) Mitochondrial-driven bicarbonate transport supports photosynthesis in a marine microalga. Plant Physiol 130:284–291

Hughes DJ, Cambell DA, Doblin MA, Kromkamp JC, Lawrenz E, Moore CM, Oxboruough K, Prášil O, Ralph PJ, Alvarez MF, Suggett DJ (2018) Roadmaps and detours: active chlorophyll-*a* assessments of primary productivity across marine and freshwater systems. Environ Sci Technol 52:12039–12054

Illik P, Pavlovic A, Kouril R, Alboresi A, Morisinotto T, Allahverdiyeva Y, Aro E-M, Yamamoto H, Shikanai T (2017) Alternative electron transport mediated by flavodiiron proteins is operational organisms from cyanobacteria up to gymnosperms. New Phytol 214:967–972

Jokel M, Kosourov S, Battchikova N, Tsygasnkov AA, Aro E-M, Allahverdiyeva Y (2015) *Chlamydomonas* flavodiron proteins facilitate acclimation to anoxia during sulfur deprivation. Plant Cell Physiol 56:1598–1607

Kana TM (1992) Relations between photosynthetic oxygen cycling and carbon assimilation in *Synechococcus* WH7805 (Cyanophyta). J Phycol 28:304–308

Kana TM (1993) Rapid oxygen cycling in *Trichodesmium thiebaultii*. Limnol Oceanogr 38:18–24

Kern R, Eisenhut M, Bauwe H, Weber APM, Hagemann M (2013) Does the *Cyanophora paradoxa* genome revise our view on the evolution of photorespiratory enzymes? Plant Biol 15:759–786

Kiefer DW, Spanswick RM (1978) Activity of the electrogenic pump in *Chara corallina* as inferred from measurements of the membrane potential, conduc-

tance and potassium permeability. Plant Physiol 62:653–661

Kolber ZS, Prasil O, Falkowski PG (1998) Measurements of variable chlorophyll fluorescence using fast repetition rate techniques: defining methodology and experimental protocols. Biochim Biophys Acta 1367(1–3):88–106

Kramer DM, Evans JR (2011) The importance of energy balance in improving photosynthetic productivity. Plant Physiol 155:70–78

Kromkamp JC, Dijkma NA, Peene J, Simis SGH, Gons HJ (2008) Estimating phytoplankton primary productivity in Lake Ijsselmeer (The Netherlands) using variable fluorescence (PAM-FRRF) and C-uptake techniques. Eur J Phycol 43:327–344

Krueger T, Becker S, Pantosch S, Dove S, Hove-Guldberg O, Leggat W, Fisher PL, Davy SK (2014) Antioxidant plasticity and thermal sensitivity in four types of *Symbiodinium* sp. J Phycol 50:1035–1047

Kuntz M (2004) Plastid terminal oxidase and its biological significance. Planta 218:686–689

Larkum AWD, Szabó M, Fizpatrick D, Raven JA (2017) Cyclic electron flow in cyanobacteria and algae. In: Barber J, Ruban AV (eds) Photosynthesis and bioenergetics. World Scientific, Singapore, pp 305–343

Laughlin TG, Bayne AN, Trempe J-F, Savage DF, Davies KM (2019) Structure of the complex I-like molecule NDH of oxygenic photosynthesis. Nature 566:411–414

Lea-Smith DJ, Bomelli P, Vasuderan R, Howe CJ (2016) Photosynthetic, respiratory and extracellular electron transport pathways in cyanobacteria. Biochim Biophys Acta 1857:247–255

Lefebvre S, Mouget J-L, Loret P, Rosa P, Tremblin G (2007) Comparison between fluorimetry and oximetry techniques to measure photosynthesis in the diatom *Skeletonema costatum* cultivated under simulated seasonal conditions. J Photochem Photobiol 86:131–139

Levin RA, Beltran VH, Hill R, Kjelleberg S, McDougall D, Steinberg PD, van Oppen MJH (2016) Sex, scavengers, and chaperones: transcriptome secrets of divergent *Symbiodinium* thermal tolerances. Mol Biol Evol 33:2201–2215

Lewitus AJ, Kana TM (1995) Light respiration in six estuarine phytoplankton species: contrasts under photoautotrophic and mixotrophic growth conditions. J Phycol 31:754–761

Li Q, Canvin DT (1997) Oxygen photoreductions and its effect on CO_2 accumulation and assimilation in air-grown cells of *Synechococcus* UTEX 625. Plant Physiol 25:274–285

Li Q, Yao Z-J, Mi H (2016) Alleviation of Photoinhibition by co-ordination of chlororespiration and cyclic electron flow mediated by NDH under heat stressed condition in tobacco. Front Plant Sci 7:285. https://doi.org/10.3389/fpls.2016.00285

Longstaff BJ, Klidea T, Runcie JW, Cheshire A, Dennison WC, Hurd C, Kana T, Raven JA, Larkum AWD (2002) An *in stu* study of photosynthetic oxygen exchange and electron transport rate in the marine macroalga *Ulva lactuca* (Chlorophyta). Photosynth Res 74:281–293

Margis R, Dunand C, Teixeira FK, Margis-Pinheiro M (2009) Glutathione peroxidase family – an evolutionary overview. FEBS J 275:3959–3970

Martin JH, Fitzwater SE (1988) Iron deficiency limits phytoplankton growth in the north-eastern Pacific subarctic. Nature 331:341–343

Maruta T, Sawa Y, Shigeoka S, Ishikawa T (2016) Diversity and evolution of ascorbate peroxidase functions in chloroplasts: more than just a classical antioxidant enzyme? Plant Cell Physiol 57:1377–1386

Masojídek J, Grobellaar JV, Pechar L, Kobliźek M (2001) Photosystem II electron transport rates and oxygen production in natural waterblooms of freshwater cyanobacteria during a diel cycle. J Plankton Res 23:57–66

McDonald A, Vanleberghe GC (2006) Origins, evolutionary history and distribution of alternative oxidase and plastoquinol terminal oxidase. Comp Biochem Physiol Part D 1:357–364

McDonald A, Amiradeghi A, Vanleberghe GC (2003) Prokaryotic orhologues of mitochondrial oxidase and plastid terminal oxidase. Plant Mol Biol 53:865–876

McDonald AE, Ivanov AG, Bode R, Maxwell DP, Rodermel SR, Huner NPA (2011) Flexibility in photosynthetic electron transport. The physiological role of plastoquinol terminal oxidase (PTOX). Biochim Biophys Acta 1807:954–967

McKew BA, Davey P, Finch SJ, Hopkins J, Lefebvre SC, Metodiev MV, Oxborough K, Raines CA, Lawson T, Geider RJ (2013) The trade-off between light-harvesting and photoprotective functions of fucoxanthin-chlorophyll proteins dominates light acclimation in *Emiliania huxleyi* (clone CCMP 1516). New Phytol 200:74–85

Miller AG, Espie GS, Canvin DT (1988) Active transport of inorganic carbon increases the rate of O_2 photoreduction by the cyanobacterium *Synechococcus* UTEX 625. Plant Physiol 88:6–9

Misumi M, Sonoike K (2017) Characterization of the influence of chlororespiration on the regulation of photosynthesis in the glaucophyte *Cyanophora paradoxa*. Sci Rep 7:46100

Miyake C, Asada K (2003) The Water-Water cycle in Algae. In: Larkum AWD, Douglas SE, Raven JA (eds) Photosynthesis in Algae, pp 183–204. Volume

14 of Advances in photosynthesis and respiration. Kluwer, Dordrecht

Miyake C, Michihata F, Asada K (1991) Scavenging of hydrogen peroxide in prokaryotic and eukaryotic algae: acquisition of ascorbate peroxidase during the evolution of cyanobacteria. Plant Cell Physiol 32:33–43

Morelle J, Claquin P (2018) Electron requirement for carbon incorporation along a diel light cycle in three marine diatom species. Photosynth Res 137:201–214

Morelle J, Shapira M, Orvain F, Riou P, Lopez PJ, Pierre-Duplessix O, Rabiller E, Maheux F, Simon B, Claquin P (2018) Annual phytoplankton primary production estimation in a temperate estuary by coupling PAM and carbon incorporation methods. Estuar Coasts 41:1337–1355

Mullineaux PM, Baker NR (2010) Oxidative stress: signalling for acclimation or cell death? Plant Physiol 154:521–525

Napoléon C, Claquin P (2012) Multi-parametric relationships between PAM measurements and carbon incorporation, an *in situ* approach. PLoS One 7:e40284

Nawrocki WJ, Touraine NJ, Taly, Rappaport E, Wollman F-A (2015) The plastid terminal oxidase: its elusive function points to multiple contributions to plastid physiology. Annu Rev Plant Biol 66:49–74

Nielsen HD, Nielsen SL (2008) Evolution of imaging and conventional PAM as a measure of photosynthesis in thin- and thick-leaved marine macroalgae. Aquat Biol 3:121–131

Oroszi S, Jakob T, Wilhelm C, Harms H, Maskow T (2011) Photosynthetic energy conversion in the diatom *Phaeodactylum tricornutum* measured by calorimetry, oxygen evolution and pulse-amplitude fluorescence. J Therm Anal Calorim 104:225–231

Peltier G, Tolleter D, Billon E, Cournac L (2010) Auxilliary electron transport pathways in chloroplasts of microalgae. Photosynth Res 106:19–31

Perkins RG, Oxborough K, Hanlon ARM, Underwood GJC, Baker NR (2002) Can chorophyll fluorescence be used to estimate the rate of photosynthetic electron transport with microphytobenthic biofilms. Mar Ecol Prog Ser 228:47–56

Petersen J, Förster K, Turina P, Gräber P (2012) Comparison of the H^+/ATP rastios from the H^+-ATP synthases from yeast and from chloroplast. Proc Natl Acad Sci USA 109:11150–11155

Pogoryelov D, Reichen C, Klyszejko AL, Brunisholz R, Muller DJ, Dimroth P, Meier T (2007) The oligomeric state of c rings from cyanobacterial F-ATP synthases varies from 13 to 15. J Bacteriol 189:5895–5902

Prasil O, Kolber Z, ,Berry JA, Falkowski G (1996) Cyclic electron flow around PSII in vivo. Photosynth Res 48: 395–410

Raven JA (1976) The quantitative role of 'dark' respiratory processes in heterotrophic and photolithotrophic growth. Ann Bot 40:587–602

Raven JA (2013) RNA function and phosphorus use by photosynthetic organisms. Front Plant Sci 4:536

Raven JA and Beardal (2005) Respiration in Aquatic Photolithotrophs. In: del Giorgio PA and Williams PJleB (eds) Respiration in Aquatic Ecosystems, pp. 36–46. Oxford University Press

Raven JA, Beardall J (2017) Consequences of the genotypic loss of Complex I in dinoflagellates and of phenotypic loss of Complex I from other photosynthetic organisms. J Exp Bot 68:2683–2692

Raven JA, Kubler JE, Beardall J (2000) Put out the light, and then put out the light. J Mar Biol Assoc UK 80:1–25

Raven JA, Beardall J, Giordano M (2014) Energy costs of carbon dioxide concentrating mechanisms in aquatic organisms. Photosynth Res 121:111–124

Raven JA, Beardall J, Sánchez-Baracaldo P (2017) The possible evolution, and future, of CO_2-concentrating mechanisms. J Exp Bot 68:3701–3716

Rech M, Mouget J-L, Tremblin G (2003) Modification of the Hansatech FMS fluorometer to facilitate measurements with microalgal cultures. Aquat Bot 77:71–80

Rizhsky L, Liang H, Mittler R (2003) The water-water cycle is essential for chloroplast protection. J Biol Chem 278:38921–38925

Roberty S, Bailleul B, Borne N, Franck F, Cardol P (2014) Photosystem I Mehler reaction is the main alternative photosynthetic electron pathway in *Symbiodinium* sp., symbiotic dinoflagellates of cnidarians. New Phytol 204:81–91

Rochaix J-D (2011) Regulation of photosynthetic electron transport. Biochim Biophys Acta 1807:247–255

Schreiber U (1994) Pulse-amplitude-modulation (PAM) Fluorometry and saturation pulse method: an overview. In: Papageorgiou GC, Govindjee G (eds) Chlorophyll a fluorescence. Dordrecht, Springer

Schuback N, Schellenberg C, Duckham C, Maldonado MT, Tortell PD (2015) Interacting effects of light and iron availability on the coupling of photosynthetic electron transport and CO_2-assimilation of marine phytoplankton. PLoS One 10:e0133235

Schuback N, Flecken M, Maldonado MT, Tortell PD (2016) Diurnal variation in the coupling of photosynthetic electron transport and carbon fixation on iron-limited phytoplankton in the NE subarctic Pacific. Biogeosciences 13:1019–1035

Shikanai T, Yamamoto H (2017) Contribution of cyclic and pseudo-cyclic electron transport to the formation of proton motive force in chloroplasts. Mol Plant 10:20–29

Shimakawa G, Shaku K, Nishi A, Hayashi R, Yamamoto H, Sakamoto K, Makino A, Miyake C (2015) FLAVODIIRON2 and FLAVODIRON4 proteins mediate an oxygen-dependent alternative electron flow in *Synechocystis* sp. PCC 6803 under CO_2-limiting conditions. Plant Physiol 167:472–480

Shimakawa G, Matsuda Y, Nakajima K, Tamoi M, Shigeoka S, Miyake C (2017a) Diverse strategies of O_2 usage for preventing photo-oxidative damage under CO_2 limitation during algal photosynthesis. Sci Rep 7:41022

Shimakawa G, Ishizaki K, Tsukamoto S, Tanaka M, Sejima T, Miyake C (2017b) The liverwort, *Marchantia*, drives alternative electron flow using a flavodiiron protein to protect PSI. Plant Physiol 173:1636–1647

Shinopoulos KE, Brudvig GW (2012) Cytochrome b_{559} and cyclic electron transfer within photosystem II. Biochim Biophys Acta 1817:66–75

Smith FA, Raven JA (1974) Energy dependent processes in *Chara coralina*: absence of light stimulation when only photosystem one is operative. New Phytol 73:1–12

Sobotka R, Esson HJ, Koník P, Trsková E, Moravcová L, Horák A, Dufková P, Oborník M (2017) Extensive gain and loss of photosystem I subunits chromerid algae, photosynthetic relatives of apicomplexans. Sci Rep 7:13214. https://doi.org/10.1038/s41598-017-13575-x

Strand DD, Fisher N, Kramer DM (2017) The higher plant plastid NAD(P)H dehydrogenase-like complex is a high efficiency proton pump that increases ATP production by cyclic electron flow. J Biol Chem 292:11850–11860

Streb P, Josse EM, Gallouet E, Baptist F, Kuntz M, Cornic G (2005) Evidence for alternative electron sinks to photosynthetic carbon assimilation in the high mountain plant species *Ranunculus glacialis*. Plant Cell Environ 28:1123–1135

Strzeprek R, Harrison PJ (2004) Photosynthetic architecture differs in coastal and oceanic diatoms. Nature 431:689–692

Suggett DJ, Oxborough K, Baker NR, MacIntyre HL, Kana TM, Geider RJ (2003) Fast repetition rate and pulse amplitude modulation chlorophyll *a* fluorescence measurements for assessment of photosynthetic electron transport for assessment of photosynthetic electron transport in marine phytoplankton. Eur J Phycol 38:371–384

Suggett DJ, MacIntyre H, Geider RJ (2004) Evaluation of biophysical and optical determination of light absorption by photosystem II. Limnol Oceanogr Methods 2:316–332

Suggett DJ, Warner ME, Smith DJ, Davey P, Hennige S, Baker NR (2008) Photosynthesis and production of hydrogen peroxide by *Symbiodinium* (Pyrrhophyta) phylotypes with different thermal tolerances. J Phycol 44:948–956

Suggett DJ, MacIntyre HL, Kana TM, Geider RJ (2009) Comparing electron transport with gas exchange: parameterising exchange rates between alternative currencies for eukaryotic phytoplankton. Aquat Microb Ecol 56:147–162

Sukenik A, Tchernov D, Kaplan A, Huertas E, Lubian A (1997) Uptake, efflux and photosynthetic utilization of inorganic carbon by the marine eustigmatophyte *Nannochloropsis* sp. 1. J Phycol 33:969–974

Sültemeyer D, Klug K, Fock HP (1986) Effect of photon fluence on oxygen evolution and uptake by *Chlamydomonas reinhardtii* suspensions grown in ambient and CO_2-enriched air. Plant Physiol 81:372–375

Sültemeyer D, Biehler K, Fock HP (1993) Evidence for the contribution of pseudocyclic photophosphorylation to the energy requirement of the mechanism for concentrating inorganic carbon in *Chlamydomonas reinhardtii*. Planta 189:235–242

Takahashi S, Badger MR (2011) Photoprotection in plants: a new light on photosystem II damage. Trends Plant Sci 16:53–60

Tchernov D, Nassidim M, Luz B, Sukenik A, Reinhold L, Kaplan A (1997) Sustained net CO_2 evolution during photosynthesis by marine microorganisms. Curr Biol 7:723–728

Torres MA, Ritchie RJ, Lilley RMC, Grillet C, Larkum AWD (2014) Measurements of photosynthetic efficiency in two diatoms. NZ J Bot 52:6–27

Turina P, Petersen J, Gräber P (2016) Thermodynamics of proton transport coupled ATP synthesis. Biochim Biophys Acta 1857:653–664

van Lis R, Mendoza-Hernández G, Groth G, Atteia A (2007) New insights into the unique structure of the F_OF_1-ATP synthase from the chlamydomonad algae *Polytomella* sp. and *Chlamydomonas reinhardtii*. Plant Physiol 144:1190–1199

Vicente JB, Gomes CM, Wasserfallen A, Teixera M (2002) Multiple fusion in an A-type flavoprotein from the cyanobacterium *Synechocystis* condenses a multiple pathway in a single polypeptide chain. Biochem Biophys Res Commun 58:336–340

Waring J, Klenell M, Bechtold U, Underwood GJC, Baker NR (2010) Light-induced responses of oxygen photoreduction, reactive oxygen species pro-

duction and scavenging in two diatom species. J Phycol 46:1206–1217

Weger HG, Herzig R, Falkowski PG, Turpin DH (1989) Respiratory losses in the light in a marine diatom: measurements by short-term mass spectrometry. Limnol Oceanogr 34:1153–1161

Wheeler G, Ishikawa T, Pornsaksit V, Smirnoff N (2015) Evolution of alternative biosynthetic pathways for Viamin C during plastid acquisition of photosynthetic organisms. Life 4:e06369

Wu T-Y, Dai C-F, Fan T-Y (2006) Effects of temperature on the oxygen- and Fluorescence-based estimates of photosynthesis parameters in the reef coral *Styllophora pistillata*. J Fish Soc Taiwan 33:253–263

Xue X, Gauthier DA, Turpin DH, Weger HG (1996) Interaction between photosynthesis and respiration in the green alga *Chlamydomonas reinhardtii*. Plant Physiol 112:1005–1014

Yu Q, Feilke K, Krieger-Liszkay A, Beyer P (2014) Functional and molecular characterization of plastid terminal oxidase from rice (*Oryza sativa*). Biochim Biophys Acta 1837:1284–1292

Zehr JP, Kudela PM (2009) Photosynthesis in the open ocean. Science 326:945–946

Zhang P, Allahverdiyeva Y, Eisenhut M, Aro E-M (2009) Flavodiiron proteins in oxygenic photosynthetic organisms: photoprotection of photosystem II by Flv2 and Flv4 in *Synechocystis* sp. PCC 6803. PLoS One 4:e5331

Chapter 9

The Algal Pyrenoid

Moritz T. Meyer*
Department of Plant Sciences, University of Cambridge, Cambridge, UK

Department of Molecular Biology, Princeton University, Princeton, NJ, USA

and

Myriam M. M. Goudet and Howard Griffiths
Department of Plant Sciences, University of Cambridge, Cambridge, UK

I. Introduction

A. *A Pyrenoid Timeline – From Microscopic Curiosity to a Key Factor in the Earth's Carbon Cycle*

The pyrenoid is an evolutionary adaptation that enables algae to fix inorganic carbon more efficiently in CO_2-limited environments. The genesis of this contemporary definition is nearly two and half centuries old. One of the earliest records of pyrenoids are un-annotated puncta in a drawing of *Conferva jugalis* (now *Spirogyra*) in Flora Danica (Müller 1782). The word pyrenoid, from the Greek *πυρηυ* (*pyren*, kernel), was coined by Schmitz a century later (1882) in a

*Author for correspondence, e-mail: mtmeyer@princeton.edu; mmmg2@cam.ac.uk

A. W. D. Larkum et al. (eds.), *Photosynthesis in Algae: Biochemical and Physiological Mechanisms*, Advances in Photosynthesis and Respiration 45, https://doi.org/10.1007/978-3-030-33397-3_9

remarkable monograph on algal chloroplasts. Schmitz observed that pyrenoids are chloroplast inclusions, that divide as chloroplasts and cells divide. He also diagnosed pyrenoid presence/absence through numerous algal lineages and astutely recorded that carbohydrate deposits around pyrenoids are highly variable, both across species and as plastic response to changes in growth conditions. Most of his observations have withstood the test of time, although the speculation that pyrenoids are akin to nucleoli was later proven unfounded (Martin and Kowallik 1999). It was the definition as a site of starch synthesis (although not all algae synthesise starch-defining α-1,4-glycosidic bonds), however, that came to dominate the literature until the early 1970s and survives to these days in some textbooks and refereed papers.

A major paradigm shift occurred after the successful isolation of pyrenoids from a green alga and the discovery that RuBisCO (then called Fraction 1) accounted for an estimated 90% of pyrenoid proteins (Holdsworth 1971). The reproducibility of this result by researchers working on other green algae as well as a brown alga, and more recent detailed work on the model Chlorophyta *Chlamydomonas reinhardtii*, has demonstrated that for those algae with a pyrenoid, the micro-compartment is the site of inorganic carbon assimilation (reviewed in Meyer and Griffiths 2013). The functional analogues in prokaryotes, carboxysomes, were isolated 2 years later (Shively et al. 1973) and some authors briefly entertained the speculation of 'calvinosomes', organelles that supposedly contained the entire CO_2- fixing Calvin-Benson-Bassham (CBB) Cycle (Beudeker and Kuenen 1981). However, contemporary data points towards RuBisCO as being the only enzyme of the CBB cycle active inside these micro-compartments, raising intriguing questions about the channelling of substrates and products (Küken et al. 2018). The physiological function of pyrenoids (and carboxysomes) was established with the clear definition in 1980 of aquatic inorganic Carbon Concentrating Mechanisms (CCMs). CCMs are discussed in detail elsewhere in this book (Chaps. 6 & 7) and a history of the CCM discovery was chronicled by Kaplan (2017). It is important to stress that the correlation of CCM with pyrenoid is not exact (Raven et al. 2017). Not all eukaryotic algae operating a CCM require a pyrenoid (*e.g.* pyrenoid-less picoplanktonic *Nannochloropsis oceanica*; Gee and Niyogi 2017), but a pyrenoid is generally taken as a marker for CCM presence in freshwater and marine algae, although further investigations are needed. Comparative studies of lineages with and without a pyrenoid support that pyrenoids enhance CO_2-assimilation efficacy (Máguas et al. 1993; Palmqvist 1993; Morita et al. 1998). The intimate association of the pyrenoid and the eukaryotic CCM have stimulated some debate regarding the evolutionary timescale for emergence of pyrenoids during algal phylogeny (Badger and Price 2003; Meyer and Griffiths 2013; Griffiths et al. 2017). Aquatic photosynthetic organisms developed a CCM in response to environmental constraints associated with the aquatic milieu and the inherently low carboxylation efficiency of RuBisCO (reviewed in Meyer and Griffiths 2013). Since the Great Oxygenation Event (2.4 billion years ago), oxygen started to compete with CO_2 for the active sites of the primary carboxylase (Blankenship and Hartman 1998), reducing the efficiency of the photosynthesis as toxic oxygenase products needed to be recycled or secreted (Griffiths et al. 2017). In addition, bicarbonate rather than free CO_2, which is needed by RuBisCO for catalysis, is typically the dominant form of inorganic carbon in the oceans (Falkowski and Raven 2007). To put things in perspective, the concentration of CO_2 is about 2200 times lower in water than air (less than 0.2 ppm *vs* 410 ppm) and diffusion is 8000 times slower, with substantial limitations imposed by surface boundary layers (Raven et al. 1985; Raven and Richardson 1985; Borges and Frankignoulle 2002; Yamano et al. 2015). Perhaps because of these limitations, pyrenoids and associated

CCMs have proved to be highly widespread adaptations. A new generation of researchers is now seeking to unravel the molecular details of the pyrenoid, foremostly in the model green alga *Chlamydomonas reinhardtii*, but also in ecologically more important species, like diatoms.

B. Pyrenoid Prevalence

There are probably over 70,000 different species of algae (Guiry 2012), classified into six much-debated clades based on chloroplast ancestry (see Chap. 2). For the purpose of this review, we follow Dorrell and Howe (2012) and interchangeably use Latin and vernacular names when still in common use. (1) Archaeplastids (comprising: red algae-Rhodophyta; green algae-Chlorophyta, Prasinophyta + Charophyta; and the Glaucophyta), have a chloroplast inherited from the primary endosymbiosis of an ancestral cyanobacterium; (2) Excavates (comprising Euglenids) and (3) Rhizaria (comprising Chlorarachniophyta), both clades with a secondary green algal chloroplast); (4) Stramenopiles (comprising Xanthophyta/yellow-green algae, Chrysophyta/golden algae, Phaeophyta/brown algae, and Bacilliarophyta/diatoms), all possessing a secondary red algal chloroplast; (5) the CCTH clade (comprising Cryptophyta and Haptophyta), also with a secondary red algal chloroplast; and finally (6) Alveolates, an evolutionary complex group with secondary or tertiary red or green chloroplasts (comprising Dinophyta/dinoflagellates) (refer to Chap. 2). The relatively recent mitochondrial and plastid sequencing of the alveolates (Chromera and Vitrella: coral endosymbiotic algae) provide yet more insights into algal diversity (Oborník and Lukeš 2015). We subsequently explore pyrenoid distribution and diversity in form and function for many of these groups below. Readers seeking to diagnose their species of interest will likely find data in phycological textbooks (Lee 2018; Hoek et al. 1996), ultrastructural monographs (e.g. green algae, Pickett-Heaps 1975), the AlgaeBase digital repository (Guiry and Guiry 2018) or specialist journals (*e.g.* Journal of Phycology, European Journal of Phycology, Phycologia, Protist, Algae, Nova Hedwigia, Cryptogamie/Algologie, etc).

Estimation of what fraction of the global net primary production is mediated by pyrenoid-possessing algae requires knowledge of species abundance. The 2009–2012 survey by the Tara Expedition is the most recent example of oceanographic surveys (De Vargas et al. 2015) and there are now hardly any bodies of water, oceans, seas or lakes, that have not been sampled. Pelagic algae are exclusively microbial, whereas macrophytes are confined to coasts or shallow waters. Pyrenoids are predominantly found in unicellular, colonial or filamentous algae, whereas frond-forming coastal algae generally lack pyrenoids (with notable exceptions like the sea lettuce *Ulva lactuca* or the edible laver, *Pyropia*). What all oceanographic and freshwater surveys agree on is the predominance of three groups of eukaryotic phytoplankton lineages: diatoms, Haptophyta with calcified scales (coccolithophores), and dinoflagellates. Some authors add a fourth clade, green algae (Not et al. 2012) including key genera from an ecological point of view: *Micromonas, Ostreococcus* and *Bathyococcus* (Prasinophytes). The dominant genera (but not necessarily species) of all four clades that were identified through metabarcoding surveys (Le Bescot et al. 2016; Malviya et al. 2016; Dos Santos et al. 2017) are generally diagnosed as having a pyrenoid (see chapter on Diversity below). Contribution to marine primary productivity from pyrenoid-less eukaryotic algae (*e.g. Ostreococcus*; Chrétiennot-Dinet et al. 1995) and cyanobacteria is, nevertheless, far from negligible (Derelle et al. 2006; Palenik et al. 2007; Not et al. 2012; Biller et al. 2015). The figure of one quarter to one third of global carbon fixation being mediated by pyrenoid-possessing families has been proposed (Mackinder et al.

2016) but more studies of CCM physiology are needed across the pyrenoid diversity.

C. *Independent Origins but Convergent Structures*

Algae are a polyphyletic assemblage of generally water dwelling photosynthetic organisms (Chap. 2). If the earliest green and red algae are about a billion years old (Butterfield et al. 1990; Yang et al. 2016), algae with secondary or tertiary chloroplasts arose much later: *Euglena* ancestors are c.450 MYA (Gray and Boucot 1989); dinoflagellates c.240 MYA (Fensome et al. 1999; Janouškovec et al. 2017); coccolithophores c.205 MYA (Gardin et al. 2012); diatoms are only c.130 MY old (Medlin 2016). There is therefore little doubt that pyrenoids are also polyphyletic, having arisen as late adaptations in established chloroplast lineages in response to declining atmospheric CO_2 concentrations (Raven et al. 2017), a process that was accelerated by the rise of the land plants from the Devonian onwards (Berner 1997). Purely from an ultrastructural perspective, pyrenoids are distinguished from one another through a limited number of characters, which the next section will explore in greater detail. The simplest pyrenoid is a homogeneous dense proteinaceous aggregate of RuBisCO, free from internal or external structures (sometimes dubbed 'naked pyrenoid', as in the unicellular red alga *Rhodella*, see Fig. 9.2b2). These instances are relatively rare. Next are pyrenoid matrices traversed by one or several membranes derived from thylakoids. These instances are the most common. Trans-pyrenoidal membranes can adopt complex morphologies, like the highly anastomosed network traversing the pyrenoid of another red alga, *Pophyridium cruentum* (Nelson and Ryan 1988) or the stellar knot at the heart of the pyrenoid of the model green alga *Chlamydomonas reinhardtii* (Engel et al. 2015; see Figs. 9.2a4 and 9.4a). Reserve material deposits at the periphery of the RuBisCO matrix can constitute a third pyrenoid feature, although there is still much debate whether these deposits have a functional role. Carbohydrate deposits can be inside the chloroplast (*e.g.* green algal starch) or in the cytosol, in which case the reserve material is separated from the RuBisCO matrix by the chloroplast envelopes (*e.g.* in all red and red-derived chloroplasts). The recent molecular characterisation of the model pyrenoid of *Chlamydomonas reinhardtii* (Mackinder et al. 2017), which will be explored in detail further on, has shown that the structure is more complex than can be resolved through conventional electron microscopy (Engel et al. 2015).

D. *Diversity*

The essential role of the pyrenoid to optimize photosynthesis in (predominantly) aquatic environments, has led to algal pyrenoids converging around the similar essential components associated with a CCM. Thus, in addition to transmembrane inorganic carbon transporters, and a spatially sensitive carbonic anhydrase (CA), a CCM is usually associated with a RuBisCO matrix enclosed within the pyrenoid, which is often traversed by thylakoid tubules, and in some green algae the pyrenoid is demarcated by a nearly all-enclosing starch sheath - Fig. 9.1 shows the typical arrangement of these characteristics in *Chlamydomonas reinhardtii*. However, despite those common elements, in various algae there can be single or multiple pyrenoids per cell which differ in size and morphology. Pyrenoid ultrastructure and distribution within the various major groups of algae has been regularly reviewed (Leyon 1954; Gibbs 1962a, b; Manton 1966; Griffiths 1970, 1980; Dodge 1973; Meyer and Griffiths 2013; Meyer et al. 2017). If pyrenoid function is presumed to be similar across all algal species, situation within the chloroplast has long been an important taxonomic feature (Griffiths 1970, 1980). The two main types are embedded (spherical or sub-spherical bodies immersed within the chloroplast) or

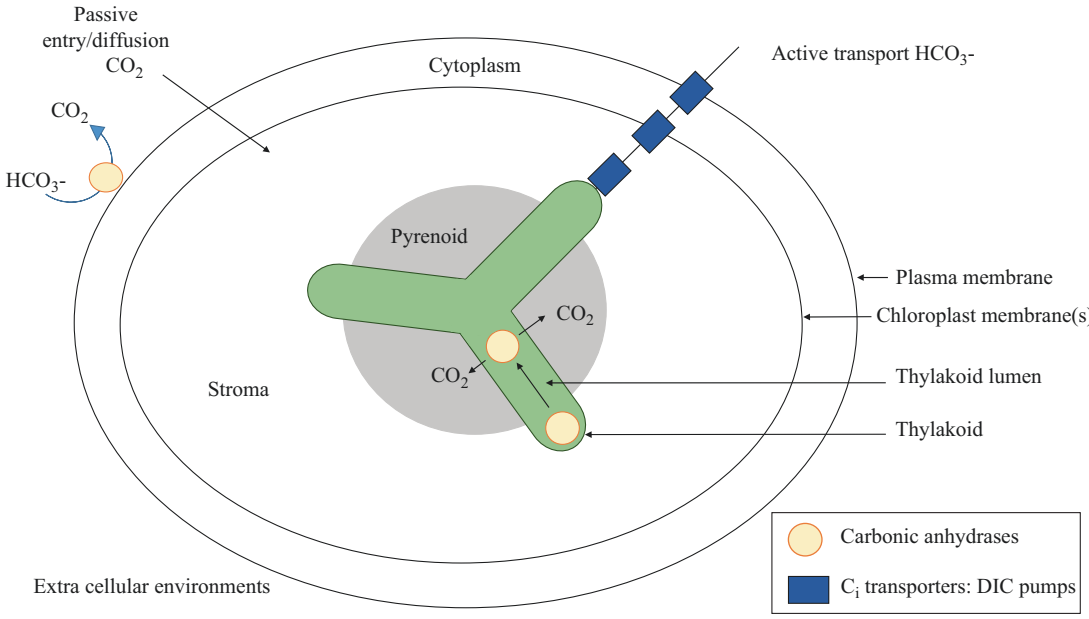

Fig. 9.1. Representative structural components of CCM and pyrenoid based on *Chlamydomonas reinhardtii*. A typical CCM includes three key elements: (1) inorganic carbon transporters, (2) carbonic anhydrases strategically localised to maximise delivery of CO_2 to RuBisCO, (3) a micro-compartment in which RuBisCO is packaged, the pyrenoid. Most pyrenoids are traversed by thylakoid membranes, sometimes in a highly organised tubular structure, with a specific carbonic anhydrase which may either be in the intrathylakoid lumen (Chlorophyta) or closely allied to the pyrenoid (diatoms)

projected (a bulge at the inner face of the chloroplast, in which case the pyrenoid can be almost entirely surrounded by chloroplast membranes). This range of traits are sketched in Fig. 9.2 (from Meyer et al. 2017), which shows representative pyrenoid outline structures from green and red algae, as well as Chlorarachniophyta, diatoms and dinoflagellates (Fig. 9.2a–e, respectively). Building from these outlines, we firstly provide an overview of pyrenoid diversity in the major algal groups and through the evolution of the plastid.

(a) *Archaeplastids: chloroplasts from the primary endosymbiosis (Chlorophyta+Charophyta, Rhodophyta)*

Green, red and Glaucophyta lineages arose from a primary endosymbiotic event when a heterotrophic host cell captured a protocyanobacterium (prokaryote) that became stably integrated and ultimately became a plastid (Archibald 2009; Keeling 2010; Martin et al. 2015; Chap. 2). This crucial event probably occurred between 1 and 1.5 billion years ago (Hedges et al. 2004; Yoon et al. 2004; Douzery et al. 2004; Shih and Matzke 2013) (Fig. 9.3). Among those three lineages, green algae from the phylum Chlorophyta are probably the best studied to date and pyrenoids are generally present, independently of life forms (unicellular, colonial, and macrophytes). The single pyrenoid of *Chlamydomonas reinhardtii*, currently the only pyrenoid which has been investigated in depth at the molecular level (Mackinder et al. 2016, 2017; Zhan et al. 2018; Küken et al. 2018) is a near spherical, starch-coated, micro-compartment traversed by a network of modified thylakoids called tubules, situated at the base of a cup-shaped chloroplast (as outlined in Figs. 9.1 and 9.2a4). Other Chlorophyta similarly have one pyrenoid per cell (e.g. *Botryococcus sp.*,

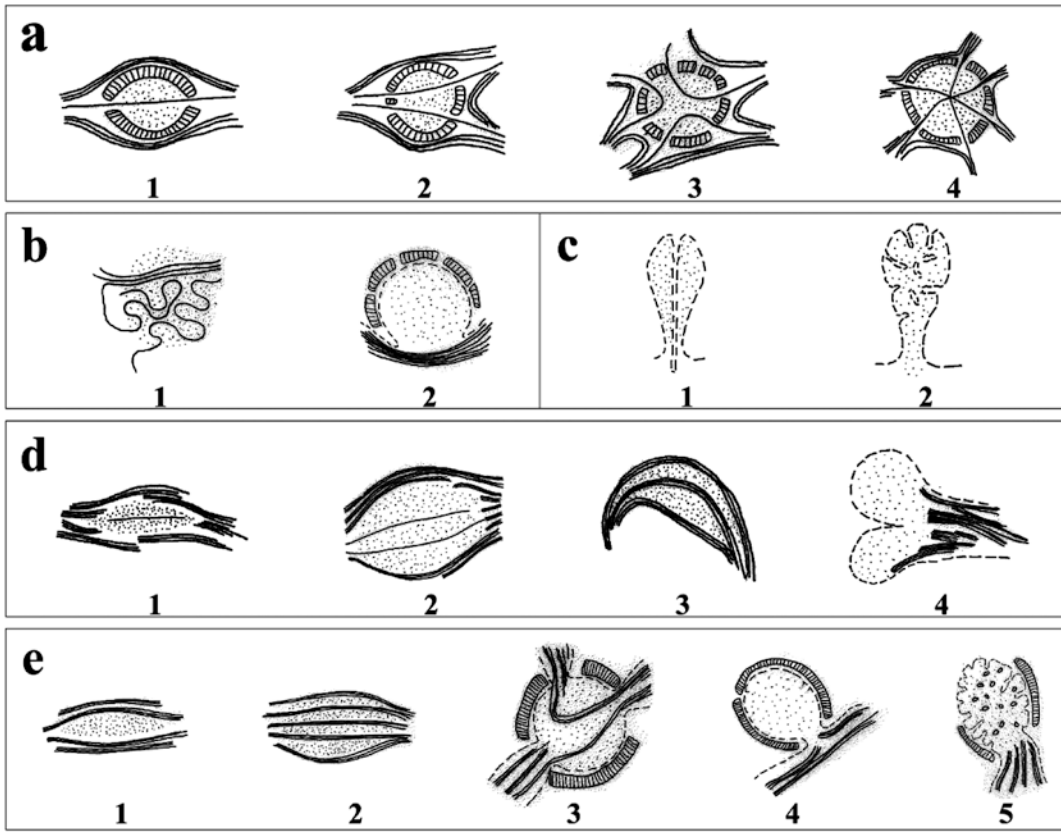

Fig. 9.2. Examples of morphological diversity of microalgal pyrenoid matrix and associated network of thylakoid membranes. (**a**) Green algae, with examples taken from Cladophorales and Siphonocladales (after Hori and Ueda 1975), and *Chlamydomonas reinhardtii*; (**b**) red algae (after Gantt and Conti 1965; Ford 1984); (**c**) Chlorarachniophyta (after Ishida et al. 1999); (**d**) diatoms (after Bedoshvili et al. 2009); (**e**) dinoflagellates (after Dodge 1973). Dots = pyrenoid matrix (mainly composed of RuBisCO); thick lines = stromal thylakoids when outside the pyrenoid matrix or transpyrenoidal membranes (tubules) when traversing the pyrenoid matrix; hatched boxes = peri-pyrenoidal carbohydrate plates, stromal in green algae and cytosolic in non-green algae; dashed lines = chloroplast envelope (composed of two lipid bilayers in Archaeplastidia, and three or more in algae that inherited a chloroplast through secondary or tertiary endosymbiosis). (Reproduced, with permission, from Meyer et al. 2017)

Komárek and Marvan 1992; *Prasinococcus cf. capsulatus*, Guillou et al. 2004; *Dunaliellia salina*, Melkonian and Preisig 1984). The subaerial Chlorella-like *Heveochlorella hainangensis* (Zhang et al. 2008), that grows on rubber trees, is a rare example of a Chlorophyta with multiple pyrenoids per chloroplast.

There is also great variability in transpyrenoidal membranes (Fig. 9.2a1–4). In *Blastophysa rhizopus* and *Cladophora glomerata* the pyrenoid is bisected by a single membrane (Chappell et al. 1991; McDonald and Pickett-Heaps 1976, respectively), whereas in *Chlamydomonas*, the pyrenoid is traversed by multiple membranes. Molecular phylogenies are, however, increasingly challenging the merit of pyrenoids as robust taxonomic markers. While *Trebouxia* pyrenoids remain useful to distinguish these common lichen photobionts (Friedl 1989), the genus *Chloromonas* no longer warrants the appellation 'pyrenoid-less' *Chlamydomonas* when considered from the angle of combined rRNA

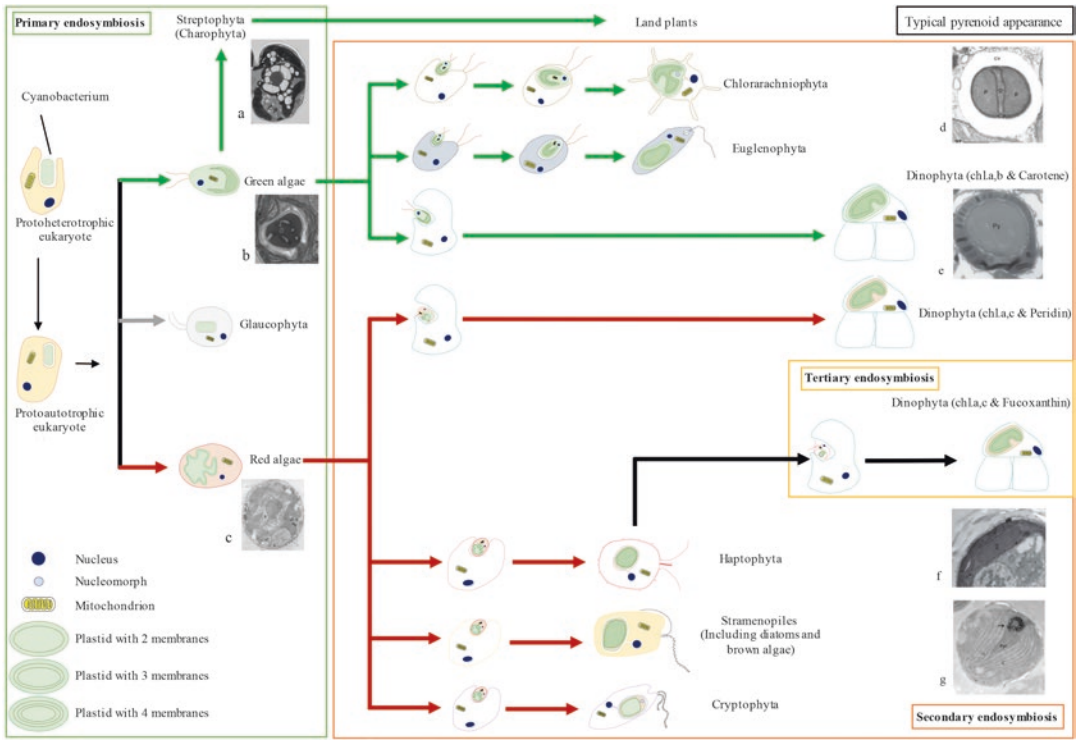

Fig. 9.3. Schematic of plastid evolution and typical pyrenoid appearance associated with the main algal lineages. Endosymbiosis events are boxed. Primary endosymbiosis gave rise to the three different types of algae with a primary chloroplast (green box), giving rise to the glaucophytes, green algae and red algae. Green algae are illustrated by a pyrenoid of *Cosmarium subtumidum* (*a*), a Streptophyta (Image courtesy: Myriam Goudet), and by a pyrenoid of *Chlamydomonas reinhardtii* (*b*), a Chlorophyta (Image courtesy: Dr. Moritz Meyer), whereas red algae are illustrated by a pyrenoid of *Porphyridium cruentum* (*c*) (Gantt and Conti 1965). Secondary endosymbioses (orange box) led to the diversification of the green lineage (green arrows) in three main groups of algae: Chlorarachniophyta (illustrated by a pyrenoid of *Chorarachnion reptans* (*d*), Hibberd and Norris 1984), Euglenophyta and Dinophyta (*e*) (illustrated by a pyrenoid of *Pseudadenoides polypyrenoides*, Hoppenrath et al. 2017). Diversification of the red lineage (red arrows) gave rise to 3 main groups: Haptophyta (illustrated by a pyrenoid of *Gephyrocapsa oceanica* (*f*) Bendif and Young 2014), Stramenopiles (illustrated by a pyrenoid of *Phaeodactylum tricornutum* (*g*), Allen et al. 2011) and Cryptophyta. Haptophyta have undergone a tertiary endosymbiosis (yellow box), with a secondary plastid membrane (black arrow) with some dinoflagellates forming a pyrenoid on a daily basis (Nassoury et al. 2001)

phylogenies and morphological studies (Pröschold et al. 2001).

Most of the species in the subphylum Prasinophyceae also contain a pyrenoid, with the notable exceptions of picoplanktonic *Ostreococcus tauri* and *O. lucimarinus*. The more efficient acquisition and usage of resources in tiny eukaryotic cells (Raven 1998) perhaps overrides the need for a pyrenoid, but it is intriguing to note that all cyanobacteria, that are equally small, package RuBisCO into a micro-compartment (Kerfeld et al. 2018). There are also numerous examples of pyrenoid-possessing species in Charophyta, the closest extant relatives of the earliest land plants (*e.g. Coleochaete scutata*, McKay et al. 1991; *Spirogyra* sp., Gibbs 1962b). Distribution of pyrenoids across the green algal diversity (Meyer and Griffiths 2013) suggested multiple independent losses and gains, similarly to what has been hypothesised for the only

example of a pyrenoid in a land plant, the hornworts (Villarreal and Renner 2012).

In contrast to green algae, the presence of a pyrenoid in red algae is restricted to certain groups, with current phylogenies possibly supporting a common origin. Following the taxonomy of Qiu et al. (2016), pyrenoids are absent from the basal lineage, the mostly extremophilic unicellular Cyanidiophytina (*e.g. Cyanidioschyzon merolae*), and from the Florideophyceae. Pyrenoids are present in families where life forms are predominantly unicellular or filamentous, including Porphyridiophyceae, Rhodellophyceae and Stylonematophyceae, but not Compsopogonophyceae (M.T. Meyer, unpublished observations). But pyrenoids are also present in macrophytic Bangiophyceae, most notably in the previously mentioned genus *Porypia* (Cole and Conway 1975; then still classified as *Porphyra*). The red algal pyrenoid differs from its green cousin most with respect to the arrangement of membranes traversing the matrix (see Fig. 9.2b1–2) and the extrachloroplastic deposition of reserve material which, when present, remains intriguingly associated with the RuBisCO matrix. Some unusual structures can also be found. In *Rhodella violacea*, the nucleus and pyrenoid are closely associated throughout the entire cell cycle. A region of the nuclear envelope runs parallel to the chloroplast envelope at the pyrenoid surface with an occasional tubular connexion between the nucleus and pyrenoid (Patrone et al. 1991).

In *Glaucophyta* plastids, RuBisCO is also packaged into a micro-compartment, but the structure (termed cyanelle) is probably akin to a vestigial carboxysome from the cyanobacterial ancestor, rather than a *bona fide* pyrenoid (Fathinejad et al. 2008).

(b) *Chloroplasts from a secondary endosymbiosis: Excavata (Euglenophyta), Rhizaria (Chlorarachniophyta), Stramenopiles (Bacilliariophyceae/diatoms, Phaeophyta/brown algae) and CCTH (Cryptophyta and Haptophyta)*

Following the primary endosymbiosis, multiple secondary endosymbiotic events gave rise to a chloroplast surrounded by, initially, four plastidic membranes, though one was occasionally lost secondarily (Fig. 9.3). Two groups dominate contemporary phytoplankton communities, diatoms and coccolithophores).

The type species of Euglenophyta, the secondary plastid lineage with the oldest fossil record, is the well-known freshwater *Euglena gracilis*, which has multiple chloroplasts. *Euglena* has a single, central pyrenoid per chloroplast (Osafune et al. 1989), traversed by widely-spaced, parallel running membranes, typically in pairs, prolonging adjacent thylakoids (Gibbs 1962a). The RuBisCO matrix is rarely if ever fully encapsulated by a sheath of carbohydrates, as typically seen in green algae, although paramylon grains do form in close proximity to the RuBisCO matrix. Freshwater photosynthetic Euglenoids are believed to have inherited a pyrenoid from their marine dwelling ancestor, but the trait was lost independently at least twice in this clade (Karnkowska et al. 2015).

The small group of Chlorarachniophyta is usually associated with pyrenoids bulging outwards from the chloroplast. Invaginations of the periplastidial compartment (a remnant of the eukaryotic endosymbiont's cytoplasm) more or less bisect the RuBisCO matrix (see Fig. 9.2c1–2). Discoveries of a species with a fully embedded pyrenoid, *Viridiuvalis adhaerens* (Shiratori et al. 2017), and a species lacking a pyrenoid altogether, *Partenskyella* glossopodia (Ota et al. 2009), suggest that here too the diversity is far from having been exhaustively explored.

Pyrenoids are ubiquitous in the ecologically important clade of diatoms, the dominant group in the Stramenopiles. The CCM-pyrenoid correlation as well their evolutionary constraints on RuBisCO kinetics have been well studied in model diatom species (Matsuda et al. 2017; Shen et al. 2017; Young and Hopkinson 2017), but must now

be extended where it is not hindered by culturing limitations to other ecologically important species. Morphological diversity was explored by Drum and Pankratz (1964), Schmid (2001) and Bedoshvili et al. (2009). Diatom pyrenoids exhibit a great variety of shape and sizes (Fig. 9.2d), probably due to the diversity of cell and chloroplast dimensions in this group. A salient feature of numerous diatom pyrenoids is a chloroplast embedded lenticular RuBisCO matrix bisected by a single or a few thylakoids. Intriguingly, some pyrenoids appear to contain a membrane that is not connected to adjacent thylakoids. A membrane entirely trapped inside a RuBisCO matrix with no continuity to the stroma is difficult to reconcile with the prevailing CCM model, that posits a continuum of bicarbonate transport from the extracellular environment to a CA at the heart of the RuBisCO matrix, within the lumen of trans-pyrenoidal membranes. This *Chlamydomonas*-type model (Fig. 9.1) appears to have been adopted by *Phaeodactylum tricornutum* too, as evidenced by a CCM-critical luminal CA, albeit of a different family than the luminal *Chlamydomonas* CA (Matsuda et al. 2017). The genera most abundant in the World's oceans, *Chaetoceros*, *Fragilariopsis*, *Thalassiosira* and *Corethron* (as confirmed by the Tara expedition, Malviya et al. 2016), comprise species that to the best of our knowledge are pyrenoid positive. Pyrenoid shape and intraplastidial position can be species-specific in some genera and therefore retain some taxonomic value (Bedoshvili et al. 2009).

In Phaeophyta (brown algae), pyrenoid occurrence has and continues to be used as a taxonomic marker along with chloroplast morphology (Delepine and Asensi 1975; Kawai and Kurogi 1992; De Reviers and Rousseau 1999; Tanaka et al. 2007). Although present in the Ectocarpales, Sphacelariales, Scytosiphonales and Dictyosiphonales, they are thought to absent in all the members of the Dictyotales and Laminariales (Evans 1966). Some brown algal chloroplasts, as in *Splachnidium rugosum*, are stellate, a shape also commonly found in red algae, and have a central pyrenoid traversed by numerous non-parallel membranes (Tanaka et al. 2007). An unusual example of pyrenoid morphology not encountered before in the present diversity survey is the bulging naked pyrenoid of *Scytosiphon lomentaria*, seemingly not connected to membranes (Nagasato and Motomura 2002).

Examples of pyrenoid bearing species of the Cryptophyta include *Rhinomonas pauca*, with a single pyrenoid which is not traversed by thylakoids but has an invagination from a protruding nucleomorph (a vestigial nucleus from the secondary endosymbiont). *Cryptomonas curvata*, has two pyrenoids, largely encased by starch (Gibbs 1962a). Pyrenoid presence/absence is however of limited taxonomic value in this clade (Hoef-Emden and Archibald 2017).

Haptophyta contain one or two chloroplasts per cell, generally with a pyrenoid which can be immersed (as in the ecologically important bloom forming *Emiliania huxleyi* and *Phaeocystis antarctica*) or bulging (Billard and Inouye 2004). The bulging can be so extreme as to form a stalk but unlike the above mentioned *Scytosiphon* bulging pyrenoid, the RuBisCO matrix is traversed by a membrane derived from thylakoids (Fresnel and Probert 2005). Most Pavlovaphyceae lack a pyrenoid (Mahdi Bendif et al. 2011).

(c) *Chloroplasts from a tertiary endosymbiosis,* Chromalveolates (*Dinophyta/dinoflagellates*)

Finally, the dinoflagellates, arising from a tertiary endosymbiosis, are mostly marine plankton. Large studies have been conducted on this group, trying to characterize the different organelle structures, including the pyrenoid (Fig. 9.2e). The detailed ultrastructural reviews by Dodge (1968) and Dodge and Crawford (1971) showed that a pyrenoid is present in about half of the species stud-

ied. These authors also classified pyrenoids into five categories: simple fusiform interlamellar, found in species like *Woloszynskia micra*; compound interlamellar (but much larger than the previous example: *Prorocentrum micans, Exuviaella mariae-lebouriae*; Kowallik 1969); a simple stalked structure surrounded by a starch sheath (*Aureodinium pigmentosum* or *Glenodinium hallii*; Dodge 1967, 1968); more complex multiple stalked supported by two or more chloroplast projections (*Peridinium trochoideum* or *Amphidinium carteri*); and finally, stalked with a matrix perforated by numerous invaginations of the envelope (*Heterocapsa triquetra*). The highly complex organization of dinoflagellate chloroplasts would benefit from the use of slice-and-view EM tools, for 3D reconstructions. This would help clarify how diverse dinoflagellate and other pyrenoids really are, and whether attempts at classification hold up. In a rare example of non-Chlorophyta pyrenoid physiology study, the Morse group showed that in *Gonyaulax polyedra*, a peridinin-containing dinoflagellate with a Form 2 RuBisCO, the pyrenoid forms diurnally. In continuous light, two distinct circadian oscillators control RuBisCO aggregation at the centre of the cell (by day, measured as maximal CO_2 assimilation) and photosynthesis (measured as O_2 exchange) (Nassoury et al. 2001).

This brief survey of pyrenoid diversity in key algae clades is far from exhaustive but give us an overview of ultrastructural variability across photosynthetic organisms. Algae are not a monophyletic clade and the presence or absence of a pyrenoid show us that developing such structure was important to survive in marine and freshwater environments. Despite such variety, it is evident that the packaging of RuBisCO into a microcompartment has convergently arisen to represent one of the three primary CCM components in most algae (alongside inorganic carbon transporters and CAs), yet understanding the interplay between pyrenoid structure and the associated molecular regulation of development is only understood for a few key model organisms. There is also a pressing need for integrative studies that seek to reconcile pyrenoid morphology with CCM effectiveness and RuBisCO kinetics, as recently published for Haptophyta (Heureux et al. 2017) and diatoms (Young and Hopkinson 2017).

II. Pyrenoid Structure & Function: Lessons from *Chlamydomonas*

Having considered the phylogenetic diversity of pyrenoid distribution, with evidence culled from rather traditional and painstaking morphological approaches, we now consider the fine structure and likely function of such microcompartments based upon the one model species *Chlamydomonas reinhardtii* (Harris 2001). Whilst hardly representative of the diverse marine ecosystems likely to harbour pyrenoid-mediated carbon concentrating processes, we have made major progress in developing novel analytical approaches to understand pyrenoid structure and function for this species. From a molecular perspective, these include genomic DNA and RNA sequencing (Merchant et al. 2007; Brueggeman et al. 2012; Fang et al. 2012; Zones et al. 2015), transformation tools associated with fluorophore and affinity tags for *in vivo* imaging and proteomic analysis of purified protein complexes (Mackinder et al. 2017), and *in situ* imaging with molecular-level precision (Engel et al. 2015). Amenability of *Chlamydomonas* to insertional mutagenesis and yeast-like suitability for genome-wide high-throughput propagation and screening (Jinkerson and Jonikas 2015; Li et al. 2016) has radically altered the pace of discovery. As an example, disrupted pyrenoid structure and/or CCM activity in mutant lines provide clues to the genetic basis of the *Chlamydomonas* system (Ma et al. 2011; Yamano et al. 2014; Mackinder et al. 2016, 2017). Traditional physiological approaches

continue to be used to evaluate the magnitude and the extent of pyrenoid-mediated CCM activity, usually following the transition from high CO_2 (cells cultured in equilibration with 2–5% CO_2 in air) to 0.04% CO_2 (air equilibration), by using the analyses of photosynthetic efficiency and CCM engagement (*e.g.* O_2 electrode dissolved inorganic carbon (DIC) responses, radio-isotopic quantification of DIC pools, $^{13}C/^{12}C$ discrimination measured concurrently with gas exchange, and immunogold labelling electron microscopy). The combination of novel and traditional analytical approaches on wildtype cells, with the new riches provided by genetically-transformed resources, has allowed substantial progress to be made in understanding *Chlamydomonas* pyrenoid structure and function.

A. Structure and Organisation

Early studies on *Chlamydomonas* using electron microscopy (Ohad et al. 1967; Goodenough and Levine 1970; Goodenough 1970) had revealed the complex interplay between the pyrenoid, consistently located centrally at the base of a cup-shaped chloroplast, with a dense matrix of RuBisCO surrounding a knotted thylakoid tubule network, enclosed by starch plates (see Figs. 9.1 and 9.4a). A few key proteins were identified, in terms of RuBisCO (Goodenough and Levine 1970; Kuchitsu et al. 1988; Rawat et al. 1996) and RuBisCO activase (McKay et al. 1991). This was enough to ground the pyrenoid as the site of CO_2 fixation. Early estimates of intracellular pools of inorganic carbon and subsequent CCM models quickly recognized the need for active transport of bicarbonate from bulk medium to chloroplast stroma (Badger et al. 1980; Spalding and Portis 1985), and at a time when experimental data was still inconclusive, the model was augmented by tentatively placing a CA in the pyrenoid (Pronina and Semenenko 1992; Badger and Price 1994). The perceptive CCM model discussed by Raven in 1997 is now accepted as being definitive for *Chlamydomonas* (see Chap. 7), with the identification of a specific CA (CAH3, Cre09.g415700), strategically located within thylakoid membranes (see Fig. 9.1), which migrates to the heart of the pyrenoid upon CCM induction (Karlsson et al. 1998; Blanco-Rivero et al. 2012), and proven absence of other CAs from the chloroplast which would tend to disperse the accumulated inorganic carbon (Terashima et al. 2010; Mackinder et al. 2017). The sub-cellular location, possible anchoring of the pyrenoid matrix around specialized thylakoid tubules acting as a point-source of CO_2 delivery is critical to CCM energetic efficacy in *Chlamydomonas* (Meyer et al. 2012; Caspari et al. 2017), as well as in other green algae (Palmqvist et al. 1994; Máguas et al. 1995; Morita et al. 1998). Furthermore, early observations were made of additional ridges or infoldings along the inner surface of tubule membranes (Ohad et al. 1967). In an exquisite *in situ* cryo-electron tomography study, these structures have now been revealed to be "minitubules" (median 5 per tubule), formed as two opposed membranes of adjacent thylakoid sheets coalesce when penetrating the starch sheath and pyrenoid matrix, thus entrapping stroma within their own lumen. As tubules proceed towards the heart of the pyrenoid, enclosed minitubules re-emerge, exposing their stromal lumina to the RuBisCO matrix (Engel et al. 2015). Thus, for *Chlamydomonas*, the gross morphological features of the pyrenoid have now been well defined: the thylakoid tubule network allows RuBisCO to aggregate as a central component around a spatially segregated carbonic anhydrase, and the minitubules allow the diffusive exchange of carboxylation substrates and reduced products between pyrenoid and stroma. The role of minitubules as a conduit for diffusion, rather than active transport across the pyrenoid-stroma boundary, gained some experimental support from a combined mass spectrometric analysis of metabolites and modelling of fluxes, comparing CCM-

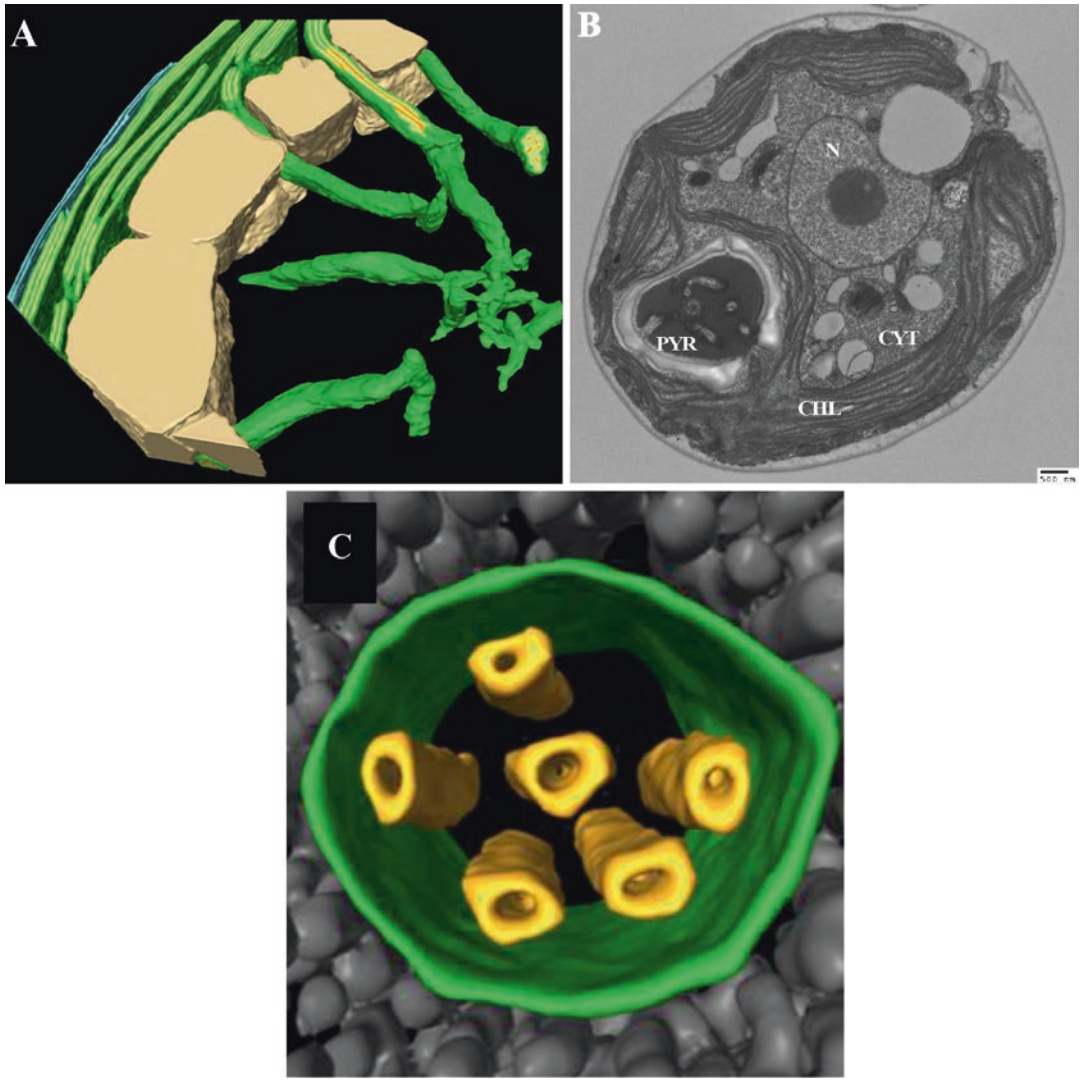

Fig. 9.4. (**a**) 3D segmentation of a tomographic volume of the pyrenoid showing thylakoid membranes (dark green), thylakoid lumina (light green), minitubules (orange), the chloroplast envelope (blue), and the pyrenoid starch sheath (tan). Cylindrical pyrenoid tubules extend from thylakoid stacks into the centre of the pyrenoid through fenestrations in the starch sheath. Once inside the pyrenoid, and narrow to form an interconnected membrane network at the pyrenoid centre. (Credit: Ben Engel et al. 2015). (**b**) Transmission electron micrograph of wild type *Chlamydomonas reinhardtii.* Grown under CCM induced conditions (low CO_2 in the light). Image courtesy of Dr. Moritz Meyer. (*N* Nucleus, *CYT* Cytosol, *CHL* Chloroplast, *PYR* Pyrenoid). (**c**) 3D segmentations of the pyrenoid matrix showing cross-sections of pyrenoid tubules (green) surrounded by RuBisCO complexes (grey). Multiple smaller minitubules (orange) are bundled within each pyrenoid tubule. The minitubules are formed within the main tubules as adjacent thylakoid sheets coalesce, and open out to provide stromal connectivity to the heart of the pyrnenoid through the tubule walls. The tomograms were 2× binned. Unbinned pixel size: 9.6 Å in **a**, 5.7 Å in **c**. Segmented tomogram thickness: 229 nm in **a**, 108 nm in **c**. (Credit: Ben Engel et al. 2015)

repressed and CCM-induced *Chlamydomonas* cultures (Küken et al. 2018). The study found only a minor concentration gradient of RuBP and no gradient of 3PGA between stroma and pyrenoid in low-CO_2 acclimated cells, despite clear increases in fluxes. The authors suggested that the starch sheath, which develops under CO_2-limited conditions, did not limit metabolite exchange and speculated that metabolite shuttling through minitubules could be regulated by charge properties, as a means to segregate between weakly anionic HCO_3^- and CO_2, and CBB intermediates.

However, there are still unresolved issues associated with the supply-side of carbon: whilst likely inorganic carbon transporters have been associated with either the plasma membrane (HLA3, Cre02.g097800; LCI1, Cre03.g162800; Ohnishi et al. 2010; Yamano et al. 2015) or chloroplast envelope (LCIA, Cre06.g309000; Duanmu et al. 2009), as yet the putative transporter required to upload bicarbonate into the intra-thylakoid space remains elusive. Elsewhere, within the stroma, LCIB/C complexes (Cre10.g452800, Cre06.g307500; Yamano et al. 2010) perhaps operate as unidirectional carbonic anhydrase moieties, to mop up CO_2 leakage from the pyrenoid complex, consistent with the structural affinity to βCA moieties (Jin et al. 2016) and preferential localisation of these complexes. Fluorescent tagging consistently situates LCIB/C where CO_2 leakage from the RuBisCO matrix would be maximal, *i.e.* near gaps between adjacent starch plates and around tubules, where these enter the RuBisCO matrix across the starch sheath (Wang et al. 2015; Mackinder et al. 2017).

One final issue, close to resolution, represents the mechanism by which RuBisCO aggregates within the pyrenoid. The pyrenoid in *Chlamydomonas* is clearly visible as a constitutive component of wildtype cells even when grown under elevated CO_2. Immunogold labelling and Yellow Fluorescent Protein (YFP) tagged confocal studies have shown that during the induction of the CCM following air-equilibration, a significant fraction of RuBisCO distributed throughout the stroma relocates to within the pyrenoid (Borkhsenious et al. 1998; Mitchell et al. 2017; Mackinder et al. 2016), suggesting the presence of an inducible RuBisCO tethering mechanism. The green algal Form 1B RuBisCO comprises a large macromolecule made up of two different subunits (8 of each, assembling into a 550 kDa hexadecameric holoenzyme with an eightfold symmetry). The large subunit (LSU) is encoded by the chloroplast genome (*rbcL*; P00877), and the small subunit (SSU) is encoded by the nuclear genome (two near-identical isoforms, *RBCS1*,*2*; Cre02.g120100, Cre02.g120150). Studies initiated on hybrid RuBisCO enzymes had shown that a range of higher plant SSUs could be engineered by nuclear transformation for assembly and catalytic functioning in *Chlamydomonas* chloroplasts (Genkov et al. 2010). However, the cells required high CO_2 for growth and seemed to lack an obvious pyrenoid structure. More detailed site-directed mutagenesis, targeted specifically towards two peripheral alpha-helices, demonstrated that the pyrenoid, and an effective CCM, could be restored by a chimeric SSU made up primarily of spinach residues, together with *Chlamydomonas* alpha-helices; in parallel, the CCM and an overt pyrenoid structure were lost in a mutant comprising *Chlamydomonas* SSU residues to which spinach alpha-helices had been inserted (Meyer et al. 2012). Confirmation that the SSU alpha-helices provide a key determinant in the RuBisCO aggregation process now awaits integration with the outputs associated with genome-wide insertional mutant libraries and screens for CCM and pyrenoid defects.

B. Functional Integration of Pyrenoid Proteome and CCM Activity

A key novel component in the RuBisCO aggregation process, as well as an essential

element of the *Chlamydomonas* CCM, is a small (c.30 kDa) intrinsically disordered chloroplast protein, with four near-identical repeats. Initially identified via traditional mutagenesis studies (LCI5, Cre10.g436550; Lavigne et al. 2002), then renamed Essential Pyrenoid Component 1 (EPYC1), it has now been characterised in detail and could indeed act as RuBisCO matrix linker protein (Mackinder et al. 2016), presumably by engaging via SSU alpha-helices. Subsequently, two major studies have characterised in more detail the dynamic nature of the pyrenoid and the extent of protein interactions associated with RuBisCO, the pyrenoid and CCM (Rosenzweig et al. 2017; Mackinder et al. 2017).

Firstly, a detailed analysis of the pyrenoid developmental dynamics during, and following cell division, has suggested that the RuBisCO-EPYC1 complexes effectively act as a liquid-like organelle (Rosenzweig et al. 2017), with properties not unlike those for example of nucleoli or P-bodies (mRNA processing bodies). This suggests that EPYC1 may act in a similar way to scaffold proteins within both major types of cyanobacterial carboxysomes (Cai et al. 2015; Rae et al. 2013), although the intriguing parallel remains in both prokaryotic (in the case of beta carboxysomes) and eukaryotic microcompartments associated with their respective CCM components, the role of the RuBisCO SSU is likely to form a key structural element.

In *Chlamydomonas*, the single pyrenoid normally divides equally between two daughter cells towards the end of the more extended chloroplast division process, although in a small proportion of cells (5%) it may be formed *de novo*, whenever the other daughter cell inherits the parent's entire pyrenoid. There is good evidence now that a significant fraction of RuBisCO molecules is released or unpackaged from the pyrenoid prior to redistribution, and that pyrenoid fission proceeds at a rapid pace (7 min) (Rosenzweig et al. 2017). Absence of dense crystalline packing of RuBisCO was validated by measuring the density of neighbouring RuBisCO molecules in high resolution cryo-EM tomograms. The observed concentration of the enzyme in the pyrenoid matrix, although extremely high (628 ± 63 μM), was less than would be represented by hexagonal close packing. Further evidence of the fluid-dynamic nature of the RuBisCO-EPYC1 complexes within the pyrenoid was given by an experiment using fluorescence recovery after photo-bleaching (FRAP) on RuBisCO and EPYC1 tagged wildtype cells, when internal remixing was shown to happen on a time scale of 20 s, thus precluding the possibility of *de novo* protein synthesis. The dynamic nature of assembly and reassembly of such liquid-like components was linked to the weak multivalent bonding, predicted to be associated with the multiple binding sites on the RuBisCO holoenzyme and their interactions with EPYC1 (Rosenzweig et al. 2017).

Secondly, Mackinder et al. (2017) localized 135 candidate CCM proteins, half of them in the chloroplast, and gained novel insight in the spatial organisation of the CCM and associated pyrenoid by identifying the interactors of 38 of these proteins through affinity tag mass spectrometry. This study showed that there might be up to 89 different proteins implicated in the *Chlamydomonas* pyrenoid, a number supported by proteomics of enriched pyrenoid fractions (Mackinder et al. 2016, identified at least 46 different pyrenoid proteins; Zhan et al. 2018, identified 190 proteins). The identity and situation, if not always function, of at least 16 pyrenoid proteins are now known. The matrix is formed, in addition to RuBisCO, RuBisCO Activase (RCA1, Cre04.g229300) and EPYC1, of three other proteins whose function is not yet entirely clear: a Ca^{2+}-sensing protein that re-localises to the pyrenoid upon CCM induction, perhaps mediating a CO_2-limiting signal (CAS1, Cre12.g497300, Wang et al. 2016; Yamano et al. 2018); a putative methyl transferase that is transcrip-

tionally upregulated under low CO_2 (SMM7, Cre03.g151650; Mackinder et al. 2017); and a protein with no know functional domain that shares some homology with proteins having a starch binding domain (Cre06.g259100; Kobayashi et al. 2015). Tubules were found to be enriched in Subunit H of Photosystem I (PSAH, Cre07.g330250), providing a suitable marker for future studies on this essential sub-compartment. Subunits of PSII were also present on tubules, challenging earlier proposals that O_2-evolving components were actively excluded from the pyrenoid. Most novel candidates were situated in discrete sub-compartments at the pyrenoid periphery, demonstrating that the pyrenoid is a more complex assemblage than previously thought. The localization of starch biosynthesis and 1,4-alpha-glucan branching enzymes (STA2, Cre17.g721500; SBE3, Cre10.g444700) coincided with that of the starch plates, whereas LCIB/C complexes matched previous reports of puncta at the entry of tubules into and across starch plates. An uncharacterized low CO_2-inducible protein (LCI9; Cre09.g394473) appeared to occupy the entire space between pyrenoid matrix and starch sheath, including spaces in-between adjacent starch plates. LCI9 is predicted to contain carbohydrate binding modules, and could therefore maybe help stabilise or organise starch plates around the matrix. A PSII sub-unit P like protein (PSBP4, Cre08.g362900) was preferentially present in the lumen of tubules, in puncta at the junction of matrix-peripheral structures. Finally, two isoforms of phosphofructokinase (PFK1, Cre06.g262900; PFK2, Cre12.g553250) were recovered in both proteomes and CCM interactome.

An urgent priority for research is to identify the function of these, and possibly other as yet unidentified proteins, and how they tether RuBisCO-EPYC1 complexes around the tubule network and how they drive the unusual shape of pyrenoid starch plates, and to identify the elusive trans-thylakoid inorganic carbon transporter(s).

C. Integrating Transcriptomics and Pyrenoid-Associated Processes

The initial molecular correlates of pyrenoid formation and regulation have focussed on known associations of CCM genes drawn from traditional mutagenesis studies or differential expression under contrasting CO_2 growth regimes (Spalding et al. 1983; Miura et al. 2004; Brueggeman et al. 2012; Fang et al. 2012). Whilst such studies have revealed intriguing interdependencies, particularly for those known CCM genes, we have made less progress in defining regulators of pyrenoid dynamics. One approach may lie in combining the detailed transcriptional time-courses across day-night cycles (Zones et al. 2015), together with the physiological evidence suggesting that such cells which show synchronised divisions a few hours into the dark period, also reveal differential expression of key CCM genes associated with recruitment of RuBisCO into the newly formed pyrenoid before "dawn", as well as gene expression and protein accumulation patterns during the transition from dark to light periods (Mitchell et al. 2014; Tirumani et al. 2014). One key missing data set to advance this question is a matching translational time-course, with quantification of protein abundance. Hammel et al. (2018) tried to overcome the non-quantitative nature of many mass spectrometry experiments with labelled standards. Their findings had RuBisCO SSU 8X more abundant than EPYC1, albeit using mixotrophically grown cells. Only every other RuBisCO binding site (assuming 8 binding sites per holoenzyme) would be linked to EPYC1 (assuming 4 binding sites per monomer, Mackinder et al. 2016) under such growth conditions (and assumptions).

Equally important are questions relating to the role of post-translational modifications in facilitating or incapacitating pyrenoid constituents to perform their function. As already mentioned, the critical luminal CA is believed to undergo phosphorylation, upon which it preferentially re-localises to the

heart of the pyrenoid. EPYC1 is also known to be phosphorylated (Turkina et al. 2006), but whether this promotes or inhibits pyrenoid matrix aggregation is currently unclear, and no kinase has been singled out yet. Answers might not be necessarily clear cut, given the propensity of *Chlamydomonas* to retain a "minimal" pyrenoid under any known growth conditions.

Our pyrenoid narrative has mainly focused on the function associated with CO_2-fixation. The downstream associated role in starch metabolism, and deposition of a conspicuous sheath around the pyrenoid matrix, is easily traceable in the numerous carbohydrate associated enzymes identified in the pyrenoid spatial interactome (Mackinder et al. 2017) and proteome (Zhan et al. 2018). Contribution of the starch sheath to CCM efficacy, and pyrenoid integrity, is an evergreen question that warrants to be settled once and for all, through (re)examination of starchless mutants, and detailed phenotyping of pyrenoid proteins containing carbohydrate binding modules.

The above exposé depicts the pyrenoid as a rather complex arrangement. Yet, experiments of *in vitro* phase separation of a binary RuBisCO-EPYC1 mixture, capable of rapid internal mixing mimicking the *in vivo* system (Wunder et al. 2018), suggests that the matrix component at least might not require many more proteins than those already known. Our greatest knowledge gap, though, is in assigning a functional role (or not) to the starch sheath and sieving from the dozens of uncharacterised pyrenoid protein candidates especially those implicated in constitutive thylakoid tubule formation.

III. When, Where, How and Whither: From Paleo-Origins to Future Synthetic Biology

From a palaeohistorical perspective, despite the diverse structural representations, a pyrenoid represents a convergent solution for many eukaryotic algal lineages, and is almost always a pre-requisite for an effective CCM (but see Giordano et al. 2005). We have a clearer understanding of when conditions favouring the emergence of a pyrenoid developed, as recent studies have developed the notions of limited CO_2 concentration and diffusive supply in the aquatic milieu.

Two recent studies have attempted to link RuBisCO aggregation within an appropriate microcompartment (such as carboxysome or pyrenoid) to kinetic properties of the extant enzyme. Meyer and Griffiths (2013) suggested that the degree of 'relaxation' in RuBisCO specificity (seen in cyanobacteria, Chlorophyta, and C_4 monocots on the one hand, relative to C_3 terrestrial plants on the other hand) could represent the time spent operating under elevated CO_2 in association with a CCM. Additionally, the origins of the CCM and shifts in RuBisCO kinetic properties in association with a pyrenoid have also been suggested to have occurred at a time when equimolar CO_2:O_2 concentrations occurred in oceanic systems, which would have occurred some 450 Mya (Heureux et al. 2017; Griffiths et al. 2017; Lenton et al. 2016). The similar relative affinities of RuBisCO for O_2 and CO_2, (K_o/K_c = 16), found in Form IB RuBisCO (Chlorophyceae) and Form ID RuBisCO (red algae, diatoms), match the modern day O_2: CO_2 proportions in oceanic waters (×16 at 12 °C) relative to current ambient availability (Griffiths et al. 2017). Furthermore, even the RuBisCO kinetics of extant C_3 and C_4 terrestrial plants (K_o/K_c = 35) were also a requirement to maintain a 1:1 ratio CO_2:O_2 at the active site of RuBisCO (Griffiths et al. 2017) at the end of the Tertiary.

In either case, the likely convergent development of pyrenoids in eukaryotic algal lineages with a primary chloroplast seems likely to have predated the Carboniferous period (Badger and Price 2003). Raven et al. (2017) also examined CO_2 concentrations needed to saturate photosynthesis with diffusive CO_2 supply alone,

and when factoring in the paleohistory of other environmental constraints (effects of temperature, incident photosynthetically active radiation and nutrient limitations) reached a similar conclusion. The fossil record of eukaryotic algae with a secondary or tertiary chloroplast, however, points to a much later emergence of CCMs and associated pyrenoids in those lines, from the Mesozoic onward (see section I). A vertical transmission to diatoms, dinoflagellates, coccolithophores, etc., is consistent with the above outlined timing of origin in the red and green parental lineages. An origin after the main lineages were established would require either horizontal gene transfer or independent *de novo* origin; a question which could be solved through comparative proteomic studies of pyrenoid from algae with a sequenced genome, starting with the investigation whether the *Chlamydomonas* linker EPYC1 presents a universal mode of RuBisCO packaging into a matrix. Preliminary bioinformatic searches found proteins with similar biophysical properties (highly disordered and basic protein, presence of repeated motifs, small size) but no sequence homology for example in diatoms (Mackinder et al. 2016).

To address the questions of 'where' and 'how' the pyrenoid is found and formed, respectively, we also require detailed phylogenetic studies on the distribution of CCM and pyrenoid across entire algal lineages whereby we link the molecular phylogeny of RuBisCO subunits to structural and kinetic correlates of pyrenoid and CCM occurrence. Of particular interest would be a more detailed comparison both across the entire green algal clade (incorporating core Chlorophyta, Prasinophyceae and Charophyta). Here, preliminary investigations suggest that some key elements of the RuBisCO subunit structure map well on to the overall phylogeny, although there is little systematic grouping of pyrenoid/CCM clades (M.M.M. Goudet, unpublished observations). The comparative phylogenetic analysis of *Chlamydomonas* and *Chloromonas*, based on *rbcL* sequences, which showed intriguing correlations between pyrenoid loss and gain (Nozaki et al. 2002) was one key study which piqued the curiosity of this Chapter's authors. *Chloromonas* species generally lack the (pyrenoid + CCM) combination, and yet the phylogeny is interleaved with closely-related *Chlamydomonas* species which do have a pyrenoid, and two *Chloromonas* species (*Chloromonas rosae*: UTEX 1137 and *Chloromonas Serbinowii*: UTEX 492) which have been reported to demonstrate a CCM in the absence of a pyrenoid (Morita et al. 1998, 1999). Detailed molecular and biochemical analyses of these species-species interactions will surely reveal key regulatory and structural correlates required for pyrenoid formation.

Additional insights into the origins and function of the pyrenoid could also be revealed by a more detailed analysis of those species in which a pyrenoid is absent and yet a CCM is still operative (Giordano et al. 2005). Additionally, for those Prasinophyceae picoplankton lacking a pyrenoid and CCM, such as *Ostreococcus* (Derelle et al. 2006), it would be interesting to identify the extent of RuBisCO close-packaging in the plastid, together with the use of acid/alkaline compartments and the boundary layer associated with each cell permit the delivery of sufficient CO_2 to RuBisCO (Raven 1991). Such features might identify fundamental mechanisms which permit RuBisCO aggregation and perhaps underpin the variety of pyrenoid forms found across the algal lineages, as depicted in Fig. 9.2.

These conclusions draw inexorably towards the question of 'whither' we should focus research to characterise pyrenoid-CCM interactions. In the previous section, we have highlighted potential lines of discovery for the *Chlamydomonas* system - namely identification of putative trans-thylakoid inorganic carbon transporters, key protein and associated post-

translational modifications needed to bind the fluid RuBisCO-EPYC1 pool, and key structural components allied with starch sheath localisation and thylakoid tubule organisation. In general, this chapter has identified a need for more detailed characterisation of well-defined pyrenoid-CCM systems, but also the huge gulf in our understanding of key pyrenoid occurrence and facilitation mechanisms, beyond that particular Chlorophyta.

An additional beneficiary of such insights would be those researchers currently hoping to introduce some minimal form of eukaryotic CCM into higher plants (for recent opinion on the feasibility and review: Meyer et al. 2016; Rae et al. 2017). Here, the challenge lies in persuading every chloroplast to integrate inorganic carbon delivery processes with some form of pyrenoid-like RuBisCO aggregation mechanism and appropriate carbonic anhydrase co-localisation. Proof of concept that higher plant chloroplast will express *Chlamydomonas* putative transporters, and that modified RuBisCO SSU variants (known to be a prerequisite for pyrenoid formation in the green alga) will assemble with native LSU, are now established (Atkinson et al. 2016, 2017). Whilst in principle this may seem a simpler engineering problem, compared to the differential cell-specificity and targeting needed to introduce the C_4 pathway into a crop such as rice (Covshoff and Hibberd 2012; Covshoff et al. 2016), ultimately we need a precise definition of molecular, structural and regulatory components needed to form an algal pyrenoid to complete this goal. We hope that the preceding chapter provides some clues to the current state of knowledge on pyrenoid and CCM interactions. Whilst our progress to date has been framed primarily by research on green algae and diatoms, the goal of the chapter has been to stimulate interest for investigating the complexities of pyrenoid structure and function across a broader range of algal lineages.

References

Allen AE, Moustafa A, Montsant A, Eckert A, Kroth PG, Bowler C (2011) Evolution and functional diversification of fructose bisphosphate aldolase genes in photosynthetic marine diatoms. Mol Biol Evol 29(1):367–379

Archibald JM (2009) The puzzle of plastid evolution. Curr Biol 19(2):R81–R88

Atkinson N, Feike D, Mackinder LC, Meyer MT, Griffiths H, Jonikas MC, Smith AM, McCormick AJ (2016) Introducing an algal carbon-concentrating mechanism into higher plants: location and incorporation of key components. Plant Biotechnol J 14(5):1302–1315

Atkinson N, Leitão N, Orr DJ, Meyer MT, Carmo-Silva E, Griffiths H, Smith AM, McCormick AJ (2017) Rubisco small subunits from the unicellular green alga Chlamydomonas complement Rubisco-deficient mutants of Arabidopsis. New Phytol 214(2):655–667

Badger MR, Price GD (1994) The role of carbonic anhydrase in photosynthesis. Annu Rev Plant Biol 45(1):369–392

Badger MR, Price GD (2003) CO_2 concentrating mechanisms in cyanobacteria: molecular components, their diversity and evolution. J Exp Bot 54(383):609–622

Badger MR, Kaplan A, Berry JA (1980) Internal inorganic carbon pool of *Chlamydomonas reinhardtii*: evidence for a carbon dioxide-concentrating mechanism. Plant Physiol 66(3):407–413

Bedoshvili YD, Popkova TP, Likhoshway YV (2009) Chloroplast structure of diatoms of different classes. Cell Tissue Biol 3(3):297–310

Bendif EM, Young J (2014) On the ultrastructure of *Gephyrocapsa oceanica* (Haptophyta) life stages. Cryptogam Algol 35(4):379–388

Bendif EM, Probert I, Hervé A, Billard C, Goux D, Lelong C, Cadoret JP, Véron B (2011) Integrative taxonomy of the Pavlovophyceae (Haptophyta): a reassessment. Protist 162(5):738–761

Berner RA (1997) The rise of plants and their effect on weathering and atmospheric CO_2. Science 276(5312):544–546

Beudeker RF, Kuenen JG (1981) Carboxysomes: 'calvinosomes'? FEBS Lett 131(2):269–274

Billard C, Inouye I (2004) What is new in coccolithophore biology? In: Coccolithophores. Springer, Berlin/Heidelberg, pp 1–29

Biller SJ, Coe A, Martin-Cuadrado AB, Chisholm SW (2015) Draft genome sequence of *Alteromonas macleodii* strain MIT1002, isolated from an enrichment culture of the marine cyanobac-

terium Prochlorococcus. Genome Announc 3(4):e00967–e00915
Blanco-Rivero A, Shutova T, Román MJ, Villarejo A, Martinez F (2012) Phosphorylation controls the localization and activation of the lumenal carbonic anhydrase in *Chlamydomonas reinhardtii*. PLoS One 7(11):e49063
Blankenship RE, Hartman H (1998) The origin and evolution of oxygenic photosynthesis. Trends Biochem Sci 23(3):94–97
Borges AV, Frankignoulle M (2002) Distribution and air-water exchange of carbon dioxide in the Scheldt plume off the Belgian coast. Biogeochemistry 59(1–2):41–67
Borkhsenious ON, Mason CB, Moroney JV (1998) The intracellular localization of ribulose-1, 5-bisphosphate carboxylase/oxygenase in *Chlamydomonas reinhardtii*. Plant Physiol 116(4):1585–1591
Brueggeman AJ, Gangadharaiah DS, Cserhati MF, Casero D, Weeks DP, Ladunga I (2012) Activation of the carbon concentrating mechanism by CO_2 deprivation coincides with massive transcriptional restructuring in *Chlamydomonas reinhardtii*. Plant Cell. https://doi.org/10.1105/tpc.111.093435
Butterfield NJ, Knoll AH, Swett K (1990) A bangiophyte red alga from the Proterozoic of arctic Canada. Science 250(4977):104–107
Cai F, Dou Z, Bernstein SL, Leverenz R, Williams EB, Heinhorst S, Shively J, Cannon GC, Kerfeld CA (2015) Advances in understanding carboxysome assembly in Prochlorococcus and Synechococcus implicate CsoS2 as a critical component. Lifestyles 5(2):1141–1171
Caspari OD, Meyer MT, Tolleter D, Wittkopp TM, Cunniffe NJ, Lawson T, Grossmann AR, Griffiths H (2017) Pyrenoid loss in *Chlamydomonas reinhardtii* causes limitations in CO_2 supply, but not thylakoid operating efficiency. J Exp Bot 68(14):3903–3913
Chappell DF, O'Kelly CJ, Floyd GL (1991) Flagellar apparatus of the biflagellate zoospores of the enigmatic marine green alga *Blastophysa rhizopus* 1. J Phycol 27(3):423–428
Chrétiennot-Dinet MJ, Courties C, Vaquer A, Neveux J, Claustre H, Lautier J, Machado MC (1995) A new marine picoeucaryote: *Ostreococcus tauri* gen. et sp. nov. (Chlorophyta, Prasinophyceae). Phycologia 34(4):285–292
Cole K, Conway E (1975) Phenetic implications of structural features of the perennating phase in the life history of Porphyra and Bangia (Bangiophyceae, Rhodophyta). Phycologia 14(4):239–245
Covshoff S, Hibberd JM (2012) Integrating C_4 photosynthesis into C_3 crops to increase yield potential. Curr Opin Biotechnol 23(2):209–214
Covshoff S, Szecowka M, Hughes TE, Smith-Unna R, Kelly S, Bailey KJ, Sage TL, Pachebat JA, Leegood R, Hibberd JM (2016) C_4 photosynthesis in the rice paddy: insights from the noxious weed *Echinochloa glabrescens*. Plant Physiol 170(1):57–73
De Reviers B, Rousseau F (1999) Towards a new classification of the brown algae. Prog Phycol Res 13:107–201
De Vargas C, Audic S, Henry N, Decelle J, Mahé F, Logares R, Lara E, Berney C, Le Bescot N, Prober I, Carmichael M, Poulain J, Romac S, Colin S, Aury J-M, Bittner L, Chaffron S, Dunthorn M, Engelen S, Flegontova O, Guidi L, Horák A, Jaillon O, Lima-Mendez G, Lukeš J, Malviya S, Morard R, Mulot M, Scalco E, Siano R, Vincent F, Zingone A, Dimier C, Picheral M, Searson S, Kandels-Lewis S, Tara Oceans Coordinators, Acinas SG, Bork P, Bowler C, Gorsky G, Grimsley N, Hingamp P, Iudicone D, Not F, Ogata H, Pesant S, Raes J, Sieracki ME, Speich S, Stemmann L, Sunagawa S, Weissenbach J, Wincker P, Karsenti E (2015) Eukaryotic plankton diversity in the sunlit ocean. Science 348(6237):1261605
Delepine R, Asensi A (1975) *Asteronema* nov. gen. nouveau genre de Phéophycée australe. Bulletin de la société botanique de France 122(7–8):295–304
Derelle E, Ferraz C, Rombauts S, Rouzé P, Worden AZ, Robbens S, Partensky F, Degroeve S, Echeynié S, Cooke R, Saeys Y, Wuyts J, Jabbari K, Bowler C, Panaud O, Piégu B, Ball SG, Ral J-P, Bouget F-Y, Piganeau G, De Baets B, Picard A, Delseny M, Demaille J, Van de Peer Y, Moreau H (2006) Genome analysis of the smallest free-living eukaryote *Ostreococcus tauri* unveils many unique features. Proc Natl Acad Sci 103(31):11647–11652
Dodge JD (1967) Fine structure of the dinoflagellate *Aureodinium pigmentosum* gen. et sp. nov. Br Phycol Bull 3(2):327–336
Dodge JD (1968) The fine structure of chloroplasts and pyrenoids in some marine dinoflagellates. J Cell Sci 3(1):41–47
Dodge JD (1973) The fine structure of algal cells. Academic, London
Dodge JD, Crawford RM (1971) A fine-structural survey of dinoflagellate pyrenoids and food-reserves. Bot J Linn Soc 64(2):105–115
Dorrell RG, Howe CJ (2012) What makes a chloroplast? Reconstructing the establishment of photosynthetic symbioses. J Cell Sci. https://doi.org/10.1242/jcs.102285

Dos Santos AL, Gourvil P, Tragin M, Noël MH, Decelle J, Romac S, Vaulot D (2017) Diversity and oceanic distribution of prasinophytes clade VII, the dominant group of green algae in oceanic waters. ISME J 11(2):512

Douzery EJ, Snell EA, Bapteste E, Delsuc F, Philippe H (2004) The timing of eukaryotic evolution: does a relaxed molecular clock reconcile proteins and fossils? Proc Natl Acad Sci 101(43):15386–15391

Drum RW, Pankratz HS (1964) Pyrenoids, raphes, and other fine structure in diatoms. Am J Bot 51:405–418

Duanmu D, Miller AR., Horken KM, Weeks DP, Spalding MH (2009) Knockdown of limiting-CO_2–induced gene HLA_3 decreases HCO_3^- transport and photosynthetic Ci affinity in *Chlamydomonas reinhardtii*. In: *Proceedings of the National Academy of Sciences*, pnas-0812885106

Engel BD, Schaffer M, Cuellar LK, Villa E, Plitzko JM, Baumeister W (2015) Native architecture of the *Chlamydomonas* chloroplast revealed by in situ cryo-electron tomography. elife 4:e04889

Evans LV (1966) Distribution of pyrenoids among some brown algae. J Cell Sci 1(4):449–454

Falkowski PG, Raven JA (2007) Photosynthesis and primary production in nature. In: Aquatic photosynthesis. Princeton University Press, Princeton, pp 319–363

Fang W, Si Y, Douglass S, Casero D, Merchant SS, Pellegrini M, Ladunga I, Liu P, Spalding MH (2012) Transcriptome-wide changes in *Chlamydomonas reinhardtii* gene expression regulated by carbon dioxide and the CO_2-concentrating mechanism regulator CIA5/CCM1. Plant Cell 24(5):1876–1893

Fathinejad S, Steiner JM, Reipert S, Marchetti M, Allmaier G, Burev SC, Ohnishi N, Fukuzawa H, Löffelhardt W, Bohmert HJ (2008) A carboxysomal carbon-concentrating mechanism in the cyanelles of the 'coelacanth' of the algal world, *Cyanophora paradoxa*? Physiol Plant 133:27–32

Fensome RA, Saldarriaga JF, Taylor M, R FJ (1999) Dinoflagellate phylogeny revisited: reconciling morphological and molecular based phylogenies. Grana 38:66–80

Ford TW (1984) A comparative ultrastructural study of *Cyanidium caldarium* and the unicellular red alga Rhodosorus marinus. Ann Bot 53(2):285–294

Fresnel J, Probert I (2005) The ultrastructure and life cycle of the coastal coccolithophorid *Ochrosphaera neapolitana* (Prymnesiophyceae). Eur J Phycol 40(1):105–122

Friedl T (1989) Comparative ultrastructure of pyrenoids in Trebouxia (Microthamniales, Chlorophyta). Plant Syst Evol 164(1–4):145–159

Gantt E, Conti SF (1965) The ultrastructure of *Porphyridium cruentum*. J Cell Biol 26(2):365–381

Gardin S, Krystyn L, Richoz S, Bartolini A, Galbrun B (2012) Where and when the earliest coccolithophores? Lethaia 45(4):507–523

Gee CW, Niyogi KK (2017) The carbonic anhydrase CAH1 is an essential component of the carbon-concentrating mechanism in *Nannochloropsis oceanica*. Proc Natl Acad Sci 114(17):4537–4542

Genkov T, Meyer M, Griffiths H, Spreitzer RJ (2010) Functional hybrid rubisco enzymes with plant small subunits and algal large subunits engineered rbcS cDNA for expression in *Chlamydomonas*. J Biol Chem 285(26):19833–19841

Gibbs SP (1962a) The ultrastructure of the pyrenoids of green algae. J Ultrastruct Res 7(3–4):262–272

Gibbs SP (1962b) Nuclear envelope-chloroplast relationships in algae. J Cell Biol 14(3):433–444

Giordano M, Beardall J, Raven JA (2005) CO_2 concentrating mechanisms in algae: mechanisms, environmental modulation, and evolution. Annu Rev Plant Biol 56:99–131

Goodenough UW (1970) Chloroplast division and pyrenoid formation in *Chlamydomonas reinhardtii* 1. J Phycol 6(1):1–6

Goodenough UW, Levine R (1970) Chloroplast structure and function in ac-20, a mutant strain of *Chlamydomonas reinhardtii*: III. Chloroplast, ribosomes and membranes organization. J Cell Biol 44(3):547–562

Gray J, Boucot AJ (1989) Is Moyeria a euglenoid? Lethaia 22(4):447–456

Griffiths DJ (1970) The pyrenoid. Bot Rev 36(1):29–58

Griffiths DJ (1980) The pyrenoid and its role in algal metabolism. Sci Prog 66:537–553

Griffiths H, Meyer MT, Rickaby RE (2017) Overcoming adversity through diversity: aquatic carbon concentrating mechanisms. J Exp Bot 68(14):3689–3695

Guillou L, Eikrem W, Chrétiennot-Dinet MJ, Le Gall F, Massana R, Romari K, Pedrós-Alió C, Vaulot D (2004) Diversity of picoplanktonic prasinophytes assessed by direct nuclear SSU rDNA sequencing of environmental samples and novel isolates retrieved from oceanic and coastal marine ecosystems. Protist 155(2):193–214

Guiry MD (2012) How many species of algae are there? J Phycol 48(5):1057–1063

Guiry MD, Guiry GM (2018) AlgaeBase [Internet]. World-Wide Electronic Publication, National University of Ireland, Galway

Hammel A, Zimmer D, Sommer F, Mühlhaus T, Schroda M (2018) Absolute quantification of major photosynthetic protein complexes in *Chlamydomonas reinhardtii* using quantification concatamers (QconCATs). Front Plant Sci 9:1265

Harris EH (2001) Chlamydomonas as a model organism. Annu Rev Plant Biol 52(1):363–406

Hedges SB, Blair JE, Venturi ML, Shoe JL (2004) A molecular timescale of eukaryote evolution and the rise of complex multicellular life. BMC Evol Biol 4(1):2

Heureux AM, Young JN, Whitney SM, Eason-Hubbard MR, Lee RB, Sharwood RE, Rickaby RE (2017) The role of Rubisco kinetics and pyrenoid morphology in shaping the CCM of haptophyte microalgae. J Exp Bot 68(14):3959–3969

Hibberd DJ, Norris RE (1984) Cytology and ultrastructure of *Chlorarachnion reptans* (Chlorarachniophyta division nova, Chlorarachniophyceae classis nova) 1. J Phycol 20(2):310–330

Hoef-Emden K, Archibald JM (2017) Cryptophyta (cryptomonads). In: Handbook of the protists. Springer, Cham, pp 851–891

Hoek CVD, Mann DC, Jahns HJ, Fogg GE (1996) Algae: an introduction to phycology. Nature 381(6584):660–660

Holdsworth RH (1971) The isolation and partial characterization of the pyrenoid protein of *Eremosphaera viridis*. J Cell Biol 51:499–513

Hoppenrath M, Yubuki N, Stern R, Leander BS (2017) Ultrastructure and molecular phylogenetic position of a new marine sand-dwelling dinoflagellate from British Columbia, Canada: Pseudadenoides polypyrenoides sp. nov.(Dinophyceae). Eur J Phycol 52(2):208–224

Hori T, Ueda R (1975) Phylogeny of algae. In: Tokida J, Hirose H (eds) Advance of phycology in Japan. Dr W. Junk b.v. Publishers, The Hague, pp 11–42

Ishida K, Green BR, Cavalier-Smith T (1999) Diversification of a chimaeric algal group, the chlorarachniophytes: phylogeny of nuclear and nucleomorph small-subunit rRNA genes. Mol Biol Evol 16(3):321–321

Janouškovec J, Gavelis GS, Burki F, Dinh D, Bachvaroff TR, Gornik SG, Bright KJ, Imanian B, Strom SL, Delwiche CF, Waller RF, Fensome RA, Leander BS, Rohwer FL, Saldarriaga JF (2017) Major transitions in dinoflagellate evolution unveiled by phylotranscriptomics. Proc Natl Acad Sci 114(2):E171–E180

Jin S, Sun J, Wunder T, Tang D, Cousins AB, Sze SK, Mueller-Cajar O, Gao YG (2016) Structural insights into the LCIB protein family reveals a new group of β-carbonic anhydrases. Proc Natl Acad Sci 113(51):14716–14721

Jinkerson RE, Jonikas MC (2015) Molecular techniques to interrogate and edit the Chlamydomonas nuclear genome. Plant J 82(3):393–412

Kaplan A (2017) On the cradle of CCM research: discovery, development, and challenges ahead. J Exp Bot 68(14):3785–3796

Karlsson J, Clarke AK, Chen ZY, Hugghins SY, Park YI, Husic HD, Moroney JV, Samuelsson G (1998) A novel a-type carbonic anhydrase associated with the thylakoid membrane in *Chlamydomonas reinhardtii* is required for growth at ambient CO_2. EMBO J 17:1208–1216

Karnkowska A, Bennett MS, Watza D, Kim JI, Zakryś B, Triemer RE (2015) Phylogenetic relationships and morphological character evolution of photosynthetic euglenids (Excavata) inferred from taxon-rich analyses of five genes. J Eukaryot Microbiol 62(3):362–373

Kawai H, Kurogi M (1992) A summary of the morphology of chloroplasts and flagellated cells in the Phaeophyceae. Korean J Phycol 7(1):33–43

Keeling PJ (2010) The endosymbiotic origin, diversification and fate of plastids. Philos Trans R Soc Lond B 365(1541):729–748

Kerfeld CA, Aussignargues C, Zarzycki J, Cai F, Sutter M (2018) Bacterial microcompartments. Nat Rev Microbiol 16:277–290

Kobayashi Y, Takusagawa M, Harada N, Fukao Y, Yamaoka S, Kohchi T, Hori K, Ohta H, Shikanai T, Nishimura Y (2015) Eukaryotic components remodeled chloroplast nucleoid organization during the green plant evolution. Genome Biol Evol 8(1):1–16

Komárek J, Marvan P (1992) Morphological differences in natural populations of the genus *Botryococcus* (Chlorophyceae). Arch Protistenkd 141(1–2):65–100

Kowallik K (1969) The crystal lattice of the pyrenoid matrix of *Prorocentrum micans*. J Cell Sci 5(1):251–269

Kuchitsu K, Tsuzuki M, Miyachi S (1988) Characterization of the pyrenoid isolated from unicellular green alga *Chlamydomonas reinhardtii*: particulate form of Rubisco protein. Protoplasma 144(1):17–24

Küken A, Sommer F, Yaneva-Roder L, Mackinder LC, Höhne M, Geimer S, Jonikas MC, Schroda M, Stitt M, Nikoloski Z, Mettler-Altmann T (2018) Effects of microcompartmentation on flux distribution and metabolic pools in *Chlamydomonas reinhardtii* chloroplasts. elife 7:e37960

Lavigne AC, Handley ER, Pollock SV, Somanchi A, Moroney JV (2002) Identification of Lci5, a novel *Chlamydomonas reinhardtii* gene induced under low CO_2 growth conditions. In: *Proceedings of the 12th international congress on photosynthesis*, vol 19. CSIRO Publishing, Collingwood

Le Bescot N, Mahé F, Audic S, Dimier C, Garet MJ, Poulain J, Wincker P, De Vargas C, Siano R (2016) Global patterns of pelagic dinoflagellate diversity across protist size classes unveiled by metabarcoding. Environ Microbiol 18(2):609–626

Lee RE (2018) Phycology. Cambridge University Press, Cambridge

Lenton A, Tilbrook B, Matear RJ, Sasse TP, Nojiri Y (2016) Historical reconstruction of ocean acidification in the Australian region. Biogeosciences 13(6):1753–1765

Leyon H (1954) The structure of chloroplasts: III. A study of pyrenoids. Exp Cell Res 6(2):497–505

Li X, Zhang R, Patena W, Gang SS, Blum SR, Ivanova N, Yue R, Robertson JM, Lefebvre P, Fitz-Gibbon ST, Grossman AR, Jonikas MC (2016) An indexed, mapped mutant library enables reverse genetics studies of biological processes in *Chlamydomonas reinhardtii*. Plant Cell 28:367–387

Ma Y, Pollock SV, Xiao Y, Cunnusamy K, Moroney JV (2011) Identification of a novel gene, CIA6, required for normal pyrenoid formation in *Chlamydomonas reinhardtii*. Plant Physiol 156:884–896

Mackinder LC, Meyer MT, Mettler-Altmann T, Chen VK, Mitchell MC, Caspari O, Freeman Rosenzweig ES, Pallesen L, Reeves G, Itakura A, Roth R, Sommer F, Geimer S, Mühlhaus T, Schroda M, Goodenough U, Stitt M, Griffiths H, Jonikas MC (2016) A repeat protein links Rubisco to form the eukaryotic carbon-concentrating organelle. Proc Natl Acad Sci 113(21):5958–5963

Mackinder LC, Chen C, Leib RD, Patena W, Blum SR, Rodman M, Ramundo S, Adams CM, Jonikas MC (2017) A spatial interactome reveals the protein organization of the algal CO_2-concentrating mechanism. Cell 171(1):133–147

Máguas C, Griffiths H, Ehleringer J, Serodio J (1993). Characterization of photobiont associations in lichens using carbon isotope discrimination techniques. In Stable Isotopes and Plant Carbon-Water Relations pp. 201–212. Academic Press

Máguas C, Griffiths H, Broadmeadow MSJ (1995) Gas exchange and carbon isotope discrimination in lichens: evidence for interactions between CO_2-concentrating mechanisms and diffusion limitation. Planta 196(1):95–102

Malviya S, Scalco E, Audic S, Vincent F, Veluchamy A, Poulain J, Wincker P, Iudicone D, De Vargas C, Bittner L, Zingone A, Bowler C (2016) Insights into global diatom distribution and diversity in the world's ocean. Proc Natl Acad Sci 113:E1516–E1525

Manton I (1966) Further observations on the fine structure of Chrysochromulina chiton with special reference to the pyrenoid. J Cell Sci 1(2):187–192

Martin W, Kowallik KV (1999) Annotated English translation of Mereschkowsky's 1905 paper 'Über Natur und Ursprung der Chromatophoren im Pflanzenreiche'. Eur J Phycol 34(3):287–295

Martin WF, Garg S, Zimorski V (2015) Endosymbiotic theories for eukaryote origin. Philos Trans R Soc B 370(1678):20140330

Matsuda Y, Hopkinson BM, Nakajima K, Dupont CL, Tsuji Y (2017) Mechanisms of carbon dioxide acquisition and CO_2 sensing in marine diatoms: a gateway to carbon metabolism. Philos Trans R Soc B 372(1728):20160403

McDonald KL, Pickett-Heaps JD (1976) Ultrastructure and differentiation in *Cladophora glomerata*. I. Cell division. Am J Bot 63:592–601

McKay RML, Gibbs SP, Vaughn KC (1991) Rubisco activase is present in the pyrenoid of green algae. Protoplasma 162(1):38–45

Medlin LK (2016) Evolution of the diatoms: major steps in their evolution and a review of the supporting molecular and morphological evidence. Phycologia 55(1):79–103

Melkonian M, Preisig HR (1984) An ultrastructural comparison between *Spermatozopsis* and *Dunaliell*a (Chlorophyceae). Plant Syst Evol 146(1–2):31–46

Merchant SS, Prochnik SE, Vallon O, Harris EH, Karpowicz SJ, Witman GB, Terry A, Salamov A, Fritz-Laylin LK, Maréchal-Drouard L, Marshall WF, Qu LH, Nelson DR, Sanderfoot AA, Spalding MH, Kapitonov VV, Ren Q, Ferris P, Lindquist E, Shapiro H, Lucas SM, Grimwood J, Schmutz J, Chlamydomonas Annotation Team, JGI Annotation Team, Grigoriev IV, Rokhsar DS, Grossman AR (2007) The Chlamydomonas genome reveals the evolution of key animal and plant functions. Science 318(5848):245–250

Meyer M, Griffiths H (2013) Origins and diversity of eukaryotic CO_2-concentrating mechanisms: lessons for the future. J Exp Bot 64(3):769–786

Meyer MT, Genkov T, Skepper JN, Jouhet J, Mitchell MC, Spreitzer RJ, Griffiths H (2012) Rubisco small-subunit α-helices control pyrenoid formation in *Chlamydomonas*. Proc Natl Acad Sci 109(47):19474–19479

Meyer MT, McCormick AJ, Griffiths H (2016) Will an algal CO_2-concentrating mechanism work in higher plants? Current Opinion in Plant Biology, 31:181–188

Meyer MT, Whittaker C, Griffiths H (2017) The algal pyrenoid: key unanswered questions. J Exp Bot 68(14):3739–3749

Mitchell MC, Meyer MT, Griffiths H (2014) Dynamics of carbon-concentrating mechanism induction and protein relocalization during the dark-to-light transition in synchronized *Chlamydomonas reinhardtii*. Plant Physiol 166(2):1073–1082

Mitchell MC, Metodieva G, Metodiev MV, Griffiths H, Meyer MT (2017) Pyrenoid loss impairs carbon-

concentrating mechanism induction and alters primary metabolism in *Chlamydomonas reinhardtii*. J Exp Bot 68(14):3891–3902

Miura K, Yamano T, Yoshioka S, Kohinata T, Inoue Y, Taniguchi F, Asamizu E, Nakamura Y, Tabata S, Yamato KT, Ohyama K, Fukuzawa H (2004) Expression profiling-based identification of CO_2-responsive genes regulated by CCM1 controlling a carbon-concentrating mechanism in *Chlamydomonas reinhardtii*. Plant Physiol 135(3):1595–1607

Morita E, Abe T, Tsuzuki M, Fujiwara S, Sato N, Hirata A, Sonoike K, Nozaki H (1998) Presence of the CO_2-concentrating mechanism in some species of the pyrenoid-less free-living algal genus Chloromonas (Volvocales, Chlorophyta). Planta 204(3):269–276

Morita E, Abe T, Tsuzuki M, Fujiwara S, Sato N, Hirata A, Sonoike K, Nozaki H (1999) Role of pyrenoids in the CO_2-concentrating mechanism: comparative morphology, physiology and molecular phylogenetic analysis of closely related strains of *Chlamydomonas* and *Chloromonas* (Volvocales). Planta 208(3):365–372

Müller OF (1782) Flora Danica, 5:15

Nagasato C, Motomura T (2002) New pyrenoid formation in the brown alga, *Scytosiphon lomentaria* (Scytosiphonales, Phaeophyceae). J Phycol 38(4):800–806

Nassoury N, Fritz L, Morse D (2001) Circadian changes in ribulose-1, 5-bisphosphate carboxylase/oxygenase distribution inside individual chloroplasts can account for the rhythm in dinoflagellate carbon fixation. Plant Cell 13(4):923–934

Nelson WA, Ryan KG (1988) *Porphyridium purpureum* (Bory) Drew et Ross (Porphyridiales, Rhodophyceae)—first record of a marine unicellular red alga in New Zealand. J R Soc N Z 18(1):127–128

Not F, Siano R, Kooistra WH, Simon N, Vaulot D, Probert I (2012) Diversity and ecology of eukaryotic marine phytoplankton. In: *Advances in botanical research*, vol 64. Academic, London, pp 1–53

Nozaki H, Onishi K, Morita E (2002) Differences in pyrenoid morphology are correlated with differences in the rbcL genes of members of the *Chloromonas* lineage (Volvocales, Chlorophyceae). J Mol Evol 55(4):414–430

Oborník M, Lukeš J (2015) The organellar genomes of *Chromera* and *Vitrella*, the phototrophic relatives of apicomplexan parasites. Annu Rev Microbiol 69:129–144

Ohad I, Siekevitz P, Palade GE (1967) Biogenesis of chloroplast membranes I. Plastid dedifferentiation in a dark-grown algal mutant (*Chlamydomonas reinhardtii*). J Cell Biol 35(3):521–552

Ohnishi N, Mukherjee B, Tsujikawa T, Yanase M, Nakano H, Moroney JV, Fukuzawa H (2010) Expression of a low CO_2-inducible protein, LCI1, increases inorganic carbon uptake in the green alga *Chlamydomonas reinhardtii*. Plant Cell 22:3105–3117

Osafune T, Sumida S, Ehara T, Hase E (1989) Three-dimensional distribution of ribulose-1, 5-bisphosphate carboxylase/oxygenase in chloroplasts of actively photosynthesizing cell of *Euglena gracilis*. Microscopy 38(5):399–402

Ota S, Vaulot D, Le Gall F, Yabuki A, Ishida K (2009) *Partenskyella glossopodia* gen. et sp. nov., the first report of a chlorarachniophyte that lacks a pyrenoid. Protist 160(1):137–150

Palenik B, Grimwood J, Aerts A, Rouzé P, Salamov A, Putnam N, Dupont C, Jorgensen R, Derelle E, Rombauts S, Zhou K, Otillar R, Merchant SS, Podell S, Gaasterland T, Napoli C, Gendler K, Manuell A, Tai V, Vallon O, Piganeau G, Jancek S, Heijde M, Jabbari K, Bowler C, Lohr M, Robbens S, Werner G, Dubchak I, Pazour GJ, Ren Q, Paulsen I, Delwiche C, Schmutz J, Rokhsar D, Van de Peer Y, Moreau H, Grigoriev IV (2007) The tiny eukaryote Ostreococcus provides genomic insights into the paradox of plankton speciation. Proc Natl Acad Sci 104(18):7705–7710

Palmqvist K (1993) Photosynthetic CO_2-use efficiency in lichens and their isolated photobionts: the possible role of a CO_2-concentrating mechanism. Planta 191(1):48–56

Palmqvist K, Máguas C, Badger MR, Griffiths H (1994) Assimilation, accumulation and isotope discrimination of inorganic carbon in lichens: further evidence for the operation of a CO_2 concentrating mechanism in cyanobacterial lichens. Cryptogam Bot 4:218–226

Patrone LM, Broadwater ST, Scott JL (1991) Ultrastructure of vegetative and dividing cells of the unicellular red algae *Rhodella violacea* and *Rhodella maculata* 1. J Phycol 27(6):742–753

Pickett-Heaps JD (1975) Green algae: structure, reproduction and evolution in selected genera. Sinauer Associates, Sunderland

Pronina NA, Semenenko VE (1992) Role of the pyrenoid in concentration, generation, and fixation of CO_2 in the chloroplast of microalgae. Sov Plant Physiol 39(4):470–476

Pröschold T, Marin B, Schlösser UG, Melkonian M (2001) Molecular phylogeny and taxonomic revision of Chlamydomonas (Chlorophyta). I. Emendation of *Chlamydomonas* Ehrenberg and *Chloromonas* Gobi, and description of

Oogamochlamys gen. nov. and Lobochlamys gen. nov. Protist 152(4):265–300

Qiu H, Yoon HS, Bhattacharya D (2016) Red algal phylogenomics provides a robust framework for inferring evolution of key metabolic pathways. PLoS Curr 8

Rae BD, Long BM, Badger MR, Price GD (2013) Functions, compositions, and evolution of the two types of carboxysomes: polyhedral microcompartments that facilitate CO_2 fixation in cyanobacteria and some proteobacteria. Microbiol Mol Biol Rev 77(3):357–379

Rae BD, Long BM, Förster B, Nguyen ND, Velanis CN, Atkinson N, Hee WY, Mukherjee B, Price GD, McCormick AJ (2017) Progress and challenges of engineering a biophysical CO_2-concentrating mechanism into higher plants. J Exp Bot 68(14):3717–3737

Raven JA (1991) Physiology of inorganic C acquisition and implications for resource use efficiency by marine phytoplankton: relation to increased CO_2 and temperature. Plant Cell Environ 14(8):779–794

Raven JA (1997) CO_2-concentrating mechanisms: a direct role for thylakoid lumen acidification? Plant Cell Environ 20(2):147–154

Raven JA (1998) The twelfth Tansley Lecture. Small is beautiful: the picoplankton. Funct Ecol 12:503–513

Raven JA, Richardson K (1985) Photosynthesis in marine environments. In: Baker NR, Long SP (eds) Photosynthesis in specific environments. Elsevier, Amsterdam

Raven JA, Osborne BA, Johnston AM (1985) Uptake of CO_2 by aquatic vegetation. Plant Cell Environ 8(6):417–425

Raven JA, Beardall J, Sánchez-Baracaldo P (2017) The possible evolution and future of CO_2-concentrating mechanisms. J Exp Bot 68(14):3701–3716

Rawat M, Henk MC, Lavigne LL, Moroney JV (1996) *Chlamydomonas reinhardtii* mutants without ribulose-1, 5-bisphosphate carboxylase-oxygenase lack a detectable pyrenoid. Planta 198(2):263–270

Rosenzweig ESF, Xu B, Cuellar LK, Martinez-Sanchez A, Schaffer M, Strauss M, Cartwright HN, Ronceray P, Plitzko JM, Förster F, Wingreen NS, Engel BD, Mackinder LCM, Jonikas MC (2017) The eukaryotic CO_2-concentrating organelle is liquid-like and exhibits dynamic reorganization. Cell 171(1):148–162

Schmid A-MM (2001) Value of Pyrenoids in the systematics of the diatoms: their morphology and ultrastructure. In: Proceedings of the 16th international diatom symposium. Amvrosiou Press, Athens, pp 1–32

Schmitz F (1882) Die Chromatophoren der Algen. Vergleichende untersuchungen über Bau und Entwicklung der Chlorophyllkörper und der analogen Farbstoffkörper der Algen. M. Cohen & Sohn (F. Cohen), Bonn

Shen C, Dupont CL, Hopkinson BM (2017) The diversity of CO_2-concentrating mechanisms in marine diatoms as inferred from their genetic content. J Exp Bot 68(14):3937–3948

Shih PM, Matzke NJ (2013) Primary endosymbiosis events date to the later Proterozoic with cross-calibrated phylogenetic dating of duplicated ATPase proteins. Proc Natl Acad Sci 110(30):12355–12360

Shiratori T, Fujita S, Shimizu T, Nakayama T, Ishida KI (2017) *Viridiuvalis adhaerens* gen. et sp. nov., a novel colony-forming chlorarachniophyte. J Plant Res 130(6):999–1012

Shively JM, Ball F, Brown DH, Saunders RE (1973) Functional organelles in prokaryotes: polyhedral inclusions (carboxysomes) of Thiobacillus neapolitanus. Science 182:584–586

Spalding MH, Portis AR (1985) A model of carbon dioxide assimilation in Chlamydomonas reinhardii. Planta 164(3):308–320

Spalding MH, Spreitzer RJ, Ogren WL (1983) Carbonic anhydrase-deficient mutant of *Chlamydomonas reinhardtii* requires elevated carbon dioxide concentration for photoautotrophic growth. Plant Physiol 73(2):268–272

Tanaka A, Nagasato C, Uwai S, Motomura T, Kawai H (2007) Re-examination of ultrastructures of the stellate chloroplast organization in brown algae: structure and development of pyrenoids. Phycol Res 55(3):203–213

Terashima M, Specht M, Naumann B, Hippler M (2010) Characterizing the anaerobic response of *Chlamydomonas reinhardtii* by quantitative proteomics. Mol Cell Proteomics 9(7):1514–1532

Tirumani S, Kokkanti M, Chaudhari V, Shukla M, Rao BJ (2014) Regulation of CCM genes in *Chlamydomonas reinhardtii* during conditions of light–dark cycles in synchronous cultures. Plant Mol Biol 85(3):277–286

Turkina MV, Blanco-Rivero A, Vainonen JP, Vener AV, Villarejo A (2006) CO_2 limitation induces specific redox-dependent protein phosphorylation in *Chlamydomonas reinhardtii*. Proteomics 6(9):2693–2704

Villarreal JC, Renner SS (2012) Hornwort pyrenoids, carbon-concentrating structures, evolved and were

lost at least five times during the last 100 million years. Proc Natl Acad Sci 109(46):18873–18878

Wang Y, Stessman DJ, Spalding MH (2015) The CO_2 concentrating mechanism and photosynthetic carbon assimilation in limiting CO_2: how *Chlamydomonas* works against the gradient. Plant J 82:429–448

Wang L, Yamano T, Takane S, Niikawa Y, Toyokawa C, Ozawa SI, Tokutsu R, Takahashi Y, Minagawa J, Kanesaki Y, Yoshikawa H, Fukuzawa H (2016) Chloroplast-mediated regulation of CO_2-concentrating mechanism by Ca^{2+}−binding protein CAS in the green alga *Chlamydomonas reinhardtii*. Proc Natl Acad Sci 113(44):12586–12591

Wunder T, Le Hung SC, Mueller-Cajar O (2018) Reconstitution of the liquid liquid phase separation underlying the microalgal Rubisco supercharger. Nat Commun 9:5076

Yamano T, Tsujikawa T, Hatano K, Ozawa S, Takahashi Y, Fukuzawa H (2010) Light and low-CO_2-dependent LCIB-LCIC complex localization in the chloroplast supports the carbon-concentrating mechanism in *Chlamydomonas reinhardtii*. Plant Cell Physiol 51:1453–1468

Yamano T, Asada A, Sato E, Fukuzawa H (2014) Isolation and characterization of mutants defective in the localization of LCIB, an essential factor for the carbon-concentrating mechanism in *Chlamydomonas reinhardtii*. Photosynth Res 121(2–3):193–200

Yamano T, Sato E, Iguchi H, Fukuda Y, Fukuzawa H (2015) Characterization of cooperative bicarbonate uptake into chloroplast stroma in the green alga *Chlamydomonas reinhardtii*. Proc Natl Acad Sci 112(23):7315–7320

Yamano T, Toyokawa C, Fukuzawa H (2018) High-resolution suborganellar localization of Ca^{2+} binding protein CAS, a novel regulator of CO_2-concentrating mechanism. Protoplasma 255:1–8

Yang EC, Boo SM, Bhattacharya D, Saunders GW, Knoll AH, Fredericq S, Graf L, Yoon HS (2016) Divergence time estimates and the evolution of major lineages in the florideophyte red algae. Sci Rep 6:21361

Yoon HS, Hackett JD, Ciniglia C, Pinto G, Bhattacharya D (2004) A molecular timeline for the origin of photosynthetic eukaryotes. Mol Biol Evol 21(5):809–818

Young JN, Hopkinson BM (2017) The potential for co-evolution of CO_2-concentrating mechanisms and Rubisco in diatoms. J Exp Bot 68(14):3751–3762

Zhan Y, Marchand CH, Maes A, Mauries A, Sun Y, Dhaliwal JS, Uniacke J, Arragain S, Jiang H, Gold ND, Martin VJJ, Lemaire SD, Zerges W (2018) Pyrenoid functions revealed by proteomics in *Chlamydomonas reinhardtii*. PLoS One 13(2):e0185039

Zhang J, Huss VA, Sun X, Chang K, Pang D (2008) Morphology and phylogenetic position of a trebouxiophycean green alga (Chlorophyta) growing on the rubber tree, *Hevea brasiliensis*, with the description of a new genus and species. Eur J Phycol 43(2):185–193

Zones JM, Blaby IK, Merchant SS, Umen JG (2015) High-resolution profiling of a synchronized diurnal transcriptome from *Chlamydomonas reinhardtii* reveals continuous cell and metabolic differentiation. Plant Cell 27(10):2743–2769

Part IV

Light-Harvesting Systems in Algae

Chapter 10

Light-Harvesting in Cyanobacteria and Eukaryotic Algae: An Overview

Anthony W D. Larkum*
Global Climate Cluster, University of Technology Sydney, Ultimo, NSW, Australia

Abbreviations

ATP	adenosine triphosphate
CAB	chlorophyll a/b binding protein
CAC	chlorophyll a/c binding protein
DCMU	3-(3,4-dichlorophenyl)-1,1-dimethylurea
Elips	early light-inducible proteins
Flvs	Flavodiiron proteins
Ga	billion years
Hlips	high light-inducible proteins
isiA	iron stress-induced protein A
LH	light-harvesting
LHC	light-harvesting complex
LHCSR	light-harvesting complex – stress related

*Author for correspondence, e-mail: a.larkum@sydney.edu.au

A. W. D. Larkum et al. (eds.), *Photosynthesis in Algae: Biochemical and Physiological Mechanisms*, Advances in Photosynthesis and Respiration 45, https://doi.org/10.1007/978-3-030-33397-3_10

MgDVP	Mg-2, 4-divinyl pheoporphyrin methyl ester
MSH	membrane spanning helix
NADP	nicotinamide adenine dinucleotide phosphate
pcb	prochlorophyte chlorophyll binding protein
PCP	peridin chlorophyll protein
PQ	plastoquinone
PSI	Photosystem I
PSII	Photosystem II
qE	fluorescence quenching due to energization of the thylakoid membrane
ROS	reactive oxygen species

I. Introduction

The Sun has been the provider of most of the energy to the biosystems of planet Earth ever since its formation (Larkum et al. 2018). Other sources of energy are from thermal reactions, radioactivity and inorganic chemical reactions, but these supply less than 1% of the total (Blankenship 2014) compared with the 99% provided by radiation from the sun. And of the Sun's radiation the greater proportion enters the biosystems of the Earth by photosynthesis and a much smaller percentage does so by energy conversion in rhodopsin, which powers photometabolic reactions in a number of bacteria, such as bacteriorhodopsin in *Halobacterium* and other genera of the Halobacteriaceae (Archaea) (Larkum et al. 2018).

Photosynthesis may also be almost as old a life itself, dating back at least 3.7 billion years (Ga) (Czaja et al. 2013). **Chlorophyll** (Chl) and **bacteriochlorophyll** (BChl) (Scheer 1991) are the two major pigment types in photosynthesis. These two pigment systems function both as primary pigments in the reaction centres and as light-harvesting pigments. With Chl there are 8 major light-harvesting systems (Larkum 2006) while in anoxygenic photosynthetic bacteria there are only five systems (Blankenship 2014). In Cyanobacteria, photosynthetic protists (algae) and land plants the photosynthetic systems of are primarily based on Chl *a*, although Chl *d* and Chl *f*, which have recently been found in certain cyanobacteria are also major photoactive pigments (Schliep et al. 2013; Nuernberg et al. 2018). All these organisms are capable of splitting water and forming oxygen in the biochemical process called **oxygenic photosynthesis** (Fig. 10.1). In contrast anoxygenic photosynthetic bacteria cannot split water to form oxygen and depend on other reactions to supply electrons to their reaction centres, which are either of Type 1 or Type 2 and never both as in oxygenic photosynthesis. There is a clear distinction also in that anoxygenic photosynthetic bacteria employ a number of BChls to carry out photosynthetic reactions [although Heliobacteria employ γ-bacteriochlorophyll, which, while it is a bacteriochlorophyll, i.e. possesses a bacteriochlorin ring, is close to chlorophyll in structure (Scheer 1991)].

Since anoxygenic photosynthetic bacteria have only one type of reaction centre (either RC1 type or RC2 type) it might be concluded that they are the "simpler" organisms and therefore that BChl preceded Chl on the early Earth. However, this logic has been challenged (Larkum 2006, 2008; Mulkidjanian et al. 2006; Cardona et al. 2019); it is quite possible that the early photosynthetic organisms possessed Chl, and had many similarities to cyanobacteria, even evolving localized concentrations of oxygen (Cardona et al. 2019). According to this view the pro-cyanobacterial organisms developed towards oxygenic photosynthesis over the billion years before the Great Oxidation Event (GOE) at 2.45 Ga (see below), with anoxygenic photosynthetic bacteria evolving from these earlier photosynthetic organisms, possibly in the period 3.5–2.0 Ga. After the GOE, anoxygenic photosynthetic bacteria which presumably would have been outcompeted by their more efficient oxygenic rela-

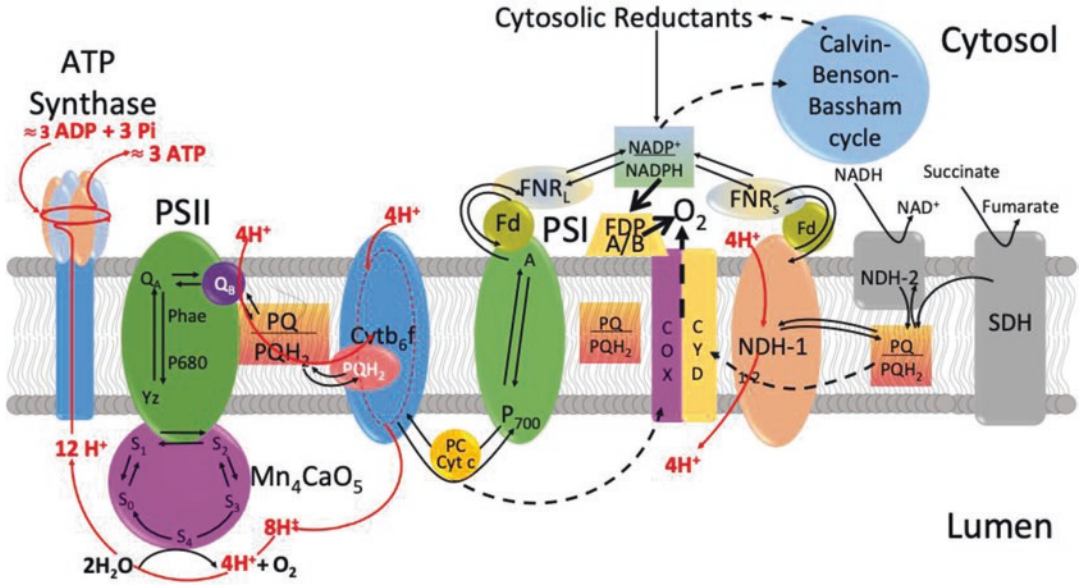

Fig. 10.1. A diagram of the generalised thylakoid membrane showing the major supercomplexes and pathways For simplicity the following pathways have been left out: Mehler-Ascorbate-Peroxidase Pathway and the formation of hydrogen peroxide; the chlororespiaratory pathway involving an Immutans oxygen-linked oxidase; other possible electron transport pathways across the thylakoid membrane that are known for cyanobacteria and play roles in balancing redox states in darkness and low light
PSI photosystem I, *PSII* photosystem II, *Mn_4CaO_5* oxygen evolving cluster, *SDH* sulphur dehydrogenase complex, *NDH-1* NADH dehydrogenase type 1, *NDH-2* NADH dehydrogenase type 2, *COX* cytochrome oxidase complex, *CYD* cytochrome b/d electron transport complex, *FNR* Ferredoxin NADP+ reductase, *Fd* Ferredoxin, *FDP* Flavodiiron protein (also known as Flv; at least two types: A/B & C/D), *PC* plastocyanin, Mn_4CaO_5 centre Oxygen evolving complex, *c* soluble cytochrome *c*, *Cyt b6/f* Cytochrome *b_6/f* complex, *P700* primary donor and acceptor of the PSI reaction centre, *PQ/PQH$_2$* Plastoquinone/reduced plastoquinone, acting as a shuttle for protons from the outside of the thylakoid membrane to the inside, *P680* primary donor of reaction centre II, *Yz* electron donor between Mn_4CaO_5 centre and P680, *Phae* phaeophytin *a* the primary acceptor of Reaction Centre II

tives, were forced to deal with a generally oxygenic environment and were pushed to the borders of habitable ecosystems, i.e. marginal habitats with low light, much of it relegated to the infrared region, and reducing conditions; although that a number of anoxygenic photosynthetic bacteria have evolved to live in aerobic environments.

It is remarkable that these two great realms of the photosynthetic world, on the one hand the cyanobacterial line leading to plastids and, on the other, anoxygenic PS bacteria do not share any similar light-harvesting systems, despite the fact that both groups have developed a wide, but not fully comprehensive, set of such pigment systems, to absorb energy from sunlight, and both share a joint origin of reaction centres (and marked similarities between Type1 and Type II reaction centres (Blankenship 2014)).

In the Cyanobacteria, eukaryotic algae and land plants, the light-harvesting systems are mainly based on the chlorophylls, with the notable exception of the phycobiliproteins (Toole and Allnutt 2003). The proteins interacting with the chlorophylls are surprisingly few: (a) the CAB proteins, (b) the relatives of the inner antennae complex (CP43 and CP47), and the novel peridinin chlorophyll complex (PCP) (see Fig. 10.2). In cyanobacteria a

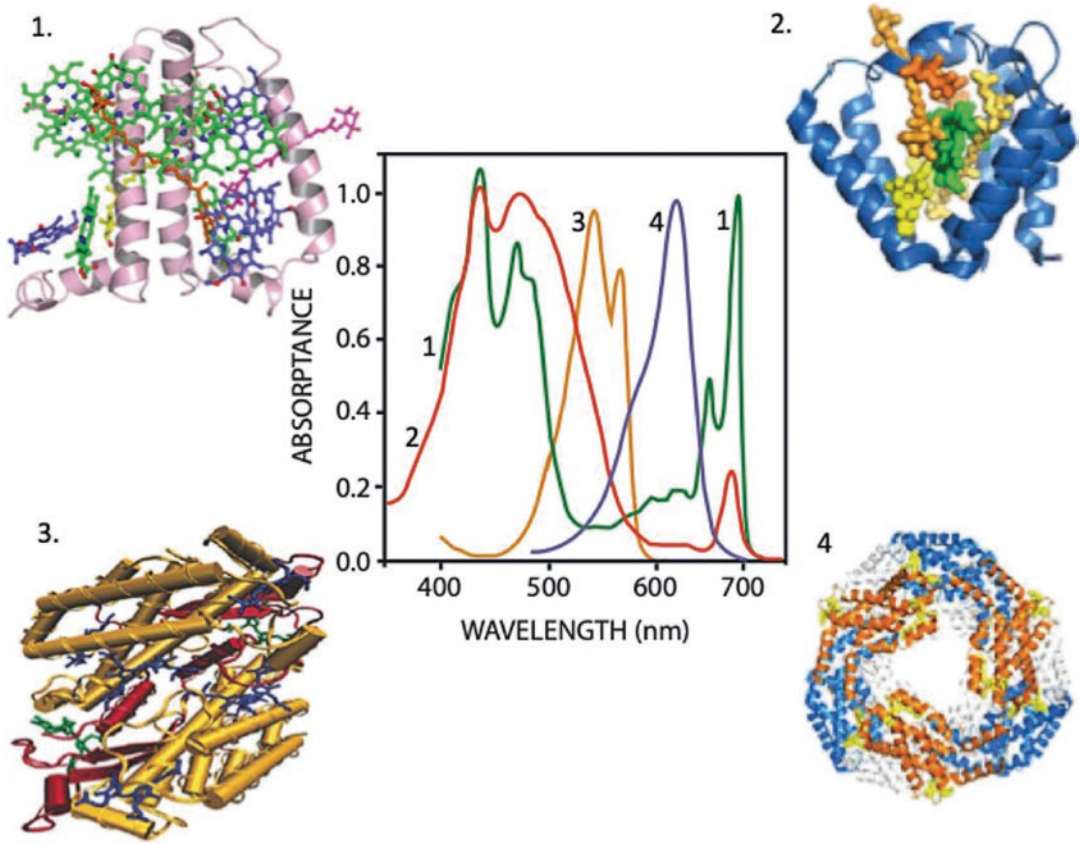

Fig. 10.2. Structure of the major light-harvesting complexes of eukaryotic algae and land plants. (1) LHCII; (2) The dinoflagellate Peridinin chlorophyll complex (PCP); (3) Phycobiliprotein subunit; (4) Novel phycoerythrin from the Cryptophyte *Chroomonas*. The detergent-extracted absorption spectra are shown in the central panel

light-harvesting ring of ~ 15 Chl *a/b*-binding antenna proteins or a ring of iron stress-induced A proteins surround a trimer of PSI centres in some species (see Zhang et al. 2010; and Sect. V) and contribute to light-harvesting. These proteins have a remarkable similarity to CP 47, from which they must have evolved. Phycobiliproteins are found in the cyanobacteria, red algae and cryptophyte algae (see below). In addition, the carotenoids have a large role to play in all photosynthetic systems (see below), although again there is little overlap between the carotenoids found in anoxygenic and oxygenic photosynthesis. For other reviews in this area the reader is referred to (Larkum and Barrett 1983; Larkum and Howe 1997; Larkum and Vesk 2003; Falkowski and Raven 2007; Hohmann-Marriott and Blankenship 2011; Blankenship 2014; Cardona et al. 2015, 2019).

II. The Photosynthetic Pigments of Cyanobacteria and Eukaryotic Algae

A. Chlorophylls

Chl *a*, and *b* were isolated and their chemical structure determined in the early twentieth century, Chl *c* was discovered in the late 1930's and Chl *d* in 1944 (see Larkum and Barrett 1983; Falkowski and Raven 2007); Chl *d* was not fully recognized until its redis-

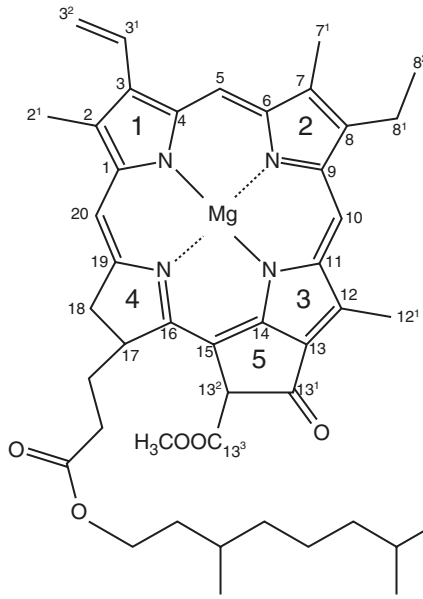

	Side chain position of formyl group	Chl biosynthesis O_2 dependent	Q_3 *(methanol)*	e^- donor in reaction centre
Chl *a*	-	yes	665 nm	yes
BChl *a*	C3	no	775 nm	yes
Chl *b*	C7	yes	650 nm	no
Chl *c1*	-	yes	630 nm	no
Chl *c2*	-	yes	630 nm	no
Chl c3	-	yes	626 nm	no
Chl *d*	C3	yes	696 nm	yes
Chl *f*	C2	unknown	706 nm	unknown

Chl *b* (C7:CHO)
Chl *d* (C3:CHO)
Chl *f* (C2:CHO)
Chl *c1* (C17: C_2H_2COOH, C18: CH_3)
Chl *c2* (C8: C_2H_3, C17: C_2H_3COOH, C18: CH_3)
Chl *c3* (C8: C_2H_3, C17: $C_2H_3COOH_3$, C18: CH_3)
BChl *a* (C3: $CHOCH_3$, C18: CH_3)

Fig. 10.3. Chemical structures and in vivo absorption spectra of Chls *a*, *b*, *c*, *d* and *f*

covery in the cyanobacterium, *Acaryochloris marina* (Miyashita et al. 1996) (Fig. 10.3). Chl *f* was discovered in a cynaobacterium of modern stromatolites from Shark Bay, Western Australia (Chen et al. 2010). With a peak *in vivo* of 735–740 nm Chl *f* can absorb light further into the NIR than Chl *d* and it has now been shown to take on a photochemical role (Nuernberg et al. 2018), but so far has only been found in rather small amounts when the algae that contain it are grown under NIR (Gan et al. 2014).

1. Chlorophyll a

Chls *a* (see Fig. 10.3) was until recently regarded as the major photoactive pigment in photosynthesis being present in the reaction centres (RCs) of Photosystem I (PSI) and Photosystem II (PSII). In RCI, which is a protein heterodimer, Chl *a* forms a special pair called P700, which is the primary donor for charge separation across the thylakoid membrane. A modified Chl *a*, Chl a_o, also acts as the special acceptor of P700. In RCII, which is also a heterodimer, a special pair of Chl *a*, P680, (attached to the polypeptides D1 and D2), acts as the primary donor and a Phaeophytin *a* (Phaeo *a*) molecule acts as the primary acceptor. In distinction to RCI, however, there is only one pathway across the thylakoid membrane and a second Phaeo *a* molecule is not used in electron transport. There are other Chls in D1 and D2 and the total is 6, in addition to phaeophytin *a*. Also there are other Chl *a* molecules in RCII; these are bound to two special proteins, which act as inner antennae, channeling excitation energy from the light-harvesting antennae to P680. These proteins are known as CP43 and CP47 and each binds 9–12 Chl *a* molecules. CP43 must be a very ancient molecule, (i) because it is phylogenetically linked to the light-harvesting part of Type I RC proteins, and (ii) because it has important structural linkages to the Mn_4CaO_5 oxygen-evolving centre (Cardona et al. 2019).

In addition to these roles in electron transport, Chl *a* is a major pigment in light-harvesting. As will be explained below a major protein family of light-harvesting chlorophyll protein complexes emerged in

Cyanobacteria and in most plastids of eukaryotic algae and land plants is found as the light-harvesting chlorophyll protein complex (LHC); the exception here is the Glaucophyta (see Fig. 10.6), which have only precursors to LHC (Fig. 10.13). It should also be noted that the LHCs also bind Chl *b* (or Chl *c*; see below). Furthermore, apart from the Prochlorophytes (see below), Cyanobacteria employ a second system of light harvesting the phycobiliproteins, that are assembled into phycobilisomes (see below), that absorb green light efficiently and pass energy on to both PSI and PSII. This evolutionary development largely replaced the need for LHC proteins, but likely evolved after the evolution of LHCs and their precursors (see below).

Chl *a* is also modified in prochlorophyte algae, most notably *Prochlorococcus marinus* and allied taxa, to Chl a_2 (8-desethyl, 8-vinyl chlorophyll a) (Goericke and Repeta 1992) which modifies the blue absorption band to absorb at 442 nm. Chl *b* is also modified to Chl b_2, a divinyl form, with an absorption peak at 478 nm, and this leads to a more optimal profile for absorbing the blue light of oceanic water.

The primary role of Chl *a* has recently been challenged by the demonstration that Chl *d* is the major photoactive pigment in the cyanobacterium, *Acaryochloris marina* (Larkum 2006; Itoh et al. 2007), Chl *d* replacing Chl *a* in the RCs with the exception that RCII still employs phaeophytin *a* rather than phaeophytin *d*. Furthermore, Chl *f* has also been shown to be photoactive in RCI and RCII of *Chroococcidiopsis* (Nuernberg et al. 2018). Chl *d* and *f* are found in organisms that rely on near infra-red (NIR) radiation for photosynthesis. It is therefore pertinent to enquire as to when these pigments and their dependent photosynthetic systems evolved? Chl *a* or protochlorophyllide *a* are the precursors to the biosynthesis of Chl *d* or Chl *f* and in both cases the addition of oxygen is required to form a formyl bond (at position R_2 or R_3, respectively) – see Fig. 10.3 and Chap. 5). In the case of Chl *d* the exact set of reactions is not known. But in the case of Chl *f* it has been shown that this reaction is catalyzed by a protein, which has a metallic centre very similar to that of the Mn_4CaO_5 of water splitting (Ho et al. 2016a, b, c). This would suggest that Chl *f* is a very ancient pigment dating back to perhaps 2.4 Ga. However, Chl *a* would likely still have preceded evolutionarily.

2. *Chlorophyll b*

Chlorophyll *b* (Fig. 10.3) is found in land plant plastids and in the plastids of a variety of "green algae", most notably the Chlorophyceae (including Trebouxiophyceae, Ulvophyceae and, recently, Palmophyllophyceae (Leliaert et al. 2016)), Euglenophyceae, Chlorarachniophyceae, Prasinophyceae, Rhizariaceae; also in this group are the streptophyte algae, including Characeae, a group of Chlorophyceae that have many features linking them to embryophyte land plants (see e.g. Turmel et al. 2013).

Chl *b* only functions as a light-harvesting pigment and it is only found in light-harvesting proteins. In the LHCs of eukaryotic algae and land plants, Chl *b* is bound in roughly similar proportions to Chl *a*, and with a total number of Chls of 12–15. The absorption peaks of Chl *b* are sufficiently separated from those of Chl *a* that it can significantly enhance the light absorption efficiency (see Fig. 10.2). However, as with Chl *c* (see below), the blue absorption peak which in comparison to Chl *a* at 436 nm is shifted to 465 nm absorbs in a region of the spectrum where many carotenoids also absorb. As we shall see below carotenoids are very efficient light-harvesting pigments and so it is not clear why Chl *b* seems to serve such an important light-harvesting function; although it must be pointed out that in the red region of the spectrum Chl *b* absorbs at a significantly different peak wavelength to Chl *a* (652 nm vs 680–720 nm).

Chl *b*, or Chl b_2, is also found in a small number of cyanobacteria: *Prochlorococcus*, *Prochlorothrix* and *Prochloron*). However, the prochlorophyte Chl *a/b* binding (Pcb) proteins are quite different in structure to the LHCs (Herbstova et al. 2010; La Roche et al. 1996). In *Prochlorococcus marinus* as mentioned above (see Chl *a*), and in allied taxa, Chl *b* is modified to the divinyl form, which shifts it absorption peak to 478 nm. This clear evolutionary development to modulate the absorption peak to a longer wavelength indicates that notwithstanding the efficiency of carotenoids in absorbing blue to blue-green light there is benefit in *Prochlorococcus marinus*, and in allied taxa, in changing the wavelength of absorption from Chl *b* to Chl b_2.

3. *Chlorophyll c and MgDVD*

The forms of Chl *c* have a Soret (blue) band not far higher than Chl *a* with peaks at 447 nm (solvent acetone) for Chl c_1, 450 nm for Chl c_2, and 452 nm for Chl c_3 (Zapata and Garrido 1997). These wavelengths are not far from the Soret peak for Chl *a* (436 nm); furthermore, considering the fact that the *in vivo* Q_Y band peak (≈630 nm) is very small, it is pertinent to ask whether they serve any light-harvesting role? However, as shown in Larkum et al. 2018 the blue absorptance peak of Chl *c*-containing organisms (*Isochrysis* and *Chaetoceros*) is conspicuously wider than in *Synechococcus* which only has Chl *a* and phycocyanin. The chlorophyte alga *Chlorella* with Chl *a* + Chl *b*, also has a much wider blue absorptance band than *Synechococcus*. The Q_Y band for Chl *b* is, however, strong and well separated from the Chl a band (645 nm vs. 665 nm, in acetone). So Chl *b* certainly serves as an efficient light-harvesting pigment in the light-harvesting chlorophyll (LHC) proteins (see Figs. 10.2 and 10.3). Chlorophyll binding proteins in the LHC family also occur in Chl *c*-containing algae and bind several Chl *c* molecules per protein. So a light-harvesting role seems certain (and the same applies to MgDVP, see below).

Nevertheless the above facts suggest that the Chl *c* pigments might perform another role in light harvesting? And the mere fact that there are three major Chls *c*, other less well Chl *c* variants and magnesium 2,4-divinyl pheoporphyrin monomethyl ester A5 (MgDVP) may suggest that they perform some other function or act in association with some special carotenoids (such as fucoxanthin in Phaeophyceae and peridinin in dinoflagellates).

MgDVP is very close to the Chls *c* biosynthetically and in molecular structure, and lies on the biosynthetic pathway to all BChls and Chl *c* ((Hunter and Coomber 1988; Burke et al. 1993) and has a Soret peak very close to that of the Chls *c*. It is found in a few chlorophyte planktonic algae in the Prasinophyceae (Rowan 1989; Kantz et al. 1990; Zingone et al. 2002; Latasa et al. 2004) and the Palmophyllophyceae (Leliaert et al. 2016) and as discussed below in two prochlorophyte algae (*Prochlorococcus* and *Prochloron*. Raven (1984, 1996) concluded that MgDVP and by implication Chls *c* do contribute to a significant degree to light harvesting in those light-harvesting chlorophyll protein complexes (LHC) where MgDVP and Chls *c* occur. Other authors, *e.g*. Larkum (2008), have speculated that these pigments play a role in energy migration from the pigment perhaps *via* specific carotenoids to the reaction centres. The latter possibility would go some way to explain why there are such a variety of Chl *c* types.

The various types of Chl *c* are found in a wide range of eukaryote chromist (chromealveolate) algae (Larkum 2006; Chap. 2), *i.e*. those algae that do not possess Chl *b* and, apart from the Cryptophyceae, do not possess PBP: the chromists (chromealveolates) are the Cryptophyta, Haptophyta, and Ochrista (= Ochrophyta) (*e.g*. brown alga and diatoms), as well as the basal, peridinin-containing, Dinoflagellata (Pyrrophyta), also including dinoflagellates with diatom tertiary endosymbiotic plastids (see Fig. 10.7 and Sect. 3). Two exceptions here are the cryptophytes which possess Chl c_2 and PBP (Larkum 2006) and

Prochloron (one of the Chl *b*-containing cyanobacteria) that also possesses MgDVP (Larkum et al. 1994). MgDVP is also found in a number of species of the Chl *b*-containing Prasinophyceae (formerly Micromonadophyceae;; Rowan 1989; Fawley 1992; Zingone et al. 2002; Latasa et al. 2004) and Palmophyllophyceae (a new group of early chlorophytes allied to the Prasinococcales and separate from the Prasinophyceae; Leliaert et al. 2016; Chap. 2).

MgDVP also occurs in the Chl *d*-containing cyanobacterium *Acaryochloris marina* ((Miyashita et al. 1997; Schliep et al. 2008), so it is now apparent that it is a rather widespread pigment in Chl *b,* Chl *c* and Chl *d*-containing algae. The PBP of Cryptophytes, however, is not in the form of a phycobilisome (see below) as is found in glaucophytes, rhodophytes, and cyanobacteria (Kaňa et al. 2009, Graham et al. 2016), but is present in a special light-harvesting antenna (Wilk et al. 1999). As mentioned above, the possession of Chl *b* in only one of the three groups, which possess primary plastids poses a problem for the proposition of a monophyletic origin of plastids; and the same is true for Chl *c* which is not present in any of the three primary plastid lines.

One possible evolutionary explanation for Chl *c* is that it arose, alongside the special carotenoids that such algae possess *de novo* to satisfy special absorption criteria; any such benefit would more likely involve blue light absorption (Soret band) rather than of 630 nm light (see Larkum et al. 2018); consistent with a rather late invasion of the oceans.

Chl *c* could have evolved independently of the evolution of the primary plastids. The shopping bag model for the evolution of plastids envisages that a good deal of variation arose at an early stage of plastid evolution (Larkum et al. 2007). Chl *c* could have been a later evolutionary event, perhaps coincident with the population of the oceans with phytoplanktonic lines. The fact that two groups of algae, the dinoflagellates, and cryptophytes have only Chl c_2 whereas the other groups that possess Chl *c* have Chl c_1 and c_2 (as well as, in some instances, Chl c_3) suggests that Chl c_2 evolved first: and this fits with the biosynthetic pathway in which Chl c_2 is a precursor to Chl c_1 (Larkum 2003, 2006). However, the fact that dinoflagellates, and cryptophytes lie on very different positions on the phylogenetic tree suggest rather that Chl c_1 has been lost subsequent to the earlier evolution of both these two forms (Fig. 10.6). Chl *c* does not usually have a phytol tail (but such forms exist in some eukaryotic algae, but not in any prokaryote with MgDVP); and this may suggest the independent evolution of light-harvesting MgDVP from Chl *c* (Zapata and Garrido 1997). As is the case in many organisms of obvious Chl *a* + *b* affinities, there are examples of chromophytes completely lacking Chl *c* such as the Eustigmatophyceae (*e.g. Nannochloropsis*) and chromerids such as *Chromera* and *Vitrella* (Pan et al. 2012). In the Apicomplexans, Chls have been lost altogether; however, loss of all Chl is not restricted to chromophytes, and is found in chlorophytes, *e.g. Prototheca*, *Polytoma*, and *Polytomella*. Thus the loss of photoautotrophy is a common secondary evolutionary event across the algae.

4. Chlorophyll *d*

Chlorophyll *d* was first discovered associated with red algae in 1943 by Manning and Strain. It was rediscovered as a pigment of a new cyanobacterium named *Acaryochloris marina* in 1996 (Miyashita et al. 1996; see also Miyashita et al. 2003) and the original observation of 1943 is best explained as the presence of *Acaryochloris marina* on the red algae that were sampled for chlorophyll analysis (see Murakami et al. 2004).

The unique Chl *d* (Fig. 10.3) serves a similar function to Chl *a* in that it functions as both a redox active special pair substituting for Chl *a* in the equivalent position of P680 (possibly at 713 nm) and P700 (P740) of cyanobacteria that possess it and additionally as a light-harvesting pigment (Larkum 2006;

Telfer et al. 2007; Mohr et al. 2010). Chl *d* replaces Chl *a* in the reaction centres, except that phaeophytin *a* is needed as the primary (acceptor of the special pair, P697) of PSII; and phaeophytin *a* is synthesised from Chl *a*, therefore requiring the formation of a small amount of Chl *a*. Apart from that and a small metabolic pool of Chl *a*, *Acaryochloris marina* seems to be able to function with mostly Chl *d* (up to ~97%); with Chl *d* also acting as a light-harvesting Chl with its own Chl *d* protein (Chen et al. 2005). The relative abundance of Chl *d* (the Chl *a/d* ratio) varies from 0.01 to 0.1 depending on the light regime under which *Acaryochloris* is grown (Miyashita et al. 1996; Chen et al. 2005; Gloag et al. 2007; Chen 2014). It has been suggested that Chl *a* may act as primary acceptor in PSI of *Acaryochloris*, as well as in PSII, but this matter is still under debate (Tomo et al. 2011). For the *in vivo* absorptance of *Acaryochloris* compared to *Synechococcus* (Chl *a*) and *Chlorella* Chl (*a* + *b*)] *see* Larkum et al. (2018). Chl *d* is synthesised from Chl *a* by substituting a methyl group on position C5 of ring A with a hydroxyl group with the oxygen derived from O_2 (*see* Fig. 10.3) (Schliep et al. 2010). How this oxygen is added is not known, but *see* Loughlin (2014).

5. *Chlorophyll f*

Chl *f* (Fig. 10.3) was discovered in a filamentous cyanobacterium from living stromatolite material collected from intertidal columnar (smooth) stromatolites from Hamelin Pool, Shark Bay, Western Australia (Chen et al. 2010; Niedzwiedzki et al. 2014; Akimoto et al. 2015). It has since been found in a number of other cyanobacteria, both filamentous and globular (Chen 2014; Itoh et al. 2015). It is found in hot spring cyanobacteria and a number of the latter organisms have been well researched by Bryant and his group (Ho et al. 2016a, 2017), who have shown that Chl *f* is induced under far-red light (Ho et al. 2016a).

The final synthetic step in Chl *f* synthesis, the addition of oxygen to a C3 methyl to form a formyl group (Fig. 10.3) has been proposed to be brought about by a primitive form of D1 protein (Ho et al. 2016b; see also Trinugroho et al. 2020). In all those organisms containing it, Chl *f* constitutes only a small proportion of the total Chl (<10%), the rest being Chl *a*; and the formation of Chl *f* is NIR-dependent, *i.e.* the amount of Chl *f* in white light is very small (Ho et al. 2016a). While most of the Chl *f* functions in a light-harvesting role (Chen 2014) it has recently been shown that Chl *f* is also found in the Reaction Centres of PSI and PSII (Nuernberg et al. 2018), where it takes on a photoactive role. The light-harvesting energy transfer mechanisms have been studied by Li et al. (2012) and Akimoto et al. (2015) and the structure of Chl *f* has been presented by Willows et al. (2013). Details on the evolution of this pigment are not known. It has a red-shifted Q_Y peak at 707 *vs.* 696 nm for Chl *d* (in organic solvents) (Chen et al. 2010), which means that it is able to function further into the NIR than Chl *d*, i.e. up to 760 nm, but this depends on conjugation to specific proteins.

In natural light fields the cyanobacteria, which have the ability to make Chl *f*, synthesise almost exclusively Chl *a*. It is only in near-infra red (NIR) radiation (>700 nm) that these organisms synthesise Chl *f* (Ho et al. 2016a). Clearly, this is a response to the altered radiation field. It is still not known how they function under these circumstances. With the discovery of Chl *f* in the RCs of PSII and PSI, it is possible that under NIR Chl *f* powers both the RCs and light-harvesting mechanisms. However, the full elucidation will have to wait for further work.

6. *Summary Comments on the Chlorophylls*

Of all the known Chls, Chl *a* has ranked supreme until recently, taking on the photochemical role in both PSI) and PSII), and featuring in light-harvesting antennae in almost

all algal groups. Chl *a* has a Soret peak at 436 nm (*in vivo*) and Q_Y peaks at 680–700 nm (*in vivo*) and is a good photosynthetic pigment for visible light, but needs augmentation in the blue, green, orange and near-infra red regions of the spectrum. However, the supremacy of Chl *a* has recently been challenged by Chl *d* (and to a limited extent Chl *f*) which appear to replace Chl *a* in a photochemical role in PSI and PSII of *Acaryochloris marina* (Schliep et al. 2013) and in *Chroococcidiopsis* (Nuernberg et al. 2018) (in *Chroococcidiopsis* Chl *f* is present in much smaller proportions than Chl *a*; nevertheless Chl *f* is the major pigment in the RCs under NIR). In *A. marina* the only known role for Chl *a* in the photosystems is the apparent need for one molecule of Chl *a* in PSII where it is converted to phaeophytin *a* and acts as the primary acceptor. Nevertheless, Chl *a* probably dominates in all known oxygenic photosynthetic organisms except for *Acaryochloris marina*, and, under NIR, Chl *f*; so *Acaryochloris marina*, constitutively, and *Chroococcidiopsis* spp., under NIR, likely eke out a restricted role in environments where mainly near-infra red (NIR) light (700–750 nm) predominates (note also that this is a region where some BChls in anoxygenic photosynthetic bacteria provide photosynthetic activity).

B. Carotenoids

The carotenoids in algae are very diverse (Fig. 10.4 and Table 10.1) and very different from those in anoxygenic bacteria. The difference may be partly due to the fact that they have to exist in a highly oxidising environment, evidenced by the fact that where anoxygenic

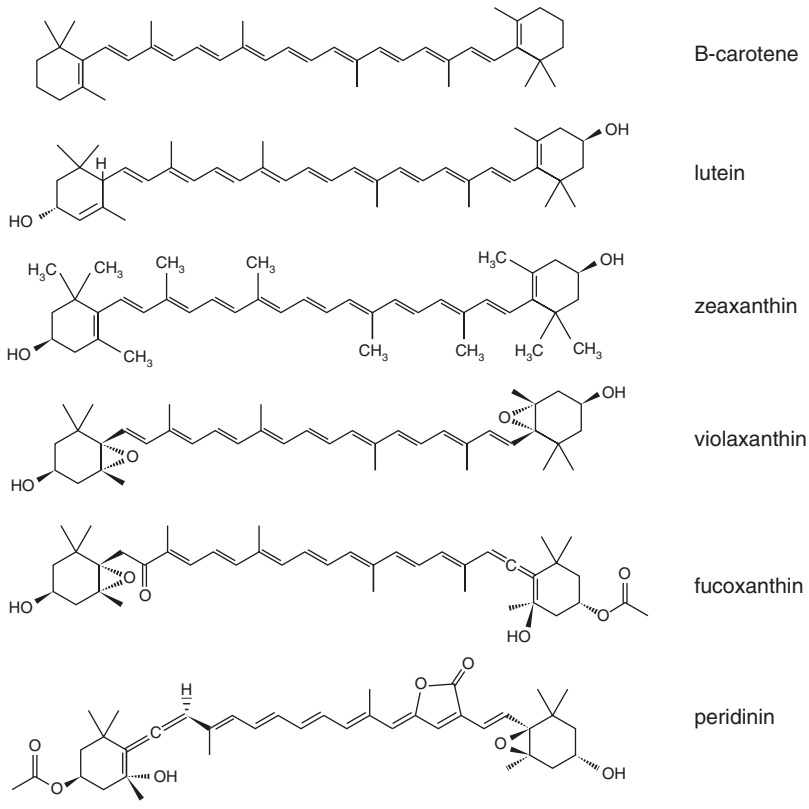

Fig. 10.4. Chemical structures of some of the more important carotenoids

Table 10.1. Absorption maxima of the carotenoids and specific absorption coefficients

Carotenoid	Absorption maxima			Ref.	$E^{1\%}_{1cm}$
Acetone					
Alloxanthin	(430)	453	483	7	–
Astaxanthin	–	472–480	–	13	
Canthaxanthin	–	466	–	20	
α-carotene	420–425	442–448	469–476	4	
β-carotene	420–432	449–454	475–480	4	
γ-carotene	(439)	461	491	15	
β-carotene 5,6 epoxide	(420–427)	441–448	470–75	4	
β-cryptoxanthin	(427–429)	450–453	475–478	4	
Cryptoxanthin depoxide	419	443	472	4	
Diadinoxanthin	(426–430)	448–449	478–479	4	2230
Diatoxanthin	(429–434)	448–454	477–482	4	
Dinoxanthin	418	442	470	21	
Echinenone	475	459–460	–	16	
Fucoxanthin	(425–428)	444–449	467–473	4, 6	1600
19’ Hex fucoxanthin	423	445–450	471–478	3	
Loroxanthin	(423)	446	473	18	
Lutein	(420)	445	473	25	
Lycopene	447–448	472–475	504–506	1, 13	
Myxoxanthophyll	450–452	475–478	508–510	13, 20	2160
Neoxanthin	413–423	436–445	463–473	5, 25	
Oscillaxanthin	466–470	490–499	522–534	16, 17	
Peridinin		465–471		6, 21	1340
Vaucherioxanthin	420	441	467	24	
Violaxanthin	401–417	440–442	469–470	24, 25	2400
Zeaxanthin	(424–425)	449–452	474–479	9, 13	2340
Hexane					
Alloxanthin	(427)	451	480	7	
Astaxanthin		466–468		9	2100
Canthaxanthin		467		9, 13	2035
α-carotene	420–422	442–445	473–479	9, 13	2710
β-carotene	423–429	447–451	472–476	13, 19	2592
γ-carotene	431–437	460–462	489–494	13, 19	2760
β-carotene 5,6 epoxide	423	444	473	9	
β-Cryptoxanthin	(422–425)	446–452	475–480	9, 19	2460
Cryptoxanthin epoxide	416	439	470	9	
Diadinoxanthin	(421–424)	439–442	470–471	13, 21	2110
Diatoxanthin		447–450	475–479	8, 13	
Dinoxanthin	416	439–442	470–471	13, 22	
Echinenone	(432)	459	483	9, 13	
Fucoxanthin	425–427	449–450	476–478	9, 13	1600
19′ Hex fucoxanthin					
Lutein	420	443–445	472–475	13, 23	
Lycopene	443–448	471–476	501–507	9, 13	3450
Myxoxanthophyll					
Neoxanthin	412–416	435–439	484–490	9, 13	

(continued)

Table 10.1. (continued)

Carotenoid	Absorption maxima			Ref.	$E^{1\%}_{1cm}$
Oscillaxanthin					
Peridinin	(431)	454–457	475	9, 13	
Vaucherioxanthin					
Violaxanthin	416–418	439–443	469–473	9, 19	
Zeaxanthin	(425–429)	447–450	474–480	9, 13	2340

(i) Shoulders shown in parentheses
(ii) Two solvents (acetone and hexane) for other solvents see Rowan (1989)
(iii) References:
1. (Aasen and Liaaen-Jensen 1966); 2. (Aihara and Yamamoto 1968); 9, 3. (Arpin et al. 1976); 10, 4. Berger et al. 1977; 12, 5. (Bjørnland 1982); 16, 6. (Bjørnland and Tangen 1979); 23, 7. (Cheng et al. 1974); 26, 8. (Davies et al. 1984); 28, 9. (Davies 1965); 31, 10. (Eskins et al. 1977); 32, 11. (Fiksdahl et al. 1984a); 33, 12. (Fiksdahl et al. 1984b); 35, 13. (Foppen 1971); 36, 14, 15. (Foss et al. 1984); 37, 39, 16. (Francis and Halfen 1972); 40, 17. (Francis et al. 1970); 41, 18. (Francis et al. 1973); 46, 19. (Hager and Meyer-Bertenrath 1966); 50, 20. (Halfen and Francis 1972); 68, 21. (Johansen et al. 1974); 73. 22. (Loeblich and Smith 1968); 76, 23. (Mues et al. 1973); 78, 24. (Norgard et al. 1974); 82, 25. (Renstrom et al. 1981); 88, 26. (Skjenstad et al. 1984)

PS bacteria exist in aerobic environments the carotenoids are very different again (Takaichi 2011). The carotenoids of phytoplanktonic algae have recently been surveyed in depth and have revealed greater details of their structure and distribution, but the taxonomic features of previous work was upheld (Serive et al. 2017).

The carotenoids are divided into carotenes, which are hydrocarbon chains with no oxygen, whereas xanthophylls have one oxygen atom or more in the hydrocarbon chain.

1. Carotenes

Carotenes (Fig. 10.4, β-carotene) are unsaturated straight hydrocarbons chains with cyclisation at one end or at both ends; they generally have chain lengths of ~20. Lycopene (not shown) is a straight chain unsaturated hydrocarbon of chain length 30. α- and β-carotenes have a cyclised head group and 40 carbons and are differentiated by the head groups, being either α-ionone and β-ionone (α) or both β-ionone (β). They play a role in light-harvesting but have specific taxonomic differentiation between algal groups; for example α-carotenes are found in many Rhodophyceae (but not all), Cryptophyceae (not all) and Glaucophyceae (not all), all of which have phycobiliproteins: in contrast Cyanobacteria have phycobiliproteins but do not have α-carotenes; they are also present in some prochlorophytes (Partensky and Garczarek 2003) and some algae with green affiliations (Larkum and Barrett 1983; Larkum and Howe 1997). Most other cyanobacteria and algae have β-carotenes (but see Serive et al. 2017).

Carotenes also quench the triplet states generated by chlorophyll and are present in antenna proteins and in RC1; however, in RCII the redox potential generated by P680 is so large that any carotene placed near to the reaction centre would be oxidized; so carotenes are not present here and triplet states generate singlet oxygen, which is why D1 protein is the protein with the highest rate of turnover of all photosynthetic proteins (Andersson and Aro 2001). Nevertheless there are plenty of carotenes in the LHCs of PSII. As discussed in Section, the xanthophylls play an important role in down-regulation of photosynthesis (principally Non-Photochemical Quenching, NPQ).

The spectral peaks of carotenes are in the blue to green region of the visible spectrum.

It should also be pointed out that **retinal** which is formed by splitting in two a Vitamin A molecule (in turn derived from β-carotene), is the photoactive part of the protein **rhodopsin**. Although rhodopsin is most familiar as the major eye pigment similar proteins are also present in microorganism and algae (bacteriorhodopsin, halorhodopsin, proteorhodopsin and xanthorhodopsin) where they can play a role in absorbing light energy that can be harnessed to drive endergonic processes, in a mechanism, which can be analogous to photosynthesis (Larkum et al. 2018).

2. *Xanthophylls*

With xanthophylls, which are basically unsaturated hydrocarbon chains with additional oxygen atoms (Fig. 10.4), there is the possibility for a large number of variants. In photosynthesis many of these variants play a light-harvesting role, such as fucoxanthin, peridinin and vaucherioxanthin (Table 10.1), which harvest light in the green region of the spectrum (500–550 nm) (Fig. 10.2). However some xanthophylls, double up by playing other roles. For example, zeaxanthin + violaxanthin (green algae and land plants) and diatoxanthin + diadinoxanthin (chromophytic algae) take part in non-photochemical quenching in the xanthophyll cycle (see Sect. VII). Also the water-soluble keto-carotenoid 3′-hydroxyechinenone is the major carotenoid in the orange carotenoid protein (Sect. A).

C. *Phycobiliproteins*

Phycobiliprotein (PBP) plays an exceptional role in light-harvesting in Cyanobacteria (see Chaps. 5, & 14) and a small number of algal classes, notably Rhodophyceae, Glaucophyceae and Cryptophyceae. PBPs harvest light in the region of 490–650 nm where the "so-called" green window is a region of the visible spectrum where Chl and carotenoid pigments absorb inefficiently (see Fig. 10.2 and Table 10.2). In fact PBPs play such a dominant role in Cyanobacteria that it is often assumed that they evolved before light-harvesting Chls, an assumption that is likely to be wrong (see above and Larkum 2006)); it is much more likely that at least some Chls apart from Chl *a* evolved before the evolution of PBPs. Larkum 2006 advanced the idea that phycobilosomes only evolved as a shading response to other algae. This has the merit that PBP is an "expensive" molecule (in terms of nitrogen) (Larkum and Howe 1997), is not a membrane intrinsic molecule and is specifically tailored for absorption of light where the Chl and, generally, carotenoids have poor absorption properties. PBPs are built into phycobilisomes and from which the energy is funneled into the thylakoid membrane via a specific stalk of additional molecules. It has recently been shown that passage of energy down this stalk is modulated in many cyanobacteria by a caroteno-protein, the orange carotenoid protein (OCP) (see Sect. A and Chap. 15). In planktonic cyanobacteria, which grow in nitrogen-limited or iron limited seas, the main light-harvesting mechanism for photosystem I is often a ring of light-harvesting chlorophyll proteins with affinities to CP47 because this is "cheaper" to produce under these circumstances (see Larkum and Howe 1997); a typical structure is shown in Fig. 10.8. Detailed chemical structures of all the important PBPs are given in Chapter 5.

The chromophores of phycobiliproteins are of three main types: phycocyanobilin (PCB), phycoerythobilin (PEB) and phycourobilin (PUB), although there are variants (Table 10.3; Toole and Allnutt 2003). The chromophores are open chain pyrroles and are formed by the same biosynthetic systems that synthesise haemoglobins, cytochromes and chlorophylls (Larkum 1992). The bilins are conjugated to specific polypeptides, which form α and β chains.

In summary PCB gives absorption properties in the red, PEB in the green-orange and PUB in the blue-green region of the visible spectrum. The main phycobiliproteins of cyanobacteria are allophycocyanin (600–660 nm peak), phycocyanin (580–630 peak) and phycoerythrin (540–575 nm). In red

Table 10.2. Distribution of the major carotenoids of Cyanobacteria and Eukaryotic Algae

	Alicyclic hydrocarbons				Dihydro Xanthophylls				Xanthophyll C-8-keto; Xanthophyll epoxides; Xanthophyll epoxides					Xanthophyll allenes		Xanthophyll acetylenes				
	α-carotene	β-carotene	γ-carotene	ε-carotene	Echinone	Lutein	Loraxanthin	Zeaxanthin	Violaxanthin	Cryptoxanthin	Siphonaxanthin (Siphonein)	Myxoxanthophyll	Neoxanthin	Vaucheriaxanthin	Fucoxanthin	Peridinin	Diatoxanthin	Diadinoxanthin	Alloxanthin	Heteroxanthin
Cyanobacteria		●	tr					○				○								
Prochlorophyta[a]	○							●		⊙									○	
Cryptophyta	○			○																
Chlorophyta	○	●				⊙	○	○	○		⊙		○							
Prasinophyta	○	●				⊙		○	○		⊙		○							
Charophyta	○	●				⊙		○					○							
Euglenophyta		●			tr								○				○	●		
Rhodophyta	●	●				●		○		○										
Dinoflagellata		●											⊙		◆[b]	●	○	○		
Haptophyta		●			○					○					●		⊙	⊙		
Chrysophyta	⊙	●	tr					○	○				○		●		○	○		
Xanthophyta		●								○			○	●			○	○		○
Chloro-monadophyta		●											○	●			○	○		
Eustigmatophyta		●							○				⊙	●			○	○		
Bacillariophyta		●		tr											●		○	○		
Phaeophyta		●							●	○					●		○	○		
Rhaphidophyta		●						○	○						●					
Chromerids		●							○						●[c]					

[a]Prochlorophyta is a group of Cyanobacteria (*Prochlorococcus*, *Prochloron*, *Prochlrothrix*) that have Chl *b* alongside Chl *a* and no phycobiliproteins

[b]◆ The fucoxanthin in these species is due to a diatom-like endosymbiont

[c]The fucoxanthin in *Chromera* has been characterized as a new form of fucoxanthin (Ifx-1) similar to Isofucoxanthin (Llansola-Portoles et al. 2016)

[d]The general references for this Table can be found in Rowan 1989 and Larkum and Barrett 1983 (Table 10.3)

[e]Symbols: ○, Low concentration; ⊙ moderate concentration; ● major pigment; tr, trace present

[f]Haptophyta: also known as Prymnesiophyta

Table 10.3. Classification and some representative properties of phycobiliproteins from Cyanobacteria (C), Rhodophyta (R) and Glaucophyta (G)

	Distribution	Absorption Max[a], nm	Fluorescence Max, nm	Chromophore number		Monomer	Protein structure aggregation
				α-chain	β-chain		
Allophycocyanin I	C, R	656	680	1PCB	1PCB	$\alpha_3\beta_3$	1
Allophycocyanin II, III	C, R	650	660	1PCB	1PCB	αβ	(1), 3, 6
Allophycocyanin B	C, R	671 > 618	680	1PCB	1PCB	αβ	(1), 3, 6
C-Phycocyanin	C, R	620	637	1PCB	1PCB	αβ	1, 3, 6
R-Phycocyanin	R	617 > 555	636	1PCB	1PCB, 1PEB	αβ	3, 6
Phycoerythrocyanin	C	535<568>590	619	1PXB	2PCB	αβ	3
C-Phycoerythrin	C	565 > 540	577	2PEB	4PEB	αβ	1, 3, 6
b-Phycoerythrin	R	545 > 563(575)	570	2PEB	4PEB	αβ	3
B-Phycoerythrin	R	545 > 563 > 498	575	2PEB	4PEB	$\alpha_6\beta_6\gamma$	1
R-Phycoerythrin	C, R	567 > 538 > 498	578	2PEB	4PEB	$\alpha_6\beta_6\gamma$	1
Phycocyanin 645[b]	G	645,625,585	660	PCB, PBV	1PCB, 1PEB	$\alpha\alpha'\beta_2$	1
Phycoerythrin 545[b]	G	545 (565)	585	PEB, PBV	PEB, PBV	αβ	1

Notes

[a]The spectra are for proteins/polypeptides in aqueous solution; therefore the wavelength may differ from other published values; for example the 680 nm fluorescence peak of allophycocyanian is for the phycobilisome-attached terminal and may differ when removed from its normal environment. The data were initially assembled by Larkum and Barratt (Larkum and Barrett 1983) and has been taken from Glazer (1977), Rüdiger (1980) and Scheer (1981); there has been some modification or provision of new data since (see e.g. Takaichi 2011; Serive et al. 2017)

[b]Glaucophyte phycobiliproteins are defined by their major absorption maximum: species either have a PC or a PE but not both. Only two PBs are shown here. In addition to PCB and PEB chromophores, phycobiliviolin (cryptoviolin) (PBV) is generally present (MacColl and Guard-Friar 1967)

algae there is an extra γ-polypeptide which binds, in addition, 2PEB and 2 PUB chromophores; giving the red algal phycobiliprotein 2 peaks and the ability to absorb as far down as 490 nm (see Toole and Allnutt 2003).

In cryptophytes – rather bizarre algae with secondary endosymbiotic plastids (see Sect. B) somewhat distantly related to red algae (see Fig. 10.6) – there is additional diversity. Each species has either a phycocyanin-type or a phycoerythrin type of PBP (Toole and Allnutt 2003). These are found in the thylakoid lumen as soluble proteins. In the case of the phycoerythrin (PE 545) of *Rhodomonas* CS24 it has been shown that the soluble phycobiliprotein is made up of two polypeptides (Wilk et al. 1999). And although the β-chain structure is similar to β chains of other known phycobiliproteins, the overall structure of PE 545 in that the α chain is novel formed of a simple extended fold with an antiparallel β-ribbon followed by an α-helix. Two doubly linked chromophore, one on each β subunit, are in van der Waals contact. Each α subunit carries a covalently linked 15,16- dihydrobiliverdin (=phycocyanobilin) chromophore and this is likely to be the final energy acceptor. Thus it is likely that the original PBP structure inherited from cyanobacteria has been evolutionarily modified during the long course of secondary symbiosis and giving rise to the present structure, with the unique α chain. It has been pointed out that the close association of the chromophores on the subunits give rise to the possibility of coherent energy transfer (Wilk et al. 1999; Collini et al. 2010; see Chap. 15 for further details).

III. The Evolution of Protists with Plastids (Algae)

A. Algae with Primary Plastids

Current evidence suggests that endosymbiosis of a cyanobacterium and an early protist organism gave rise to the ancestral line of plastids over 1 Ga ago (e.g. (Price et al. 2012; Keeling 2013; Ochoa de Alda et al. 2014; Archibald 2015; Chap. 2) (Fig. 10.5); there has even been some speculation as to from which group of Cyanobacteria the first endosymbionts came, although no definitive answer has been provided at this stage (Ochoa de Alda et al. 2014; Archibald 2015). A single endosymbiosis is generally held to be the most likely, because such an occurrence is held to be a very unlikely event; this is called the **monophyletic hypothesis**. And this hypothesis is embodied in the concept of the Archaeplastida, in which it is stated that this single endosymbiosis gave rise to the modern Glaucophyceae (Glaucocystophyceae), Rhodophyceae and Chlorophyceae. These three phyla all have plastids with only two outer envelope membranes i.e. **primary plastids**, in contradistinction to the secondary plastids, which have three or four envelope membranes (Larkum and Vesk 2003) (Fig. 10.5). Since in the present Era the primary plastids contain only a few genes (usually much less than 250) it is assumed that the original nucleus lost most of its genes, some to the host nucleus and others altogether.

An alternative **polyphyletic hypothesis** states that there were several independent endosymbioses during an early period during which endosymbiosis took place (at a time of ~1–2 Ga), but that reticulate evolution, occurring over many Ma, gave rise to the three modern classes with primary plastids, i.e. the Glaucophyceae, the Rhodophyceae and the Chlorophyceae; this is represented by the **shopping bag model** (Larkum et al. 2007), but there are other proposals. It has gained support recently from evidence that cyanobacterial endosymbioses have occurred much more recently than the period when primary plastids evolved, and have given rise to endosymbionts, where some genes have been transferred to the host nucleus, e.g. *Paulinella* (Nowack and Grossman 2012) and other examples (Dorrell and Howe 2012). It was also supported by an analysis of slowly evolving genes (Nozaki et al. 2009).

A further point to notice is that the protistan organism(s) into which this endosymbiosis occurred, already possessed a

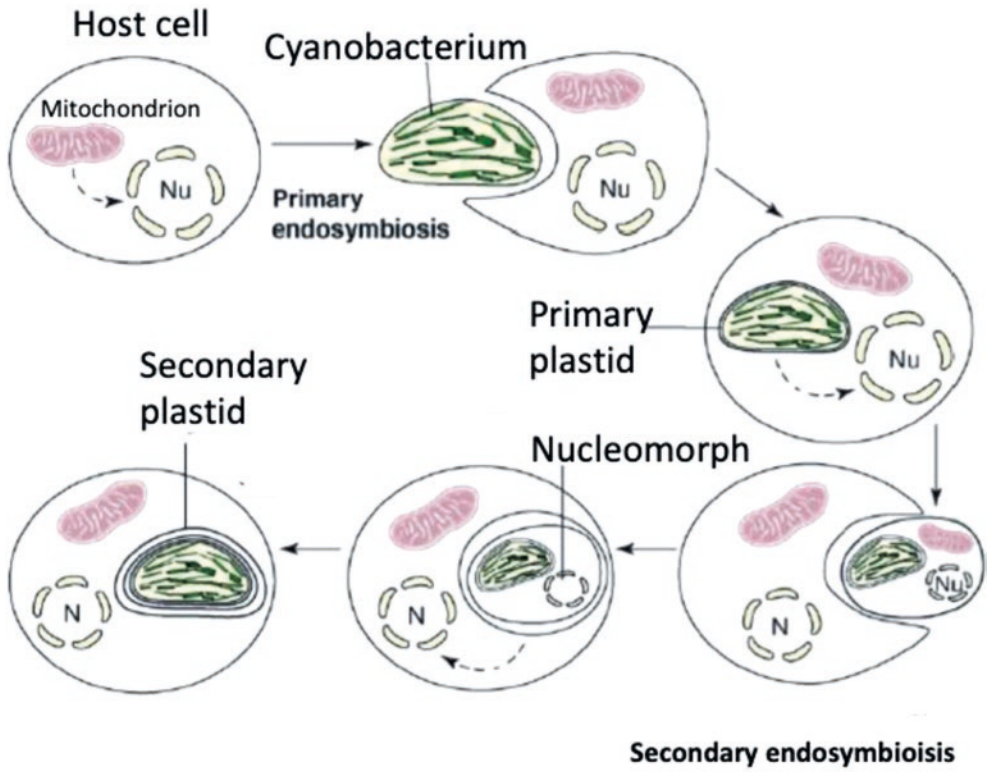

Fig. 10.5. The monophyletic endosymbiotic model of plastid evolution
Secondary endosymbiosis occurred in a number of photosynthetic groups, where an alga with primary plastids was engulfed by another eukaryotic unicellular organism, leading to the formation of a plastid with 4 (or 3) outer plastid membranes. In Cryptophyceae there is a relic nucleus, nucleomorph, of the primary host between the two sets of plastid membranes (Douglas et al. 2001)

mitochondrial endosymbiont, since all protists have been shown to possess at least a relict mitochondrion (Fehling et al. 2007) and likely a chlamydial endosymbiont, too (Ball et al. 2013; Chap. 2).

Thus a key feature of modern research is to identify the cyanobacterial organism(s) and those original cyanobacterial genes which have survived (either in retained in the plastid, that have migrated to the host nuclear DNA and that which has been lost altogether).

In the following sections the major groups of eukaryotic algae and their photosynthetic systems are described.

1. Glaucophyceae

Glaucophyceae are protist organisms (eukaryotic algae), whose affinities are not clear (Reyes-Prieto et al. 2018). There are about a dozen species, none of which is common. *Cyanophora paradoxa* is the most studied and consists of a motile cell without a cell wall. Another species, *Glaucocystis* is immotile, although it retains vestigial flagella. It has a cellulose cell wall. *Gloeochaete* has both motile and immotile stages and it appears that its cell wall is not composed of cellulose. The structure of the flagellum root and the presence of two unequal flagella suggests links with Chlorophyceae, although the presence of cortical alveoli is a difficulty with such a suggestion (Berner 1993).

The primary plastid, known as a cyanelle, has by definition two outer membranes, but in addition there is a vestigial cell wall, a peptidoglycan layer lying between the two bounding membranes. The latter layer could

be the vestige of the cell wall of the cyanobacterium, which gave rise to the symbiosis.

Of all the plastids, the photosynthetic machinery of the cyanelles is most similar to Cyanobacteria. Of the Chls, only Chl *a* is present and the major light-harvesting proteins are phycobiliproteins, which lie in the plastid matrix and funnel energy down to the thylakoid membrane via a stalk. There are no LH proteins in the CAB family present; but as might be expected with the close link to Cyanobacteria there are proteins, which are relatives of the Hlip proteins of Cyanobacteria (Komenda and Sobodka 2016), and which have one alpha-helix and, in addition, there are the Stress Enhanced Proteins (SEP), with two helices, which occur in Glaucophyceae, Rhodophyceae and diatoms (Engelken et al. 2010; Sturm et al. 2013). The plastid genome of Cyanophora has a size of 139 Kb and holds 192 genes, one of the largest plastid genomes.

If the concept of Archaeplastida is upheld then Glaucophyceae, Rhodophyceae and Chlorophyceae share a common origin. Recently the whole genome of *Cyanophora paradoxa* was accomplished (Price et al. 2012). While this work indicated many shared characteristics between these three mentioned phyla there are many differences, which still cannot easily be explained (Reyes-Prieto et al. 2018); for example the lack of any LHC genes is not readily explained on a shared origin.

2. *Rhodophyceae*

The Rhodophyceae is a group of non-flagellate protists with affinities with Amoebozoa (Larkum and Vesk 2003; Fehling et al. 2007). The presence of two outer membranes places their plastids with the primary plastids and the presence of phycobiliproteins must be a strong clue; however, there are many features, which separate rhodophyte plastids from the plastids of glaucophytes. Firstly their phycobiliproteins show considerable evolution as compared with Cyanobacteria and glaucophytes. For example, many rhodophytes have an extra pigment group, the gamma phycobiliprotein (Table 10.2). They also have a CAB protein, attached to PSI, with affinities with the CAB proteins of green algae and many Chl *c*-containing algae (Chromalveolates; see Chap. 2), although the only chlorophyll in rhodophytes is Chl *a*. They also have a special form of starch known as floridean starch. The thylakoids are non-appressed and bear phycobilisomes on their outer surface (Figs. 10.6, 10.7, and 10.8), as with Cyanobacteria.

Ten whole genomes of rhodophyte algae are at present available, and more are on the way: the primitive hot springs alga, *Cyanidioschyzon merolae* ((Matsuzaki et al. 2004) and the advanced red alga (Floridiophyceae) *Porphyridium purpureum* (Bhattacharya et al. 2013) were the first. However since then, eight other species have been sequenced including *Porphyra* (*Pyropia*) and *Gracilaria chilensis* (refer to the NCBI database). In addition many plastid genomes are now available; from *Cyanidioschyzon merulae,* from two bangiophyte algae and from many advanced red algae (DePriest et al. 2013). It should therefore be possible to trace the evolutionary inheritance of the cyanobacterial symbiont that gave rise to the red algal plastid. However, this has not been achieved to date; see (Li et al. 2014).

The plastid genome, although varying between the different red algae, shows generally similar features in having a size of 150–190 Kb and a protein coding gene number of 193–234 (DePriest et al. 2013). This is a much larger size than is found in green plastids.

3. *Chlorophyceae*

The third group of algae possessing primary plastids are the Chlorophyceae. In this group of protists the ancestral host was flagellated with two unequal flagella. The outer membranes of the plastid enclose many thylakoid

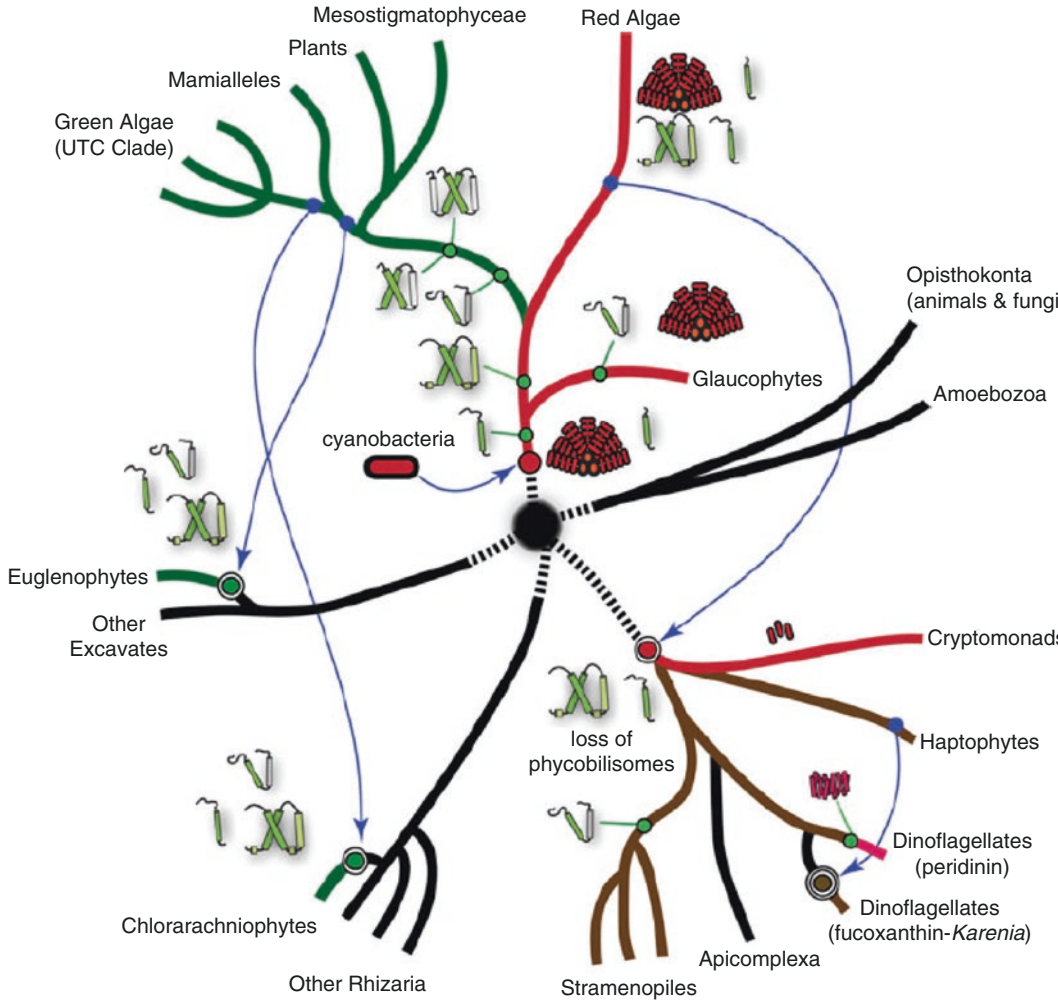

Fig. 10.6. The evolution of light-harvesting Chl *a*, *b* and *c* systems in cyanobacteria, eukaryotic algae and land plants. (Reproduced from Neilson and Durnford 2010, with permission)
The hypothetical endosymbiotic event of a cyanobacterium being taken up by a eukaryotic host cell (see Fig. 10.5 is shown by a red circle. This must have been followed by the transfer of HLIP genes into the nucleus of the eukaryote host and the subsequent evolution of the family of LHC proteins at different points along the evolutionary tree as indicated (green dots plus icons as explained in the key, below)). In Chl *b*-containing algae, CAB proteins with 3-membrane spanning helices were involved; but there was also some spread laterally to other eukaryotic lineages via secondary or tertiary endosymbiosis (blue arrows plus symbol) after which the LH antenna systems continued to diversify; euglenophytes and chloarachniophytes acquired plastids independently through a secondary endosymbiosis with a green alga. The Chl *a/c*-containing organisms seem to have acquired a plastid from an organism with affinities to red algae (but as pointed out in the text, this clearly is problematic for the monophyletic hypothesis of endosymbiosis); here the phycobilisomes were lost and replaced by a CAC-like antenna system, with 3-membrane spanning helices with Chl *a/c*. In cryptophytes, phycobiliprotein remains but does not assemble into phycobilisomes. In peridinin-containing dinoflagellates, a novel, soluble chlorophyll protein (Peridinin-Chl Protein, PCP) evolved to supplement the membrane-integral CAC system
For a somewhat revised phylogenetic scheme see Fig. 10.7 and Key to figure

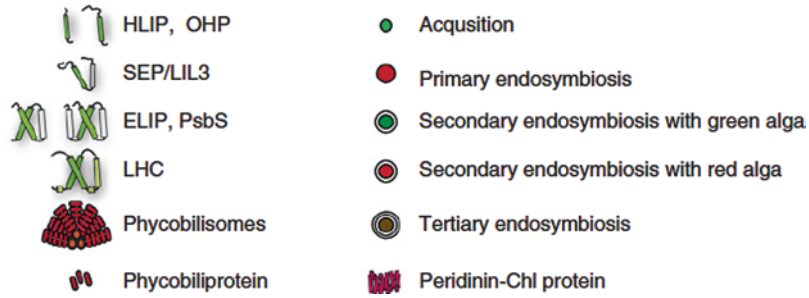

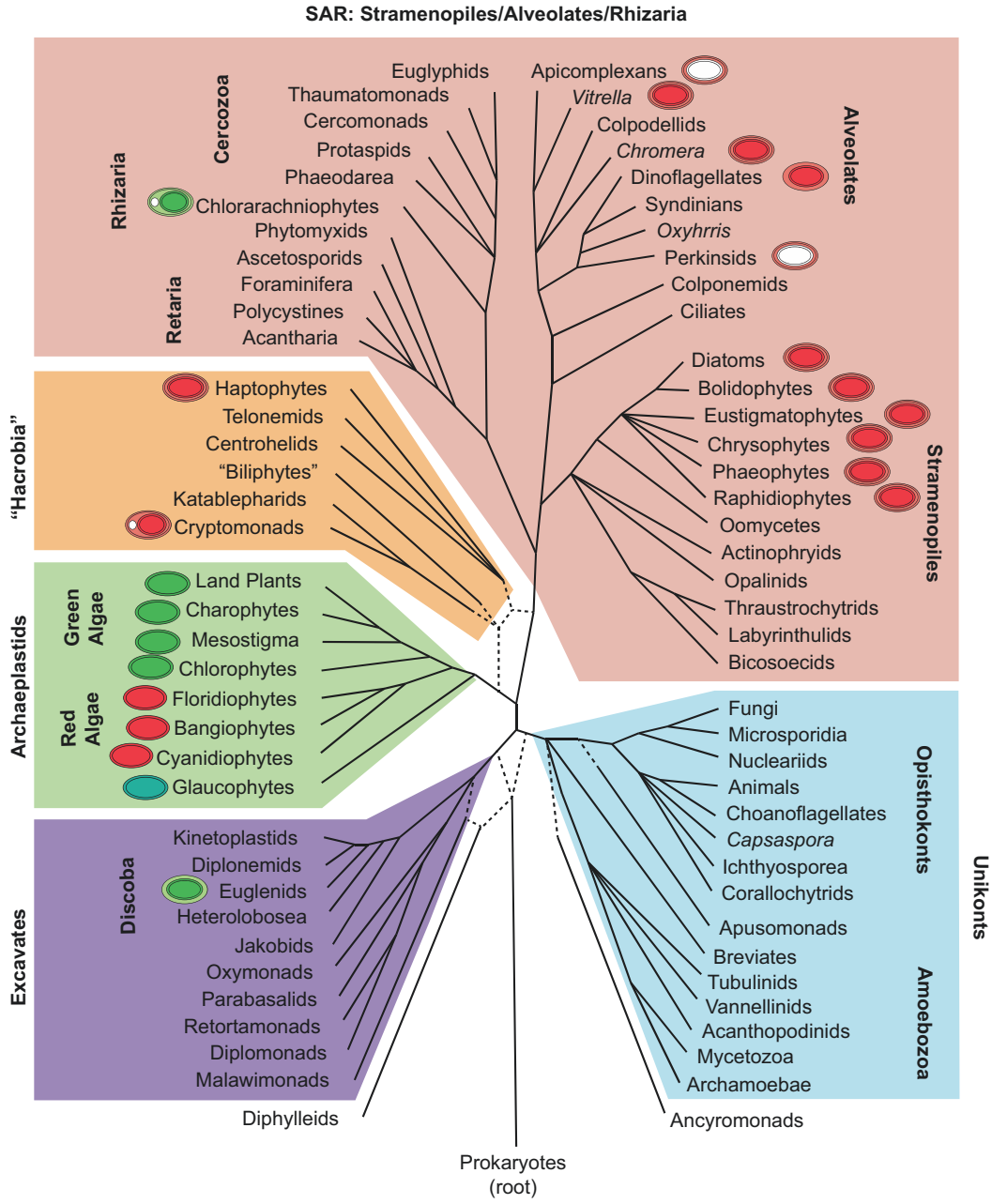

Fig. 10.7. The photosynthetic eukaryotic algae arranged phylogenetically, based on the arrangement of Keeling 2013

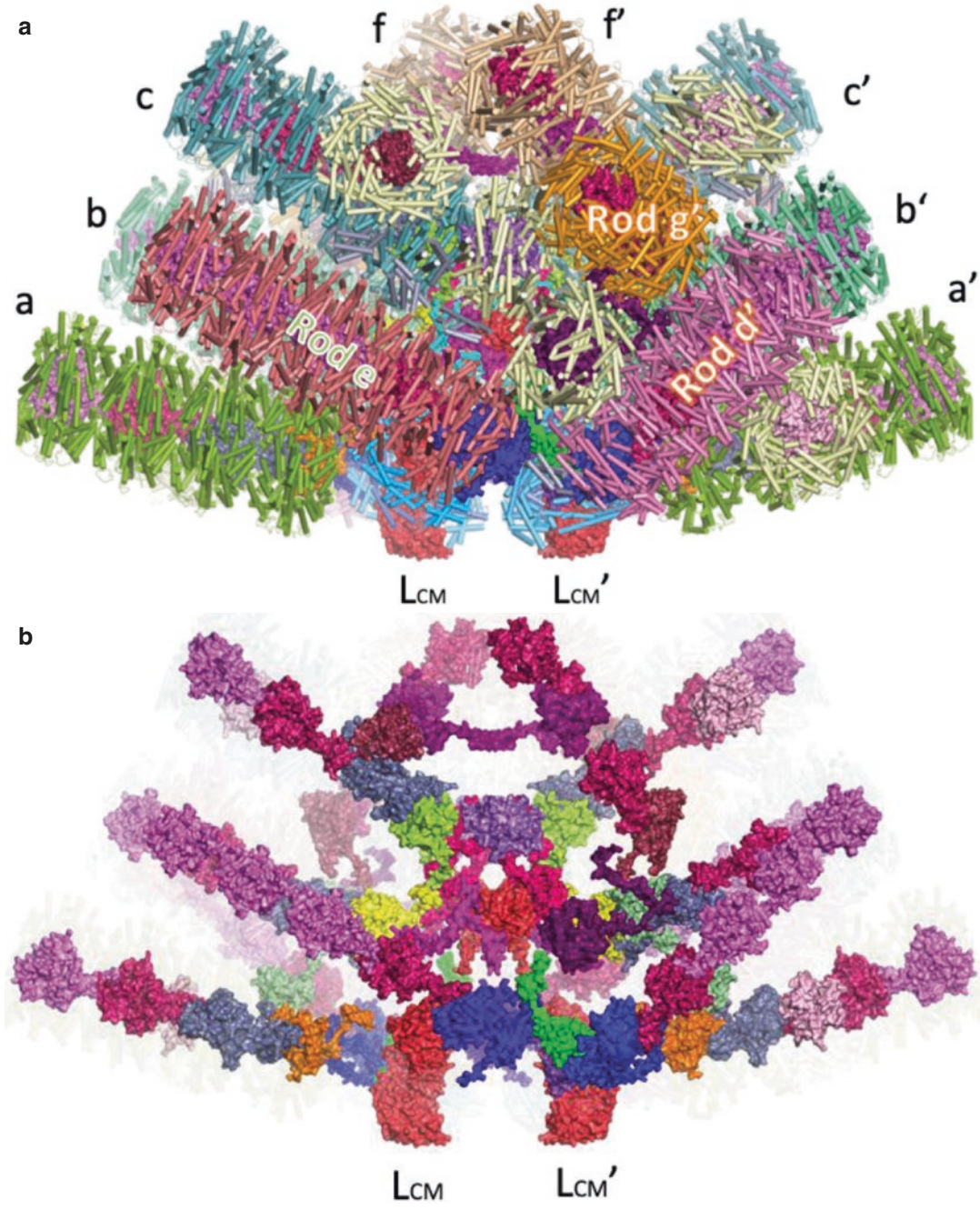

Fig. 10.8. Space-filling model of the phycobilisome of *Griffithsia monilis*. (**a**) Side view of phycobilisome showing peripheral rods of 3 phycoerythrins (salmon) and 1 phycocyanin (blue). (**b**) Side view of phycobilisome with side phycobiliprotein rods removed. Taken from Zhang et al. 2017. With permission from Nature Publishing

membranes, which are closely positioned to each other over significant portions, but the term appression has been reserved for the grana of higher plants (Larkum and Vesk 2003). Unlike the plastids of glaucophytes and rhodophytes, the light-harvesting system is based on membrane integral proteins, and does not bear phycobiliptoteins. Many of these pigment-proteins are in the Chlorophyll a/b (CAB) family of proteins (often called LHC proteins) binding Chl *a* and Chl *b* (see Sect. V and Fig. 10.6). In addition there are a number of other differences with Glaucophyceae and Rhodophyceae: e.g. the presence of starch, the close positioning of thylakoid membranes, the presence directly in the cytoplasmic compartment, and not enclosed by any other membranes. It should be noted, however, that in Rhodophyceae there is a CAB-type gene targetted to and located in PSI (see above), an occurrence which might be explained either by vertical or lateral gene transfer. It should also be pointed out that eukaryotic algae in the chromophyte lineages (chomalveolates) (Fig. 10.7), which bear secondary plastids, have proteins in the same family as CAB proteins, but they carry Chl *c,* not Chl *b,* and are referred to as CAC light-harvesting proteins (see Fig. 10.6).

The chlorophyceae gave rise to land plants (embryophytes). This happened in one lineage of the Chlorophyta, the Streptophyta, where a number of significant evolutionary changes paved the way to the development of land plants (embryophytes) via the evolution of bryophytes (Turmel et al. 2013)).

The genomes of many chlorophyte plastids have been sequenced and range in size from 118–204 kb, with 94–107 genes (Green 2011b).

A number of chlorophyte genomes have been fully sequenced. The size ranges from 12 Mb to 121 Mb (Blanc et al. 2010), with *Chlamydomonas reindardtii* being the largest by far. Interestingly, *Chlorella* (*Chlorella variabilis*) turns out to be a member of the Trebouxiaceae, with a history of endosymbiosis of the alga in other protists and metazoans, cryptic sex and cryptic/residual flagella (Blanc et al. 2010).

B. Secondary and Tertiary Plastids

All other plastids (it is hypothesized) evolved through secondary symbioses, followed in some cases by tertiary symbioses (Figs. 10.5 and 10.7; see also Chap. 2). Good evidence for this comes from the cryptophytes, where there are four membranes around the plastid and the presence of a nucleomorph, bearing three reduced chromosomes, between the two sets of outer membranes: this nucleomorph has been sequenced and indicates that the primary host was a relative of a red alga (Douglas et al. 2001). The cryptophyte plastid genome of *Guillardia theca* also bears strong similarities to rhodophyte plastids (Douglas and Penny 1999). This is important information because the primary light-harvesting protein of cryptophytes is quite distinct (see below). In addition cryptophytes, in contradistinction to Rhodophyceae, have acquired Chl *c,* in this case Chl c_2 (without Chl c_1), the same situation as in dinoflagellates: information that might suggest a link in the origins of these two phyla, but reference to Fig. 10.7 indicates that the phylogenies of the hosts and the properties of the plastids (see Larkum and Vesk 2003) are very different; see also the comments in Sect. 4. As an interesting aside here, the Haptophyceae (containing the coccolithophores) are on a similar line to cryptomonads but have both Chl c_1 and Chl c_2, indicating that the plastids in Haptophyceae were "captured" from a very different organism, although also related to red algae.

For most of the secondary plastids, largely in the chromophyte lineage (also called the chromalveolate branch; see Chap. 2), no equivalent of the nucleomorph has been found (but it is assumed that these secondary plastids evolved in a similar way by two serial endosymbioses): four outer membranes usually exist, although in the case of dinoflagellates only 3 are found today. A case

for tertiary endosymbiosis can also be made out in certain limited instances (e.g. in some dinoflagellates – (Keeling 2013)).

1. *Diatoms (Bacillariophyceae) and Related Phyla Including the Phaeophyceae*

The LHCs of diatoms, the fucoxanthin chlorophyll proteins (FCPs) form the most recalcitrant and least understood of all the LHCs (Chap. X) (Gundermann and Büchel 2014) see Fig. 10.6. While in other algae it has been relatively easy to assign LHCs to PSI or PSII, this has not been so easy in diatoms.

The LHCs of diatoms have been classified into three major groups (Chap. 16) (Caron et al. 1988; Gundermann and Büchel 2014):

Group 1, coded by Lhcr genes, is equated with a pure light-harvesting component of PSI,
Group 2, coded by Lhcf, gives rise to the major fraction of light-harvesting proteins (FCPs, attached to PSII and PSI), and
Group 3, coded by Lhcx, is similar to the LI818 (LHCSR) (see below and Fig. 10.13) proteins of other algae (Gundermann et al. 2013), which have a controlling role in non-photochemical quenching (Lepetit et al. 2013) (see Sect. A and Chaps. 3 & 16).

The levels of subpopulations of Lhcf change with light conditions: recently two groups have proposed models to describe changes to the thylakoid membranes under low and high light (Gundermann et al. 2013; Lepetit et al. 2013). Nevertheless it is broadly true that neither state transitions nor spillover of excitation energy from one photosystem to the other have been conclusively observed in diatoms (Arsalane et al. 1994).

Nevertheless, diatoms have the ability to respond to rapid changes in light intensity (Wagner et al. 2006) as a result of non-photochemical quenching (NPQ) mechanisms (see Chaps. 3 & 16).

The situation in diatoms is atypical because they have both the diadinoxanthin cycle (DdC) and the violaxanthin cycle (Lohr and Wilhelm 1999). And, indeed, in the diatoms it has recently been shown that there are two NPQ mechanisms, one associated with antenna units attached to PSII and the other associated with antenna units that detach from PSII and remain isolated during high light conditions (Miloslavina et al. 2009). Neither of these NPQ mechanisms would be expected to affect the maximum efficiency of photosynthesis in diatoms, which has been shown to be high (Torres et al. 2013).

Diatoms have a unique outer wall formed of silica and arranged in two abutting frustules. The function of the frustules is most probably protection but LH has also been proposed: the frustule has a unique architecture with sculpturing giving rise to small perforations which are the right distance apart to affect coherent laser light at wavelengths of >1000 nm; as a result frustules have become a favourite tool for laser studies (Hsu et al. 2012); however, to date there is only circumstantial evidence to suggest that there is any connection to photosynthesis and light-haresting (Goessling et al. 2018).

All these unknowns make diatoms one of the most intriguing systems in the field of algal light-harvesting today.

2. *Related Phyla*

In very general terms the following phyla fit into the diatom pattern, having, in addition to Chl *a*, Chl c_1 and c_2, (and in some cases Chl c_3), the xanthophylls, diatoxanthin and diadinoxanthin, and LHC light-harvesting proteins:

Phaeophyceae, Rhaphidophyceae, Chrysophyceae, Bolidophyceae (see Fig. 10.7).

In many respects the Eustigmatophyceae (in which *Nannochloropsis* occurs) also share similarities with this group but retain only Chl *a*.

3. *Dinoflagellates*

Dinoflagellates (Dinophyceae) evolved within the chromalveolate group of algae and gave rise, via *Chromera* ((Quigg et al.

2012)) to their non-photosynthetic relatives, the Apicomplexans, according to modern phylogenetic studies (Fig. 10.7; Chap. 2). In the botanical system they form part of the Chromophyceae.

In terms of LH, dinoflagellates have a fascinating array of pigments and pigment proteins arranged in a unique thylakoid membrane and unique plastid. In addition, the molecular biology of the chloroplast, in dinoflagellates, with its DNA minicircles, is quite unique i (Larkum and Vesk 2003).

There are two major types of LHPs in dinoflagellates, (i) a membrane bound protein (Chl *a*, Chl c_2, peridinin protein complex: acpPC, allied to CAC proteins) and (ii) a water-soluble peridinin-chlorophyll protein (PCP) complex. Of these two proteins much more is known on the PCP complex, which has been resolved to a crystal structure of 1.63 Å (Wilk et al. 1999) and studied in considerable molecular detail (Hofmann et al. 1996; Schulte et al. 2009; see Chaps. 3 & 17).

The gene sequence for PCP was established by Hofmann et al. 1996, and has no homology to any other known protein. The crystal structure indicates a protein with the monomer binding 2 Chl *a* molecules and 2 peridinin molecules (Hofmann et al. 1996) (Fig. 10.2), essentially as predicted from CD spectra by Song et al. 1976. Peridinin has an *in vivo* absorption spectrum extending up to 540 nm and adds greatly to the absorption capacity of dinoflagellates by light absorption in the blue-green region of the spectrum; thus PCP significantly augments the light-harvesting capacity of the dinoflagellate CAC proteins and does this at low nitrogen cost (Larkum 2003), and can attain concentrations of up to 50% of the total peridinin, i.e. 50% of the concentration of acpPC (Hofmann et al. 1996).

The functioning of PCP is still not well resolved. PCP lies in the thylakoid lumen space and is extracted as a soluble protein. However, if it is to function as an efficient LH protein, it presumably interacts efficiently with adjacent PCPs. This suggests that there may be a semi-crystalline state *in vivo*, which aids resonance (or even coherent energy transfer – see Chap. 15) otherwise energy transfer would be very slow. Recent work on PCP indicates that energy transfer is efficient and is directed efficiently into the thylakoid membrane at specific sites (Hill et al. 2012; Reynolds et al. 2008). Earlier it was suggested that there were two types of PCP and that one of these, a high-salt PCP, might play a role in directing energy into the thylakoid membrane; however, now, the evidence is less compelling (Schulte et al. 2009).

In hermatypic corals, where coral bleaching occurs, and is triggered via the photosynthetic machinery, there is a definite effect of coral bleaching temperatures (30–34 °C) on the interaction of PCP with the thylakoid membrane, as indicated by changes in the wavelength of fluorescence emission (Hill et al. 2012; Reynolds et al. 2008). Kanazawa et al. (2014) have suggested that energy transfer into the membrane is increased by coral bleaching temperatures in Clade C *Symbiodinium* (the heat sensitive clade of hermatypic corals). Furthermore, Slavov et al. (2016) have proposed that a special kind of super-quenching occurs in *Symbiodinium* clades at coral bleaching temperatures, which presumably would involve light-harvesting proteins (Slavov et al. 2016).

4. *Cryptophytes (Cryptophyceae)*

Cryptophytes belong to a phylogenetic group of biflagellate protists, only a part of which are photosynthetic algae and to which the name "Hacrobians" has recently been given (see Keeling 2013) (Fig. 10.7). Previously this group would have been placed in the Chromophyta (Chromalveolates). In broad terms, cryptomonads have a secondary plastid that has engulfed an organism with a primary plastid allied to a red alga (Douglas et al. 2001). However, this cannot be the complete story because the plastid bears an LHC (CAC protein) with Chl *a* and Chl c_2. In addition the plastid bears phycobiliproteins (PBPs), which are unique and quite different,

at least in the alpha chain, from red algal PBPs (Wilk et al. 1999): these have a β polypeptide with distinct affinities to red algal PBPs but an α chain with no affinity to any other protein (see Sect. C); and some of the chromophores of the phycobiliproteins are quite unique as well (Glazer and Wedemeyer 1995). Thus there is much evolutionary history in the production of these PBPs and it is not at all clear that there is any direct, linear descent from red algae.

As in dinoflagellates the water-soluble PBPs are in the lumen of the thylakoids. Thus photons that are harvested must be passed onto the thylakoid membrane through interaction of these protein units. Recently there has been much excitement with the suggestion from several laboratories that coherent energy transfer may take place, i.e. that the migration of excitation energy is by exciton coherent wave transfer (refer to Chap. 15). Exactly how this can take place is being taken up as a challenge by these laboratories.

5. *Other Stramenopiles, Haptophytes and Apicomplexans*

Haptophytes, eustigmatophytes, bolidophytes, chrysophytes, phaeophytes, raphidophytes, chromerids, vitrellids, perkinsids and apicomplexans make up a diversity of plastidial groups (see Fig. 10.6), with evolutionary affinities but distinct differences. In the Hacrobia, haptophytes share a place with cryptophytes; see Chap. 2; however there is little similarity between their photosynthetic and structural characteristics (Larkum and Vesk 2003): haptophytes share more similarity with photosynthetic stramenopiles and this is where their plastids may have come from (by tertiary symbiosis?). Thus the diatoms, bolidophytes, chrysophyes, phaeophytes and raphidophytes all have Chl a/c (CAC) proteins, which bind Chl c_1 + c_2 (and in some cases c_3). The eustigmatophytes, which share many similarities with these phyla, lack Chl c_1 + c_2. The latter small, mainly freshwater, phylum contains the important Eustigmataceae genus *Nannochloropsis,* which is marine.

Finally in the Alveolates (Fig. 10.6) along with the dinoflagellates are the chromerids and vitrellids that possess only Chl *a*; and in addition the Perkinsids and Apicomplexans, which have lost all chlorophylls and do not carry out autotrophic photosynthesis. *Perkinsus* is the type genus of the perkinsids, and is parasitic in shell fish. The Apicomplexans are more diverse and are involved in a number of parasitic infections, including, in humans, malaria, babesiosis and toxoplamosis.

IV. The Need for Light-Harvesting Antennas

Figure 10.1 shows the molecular layout of the reaction centres (RCs) of photosystem I and photosystem II as currently configured from molecular X-ray diffraction studies. The two centres are built around a scaffold, which takes an absorbed photon of light and uses this to drive an electron through the reaction centre, from one side to the other (inside to outside), forming per reaction a primary reductant and a primary oxidant molecule. From there the primary sites are stabilised by electron transfers to and from secondary sites. And from there an electron transport chain carries out the fixation of energy as ATP and NADPH (by which CO_2 is fixed into organic form).

The RCs have few pigment molecules and a large number of cofactors and are expensive in terms of light capture vs. the amount of protein per absorbed photon. It is therefore an attendant imperative of all photosynthetic systems to build light-harvesting centres with a much greater concentration of pigments per protein molecule. These pigment protein complexes are arranged around the reaction centres and give a density of perhaps up to 1000 pigment molecules per RC. Under these conditions the absorption cross-section of the RC increases by up to 1000 and for Chl molecules this results in a

turnover of the RC of about once every 0.1s under medium light intensities.

Clearly the absorption cross-section will be affected by the pigments (Chl, carotenoid, PBP) that are linked into the light-harvesting pigment protein complexes and the quality of the incident light, e.g. whether this is in full sunlight, or the shade of a forest or the depths of the ocean.

Under low light conditions the need for more light-harvesting molecules and a greater absorption cross-section is high. Thus it is not surprising that algal and plant systems adjust to lowered light by incorporating a higher density of pigments and thereby increase the absorption cross-section. Thus algae also have evolved the ability to place a large number of pigments in their LH antennae. However, surprisingly, few have evolved pigments that can absorb in the green region: here phycobiliproteins (PBP) are the example, *par excellence*; there are also the oxygenated carotenoids, fucoxanthin and peridinin, which are exceptional in terms of carotenoids by the extension of their absorption spectra out to ~550 nm; and both seem to have evolved rather recently in world history, e.g. <300 Ma ((Dautermann and Lohr 2017). The obverse to the low light situation is the high light situation where algae and plants appear to have evolved special proteins such as **Flavodiirons** and **LHCSR** to avoid over-reduction of the reducing side of PSI and PSII (see below).

V. Light-Harvesting Antennas in Cyanobacteria and Eukaryotic Algae

In Cyanobacteria, phycobiliproteins are the light-harvesting antenna *par excellence*. However, it seems likely that these are a secondary, although very successful, evolutionary development. PBPs are also water soluble and extrinsic to the thylakoid membrane. It is more likely that they were preceded by membrane intrinsic light-harvesting antennae; of which there are still some in existence. The isiA antenna, containing only Chl *a* (Fig. 10.8), the pcb antenna, containing Chl *a* + *b* and similar antennae which bind Chls *d* and *f* (see Sects. 4 and 5) are examples of such antennae, although whether these preceded PBPs is not known. It seems clear too that these pigments if not their antennae were inherited by plastids, although the LHC (CAB/CAC) proteins seem to have evolved from high-light protection proteins (HLIP; see below) (Fig. 10.13; Engelken et al. 2010; Niyogi and Truong 2013). There are also HLIP proteins or equivalent in cyanobacteria, which almost certainly gave rise to the light-harvesting chlorophyll (LHC) proteins of algae and land plants (discussed below).

In all primary plastids, except the cyanelles of Glaucophyta, a related family of LHC membrane intrinsic proteins exists each with three membrane-spanning protein helices (Figs. 10.2 and 10.5). These bind ~8 Chl *a* and ~6 Chl *b* or *c* and 4 xanthophyll molecules (Rochaix 2014). In nearly all plastids the LHCs are divided into those attached to PSI (LHCI), and those attached to PSII (LHCII). However it has long been known that LHCII is mobile and can reattach to PSI under conditions where this evens up the activity of the PSs (see e.g. Larkum 2003). Much is known on the subdistribution of LHCI and LHCII in different plastids, particularly land plants. In eukaryotic algae most is known for *Chlamydomonas reinhardtii* (Rochaix 2014; Chap. 4): here 15 LHCII- and 6 LHCI-encoding genes have been identified. Clearly, there is much latitude here for adaptive responses in light-harvesting strategies. In eukaryotic algae, LHCII trimers are connected to RCII (a dimer of D1 & D2 which together with CP43 and CP47 form the core of RCII and bind to two monomeric LHCII proteins, CP26 and CP29 (see Fig. 10.11).

PSI RC complex is monomeric in algae, in contrast to Cyanobacteria, and a number of Chls bound to extra LHC an5ennae, which act as antennae: in *Chlamydomonas reinhardtii* there are up to 6 LHCI proteins,

bound asymmetrically in a crescent-shaped arc, and, during state transitions (see below), an additional number of LHCII molecules (Chap. 4). PSII RCII is dimeric with a D1 and a D2 core attached to a pair of CP43 and CP47 inner core antennae (Fig. 10.11). LHCII antennae are attached to this core, of which some are mobile and can move to PSI (Fig. 10.11; Chap. 4).

In secondary plastids, i.e. plastids that have evolved through two or more endosymbioses (see Sect. B), chlorophyll *a/c* (CAC) antenna proteins commonly exist (Figs. 10.6 and 10.7). These CAC proteins form a subfamily with CAB antenna proteins and clearly share an evolutionary history (Fig. 10.6; Neilson and Durnford 2010). However, in two closely related evolutionary lines either Chl *c,* or Chl *c* and Chl *a,* has been lost; these are **Chromerids** (loss of Chl *c*) and **Apicomplexans** (loss of Chl *c* and Chl *a*) (Larkum 2003, 2006, 2008; Keeling 2013; Chen 2014). In the Apicomplexans photosynthesis has been entirely lost and the reduced, non-photosynthetic relict plastid (a**picoplast**) is nevertheless retained and redeployed to produce vital organic compounds for the host (McFadden and Yeh 2017).

VI. Control of Energy Supply to PSI and PSII: State Transitions, Absorption Cross-Sectional Changes and Spillover

A. Overview

Photosynthetic organisms must often be able to adapt to light intensities that may range over a thousand fold intensity. Such environmental changes may be slow, such as weather–based or seasonal changes. Or they may be fast, ranging from moderately fast, as between dawn and noon time, to very fast as between clouds and full sunlight, or light flecks that occur in forests and in the sea. To meet these circumstances photosynthetic organisms put in place two kinds of adaptation/acclimation mechanisms: long-term changes brought about by DNA mechanisms and protein formation (and accompanying pigments) to produce new pigment levels (adaptation) and short term changes, which reassign the concentration of pigments already entrained (acclimation). Here we concentrate more on the short-term, acclimative changes. Long–term adaptive changes, which are well known in Cyanobacteria, eukaryotic algae and land plants, have been dealt with elsewhere (Larkum 2003; Falkowski and Raven 2007).

The ultimate benefit of all these mechanisms is to optimise the energy received by PSI and PSII so that the optimum levels of ATP and NADPH are produced, and thus to maximize efficiency. Note that where cyclic electron transport (CET) is involved, as it often is, to balance the need of the Calvin-Benson Cycle for more ATP than NADPH (Lucker and Kramer 2013; Chap. 12), there is a need to have PSI operating faster overall than PSII. Also note that under high light where damage to the photosynthetic apparatus might occur there is often a trade-off between efficiency and protection of the photosystems (Belgio et al. 2014).

B. State Transitions

State transitions were one of the first light-harvesting mechanisms to be documented (Murata 1969; Bonaventura and Myers 1989). The work of Murata (Murata 1969, 1970), showed, in red algae and in spinach chloroplasts, that the amount of variable fluorescence (assigned to PSII) was affected by the previous conditions of illumination. However, it was Bonaventura and Myers (1989) who first defined the phenomenon, albeit in a spillover model, which may be restated, as follows:

State I in which there is an excess of light available to and absorbed by PSI (light I) and a decrease in the amount of excitation energy distributed from the light-harvesting pigments to PSI; and

State II in which there is an excess of light available to and absorbed by PSII (light II) and an increase in the amount of excitation energy distributed from the light-harvesting pigments and PSII to PSI (Fork and Satoh 1986) (refer to Fig. 10.10). In darkness a State I condition is usually found.

Satoh and Fork (1983) proposed a putative third state (State III) from evidence using the green alga *Scenedesmus obliqua* and the red alga *Porphyra perforata* (now *Pyropia*). Illumination of this alga either in state I or state II with light II produced state III in which light energy reaching PSII was decreased with no attendant increase in the energy supply to PSI. This is similar to what has recently been proposed for diatoms by Drop et al. (2014a, b and see below). In *Pyropia (Porphyra)*, although there was no change in the distribution of energy between the two photosystems there was a decrease in the overall amount of excitation energy migrating to RCII from the light-harvesting pigments. This phenomenon is probably a photoinhibitory response whereby some phycobilisomes are decoupled under high light to protect the RCs from over-activity. Similarly, LHCs could be decoupled from PSII in *Scenedesmus* and diatoms.

The first physical model of the fluorescence changes in State Transitions came from Butler and coworkers (see Butler 1978) again in terms of a spillover model. It now seems more likely that the changes are effected in terms of re-association of light-harvesting complexes between the two PSs (rather than channelling of energy absorbed by one PS to the other – the latter is **Spillover**: it is still a possible explanation in some circumstances and is discussed in Sect. D). While there is strong evidence that redistribution of antenna complexes occurs in algae and higher plants, other mechanisms also seem to play a part. Thus down-regulation of PSII occurs, which is brought about, both by the xanthophyll cycle and by delta pH quenching (see below). But other unknown mechanisms also likely play a part.

A generalized model for changes in absorption cross-section in higher plants has been available for over 20 years (Allen et al. 1981; Allen 1992). As summarised in Fig. 10.10, the mechanism is thought, in streptophyte algae and land plants, to be as follows. In the dark or under **Light 1** (i.e. light that is preferentially absorbed by PSI – near infra red radiation >700 nm) PSII is in **State 1**, where the major LHCIIs are associated with PSII in appressed thylakoids (and grana in higher plants). Then upon preferential illumination of PSII under **Light 2** (i.e. light preferentially absorberd by PSII – red light), or high light, a transition to **State 2** occurs. Here evidence points to activation by a reduction of the plastoquinone (PQ) pool, which lies between the two PSs; and under these conditions, and through the mediation of the Q_o site of the cyt b_6f complex, at least one, and possibly more than one, membrane-bound protein kinase(s) becomes activated leading to the phosphorylation of mobile LHCII and other polypeptides. Phosphorylated LHCII then moves away from the appressed thylakoid regions, to unappressed thylakoids (in higher plants on the outside of grana or in the stroma lamellae, where it associates with PSI, leading to **State 2**. The membrane bound kinase is deactivated in the dark or in **Light 1** (and a latent phosphatase continually reverses the action of the kinase (Allen 1992), leading back to **State 1** (Fig. 10.10).

It should be remembered in consideration of algae that there is much less appression of thylakoids and lateral heterogeneity in algae; and that the photosystems are more homogeneously distributed in algae (Larkum and Vesk 2003). This even goes for many green algae including *Chlamydomonas reinhardtii*. It is only in the green algal group leading to the land plants, the streptophytes, that the strict lateral separation found in tracheophytes first began to appear (Larkum and Vesk 2003). Phosphorylation mechanisms have ceratainly been advanced for green algae (Escoubas et al. 1996) and there is some evidence that they may also exist in

dinoflagellates (ten Lohuis and Miller 1998). However, the greatest advance in the area of algae has come over the last two decades from studies of *Chlamydomonas reinhardtii* (Rochaix 2014; Chap. 4), an alga that can be transformed and has become the alga of choice, similar to the choice of *Arabidopsis thaliana* in higher plants (see next Sect. 1). Here state transitions are clearly connected with changes in absorption cross-section brought about by reassignment of LHCs as a result of short-term rearrangements and long–term production. Particularly important here is the realization that changes are brought about in going from low light to high light (and vice-versa) and that much can be learnt from such an approach. One recent example for *C. reinhardtii* is where changes in the LHCs have been physically mapped onto PSI and PSII (Drop et al. 2014a, b; Unlu et al. 2014; see Fig. 10.11); this is possible because through microscopy it is possible to carry out electron density scans of light-harvesting particles obtained from developed sucrose density gradients. What these investigations show is that the standard model of state transitions needs changing: **thus phosphorylation does not necessarily induce a State 1 to State 2 transition**.

All oxygenic photosynthetic organisms appear to display some form of state transitions: largest in Cyanobacteria and red algae and lowest in land plants. Changes in optical cross-section of the PSs (see below) can best explain the mechanism of state transitions. However changes in optical cross-section and state transitions do not seem to be quantitatively correlated (Haldrup et al. 2001; Wollman 2001) and other mechanisms need to be invoked. Thus, although, state transitions have been a simple way to study responses to short-term changes in energy distribution to PSI and PSII and have been used extensively for this purpose (see e.g. Haldrup et al. 2001; Wollman 2001), better descriptions need to be formulated in the future. Here, we concentrate on what is known from *Chlamydomonas reinhardtii* because this is where most recent advances in algae have been made as a result of the greater genetic information and transformability of this organism (see reviews e.g. by Rochaix (2014) and Chap. 4).

1. State Transitions in Chlamydomonas

In *Chlamydomonas reinhardtii* state transitions involve 80% mobile LHCII as compared with 15–20% in *Arabidopsis thaliana* (Delosme et al. 1996; see Chap. 4). Work on mutants has revealed a mutant, Stt7, in which State 1 is blocked, is deficient in LHCII phosphorylation in State 2 and lacks Stt7 protein kinase (Depege et al. 2003); this has an equivalent in *A. thaliana* STN7. There is also an additional mutant Stt1 (STN8 in *A. thaliana* (Rochaix 2014)). It is likely that in the mutant Stt7/STN7 a protein kinase is deficient and cannot phosphorylate LHCII. Thus the mutant is locked under State 1 conditions, with mobile LHCII on PSII and blocked from transferring mobile LHCII from PSII to PSI (Chap. 2).

In a another study of structural rearrangements during State Transitions in *C. reinhardtii* (Drop et al. 2014b), it was shown that under State 2 conditions, PSI is able to bind two LHCII trimers that contain all four LHCII types, and one monomer, most likely CP29, in addition to its Lhca. This structure is the largest PSI complex ever observed, having an antenna size of 340 Chls/P700. Moreover, all PSI-bound Lhcs were efficient in transferring energy to PSI. Interestingly, only LHCII type I, II and IV were phosphorylated when associated with PSI, while LHCII type III and CP29 were not, but CP29 was phosphorylated when associated with PSII in state 2. In another study from the same group (Unlu et al. 2014), it has been shown that although some LHCII reattaches to PSI under State 2 conditions the majority becomes detached from PSII but does not reattach to PSI. These studies underscore what has become clear from a number of recent studies, that the classical view of

phosphorylation of LHCII under reduced PQH conditions and its reattachment to PSI is an oversimplification.

2. An Aside on Cyclic Electron Transport (CET)

It should be pointed out that the suggested function of State Transitions in bringing about equal activity of the PSs was challenged long ago by Bulté et al. (1990), who suggested that the main function of State Transitions might be to balance the production of ATP and $NADPH_2$, which, therefore, has to accommodate cyclic electron transport around PSI (and this is further discussed in Chap. 12). They showed that inhibition of ATP production in intact cells in *Chlamydomonas reihardtii* led to a transition to State II while an increase of ATP production caused a change to State I. This proposal seems to have been upheld by later investigations (Delosme et al. 1996). Recent work has shown that CET is controlled by redox chemistry and not by State Transitions; for example State 2 was not required for inducing CET, since anoxic conditions enhanced CET, both in wild type and in an stt7 mutant blocked in State 1 and the PSI-$Cytb_6f$ supercomplex involved in CET was formed independently of State Transitions (Takahashi et al. 2013). In the unicellular red alga *Rhodella* violacea, in contrast to *Chlamydomonas,* State Transitions were not accompanied by phosphorylation of thylakoid proteins (Delphin et al. 1995). Also ST occurred under conditions where the activity of PSI did not change and it was suggested that ΔpH changes across the thylakoid membrane triggered "state II" quenching possibly through a down-regulation process of RCII (Delphin et al. 1996).

3. State Transitions in Other Algae

State Transitions have been investigated in a number of other algae since the early work, which was mainly directed to cyanobacteria, green algae and higher plants: the groups investigated include brown algae (Fork et al. 1991); *Chromera velia* (Belgio et al. 2018; Llansola-Portoles et al. 2016, 2017; Quigg et al. 2012); chlorophytes (*Dunaliella*) (Ihnken et al. 2014); cryptophytes (Bruce et al. 1986); chrysophytes (Gibbs and Biggins 1991); *Nannochloropsis* (Eustimatophyceae) (Bina et al. 2017; Chukhutsina et al. 2017; Litvin et al. 2016; Szabo et al. 2014; Umetani et al. 2018); *Pleurochloris* (Xanthophyceae) (Büchel and Wilhelm 1990). In *Pleurochloris* the state transitions were wavelength-independent.

In many cases the extent of State Transitions is much more pronounced in algae than in plastids of higher plants (Schreiber et al. 1995). Furthermore, apart from the streptophyte algae, it appears that there is little lateral heterogeneity in the thylakoids of algae (Larkum and Vesk 2003; Larkum 2003). As a result there is the possibility of energy transfer between the PSs. Thus further scrutiny of light energy distribution to the PSs in algal plastids is more than justified., especially as concerns Spillover (Sect. D).

C. Absorption Cross-Sectional Changes

As shown above state transitions can be understood in higher plants in general terms as brought about by changes in the oxidation-reduction potential of plastoquinone and the resultant phosphorylation/dephosphorylation of LHCII, although many fine details remain to be worked out. Such changes are largely artificial in that they do not occur naturally, and have been used only to examine the mechanisms behind these changes, using rather artificial lighting conditions. A much more natural effect is the short-term change from high light to low light and vice versa, an occurrence which is very normal for an alga undergoing changes in shading due to clouds, diurnal events, sun flecks and wave/wind effects, etc. Such changes have become a focus of several recent studies, the

most insightful of which have been carried out on *Chlamydomonas reinhardtii* (see Chap. 4). As mentioned in Sect. 1, several genes have been identified which influence the placement of LHCII between PSI and PSII. Also by analogy with *Arabidopsis,* it appears that the placement of LHCI and LHCII in the two PSs is regulated in different ways when the light intensity changes (Chap. 4, Rochaix 2014). The recent demonstration of large changes in the antenna size and distribution of LHCI and LHCII in *C. reinhardtii* (Drop et al. 2014a, 2014b; Unlu et al. 2014) indicate the potential of these technique; and the effects of light intensity changes will be awaited with interest.

Of course, changes in absorption cross-section in response to light intensity changes is only one mechanism of dealing with changes in light intensity. Another important mechanism is to down-regulate light energy uptake by the process of non-photochemical quenching (NPQ) and this phenomenon is dealt with next.

When the flux of photons to PSI and PSII is not equal, one way of effecting equal activity of PSI and PSII, is to reduce the excitation energy flowing to one PS and to increase it to the other. Initially it was supposed that there was a mechanism ("**spillover**"), which simply diverted energy from one photosystem to the other – predominantly from PSII to PSI (Larkum and Barrett 1983). However, the mechanism now generally proposed is in terms of mobile light-harvesting units, which change the optical cross-section, and also maybe change the spectral properties, of one or both photosystems (Fosberg and Allen 2001; Minagawa 2013; Rochaix 2014). However, proposals of spillover are still being put forward in special circumstances (see next Sect. D).

While the general principles of this proposed mechanism have been supported, in the interval there has been much progress in many areas – both in higher plant and in algal studies. In higher plants it has been shown that there is a specific LHCI, which acts to harvest light specifically for PSI (Green and Durnford 1996). Thus changes in cross-sectional area of PSI and PSII due to re-association of mobile LHCII can only contribute a small fraction of change in cross-sectional areas (usually <20%). In higher plants too it has been shown that the PSI subunit H polypeptide is essential for docking of phosphorylated LHCII and in mutants lacking the H subunit phosphorylated LHCII stays associated with PSII – with no changes in cross-sectional area (Lunde et al. 2000; Haldrup et al. 2001). Furthermore it has been shown that phosphorylation of LHCII is not linearly dependent on the reduction of PQ (Haldrup et al. 2001): the degree of phosphorylation reaches a peak at rather low light intensities (of light which preferentially activates PSII).

In algae in general (other than streptophyte green algae) the distribution of PSI and PSII often appears to be quite homogeneous (Larkum and Vesk 2003). Here there is less evidence for phosphorylation of LHCs driven by Light 1 and Light 2 (and the involvement of a PQ-driven mechanism). Gibbs and Biggins 1991 argued against such a phosphorylation mechanism in the Chl *c*-containing chrysophyte alga, *Ochromonas*. Allen (1992) gives a review of this early work on eukaryotic algae. Figure 10.9 summarises the current thinking on state transitions in streptophyte algae and land plants. There the appression of thylakoids into grana causes the separation of PSI complexes into sites on the grana margin or in stroma lamellae (**lateral heterogeneity**). In these circumstances, state transitions effect a redistribution of energy to PSI from PSII by rearranging LHCs (refer to Larkum 2003). In *Chlamydomonas reinhardtii*, as mentioned in Sect. 1, there appears to be a much greater lability in rearranging LHCs (see also Chap. X). In other algae the association of thylakoids can be even freer than in *C. reinhardtii* and here it is possible to envisage energy migration from PSII to PSI and vice versa over

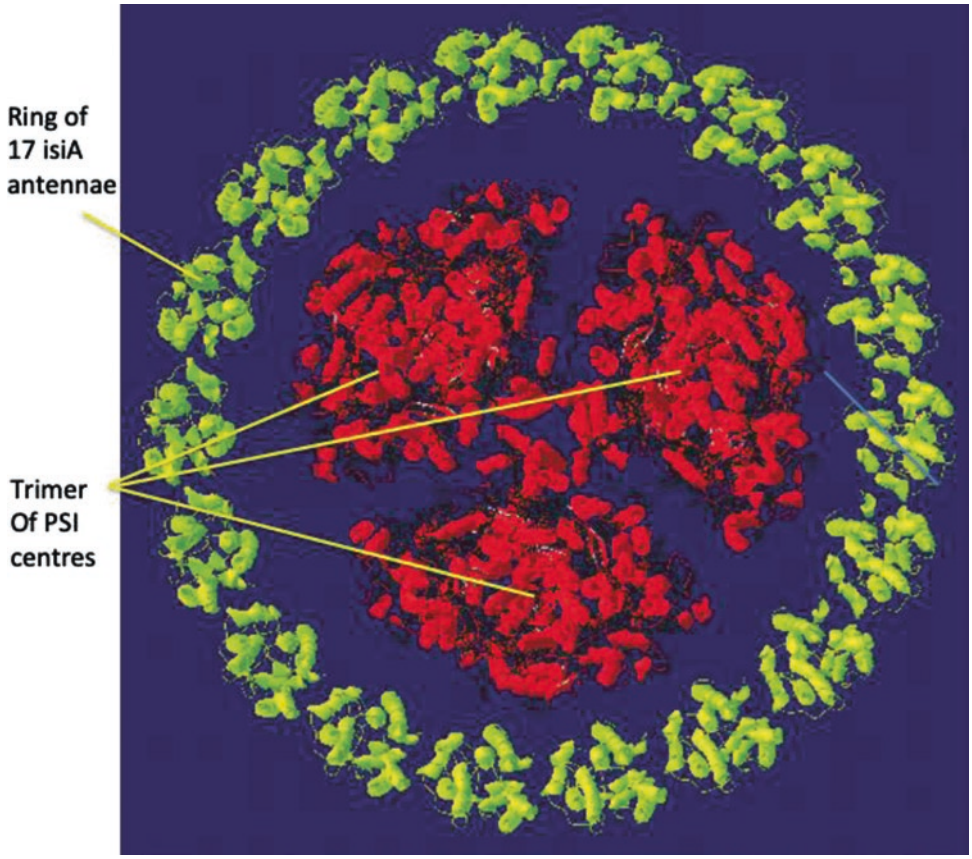

Fig. 10.9. Space-filling model of the structure of the isiA-photosystem I supercomplex of *Synechococcus elongatus* PCC 7942, with a 17-mer isiaA ring. Taken from the work of Yinan Zhang and Anthony Larkum (see also e.g. Zhang et al. 2010)

short distances, encompassing "**spillover**" (see below).

In Cyanobacteria and red algal plastids, the main light-harvesting system is the phycobilisome (PBS) and there has been much debate over whether the attachment of PBS to PSII or PSI is driven by the redox state of PQ involving phosphorylated proteins (for a detailed review see Allen 1992). Certainly there is good evidence that the absorption cross-sections of PSI and PSII change in response to Light 1 and Light 2 and this has been amply borne out by many recent publications on the rearrangement of LHCs in response to changes in light intensity or quality (see, e. g. Figure 10.10). Many proteins are also phosphorylated in the light. Recent evidence seems to suggest that the PBS physically move between PSII and PSI sites (Mullineau and Sarcina 2002; Sarcina et al. 2001). However, there is certainly evidence for a protective mechanism in red algae whereby energy is directed from one PS to the other in what has been called **spillover** (see below, and Kowalczyk et al. 2013) and of course there is the Orange Carotenoid Protein which can cause non-photochemical quenching of light energy before it arrives at the thylakoid membrane (see Sect. C and Chap. X) (Fig. 10.11).

Almost certainly there are distinct differences in the mechanisms by which short-term accommodation of Light 1 and Light 2 effects changes in the cross-sectional areas of PSI and PSII in cyanobacteria, algae and

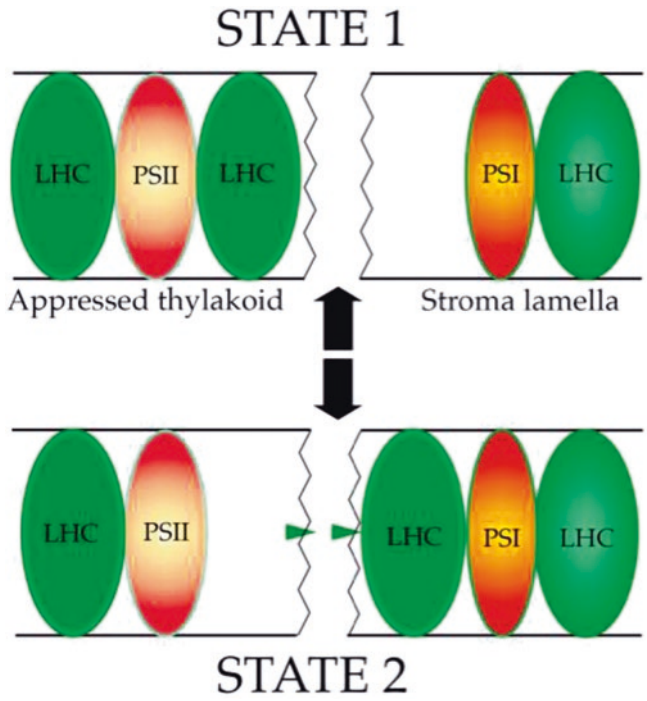

Fig. 10.10. A simplified model of State I/State II transitions in streptophyte green algae and land plants. The scheme is based on the phosphorylation model first proposed by Allen et al. 1981 (see also Allen 1992)
Light 1 (generally near-infra red radiation <700 nm), or darkness, causes the movement of mobile LHCII from PSI in non-appressed membranes to PSII in appressed membranes, to generate **State 1**
Light 2 (generally red light) or high light, drives the movement of LHCIIs to PSI to form **State 2;** thus the mobile LHCII moves to non-appressed thylakoids membranes and PSI, from PSII in appressed membranes
In *Chlamydomonas reinhardtii,* as mentioned in Sect. 1, there is much greater mobility of the LHCs. In other algae the strict separation of PSII and PSI is much looser. And in many groups of algae it is possible to envisage local migration of energy from PSII to PSI and vice versa in a process of "spillover" (see Sect. D)

land plants. Pursiheimo et al. (1998) proposed three categories: **Group 1**, Cyanobacteria and red algae, which did not show phosphorylation of any of the PSII proteins; **Group 2** consisting of some of the remaining eukaryotic algae, mosses, liverworts and ferns, which phosphorylated both the light-harvesting CAB proteins (LHCII) and the PSII core proteins D2 and CP43, but not the D1 protein, and **Group 3** where reversible phosphorylation of the D1 protein of PSII was found only in seed plants and was seen as the most recent evolutionary event in the series. In terms of phosphorylation of LHCII they found that Groups 2 and 3 were similar with maximal phosphorylation of LHCII at low light and nearly complete de-phosphorylation at high light. Clearly this survey did not include any algae dependent on CAC light-harvesting systems. However, the large number of studies of *Chlamydomonas reinhardtii* over the last two decades has provided a solid base for understanding this system (see Sect. 1, Rochaix 2014 and Chap. 4), with some recent revaluation of the finer details of the mechanisms (Tikkanen et al. 2012; Croce and van Amerongen 2014; Steinbeck et al. 2018).

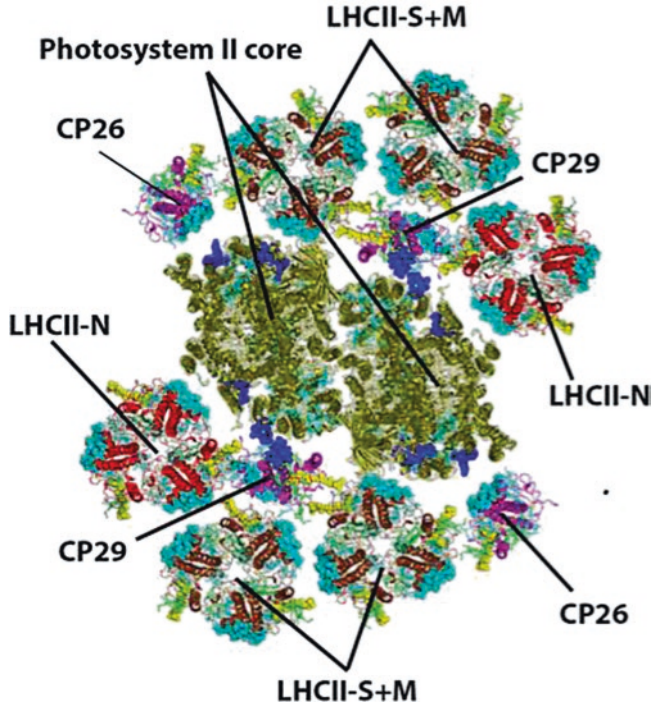

Fig. 10.11. Space-filling model for *Chlamydomonas reinhardtii* of PSII with LHC units in State I before transfer of subunits in State II. The model was assembled using crystal stuctures of cyanobacterial PSII core, LHCII trimer and CP 29. For CP26, the structure of monomeric LHCII has been used. Proteins of the PSII core (lime green), LHCII-S and –M (brown), novel LHCII-N (red), CP29 and CP26 (magenta), Chl a (cyan), Chl b (green), neoxanthin (yellow spheres), lutein L1 (orange), lutein L2 (dark yellow sticks). (Taken from Drop et al. 2014a)

D. Spillover

Spillover is a term first used by Butler in the 1950s to denote a physical migration of excitation energy along subunits in the thylakoid membrane from one photosystem to the other (usually from PSII to PSI). In its earliest formulations it can probably be seen as a process that was confused with changes in absorption cross-section, brought about by reassignment of antenna unit or subunits. Nevertheless, a valid use of the term seems to have been that of Ley and Butler (1980) who studied the fluorescence changes in the unicellular red alga *Porphyridium cruentum*. As recently reported in the high-light-stressed intertidal red alga, *Chondrus crispus* (Kowalczyk et al. 2013), a real migration of energy from PSII to PSI can be detected, rather than a deactivation through an NPQ pathway. Another situation, where spillover has been shown is in the Lichen *Parmelia sulcata*, which harbours a unicellular Trebouxian green alga ((Slavov et al. 2013) where a process been called "superquenching" has been shown and this has also been shown to occur in dinoflagellate symbionts of a coral species (Slavov et al. 2016) under enhanced temperature (coral bleaching) conditions. It should be pointed out that few eukaryotic algae have thylakoids with grana, and true appression has not been documented (Larkum and Vesk 2003), i.e. where PSII is physically segregated from PSI (see e.g. (Rochaix 2014). It is therefore possible in algae, and in Cyanobacteria, for PSI and PSII to be physically close to one another, and therefore, theoretically, for energy to

migrate from one photosystem to the other. How widespread this phenomenon is has yet to be shown.

E. Complementary Chromatic Adaptation

Phylogenetic complementary chromatic adaptation (CCA) was an early hypothesis which explained that in seas and oceans, red algae (Rhodophceae) grew better at greater depth because the red pigments (phycobiliproteins) allowed these algae to capture more light than green or brown algae (Larkum and Barrett 1983). As first shown by Crossett et al. (1965) in oceanic water, where the maximum wave length of penetration is in the blue region of the visible spectrum, there is no advantage to red algae or Cyanobacteria and most classes of benthic algae grow at depth, including the forests of brown algae such as *Laminaria*. However, it is true that in coastal waters with extreme levels of "yellow substance" such as the Baltic Sea, phytoplanktonic cyanobacteria and benthic red algae grow more efficiently than other algae at greater depths in the green light (of inshore waters) more efficiently than other algae (Larkum and Barrett 1983).

Ontogenetic CCA was first shown in elegant detail by Tandeau de Marsac (1977) in Cyanobacteria. They showed that under green light as opposed to blue light (i.e. under inshore spectral conditions vs. oceanic conditions) certain (but not all) Cyanobacteria had the ability to switch the production of phycobiliproteins from phycocyanins (PC) to phycoerythins (PE) enhancing the absorption of green light, which theoretically gave these algae the ability to grow better in inshore waters where "yellow substance" was in higher concentration (sse Larkum and Barrett 1983). Further research using modeling and laboratory experiments has shown that this model can explain why two *Synechococcus spp,* one with PE can grow better in inshore waters than another with phycocyanin and how a cyanobacterium such as *Tolypothrix tenuis*, which can change its PBP from PC in blue light and to PE in green light can compete better to changes in light quality than cyanobacteria, which constitutively produce only PC or only PE. This hypothesis of ontogenetic CCA has also been further developed by Kehoe (2010). And Kehoe and Grossman (1996) showed that biosynthesis of PBP was under the control of a sensor system similar to phytochrome. The laboratory of Jeff Huisman has made several important contributions to understanding of the growth of phytoplankton at different depths in oceans and inshore waters; for example they showed that the vibrations of the water molecule itself makes an important contribution to the success of various phytoplankton organisms in the sea (Stomp et al. 2007). Thus the simple story of CCA has many nuances in the real world (Stomp et al. 2004). In marine *Synechocccus* it has been shown that there can be up to four different types of CCA (Sanfilippo et al. 2019).

Ontogenetic CCA is not just restricted to the PBPs of Cyanobacteria. Recently Don Bryant's laboratory has shown that NIR radiation induces a FaRLiP system controlling the production of Chl *f* and special PBPs that are able to absorb radiation in the Red and NIR region of the spectrum (Gan et al. 2014, 2015; Ho et al. 2016a, b, c; Shen et al. 2019).

CCA is probably widespread in the eukaryotic algae, although not a great deal of research has been carried out. Even in Chl *a/b* organisms it has recently been found that changes in visible light quality can effect changes in the LHCs (see Chap. 3). And it has been well known for several decades that deep water green algae have extremely large amounts of special LHCs with high ratios of Chl *b* to Chl *a.* However, as discussed by Larkum and Barrett (1983) it is often difficult to separate out effects of low light from changed spectral quality at depth.

F. Non-photochemical Quenching – Sensu Lato

Non-photochemical quenching is a set of processes, whereby light energy is deactivated as heat before it is channeled to the reaction centres; it is a protective mechanism that is activated under high light, protecting the reaction centres from damaging levels of excitation, which can give rise to photoinhihibition, through the degradation of key peptides and the activities of Reactive Oxygen Species (ROS). The oldest known process is the Xanthophyll Cycle, which is activated by key carotenoids and triggered though the polypeptide PSBS, in land plants or LHCSR (LHCX) in most algae (Lepetit et al. 2013; Niyogi and Truong 2013). There is another process, which is simply triggered by low pH and involves a number of xanthophylls – see Chap. 12. Additionally in some Cyanobacteria there is a specific mechanism brought about by the Orange Carotenoid Protein (OCP), which acts similarly to deactivate excitation energy as heat – see Chap. 14.

VII. Non-photochemical Quenching

A. The Xanthophyll Cycle

The Xanthophyll Cycle in its generally recognised form occurs in most eukaryotic algae and in higher plants (Demmig-Adams et al. 2014).

There is a general lack of evidence for a conventional Xanthophyll Cycle in Cyanobacteria: a limited epoxide cycle takes place with changes in levels of zeaxanthin (see 1A, below): however, there an Orange Carotenoid Protein (OCP), occurs in about 50% of Cyanobacteria (Chap. 14) and this protein modulates the down-regulation of light energy from the phycobilisomes to the PSs; also in those cyanobacteria where the OCP mechanism does not occur or where PBS do not occur down-regulation of light energy may well occur through through the rings of protein-binding Chl *a* or Chl *a* + Chl *b* (Fig. 10.9) (Zhang et al. 2010).

The xanthophylls involved are violaxanthin, antheraxanthin and zeaxanthin or diatoxanthin and diadinoxanthin (Figs. 10.4 and 10.12). In the conventional Xanthophyll Cycle light causes violaxanthin to transform into zeaxanthin (via antheraxanthin), and diadinoxanthin to diatoxanthin, (Demmig-Adams and Adams III 1993; Larkum 2003).

Much less work has been carried out on algae in general, other than some green algae such as *Chlamydomonas reinhardtii* (Rochaix 2014; Chap. 4) and diatoms (see below). Nevertheless there is good evidence to believe that a xanthophyll cycle does exists throughout the eukaryotic algae (Lichtle et al. 1995; Goss and Bohme 1998; Brown et al. 1999; Lohr and Wilhelm 1999).

In the xanthophyll cycle the changes in the light are brought about by enzymic de-epoxidases and subsequently, in the dark or shade, by epoxidases (Fig. 10.12) and these have been well documented, (see e.g. Yamamoto 1979; Mohanty et al. 1995; Demmig-Adams and Adams III 1993; Demmig-Adams et al. 2014). Thus one molecule of oxygen is liberated (de-epoxidated) or taken up (epoxidated) for a complete transition. In algae these changes were worked out in some detail by Stransky and Hager as long ago as Stransky and Hager 1970 and their general conclusions, shown in Fig. 10.12 have been substantiated as follows:

Group 1A (Cyanobacteria, Glaucophyta) only a limited epoxide cycle takes place with changes in levels of zeaxanthin;

Group 1B: the situation in Rhodophyta, has recently been unraveled by Dautermann and Lohr (2017); here it has been shown that red algae have inherited a zeaxanthin de-epoxidase (ZEP) from a joint ancestor of red algae and green algae and have passed this on to stramenopiles and photosynthetic alveolates (Chromalveolates). However in the case of Rhodophyta only some groups have a ZEP, and those that have, only transform zeathanthin to antheraxanthin, and not violaxanthin; but as a

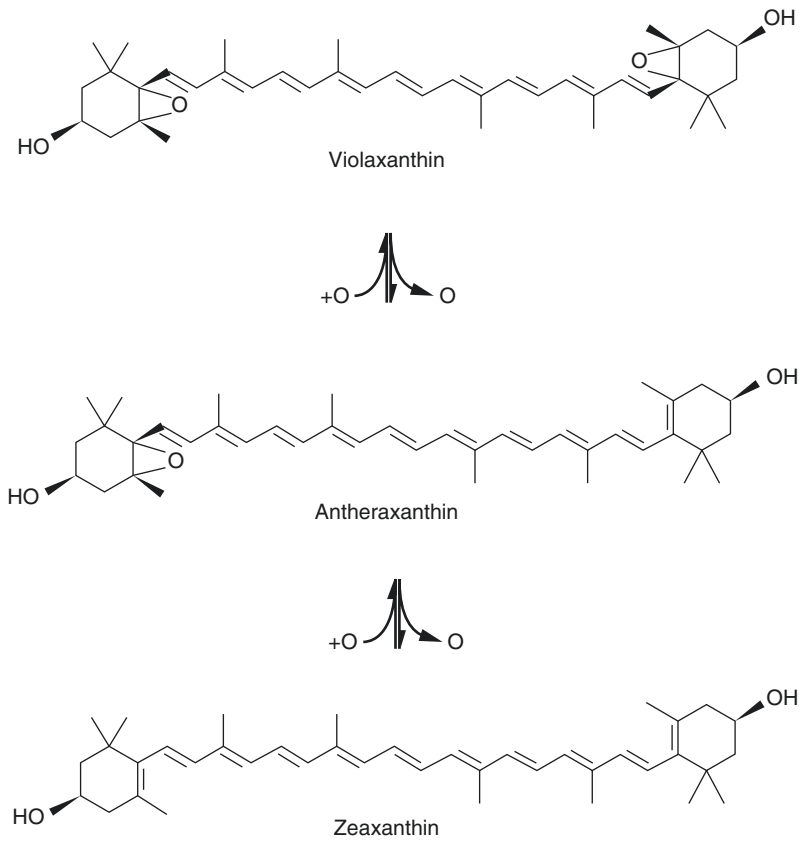

Fig. 10.12. The basic xanthophyll cycle: the interconversion of violaxanthin and zeaxanthin, with light triggering the conversion of violaxanthin to zeathanthin (or diadinoxanthin to diatoxanthin in those algae which possess these xanthophylls). In some diatoms and Chl *c*-containing algae a more complex situation occurs (see text, Sect. A)

result at least some red algae probably have a reduced xanthophyll cycle; whereas in the next group (2) diadinoxanthin is de-epoxidated by a ZEP to diatoxanthin (the equivalent of violaxanthin) in a full xanthophyll cycle;

Group 2 (Bacillariophyta, Chrysophyta, Xanthophyta, Chloromonadophyta, Dinophycta and Eugelenophyta), diadinoxanthin is the oxygenated carotenoid and diatoxanthin is the de-epoxidated carotenoid, which are derived from neoxanthin (which in turn are derived from violaxanthin). In addition it may be noted that the allenic xanthophylls, peridinin fucoxanthin and vaucherioxanthin acyl esters are derived from neoxanthin.

Group 3 (Phaeophyta and Chlorophyta and a few species of some other Classes), the full Xanthophyll Cycle is present. In micromonadophyte algae (Mamieliaceae) only a part of the conventional Xanthophyll Cycle is present – that converting violaxanthin to antheraxanthin (Goss and Jakob 2010); furthermore, Lohr and Wilhelm (1999) have shown that some algae displaying the diadinoxanthin type of a Xanthophyll Cycle also display features of the violaxanthin-based cycle. In addition, a caution has been put forward for not taking conventional NPQ for granted in all algal classes by Berne et al. (2018).

In general as light levels increase so the level of violaxanthin/diadinoxanthin decreases, reaching a steady level, and, conversely, the level of zeaxanthin/diatoxanthin

increases to an asymptote (Demmig-Adams and Adams III 1993) and this stimulates NPQ.

The Xanthophyll Cycle involves, generally, three factors in the stimulation of a non-photochemical quenching (NPQ) of energy in the PSII/LHCII assemblage:

(i) an increased concentration of zeaxanthin (or diatoxanthin),

(ii) the presence of LHCSR in eukaryotic algae (and to a lesser extent in (liverworts, mosses and other non-vascular plants i.e., non tracheophytes), and PSBS, in green algae and land plants,

(iii) a ΔpH across the thylakoid membrane. Here the low pH of the thylakoid lumen acts on the PSBS protein or the LHCSR (see, e.g. Allorent et al. 2013; Chap. 12).

With these three factors in operation, and in the presence of LHCII, excitation energy is transferred to the carotenoid and excitation energy is transduced to heat, presumably in one of the LHCs.

It appears that in algae with phycobiliprotein-dependent primary plastids, i.e. in some Rhodophyta (without a ZEP) and in all Glaucophyta, energy dependent quenching is controlled by a mechanism allied to OCP quenching in Cyanobacteria (Chap. 14). However on the green line and in secondary plastids there has been the evolution of the three-helix LHCs and the evolution of the special quenching protein LHCSR (Niyogi and Truong 2013). In *Chlamydomonas* it has been shown by Minagawa and coworkers (see below) that there are two controls on LHCSR.

In streptophyte and land plants, the non-chlorophyll-binding, 22 kDa 4-helix protein, PSBS, has been shown to have been independently evolved (Li et al. 2002; Niyogi and Truong 2013); so LHCSR and PSBS are present together in streptophyte algae, liverworts, mosses and some ferns. In these taxa the evidence suggests that both LHCSR and PSBS are involved in energy-dependent quenching, qE (defined as that component of the total non-photochemical quenching, qN, directly attributable to the energisation of the thylakoid membrane (i.e. linked to a rapid change in ΔpH; see Sect. B on "pH Quenching", below) and therefore the rapidly entrained component of qN). PSBS protein may lie in an intermediate position between LHCII and the inner antennae of RCII (Belgio et al. 2014).

Light-harvesting complex-stress-related (LHCSR) proteins are a protein family allied to the 3-helix LHCs (Figs. 10.12 and 10.13) and evolved from them specifically as energy quenchers, to reduce the formation of ROS upon transitions from low to high light. There are two types of LHCSR, LHCSR1 and LHCSR3 (Allorent et al. 2013; Niyogi and Truong 2013; Kosuge et al. 2018). In *Chlamydomonas*, LHCSR3 is triggered by blue light and activates a low-pH-dependent NPQ of PSII (Allorent et al. 2013; Niyogi and Truong 2013), whereas LHCSR1 is triggered by UV light as well as visible light in the presence of CO_2 (where the stimulation is five to ten fold) and triggers a low pH dependent spillover of excitation energy from PSII to PSI and NPQ in the LHC of PSI (Pinnola et al. 2015: Kosuge et al. 2018) (see Fig. 10.13). In contrast in *C. reinhardti,* LHCSR3 is completely repressed by CO_2 in the light. Kosuge et al. (2018) speculate that "LHCSR1-mediated fluorescence quenching by PSI in green algae is the primitive photoprotection mechanism of green photosynthetic eukaryotes". Also recently, Girolomoni et al. (2019) have shown that LHCSR3 is involved in NPQ in both PSI and PSII in *Chlamydomonas reinhardtii*.

A number of specific details are known concerning the reactions involved in quenching by zeaxanthin (and diatoxanthin). For instance, dibucaine stimulates the quenching and antimycin A, dithiothreitol (DTT) and the protein carboxyl-modifying agent dicyclohexylcarbodiimide (DCCD) inhibit the quenching. Horton et al. (1996) suggested that there is a pocket extending from the

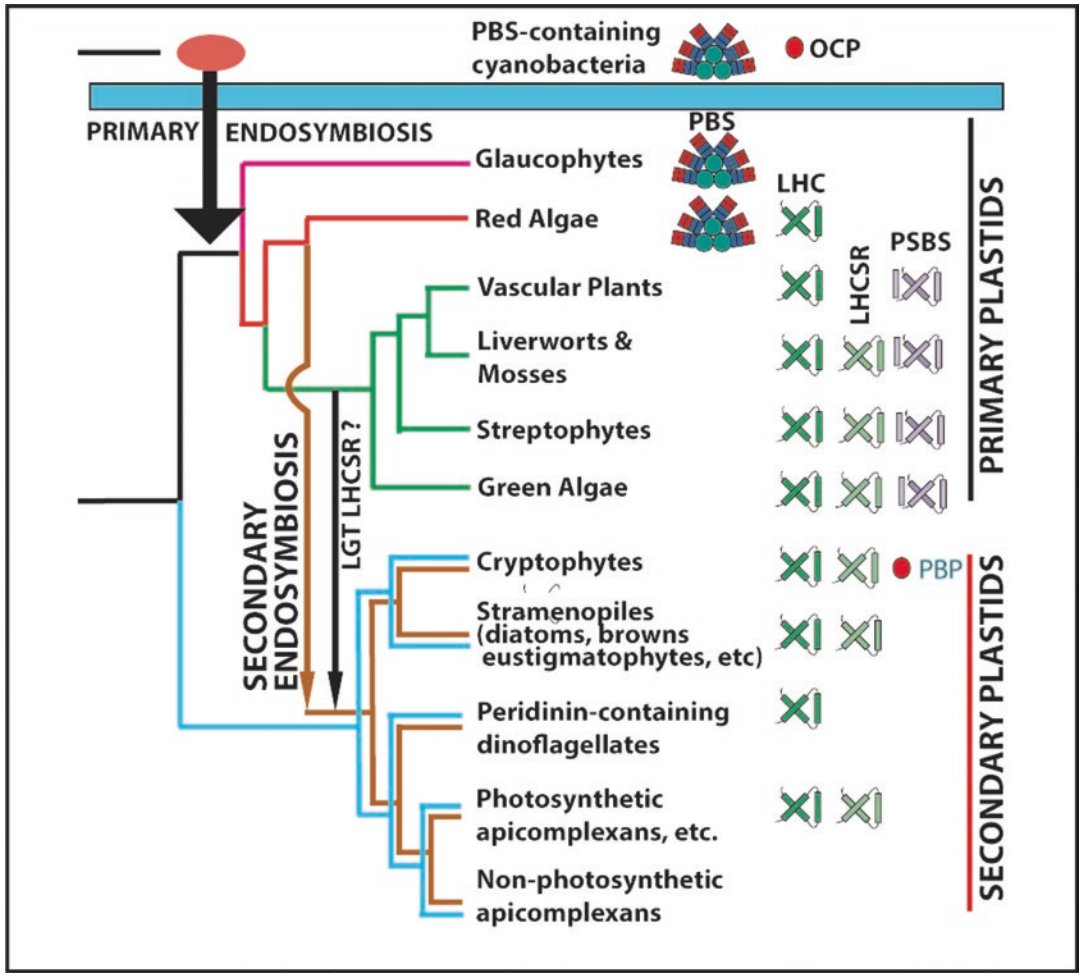

Fig. 10.13. Scheme showing the likely evolutionary events in the formation of photosynthetic proteins involved in light-harvesting and photoprotection (based on the scheme of Engelken et al. (2010) and Niyogi and Truong (2013). For simplicity the evolution of HLIP, OMP and SEP proteins has been omitted (but see Engelken et al. 2010 and Sturm et al. 2013). According to Engelken et al. (2010) PSBS/LHCSR evolved independently of LHC proteins. LGT lateral gene transfer, PBP phycobiliprotein

intrathylakoid lumen into the membrane by which low pH in the thylakoid lumen can influence a critical site in the thylakoid membrane. Since PSBS is essential for qE to occur it may be that protein, which senses the low pH and the binds zeaxanthin or it may play a crucial structural role in energy transfer/dissipation (Li et al. 2002). The mechanistic details of energy quenching have yet to be fully worked out. Clearly if the mechanism is to work zeaxanthin has to be able to change its molecular excitation states, which would then allow it to dissipate excitation energy as heat when triggered by low pH. Work by the group of Frank (see Josue and Frank 2002) suggested that the S1 state of carotenoids is important for this kind of down-regulation.

The situation in algae is even more complicated in comparison with higher plants. Firstly chlororespiration may make up a larger component of electron flow than in higher plant plastids (Minagawa 2013; Rochaix 2014, Chaps. 4, 8 & 12) and chlororespiration may induce a pH gradient even in

the dark (e.g. in *Euglena,* Doege et al. 2000). Secondly, qE seems to be independent of the xanthophyll cycle in *Euglena* (Doege et al. 2000). Thirdly, Cyanobacteria, admittedly oxygenic photosynthetic bacteria and not algae, but nevertheless with similar photosynthetic mechanisms, and sharing an ancestry, do not have the conventional xanthophyll cycle and yet carry out down-regulation of photosynthesis, both by conventional carotenoids (Schreiber et al. 1995) and by the orange carotenoid protein (see Chap. 14). Fourthly, it is clear that in Chromealveolates the equivalent of a Zeaxanthin (ZEP), forming diatoxanthin from didinoxanthin, has been inherited from a red algal/green algal ancestor and that this has led not only to NPQ under high light by a Diadinoxanthin Epoxidase but also to the evolution of the special allenic and acetylenic xanthophylls such as fucoxanthin, peridinin and vaucheriaxanthin, which are such a notable feature of diatoms and allied algae (Table 10.2) (Dauterman and Lohr 2017; Chap. 12).

B. pH Quenching

Low pH is clearly involved in conventional NPQ quenching. However, many workers in the field have suggested that there are other mechanisms by which eukaryotic algae and land plants can quench excitation energy; this is through the action of low pH on ATP synthase (Kanazawa et al. 2017; Kohzuma et al. 2017; Davis et al. 2017; Chap. 12) and on proteins involved with the intermediate pathway of electron transport between PSII and PSI (Chap. X). More recently it has been shown in *Chlamydomonas reinhardtii* that low pH also causes LHSCR1 to initiate spillover from PSII → PSI and also to activate excitation energy down-regulation in the LHC of PSI as well as in P700 (Kosuge et al. 2018). In diatoms, LHSX a variant of LHSR light-harvesting proteins plays an important role in NPQ associated with changes in ΔpH (Bailleul et al. 2010; Taddei et al. 2018).

C. Orange Carotenoid Protein

The orange carotenoid protein was discovered relatively recently (Kirilovsky and Kerfeld 2012; see Chap. 14). It is, as its name suggests, a caroteno-protein, which is produced under high light in Cyanobacteria; initially it was thought that it occurred in only certain Cyanobacteria but it has been found to exist quite widely; and as mentioned above has a counterpart in Glaucophyceae. The OCP is located on the stalk of the phycobilisosome under high light and channels excitation energy into the carotenoid where the energy is dissimulated as heat. However, the OCP has a second role in quenching singlet oxygen (Sedoud et al. 2014).

When the light intensity is reduced to non-stressful levels a Fluorescence Recovery Protein (FRP) decouples the OCP and excitation energy is once again passed on to the local reaction centre (Gwizdala et al. 2013; Chap. 14).

VIII. Reactive Oxygen Species (ROS) and Other Photoprotective Mechanisms

Reactive oxygen species (ROS) are comprised of singlet oxygen ($^1O_2$), hydroxyl radical (OH∗), hydrogen peroxide (H_2O_2) and a number of smaller constituents (Schmitt et al. 2014). All of these radicals have short half-lives and degrade organic molecules to form oxidation products; singlet oxygen has a half-life of ~ 3.5 μs at normal temperatures. With lipids, lipid peroxides are formed which may be strongly detrimental to normal membrane-based reactions. Thus the formation of ROS, which is unavoidable when electron transport processes are involved, is an activity, which is a) curtailed as far as possible and b) mitigated

by repair processes. A prime example is in PSII where for reasons of proper functioning of P680 a carotenoid triplet valve cannot be put in place and D1 protein is actively degraded during photosynthesis and must be actively replaced (Andersson and Aro 2001; Larkum 2003; see Sect. 1).

To mitigate the formation of ROS, a set of protective measures are set in place in eukaryotic algal systems. One of these is the alternate oxygenase (NOX); another is Mehler Ascorbate Peroxidase (MAP) pathway, whereby electrons are channeled out of the reducing side of PSI to oxygen, rather than feeding into NADP reduction (Miyake and Asada 2003). And another are the flavodiiron proteins, which have a limited capacity to mop up excess electrons arriving at the reducing side of PSI (Gerotto et al. 2016).

However, just as importantly ROS (H_2O_2, singlet oxygen and hydroxyl radical) have been implicated in the turning on of various second messenger enzymic pathways through transcription factors, etc. Coral bleaching, for example, has been assigned to the overproduction of H_2O_2 in the zooxanthellae of hermatypic corals when PSI becomes overreduced, and when this triggers a second messenger system that leads to the expulsion of the zooxanthellae (Hill et al. 2014; Roberty et al. 2015; Goyen et al. 2017; Chap. 17). These reactions have only attracted attention relatively recently and their true importance is only now being realized by an increasing number of sophisticated investigations.

Dark to light transitions and fluctuating light (light flecks and clouds, on land, waves in lakes and at sea) create special problems for photoprotection and to minimise generation of ROS. Flavodoiiron proteins (FLVs) are attached to the stroma side of thylakoids close to PSI (Allahverdiyeva et al. 2015; Gerotto et al. 2016). It takes up electrons from ferredoxin and oxygen to form water. While there is not a great amount of this protein it is able to buffer the reducing side of PSI from over-reduction for several minutes and so minimise the production of superoxide (and hence H_2O_2 in the ubiquitous presence of superoxide dismutase); this therefore buffers thylakoids against suddene dark to light transitions when it takes the Calvin-Benson cycle several minutes to become activated during which it cannot soak up reduced NADPH and there is an over-supply of reduced ferredoxin; and another example would be in fluctuating light where the down-regulation systems available to thylakoids is overwhelmed. Another system which seems to have evolved to cope with imbalances in light-harvesting system and its feedback into the intersystem (PSII-PSI) electrochemical balance (see Chaps. 4 and 12) is the PTOX mechanism (Chap. 8). Here too electrons can be fed into oxygen to form water and so alleviate excess imbalance of reducing equivalents across the thylakoid membrane (Krieger-Liskay and Feilke 2016). Likewise there can be cross talk between mitochondria and plastids to alleviate the same problem, such as in diatoms (Bailleul et al. 2015).

Evolution of Photosynthetic Proteins Involved in Photoprotection and Light Harvesting

Balancing efficient capture of light against the damaging effects of high light is a problem faced by all photosynthetic organisms and not only results in the phenomenon of photoinhibition (Andersson and Aro 2001; Raven 2011) but also several photoprotective mechanisms which down-regulate the supply of energy to the photosystems (see above and Chaps. 3 and 12). It is therefore clear why both oxygenic and anoxygenic photosynthetic organisms have evolved mechanism to deal with situations of low light and high light. As discussed at the beginning of this

article curiously there is no phylogenetic link between the light-harvesting proteins of oxygenic and anoxygenic photosynthetic organisms. This is despite a clear connection between the proteins of their Reaction Centres (Blankenship 2014). However it should be remembered that oxygenic and anoxygenic photosynthetic organisms separated at least 3 Ga ago and probably 3.5 Ga ago (Cardona et al. 2015).

In oxygenic photosynthetic organisms there are some clear links with the proteins involved in light harvesting and photoprotection. Furthermore, it is likely that in Cyanobacteria, light-harvesting proteins involving Chl evolved before phycobiliproteins; however, the Chls involved attached to isiA proteins (see Fig. 10.9) bear no relation to the light-harvesting proteins of eukaryotic algae and land plants, and are in fact related to CP47 protein. Nevertheless there is a clear link back to Cyanobacteria both for the light-harvesting proteins of eukaryotic algae (and land plants) and the photoprotective proteins (Figs. 10.6 and 10.13); there is also good evidence that the HLIP proteins, with a single membrane spanning helix, of cyanobacteria gave rise to the three- and four-membrane-spanning light-harvesting chlorophyll proteins (LHC) of algae and land plants (see next paragraph).

Some important recent advances have been made by the group of Adamska (Engelken et al. 2010; Sturm et al. 2013; Shukla et al. 2018) and in terms of LHCSR proteins (see Sect. A and Figs. 10.13 and 10.14). It has long been known that Cyanobacteria have a group of proteins, which broadly fit into the category of High Light-Inducible Proteins (Hlips). These have a single membrane spanning helix, which binds Chl *a*, probably acts as a store of Chl under high light stress and are absolutely essential under under high light stress (Komenda and Sobodka 2016). These proteins are homologous with small Chlorophyll-Binding (CB) proteins (OHP1, OHP2); also with a single membrane spanning helix, which occur in plastids of eukaryotic algae and land plants (OHP1 occurs in green algae and land plants, OHP2 occurs in almost all algae and in land plants). Two-helix Stress Enhanced proteins (SEP) also occur in most

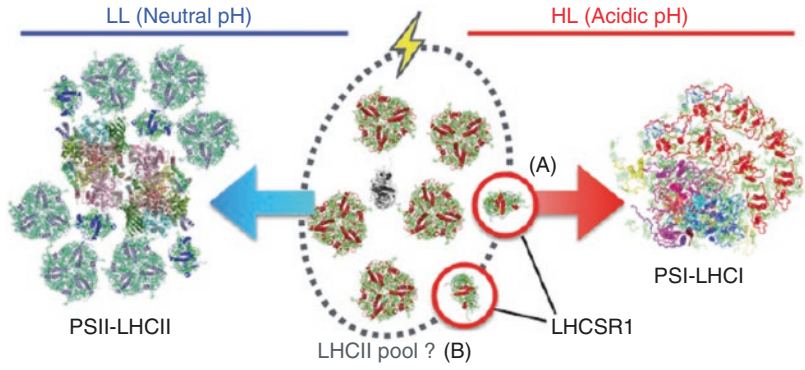

Fig. 10.14. A tentative model of LHCSR-dependent energy quenching in *Chlamydomonas reinhardtii*. The light captured by LHCIIs is transferred to the PSII−LHCII or PSI − LHCI supercomplexes under low lightt (representing neutral pH in the lumen, blue arrow) or high light (representing acidic pH in the lumen, red arrow), respectively. When the lumen is acidified, LHCSR1 (**a**) mediates excitation energy transfer from LHCIIs in the pool to PSI-LHCI (this study) and/or (**b**) triggers energy-dependent quenching in the LHCII pool. Icons surrounded by a red line represent LHCSR1.LHCSR1 and LHCSR3. Taken from Kosuge *et al.,* 2018, with permission from Proceedings of National Academy of Sciences (USA)

eukaryotic algae and land plants and can be seen as gene duplications from Hlips/OHP. These two-helix proteins almost certainly gave rise by gene duplication to four-helix proteins, of which PSBS is the only extant member, somewhat paradoxically since PSBS is found only in some green algae and land plants and bears no Chl molecules. Whereas its equivalent in most algae, LHCSR (see Fig. 10.13), is a 3-helix protein and binds Chl molecules. Thus the four helix proteins must have evolved early on into 3-helix proteins which include LHCSR proteins, CAB/CAC proteins of many algae and land plants (Fig. 10.6), and the early light induced protein (ELIP) of green algae and land plants. They also gave rise to RedCAP (red lineage Chl *a/b* binding-like) protein of red algae, cryptophytes, haptophytes and stramenopiles, including diatoms (Sturm et al. 2013) – see Fig. 10.13. The evolutionary development of the RedCAP protein is not clear, and is probably lost in the events that led up to the formation of the primary plastids, over 1 Ga ago. During these early events, glaucophytes did not inherit any of the new CAB/CAC proteins. Red algae did inherit an LHC (but PSI only) and red algal secondary lineages (Chromalveolates) inherited RedCAP proteins (Figs. 10.6 and 10.13). Green alga inherited CAB proteins (and associated, LHCSR, PSBS, ELIP and SEP proteins) (Figs. 10.6 and 10.13). During this time Chl *c* evolved and became the Chl that accompanied Chl *a* on the three-helix RedCAP (CAC) proteins – but not in red algae where only Chl *a* is bound – Chl c_1 & c_2 (and where it occurs Chl c_3) are bound to all RedCap CACs (Buchel 2015: and in cryptophytes where only Chl c_2 occurs it too is bound (Fig. 10.13). As pointed out by Sturm et al. 2013) this would have required considerable genetic readjustment in the lineages with secondary plastids. However, why Chl *c* was used and not Chl *b* is unclear (Green 2011a).

In the green lineage, which includes Chlorophyceae, Euglenophyceae, Chlorarachniophyceae and land plants, CAB proteins with associated LHCSR, PSBS, Elip and SEP proteins were inherited. However, during the evolution of land plants LHCSR proteins, although occurring in liverworts, mosses and some ferns, were discarded in favour of PSBS in the evolution of vascular plants (Niyogi and Truong 2013). Furthermore, an interesting development in flowering plants was the abandonment of flavodiiron proteins, which regulate and protect PSI in fluctuating light (Gerotto et al. 2016) in favour of other systems which are still under investigation. The abandonment of flavodiirons after such a long evolutionary history is interesting and possibly points to more flexibility in the angiosperm line.

Outlook

Currently it is apparent that our understanding of photosynthesis and light-harvesting are continuing to undergo radical changes. This is being brought about by new techniques such as molecular biology, electron diffraction, single particle electron microscopy, fast fluorescence and new chromatographic techniques. As a result what we saw as unifying concepts in the past are opening up to more detailed study, e.g. changes in absorption cross-section of PSI and PSII. Furthermore it is becoming clear that the rather crude understanding of the unity of primary plastids needs a radical overhaul and that this will pass valuable insights into our understanding of secondary (and tertiary) plastids. The discovery (or rediscovery) of Chl *d* and Chl *f* over the last fifteen years is yielding much to our understanding of the role of Chl *a*, *b* and *c*, both in the modern and in the Archean world. And, most surprisingly of all, it appears that through the discovery of *Gloeobacter kilaueensis* (Saw et al. 2013) we may be able to glimpse some of the evolutionary events that gave rise to the mechanism by which water was split by a newly evolving PSII (Ho et al. 2016b; Trinugroho et al. 2020) (Box 10.1).

Box 10.1: Glossary

Archaeplastida
A eukaryotic supergroup of organisms with primary plastids. Includes Chlorophyceae (including streptophytes) Rhodophyceae and Glaucophyceae.

Chromalveolates
A group of algae proposed by Cavalier Smith, which are in the lineage which inherited genes from red algae and have secondary (and tertiary) plastids. Depending on how it is defined it includes Cryptophyceae, Haptophyceae, Heterokontophyceae (including diatoms), Chromerids and Apicomplexans (see Chap. 2).

CAB/CAC proteins
As used here, this term refers specifically to the CAB/CAC superfamily that contain three transmembrane α-helices binding Chl *a* and Chl *b* or Chl *c*. Coded for by Lhc genes.

LHC superfamily
Proteins that contain a characteristic transmembrane domain called the LHC motif, but do not necessarily bind Chls.

LHCSR
Stress-induced LHC protein involved in flexible NPQ in algae, liverworts and mosses.

NPQ
Non-photochemical quenching of chlorophyll fluorescence. Used as a proxy for photoprotective thermal dissipation of excess light energy in photosynthesis.

OCP
Orange carotenoid protein involved in flexible NPQ in many phycobilisome-containing cyanobacteria.

PBS
Phycobilisome, the major soluble light-harvesting antenna in many Cyanobacteria, red algae and glaucophytes. It is composed of water-soluble phycobiliproteins and is peripherally attached to thylakoids, where it transfers absorbed light energy to the reaction centers of PSII and PSI.

PSBS
A four-helix protein in the LHC superfamily that is involved inflexible NPQ in green algae and land plants. This protein does not appear to bind pigments.

Xanthophyll cycle
An interconversion of xanthophylls that involves one or two deepoxidation reactions occurring in high light (with a reverse epoxidation reaction in limiting light). Three types of xanthophyll cycles are known: violaxanthin cycle, diadinoxanthin cycle, and lutein epoxide cycle (see Sect. VIIA).

Acknowledgements

I wish to thank my many colleagues at the University of Sydney and the University of Technology Sydney, and elsewhere, for their support and stimulating discussions over many past years. I also wish to acknowledge the generous support given by the University of Technology Sydney, during the writing of this review.

References

Aasen AJ, Liaaen-Jensen S (1966) The carotenoids of the flexbacteria. II. A new xanthophyll from *Saphrospira grandis*. Acta Chem Scand 20:811–819

Aihara MS, Yamamoto HY (1968) Occurrence of antheraxanthin in two Rhodophyceae, *Acanthophora specifera* and *Gracilaria lichenoides*. Phytochemistry 7:497–499

Akimoto S, Shinoda T, Chen M, Allakhverdiev SI, Tomo T (2015) Energy transfer in the chlorophyll f-containing cyanobacterium, Halomicronema hongdechloris, analyzed by time-resolved fluorescence spectroscopies. Photosynth Res 125:115–122

Allahverdiyeva Y, Isojärvi J, Zhang P, Aro E-M (2015) Cyanobacterial oxygenic photosynthesis is protected by flavodiiron proteins. Life 5:716-43. https://doi.org/10.3390/life5010716

Allen JF (1992) Protein phoshorylation in regulation of photosynthesis. Biochim Biophys Acta 1098:275–335

Allen JF, Bennett J, Steinbeck KE, Arntzen CJ (1981) Chloroplast protein phosphorylation couples plastoquinone redox state to distribution of excitation energy between photosystems. Nature 291:482–492

Allorent G, Tokutsu R, Roach T, Peers G, Cardol P et al (2013) A dual strategy to cope with high light in *Chlamydomonas reinhardtii*. Plant Cell 25:545–557

Andersson B, Aro EM (2001) Photodamage and D1 protein turnover in photosystem II. In: Aro EM, Andersson B (eds) Regulation of photosynthesis. Springer, Berlin, pp 377–393

Archibald JM (2015) Genomic perspectives on the birth and spread of plastids. Proc Natl Acad Sci U S A 112:10147–10153

Arpin N, Svec WA, Liaaen-Jensen S (1976) New fucoxanthin-related carotenoids from *Coccolithus huxleyi*. Phytochemistry 15:529–532

Arsalane W, Rousseau B, Duval J (1994) Influence of the pool size of the xanthophyll cycle on the effects of light stress in a diatom: competition between photoprotection and photoinhibition. Photochem Photobiol 60:237–243

Bailleul B, Rogato A, de Martino A, Coesel S, Cardol P et al (2010) An atypical member of the light-harvesting complex stress-related protein family modulates diatom responses to light. Proc Natl Acad Sci U S A 107:18214–18219

Bailleul B, Berne N, Murik O, Petrosoulos D et al (2015) Energetic coupling between plastids and mitochondria drives CO_2 assimilation in diatoms. Nature 524:366–369

Ball SG, Subtil A, Bhattacharya D, Moustafa A, Weber APM et al (2013) Metabolic effectors secreted by bacterial pathogens: essential facilitators of plastid endosymbiosis? Plant Cell 25:7–21

Belgio E, Kapitonova E, Chmeliov J, Duffy CDP, Ungerer P et al (2014) Economic photoprotection in photosystem II that retains a complete light-harvesting system with slow energy traps. Nat Commun 5:4433

Belgio E, Trskova E, Kotabova E, Ewe D, Prasil O, Kana R (2018) High light acclimation of *Chromera velia* points to photoprotective NPQ. Photosynth Res 135:263–274

Berger R, Liaaen-Jensen S, McAlister V, Guillard RRL (1977) Carotenoids of Prymnesiophyceae (Haptophyceae). Biochem Syst Ecol 5:71–75

Berne N, Fabryova T, Bistaz F, Cardol P, Bailleul B (2018) The peculiar NPQ regulation in the stramenopile Phaeomonas sp. challenges the xanthophyll cycle dogma. Biochim Biophys Acta (Bioenergetics) 1859:491–500

Berner T (1993) Ultrastructure of microalgae. CRC Press, Boca Raton, p 320

Bhattacharya D, Price DC, Chan CX, Qiu H, Rose N et al (2013) Genome of the red alga *Porphyridium purpureum*. Nat Commun 4:1941

Bina D, Gardian Z, Herbstova M, Litvin R (2017) Modular antenna of photosystem I in secondary plastids of red algal origin: a Nannochloropsis oceanica case study. Photosynth Res 131:255–266

Bjørnland T (1982) Chlorophylls and carotenoids of the marine alga *Eutreptiella gymnastica*. Phyochemistry 21:1715–1719

Bjørnland T, Tangen K (1979) Pigmentationand morphology of a marine *Gyrodinium* (Dinophyceae) with a major carotenoid different from peridinin and fucoxanthin. J Phycol 15:457–463

Blanc G, Duncan G, Agarkova I, Borodovsky M, Gurnon J et al (2010) The *Chlorella variabilis* NC64A genome reveals adaptation to photosymbio-

sis, coevolution with viruses, and cryptic sex. Plant Cell 22:2943–2955
Blankenship RE (2014) Molecular mechanisms of photosynthesis, 2nd edn. Wiley-Blackwell, New York
Bonaventura CJ, Myers J (1989) Fluorescence and oxygen evolution from *Chlorella Pyrenoidosa*. Biochim Biophys Acta 301:227–248
Brown BE, Ambarsari I, Warner ME, Fitt WK, Dunne RP et al (1999) Diurnal changes in photochemical efficiency and xanthophyll concentrations in shallow water reef corals: evidence for photoinhibition and photoprotection. Coral Reefs 18:99–105
Bruce D, Biggins J, Steiner T, Thewalt M (1986) Exctation energy tansfer in cryptophytes. Fluorescence excitation spectra and picosecond time-resolved emeission spectra of intact alga at 77K. Photochem Photobiol 44:519–525
Buchel C (2015) Evolution and function of light harvesting proteins. J Plant Physiol 172:62–75
Büchel C, Wilhelm C (1990) Wavelength independent state transitions and light regulated chlororespiration as mechanisms to control the energy status in teh chloroplast of *Pleurochloris meiringensis*. Plant Physiol Biochem 28:307–314
Bulté L, Gans P, Rebéille F, Wollman F-A (1990) ATP control of state transitions *in vivo* in *Chlamydomonas reinhardtii*. Biochim Biophys Acta 1020:72–80
Burke DH, Alberti M, Hearst JE (1993) bchFNBH bacteriochlorophyll synthesis genes of *Rhodobacter capsulatus* and identification of the third subunit of light-independent protochlorophyllide reductase in bacteria and plants. J Bacteriol 175:2414–2422
Butler WL (1978) Energy distribution in the photochemical apparatus of photosynthesis. Annu Rev Plant Physiol 29:345–378
Cardona T, Murray JW, Rutherford AW (2015) Origin and evolution of water oxidation before the last common ancestor of the cyanobacteria. Mol Biol Evol 32:1310–1328
Cardona T, Sanchez-Baracaldo P, Rutherford W, Larkum AWD (2019) Early Archean origin of photosystem II. Geobiology 17:127–150
Caron L, Remy R, Berkaloff C (1988) Polypeptide composition of light-harvesting complexes from some brown-algae and diatoms. FEBS Lett 229:11–15
Chen M (2014) Chlorophyll modifications and their spectral extension in oxygenic photosynthesis. Annu Rev Biochem 83:317–340
Chen M, Hiller RG, Howe CJ, Larkum AWD (2005) Unique origin and lateral transfer of prokaryotic chlorophyll-b and chlorophyll-d light-harvesting systems. Mol Biol Evol 22:21–28
Chen M, Schliep M, Willows D, Cai Z-L, Neilan BA, Scheer H (2010) A red shifted chlorophyll. Science 329:1318
Cheng JY, Don-Paul M, Antia SJ (1974) Isolationof an usually stable cis-isomer of alloxanthin from a bleached autolysed culture of *Chroomonas salina* grown photoheterotrophically on glycerol. Observations of cis-trans isomerization of alloxanthin. J Protozool 21:761–768
Chukhutsina VU, Fristedt R, Morosinotto T, Croce R (2017) Photoprotection strategies of the alga *Nannochloropsis gaditana*. Biochim Biophys Acta 1858:544–552
Collini E, Wong CY, Wilk KE, Curmi PMG, Brumer P, Scholes GD (2010) Coherently wired light-harvesting in photosynthetic marine algae at ambient temperature. Nature 463:644–647
Croce R, van Amerongen H (2014) Natural strategies for photosynthetic light harvesting. Nat Chem Biol 10:492–501
Crossett RN, Drew EA, Larkum AWD (1965) Chromatic adaptation in benthic marine algae. Nature 207:547. https://doi.org/10.1038/207547a0
Czaja AD, Johnson CM, Beard BL, Roden EE, Li W, Moorbath S (2013) Biological Fe oxidation controlled deposition of banded iron formation in the ca. 3770 Ma Isua Supracrustal Belt (West Greenland). Earth Planet Sci Lett 363:192–203
Dautermann O, Lohr M (2017) A functional Zeaxanthin epoxidase from red algae shedding light on the evolution of light-harvesting carotenoids and the xanthophyll cycle in photosynthetic eukaryotes. Plant J 92:879–891. https://doi.org/10.1111/tpj.13725
Davies BH (1965) Analysis of carotenoid pigments. In: Goodwin TW (ed) Chemistry and biochemistry of plant pigments. Academic, London, pp 489–532
Davies AJ, Khare A, Mallams AK, Massy-Westropp RA, Moss GP, Weedon BCL (1984) Carotenoids and related compounds, 38. Synthesis of 3RS, 3′ RS alloxanthin and other acetylenes. J Chem Soc Perkin Trans 1:2147–2158
Davis GA, Rutherford AW, Kramer DM (2017) Hacking the thylakoid proton motive force for improved photosynthesis: modulating ion flux rates that control proton motive force partitioning into Delta psi and Delta pH. Philos Trans R Soc London B Biol Sci 372:20160381
Delosme R, Olive J, Wollman FA (1996) Changes in light energy distribution upon state transitions: an in vivo photoacoustic study of the wild type and photosynthesis mutants from *Chlamydomonas reinhardtii*. BBA-Bioenergetics 1273:150–158
Delphin E, Duval JC, Kirilovsky D (1995) Comparison of state 1-state 2 transitions in the green alga *Chlamydomonas reinhardtii* and in the red alga *Rhodella violacea*. Effect of kinase and phospha-

tase inhibitors. Biochim Biophys Acta Bioenerg 1232:91–95

Delphin E, Duval L, Etienne A, Kiirilovsky D (1996) State transitions or ΔpH-dependent quenching of photosystem II fluorescence in red algae. Biochemistry 35:9435–9443

Demmig-Adams B, Adams WW III (1993) The xanthophyll cycle. In: Young A, Britton G (eds) Carotenoids in photosynthesis. London, Chapman & Hall

Demmig-Adams B, Garab G, Adams W, Govindjee (eds) (2014) Non-photochemical quenching and energy dissipation in plants algae and cyanobacteria, Advances in photosynthesis and respiration, vol 40. Springer, Berlin

Depege N, Bellafiore S, Rochaix JD (2003) Role of chloroplast protein kinase Stt7 in LHCII phosphorylation and state transition in *Chlamydomonas*. Science 299:1572–1575

DePriest MS, Bhattacharya D, Lopez-Bautista JM (2013) The plastid genome of the red macroalga Grateloupia taiwanensis (Halymeniaceae). PLoS One 8:e68246

Doege M, Ohmann E, Tschiersch H (2000) Chlorophyll fluorescence quenching in the alga *Euglena gracilis*. Photsynth Res 63:159–170

Dorrell RG, Howe CJ (2012) What makes a chloroplast? Reconstructing the establishment of photosynthetic symbioses. J Cell Sci 125:1865–1875

Douglas SE, Penny SL (1999) The plastid genome of the cryptophyte alga, *Guillardia theta*: complete sequence and conserved synteny groups confirm its common ancestry with red algae. J Mol Evol 48:236–244

Douglas S, Zauner S, Fraunholz M, Beaton M, Penny S et al (2001) The highly reduced genome of an enslaved algal nucleus. Nature 410:1091–1096

Drop B, Webber-Birungi M, Yadav SKN, Filipowicz-Szymanska A, Fusetti F et al (2014a) Light-harvesting complex II (LHCII) and its supramolecular organization in *Chlamydomonas reinhardtii*. BBA-Bioenergetics 1837:63–72

Drop B, Yadav KNS, Boekema EJ, Croce R (2014b) Consequences of state transitions on the structural and functional organization of photosystem I in the green alga *Chlamydomonas reinhardtii*. Plant J 78:181–191

Engelken J, Brinkmann H, Adamska I (2010) Taxonomic distribution and origins of the extended LHC (light-harvesting complex) antenna protein superfamily. BMC Evol Biol 10:233

Escoubas JM, Lomas M, Laroche J, Falkowski PG (1996) Light intensity regulation of CAB gene transcription is signaled by redox state of plastoquinone pool. Proc Natl Acad Sci U S A 92:10237–10241

Eskins K, Schoefield CR, Dutton HJ (1977) High performance chromatograhy of plant pigments. J Chromatogr 135:217–220

Falkowski PG, Raven JA (2007) Aquatic photosynthesis, 2nd edn. Princeton University Press, Princeton

Fawley MW (1992) Photosynthetic pigments of *Pseudoscourfieldia marina* and select green flagellates and coccoid ultraphytoplankton: implications for the systematics of the Micromonadophyceae (Chlorophyta). J Phycol 28:26–31

Fehling J, Stoeker D, Baldauf SL (2007) Photosynthesis and the eukaryote tree of life. In: Falkowski PG, Knoll AH (eds) Evolution of primary producers in the sea. Elsevier Academic Press, Amsterdam, pp 75–107

Fiksdahl A, Bjornland T, Liaaen-Jensen S (1984a) Algal carotenoids with novel end groups. Phytochemistry (Oxford) 23:649–656

Fiksdahl A, Withers N, Liaaen-Jensen S (1984b) Carotenoids of *Heterosigma akashiwo*: a chemosytematic contribution. Biochem Syst Ecol 12:355–356

Foppen FH (1971) Tables for the identifcation of carotenoid pigments. Chromatogr Rev 14:133–298

Fork DC, Satoh K (1986) The control of state transitions of the distribution of excitation energy in photosysnthesis. Ann Rev Plant Physiol 37:335–361

Fork DC, Herbert SK, Malkin S (1991) Light energy distribution in the brown alga *Macrocystis pyrifera* (giant kelp). Plant Physiol 95:731–739

Fosberg J, Allen JF (2001) Molecular recognition in thylakoid structure and function. Trends Plant Sci 6:317–326

Foss P, Guillard RRL, Liaaen-Jensen S (1984) Prasinoxanthin. A Chemosystematic Marker for Algae. *Phytochemistry* 23:1629–1633

Francis GW, Halfen LN (1972) Cyanophyta. Oscillatoriaceae. γ-carotene and lycopene. Phytochemistry 11:2347–2348

Francis GW, Hertzberg S, Andersen K, Liaaen-Jensen S (1970) New carotenoid glycosides from *Oscillatoria limosa*. Phytochemistry (Oxford) 9:629–635

Francis GW, Knutsen G, Lien T (1973) Loroxanthin from *Chlamydomonas reinhardtii*. Acta Chem Scand 27:3599–3600

Gan F, Zhang SY, Rockwell NC, Martin SS, Lagarias JC, Bryant DA (2014) Extensive remodeling of a cyanobacterial photosynthetic apparatus in far-red light. Science 345:1312–1317

Gan F, Shen G, Bryant DA (2015) Occurrence of far-red light photoacclimation (FaRLiP) in diverse cyanobacteria. Life 5:4–24

Gerotto C, Alboresi A, Meneghesso A, Jokel M, Suorsa M et al (2016) Flavodiiron proteins act as

safety valve for electrons in *Physcomitrella patens*. Proc Natl Acad Sci U S A 113:12322–12327

Gibbs PB, Biggins J (1991) *In vivo* and *in vitro* protein phosphorylation studies in *Ochromonas danica*, an alga with chlorophyll a/c/fucoxanthin binding protein. Plant Physiol 97:388–395

Girolomoni L, Cazzaniga S, Pinnola A, Perozeni F, Ballottari M, Bassi R (2019) LHCSR3 is a nonphotochemical quencher of both photosystems in *Chlamydomonas reinhardtii*. Proc Natl Acad Sci, U S A 116:4212–4217

Glazer AN (1977) Structure and molecular organization of the photosynthetic accessory pigments of cyanobacteria and red algae. Mol Cell Biochem 18:125–140

Glazer AN, Wedemeyer GJ (1995) Cryptomonad biliproteins – an evolutionary perspective. Photosynth Res 46:93–105

Gloag RS, Ritchie RJ, Chen M, Larkum AWD, Quinnell RG (2007) Chromatic photoacclimation, photosynthetic electron transport and oxygen evolution in the chlorophyll *d*-containing oxyphotobacterium Acaryochloris marina. BBA-Bioenergetics 1767:127–135

Goericke R, Repeta DJ (1992) The pigments of *Prochlorococcus marinus:* the presence of Divinylchlorophyll *a* and *b* in a marine prokaryote. Limnol Oceanogr 37:425–433

Goessling JW, Su Y, Cartaxana P, Maibohm C, Rickelt LF et al (2018) Structure-based optics of centric diatom frustules: modulation of the *in vivo* light field for efficient diatom photosynthesis. New Phytol 219:122–134

Goss R, Bohme KC (1998) The xanthophyll cycle of *Mantoniella squamata* converts violaxanthin into antheraxanthin but not to zeaxanthin – consequences for the mechanism of enhanced non-photochemical energy dissipation. Planta 205:613–621

Goss R, Jakob T (2010) Regulation and function of xanthophyll cycle-dependent photoprotection in algae. Photosynth Res 106:103–122

Goyen S, Pernice M, Szabo M, Warner ME, Ralph PJ, Suggett DJ (2017) A molecular physiology basis for functional diversity of hydrogen peroxide production amongst *Symbiodinium* spp. (Dinophyceae). Mar Biol (Berlin) 164:46

Graham JE, Wilcox LW, Cook M (2016) Algae. LJLM Press, Madison

Green BR (2011a) After the primary endosymbiosis: an update on the chromalveolate hypothesis and the origins of algae with Chl c. Photosynth Res 107:103–115

Green BR (2011b) Chloroplast genomes of photosynthetic eukaryotes. Plant J 66:34–44

Green BR, Durnford DG (1996) The chlorophyll-carotenoid proteins of oxygenic photosynthesis. Annu Rev Plant Physiol Plant Molec Biol 47:685–714

Gundermann K, Büchel C (2014) Structure and functional heterogeneity of fucoxanthin-chlorophyll proteins in diatoms. In: Hohmann-Marriott MF (ed) The structural basis of biological energy generation, vol 21. Springer, Dordrecht, pp 21–37

Gundermann K, Schmidt M, Weisheit W, Mittag M, Buchel C (2013) Identification of several subpopulations in the pool of light harvesting proteins in the pennate diatom *Phaeodactylum tricornutum*. BBA-Bioenergetics 1827:303–310

Gwizdala M, Wilson A, Omairi-Nasser A, Kirilovsky D (2013) Characterization of the *Synechocystis* PCC 6803 fluorescence recovery protein involved in photoprotection. BBA-Bioenergetics 1827:348–354

Hager A, Meyer-Bertenrath T (1966) Extraction and quantitative determination of carotenoids and chlorophylls from leaves, algae and isolated chloroplasts with the aid of thin-layer chromatography. Planta 69:198–217

Haldrup A, Jensen PE, Lunde C, Scheller HV (2001) Balance of power: a view of the mechanism of photosynthetic state transitions. Trends Plant Sci 6:301–305

Halfen LN, Francis GW (1972) The influence of culture temperature on the carotenoid composition of the blue-green alga *Anacystis nidulans*. Archiv f Mikrobiol 81:25–35

Herbstova M, Litvin R, Gardian Z, Komenda J, Vacha F (2010) Localization of Pcb antenna complexes in the photosynthetic prokaryote *Prochlorothrix hollandica*. Biochim Biophys Acta 1797:89–97

Hill R, Larkum AWD, Prášil O, Kramer DM, Szabo M, Kumar V, Ralph PJ (2012) Light-induced dissociation of antenna complexes in the symbionts of Scleractinian corals correlates with sensitivity to coral bleaching. Coral Reefs 31:963–975

Hill R, Szabo M, Rehman AU, Vass I, Ralph PJ, Larkum AWD (2014) Inhibition of photosynthetic CO_2 fixation in the coral *Pocillopora damicornis* and its relationship to thermal bleaching. J Exp Biol 217:2150–2162

Ho M, Gan F, Shen G, Zhao C, Bryant DA (2016a) Far-red light photoacclimation (FaRLiP) in *Synechococcus* sp. PCC 7335: I. Regulation of FaRLiP gene expression. Photosynth Res 131:173–186

Ho M, Gan F, Shen G, Bryant DA (2016b) Far-red light photoacclimation (FaRLiP) in *Synechococcus* sp. PCC 7335. II. Characterization of phycobilipro-

teins produced during acclimation to far-red light. Photosynth Res 131:187–202

Ho M-Y, Shen G, Canniffe DP, Zhao C, Bryant DA (2016c) Light-dependent chlorophyll *f* synthase is a highly divergent paralog of PsbA of photosystem II. Science 353:886–893

Ho M-Y, Soulier NT, Canniffe DP, Shen G, Bryant DA (2017) Light regulation of pigment and photosystem biosynthesis in cyanobacteria. Curr Opin Plant Biol 37:24–33

Hofmann E, Wrench PM, Sharples FP, Hiller RG, Welte W, Diederichs K (1996) Structural basis of light harvesting by carotenoids: Peridinin-chlorophyll-protein from *Amphidinium carterae*. Science 272:1788–1791

Hohmann-Marriott MF, Blankenship RE (2011) Evolution of photosynthesis. In: Merchant SS, Briggs WR, Ort D (eds) *Annual Review of Plant Biology*, vol 62, pp 515–548

Horton P, Ruban AV, Walters RG (1996) Regulation of light harvesting in green plants. Annu Rev Plant Physiol Plant Molec Biol 47:655–684

Hsu SH, Paoletti C, Torres M, Ritchie RJ, Larkum AWD, Grillet C (2012) Light transmission of the marine diatom *Coscinodiscus wailesii*. In: Lakhtakia A, MartinPalma RJ (eds) Bioinspiration, biomimetics, and bioreplication. https://doi.org/10.1117/12.915044

Hunter CN, Coomber SA (1988) Cloning and oxygen-regulated expression of the bacteriochlorophyll biosynthesis genes BChl e, b, a and c of *Rhodobacter spheroides*. J Gen Microbiol Rev 134:1491–1497

Ihnken S, Kromkamp JC, Beardall J, Silsbe GM (2014) State-transitions facilitate robust quantum yields and cause an over-estimation of electron transport in *Dunaliella tertiolecta* cells held at the CO2 compensation point and re-supplied with DIC. Photosynth Res 119:257–272

Itoh S, Mino H, Itoh K, Shigenaga T, Uzumaki T, Iwaki M (2007) Function of chlorophyll d in reaction centers of photosysterns I and II of the oxygenic photosynthesis of acaryochloris marina. Biochemistry 46:12473–12481

Itoh S, Ohno T, Noji T, Yamakawa H, Komatsu H et al (2015) Harvesting far-red light by chlorophyll *f* in photosystems I and II of unicellular cyanobacterium strain KC1. Plant Cell Physiol 56:2024–2034

Johansen JE, Svec WA, Liaaen-Jensen S, Haxo FT (1974) Carotenoids of the Dinophyceae. Phytochemistry (Oxford) 13:2261–2272

Josue JS, Frank HA (2002) Direct determination of the S-1 excited-state energies of xanthophylls by low-temperature fluorescence spectroscopy. J Phys Chem A 106:4815–4824

Kaňa R, Prášil O, Mullineaux CC (2009) Immobility of phycobilins in the thylakoid lumen of as cryptophyte suggests that protein diffusion in the lumen is very restricted. FEBS Lett 583:670–674

Kanazawa A, Blanchard GJ, Szabo M, Ralph PJ, Kramer DM (2014) The site of regulation of light capture in Symbiodinium: does the peridinin-chlorophyll alpha-protein detach to regulate light capture? BBA-Bioenergetics 1837:1227–1234

Kanazawa A, Ostendorf E, Kohzuma K, Hoh D, Strand DD et al (2017) Chloroplast ATP synthase modulation of the thylakoid proton motive force: implications for photosystem I and photosystem II photoprotection. Front Plant Sci 8:719

Kantz TS, Theriot EC, Zimmer EA, Chapman RL (1990) The Pleurastrophyceae and Micromonadophyceae a cladistic analysis of nuclear ribosomal RNA sequence data. J Phycol 26:711–721

Keeling PJ (2013) The number, speed, and impact of plastid endosymbioses in eukaryotic evolution. Annu Rev Plant Biol 64:583–607

Kehoe DM (2010) Chromatic adaptation and the evolution of light color sensing in cyanobacteria. Proc Natl Acad Sci U S A 107:9029–9030

Kehoe DM, Grossman AR (1996) Similarity of a chromatic adaptation sensor to phytochrome and ethylene receptors. Science 273:1409–1412

Kirilovsky D, Kerfeld CA (2012) The orange carotenoid protein in photoprotection of photosystem II in cyanobacteria. BBA-Bioenergetics 1817:158–166

Kohzuma K, Froehlich JE, Davis GA, Temple JA, Minhas D et al (2017) The role of light-dark regulation of the chloroplast ATP synthase. Front Plant Sci 8:1248

Komenda J, Sobodka H (2016) Cyanobacterial high light-inducible proteins: protectors of chlorphyll biosynthesis and assembly. Biochim Biophys Acta-Bioenegetics 1857:288–295

Kosuge K, Tokutsu R, Kim E, Akimoto S, Yokono M et al (2018) LHCSR1-dependent fluorescence quenching is mediated by excitation energy transfer from LHCII to photosystem I in *Chlamydomonas reinhardtii*. Proc Natl Acad Sci U S A 115:3722–3727

Kowalczyk N, Rappaport F, Boyen C, Wollman FA, Collen J, Joliot P (2013) Photosynthesis in *Chondrus crispus*: the contribution of energy spill-over in the regulation of excitonic flux. BBA-Bioenergetics 1827:834–842

Krieger-Liskay A, Feilke K (2016) The dual role of plastid terminak oxidase PTOX: between a protective and a pro-oxidant function. Front Plant Sci 6:1147

La Roche J, Van Der Staay GWM, Partensky F, Ducret A, Aebersold R et al (1996) Independent evolution

of the prochlorophyte and green plant chlorophyll a/b light-harvesting proteins. Proc Natl Acad Sci U S A 93:15244–15248

Larkum AWD (1992) The evolution of chlorophylls, light-harvesting systems and photoreaction centers. In: Murata N (ed) Research in photosynthesis. Kluwer, Dordrecht, pp 475–482

Larkum AWD (2003) Light-harvesting systems in algae. In: Govidjee (ed) Photosynthesis in algae. Kluwer, Dordrecht, pp 277–304

Larkum AWD (2006) The evolution of chlorophylls and photosynthesis. In: Grimm B, Porra RJ, Rudiger W, Scheer H (eds) Chlorophylls and bacteriochlorophylls. Springer, Berlin, pp 261–282

Larkum AWD (2008) Evolution of the reaction centers and photosystems. In: Renger G (ed) Primary processes of photosynthesis: principles and apparatus. Royal Society of Chemistry, Cambridge, pp 489–521

Larkum AWD, Barrett J (1983) Light harvesting processes in algae. In: Woolhouse HW (ed) Advances in botanical research. Academic Press, New York, pp 1–219

Larkum AWD, Howe CJ (1997) Molecular aspects of light harvesting processes in algae. In: Callow JA (ed) Advances in botanical research. Academic, New York, pp 257–330

Larkum AWD, Vesk M (2003) Algal plastids: Their fine structure and properties. In: Larkum AWD, Douglas SE, Raven JA (eds) Photosynthesis of algae. Kluwer, Dordrecht, pp 11–28

Larkum AWD, Scaramuzzi C, Cox GC, Hiller RG, Turner AG (1994) Light-harvesting chlorophyll *c*-like pigment in *Prochloron*. Proc Natl Acad Sci U S A 91:679–683

Larkum A, Lockhart P, Howe C (2007) Shopping for plastids. Trends Plant Sci 12(12):189–195

Larkum AWD, Ritchie RJ, Raven JA (2018) Living off the Sun: chlorophylls, bacteriochlorophylls and rhodopsins. Photosynthetica (Prague) 56:11–43

Latasa M, Scharek R, Le Gall F, Guillou L (2004) Pigment suites and taxonomic group in Prasinophyceae. J Phycol 40:1149–1155

Leliaert F, Tronholm A, Lemieux C, Turmel M, DePriest MS, Bhattacharya D, Karol KG et al (2016) Chloroplast Phylogenomic analyses reveal the deepest-branching lineage of the Chlorophyta, Palmophyllophyceae class. Nov Sci Rep 6:25367. https://doi.org/10.1038/srep25367

Lepetit B, Sturm S, Rogato A, Gruber A, Sachse M et al (2013) High light acclimation in the secondary plastids containing diatom *Phaeodactylum tricornutum* is triggered by the redox state of the plastoquinone pool. Plant Physiol 161:853–865

Ley AC, Butler WL (1980) Energy distribution in the photchemical apparatus of *Porphyridium cruentum* in state 1 and state 2. Biochim Biophys Acta Bioenerg 592:349–363

Li XP, Muller-Moule P, Gilmore AM, Niyogi KK (2002) PsbS-dependent enhancement of feedback de-excitation protects photosystem II from photoinhibition. Proc Natl Acad Sci U S A 99:15222–15227

Li YQ, Scales N, Blankenship RE, Willows RD, Chen M (2012) Extinction coefficient for red-shifted chlorophylls: chlorophyll d and chlorophyll f. BBA-Bioenergetics 1817:1292–1298

Li B, Lopes JS, Foster PG, Embley TM, Cox CJ (2014) Compositional biases among synonymous substitutions cause conflict between gene and protein trees for plastid origins. Mol Biol Evol 7:1697–1709

Lichtle C, Arsalane W, Duval JC, Passaquet C (1995) Characterization of the light-harvesting complex of *Giraudyopsis stellifer* (Chrysophyceaeae) and effects of light stress. J Phycol 31:380–387

Litvin R, Bina D, Herbstova M, Gardian Z (2016) Architecture of the light-harvesting apparatus of the eustigmatophyte alga *Nannochloropsis oceanica*. Photosynth Res 130:137–150

Llansola-Portoles MJ, Uragami C, Pascal AA, Bina D, Litvin R, Robert B (2016) Pigment structure in the FCP-like light-harvesting complex from Chromera velia. Biochim Biophys Acta 1857:1759–1765

Llansola-Portoles MJ, Litvin R, Ilioaia C, Pascal AA, Bina D, Robert B (2017) Pigment structure in the violaxanthin-chlorophyll-a-binding protein VCP. Photosynth Res 134:51–58

Loeblich LA, Smith VE (1968) Chloropalst pigmentsof a marine dinoflagellate *Gyrodinium resplendens*. Lipids 3:5–13

Lohr M, Wilhelm C (1999) Algae displaying the diadinoxanthin cycle also possess the violaxanthin cycle. Proc Natl Acad Sci U S A 96:8784–8789

Loughlin PC, Willows RD, Chen M (2014) In vitro conversion of vinyl to formyl groups in naturally occurring chlorophylls. Sci Rep 4:6069

Lucker B, Kramer DM (2013) Regulation of cyclic electron flow in *Chlamydomonas reinhardtii* under fluctuating carbon availability. Photosynth Res 117:449–459

Lunde C, Jensen PE, Haldrup A, Knoezel J, Scheller HV (2000) The PS I-H subunit of photosystem I is essential for state transitions in *plant photosynthesis*. Nature 408:613–615

MacColl R, Guard-Friar D (1967) Phycobiliproteins. CRC Press, Boca Raton

Manning WM, Srtrain HH (1943) Chlorophyll *d*, a green pigment of red algae. J Biol Chem 151:1–19

Matsuzaki M, Misumi O, Shin-I T, Maruyama S, Takahara M et al (2004) Genome sequence of the ultrasmall unicellular red alga *Cyanidioschyzon merolae* 10D. Nature 428:653–657

McFadden GI, Yeh E (2017) The apicoplast: now you see it, now you don't. Int J Parasitol 47:137–144

Miloslavina Y, Grouneva I, Lambrev PH, Lepetit B, Goss R et al (2009) Ultrafast fluorescence study on the location and mechanism of non-photochemical quenching in diatoms. BBA-Bioenergetics 1787:1189–1197

Minagawa J (2013) Dynamic reorganization of photosynthetic supercomplexes during environmental acclimation of photosynthesis. Front Plant Sci 4:513

Miyake C, Asada K (2003) The water water cycle in algae. In: Larkum AWD, Douglas SE, Raven JA (eds) Photosynthesis of algae. Kluwer Academic Publisher, Dordrecht, pp 11–28

Miyashita H, Ikemoto H, Kurano N, Adachi K, Chihara M, Miyachi S (1996) Chlorophyll *d* as a major pigment. Nature 383:402–402

Miyashita H, Adachi K, Kurano N, Ikemoto H, Chihara M, Miyachi S (1997) Pigment composition of a novel oxygenic photosynthetic prokaryote containing chlorophyll d as the major chlorophyll. Plant Cell Physiol 38:274–281

Miyashita H, Ikemoto H, Kurano N, Miyachi S, Chihara M (2003) *Acaryochloris marina* gen. et sp nov (cyanobacteria), an oxygenic photosynthetic prokaryote containing Chl d as a major pigment. J Phycol 39:1247–1253

Mohanty N, Gilmore AM, Yamamoto HY (1995) Mechanism of non-photochemical chlorophyll fluorescence quenching. 2. Resolution of rapidly reversible absorbance changes at 530nm and fluorescence quenching by the effects of antimycin, dibucaine and cation exchanger A23187. Aust J Plant Physiol 22:239–247

Mohr R, Voss B, Schliep M, Kurz T, Maldener I et al (2010) A new chlorophyll d-containing cyanobacterium: evidence for niche adaptation in the genus Acaryochloris. ISME J 4:1456–1469

Mues R, Edelbluth E, Zinsmeister HD (1973) The carotenoid pattern of *Lophocolea bidentata*. Oesterreichische Botanische Zeitschrift 122:177–184

Mulkidjanian AY, Koonin EV, Makarova KS, Mekhedov SL, Sorokin A et al (2006) The cyanobacterial genome core and the origin of photosynthesis. Proc Natl Acad Sci U S A 103:13126–13131

Mullineau CW, Sarcina M (2002) Pprobing the dynamic of photsynthetic mebranes with fluorescence recovery after photobleaching. Trends Plant Sci 7:27–42

Murakami A, Miyashita H, Iseki M, Adachi K, Mimuro M (2004) Chlorophyll d in an epiphytic cyanobacterium of red algae. Science 303:1633–1633

Murata N (1969) Control of excitation transfer in photosynthesis. I. Light-induced changes of chlorophyll *a* fluorescence in *Porphyridium cruentum*. Biochim Biophys Acta 189:171–181

Murata N (1970) Control of excitation transfer in photosynthesis. IV. Kinetics of chlorophyll *a* fluorescence in *Porphyra yezoensis*. Biochim Biophys Acta 205:379–389

Neilson JAD, Durnford DG (2010) Structural and functional diversification of the light-harvesting complexes in photosynthetic eukaryotes. Photosynth Res 106:57–71

Niedzwiedzki DM, Liu H, Chen M, Blankenship RE (2014) Excited state properties of chlorophyll f in organic solvents at ambient and cryogenic temperatures. Photosynth Res 121:25–34

Niyogi KK, Truong TB (2013) Evolution of flexible non-photochemical quenching mechanisms that regulate light harvesting in oxygenic photosynthesis. Curr Opin Plant Biol 16:307–314

Norgard S, Svec WA, Liaaen-Jensen S, Jensen A, Guillard RRL (1974) Chloroplast pigments and algal systematics. Biochem Syst Ecol 2:3–6

Nowack ECM, Grossman AR (2012) Trafficking of protein into the recently established photosynthetic organelles of *Paulinella* chromatophora. Proc Natl Acad Sci U S A 109:5340–5345

Nozaki H, Maruyama S, Matsuzaki M, Nakada T, Kato S, Misawa K (2009) Phylogenetic positions of Glaucophyta, green plants (Archaeplastida) and Haptophyta (Chromalveolata) as deduced from slowly evolving nuclear genes. Mol Phylogenet Evol 53:872–880

Nuernberg DJ, Morton J, Santabarbara S, Telfer A, Joliot P et al (2018) Photochemistry beyond the red limit in chlorophyll f-containing photosystems. Science (Washington D C) 360:1210–1213

Ochoa de Alda JAG, Esteban R, Diago ML, Houmard J (2014) The plastid ancestor originated among one of the major cyanobacterial lineages. Nat Commun. https://doi.org/10.1038/ncomms5937

Pan H, Slapeta J, Carter D, Chen M (2012) Phylogenetic analysis of the light-harvesting system in Chromera velia. Photosynth Res 111:19–28

Partensky F, Garczarek l (2003) The photosynthetic apparatus of chlorophyll B- and D-Containing Oxyphotobacteria. In: Larkum AWD, Douglas SE, Raven JA (eds) *Photosynthesis in Algae*, Advances in Photsynthesis and respiration. Springer, Berlin, pp 29–62

Pinnola A, Ghin L, Gecchele E, Merlin M, Alboresi A et al (2015) Heterologous expression of Moss light-harvesting complex stress-related 1 (LHCSR1), the chlorophyll a-xanthophyll pigment-protein complex catalyzing non-photochemical quenching, in Nicotiana sp. J Biol Chem 290:24340–24354

Price DC, Chan CX, Yoon HS, Yang EC, Qiu H et al (2012) *Cyanophora paradoxa* genome elucidates origin of photosynthesis in algae and plants. Science 335:843–847

Pursiheimo S, Rintamaki E, Baena-Gonzalez E, Aro EM (1998) Thylakoid protein phosphorylation in evolutionally divergent species with oxygenic photosynthesis. FEBS Lett 423:178–182

Quigg A, Kotabova E, Jaresova J, Kana R, Setlik J et al (2012) Photosynthesis in *Chromera velia* represents a simple system with high efficiency. PLoS One 7:e47036

Raven JA (1984) A cost-benefit analysis of photon absorption by photosynthetic unicells. New Phytol 98:593–626

Raven JA (1996) The bigger the fewer: size, taxonomic diversity and the range of chlorophyll(ide) pigments in oxygen evolving marine photolithotrophs. J Mar Biol Assoc UK 76:211–217

Raven JA (2011) The cost of photoinhibition. Physiol Plant 142:87–104

Renstrom S, Borsch G, Skulberg OM, Liaaen-Jensen S (1981) Optical purity of 3S, 3′S-astaxanthin from *Haematococcus fluvialis*. Phyochemistry 20:2561–2564

Reyes-Prieto A, Russell S, Figueroa-Martinez F, Jackson C (2018) Comparative plastid genomics of glaucophytes. Ad Bot Res 85:95–127

Reynolds JM, Bruns BU, Fitt WK, Schmidt GW (2008) Enhanced photoprotection pathways in symbiotic dinoflagellates of shallow-water corals and other cnidarians. Proc Natl Acad Sci U S A 105:13674–13678

Roberty S, Fransolet D, Cardol P, Plumier JC, Franck F (2015) Imbalance between oxygen photoreduction and antioxidant capacities in *Symbiodinium* cells exposed to combined heat and high light stress. Coral Reefs 34:1063–1073

Rochaix JD (2014) Regulation and dynamics of the light-harvesting system. Annu Rev Plant Biol 65(65):287–309

Rowan KS (1989) Photosynthetic pigments of algae. Cambridge Univesity Press, Cambridge. 334 pp

Rüdiger W (1980) Phycolibiproteins. In: Cyzan FC (ed) Pigments in plants. Gustav Fisher, Stuttgart, pp 314–351

Sanfilippo JE, Nguyen AA, Garczarek L, Karty JA, Pohkrel S, Strnat JA, Partensky F, Schluchter WM, Kehoe DM (2019) Interplay between differentially expressed enzymes contributes to light color acclimation in marine Synechococcus. Proc Natl Acad Sci, US 116:6457–62

Sarcina M, Tobin MJ, Mullineaux CW (2001) Diffusion of phycobilisomes on the thylakoid membranes of the cyanobacterium *Synechococcus* 7942 – effects of phycobilisome size, temperature, and membrane lipid composition. J Biol Chem 276:46830–46834

Satoh K, Fork DC (1983) State I – sate II transitions in the green alga *Scanedesmus obliqus*. Photochem Photobiol 37:429–434

Saw JHW, Schatz M, Brown MV, Kunkel DD, Foster JS et al (2013) Cultivation and complete genome sequencing of Gloeobacter kilaueensis sp nov., from a Lava Cave in Kilauea Caldera, Hawai'i. PLoS One 8:e76376

Scheer H (1981) Biliproteins. Angew Chem (English ed) 20:241–261

Scheer H (ed) (1991) Chlorophylls. CRC Press, Boca Raton, p 1257

Schliep M, Chen M, Larkum A, Quinnell R (2008) Photosynthesis. Energy from the Sun, Montreal, 2008. Springer, Dordrecht, pp 1125–1128

Schliep M, Crossett B, Willows RD, Chen M (2010) O-18 labeling of chlorophyll d in *Acaryochloris marina* reveals that chlorophyll *a* and molecular oxygen arre precursors. J Biol Chem 285:28450–28456. https://doi.org/10.1074/jbc.M110.146753

Schliep M, Cavigliasso G, Quinnell RG, Stranger R, Larkum AWD (2013) Formyl group modification of chlorophyll a: a major evolutionary mechanism in oxygenic photosynthesis. Plant Cell Environ 36:521–527

Schmitt FJ, Renger G, Friedrich T, Kreslavski VD, Zharmukhamedov SK et al (2014) Reactive oxygen species: re-evaluation of generation, monitoring and role in stress-signaling in phototrophic organisms. Biochim Biophys Acta-Bioenerg 1837:835–848

Schreiber U, Endo T, Mi HL, Asada K (1995) Quenching analysis of chlorophyll fluorescence by the saturation pulse method – particular aspects relating to the study of eukaryotic algae and cyanobacteria. Plant Cell Physiol 36(5):873–882

Schulte T, Sharples FP, Hiller RG, Hofmann E (2009) X-ray structure of the high-salt form of the peridinin-chlorophyll a-protein from the dinoflagellate *Amphidinium carterae*: modulation of the spectral properties of pigments by the protein environment. Biochemistry 48:4466–4475

Sedoud A, Lopez-Igual R, Rehman AU, Wilson A, Perreau F et al (2014) The cyanobacterial photoactive orange carotenoid protein is an excellent singlet oxygen quencher. Plant Cell 26:1781–1791

Serive B, Nicolau E, Berard J-B, Kaas B, Pasquet V et al (2017) Community analysis of pigment

patterns from 37 microalgae strains reveals new carotenoids and porphyrins characteristic of distinct strains and taxonomic groups. In: PLOS One, vol 12, p e0171872

Shen G, Canniffe DP, Ho M-Y et al (2019) Characterization of chlorophyll *f* synthase heterologously produced in *Synechococcus* sp. PCC 7002. Photosynth Res 140:77–92

Shukla MK, Llansola-Portoles MJ, Tichý M, Pascal AA, Robert B, Sobotka R (2018) Binding of pigments to the cyanobacterial high-light-inducible protein HliC. Photosynth Res 137:29–39

Skjenstad T, Haxo FT, Liaaen-Jensen S (1984) Carotenoids of clam coral and nudibranch zooxanthellae in aposymbiotic culture. Biochem Syst Ecol 12:149–154

Slavov C, Reus M, Holzwarth AR (2013) Two different mechanisms cooperate in the desiccation-induced excited state quenching in Parmelia Lichen. J Phys Chem B 117:11326–11336

Slavov C, Schrameyer V, Reus M, Ralph PJ, Hill R et al (2016) "Super-quenching" state protects Symbiodinium from thermal stress – implications for coral bleaching. Biochim Biophys Acta 1857:840–847

Song P-S, Koka P, Prezelin BB, Haxo FT (1976) Molecular topology of the photosynthetic light-harvesting pigment complex, peridinin-chlorophyll a-protein, from marine dinoflagellates. Biochemistry 15:4422–4427

Steinbeck J, Ross IL, Rothnagel R, Gäbelein P, Schulze S et al (2018) Structure of a PSI–LHCI–cyt b6f supercomplex in *Chlamydomonas reinhardtii* promoting cyclic electron flow under anaerobic conditions. Proc Natl Acad Sci U S A 115(41):10517–10522

Stomp M, Huisman J, De Jongh F et al (2004) Adaptive divergence in pigment composition promotes phytoplankton biodiversity. Nature 432:104–107

Stomp M, Huisman J, Stal LJ, Matthijs HCP (2007) Colorful niches of phototrophic microorganisms shaped by vibrations of the water molecule. ISME J 1:271–282

Stransky H, Hager A (1970) Das Carotenoidmuster und die Verbreitung des lichtinduzerten Xanthophyll-Cyclus in verschiedenen Algenklassen. Bertrachtung Arkiv Mikrobiol 73:315–323

Sturm S, Engelken J, Gruber A, Vugrinec S, Kroth PG et al (2013) A novel type of light-harvesting antenna protein of red algal origin in algae with secondary plastids. BMC Evol Biol 13:159

Szabo M, Parker K, Guruprasad S, Kuzhiumparambil U, Lilley RM et al (2014) Photosynthetic acclimation of Nannochloropsis oculata investigated by multi-wavelength chlorophyll fluorescence analysis. Bioresour Technol 167:521–529

Taddei L, Chukhutsina VU, Lepetit B, Stella GR, Bassi R et al (2018) Dynamic changes between two LHCX-related energy quenching sites control diatom photoacclimation. Plant Physiol (Rockville) 177:953–965

Takahashi H, Clowez S, Wollman FA, Vallon O, Rappaport F (2013) Cyclic electron flow is redox-controlled but independent of state transition. Nat Commun 4:1954

Takaichi S (2011) Carotenoids in algae: distributions, biosyntheses and functions. Mar Drugs 9:1101–1118

Tandeau de Marsac N (1977) Occurrence and nature of chromatic adaptation in cyanobacteria. J Bacteriol 130:82–91

Telfer A, Pascal A, Barber J, Schenderlein M, Schlodder E, Cetin M (2007) Electron transfer reactions in photosystem I and II of the chlorophyll *d* containing cyanobacterium, Acaryochloris mari. Photosynth Res 91:143–143

ten Lohuis MR, Miller DJ (1998) Light-regualted transcription of genes encoding peridinin chlrophyll a proteins and eh major inrinsic light-harvesting complex proteins inthe dinoflagellate *Amphidinium carterae* Hulbert (Dinophyceae) – changes in cytosine methylaion accompany photadaptation. Plant Physiol 117:189–196

Tikkanen M, Suorsa M, Gollan PJ, Aro EM (2012) Post-genomic insight into thylakoid membrane lateral heterogeneity and redox balance. FEBS Lett 586:2911–2916

Tomo T, Allakhverdiev SI, Mimuro M (2011) Constitution and energetics of photosystem I and photosystem II in the chlorophyll *d*-dominated cyanobacterium *Acaryochloris marina*. J Photochem Photobiol B-Biol 104:333–340

Toole CM, Allnutt FCT (2003) Red, cryptomonad and glaucocystophyte phycolbiliproteins. In: Larkum AWD, Douglas SE, Raven JA (eds) Photosynthesis in algae. Kluwer Academic Publishers, Dordrecht, pp 305–334

Torres M, Ritchie RJ, Lilley RM, Grillet C, Larkum AWD (2013) Measurement of photosynthesis and photosynthetic efficiency in two diatoms. N Z J Bot 52. https://doi.org/10.1080/00288825X.2013.831917

Trinugroho JP, Bečková M, Shao S, Yu J, Zhao Z, Murray JW, Sobotka R, Komenda J, Nixon PJ (2020) Chlorophyll f synthesis by a super-rogue photosystem II complex. Nature Plants 6(3):238–244

Turmel M, Otis C, Lemieux C (2013) Tracing the evolution of streptophyte algae and their mitochondrial genome. Genome Biol Evol 5:1817–1835

Umetani I, Kunugi X, Yokono M, Takabayashi A, Tanaka A (2018) Evidence of the supercomplex organization of photosystem II and light-harvesting complexes in *Nannochloropsis granulata*. Photosynth Res 136:49–61

Unlu C, Drop B, Croce R, van Amerongen H (2014) State transitions in *Chlamydomonas reinhardtii* strongly modulate the functional size of photosystem II but not of photosystem I. Proc Natl Acad Sci U S A 111:3460–3465

Wagner H, Jakob T, Wilhelm C (2006) Balancing the energy flow from captured light to biomass under fluctuating light conditions. New Phytol 169:95–108

Wilk KE, Harrop SJ, Jankova L, Edler D, Keenan G et al (1999) Evolution of a light-harvesting protein by addition of new subunits and rearrangement of conserved elements: crystal structure of a cryptophyte phycoerythrin at 1.63-angstrom resolution. Proc Natl Acad Sci U S A 96:8901–8906

Willows RD, Li YQ, Scheer H, Chen M (2013) Structure of chlorophyll f. Org Lett 15:1588–1590

Wollman FA (2001) State transitions reveal the dynamics and flexibility of the photosynthetic apparatus. EMBO J 20:3623–3630

Yamamoto HY (1979) Biochemistry of the violaxanthin cycle in higher plants. Pure Appl Chem 51:639–648

Zapata M, Garrido JL (1997) Occurrence of phytylated chlorophyll c in *Isochrysis galbana* and Isochrysis sp. (clone t-iso) (Prymnesiophyceae). J Phycol 33:209–214

Zhang YA, Chen M, Church WB, Lau KW, Larkum AWD, Jermiin LS (2010) The molecular structure of the IsiA-photosystem I supercomplex, modelled from high-resolution, crystal structures of photosystem I and the CP43 protein. BBA-Bioenergetics 1797:457–465

Zhang J, Ma J, Liu D, Qin S, Sun S et al (2017) Structure of phycobilisome from the red alga *Griffithsia pacifica*. Nature (London) 551:57–63

Zingone A, Borra M, Brunet C, Forlani G, Kooistra WHCF, Procaccini G (2002) Phylogenetic position of *Crustomastix stigmata* sp. nov. and *Dolichomastix tenuilepis* in relation to the Mamiellales. *J*. Phycologia 38:1024–1039

Chapter 11

Light Harvesting by Long-Wavelength Chlorophyll Forms (Red Forms) in Algae: Focus on their Presence, Distribution and Function

Stefano Santabarbara*
Centre for Fundamental Research in Photosynthesis, Vergiate, Varese, Italy

Photosynthesis Research Unit, Centro Studi sulla Biologia Cellulare e Molecolare delle Piante, Milan, Italy

Anna Paola Casazza
Istituto di Biologia e Biotecnologia Agraria, Consiglio Nazionale delle Ricerche, Milan, Italy

Erica Belgio and Radek Kaňa
Centre Algatech, Institute of Microbiology, Academy of Sciences of the Czech Republic, Třeboň, Czech Republic

and

Ondřej Prášil
Centre Algatech, Institute of Microbiology, Academy of Sciences of the Czech Republic, Třeboň, Czech Republic

Faculty of Science, University of South Bohemia, České Budějovice, Czech Republic

*Author for correspondence, e-mail: stefano.santabarbara@cnr.it

A. W. D. Larkum et al. (eds.), *Photosynthesis in Algae: Biochemical and Physiological Mechanisms*, Advances in Photosynthesis and Respiration 45, https://doi.org/10.1007/978-3-030-33397-3_11

I. Long Wavelength ("Red") Chlorophyll *a* Forms: Historical Perspective on Their Discovery and General Overview

Probably the first evidence for an important role of light absorbed by Chlorophyll (Chl) at wavelengths above 700 nm in the photosynthetic process stems from the pivotal experiments of Emerson and coworkers (Emerson and Arnold 1932; Emerson and Lewis 1943; Emerson et al. 1957; Emerson and Rabinowitch 1960) demonstrating, in the green alga *Chlorella*, a sharp decrease in the yield of oxygen evolution per absorbed quanta of monochromatic radiation at wavelengths longer than about 695 nm. This phenomenon which was then called "red drop" was shown to be significantly compensated when a background illumination at shorter wavelengths was superimposed to near-infrared single turnover excitation flashes. This evidence, together with the monitoring of antagonistic effects of short-wavelength visible and near-infrared radiations on the oxidation/reduction of cytochromes performed by Duysens et al. (1961), provided the first solid experimental support for the now amply accepted Z-scheme of electron transport, involving the action of two photocatalytic centres, Photosystem I (PSI) and Photosystem II (PSII), which was originally proposed by Hill (Hill and Bendall 1960). Simultaneously, Govindjee and Rabinowitch (1960) noted that the steady state Chl *a* fluorescence of *Chlorella* upon excitation with combined blue and far-red light (436 and 700 nm) was smaller than the sum of the fluorescence intensities measured separately, also suggesting the existence of two forms of Chl *a in vivo* with distinct photochemical functions reflecting two photosystems catalysing two light-driven reactions. These findings correlated rather well with the observation that the meta-stable electron donor of PSI exhibited a maximal different absorption bleaching centred at about 700–705 nm, as originally reported by Kok (1956), whereas photoreactions associated with PSII led to an absorption bleaching due to Chl oxidation at about 680–684 nm, as originally reported by Witt and coworkers (Döring et al. 1967, 1968; Witt 1979). Hence the two photoactive Chl pigment species, now commonly referred to as P_{700} and P_{680} for PSI and PSII, respectively, manifested a parallel shift in photon energy absorption to the one observed for functional light harvesting utilisation measurements. This evidence, gathered well before biochemical purification and isolation methods for the individual photosystems were developed, indicated, although indirectly, that one of the two photocatalytic centres, PSI, was able to absorb and utilise near infrared radiation more efficiently than its counterpart, PSII.

With the improvement of biochemical procedures for photosystems isolation, it became immediately clear that indeed, at least in higher plants, most of the absorption above 700 nm, which can be considered as a first-order approximation threshold to define long wavelength ("red") Chl spectral forms, were indeed bound to Photosystem I. The contribution of the red forms was observable both as a pronounced absorption tail extending up to approximately 740 nm (French 1971; Litvin and Sinechchekov 1975), and as an intense, but rather broad, fluorescence emission band centred at ~735 nm observable at cryogenic (liquid nitrogen) temperatures (Butler (1960),

Butler (1961), Kitajima and Butler (1975), Murata et al. (1966), Rijgersberg & Amesz (1978). Butler 1978 and references therein).

The presence of a distinct spectral feature centred in the 715–740 nm range in the fluorescence emission spectra recorded in several photosynthetic organisms other than higher plants, including model green and red algae, such as *Chlorella* and *Porphyridium*, and cyanobacteria, such as *Synechocystis* and *Anabaena*, could then be readily interpreted as being associated specifically to PSI, whereas the low temperature emission stemming from PSII gave rise to peaks at 685 and 695 nm instead (*e.g* Murata et al. (1966), Rijgersberg & Amesz (1978), Butler 1978 and references therein). A few representative examples are shown in Fig. 11.1. Even though the exact maximal value depends on the specific species studied, the red-shifted emission of PSI with respect to PSII appeared therefore to be a general property of the PSI light harvesting apparatus. This conclusion was successively supported by development of protocols for the purification of PSI (Boardman and Anderson 1964; Anderson and Boardman 1965), and specific mutants suppressing either the assembly of PSII or, when present, the external light harvesting complexes (Butler 1978; Rijgersberg et al. 1979 and references therein). The presence of red Chl forms, their spectroscopic characteristics and molecular nature in PSI will be treated in further detail in the successive paragraph.

Still, despite the broad acceptance that the presence of Chls absorbing in the far red region of the incident spectrum was almost uniquely and ubiquitously associated to PSI, recent surveys of open water environments challenged this view, as, in the field, red forms appear to be less diffused than in laboratory grown model organisms. A survey of the ecophysiological distribution of red-forms will be discussed in Section IV.

More recently, evidence started to emerge concerning the presence of moderately red-shifted forms, generally centred at around

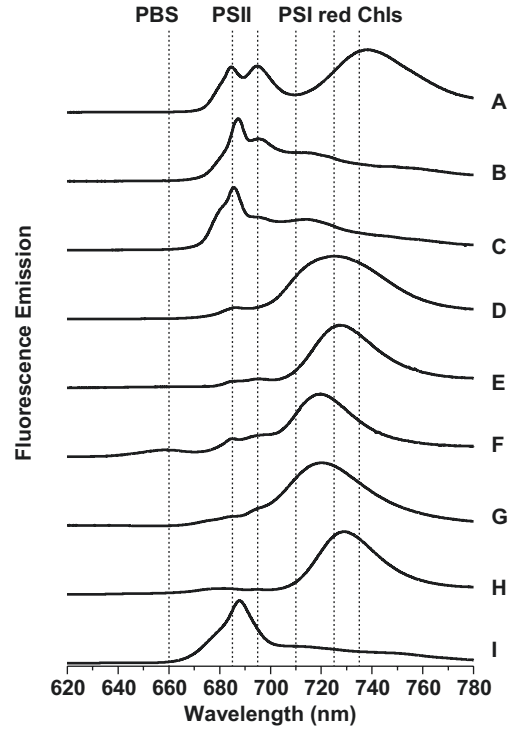

Fig. 11.1. Low temperature (80 K) fluorescence emission spectra recorded in different algal species (B-I) compared with isolated spinach thylakoids (**a**). The emission bands from PBS (660 nm), PSII (685 and 695 nm) and PSI red chls (710 nm, 725 nm and 735 nm) are marked by vertical dashed lines. Species shown are representative of green algae: *Chlorella sorokiniana* (**b**), *Chlamydomonas reinhardtii* (**c**); the protist, green-algae like, *Euglena gracilis* (**d**); cyanobacteria: *Synechocystis sp.* PCC6803 (**e**) and *Synechococcus sp.* PCC7942 (**f**); red algae having PBS antenna: *Phorphyridium cruentum* (**g**), *Cyanidioschyzon merolae* (**h**); and diatoms: *Phaeodactylum tricornutum* (**i**). All spectra were acquired upon excitation at 435 nm and corrected for the detector sensitivity

705–710 nm, also in the light harvesting apparatus of PSII. The first report of PSII-associated red forms was, to our knowledge, demonstrated in the green alga *Ostreobium sp.* (Koehne et al. 1999). More recently the presence of red forms coupled to PSII antenna was also observed in two red clade algae, the diatom *Pheodactylum tricornutum* (Fujita and Ohki 2004; Herbstova et al. 2017) and the apicomplexan-related *Chromera velia* (Bina et al. 2014; Kotabová et al. 2014). In both of these organisms the presence of PSII

red forms was induced by either specific growth under far-red illumination as well as by growth under culture self-shading conditions. In paragraph 3 the occurrence of PSII red forms will be discussed in further detail.

The presence of red Chl forms poses an interesting physiological puzzle. Long wavelength Chls extend the absorption cross-section of either one or both photosystems. On the other hand, laying at a lower energy than the photochemical active pigments composing the reaction centre, they effectively compete for excited state localisation. As a consequence they are expected to lower the yield of the absorbed photon conversion into electrochemical potential. In the most investigated case of PSI red forms, it has been proven that the losses induced to quantum conversion yield are limited (Gobets and van Grondelle 2001; Croce and van Amerongen 2013; Caffarri et al. 2014 and references therein). On the other hand, the situation in which red forms are present in PSII has not been investigated in detail yet. This, however, represents a general problem. Thus, in Section V of this review chapter, a minimal kinetic model is presented addressing the effect of red forms on the yield of photochemical charge separation. Both the role of red forms energy and stoichiometry with respect to the bulk of antenna chromophores, as well as with respect to the effective rate of photochemical trapping, will be explored in order to extract first order, but general, principles concerning the balance between antenna bandwidth and photochemical efficiency. Finally, also based on this simple modelling analysis, the physiological role of red forms will be discussed.

II. Long Wavelength Chlorophyll Forms Associated to Photosystem I

Long wavelength Chl forms have been reported to be present both in the core complex of PSI as well as in the external antenna, particularly in the transmembrane Chl *a*/*b* binding complexes (hereafter referred as LHCI – Light Harvesting Complex I). The PSI core-associated red forms are better characterised in cyanobacteria where the external antenna is constituted by phycobilisomes (PBS), which are extrinsic megacomplexes located on the membrane surface. On the other hand, long wavelength Chl forms associated to the LHCI complement are better described in green algae and in land plants. Figure 11.2 shows a comparison of the pigments arrangement in PSI according to the structural models of a cyanobacterium (*Thermosynechococcus elongatus*, Jordan et al. 2001) and a higher plant (*Pisum sativum*, Qin et al. 2015). The diagram highlights the similarity of the overall chromophore organisation in the core complexes and shows the specific location of transmembrane light harvesting complexes, in the land plants structural model.

A. Photosystem I Core Red Forms

The overall organisation of the PSI core supercomplex (Fig. 11.2) is well conserved through evolution (e.g. Schubert et al. 1998; Fromme et al. 2001; Nelson and Yocum 2006; Caffarri et al. 2014 and reference therein), being most of the differences amongst species found at the level of the so-called minor subunits. The structural architecture and the protein sequences of essential PSI subunits are remarkably similar probably due to their involvement in photochemical and electron transfer reactions. However, there are notable differences in the oligomerisation state of PSI between species. In the majority of land plants and green algae the PSI-LHCI supercomplex is present as a monomer (Croce and van Amerongen 2013; Caffarri et al. 2014) whereas, in cyanobacteria, the most common oligomeric state is represented by trimers, with even higher-order oligomers reported (Fromme et al. 2001; Gobets and van Grondelle 2001). A dynamic equilibrium between monomers and oligomers might

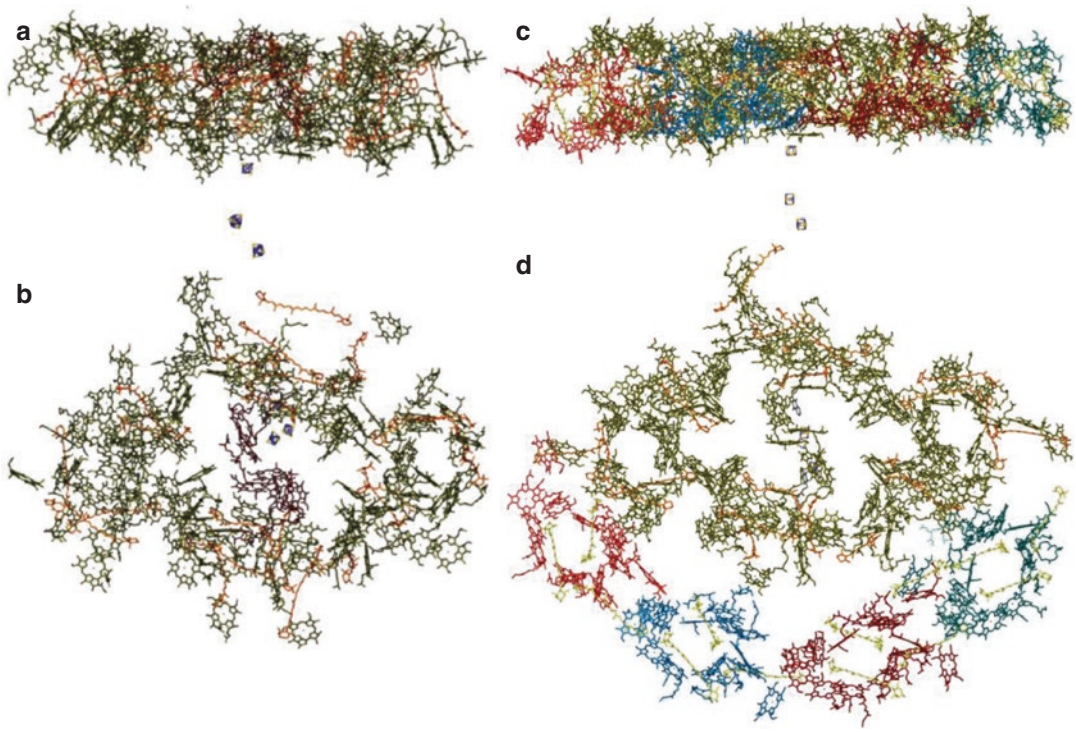

Fig. 11.2. Schematic representation of the pigments arrangement in PSI core complex of cyanobacteria (**a** and **b**, pdb:1jb0) and in the PSI-LHCI supercomplex of higher plants (**c** and **d**, pdb: 4xk8). Panels **a** and **c** show a side view, parallel to the putative membrane plane, whereas Panels **b** and **d** show a top view, perpendicular to the membrane plane (stromal side). Chlorophyll *a* molecules coordinated by the core complex are shown in green, and *β*-carotene is shown in orange. In panel **a** and **b**, Chls in dark-red represent those active in primary photochemistry and electron transfer processes. In the PSI-LHCI supercomplex (**c** and **d**) Chl bound to individual antenna complexes are marked in different colours (pink: Lhca3; light blue: Lhca2; red: Lhca4; dark blue: Lhca1). Carotenoids bound to the LHCI complement are shown in yellow

exist and it has been suggested to be determined by environmental conditions (Shubin et al. 1993; Kruip et al. 1994, reviewed by Yang et al. 2015) and also to participate in state transitions (Bald et al. 1996), a process balancing excitation between the photosystems (Kirilovsky et al. 2014).

Irrespective of the oligomeric organisation, in all species, the majority of core chromophores are bound to the hetero-dimer composed by the PsaA:PsaB subunits (containing 85 Chl *a* and ~30 β-carotene), together with the phylloquinones and the iron-sulphur centre F_X that are essential components of the electron transfer chains (Brettel 1997; Fromme et al. 2001; Santabarbara et al. 2005 and references therein). As only 6 Chl molecules are directly involved in electron transfer reactions, the vast majority of bound pigments serve as an inner antenna system (Fig. 11.2, where the Chls involved in electron transfer processes are marked in a different colour with respect to antenna pigments). Despite the large degree of PSI core structural homology, the light harvesting properties of these core complexes significantly vary between species, particularly in respect to the presence of red forms and their transition energies (Gobets and van Grondelle 2001; Croce and van Amerongen 2013; Caffarri et al. 2014). As in cyanobacteria the PBS antenna do not absorb significantly above 685 nm, the presence of long wavelength absorption/emission forms in PSI has

to be straightforwardly associated to Chl *a* coordinated by the PSI core complex. On the other hand, the presence and function of core red forms in organisms containing a transmembrane antenna system (*e.g.* algae and plants) is more controversial. Therefore here we focus our attention on cyanobacterial core PSI which has been most extensively investigated. Interestingly, significant species-specific differences have been noticed even within this single class of organisms (Shubin et al. 1991; Wittmershaus et al. 1992; van der Lee et al. 1993; Gobets et al. 1994; Palsson et al. 1996; Rätsep et al. 2000; Hayes et al. 2000; Cometta et al. 2000; Zazubovich et al. 2003), with transition energies of red forms ranging from ~705 to over 730 nm, depending on the species and on the oligomeric state of the core complex.

Gobets and coworkers (Gobets and van Grondelle 2001) presented a critical detailed comparative analysis of PSI cores isolated from several cyanobacterial species indicating that, although the relative abundance of specific forms does depend on the species, there are also some common characteristics. The comparison of *Synechocystis sp.* PCC6803, *Synechococcus elongatus* and *Spirulina platensis* highlighted the presence of red forms with absorption centred at about 708 nm (702 at room temperature), giving rise to a low temperature emission centred at about 720 nm. It has been suggested that a variable number of Chls are involved in the formation of the 708 nm absorption (F720 low-temperature emission) form, ranging from ~3 in monomeric PSI core of *Synechocystis* to ~7 in the trimeric core of *Spirulina*. In general, switching from monomeric to trimeric form, leads to a stoichiometric enhancement of the 708/720 absorption/emission form (Gobets and van Grondelle 2001 and references therein), suggesting these forms results from interacting chromophores at the core monomer-monomer interfaces. The large number of Chl molecules involved and the broadness of the red forms spectral band had also led to the suggestion that the 708 nm form might be actually composed of two bands, one centred at 706 nm and the other at 714 nm, both originating from dimers (Hayes et al. 2000). Absorption forms further shifted to the red edge are present in the core complexes of *Synechocuccus elongatus* and *Spirulina platensis*, showing transitions at 719 nm in both, and up to 740 nm in the trimeric form of the latter (Gobets and van Grondelle 2001; Shubin et al. 1991, 1993; Karapetyan et al. 1997; Koehne and Trissl 1988). The 740 nm absorption form detected in the core of *Spirulina* gives rise to a near-infrared emission centred at ~760 nm, that, to our knowledge, is the red-most Chl *a* emission form present in nature. However, Karapetyan and coworkers (Karapetyan et al. 1997) suggested that also this spectral form could be due to the superimposition of bands centred at 725 nm and 745 nm. Upon trimer monomerisation the 740 nm absorption (F760 emission form) is lost and the amplitude of the 719 nm band, also observed in *Synechococcus*, increases dramatically instead. The number of Chls contributing to the ~719 and ~740 nm red states is in the order of 3–4 Chl molecules (Gobets and van Grondelle 2001). If the latter were to be due to two transitions at ~725 and 745 nm, this would also correspond to approximately two chlorophyll molecules for each band, pointing towards a dimeric origin of these spectral features.

Thus, the core complex of PSI of several model cyanobacterial species harbours Chl *a* forms capable of extending the absorption cross section to the near infrared, spanning a broad range with limits exceeding even 780 nm when considering the long-wavelength tail of the red-most form of *S. platensis*. On the other hand, there are several cyanobacterial species which display almost no absorption over 700 nm, excluding the terminal donor P_{700}. The best characterised species is the marine *Synechococcus* WH 7803 that has also the least red-shifted PSI amongst cyanobacteria (van Stokkum et al. 2013; Acuña et al. 2018). The absence of red

forms in cyanobacterial species inhabiting oceanic water might in fact be more common than generally perceived. This issue will be dealt in further detail in Section IV.

B. *Photosystem I External Antenna Red Forms*

Amongst algal species possessing a transmembrane external antenna complement, the best characterised is the green alga *Chlamydomonas reinhardtii*. It represents a good model organism due to the relative ease of obtaining mutants and, more recently, biochemical preparations of PSI-LHCI supercomplexes, cores and isolated LHCI. However, results obtained from mutants lacking the PSI core complex (Chua et al. 1975; Girard et al. 1980; Wollman and Bennoun 1982) and biochemical analysis of either isolated (Croce and van Amerongen 2013 and references therein), or *in vitro* reconstituted antenna complexes are not in full agreement. Therefore it is useful to compare the evidence gathered in *C. reinhardtii* with the better characterised LHCI of land plants, as they have a similar Chl *a/b*-binding transmembrane antenna system.

Photosystem I of land plants harbours four LHCI antenna complexes, binding 13–14 Chl (*a* + *b*) each, attached to one side of PSI core forming a half moon (Ben-Shem et al. 2003; Jensen et al. 2007; Amunts et al. 2010; Qin et al. 2015). The four LHCI monomers are organised as pairs of dimers, each composed by the Lhca1/Lhca4 and the Lhca2/Lhca3 antenna subunits (Fig. 11.2). It has been recently shown that each of these dimers harbours a long wavelength Chl *a* form, reflecting in a low temperature emission maximum centred at ~730 nm (Wientjes and Croce 2011) and that the red-most transition form is present in the Lhca1/Lhca4 heterodimer (Wientjes and Croce 2011; Croce and van Amerongen 2013). These results are in agreement with studies on reconstituted complexes (Lhca3 and Lhca4 monomers) that contain long wavelength spectral forms diplaying a maximal fluorescence emission centred at ~720 and ~730 nm (*e.g.* Morosinotto et al. 2003; Castelletti et al. 2003; Zucchelli et al. 2005; Croce et al. 2007; Wientjes and Croce 2011), respectively. Moreover, all LHCI complexes of land plants are red-shifted with respect to the bulk (core) emission, that is centred at 685-690 nm. Thus also the *in vitro* reconstituted Lhca2 has a maximal emssion at 702 nm whereas Lhca1 emission peaks at 695 nm (Morosinotto et al. 2003; Castelletti et al. 2003; Croce et al. 2002, 2004, 2007). Furthermore, the comparative analysis of the isolated core and the full LHCI complement (*i.e.* a mixture of the Lhca1/Lhca4 and Lhca2/Lhca3 dimers) of land plants indicated that the majority of PSI red-forms were indeed localised in the external antenna (Croce et al. 1996, 1998; Jennings et al. 2004). The core was almost devoid of red forms which were in any case less red-shifted than in LHCI (Croce et al. 1998). The isolated supercomplex (PSI-LHCI) contains three red forms having maximal emission at 720, 730, and 742 nm (Croce et al. 1996), and being therefore more red-shifted than those observed in the isolated antenna complexes. It was estimated that their absorption transitions fell at 714, 725, and 738 nm and that about 10–12 Chl *a* molecules per photosystem participated to these spectral forms (Croce et al. 1996).

In contrast to higher plants, the PSI-LHCI supercomplex of *C. reinhardtii* has a larger antenna network, with nine LHCI monomers concentrically arranged into two half-moon shaped arrays around the core (Drop et al. 2014). The inner array resembles the LHCI organisation observed in land plants (with four monomers) while the outer array comprises the remaining five monomers. It was suggested that the inner half-ring is formed by the Lhca1, Lhca2, Lhca3, Lhca7 and/or Lhca8 subunits, with Lhca2 being the weakest bound one (Drop et al. 2014; Croce and van Amerongen 2013; Caffarri et al. 2014). Lhca4, which is found in the inner ring in plants, is part of the additional peripheral complement in *C. reinhardtii* together with

the Lhca5, Lhca6, Lhca9 and/or Lhca8 subunits. The low temperature fluorescence emission of whole PSI-LHCI supercomplex from *C. reinhardtii* has a maximum at ~715 nm (Germano et al. 2002; Gibasiewicz et al. 2005; Santabarbara et al. 2007; Croce and van Amerongen 2013 and references therein), that is blue-shifted with respect to what usually is observed in most land plants (735 nm). As the same blue shift can be observed also in whole cells, it is not just an artefact due to PSI supercomplex purification. It shall be noticed that similar blue-shifts *in vivo* (by 15–20 nm) are present also in other green algal species (*Chlorella sorokiniana, Chlorella vulgaris*) (*e.g.* Cho and Govindjee 1970a, b) whose PSI-LHCI complexes have not yet been biochemically characterised in detail.

It was observed that in mutants of *C. reinhardtii* incapable of assembling a stable PSI core complex but still capable of assembling the LHCI complement, the low temperature emission maxima shifted to ~708 nm, *i.e.* by approximately 10 nm with respect to the wild type strain (Girard et al. 1980; Wollman and Bennoun 1982). This observation was taken as an indication that the red-most Chl *a* spectral form in this organism was associated to the core complex, similarly to what observed in model cyanobacterial species. The LHCI antenna still harboured some long wavelength emission forms, albeit less red-shifted than those bound to the core.

On the other hand, the biochemical isolation (Bassi et al. 1992) and *in vitro* reconstitution (Mozzo et al. 2006) of the Lhca complexes of *C. reinhardtii* indicated the presence of long wavelength Chl *a* forms in at least three monomeric complexes, Lhca2, Lhca4 and Lhca9, displaying low temperature emission peaks at 717 nm, 708 nm, 710 nm, respectively. Moreover, it was shown that also the Lhca5, Lhca6 and Lhca8 monomers displayed significant emission above 700 nm, due to very broad bands centred in the 695–700 nm range (Mozzo et al. 2006). At the same time, the relative abundance of these moderately red-shifted forms and the influence of subunits dimerisation (and/or higher oligomerisation states formation) on the emission properties are not well understood yet.

The apparent discrepancies between PSI core-lacking mutants and monomeric *in vitro* reconstituted complexes could be explained by the presence of fine-scale interactions among individual LHCI monomers, as well as amonsgt monomers and the core complex that, in turn, affect the red-forms properties of the intact, fully assembled, PSI-LHCI supercomplex. This argument could also apply to core-lacking mutants where the super-structural assembling of the antenna subunits in the absence of the core complex might be altered, causing the blue-shifted emission at 708 nm observed in mutants cells.

C. *Nature of Long Wavelength Chlorophyll Forms*

Long wavelength spectral forms are characterised by their significantly broader bandwidth with respect to the vast majority of other protein-bound Chls. Based on experiments on Chl (*a*) dissolved in organic solvents, the red spectral forms were initially attributed to excitonically interacting dimers, trimers or even higher-order oligomers, as these would explain both the red-shift and the band broadness (Vernon and Seely 1966 and references therein). Most of the detailed information concerning the nature of long wavelength Chl forms in cyanobacterial PSI core complex came from site selective spectroscopic techniques, either Fluorescence Line Narrowing (FLN) or Hole Burning (HB), at very low temperatures (below 10 K), which allow to resolve fine spectral characteristics even within crowded chromophore systems. HB and FLN data on cyanobacterial PSI confirmed that, even upon their direct excitation, the long wavelength spectral forms have both a remarkably large Stokes' shift of about 12–15 nm, i.e. ~200–300 cm^{-1} (Palsson et al. 1996; Rätsep et al. 2000; Hayes et al. 2000; Zazubovich et al.

2003; Gobets and van Grondelle 2001), as well as an unusually broad bandwidth. For higher plants PSI-LHCI and isolated LHCI only results from FLN spectroscopy are available, indicating that however the Stokes shift of the red-most energy transitions were close to those reported for cyanobacteria.

The Stokes shift is mainly due to two parameters: (i) the frequency of the phonon mode (*i.e.* generally low frequency vibration of the embedding, protein, surroundings) that is coupled to the electronic transitions and (ii) the strength of the electron–phonon coupling, which is described by the so-called Huang-Rhys factor (*S*). Site-selective spectroscopy studies indicate that the mean coupled phonon mode is in the ~20–25 cm^{-1} range (Gobets and van Grondelle 2001 and references therein) for cyanobacteria red-forms, close to those typical retrieved for Chl *a* antenna molecules (Jankowiak et al. 1993 and reference therein). Coupling with higher frequency modes, of about 100–150 cm^{-1}, has however also been invoked (Rätsep et al. 2000). Thus, to explain a 200–300 cm^{-1} Stokes shift, the Huang-Rhys factor for red forms needs to be rather large (between 2–4) in contrast to the typical low value of *S* associated with antenna Chls (around 0.5). The proposed large values of *S* are consistent with the original hypothesis attributing the long wavelength forms to excitonically coupled dimers or higher oligomers. However this might not be sufficient to lead to such a strong electron–phonon coupling. To explain the observed red-shift, other mechanisms, like electron–exchange coupling between closely spaced Chl *a* molecules, need to be invoked (Gobets et al. 2001; Hayes et al. 2000; Zazubovich et al. 2003). This process would provide significant charge transfer (CT) character to the electronic states involved (Hayes et al. 2000; Zazubovich et al. 2003). Mixing of CT states with the electronic transitions can result in significant changes in the dipole moment between the ground and the excited states (Lathrop and Friesner 1994), leading to a permanent dipole which shall therefore be sensitive to an externally applied electric fields. This was shown indeed to be the case, both through Stark spectroscopy (Rätsep et al. 2000) as well as field-dependent HB experiments (Zazubovich et al. 2003). Hence, it appears that the spectral characteristics of the long wavelength Chl forms are the results of different interactions, including both excitonic and the establishment of CT states.

There is no conclusive model that would localise red chlorophyll forms to particular pigments in the PSI core complexes of cyanobacteria. The assignments depended on whether the conclusions were derived primarily from spectroscopic evidences (Byrdin et al. 2002; Zazubovich et al. 2003) or from theoretical/computational methods (Damjanovic et al. 2002; Sener et al. 2002, 2005). The only substantial agreement concerns the involvement of the A32 – B07 pair (nomenclature according to Jordan et al. 2001) located at the PsaA:PsaB subunits interface. Figure 11.3a shows the organisation of the A32 – B07 dimer. It is however worth mentioning that quantum chemical methods predicted that the Chl-protein interactions that tune the individual Chl site energies might have a dominant effect with respect to excitonic (Chl-Chl) interactions in determining the long wavelength states (Damjanovic et al. 2002; Sener et al. 2005).

More detailed information about the localisation of red chlorophyll forms are instead available for the LHCI complexes of higher plants and *C. reinhardtii*, thanks to the ability to reconstruct these antenna complexes *in vitro*. This approach proved to be a very useful tool for mutating specific residues involved in Chl coordination (Morosinotto et al. 2003; Castelletti et al. 2003; Croce et al. 2002, 2007; Croce and van Amerongen 2013). Through a survey of the putative Chl ligands, it was shown that the asparagine coordinating Chl 603 (numbering as in the PSI-LHCI structure of Qin et al. 2015) is of fundamental importance to observe a red state in reconstituted LHCI (Morosinotto et al. 2003; Castelletti et al. 2003; Croce and van Amerongen 2013).

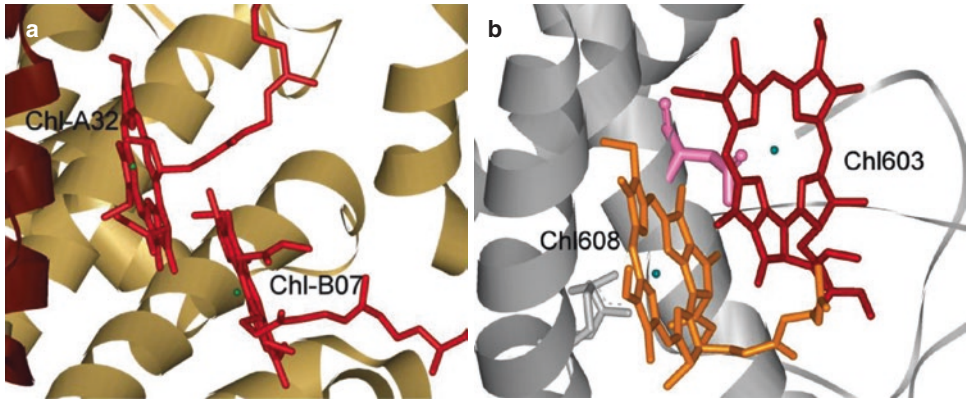

Fig. 11.3. (**a**): Structural arrangements of the putative red-most form in the core of cyanobacteria (Chl-A32/Chl-B07) located at the interface of the PsaA (dark brown) and PsaB (light brown) reaction centre subunits. (**b**): geometrical arrangements of the Chl603:Chl608 pair, identified at the red-most state in Lhca4 of land plants, also showing the main protein ligands for Chl603 (Asn98 in pink) and for Chl608 (Glu153 and Arg156 in light grey). Nomenclature and amino-acid numbering according to Qin et al. 2015 (pdb: 4xk8)

The red form results then from the interaction of Chl 603 with the nearby Chl 608, where structural arrangement is depicted in Fig. 11.3b; although the effect of the asparagine substitution is more evident for the Lhca4 complex of land plants (Asn98, also shown in Fig. 11.3b), which harbours the red-most shifted transition, similar effects were also observed for other Lhca complexes, particularly Lhca3 (Croce and van Amerongen 2013), as well as the reconstituted LHCI complexes of *C. reinhardtii* (Mozzo et al. 2006). The authors interpreted the role of the unusual asparagine coordination in terms of setting the correct geometrical arrangement of the Chl 603–608 pair. This would favour the establishment of both excitonic interactions and, in particular, the mixing with CT states (Croce et al. 2007; Croce and van Amerongen 2013), rather than causing a direct red-shift of the unperturbed site energy.

More investigations, employing both experimental and computational methods, appear to be required to fully elucidate the origin of the intriguing properties of long wavelength Chl forms, possibly also by extending their study to yet poorly explored microalgal species, which display larger variability with respect to the classical models investigated so far.

III. Long Wavelength Chlorophyll Forms Associated to Photosystem II

Long wavelength Chl forms have been mainly associate to pigments present either in the PSI core of cyanobacteria (see paragraph II.A) or in the external antenna of green algae and higher plants (see paragraph II.B). However, there is a rising amount of experimental evidences (see *e.g.* Koehne et al. 1999; Kotabová et al. 2014) indicating the existence of new, far-red light absorbing spectral forms also in the external antenna of PSII. Hereafter these will be referred to as "*PSII-associated red forms*". The first experimental proof of their existence was gathered in the green chlorophyte alga *Ostreobium sp.* (Halldal 1968; Koehne et al. 1999; Wilhelm and Jakob 2006), a phototrophic endolith growing within the scleractinian corals *Porites cylindrica* and *Montipora monasteriata* (Magnusson et al. 2007). Later, PSII-associated red Chl forms have also been identified in other algal species from the red-clade including *Pheodactylum tricornutum* (Fujita and Ohki 2004; Herbstova et al. 2017) and *Chromera velia* (Bina et al. 2014; Kotabová

et al. 2014). The latter is a novel unicellular alga, isolated from the Sydney bay, that belongs to the colpodellids (Obornik and Lukes 2013) and that is closely related to non-photosynthetic apicomplexan parasites (Moore et al. 2008).

At the same time, several species of cyanobacteria and algae, mostly inhabiting pelagic zones, do not have any type of long wavelength absorbing Chl forms (see paragraph IV). It is important to note, that several cyanobacterial species can adjust their pigmentation to red light by synthesising different types of chlorophylls (see *e.g.* Averina et al. 2018 for a recent review), having an inhrently red-shifted absorption, such as Chl *d* and Chl *f*. In particular, Chl *d* represents, constitutively, the main pigment in the cyanobacterium *Acaryochloris marina* (Kuhl et al. 2005) whereas Chl *f* synthesis can be induced by far-red light in several cyanobacteria (Chen et al. 2010; Ho et al. 2017; Nürnberg et al. 2018), including some extremophilic strains, such as *Chroococcidiopsis thermalis* (Nürnberg et al. 2018), that contain both Chl *f* and *d*. Therefore, it has been proposed that various Chl *d*-containing cyanobacteria have an important role in special far-red enriched niches, like endolithic habitats (Behrendt et al. 2011). Moreover, the cyanobacteria exhibiting inducible alternative Chl synthesis (reviewed in Gan and Bryant 2015) have adopted even more complex photo-acclimative responses to far-red-light growth (Gan et al. 2014) as they not only accumulate far-red absorbing Chls *d* and *f* but also remodel their photosystems and phycobilisome antenna by the expression of specific subunits isoforms, in a process defined as Far-red light photoacclimation (FaRLiP, see *e.g.* Ho et al. 2017 for review). However, this FaRliP adaptation will not be discussed in further detail although it will be considered within the larger framework of general far-red light photoacclimation strategies of algae (see paragraph IV).

A. PSII-Associated Long Wavelength Chlorophylls in Algae

Although the association of Chl *a* red forms with PSI is well established (see paragraph II), far-red Chl forms need to be also involved in supporting PSII photochemical activity, due to the observation that oxygen evolution occurred also for irradiation well above 700 nm in several phototrophs including the green alga *Chlorella vulgaris* (Greenbaum and Mauzerall 1991; Myers and Graham 1963) and higher plant species, including sunflower, bean and spinach (Pettai et al. 2005a, b; Thapper et al. 2009). Therefore, the so-called red limit of PSII activity has been recently reconsidered by several authors (Pettai et al. 2005a, b, Thapper et al. 2009).

The presence of long-wavelength Chls associated to PSII was also strongly supported by the unusually intense far-red fluorescence emission band, centred at 710 nm (F710), observed at room temperature the diatoms *Phaeodactylum tricornutum* (Fujita and Ohki 2004) as well as in *Chromera velia* (Kotabová et al. 2014). Measurements of variable fluorescence parameters (Fujita and Ohki 2004) and the application of spectrally resolved fluorescence induction methods, allowing detection over a wide spectral range (Kaňa 2018; Kaňa et al. 2012), confirmed the functional connection of the F710 fluorescence with PSII (Kotabová et al. 2014). In fact, the kinetic behaviour of the F710 band induction curve at room temperature was very similar to that of the typical PSII emission peak centred at 685 nm, F685 (Kotabová et al. 2014).

The appearance of far-red absorbing and emitting forms during chromatic adaptation (especially in diatoms) has been discussed since the 60's (see *e.g.* Brown 1967; French 1967; Shimura and Fujita 1973). However, only recently their characterization on a molecular level has been undertaken (Fujita and Ohki 2004; Kotabová et al. 2014). These authors have noted, that the presence of these red-shifted PSII-associated forms is condi-

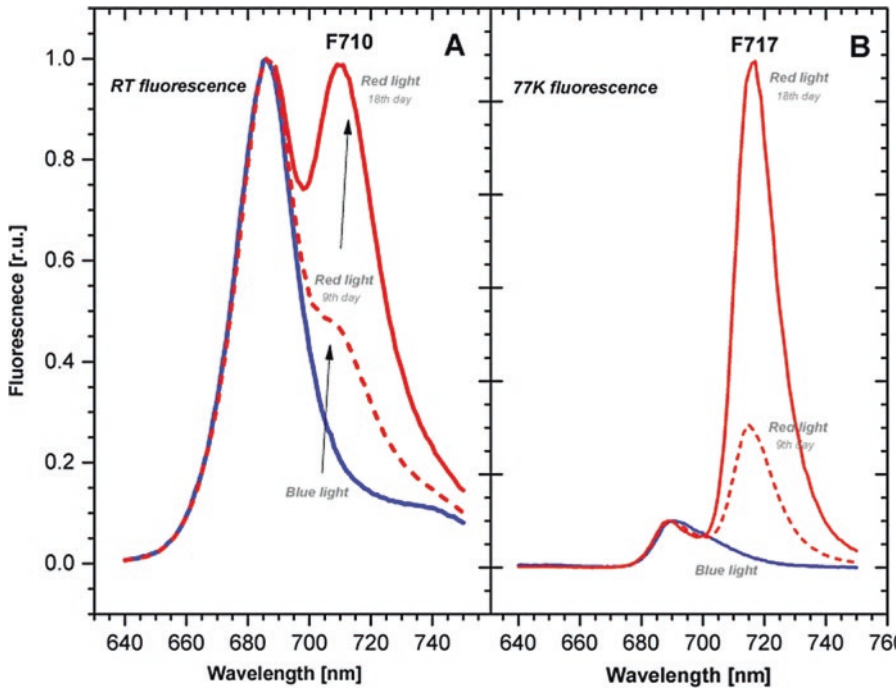

Fig. 11.4. Fluorescence emission of long wavelength Chlorophyll forms associated with PSII in *Chromera velia.* The PSII-associated red forms are present in *C. velia* cells grown for several days on red light (λ = 635 nm) in comparison to blue light grown cells (λ = 460 nm). The long-term adaptation on red light caused synthesis of specific PSII antenna subunits (Red-CLH antenna protein of 15 kDa) in comparison to standard CLH. Red light conditions resulted in the appearance of additional fluorescence bands situated at 710 nm at room temperature (**a**) or at 717 nm for measurements at 77 K (**b**). For further details, see *e.g.* Kotabová et al. (2014)

tional, as their presence became obvious only for cells grown under red/near-far-red enriched lights. This chromatic adaptation is rather slow as several days of far-red light growth are required to detect the typical 710 nm centred fluorescence band (F710). Figure 11.4 shows exemplificative spectra of the F710 band appearance as a function of adaptation to red-light growth. It is worth to notice that the F710 emission form is already well evident at room temperature. Although visible at 77 K as well, it would be difficult to discriminate it from typical PSI red forms without a comparison with emission spectra acquired at higher temperatures.

Whereas the onset of PSII far-red emission is a rather slow adaptation, its disappearance is much faster, requiring a few hours only, when cells were moved to standard light conditions without red light enrichment (Fujita and Ohki 2004; Kotabová et al. 2014). All these characteristic features would explain why this type of chromatic adaptation, giving rise to F710 emission at room temperature, has been widely overlooked recently, particularly in studies employing cultivation under white light conditions, despite the above discussed evidences strongly confirm the original suggestion of earlier literature (Brown 1967; French 1967; Shimura and Fujita 1973).

The association of the F710 fluorescence form to specific PSII antenna subunits was initially demonstrated in experiments using the protein synthesis inhibitor cycloheximide (Bina et al. 2014; Kotabová et al. 2014). In these studies it was shown that the appearance of far-red emission at room temperature under red-light growth conditions required protein synthesis. Indeed, specific PSII

antenna complexes giving rise to the F710 room temperature fluorescence were later biochemically identified not only in *C. velia* (Bina et al. 2014; Kotabová et al. 2014) but also in the pennate diatom *Phaeodactylum tricornutum* (Herbstova et al. 2015, 2017). The red-shifted emission from the pigment-protein complex isolated from *C. velia* and defined as *Red-CLH* complex resulted from the oligomeric organisation of a 17 kDa protein (Kotabová et al. 2014). This protein belongs to the LHC family but has a different origin with respect to the typical LHCI antennae of higher plants or green algae (Bina et al. 2014). The *Red-CLH* complex also differs from both the typical PSI and PSII light-harvesting antennae complexes of *C. velia* (Tichy et al. 2013). In fact, the PSII antenna complexes of *C. velia* (CLH) have been identified as FCP-like antennae belonging to the LHCf/FCP family, common in diatoms, while the PSI antenna complexes phylogenetically belong to the LHCr antennae typical of red algae (Tichy et al. 2013). Interestingly, the isolated PSI-LHCr complex of *C. velia* displays only a limited red-shift with respect to the bulk of PSI core pigments (Belgio et al. 2017). Therefore, during red/near-far red chromatic adaptation the light-harvesting system in *C. velia* has almost unique characteristics because the *Red-CLH* complex shifts PSII absorption (Bina et al. 2014) close to isoenergetic, or even further red shifted than that of PSI (Belgio et al. 2017).

The CLH antennae of *C. velia* contain Chl *a*, violaxanthin and isofucoxanthin but does not bind Chl *c*, as no accessory Chls are present in this organism (Moore et al. 2008; Quigg et al. 2012). This represents the main difference with diatoms, the other algal group possessing PSII-associated red forms (Fujita and Ohki 2004; Herbstova et al. 2015, 2017). In diatoms, the presence of a variable F710 fluorescence at room temperature (which is a signature of PSII-associated long-wavelength Chls, *e.g.* Fujita and Ohki 2004; Kotabová et al. 2014) has been attributed to the supramolecular oligomeric state of the Chl *a*/*c*-binding Lhcf15 complex (Herbstova et al. 2015, 2017), which belongs to the fucoxanthin-Chl *a*/*c* binding protein (FCP) family (Nymark et al. 2013). The Lhcf15 protein is strongly up-regulated in red light and down-regulated in blue light (Schellenberger Costa et al. 2013) and it is not phylogenetically related to the *Red-CLH* complex of *C. velia* (Herbstova et al. 2015).

Another group, already mentioned above, in which red-shifted antenna complexes have been observed and biochemically identified, is the green prasinophytes endolithic alga *Ostreobium sp.* where PSII red antennae were shown to belong to the LHCa family (Koehne et al. 1999). The detailed phylogenetical analysis of Lhc sequences has identified several other protein candidates that could act as PSII red-form antenna complexes, based on their sequence similarity with Lhcf15. These include antenna proteins of the chrysophycean alga *Ochromonas sp.* and members of haptophytes (Herbstova et al. 2015), a group of organisms that is clearly evolutionary distant from the heterokont linage of diatoms (Burki et al. 2012). Moreover, PSII-associated red forms have been recently identified also in several Eustigmatophytes (Pazdernik 2015; Wolf et al. 2018), that are similar to *C. velia* as they lack any accessory chlorophylls, including Chl *c* (Litvin et al. 2016). Finally, the red-shifted antenna protein LHCb9, which has a typical motif of PSI antennae but is however functionally associated with PSII, has been identified in the moss *Physcomitrella patens* (Alboresi et al. 2008, 2011).

On the other hand, all the experimental data collected until now cannot exclude the possibility that when PSII associated red-forms are observed, some of the long-wavelength Chl forms harbouring complexes could also be functionally connected to PSI. Moreover, another scenario which needs to be considered is that, whereas the F710 forms are specifically harboured by PSII antennae, it is possible that in diatoms and in other organism in which there is no

specific separation of photosystems into well defined physical domains, like grana and stromal lamellae typical for plant thylakoids, that these antennae could serve both photosystems because of energy spillover (Butler 1978 and reference therein) between them. It is worth mentioning moreover that whereas the F710 antenna red-forms are almost isoenergetic with the PSI primary donor (centred at ~ 705 nm), thermal activation will in general be required for energy transfer from these forms to the reaction centre of PSII (see discussion in Bina et al. 2014).

All the above-mentioned evidence demonstrates the presence of PSII-associated red forms in various organisms, raising the question of the general importance of these red forms in photothrophs. They seem to be the result of specific adaptations to lights of different spectral quality, specifically enriched in red and/or near-far red radiation. Such spectral enrichment could be caused by self-shading, shading by other organisms for corals-accompanied algae, permanently red-light enriched niches like endolithic habitats and also during the switch between planktonic and benthic living strategies. This adaptation can then be accompanied by a substantial re-organisation of the photosynthetic apparatus and by distinct changes in cell morphology (Herbstova et al. 2017).

IV. Survey of Cyanobacterial and Algal Species for the Presence of Long-Wavelength Chlorophyll Forms

Fluorescence emission spectroscopy at low temperatures (most frequently at liquid nitrogen temperature, 77k) has represented the method of choice for the semi-quantitative determination of the presence of long-wavelength Chls in algal and cyanobacterial samples. Currently, portable low temperature spectrophotometers with LED excitation have been developped (Prášil et al. 2009; Hill et al. 2012; Lamb et al. 2015, 2018), allowing to survey the presence of red forms among phytoplankton and macroalgal communities either grown in the laboratory or collected *in situ*. The emission spectra of representative model species studied in the laboratory (the diatom *Thalassiosira pseudonana*, the green alga *Dunaliella teriolecta* and the cyanobacteria *Synechococcus sp.* and *Cyanothece sp.*) measured using the portable spectrometer (Fig. 11.5) can be used as a standard reference for the interpretation of field data from mixed communities. All reference cultures show a major emission band associated to Photosystem II (685 nm and a shoulder at 695 nm). Cyanobacteria also show emission from phycobiliproteins (allophycocyanines at 655 nm). The red forms assigned to Photosystem I can be clearly revealed as long-wavelength emission bands with peaks at 710 nm (in the model green alga) or even at 730 nm in cyanobacteria. In the model diatom, there is only a shoulder visible at 715 nm

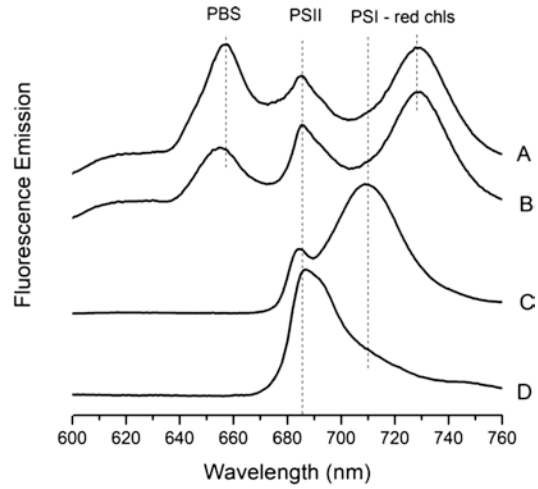

Fig. 11.5. Reference low temperature emission spectra of standard laboratory model species of cyanobacteria (*Cyanothece sp. ATCC 51142* (**a**) and *Synechococcus sp.* (**b**)), green algae (*Dunaliella tertiolecta* (**c**)) and diatoms (*Thalssiosira pseudonana* (**d**)). The emission bands from phycobilisomes (PBS, 657 nm), Photosystem II (PSII, 685 nm) and long wavelength (>700 nm) Photosystem I (PSI, 710 and 728 nm) are marked by vertical dashed lines. Spectra are recorded upon broad-band excitation from a white LED. The stray background from the excitation source has been subtracted from the spectra

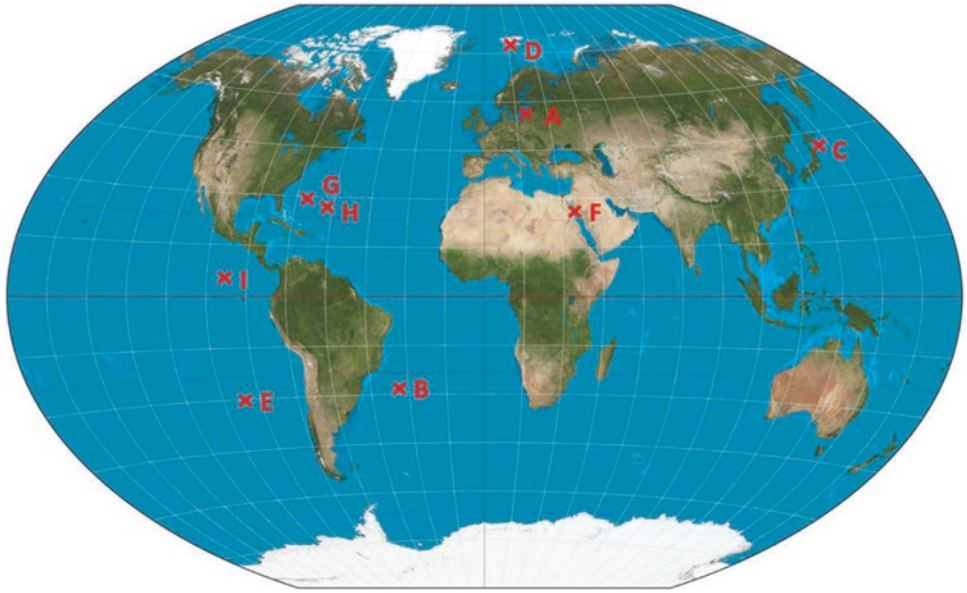

Fig. 11.6. Sampling sites for field survey of the presence of long-wavelength Chls. Samples were collected during oceanographic cruises in the Baltic sea (**A**, BioOptics – SY Oceania, 2004), South Atlantic (**B**, AMT20 – RRS James Cook, 2010), North Pacific Oyashio current (**C**, KH15/1 – RV Hakuho Maru, 2015), North Atlantic, Isfjorden in Svalbard (**D**, UNIS, 2018), South Pacific Gyre (**E**, Biosope – RV L'Atalante, 2004), Red Sea (**F**, 8thGAP workshop, 2008), Atlantic, Sargasso sea (**G**, AMT16 – RRS Discovery, 2005), Atlantic, Sargasso sea (**H**, FeAST6 – RV Atlantic Explorer, 2008), Equatorial East Pacific (**I**, TAO/TRITON – RV Ron Brown, 2003). The respective emission spectra from the locations are shown in Fig. 11.5

instead. The minor band around 745 nm that is often observed in the emission spectra has been assigned to the vibrational satellites of the major PSII bands at 685 and 695 nm. The spectra shown in Fig. 11.5, (and succesiveli in Figs 11.7 and 11.8) are obtained using the simple portable emission spectrofluorometer employing broadband LED excitation (Prášil et al. 2009). They might therefore qualitatively differ from the spectra obtained using more sophisticated instruments emplying monochromatic excitation. For the purpose of this chapter, we are interested only in the qualitative analysis of the emission spectra as red-forms presence indicators.

An environmental field survey on the presence of red forms among aquatic phytoplankton using portable low temperature emission spectroscopy has been performed (Fig. 11.6); in most cases, the pelagic samples were collected by standard methods of oceanographic field sampling (Niskin bottles), filtered on GF/F filters and immediately measured on board of the oceanographic vessels. The freshwater samples were collected using buckets from piers or boats and processed and measured in the laboratory within few hours after sampling.

The oceanic sampling sites in Fig. 11.6 varied in their geographic location, trophic status, salinity, temperature, season of sampling and phytoplankton species composition and abundance – from mesotrophic/eutrophic brackish southern Baltic sea stations dominated by filamentous cyanobacteria or Arctic coastal bays (Svalbard, diatoms and flagellates), through oligotrophic coastal areas dominated by diatoms (Oyashio current) and open ocean of Sargasso sea dominated by cyanobacteria and picoeukaryotes to extremely oligotrohic ocean deserts (South Pacific Gyre) where the remaining biomass was composed of picocyanobacteria *Prochlorococcus* and *Synechoccocus*.

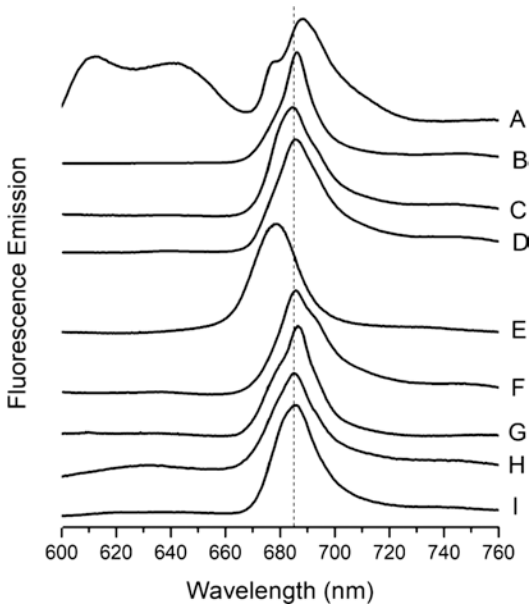

Fig. 11.7. Low temperature emission spectra of phytoplankton field samples. Samples were collected in the Baltic sea (**a**), South Atlantic Gyre (**b**), North Pacific Oyashio current (**c**), Isfjorden inside Svalbard (**d**), South Pacific Gyre (**e**), Gulf of Aquaba, Red Sea (**f**), Atlantic, Sargasso sea (**g**), Atlantic, Sargasso sea (**h**), Equatorial East Pacific (**i**). For sample location, see Fig. 11.2. The dashed line indicates emission at 685 nm. Data were collected by M. Koblížek (**a**, **g**), B. Šedivá (**b**), K. Suzuki (**c**), O. Prášil (**d**, **e**, **f**), T. Bibby (**h**) and M. Behrenfeld (**i**) using the 77 K portable emission spectrofluorometer (Prášil et al. 2009)

Examples of emission spectra of oceanic, open water, phytoplankton collected from their natural environments are shown in Fig. 11.7. Although collected from a wide variety of geographical locations and environmental conditions, the spectra are surprisingly similar. Unlike the reference spectra of laboratory strains, the emission spectra of the field samples show usually only one major emission band peaking in the region 670–690 nm and no, or very little, contribution by emission from red chlorophylls (i.e. emission peaking above 700 nm). The dominant emission band of field samples, centred at around 685 nm is the emission from photosynthetic reaction centres. It is composed from several bands, with the major peak at 685 nm stemming from PSII emission and clear shoulders also observable at about 695 nm and 676 nm. The shoulder at 695 nm was interpreted as an additional signal associated to intact PSII reaction centres, whereas the 676 nm band was assigned to reaction centres-uncoupled antenna, originating from cells either stressed by lack of nutrients (line E, Fe limitation in the South Pacific Gyre) or by excessive irradiance. As can be seen by detailed inspection of the spectra, the proportion of the individual bands that contribute to the major emission at 685 nm varied. The phycobilisome emission (below 665 nm) was visible just in a few samples (here only samples from the Baltic sea are shown, line A). Although the characteristic long-wavelength emission peak associated to red-Chls, was missing from in field samples (Fig. 11.7), a clearly distinct small emission shoulder was present at around 710 nm. However, its intensity was never above 20% of the major band at 685 nm.

The field data shown in Fig. 11.7 clearly indicate the absence, or the significant decrease, of red Chls emission in pelagic, open ocean, phytoplankton. Since the red forms of Chl are usually associated with PSI, the standard interpretation of the low intensity of long-wavelength emission would be that the relative concentration of active PSI is significantly decreased in the open ocean phytoplankton. This is clearly not the case, as proved by several quantitative biochemical protein analyses. In some strains of *Prochlorococcus*, the dominant phytoplankton from oligotrophic regions, the PSI/PSII ratio is even higher than in the reference cultures shown in Fig. 11.5 (Zorz et al. 2015). Therefore the absence of Chl red forms can be instead interpreted as an intrinsic property of algae and cyanobacteria living in the aquatic environment that strongly absorbs all the near infrared irradiance.

In order to verify that the absence of the long-wavelength Chl forms observed in

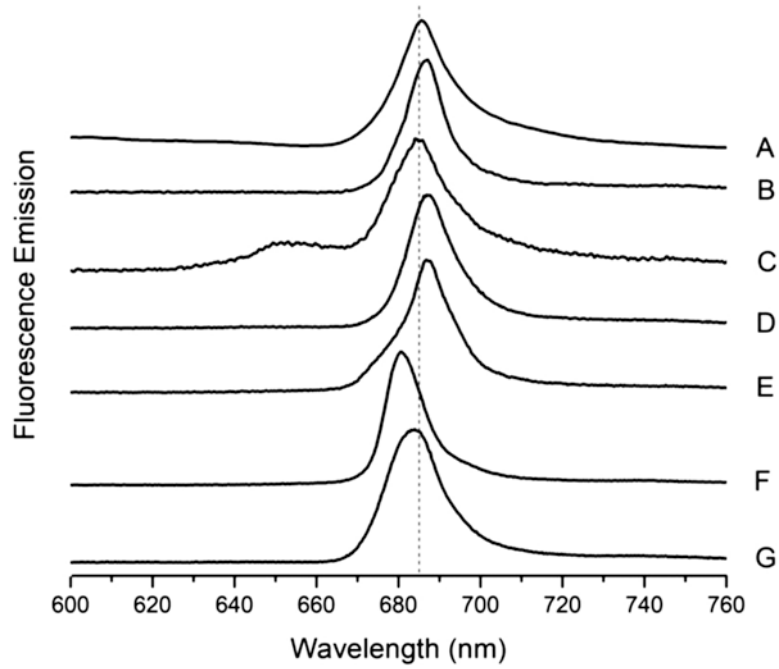

Fig. 11.8. Fluorescence emission spectra of selected phytoplankton species isolated from natural environments: diatom *Thalassiosira oceanica* (**a**, spectrum provided by *R. Strzepek*), cyanobacterium *Prochlorococcus sp. PCC9511* (**b**), cyanobacterium *Synechococcus sp. WH7805* (**c**), dinoflagellate *Prorocentrum minimum RCC291* (**d**), prymnesiophyte *Chrysotila carterae RCC190* (**e**), flagellate prasinophyte *Micromonas commode RCC299* (**f**) and heterokont flagellate *Pelagomonas calceolata RCC102* (**g**). The vertical dashed line indicates the 685 nm emission

Fig. 11.7 was not due to nutrient or light stresses present in the natural environment, the emission spectra of the individual phytoplankton species that are known to be dominant in the natural pelagic or coastal phytoplankton assemblages (picocyanobacteria, diatoms and picoeukaryotes) were also measured in laboratory-grown cultures. Representative low-temperature emission spectra from several species of each taxonomic group are shown in Fig. 11.8. Similarly to field data from mixed communities (Fig. 11.7), all spectra of single species have a dominant band around 685 nm and very little emission from red Chls above 710 nm. These data seem therefore to support that the absence, or the only moderate red-shift, of long-wavelenght Chl forms is indeed a very common characteristic of organisms inhabiting pelagic, open ocean, waters.

A. Physiological and Environmental Consequences of the Presence of Red Forms (or Their Absence)

More than 40% of solar photons reaching the Earth surface are in the infrared region (> 700 nm). It is generally considered that these wavelengths are only minimally absorbed by oxygenic photoautotrophs that contain PSI and PSII. In general, the limited abundance of long-wavelength spectral forms, even in organisms displaying a marked low-temperature emission in the 710–740 nm window, is due to bioenergetic constraints impacting on the overall photochemical quantum conversion efficiency of reaction centres that will be discussed in detail in Section V. Nonetheless, on the surface of Earth there are many ecological situations where the availability of visible light is limited, while the number of photons in the near

infrared is still relative large. Then, the ability to absorb light in the near infrared region can be decisive for ecological success. Such situations occur under dense plant canopy, in the sand or soil and in general whenever photosynthetic organisms are densely layered, such as in microbial mats, corals, biofilms or shallow benthic communities. Under these conditions it is expected to find phytoplankton with "red" Chls that can utilize the available near infrared radiation. On the other hand, in open ocean (pelagic) water the spectrum of available light is governed by the optical properties of water and by the dissolved organic and inorganic matter as well as by the absorption of phytoplankton itself. Here the strongest absorption of water molecules is in the near infrared and red part of the spectrum. In clear, oligotrophic, waters illuminated by the Sun at noon, below the depth of 10 m there are almost no "red" photons available (Fig. 11.9). In deeper layers of the euphotic zone the spectrum becomes dominated by photons in the blue-green region instead (Fig. 11.9). Therefore, in pelagic (open sea) waters and in deep freshwater lakes, it is expected, as observed, that long-wavelength spectral forms are basically absent in organisms colonising these habitats.

V. Effect of Long Wavelength Chlorophyll Forms on the Photochemical Quantum Efficiency

The long wavelength Chl spectral forms absorb at lower energies than the terminal electron donor as well as, on average, the chromophores of a the reaction centre (RC). Therefore energy transfer from the red forms to both the photochemically active and the bulk antenna pigments is energetically unfa-

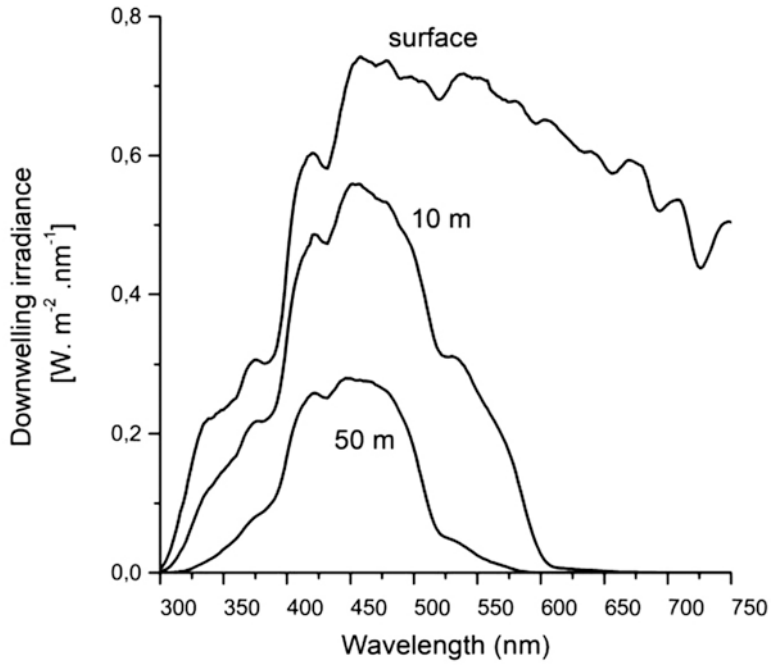

Fig. 11.9. Example spectra of downward irradiance in oceanic clear waters determined at discrete depths (m) as indicated. Data were obtained by A. Morel during the Biosope cruise in South Pacific, near Easter Island. Note the almost absence of red (>600 nm) photons already in 10 m of water. Contrary, the blue-green part of the spectrum (400–500 nm) propagates well into the deep. All the spectra are normalized for a constant incident irradiation at the surface and thus are directly comparable. The acquisition of Biosope data where funded through CNRS-INSU grants

vourable. In a rather simple framework, the red forms can be seen as being in competition for excited state localisation with the RC even though the most of the excitation is, statistically, initially localised in the bulk antenna pigments because of their larger stoichiometric abundance. Red forms are thus expected to impose some kinetic limitations on the mean time required for photochemical conversion and, therefore, reduce the "effective" photochemical trapping efficiency. It was shown that the estimation of the average fluorescence lifetime represents a good indicator of the effective photochemical trapping rate (Jennings et al. 2003): "fast" decay corresponds to rapid (*i.e.* efficient) energy conversion and *vice versa*. This parameter can be relatively straightforwardly determined from the analysis of the excited state decay kinetics (*i.e.* fluorescence lifetime) by monitoring "bulk" or red shifted emitted photons in different spectral regions.

In fluorescence decay investigations of energy trapping in PSI containing red forms, it was observed that, irrespectively of the detailed model utilised to describe the data, the average fluorescence lifetime increased when monitored on the long wavelengths emission tail above 700 nm (Croce et al. 2000; Jennings et al. 2003, 2013; Engelmann et al. 2006; Gobets and van Grondelle 2001; Gobets et al. 2001, 2003; Le Quiniou et al. 2015a, b; Slavov et al. 2008; Wientjes et al. 2011a, b). This common trend was valid for both, cyanobacterial PSI core complexes (e.g. Byrdin et al. Turconi et al. Gobets and van Grondelle 2001; Gobets et al. 2001) as well as for the PSI-LHCI supercomplexes of green algae (*e.g.* Owens et al. 1987; Ihalainen et al. 2005a; Le Quiniou et al. 2015a, b; Giera et al. 2014) and land plants (e.g. Croce et al. 2000; Jennings et al. 2003, 2013; Engelmann et al. 2006; Slavov et al. 2008; Wientjes et al. 2011a, b; Galka et al. 2012; Santabarbara et al. 2017). The average lifetimes measured in the spectral emission window dominated by bulk pigments is between 10–30 ps (Turconi et al. 1996; Byrdin et al. 2000; Gobets and van Grondelle 2001; Croce and van Amerongen 2013; Caffarri et al. 2014) where when monitored on the red forms emission tail it falls in the 40–100 ps interval (Croce and van Amerongen 2013, Caffarri et al. 2014). The increase in the fluorescence average lifetime (up to about fivefold) monitored on the red forms emissions correlates with the energy and the relative stoichiometric abundance of long-wavelength Chl forms, which are characteristics of specific PSI systems (*e.g.* Gobets and van Grondelle 2001; Caffarri et al. 2014 and references therein). For instance, the longest decay component specifically associated to the red-most spectral form present in different cyanobacterial core complexes varies from ~25 ps in the trimeric core of *Syncochocystis sp.* PPC6803 to ~40 ps in that of *Synechococcus elongatus,* correlating with the red forms transitions being dominated by the 708 nm- and the 719 nm-absorbing forms, respectively. Moreover in the PSI trimer of *S. platensis* a biphasic decay in the red tail was reported, characterised by lifetimes of ~30 ps and ~65 ps, which appear to be predominantly associated to the 719 nm and the 740 nm forms, respectively (Gobets and van Grondelle 2001; Gobets et al. 2001). Similarly, in the core of land plants the longest decay was shown to have values of ~20 ps whereas, when the red form-harbouring LHCI complex is associated to it, two additional phases of ~30–45 and ~80–120 ps are observed (Croce et al. 2000; Jennings et al. 2003, 2013; Engelmann et al. 2006; Slavov et al. 2008; Galka et al. 2012; Santabarbara et al. 2017). An analogous trend of the fluorescence decay was observed in the larger PSI-LHCI supercomplex of *C. reinhardtii*. However, for this supercomplex a rather broad range of values associated with the slowest decay lifetime (~80–200 ps) have been reported, depending on both the overall external antenna dimensions (Gibasiewicz et al. 2001; Holzwarth et al. 2005; Ihalainen et al. 2005a; Le Quiniou et al. 2015a, b) as well as the relative red form abundances (Giera et al. 2014). On the other hand, the average lifetime

is almost wavelength independent in PSI systems with low red form content, for instance the core complexes of land plants (Engelmann et al. 2006; Ihalainen et al. 2005b; Wientjes et al. 2011b) and of *Synechococcus* WH 7803 (van Stokkum et al. 2013), as well as in the PSI-LHCI supercomplexes isolated from red-clade algae, such as *P. tricornutum* and *C. velia* (Belgio et al. 2017).

The increase in the average lifetime in the long wavelength emission tail of red-form harbouring systems indicates a decrease in the photochemical efficiency linked to the uphill energy transfer from the long wavelength absorbing/emitting pigments to both the bulk antenna and the RC pigments. However, the overall loss in quantum efficiency caused by the presence of the red forms is rather low, because the average lifetime of fluorescence decay remains always much faster (<100 ps) than the natural excited state relaxation (~ 2 ns) in antenna pigments (see Santabarbara et al. 2017 and Molotokaite et al. 2017 for further detail). The species containing PSI red forms thus rather benefit from the increased absorption in the far-red/near-infrared regions, since this compensates the possible small losses in photochemical quantum efficiency. This is especially the case under environmental conditions in which the incident light is very enriched in red/far red spectral components (Rivadossi et al. 1999), for instance because of shading and filtering effects caused by other photosynthetic phototrophs.

Whereas experimental evidence gathered on red-forms harbouring PSI are generally consistent, much less detailed information is available concerning red forms associated to PSII antenna as their presence and relevance has emerged only in recent years (Bina et al. 2014; Fujita and Ohki 2004; Herbstova et al. 2017; Koehne et al. 1999; Kotabová et al. 2014; Wilhelm and Jakob 2006). It is nonetheless interesting to address the question relating to the balance between the presence of long wavelength spectral forms and the limits that they can impose on photochemical efficiency. In other words, what is the maximal number and/or energy red-shift that a photosystem can tolerate before quantum efficiency losses will exceed, significantly, the increased photon absorption of radiation at wavelength longer than 700 nm. The question of long-wavelength limit of photosynthetic efficiency, especially in a view of PSII catalysed O_2 evolution, represents an open question (see *e.g.* Pettai et al. 2005a, b; Thapper et al. 2009) that still needs to be solved (see also Sect. III.A).

In order to derive some general conclusions on this intriguing issue, which is of obvious relevance under an adaptive perspective, we have developed a minimal compartmental kinetic model which allows to threat in relatively simple and physically intuitive terms the role of red forms stoichiometry, transition energies and effective energy transfer rates on the excited state trapping dynamics. We would like to stress that, although this represents a reasonable model stemming from literature reports, it does not aim or have the ambition to describe any system *accurately*. Rather, it is meant at restricting the number of variables, so that the most relevant ones can be more straightforwardly approached in the future.

A. Simulations of the Impact of Red Forms on Excited State Energy Trapping

In the minimal kinetic model, schemat ically represented in Fig. 11.10, most of the photosystems' chromophores are represented by two functional excited compartments only, one being the "bulk" of the antenna [Bulk*], the other the reaction centre [RC*], which are coupled by pair-wise rates of energy transfer, linked by so-called detailed balance (*i.e.* site degeneracy-weighted Boltzmann factors). Photochemical reactions are described by an "output" rate from the [RC*] compartment, therefore the exact mechanisms of charge separation and charge stabilisation are neglected. The photochemical rate then just describes the average time required to popu-

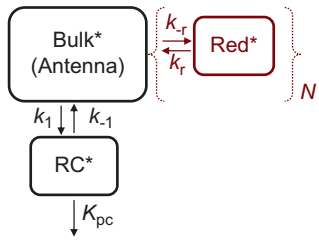

Fig. 11.10. Minimal kinetic model utilised to describe the effect of long wavelength Chl forms on the effective photochemical trapping and photochemical quantum efficiency in PSI-like and PSII-like scenarios. The model considers two red-form-less compartments, describing the bulk of the antenna (Bulk*) and the reaction centre (RC*). In all simulations the number of Chls involved in RC* is 6. The number of molecules involved in Bulk* depends on the known biochemical/structural binding stoichiometries of the core and the core-LHC supercomplexes. The RC* and Bulk* communicate through the pair of excited state energy transfer rate constants k_1/k_{-1} linked by so-called detailed balance. Photochemistry is accounted by a single *effective* constant K_{PC}. The values of k_1 and K_{PC} were chosen to describe qualitatively the experimental decays in PSI and PSII core complexes, and not changed further. Hence only $k-_1$ varies when changing the number of pigment in Bulk*

The presence of long wavelength Chl forms is accounted by the additional compartment Red*, connected uniquely to Bulk* by the pair-wise rates k_r/k_{-r}. In the simulations different energies of the Red* compartment, corresponding to transitions having maximal emission centred from 700 to 750 nm, were considered. Moreover the number of forms coupled to the bulk (N) was varied from 0 to 6 (considering two Chls for each state) all being isoenergetic. Hence the number of compartment considered was from 2 (no red forms) to 8 (maximal number of red forms). The red forms compartments are considered not to be in direct energy transfer amongst themselves, but they communicate through Bulk*, to which they are directly coupled only. For the simulations the value of k_r was changed from 15 to 180 ns^{-1} whereas the one of k_{-r} varied according to detail balance

All simulations were performed considering unselective excitation conditions. That is, the initial population in each compartment equals $n_i\left(\sum_i n_i\right)^{-1}$ where n_i are the number of Chls in a given compartment and $\sum_i n_i$ is the total number of Chls

late a radical pair whose recombination lifetime (to [RC*]) exceeds by at least an order of magnitude the compartment de-excitation by natural processes.

1.. *Photosystem I*

We start to discuss a PSI-like system for which we consider three different situations. The simplest situation being the one resembling the core complex which binds 90 Chl molecules in total (PSI $core_{90}$), 6 of which compose the reaction centre. This number is kept fixed for all simulations. When the presence of a variable number of red forms is considered, the number of Chls in the bulk antenna decreases accordingly, so that the total number of pigments remains constant. The other two situations consider a larger overall antenna size, corresponding to 150 and 200 Chls in total (PSI-LHC_{150} and PSI-LHC_{200}) These two scenarios approach the physical antenna dimension of land plants and of the green alga *C. reinhardtii*, respectively (Croce and van Amerongen 2013; Caffarri et al. 2014 and reference therein). We deliberately avoided to use the exact experimental estimates for the antenna size and rather opted to use round numbers to maintain generality and to stress that the results obtained by the present simulations are intended only to be indicative and not to reproduce any specific experimental dataset. Initially simulations were performed for a system in which red forms are not present, the average bulk antenna emission is set at 690 nm (1.8 eV) and the energy of RC* at 705 nm (1.76 eV), which accounts for the presence of red-shifted Chl at least in P_{700}. In all simulations, the value of the rate describing the excited state delivery to the RC is kept constant (k_1) whereas the back-transfer rate (k_{-1}) scales with antenna dimension instead. We consider this as a reasonable approximation which limits the model parameter changes, because the average energy transfer rate to RC* would be mainly (although not exclusively) determined by chromophores which are in closer proximity to it and this shall not be strongly affected by increasing the dimension of the antenna array at the periphery. When considering an effective photochemical constant (K_{pc}) of 165 ns^{-1} and a rate of transfer from the

Bulk* to the RC* of 350 ns^{-1}, the estimated biphasic decays for the three situations having a progressively larger antenna are characterised by average lifetimes ($\tau_{av} = \sum_i A_i\tau_i / \sum_i A_i$, where A_i is the sum of the population amplitudes associated to the i-th lifetime, τ_i) of 25, 37 and 47 ps, respectively. These values are in rather fair agreement with those estimated experimentally (Gobets and van Grondelle 2001; Croce and van Amerongen 2013; Caffarri et al. 2014). It is rather well established that PSI does not display any significant change in fluorescence yield in response to the redox state of the terminal donors, *i.e.* when P_{700} is either oxidised or reduced, with maximal changes being in the order of 10% (*e.g.* Byrdin et al. 2000). This is generally attributed to the fact that the oxidised species P_{700}^+ is an efficient fluorescence quencher. The possibility that an open photochemical channel is present even when P_{700} is already oxidised, has also been considered as a reasonable explanation for the absence of significant changes in average lifetime between "open" and "closed" centres (Giera et al. 2010). A detailed discussion of this issues is beyond the scope of the present chapter. However, the small changes in fluorescence yield preclude a simple estimation of PSI photochemical quantum yield (ϕ_{pc}), contrary to what routinely discussed for the case of PSII where a sizable fluorescence induction is observed instead (*e.g.* Butler 1978; Duysens 1978). To estimate the yield at "closed", photochemically inactive, centres we then consider an average decay lifetime of 1.6 ns ($\tau_{av,c}$) that is to close to what observed for PSII embedded in native membranes in the absence of photochemical quenching (*e.g.* Searle et al. 1979; Karukstis and Sauer 1985; Holzwarth et al. 1985; Hodges and Moya 1986; Roelofs et al. 1992). This is equivalent, in the minimal model of Fig. 11.10 to set the value of K_{pc} to zero, since natural relaxation remains the only de-excitation channel available. Following the simple relation $\phi_{pc} = 1 - \tau_{av}/\tau_{av,c}$, which is analogous to the well-known F_V/F_M parameter commonly employed to evaluated PSII maximal photochemical efficiency, PSI quantum efficiency is estimated to be 0.984, 0.977 and 0.970 for red-form-less PSI $core_{90}$, PSI-LHC_{150} and PSI-LHC_{200}. This corresponds to less than 1% efficiency loss for the doubling of antenna dimension.

Two factors associated to the presence of the red forms are considered in the simulations, their mean energy, which is varied from 705 to 750 nm (1.76 to 1.65 eV) and their abundance, that is changed from 1 to 6 forms per photosystem, each being composed by 2 Chl molecules, *i.e.* the maximal number of long wavelength pigments (n_{red}) considered is 12. Moreover, the rate of energy transfer from each red spectral form to the bulk (k_r) is changed from 15 to 180 ns^{-1} (*i.e.* from ~67–5.5 ps)$^{-1}$), which covers most of the broad range of values present in the literature (Gobets and van Grondelle 2001; Croce and van Amerongen 2013; Caffarri et al. 2014). Upon increasing the number of red forms, which are considered to be in energy transfer contact with the bulk but not amongst themselves, the value of k_r is held constant, whereas that of the back-transfer rate *from* the bulk (k_{-r}) varies according to detailed balance. The absence of *direct* energy transfer amongst the red forms (all at a given energy for each scenario) is a reasonable assumption as long as their number is low, *i.e.* the goodness of this approximation decreases by increasing the number of red states. Moreover, we consider the red forms to be in direct energy transfer contact with the bulk only. Gobets et al. (2003; Gobets and van Grondelle 2001) suggested that for the core of cyanobacteria direct energy transfer from the red states to the RC might instead be present. However, this is less likely for LHC binding systems as the red states are physically further away from the photochemical active chromophores. This is still another simplification that is introduced for the sake of generality, but might affect the

detailed dynamics of transfer and trapping in core simulations.

Upon considering the presence of red forms in the model, the excited state decay becomes polyphasic. However, for unselective excitation, *i.e.* by setting the initial population in each compartment accordingly to its relative stoichiometric abundance, most decay components vanish at a photosystem level, as they correspond to pure energy transfer processes. Thus, for these specific excitation conditions (equivalent to a broadband incident spectrum) the decay is described by three lifetimes only, the fastest of which has a very small residual amplitude. Then, these overall scenarios are similar to the one of the core complex, which is characterised by a biphasic decay. Therefore, we will focus the discussion mainly on the average lifetime, rather than on the specific lifetime components, as τ_{av} can be computed for all scenarios.

Figure 11.11 shows the simulations outcomes in terms of average lifetimes considering the range of values associated to the model parameters (red form mean energies, stoichiometries and energy transfer rates) already discussed above. As expected, and in accordance to the experimental reports discussed above, the presence and stoichiometry of long wavelength spectral forms lead to an increase in the value of τ_{av} in all the scenarios considered. Although a rather smooth increase in the τ_{av} value is simulated upon increasing the relative number of a given red state, it is the energy of the state which is by far the most impacting factor. The exact value of the k_r transfer rate has however only a marginal effect on the average lifetime simulations. Yet the k_r value does influence the detail of excites state relaxation, when the individual lifetimes, rather than τ_{av}, are considered. As an example, considering a scenario in which a single form centred at 715 nm is present in the PSI core complex, by changing the value of k_r from 15 ns^{-1} to 180 ns^{-1} a significant shortening of the slowest decay lifetime, from 73 to 32 ps, is simulated. This is however compensated by a loss of relative amplitude, which transits to the faster component having lifetimes in the 21 to 3 ps range. As a result, the τ_{av} value changes only slightly.

Thus, the precise value of k_r is important for describing experimental data correctly when the relative amplitudes of the different kinetic phases are observed. Yet, on average, it appears to have a much less drastic impact on the overall, photosystem level, *effective* trapping time. It is worth stressing that the here performed simulations are equivalent to measurements integrated over the entire emission bandwidth. Changing the energy of the red state can have very radical effects instead, as it is most obvious for forms having mean energy at 730 nm and 750 nm, *i.e.* 100 meV and 145 meV gap from the bulk, corresponding to ~ 4–6 time the thermal energy (k_BT ~ 25 meV at physiological relevant temperatures). The substantial increase in the τ_{av} is particularly apparent for the 750 nm forms, as this value varies from ~180 ps to ~700 ps when considering 1–6 states, respectively. We stress that the values estimated here exceed significantly those reported by Gobets and coworkers for the reddest state in *S. platensis* (Gobets et al. 2001). This is due to the fact that the authors considered both an higher energy for RT conditions (733 nm) as well as direct coupling between this state and RC^* (actual direct trapping from the state), which is consistent with its direct quenching by P_{700} at cryogenic temperatures (Karapetian 2004; Karapetyan et al. 1997).

We conclude the discussion on the simulations of PSI long wavelength forms, considering the effect of their presence on the photochemical yield, which is the most crucial physiological parameter. This is shown in Fig. 11.12, where it appears that a PSI-like system can robustly tolerate the presence of low energy states up to 730 nm with the quantum yield remaining generally larger than 0.9. Moreover, for red forms centred at 705 and 715 nm the quantum yield is always

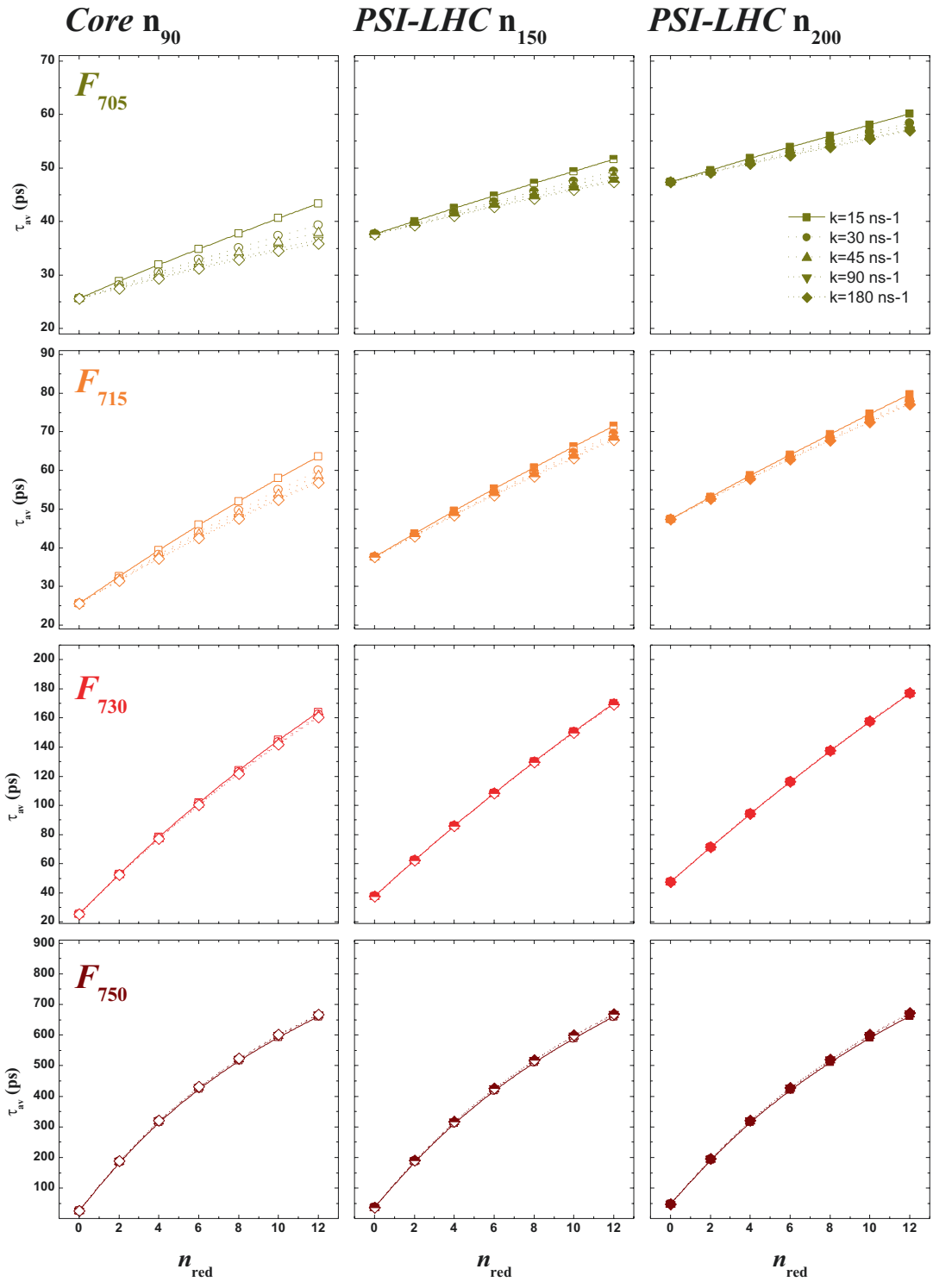

Fig. 11.11. Outcome of simulations for a minimal kinetic model aiming at describing the effect of long wavelength spectral forms in PSI-like photosystems. Three general cases are considered, one mimicking the core (90 Chls, open symbols), the other two representing core-LHC supercomplexes of different antenna

larger than 0.95. The only clear exception is when the F_{750} form is considered, as the quantum efficiency loss is then remarkable. Only when a single F750 form is present the photochemical yield remains around ~0.90. Yet, from two or more red states involved, it drops from 0.8, which will still be physiologically sustainable, to 0.5, which appears too high a penalty to pay for increasing the absorption cross-section. Interestingly, very red-shifted forms are indeed not very abundant in the known PSI complexes. Moreover, these forms might be in direct energy coupling with the RC, thereby releasing, in part, the photochemical yield losses predicted by the minimal kinetic model considered here. On the same line of thoughts, however, the number of pigments which could directly communicate to the RC cannot be very large for physical constraint reasons. Therefore the number of 1–2 red forms with energy equivalent to 750 nm, or better an energy gap of ~5–6 k_BT with respect to the bulk, might well represent an upper limit of bandwith increase in the near infrared region for a typical Chl *a*-based, PSI-like, photosystem.

2.. *Photosystem II*

The simulations for PSII-like systems were performed, in general terms, as discussed above for PSI. Therefore, we initially began by considering a core complex scenario, binding 45 Chls in total and in the absence of long wavelength spectral forms (PSII $core_{45}$). The energy of the bulk antenna and of the RC* was in this case set at 685 nm (1.81 eV) for both compartments. Considering a rate of energy transfer from the bulk to RC of 60 ns^{-1} and an effective photochemical rate of 100 ns^{-1} (10 ps)$^{-1}$, *i.e.* about half the value utilised for PSI simulations above, τ_{av} equals

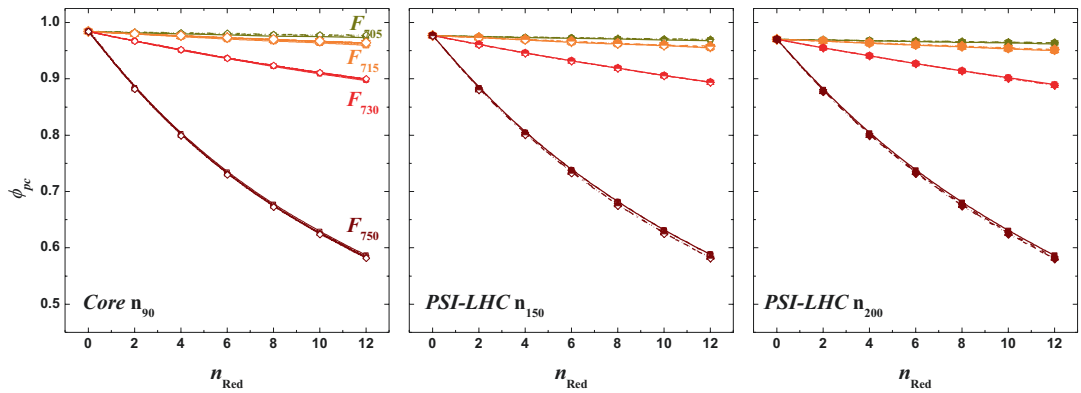

Fig. 11.12. Simulated quantum efficiencies for a minimal kinetic model aiming at describing the core of PSI (90 Chls, open symbols) and the two core-LHC supercomplexes of different antenna dimension (150 Chls, half-filled symbols, and 200 Chls, solid symbols). Simulations of the photochemical quantum yield are presented for red forms centred at 705 nm (gold), 715 nm (orange), 730 nm (red) and 750 nm (crimson), involving 0–12 Chls in total, and for transfer rates from the red forms to the bulk antenna of 15 ns^{-1} (squares), 30 ns^{-1} (circles), 45 ns^{-1} (up triangles), 90 ns^{-1} (down triangles) and 180 ns^{-1} (diamonds)

Fig. 11.11. (continued) dimension (150 Chls, half-filled symbols, and 200 Chls, solid symbols). Shown are the average lifetimes (τ_{av}) resulting from the presence of red forms centred at 705 nm (gold), 715 nm (orange), 730 nm (red) and 750 nm (crimson). The number of forms is varied from 1 to 6, comprising 2 Chls each, *i.e.* the total number of Chls involved (n_{red}) varies from 0 to 12. Moreover, the rate of transfer from the red forms to the bulk antenna was considered to be 15 ns^{-1} (squares), 30 ns^{-1} (circles), 45 ns^{-1} (up triangles), 90 ns^{-1} (down triangles) and 180 ns^{-1} (diamonds). Please notice the change in the τ_{av} scale upon varying the red-state energy

84.6 ps. This value falls in the middle of the literature spread ranging from ~50 to ~120 ps (*e.g.* Schatz et al. 1988; Barter et al. 2003; Miloslavina et al. 2006; Holzwarth et al. 2006; Broess et al. 2008; Tumino et al. 2008; van Oort et al. 2010; Caffarri et al. 2011), with the fastest values typically referring to cyanobacterial core complexes.

The excited state decay in the red-formless PSII core is described, analogously to the PSI core simulations, by a bi-exponential function. However, whereas this represents a rather good approximation for PSI core complexes, the experimental decay of PSII cores is generally reported to be more complex, involving at least three decay phases or more (Schatz et al. 1988; Barter et al. 2003; Miloslavina et al. 2006; Holzwarth et al. 2006; Tumino et al. 2008). Nevertheless, we considered that, for sake of generality and because of the limited number of simulation parameters considered, the minimal model here employed is adequate for the scope. The simulation predictions will, however, be unavoidably less accurate for PSII-like than for PSI-like systems. This also apply to the increase of the antenna dimension. In fact, kinetic energy transfer bottleneck were reported to be significant when coupling LHCII to the core of PSII. In the present model these bottlenecks are neglected and an uniform antenna increase is considered instead. For PSII simulations we thus limit to consider only an increase in the overall antenna dimension to 150 Chls in total (PSII-LHC_{150}), which is the size of a typical PSII-LHCII supercomplex of land plants and green algae (van Amerongen and Croce 2013; Caffarri et al. 2014 and references therein). Using the rate constants discussed above, the simulated value of τ_{av} of PSII-LHC_{150} is 228 ps, *i.e.* ~threefold larger than for the core, which is, despite the model simplification, in good agreement with experimental observables (*e.g.* Engelmann et al. 2005; van Oort et al. 2010; Caffarri et al. 2011). The computed quantum yields of charge separation are 0.95 and 0.86 for the core and PSII-LHC_{150}, respectively, *i.e.* almost a 10% decrease brought about by the antenna size enlargement.

For the coupling of red forms we considered a different energy range spanning from 700 to 730 nm (i.e. 1.77 to 1.70 eV), because the PSII coupled red-forms were shown to be less red-shifted with respect to those of PSI (as discussed in paragraph 3). Moreover the mean energy of the bulk antenna is also blue-shifted in PSII. Simulations were again performed for variable stoichiometries of Chls involved in the red states (from 0 to 12, with 2 Chls per state) and for a range of energy transfer rates from the red form to the bulk antenna (from 15 to 180 ns^{-1}). The simulation outcomes are presented in Fig. 11.13 where the dependency of τ_{av} on the variable simulation parameters for the PSII $core_{45}$ and PSII-LHC_{150} are compared. The accompanying impact on the photochemical quantum yield is shown in Fig. 11.14 instead. Similarly to what predicted for PSI-like systems, increasing the number of the red spectral forms at a given energy, lead to a progressive increase in the value of τ_{av}, with the increase becoming more sizable for the red-most shifted ones. Again, however, the factor which most strongly affects τ_{av} is the energy of the red-form. Whereas for forms up to 715 nm the lengthening of τ_{av} is overall contained, at least for up to two forms per photosystem, it becomes sizable when even a single energy state centred at 730 nm is con-

Fig. 11.13. (continued) open symbols), the other representing core-LHC supercomplexes comprising 150 Chls in total (half-filled symbols). Shown are the average lifetimes (τ_{av}) resulting from unselective excitation and as a function of the presence of red forms centred at 700 (yellow), 705 nm (gold), 715 nm (orange) and 730 nm (red). The number of forms is varied from 1 to 6, comprising 2 Chls each, *i.e.* the total number of Chls involved in red states (n_{red}) varies from 0 to 12. Moreover, the rate of transfer from the red forms to the bulk antenna was considered to be 15 ns^{-1} (squares), 30 ns^{-1} (circles), 45 ns^{-1} (up triangles), 90 ns^{-1} (down triangles) and 180 ns^{-1} (diamonds). Please notice the change in the τ_{av} scale upon varying the red-state energy

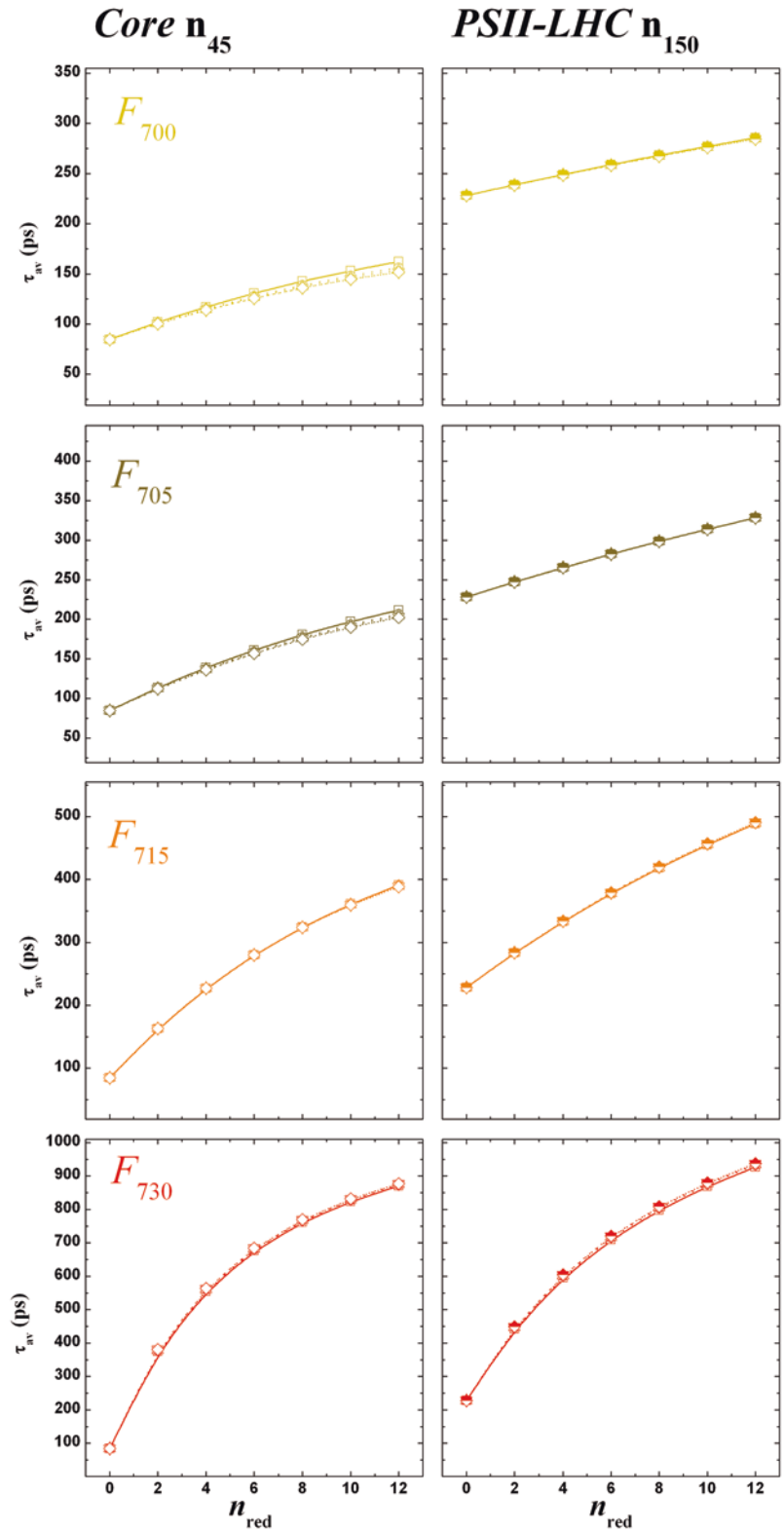

Fig. 11.13. The outcome of simulations for a minimal kinetic model aiming at describing the effect of long wavelength spectral forms in PSII-like photosystems. Two cases are considered, one mimicking the core (45 Chls,

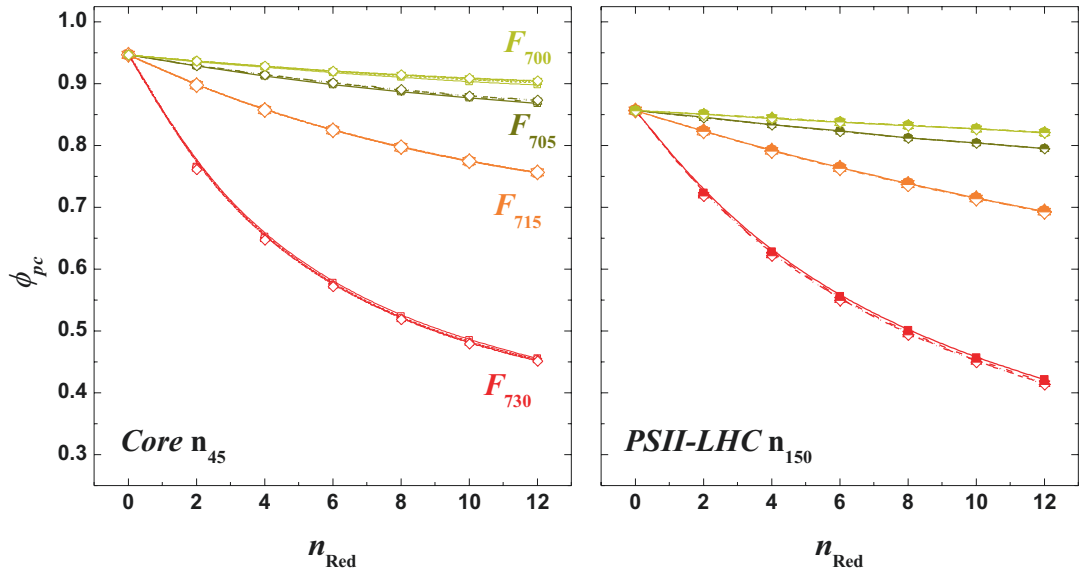

Fig. 11.14. Simulated quantum efficiencies for a minimal kinetic model aiming at describing the core of PSII (45 Chls, open symbols) and the PSII-LHC supercomplexes having an antenna dimension of 150 Chls in total. Simulations of the photochemical quantum yield are presented for red forms centred at 700 (yellow), 705 nm (gold), 715 nm (orange) and 730 nm (red), involving 0–12 Chls (n_{red}) in total, and for transfer rates from the red forms to the bulk antenna of 15 ns^{-1} (squares), 30 ns^{-1} (circles), 45 ns^{-1} (up triangles), 90 ns^{-1} (down triangles) and 180 ns^{-1} (diamonds)

sidered instead. The latter leads to a four-folds increase in τ_{av} that exceeds the pure antenna size effect for similar dimensional scaling. A single red state centred at 750 nm would bring τ_{av} to a value of ~1 ns, *i.e.* close to a tenfold increase (not shown). Although present also in the simulations of PSI-mimicking systems, the effect of red forms presence in the PSII core complex is much more pronounced than when coupled to the larger antenna scenario described by PSII-LHC_{150}. This is in part due to the smaller dimensions of the core of PSII, where each red state represents a larger relative fraction of the overall antenna. Still, the coupling of red forms to PSII cores causes a slowing of τ_{av} which is far larger than for the core of PSI even when the relative ratio of red-to-bulk pigments are compensated (*i.e.*, for instance one state in PSII- vs. two states in PSI-like scenarios). When red forms are coupled in the larger PSI-LHC_{150} model, the lengthening of τ_{av} is less sensitive to the number of states present, as these are "diluted" over the more extended bulk antenna. Yet, since in this scenario a large increase of τ_{av} is simulated due to the antenna increase alone, the systems starts from what could be considered an initial penalty. As observed for PSI, the parameter which appears to be less important in defining τ_{av} for broadband, unselective, excitation conditions is the rate of energy transfer from the red forms to the bulk (k_r). In very close analogy to what discussed in the previous paragraph, this is due to a cross-compensation effect between the amplitudes associated to each of the specific lifetime components.

We conclude this general discussion based on a generalised minimal kinetic model, considering the effect of red-forms coupled to PSII-like systems on their photochemical quantum yield (Fig. 11.13). In this case, the decrease in quantum efficiency is clearly more obvious with respect to that predicted (and observed) for PSI, with the yield readily dropping below 0.9 even for a relatively small number (3) of moderately red-shifted forms

(F705) in the PSII core. The photochemical yield also drops readily below 0.8 when more than 4 Chl forms centred at 715 nm are considered in PSII-core$_{45}$ and PSI-LHC$_{150}$ model scenarios. Coupling of even a single form centred at 730 nm causes a quantum yield decrease of more than 30% and a further decrease is predicted when increasing the number of red states is considered. Thus, in general, PSII appears to pay a greater price in terms of photochemical yield losses upon coupling of red states in comparison with PSI. In order for the quantum yield drop to be contained, the forms need to be only moderately red shifted with a low abundance of bands centred at about 715 nm representing a sensible upper limit for the antenna red-shift. Moreover, in relative terms, the quantum yield loss is less sizable for larger antenna systems than for the core alone. Hence, despite the relative simplicity of the model it seems to provide consistent description/prediction of the experimental observables, since PSII-associated red forms in algae of the red lineage were indeed shown to be associated with specific polypeptides of the external antennae, being characterised by red-most states peaking at 710–715 nm. Note, the presence of PSII red forms was observed originally as a result of culture self-shading, which also leads to low incident photon fluence, and therefore to conditions in which maintaining a high photochemical yield is important in order to sustain electron transfer.

VI. Concluding Remarks

The presence of Chl spectral forms absorbing at wavelengths longer than 700 nm allows photosynthetic organisms to extend their absorption cross-section to the near infrared. In several model organisms, the presence of red spectral forms appears to be confined to the PSI antenna only, where the mean energies of absorption of these spectral forms is centred at ~702, 705, 715 and up to 735 nm, with the peak emission having a Stokes shift of ~15 nm. Photosystem I appears to tolerate quite robustly the presence of long-wavelength forms, even up to 20–30 nm red-shifted to the RC, as long as their stoichiometric abundance is not too large, *i.e.* one-two forms depending on the exact energy. Red spectral forms which lie at higher energies than those of PSI have been reported also for PSII antenna systems. The lower abundance and the reduced shift seem to be linked to the different intrinsic efficiency of trapping, determined either by the slower energy transfer to the reaction centre or the slower photochemical energy conversion of PSII, or both. Hence, the relative number and transition energy of long wavelength forms coupled to each photosystem appear to be tailored in order to balance the increase in absorption cross-section of the incident light and concomitantly minimise the quantum efficiency losses in the antennae.

This situation is crucial under adaptation, since long-wavelength Chl forms represent only a relative small portion of the photosystem cross-section for broad, direct, daylight irradiation, such as on the land surface or the upper layers of a vegetation canopy, or algal mats. However, the near infrared portion of incident radiation will progressively increase, in relative terms, due to vegetation shading, being less absorbed by the upper/outer vegetation layers (Rivadossi et al. 1999), and could even become one of the most prominent spectral regions as a result of deep shading conditions. Yet, these very same conditions would determine also a low light fluence regime, which is when the light dependent electron transport reactions become limiting for the cellular metabolism. Generally, downstream light-independent processes are limiting for higher light intensities instead. It is therefore physiologically important that, when long-wavelength Chl forms become significant in terms of photon capture, they are only weakly impacting on the photo-conversion yields.

The prominent role of red forms in light harvesting under vegetation shading conditions appears also to correlate well with the absence or marked blue shift of these antenna

Chls in organisms living in open waters, especially oceanic. In fact, in these habitats the algal population hardly ever reach densities which can cause significant shading at the surface, or even across the water column. Moreover, the near infrared portion of the solar radiation incident on the water surface will be deeply attenuated through the column because of absorption, refraction and reflection by water itself.

Another argument in favour of the role of long-wavelength spectral forms in light capture under vegetation shading conditions stems from the discovery of oxygenic organisms synthesising different types of Chls having, intrinsically, a red-shifted absorption with respect to Chl *a*. The first organism of this kind isolated was *Acaryochloris marina* in which Chl *d,* that is about 20 nm red-shifted with respect to Chl *a*, constitutes the main pigment, composing in general more than 90% of the total Chl pool, the remaining being Chl *a* (*e.g.* Miyashita et al. 1996; Kuhl et al. 2005; Ohashi et al. 2008). *A. marina* inhabits an ecological niche in which the organism experiences, predominantly and almost constantly, a vegetation (cyanobacterial) shaded light. It has therefore constitutively adapted to these conditions by bulk-shifting its absorption towards the near infrared and, at least in PSI, also by replacing Chl *a* with Chl *d* in most of the photochemically active pigments, so that the characteristic P_{700} absorption shifts to P_{740} in this organism (Hu et al. 1998; Kumazaki et al. 2002; Itoh et al. 2007; Tomo et al. 2008; Schenderlein et al. 2008) (see Chaps. 5 & 10).

More recently it has been shown that other cyanobacteria are capable of synthesising, upon specific induction by far-red light, Chl *f*, which is also intrinsically red-shifted with respect to Chl *a* (Chen et al. 2010). The conditional expression level of Chl *f* however never reaches large values, with the maximal amount being around 10% of the total Chl pool (Gan et al. 2014; Gan and Bryant 2015; Ho et al. 2017; Nürnberg et al. 2018; Chaps. 5 & 10). Upon the accumulation of Chl *f*, spectral forms absorbing up to ~730 nm where observed in PSII and above 760 nm in PSI (Nürnberg et al. 2018). Interestingly, also for this special and still not fully understood adaptive strategy, PSI appears to bind and, it can be argued, tolerate in terms of quantum yield losses, Chl *f* spectral forms that are more red shifted than for PSII, *i.e.* this appears to be a general difference in properties of the two oxygenic reaction centres. Moreover, it has been recently shown that when Chl *f* is induced by far-red light illumination, it does not exclusively act as a light harvesting pigment but does also replace Chl *a* in key positions within the reaction centres (Nürnberg et al. 2018). Changing the energy of the RC excited state might therefore be necessary to prevent excessive "dilution" of the excited population in the long-wavelength antenna pigment, so that part of the unavoidable energy losses due to lower photon energy of Chl *f* (or *d*) with respect to Chl *a* is mitigated, thereby maintaining the extremely high efficiencies in photochemical quantum conversion characterising photosynthetic reaction centres (see Chaps. 5 & 10 and references therein).

Acknowledgements

SS and APC acknowledge support from Fondazione Cariplo through the project "Cyanobacterial Platform Optimised for Bioproductions" (CYAO, ref. 2016-0667). S.S also acknowledge support from the S.a.C program of the CFRP (SaC2018. mkII/b). RK and OP acknowledge support from the Czech Science Foundation GACR (Grantová Agentura Ceské Republiky), projects GACR 16-10088S to RK and GACR 16-15467S to OP. The work at center ALGATECH has been also supported by the institutional projects Algatech Plus (MSMT LO1416) and Algamic (CZ 503

1.05/2.1.00/19.0392) from the Czech Ministry of Education, Youth and Sport.

References

Acuña AM, Lemaire C, van Grondelle R, Robert B, van Stokkum IHM (2018) Energy transfer and trapping in *Synechococcus* WH7803. Photosynth Res 135:115–124

Alboresi A, Caffarri S, Nogue F, Bassi R, Morosinotto T (2008) *In Silico* and biochemical analysis of *Physcomitrella patens* photosynthetic antenna: identification of subunits which evolved upon land adaptation. PLoS One 3:e2033

Alboresi A, Gerotto C, Cazzaniga S, Bassi R, Morosinotto T (2011) A red-shifted antenna protein associated with photosystem II in *Physcomitrella patens*. J Biol Chem 286:28978–28987

Amunts A, Toporik H, Borovikova A, Nelson N (2010) Structure determination and improved model of plant photosystem I. J Biol Chem 285:3478–3486

Anderson JM, Boardman NK (1965) Fractionation of photochemical systems of photosynthesis. I. Chlorophyll contents and photochemical activities of particles isolated from spinach chloroplasts. Biochim Biophys Acta 112:403–421

Averina S, Velichko N, Senatskaya E, Pinevich A (2018) Far-red light photoadaptations in aquatic cyanobacteria. Hydrobiologia 813:1–17

Bald D, Kruip J, Rögner M (1996) Supramolecular architecture of cyanobacterial thylakoid membranes: how is the phycobilisome connected with the photosystems? Photosynth Res 49:103–118

Barter LCM, Durrant JR, Klug DR (2003) A quantitative structure-function relationship for the Photosystern II reaction center: supermolecular behavior in natural photosynthesis. Proc Natl Acad Sci U S A 100:946–951

Bassi R, Soen SY, Frank G, Zuber H, Rochaix JD (1992) Characterization of chlorophyll a/b proteins of photosystem I from *Chlamydomonas reinhardtii*. J Biol Chem 267:25714–25721

Behrendt L, Larkum AWD, Norman A, Qvortrup K, Chen M, Ralph P, Sorensen SJ, Trampe E, Kuhl M (2011) Endolithic chlorophyll *d*-containing phototrophs. ISME J 5:1072–1076

Belgio E, Santabarbara S, Bína D, Trsková E, Herbstová M, Kaňa R, Zucchelli G, Prášil O (2017) High photochemical trapping efficiency in photosystem I from the red clade algae *Chromera velia* and *Phaeodactylum tricornutum*. Biochim Biophys Acta 1858:56–66

Ben-Shem A, Frolow F, Nelson N (2003) Crystal structure of plant photosystem I. Nature 426:630–635

Bina D, Gardian Z, Herbstova M, Kotabova E, Konik P, Litvin R, Prášil O, Tichy J, Vacha F (2014) Novel type of red-shifted chlorophyll *a* antenna complex from *Chromera velia*: II. Biochemistry and spectroscopy. Biochim Biophys Acta 1837:802–810

Boardman NK, Anderson JM (1964) Isolation from spinach chloroplasts of particles containing different proportions of chlorophyll a and chlorophyll b and their possible role in the light reaction of photosynthesis. Nature 203:166–167

Brettel K (1997) Electron transfer and arrangement of the redox cofactors in photosystem I. Biochim Biophys Acta 1318:322–373

Broess K, Trinkunas G, van Hoek A, Croce R, van Amerongen H (2008) Determination of the excitation migration time in photosystem II – consequences for the membrane organization and charge separation parameters. Biochim Biophys Acta 1777:404–409

Brown JS (1967) Fluorometric evidence for the participation of chlorophyll *a*-695 in system 2 of photosynthesis. Biochim Biophys Acta 143:391–398

Burki F, Okamoto N, Pombert J-F, Keeling PJ (2012) The evolutionary history of haptophytes and cryptophytes: phylogenomic evidence for separate origins. Proc R Soc B Biol Sci 279(2012):2246–2254

Butler WL (1960) A far red absorbing form of chlorophyll. Biochem Biophys Res Commun 3:685–688

Butler WL (1961) A far-red absorbing form of chlorophyll, in vivo. Arch Biochem Biophys 93:413–422

Butler WL (1978) Energy distribution in the photochemical apparatus of photosynthesis. Annu Rev Plant Physiol 29:345–378

Byrdin M, Rimke I, Schlodder E, Stehlik D, Roelofs TA (2000) Decay kinetics and quantum yields of fluorescence in photosystem I from *Synechococcus elongatus* with P_{700} in the reduced and oxidized state: are the kinetics of excited state decay trap-limited or transfer-limited? Biophys J 79:992–100

Byrdin M, Jordan P, Krauss N, Fromme P, Stehlik D, Schlodder E (2002) Light harvesting in photosystem I: modeling based on the 2.5-angstrom structure of photosystem I from *Synechococcus elongatus*. Biophys J 83:433–457

Caffarri S, Broess K, Croce R, van Amerongen H (2011) Excitation energy transfer and trapping in higher plant photosystem II complexes with different antenna sizes. Biophys J 100:2094–2103

Caffarri S, Tibiletti T, Jennings RC, Santabarbara S (2014) A comparison between plant photosystem I and photosystem II architecture and functioning. Curr Protein Pept Sci 15:296–331

Castelletti S, Morosinotto T, Robert B, Caffarri S, Bassi R, Croce R (2003) Recombinant Lhca2 and Lhca3 subunits of the photosystem I antenna system. Biochemistry 42:4226–4234

Chen M, Schliep M, Willows RD, Cai ZL, Neilan BA, Scheer H (2010) A red-shifted chlorophyll. Science 329:1318–1319

Cho F, Govindjee (1970a) Fluorescence spectra of Chlorella in the 295-77°K range. Biochim Biophys Acta 205:371–378

Cho F, Govindjee (1970b) Low-temperature (4-77°K) spectroscopy of Chlorella; temperature dependence of energy transfer efficiency. Biochim Biophys Acta 216:139–150

Chua NH, Matlin K, Bennoun P (1975) A chlorophyll-protein complex lacking in photosystem I mutants of *Chlamydomonas reinhardtii*. J Cell Biol 67:361–377

Cometta A, Zucchelli G, Karapetyan NV, Engelmann E, Garlaschi FM, Jennings RC (2000) Thermal behavior of long wavelength absorption transitions in *Spirulina platensis* photosystem I trimers. Biophys J 79:3235–3243

Croce R, van Amerongen H (2013) Light-harvesting in photosystem I. Photosynth Res 116:153–166

Croce R, Zucchelli G, Garlaschi FM, Bassi R, Jennings RC (1996) Excited state equilibration in the photosystem I-light-harvesting I complex: P700 is almost isoenergetic with its antenna. Biochemistry 35:8572–8579

Croce R, Zucchelli G, Garlaschi FM, Jennings RC (1998) A thermal broadening study of the antenna chlorophylls in PSI-200, LHCI, and PSI core. Biochemistry 37:17355–17360

Croce R, Dorra D, Holzwarth AR, Jennings RC (2000) Fluorescence decay and spectral evolution in intact photosystem I of higher plants. Biochemistry 39:6341–6348

Croce R, Morosinotto T, Castelletti S, Breton J, Bassi R (2002) The Lhca antenna complexes of higher plants photosystem I. Biochim Biophys Acta 1556:29–40

Croce R, Morosinotto T, Ihalainen JA, Chojnicka A, Breton J, Dekker JP, van Grondelle R, Bassi R (2004) Origin of the 701-nm fluorescence emission of the Lhca2 subunit of higher plant photosystem I. J Biol Chem 279:48543–48549

Croce R, Chojnicka A, Morosinotto T, Ihalainen JA, van Mourik F, Dekker JP, Bassi R, van Grondelle R (2007) The low-energy forms of photosystem I light-harvesting complexes: spectroscopic properties and pigment-pigment interaction characteristics. Biophys J 93:2418–2428

Damjanovic A, Vaswani HM, Fromme P, Fleming GR (2002) Chlorophyll excitations in photosystem I of *Synechococcus elongatus*. J Phys Chem B 106:10251–10262

Döring G, Stiel HH, Witt HT (1967) A second chlorophyll reaction in the electron chain of photosynthesis – registration by the repetitive excitation technique. Z Naturforsch 22B:639–644

Döring G, Bailey JR, Weikara J, Witt HT (1968) Some new results in photosynthesis, the action of two chlorophyll a molecules in light reaction I of photosynthesis. Naturwissenschaften 5:219–224

Drop B, Yadav SKN, Boekema EJ, Croce R (2014) Consequences of state transitions on the structural and functional organization of photosystem I in the green alga *Chlamydomonas reinhardtii*. Plant J 78:181–191

Duysens LNM (1978) Transfer and trapping of excitation energy in photosystem II. CIBA Found Symp 323–340

Duysens LNM, Amesez J, Kamp BM (1961) Two photochemical system in photosynthesis. Nature 190:510–511

Emerson R, Arnold W (1932) Separation of the reactions in photosynthesis by means of intermittent light. J Gen Physiol 15:391–420

Emerson R, Lewis CM (1943) The dependence of the quantum yield of chlorella photosynthesis on wavelength of light. Am J Bot 30:165–178

Emerson R, Rabinowitch E (1960) Red drop and the role of auxiliary pigments in photosynthesis. Plant Physiol 35:477–485

Emerson R, Chalmers RV, Cederstrand C (1957) Some factors influencing the long-wave limit of photosynthesis. Proc Natl Acad Sci U S A 43:133–143

Engelmann ECM, Zucchelli G, Garlaschi FM, Casazza AP, Jennings RC (2005) The effect of outer antenna complexes on the photochemical trapping rate in barley thylakoid photosystem II. Biochim Biophys Acta 1706:276–286

Engelmann ECM, Zucchelli G, Casazza AP, Brogioli D, Garlaschi FM, Jennings RC (2006) Influence of the photosystem I-light harvesting complex I antenna domains on fluorescence decay. Biochemistry 45:6947–6955

French CS (1967) Changes with age in absorption spectrum of chlorophyll *a* in a diatom. Archiv Fur Mikrobiologie 59:93–103

French CS (1971) The distribution and action in photosynthesis of several forms of chlorophyll. Proc Natl Acad Sci U S A 68:2893–2897

Fromme P, Jordan P, Krauss N (2001) Structure of photosystem I. Biochim Biophys Acta 1507:5–31

Fujita Y, Ohki K (2004) On the 710 nm fluorescence emitted by the diatom *Phaeodactylum tricornutum* at room temperature. Plant Cell Physiol 45:392–397

Galka P, Santabarbara S, Khuong TT, Degand H, Morsomme P, Jennings RC, Boekema EJ, Caffarri S (2012) Functional analyses of the plant photosystem

I-light-harvesting complex II supercomplex reveal that light-harvesting complex II loosely bound to photosystem II is a very efficient antenna for photosystem I in state II. Plant Cell 24:2963–2978

Gan F, Bryant DA (2015) Adaptive and acclimative responses of cyanobacteria to far-red light. Environ Microbiol 17:3450–3465

Gan F, Zhang S, Rockwell NC, Martin SS, Lagarias JC, Bryant DA (2014) Extensive remodeling of a cyanobacterial photosynthetic apparatus in far-red light. Science 345:1312–1317

Germano M, Yakushevska AE, Keegstra W, van Gorkom HJ, Dekker JP, Boekema EJ (2002) Supramolecular organization of photosystem I and light-harvesting complex I in *Chlamydomonas reinhardtii*. FEBS Lett 525:121–125

Gibasiewicz K, Ramesh VM, Melkozernov AN, Lin S, Woodbury NW, Blankenship RE, Webber AN (2001) Excitation dynamics in the core antenna of PSI from *Chlamydomonas reinhardtii* CC2696 at room temperature. J Phys Chem B 105:11498–11506

Gibasiewicz K, Szrajner A, Ihalainen JA, Germano M, Dekker JP, van Grondelle R (2005) Characterization of low-energy chlorophylls in the PSI-LHCI supercomplex from *Chlamydomonas reinhardtii*. A site-selective fluorescence study. J Phys Chem B 109:21180–21186

Giera W, Ramesh VM, Webber AN, van Stokkum IHM, van Grondelle R, Gibasiewicz K (2010) Effect of the P_{700} pre-oxidation and point mutations near A_0 on the reversibility of the primary charge separation in photosystem I from *Chlamydomonas reinhardtii*. Biochim Biophys Acta 1797:106–112

Giera W, Szewczyk S, McConnell MD, Snellenburg J, Redding KE, van Grondelle R, Gibasiewicz K (2014) Excitation dynamics in photosystem I from *Chlamydomonas reinhardtii*. Comparative studies of isolated complexes and whole cells. Biochim Biophys Acta 1837:1756–1768

Girard J, Chua NH, Bennoun P, Schmidt G, Delosme M (1980) Studies on mutants deficient in the photosystem I reaction centers in *Chlamydomonas reinhardtii*. Curr Genet 2:215–221

Gobets B, van Grondelle R (2001) Energy transfer and trapping in photosystem I. Biochim Biophys Acta 1057:80–99

Gobets B, van Amerongen H, Monshouwer R, Kruip J, Rogner M, van Grondelle R, Dekker JP (1994) Polarised site-selected fluorescence of isolated photosystem I. Biochim Biophys Acta 1188:75–85

Gobets B, van Stokkum IHM, Rogner M, Kruip J, Schlodder E, Karapetyan NV, Dekker JP, van Grondelle R (2001) Time-resolved fluorescence emission measurements of photosystem I particles of various cyanobacteria: a unified compartmental model. Biophys J 81:407–424

Gobets B, Valkunas L, van Grondelle R (2003) Bridging the gap between structural and lattice models: a parameterization of energy transfer and trapping in photosystem I. Biophys J 85:3872–3882

Govindjee, Rabinowitch E (1960) Two forms of chlorophyll *a* in vivo with distinct photochemical functions. Science 132:355–356

Greenbaum NL, Mauzerall D (1991) Effect of irradiance level on distribution of chlorophylls between PS II and PS I as determined from optical cross-sections. Biochim Biophys Acta 1057:195–207

Halldal P (1968) Photosynthetic capacities and photosynthetic action spectra of endozoic algae of the massive coral favia. Biol Bull 134(3):411–424

Hayes JM, Matsuzaki S, Rätsep M, Small GJ (2000) Red chlorophyll a antenna states of photosystem I of the cyanobacterium *Synechocystis sp.* PCC 6803. J Phys Chem B 104:5625–5633

Herbstova M, Bina D, Konik P, Gardian Z, Vacha F, Litvin R (2015) Molecular basis of chromatic adaptation in pennate diatom Phaeodactylum tricornutum. Biochim Biophys Acta 1847:534–543

Herbstova M, Bina D, Kana R, Vacha F, Litvin R (2017) Red-light phenotype in a marine diatom involves a specialized oligomeric red-shifted antenna and altered cell morphology. Sci Rep 7:10

Hill R, Bendall F (1960) Function of the two cytochrome components in chloroplasts: a working hypothesis. Nature 186:136

Hill R, Larkum AWD, Prášil O, Kramer DM, Szabo M, Kumar V, Ralph PJ (2012) Light-induced dissociation of antenna complexes in the symbionts of scleractinian corals correlates with sensitivity to coral bleaching. Coral Reefs 31:963–975

Ho MY, Soulier NT, Canniffe DP, Shen G, Bryant DA (2017) Light regulation of pigment and photosystem biosynthesis in cyanobacteria. Curr Opin Plant Biol 37:24–33

Hodges M, Moya I (1986) Time-resolved chlorophyll fluorescence studies of photosynthetic membranes: resolution and characterization of four kinetic components. Biochim Biophys Acta 849:193–202

Holzwarth AR, Wendler J, Haehnel W (1985) Time-resolved picosecond fluorescence spectra of the antenna chlorophylls in *Chlorella vulgaris*. Resolution of photosystem I fluorescence. Biochim Biophys Acta 807:155–167

Holzwarth AR, Müller MG, Niklas J, Lubitz W (2005) Charge recombination fluorescence in photosystem I reaction centers from *Chlamydomonas reinhardtii*. J Phys Chem B 109:5903–5911

Holzwarth AR, Muller MG, Reus M, Nowaczyk M, Sander J, Rogner M (2006) Kinetics and mechanism of electron transfer in intact photosystem II and in the isolated reaction center: Pheophytin is the primary electron acceptor. Proc Natl Acad Sci U S A 103:6895–6900

Hu Q, Miyashita H, Iwasaki I, Kurano N, Miyachi S, Iwaki M, Itoh S (1998) A photosystem I reaction center driven by chlorophyll *d* in oxygenic photosynthesis. Proc Natl Acad Sci U S A 95:13319–13323

Ihalainen JA, van Stokkum IH, Gibasiewicz K, Germano M, van Grondelle R, Dekker JP (2005a) Kinetics of excitation trapping in intact photosystem I of *Chlamydomonas reinhardtii* and *Arabidopsis thaliana*. Biochim Biophys Acta 1706:267–275

Ihalainen JA, Klimmek F, Ganeteg U, van Stokkum IH, van Grondelle R, Jansson S, Dekker JP (2005b) Excitation energy trapping in photosystem I complexes depleted in Lhca1 and Lhca4. FEBS Lett 579:4787–4791

Itoh S, Mino H, Itoh K, Shigenaga T, Uzumaki T, Iwaki M (2007) Function of chlorophyll *d* in reaction centers of photosystems I and II of the oxygenic photosynthesis of *Acaryochloris marina*. Biochemistry 46:12473–12481

Jankowiak R, Hayes JM, Small GJ (1993) Spectral hole burning spectroscopy in amorphous molecular solids and proteins. Chem Rev 93:1471–1502

Jennings RC, Zucchelli G, Croce R, Garlaschi FM (2003) The photochemical trapping rate from red spectral states in PSI-LHCI is determined by thermal activation of energy transfer to bulk chlorophylls. Biochim Biophys Acta 1557:91–98

Jennings RC, Zucchelli G, Engelmann ECM, Garlaschi FM (2004) The long-wavelength chlorophyll states of plant LHCI at room temperature: a comparison with PSI-LHCI. Biophys J 87:488–497

Jennings RC, Zucchelli G, Santabarbara S (2013) Photochemical trapping heterogeneity as a function of wavelength in plant photosystem I (PSI-LHCI). Biochim Biophys Acta 1827:779–785

Jensen PE, Bassi R, Boekema EJ, Dekker JP, Jansson S, Leister D, Robinson C, Scheller HV (2007) Structure, function and regulation of plant photosystem I. Biochim Biophys Acta 1767:335–352

Jordan P, Fromme P, Witt HT, Klukas O, Saenger W, Krauss N (2001) Three-dimensional structure of Cyanobacterial photosystem I at 2.5 Å resolution. Nature 411:909–917

Kaňa R (2018) Application of spectrally resolved fluorescence induction to study light-induced non-photochemical quenching in algae. Photosynthetica 56:132–138

Kaňa R, Kotabová E, Komárek O, Šedivá B, Papageorgiou GC, Govindjee, Prášil O (2012) The slow S to M fluorescence rise in cyanobacteria is due to a state 2 to state 1 transition. Biochim Biophys Acta 1817:1237–1247

Karapetian NV (2004) Dynamics of excitation in the photosystem I of cyanobacteria: transfer in the antenna, capture by the reaction site, and dissipation. Biofizika 49:212–226

Karapetyan NV, Dorra D, Schweitzer G, Bezsmertnaya IN, Holzwarth AR (1997) Fluorescence spectroscopy of the longwave chlorophylls in trimeric and monomeric photosystem I core complexes from the cyanobacterium *Spirulina platensis*. Biochemistry 36:13830–13837

Karukstis KK, Sauer K (1985) The effects of cation-induced and pH-induced membrane stacking on chlorophyll fluorescence decay kinetics. Biochim Biophys Acta 806:374–388

Kirilovsky D, Kaňa R, Prášil O (2014) Mechanisms modulating energy arriving at reaction centers in cyanobacteria. In: Demmig-Adams B, Garab G, Adams W III, Govindjee (eds) Non-photochemical quenching and energy dissipation in plants, algae and cyanobacteria. Springer, Dordrecht, pp 471–501

Kitajima M, Butler WL (1975) Excitation spectra for photosystem I and photosystem II in chloroplasts and the spectral characteristics of the distribution of quanta between the two photosystems. Biochim Biophys Acta 408:297–305

Koehne B, Trissl HW (1988) The cyanobacterium Spirulina platensis contains a long wavelength-absorbing pigment C738 (F76077K) at room temperature. Biochemistry 37:5494–5500

Koehne B, Elli G, Jennings RC, Wilhelm C, Trissl HW (1999) Spectroscopic and molecular characterization of a long wavelength absorbing antenna of *Ostreobium sp*. Biochim Biophys Acta 1412:94–107

Kok B (1956) On the reversible absorption change at 705 nm in photosynthetic organisms. Biochim Biophys Acta 22:399–401

Kotabová E, Jarešova J, Kaňa R, Sobotka R, Bína D, Prášil O (2014) Novel type of red-shifted chlorophyll a antenna complex from *Chromera velia*. I. Physiological relevance and functional connection to photosystems. Biochim Biophys Acta 1837:734–743

Kruip J, Bald D, Boekema E, Rögner M (1994) Evidence for the existence of trimeric and monomeric photosystem I complexes in thylakoid membranes from cyanobacteria. Photosynth Res 40:279–286

Kuhl M, Chen M, Ralph PJ, Schreiber U, Larkum AWD (2005) A niche for cyanobacteria containing chlorophyll *d*. Nature 433:820

Kumazaki S, Abiko K, Ikegami I, Iwaki M, Itoh S (2002) Energy equilibration and primary charge

separation in chlorophyll *d*-based photosystem I reaction center isolated from *Acaryochloris marina*. FEBS Lett 530:153–157

Lamb J, Forfang K, Hohmann-Marriott M (2015) A practical solution for 77 K fluorescence measurements based on LED excitation and CCD array detector. PLoS One 10:e0132258

Lamb JJ, Røkke G, Hohmann-Marriott MF (2018) Chlorophyll fluorescence emission spectroscopy of oxygenic organisms at 77 K. Photosynthetica 56:105–124

Lathrop EJP, Friesner RA (1994) Vibronic mixing in the strong electronic coupling limit. Spectroscopic effects of forbidden transitions. J Phys Chem 98:3050–3055

Le Quiniou C, van Oort B, Drop B, van Stokkum IH, Croce R (2015a) The high efficiency of photosystem I in the green alga *Chlamydomonas reinhardtii* is maintained after the antenna size is substantially increased by the association of light-harvesting complexes II. J Biol Chem 290:30587–30595

Le Quiniou C, Tian L, Drop B, Wientjes E, van Stokkum IHM, van Oort B, Croce R (2015b) PSI-LHCI of *Chlamydomonas reinhardtii*: increasing the absorption cross section without losing efficiency. Biochim Biophys Acta 1847:458–467

Litvin FF, Sinechchekov VV (1975) Molecular organisation of chlorophyll and energetics of the initial stages in photosynethesis. In: Govindjee (ed) Bioenegetics of photosynthesis. Academi Press, New York

Litvin R, Bina D, Herbstova M, Gardian Z (2016) Architecture of the light-harvesting apparatus of the eustigmatophyte alga *Nannochloropsis oceanica*. Photosynth Res 130:137–150

Magnusson SH, Fine M, Kuhl M (2007) Light microclimate of endolithic phototrophs in the scleractinian corals *Montipora monasteriata* and *Porites cylindrica*. Mar Ecol Prog Ser 332:119–128

Miloslavina Y, Szczepaniak M, Muller MG, Sander J, Nowaczyk M, Rogner M, Holzwarth AR (2006) Charge separation kinetics in intact photosystem II core particles is trap-limited. A picosecond fluorescence study. Biochemistry 45:2436–2442

Miyashita H, Ikemoto H, Kurano N, Adachi K, Chihara M, Miyachi S (1996) Chlorophyll *d* as a major pigment. Nature 383:402

Molotokaite E, Remelli W, Casazza AP, Zucchelli G, Polli D, Cerullo G, Santabarbara S (2017) Trapping dynamics in photosystem I-light harvesting complex I of higher plants is governed by the competition between excited state diffusion from low energy states and photochemical charge separation. J Phys Chem B 121:9816–9830

Moore RB, Obornik M, Janouskovec J, Chrudimsky T, Vancova M, Green DH, Wright SW, Davies NW, Bolch CJS, Heimann K, Slapeta J, Hoegh-Guldberg O, Logsdon JM Jr, Carter DA (2008) A photosynthetic alveolate closely related to apicomplexan parasites. Nature 451:959–963

Morosinotto T, Breton J, Bassi R, Croce R (2003) The nature of a chlorophyll ligand in Lhca proteins determines the far red fluorescence emission typical of photosystem I. J Biol Chem 278:49223–49229

Mozzo M, Morosinotto T, Bassi R, Croce R (2006) Probing the structure of Lhca3 by mutation analysis. Biochim Biophys Acta 1757:1607–1613

Murata N, Nishimura M, Takamiya A (1966) Fluorescence of chlorophyll in photosynthetic systems III. Emission and action spectra of fluorescence-three emission bands of cholophyll *a* and the energy transfer between two pigment systems. Biochim Biophys Acta 126:234–243

Myers J, Graham J-R (1963) Enhancement in chlorella. Plant Physiol 38:105–116

Nelson N, Yocum CF (2006) Structure and function of photosystems I and II. Annu Rev Plant Biol 57:521–565

Nürnberg DJ, Morton J, Santabarbara S, Telfer A, Joliot P, Antonaru LA, Ruban AV, Cardona T, Krausz E, Boussac A, Fantuzzi A, Rutherford AW (2018) Photochemistry beyond the red limit in chlorophyll *f*–containing photosystems. Science 360:1210–1213

Nymark M, Valle KC, Hancke K, Winge P, Andresen K, Johnsen G, Bones AM, Brembu T (2013) Molecular and photosynthetic responses to prolonged darkness and subsequent acclimation to re-illumination in the diatom *Phaeodactylum tricornutum*. PLoS One 8:e58722

Obornik M, Lukes J (2013) Cell biology of chromerids: autotrophic relatives to apicomplexan parasites. In: Jeon KW (ed) International review of cell and molecular biology, vol 306, pp 333–369

Ohashi S, Miyashita H, Okada N, Iemura T, Watanabe T, Kobayashi M (2008) Unique photosystems in *Acaryochloris marina*. Photosynth Res 98:141–149

Owens TG, Webb SP, Mets L, Alberte RS, Fleming GR (1987) Antenna size dependence of fluorescence decay in the core antenna of photosystem I: estimates of charge separation and energy transfer rates. Proc Natl Acad Sci U S A 84:1532–1536

Palsson LO, Dekker JP, Schlodder E, Monshouwer R, van Grondelle R (1996) Polarised site-selected fluorescence spectroscopy of long-wavelength emitting chlorophyll in isolated photosytem I particles of *Synechococcus elongates*. Photosynth Res 48:239–246

Pazdernik M (2015) Light harvesting complexes and chromatic adaptation of Eustigmatophyte alga *Trachydiscus minutus*. University of Southern Bohemia, Ceske Budejovice

Pettai H, Oja V, Freiberg A, Laisk A (2005a) The long-wavelength limit of plant photosynthesis. FEBS Lett 579:4017–4019

Pettai H, Oja V, Freiberg A, Laisk A (2005b) Photosynthetic activity of far-red light in green plants. Biochim Biophys Acta 1708:311–321

Prášil O, Bina D, Medova H, Rehakova K, Zapomelova E, Vesela J, Oren A (2009) Emission spectroscopy and kinetic fluorometry studies of phototrophic microbial communities along a salinity gradient in solar saltern evaporation ponds of Eilat, Israel. Aquat Microb Ecol 56:285–296

Qin X, Suga M, Kuang T, Shen JR (2015) Photosynthesis. Structural basis for energy transfer pathways in the plant PSI-LHCI supercomplex. Science 348:989–995

Quigg A, Kotabová E, Jarešova J, Kaňa R, Šetlik J, Šediva B, Komárek O, Prášil O (2012) Photosynthesis in *Chromera velia* represents a simple system with high efficiency. PLoS One 7:e47036

Rätsep M, Johnson TW, Chitnis PR, Small GJ (2000) The red-absorbing chlorophyll *a* antenna states of photosystem I: a hole-burning study of *Synechocystis sp.* PCC 6803 and its mutants. J Phys Chem B 104:836–847

Rijgersberg CP, Amesz J (1978) Changes in light absorbance and chlorophyll fluorescence in spinach choloplasts between 5 and 80°K. Biochim Biophys Acta 502:152–160

Rijgersberg CP, Melis A, Amesz J, Swager JA (1979) Quenching of cholophyll fuorescence and photochemical activity of chloroplasts at low temperature in chlorophyll organization and energy transfer in photosynthesis. Ciba Foundation Symposium 61:305–322, Excerpta Medica, Amsterdam

Rivadossi A, Zucchelli G, Garlaschi FM, Jennings RC (1999) The importance of PS I chlorophyll red forms in light-harvesting by leaves. Photosynth Res 60:209–215

Roelofs TA, Lee CH, Holzwarth AR (1992) Global target analysis of picosecond chlorophyll fluorescence kinetics from pea chloroplasts. A new approach to the characterization of the primary processes in photosystem II alfa- and beta-units. Biophys J 61:1147–1163

Santabarbara S, Heathcote P, Evans MCW (2005) Modelling of the electron transfer reactions in photosystem I by electron tunnelling theory: the phylloquinones bound to the PsaA and the PsaB reaction centre subunits of PS I are almost isoenergetic to the iron-sulfur cluster F_X. Biochim Biophys Acta 1708:283–310

Santabarbara S, Agostini G, Casazza AP, Syme CD, Heathcote P, Böhles F, Evans MC, Jennings RC, Carbonera D (2007) Chlorophyll triplet states associated with photosystem I and photosystem II in thylakoids of the green alga *Chlamydomonas reinhardtii*. Biochim Biophys Acta 1767:88–105

Santabarbara S, Tibiletti T, Remelli W, Caffarri S (2017) Kinetics and heterogeneity of energy transfer from light harvesting complex II to photosystem I in the supercomplex isolated from Arabidopsis. Phys Chem Chem Phys 19:9210–9222

Schatz GH, Brock H, Holzwarth AR (1988) A kinetic and energetic model for the primary processes in photosystem II. Biophys J 54:397–405

Schellenberger Costa B, Jungandreas A, Jakob T, Weisheit W, Mittag M, Wilhelm C (2013) Blue light is essential for high light acclimation and photoprotection in the diatom *Phaeodactylum tricornutum*. J Exp Bot 64:483–493

Schenderlein M, Çetin M, Barber J, Telfer A, Schlodder E (2008) Spectroscopic studies of the chlorophyll d containing photosystem I from the cyanobacterium *Acaryochloris marina*. Biochim Biophys Acta 1777:1400–1408

Schubert WD, Klukas O, Saenger W, Witt HT, Fromme P, Krauss N (1998) A common ancestor for oxygenic and anoxygenic photosynthetic system: a comparison based on the structural model of photosystem I. J Mol Biol 280:297–314

Searle GF, Tredwell CJ, Barber J, Porter G (1979) Picosecond time-resolved fluorescence study of chlorophyll organisation and excitation energy distribution in chloroplasts from wild-type barley and a mutant lacking chlorophyll *b*. Biochim Biophys Acta 545:496–507

Sener MK, Lu DY, Park SH, Schulten K, Fromme P (2002) Spectral disorder and excitation transfer dynamics in cyanobacterial photosystem I. Biophys J 82:292–302

Sener MK, Jolley C, Ben-Shem A, Fromme P, Nelson N, Croce R, Schulten K (2005) Comparison of the light-harvesting networks of plant and cyanobacterial photosystem I. Biophys J 89(3):1630–1642

Shimura S, Fujita Y (1973) Some properties of the chlorophyll fluorescence of the diatom *Pheodactylum tricornutum*. Plant Cell Physiol 14:341–352

Shubin VV, Murthy SDS, Karapetyan NV, Mohanty P (1991) Origin of the 77 K variable fluorescence at 758 nm in the cyanobacterium *Spirulina platensis*. Biochim Biophys Acta 1060:28–36

Shubin VV, Tsuprun VL, Bezsmertnaya IN, Karapetyan NV (1993) Trimeric forms of the photosystem I

reaction center complex pre-exist in the membranes of the cyanobacterium *Spirulina platensis*. FEBS Lett 334:79–82

Slavov C, Ballottari M, Morosinotto T, Bassi R, Holzwarth AR (2008) Trap-limited charge separation kinetics in higher plant photosystem I complexes. Biophys J 94:3601–3612

Thapper A, Mamedov F, Mokvist F, Hammarstrom L, Styring S (2009) Defining the far-red limit of photosystem II in spinach. Plant Cell 21:2391–2401

Tichy J, Gardian Z, Bina D, Konik P, Litvin R, Herbstova M, Pain A, Vacha F (2013) Light harvesting complexes of *Chromera velia*, photosynthetic relative of apicomplexan parasites. Biochim Biophys Acta 1827:723–729

Tomo T, Kato Y, Suzuki T, Akimoto S, Okubo T, Noguchi T, Hasegawa K, Tsuchiya T, Tanaka K, Fukuya M, Dohmae N, Watanabe T, Mimuro M (2008) Characterization of highly purified photosystem I complexes from the chlorophyll *d*-dominated cyanobacterium *Acaryochloris marina* MBIC 11017. J Biol Chem 283:18198–18208

Tumino G, Casazza AP, Engelmann ECM, Garlaschi FM, Zucchelli G, Jennings RC (2008) Fluorescence lifetime spectrum of the plant photosystem II core complex: photochemistry does not induce specific reaction center quenching. Biochemistry 47:10449–10457

Turconi S, Kruip J, Schweitzer G, Rögner M, Holzwarth AR (1996) A comparative fluorescence kinetics study of photosystem I monomers and trimers from *Synechocystis* PCC 6803. Photosynth Res 49:263–268

van Amerongen H, Croce R (2013) Light harvesting in photosystem II. Photosynth Res 116:251–263

van der Lee J, Bald D, Kwa SLM, van Grondelle R, Rogner M, Dekker JP (1993) Steady-state polarized-light spectroscopy of isolated photosystem-I complexes. Photosynth Res 35:311–321

van Oort B, Alberts M, de Bianchi S, Dall'Osto L, Bassi R, Trinkunas G, Croce R, van Amerongen H (2010) Effect of antenna-depletion in photosystem II on excitation energy transfer in *Arabidopsis thaliana*. Biophys J 98:922–931

van Stokkum IHM, Desquilbet TE, van der Weij-de Wit CD, Snellenburg JJ, van Grondelle R, Thomas JC, Dekker JP, Robert B (2013) Energy transfer and trapping in red-chlorophyll-free photosystem I from *Synechococcus* WH 7803. J Phys Chem B 117:11176–11183

Vernon LP, Seely GR (1966) The chlorophylls. Academic, New York City

Wientjes E, Croce R (2011) The light-harvesting complexes of higher plant photosystem I: Lhca1/4 and Lhca2/3 form two red-emitting heterodimers. Biochem J 433:477–485

Wientjes E, van Stokkum IHM, van Amerongen H, Croce R (2011a) Excitation-energy transfer dynamics of higher plant photosystem I light-harvesting complexes. Biophys J 100:1372–1380

Wientjes E, van Stokkum IHM, van Amerongen H, Croce R (2011b) The role of the individual Lhcas in photosystem I excitation energy trapping. Biophys J 101:745–754

Wilhelm C, Jakob T (2006) Uphill energy transfer from long-wavelength absorbing chlorophylls to PS II in *Ostreobium sp.* is functional in carbon assimilation. Photosynth Res 87:323–329

Witt HT (1979) Energy conversion in the functional membrane of photosynthesis. Analysis by light pulse and electric pulse methods. The central role of the electric field. Biochim Biophys Acta 505:355–427

Wittmershaus BP, Woolf VM, Vermaas WJF (1992) Temperature dependence and polarization of fluorescence from photosystem I in the cyanobacterium *Synechocystis sp.* PCC 6803. Photosynth Res 31:75–87

Wolf BM, Niedzwiedzki DM, Magdaong NCM, Roth R, Goodenough U, Blankenship RE (2018) Characterization of a newly isolated freshwater Eustigmatophyte alga capable of utilizing far-red light as its sole light source. Photosynth Res 135:177–189

Wollman F-A, Bennoun P (1982) A new chlorophyll-protein complex related to photosystem I in *Chlamydomonas reinhardii*. Biochim Biophys Acta 680:352–360

Yang H, Liu J, Wen X, Lu C (2015) Molecular mechanism of photosystem I assembly in oxygenic organisms. Biochim Biophys Acta 1847:838–848

Zazubovich V, Matsuzaki S, Johnson TW, Hayes JM, Chitnis P, Small GJ (2003) Red antenna states of photosystem I from the cyanobacterium *Synechococcus elongatus*: a spectral hole burning study. Chem Phys 275:47–59

Zorz JK, Allanach JR, Murphy CD, Roodvoets MS, Campbell DA, Cockshutt AM (2015) The RUBISCO to photosystem II ratio limits the maximum photosynthetic rate in picocyanobacteria. Life (Basel) 5:403–417

Zucchelli G, Morosinotto T, Garlaschi FM, Bassi R, Jennings RC (2005) The low energy emitting states of the Lhca4 subunit of higher plant photosystem I. FEBS Lett 579:2071–2076

Chapter 12

Diversity in Photoprotection and Energy Balancing in Terrestrial and Aquatic Phototrophs

Atsuko Kanazawa, Peter Neofotis, Geoffry A. Davis, Nicholas Fisher and David M. Kramer*
DOE Plant Research Laboratory, Department of Chemistry and Department of Biochemistry and Molecular biology, Michigan State University, East Lansing, MI, USA

I. Introduction

Photosynthesis likely evolved because it gave living systems the survival advantages of solar energy, obviating the need for localized energy sources. At the same time, nature places very specific constraints on photosynthesis because the light reactions involve highly energetic intermediates that can generate highly toxic side products, especially reactive oxygen species (ROS), that can kill the organisms it powers. Thus, the energy input into photosynthesis must be tightly regulated by photoprotective nonphotochemical quenching (NPQ) and control of electron transfer, to balance the need for efficient energy conversion with the avoidance of photodamage (Gust et al. 2008; Aro et al. 1993; Raven 2011; Sonoike 2010; Long et al. 1994; Kanazawa et al. 2017; Davis et al. 2016, 2017; Alboresi et al. 2018). A related constraint on photosynthesis is the need to balance energy storage into ATP and NADPH to *precisely* meet biochemical

*Author for correspondence, e-mail: kramerd8@cns.msu.edu

A. W. D. Larkum et al. (eds.), *Photosynthesis in Algae: Biochemical and Physiological Mechanisms*, Advances in Photosynthesis and Respiration 45, https://doi.org/10.1007/978-3-030-33397-3_12

demands. If this balancing does not occur, the system will fail, leading to metabolic congestion and photodamage (Kramer and Evans 2011). It is also becoming clear that energy balancing mechanisms must not only be robust, but respond to rapid and unpredictable fluctuations in environmental conditions that are encountered in the field, and that lagging responses can lead to severe photodamage (e.g. when light is suddenly increased) (Davis et al. 2016) or substantial losses of photosynthetic efficiency (e.g. when light is suddenly decreased) (Kromdijk et al. 2016). This chapter discusses the impact of recent research that reveals unexpected connections between photoprotection and energy balancing, focusing on the impact of photoprotection on energy balance and *vice versa*.

II. Energy Storage and Regulation in Oxygenic Photosynthesis

In its simplest formulation, oxygenic photosynthesis consists of the light-driven transfer of electrons from water to CO_2, to form O_2 and reduced forms of carbon. This reaction could also be performed in two discrete steps by human-made "artificial leaves," using a set of appropriate catalysts and photovoltaic cells to generate electrical potential, to directly oxidize water at one electrode, and reduce CO_2 at another. By contrast, natural photosynthesis is much more complex, mainly because it evolved within pre-existing living systems. For example, natural photosynthesis systems are quite sensitive to ROS so it is critical for photosynthesis to minimize the production of high energy excited states or electron transfer intermediates that can interact with O_2 (Foyer and Shigeoka 2011; Rutherford et al. 2012) As will be discussed below, minimizing ROS-producing side reactions involves downregulation of energy capture that necessarily results in loss of energy, leading to tradeoffs between energy efficiency and the avoidance of ROS. These tradeoffs are compounded by the fact that natural photosynthesis evolved to "plug into" ancient biochemical pathways that require energy in bio-compatible forms, including redox energy stored in the NAD(P)H/O_2 couple, and phosphorylation potential stored in the ATP/ADP + P_i couple (Gust et al. 2008). As discussed below, the ratios of the production of ATP and NADPH must be balanced to match metabolic needs and thus avoid metabolic congestion (Kramer and Evans 2011).

We first describe the well-known, and highly conserved core components of the light reactions, and then discuss why a photosynthetic system based solely on these components will fail under real world conditions. We then introduce a series of additional components that have evolved that act to "tune" the activities of the core components, making them biocompatible. The text will focus mainly on how the interactions of electron, proton and counterion transport play pivotal roles in tuning both energy capture and energy balancing, and how diverse tuning mechanisms impose different constrains on these interactions.

The core reactions of oxygenic photosynthesis involve a processes called "linear electron flow" (LEF), in which light is used to extract electrons from water and transfer them to $NADP^+$ while generating ATP from ADP and P_i (reviewed in e.g. Kramer et al. 2004a; Ort and Yocum 1996). Light is initially captured by an array of pigments in light harvesting protein complexes, and delivered to a special subset of chlorophyll molecules in photosystem I (PSI) and photosystem II (PSII). The absorption of a photon of visible light result in the photochemical excitation of chlorophylls in PSII, producing a state termed P_{680}^*, which allows for the formation of a charge separated state, with an electron being transferred through a series of electron carriers within PSII to a plastoquinone (PQ) molecule, Q_B, and an electron hole remaining on P_{680}. The oxidized P_{680}^+ is a very strong electron oxidant (~1.25 eV (Grabolle and Dau 2005)), that extracts electrons from a redox active tyrosine, which in

turn allows oxidation of the manganese cluster of the oxygen evolving complex, releasing one molecule of O_2 and 4 H^+ into the lumen for each 4 turnovers of PSII. Upon successive excitation of PSII, electrons on Q_B are transferred through a cascade of exergonic electron transfer reactions through a mobile pool of PQ, the cytochrome b_6f complex, plastocyanin (PC), and to the primary electron donor in PSI, P_{700}^+ (orange arrows in Fig. 12.1). An additional photon is required to excite an electron on P_{700} to reach the P_{700}^* state, which initiates a second cascade of energetically downhill electron transfer reactions in PSI, then to ferredoxin (Fd) and finally to NADPH.

Through these core processes, energy is initially stored in two forms. Extracting electrons from water and transferring them to $NADP^+$, energy is stored in the two redox half reactions $4H^+ + O_2$ / H_2O and $NADP^+ + H^+$/NADPH. In addition, the transfer of electrons results in the storage of an electrochemical gradient of protons across the thylakoid membrane, termed the proton motive force (*pmf*). The vectorial electrogenic transfer (from the lumenal to the stromal face of the thylakoid membrane, within PSII, the cytochrome b_6f complex—via the Q-cycle mechanism (reviewed in Cape et al. 2006) and PSI) results in the formation of the electric field component of *pmf*. The *pmf* represents the driving force for moving protons across the thylakoid membrane, which can have two distinct energetic components. The ΔpH component, sometimes called the proton gradient, is the free energy stored in the difference of free proton concentrations between the lumen and stroma. Because protons are charged, they will also tend to move

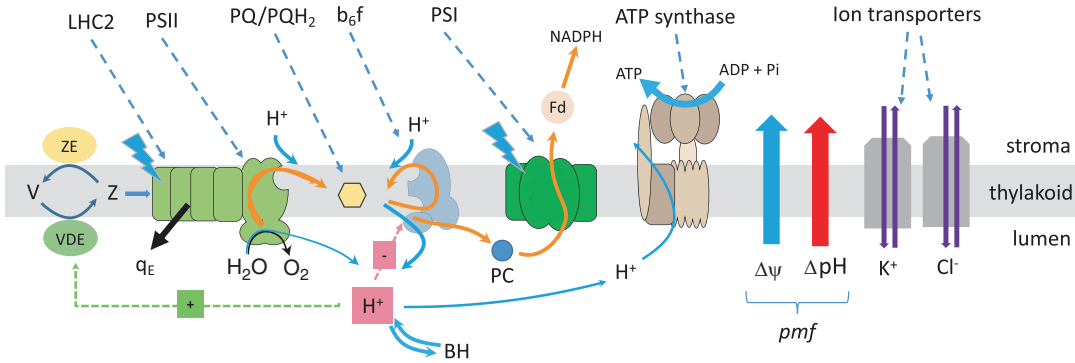

Fig. 12.1. **Basic Z-scheme model for the electronic and protonic circuits of the light reactions of photosynthesis, and the pmf paradigm for regulation of the light reactions.** *Scheme of linear electron flow (LEF) in oxygenic photosynthesis, in which light energy is captured by light harvesting complexes associated with photosystem II (PSII light green) and photosystem I (PSI, dark green) initiate electron flow (orange arrows) from PSII, through the cytochrome* ***b6f*** *complex (dark grey), plastocyanin (PC, turquois), to PSI and ferredoxin (brown) and finally to NADPH.* LEF is coupled to proton flow (blue arrows) at PSII and the cytochrome b_6f complex, storing energy in the thylakoid proton motive force (*pmf*). Transfer of electrons from the lumenal (pink) to the stromal side of the thylakoid (grey) forms a transmembrane electric field (Δψ, blue arrow), while proton uptake from the stroma and deposition in the lumen lead to the formation of a transthylakoid pH gradient (ΔpH, red arrow), which together drive the synthesis of ATP from ADP + P_i at the thylakoid ATP synthase, storing energy in ΔG_{ATP}. The orange and blue lines describe the pathways of electron and proton fluxes, leading to the reduction of NADPH and the synthesis of ATP. The acidification of the lumen (indicated by the H^+ in the red box) activates violaxanthin deepoxidase (VDE) which converts violaxanthin (V) to zeaxanthin (Z) and protonates the PsbS protein, which triggers the photoprotective dissipation of light energy by the q_E (black arrow). Lumen pH also regulates electron flow (red box with '-') to PSI by slowing the rate of PQH_2 oxidation at the cytochrome b_6f complex. Abbreviations: ATP synthase, chloroplast ATP synthase; b_6f, cytochrome b_6f complex; LHC2, light harvesting complexes associated with PSII; PSI/PSII, photosystem I and photosystem II; PQ/PQH_2, plastoquinone, plastoquinol; *pmf*, proton motive force, ZE: zeaxanthin epoxidase

down an electric field (from more positively to more negatively charged faces of the membrane), and thus a second term, $\Delta\psi$, represents the differences in charge between the lumenal and stromal faces. The ATP synthase is driven by the sum of $\Delta\psi$ and ΔpH, and both forms are energetically equivalent (Fischer and Graber 1999; Hangarter and Good 1982), so that

$$pmf = \Delta\psi\left(1-s\right) - 2.3RT / F\,\Delta pH\left(1-s\right)a_b$$

where l and s are the lumenal and stromal facing sides of the thylakoid membrane, R is the universal gas constant, F is Faraday's constant, and T is the absolute temperature in Kelvin. Note that the RT/F term simply converts the energies of two components of *pmf* into the same units.

The $\Delta\psi$ component is sometimes called the "electric field," though a field is defined with units of V/m or N/C, whereas $\Delta\psi$ is typically expressed simply as V. If we assume that the thylakoid membrane is approximately 5 nm thick (Daum et al. 2010), then a typical $\Delta\psi$ of 60 mV would be approximately 120,000 V/cm. This calculation demonstrates that the electric fields experienced by the photosynthetic machinery are not trivial. Indeed, the fields are strong enough to shift the redox potentials of electron transfer components (Drachev et al. 1989; van Gorkom 1996) as well as the absorption spectra (colors) of pigments (via Stark shift) of light harvesting complexes embedded in the thylakoid membranes (Kakitani et al. 1982; Witt and Zickler 1974; Bailleul et al. 2010).

III. The pmf Paradigm for Regulation of the Photosynthetic Light Reactions

A series of mechanisms for photoprotection have evolved to avoid over-excitation of reaction centers that can lead to accumulation of electrons on highly reducing carriers and production of ROS, when light input exceeds the capacity of system to process it (e.g. Hideg et al. 2006; Asada 2006; Nishiyama et al. 2006; Tyystjärvi and Aro 1996; Aro et al. 1993). We will focus here on what we call the "*pmf* paradigm" of feedback regulation, in which the *pmf* plays central role in both energy storage and feedback regulation, and has been extensively studied in chloroplasts of higher plants and some algae. A major photoprotective mechanism in chloroplasts which acts to dissipate light energy from antenna complexes is through "non-photochemical quenching" (NPQ) (Anderson and Barber, 1996; Aro et al. 1993; Baker and Bowyer, 1994; Demmig-Adams and Adams, 1996; Müller et al. 2001). There are several NPQ mechanisms, all of which can contribute to photoprotection, and are triggered by diverse regulatory mechanisms, as discussed in more detail in Chap. 10. We will first describe components of this paradigm, focusing on what has been established for plant chloroplasts, in particular the NPQ mechanism termed q_E (for 'energy dependent' quenching), which is triggered by acidification of the lumen imposed by the ΔpH component of *pmf*. Activation of q_E in higher plant chloroplasts involves at least two reactions: the conversion of violaxanthin (V) to antheraxanthin and zeaxanthin (Z) (see Eskling et al. 2001), which is controlled by the lumen pH-sensitive violaxanthin deepoxidase (VDE), and the stromal redox-sensitive zeaxanthin epoxidase, which catalyzes the reverse reaction; and the protonation of the antenna protein PsbS (Li et al. 2002; Niyogi et al. 2004). Various models have been proposed for both the biophysical mechanism of q_E and how the two reactions interact (Kiss et al. 2008; Crouchman et al. 2006; Zaks et al. 2012; Li et al. 2004). For the purposes of the current discussion, we can assume that Z accumulation and PsbS protonation are both required for full q_E activity, and both are controlled by the lumen pH, which is consistent with phenomenological behavior of q_E in plants (Takizawa et al.

2007). The ΔpH component of *pmf* also down-regulates electron flow by slowing PQH_2 oxidation by the cytochrome b_6f complex (in a process termed 'photosynthetic control'), preventing accumulation of electrons on highly reducing components of PSI, and subsequent PSI photodamage (reviewed in Takizawa et al. 2007).

IV. The Need to Coordinate q_E and Photosynthetic Control

Photosynthetic control in the absence of NPQ can lead to buildup of electrons in the PQ pool, leading to accumulation of reduced Q_A, which is expected to accentuate photodamage to PSII (Vass et al. 1992). To prevent this situation, q_E should be initiated prior to the onset of photosynthetic control, by tuning the lumen pH-dependencies of VDE, PsbS and PQH_2 turnover at the b_6f complex. Indeed, detailed *in vivo* spectroscopic characterization (Takizawa et al. 2007) showed that, as the lumen pH decreases, PsbS and VDE are partially activated prior to onset of photosynthetic control at the b_6f complex (Takizawa et al. 2007). By contrast, the *pgr1* mutant in *Arabidopsis thaliana*, which contains a point mutation in the Rieske FeS protein of the b_6f complex conferring altered pH-dependence of PQH_2 oxidation so that photosynthetic control is induced at a more moderate (higher) lumen pH than q_E can be activated (Jahns et al. 2002), leads to the buildup of reduced Q_A^- and accelerated photoinhibition of PSII (Okegawa et al. 2005).

V. The Critical Need to Balance the Chloroplast Energy Budget

The pool sizes of ATP and NADPH are small relative to the high fluxes of energy from the light reactions. Thus, any imbalance in the production and consumption of ATP or NADPH can rapidly lead to "metabolic congestion" (indigestion), depletion or buildup of metabolic intermediates, followed by the accumulation of high energy intermediates of the light reactions (Avenson et al. 2005). A major issue with a simple Z-scheme model for the light reactions is the lack of flexibility in the output ratios of ATP and NADPH because the proton and electron transfer reactions of LEF are tightly coupled, so that the ratio of ATP and NADPH outputs is fixed. For the light reactions, NADPH production cannot take place without ATP synthesis and vice versa (Kramer and Evans 2011). Similarly, metabolic pathways will consume ATP and NADPH at specific, different ratios than the output of LEF. For instance, if the ratio of ATP/NADPH produced by the light reactions is even slightly smaller than that used by downstream biochemistry, ATP will be depleted in a few seconds, shutting down both LEF and the Calvin-Benson-Bassham (CBB) cycle.

The potential problems associated with ATP/NADPH balance, and some solutions, are illustrated in Fig. 12.2. Three protons are expected to be transferred to the lumen for an electron transferred through LEF (Sacksteder et al. 2000). The number of protons required to be transferred through the ATP synthase to generate one ATP is thought to be determined by the stoichiometry of *c*-subunits per ATP synthase. Higher plant chloroplast ATP synthase has 14 *c*-subunits, suggesting that 14 protons are required to make a full rotation, which should produce 3 ATPs (Stock et al. 1999), but see below (Turina et al. 2003)), so that we expect $H^+/ATP = 4.67$ and the ratio of ATP/NADPH produced by LEF is expected to be 2.66, 13% lower than that needed to drive assimilation, requiring supplementary ATP production even under permissive conditions (Avenson et al. 2005; Noctor and Foyer 1998). Active transport of metabolites or ions across the chloroplast envelope can consume additional ATP, either directly as is the case for ATP-binding cassette transporters (Verrier et al. 2008), lipid transporters (Lu et al. 2007), or by consuming the proton motive force across the thylakoid or chloro-

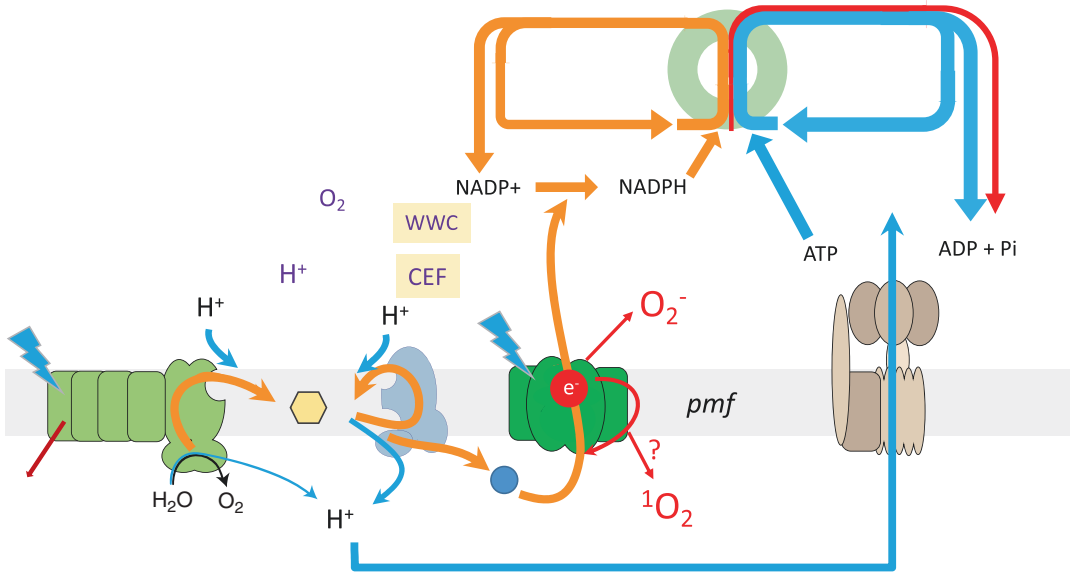

Fig. 12.2. **The problem of ATP/NADPH mismatch and possible solutions.** Alternative electron transfer pathways that can generate ATP without production of NADPH, thus augmenting the ATP/NADPH output ratio to match that of consumption. The orange arrows show the fluxes of energy through the electronic circuit of photosynthesis, starting with electron transfer (ET) through linear electron flow (LEF) to the reduction of substrates in the Calvin-Benson-Bassham (CBB) cycle. The blue arrows show the flux of energy through the proton circuit of photosynthesis, starting with the ET-coupled proton translocation into the lumen, through the ATP synthase to form ATP, which is used in phosphorylation-driven reactions in the CBB. The red arrow shows a mismatch in the supply of ATP relative to NADPH supplied by LEF with the ratio required to run CBB. The purple arrow represent possible mechanisms to augment the production of ATP without net production of NADPH, thus balancing the supply and demand for these energy-containing substrates

plast inner envelope, as is the case with ion transporters involved ion homeostasis (Spetea et al. 2016; Chap. 6). ATP/NADPH demands will be further altered by activation of other metabolic processes, so that adjustments to the energy budget should be quite flexible (Kramer et al. 2004a; Cruz et al. 2005a; Scheibe 2004). Some metabolic processes preferentially oxidize NADPH (e.g. nitrite reduction), while others preferentially consume ATP (e.g. transport of substrates, ions and proteins, and synthesis of DNA or proteins). Thus, the chloroplast needs energy balancing mechanisms that adjust both the production and consumption of ATP/NADPH.

Several processes have been proposed to overcome a deficit of ATP in the chloroplast (Backhausen et al. 1994; Kramer and Evans 2011), including the 'malate valve' (Scheibe 2004), the Mehler peroxidase reaction (MPR) (Asada 1999), the plastid terminal oxidase (PTOX) in some species, (reviewed in Joet et al. 2002b) and cyclic electron flow (CEF) (see Chap. 8). (Note that the MPR is also termed the water-water cycle because electrons are extracted from water, forming O_2, but are returned to O_2, reforming water; because other pathways, including PTOX and FLV, perform the same reaction, we thus prefer to use the term MPR). By far the most studied process is cyclic electron flow around PSI (CEF) (Kramer and Evans 2011). This process involves excitation of PSI, but not PSII, eliminating the participation of PSII (Fig. 12.2, purple curved arrows). Light-driven electron flow from PSI through Fd is shunted back to the PQ pool by several possible PQ reductases. Once PQH_2 is formed by PQ reductase activity, it is oxidized

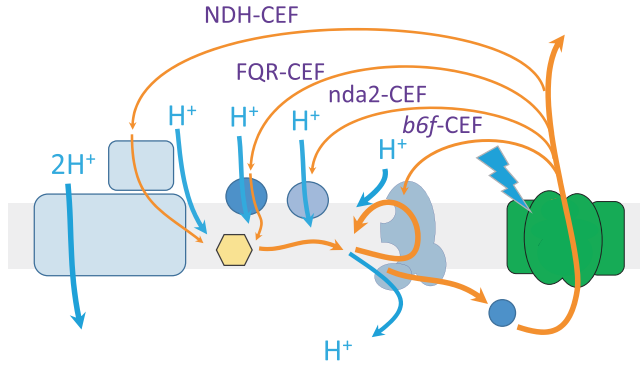

Fig. 12.3. **Cyclic Electron Flow (CEF) electron flow routes.** NDH-CEF, CEF through the NDH complex; FQR-CEF, CEF through the antimycin-A sensitive PGR5/PGRL1 pathway; nda2-CEF, CEF through the type 2 (non-proton pumping) PQ reductase; b_6f-CEF, CEF directly to redox carriers in the cytochrome b_6f complex

through the Q-cycle via the cytochrome b_6f complex, resulting in proton translocation, and delivery of electrons back to PSI. The specific mechanisms for CEF have been under intense debate, and at least four pathways have been proposed, differing at the PQ reductase step (Fig. 12.3). These pathways may operate in parallel (Scheller 1996; Holser and Yocum 1987; Munekage et al. 2004; Ducruet et al. 2005) or in species-specific ways (Havaux et al. 2005). Thylakoids from higher plants contain a type 1 (proton pumping) NADPH/Fd: plastoquinone reductase, termed the NDH complex (also NDH-like or chloroplast Complex I), which is proposed to participate in CEF. NDH is homologous to bacterial and mitochondrial (respiratory) complex I (Lascano et al. 2003). However, it is important to note that chloroplast NDH has a number of distinct properties. For example, it lacks the complex I NAD(P)H binding site, and uses Fd, rather than NAD(P)H, as its substrate (Ifuku et al. 2011). Recent work demonstrated that the higher plant NDH complex is a thermodynamically reversible proton pump that enables highly efficient ATP production by CEF (Strand et al. 2017), with a H^+/e^- stoichiometry matching that predicted for respiratory complex I (Burrows et al. 1998; Friedrich et al. 1995) that pumps up to two protons across the energetic membrane for each electron transferred to quinone (Efremov et al. 2010). The added proton pumping through NDH is expected to double the proton-to-electron stoichiometry for CEF compared to CEF through non-proton pumping pathways (Strand et al. 2017) allowing for more efficient balancing of the ATP/NADPH budget.

Other CEF pathways have been proposed that likely involve non-proton pumping PQ reductases. (It is important to note that even if these pathways do not involve a proton pumping PQ reductase, CEF will still translocate protons into the lumen through reduction and oxidation of PQ, mediated by the b_6f complex.) A distinct Ferredoxin:PQ oxidoreductase (FQR) was introduced by study of the *pgr5* mutant in *Arabidopsis*, which shows low *pmf* and slow *in vitro* PQ pool reduction by NADPH and Fd (Munekage et al. 2004). It was subsequently found that the PGRL1 protein is required for this activity (DalCorso et al. 2008). It has been proposed that PGR5:PGRL1 may act as the PQ reductase itself (Hertle et al. 2013), though other studies (Nawrocki et al. 2019) argue that PGR5:PGRL1 cannot account for the observed rates of CEF, suggesting that these proteins may play a regulatory role in CEF (Shikanai 2007). In line with this view, *pgr5* also shows a remarkably high ATP synthase activity, preventing the buildup of sufficient

lumen acidification to activate q_E. This observation implies that, while PGR5 is clearly involved in maintaining ΔpH, these effects cannot be completely accounted for by decreased CEF.

In *Chlamydomonas*, a CEF pathway has been proposed that involves a type 2 (non-proton pumping) NADPH:PQ oxidoreductase, termed Nda2, related to those found in bacteria and mitochondria (Desplats et al. 2009). Cramer and co-workers (Zhang et al. 2004), Minagawa and coworkers (Iwai et al. 2010) and Joliot and coworkers (Joliot and Joliot 2006) have proposed that CEF might occur directly through the participation of cytochrome b_6f complex c_i heme, after formation of a supercomplex containing FNR and cytochrome b_6f complex (Furbacher et al. 1989), with electrons being passed from the bound FNR to the Q_i (PQ reductase) site. Consistent with these models, the crystal structure of the b_6f complex (Kurisu et al. 2003; Stroebel et al. 2003) showed that heme c_i, to which PQ is presumably bound and reduced, is located very near the stromal surface, suggesting that it might be able to conduct electron transfer from stromal reductants. On the other hand, efforts to directly detect the reduction of the c_i/b hemes of b_6f in plant chloroplasts found only very slow rates (Fisher et al. 2018), implying that this pathway may not be rapid enough to account for all CEF.

In all cases, *pmf* produced by CEF can drive ATP synthesis to increase the ATP/NADPH output ratio, and thus activation of CEF is primarily thought to act as an energy balancing mechanism (Strand et al. 2016b). However, excessive activation of CEF will produce imbalance in the ATP/NADPH output ratio (i.e. excess ATP or NADPH deficit), that can also lead to metabolic congestion. It is thus essential that CEF be finely tuned to produce the correct amount of ATP, but not more. CEF may also play a regulatory role via its acidification of the thylakoid lumen (Kramer et al. 2004a; Golding et al. 2004; Joliot and Johnson 2011), but the coupling of any increased CEF to ATP production may also restrict the extent to which CEF can induce sufficient ΔpH to initiate q_E, without also leading to ATP/NADPH imbalances, suggesting that CEF may play a predominant role in ATP/NADPH balancing (but see below).

Consistent with the view that CEF is highly regulated, measurements in C3 plants show only small rates of CEF under steady-state, non-stressed conditions when presumably LEF by itself can nearly meet the ATP/NADPH demand required for assimilation (Laisk et al. 2007; Cruz et al. 2005a; Livingston et al. 2010b; Livingston et al. 2010a; Harbinson et al. 1989; Avenson et al. 2005). CEF is observed to increase under conditions of high ATP demand, e.g. under environmental stress (e.g. Rumeau et al. 2007; Kohzuma et al. 2009; Jia et al. 2008), when carbon concentrating mechanisms or C_4 photosynthesis are engaged (Finazzi et al. 2002; Kubicki et al. 1996), or during induction of photosynthesis in dark-adapted plants (Joet et al. 2002a; Joliot et al. 2004). These ATP/NADPH balancing and regulatory roles for CEF are not independent, since ATP/NADPH balance is critical for maintaining *pmf*, and thus regulating q_E or b_6f complex. However, CEF is clearly not essential for q_E since it is observed in its absence (Avenson et al. 2005; Ishikawa et al. 2008), while other processes can contribute to the regulation of q_E responses (Kanazawa and Kramer 2002; Kramer et al. 2004b; Avenson et al. 2004; Cruz et al. 2005b).

VI. Regulation of CEF

A previously accepted model for CEF regulation (Finazzi et al. 2002; Iwai et al. 2010) stated that CEF is linked to antenna state transitions, and is inactive in state 1, but activated in state 2. However, more recent work (Takahashi et al. 2013; Shikanai 2010) showed that CEF can occur in the complete absence of state transitions, both in algae

(Lucker and Kramer 2013; Takahashi et al. 2013) and plants (Strand et al. 2013) and that state transitions, which occur on the minutes timescale, are too slow to account for rapid regulation of CEF required to respond to abrupt changes in metabolic demands (Lucker and Kramer 2013). These results suggested CEF is regulated by other signals, such as redox status (Breyton et al. 2006), ATP levels (Joliot and Joliot 2002, 2006), and ROS production (Livingston et al. 2010b). It is also possible that these processes differentially affect different CEF pathways (Livingston et al. 2010b). A detailed regulatory pathway, a chloroplast-localized Ca^{2+} sensor (CAS) protein has been proposed for *Chlamydomonas reinhardtii*, and is posited to interact with the PGRL1 protein (and also control expression of the LHCSR3 antenna protein) (Hochmal et al. 2015; Terashima et al. 2012), but the means by which CEF is regulated in plants and cyanobacteria is, in general, not well understood. Very recently we found (Fisher et al. 2019) that, in plants, the chloroplast NDH and FQR pathways are inhibited by stromal adenylates (ATP and ADP) at physiologically relevant concentrations (K_i (ATP) *in vitro* ≈ 0.5 mM), with ADP a two- to threefold weaker inhibitor of these pathways. Importantly, ATP appears a stronger inhibitor of FQR compared to NDH, such that the more energy efficient CEF pathway afforded by NDH ($8H^+/2e^-$, compared to the predicted $4H^+/2e^-$ for the FQR pathway) would be operational under conditions when ATP concentrations may be expected to be limiting for downstream metabolism.

In our previous work, we identified a series of mutants with constitutively high rates of CEF, and used these to assess possible regulatory mechanisms (Strand et al. 2015, 2016c; Livingston et al. 2010a, b). We noticed a striking pattern in which essentially all of these mutants showed elevated production of H_2O_2 and pondered whether these effects were functionally linked. We thus tested the hypothesis that CEF is activated by H_2O_2 *in vivo* (Strand et al. 2015). We found that CEF through the type 1 NDH pathway was strongly increased by H_2O_2, both by infiltration or *in situ* production by chloroplast-localized glycolate oxidase, implying that H_2O_2 can activate CEF either directly by redox modulation of key enzymes, or indirectly by affecting other photosynthetic enzymes. We propose that H_2O_2 may be a "missing link" between environmental stress, metabolism, and redox regulation of CEF in higher plants. Relatedly, we have found recently that including reduced dithiothreitol (DTT) in spinach thylakoid preparations (where the FQR-mediated CEF pathway is dominant) preserves *in vitro* CEF activity (where it is normally rapidly lost on tissue disruption). The midpoint potential of this preservatory component was determined to be −306 mV at pH 7.6, titrating as an $n = 2(e^-)$ species, therefore most likely a thiol (Strand et al. 2016a). As such, the apparent thiol-mediated regulation of FQR CEF would allow this particular pathway to respond more rapidly to metabolic demands under conditions of oxidative stress given the slower activation of NDH CEF in response to exposure to H_2O_2 (halftime for activation of approximately 20 min) (Strand et al. 2015).

VII. Modulation of *pmf* Feedback Regulation and Its Impact on Energy Balancing

In the simplest formation of the *pmf* paradigm, lumen acidification is determined by the rate of proton translocation, explaining why q_E responds to increasing light, i.e. higher increased proton flux, which increases lumen acidification. However, photoprotection must also respond to changes in downstream capacity to utilize the products of the light reactions. Indeed, increased q_E is observed under adverse environmental conditions when the LEF and associated proton fluxes decrease (Kramer et al. 2004a). These observations imply that *pmf* feedback is modulated (or regulated) by downstream pro-

cesses either by modulating the extent or sensing of lumen acidification. For the purposes of this review, we divide these processes into two distinct classes of mechanism (Kramer et al. 2004a): Type 1 modulation involves processes that change the production or sensing of lumen pH without affecting the ratios of production of ATP and NADPH. For example, altering the concentrations of Z by regulating biosynthesis of xanthophylls or the activities of VDE or ZE should change the activation of q_E at a particular lumen pH without directly affecting the relative output of ATP/NADPH, as is seen in a number of mutants affecting these enzymes (Zhang et al. 2009; Murchie and Niyogi 2011; Li et al. 2004), or under diverse environmental conditions (Demmig-Adams et al. 2017). Another type 1 mechanism involves adjusting the activity of the ATP synthase, which is known to be modulated by metabolic or environmental factors (e.g. low CO_2 levels (Kanazawa and Kramer 2002), drought (Kohzuma et al. 2009), and feedback limitations (Takizawa et al. 2008)). Slowing the ATP synthase decreases the conductivity of the thylakoid to protons (g_{H^+}), leading to buildup of the *pmf* even at similar proton input rates, and subsequent acidification of the lumen and enhanced q_E and photosynthetic control (Avenson et al. 2005; Cruz et al. 2005a; Kanazawa and Kramer 2002).

Type 2 mechanisms modulate lumen pH by activating non-LEF light-driven processes, such as CEF and MPR. These processes necessarily alter the ratio of ATP/NADPH produced by the light reactions. In principle, the acidification of the lumen associated with these processes should activate q_E or induce photosynthetic control (Shikanai and Yamamoto 2017; Shikanai 2007; Johnson 2004). However, they also alter the ATP/NADPH output ratio of the light reactions, which as discussed above, can lead to mismatches in the energy budget of the chloroplast, likely limiting the degree to which these processes can be activated, as will be discussed in more detail below.

A special case of feedback modulation is partitioning of *pmf* into $\Delta\psi$ and ΔpH. Because ΔpH, but not $\Delta\psi$, results in lumen acidification, changing the fraction of *pmf* stored in these two forms should control the regulatory impact of a particular extent of *pmf* (Kramer et al. 2003; Avenson et al. 2004). For instance, suppose that the steady state *pmf* is held at 180 mV. If this *pmf* was stored exclusively as $\Delta\psi$, then ΔpH = 0. With no ΔpH, and stromal and lumen pH of 7.8, no q_E should be activated. If, instead, this *pmf* is equally partitioned, $\Delta\psi$ and ΔpH should be approximately 90 mV and 1.5 pH units respectively, and lumen pH should thus reach about 6.3, where q_E should be substantially activated (Takizawa et al. 2007). If all *pmf* is stored as ΔpH, lumen pH should reach 4.8, which should induce maximal activation of q_E as well as very strong slowing of PQH_2 oxidation, such that LEF would become very slow (Kramer et al. 2003), and possible acid-induced photodamage to PSII centers (Krieger and Weis 1993; Spetea et al. 1997; Kramer et al. 1999). Further, the need to sustain a sufficiently large *pmf* to maintain stromal ΔG_{ATP} should preclude 100% ΔpH storage, as this would lead to induction of q_E in the dark and such extreme lumen acidities that the system could not work efficiently (Kramer et al. 1999). It is thus likely that *pmf* partitioning is adjusted to balance the needs for energy storage and regulation, as is seen under adverse environmental conditions (e.g. Avenson et al. 2004; Zhang et al. 2011; Davis et al. 2017).

It was originally suggested (Kramer et al. 2003) that *pmf* partitioning would act as a Type 1 regulator, because under steady state conditions, changing the fraction of *pmf* stored as ΔpH should not affect ATP/NADPH output. However, a detailed computational model of the light reactions (Davis et al. 2017) showed that abrupt changes in light intensity should transiently affect ATP/NADPH output. As illustrated in Fig. 12.4, the simulations showed that, under many conditions, the rate of q_E formation will

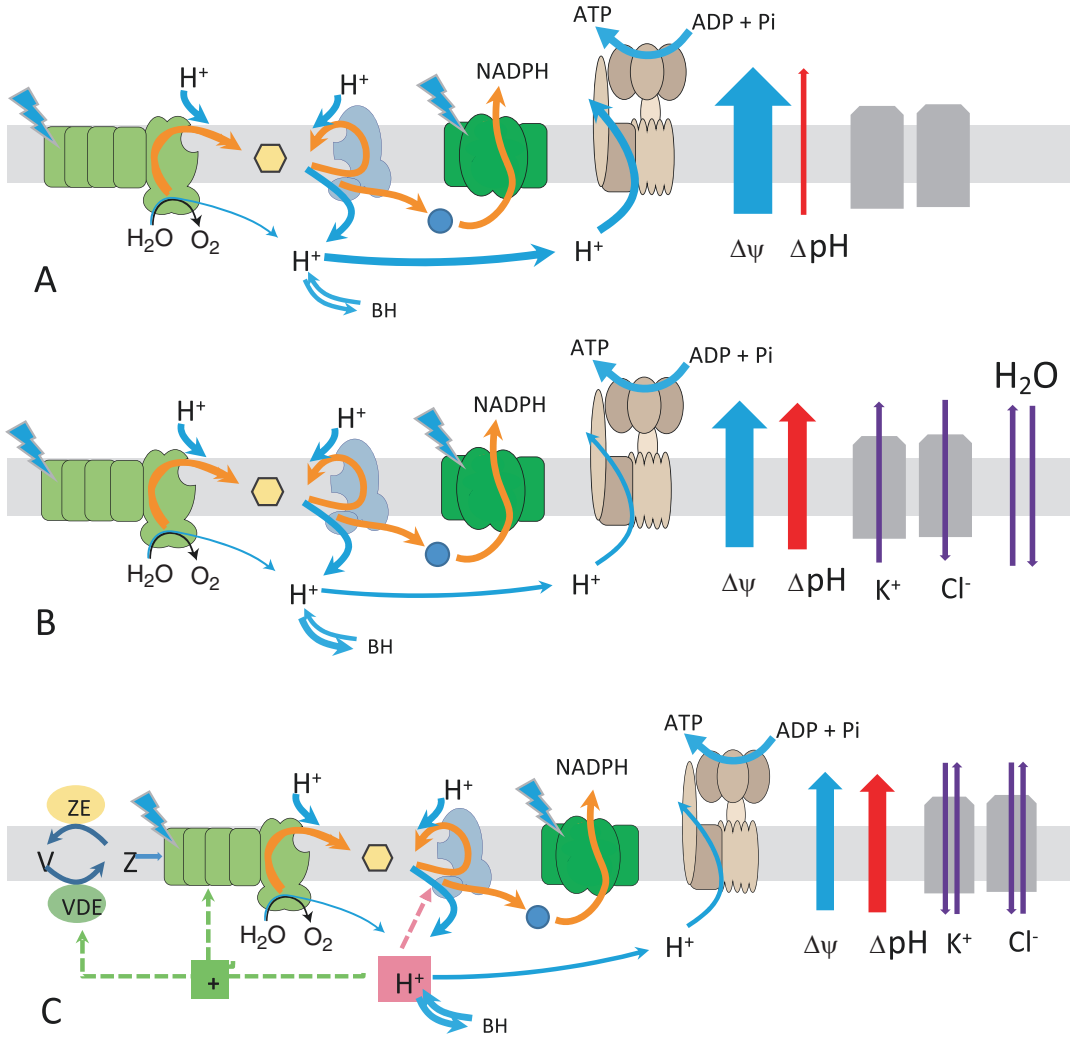

Fig. 12.4. **Counterion exchange modulates Δ*p*H, resulting in activation of qE, but imposing deficits in proton translocation and ATP synthesis.** *The blue arrows on the upper thylakoid membrane show the directions of transmembrane electron flow that generates Δψ, while the red arrows show the uptake and deposition of protons that generates ΔpH.* The semi-transparent arrows passing over the ATP synthase indicate the relative contributions of Δ*ψ* (blue) and ΔpH (red) to the ATP synthase reaction. (**a**) At early times after illumination, *pmf* is stored predominantly in Δ*ψ*, owing to the low electrical capacitance of the thylakoid membrane and the large proton buffering capacity of the lumen. The high Δ*ψ* effectively drives the efflux of protons from the lumen through the ATP synthase, maintaining a low ΔpH. Without counterion fluxes, the *pmf* would remain predominantly in Δ*ψ*. (**b**) Activating counter-ion fluxes dissipates a fraction of Δ*ψ*, allowing additional proton influx and less efflux, which gradually protonates lumenal buffering groups, forming a ΔpH. (**c**) Counter-ion fluxes establish ion gradients that eventually reach a local equilibrium with Δ*ψ*, leading to a steady-state ratio of Δ*ψ*: ΔpH. The acidification of the lumen due to the generation of ΔpH can then downregulate the cytochrome b_6f turnover (triangle) and activate q_E (dark blue circle). However, the dissipation of Δ*ψ* by counterion transport results in loss of *pmf*. We propose that the proton (ATP) deficit is filled by activating CEF.

likely be limited by protonation of PsbS, which is determined by ΔpH formation, in turn controlled by the (slow) rates of counter-ion fluxes across the thylakoid (Davis et al. 2016, 2017). Owing to the low electrical capacitance of the thylakoid membrane (Junge and Witt 1968) and the large proton buffering capacity of the lumen (Junge et al. 1979), the initial charge separations at PSI and PSII induce a large *pmf* almost exclusively in the form of Δψ (Cruz et al. 2001). The large Δψ is sufficient to force protons to exit through the ATP synthase, preventing the formation of ΔpH, and limiting the rate of q_E activation (Fig. 12.4, panel A). Only when counterions are allowed to pass across the thylakoid membrane (Fig. 12.4, panel B), collapsing part of Δψ, can protons accumulate to overcome the lumen buffering capacity (Fig. 12.4, panel C). Thus, counter-ion translocation that dissipates Δψ is not only *essential* for lumen acidification-induced photoprotection, it is likely the limiting step under many conditions (Davis et al. 2017). Dissipation of Δψ requires either an influx of anions (probably Cl^-) into the lumen, or effluxes of cations (K^+, Na^+, Mg^{2+}, Ca^{2+} etc.) from the lumen (Pottosin and Schönknecht 1996; Cruz et al. 2001; Barber 1976). The extent and kinetics of Δψ dissipation are finely controlled by a series of additional ion transporters, including K^+ and Cl^- channels and a K^+/H^+ antiporter (Spetea et al. 2016; Armbruster et al. 2016). In addition, mobile buffers, such as the polyamine putrescine or bicarbonate may play a role in modulating Δψ/ΔpH by altering the proton buffering capacity of the lumen (Ioannidis et al. 2012).

Along with the metabolic and regulatory processes involved in the generation and dissipation of the *pmf,* the movement of protons and ions into the thylakoid lumen during photosynthesis results in ultrastructural changes in thylakoids (Deamer et al. 1966; Kirchhoff et al. 2011), as illustrated in Fig. 12.4, panel B. Experiments with isolated chloroplasts with addition of various salt concentrations or ionophores to intact or broken chloroplasts showed that the thylakoid was permeable to specific ionic species, and that these had large effects on photosynthetic electron transfer and light absorbing properties of the antenna complexes (Barber 1976), including grana stacking (Mg^{2+}), Rubisco activity (Mg^{2+}), and oxygen evolution (Cl^- and Ca^{2+}). Thus, at a minimum, ion transporter systems must be present to facilitate delivery of necessary ions into the chloroplast compartments. In higher plant chloroplasts, illumination of dark-adapted samples results in expansion of the internal lumen volume of thylakoids (Kirchhoff et al. 2011), likely accomplished by light-induced chloride influx into the lumen (Schönknecht et al. 1988; Cruz et al. 2001), followed by water influx (see arrows indicating H_2O flux in Fig. 12.4, panel B), altering the diffusion rates of soluble lumen proteins. Very recently, a connection has been identified between hyperosmotic stress responses and the chloroplast ionic homeostatic machinery triggered through a Ca^{2+}-signaling pathway (Stephan et al. 2016). Therefore, the chloroplast must simultaneously modulate the Δψ and ΔpH components of *pmf*, prevent fluctuations in osmotic balance, and ensure that the concentrations of ionic cofactors are maintained.

The simulations show an additional effect of ion translocation on energy balance. Overcoming the buffering capacity of the lumen requires the electrogenic transport of an ion, which diverts one proton from ATP synthesis to counterion transport, leading to a deficit of ATP relative to NADPH (see Fig. 12.4 panel B). In other terms, the dissipation of Δψ by counterion fluxes, required to build ΔpH, results in a loss of *pmf* that would otherwise drive the ATP synthase (Davis et al. 2017). The simulations predict that the ATP deficit can be substantial, and generating a ΔpH of one unit should consume the equivalent of ATP needed to fix 140 CO_2 molecules per PSII complex. This deficit must be balanced in some way to prevent metabolic congestion, and we proposed that

CEF may be transiently activated to meet this limitation. Because of the slow relaxation of the $\Delta\psi$ component during photosynthesis, as well as the slow decay of the $\Delta\psi$ in plants or algae under conditions where synthase is inactive (Cruz et al. 2001, 2005b), it can be concluded that the counterion movements across thylakoids in plants and green algae are 2–3 orders of magnitude slower than movements of protons (see Chap. 6), so that ATP deficit induced by ΔpH formation is spread out over a lengthy time (tens of seconds to minutes), requiring only a small contribution from CEF. However, speeding up the formation and recovery of q_E, as has been suggested, could increase plant productivity (Kromdijk et al. 2016), should impose an acute, albeit transient, ATP deficit. Without an equally rapid mechanism to refill the proton pool, this proton drain may disable photoprotection, and lead to the accumulation of electrons on PSI and PSII. Thus, this tradeoff may explain the rather slow onset and decay of q_E. One possible remedy to circumvent this problem would be to introduce a mechanism to replenish the lost protons; for example, a very rapidly activated and robust form of CEF, though it is an open question whether such mechanisms have already evolved.

VIII. How Diverse Photoprotective Mechanisms Challenge the *pmf* Paradigm and Open Up New Questions

Above, we described how cross talk between the two critical roles of *pmf*, storing energy and activating photoprotection, require multiple levels of regulation. A key lesson is that there will be far-reaching and unexpected consequences of changing any one component of this hub. It is also clear from genetic and physiological analyses that some of these components are likely not conserved across the diversity of photosynthetic species, leading to questions about how a *pmf*-feedback regulatory system could work, or if the *pmf* paradigm may be replaced with completely different modes of regulation.

It is important to point out that, the overall *pmf* paradigm can still operate even if specific components behave differently (Goss and Lepetit 2015). Even in plants, different forms of NPQ occur simultaneously with q_E, including the long-lived forms q_I and q_Z, related to the damage-repair cycle of PSII and the accumulation of Z (Adams III et al. 2006). In diverse species, the mechanistic details can vary. For example, q_E in *Chlamydomonas* involves "light stress" forms of light harvesting complexes, LHCSR1, LHCSR3, rather than PsbS (Peers et al. 2009; Tokutsu and Minagawa 2013; Bonente et al. 2011; Chap. 4), though these are similarly responsive to acidification of the lumen, which is controlled by changes in *pmf* partitioning (Cruz et al. 2005a) and activation of CEF (Lucker and Kramer 2013). The moss *Physcomitrella patens* contains both the PsbS and LHCSR3 system (Gerotto et al. 2011). In the stramenopile *Phaeomonas* sp., the extent of NPQ is strictly proportional to the accumulation of Z, i.e. it lacks the more rapid adjustment of NPQ by protonation of PsbS or LHCSR3 (Berne et al. 2018). In diatoms and dinoflagellates, the xanthophyll cycle is replaced by a diadinoxanthin cycle, in which the lumen pH-activated diadinoxanthin de-epoxidase catalyzes the one-step de-epoxidation of diadinoxanthin into diatoxanthin (Goss and Lepetit 2015). In the red alga, *Cyanidioschyzon merolae*, lumen acidification apparently induces NPQ within the reaction center complex itself (Krupnik et al. 2013).

Ion movement across the thylakoid, in general, has been observed for decades (Barber 1976), yet there appears to be evidence for more ion transport activities from experimental data than can be accounted for by the small number of transport proteins thus far identified (Chap. 6). This mismatch means that either the transporters are not very specific or that their low content in the membranes has prevented unam-

biguous identification by bulk proteomic analyses (van Wijk 2004). Genetics and reverse genetics approaches have identified a limited number of mutants in *Arabidopsis thaliana* ion channels and transporters at both the thylakoid and chloroplast inner envelope membranes (Spetea et al. 2017). We know even less about ion transporters in algae and cyanobacteria (Pfeil et al. 2014). In *Chlamydomonas reinhardtii*, in which electrochromic shift measurements of the *pmf* are well-developed, alterations in the $\Delta\psi$:ΔpH ratio have been observed (Cruz et al. 2005b), similar to that seen in higher plant chloroplasts (see above). Comparative genomic analyses suggest that *Chlamydomonas* contains ion channels with similar sequences to those in Arabidopsis (Marchant et al. 2018), but their activities have yet been demonstrated. In the model cyanobacterium *Synechocystis* sp. PCC 6803, the demonstration of ion channel activities have been limited to observations that altering the expression of a putative potassium channel affects the turnover rate of b_6f complex, consistent with a role in lumen pH homeostasis (Checchetto et al. 2012).

Prokaryotic phototrophs have evolved a wide range of antenna systems, some of which are unlikely to interact with the *pmf* in the same way as those in plants (Kirilovsky and Kerfeld 2012). In some cyanobacteria, light capture by the cytosolic phycobilisomes (PBS) is regulated by the orange carotenoid protein (OCP) and the fluorescence recovery protein (FRP) system, in which strong excitation with blue-green light leads to the conversion of the orange to the red form of the protein, allowing it to attach to PBS and quench excitons (Wilson et al. 2006). The process is reversed by the activity of the FRP, which converts OCP back from the red to the orange form (Kirilovsky and Kerfeld 2016). PBS can also shunt energy to either PSII or PSI through state transitions that appear to be responsive to the redox state of the cell (Ranjbar Choubeh et al. 2018).

Photoprotection in these systems are not directly induced by lumen acidification, opening the question of whether the *pmf* paradigm is needed. Of particular interest is whether photosynthetic control in cyanobacteria is needed to prevent PSI photodamage. Evidence for a substantially acidified lumen and subsequent photosynthetic control was presented by Trubitsin et al. (2005) and it was further suggested that the formation of ΔpH involves dissipation of $\Delta\psi$ by ion transporters (Checchetto et al. 2012). However, it has also been suggested that, at least in some cases, photosynthetic control is not needed or would hinder efficient photosynthesis (Badger et al. 2000/see also below).

Under some conditions, e.g. low temperature, high temperature (Diaz et al. 2007; Quiles 2006), or high salt (Stepien and Johnson 2009), plant chloroplasts can dissipate small amounts of energy by diverting electrons from the light reactions to O_2 but this mechanism appears to be much more robust in cyanobacteria and algae (Houille-Vernes et al. 2011; Peltier et al. 2010), and can account for a substantial fraction photoprotection in green algae, red algae, and dinoflagelletes (Badger et al. 2000). There are at least three mechanisms for dissipating photosynthetic energy to O_2, the Mehler-peroxidase or Water-Water cycle (Asada 1999), oxidation of PQH_2 by the plastid terminal oxidase (PTOX) (Krieger-Liszkay and Feilke 2015), and the flavodiiron proteins (FLV) (Chukhutsina et al. 2015; Allahverdiyeva et al. 2013).

The FLV system is found in the cytoplasm of many (but not all) cyanobacterial species, in most eukaryotic algae icluding green algae and in moss stroma (Chaux et al. 2017; Dang et al. 2014). FLV1- and 3, functioning as a heterodimeric enzyme, can accept four electrons (sequentially) from PSI-reduced Fd, and reduce O_2 to two molecules of water. Much like NPQ, which dissipates light energy, the diversion of electron flow from PSI to O_2 effectively prevents the buildup of highly reducing electron carriers, minimiz-

ing production of ROS (Jokel et al. 2018). In contrast to the Mehler-peroxidase cycle, the 4-electron oxygen reductase chemistry of FLV1/3 probably results in the formation of water, not superoxide, though there is some question about the precise mechanism (see Chap. 8 by Raven, Beardall and Quigg). It has been proposed that upwards of 30% of the electrons derived from water oxidation may be shunted through the FLV1/3 system under high light conditions in cyanobacteria (Helman et al. 2003). It has been demonstrated in both cyanobacteria and green algae that knocking out FLV proteins can lead to severe photodamage, especially under high or fluctuating light (Shimakawa et al. 2016; Jokel et al. 2018). It can also be argued that electron flow through FLV can augment ATP synthesis and replace the need for CEF (Dang et al. 2014). Intriguingly, the FLV2- and − 4 proteins, which are unique to β-cyanobacteria, have been posited to have a photoprotective role for PSII, either *via* direct oxidation of the Q_B-site semiquinone (i.e. functioning as an electron sink) or through modification of PBS association with PSII (Zhang et al. 2012).

In higher plant tissues, PTOX plays an essential role in plastid development as its plastoquinol oxidase activity is required for carotenoid biosynthesis (a role which is undertaken by the cytochrome b_6f complex in mature chloroplasts) (Josse et al. 2000). PTOX is also likely to participate in a 'chlororespiratory' pathway within the thylakoid (the light-independent linear electron flow of electrons from NADPH (or Fd) to oxygen), of which NDH has also been proposed to be a component of in plants (Bennoun 2002). While a role for PTOX in plastid development has been established, its role in photosynthesis and stress responses remains unclear, likewise the importance of chlororespiratory processes within the chloroplast. PTOX has been proposed to function as an alternative electron sink under conditions where the acceptor side of PSI is limited (McDonald et al. 2011), and it has been shown to be induced by a variety of stress conditions, including cold, heat, salinity, drought (Diaz et al. 2007; Quiles 2006; Ibanez et al. 2010), low temperature and high light (Ivanov et al. 2012), and combinations of low temperature and high UV exposure (Streb et al. 2005; Laureau et al. 2013). According to the original model proposed (Huner et al. 1998), a single stress alone does not induce the response. Rather, the acclimation response occurs when a high excitation pressure is coupled with an environmental stress.

Several groups have proposed that PTOX in eukaryotic algae and higher plants acts as a safety valve in the light under abiotic stress conditions by preventing the "over-reduction" of the PQ pool, which would lead to accumulation of electrons on PSII (see Chap. 8). For example, when PTOX was found to be upregulated in sun vs. shade leaves in the alpine plant *Ranunculus glacialis* L., it was concluded that the adaptation may help ameliorate the rapid light and temperature changes that occur in the plant's climate. The work showed that PTOX content correlated with the magnitude of electron flow unrelated to the carboxylation and oxygenation of rubisco, strongly suggesting that PTOX acts as safety valve to relieve pressure on the electron transport chain when the PQ pool is highly reduced (Laureau et al. 2013). Similarly, when rice PTOX was overexpressed in the cyanobacteria *Synechocystis* sp. PCC 6803, the NAD(P)H/NAD(P)$^+$ pool became highly oxidized, consistent with the model of PTOX being a redox release valve, although care is needed in interpreting these data due to the highly branched nature of competing electron transfer pathways in cyanobacterial thylakoids, which also contain respiratory complexes (Ermakova et al. 2016). The overexpression of PTOX also led to decreases in the ratio of PSII/PSI suggesting that PTOX may play a role in (direct or indirect) signaling that regulates PSI and PSII biosynthesis, perhaps by altering the thiol redox state (Feilke et al. 2017). PTOX has also been shown to func-

tion as an electron sink in Chlamydomonas and its loss decreases fitness under low (40 μmol photons m^{-2} s^{-1}) light (Houille-Vernes et al. 2011).

Other studies cast some doubt on the PTOX is a safety valve model, or at least call into question whether introducing PTOX into exotic species will lead to "safer" photosynthesis. A study in tomato demonstrated that the enzymatic properties of PTOX are not compatible with high fluxes required for a robust safety valve (Trouillard et al. 2012). Overexpression of PTOX in *A. thaliana* did not decrease light-induced photodamage (Rosso et al. 2006), and over-expression in tobacco (Krieger-Liszkay and Feilke 2015) resulted in higher photoinhibition and ROS production under high light. Also, PTOX overexpressing plant thylakoids showed decreases in oxygen evolving activity beyond that accounted for by diversion of electrons to O_2 through PTOX, and higher levels of superoxide ($O_2^{\cdot -}$) production. Experiments with *E. coli* expressing PTOX showed that PTOX activity leads to the generation of ROS when the quinone pool is over-reduced (Heyno et al. 2009). Overall, these results suggest that in plants, PTOX mainly plays a role in maintaining the redox state of the PQ pool during chloroplast biogenesis and the assembly of the photosynthetic apparatus, but in high light may result in $O_2^{\cdot -}$ production (Heyno et al. 2009).

The emerging picture seems to be that, in higher plants, PTOX is highly regulated to operate only under specific stress conditions (Stepien and Johnson 2018; Feilke et al. 2016). This view reconciles discrepancies between earlier work because PTOX activities are kept low, either by low expression levels of regulation at the enzyme level, under non-stressed conditions (Feilke et al. 2016). Consistent with this view, overexpressing PTOX does not necessarily increases its overall activity (Stepien and Johnson 2018), whereas exposure to abiotic stresses does (Feilke et al. 2016). In dark adapted tomato plants, PTOX showed sluggish activity (Trouillard et al. 2012), but under abiotic stress, its activity increases to the point where it could account for a substantial fraction of LEF (Feilke et al. 2016) and in stressed *Extrema* (previously *Thellungiella halophila*), PTOX-dependent electron flow accounted for up to 30% of the total LEF (Stepien and Johnson 2009).

The mode of regulation of PTOX is not yet settled, but it has been proposed that the association of PTOX (which is a monotopic membrane protein) with the stromal face of the thylakoid membrane, and therefore its activity, is controlled by pH, which in turn is responsive to the metabolic state of the stroma, especially the activity of the Calvin-Benso-Bassham cycle (Feilke et al. 2016). Another hypothesis is that PTOX regulation involves translocation of the protein from the stroma lamellae into proximity with the PQ pool associated with PSII (Stepien and Johnson 2018). In any case, the flux of electrons through PTOX should also be responsive to the redox state of the PQ pool, which is determined by the flux of electrons into the pool through PSII and out of the pool through the b_6f complex, which are both regulated by the *pmf* through effects on NPQ and photosynthetic control (Strand and Kramer 2014).

IX. Coping with ATP Excess or NADPH Deficit

The previous section emphasizes an important theme of this paper: that while O_2 reduction by PTOX, FLV and MPR have been considered to act as safety valves for the electronic circuit of photosynthesis, these valves may themselves be unsafe in that they perturb the energy balance of the photosynthetic system, and thus may impose the need for a second safety valves for the protonic circuit. Badger et al. (2000) recognized this potential problem, and suggested that, in algae and cyanobacteria that have larger capacity for O_2 reduction, the additional LEF needed to rebalance the energy budget may not be uncoupled from ATP pro-

duction, e.g. if electron transport through the cytochrome b_6f complex was not controlled by lumen pH, but by stromal side regulatory processes, such as the redox state of NADPH or the presence of CO_2/bicarbonate. Indeed, one could imagine adaptations that decreased the canonical photosynthetic control mechanisms, e.g. changing the pH dependence of the cytochrome b_6f complex or storing more *pmf* in the form of $\Delta\psi$. However, in our view, the thylakoid would still need to dissipate $\Delta\psi$ to prevent accelerated recombination reactions that produce $^1O_2$ (Rutherford et al. 2012; Davis et al. 2016).

While much research has been reported on responses to ATP deficits, little is known about how photosynthetic systems cope with the opposite: excess ATP or limiting NADPH (Fig. 12.5). One way to adjust cellular ATP/NADPH would be to decrease the rate of ATP synthesis under NADPH deficit (or ATP excess) and there is some evidence that mitochondrial respiration through complex IV is inhibited by ATP levels (Ramzan et al. 2010; Bender and Kadenbach 2000; Kadenbach and Arnold 1999), though to our knowledge this has not been tested in photosynthetic systems. Also, thylakoids from cyanobacteria (Vermaas 2001) and (in likelihood) green alga (Bennoun 2002) contain respiratory enzymes and there is evidence that these interact (Pringault et al. 2005; Scherer et al. 1988; Binder 1982) possibly leading to regulation of ATP/NADPH balance. Of course, this type of mechanism could only account for imbalances smaller than ATP formation by these respiratory pathways, and given that for a phototroph, photosynthesis must run faster than respiration, there would seem to be situations where additional balancing is needed.

It may also be that the production of ATP is decreased or that ATP sinks are upregulated. However, because productive sinks are likely to become saturated at high rates, it seems more likely that these processes act more like safety valves that dissipate excess energy, rather than productive energy stor-

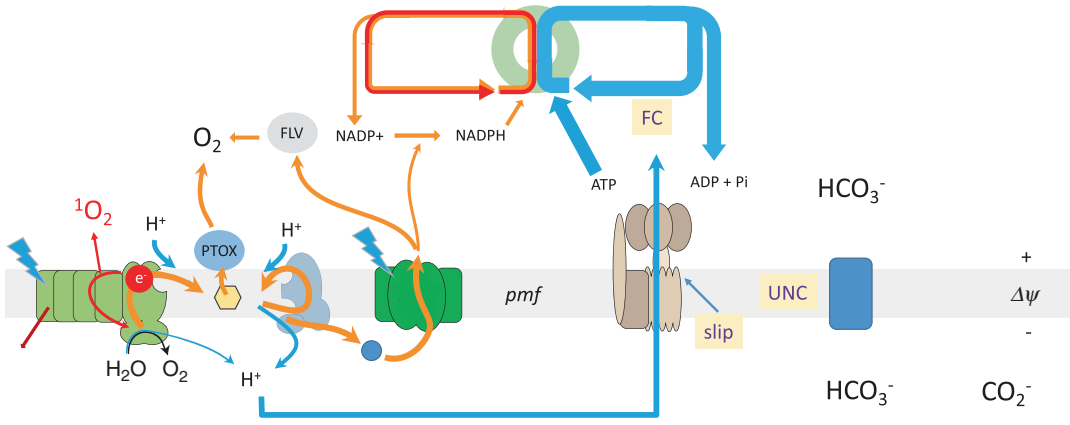

Fig. 12.5. **Energy imbalances caused by excess ATP or insufficient NADPH production.** The production ratio of NADPH/ATP may at times be insufficient to maintain metabolic pathways, e.g. when rates of O_2 reduction by PTOX or FLV are rapid, leading to a decrease in NADPH and increase in ATP, leading to mismatches between production and consumption of ATP (blue arrows) and NADPH (red curves). The depletion of ADP and P_i would be expected to slow the ATP synthase, increase *pmf*, slow electron flow at the cytochrome b_6f complex and lead to accelerated recombination reactions in PSII, leading to $^1O_2$ production (red arrows). Several processes may allow rebalancing of the energy budget (purple arrows) including uncoupling (leakage) protons across the thylakoid or through the ATP synthase, and various *pmf* or ATP-consuming futile cycles, e.g. the pumping of bicarbonate into the lumen, followed by escape of CO_2

age. Early evidence in favor of high rates of slippage (Schonfeld and Neumann 1977; Braun et al. 1991) were shown to be artifacts of isolation in the absence of nucleotides and Mg^{2+} (Groth and Junge 1993), though it has also been argued that such conditions are physiologically relevant (Feniouk et al. 1999). Indeed, the structural/mechanistic basis for proton-driven ATP synthesis involves mechanical coupling between two rotating subcomplexes, and it seems conceivable that slippage could occur, and it has been proposed that such slippage may be beneficial (Nelson et al. 2002). Another possibility is partially uncoupling the thylakoid membrane, as seen with uncoupler proteins (UCPs) (Jarmuszkiewicz 2001), which allow protons to pass through a membrane, bypassing ATP synthesis. UCPs have been found in animals, higher plants and some microorganisms, but as far we know, not in thylakoids. In plants, mitochondrial UCPs have been shown to be important for responses of photosynthesis to abiotic stresses, most likely by relieving oxidative stress during photorespiration (Sweetlove et al. 2006), but a recent paper showed that these proteins are more likely to act as transporters of aspartate, glutamate and dicarboxylates (Monne et al. 2018). To our knowledge, no canonical UCPs have not been found in cyanobacteria, though it is possible that unrelated proteins with similar functions have evolved.

Futile cycling may also be induced to consume ATP. One possible futile cycle involves the carbon concentrating mechanism, which under certain conditions may conduct a futile cycle that dissipates *pmf* and thus ATP (Fig. 12.5, purple arrows). In green algae, such a futile cycle could involve transport of bicarbonate across the thylakoid into the lumen (via an electrogenic transporter), followed by hydrolysis in the lumen of bicarbonate + H^+ to CO_2 + H_2O, and escape of the CO_2 across the non-pyrenoid segments of the thylakoid membrane (Wang et al. 2011; Badger 2003). Similarly, the uptake of HCO_3^- by cyanobacteria involves active transport down the ATP-hydrolysis-driven electrochemical potential gradient of the cell membrane, and therefore will consume ATP (Mangan and Brenner 2014). Metabolic futile cycles are also possible. For example we previously proposed (Livingston et al. 2010b) that in the Calvin-Benson cycle, 3-phosphoglycerate (3-PGA) is phosphorylated to 1,3-bisphosphoglycerate (1,3-BPG), which is reduced to glyceraldehyde-3-phosphate (GAP) via GAP dehydrogenase (GAPDH). However, 1,3-BPG is very unstable and if GAPDH activity is low, e.g. when NADPH is limiting, should decay with loss of P_i, to reform 3-PGA, forming an effective ATP-consuming futile cycle activated when NADPH content is low. It is unclear whether any of these reactions occur in cyanobacteria.

A. Energy Balancing by Interactions Between Photosynthetic and Respiratory Machinery

For cyanobacteria, it is likely that when Flv1/3 complexes are functional, other respiratory chain oxidases are not essential (Ermakova et al. 2016). However, under conditions of increased ATP requirements, e.g. under fluctuating light, when presumably repair of cellular machinery is required, the cytochrome c oxidase (COX) and/or the cytochrome bd quinol oxidase (Cyd), two membrane-localized respiratory terminal oxidases (RTOs), are necessary for survival. The Cyd oxidizes PQ/PQH_2 directly, and is not in itself a proton pump, but participates in proton translocation by reducing O_2 on the stromal side of the thylakoid, taking up 1 H^+/e^-. COX oxidizes PC or cytochrome c_6 and reduces O_2 to H_2O, like Cyd, but also directly pumps 2 H^+/e^- (Iwata et al. 1995; Branden et al. 2006). In respiration, PQ is reduced by a non-photoactive reductase, e.g. complex I or II, but because the respiratory enzymes are localized in the thylakoid in cyanobacteria, it is possible that electrons from PSII can also participate in respiration, through the activi-

ties of Cyd or the combination of b_6f complex PC/c6 and COX, leading to the generation of a *pmf* and ATP, without the reduction of $NADP^+$ (essentially another water-water-like cycle). Evidence has been presented that such alternative electron transfer pathways can occur in cyanobacteria, for example when the b_6f complex is blocked, PQH_2 can be oxidized by Cyd, and in mutants lacking PSI electron flow can occur to COX (Ermakova et al. 2016).

There is evidence that some eukaryotic algae have evolved energy balancing mechanisms that rely on cross talk between the chloroplast and the mitochondria. In diatoms, the chloroplast-localized energy balance mechanisms (i.e. CEF, MPR, FLV) do not appear active enough to modulate ATP/NADPH energy fluxes (Wilhelm et al. 2006; Lepetit et al. 2012; Bailleul et al. 2015), but instead appear to channel excess reducing power generated in the chloroplast to the mitochondria, where the reductant is utilized to generate ATP via oxidative phosphorylation. This ATP is then brought back to the chloroplast, to power processes such as the carbon assimilation (Bailleul et al. 2015). This rerouting of the electronic circuit of photosynthesis appears to involve the malate shuttle, which transfers reducing equivalents by transporting the malate/aspartate redox couple across the chloroplast and mitochondrial membranes, allowing equilibration of redox potentials of the $NAD(P)^+$/NAD(P)H couples in the two compartments. The rapid fluxes needed to balance the photosynthetic energy budget may be facilitated by the close proximity of the chloroplast and mitochondria in these organisms (Prihoda et al. 2012).

An intriguing, but relatively unrecognized bioenergetic complex is the the pyridine nucleotide transhydrogenase (PntAB), which catalyzes the reversible hydride transfer between NAD^+ and NADPH, coupled to the pumping of protons across a bioenergetic membrane (Jackson 2012). In mitochondria, PntAB is thought to use the *pmf* to maintain the NADPH and NADH out of equilibrium, favoring the reduction of NADPH, which in heterotrophic organisms is used to power reductive (anabolic) reactions, whereas NADH tends to be involved in breaking down molecules to supply energy for cellular processes. Interestingly, PntAB is also found in some cyanobacteria, in which it is expressed in the same bioenergetic membrane (thylakoid) as both the photosynthetic and respiratory reactions occur. During photosynthesis, LEF will reduce $NADP^+$ to NADPH. Transferring the hydride from NADPH to NAD^+ will result in the pumping of a proton from the lumen to the cytoplasm, storing energy in the *pmf*, and possibly contributing to ATP synthesis, though it is not clear how large fluxes of electrons to NAD^+ could be maintained. It is more likely that PntAB plays a role under respiratory conditions, where *pmf* formed during oxidative phosphorylation will be used to maintain a more reducing NADPH pool, as would be required to power biosynthetic reactions, presumably at night when photosynthesis is not actively reducing NADPH. Consistent with this interpretation, mutants of *Synechocystis* deficient in PntAB exhibit growth defects when grown under hetertropic, low light conditions, but not under autotrophic conditions (Kamarainen et al. 2017).

X. Conclusions and Perspective

The photoprotective and energy balancing mechanisms of photosynthesis are interconnected in complex ways, such that diversity of one component will have far reaching consequences that need to be recognized to understand the efficiency and robustness of photosynthesis in different environments. The *pmf* paradigm is probably partly, but not completely, conserved across evolutionarily diverse phototrophs. For example, while the ΔpH-induced regulation of light capture in plants is not conserved in cyanobacteria, the need to maintain *pmf* in a range

that allows efficient production of ATP but does not induce photodamage still exists. Though relatively little is currently known about these systems in diverse algal organisms, there will almost certainly be unexpected mechanisms.

Acknowledgements

The authors are funded by grant DE-FG02-11ER16220 from the Division of Chemical Sciences, Geosciences, and Biosciences, Office of Basic Energy Sciences of the US Department of Energy with foundations support from grants DE-FG02-04ER15559 (for AK, GD) and Grant DE-FG02-91ER2002 (for AK and NF). A portion of DMK's salary is supported by the MSU AgBioResearch.

References

Adams WW III, Zarter CR, Mueh KE, Amiard V, Demmig-Adams B (2006) Energy dissipation and photoinhibition: a continuum of photoprotection. In: Demmig-Adams B, Adams W III, Mattoo AK (eds) Photoprotection, photoinhibition, gene regulation, and environment. Springer, Dordrecht

Alboresi A, Storti M, Morosinotto T (2018) Balancing protection and efficiency in the regulation of photosynthetic electron transport across plant evolution. New Phytol 221:105–109

Allahverdiyeva Y, Mustila H, Ermakova M, Bersanini L, Richaud P, Ajlani G, Battchikova N, Cournac L, Aro EM (2013) Flavodiiron proteins Flv1 and Flv3 enable cyanobacterial growth and photosynthesis under fluctuating light. Proc Natl Acad Sci U S A 110(10):4111–4116. https://doi.org/10.1073/pnas.1221194110

Anderson B, Barber J (1996) Mechanisms of photodamage and protein degradation during photoinhibition of photosystem II. In Photosynthesis and the Environment, Baker NR (ed), pp 101–121. The Netherlands: Kluwer Academic Publishers

Armbruster U, Leonelli L, Correa Galvis V, Strand D, Quinn EH, Jonikas MC, Niyogi KK (2016) Regulation and levels of the thylakoid K+/H+ antiporter KEA3 shape the dynamic response of photosynthesis in fluctuating light. Plant Cell Physiol 57:1557–1567. https://doi.org/10.1093/pcp/pcw085

Aro E-M, Virgin I, Andersson B (1993) Photoinhibition of photosystem II. Inactivation, protein damage and turnover. BBA 1143:113–134

Asada K (1999) The water-water cycle in chloroplasts: scavenging of active oxygens and dissipation of excess photons. Annu Rev Plant Physiol 50:601–639

Asada K (2006) Production and scavenging of reactive oxygen species in chloroplasts and their functions. Plant Physiol 141(2):391–396

Avenson T, Cruz JA, Kramer D (2004) Modulation of energy dependent quenching of excitons (q_E) in antenna of higher plants. Proc Natl Acad Sci U S A 101:5530–5535

Avenson TJ, Kanazawa A, Cruz JA, Takizawa K, Ettinger WE, Kramer DM (2005) Integrating the proton circuit into photosynthesis: progress and challenges. Plant Cell Environ 28:97–109

Backhausen JE, Kitzmann C, Scheibe R (1994) Competition between electron acceptors in photosynthesis – regulation of the malate valve during Co2 fixation and nitrite reduction. Photosynth Res 42(1):75–86

Badger M (2003) The roles of carbonic anhydrases in photosynthetic CO(2) concentrating mechanisms. Photosynth Res 77(2–3):83–94. https://doi.org/10.1023/A:1025821717773

Badger MR, von Caemmerer S, Ruuska S, Nakano H (2000) Electron flow to oxygen in higher plants and algae: rates and control of direct photoreduction (Mehler reaction) and rubisco oxygenase. Philos Trans R Soc Lond Ser B Biol Sci 355(1402):1433–1446. https://doi.org/10.1098/rstb.2000.0704

Bailleul B, Cardol P, Breyton C, Finazzi G (2010) Electrochromism: a useful probe to study algal photosynthesis. Photosynth Res 106(1–2):179–189. https://doi.org/10.1007/s11120-010-9579-z

Bailleul B, Berne N, Murik O, Petroutsos D, Prihoda J, Tanaka A, Villanova V, Bligny R, Flori S, Falconet D, Krieger-Liszkay A, Santabarbara S, Rappaport F, Joliot P, Tirichine L, Falkowski PG, Cardol P, Bowler C, Finazzi G (2015) Energetic coupling between plastids and mitochondria drives CO2 assimilation in diatoms. Nature 524(7565):366–369. https://doi.org/10.1038/nature14599

Baker NR, Bowyer JR (1994) Photoinhibition of photosynthesis from molecular mechanisms to the field. In Environmental Plant Biology series, Davies WJ (ed), pp 1–471. Institute of Environmental and Biological Sciences, Division of Biological Sciences, University of Lancaster, Lancaster LA1 4YQ,UK: Bios Scientific Publishers

Barber J (1976) Ionic regulation in intact chloroplasts and its effect on primary photosynthetic processes. In: Barber J (ed) The intact chloroplast. Elsevier/

North Holland Biomedical Press, Amsterdam, pp 89–134

Bender E, Kadenbach B (2000) The allosteric ATP-inhibition of cytochrome c oxidase activity is reversibly switched on by cAMP-dependent phosphorylation. FEBS Lett 466(1):130–134

Bennoun P (2002) The present model for chlororespiration. Photosynth Res 73(1–3):273–277. https://doi.org/10.1023/A:1020479920622

Berne N, Fabryova T, Istaz B, Cardol P, Bailleul B (2018) The peculiar NPQ regulation in the stramenopile phaeomonas sp. challenges the xanthophyll cycle dogma. Biochim Biophys Acta Bioenerg 1859(7):491–500. https://doi.org/10.1016/j.bbabio.2018.03.013

Binder A (1982) Respiration and photosynthesis in energy-transducing membranes of cyanobacteria. J Bioenerg Biomembr 14(5–6):271–286

Bonente G, Ballottari M, Truong TB, Morosinotto T, Ahn TK, Fleming GR, Niyogi KK, Bassi R (2011) Analysis of LhcSR3, a protein essential for feedback de-excitation in the green alga Chlamydomonas reinhardtii. PLoS Biol 9(1):e1000577. https://doi.org/10.1371/journal.pbio.1000577

Branden G, Gennis RB, Brzezinski P (2006) Transmembrane proton translocation by cytochrome c oxidase. BBA-Bioenergetics 1757(8):1052–1063. https://doi.org/10.1016/j.bbabio.2006.05.020

Braun G, Evron Y, Malkin S, Avron M (1991) Proton flow through the ATP synthase in chloroplasts regulates the distribution of light energy between PS I and PS II. FEBS Lett 280:57–60

Breyton C, Nandha B, Johnson GN, Joliot P, Finazzi G (2006) Redox modulation of cyclic electron flow around photosystem I in C_3 plants, Biochemistry 45, 13465–13475

Burrows PA, Sazanov LA, Svab Z, Maliga P, Nixon PJ (1998) Identification of a functional respiratory complex in chloroplasts through analysis of tobacco mutants containing disrupted plastid ndh genes. EMBO J 17(4):868–876

Cape JL, Bowman MK, Kramer DM (2006) Understanding the cytochrome *bc* complexes by what they don't do. The Q-cycle at 30. Trends Plant Sci 11:46–55

Chaux F, Burlacot A, Mekhalfi M, Auroy P, Blangy S, Richaud P, Peltier G (2017) Flavodiiron proteins promote fast and transient O2 photoreduction in chlamydomonas. Plant Physiol 174(3):1825–1836. https://doi.org/10.1104/pp.17.00421

Checchetto V, Segalla A, Allorent G, La Rocca N, Leanza L, Giacometti GM, Uozumi N, Finazzi G, Bergantino E, Szabo I (2012) Thylakoid potassium channel is required for efficient photosynthesis in cyanobacteria. Proc Natl Acad Sci U S A 109(27):11043–11048. https://doi.org/10.1073/pnas.1205960109

Chukhutsina V, Bersanini L, Aro EM, van Amerongen H (2015) Cyanobacterial flv4-2 operon-encoded proteins optimize light harvesting and charge separation in photosystem II. Mol Plant 8(5):747–761. https://doi.org/10.1016/j.molp.2014.12.016

Crouchman S, Ruban A, Horton P (2006) PsbS enhances nonphotochemical fluorescence quenching in the absence of zeaxanthin. FEBS Lett 580(8):2053–2058. https://doi.org/10.1016/j.febslet.2006.03.005

Cruz JA, Sacksteder CA, Kanazawa A, Kramer DM (2001) Contribution of electric field (Dy) to steady-state transthylakoid proton motive force *in vitro* and *in vivo*. Control of *pmf* parsing into Dy and DpH by counterion fluxes. Biochemistry 40:1226–1237

Cruz JA, Avenson TJ, Kanazawa A, Takizawa K, Edwards GE, Kramer DM (2005a) Plasticity in light reactions of photosynthesis for energy production and photoprotection. J Exp Bot 56:395–406

Cruz JA, Kanazawa A, Treff N, Kramer DM (2005b) Storage of light-driven transthylakoid proton motive force as an electric field Dy under steady-state conditions in intact cells of *Chlamydomonas reinhardtii*. Photosynth Res 85(2):221–233

DalCorso G, Pesaresi P, Masiero S, Aseeva E, Schunemann D, Finazzi G, Joliot P, Barbato R, Leister D (2008) A complex containing PGRL1 and PGR5 is involved in the switch between linear and cyclic electron flow in Arabidopsis. Cell 132(2):273–285

Dang KV, Plet J, Tolleter D, Jokel M, Cuine S, Carrier P, Auroy P, Richaud P, Johnson X, Alric J, Allahverdiyeva Y, Peltier G (2014) Combined increases in mitochondrial cooperation and oxygen photoreduction compensate for deficiency in cyclic electron flow in Chlamydomonas reinhardtii. Plant Cell 26(7):3036–3050. https://doi.org/10.1105/tpc.114.126375

Daum B, Nicastro D, Austin J 2nd, McIntosh JR, Kuhlbrandt W (2010) Arrangement of photosystem II and ATP synthase in chloroplast membranes of spinach and pea. Plant Cell 22(4):1299–1312. https://doi.org/10.1105/tpc.109.071431

Davis GA, Kanazawa A, Schöttler MA, Kohzuma K, Froehlich JE, Rutherford AW, Satoh-Cruz M, Minhas D, Tietz S, Dhingra A, Kramer DM (2016) Limitations to photosynthesis by proton motive force-induced photosystem II photodamage. elife 5:e16921

Davis GA, Rutherford AW, Kramer DM (2017) Hacking the thylakoid proton motive force (pmf) for

improved photosynthesis: possibilities and pitfalls. Philos Trans R Soc B 372:20160381

Deamer DW, Crofts AR, Packer L (1966) Mechanisms of light-induced structural changes in chloroplasts. I. Light-scattering increments and ultrastructural changes mediated by proton transport. Biochim Biophys Acta 131:81–96

Demmig-Adams B, Adams W (1996) The role of xanthophyll cycle carotenoids in the protecion of photosynthesis. Trends Plant Sci 1:21–26

Demmig-Adams B, Stewart JJ, Adams WW 3rd (2017) Environmental regulation of intrinsic photosynthetic capacity: an integrated view. Curr Opin Plant Biol 37:34–41. https://doi.org/10.1016/j.pbi.2017.03.008

Desplats C, Mus F, Cuine S, Billon E, Cournac L, Peltier G (2009) Characterization of Nda2, a plastoquinone-reducing type II NAD(P)H dehydrogenase in chlamydomonas chloroplasts. J Biol Chem 284(7):4148–4157

Diaz M, de Haro V, Munoz R, Quiles MJ (2007) Chlororespiration is involved in the adaptation of Brassica plants to heat and high light intensity. Plant Cell Environ 30(12):1578–1585. https://doi.org/10.1111/j.1365-3040.2007.01735.x

Drachev LA, Kaurov BS, Mamedov MD, Mulkidjanian AY, Semenov AY, Shinkarev VP, Skulachev VP, Verkhovsky MI (1989) Flash-induced electrogenic events in the photosynthetic reaction center and bc1complexes of rhodobacter sphaeroides chromatophores. Biochim Biophys Acta 973:189–197

Ducruet JM, Roman M, Havaux M, Janda T, Gallais A (2005) Cyclic electron flow around PSI monitored by afterglow luminescence in leaves of maize inbred lines (Zea mays L.): correlation with chilling tolerance. Planta 221(4):567–579

Efremov RG, Baradaran R, Sazanov LA (2010) The architecture of respiratory complex I. Nature 465(7297):441–445

Ermakova M, Huokko T, Richaud P, Bersanini L, Howe CJ, Lea-Smith DJ, Peltier G, Allahverdiyeva Y (2016) Distinguishing the roles of thylakoid respiratory terminal oxidases in the cyanobacterium synechocystis sp PCC 6803. Plant Physiol 171(2):1307–1319. https://doi.org/10.1104/pp.16.00479

Eskling M, Emanuelsson A, Akerlund H-E (2001) Enzymes and mechanisms for violaxanthin-zeaxanthin conversion. In: Aro E-M, Anderson B (eds) Regulation of photosynthesis, vol 100. Kluwer Academic Publishers, Dordrecht, pp 806–816

Feilke K, Streb P, Cornic G, Perreau F, Kruk J, Krieger-Liszkay A (2016) Effect of chlamydomonas plastid terminal oxidase 1 expressed in tobacco on photosynthetic electron transfer. Plant J 85(2):219–228. https://doi.org/10.1111/tpj.13101

Feilke K, Ajlani G, Krieger-Liszkay A (2017) Overexpression of plastid terminal oxidase in synechocystis sp. PCC 6803 alters cellular redox state (vol 372, 20160379, 2017). Philos Trans R Soc B Biol Sci 372(1736):20160379. https://doi.org/10.1098/rstb.2017.0277

Feniouk BA, Cherepanov DA, Junge W, Mulkidjanian AY (1999) ATP-synthase of Rhodobacter capsulatus: coupling of proton flow through F0 to reactions in F1 under the ATP synthesis and slip conditions. FEBS Lett 445(2–3):409–414

Finazzi G, Rappaport F, Furia A, Fleischmann M, Rochaix JD, Zito F, Forti G (2002) Involvement of state transitions in the switch between linear and cyclic electron flow in *Chlamydomonas reinhardtii*. EMBO Rep 3(3):280–285

Fischer S, Graber P (1999) Comparison of DpH- and Dy-driven ATP synthesis catalyzed by the H(+)-ATPases from Escherichia coli or chloroplasts reconstituted into liposomes. FEBS Lett 457:327–332

Fisher N, Quevedo V, Kramer DM (2018) To b or not to b: direct reduction of cytochrome b-563 by ferredoxin in higher plant cyclic electron flow in vitro? Biochim Biophys Acta 1859:e106

Fisher N, Bricker T, Kramer DM (2019) Regulation of cyclic electron flow pathways by adenylate status in higher plant chloroplasts. Proc Natl Acad Sci U S A submitted

Foyer CH, Shigeoka S (2011) Understanding oxidative stress and antioxidant functions to enhance photosynthesis. Plant Physiol 155(1):93–100. https://doi.org/10.1104/pp.110.166181

Friedrich T, Steinmuller K, Weiss H (1995) The proton-pumping respiratory complex I of bacteria and mitochondria and its homologue in chloroplasts. FEBS Lett 367(2):107–111

Furbacher PN, Girvin ME, Cramer WA (1989) On the question of interheme electron transfer in the chloroplast cytochrome b6 in situ. Biochemistry 28:8990–8998

Gerotto C, Alboresi A, Giacometti GM, Bassi R, Morosinotto T (2011) Role of PSBS and LHCSR in Physcomitrella patens acclimation to high light and low temperature. Plant Cell Environ 34(6):922–932. https://doi.org/10.1111/j.1365-3040.2011.02294.x

Golding AJ, Finazzi G, Johnson GN (2004) Reduction of the thylakoid electron transport chain by stromal reductants-evidence for activation of cyclic electron transport upon dark adaptation or under drought. Planta 220(2):356–363

Goss R, Lepetit B (2015) Biodiversity of NPQ. J Plant Physiol 172:13–32. https://doi.org/10.1016/j.jplph.2014.03.004

Grabolle M, Dau H (2005) Energetics of primary and secondary electron transfer in photosystem II membrane particles of spinach revisited on basis of recombination-fluorescence measurements. Biochim Biophys Acta 1708(2):209–218. https://doi.org/10.1016/j.bbabio.2005.03.007

Groth G, Junge W (1993) Proton slip of the chloroplast ATPase: its nucleotide dependence, energetic threshold, and relation to an alternating site mechanism of catalysis. Biochemistry 32:8103–8111

Gust D, Kramer D, Moore A, Moore T, Vermaas W (2008) Engineered and artificial photosynthesis: human ingenuity enters the game. Mater Res Bull 33:383–389

Hangarter RP, Good ND (1982) Energy thresholds for ATP synthesis in chloroplasts. Biochim Biophys Acta 681:396–404

Harbinson J, Genty B, Baker NR (1989) Relationship between the quantum efficiencies of photosystem I and II in pea leaves. Plant Physiol 90:1029–1034

Havaux M, Rumeau D, Ducruet JM (2005) Probing the FQR and NDH activities involved in cyclic electron transport around photosystem I by the 'afterglow' luminescence. BBA-Bioenergetics 1709(3):203–213

Helman Y, Tchernov D, Reinhold L, Shibata M, Ogawa T, Schwarz R, Ohad I, Kaplan A (2003) Genes encoding A-type flavoproteins are essential for photoreduction of O2 in cyanobacteria. Curr Biol 13(3):230–235

Hertle AP, Blunder T, Wunder T, Pesaresi P, Pribil M, Armbruster U, Leister D (2013) PGRL1 is the elusive ferredoxin-plastoquinone reductase in photosynthetic cyclic electron flow. Mol Cell 49(3):511–523. https://doi.org/10.1016/j.molcel.2012.11.030

Heyno E, Gross CM, Laureau C, Culcasi M, Pietri S, Krieger-Liszkay A (2009) Plastid alternative oxidase (PTOX) promotes oxidative stress when overexpressed in tobacco. J Biol Chem 284(45):31174–31180. https://doi.org/10.1074/jbc.M109.021667

Hideg E, Kalai T, Kos PB, Asada K, Hideg K (2006) Singlet oxygen in plants- its significance and possible detection with double (fluorescent and spin) indicator reagents. Photochem Photobiol 82(5):1211–1218

Hochmal AK, Schulze S, Trompelt K, Hippler M (2015) Calcium-dependent regulation of photosynthesis. Biochim Biophys Acta 1847(9):993–1003. https://doi.org/10.1016/j.bbabio.2015.02.010

Holser JP, Yocum CF (1987) Regulation of cyclic photophosphorylation during ferredoxin-mediated electron transport. Plant Physiol 83:965–969

Houille-Vernes L, Rappaport F, Wollman FA, Alric J, Johnson X (2011) Plastid terminal oxidase 2 (PTOX2) is the major oxidase involved in chlororespiration in Chlamydomonas. Proc Natl Acad Sci U S A 108(51):20820–20825. https://doi.org/10.1073/Pnas.1110518109

Huner NPA, Oquist G, Sarhan F (1998) Energy balance and acclimation to light and cold. Trends Plant Sci 3(6):224–230. https://doi.org/10.1016/s1360-1385(98)01248-5

Ibanez H, Ballester A, Munoz R, Quiles MJ (2010) Chlororespiration and tolerance to drought, heat and high illumination. J Plant Physiol 167(9):732–738. https://doi.org/10.1016/j.jplph.2009.12.013

Ifuku K, Endo T, Shikanai T, Aro EM (2011) Structure of the chloroplast NADH dehydrogenase-like complex: nomenclature for nuclear-encoded subunits. Plant Cell Physiol 52(9):1560–1568. https://doi.org/10.1093/pcp/pcr098

Ioannidis N, Cruz J, Kotzabasis K, Kramer DM (2012) Does putrescine regulate the higher plant photosynthetic proton circuit? PLoS One 7(1):1–6

Ishikawa N, Endo T, Sato F (2008) Electron transport activities of Arabidopsis thaliana mutants with impaired chloroplastic NAD(P)H dehydrogenase. J Plant Res 121(5):521–526

Ivanov AG, Rosso D, Savitch LV, Stachula P, Rosembert M, Oquist G, Hurry V, Huner NPA (2012) Implications of alternative electron sinks in increased resistance of PSII and PSI photochemistry to high light stress in cold-acclimated Arabidopsis thaliana. Photosynth Res 113(1–3):191–206. https://doi.org/10.1007/s11120-012-9769-y

Iwai M, Takizawa K, Tokutsu R, Okamuro A, Takahashi Y, Minagawa J (2010) Isolation of the elusive supercomplex that drives cyclic electron flow in photosynthesis. Nature 464(7292):1210–1213

Iwata S, Ostermeier C, Ludwig B, Michel H (1995) Structure at 2.8-Angstrom resolution of cytochrome-c-oxidase from *Paracoccus denitrificans*. Nature 376(6542):660–669. https://doi.org/10.1038/376660a0

Jackson JB (2012) A review of the binding-change mechanism for proton-translocating transhydrogenase. Biochem Biophys Acta 1817:1839–1846

Jahns P, Graf M, Munekage Y, Shikanai T (2002) Single point mutation in the Rieske iron-sulfur subunit of cytochrome b6/f leads to an altered pH dependence of plastoquinol oxidation in Arabidopsis. FEBS Lett 519(1–3):99–102

Jarmuszkiewicz W (2001) Uncoupling proteins in mitochondria of plants and some microorganisms. Acta Biochim Pol 48(1):145–155

Jia H, Oguchi R, Hope AB, Barber J, Chow WS (2008) Differential effects of severe water stress on linear and cyclic electron fluxes through photosystem I

in spinach leaf discs in CO2-enriched air. Planta 228(5):803–812

Joet T, Cournac L, Peltier G, Havaux M (2002a) Cyclic electron flow around photosystem I in C-3 plants. In vivo control by the redox state of chloroplasts and involvement of the NADH-dehydrogenase complex. Plant Physiol 128(2):760–769

Joet T, Genty B, Josse EM, Kuntz M, Cournac L, Peltier G (2002b) Involvement of a plastid terminal oxidase in plastoquinone oxidation as evidenced by expression of the Arabidopsis thaliana enzyme in tobacco. J Biol Chem 277(35):31623–31630

Johnson G (2004) Controversy remains: regulation of pH gradient across the thylakoid membrane. Trends Plant Sci 9(12):570–571. author reply 571–572

Jokel M, Johnson X, Peltier G, Aro EM, Allahverdiyeva Y (2018) Hunting the main player enabling Chlamydomonas reinhardtii growth under fluctuating light. Plant J 94(5):822–835. https://doi.org/10.1111/tpj.13897

Joliot P, Johnson GN (2011) Regulation of cyclic and linear electron flow in higher plants. Proc Natl Acad Sci U S A 108(32):13317–13322. https://doi.org/10.1073/Pnas.1110189108

Joliot P, Joliot A (2002) Cyclic electron transfer in plant leaf, Proc Natl Acad Sci U S A 99, 10209–10214.

Joliot P, Joliot A (2006) Cyclic electron flow in C_3 plants, Biochim Biophys Acta 1757, 362–368

Joliot P, Beal D, Joliot A (2004) Cyclic electron flow under saturating excitation of dark-adapted Arabidopsis leaves. Biochim Biophys Acta 1656(2–3):166–176

Josse EM, Simkin AJ, Gaffe J, Laboure AM, Kuntz M, Carol P (2000) A plastid terminal oxidase associated with carotenoid desaturation during chromoplast differentiation. Plant Physiol 123(4):1427–1436

Junge W, Witt HT (1968) On the ion transport system of photosynthesis–investigations on a molecular level. Z Naturforsch B 23(2):244–254

Junge W, Ausländer W, McGeer AJ, Runge T (1979) The buffering capacity of the internal phase of thykaloids and the magnitude of the pH changes inside under flashing light. Biochim Biophys Acta 546:121–141

Kadenbach B, Arnold S (1999) A second mechanism of respiratory control. FEBS Lett 447(2–3):131–134

Kakitani T, Honig B, Crofts AR (1982) Theoretical studies of the electrochromic response of carotenoids in photosynthetic membranes. Biophys J 39:57–63

Kamarainen J, Huokko T, Kreula S, Jones PR, Aro EM, Kallio P (2017) Pyridine nucleotide transhydrogenase PntAB is essential for optimal growth and photosynthetic integrity under low-light mixotrophic conditions in *Synechocystis* sp PCC 6803. New Phytol 214(1):194–204. https://doi.org/10.1111/nph.14353

Kanazawa A, Kramer DM (2002) *In vivo* modulation of nonphotochemical exciton quenching (NPQ) by regulation of the chloroplast ATP synthase. Proc Natl Acad Sci U S A 99:12789–12794

Kanazawa A, Ostendorf E, Kohzuma K, Hoh D, Strand DD, Sato-Cruz M, Savage L, Cruz JA, Froehlich JE, Kramer DM (2017) Chloroplast ATP synthase modulation of the thylakoid proton motive force: implications for photosystem I and photosystem II photoprotection. Front Plant Physiol 8:719. https://doi.org/10.3389/fpls.2017.00719

Kirchhoff H, Hall C, Wood M, Herbstova M, Tsabari O, Nevo R, Charuvi D, Shimoni E, Reich Z (2011) Dynamic control of protein diffusion within the granal thylakoid lumen. Proc Natl Acad Sci U S A 108(50):20248–20253. https://doi.org/10.1073/pnas.1104141109

Kirilovsky D, Kerfeld CA (2012) The orange carotenoid protein in photoprotection of photosystem II in cyanobacteria. Biochim Biophys Acta 1817(1):158–166. https://doi.org/10.1016/j.bbabio.2011.04.013

Kirilovsky D, Kerfeld CA (2016) Cyanobacterial photoprotection by the orange carotenoid protein. Nat Plants 2(12):16180. https://doi.org/10.1038/nplants.2016.180

Kiss AZ, Ruban AV, Horton P (2008) The PsbS protein controls the organization of the photosystem II antenna in higher plant thylakoid membranes. J Biol Chem 283(7):3972–3978

Kohzuma K, Cruz JA, Akashi K, Hoshiyasu S, Munekage Y, Yokota A, Kramer DM (2009) The long-term responses of the photosynthetic proton circuit to drought. Plant Cell Environ 32:209–219

Kramer DM, Evans JR (2011) The importance of energy balance in improving photosynthetic productivity. Plant Physiol 155:70–78

Kramer DM, Sacksteder CA, Cruz JA (1999) How acidic is the lumen? Photosynth Res 60:151–163

Kramer DM, Cruz JA, Kanazawa A (2003) Balancing the central roles of the thylakoid proton gradient. Trends Plant Sci 8:27–32

Kramer DM, Avenson TJ, Edwards GE (2004a) Dynamic flexibility in the light reactions of photosynthesis governed by both electron and proton transfer reactions. Trends Plant Sci 9:349–357

Kramer DM, Kanazawa A, Cruz JA, Ivanov B, Edwards GE (2004b) The relationship between photosynthetic electron transfer and its regulation. In: Govindjee, Papageorgiou GC (eds) Chlorophyll fluorescence: the signature of green plant photosynthesis, vol 251–278. Kluwer Publishers, Dordrecht

Krieger A, Weis E (1993) The role of calcium in the pH-dependent control of photosystem II. Photosynth Res 37:117–130

Krieger-Liszkay A, Feilke K (2015) The dual role of the plastid terminal oxidase PTOX: between a protective and a pro-oxidant function. Front Plant Sci 6:1147. https://doi.org/10.3389/fpls.2015.01147

Kromdijk J, Glowacka K, Leonelli L, Gabilly ST, Iwai M, Niyogi KK, Long SP (2016) Improving photosynthesis and crop productivity by accelerating recovery from photoprotection. Science 354(6314):857–861. https://doi.org/10.1126/science.aai8878

Krupnik T, Kotabova E, van Bezouwen LS, Mazur R, Garstka M, Nixon PJ, Barber J, Kana R, Boekema EJ, Kargul J (2013) A reaction center-dependent photoprotection mechanism in a highly robust photosystem II from an extremophilic red alga, Cyanidioschyzon merolae. J Biol Chem 288(32):23529–23542. https://doi.org/10.1074/jbc.M113.484659

Kubicki A, Funk E, Westhoff P, Steinmueller K (1996) Differential expression of plastome-encoded ndh genes in the mesophyll and bundle sheath chloroplasts of the C-4 plant *Sorgum bicolor* indicates that the complex I-homologous NAD(P)H-plastoquinone oxidoreductase is involved in cyclic electron transport. Planta 199:276–281

Kurisu G, Zhang H, Smith JL, Cramer WA (2003) Structure of the cytochrome b_6f complex of oxygenic photosynthesis: tuning the cavity. Science 302(5647):1009–1014

Laisk A, Eichelmann H, Oja V, Talts E, Scheibe R (2007) Rates and roles of cyclic and alternative electron flow in potato leaves. Plant Cell Physiol 48(11):1575–1588

Lascano H, Casano L, Martin M, Sabater B (2003) The activity of the chloroplastic Ndh complex is regulated by phosphorylation of the NDH-F subunit. Plant Physiol 132:256–262

Laureau C, De Paepe R, Latouche G, Moreno-Chacon M, Finazzi G, Kuntz M, Cornic G, Streb P (2013) Plastid terminal oxidase (PTOX) has the potential to act as a safety valve for excess excitation energy in the alpine plant species Ranunculus glacialisL. Plant Cell Environ 36(7):1296–1310. https://doi.org/10.1111/pce.12059

Lepetit B, Goss R, Jakob T, Wilhelm C (2012) Molecular dynamics of the diatom thylakoid membrane under different light conditions. Photosynth Res 111(1–2):245–257. https://doi.org/10.1007/s11120-011-9633-5

Li XP, Muller-Moule P, Gilmore AM, Niyogi KK (2002) PsbS-dependent enhancement of feedback de-excitation protects photosystem II from photoinhibition. Proc Natl Acad Sci U S A 99(23):15222–15227

Li XP, Gilmore AM, Caffarri S, Bassi R, Golan T, Kramer D, Niyogi KK (2004) Regulation of photosynthetic light harvesting involves intrathylakoid lumen pH sensing by the PsbS protein. J Biol Chem 279(22):22866–22874

Livingston AK, Cruz JA, Kohzuma K, Dhingra A, Kramer DM (2010a) An Arabidopsis mutant with high cyclic electron flow around photosystem I (*hcef*) involving the NDH complex. Plant Cell 22:221–233

Livingston AK, Kanazawa A, Cruz JA, Kramer DM (2010b) Regulation of cyclic electron transfer in C3 plants: differential effects of limiting photosynthesis at rubisco and glyceraldehyde-3-phosphate dehydrogenase. Plant Cell Environ 33(11):1779–1788

Long SP, Humphries S, Falkowski PG (1994) Photoinhibition of photosynthesis in nature. Annu Rev Plant Physiol 45:633–662. https://doi.org/10.1146/Annurev.Pp.45.060194.003221

Lu B, Xu C, Awai K, Jones AD, Benning C (2007) A small ATPase protein of Arabidopsis, TGD3, involved in chloroplast lipid import. J Biol Chem 282(49):35945–35953. https://doi.org/10.1074/jbc.M704063200

Lucker B, Kramer DM (2013) Regulation of cyclic electron flow in *Chlamydomonas reinhardtii* under fluctuating carbon availability. Photosynth Res 117:449–459. https://doi.org/10.1007/s11120-013-9932-0

Mangan N, Brenner M (2014) Systems analysis of the CO2 concentrating mechanism in cyanobacteria. elife 3:e02043. https://doi.org/10.7554/eLife.02043

Marchant J, Heydarizadeh P, Schoefs B, Spetea C (2018) Ion and metabolite transport in the chloroplast of algae: lessons from land plants. Cell Mol Life Sci 75(12):2153–2176. https://doi.org/10.1007/s00018-018-2793-0

McDonald AE, Ivanov AG, Bode R, Maxwell DP, Rodermel SR, Huner NP (2011) Flexibility in photosynthetic electron transport: the physiological role of plastoquinol terminal oxidase (PTOX). Biochim Biophys Acta 1807(8):954–967. https://doi.org/10.1016/j.bbabio.2010.10.024

Monne M, Daddabbo L, Gagneul D, Obata T, Hielscher B, Palmieri L, Miniero DV, Fernie AR, Weber APM, Palmieri F (2018) Uncoupling proteins 1 and 2 (UCP1 and UCP2) from Arabidopsis thaliana are mitochondrial transporters of aspartate, glutamate, and dicarboxylates. J Biol Chem 293(11):4213–4227. https://doi.org/10.1074/jbc.RA117.000771

Müller P, Li X-P, Niyogi KK (2001) Non-photochemical quenching. A response to excess light energy. Plant Physiology 125: 1558-1566

Munekage Y, Hashimoto M, Miyake C, Tomizawa K, Endo T, Tasaka M, Shikanai T (2004) Cyclic electron flow around photosystem I is essential for photosynthesis. Nature 429(6991):579–582

Murchie EH, Niyogi KK (2011) Manipulation of photoprotection to improve plant photosynthesis. Plant Physiol 155(1):86–92. https://doi.org/10.1104/pp.110.168831

Nawrocki WJ, Bailleul B, Cardol P, Rappaport F, Wollman FA, Joliot P (2019) Maximal cyclic electron flow rate is independent of PGRL1 in Chlamydomonas. Biochim Biophys Acta Bioenerg 1860:425–432. https://doi.org/10.1016/j.bbabio.2019.01.004

Nelson N, Sacher A, Nelson H (2002) The significance of molecular slips in transport systems. Nat Rev Mol Cell Biol 3(11):876–881. https://doi.org/10.1038/nrm955

Nishiyama Y, Allakhverdiev SI, Murata N (2006) A new paradigm for the action of reactive oxygen species in the photoinhibition of photosystem II. BBA-Bioenergetics 1757(7):742–749

Niyogi KK, Li X-P, Rosenberg V, Jung H-S (2004) Is PsbS the site of non-photochemical quenching in photosynthesis? J Exp Bot 56:375–382

Noctor G, Foyer C (1998) A re-evaluation of the ATP: NADPH budget during C3 photosynthesis: a contribution from nitrate assimilation and its associated respiratory activity? J Exp Bot 49:1895–1908

Okegawa Y, Tsuyama M, Kobayashi Y, Shikanai T (2005) The pgr1 mutation in the Rieske subunit of the cytochrome b6f complex does not affect PGR5-dependent cyclic electron transport around photosystem I. J Biol Chem 280(31):28332–28336. https://doi.org/10.1074/jbc.M505703200

Ort DR, Yocum CF (1996) Light reactions of oxygenic photosynthesis. In: Ort DR, Yocum CF (eds) Oxygenic photosynthesis: the light reactions. Kluwer Academic Publishers, Dordrecht, pp 1–9

Peers G, Truong TB, Ostendorf E, Busch A, Elrad D, Grossman AR, Hippler M, Niyogi KK (2009) An ancient light-harvesting protein is critical for the regulation of algal photosynthesis. Nature 462(7272):518–521. https://doi.org/10.1038/nature08587

Peltier G, Tolleter D, Billon E, Cournac L (2010) Auxiliary electron transport pathways in chloroplasts of microalgae. Photosynth Res 106(1–2):19–31. https://doi.org/10.1007/s11120-010-9575-3

Pfeil BE, Schoefs B, Spetea C (2014) Function and evolution of channels and transporters in photosynthetic membranes. Cell Mol Life Sci 71(6):979–998. https://doi.org/10.1007/s00018-013-1412-3

Pottosin II, Schönknecht G (1996) Ion channel permeable for divalent and monovalent cations in native spinach thylakoid membranes. J Membr Biol 152:223–233

Prihoda J, Tanaka A, de Paula WBM, Allen JF, Tirichine L, Bowler C (2012) Chloroplast-mitochondria cross-talk in diatoms. J Exp Bot 63(4):1543–1557. https://doi.org/10.1093/jxb/err441

Pringault O, de Wit R, Camoin G (2005) Irradiance regulation of photosynthesis and respiration in modern marine microbialites built by benthic cyanobacteria in a tropical lagoon (New Caledonia). Microb Ecol 49(4):604–616. https://doi.org/10.1007/s00248-004-0102-y

Quiles MJ (2006) Stimulation of chlororespiration by heat and high light intensity in oat plants. Plant Cell Environ 29(8):1463–1470

Ramzan R, Staniek K, Kadenbach B, Vogt S (2010) Mitochondrial respiration and membrane potential are regulated by the allosteric ATP-inhibition of cytochrome c oxidase. Biochim Biophys Acta 1797(9):1672–1680. https://doi.org/10.1016/j.bbabio.2010.06.005

Ranjbar Choubeh R, Wientjes E, Struik PC, Kirilovsky D, van Amerongen H (2018) State transitions in the cyanobacterium Synechococcus elongatus 7942 involve reversible quenching of the photosystem II core. Biochim Biophys Acta Bioenerg 1859:1059–1066. https://doi.org/10.1016/j.bbabio.2018.06.008

Raven JA (2011) The cost of photoinhibition. Physiol Plant 142:87–104. https://doi.org/10.1111/j.1399-3054.2011.01465.x

Rosso D, Ivanov AG, Fu A, Geisler-Lee J, Hendrickson L, Geisler M, Stewart G, Krol M, Hurry V, Rodermel SR, Maxwell DP, Huner NPA (2006) IMMUTANS does not act as a stress-induced safety valve in the protection of the photosynthetic apparatus of arabidopsis during steady-state photosynthesis. Plant Physiol 142(2):574–585. https://doi.org/10.1104/pp.106.085886

Rumeau D, Peltier G, Cournac L (2007) Chlororespiration and cyclic electron flow around PSI during photosynthesis and plant stress response. Plant Cell Environ 30:1041–1051

Rutherford AW, Osyczka A, Rappaport F (2012) Back-reactions, short-circuits, leaks and other energy wasteful reactions in biological electron transfer: redox tuning to survive life in O-2. FEBS Lett 586(5):603–616. https://doi.org/10.1016/J.Febslet.2011.12.039

Sacksteder CA, Kanazawa A, Jacoby ME, Kramer DM (2000) The proton to electron stoichiometry

of steady-state photosynthesis in living plants: a proton-pumping Q-cycle is continuously engaged. Proc Natl Acad Sci U S A 97:14283–14288

Scheibe R (2004) Malate valves to balance cellular energy supply. Physiol Plant 120(1):21–26

Scheller HV (1996) In vitro cyclic electron transport in barley thykaloids follows two independent pathways. Plant Physiol 110:187–194

Scherer S, Almon H, Boger P (1988) Interaction of photosynthesis, respiration and nitrogen fixation in cyanobacteria. Photosynth Res 15(2):95–114. https://doi.org/10.1007/BF00035255

Schonfeld M, Neumann J (1977) Proton conductance of the thylakoid membrane: modulation by light. FEBS Lett 73(1):51–54

Schönknecht G, Hedrich R, Junge W, Raschke K (1988) A voltage-dependent chloride channel in the photosynthetic membrane of a higher plant. Nature 336:589–592

Shikanai T (2007) Cyclic electron transport around photosystem I: genetic approaches. Annu Rev Plant Biol 58:199–217

Shikanai T (2010) Regulation of photosynthetic electron transport. In: Rebeiz C, Benning C, Bohnert H et al (eds) Chloroplast: basics and applications, Advances in photosynthesis and respiration, vol 31. Springer, Dordrecht, pp 347–362

Shikanai T, Yamamoto H (2017) Contribution of cyclic and pseudo-cyclic electron transport to the formation of proton motive force in chloroplasts. Mol Plant 10(1):20–29. https://doi.org/10.1016/j.molp.2016.08.004

Shimakawa G, Shaku K, Miyake C (2016) Oxidation of P700 in photosystem I is essential for the growth of cyanobacteria. Plant Physiol 172(3):1443–1450. https://doi.org/10.1104/pp.16.01227

Sonoike K (2010) Photoinhibition of photosystem I. Physiol Plant 142:56–64. https://doi.org/10.1111/j.1399-3054.2010.01437.x

Spetea C, Hidge E, Vass I (1997) Low pH accelerates light-induced damage of photosystem II by enhancing the probability of the donor-side mechanism of photoinhibition. Biochim Biophys Acta 1318:275–283

Spetea C, Szabo I, Kunz HH (2016) Editorial: ion transport in chloroplast and mitochondria physiology in green organisms. Front Plant Sci 7:2003. https://doi.org/10.3389/fpls.2016.02003

Spetea C, Herdean A, Allorent G, Carraretto L, Finazzi G, Szabo I (2017) An update on the regulation of photosynthesis by thylakoid ion channels and transporters in Arabidopsis. Physiol Plant 161(1):16–27. https://doi.org/10.1111/ppl.12568

Stephan AB, Kunz HH, Yang E, Schroeder JI (2016) Rapid hyperosmotic-induced Ca2+ responses in Arabidopsis thaliana exhibit sensory potentiation and involvement of plastidial KEA transporters. Proc Natl Acad Sci U S A 113(35):E5242–E5249. https://doi.org/10.1073/pnas.1519555113

Stepien P, Johnson GN (2009) Contrasting responses of photosynthesis to salt stress in the glycophyte Arabidopsis and the halophyte thellungiella: role of the plastid terminal oxidase as an alternative electron sink. Plant Physiol 149(2):1154–1165. https://doi.org/10.1104/pp.108.132407

Stepien P, Johnson GN (2018) Plastid terminal oxidase requires translocation to the grana stacks to act as a sink for electron transport. Proc Natl Acad Sci U S A 115(38):9634–9639. https://doi.org/10.1073/pnas.1719070115

Stock D, Leslie AG, Walker JE (1999) Molecular architecture of the rotary motor in ATP synthase. Science 286(5445):1700–1705

Strand DD, Kramer DM (2014) Control of non-photochemical exciton quenching by the proton circuit of photosynthesis. In: Demmig-Adams B, Garab G, Adams W III, Govindjee (eds) Non-photochemical quenching and energy dissipation in plants, algae and cyanobacteria, Advances in photosynthesis, vol XXXVIII. Springer, Dordrecht, pp 387–408

Strand DD, Livingston AK, Kramer DM (2013) Do state transitions control cef1 in higher plants? In: Kuang T, Lu C, Zhang L (eds) Photosynthesis for food, fuel and future. Springer, Beijing, pp 286–289

Strand DD, Livingston AK, Satoh-Cruz M, Froehlich JE, Maurino VG, Kramer DM (2015) Activation of cyclic electron flow by hydrogen peroxide in vivo. Proc Natl Acad Sci U S A 112:5539–5544

Strand DD, Fisher N, Davis GA, Kramer DM (2016a) Redox regulation of the antimycin A sensitive pathway of cyclic electron flow around photosystem I in higher plant thylakoids. Biochim Biophys Acta 1857:1–6. https://doi.org/10.1016/j.bbabio.2015.07.012

Strand DD, Fisher N, Kramer DM (2016b) Distinct energetics and regulatory functions of the two major cyclic electron flow pathways in chloroplasts. In: Kirchhoff H (ed) Chloroplasts: current research and future trends, vol 978-1-910190-47-0. Horizon Press, Norforlfk

Strand DD, Livingston AK, Satoh-Cruz M, Koepke T, Enlow HM, Fisher N, Froehlich JE, Cruz JA, Minhas D, Hixson KK, Kohzuma K, Lipton M, Dhingra A, Kramer DM (2016c) Defects in the expression of chloroplast proteins leads to H2O2 accumula-

tion and activation of cyclic electron flow around photosystem I. Front Plant Sci 7:2073. https://doi.org/10.3389/fpls.2016.02073

Strand DD, Fisher N, Kramer DM (2017) The higher plant plastid complex I (NDH) is a thermodynamically reversible proton pump that increases ATP production by cyclic electron flow around photosystem I. J Biol Chem 292(28):11850–11860

Streb P, Josse EM, Gallouet E, Baptist F, Kuntz M, Cornic G (2005) Evidence for alternative electron sinks to photosynthetic carbon assimilation in the high mountain plant species Ranunculus glacialis. Plant Cell Environ 28(9):1123–1135

Stroebel D, Choquet Y, Popot JL, Picot D (2003) An atypical haem in the cytochrome b(6)f complex. Nature 426(6965):413–418

Sweetlove L, Lytovchenko A, Morgan M, Nunes-Nesi A, Taylor N, Baxter C, Eickmeier I, Fernie A (2006) Mitochondrial uncoupling protein is required for efficient photosynthesis. Proc Natl Acad Sci 103:19587–19592

Takahashi H, Clowez S, Wollman FA, Vallon O, Rappaport F (2013) Cyclic electron flow is redox-controlled but independent of state transition. Nat Commun 4:1954. https://doi.org/10.1038/ncomms2954

Takizawa K, Kanazawa A, Cruz JA, Kramer DM (2007) In vivo thylakoid proton motive force. Quantitative non-invasive probes show the relative lumen pH-induced regulatory responses of antenna and electron transfer. Biochim Biophys Acta 1767:1233–1244

Takizawa K, Cruz JA, Kramer DM (2008) Depletion of stromal inorganic phosphate induces high 'energy-dependent' antenna exciton quenching (q_E) by decreasing proton conductivity at CF_O-CF_1 ATP synthase. Plant Cell Environ 31:235–243

Terashima M, Petroutsos D, Hudig M, Tolstygina I, Trompelt K, Gabelein P, Fufezan C, Kudla J, Weinl S, Finazzi G, Hippler M (2012) Calcium-dependent regulation of cyclic photosynthetic electron transfer by a CAS, ANR1, and PGRL1 complex. Proc Natl Acad Sci U S A 109(43):17717–17722. https://doi.org/10.1073/pnas.1207118109

Tokutsu R, Minagawa J (2013) Energy-dissipative supercomplex of photosystem II associated with LHCSR3 in Chlamydomonas reinhardtii. Proc Natl Acad Sci U S A 110(24):10016–10021. https://doi.org/10.1073/pnas.1222606110

Trouillard M, Shahbazi M, Moyet L, Rappaport F, Joliot P, Kuntz M, Finazzi G (2012) Kinetic properties and physiological role of the plastoquinone terminal oxidase (PTOX) in a vascular plant. BBA-Bioenergetics 1817(12):2140–2148. https://doi.org/10.1016/j.bbabio.2012.08.006

Trubitsin BV, Ptushenko VV, Koksharova OA, Mamedov MD, Vitukhnovskaya LA, Grigor'ev IA, Semenov AY, Tikhonov AN (2005) EPR study of electron transport in the cyanobacterium Synechocystis sp. PCC 6803: oxygen-dependent interrelations between photosynthetic and respiratory electron transport chains. Biochim Biophys Acta 1708(2):238–249. https://doi.org/10.1016/j.bbabio.2005.03.004

Turina P, Samoray D, Graber P (2003) H+/ATP ratio of proton transport-coupled ATP synthesis and hydrolysis catalysed by CF0F1-liposomes. EMBO J 22(3):418–426

Tyystjärvi E, Aro E (1996) The rate constant of photoinhibition, measured in lincomycin- treated leaves, is directly proportional to light intensity. Proc Natl Acad Sci U S A 93(5):2213–2218

van Gorkom HJ (1996) Electroluminescence. Photosynth Res 48:107–116

van Wijk KJ (2004) Plastid proteomics. Plant Physiol Biochem 42(12):963–977. https://doi.org/10.1016/j.plaphy.2004.10.015

Vass I, Styring S, Hundal T, Koivuniemi A, Aro E, Andersson B (1992) Reversible and irreversible intermediates during photoinhibition of photosystem II: stable reduced QA species promote chlorophyll triplet formation. Proc Natl Acad Sci U S A 89(4):1408–1412

Vermaas WF (2001) Photosynthesis and respiration in cyanobacteria. Encyclopedia of Life Sciences. https://doi.org/10.1038/npg.els.0001670

Verrier PJ, Bird D, Burla B, Dassa E, Forestier C, Geisler M, Klein M, Kolukisaoglu U, Lee Y, Martinoia E, Murphy A, Rea PA, Samuels L, Schulz B, Spalding EJ, Yazaki K, Theodoulou FL (2008) Plant ABC proteins–a unified nomenclature and updated inventory. Trends Plant Sci 13(4):151–159. https://doi.org/10.1016/j.tplants.2008.02.001

Wang Y, Duanmu D, Spalding MH (2011) Carbon dioxide concentrating mechanism in Chlamydomonas reinhardtii: inorganic carbon transport and CO2 recapture. Photosynth Res 109(1–3):115–122. https://doi.org/10.1007/s11120-011-9643-3

Wilhelm C, Buchel C, Fisahn J, Goss R, Jakob T, LaRoche J, Lavaud J, Lohr M, Riebesell U, Stehfest K, Valentin K, Kroth PG (2006) The regulation of carbon and nutrient assimilation in diatoms is significantly different from green algae. Protist 157(2):91–124. https://doi.org/10.1016/j.protis.2006.02.003

Wilson A, Ajlani G, Verbavatz JM, Vass I, Kerfeld CA, Kirilovsky D (2006) A soluble carotenoid protein involved in phycobilisome-related energy dissipation in cyanobacteria. Plant Cell 18(4):992–1007. https://doi.org/10.1105/tpc.105.040121

Witt HT, Zickler A (1974) Vectorial electron flow across the thylakoid membrane, further evidence by kinetic measurements with an electrochromic and electrical method. FEBS Lett 39(2):205–208

Zaks J, Amarnath K, Kramer DM, Niyogi KK, Fleming GR (2012) A kinetic model of rapidly reversible nonphotochemical quenching. Proc Natl Acad Sci U S A 109(39):15757–15762

Zhang H, Primak A, Cape J, Bowman MK, Kramer DM, Cramer WA (2004) Characterization of the high-spin heme x in the cytochrome b6f complex of oxygenic photosynthesis. Biochemistry 43(51):16329–16336. https://doi.org/10.1021/bi048363p

Zhang R, Cruz JA, Kramer DM, Magallanes-Lundback M, DellaPenna D, Sharkey TD (2009) Heat stress reduces the pH component of the transthylakoid proton motive force in light-adapted intact tobacco leaves. Plant Cell Environ 32:1538–1547

Zhang R, Kramer DM, Cruz JA, Struck KR, Sharkey TD (2011) The effects of moderately high temperature on zeaxanthin accumulation and decay. Photosynth Res 108:171–181. https://doi.org/10.1007/s11120-011-9672-y

Zhang P, Eisenhut M, Brandt AM, Carmel D, Silen HM, Vass I, Allahverdiyeva Y, Salminen TA, Aro EM (2012) Operon flv4-flv2 provides cyanobacterial photosystem II with flexibility of electron transfer. Plant Cell 24(5):1952–1971. https://doi.org/10.1105/tpc.111.094417

Chapter 13

Photoinhibition of Photosystem II in Phytoplankton: Processes and Patterns

Douglas A. Campbell*
Department of Biology, Mount Allison University, Sackville, NB, Canada

and

João Serôdio
Department of Biology and CESAM – Centre for Environmental and Marine Studies, University of Aveiro, Aveiro, Portugal

I. Introduction: Scope & Terms

Photoinhibition of photosynthesis in phytoplankton has been long studied (Kok 1956; Osmond and Chow 1988) using diverse model organisms and experimental approaches. The term photoinhibition is used differently depending upon context. When modelling light response curves photoinhibition is used for short-term light- and time- (Henley 1993; Perkins et al. 2006) dependent down regulations of photosynthesis or electron transport rate, as for example captured in the β^{ETR} parameter (Webb et al. 1974; Platt et al. 1981). This phenomenological parameterization is mechanistically agnostic, although under a given circumstance a particular mechanism may be known or suspected to dominate the response, and in some cases authors conflate assumed mechanisms with measured phenomena.

Photoinhibition is used more narrowly to describe a light-dependent loss of photosynthetic activity (Kok 1956) modelled as the outcome of a light dependent inactivation and a counteracting reactivation or repair process

*Author for correspondence, e-mail: dcampbell@mta.ca

A. W. D. Larkum et al. (eds.), *Photosynthesis in Algae: Biochemical and Physiological Mechanisms*, Advances in Photosynthesis and Respiration 45, https://doi.org/10.1007/978-3-030-33397-3_13

(Ross et al. 2008; Keren and Krieger-Liszkay 2011). This phenomenon is now understood as the outcome of the balance between photoinactivation of Photosystem II (PSII) and the counteracting repair through replacement of protein subunits (Kyle et al. 1984; Greer et al. 1986; Keren and Krieger-Liszkay 2011; Nishiyama and Murata 2014). In this chapter we use 'photoinhibition' as the net outcome of 'photoinactivation' and counteracting 'repair', all with respect to PSII (Campbell and Tyystjärvi 2012), while acknowledging other usages in other contexts.

All phytoplankters carry a pool of PSII complexes, which are structurally and functionally highly conserved across taxa (Campbell et al. 2003; Falkowski et al. 2008). These PSII mediate the photochemical extraction of electrons from water, with concomitant release of oxygen. Aside from specialized desert crust chlorophytes (Treves et al. 2013), in all oxygenic photoautotrophs studied to date PSII shows susceptibility to light-dependent photoinactivation, which is countered by a process of protein subunit removal and replacement (Silva et al. 2003). The photoinactivation and counteracting repair of PSII imposes direct costs upon energy (Murata et al. 2007; Miyata et al. 2012; Murata and Nishiyama 2018) and protein metabolism (Campbell et al. 2013; Li et al. 2015) but also opportunity costs when down-regulation of PSII under transient conditions (Oliver et al. 2003) results in a lingering loss of photosynthetic capacity (Raven 2011).

The currently extant phytoplankton include representatives from most of the major eukaryotic lineages, along with cyanobacteria (Falkowski et al. 2004). Across this vast genomic and cellular diversity PSII functions within a wide range of membrane organizations, metabolic and pigment contexts (Neilson and Durnford 2010; Lepetit et al. 2011; Bailleul et al. 2015; Rast et al. 2015) (Chaps. 1, 2 and 3, this volume). In this review we first survey approaches and pitfalls of measuring PSII photoinactivation and repair processes in phytoplankton. We then review the diversity of PSII photoinactivation and repair patterns across the studied evolutionary, structural and ecological diversity of phytoplankton lineages. In particular we review the evidence around outstanding issues including:

1. Do quantum yields for PSII photoinactivation vary with growth irradiance or other environmental conditions, or are they taxonomically defined quantitative traits.
2. Do PSII repair rates and responses vary systematically across phytoplankton
3. Do these photophysiological parameters systematically relate to habitat, taxonomy or photosynthetic architecture?

We place the processes of photoinactivation and repair of PSII in phytoplankton in the wider context of photoacclimation, because in many cases the fastest photoacclimation strategy is rapid change in the cellular content of PSII. We emphasize responses to changes in photosynthetically active radiation, although ultraviolet radiation is also a significant driver of photoinhibition (Vassiliev et al. 1994; Heraud and Beardall 2000; Litchman et al. 2002; Tyystjärvi 2008, 2013; Hakala-Yatkin et al. 2010; Neale et al. 2014; Neale and Thomas 2016). We draw concepts from the homologous processes in the plant literature, but emphasize the biooptical, biophysical, and metabolic contexts that distinguish phytoplankton photophysiology. Our coverage is biased towards our experience with mechanism-oriented culture studies, while recognizing the long history of modelling and field studies (Schofield et al. 1995; Platt et al. 1981; Litchman et al. 2002; Ross et al. 2008; Neale and Thomas 2016).

II. Mechanisms of Photoinactivation

Extensive experimentation and debate shows that *in vivo* photoinactivation of PSII can be driven by two, non-exclusive, mechanistic paths, which can occur in parallel in the same

cell (Vass 2012; Tyystjärvi 2013; Murphy et al. 2017). The conditional balance between the paths generates distinct implications for analyses and parameterization (Oguchi et al. 2011; Campbell and Tyystjärvi 2012; He et al. 2015). Firstly, artificial manganese cluster models of the water oxidizing subcomplex of PSII have a strong absorption cross section in the UV and blue regions of the spectra (Tyystjärvi 2008). Absorbance of a photon by the natural Mn cluster can disrupt the water splitting function. Subsequent excitation of the P_{680} of PSII through the photosynthetic antenna then leads to photooxidative damage to PSII when re-reduction from water is lost. Photoinactivation through this path shows an action spectra peaking in the UV with a blue tail extending into the PAR region, and only marginal susceptibility to photoinactivation driven by red light. The susceptibility to photoinactivation shows only weak, secondary dependence upon the size or spectra of the light harvesting antenna serving PSII, because the primary photoinactivation is through a direct hit to the Mn cluster. Biooptical properties of cells can, however, alter the screening of the Mn cluster from photoinactivation, generating a size-dependence in primary susceptibility to photoinactivation (Key et al. 2010). This path wholly dominates photoinactivation driven by UVB (Tyystjärvi 2008), and likely dominates photoinactivation in phytoplankton under low to moderate light regimes (Murphy et al. 2017), particularly since the sub-surface spectral environment is biased towards blue and green, and away from red.

Alternatively, photochemical closure of PSII by excitation delivered through the light harvesting antenna can increase the lifetime of excited states, leading to increased production of reactive oxygen which can, in turn, inactive PSII photochemistry. This path shows a dependence upon excitation pressure (Huner et al. 1998; Murphy et al. 2017); the balance between incoming excitation delivered through the photosynthetic antenna, excitation dissipation and photochemical flux away from PSII. The photoinactivation action spectra through this path mirrors the photosynthetic action spectra (Soitamo et al. 2017), since both are driven through absorption of photons by the antennae. In optically simple picocyanobacteria we distinguished conditionally dependent contributions from both of these paths (Murphy et al. 2017). Under red light the quantum yield for photoinactivation, on the basis of excitation delivered to PSII ($\Phi_{I\ PSII}$) showed an intercept near 0 at excitation pressure of 0, with all PSII open. Photoinactivation then increased linearly with PSII closure driven by increasing light. Thus red light showed no direct toxicity to PSII; inactivation was a by-product of PSII closure driven by absorbance through the photosynthetic antenna. In contrast, under blue light a significant susceptibility to photoinactivation remained even when all PSII were open at excitation pressure of 0. Blue light thus shows a direct toxicity to PSII, even in the absence of PSII closure. As PSII closed under increasing blue light susceptibility to photoinactivation increased, with a slope equal to that observed under red light (Fig. 13.1). Induction of non-photochemical dissipation of excess excitation to lower excitation pressure can protect against photoinactivation mediated through excitation pressure, but should not alter the susceptibility to direct hit photoinactivation of the Mn cluster. Elegant work on leaves (Oguchi et al. 2011; He et al. 2015) supports these interpretations.

Note that in natural settings these analyses are complicated because photoinactivation of PSII occurs in parallel with counter-acting PSII repair, and with down-regulation through induction of non-photochemical quenching. An extensive series of studies (Allakhverdiev and Murata 2004; Nishiyama et al. 2005; Murata et al. 2007, 2012; Nishiyama and Murata 2014) demonstrate that the repair of photoinactivated PSII is itself susceptible to inactivation by Reactive Oxygen Species (ROS). Thus under natural

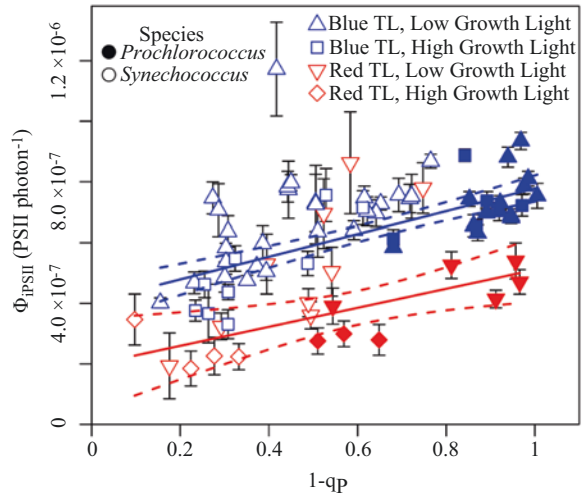

Fig. 13.1. $\Phi_{I\,PSII}$ versus excitation pressure on Photosystem II in Picocyanobacteria *Synechococcus sp.* WH8102 (open symbols) and *Prochlorococcus marinus* MED4 (closed symbols) fell on a common regression for $\Phi_{I\,PSII}$ (PSII photon^{-1}) measured under red light treatment (solid red line, slope = 3.1 42 × 10^{-7} ± 1.110 × 10^{-7}, intercept = 1.968 × 10^{-7} ± 7.308 × 10^{-8}, R^2 = 0.2968, dotted red lines denote 95% confidence intervals). *Synechococcus sp.* WH8102 and *Prochlorococcus marinus* MED4 also fell on a common regression for $\Phi_{I\,PSII}$ measured under blue light treatment (solid blue line, slope = 3.731 × 10^{-7} ± 4.921 × 10^{-8}, intercept = 4.046 × 10^{-7} ± 3.458 × 10^{-8}, R^2 = 0.5156, dotted red lines denote 95% confidence intervals on the regressions). Species (open symbols, *Synechococcus*; closed symbols, *Prochlorococcus*) had no statistically significant effect on the regressions of $\Phi_{I\,PSII}$ versus excitatation pressure, nor did low (upward or downward triangles) versus high (squares or diamonds) growth light when either species or growth light was included in a linear model of the data as a binary interaction term. (Reproduced from Murphy et al. 2017)

conditions photoinhibition (Lesser et al. 1994; Litchman et al. 2002; Bouchard et al. 2005a, b) can often be attributed primarily to ROS dependent inactivation of PSII repair, rather than to blue light or ROS dependent direct photoinactivation of PSII itself. Furthermore, non-photochemical excitation dissipation may serve primarily to protect the PSII repair process (Murata et al. 2012), rather than to protect PSII itself from photoinactivation (Havurinne and Tyystjärvi 2017) . Furthermore the induction or suppression of particular ROS defence paths can lead to compensatory hormetic changes in resistance to photoinactivation, through activation of other dissipatory or quenching paths (Hakkila et al. 2014)

III. Measurement and Parameterization of PSII Photoinactivation and Counteracting PSII Repair

Photoinactivation and counteracting repair have been tracked using different metrics of PSII function, applied over different time scales, sequences of light levels and spectral regimes. In all cases quantifying the photoinactivation of PSII in the narrow sense requires discrimination of gross photoinactivation of PSII from the counter-acting process of PSII repair, and from over-lapping processes of down-regulation of PSII function through induction of non-photochemical quenching mechanisms (Ruban 2016).

Depending upon the study organism and the experimental approach, these processes may be distinguished through kinetic analyses under step changes in light (Kok 1956; Oliver et al. 2003; Serôdio et al. 2017). For example, cells can be exposed to a level of light so high that the instantaneous repair rate is negligible in comparison to photoinactivation. Then a subsequent low light or dark period can be used to track recovery with the instantaneous rate of photoinactivation nearly negligible (Serôdio et al. 2017). The practicality of such purely kinetic analyses can be limited by overlapping mechanisms such as induction of sustained phases of non-photochemical quenching. Alternately inhibitor treatments to block chloroplastic (or cyanobacterial) protein synthesis can be used to block the synthesis of PSII subunits (Bilger and Björkman 1990; Heraud and Beardall 2000; Bachmann et al. 2004; Aro et al. 2005; Murata et al. 2007; Ragni et al. 2008) and thereby pre-empt PSII repair. Many studies assemble input from complementary experimental approaches (Lavaud et al. 2016; Ni et al. 2017). Inhibiting chloroplast (or cyanobacterial) protein synthesis places a practical limit on the duration of light treatment experiments to track photoinactivation in the absence of repair, because inhibiting protein synthesis is ultimately lethal within a cellular generation or less. This in turn places limits on the practical range of irradiances that can be tested because slow photoinactivation under low light can result in treatments so slow as to be lethal before generating a detectable change resulting from PSII photoinactivation.

Photosynthetic oxygen evolution is an integrative measure of the activity of PSII, and net, or inferred gross, oxygen evolution under light saturating conditions has been used to track changes in PSII activity (Nagy et al. 1995). Steady state oxygen evolution has the advantage of being an integrative measure of the photosynthetic metabolism of the cell. For mechanistic studies, however, this integrative nature means that steady state oxygen evolution can respond to multiple limiting factors depending upon the exact circumstances. Therefore changes in steady oxygen evolution do not necessarily reflect changes in the inactivation of PSII. Alternately electron flow from water through PSII to an artificial electron acceptor can be measured by monitoring oxygen evolution (Soitamo et al. 2017; Havurinne and Tyystjärvi 2017).

A well established approach to quantitation of [$PSII_{active}$] (Chow et al. 1989; Suggett et al. 2009; Murphy et al. 2016) uses a train of single turnover saturating flashes to provoke repeated charge separations in PSII, with the time between flashes long enough to allow clearance of the photochemical electron from PSII (>1 ms), but short enough so that the oxygen evolving complex does not slip back an oxidation state between sequential flashes (<1 s) (Keren et al. 1997). In principle, and with caution in practice, each 4 flashes will then provoke release of 1 O_2 from each $PSII_{active}$. The content of [$PSII_{active}$] can then be estimated from the rate of O_2 evolution per saturating, single turnover flash. The method is suitable for start and end point measures of [$PSII_{active}$], or for comparisons of [$PSII_{active}$] across cultures or taxa, but is generally too slow for repeated kinetic measures within a time course. The sensitivity is limited so the measures must be conducted at cell densities higher than typically achieved for marine cultures. Correcting for background rates of respiration can be problematic unless isotopic discrimination is achieved by using a membrane inlet mass spectrophotometer (MIMS) (Suggett et al. 2009).

The widely used chlorophyll fluorescence induction parameter (van Kooten and Snel 1990; Kalaji et al. 2017):

$$F_V / F_M = \left(F_M - F_0\right) / F_M$$

is the mostly widely deployed metric to track changes in PSII function, and to thereby infer PSII photoinactivation and repair pro-

cesses. F_V/F_M is taken to represent the maximum quantum yield of PSII (van Kooten and Snel 1990). F_V/F_M can be measured rapidly, repeatedly, and fairly non-invasively (Tyystjarvi and Vass 2004), with an individual determination possible within milliseconds using single turnover induction approaches such as the Fast Repetition & Relaxation (FRR) fluorometer (Kolber et al. 1998) or within seconds using multiple turnover inductions as with a Pulse Amplitude Modulated fluorometer (Schreiber and Klughammer 2013). Many instruments are available, spanning wide ranges of precision, sensitivity and spatial integration from single cell responses to whole culture or mesocosm measures. Alternately, the parameter $1/F_O - 1/F_M$ can be extracted from the same fluorescence signals used to generate F_V/F_M, as a measure of the rate constant of excitation trapping by the PSII reaction centre (Havaux et al. 1991; Walters and Horton 1993; Park et al. 1995). Under many circumstances changes in F_V/F_M or $1/F_O - 1/F_M$ correlate with measures of the content of $[PSII_{active}]$ (Park et al. 1995; Wu et al. 2012). Both measures are intrinsically normalized and, to a first approximation, are not altered by changes in cell suspension density, nor by changes in the exact optical configuration of the measuring system.

Although widely used, both F_V/F_M and $1/F_O - 1/F_M$ suffer methodological and conceptual drawbacks and limitations, which are often under-appreciated. Firstly, the underlying interpretations of these parameters assume that the F_O, F_V, and thus F_M (= $F_O + F_V$) signals originate exclusively from PSII (van Kooten and Snel 1990; Kramer et al. 2004). This simplifying assumption is widely and variably broken across phytoplankters (Campbell et al. 1998; Simis et al. 2012) because, depending upon the excitation and emission wavebands used for fluorescence detection, fluorophores including dissolved organic matter, phycobiliproteins (if present) and PS I make significant contributions to the measured F_O. Although F_V is derived quite cleanly from $[PSII_{active}]$ the non-PSII contributions to F_O distort the interpretations of both F_V/F_M and $1/F_O - 1/F_M$. Emerging multi-spectral fluorometers are beginning to address these issues (Simis et al. 2012; Schreiber and Klughammer 2013; Schuback et al. 2016) by supporting better discrimination of fluorescence emitted from PSII from other fluorophors in the cell. The diversity of pigment contents across phytoplankton means there is, however, no generalized protocol to cleanly extract a pure PSII fluorescence signal.

Secondly the operational definition of F_M is problematic in many phytoplankton. Both cyanobacteria (Campbell et al. 1998) and diatoms (Serôdio et al. 2005) can show, for different mechanistic reasons, progressive down regulation of F_M under darkness, compared to levels measured under low to moderate light. Furthermore diatoms (Wu et al. 2012; Lavaud and Goss 2014), and probably other phytoplankters, show induction of sustained forms of non-photochemical quenching that can persist under subsequent dark or low light relaxation periods. From a functional perspective of estimating productivity (Raven 2011) these forms of sustained down regulation of PSII can perhaps be considered ecophysiologically similar to actual photoinactivation. But for mechanistic studies they should be distinguished because reversal of sustained non-photochemical quenching does not involve proteolytic removal and translational replacement of PSII subunits, but rather changes in the functional organization of existing antenna or PSII units (Ivanov et al. 2008; Gorbunov et al. 2011; Lavaud and Goss 2014). Furthermore at the PSII level the maximum fluorescence yield varies with the S-state of the oxygen evolving complex, with the reduction status of the Q_A and Q_B electron acceptors (Prášil et al. 2018) and with rapidly changing charge distributions within the PSII complex (Magyar et al. 2018) . Thus the measured level of F_M can depend sensitively upon the exact duration and repetition of saturating flashes

applied. Some forms of non-photochemical quenching are induced or relax very quickly, within less than a second, so that obtaining internally consistent measures of F_O and F_M can be problematic even from a single FRRf induction curve (Xu et al. 2017). Therefore achieving a generalized protocol for consistent determination of F_M across diverse phytoplankton or different instrumentation is problematic.

Thirdly, the intrinsic normalization of F_V/F_M can itself be problematic. The measure of the quantum yield of the PSII pool can diverge from measures of the content of $[PSII_{active}]$ under conditions where pool sizes of $[PSII_{active}]$ and $[PSII_{inactive}]$ are both changing during a time course measurement (Wu et al. 2012), or where net synthesis of $[PSII_{total}]$ is a significant factor over the course of a treatment protocol (Campbell et al. 2013).

Fourthly, measures of F_V/F_M often show a remaining signal even when $[PSII_{active}]$ measured through oxygen flash yields have dropped to 0 ((Wu et al. 2012), which could reflect differences in the sensitivity of the measures, or the contribution to F_V/F_M of PSIIβ centres capable of a single charge separation, but not contributing to sustained electron transport (Cao and Govindjee 1990).

In spite of these issues, with caution, short term repeated measures of F_V/F_M, or F_V'/F_M' in a light acclimated state, are widely deployed to track changes in PSII function, and to infer photoinactivation and repair processes. In many cases (Six et al. 2007; Key et al. 2010; Wu et al. 2011, 2012; Li et al. 2016; Ni et al. 2017) we have used versions of F_V'/F_M' corrected for the influence of sustained non-photochemical quenching, as inferred by recovery of F_V'/F_M' during dark or low light recovery periods in the presence of lincomycin.

In the context of estimating ocean productivity from fluorescence metrics Oxborough et al. (2012) and Silsbe et al. (2015) introduced fluorescence based estimates for $[PSII_{active}]$ derived from the ratio of F_O: σ_{PSII}, with an instrument specific calibration factor. The concept is that F_O reflects the total pigment bed associated with PSII, while σ_{PSII} reflects the pigment bed associated with an individual PSII, therefore F_O: σ_{PSII} is a proxy for the number of PSII. (Murphy et al. 2016) then extended these efforts to studies of changes in $[PSII_{active}]$ during stress treatments. This metric shows promise for productivity studies, but is limited for studies of photoinactivation by the cross taxon variation in non-PSII contributions to F_O, noted above. Furthermore, photoinactivation of PSII provokes an increase in F_O (Ware et al. 2015a, b), which has itself been used as a metric for photoinactivation. This led us to attempt to correct the measured F_O for the short term influence of photoinactivation (Oxborough and Baker 1997; Ware et al. 2015a, b), but the effort became circular. In leaves PSII photoinactivation has been analyzed (Losciale et al. 2008) through changes in the delivery of electrons to PSI monitored using differential absorbance. This approach proved valuable in the optically complex environment of a leaf but has not yet, to our knowledge, been attempted with phytoplankton suspensions.

To complement functional measures we and many others have tracked changes in protein subunits of PSII, in particular PsbA (Aro et al. 1993; Baroli and Melis 1996; Six et al. 2007; Edelman and Mattoo 2008; Wu et al. 2011, 2012; Campbell et al. 2013). These changes in protein subunit content reflect the outcomes of PSII biosynthesis and the PSII repair cycle, and not necessarily changes in $[PSII_{active}]$. In particular photoinactivation does not, in itself, provoke loss of PsbA, rather PsbA removal follows photoinactivation, sometimes at a considerable temporal remove (Li et al. 2016), while accumulation of PsbA does not necessarily immediately flow through to an increase in $[PSII_{active}]$. This distinction between $[PSII_{active}]$ and [PsbA] is frequently obscured, particularly in the field literature. Every $PSII_{active}$ contains a PsbA, but not every PsbA is part of a $PSII_{active}$.

Whatever metric is used to track changes in [$PSII_{active}$] we, and others (Kok 1956; Lesser et al. 1994; Nagy et al. 1995; Sinclair et al. 1996; Oliver et al. 2003; Campbell and Tyystjärvi 2012) have used multiple parameterizations to express the susceptibility of PSII to photoinactivation.

k_{PI} is a first order exponential rate constant formulation (Kok 1956) expressing the exponential change in PSII function vs. time under conditions where counteracting PSII repair is either blocked or negligible, relative to the rate of photoinactivation.

$$\left[\mathrm{PSII_{active}}\right](t) = \left[\mathrm{PSII_{active}}\right](t_0)\, e^{-k_{PI}t} \qquad (13.1)$$

If PSII repair is continuing at a non-neglible rate during the treatment the Kok (1956) model of photoinactivation, parameterized by k_{PI}, and repair, parameterized by a first order rate constant, k_{REC}, can be used:

$$\mathrm{PSII_{active}} \underset{k_{REC}}{\overset{k_{PI}}{\rightleftharpoons}} \mathrm{PSII_{inactive}}$$

Under some situations an integrated form of the resulting rate equation can then be used to solve for k_{PI} and k_{REC} simultaneously:

$$\left[\mathrm{PSII_{active}}\right](t) = \left[\mathrm{PSII_{active}}\right](t_0)\frac{k_{REC} + k_{PI}e^{-(k_{PI}+k_{REC})t}}{k_{PI} + k_{REC}} \qquad (13.2)$$

This integrated form assumes that at T0 [$PSII_{active}$] = [$PSII_{total}$]; that [$PSII_{total}$] is constant over the course of the measurement, usually normalized to 1; and that [$PSII_{inactive}$] at time t = [$PSII_{total}$]- [$PSII_{active}$]t. That is, [$PSII_{inactive}$] only accumulates during the treatment time course t, as k_{PI} acts upon [$PSII_{active}$]. This [$PSII_{inactive}$] then becomes the substrate pool acted upon by the repair rate constant k_{REC}. The model thus explains any changes in repair rate as resulting solely from fluctuations in the pool of [$PSII_{inactive}$] and does not directly account for regulatory responses modulating the rate constant or capacity. If the treatment conditions are not too severe and k_{PI} is moderate relative to the value of k_{REC}, then at some point the loss of [$PSII_{active}$] and accumulation of [$PSII_{inactive}$] can result in:

$$\left[\mathrm{PSII_{active}}\right]k_{PI} = \left[\mathrm{PSII_{inactive}}\right]k_{REC} \qquad (13.3)$$

The pool of [$PSII_{active}$] then stabilizes and stops changing with time (Fig. 13.2a).

Under more severe conditions where k_{PI} is larger relative to k_{REC}:

$$\left[\mathrm{PSII_{active}}\right]k_{PI} > \left[\mathrm{PSII_{inactive}}\right]k_{REC} \qquad (13.4)$$

and [$PSII_{active}$] continues to decline towards zero (Fig. 13.2b).

In some data sets when repair is blocked linear vs. exponential equations give statistically indistinguishable fits to the decline in the metric of [$PSII_{active}$] with respect to time (Schreiber and Klughammer 2013). An apparent linear relationship can simply reflect a very low k_{PI} relative to the measurement period, in which case the exponential curvature of [PSIIactive] becomes indistinguishable from linearity (Fig. 13.2c). These pseudo-linear cases could, however, reflect underlying mechanistic complexities, if, for example, accumulation of [$PSII_{inactive}$] imparts progressive photoprotection to

Fig. 13.2. (continued) (**b**) Photoinactivation dominates over limited PSII repair capacity ($k_{PI} > k_{REC}$). Cells suffer progressive loss of [$PSII_{active}$] towards zero
(**c**) PSII repair capacity is limited but susceptibility to PSII photoinactivation is low relative to the measurement period ($k_{PI} \approx k_{REC}$), so loss of instantaneous repair has little effect, and the exponential curvature of [PSIIactive] becomes indistinguishable from linearity
(**d**) PSII repair capacity is limited but cells stabilize [$PSII_{active}$] by maintaining a significant pool of [$PSII_{inactive}$], prior to the beginning of light exposure ([$PSII_{inactive}$] > 0), providing a large substrate reserve for PSII repair

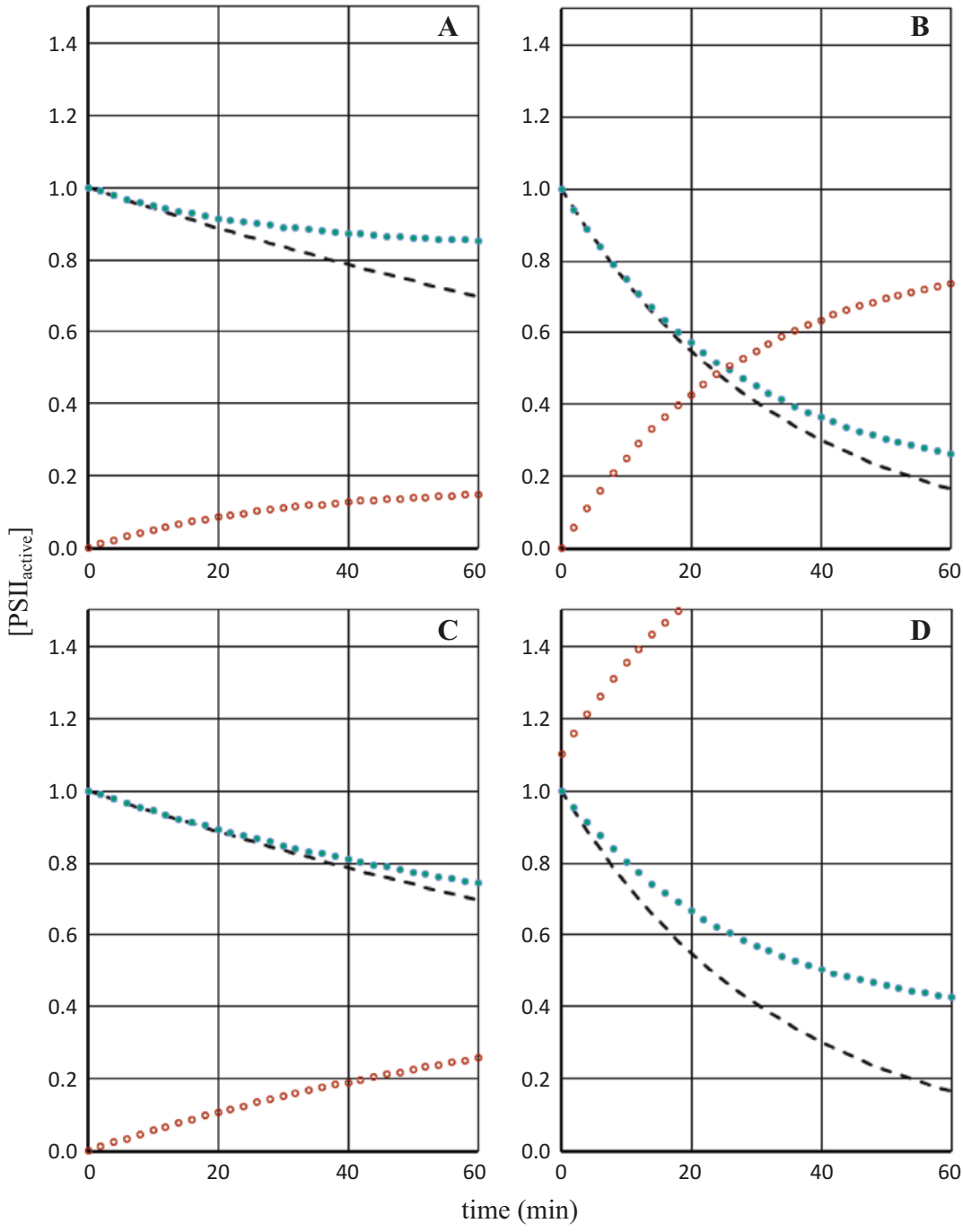

Fig. 13.2. Simulations of the variation over time during light exposure of the concentration of [$PSII_{inactive}$] and [$PSII_{active}$] (normalized to initial value of [$PSII_{active}$]), as a function of the rate constants of PSII inactivation (k_{PI}) and repair (k_{REC}). Simulations based on the model from Ni et al. (2017), which collapses to the simpler first-order model (Kok 1956) when initial [$PSII_{inactive}$] = 0 (**a**–**c**). k_{PI} depends upon the imposed light environment, but also varies depending upon the susceptibility of the cells to photoinactivation
Green dots track [$PSII_{active}$]; Open red dots track [$PSII_{inactive}$]; dashed line tracks [$PSII_{active}$] expected in the absence of PSII repair, as in the presence of a protein synthesis inhibitor
(**a**) Photoinactivation is moderate relative to the repair capacity ($k_{PI} < < k_{REC}$). Cells rely upon significant repair to stabilize the pool of [$PSII_{active}$]

remaining $PSII_{active}$ (Chow et al. 2002; Petrou et al. 2012) leading to a progressive increase in the instantaneous k_{PI} over the course of the measurement period. In our experiments to estimate k_{PI} under growth or near-growth conditions we generally avoid driving cells below ~50% of the their starting $[PSII_{active}]$ to limit this putative photoprotective effect. Alternately, a pseudo-linear decay could reflect issues with the metric used to estimate change in $[PSII_{active}]$. For example many samples show a residual F_V/F_M even when all measurable $[PSII_{active}]$ is lost (Wu et al. 2012). This residual F_V/F_M could reflect a pool of PSII that contribute to F_V/F_M but not to sustained electron transport, sometimes termed PSIIβ (see below). Or, a small residual F_V/F_M can arise from optical or electronic instrumental artefacts.

Comparing pools of PsbA and PsbD protein with content of functionally determined $[PSII_{active}]$, shows that multiple taxa of marine phytoplankton can maintain significant pools of $[PSII_{inactive}]$ that even under moderate growth conditions (Wu et al. 2011, 2012; McCarthy et al. 2012; Campbell et al. 2013; Lavaud et al. 2016; Ni et al. 2017). $[PSII_{inactive}]$ can be equivalent or even larger than the steady state pool of $[PSII_{active}]$. These findings from marine phytoplankton run counter to the patterns in eutrophile model species and plants where the $[PSII_{inactive}]$ is often kept lower (Aro et al. 2005), although transient pools of $[PSII_{inactive}]$ accumulate under some situations (Osmond and Chow 1988; Chow et al. 2002). If a cell population indeed contains a significant initial content of $[PSII_{inactive}]$ it forms a pre-existing substrate for PSII repair, before any light treatment begins (Fig. 13.2d). Under these conditions applying the simple (Kok 1956) model results in an over-estimate of the actual capacity for PSII repair, because the (Kok 1956) model accounts for all PSII repair in terms of k_{REC} acting only upon the pool of $[PSII_{inactive}]$ generated from the initial pool of $[PSII_{active}]$, and measured as the drop in $[PSII_{active}]$ from the initial value.

In one such situation we used a data set of parallel estimates of k_{PI} from treatments with lincomycin to block PSII repair, and $k_{PsbA,}$ the rate constant for clearance of the key PsbA protein (Lavaud et al. 2016). We assumed that k_{PsbA} approximates the actual rate constant for PSII repair, k_{rec}. We could then rearrange (Eq. 13.4) to get

$$\frac{k_{PsbA}}{k_{PI}} = \frac{[PSII_{active}]}{[PSII_{inactive}]} \tag{13.5}$$

We (Ni et al. 2017) then derived a more generalized version of the integrated model that allows for an initial pool of $[PSII_{inactive}]$ and generates a k_{REC} that accounts for $[PSII_{inactive}]$ $t_0 > 0$, (termed '$k_{RECINACT}$' in the original paper):

$$[PSII_{active}](t) = [PSII_{active}](t_0)\frac{k_{REC} + k_{PI}e^{-(k_{PI}+k_{REC})t}}{k_{PI}+k_{REC}} + [PSII_{inactive}](t_0)\frac{k_{REC}}{k_{PI}+k_{REC}}\left[1 - e^{-(k_{PI}+k_{REC})t}\right] \tag{13.6}$$

Please note that Ni et al. (2017) was plagued by typing errors in the presentation of Eq. 13.6, for which DC apologizes. This equation includes three fit parameters, k_{PI}, k_{REC} and $[PSII_{inactive}](t_0)$. Under conditions where $[PSII_{inactive}](t_0)$ is negligible the Ni et al. (2017) fit collapses to the original fit (Kok 1956). To usefully constrain the fit k_{PI} can be determined separately under conditions where repair is blocked or negligible. For mechanistically informative fits k_{REC} or $[PSII_{inactive}](t_0)$ can also be constrained using separate data. We have tracked the rate of change in the PsbA protein subunit in the

absence of repair, as a measure of the upper limit for k_{REC} imposed by clearance of PsbA from photoinactivated PSII.

Alternately, we have constrained fits by using estimates of $[PSII_{inactive}](t_0)$ as the difference between content of representative protein subunits and the functional content of protein based estimates of $[PSII_{active}](t_0)$. Interestingly a sub-population of PSII are detectable as contributing a slow kinetic phase in the decay of F_V upon re-opening of PSII after a single turnover saturating flash (Melis 1985; Cao and Govindjee 1990; Tyystjarvi and Vass 2004) . This population sometimes termed PSIIβ centers have been interpreted as capable of only a single charge separation, and not contributing to the sustained electron transport mediated by $[PSII_{active}]$. In our re-analyses of datasets these PSIIβ represent only a fraction of the $[PSII_{inactive}]$ quantified through comparison of protein subunit contents to $[PSII_{active}]$. $[PSII_{inactive}]$ thus comprises multiple sub-pools, likely representing different assembly/disassembly intermediates of the PSII repair cycle (Aro et al. 2005; Grouneva et al. 2011; Järvi et al. 2015). Sub-pools of $[PSII]_{inactive}$ also contribute to F_O (Ware et al. 2015b, a) but not to F_V, and may thus contribute to the generally low values of F_V/F_M found in many phytoplankton.

Both the Kok (1956) fit, and to an extent the Ni et al. (2017) fit are applicable only under restricted conditions where a time course treatment induces a significant initial drop in measured $[PSII_{active}]$, followed by significant repair to partially or fully counter photoinactivation during the ongoing light treatment. If the treatment is insufficient to drive an initial drop in $[PSII_{active}]$, or if a subsequent induction of PSII repair drives $[PSII_{active}]$ above initial levels during the light treatment, the curve fits become unconstrained and uninformative for extraction of rate constants. Thus the light level, spectral regime and measurement period must be matched to the photophysiology of the subject, which in turn varies with taxon and with prior growth conditions. Oliver et al. (2003) and many others have fit a PSII recovery rate under low light, following a period of photoinhibition, using an exponential rate constant acting upon the difference between $[PSII_{active}]$ and a plateau set as the maximum estimate of $[PSII_{active}]$ for the sample. This formulation is mathematically equivalent to k_{REC} and is applicable under situations where a simultaneous determination of k_{PI} and k_{REC} is impractical. In a simpler approach we (Key et al. 2010) and others have used the difference between an exponential decay in the presence of repair, and the exponential decay (k_{PI}) in the absence of repair, as an estimate of PSII repair capacity. This difference parameter does not directly connect to an underlying mechanistic hypothesis (Campbell and Tyystjärvi 2012) and departs from k_{REC} as k_{PI} increases, but avoids the need for a recovery period after the photoinhibitory period.

To achieve steady state under a given condition, Eq. (13.4) the must be balanced. If k_{PI} is imposed by the light environment and the biooptical properties of the cell (see below) then Eq. (13.4) can be balanced by compensatory changes in k_{REC} or by changes in $[PSII_{inactive}]$. These strategies have differing resource, metabolic and temporal allocation implications (Fig. 13.3).

The preceding models use a simple first order rate constant k_{REC} or to summarize cellular capacity for repair, but this is a gross over-simplification in light of our growing understanding of the layers of regulation involved in transcription, translation, proteolysis and PSII subunit assembly (Aro et al. 1993; Silva et al. 2003; Nixon et al. 2010; Grouneva et al. 2011; Komenda et al. 2012; Campbell et al. 2013; Gollan et al. 2015; Murata and Nishiyama 2018).

In particular, the capacity for repair is not fixed and can be modulated even over fairly short time periods. This can lead to responses showing an initial drop in $[PSII_{active}]$ followed by recovery or even net increases as repair processes are induced. Although the

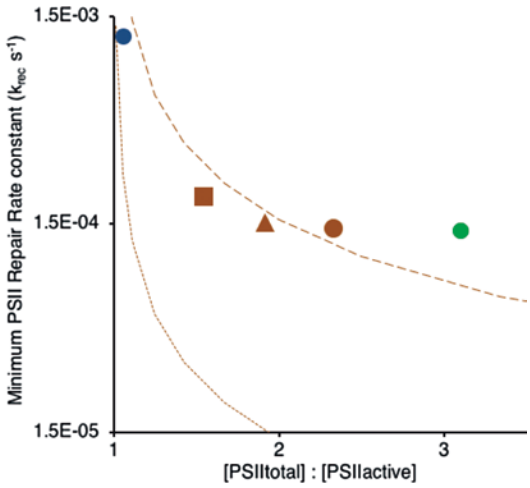

Fig. 13.3. Trade off between PSII repair capacity (k_{REC}, s^{-1}) and [$PSII_{total}$]:[$PSII_{active}$]
Symbols show data points. Blue circle: *Synechococcus* WH8102 growing at 260 μmol photons m^{-2} s^{-1}; Brown: *Thalassiosira pseudonana* CCMP 1335 growing at 30 (circle); 166 (triangle); or 385 μmol photons m^{-2} s^{-1}; Green circle: *Prochlorococcus* MED4 growth at 30 μmol photons m^{-2} s^{-1}
Lines indicate tradeoff thresholds to maintain a pool of [$PSII_{active}$] = 1, in the face of PSII photoinactivation imposed by k_{PI} (s^{-1}) for *Thalassiosira pseudonana* CCMP 1335 under 385 (dashed line) or 30 (dotted line) μmol photons m^{-2} s^{-1}. To generate the tradeoff threshold we estimated k_{PI} for the given irradiance. Then at steady state:
$[PSII_{active}]k_{PI} = [PSII_{inactive}]k_{REC}$
$[PSII_{active}]k_{PI} = ([PSII_{total}] - [PSII_{active}])k_{REC}$
For $[PSII_{active}] = 1$
$k_{PI} = ([PSII_{total}] - 1)k_{REC}$

preceding models do not account for **short-term** regulatory changes in k_{REC} during the course of a treatment, they clearly detect differences in k_{REC} across different taxa or after different growth regimes.

PSII repair involves multiple steps that require ATP, including transcription, ribosomal synthesis of protein and FtsH mediated proteolytic removal of photoinactivated proteins (Aro et al. 1993; Silva et al. 2003; Nixon et al. 2010; Komenda et al. 2012; Campbell et al. 2013). Although PSII repair responds to increasing light, the repair rate tends to saturate at fairly low light (Allakhverdiev and Murata 2004; Edelman and Mattoo 2008; Campbell et al. 2013; Li et al. 2016), so that under excess light the transient rate of PSII inactivation frequently outruns the instantaneous repair rate (Behrenfeld et al. 1998). These limitations on PSII repair are particularly evident in studies at low temperature (Osmond and Chow 1988; Ni et al. 2017) or on taxa genomically adapted to low light regimes (Six et al. 2007). The tight integration of photosynthetic and respiratory metabolism in unicellular phytoplankton (Bailleul et al. 2015) can also support significant rates of PSII repair in darkness, at least in diatoms (Li et al. 2016). Some phytoplankton can thus temporally offset episodes of net photoinactivation (Behrenfeld et al. 1998) from later repair under lower light or even darkness. In centric diatoms (Wu et al. 2011, 2012) these patterns can result in cells growing with significant pools of [$PSII_{inactive}$] protein intermediates, in excess of the pool of [$PSII_{active}$] (Fig. 13.3).

We (Six et al. 2007; Lavaud et al. 2016) and others (Neale et al. 2014; Neale and Thomas 2016) realized that these interacting processes generate acclimation trade off thresholds or surfaces (Fig. 13.3). To maintain a given steady state pool of [$PSII_{active}$] in the face of a rate of photoinactivation imposed by irradiance driving k_{PI}, a cell can invest in sufficient repair capacity of proteases, ribosomes, translational machinery and ATP to sustain rapid repair of a small pool of [$PSII_{inactive}$]. Alternately, at the same photoinactivation rate, the cell can tolerate the accumulation of a significant standing pool of [$PSII_{inactive}$] to provide a large substrate reserve for PSII repair. This tradeoff can be expressed as a threshold line on a plot of k_{REC} vs. [$PSII_{Total}$]: [$PSII_{active}$]. Cells with a large k_{REC} can function with only a small standing pool of [$PSII_{inactive}$], so that [$PSII_{Total}$]: [$PSII_{active}$] is near 1, with most of the [$PSII_{Total}$] in the form of [$PSII_{active}$]. Or, cells can cope with comparable rates of photoinactivation with a lower k_{REC} by allowing [$PSII_{Total}$]: [$PSII_{active}$] to increase, by accumulating a standing pool of [$PSII_{inactive}$]. In multiple

datasets we are finding that cells indeed shift along these threshold lines (Lavaud et al. 2016) (Fig. 13.3), reflecting different acclimatory strategies across taxa, or under different environmental constraints. For example we (Ni et al. 2017) found that the arctic psychrophile *Micromonas* CCMP 2099 (Lovejoy et al. 2007) maintained measurable PSII repair rates even at low temperatures by maintaining large pools of $[PSII_{inactive}]$ to counter kinetic limitations on enzymatic repair processes. We also found that onshore diatoms achieved faster PsbA protein clearance and functional k_{REC} by accumulating larger pools of the key proteolytic complex FtsH (Campbell et al. 2013), in comparison to related offshore diatoms from more stable offshore light environments (MacIntyre et al. 2000) with less investment in PSII repair capacity.

In contrast to metabolically constrained PSII repair, PSII photoinactivation is driven by instantaneous light, so a given determination of k_{PI} is only applicable to a particular light level and biooptical configuration; an identical sample measured at a different light level will yield a different k_{PI} (ex. Fig. 13.3, thresholds for 30 vs. 385 μmol photons m^{-2} s^{-1}).

In most experimental conditions, PSII inactivation follows a photon dose reciprocity between irradiance and time (Nagy et al. 1995; Tyystjärvi and Aro 1996; Allakhverdiev and Murata 2004; Sarvikas et al. 2010; Serôdio et al. 2017). That is, the number of photoinactivated PSII depends on the number of photons absorbed, regardless of the particular combination of irradiance and duration of exposure applied. When these conditions are fulfilled, a plot of k_{PI} values determined at different irradiances will show a linear relation, with zero intercept (Park et al. 1995; Sinclair et al. 1996; Hakala et al. 2005; Tyystjärvi 2008; McKew et al. 2013; Soitamo et al. 2017; Havurinne and Tyystjärvi 2017). In our hands (Murphy et al. 2017) (Fig. 13.1) PSII photoinactivation on the basis of photons delivered to PSII shows some departure from photon dose reciprocity, increasing with higher PSII closure.

The slope of the k_{PI} vs irradiance relationship can be used to derive generalized, irradiance-independent parameters that quantify the susceptibility of PSII to photoinactivation on a photon basis. Two interconvertible parameters are then the quantum yield of photoinactivation, Φ_{PI} and the effective absorption cross section driving photoinactivation, σ_I (Nagy et al. 1995; Sinclair et al. 1996; Oliver et al. 2003; Six et al. 2007; Key et al. 2010; Campbell and Tyystjärvi 2012).

In its simplest formulation, Φ_{PI} is determined based on incident irradiance (I_i) and on some metric of PSII inactivation (e.g. F_V/F_M) normalized to pre-illumination levels (units of m^2 $photons^{-1}$) (Campbell and Tyystjärvi 2012):

$$rel.\Phi_{PI} = \frac{k_{PI}}{I_i} \tag{13.7}$$

Because k_{PI} ultimately depends on the photons absorbed by the sample, this relative Φ_{PI} should be limited to comparing samples with similar optical and light absorption properties. A more precise formulation takes into account the fraction of incident photons absorbed by the sample, measured in terms of absorptance (Campbell and Tyystjärvi 2012):

$$\Phi_{PI} = \frac{k_{PI}}{I_i\, abs} \tag{13.8}$$

An absolute Φ_{PI} can be determined considering the amount of active PSII (not normalized) prior to the start of light treatment (Campbell and Tyystjärvi 2012):

$$\Phi_{PI} = \left[PSII_{active}\right](t_0)\frac{k_{PI}}{I_i\, abs} \tag{13.9}$$

For flat samples such as leaves, macroalgae thalli, lichens or biofilms, [$PSII_{active}$] is conveniently expressed on an area basis (mol PSII m^{-2}) in which case, Φ_{PI} becomes dimensionless, being interpreted as the probability of incident photon causing inactivation of a PSII reaction center (Campbell and Tyystjärvi 2012).

σ_I is the first order exponential rate constant derived from a plot of PSII function vs. cumulative photon dose:

$$\left[\mathrm{PSII}_{\mathrm{active}}\right](t) = \left[\mathrm{PSII}_{\mathrm{active}}\right](t_0)\, e^{-\sigma_I I_i t} \qquad (13.10)$$

σ_I has units of m^2 $quanta^{-1}$, giving a target size parameterization of the susceptibility to photoinactivation. Under conditions of constant incident irradiance, I_i:

$$\sigma_I = \frac{k_{PI}}{I_i} \qquad (13.11)$$

If dose reciprocity holds then σ_I determined under a given irradiance can be used to calculate the rate constant for photoinactivation expected under a different irradiance. σ_I is also useful for fitting photoinactivation when instantaneous irradiance varies over time (Oliver et al. 2003). σ_I has the same units as σ_{PSII}', the effective absorption cross section for PSII photochemistry (Kolber et al. 1998). The ratio of σ_{PSII}'/σ_I then represents photochemical cycles per photoinactivation cycle and is thus a gross estimate of return on investment per PSII unit under low light. As excitation pressure ($1\text{-}q_P$) increases and PSII closes the ratio of achieved photochemical cycles per photoinactivation decreases ($\sigma_{PSII}' \times q_P$), until at some point maintaining the PSII pool becomes uneconomic (Murphy et al. 2017). This transition from net productivity to unsustainable photoinactivation depends upon both the current physiological state and the genomically encoded properties of the cell, and underpins distinctions in light acclimation and niche partitioning across taxa (Six et al. 2007).

Alternately, in analogy with the Φ_{PI} quantum yield for photoinactivation on the basis of absorbed photons, $\Phi_{I\ PSII}$ is the quantum yield for photoinactivation per photon delivered to PSII (Campbell and Tyystjärvi 2012; Murphy et al. 2017).

$$\begin{aligned}\left[\mathrm{PSII}_{\mathrm{active}}\right](t) &= \left[\mathrm{PSII}_{\mathrm{active}}\right](t_0)\, e^{-\Phi_{I\mathrm{PSII}}} \\ &= \left[\mathrm{PSII}_{\mathrm{active}}\right](t_0)\, e^{-\sigma_I \sigma_{\mathrm{PSII}}}\end{aligned} \qquad (13.12)$$

To estimate $\Phi_{I\ PSII}$ we plot change in PSII function vs. photons delivered to PSII, estimated by multiplying cumulative incident photons m^{-2} by σ_{PSII}' (m^2 $PSII^{-1}$). Algebraically,

$$\Phi_{I\mathrm{PSII}} = \frac{\sigma_I}{\sigma_{PSII'}} \qquad (13.13)$$

In comparison to the simpler σ_I that expresses photoinactivation per incident photon, $\Phi_{I\ PSII}$ proves useful in reconciling taxonomic and light colour effects upon responses to changing irradiance because $\Phi_{I\ PSII}$ accounts for taxonomic or regulatory differences in the delivery of incident photons to PSII (Fig. 13.1).

IV. Patterns of Photoinactivation and Repair Across Phytoplankton

Phytoplankton are exposed to fluctuating light levels through mixing through the water column, diel cycles and variations in sunlight (Oliver et al. 2003) and annual changes in photoperiod and solar angle (Sathyendranath and Platt 1988; Kvernvik et al. 2018). Thus at the cell-level variability in instantaneous and integrated light differs across different habitats (MacIntyre et al. 2000). This variable light imposes costs and risks on phytoplankton (Raven 2011), and influences niche partitioning (Six et al. 2007; Neale and Thomas 2016).

Across tested strains the primary susceptibility to photoinactivation on the basis of

incident photons varies at least eight fold (Table 13.2). Centric diatoms span a wide range of cell sizes, and larger diatoms show low intrinsic susceptibility to photoinactivation (Fig. 13.4) and thus potentially lower costs for counteracting PSII repair (Key et al. 2010; Wu et al. 2011). The lower susceptibility in larger diatoms likely reflects optical screening (Finkel 2001) (Fig. 13.5), which also affects their σ_{PSII}. It is also tempting to speculate on the optical properties of the siliceous frustule (Fuhrmann et al. 2004), given the low susceptibility to photoinactivation of even small diatoms relative to other phytoplankton (Fig. 13.4). It remains to be seen if the pattern of low susceptibility to photoinactivation holds across other larger phytoplankton cells; we have only limited data to date from other large taxa (Fig. 13.4). Furthermore some centric diatoms maintain pre-emptive or luxury cycling of [$PSII_{active}$] protein subunits (Li et al. 2016) and so may not realize the potential metabolic savings of lower susceptibility to photoinactivation. Interestingly the vaunted capacity of some diatoms for very high inducible NPQ (Bailleul et al. 2010) does not appear to directly protect their PSII from photoinactivation (Havurinne and Tyystjärvi 2017). This corroborates the hypothesis that NPQ acts primarily to protect against secondary ROS generated by excitation of the photosynthetic antenna, rather than against direct photoinactivation.

In comparison to other groups diatoms tested show a generally slow rate constant for removal of the key PsbA protein (Fig. 13.6), possibly related to their triply stacked thylakoid morphology (Campbell et al. 2013; Li et al. 2016), but also in keeping with their generally low susceptibility to photoinactivation (Fig. 13.4). Interestingly the coccolithophore *Emiliania huxleyi* also strongly resists photoinhibition (Ragni et al. 2008) but adopts the mirror image strategy of high repair capacity to reverse fairly rapid photoinactivation of PSII, at least under nutrient repletion (Loebl et al. 2010). Growth (and matching treatment) temperature, over a moderate range of 12-24C, had little influence on susceptibility to photoinactivation or indeed upon the counteracting achieved repair rates in centric diatoms (Wu et al. 2012). Instead achieved repair was maximal at the optimal growth temperature for the tested strains. Under low polar water temperatures PSII repair is indeed temperature limited (Ni et al. 2017) forcing a prasinophyte psychrophile to adopt large pools of [$PSII_{inactive}$] reserves and strong non-photochemical quenching to cope with changing irradiance, rather than relying upon dymamic regulation of PSII repair capacity. These patterns mirror those of some leaves under low temperature restrictions (Osmond and Chow 1988).

Nutrient status (N) can strongly alter cellular responses to variable light, as for example in coccolithophores (Loebl et al. 2010), by restricting repair rates but also by lowering susceptibility to photoinactivation (Fig. 13.4). This change may relate to large changes in PSII content per cell, with cells with low [$PSII_{active}$] showing resistance to further inhibition of their residual pool of PSII (Chow et al. 2002; Petrou et al. 2012), although this mechanism is debated in the literature (Sarvikas et al. 2010). Higher CO_2 alters responses to variable light. In some cyanobacteria and diatoms increased CO_2 increases susceptibility to photoinactivation, possibly by suppressing the dissipation of excitation through the Carbon Concentrating Mechanism (Mackenzie 2004; McCarthy et al. 2012; Gao and Campbell 2014). Furthermore increased CO_2 alters allocation patterns of cellular resources and thus differentially alters incurred running and acclimation costs across ranges of growth light (Li et al. 2015).

Across strains of picocyanobacteria capacity for PSII repair varies with original habitat, with strains from more dynamic light environments showing a greater short-term amplitude of regulation of PSII repair (Six et al. 2007) (Fig. 13.5). Soitamo et al.

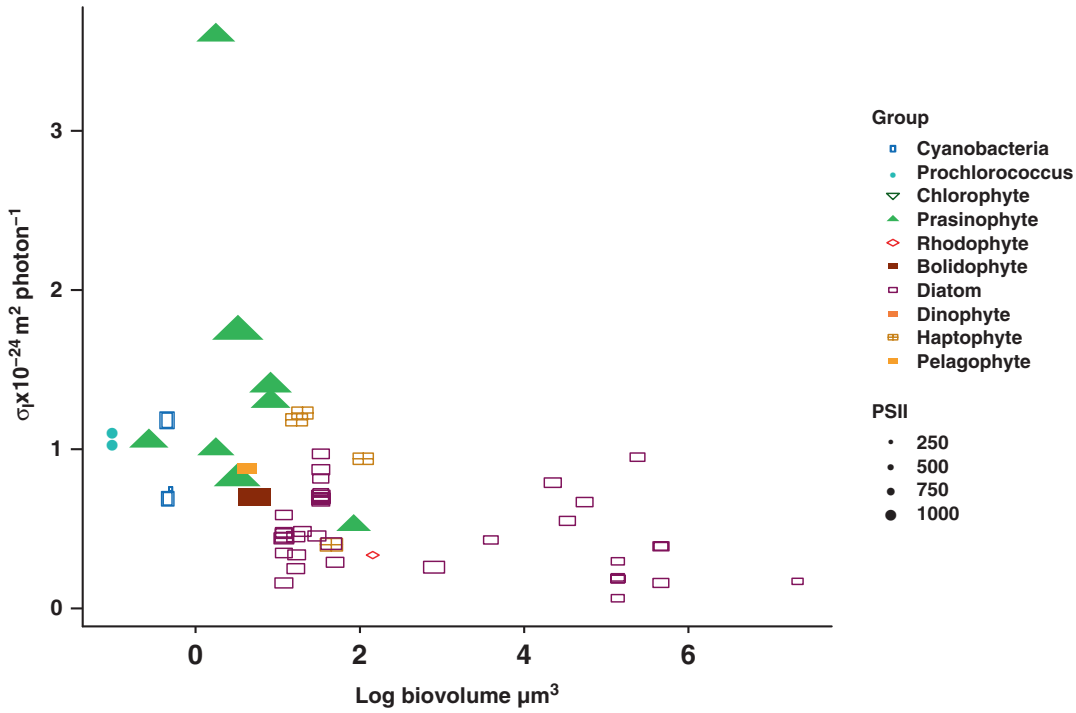

Fig. 13.4. Susceptibility to photoinactivation (σ_I) of Photosystem II vs. log cell volume for a panel of marine phytoplankton
Blue open rectangles: phycobilin containing picocyanobacteria
Blue closed circles: Prochlorococcus
Green closed triangles: marine Prasinophytes
Large range across prasinophytes reflects low light vs. high light strains.
Red open diamond: Rhodophyte, *Porphyridium cruentum* (C. Dubois & D. Campbell, unpub)
Red closed squares: Bolidophyte
Purple open squares: centric diatoms from *Thalassiosira* & *Coscinodiscus*
Scatter among determinations for diatoms of the same size largely reflects growth under low vs. higher pCO_2
Orange filled square: Dinophyte
We need additional data from dinoflagellates outside the optically complex symbiotic associations
Brown Square with cross: Haptophyte coccolithophore (*Emiliania huxeyli*). Range reflects strong downward shift in photoinactivation susceptibility in *Emiliania huxeyli* from nutrient repletion (high susceptibility) to nitrogen depletion (low susceptibility of small remaining pool of [PSIIactive]
Light Orange filled square: Pelagophyte *Pelagococcus* (C. Dubois & D. Campbell, unpub)
Symbol size proportional to effective absorption cross section for Photosystem II photochemistry(σ_{PSII} 10^{-20} m^2 $photon^{-1}$) measured under the same spectral quality as σ_I
Citations for underlying data in Table 13.2.

(2017) used action spectra for loss of oxygen evolution to show that marine picocyanobacteria show lower relative blue sensitivity to photoinactivation, compared to broad band irradiance, than expected from comparisons with freshwater eutrophilic cyanobacteria. The data thus support a mixed-model of photoinactivation as a function of both direct photoinactivation dominated by blue light and photoinactivation driven by excitation delivered through the photosynthetic antenna (Fig. 13.1). We suspect the antenna-driven component of photoinactivation in marine picocyanobacteria is a function of down-

Table 13.1. Terms and definitions

Term	Definition	Representative citations
$PSII_{active}$	A PSII complex capable of sustained charge separation under illumination	Melis (1985) and Cao and Govindjee (1990)
$PSII_{inactive}$	A PSII complex or sub-complex which is incapable of sustained charge separation under illumination. By some definitions $PSII_{\beta}$ represents a subset of $PSII_{inactive}$ capable of a single round of charge separation but not sustained electron transport	Melis (1985), Cao and Govindjee (1990), Chow et al. (2002) and Sarvikas et al. (2010)
Photoinactivation (of PSII)	A physico-chemical change in the structure of $PSII_{active}$ that generates a $PSII_{inactive}$	Aro et al. (1993)
k_{PI}	Apparent first order rate constant for photoinactivation of $PSII_{active}$ generating $PSII_{inactive}$	Kok (1956)
PSII repair	The coordinated proteolytic removal of protein subunits, gene transciption, protein subunit translation and sub-complex re-assembly that re-generates a $PSII_{active}$ from a $PSII_{inactive}$	Aro et al. (1993) and Järvi et al. (2015)
k_{REC}	Apparent first order rate constant for repair of $PSII_{inactive}$ to $PSII_{active}$. $k_{RECINACT}$ accounts for a starting pool of $PSII_{inactive}$, which if present leads to over-estimates of simple k_{REC}	Kok (1956) and Ni et al. (2017)
k_{PsbA}	Apparent first order rate constant for removal of the PsbA (D1) protein of PSII PSII. k_{PsbA} is a mechanistic proxy for the overall k_{REC} because in at least some determinations removal of PsbA protein is the limiting step on PSII repair.	Campbell et al. (2013)
PSII synthesis	Complete *de novo* synthesis and assembly of a PSII unit; mechanistically overlaps with PSII repair	Järvi et al. (2015)
Photoinhibition (of PSII)	Net loss of PSII activity when photoinactivation outruns PSII repair. Note that depending upon context and field, photoinhibition is also used to refer to light-dose dependent drops in the quantum yield of electron transport, or to drops in electron transport or photosynthesis under high light.	Platt et al. (1981), Greer et al. (1986) and Henley (1993)
Non-photochemical quenching	Dissipation of incident excitation as heat. Induction and relaxation of non-photochemical quenching operates through multiple paths, over wide kinetic ranges. Non-photochemical quenching can overlap kinetically and phenomenologically with the broader definition of photoinhibition. In particular q_I is a kinetically defined subset of non-photochemical quenching	Horton and Hague (1988)
Φ_{PI}	Quantum yield for photoinactivation on the basis of absorbed photons	Campbell and Tyystjärvi (2012)
σ_I	Target size parameterization of susceptibility to photoinactivation	Sinclair et al. (1996), Oliver et al. (2003) and Campbell and Tyystjärvi (2012)
$\Phi_{I\ PSII}$	Quantum yield for photoinactivation on the basis of photons delivered to PSII through the effective absorption cross section	Campbell and Tyystjärvi (2012), and Murphy et al. (2017)

Table 13.2. Summary of published parameters for photoinactivation and repair of phytoplankton

Group	Species	Biovol_µm^3	Growth_µE	Treatment_µE	Treatment_nm	Stress	σpsii_10_20_m^{-2}	σi_10_-24_m^{-2} quanta^{-1}	Φpi_10_-7_m-2_µmol	kpi_10_-4_s^{-1}	Krec_10_-4_s^{-1}	Difference_10_-4	kpsba_10_-4_s^{-1}	Reference
Bolidophyte	*Bolidomonas pacifica* CCMP1866	5.2	30	150	455		900	0.7	*4.2*				0.1	Thomas et al. (2013)
Bolidophyte	*Bolidomonas pacifica* CCMP1866	5.4	150	450	455		944	0.7	*4.2*					Thomas et al. (2013)
Bolidophyte	*Bolidomonas pacifica* CCMP1866	5.4	250	250	455		810	0.7	*4.2*				1.7	Thomas et al. (2013)
Chlorophyte	*Chlorella vulgaris* ACOI2919		15		Mercury arc	–		*0.3*	2.0					Serôdio et al. (2017)
Chlorophyte	*Chlorella vulgaris* ACOI2919		150		Mercury arc	–		*0.6*	3.5					Serôdio et al. (2017)
Chlorophyte	*Chlorella vulgaris* ACOI2919		15	1460	Mercury arc	–					1.7			Serôdio et al. (2017)
Chlorophyte	*Chlorella vulgaris* ACOI2919		150	1460	Mercury arc	–					5.3			Serôdio et al. (2017)
Chlorophyte	*Dunaliella salina* Teod.	220.9	50	50	Tungsten halogen	–							0.1	Baroli and Mellis (1996)
Chlorophyte	*Dunaliella salina* Teod.	220.9	1500	1500	Tungsten halogen	–							1.9	Baroli and Mellis (1996)
Chlorophyte	*Dunaliella salina* Teod.	220.9	2500	2500	Tungsten halogen	–							3.3	Baroli and Mellis (1996)
Chlorophyte	*Botryococcus braunii*				Solar	–		*0.3*	1.6		1.9			Oliver et al. (2003)
Chlorophyte	*Botryococcus braunii*				Solar			*0.1*	0.3		0.7			Oliver et al. (2003)
Chlorophyte	*Oocystis*			1600	Solar	–		*0.4*	2.2		4.3			Oliver et al. 2003
Chlorophyte	*Chlamydomonas reinhardtii* CC-425	113.1	100	1100	Halogen	–				9.6				Elrad et al. (2002)
Chlorophyte	*Chlamydomonas reinhardtii* CC-425	113.1	100	1100	Halogen	np5 mutant				12.4				Elrad et al. (2002)
Chlorophyte	*Dunaliella tertiolecta* butcher CS175	220.9	150		UVBR	–				4.8				Heraud & Beardall (2000)
Chlorophyte	*Chlorella vulgaris*		30	1750	440					4.2				Schreiber & Klughammer (2013)
Chlorophyte	*Chlorella vulgaris*		30	1750	480					2.2				Schreiber & Klughammer (2013)
Chlorophyte	*Chlorella vulgaris*		30	1750	540					0.4				Schreiber & Klughammer (2013)
Chlorophyte	*Chlorella vulgaris*		30	1750	590					0.5				Schreiber & Klughammer (2013)
Chlorophyte	*Chlorella vulgaris*		30	1750	625					0.7				Schreiber & Klughammer (2013)
Chlorophyte	*Dunaliella tertiolecta* butcher CS175	220.9	150		UVBR 1.1 W/m2	Ctrl				0.3	0.0			Shelly et al. (2002)

Chlorophyte	*Dunaliella tertiolecta* butcher CS175	220.9	150		UVBR 1.1 W/m2	N-depleted			0.0	0.0			Shelly et al. (2002)
Chlorophyte	*Dunaliella tertiolecta* butcher CS175	220.9	150		UVBR 2.1 W/m2	Ctrl			1.2	0.2			Shelly et al. (2002)
Chlorophyte	*Dunaliella tertiolecta* butcher CS175	220.9	150		UVBR 2.1 W/m2	N-depleted			3.1	4.2			Shelly et al. (2002)
Chlorophyte	*Dunaliella tertiolecta* butcher CS175	220.9	150		UVBR 2.8 W/m2	Ctrl			3.0	1.6			Shelly et al. (2002)
Chlorophyte	*Dunaliella tertiolecta* butcher CS175	220.9	150		UVBR 2.8 W/m2	N-depleted			13.9	7.7			Shelly et al. (2002)
Cyanobacteria	*Synechococcus* WH8102	0.5	30		455		1.6	9.6					Murphy et al. (2017)
Cyanobacteria	*Synechococcus* WH8102	0.5	260		455		0.7	4.2					Murphy et al. (2017)
Cyanobacteria	*Synechocystis* PCC6803	3.1	70	1000	Incandescent	H2O2 1.0 M			1.5				Allakhverdiev and Murata (2004)
Cyanobacteria	*Synechocystis* PCC6803	3.1	70	2000	Incandescent	H2O2 1.0 M			3.2				Allakhverdiev and Murata (2004)
Cyanobacteria	*Synechocystis* PCC6803	3.1	70	1000	Incandescent	Cold 10 °C			1.7				Allakhverdiev and Murata (2004)
Cyanobacteria	*Synechocystis* PCC6803	3.1	70	2000	Incandescent	Cold 10 °C			3.4				Allakhverdiev and Murata (2004)
Cyanobacteria	*Synechocystis* PCC6803	3.1	70		Incandescent	–	0.3	1.8					Allakhverdiev and Murata (2004)
Cyanobacteria	*Synechocystis* PCC6803	3.1		1500		–			3.2				Nishiyama et al. (2005)
Cyanobacteria	*Synechocystis* PCC6803	3.1				–	0.3	1.8					Nishiyama et al. (2005)
Cyanobacteria	*Synechocystis* PCC6803	3.1		2000					1.4				Bentley & Eaton-Rye (2008)
Cyanobacteria	*Synechocystis* PCC6803 ΔPsbM	3.1		2000					2.4				Bentley & Eaton-Rye (2008)
Cyanobacteria	*Synechocystis* PCC6803 ΔPsbT	3.1		2000					4.0				Bentley & Eaton-Rye (2008)
Cyanobacteria	*Synechocystis* PCC6803	3.1		*1800*			0.4	*2.5*					Nagy et al. (1995)
Cyanobacteria	*Synechocystis* PCC6803	3.1		*1800*			0.1	*0.6*					Nagy et al. (1995)
Cyanobacteria	*Synechococcus* RCC 307	0.5	25	270	455	382	0.7	*4.2*					Six et al. (2007)
Cyanobacteria	*Synechococcus* WH8102	0.5	30	270	455	546	1.2	*7.2*				3.1	Six et al. (2007)
Cyanobacteria	*Synechococcus* SR9917	0.5	30	270	455	56	0.8	*4.5*				2.0	Six et al. (2007)
Cyanobacteria	*Synechococcus* WH7803	33.5	18	18	Fluorescent				0.0		0.0		Blot et al. (2011)

(continued)

Table 13.2. (continued)

Group	Species	Biovol_μm^3	Growth_μE	Treatment_μE	Treatment_nm	Stress	σpsii_10_20_m^{-2}	σi_10_-24_m^{-2} quanta^{-1}	Φpi_10_-7_m-2_μmol	kpi_10_-4_s_$^{-1}$	Krec_10_-4_s^{-1}	Difference_10_-4	kpsba_10_-4_s_$^{-1}$	Reference
Cyanobacteria	*Synechococcus* WH7803	33.5	250	250	Fluorescent					0.0		0.0		Blot et al. (2011)
Cyanobacteria	Ubatuba (231,450 S, 451060 W)		1960	1750	Sunlight					8.9		9.2	48.0	Bouchard et al. (2005b)
Cyanobacteria	Ubatuba (231,450 S, 451060 W)		1960	1960	Sunlight					15.7		13.8	54.0	Bouchard et al. (2005b)
Prochlorococcus	*Prochlorococcus* MIT9313	0.3	13	300	450					0.0				Soitamo et al. (2017)
Cyanobacteria	*Synechococcus* WH8103	0.5	24	150	PAR					2.7				Soitamo et al. (2017)
Cyanobacteria	*Synechococcus* WH8103	0.5	24	300	PAR					4.3				Soitamo et al. (2017)
Cyanobacteria	*Synechococcus* WH8103	0.5	24	600	PAR					8.2				Soitamo et al. (2017)
Cyanobacteria	*Synechococcus* WH8103	0.5	24	300	450					2.7				Soitamo et al. (2017)
Prochlorococcus	*Prochlorococcus* MED4	0.1	30		455			1.3	7.8					Murphy et al. (2017)
Prochlorococcus	*Prochlorococcus* MED4	0.1	260		455			1.3	7.8					Murphy et al. (2017)
Prochlorococcus	*Prochlorococcus* SS120	0.1	30	270	455		462	1.0	*6.1*				0.9	Six et al. (2007)
Prochlorococcus	*Prochlorococcus* PCC9511	0.1	25	270	455		404	1.1	*6.6*				2.7	Six et al. (2007)
Prochlorococcus	*Prochlorococcus* PSS120	0.1	13	150	PAR					4.9				Soitamo et al. 2017
Prochlorococcus	*Prochlorococcus* PSS120	0.1	13	300	PAR					6.0				Soitamo et al. (2017)
Prochlorococcus	*Prochlorococcus* PSS120	0.1	13	600	PAR					11.4				Soitamo et al. (2017)
Prochlorococcus	*Prochlorococcus* PSS120	0.1	13	300	450					4.9				Soitamo et al. (2017)
Prochlorococcus	*Prochlorococcus* MIT9313	0.3	13	300	PAR					5.0				Soitamo et al. (2017)
Diatom	*Phaeodactylum tricornutum* Bohlin ALISU108–01	77.4	40	1250		–				2.2				Domingues et al. (2012)

Diatom	*Phaeodactylum tricornutum* Bohlin ALISU108–01	77.4	40			–		*0.3*	1.8					Domingues et al. (2012)
Diatom	*Phaeodactylum tricornutum* CCMA106		35	900	Fluorescent	18 °C		0.7	4.1					Xu et al. (2016)
Diatom	*Phaeodactylum tricornutum* CCMA106		35	900	Fluorescent	24 °C		0.4	2.6					Xu et al. (2016)
Diatom	*Thalassiosira weissflogii* CCMA102	696.9	200	706	Xenon arc (PAR)	–				1.2	0.0			Wu et al. (2015)
Diatom	*Thalassiosira pseudonana* CCMP1335	33.5	200	706	Xenon arc (PAR)	–				2.9	0.7			Wu et al. (2015)
Diatom	*Thalassiosira punctigera* CCAP 1085/19	54361.6	200	706	Xenon arc (PAR)	–				7.2	17.6			Wu et al. (2015)
Diatom	*Thalassiosira weissflogii* CCMA102	696.9	200	706	PAR + UVA + UVB	UVA + UVB				4.1	0.0			Wu et al. (2015)
Diatom	*Thalassiosira pseudonana* CCMP1335	33.5	200	706	PAR + UVA + UVB	UVA + UVB				4.7	0.4			Wu et al. (2015)
Diatom	*Thalassiosira punctigera* CCAP 1085/19	54361.6	200	706	PAR + UVA + UVB	UVA + UVB				9.9	4.1			Wu et al. (2015)
Diatom	*Fragilariopsis cylindrus* (CCMP 1102)	0.0	65	65						0.1				Kropuenske et al. (2009)
Diatom	*Fragilariopsis*	1800.0		50	PAR			0.3	*1.9*			0.1		Petrou et al. (2010)
Diatom	*Fragilariopsis*	1800.0		100	PAR			0.3	*1.9*			0.1		Petrou et al. (2010)
Diatom	*Fragilariopsis*	1800.0		200	PAR			0.3	*1.9*			0.2	0.6	Petrou et al.2010
Diatom	*Thalassiosira pseudonana* CCMP1014	11.9	95	450	455		270	0.5	*2.8*			1.2		Loebl et al. (2010)
Diatom	*Thalassiosira pseudonana* CCMP1014	11.9	95	450	455	N-depleted	380	0.4	*2.6*			0.8		Loebl et al. (2010)
Diatom	*Coscinodiscus* CCMP1583	462000.0	95	450	455		160	0.4	*2.3*			1.0		Loebl et al. (2010)

(continued)

Table 13.2. (continued)

Group	Species	Biovol_µm^3	Growth_µE	Treatment_µE	Treatment_nm	Stress	σpsii_10_20_m^{-2}	σi_10_-24_m^{-2} quanta^{-1}	Φpi_10_-7_m-2_µmol	kpi_10_-4_s_$^{-1}$	Krec_10_-4_s^{-1}	Difference_10_-4	kpsba_10_-4_s_$^{-1}$	Reference
Diatom	*Coscinodiscus* CCMP1583	462000.0	95	450	455	N-depleted	230	0.4	*2.3*			0.3		Loebl et al. (2010)
Diatom	*Coscinodiscus* CCMP2513	21300000.0	30	450	455		99	0.2	*1.0*			0.3	0.7	Key et al. (2010)
Diatom	*Coscinodiscus* CCMP1583	462000.0	30	450	455		226	0.2	*1.0*			0.3		Key et al. (2010)
Diatom	*Coscinodiscus radiatus* CCMP312	138000.0	30	450	455		160	0.2	*1.1*				1.3	Key et al. (2010)
Diatom	*Coscinodiscus* CCMP2063	3930.0	30	450	455		181	0.4	*2.6*					Key et al. (2010)
Diatom	*Thalassiosira weissflogii* CCMP1010	801.0	30	300	455		447	0.3	*1.6*				1.0	Key et al. (2010)
Diatom	*Thalassiosira pseudonana* CCMP1335	45.0	30	450	455		429	0.4	*2.5*			1.2	0.4	Key et al. (2010)
Diatom	*Thalassiosira pseudonana* CCMP1014	16.6	30	450	455		291	0.3	*1.5*			1.2		Key et al. (2010)
Diatom	*Thalassiosira pseudonana* CCMP1014	16.6	30	450	455		303	0.5	*2.7*			1.2		Key et al. (2010)
Diatom	*Coscinodiscus radiatus* CCMP312	138000.0	30	450	455		143	0.3	*1.8*				0.8	Wu et al. (2012)
Diatom	*Coscinodiscus radiatus* CCMP312	138000.0	30	450	455		160	0.2	*1.1*				0.6	Wu et al. (2011)
Diatom	*Coscinodiscus radiatus* CCMP312	138000.0	30	450	625		138	0.1	*0.4*				0.3	Wu et al. (2011)
Diatom	*Coscinodiscus radiatus* CCMP312	138000.0	30	1400	Fluorescent		147	0.2	*1.2*				0.7	Wu et al. (2011)
Diatom	*Thalassiosira pseudonana* CCMP1014	11.9	30	450	455		286	0.4	*2.7*				0.4	Wu et al. (2012)
Diatom	*Thalassiosira pseudonana* CCMP1014	11.9	30	450	455		260	0.5	*2.9*				0.5	Wu et al. (2012)

Diatom	*Thalassiosira pseudonana* CCMP1014	11.9	30	1400	Fluorescent	258	0.3	*2.1*		0.7	Wu et al. (2011)
Diatom	*Thalassiosira pseudonana* CCMP1014	11.9	30	450	455	256	0.6	*3.5*		0.9	Wu et al. (2011)
Diatom	*Thalassiosira pseudonana* CCMP1014	11.9	30	450	625	299	0.2	*1.0*		0.7	Wu et al. (2011)
Diatom	*Phaeodactylum tricornutum*		30	450	455	267	0.7	*4.2*		1.0	Lavaud et al. (2016)
Diatom	*Skeletonema costatum*		30	450	455	253	0.9	*5.1*		0.8	Lavaud et al. (2016)
Diatom	*Ditylum brightwelli* P1 small	22300.0	287	450	455		0.8	*4.8*	2.0		Sharpe et al. (2012)
Diatom	*Ditylum brightwelli* P1 small	22300.0	37	450	455	261	0.8	*4.8*	1.9		Sharpe et al. (2012)
Diatom	*Ditylum brightwelli* P1 big	54500.0	287	450	455		0.9	*5.2*	2.4		Sharpe et al. (2012)
Diatom	*Ditylum brightwelli* P1 big	54500.0	37	450	455	255	0.7	*4.0*	1.8		Sharpe et al. (2012)
Diatom	*Ditylum brightwelli* P2 small	33610.0	287	450	455		0.9	*5.2*	2.5		Sharpe et al. 2012
Diatom	*Ditylum brightwelli* P2 small	33610.0	37	450	455	232	0.6	*3.3*	1.4		Sharpe et al. (2012)
Diatom	*Ditylum brightwelli* P2 big	240300.0	287	450	455		0.9	*5.4*	2.5		Sharpe et al. (2012)
Diatom	*Ditylum brightwelli* P2 big	240300.0	37	450	455	189	1.0	*5.7*	1.4		Sharpe et al. (2012)
Diatom	*Thalassiosira pseudonana* CCMP1335	33.5	31	450	455	327	0.7	*4.3*		1.4	Li et al. (2015)
Diatom	*Thalassiosira pseudonana* CCMP1335	33.5	81	450	455	299	0.9	*5.2*		1.0	Li et al. (2015)
Diatom	*Thalassiosira pseudonana* CCMP1335	33.5	167	450	455	266	1.0	*5.8*		1.6	Li et al. (2015)
Diatom	*Thalassiosira pseudonana* CCMP1335	33.5	242	450	455	230	0.8	*4.9*		2.1	Li et al. (2015)

(continued)

Table 13.2. (continued)

Group	Species	Biovol_µm^3	Growth_µE	Treatment_µE	Treatment_nm	Stress	σpsii_10_20_m^{-2}	σi_10_-24_m^{-2} quanta^{-1}	Φpi_10_-7_m-2_µmol	kpi_10_-4_s_$^{-1}$	Krec_10_-4_s^{-1}	Difference_10_-4	kpsba_10_-4_s_$^{-1}$	Reference
Diatom	*Thalassiosira pseudonana* CCMP1335	33.5	380	450	455		208	0.7	*4.4*				2.1	Li et al. (2015)
Diatom	*Thalassiosira pseudonana* CCMP1335	33.5	31	450	455		313	0.7	*4.1*				1.4	Li et al. (2015)
Diatom	*Thalassiosira pseudonana* CCMP1335	33.5	81	450	455		300	0.7	*4.1*				1.7	Li et al. (2015)
Diatom	*Thalassiosira pseudonana* CCMP1335	33.5	167	450	455		275	0.7	*4.2*				1.7	Li et al. (2015)
Diatom	*Thalassiosira pseudonana* CCMP1335	33.5	242	450	455		227	0.7	*4.2*				1.7	Li et al. (2015)
Diatom	*Thalassiosira pseudonana* CCMP1335	33.5	380	450	455		214	0.7	*4.1*				2.1	Li et al. (2015)
Diatom	Rimouski (481,300 N, 681290 W)		1750	1750	Sunlight					0.1		0.4	1.8	Bouchard et al. (2005b)
Diatom	Rimouski (481,300 N, 681290 W)		1750	1750	Sunlight					0.8		0.9	4.0	Bouchard et al. (2005b)
Diatom	Ushuaia (541,470 S, 681200 W)		2000	2000	Sunlight					8.8		8.8	33.0	Bouchard et al. (2005b)
Diatom	Ushuaia (541,470 S, 681200 W)		2000	2000	Sunlight					8.0		8.0	15.8	Bouchard et al. (2005b)
Diatom	*Thalassiosira pseudonana* CCMP1014	17.0	30	450	455		292	0.3	*2.0*					McCarthy et al. (2012)
Diatom	*Thalassiosira pseudonana* CCMP1014	20.0	30	450	455		286	0.5	*2.9*					McCarthy et al. (2012)
Diatom	*Thalassiosira pseudonana* CCMP1335	50.0	30	450	455		289	0.3	*1.7*					McCarthy et al. (2012)
Diatom	*Thalassiosira pseudonana* CCMP1335	30.0	30	450	455		299	0.5	*2.7*					McCarthy et al. (2012)

Diatom	*Thalassiosira punctigera* CCAP1085/19	54361.6	150	75	Fluorescent	399	0.0	Li et al. (2016)
Diatom	*Thalassiosira punctigera* CCAP1085/19	54361.6	300	75	Fluorescent	393	0.5	Li et al. (2016)
Diatom	*Thalassiosira punctigera* CCAP1085/19	54361.6	75	75	Fluorescent	460	0.1	Li et al. (2016)
Diatom	*Thalassiosira punctigera* CCAP1085/19	54361.6	25	300	Fluorescent	385	0.0	Li et al. (2016)
Diatom	*Thalassiosira punctigera* CCAP1085/19	54361.6	600	300	Fluorescent	462	1.6	Li et al. (2016)
Diatom	*Thalassiosira punctigera* CCAP1085/19	54361.6	300	300	Fluorescent	577	0.2	Li et al. (2016)
Diatom	*Thalassiosira punctigera* CCAP1085/19	54361.6	150	300	Fluorescent	451	0.0	Li et al. (2016)
Diatom	*Thalassiosira punctigera* CCAP1085/19	54361.6	75	300	Fluorescent	489	0.1	Li et al. (2016)
Diatom	*Thalassiosira punctigera* CCAP1085/19	54361.6	300	300	Fluorescent	469	0.5	Li et al. (2016)
Diatom	*Thalassiosira punctigera* CCAP1085/19	54361.6	150	300	Fluorescent	516	0.2	Li et al. 2016
Diatom	*Thalassiosira punctigera* CCAP1085/19	54361.6	75	300	Fluorescent	471	0.0	Li et al. (2016)
Diatom	*Thalassiosira punctigera* CCAP1085/19	54361.6	300	300	Fluorescent	445	0.4	Li et al. (2016)
Diatom	*Thalassiosira punctigera* CCAP1085/19	54361.6	150	300	Fluorescent	459	0.1	Li et al. (2016)
Diatom	*Thalassiosira punctigera* CCAP1085/19	54361.6	75	300	Fluorescent	494	0.0	Li et al. (2016)

(continued)

Table 13.2. (continued)

Group	Species	Biovol_µm^3	Growth_µE	Treatment_µE	Treatment_nm	Stress	σpsii_10_20_m^{-2}	σi_10_-24_m^{-2} quanta^{-1}	Φpi_10_-7_m-2_µmol	kpi_10_-4_s_$^{-1}$	Krec_10_-4_s^{-1}	Difference_10_-4	kpsba_10_-4_s_$^{-1}$	Reference
Diatom	*Thalassiosira weissflogii* CCMA102	696.9		800	PAR									Gao et al. (2018)
Diatom	*Thalassiosira weissflogii* CCMA102	696.9		800	PAR									Gao et al. (2018)
Diatom	*Thalassiosira weissflogii* CCMA102	696.9		800	PAR									Gao et al. (2018)
Diatom	*Thalassiosira weissflogii CCMA102*	696.9		800	PAR									Gao et al. (2018)
Diatom	*Phaeodactylum tricornutum* CCAP 1055/1		40	150	PAR					1.0				Havurinne and Tyystjärvi, (2017)
Diatom	*Phaeodactylum tricornutum* CCAP 1055/1		40	300	PAR					2.1				Havurinne and Tyystjärvi, (2017)
Diatom	*Phaeodactylum tricornutum* CCAP 1055/1		40	600	PAR					3.7				Havurinne and Tyystjärvi, (2017)
Diatom	*Phaeodactylum tricornutum* CCAP 1055/1		40	300	450					2.5				Havurinne and Tyystjärvi, (2017)
Dinophyte	*Ceratium*										6.3			Oliver et al. (2003)
Dinophyte	*Symbiodinium* A1.1		100	100	465					0.1	0.1			Ragni et al. (2010)
Dinophyte	*Symbiodinium* A1.1		100	1600	465					0.8	0.1			Ragni et al. (2010)
Dinophyte	*Symbiodinium* A1		100	100	465					0.2	0.1			Ragni et al. (2010)
Dinophyte	*Symbiodinium* A1		100	1600	465					0.7	0.3			Ragni et al. (2010)
Dinophyte	*Symbiodinium* A1		650	650	465					0.0	0.1			Ragni et al. (2010)
Dinophyte	*Symbiodinium* A1		650	1600	465					0.2	0.2			Ragni et al. (2010)
Haptophyte	*Emiliania huxleyi* B11	65.4	30	50	465					0.0	0.1			Ragni et al. (2008)
Haptophyte	*Emiliania huxleyi* B11	65.4	30	90	465					0.1	0.2			Ragni et al. (2008)
Haptophyte	*Emiliania huxleyi* B11	65.4	30	250	465					0.4	0.4			Ragni et al. (2008)
Haptophyte	*Emiliania huxleyi* B11	65.4	30	520	465					0.6	0.6			Ragni et al. (2008)
Haptophyte	*Emiliania huxleyi* B11	65.4	30	980	465					0.7	0.6			Ragni et al. (2008)
Haptophyte	*Emiliania huxleyi* B11	65.4	30	1980	465					0.9	0.4			Ragni et al. (2008)
Haptophyte	*Emiliania huxleyi* B11	65.4	300	50	465					0.0	0.1			Ragni et al. (2008)
Haptophyte	*Emiliania huxleyi* B11	65.4	300	90	465					0.2	0.3			Ragni et al. (2008)
Haptophyte	*Emiliania huxleyi* B11	65.4	300	250	465					0.5	0.6			Ragni et al. (2008)
Haptophyte	*Emiliania huxleyi* B11	65.4	300	520	465					0.9	0.9			Ragni et al. (2008)
Haptophyte	*Emiliania huxleyi* B11	65.4	300	980	465					1.1	1.1			Ragni et al. (2008)

Haptophyte	*Emiliania huxleyi* B11	65.4	300	1980	465					1.1	1.0			Ragni et al. (2008)
Haptophyte	*Emiliania huxleyi* CCMP1516	38.0	30	1200						16.5		13.6		McKew et al. (2013)
Haptophyte	*Emiliania huxleyi* CCMP1516	38.0	30	550						5.7		5.6		McKew et al. (2013)
Haptophyte	*Emiliania huxleyi* CCMP1516	38.0	30	300						2.2		2.2		McKew et al. (2013)
Haptophyte	*Emiliania huxleyi* CCMP1516	38.0	30	150						0.6		0.6		McKew et al. (2013)
Haptophyte	*Emiliania huxleyi* CCMP1516	70.7	1000	1200						7.5		7.2		McKew et al. (2013)
Haptophyte	*Emiliania huxleyi* CCMP1516	70.7	1000	550						2.8		2.8		McKew et al. (2013)
Haptophyte	*Emiliania huxleyi* CCMP1516	70.7	1000	300						1.0		1.1		McKew et al. (2013)
Haptophyte	*Emiliania huxleyi* CCMP1516	70.7	1000	150						0.3		0.3		McKew et al. (2013)
Haptophyte	*Emiliania huxleyi* CCMP1516	70.7	1000					1.2	7.0					McKew et al. (2013)
Haptophyte	*Phaeocystis antarctica* (CCMP 1841)	0.0	65	65						0.1				Kropuenske et al. (2009)
Haptophyte	*Emiliania huxleyi* CCMP1516	*110.0*	95	450	455		300	0.9	*5.7*			2.0		Loebl et al. (2010)
Haptophyte	*Emiliania huxleyi* CCMP1516	*45.0*	95	450	455	N-depleted	390	0.4	*2.4*			0.5		Loebl et al. (2010)
Haptophyte	*Emiliania huxleyi* AWI (CCMP 1516)	20.0	30	450	455		344	1.2	*7.4*					McCarthy et al. (2012)
Haptophyte	*Emiliania huxleyi* AWI (CCMP 1516)	17.0	30	450	455		366	1.2	*7.1*					McCarthy et al. (2012)
Pelagophyte	*Pelagococcus* CCMP2414	4.2	30	300	455		281	0.9	*5.3*				1.1	Campbell & Tyystjarvi (2012)
Prasinophyte	*Ostreococcus tauri* OTH95	0.3	30	300	455		765	1.1	*6.3*				1.4	Six et al. (2009)
Prasinophyte	*Ostreococcus lucimarinus* CCMP2514	3.2	30	300	455		1170	0.8	*4.9*				2.4	Six et al. (2009)
Prasinophyte	*Ostreococcus* sp. RCC809	3.3	30	300	455		1450	1.7	*10.5*				1.8	Six et al. (2009)
Prasinophyte	*Pyramimonas obovata* CCMP722	84.0	30	300	455		567	0.5	*3.1*				0.6	Six et al. (2009)

(continued)

Table 13.2. (continued)

Group	Species	Biovol_µm^3	Growth_µE	Treatment_µE	Treatment_nm	Stress	σpsii_10_20_m^{-2}	σi_10_-24_m^{-2} quanta^{-1}	Φpi_10_-7_m-2_µmol	kpi_10_-4_s_$^{-1}$	Krec_10_-4_s^{-1}	Difference_10_-4	kpsba_10_-4_s_$^{-1}$	Reference
Prasinophyte	*Micromonas* NCMA 1646	8.2	28	797	455		934	1.4	*8.4*		2.0		1.9	Ni et al. (2017)
Prasinophyte	*Micromonas* NCMA 1646	8.2	185	797	455		791	1.3	*7.8*		5.0		2.9	Ni et al. (2017)
Prasinophyte	*Micromonas* NCMA 2099	1.8	28	400	455		747	3.6	*21.7*		0.7		0.6	Ni et al. (2017)
Prasinophyte	*Micromonas* NCMA 2099	1.8	28	400	455		667	1.0	*6.0*		0.2		0.4	Ni et al. (2017)
Small flagellates	Melchior (64° 20′ S, 62° 59′ W)		464	4.64E+02	Sunlight					0.6		0.6		Bouchard et al. (2005a)
Small flagellates	Melchior (64° 20′ S, 62° 59′ W)		181	1.81E+02	Sunlight					0.7		0.7		Bouchard et al. (2005a)
Small flagellates	Melchior (64° 20′ S, 62° 59′ W)		600	6.00E+02	Sunlight					20.4		20.4		Bouchard et al. (2005a)
Small flagellates	Melchior (64° 20′ S, 62° 59′ W)		33	3.33E+01	Sunlight					0.6		0.6		Bouchard et al. (2005a)
Small flagellates	Melchior (64° 20′ S, 62° 59′ W)		461	4.61E+02	Sunlight					8.5		7.1		Bouchard et al. (2005a)

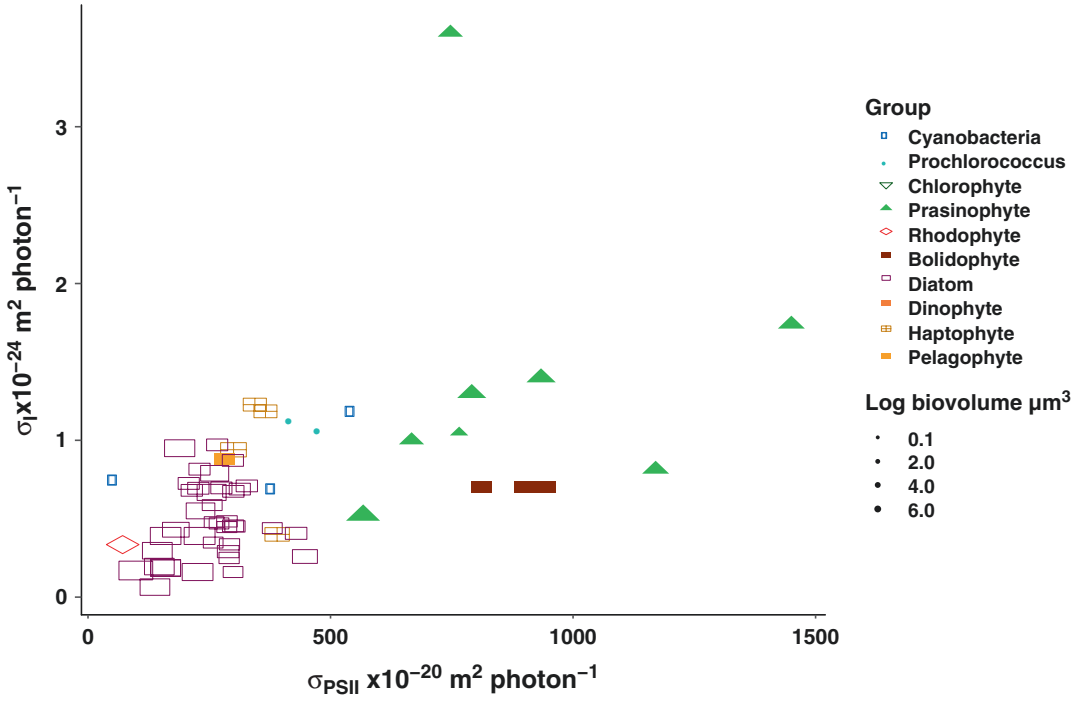

Fig. 13.5. Susceptibility to photoinactivation (σ_I) of Photosystem II vs. effective absorption cross section for photochemistry of Photosystem II (σ_{PSII}) for a panel of marine phytoplankton
Porphyridium cruentum (C. Dubois & D. Campbell, unpub)
Blue open rectangles: phycobilin containing picocyanobacteria
Blue closed circles: *Prochlorococcus*
Green closed triangles: marine Prasinophytes
Red open diamond: Rhodophyte, Porphyridium cruentum (C. Dubois & D. Campbell, unpub)
Red closed squares: Bolidophyte
Purple open squares: centric diatoms from *Thalassiosira* & *Coscinodiscus*
Orange filled square: Dinophyte
Orange square with cross: Haptophyte Coccolithophore (*Emiliania huxeyli*).
Light Orange filled square: Pelagophyte *Pelagococcus* (C. Dubois & D. Campbell, unpub).
Symbol size proportional to log10 cell volume
Citations for underlying data in Table 13.2.

stream limitations on their metabolism (Zorz et al. 2015) and their limited capacity to detoxify reactive oxygen species (Morris et al. 2011) which increase the risk of deleterious side reactions from photosynthetic light capture.

V. Summary

The process(es) dominating the functional responses of phytoplankton PSII to environmental fluctuations are conditionally dependent upon multiple factors. The spectral

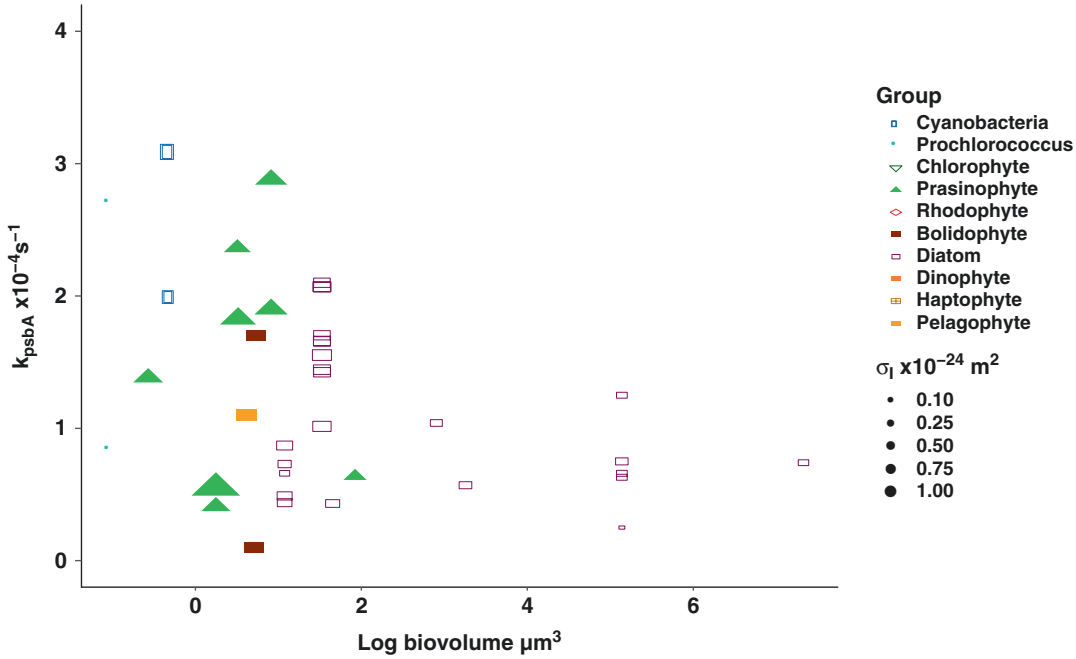

Fig. 13.6. Capacity for removal of the PSII PsbA subunit k_{PsbA}, vs. cell volume for a panel of marine phytoplankton
Blue open rectangles: phycobilin containing picocyanobacteria
Blue closed circles: Prochlorococcus
Green closed circles: marine Prasinophytes
Red open diamond: Rhodophyte, Porphyridium cruentum (C. Dubois & D. Campbell, unpub)
Red closed squares: Bolidophyte
Purple open squares: centric diatoms from *Thalassiosira* & *Coscinodiscus*
Orange filled square: Dinophyte
Orange square with cross: Haptophyte Coccolithophore (*Emiliania huxeyli*).
Light Orange filled square: Pelagophyte *Pelagococcus* (C. Dubois & D. Campbell, unpub).
Symbol size proportional to $\sigma_I(10^{-24}$ m^2 photon$^{-1})$
Citations for underlying data in Table 13.2.

regime is generally blue biased in the water column, favouring the direct hit path for photoinactivation. Light levels are exponentially attenuated with depth, again favouring the direct hit path by acting to lower excitation pressure upon PSII, although low temperature or metabolic factors constraining down stream metabolism (Zorz et al. 2015) can drive up excitation pressure even under moderate light (Ni et al. 2017). These interacting factors generate a large range of susceptibilities to photoinactivation across small phytoplankton cells, even within a lineage. Large cells, and diatoms in particular, enjoy higher biooptical screening (Key et al. 2010; Wu et al. 2011) and thus lower intrinsic susceptibility to photoinactivation at a given light level. This apparent benefit of large cell size is not always matched by a decrease in PSII protein complex recycling (Li et al. 2016) because, at least under nutrient replete conditions, diatoms may engage in luxury or pre-emptive recycling of PSII before photoinactivation occurs. PSII repair may be

restricted by low temperatures, or by salinity or nutrient stress (Nishiyama et al. 2005; Murata et al. 2007). Furthermore, environmental shifts in nutrients or CO_2 can alter resource allocations or electron flows, with sometimes counter-intuitive effects upon susceptibility to photoinactivation across taxa (Loebl et al. 2010; McCarthy et al. 2012; Gao and Campbell 2014; Li et al. 2015; Gao et al. 2018).

Acknowledgements

The authors thank their many colleagues and associates who have contributed data and concepts, in particular, E. Tyystjärvi, A. Cockshutt, J. Bouchard, W. Schmidt, T. Key, R. Sherrard, S. Thomas, T. Loebl, C. Six, C. DuBois, A. McCarthy, H. Wu, Y. Wu, G. Li, G. Ni., C. Murphy, M. Roodvoets, S. Frankenbach, A. Dolan. N. Duff assisted with generation of figures. A. Irwin & RL Cockshutt assisted with the derivation of Equation 13.6.

DC was supported by a Canada Research Chair in Phytoplankton Ecophysiology and by a Visiting Professor position at Centrum ALGATECH of the Czech Academy of Sciences, Třeboň, Czech Republic.

The chapter benefited from review by Dr. W.S. Chow.

References

Allakhverdiev SI, Murata N (2004) Environmental stress inhibits the synthesis de novo of proteins involved in the photodamage–repair cycle of Photosystem II in Synechocystis sp. PCC 6803. Biochim Biophys Acta BBA – Bioenerg 1657:23–32. https://doi.org/10.1016/j.bbabio.2004.03.003

Aro E, Virgin I, Andersson B (1993) Photoinhibition of photosystem II. Inactivation, protein damage and turnover. Biochim Biophys Acta Bioenerg 1143:113–134

Aro E-M, Suorsa M, Rokka A et al (2005) Dynamics of photosystem II: a proteomic approach to thylakoid protein complexes. J Exp Bot 56:347–356. https://doi.org/10.1093/jxb/eri041

Bachmann KM, Ebbert V, Adams WW III et al (2004) Effects of lincomycin on PSII efficiency, non-photochemical quenching, D1 protein and xanthophyll cycle during photoinhibition and recovery. Funct Plant Biol 31:803–813

Bailleul B, Rogato A, de Martino A et al (2010) An atypical member of the light-harvesting complex stress-related protein family modulates diatom responses to light. Proc Natl Acad Sci 107:18214–18219. https://doi.org/10.1073/pnas.1007703107

Bailleul B, Berne N, Murik O et al (2015) Energetic coupling between plastids and mitochondria drives CO2 assimilation in diatoms. Nature 524:366–369. https://doi.org/10.1038/nature14599

Baroli I, Melis A (1996) Photoinhibition and repair in *Dunaliella salina* acclimated to different growth irradiances. Planta 198:640–646. https://doi.org/10.1007/BF00262653

Behrenfeld MJ, Prasil O, Kolber ZS et al (1998) Compensatory changes in photosystem II electron turnover rates protect photosynthesis from photoinhibition. Photosynth Res 58:259–268

Bentley FK, Eaton-Rye JJ (2008) The effect of protein synthesis inhibitors on recovery of Photodamaged photosystem II in Synechocystis sp. PCC 6803 lacking PsbM or PsbT. In: Allen JF, Gantt E, Golbeck JH, Osmond B (eds) Photosynthesis. Energy from the Sun. Springer Netherlands, Dordrecht, pp 711–714

Bilger W, Björkman O (1990) Role of the xanthophyll cycle in photoprotection elucidated by measurements of light-induced absorbance changes, fluorescence and photosynthesis in leaves of *Hedera canariensis*. Photosynth Res 25:173–185. https://doi.org/10.1007/BF00033159

Blot N, Mella-Flores D, Six C et al (2011) Light history influences the response of the marine Cyanobacterium Synechococcus sp. WH7803 to oxidative stress. Plant Physiol 156:1934–1954. https://doi.org/10.1104/pp.111.174714

Bouchard JN, Campbell DA, Roy S (2005a) Effects of UV-B radiation on the D1 protein repair cycle of natural phytoplankton communities from three latitudes (Canada, Brazil and Argentina). J Phycol 41:273–286. https://doi.org/10.1111/j.1529-8817.2005.04126.x

Bouchard JN, Roy S, Ferreyra G et al (2005b) Ultraviolet-B effects on photosystem II efficiency of natural phytoplankton communities from Antarctica. Polar Biol 28:607–618. https://doi.org/10.1007/s00300-005-0727-4

Campbell D, Hurry V, Clarke AK et al (1998) Chlorophyll fluorescence analysis of cyanobacterial photosynthesis and acclimation. Microbiol Mol Biol Rev 62:667–683

Campbell DA, Cockshutt AM, Porankiewicz-Asplund J (2003) Analysing photosynthetic complexes in uncharacterized species or mixed microalgal communities using global antibodies. Physiol Plant 119:322–327

Campbell DA, Hossain Z, Cockshutt AM et al (2013) Photosystem II protein clearance and FtsH function in the diatom *Thalassiosira pseudonana*. Photosynth Res 115:43–54. https://doi.org/10.1007/s11120-013-9809-2

Campbell DA, Tyystjärvi E (2012) Parameterization of photosystem II photoinactivation and repair. Biochim Biophys Acta 1817:258–265. https://doi.org/10.1016/j.bbabio.2011.04.010

Cao J, Govindjee (1990) Chlorophyll a fluorescence transient as an indicator of active and inactive photosystem II in thylakoid membranes. Biochim Biophys Acta BBA – Bioenerg 1015:180–188. https://doi.org/10.1016/0005-2728(90)90018-Y

Chow WS, Hope AB, Anderson JM (1989) Oxygen per flash from leaf disks quantifies photosystem II. Biochim Biophys Acta BBA – Bioenerg 973:105–108. https://doi.org/10.1016/S0005-2728(89)80408-6

Chow WS, Lee H-Y, Park Y-I et al (2002) The role of inactive photosystem–II–mediated quenching in a last–ditch community defence against high light stress in vivo. Philos Trans R Soc Lond Ser B Biol Sci 357:1441–1450. https://doi.org/10.1098/rstb.2002.1145

Domingues N, Matos AR, da Silva JM, Cartaxana P (2012) Response of the diatom *Phaeodactylum tricornutum* to Photooxidative stress resulting from high light exposure. PLoS One 7:e38162. https://doi.org/10.1371/journal.pone.0038162

Edelman M, Mattoo AK (2008) D1-protein dynamics in photosystem II: the lingering enigma. Photosynth Res 98:609–620. https://doi.org/10.1007/s11120-008-9342-x

Elrad D, Niyogi KK, Grossman AR (2002) A major light-harvesting polypeptide of photosystem II functions in thermal dissipation. Plant Cell 14:1801–1816. https://doi.org/10.1105/tpc.002154

Falkowski PG, Katz ME, Knoll AH et al (2004) The evolution of modern eukaryotic phytoplankton. Science 305:354–360. https://doi.org/10.1126/science.1095964

Falkowski P, Fenchel T, Delong E (2008) The microbial engines that drive earth's biogeochemical cycles. Science 320:1034–1039. https://doi.org/10.1126/science.1153213

Finkel ZV (2001) Light absorption and size scaling of light-limited metabolism in marine diatoms. Limnology and Oceanography 46:86–94. https://doi.org/10.4319/lo.2001.46.1.0086

Fuhrmann T, Landwehr S, El Rharbi-Kucki M, Sumper M (2004) Diatoms as living photonic crystals. Appl Phys B Lasers Opt 78:257–260. https://doi.org/10.1007/s00340-004-1419-4

Gao K, Campbell DA (2014) Photophysiological responses of marine diatoms to elevated CO_2 and decreased pH: a review. Funct Plant Biol 41:449. https://doi.org/10.1071/FP13247

Gao G, Shi Q, Xu Z et al (2018) Global warming interacts with ocean acidification to alter PSII function and protection in the diatom Thalassiosira weissflogii. Environ Exp Bot 147:95–103. https://doi.org/10.1016/j.envexpbot.2017.11.014

Gollan PJ, Tikkanen M, Aro E-M (2015) Photosynthetic light reactions: integral to chloroplast retrograde signalling. Curr Opin Plant Biol 27:180–191. https://doi.org/10.1016/j.pbi.2015.07.006

Gorbunov MY, Kuzminov FI, Fadeev VV et al (2011) A kinetic model of non-photochemical quenching in cyanobacteria. Biochim Biophys Acta BBA – Bioenerg 1807:1591–1599. https://doi.org/10.1016/j.bbabio.2011.08.009

Greer DH, Berry JA, Björkman O (1986) Photoinhibition of photosynthesis in intact bean leaves: role of light and temperature, and requirement for chloroplast-protein synthesis during recovery. Planta 168:253–260. https://doi.org/10.1007/BF00402971

Grouneva I, Rokka A, Aro E-M (2011) The thylakoid membrane proteome of two marine diatoms outlines both diatom-specific and species-specific features of the photosynthetic machinery. J Proteome Res 10:5338–5353. https://doi.org/10.1021/pr200600f

Hakala M, Tuominen I, Keränen M et al (2005) Evidence for the role of the oxygen-evolving manganese complex in photoinhibition of Photosystem II. Biochim Biophys Acta BBA – Bioenerg 1706:68–80. https://doi.org/10.1016/j.bbabio.2004.09.001

Hakala-Yatkin M, Mäntysaari M, Mattila H, Tyystjärvi E (2010) Contributions of visible and ultraviolet parts of sunlight to photoinhibition. Plant Cell Physiol 51:1745–1753. https://doi.org/10.1093/pcp/pcq133

Hakkila K, Antal T, Rehman AU et al (2014) Oxidative stress and photoinhibition can be separated in the cyanobacterium Synechocystis sp. PCC 6803. Biochim Biophys Acta BBA – Bioenerg 1837:217–225. https://doi.org/10.1016/j.bbabio.2013.11.011

Havaux M, Strasser RJ, Greppin H (1991) A theoretical and experimental analysis of the qP and q N coefficients of chlorophyll fluorescence quenching and their relation to photochemical and nonphotochemical events. Photosynth Res 27:41–55. https://doi.org/10.1007/BF00029975

Havurinne V, Tyystjärvi E (2017) Action spectrum of photoinhibition in the diatom phaeodactylum tricor-

nutum. Plant Cell Physiol 58:2217–2225. https://doi.org/10.1093/pcp/pcx156

He J, Yang W, Qin L et al (2015) Photoinactivation of Photosystem II in wild-type and chlorophyll b-less barley leaves: which mechanism dominates depends on experimental circumstances. Photosynth Res 126:399–407. https://doi.org/10.1007/s11120-015-0167-0

Henley WJ (1993) Measurement and interpretation of photosynthetic light-response curves in algae in the context of photoinhibition and diel changes. J Phycol 29:729–739. https://doi.org/10.1111/j.0022-3646.1993.00729.x

Heraud P, Beardall J (2000) Changes in chlorophyll fluorescence during exposure of Dunaliella tertiolecta to UV radiation indicate a dynamic interaction between damage and repair processes. Photosynth Res 63:123–134. https://doi.org/10.1023/A:1006319802047

Horton P, Hague A (1988) Studies on the induction of chlorophyll fluorescence in isolated barley protoplasts. IV. Resolution of non-photochemical quenching. Biochim Biophys Acta BBA – Bioenerg 932:107–115. https://doi.org/10.1016/0005-2728(88)90144-2

Huner NPA, Öquist G, Sarhan F (1998) Energy balance and acclimation to light and cold. Trends Plant Sci 3:224–230. https://doi.org/10.1016/S1360-1385(98)01248-5

Ivanov AG, Sane PV, Hurry V et al (2008) Photosystem II reaction centre quenching: mechanisms and physiological role. Photosynth Res 98:565–574. https://doi.org/10.1007/s11120-008-9365-3

Järvi S, Suorsa M, Aro E-M (2015) Photosystem II repair in plant chloroplasts — Regulation, assisting proteins and shared components with photosystem II biogenesis. Biochim Biophys Acta BBA – Bioenerg 1847:900–909. https://doi.org/10.1016/j.bbabio.2015.01.006

Kalaji HM, Schansker G, Brestic M et al (2017) Frequently asked questions about chlorophyll fluorescence, the sequel. Photosynth Res 132:13–66. https://doi.org/10.1007/s11120-016-0318-y

Keren N, Krieger-Liszkay A (2011) Photoinhibition: molecular mechanisms and physiological significance. Physiol Plant 142:1–5. https://doi.org/10.1111/j.1399-3054.2011.01467.x

Keren N, Berg A, van Kan PJM et al (1997) Mechanism of photosystem II photoinactivation and D1 protein degradation at low light: the role of back electron flow. Proc Natl Acad Sci U S A 94:1579–1584

Key T, McCarthy A, Campbell D et al (2010) Cell size trade-offs govern light exploitation strategies in marine phytoplankton. Environ Microbiol 12:95–104. https://doi.org/10.1111/j.1462-2920.2009.02046.x

Kok B (1956) On the inhibition of photosynthesis by intense light. Biochim Biophys Acta 21:234–244

Kolber ZS, Prášil O, Falkowski PG (1998) Measurements of variable chlorophyll fluorescence using fast repetition rate techniques: defining methodology and experimental protocols. Biochim Biophys Acta BBA – Bioenerg 1367:88–106. https://doi.org/10.1016/S0005-2728(98)00135-2

Komenda J, Sobotka R, Nixon PJ (2012) Assembling and maintaining the Photosystem II complex in chloroplasts and cyanobacteria. Curr Opin Plant Biol 15:245–251. https://doi.org/10.1016/j.pbi.2012.01.017

Kramer DM, Johnson G, Kiirats O, Edwards GE (2004) New fluorescence parameters for the determination of QA redox state and excitation energy fluxes. Photosynth Res 79:209–218

Kropuenske LR, Mills MM, van DGL et al (2009) Photophysiology in two major Southern Ocean phytoplankton taxa: Photoprotection in Phaeocystis antarctica and *Fragilariopsis cylindrus*. Limnol Oceanogr 54:1176–1196. https://doi.org/10.4319/lo.2009.54.4.1176

Kvernvik AC, Hoppe CJM, Lawrenz E et al (2018) Fast reactivation of photosynthesis in arctic phytoplankton during the polar night. J Phycol. https://doi.org/10.1111/jpy.12750

Kyle DJ, Ohad I, Arntzen CJ (1984) Membrane protein damage and repair: Selective loss of a quinone-protein function in chloroplast membranes. Proc Natl Acad Sci 81:4070–4074. https://doi.org/10.1073/pnas.81.13.4070

Lavaud J, Goss R (2014) The peculiar features of non-photochemical fluorescence quenching in diatoms and brown algae. In: Demmig-Adams B, Garab G, Adams III WA, Govindjee (eds) Non-photochemical quenching and energy dissipation in plants, algae and cyanobacteria. Springer Netherlands, pp 421–443

Lavaud J, Six C, Campbell DA (2016) Photosystem II repair in marine diatoms with contrasting photophysiologies. Photosynth Res 127:189–199. https://doi.org/10.1007/s11120-015-0172-3

Lepetit B, Goss R, Jakob T, Wilhelm C (2011) Molecular dynamics of the diatom thylakoid membrane under different light conditions. Photosynth Res 111:245–257. https://doi.org/10.1007/s11120-011-9633-5

Lesser MP, Cullen JJ, Neale PJ (1994) Carbon uptake in a marine diatom during acute exposure to ultraviolet B radiation: relative importance of damage and repair. J Phycol 30:183–192. https://doi.org/10.1111/j.0022-3646.1994.00183.x

Li G, Brown CM, Jeans JA et al (2015) The nitrogen costs of photosynthesis in a diatom under current and future pCO_2. New Phytol 205:533–543. https://doi.org/10.1111/nph.13037

Li G, Woroch AD, Donaher NA et al (2016) A hard day's night: diatoms continue recycling photosystem II in the dark. Front Mar Sci 3. https://doi.org/10.3389/fmars.2016.00218

Litchman E, Neale PJ, Banaszak AT (2002) Increased sensitivity to ultraviolet radiation in nitrogen-limited dinoflagellates: photoprotection and repair. Limnol Oceanogr 47:86–94. https://doi.org/10.4319/lo.2002.47.1.0086

Loebl M, Cockshutt AM, Campbell DA, Finkel ZV (2010) Physiological basis for high resistance to photoinhibition under nitrogen depletion in *Emiliania huxleyi*. Limnol Oceanogr 55:2150–2160. https://doi.org/10.4319/lo.2010.55.5.2150

Losciale P, Oguchi R, Hendrickson L et al (2008) A rapid, whole-tissue determination of the functional fraction of PSII after photoinhibition of leaves based on flash-induced P700 redox kinetics. Physiol Plant 132:23–32. https://doi.org/10.1111/j.1399-3054.2007.01000.x

Lovejoy C, Vincent WF, Bonilla S et al (2007) Distribution, phylogeny, and growth of cold-adapted picoprasinophytes in arctic seas. J Phycol 43:78–89

MacIntyre HL, Kana TM, Geider RJ (2000) The effect of water motion on short-term rates of photosynthesis by marine phytoplankton. Trends Plant Sci 5:12–17. https://doi.org/10.1016/S1360-1385(99)01504-6

Mackenzie T (2004) Carbon status constrains light acclimation in the cyanobacterium *Synechococcus elongatus*. Plant Physiol 136:3301–3312. https://doi.org/10.1104/pp.104.047936

Magyar M, Sipka G, Kovács L et al (2018) Rate-limiting steps in the dark-to-light transition of Photosystem II – revealed by chlorophyll-a fluorescence induction. Sci Rep 8. https://doi.org/10.1038/s41598-018-21195-2

McCarthy A, Rogers SP, Duffy SJ, Campbell DA (2012) Elevated carbon dioxide differentially alters the photophysiology of *Thalassiosira pseudonana* (Bacillariophyceae) and *Emiliana huxleyi* (Haptophyta). J Phycol 48:635–646. https://doi.org/10.1111/j.1529-8817.2012.01171.x

McKew BA, Davey P, Finch SJ et al (2013) The trade-off between the light-harvesting and photoprotective functions of fucoxanthin-chlorophyll proteins dominates light acclimation in *Emiliania huxleyi* (clone CCMP 1516). New Phytol 200:74–85. https://doi.org/10.1111/nph.12373

Melis A (1985) Functional properties of Photosystem II? in spinach chloroplasts. Biochim Biophys Acta BBA – Bioenerg 808:334–342. https://doi.org/10.1016/0005-2728(85)90017-9

Miyata K, Noguchi K, Terashima I (2012) Cost and benefit of the repair of photodamaged photosystem II in spinach leaves: roles of acclimation to growth light. Photosynth Res 113:165–180. https://doi.org/10.1007/s11120-012-9767-0

Morris JJ, Johnson ZI, Szul MJ et al (2011) Dependence of the cyanobacterium *Prochlorococcus* on hydrogen peroxide scavenging microbes for growth at the ocean's surface. PLoS One 6:e16805. https://doi.org/10.1371/journal.pone.0016805

Murata N, Nishiyama Y (2018) ATP is a driving force in the repair of photosystem II during photoinhibition. Plant Cell Environ 41:285–299. https://doi.org/10.1111/pce.13108

Murata N, Takahashi S, Nishiyama Y, Allakhverdiev SI (2007) Photoinhibition of photosystem II under environmental stress. Biochim Biophys Acta BBA – Bioenerg 1767:414–421. https://doi.org/10.1016/j.bbabio.2006.11.019

Murata N, Allakhverdiev SI, Nishiyama Y (2012) The mechanism of photoinhibition *in vivo*: Re-evaluation of the roles of catalase, α-tocopherol, non-photochemical quenching, and electron transport. Biochim Biophys Acta BBA – Bioenerg 1817:1127–1133. https://doi.org/10.1016/j.bbabio.2012.02.020

Murphy CD, Ni G, Li G et al (2016) Quantitating active photosystem II reaction center content from fluorescence induction transients: PSII calibration. Limnol Oceanogr Methods. https://doi.org/10.1002/lom3.10142

Murphy CD, Roodvoets MS, Austen EJ et al (2017) Photoinactivation of Photosystem II in Prochlorococcus and Synechococcus. PLoS One 12:e0168991. https://doi.org/10.1371/journal.pone.0168991

Nagy L, Bálint E, Barber J et al (1995) Photoinhibition and law of reciprocity in photosynthetic reactions of Synechocystis sp. PCC 6803. J Plant Physiol 145:410–415. https://doi.org/10.1016/S0176-1617(11)81763-3

Neale PJ, Thomas BC (2016) Inhibition by ultraviolet and photosynthetically available radiation lowers model estimates of depth-integrated picophytoplankton photosynthesis: global predictions for *Prochlorococcus* and *Synechococcus*. Glob Chang Biol. https://doi.org/10.1111/gcb.13356

Neale PJ, Pritchard AL, Ihnacik R (2014) UV effects on the primary productivity of picophytoplankton: biological weighting functions and exposure response curves of *Synechococcus*. Biogeosciences 11:2883–2895. https://doi.org/10.5194/bg-11-2883-2014

Neilson JAD, Durnford DG (2010) Structural and functional diversification of the light-harvesting complexes in photosynthetic eukaryotes. Photosynth Res 106:57–71. https://doi.org/10.1007/s11120-010-9576-2

Ni G, Zimbalatti G, Murphy CD et al (2017) Arctic Micromonas uses protein pools and non-photochemical quenching to cope with temperature restrictions on Photosystem II protein turnover. Photosynth Res 131:203–220. https://doi.org/10.1007/s11120-016-0310-6

Nishiyama Y, Murata N (2014) Revised scheme for the mechanism of photoinhibition and its application to enhance the abiotic stress tolerance of the photosynthetic machinery. Appl Microbiol Biotechnol:1–20. https://doi.org/10.1007/s00253-014-6020-0

Nishiyama Y, Allakhverdiev SI, Murata N (2005) Inhibition of the repair of Photosystem II by oxidative stress in cyanobacteria. Photosynth Res 84:1–7. https://doi.org/10.1007/s11120-004-6434-0

Nixon PJ, Michoux F, Yu J et al (2010) Recent advances in understanding the assembly and repair of photosystem II. Ann Bot 106:1–16. https://doi.org/10.1093/aob/mcq059

Oguchi R, Terashima I, Kou J, Chow WS (2011) Operation of dual mechanisms that both lead to photoinactivation of Photosystem II in leaves by visible light. Physiol Plant 142:47–55. https://doi.org/10.1111/j.1399-3054.2011.01452.x

Oliver RL, Whittington J, Lorenz Z, Webster IT (2003) The influence of vertical mixing on the photoinhibition of variable chlorophyll a fluorescence and its inclusion in a model of phytoplankton photosynthesis. J Plankton Res 25:1107–1129. https://doi.org/10.1093/plankt/25.9.1107

Osmond C, Chow W (1988) Ecology of photosynthesis in the sun and shade: summary and prognostications. Aust J Plant Physiol 15:1–9

Oxborough K, Baker NR (1997) Resolving chlorophyll a fluorescence images of photosynthetic efficiency into photochemical and non-photochemical components – calculation of qP and Fv'/Fm'; without measuring Fo'. Photosynth Res 54:135–142. https://doi.org/10.1023/A:1005936823310

Oxborough K, Moore CM, Suggett DJ et al (2012) Direct estimation of functional PSII reaction center concentration and PSII electron flux on a volume basis: a new approach to the analysis of Fast Repetition Rate fluorometry (FRRf) data. Limnol Oceanogr Methods 10:142–154. https://doi.org/10.4319/lom.2012.10.142

Park Y-I, Chow WS, Anderson JM (1995) Light inactivation of functional photosystem II in leaves of peas grown in moderate light depends on photon exposure. Planta 196:401–411. https://doi.org/10.1007/BF00203636

Perkins RG, Mouget J-L, Lefebvre S, Lavaud J (2006) Light response curve methodology and possible implications in the application of chlorophyll fluorescence to benthic diatoms. Mar Biol 149:703–712. https://doi.org/10.1007/s00227-005-0222-z

Petrou K, Hill R, Brown CM et al (2010) Rapid photoprotection in sea-ice diatoms from the East Antarctic pack ice. Limnol Oceanogr 55:1400–1407. https://doi.org/10.4319/lo.2010.55.3.1400

Petrou K, Kranz SA, Doblin MA, Ralph PJ (2012) Photophysiological responses of *Fragilariopsis cylindrus* (Bacillariophyceae) to nitrogen depeletion at two temperatures 1: nitrogen stress in *F. cylindrus*. J Phycol 48:127–136. https://doi.org/10.1111/j.1529-8817.2011.01107.x

Platt T, Gallegos C, Harrison W (1981) Photoinhibition of photosynthesis in natural assemblages of marine phytoplankton. Inst Mar Peru Boletin volumen extraordinario:103–111

Prášil O, Kolber ZS, Falkowski PG (2018) Control of the maximal chlorophyll fluorescence yield by the QB binding site. Photosynthetica 56:150–162. https://doi.org/10.1007/s11099-018-0768-x

Ragni M, Airs R, Leonardos N, Geider R (2008) Photoinhibition of PSII in *Emiliania huxleyi* (Haptophyta) under high light stress: the roles of photoacclimation, photoprotection and photorepair. J Phycol 44:670–683. https://doi.org/10.1111/j.1529-8817.2008.00524.x

Ragni M, Airs RL, Hennige SJ et al (2010) PSII photoinhibition and photorepair in Symbiodinium (Pyrrhophyta) differs between thermally tolerant and sensitive phylotypes. Mar Ecol Prog Ser 406:57–70. https://doi.org/10.3354/meps08571

Rast A, Heinz S, Nickelsen J (2015) Biogenesis of thylakoid membranes. Biochim Biophys Acta BBA – Bioenerg 1847:821–830. https://doi.org/10.1016/j.bbabio.2015.01.007

Raven JA (2011) The cost of photoinhibition. Physiol Plant 142:87–104. https://doi.org/10.1111/j.1399-3054.2011.01465.x

Ross ON, Moore CM, Suggett DJ et al (2008) A model of photosynthesis and photo-protection based on reaction center damage and repair. Limnol Oceanogr 53:1835–1852

Ruban AV (2016) Nonphotochemical chlorophyll fluorescence quenching: mechanism and effectiveness in protecting plants from photodamage. Plant Physiol 170:1903–1916. https://doi.org/10.1104/pp.15.01935

Sarvikas P, Tyystjärvi T, Tyystjärvi E (2010) Kinetics of prolonged photoinhibition revisited: photoinhibited Photosystem II centres do not protect the active ones against loss of oxygen evolution.

Photosynth Res 103:7–17. https://doi.org/10.1007/s11120-009-9496-1

Sathyendranath S, Platt T (1988) The spectral irradiance field at the surface and in the interior of the ocean: a model for applications in oceanography and remote sensing. J Geophys Res 93:9270. https://doi.org/10.1029/JC093iC08p09270

Schofield O, Kroon BMA, Prézelin BB (1995) Impact of ultraviolet-B radiation on photosystem li activity and its relationship to the inhibition of carbon fixation rates for Antarctic ice algae communities. J Phycol 31:703–715. https://doi.org/10.1111/j.0022-3646.1995.00703.x

Schreiber U, Klughammer C (2013) Wavelength-dependent photodamage to Chlorella investigated with a new type of multi-color PAM chlorophyll fluorometer. Photosynth Res 114:165–177. https://doi.org/10.1007/s11120-013-9801-x

Schuback N, Flecken M, Maldonado MT, Tortell PD (2016) Diurnal variation in the coupling of photosynthetic electron transport and carbon fixation in iron-limited phytoplankton in the NE subarctic Pacific. Biogeosciences 13:1019–1035. https://doi.org/10.5194/bg-13-1019-2016

Serôdio J, Cruz S, Vieira S, Brotas V (2005) Non-photochemical quenching of chlorophyll fluorescence and operation of the xanthophyll cycle in estuarine microphytobenthos. J Exp Mar Biol Ecol 326:157–169. https://doi.org/10.1016/j.jembe.2005.05.011

Serôdio J, Schmidt W, Frankenbach S (2017) A chlorophyll fluorescence-based method for the integrated characterization of the photophysiological response to light stress. J Exp Bot 68:1123–1135. https://doi.org/10.1093/jxb/erw492

Sharpe SC, Koester JA, Loebl M et al (2012) Influence of cell size and DNA content on growth rate and photosystem II function in cryptic species of *Ditylum brightwellii*. PLoS One 7:e52916. https://doi.org/10.1371/journal.pone.0052916

Shelly K, Heraud P, Beardall J (2002) Nitrogen limitation in *Dunaliella tertiolecta* (Chlorophyceaea) leads to increased susceptibility to damage by ultraviolet-B radiation but also increased repair capacity. J Phycol 38:713–720. https://doi.org/10.1046/j.1529-8817.2002.01147.x

Silsbe GM, Oxborough K, Suggett DJ et al (2015) Toward autonomous measurements of photosynthetic electron transport rates: an evaluation of active fluorescence-based measurements of photochemistry. Limnol Oceanogr Methods 13:138–155. https://doi.org/10.1002/lom3.10014

Silva P, Thompson E, Bailey S et al (2003) FtsH is involved in the early stages of repair of photosystem II in *Synechocystis* sp PCC 6803. Plant Cell Online 15:2152–2164. https://doi.org/10.1105/tpc.012609

Simis SGH, Huot Y, Babin M et al (2012) Optimization of variable fluorescence measurements of phytoplankton communities with cyanobacteria. Photosynth Res 112:13–30. https://doi.org/10.1007/s11120-012-9729-6

Sinclair J, Park YI, Chow WS, Anderson JM (1996) Target theory and the photoinactivation of Photosystem II. Photosynth Res 50:33–40

Six C, Finkel Z, Irwin A, Campbell D (2007) Light variability illuminates niche-partitioning among marine picocyanobacteria. PLoS One 2:e1341

Six C, Sherrard R, Lionard M et al (2009) Photosystem II and pigment dynamics among ecotypes of the green alga Ostreococcus. Plant Physiol 151:379–390

Soitamo A, Havurinne V, Tyystjärvi E (2017) Photoinhibition in marine picocyanobacteria. Physiol Plant. https://doi.org/10.1111/ppl.12571

Suggett D, MacIntyre H, Kana T, Geider R (2009) Comparing electron transport with gas exchange: parameterising exchange rates between alternative photosynthetic currencies for eukaryotic phytoplankton. Aquat Microb Ecol 56:147–162. https://doi.org/10.3354/ame01303

Thomas SL, Campbell DA (2013) Photophysiology of Bolidomonas pacifica. J Plankton Res 35:260–269. https://doi.org/10.1093/plankt/fbs105

Treves H, Raanan H, Finkel OM et al (2013) A newly isolated Chlorella sp. from desert sand crusts exhibits a unique resistance to excess light intensity. FEMS Microbiol Ecol 86:373–380. https://doi.org/10.1111/1574-6941.12162

Tyystjärvi E (2008) Photoinhibition of Photosystem II and photodamage of the oxygen evolving manganese cluster. Coord Chem Rev 252:361–376. https://doi.org/10.1016/j.ccr.2007.08.021

Tyystjärvi E (2013) Chapter seven – photoinhibition of photosystem II∗. In: Jeon KW (ed) International review of cell and molecular biology. Academic Press, pp 243–303

Tyystjärvi E, Aro E-M (1996) The rate constant of photoinhibition, measured in lincomycin-treated leaves, is directly proportional to light intensity. Proc Natl Acad Sci USA 93:2213–2218

Tyystjarvi E, Vass I (2004) Light emission as a probe of charge separation and recombination in the photosynthetic apparatus: relation of prompt fluorescence

to delayed light emission and thermoluminescence. In: Papageorgiou GC, Govindjee (eds) Chlorophyll a fluorescence. Springer Netherlands, Dordrecht, pp 363–388

van Kooten O, Snel JFH (1990) The use of chlorophyll fluorescence nomenclature in plant stress physiology. Photosynth Res 25:147–150. https://doi.org/10.1007/BF00033156

Vass I (2012) Molecular mechanisms of photodamage in the Photosystem II complex. Biochim Biophys Acta BBA – Bioenerg 1817:209–217. https://doi.org/10.1016/j.bbabio.2011.04.014

Vassiliev IR, Prasil O, Wyman KD et al (1994) Inhibition of PS II photochemistry by PAR and UV radiation in natural phytoplankton communities. Photosynth Res 42:51–64. https://doi.org/10.1007/BF00019058

Walters RG, Horton P (1993) Theoretical assessment of alternative mechanisms for non-photochemical quenching of PS II fluorescence in barley leaves. Photosynth Res 36:119–139. https://doi.org/10.1007/BF00016277

Ware MA, Belgio E, Ruban AV (2015a) Comparison of the protective effectiveness of NPQ in Arabidopsis plants deficient in PsbS protein and zeaxanthin. J Exp Bot 66:1259–1270. https://doi.org/10.1093/jxb/eru477

Ware MA, Belgio E, Ruban AV (2015b) Photoprotective capacity of non-photochemical quenching in plants acclimated to different light intensities. Photosynth Res 126:261–274. https://doi.org/10.1007/s11120-015-0102-4

Webb WL, Newton M, Starr D (1974) Carbon dioxide exchange of *Alnus rubra*. Oecologia 17:281–291. https://doi.org/10.1007/BF00345747

Wu H, Cockshutt AM, McCarthy A, Campbell DA (2011) Distinctive photosystem II photoinactivation and protein dynamics in marine diatoms. Plant Physiol 156:2184–2195. https://doi.org/10.1104/pp.111.178772

Wu H, Roy S, Alami M et al (2012) Photosystem II Photoinactivation, repair, and protection in marine centric diatoms. Plant Physiol 160:464–476. https://doi.org/10.1104/pp.112.203067

Wu Y, Li Z, Du W, Gao K (2015) Physiological response of marine centric diatoms to ultraviolet radiation, with special reference to cell size. J Photochem Photobiol B Biol 153:1–6. https://doi.org/10.1016/j.jphotobiol.2015.08.035

Xu X, Liu J, Shi Q et al (2016) Ocean warming alters photosynthetic responses of diatom *Phaeodactylum tricornutum* to fluctuating irradiance. Phycologia 55:126–133. https://doi.org/10.2216/15-64.1

Xu K, Grant-Burt JL, Donaher N, Campbell DA (2017) Connectivity among Photosystem II centers in phytoplankters: patterns and responses. Biochim Biophys Acta BBA – Bioenerg. https://doi.org/10.1016/j.bbabio.2017.03.003

Zorz JK, Allanach JR, Murphy CD et al (2015) The RUBISCO to photosystem II ratio limits the maximum photosynthetic rate in picocyanobacteria. Life 5:403–417. https://doi.org/10.3390/life5010403

Chapter 14

Modulating Energy Transfer from Phycobilisomes to Photosystems: State Transitions and OCP-Related Non-Photochemical Quenching

Diana Kirilovsky*
Institute for Integrative Biology of the Cell (I2BC), CNRS, CEA, Université Paris-Sud, Université Paris-Saclay, Gif sur Yvette, France

I. Introduction

Photosynthesis is the most important biosynthetic pathway that makes use of nature's most plentiful resources: solar light, water and inorganic carbon. Photosynthetic organisms harvest solar energy and convert the absorbed light energy into chemical energy (ATP) and reducing power (NADPH) which are used in the assimilation of CO_2 and synthesis of organic carbon molecules. In this process, they capture atmospheric CO_2 and produce molecular oxygen. They hold the potential for the production of clean and renewable energy.

Photosynthetic organisms do not have the possibility to control the incoming flux of light. Indeed the absorption of a photon cannot

*Author for correspondence, e-mail: diana.kirilovsky@cea.fr

A. W. D. Larkum et al. (eds.), *Photosynthesis in Algae: Biochemical and Physiological Mechanisms*, Advances in Photosynthesis and Respiration 45, https://doi.org/10.1007/978-3-030-33397-3_14

be switched off. When the photon flux exceeds the photo-converting capacities of the cell, the entire photosynthetic chain gets over-reduced. This promotes the accumulation of high energy reactive intermediates and induced secondary reactions. The most unwanted and dangerous side-reactions are those involving oxygen which produces singlet oxygen and oxygen radicals (ROS). The disequilibrium between the energy absorbed and energy consumed occurs at high irradiance but it can also occur at lower irradiance, under nutrient starvation or low CO_2 conditions. Changes in light quality also affect photosynthetic organisms by misbalancing the photosystem activities and leading to a decrease in the efficiency of photosynthesis and/or a reduction of the electron transport chain and production of ROS. Finally, changes in environmental conditions can also induce an imbalance in the needs of chemical energy (ATP) versus reducing power (NADPH). To avoid increased production of ROS, the quantity of energy arriving at the reaction centers and the photosynthetic production of ATP and NADPH are continuously adjusted. Plants, algae and cyanobacteria possess mechanisms that sense the quality and quantity of incident light and rapidly induce a reorganization of the photosynthetic apparatus and the interaction between antennae and reaction centers to adjust light absorption and utilization. In cyanobacteria, non-photochemical-quenching (NPQ) mechanisms (including Orange Carotenoid Protein (OCP)-related NPQ and state transitions), cyclic electron transport and flavodiirons proteins are key actors in the regulation of photosynthesis. Both, OCP-related NPQ and state transitions regulate the energy transfer from the phycobilisome (PBS), the extra-membrane cyanobacterial antenna, to the photosystems. While the OCP-related NPQ mechanism simultaneously decreases the energy arriving to both photosystems (PSII and PSI) under high light conditions, the "State Transition" mechanism decreases (or increases) the energy transfer from the PBS to one or the other photosystem. This review will describe these two mechanisms that regulate energy transfer from PBSs to the photosystems (regulation between the two photosystems is also dealt with in Chaps. 4, 10 & 12).

II. The Phycobilisome

The phycobilisome is a supercomplex attached to the cytoplasmic side of thylakoid membranes (Gantt and Conti 1966). It is formed by water soluble phycobiliproteins (PBPs) and linker proteins (for reviews, see (Glazer 1984; Grossman et al. 1993; MacColl 1998; Tandeau de Marsac 2003; Watanabe and Ikeuchi 2013; Adir 2005, 2008). The most common PBS is hemidiscoidal, organized as a core from which peripheral cylindrical rods (6–8) radiate (Fig. 14.1). The core is formed by two (ex *Synechococcus elongatus* (Yamanaka et al. 1978)), three (ex *Synechococcus* PCC7002 and *Synechocystis PCC6803* and PCC6701 (Arteni et al. 2009; Bryant et al. 1990; Elmorjani et al. 1986; Williams et al. 1980)) or five (*Anabaena PCC7120, Mastigocladus laminosus* (Ducret et al. 1998; Glauser et al. 1992)) cylindrical substructures. Two of the cylinders are basal and attached to the thylakoid.

The PBPs covalently bind different types of bilins which are open-chain tetrapyrroles with colors going from bleu to red. The bilins (phycocyanobilin (PCB), phycoerythrobilin (PEB), phycourobiline (PUB) and phycobilivioline (PXB)) bind the protein via a thioester bond to a cysteine. The maximum absorbance and emission of these chromophores are largely influenced by their interaction with the surrounding amino acids in the protein. Each PBP is formed by two subunits: the α subunit and the β subunit. This heterodimer (conventionally called monomer) is assembled in disc-shaped trimers $(\alpha\beta)_3$ and hexamers $(\alpha\beta)_6$ enclosing a central channel (Fig. 14.1). Most of PBSs from fresh water cyanobacteria contains only phycocya-

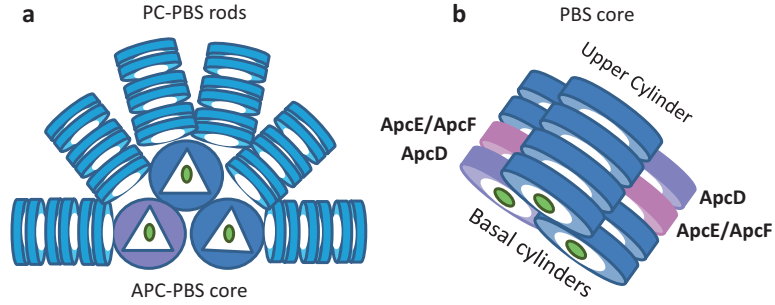

Fig. 14.1. **The *Synechocystis* PCC 6803 phycobilisome**
(**a**) In *Synechocystis* PCC 6803, the strain mostly used to study the cyanobacterial NPQ mechanism, the PBS is hemidiscoidal. Six rods radiates from a core. Each rod is composed by 3 hexamers of the blue phycocyanin (PC). Colorless linker proteins stabilize the PBS structure and optimize directional energy transfer. Energy transfer occurs from the external rod-PC hexamer to the PBS-core. (**b**) The core is formed by 2 basal cylinders and 1 upper cylinder. Each cylinder contains 4 trimers of allophycocyanin (APC). All the trimers in the upper cylinder are formed by heterodimer αAPC-βAPC emitting at 660 nm (blue trimer). In the basal cylinders, in one of the external trimers one αAPC subunit is replaced by a special αAPC-like subunit called ApcD (violet) and in another trimer one β subunit is replaced by ApcF, a βAPC-like subunit, and one α subunit is replaced by the N-terminal domain of ApcE, a αAPC-like domain (rose). The bilins attached to ApcD and ApcE have a maximal fluorescence at 680 nm and are the terminal energy acceptors of the PBS. In each cylinder the 2 external trimers are stabilized by the ApcC linker protein (green)

nin (PC) hexamers in the rods. The PC is blue (Abs_{max} = 620 nm) and binds 1 PCB in the α subunit and 2 PCB in the β subunit. In most of marine cyanobacteria and some fresh water strains, the core-distal rod hexamers are formed by phycoerytrin (PE) and/or phycoerytrocyanine (PEC). The PE is red (Abs_{max} = 495 and/or 565–575 nm) and binds 2 PEB in the α subunit and 3 PB (or PUB) in the β subunit. The PEC is violet (Abs_{max} = 567 nm) and binds 1 PXB in α and 2 PCB in β. The core-adjacent hexamers contain PC. The rods are stabilized by colorless linker proteins (L_R (rod extension), L_{RT} (distal termination), L_{RC} (rod-core interaction)) (review (Liu et al. 2005). The linker proteins bind in the central cavity of the PBPs trimers (Yu and Glazer 1982). They participate in the assembly of PBSs and optimize directional energy transfer (Glazer 1989).

The core cylindrical structures contain 4 allophycocyanin (APC) trimers. The APC heterodimer formed by an α and a β subunit has a maximum absorbance at 650 nm and a maximum emission at 660 nm (APC_{660}). Each subunit binds 1 PCB. In the basal cylinders, in one external APC trimer, one α subunit is replaced by a special αAPC-like subunit called ApcD. In addition, in one internal APC trimer, one β subunit is replaced by ApcF, a βAPC-like subunit, and one α subunit is replaced by the N-terminal domain of ApcE (or Lcm), an αAPC-like domain (Lundell and Glazer 1983a, b, c) (Fig. 14.1b). ApcD and ApcE are the last energy acceptors of the PBS and have a maximal emission at 680 nm (APC_{680}). In each cylinder the 2 external trimers are stabilized by an 8.7 kDa linker protein (ApcC) which is in the central channel (Reuter et al. 1999). The ApcE protein also determines the number of APC cylinders that form the PBS core (Capuano et al. 1991, 1993). The C-terminal part of ApcE contains 2, 3 or 4 interconnected repeated domains of about 120 residues (called Rep) which are similar to the conserved domains of rod linkers. Each Rep domain interacts with an APC trimer situated in different cylinders and stabilizes the PBS

core (Ajlani and Vernotte 1998; Ajlani et al. 1995; Shen et al. 1993; Zhao et al. 1992). ApcE is also involved in the interaction between the PBS and the thylakoids (Redlinger and Gantt 1982). The structures of *Synechocystis* PCC6803 PBS (Arteni et al. 2009) and *Anabaena* PCC7120 PBS (Chang et al. 2015) were resolved at low resolution using single-particle electron microscopy.

The light energy absorbed by the PBS could be directly transferred to both photosystems, PSII and PSI (Mullineaux 1992; Rakhimberdieva et al. 2001). The excitation energy is transferred from the PBS terminal emitters, ApcD and ApcE, to the Chl antennae and also maybe directly to reaction centers. In *Synechococcus* PCC 7002, ApcD seems to be preferentially involved in energy transfer to PSI and ApcF/ApcE preferentially involved in energy transfer to PSII (Dong et al. 2009; Gindt et al. 1992). In contrast, in *Synechocystis* PCC 6803, the ApcE/ApcF dimer is the principal energy transmitter from PBS to both PSI and PSII. The lack of ApcD only slightly perturbed the energy transfer to both photosystems (Ashby and Mullineaux 1999).

III. The OCP-Related NPQ Mechanism

A. *The Discovery of the OCP-Related NPQ Mechanism in Cyanobacteria*

In 2000, it was reported that strong blue-green light induced a large quenching of fluorescence in *Synechocystis* PCC 6803 (hereafter called *Synechocystis*) (El Bissati et al. 2000). This decrease of fluorescence was not related to photoinhibition or to State 1 to State 2 transition. The authors proposed that it could be related to PBS fluorescence quenching and a concomitant decrease of energy transfer from the PBS to the photosystems (El Bissati et al. 2000). This proposition was later demonstrated by three different laboratories (Rakhimberdieva et al. 2004; Scott et al. 2006; Wilson et al. 2006). They showed that strong blue-green also induced a large quenching fluorescence in *Synechocystis* mutants lacking the chlorophyll antennae CP47 and CP43 and the Reaction Center II (Rakhimberdieva et al. 2004; Scott et al. 2006; Wilson et al. 2006). In addition, it was demonstrated that in the "quenched state", the effective size of the antenna was smaller than in the "unquenched state" and less energy was transmitted to both photosystems (Wilson et al. 2006; Gorbunov et al. 2011; Rakhimberdieva et al. 2010). Thus, in *Synechocystis* strong blue-green light induces a mechanism that decreases PBS fluorescence and energy transfer to photosystems by increasing thermal dissipation of excess excitation energy absorbed. This mechanism is photoprotective. Cyanobacteria strains and cyanobacteria mutants lacking this mechanism are more sensitive to high light conditions (Wilson et al. 2006, 2007; Boulay et al. 2008). First results suggesting that a carotenoid protein is involved in this mechanism were published in 2004 by Rakhimberdieva et al. (2004). Then, in 2006, it was demonstrated that a soluble carotenoid protein known as Orange Carotenoid Protein (OCP) and first described by David Krogmann and collaborators (Holt and Krogmann 1981) is essential for the blue-green light induced photoprotective mechanism (Wilson et al. 2006). This mechanism that was first called NPQcya, is now known as the OCP-related (triggered) NPQ mechanism. Details about the discovery of this mechanism and its first characterization are described in Karapetyan (2007) and Kirilovsky (2007).

B. *The OCPs and their Homologs*

The discovery of the OCP and its first characterization (including its structure) were largely described by Cheryl A Kerfeld in two reviews in 2004 (Kerfeld 2004a, b). In 1981, David Krogmann's group reported the exis-

tence of a soluble carotenoid protein in several cyanobacteria strains (Holt and Krogmann 1981) and then in 1997, they showed that in *Synechocystis*, the *slr1963* open reading frame code the OCP (Wu and Krogmann 1997). Genes coding for OCP have been frequently identified in a large number of PBS-containing cyanobacteria strains (Kerfeld 2004b; Bao et al. 2017a, b; Kerfeld and Kirilovsky 2013; Kerfeld et al. 2003, 2017). Recently, cyanobacterial phylogenomic analysis (333 sequenced strains) revealed the existence of at least three paralogs families of OCP (Bao et al. 2017a, b). Most of OCP (139) belongs to a family named 1 (OCP1) to which belongs the well characterized *Synechocystis PCC 6803*, *Arthrospira maxima* and *Anabaena PCC 7120* OCPs. The other two clade paralogous to OCP1 were named OCP2 (18) and OCPX (35) (Bao et al. 2017a, b). One OCP that belongs to the OCP2 clade (the OCP2 of *Tolypothrix* sp. PCC 7601 (also known as *Fremyella diplosiphon*) (Bao et al. 2017b; Lechno-Yossef et al. 2017)) and one OCP that belongs to the OCPX clade (the OCPX of *Scytonema* sp. PCC 7110 (Muzzopappa et al. 2019) were characterized. OCPs belonging to different clades are present in some strains (Bao et al. 2017a, b). The OCP-related mechanism was mostly characterized in strains containing at least one copy of OCP1. Thus, this review will principally describe the characteristics of the OCP1 family.

One third of sequenced cyanobacteria strains had no *ocp* genes. For example, *Synechococcus elongatus* and *Termosynechoccocus elongatus* lack *ocp*-like genes and lack photoprotective mechanisms decreasing the energy arriving to the reaction centers (Boulay et al. 2008). OCP is completely absent in the PBS-lacking cyanobacteria (alpha clade including *Prochlorococcus marinus* strains) (Kerfeld 2004b; Kerfeld and Kirilovsky 2013; Kerfeld et al. 2003). In red algae, eukaryotic PBS-containing algae, no *ocp*-like genes were found. However, red algae also possess NPQ mechanisms. They are triggered by low lumen pH (like in plants and green algae) (Delphin et al. 1996, 1998). The presence of a reaction center type NPQ mechanism was recently described in a thermophilic red alga having a strong interaction PBS-photosystems (Krupnik et al. 2013). The existence of PBS-related NPQ mechanisms in red algae is uncertain (Kana et al. 2014).

In addition to OCPs, many cyanobacterial strains contain homologous to the N-terminal (NTD) and C-terminal (CTD) domains of the OCP (Bao et al. 2017a, b; Kirilovsky and Kerfeld 2012, 2013; Lopez-Igual et al. 2016; Melnicki et al. 2016; Muzzopappa et al. 2017). The family of NTD-like proteins (named Helical Carotenoid proteins (HCPs)) contains at least nine different sub-clades (HCP1 to 9, (Melnicki et al. 2016)) while the family of CTD-like proteins (CTDH) contains only two sub-clades (Muzzopappa et al. 2017). The *ctdh* genes are present in all the strains containing HCPs. Moreover, the *hcp4* gene is located adjacent or near the *ctdh* gene. It was proposed that the fusion of *hcp4* (the one presented the higher identity with NTD-OCP) and *ctdh* genes could form an ancient OCP (Lechno-Yossef et al. 2017; Melnicki et al. 2016). Both, HCPs and CTDHs bind carotenoids (Lopez-Igual et al. 2016; Muzzopappa et al. 2017). Although, these proteins can bind different carotenoids, the keto carotenoid canthaxanthin seems to be the preferred one (Lopez-Igual et al. 2016; Muzzopappa et al. 2017). While several HCPs from different subclades could co-exist in a cell of some strains, only one CTDH is present (Bao et al. 2017a; Melnicki et al. 2016; Muzzopappa et al. 2017). The HCPs and CTDHs from *Anabaena* PCC7120 (HCP1 to 4 and CTDH2) and *Termosynechococus elongatus* (HCP4/5 and CTDH1) were characterized. The structures of *Anabaena* canthaxanthin containing HCP1 (Melnicki et al. 2016) and of the *Anabaena* apo-CTDH (Harris et al. 2018) were resolved. HCPs are monomers while

CTDHs are dimers sharing one canthaxanthin molecule (Muzzopappa et al. 2017). The *Anabaena* HCPs have different activities, at least in vitro (Lopez-Igual et al. 2016): only HCP4 (All4941) is able to bind to PBS and to induce energy quenching like the OCP (see below). HCP2 (All3221) and HCP3 (Alr4873) are good singlet oxygen quenchers and HCP1 could be a carotenoid carrier. CTDHs are also good singlet oxygen quenchers but their principal role is as carotenoid carrier from the membranes to the HCPs (Muzzopappa et al. 2017; Harris et al. 2018).

C. *OCP1 Photoactivity*

The first crystal structure of the OCP was reported in 2003 (Kerfeld et al. 2003). It was the tridimensional structure of OCP isolated from *Arthrospira maxima*. The OCP *Synechocystis* (Wilson et al. 2010) and the OCP *Anabaena* PCC7120 (Lopez-Igual et al. 2016) crystal structures were also resolved by Kerfeld's group. The three structures are similar (Lopez-Igual et al. 2016). The OCP is a soluble protein of 35 kDa composed by two globular domains: an α-helical N-terminal domain (NTD, residues 18–165) unique for cyanobacteria and an α helix/β sheet C-terminal domain (CTD, residues 190–317) that is member of the nuclear transport factor twofold superfamily (Fig. 14.2a) (Kerfeld et al. 2003; Wilson et al. 2010). The two domains are connected by a long flexible linker (about 25 residues). Strong interactions between the domains maintain the protein in a closed globular conformation. The interactions occur in the principal interface between the domains, in the middle of the protein (including a salt bridge between residues R155 and E244), and in the interface between the N-terminal arm (residues 1–20, containing a small α helix) and the β-sheet of the CTD (Kerfeld et al. 2003; Wilson et al. 2010) (Fig. 14.2a). In *Synechocystis* and *Arthrospira* cells, the OCP binds a keto-carotenoid, the hydroxyechinenone (hECN), which has a

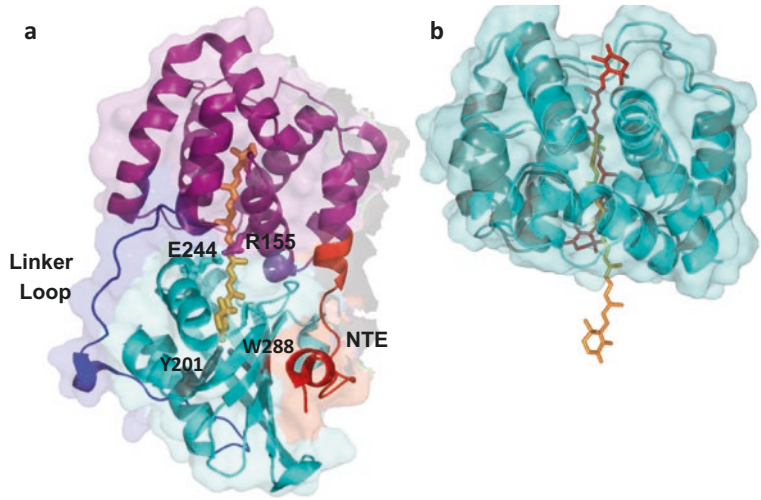

Fig. 14.2. **The crystal structures of the *Synechocystis* OCP and the isolated *Synechocystis* RCP**. (**a**) OCP structure (Protein Data Bank identifier: 3MG1). The OCP monomer is represented in the orange state. The N-terminal domain (residues 1–165) is violet. The C-terminal domain (residues 196–315) is light blue-green. The N-terminal arm (NTE) is represented in red and the linker loop in blue. The carotenoid is represented as orange sticks. Y201 and W288 residues forming H-bonds with the carotenoid carbonyl are represented as grey sticks. E244 and R155 forming a salt bridge between the two domains are also shown (**b**) Comparison of the structures of *Synechocystis* NTD in OCP^o (grey) and of the NTD in OCP^r (light blue-green) (Protein Data Bank identifier: 4xb4). The carotenoid in red sticks is in the position in OCP^r and in orange in the position in OCP^o

carbonyl (keto) group in one of the rings and an hydroxyl group in the other (Kerfeld et al. 2003; Wilson et al. 2010). The hECN spans both domains and it is in all trans configuration with the carbonyl group in a hydrophobic pocket of the CTD (Kerfeld et al. 2003; Polivka et al. 2005). In the absence of hECN, OCP can bind other keto-carotenoids as echinenone (ECN) and cantaxanthin (CAN) and non-keto-carotenoids as zeaxanthin (Bourcier de Carbon et al. 2015; Punginelli et al. 2009). However, the nature of the carotenoid is essential for OCP activity: only the OCPs carrying a ketocarotenoid are able to trigger the NPQ mechanism (Bourcier de Carbon et al. 2015; Punginelli et al. 2009).

The OCP is a photoactive protein (Wilson et al. 2008). The presence of a ketocarotenoid molecule is essential for OCP photoactivation (Bourcier de Carbon et al. 2015; Punginelli et al. 2009; Wilson et al. 2008). In darkness, the OCP is orange (OCP^o) and its absorbance spectrum presents two maxima at 496 and 467 nm with a shoulder at 440 nm. The bands at 496 and 467, related to 0–0 and 0–1 vibrational transitions, have similar strength (Fig. 14.3). This is unusual for carotenoids; typically the 0–1 vibrational band is the strongest one. It was recently demonstrated that this feature is due to the existence of two OCP^o subpopulations: a main population having the maximum of the spectrum at around 467 nm and a red-shifted form (Kish et al. 2015a; Slouf et al. 2017). Different configurations of the carotenoid β1-ring (carrying the carbonyl) in each population can explain the differences in the excited states of these two forms (Kish et al. 2015a; Slouf et al. 2017).

Conformational changes in the carotenoid and the protein are induced by strong blue-green light absorbed by the carotenoid and the orange form is converted into a metastable active red form (OCP^r) (Wilson et al. 2008). The spectrum of the red form loses the resolution of the vibrational bands and presents a large maximum at 510 nm (Fig. 14.3). The photoconversion reaction has a very low yield and accumulation of the red form occurs only under high irradiance (Wilson et al. 2008).

In OCP^o, the hydrogen bonds between the carotenoid carbonyl and the conserved Y201 and W288 (*Synechocystis* numeration) residues situated in a hydrophobic pocket in the core of the CTD-OCP (Fig. 14.2a) stabilize the position of the carotenoid, which by spanning both domains stabilizes the closed globular structure of OCP^o (Maksimov et al. 2015a; Wilson et al. 2011). As already said, this closed conformation is also stabilized by interactions in the principal interface between the domains, in the middle of the protein and in the interface between the N-terminal arm (NTE) and the β-sheet of the CTD. The energy absorbed by the carotenoid and the induced conformational changes provoke the breakage of these hydrogen bonds. The exact mechanism inducing the breakage of the H-bond remains to be elucidated. The liberation of the carotenoid induces slight changes in the β-sheet CTD and the signal is translated to the surface of the protein inducing the detachment of the N-terminal arm (including the αA-helix) from the CTD and the complete separation of the CTD from the NTD. The C-terminal tail (CTT) also seems to move accompanying the movement of the N-terminal arm. In OCP^o, the CTT interacts with the β-sheet while in OCP^r more probably caps the carotenoid tunnel that is now empty (Harris et al. 2018). OCP mutants lacking W288 (Maksimov et al. 2016; Sluchanko et al. 2017a), and/or weaker interactions between the domains (Wilson et al. 2012) and/or lacking the N-terminal arm (Sluchanko et al. 2017b; Thurotte et al. 2015) have a much less stable OCP^o and OCP^r is accumulated much faster and at lower light intensities.

The fact that R155 (NTD), which forms a salt bridge with E244 (CTD) (Fig. 14.2a), is essential for the binding of OCP^r to PBS (see next chapter) already strongly suggested that the domains separate upon OCP photoactivation (Wilson et al. 2012). Then, an increased

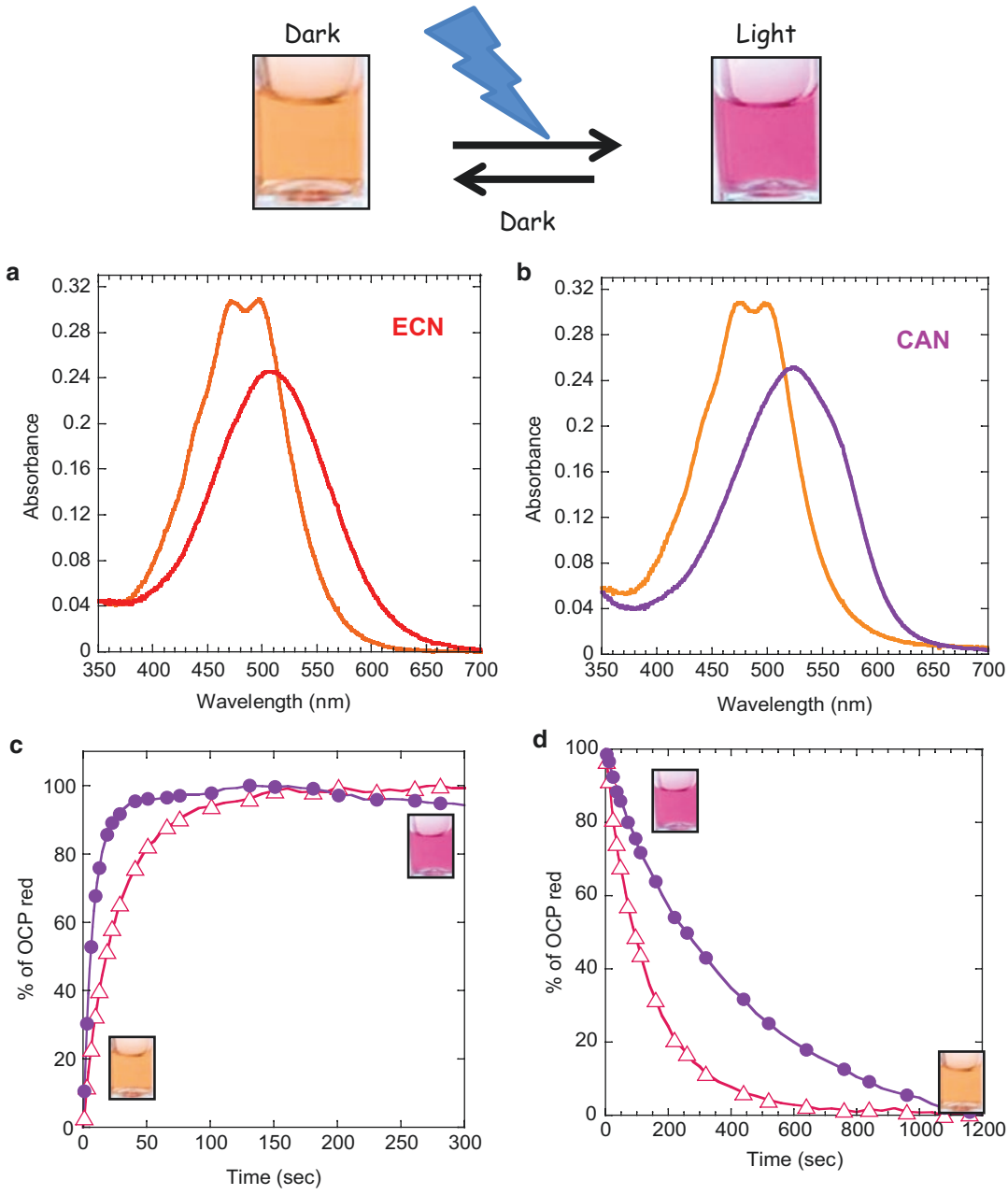

Fig. 14.3. Absorbance spectra OCP-ECN (**a**) and OCP-CAN (**b**) in darkness(orange) and after 5 min of strong white illumination at 18 °C (red and violet). The OCP is orange in darkness and red under strong illumination. (**c** and **d**) Photoactivation (**c**) and recovery (**d**) kinetics of OCP-ECN (red) and OCP-CAN at 18 °C

surface exposure of the large inter-domain interface in OCP^r was shown (Liu et al. 2014). More recently, a study combining MS methods with CD and SAXS and focusing on the structural changes induced during OCP photoactivation clearly confirmed the complete separation of NTD and CTD in OCP^r (Gupta et al. 2015). They also showed that the N-terminal αA helix not only dissociates from the CTD but also becomes disor-

dered upon OCP photoactivation (Gupta et al. 2015). Subsequently, other results consistent with separation of NTD and CTD were also described (Maksimov et al. 2016; Sluchanko et al. 2017a; Liu et al. 2016). The secondary structures of each individual domain are rather similar in OCP^o and OCP^r (Gupta et al. 2015; Leverenz et al. 2015). In the NTD, the αA-helix of the N-terminal arm unfolds and at least one α-helix slightly rotates inducing a rearrangement of some amino acids in the CTD, the movement of a loop (Gupta et al. 2015) and of the C-terminal tail cap the carotenoid binding pocket (Harris et al. 2018).

Upon photoactivation an unprecedented movement of the carotenoid 12A deeper into the NTD occurs (Leverenz et al. 2015; Maksimov et al. 2017a). In OCP^r, the carotenoid is completely buried in the NTD. Only in the vicinity of the rings is solvent exposed (Fig. 14.2b). As a consequence of its movement, the carotenoid interaction with the protein changes. New amino acids are in contact with it in the OCP^r including E34, Y129, P126 (Leverenz et al. 2015). For the moment, it is not clear if the movement of the carotenoid precedes the opening of the protein or both processes occur simultaneously. Intermediary orange and red forms in the OCP photocycle were recently described showing asynchronous changes in carotenoid and protein components (Maksimov et al. 2017b; Konold et al. 2019). These results strongly suggested that the carotenoid becomes red much faster than the opening of the protein. In addition, during recovery, the carotenoid becomes orange (by attachment to Tyr201 and Trp288) before the domains are completely closed (Maksimov et al. 2017b).

Spectroscopic studies indicated that upon OCP photoactivation, conformational changes are induced in the carotenoid rendering the carotenoid molecule more planar with a larger effective conjugation (Wilson et al. 2008). The carotenoid is in an all-trans configuration in both OCP^o and OCP^r and no trans-cis double bound isomerization of the polyene chain is involved in photoactivation (Wilson et al. 2008; Leverenz et al. 2014, 2015; Kish et al. 2015b). The longer conjugation length was proposed to be related to different positions of the rings around the single bonds C6-C7 (C6′-C7′) and a less bent polyene chain (Kish et al. 2015b). In OCP^o, the C6-C7 single bond is in the anti-conformation, which set the double bond in the β1 ring off of the conjugation plane of the polyene chain by 53° instead of the 34° in the isolated NTD (Leverenz et al. 2015; Bandara et al. 2017). It had been proposed that the first step in OCP photoactivation involves this rotation of the β-ionone ring, however, structural results of Bandara et al. (Bandara et al. 2017) did not support this hypothesis (Bandara et al. 2017). They did not observe significant rotational movement of the ring. The torsion angles C6′-C7′ around β2 ring also changes from 69° in OCP^o to 40 in the isolated NTD (Leverenz et al. 2015). In addition, in OCP^o, the polyene chain of the carotenoid is twisted and bowed while in OCP^r, it is more planar (Leverenz et al. 2015; Bandara et al. 2017).

D. The OCP-Related NPQ: OCP-PBS Interaction and Fluorescence and Energy Quenching

OCP^r is the active form of the protein because only OCP^r is able to bind to PBS (Wilson et al. 2008; Gwizdala et al. 2011). All OCPs, OCP1, OCP2 and OCPX, are able to interact with the PBS (Bao et al. 2017b; Muzzopappa et al. 2019). OCP is a modular protein in which each domain has its own essential role. The NTD is the effector domain that interacts with PBS: it is constitutively active in fluorescence and energy quenching, even in darkness (Leverenz et al. 2014). The CTD is the light sensing and activity regulator domain (Sutter et al. 2013). In darkness, its interaction with the NTD inhibits the OCP binding to PBS. Upon strong illumination the conformational

changes induced in specific amino acids of the CTD, provoke the separation of the CTD from the NTD and the "free" NTD is able to interact with the PBS (Leverenz et al. 2014; Sutter et al. 2013).

Binding of only one molecule of OCP^r to the PBS is sufficient to quench the entire PBS fluorescence suggesting the existence of a specific OCP binding site (Gwizdala et al. 2011). OCP^r interacts with one of the basal cylinders of the PBS (Gwizdala et al. 2011; Jallet et al. 2014). However, the exact site of binding is still matter of discussion. Three different models were proposed (Harris et al. 2016; Stadnichuk et al. 2012; Zhang et al. 2013). The most recent and complete model is based on cross-linking and mutant characterization (Harris et al. 2016) (Fig. 14.4). Harris and coworkers identified 18 cross-links between the OCP and the PBS in a OCP-PBS complex; 4 residues of the flexible linker (R167, K170, R171, K185) and one of the C-terminal domain (K249, adjacent to the linker) crosslinked with 13 residues from ApcB (5 residues), CpcG (4 residues), ApcC (3 residues) and CpcB (one residue) (Harris et al. 2016). The fact that none of the potentially active residues of the NTD cross-linked with PBS residues was interpreted as a tight interaction between the NTD and the PBS (Harris et al. 2016). The model proposes that the NTD is buried between two APC rings in a basal cylinder: the trimer containing ApcF-ApcE (disc 3) and the external trimer containing ApcD (disc 4) (Harris et al. 2016). The OCP binding alters the structure of one core cylinder, separating the rings. This alteration could hinder the binding of a second OCP in the other basal cylinder. The OCP-binding model was based on three observations: (1) OCP^r cross-linked with ApcC present in the external trimer, (2) upon OCP binding, ApcC slightly moves closer to ApcF and (3) in the ΔApcC mutant the OCP binding is destabilized (Harris et al. 2016). These results clearly showed that one APC trimer containing the ApcC linker protein and the APC trimer containing ApcF are involved in OCP^r binding. However, the involvement of the APC trimer containing ApcD remains to be confirmed. In all PBS models, the ApcD containing trimer forms an hexamer with the one containing ApcE (Fig. 14.1) but this was not demonstrated (Chang et al. 2015). The absence of ApcD or ApcF affects the rates of fluorescence recovery by lowering the activation energy barrier of the recovery reaction (Maksimov et al. 2015b). This can be interpreted as a weaker OCP^r binding in the absence of ApcD or ApcF. However, the absence of ApcD does not inhibit PBS fluorescence quenching (Dong and Zhao 2008; Jallet et al. 2012). Harris et al. also proposed that the CTD-OCP might be relatively mobile

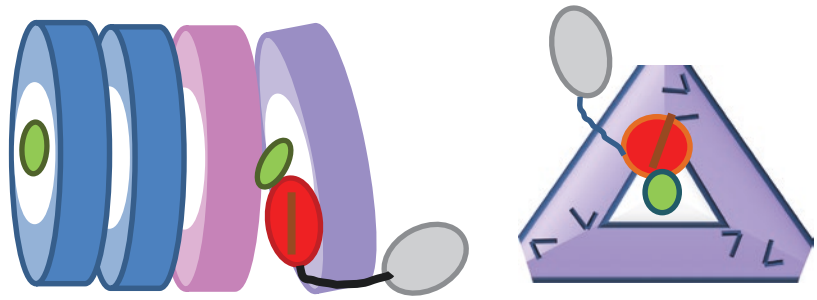

Fig. 14.4. **Model of OCP binding to the phycobilisomes**
Model proposed by Harris et al.: In this model, the NTD is buried between the (αApcβApc)(αApcApcF) (ApcEβApc) trimer (rose) and the $(\alpha ApcB\beta Apc)_2$ (ApcDApcB) trimer (violet) of one of the basal APC cylinders of the PBS core. The binding is stabilized by the core linker ApcC. The OCP binding to the PBS alters the structure of one core cylinder, separating the terminal ring from the second ring. The CTD floats in solution located on the outer surface of the cylinder

in the attached OCP^r, floating in solution located on the outer surface of one basal core cylinder (Harris et al. 2016). This remains to be confirmed since only one CTD residue cross-linked with a PBS residue (Harris et al. 2016). Further studies must be realized to elucidate the exact position of OCP^r in the PBS.

Spectrally resolved picosecond fluorescence measurements in quenched and unquenched WT and mutant cells of *Synechocystis* and isolated OCP-PBS complexes demonstrated that the first site of fluorescence quenching is an APC bilin emitting at 660 nm (APC_{660}) (Tian et al. 2011, 2012). This is not in contradiction with the OCP binding model proposed in Harris et al. (2016) because the trimers containing ApcD and ApcE also contain two pairs of bilins emitting at 660 nm. It was proposed that in addition to an APC_{660} also an APC_{680} could be primarily quenched (Kuzminov et al. 2012). However, the absence of ApcD and ApcF means that they do not inhibit the OCP-related NPQ (Dong and Zhao 2008; Jallet et al. 2012). OCP^r is also able to quench PBS fluorescence in the absence of ApcE bilin suggesting that ApcE chromophore is not essential (or not involved) in this mechanism (Jallet et al. 2012). In *Synechocystis* cells, the overall quenching rate is around 16 ps^{-1} (Tian et al. 2011). This very fast quenching, which is competitive with energy transfer to the photosystems, leads to efficient quenching (80%) of PBS absorbed energy. The role of the carotenoid in the quenching mechanism remains to be elucidated. The structural modification of the core cylinder, affecting the environment of one or more bilin could also be at the origin of NPQ by hindering energy propagation and/or converting one α or β bilin into an energy dissipating state (Wang and Moerner 2015). Although there is no clear evidence for the participation of the carotenoid, different laboratories proposed that energy transfer (Maksimov et al. BBA 2014; Berera et al. 2012; Polivka et al. 2013) or charge transfer (Tian et al. 2011, 2012) between the bilin and the carotenoid are involved in the OCP-related NPQ mechanism. The excited states of the keto-carotenoids (hECN, ECN and CAN) in OCP^o and OCP^r present different characteristics (Slouf et al. 2017; Berera et al. 2012, 2013; Niedzwiedzki et al. 2014; Polivka et al. 2013); however, both OCP^o and OCP^r could efficiently quench PBS (Slouf et al. 2017; Niedzwiedzki et al. 2014; Polivka et al. 2013). Further spectroscopic experiments will be needed to elucidate the energy quenching mechanism.

E. The Fluorescence Recovery Protein

Once activated, the OCP-related NPQ mechanism decreases the excess excitation energy arriving at the reaction centers diminishing the formation the ROS under strong light conditions. However, when low light conditions come back, to increase photosynthetic efficiency, the effective size of antennae must be increased. To reverse OCP-related NPQ a protein called Fluorescence Recovery Protein (FRP) is needed (Boulay et al. 2010). In vitro, the isolated OCP^r spontaneously reverts to OCP^o in darkness (Wilson et al. 2008). Depending on experimental conditions, it can also spontaneously detach from the PBS (Bourcier de Carbon et al. 2015; Gwizdala et al. 2011). In contrast, in vivo, FRP is essential for the recovery of PBS fluorescence (and full antenna capacity) (Boulay et al. 2010). The fluorescence recovery is relatively slow (10–20 min) and its rate depends on the amplitude of fluorescence quenching: larger the fluorescence quenching, slower the fluorescence recovery (Boulay et al. 2008, 2010; Maksimov et al. 2015b). FRP interacts with high affinity with the CTD of free and bound $OCP1^r$ (Sluchanko et al. 2017a; Sutter et al. 2013; Boulay et al. 2010; Moldenhauer et al. 2018). Although the first and essential FRP-binding site is located on the CTD, secondary sites on the NTD were suggested that could also be important for FRP activity (Sluchanko et al. 2017a, b, 2018; Lu et al. 2017a). In *in vitro* experiments, the presence of FRP accel-

erates OCP1^r to OCP^o conversion (Sutter et al. 2013; Boulay et al. 2010; Thurotte et al. 2017) and recovery of PBS fluorescence (Thurotte et al. 2015, 2017; Gwizdala et al. 2011). FRP activity is independent of light: it is active in the dark but also under high light conditions (Sluchanko et al. 2017a; Thurotte et al. 2017). FRP affinity to OCP1^r is strong and its presence during illumination decreases the amplitude of OCP-triggered fluorescence quenching by accelerating the OCP1^r to OCP1^o conversion (Sluchanko et al. 2017a; Gwizdala et al. 2011, 2013; Kuzminov et al. 2012; Thurotte et al. 2017). It was also shown that FRP can interact with OCP1^o (with low affinity) preventing its photoactivation (Sluchanko et al. 2017a). In the cells, the concentration of FRP is largely lower than that of OCP. This is important since high FRP concentrations completely inhibit PBS fluorescence quenching (Gwizdala et al. 2013). Thus, the concentration of FRP controls not only the rate of PBS fluorescence recovery but also the amplitude of PBS fluorescence quenching (Gwizdala et al. 2013). FRP does not interact with OCP2 and OCPX and as a consequence does not accelerate OCP2^r to OCP2^o and OCPX^r to OCPX^o reconversions (Bao et al. 2017b; Muzzopappa et al. 2019).

In *Synechocystis*, the FRP is encoded by the *slr1964* open reading frame which is adjacent to the *ocp* gene (*slr1963*) (Boulay et al. 2010). Already in 2004, this conserved open reading frame was identified in the vicinity of the *ocp* gene in several cyanobacteria strains (Kerfeld 2004a) but only in 2010 its role was elucidated (Boulay et al. 2010). Genes encoding *frp* like genes are present in all of cyanobacteria strains possessing an *ocp1* gene (Bao et al. 2017a, b; Kerfeld and Kirilovsky 2013; Kerfeld et al. 2009, 2017; Kirilovsky and Kerfeld 2013). *Frp* genes are absent from strains containing only OCP2 and OCPX paralogs (Bao et al. 2017a, b).

At least in *Synechocystis*, the *ocp* and *frp* genes do not form an operon and they have their own promoters (Gwizdala et al. 2013). Moreover, analysis of transcriptome data sets showed that the expression of *ocp* and *frp* genes are sometimes inversely correlated (Ludwig and Bryant 2011, 2012; Singh et al. 2009; Straub et al. 2011). Under stress conditions (salt stress, low CO2, nutrient limitations, LL to HL transitions), OCP is highly up-regulated while FRP expression is concurrently down regulated. This is important to create a high OCP to FRP ratio under conditions in which photoprotection is needed.

FRP is structurally unique (Sutter et al. 2013) (Fig. 14.5). In the crystals, the FRP molecules were in two oligomeric (dimer and tetramer) and conformational states (Sutter et al. 2013). In the tetramer, the FRP consisted of an extended α helix with a small helical cap and in the dimer, there is a most compact fold of helices (Fig. 14.5) (Sutter et al. 2013). In solution, the FRP is mostly present as dimer (Sluchanko et al. 2017a, b; Sutter et al. 2013; Lu et al. 2017b; Slonimskiy et al. 2018). The dimer was proposed to be the active form of the FRP that binds to the OCP (Sutter et al. 2013; Lu et al. 2017a; Sluchanko et al. 2018). Results on FRP binding to OCP, which were obtained, using a permanent OCP^r mutant, strongly suggested that FRP dimer monomerizes upon (or after) binding to OCP (Sluchanko et al. 2017a). Then, Sluchanko and coworkers (Sluchanko et al. 2018) clearly confirmed that it is the FRP dimer (and not the monomer) that binds the OCP. Then, this binding and/or the binding of a second OCP breaks the interaction between the two monomers and each monomer attaches one OCP (Sluchanko et al. 2018) (Fig. 14.6).

On one surface of the FRP dimer, there is a patch of highly conserved amino acids. Some of them are involved in intermolecular interactions. For example, R60 of one monomer interacts with W50 and D54 of the other monomer. A cation-pi interaction between R60 and W50 allows the formation of a salt bridge between D54 and R60 (Sutter et al. 2013). The FRP interface is also stabilized by hydrophobic interactions and replacement of L49 by a glutamate renders the FRP to a permanent monomer (Sluchanko et al. 2018). The conserved R60, W50, D54 are

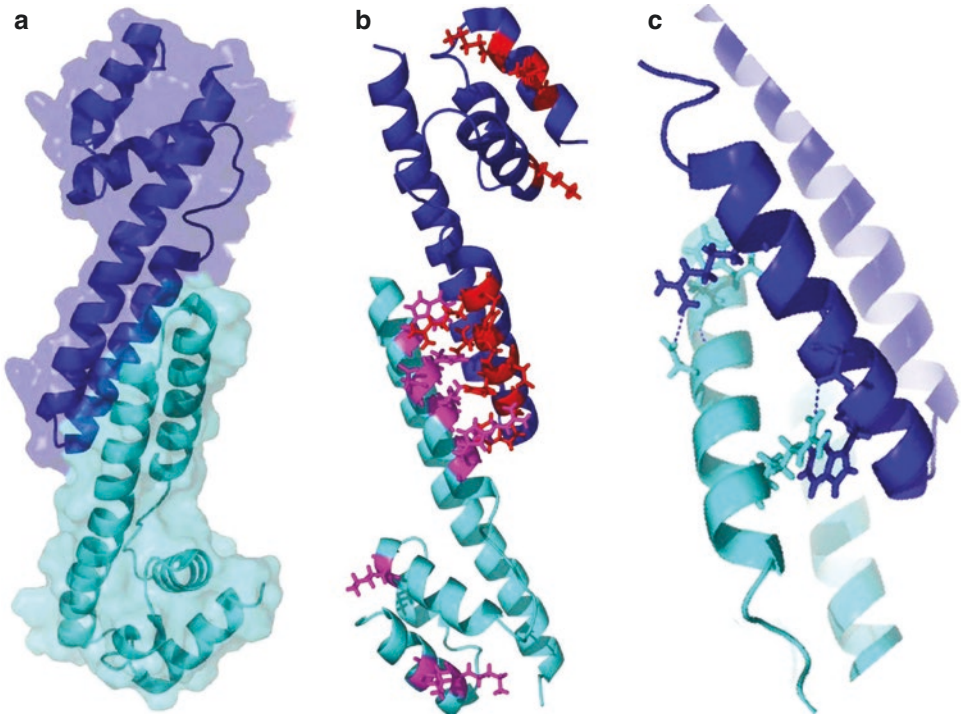

Fig. 14.5. **Crystal structure of the Fluorescence Recovery Protein (FRP)** (Protein Data Bank identifier: 4JDX). (**a**) Cartoon representation of the dimer form of the FRP present in the crystal. (**b**) The conserved amino acids are shown. In the proposed active site: R60, W50, D54, H61, H53, L56, S57. In the extreme: K83, K99, K102. (**c**) Details of the interaction between R60 of one monomer with D54 and W50 of the other monomer to stabilize the dimer

also important for the FRP activity as accelerator of the OCP^r to OCP^o conversion, especially R60 (Sutter et al. 2013; Thurotte et al. 2017). However, it seems that they are not involved in FRP binding to OCP (Lu et al. 2017a; Sluchanko et al. 2018). The FRP binding face involves F76 and K102 located in the C-terminal head (Lu et al. 2017a; Sluchanko et al. 2018). In the isolated OCP, the main (primary) FRP binding site in the CTD overlaps with the surface that is occupied by the NTE on the orange closed OCP including F299 and D220 OCP amino acids (Sluchanko et al. 2017b). These two amino acids were demonstrated to be important for the FRP activity as OCP deactivator (Thurotte et al. 2017). However, F299K and D220K OCP mutations did not prevent FRP dependent acceleration of OCP^r detachment from the PBS (Thurotte et al. 2017). Moreover, R60L FRP is still able to accelerate the recovery of PBS fluorescence (Thurotte et al. 2017). These results indicate that FRP has two distinct activities: OCP^r deactivation and OCP^r detachment from PBS. In addition, these two activities seem to involve different FRP and OCP amino acids (Thurotte et al. 2017). The molecular mechanisms related to these distinct activities remain to be elucidated. However, it was already demonstrated that FRP does not reduce the activation energy barrier of the OCP^r to OCP^o conversion (Sluchanko et al. 2017a). FRP seems to bring together the NTD and CTD stabilizing an intermediary state that facilitates the OCP^r to OCP^o conversion (Sluchanko et al. 2017a; Lu et al. 2017a). For this process, F299 OCP and R60 FRP are essential (Sutter et al. 2013; Thurotte et al. 2017). It was also proposed that there is

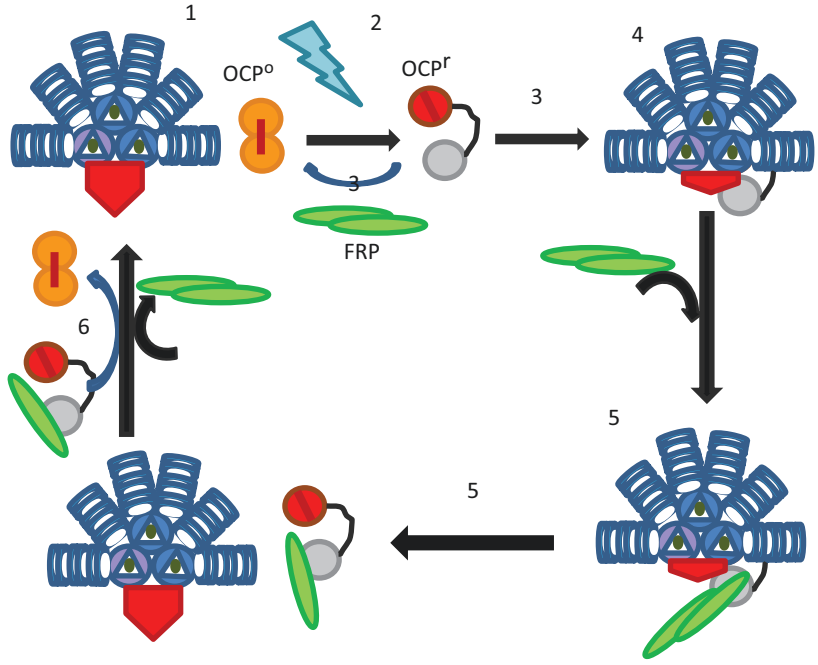

Fig. 14.6. **The working model of OCP-related NPQ**
(1) In darkness, the OCP is not bound and most of the energy absorbed by the PBS arrives at the reaction centers and is used for photosynthesis. (2) Strong blue-green (or white) light induces OCP photoactivation converting the inactive orange form (OCP^o) to the active red form (OCP^r). (3) OCP^r can come back to the orange form by interaction with the FRP or bind to the PBS. Both reactions are light independent. (4) OCP^r binding to PBS induces energy and fluorescence quenching (NPQ). The extent of NPQ depends on the concentration of OCP^r. (5) The FRP which is present as a dimer interacts with the CTD-OCP helping the detachment of OCP^r from the PBS. Possible monomerization of FRP upon interaction with OCP. (6) Once OCP^r is detached, FRP accelerates its conversion into the inactive OCP^o. In the dark (or low light), the concentration of OCP^r decreases and the concentration of unquenched PBS increases. Again most energy arrives at reaction centers

a partial unfolding of the FRP C-terminal region upon binding to the OCP (Lu et al. 2017a). Nothing is known about the FRP interaction with PBS-bound-OCP^r and how it helps the OCP^r to detach from PBS. Nevertheless, it was shown that in the absence of the N-terminal arm (including the αA helix) of the OCP, the action of the FRP in detaching OCP^r from PBS was largely increased (Thurotte et al. 2015).

F. The Working Model of the OCP-Related NPQ Mechanism

Based on the results described in this review, we propose here a working model of the OCP-related NPQ mechanism. In darkness (and low light) the OCP is in its non-active orange form. It is not attached to the PBS but has strong interactions with the thylakoid membrane. Under strong light, OCP is photoactivated and converted to its red active form. This reaction has a very low yield and accumulation of OCP^r occurs only under high light intensities. The redox state of the PQ pool and low lumen pH do not influence the amplitude or yield of the photoactivation reaction. In contrast, under stress conditions which induce reduction of the PQ pool, OCP synthesis is increased. During OCP photoactivation, absorption of light by the carotenoid induces conformational changes in the carotenoid and the breakage of the hydrogen bonds between the carotenoid carbonyl and

the Y201 and W288 residues of the OCP-CTD. The signal is transmitted to the surface of the protein leading to the breakage of the interactions between the N-terminal arm and the CTD and between the NTD and CTD in the major domain interface. An opening of the protein occurs with a complete separation of the NTD and CTD. Previously or simultaneously with the opening of the protein there is a movement of 12 A of the carotenoid into the NTD. Several intermediary red states are formed during photoactivation. In OCP^r, the carotenoid is completely buried in the NTD. Only the carotenoid rings are partially exposed. For more details in photoactivation see specially (Gupta et al. 2015; Leverenz et al. 2015; Maksimov et al. 2017b; Bandara et al. 2017; Konold et al. 2019). OCP^r attaches to the core of PBS inducing PBS fluorescence and excitation energy quenching. When bound to PBS, the NTD of OCP^r is buried between two APC trimers of one of the basal APC cylinders causing a deformation of the cylinder that hinders the interaction of a second OCP with the PBS. Most probably the NTD is bound between the APC trimers containing ApcD and ApcF/ApcE dimer. Free OCP^r can spontaneously convert to OCP^o. This OCP deactivation is accelerated by the presence of FRP. When OCP^r is buried in the PBS, it is stabilized and FRP is needed to detach it from the PBS. Then, FRP accelerates its deactivation. In the cell, FRP concentration is very low. A high FRP concentration prevents the OCP-related NPQ. FRP binds as a dimer to the OCP but after binding it monomerizes. This monomerization can be induced by the binding of a second OCP to the FRP dimer (Sluchanko et al. 2018).

IV. Cyanobacterial State Transitions

Specific illumination of Photosystem I (PSI) or Photosystem II (PSII) creates an imbalance in the electron transport chain rendering the plastoquinone (PQ) pool more oxidized or more reduced. In plants and green algae, "State transitions" is a proposed mechanism which is triggered by changes in the redox state of the PQ pool and regulates the relative extent of excitation energy arriving at PSI and PSII. This mechanism which rebalances the activity of photosystems under specific PSI or PSII lights was first described in red (Murata 1969) and green algae (Bonaventura and Myers 1969). In cyanobacteria, this specific illumination is possible not only by the fact that only PS I absorbs far-red light but also because the distribution and pigment composition of photosystems are different. Cyanobacteria contain between two to ten PSI per one PSII. In the cells, they are distributed in three dominant domains containing only PSI, or PSII-PBS complexes or PSI-PSII-PBS (Steinbach et al. 2015). Only 35 Chl *a* molecules are present in PSII (Umena et al. 2011) while PSI contains 96 Chl *a* molecules (Jordan et al. 2001). Thus, illumination of cyanobacteria cells with blue light, principally absorbed by Chl *a*, induces higher activity of PSI than of PSII. The activity of PSII is increased when the cells are illuminated with green-orange light principally absorbed by the phycobiliproteins since although PBS can transfer energy to both photosystems there is a preferential energy transfer from the PBS to PS II. There are rather large quantities of PSI that are not connected to PBS (Steinbach et al. 2015).

As in higher plants and green algae, in cyanobacteria, state transitions are triggered by changes in the redox state of the PQ pool induced by specific PSI and PSII light and by dark-light transitions (Mullineaux and Allen 1986, 1990). Two "States" were defined: State II induced by light preferentially absorbed by the PSII and characterized by low PSII fluorescence (observed at room temperature and 77 K) and State I induced by light preferentially absorbed by PSI characterized by high PSII fluorescence (see Chap. 10). In 77 K fluorescence spectra is also clearly observed that PSI to PSII fluorescence ratio changes during state transi-

tions, being higher in State I than in State II. It was proposed that in cyanobacteria these changes in fluorescence levels are related to rearrangement of the interactions between the PBSs and the photosystems (like in plants and green algae) and/or between the photosystems (changes in spillover like in red algae) and/or a PSII quenching (see below for details and references).

A. Dark-Light Transitions

Cyanobacteria cells, in contrast to eukaryotic algae and plants, are commonly in State II in the dark (Mullineaux and Allen 1986; Aoki and Katoh 1982). This occurs because both respiration and photosynthesis occur in thylakoid membranes. PQ, cytochrome b_6f (cyt b_6f) and plastocyanin (or cytochrome c_6) are electron carriers common to both electron transport chains (review (Mullineaux 2014)). In the respiratory chain, the homologs of mitochondrial Complex I (NDH-1) and Complex II (Succinate dehydrogenase, SDH) reduce the PQ pool and the electrons of PQH_2 are transferred to terminal oxidases or/ and to PSI (review (Mullineaux 2014)). Thus, respiration also affects the redox state of the PQ pool (Mullineaux and Allen 1986; Aoki and Katoh 1982). The reduction of the PQ pool in the dark is generally faster than its oxidation and as a consequence the PQ pool is reduced and the cells are in State II (Mullineaux and Allen 1986; Aoki and Katoh 1982). However, the balance between reduction and oxidation is not identical in all cyanobacteria strains (Misumi et al. 2016). This gives different "levels" of State II in the dark. Also mutations of NDH-1, SDH, and terminal oxidases change the "level" of dark State II. Disruption of *ndh* genes, which are involved in PQ pool reduction and are essential for respiration, resulted in *Synechocystis* cells almost in State I in the dark (Ogawa and Sonoike 2015). Benzoquinone analogues, phenyl-1,4 benzoquinone (PBQ) and 2,5 dimethyl benzoquinone (DMBQ), oxidize the PQ pool even in darkness. Addition of these chemicals to dark-adapted cyanobacteria cells induced State I transition even in dark (Huang et al. 2003; Mao et al. 2003).

Upon illumination, PSI is activated and the PQ pool becomes more oxidized. Illumination of dark adapted cells with any kind of light (even green-orange light, mostly absorbed by phycobiliproteins) induces an increase of PSII fluorescence yield characteristic of a State II to State I transition (see (Mullineaux and Allen 1990)). However, blue light preferentially absorbed by chlorophyll and PSI is more effective than yellow-orange light to induce this transition (Mullineaux and Allen 1990). For a long time, it was considered that the rearrangement of the photosynthetic apparatus triggered by dark-light (light–dark) transition or orange-blue (blue-orange) light transition were identical. Thus, some studies were realized changing light quality (wavelength) and others inducing dark-light transitions. Moreover, some researchers induced State II by incubating the cells in darkness under anaerobiosis conditions and State I, by illuminating the cells in the presence of DCMU. These treatments largely reduce or oxidize (respectively) the PQ pool generating extreme States. Nowadays, doubts are emerging about the idea that all these conditions induce an unique mechanism and the conclusions obtained using one or other condition are not more generalized. It has been already proposed that while changes in light quality induce only movement of PBS, dark-light transition involves changes in concentration of PSI trimers and movement of photosystems in addition to movements of PBS (Li et al. 2006). Moreover, the authors proposed that the fluorescence changes observed upon dark to light or light to dark transitions are regulated (at least partially) by changes in proton concentration on the cytosol side of thylakoids and not by only the redox state of the PQ pool (Li et al. 2006). More recently, results were published suggesting that in dark-light transitions functional detachment of PBS from PSII and PSI or only PSI is the responsible of the increase of fluorescence yield (Chukhutsina et al. 2015; Kana et al. 2009).

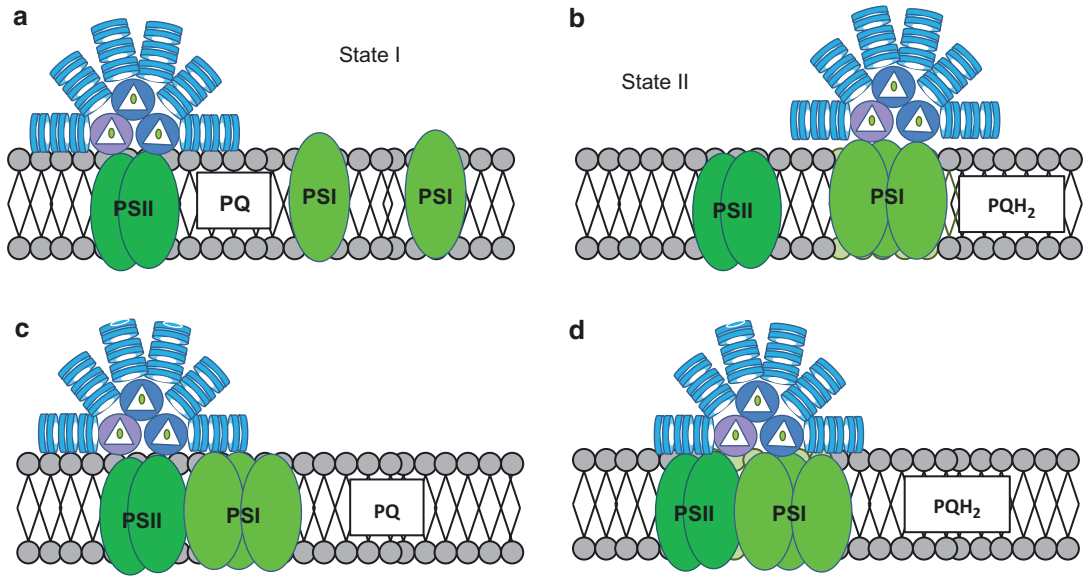

Fig. 14.7. **State Transitions. The Phycobilisome movement model**. (**a** and **b**) Long-scale movement. In State I, the PBS is attached to PSII. In State II, upon movement of the PBS, it attaches PSI trimers. (**c** and **d**) Short-scale PBS movement. State transitions occur in the region containing PSII-PSI-PBS. In State I, the PBS is attached to the PSII. In State I a small movement of the PBS allows energy transfer from PBS to PSI. No spillover or photosystem movement is considered in these models

B. Phycobilisome Versus Photosystem Movement

The changes in fluorescence yield observed during State Transitions were related to different mechanisms: (1) changes in direct energy transfer from PBS to PSII and PSI (Mullineaux and Allen 1990; Allen et al. 1985; Mullineaux et al. 1997); (2) reorganization of photosystems in the membranes and changes in spillover (direct energy transfer from PSII to PSI chlorophylls; PBS is not needed) (El Bissati et al. 2000; Biggins and Bruce 1989; Biggins et al. 1989; Bruce and Biggins 1985; Federman et al. 2000; Ley and Butler 1980; Olive et al. 1986; Vernotte et al. 1992); and (3) functional detachment of PBS from photosystems (Mullineaux 1992; Chukhutsina et al. 2015; Kana et al. 2009). The mobile-PBS model attributes the low PSII fluorescence yield in State II to a smaller effective antenna due to smaller energy transfer from PBSs to PSII and larger direct energy transfer to PSI (Fig. 14.7). In the spillover model, the energy transfer from PBS to PSII remains equal in both states, but the excess energy absorbed by PSII is transferred to PSI and the effective cross-section of PSI increases (Fig. 14.8). In the third model, the increase of fluorescence yield in State I is attributed to a larger concentration of detached PBS.

1. The Mobile-Phycobilisome Model

First, it was demonstrated that PBSs can rapidly diffuse at the surface of the thylakoids ((Mullineaux et al. 1997; Yang et al. 2007); review (Kana 2013)) while the movement of PSII seemed to be largely restricted (Sarcina et al. 2001). Then, it was shown that presence of high concentrations of chemicals that inhibit the movement of PBSs also inhibit state transition (see e.g., (Li et al. 2006; Joshua and Mullineaux 2004; Li et al. 2004).). These results convinced a large

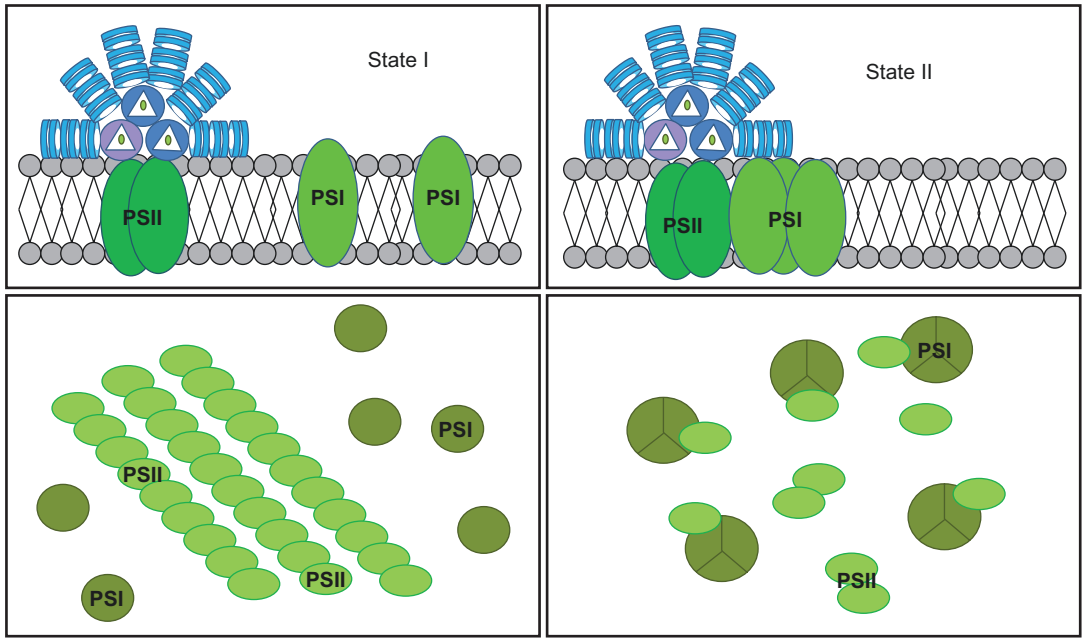

Fig. 14.8. **State Transitions. The spillover model.** In State I, the PBS are attached to PSII. The PSII is organized in rows and the PSI are monomers. Light II induces the movement of PSI and their trimerization. The interaction between PSII and PSI induces spillover from PSII to PSI

majority of workers in the field that during state transition, PBSs move changing the portion of energy directed to PSII and PSI. In order to move, the PBS must be able to disconnect from the membrane (Kana et al. 2012). It was proposed that the ΔApcD mutant is unable to perform state transitions because the PBSs are strongly attached to PSII in the absence of ApcD (Dong et al. 2009). Moreover, the absence of the RpaC protein, which is involved in the stability of the PSII-PBS interaction (Joshua and Mullineaux 2005), also inhibits state transitions in *Synechocystis* cells (Emlyn-Jones et al. 1999; Mullineaux and Emlyn-Jones 2005). The hypotheses about the roles of ApcD and RpaC in state transition remain to be confirmed.

This mechanism does not obligatorily require long-scale mobility of PBSs as only a slight shift would be sufficient to modify the protein coupling in the thylakoid regions containing PBS, PSII and PSI (Kana 2013) (Fig. 14.6c, d). Decoupling of PBSs and their slight movement could change the interaction of the PBS terminal emitters, ApcD and ApcE, with one and the other photosystem (Liu et al. 2013). Alternatively, it was proposed that in State I, all PBSs transfer energy to PSII via the APC core, while in State II the PBSs move away from PSII and become closer to PSI to which they transfer energy via the PC rods (Yang et al. 2007, 2009; Billsten et al. 2003). This hypothesis is improbable. An alternative PBS consisting in one PC rod with a linker protein which preferentially transfer energy to PSI was recently discovered (Kondo et al. 2005, 2007; Watanabe et al. 2014). This PBS is not involved in state transitions (Kondo et al. 2009).

2. *The Spillover Model*

The spillover model (see Chap. 10) does not require PBS movement (Fig. 14.7). It involves a variable coupling between the chlorophylls of PSII and PSI: low PS II-PS I

coupling in State I, and high coupling in State II. Thus, in State II the excess energy absorbed by PSII is transferred to the PSI via the chlorophylls. The spillover mechanism requires a reorganization of the thylakoid membranes and changes in the interaction between the photosystems during state transitions. Several results described in the literature go in this direction. State transitions occur in mutants lacking PBSs (Bruce et al. 1989; El Bissati and Kirilovsky 2001; Olive et al. 1997). State transitions are accompanied by ultrastructural membrane changes: in State I, larger quantities of PSII are arranged in rows compared to State II (40% versus 20%) (Olive et al. 1986, 1997). These thylakoids regions in which PSII particles are associated in multiple rows and PSI is absent were also observed by (Folea et al. 2008). Spillover must be prevented in these thylakoids regions. Both research groups proposed that rearrangements of PSII and PSI domains could be involved in state transitions. In a *Synechocystis* mutant in which the membranes are more rigid due to the absence of di- and tri-unsaturated fatty acids, state transitions are completely inhibited already at 18 °C (El Bissati et al. 2000). In contrast, the OCP-related mechanism (involving PBS) was not affected in this mutant (El Bissati et al. 2000). These results also suggested the involvement of photosystem rearrangements in state transitions. It was also proposed that PSI monomerization/trimerization could be involved in state transitions being PSI trimers more abundant in State II than in State I. The trimers have a stronger interaction with the PBSs than the monomers (Aspinwall et al. 2004). A mutant containing only PSI monomers performs state transitions faster than the WT containing mostly PSI trimers (Schluchter et al. 1996). Although the PSII supercomplex has been found to be rather immobile in cyanobacteria cells (Sarcina et al. 2001), the IsiA chlorophyll binding protein was demonstrated to be mobile (Sarcina and Mullineaux 2004). Thus, although there is no data regarding the mobility of PSI (Mullineaux 2008) we cannot exclude the possibility that PSI moves during state transitions.

3. *Mixed Models*

Bald et al. (1996) proposed the first mixed model in which PSII particles are aligned in rows without contact to monomeric PSI in State I and in State II the trimeric PSI is in contact with disorganized PSII complexes. In this model, in State I the PBSs are attached principally to PSII and in State II the PBS attaches PSI trimers. This is a mixed model. Movement of PBSs and photosystems are involved. (Fig. 14.7)

In McConnell et al. (2002) it was also proposed that state transitions could be simultaneously controlled by variations in direct energy transfer from PBSs to PS I (and PSII) and in energy spillover from PSII to PSI. They showed that in two cyanobacteria mutants (ΔApcD and ΔRpaC) in which the PBS involving process was inhibited still changes in spillover were detected. Rates of both processes would increase in State II and decrease in State I. In State II, an increase of energy spillover from PS II to PSI due to a physical coupling of Chls of PSII and of PSI and an increase in energy transfer from PBSs to PSI is responsible for the decrease of PSII fluorescence (McConnell et al. 2002).

4. *PBS Decoupling*

Decoupling of PBS from photosystems is another process which was proposed to be involved in state transitions, at least in dark-light transitions (Chukhutsina et al. 2015; Kana et al. 2009, 2012). Indeed, the higher 685 nm fluorescence observed in 77 K fluorescence spectra of cyanobacteria cells in State I can be explained also by a disconnection of PBS from photosystems. Decoupling of PBS from photosystems was proposed to occur under different stress conditions: like high light and temperatures (Kana et al. 2009, 2012; Stoitchkova et al. 2007; review,

Kirilovsky et al. 2014, low temperature, Li et al. 2001, and iron starvation, Wilson et al. 2007. Also modifications in the PSII structure could lead to unbinding of PBS (Sakurai et al. 2007a, b; Veerman et al. 2005). Finally, decoupling of PBS from photosystems was also observed during dark-light transitions (Chukhutsina et al. 2015; Kana et al. 2009, 2012). Moreover, it was recently proposed that during dark-light transitions, around 13% of total PBSs uncouple from PSI and only 2% reattach to PSII (Chukhutsina et al. 2015). These results remain to be confirmed.

5. PSII Quenching

Recently, 77 K time-resolved fluorescence spectroscopy on *Synechococcus elongatus* 7942 was used to test the different models for cyanobacterial state transitions. Their results showed that state transitions are not due to changes in spillover or to large PBS movement from one to the other photosystem. They demonstrated that PSII core becomes largely quenched in State II as compared to State I. In addition a small disconnection of PBS from both photosystems was observed (Ranjbar Choubeh et al. 2018).

Thus, PBS uncoupling, PBS movement, spillover between PSII and PSI and PSII core quenching are possibly involved in state transitions.

C. The Signal Transmission from PQ Pool to Complex Movements Is Still an Open Question in Cyanobacteria State Transitions

The signal cascade connecting changes in PQ pool and the rearrangement of the photosynthetic apparatus is unknown and remains to be elucidated in cyanobacteria. In higher plants and green algae, the redox sensor of the PQ pool is the cyt b_6f complex (Wollman and Lemaire 1988). The occupancy of the cyt b_6f Qo site by a PQH_2 molecule (Vener et al. 1995, 1997; Zito et al. 1999) and the conformational changes induced in the complex, especially in the Rieske protein (Zito et al. 1999; Breyton 2000; Finazzi et al. 2001; Zhang et al. 1998), activates a kinase (STN7/Stt7) (Bellafiore et al. 2005; Depege et al. 2003)) that by phosphorylating the mobile trimers of the LHCII induces their detachment from PSII. The Chl molecule attached to the cyt b_6f complex could also have a role in the activation of the LHCII kinase (Lacroix de Lavalette et al. 2008; Hasan et al. 2013; Stroebel et al. 2003; Vladkova 2016).

In cyanobacteria the role of cyt b_6f in state transitions has remained unclear over a long time. In the past, two publications proposed its involvement in this mechanism (Huang et al. 2003; Mao et al. 2002). In cyanobacteria, 2,5-dibromo-3-methyl-6-isopropyl-1,4, benzoquinone (DBMIB) which binds to the Qo site of the cytb_6f and inhibits PQH_2 oxidation induces State II transition even in the presence of DCMU (inhibitor of PQ reduction via PSII) and PQ and DMQ (two electron acceptors from PSII and the PQ pool) (Huang et al. 2003; Mao et al. 2002). The authors considered that the PQ pool was oxidized in the two latter conditions. However, this was not clearly demonstrated. In darkness or in the presence of DCMU and DMQ, the PQ pool continues to be reduced by NDH and SDH enzymes and oxidized by the respiratory oxidases (review (Mullineaux 2014)). In the dark, in the absence of DBMIB, the concentrations used of PQ and DMQ were sufficient to re-oxidase the PQ pool and to induce State I transition (Huang et al. 2003; Mao et al. 2002). In the presence of DBMIB this was inhibited (Huang et al. 2003; Mao et al. 2002). The authors concluded that the binding of DBMIB to the Qo site of the cyt b_6f complex inhibits transition to State II even when the PQ pool is oxidized in the presence of PQ and DMQ. However, in the presence of DMIB, the reoxidation of the PQ pool by respiratory oxidases is also inhibited and even in the dark, the PQ pool could be more reduced in the presence of DMIB than in its absence. Thus, it is possible that the concentrations of PQ and DMQ used were

not sufficient to maintain an oxidized PQ pool in the presence of DBMIB. Indeed, it has been just demonstrated that the PQ pool becomes reduced upon addition of DBMIB even in the presence of DMBQ (Calzadilla et al. 2019). In addition, the same concentration of DBMIB has different effects on state transitions in darkness and under illumination. For instance, DBMIB at 5 μM is unable to induce transition to State II in dark-adapted cells in the presence of DMBQ whereas it induces a large quenching in blue-green light adapted cells in the absence or presence of DMBQ. The amplitude of fluorescence quenching induced by 10 μM DBMIB is also larger under illumination than in darkness in the presence of DMBQ. These experiments strongly suggested that the cyt b_6f complex is not involved in cyanobacterial state transitions. This was clearly demonstrated in an experiment using *N*,*N*′,*N*′-tetramethyl-*p*-phenylenediamine (TMPD). This compound accepts electrons from the PQ pool and directly donates them to $P700^+$, bypassing the DBMIB-poisoned cyt b_6f complex (Draber et al. 1970; Nanba and Katoh 1985). When TMPD was added to largely quenched DBMIB-poisoned cells, it induced a large increase of fluorescence related to transition to State 1. Thus, TMPD is able to reverse the effect of DBMIB by taking electrons from PQ and giving them to PSI, bypassing the inhibited cyt b_6f complex. In conclusion, transition to State I can be induced even when the cyt b_6f is inhibited by DBMIB, by partial oxidation of the PQ pool demonstrating that DBMIB binding to the Qo site of cyt b_6f is not involved in transition to State II.

As an alternative, it was recently proposed that the single Chl *a* in the cyt b_6f complex could be the redox sensor. A change of Chl volume could induce modifications in the hydrophobic thickness of cyt b_6f complex and induce hydrophobic mismatches in thylakoids. This will induce lipid sorting around cyt b_6f and change the lipid composition in other membrane regions leading to changes in the photosystems interactions and PBS-Photosystems binding (Vladkova 2016). However, based on the results obtained with TMPD, the involvement of this Chl *a* in cyanobacterial state transitions is not likely.

A long time ago, Allen and coworkers suggested that specific protein phosphorylations could be involved in cyanobacterial state transitions (Allen et al. 1985). More recently phosphoproteomes showed that PBS and photosystems proteins are phosphorylated (Chen et al. 2015; Spat et al. 2015; Yang et al. 2013) and state transitions seemed to be affected when the Ser and Thr of phycocyanin were replaced by non-phosphorylable amino acids (Chen et al. 2015). However, the recent characterization of 12 kinase and 9 phosphatase single mutants clearly showed that there is not a specific protein kinase and/or phosphatase that is necessary for cyanobacterial state transitions (Calzadilla et al. 2019). Moreover, the use of kinase and phosphatase inhibitors demonstrated that phosphorylation reactions are not essential in cyanobacterial state transitions (Calzadilla et al. 2019). Thus, the signal transduction from the PQ pool to the antenna and the photosystems is completely different in cyanobacteria and green algae and higher plants.

V. Perspectives and Conclusions

To adjust the amount of energy arriving at the reaction centers under different conditions cyanobacteria use three different mechanisms that involves the interaction between the PBSs and the photosystems: OCP-related NPQ, PBS decoupling and state transitions. The latter mechanism optimizes the relative activity of the photosystems while the first two mechanisms are involved in photoprotection. PBS decoupling was also proposed to be involved in state transitions.

The cyanobacterial OCP-related NPQ was discovered and first characterized around

10 years ago. During the last 10 years, important discoveries allowed a large progress in the understanding of the photoprotective mechanism: the three elements that are involved were discovered and their interaction was studied, the roles of the photoactivity of the OCP and of the FRP were elucidated. Nevertheless, important points remain to be elucidated including: (1) confirmation of the site of OCP binding in the core of PBSs; (2) elucidation of the quenching mechanism; (3) resolution of OCP^r structure; (4) molecular mechanism of the FRP; (5) elucidation of the OCP photocycle.

The cyanobacterial state transitions mechanisms has been studied for more of 40 years and still a lot of questions remain without answer and many points are still controversial. The most intriguing open question about state transition mechanism is the transmission of the signal. Nothing is known about the element that links changes in the redox state of the PQ pool and the movement of PBSs and/or photosystems. This is an important question that must be answered in the future.

It is also important to know if the fluorescence changes induced in dark-light transitions and those generated by orange-blue transitions have the same origin and the same trigger. The relative importance of the PBS mobile mechanism versus membrane related mechanisms must be elucidated. The role of PBS detachment in state transitions must also be further studied.

Finally, preliminary observations suggest that the OCP-dependent NPQ and state transitions are complementary photoprotective mechanisms; their particular importance differs between species and conditions. In some strains, like *Synechocystis*, the OCP-related NPQ mechanism seems to be the most important mechanism; in other strains of cyanobacteria, which lack OCP, such as in *Synechococcus elongatus* state transitions become the principal photoprotective mechanism. It will be interesting to further investigate this complementary.

References

Adir N (2005) Elucidation of the molecular structures of components of the phycobilisome: reconstructing a giant. Photosynth Res 85:15–32

Adir N (2008) Structure of the phycobilisome antennae in cyanobacteria and red algae. In: Fromme P (ed) Photosynthetic protein complexes: a structural approach. WILEY-VCH Verlag GmbH & Co. KGaA, Weinheim, pp 243–274

Ajlani G, Vernotte C (1998) Deletion of the PB-loop in the Lcm subunit does not affect phycobilisome assembly or energy transfer functions in the cyanobacterium *Synechocystis* sp. PCC6714. Eur J Biochem 257:154–159

Ajlani G, Vernotte C, Dimagno L, Haselkorn R (1995) Phycobilisome Core mutants of *Synechocystis* PCC 6803. Biochim Biophys Acta 1231:189–196

Allen JF, Sanders CE, Holmes NG (1985) Correlation of membrane-protein phosphorylation with excitation-energy distribution in the cyanobacterium *Synechococcus* 6301. FEBS Lett 193:271–275

Aoki M, Katoh S (1982) Oxidation and reduction of plastoquinone by photosynthetic and respiratory electron transport in a cyanobacterium *Synechococcus* sp. Biochim Biophys Acta 682:307–314

Arteni AA, Ajlani G, Boekema EJ (2009) Structural organisation of phycobilisomes from *Synechocystis* sp. strain PCC6803 and their interaction with the membrane. Biochim Biophys Acta 1787:272–279

Ashby MK, Mullineaux CW (1999) The role of ApcD and ApcF in energy transfer from phycobilisomes to PSI and PSII in a cyanobacterium. Photosynth Res 61:169–179

Aspinwall CL, Sarcina M, Mullineaux CW (2004) Phycobilisome mobility in the cyanobacterium Synechococcus sp. PCC7942 is influenced by the trimerisation of photosystem I. Photosynth Res 79:179–187

Bandara S, Ren Z, Lu L, Zeng X, Shin H, Zhao KH, Yang X (2017) Photoactivation mechanism of a carotenoid-based photoreceptor. Proc Natl Acad Sci U S A 114:6286–6291

Bao H, Melnicki MR, Kerfeld CA (2017a) Structure and functions of orange carotenoid protein homologs in cyanobacteria. Curr Opin Plant Biol 37:1–9

Bao H, Melnicki MR, Pawlowski EG, Sutter M, Agostoni M, Lechno-Yossef S, Cai F, Montgomery BL, Kerfeld CA (2017b) Additional families of orange carotenoid proteins in the photoprotective system of cyanobacteria. Nat Plants 3:17089

Bellafiore S, Barneche F, Peltier G, Rochaix JD (2005) State transitions and light adaptation require chloroplast thylakoid protein kinase STN7. Nature 433:892–895

Berera R, van Stokkum IH, Gwizdala M, Wilson A, Kirilovsky D, van Grondelle R (2012) The photophysics of the orange carotenoid protein, a light-powered molecular switch. J Phys Chem 116:2568–2574

Berera R, Gwizdala M, van Stokkum IH, Kirilovsky D, van Grondelle R (2013) Excited states of the inactive and active forms of the orange carotenoid protein. J Phys Chem 117:9121–9128

Biggins J, Bruce D (1989) Regulation of excitation-energy transfer in organisms containing phycobilins. Photosynth Res 20:1–34

Biggins J, Tanguay NA, Frank HA (1989) Electron-transfer reactions in photosystem-I following vitamin-K1 depletion by ultraviolet-irradiation. FEBS Lett 250:271–274

Billsten HH, Bhosale P, Yemelyanov A, Bernstein PS, Polivka T (2003) Photophysical properties of xanthophylls in carotenoproteins from human retinas. Photochem Photobiol 78:138–145

Bonaventura C, Myers J (1969) Fluorescence and oxygen evolution from Chlorella pyrenoidosa. Biochim Biophys Acta 189:366–383

Boulay C, Abasova L, Six C, Vass I, Kirilovsky D (2008) Occurrence and function of the orange carotenoid protein in photoprotective mechanisms in various cyanobacteria. Biochim Biophys Acta 1777:1344–1354

Boulay C, Wilson A, D'Haene S, Kirilovsky D (2010) Identification of a protein required for recovery of full antenna capacity in OCP-related photoprotective mechanism in cyanobacteria. Proc Natl Acad Sci U S A 107:11620–11625

Bourcier de Carbon C, Thurotte A, Wilson A, Perreau F, Kirilovsky D (2015) Biosynthesis of soluble carotenoid holoproteins in Escherichia coli. Sci Rep 5:9085

Breyton C (2000) Conformational changes in the cytochrome b6f complex induced by inhibitor binding. J Biol Chem 275:13195–13201

Bruce D, Biggins J (1985) Mechanism of the light-state transition in photosynthesis : V. 77 K linear dichroism of *Anacystis nidulans* in state 1 and state 2. Biochim Biophys Acta 810:295–301

Bruce D, Brimble S, Bryant DA (1989) State transitions in a phycobilisome-less mutant of the cyanobacterium *Synechococcus* sp. PCC 7002. Biochim Biophys Acta 974:66–73

Bryant DA, de Lorimier R, Guglielmi G, Stevens SE Jr (1990) Structural and compositional analyses of the phycobilisomes of Synechococcus sp. PCC 7002. Analyses of the wild-type strain and a phycocyanin-less mutant constructed by interposon mutagenesis. Arch Microbiol 153:550–560

Calzadilla PI, Zhan J, Setif P, Lemaire C, Solymosi D, Battchikova N, Wang Q, Kirilovsky D (2019) The cytochrome b6f complex is not involved in cyanobacterial state transitions. Plant Cell 31: 911–931

Capuano V, Braux AS, Tandeau de Marsac N, Houmard J (1991) The "anchor polypeptide" of cyanobacterial phycobilisomes. Molecular characterization of the *Synechococcus* sp. PCC 6301 apce gene. J Biol Chem 266:7239–7247

Capuano V, Thomas JC, Tandeau de Marsac N, Houmard J (1993) An *in vivo* approach to define the role of the L_{CM}, the key polypeptide of cyanobacterial phycobilisomes. J Biol Chem 268:8277–8283

Chang L, Liu X, Li Y, Liu C-C, Yang F, Zhao J, Sui S-F (2015) Structural organization of an intact phycobilisome and its association with photosystem II. Cell Res 25:726

Chen Z, Zhan J, Chen Y, Yang M, He C, Ge F, Wang Q (2015) Effects of phosphorylation of beta subunits of Phycocyanins on state transition in the model cyanobacterium *Synechocystis* sp. PCC 6803. Plant Cell Physiol 56:1997–2013

Chukhutsina V, Bersanini L, Aro EM, van Amerongen H (2015) Cyanobacterial light-harvesting Phycobilisomes uncouple from photosystem I during dark-to-light transitions. Sci Rep 5:14193

de Lacroix De Lavalette A, Finazzi G, Zito F (2008) b6f-Associated chlorophyll: structural and dynamic contribution to the different cytochrome functions. Biochemistry 47:5259–5265

Delphin E, Duval JC, Etienne AL, Kirilovsky D (1996) State transitions or Delta pH-dependent quenching of photosystem II fluorescence in red algae. Biochemistry 35:9435–9445

Delphin E, Duval JC, Etienne AL, Kirilovsky D (1998) Delta pH-dependent photosystem II fluorescence quenching induced by saturating, multiturnover pulses in red algae. Plant Physiol 118:103–113

Depege N, Bellafiore S, Rochaix JD (2003) Role of chloroplast protein kinase Stt7 in LHCII phosphorylation and state transition in *Chlamydomonas*. Science 299:1572–1575

Dong C, Zhao J (2008) ApcD is required for state transition but not involved in blue-light induced quenching in the cyanobacterium *Anabaena* sp. PCC7120. Chin Sci Bull 53:3422–3424

Dong C, Tang A, Zhao J, Mullineaux CW, Shen G, Bryant DA (2009) ApcD is necessary for efficient energy transfer from phycobilisomes to photosystem I and helps to prevent photoinhibition in the

cyanobacterium *Synechococcus* sp. PCC 7002. Biochim Biophys Acta 1787:1122–1128

Draber W, Trebst A, Harth E (1970) On a new inhibitor of photosynthetic electron-transport in isolated chloroplasts. Z Naturforsch B 25:1157–1159

Ducret A, Muller SA, Goldie KN, Hefti A, Sidler WA, Zuber H, Engel A (1998) Reconstitution, characterisation and mass analysis of the pentacylindrical allophycocyanin core complex from the cyanobacterium Anabaena sp. PCC 7120. J Mol Biol 278:369–388

El Bissati K, Kirilovsky D (2001) Regulation of *psbA* and *psaE* expression by light quality in *Synechocystis* species PCC 6803. A redox control mechanism. Plant Physiol 125:1988–2000

El Bissati K, Delphin E, Murata N, Etienne A, Kirilovsky D (2000) Photosystem II fluorescence quenching in the cyanobacterium *Synechocystis* PCC 6803: involvement of two different mechanisms. Biochim Biophys Acta 1457:229–242

Elmorjani K, Thomas JC, Sebban P (1986) Phycobilisomes of wild-type and pigment mutants of the cyanobacterium *Synechocystis* PCC 6803. Arch Microbiol 146:186–191

Emlyn-Jones D, Ashby MK, Mullineaux CW (1999) A gene required for the regulation of photosynthetic light harvesting in the cyanobacterium *Synechocystis* 6803. Mol Microbiol 33:1050–1058

Federman S, Malkin S, Scherz A (2000) Excitation energy transfer in aggregates of photosystem I and photosystem II of the cyanobacterium *Synechocystis* sp. PCC 6803: can assembly of the pigment-protein complexes control the extent of spillover? Photosynth Res 64:199–207

Finazzi G, Zito F, Barbagallo RP, Wollman FA (2001) Contrasted effects of inhibitors of cytochrome b6f complex on state transitions in *Chlamydomonas reinhardtii:* the role of Qo site occupancy in LHCII kinase activation. J Biol Chem 276:9770–9774

Folea IM, Zhang P, Aro EM, Boekema EJ (2008) Domain organization of photosystem II in membranes of the cyanobacterium *Synechocystis* PCC6803 investigated by electron microscopy. FEBS Lett 582:1749–1754

Gantt E, Conti SF (1966) Granules associated with the chloroplast lamellae of Porphyridium cruentum. J Cell Biol 29:423–434

Gindt YM, Zhou J, Bryant DA, Sauer K (1992) Core mutations of Synechococcus sp. PCC 7002 phycobilisomes: a spectroscopic study. J Photochem Photobiol 15:75–89

Glauser M, Bryant DA, Frank G, Wehrli E, Rusconi SS, Sidler W, Zuber H (1992) Phycobilisome structure in the cyanobacteria Mastigocladus laminosus and Anabaena sp. PCC 7120. Eur J Biochem 205:907–915

Glazer AN (1984) Phycobilisome – a macromolecular complex optimized for light energy-transfer. Biochim Biophys Acta 768:29–51

Glazer AN (1989) Light guides. Directional energy transfer in a photosynthetic antenna. J Biol Chem 264:1–4

Gorbunov MY, Kuzminov FI, Fadeev VV, Kim JD, Falkowski PG (2011) A kinetic model of non-photochemical quenching in cyanobacteria. Biochim Biophys Acta 1807:1591–1599

Grossman AR, Schaefer MR, Chiang GG, Collier JL (1993) The phycobilisome, a light-harvesting complex responsive to environmental-conditions. Microbiol Rev 57:725–749

Gupta S, Guttman M, Leverenz RL, Zhumadilova K, Pawlowski EG, Petzold CJ, Lee KK, Ralston CY, Kerfeld CA (2015) Local and global structural drivers for the photoactivation of the orange carotenoid protein. Proc Natl Acad Sci U S A 112:E5567–E5574

Gwizdala M, Wilson A, Kirilovsky D (2011) *In vitro* reconstitution of the cyanobacterial photoprotective mechanism mediated by the orange carotenoid protein in *Synechocystis* PCC 6803. Plant Cell 23:2631–2643

Gwizdala M, Wilson A, Omairi-Nasser A, Kirilovsky D (2013) Characterization of the Synechocystis PCC 6803 fluorescence recovery protein involved in photoprotection. Biochim Biophys Acta 1827:348–354

Harris D, Tal O, Jallet D, Wilson A, Kirilovsky D, Adir N (2016) Orange carotenoid protein burrows into the phycobilisome to provide photoprotection. Proc Natl Acad Sci U S A 113:E1655–E1662

Harris D, Wilson A, Muzzopappa F, Sluchanko NN, Friedrich T, Maksimov EG, Kirilovsky D, Adir N (2018) Structural rearrangements in the C-terminal domain homolog of Orange carotenoid protein are crucial for carotenoid transfer. Commun Biol 1:125

Hasan SS, Yamashita E, Cramer WA (2013) Transmembrane signaling and assembly of the cytochrome b6f-lipidic charge transfer complex. Biochim Biophys Acta 1827:1295–1308

Holt TK, Krogmann DW (1981) A carotenoid-protein from cyanobacteria. Biochim Biophys Acta 637:408–414

Huang C, Yuan X, Zhao J, Bryant DA (2003) Kinetic analyses of state transitions of the cyanobacterium *Synechococcus* sp. PCC 7002 and its mutant strains impaired in electron transport. Biochim Biophys Acta 1607:121–130

Jallet D, Gwizdala M, Kirilovsky D (2012) ApcD, ApcF and ApcE are not required for the orange carotenoid protein related phycobilisome fluorescence quench-

ing in the cyanobacterium Synechocystis PCC 6803. Biochim Biophys Acta 1817:1418–1427

Jallet D, Thurotte A, Leverenz RL, Perreau F, Kerfeld CA, Kirilovsky D (2014) Specificity of the cyanobacterial orange carotenoid protein: influences of orange carotenoid protein and phycobilisome structures. Plant Physiol 164:790–804

Jordan P, Fromme P, Witt HT, Klukas O, Saenger W, Krauss N (2001) Three-dimensional structure of cyanobacterial photosystem I at 2.5 A resolution. Nature 411:909–917

Joshua S, Mullineaux CW (2004) Phycobilisome diffusion is required for light-state transitions in cyanobacteria. Plant Physiol 135:2112–2119

Joshua S, Mullineaux CW (2005) The rpaC gene product regulates phycobilisome-photosystem II interaction in cyanobacteria. Biochim Biophys Acta 1709:58–68

Kana R (2013) Mobility of photosynthetic proteins. Photosynth Res 116:465–479

Kana R, Prasil O, Komarek O, Papageorgiou GC (2009) Govindjee, spectral characteristic of fluorescence induction in a model cyanobacterium, *Synechococcus* sp. PCC 7942. Biochim Biophys Acta 1787:1170–1178

Kana R, Kotabova E, Komarek O, Sediva B, Papageorgiou GC, Govindjee OP (2012) The slow S to M fluorescence rise in cyanobacteria is due to a state 2 to state 1 transition. Biochim Biophys Acta 1817:1237–1247

Kana R, Kotabova E, Lukes M, Papacek S, Matonoha C, Liu LN, Prasil O, Mullineaux CW (2014) Phycobilisome mobility and its role in the regulation of light harvesting in red algae. Plant Physiol 165:1618–1631

Karapetyan NV (2007) Non-photochemical quenching of fluorescence in cyanobacteria. Biochemistry 72:1127–1135

Kerfeld CA (2004a) Structure and function of the water-soluble carotenoid-binding proteins of cyanobacteria. Photosynth Res 81:215–225

Kerfeld CA (2004b) Water-soluble carotenoid proteins of cyanobacteria. Arch Biochem Biophys 430:2–9

Kerfeld CA, Kirilovsky D (2013) Structural, mechanistic and genomic insights into OCP-mediated photoprotection. In: Chauvat F, Cassier-Chauvat C (eds) Advances in botanical research: genomics in cyanobacteria. Elsevier, Oxford, pp 1–26

Kerfeld CA, Sawaya MR, Brahmandam V, Cascio D, Ho KK, Trevithick-Sutton CC, Krogmann DW, Yeates TO (2003) The crystal structure of a cyanobacterial water-soluble carotenoid binding protein. Structure 11:55–65

Kerfeld CA, Alexandre M, Kirilovsky D (2009) The orange carotenoid protein in cyanobacteria. In: Landrum J (ed) Carotenoids: Physical, chemical and biological functions and properties. Taylor and Francis group, Boca Raton, pp 3–19

Kerfeld CA, Melnicki MR, Sutter M, Dominguez-Martin MA (2017) Structure, function and evolution of the cyanobacterial orange carotenoid protein and its homologs. New Phytol 215:937–951

Kirilovsky D (2007) Photoprotection in cyanobacteria: the orange carotenoid protein (OCP)-related non-photochemical-quenching mechanism. Photosynth Res 93:7–16

Kirilovsky D, Kerfeld CA (2012) The orange carotenoid protein in photoprotection of photosystem II in cyanobacteria. Biochim Biophys Acta 1817:158–166

Kirilovsky D, Kerfeld CA (2013) The orange carotenoid protein: a blue-green light photoactive protein. Photochem Photobiol Sci 12:1135–1143

Kirilovsky D, Kana R, Prasil O (2014) Mechanisms modulating energy arriving at reaction centers in cyanobacteria. In: Demmig-Adams B, Garab G, Adams W, Govindjee (eds) Non-Photochemical Quenching and energy dissipation in plants, algae and cyanobacteria. Springer, Dordrecht/Heidelberg/New York/London, pp 471–501

Kish E, Kos PB, Chen M, Vass I (2015a) A unique regulation of the expression of the psbA, psbD, and psbE genes, encoding the 01, 02 and cytochrome b559 subunits of the photosystem II complex in the chlorophyll d containing cyanobacterium Acaryochloris marina. Biochim Biophys Acta 1817:1083–1094

Kish E, Pinto MM, Kirilovsky D, Spezia R, Robert B (2015b) Echinenone vibrational properties: from solvents to the orange carotenoid protein. Biochim Biophys Acta 1847:1044–1054

Kondo K, Geng XX, Katayama M, Ikeuchi M (2005) Distinct roles of CpcG1 and CpcG2 in phycobilisome assembly in the cyanobacterium Synechocystis sp. PCC 6803. Photosynth Res 84:269–273

Kondo K, Ochiai Y, Katayama M, Ikeuchi M (2007) The membrane-associated CpcG2-phycobilisome in Synechocystis: a new photosystem I antenna. Plant Physiol 144:1200–1210

Kondo K, Mullineaux CW, Ikeuchi M (2009) Distinct roles of CpcG1-phycobilisome and CpcG2-phycobilisome in state transitions in a cyanobacterium Synechocystis sp. PCC 6803. Photosynth Res 99:217–225

Konold PE, van Stokkum IHM, Muzzopappa F, Wilson A, Groot M-L, Kirilovsky D and Kennis JTM (2019) Photoactivation mechanism, timing of protein secondary structure dynamics and carotenoid translocation in the Orange carotenoid protein. J Am Chem Soc J Am Chem Soc 141:520–530

Krupnik T, Kotabova E, van Bezouwen LS, Mazur R, Garstka M, Nixon PJ, Barber J, Kana R, Boekema EJ, Kargul J (2013) A reaction center-dependent photoprotection mechanism in a highly robust photosystem II from an extremophilic red alga, *Cyanidioschyzon merolae*. J Biol Chem 288:23529–23542

Kuzminov FI, Karapetyan NV, Rakhimberdieva MG, Elanskaya IV, Gorbunov MY, Fadeev VV (2012) Investigation of OCP-triggered dissipation of excitation energy in PSI/PSII-less Synechocystis sp. PCC 6803 mutant using non-linear laser fluorimetry. Biochim Biophys Acta 1817:1012–1021

Lechno-Yossef S, Melnicki MR, Bao H, Montgomery BL, Kerfeld CA (2017) Synthetic OCP heterodimers are photoactive and recapitulate the fusion of two primitive carotenoproteins in the evolution of cyanobacterial photoprotection. Plant J 91:646–656

Leverenz RL, Jallet D, Li MD, Mathies RA, Kirilovsky D, Kerfeld CA (2014) Structural and functional modularity of the orange carotenoid protein: distinct roles for the N- and C-terminal domains in cyanobacterial photoprotection. Plant Cell 26:426–437

Leverenz RL, Sutter M, Wilson A, Gupta S, Thurotte A, Bourcier de Carbon C, Petzold CJ, Ralston C, Perreau F, Kirilovsky D, Kerfeld CA (2015) PHOTOSYNTHESIS. A 12 a carotenoid translocation in a photoswitch associated with cyanobacterial photoprotection. Science 348:1463–1466

Ley AC, Butler WL (1980) Energy distribution in the photochemical apparatus of *Porphyridium cruentum* in state-I and state-II. Biochim Biophys Acta 592:349–363

Li Y, Zhang J, Xie J, Zhao J, Jiang L (2001) Temperature-induced decoupling of phycobilisomes from reaction centers. Biochim Biophys Acta 1504:229–234

Li D, Xie J, Zhao J, Xia A, Li D, Gong Y (2004) Light-induced excitation energy redistribution in Spirulina platensis cells: "spillover" or "mobile PBSs". Biochim Biophys Acta 1608:114–121

Li H, Li D, Yang S, Xie J, Zhao J (2006) The state transition mechanism – simply depending on light-on and -off in Spirulina platensis. Biochim Biophys Acta 1757:1512–1519

Liu LN, Chen XL, Zhang YZ, Zhou BC (2005) Characterization, structure and function of linker polypeptides in phycobilisomes of cyanobacteria and red algae: an overview. Biochim Biophys Acta 1708:133–142

Liu H, Zhang H, Niedzwiedzki DM, Prado M, He G, Gross ML, Blankenship RE (2013) Phycobilisomes supply excitations to both photosystems in a megacomplex in cyanobacteria. Science 342:1104–1107

Liu H, Zhang H, King JD, Wolf NR, Prado M, Gross ML, Blankenship RE (2014) Mass spectrometry footprinting reveals the structural rearrangements of cyanobacterial orange carotenoid protein upon light activation. Biochim Biophys Acta 1837:1955–1963

Liu H, Zhang H, Orf GS, Lu Y, Jiang J, King JD, Wolf NR, Gross ML, Blankenship RE (2016) Dramatic domain rearrangements of the cyanobacterial orange carotenoid protein upon photoactivation. Biochemistry 55:1003–1009

Lopez-Igual R, Wilson A, Leverenz RL, Melnicki MR, Bourcier de Carbon C, Sutter M, Turmo A, Perreau F, Kerfeld CA, Kirilovsky D (2016) Different functions of the Paralogs to the N-terminal domain of the orange carotenoid protein in the Cyanobacterium Anabaena sp. PCC 7120. Plant Physiol 171:1852–1866

Lu Y, Liu H, Saer R, Li VL, Zhang H, Shi L, Goodson C, Gross ML, Blankenship RE (2017a) A molecular mechanism for nonphotochemical quenching in cyanobacteria. Biochemistry 56:2812–2823

Lu Y, Liu H, Saer RG, Zhang H, Meyer CM, Li VL, Shi L, King JD, Gross ML, Blankenship RE (2017b) Native mass spectrometry analysis of Oligomerization states of fluorescence recovery protein and orange carotenoid protein: two proteins involved in the cyanobacterial photoprotection cycle. Biochemistry 56:160–166

Ludwig M, Bryant DA (2011) Transcription profiling of the model cyanobacterium *Synechococcus* sp strain PCC 7002 by next-gen (SOLiD™) sequencing of cDNA. Front Microbiol 2(41). https://doi.org/10.3389/fmicb.2011.00041

Ludwig M, Bryant DA (2012) Acclimation of the global transcriptome of the cyanobacterium sp strain PCC 7002 to nutrient limitations and different nitrogen sources. Front Microbiol 3:145. https://doi.org/10.3389/fmicb.2012.00145

Lundell DJ, Glazer AN (1983a) Molecular architecture of a light-harvesting antenna. Quaternary interactions in the Synechococcus 6301 phycobilisome core as revealed by partial tryptic digestion and circular dichroism studies. J Biol Chem 258:8708–8713

Lundell DJ, Glazer AN (1983b) Molecular architecture of a light-harvesting antenna. Core substructure in Synechococcus 6301 phycobilisomes: two new allophycocyanin and allophycocyanin B complexes. J Biol Chem 258:902–908

Lundell DJ, Glazer AN (1983c) Molecular architecture of a light-harvesting antenna. Structure of the 18 S core-rod subassembly of the Synechococcus 6301 phycobilisome. J Biol Chem 258:894–901

MacColl R (1998) Cyanobacterial phycobilisomes. J Struct Biol 124:311–334

Maksimov EG, Shirshin EA, Sluchanko NN, Zlenko DV, Parshina EY, Tsoraev GV, Klementiev KE, Budylin GS, Schmitt FJ, Friedrich T, Fadeev VV, Paschenko VZ, Rubin AB (2015a) The signaling state of orange carotenoid protein. Biophys J 109:595–607

Maksimov EG, Klementiev KE, Shirshin EA, Tsoraev GV, Elanskaya IV, Paschenko VZ (2015b) Features of temporal behavior of fluorescence recovery in Synechocystis sp. PCC6803. Photosynth Res 125:167–178

Maksimov EG, Moldenhauer M, Shirshin EA, Parshina EA, Sluchanko NN, Klementiev KE, Tsoraev GV, Tavraz NN, Willoweit M, Schmitt FJ, Breitenbach J, Sandmann G, Paschenko VZ, Friedrich T, Rubin AB (2016) A comparative study of three signaling forms of the orange carotenoid protein. Photosynth Res 130:389–401

Maksimov EG, Sluchanko NN, Mironov KS, Shirshin EA, Klementiev KE, Tsoraev GV, Moldenhauer M, Friedrich T, Los DA, Allakhverdiev SI, Paschenko VZ, Rubin AB (2017a) Fluorescent labeling preserving OCP photoactivity reveals its reorganization during the photocycle. Biophys J 112:46–56

Maksimov EG, Sluchanko NN, Slonimskiy YB, Slutskaya EA, Stepanov AV, Argentova-Stevens AM, Shirshin EA, Tsoraev GV, Klementiev KE, Slatinskaya OV, Lukashev EP, Friedrich T, Paschenko VZ, Rubin AB (2017b) The photocycle of orange carotenoid protein conceals distinct intermediates and asynchronous changes in the carotenoid and protein components. Sci Rep 7:15548

Mao HB, Li GF, Ruan X, Wu QY, Gong YD, Zhang XF, Zhao NM (2002) The redox state of plastoquinone pool regulates state transitions via cytochrome b_6f complex in *Synechocystis* sp. PCC 6803. FEBS Lett 519:82–86

Mao L, Wang Y, Hu X (2003) pi-pi stacking interactions in the peridinin-chlorophyll-protein of *Amphidinium carterae*. J Phys Chem B 107:3963–3971

McConnell MD, Koop R, Vasil'ev S, Bruce D (2002) Regulation of the distribution of chlorophyll and phycobilin-absorbed excitation energy in cyanobacteria. A structure-based model for the light state transition. Plant Physiol 130:1201–1212

Melnicki MR, Leverenz RL, Sutter M, Lopez-Igual R, Wilson A, Pawlowski EG, Perreau F, Kirilovsky D, Kerfeld CA (2016) Structure, diversity, and evolution of a new family of soluble carotenoid-binding proteins in cyanobacteria. Mol Plant 9:1379–1394

Misumi M, Katoh H, Tomo T, Sonoike K (2016) Relationship between photochemical quenching and non-photochemical quenching in six species of cyanobacteria reveals species difference in redox state and species commonality in energy dissipation. Plant Cell Physiol 57:1510–1517

Moldenhauer M, Sluchanko NN, Tavraz NN, Junghans C, Buhrke D, Willoweit M, Chiappisi L, Schmitt FJ, Vukojevic V, Shirshin EA, Ponomarev VY, Paschenko VZ, Gradzielski M, Maksimov EG, Friedrich T (2018) Interaction of the signaling state analog and the apoprotein form of the orange carotenoid protein with the fluorescence recovery protein. Photosynth Res 135:125–139

Mullineaux CW (1992) Excitation energy transfer from phycobilisomes to photosystem-I and photosystem-II in a Cyanobacterium. Photosynth Res 34:114–114

Mullineaux CW (2008) Factors controlling the mobility of photosynthetic proteins. Photochem Photobiol 84:1310–1316

Mullineaux CW (2014) Co-existence of photosynthetic and respiratory activities in cyanobacterial thylakoid membranes. Biochim Biophys Acta 1837:503–511

Mullineaux CW, Allen JF (1986) The state 2 transition in the cyanobacterium *Synechococcus* 6301 can be driven by respiratory electron flow into the plastoquinone pool. FEBS Lett 205:155–160

Mullineaux CW, Allen JF (1990) State 1 – State 2 transitions in the cyanobacterium *Synechococcus* 6301 are controlled by the redox state of electron carriers between photosystem I and photosystem II. Photosynth Res 23:297–311

Mullineaux CW, Emlyn-Jones D (2005) State transitions: an example of acclimation to low-light stress. J Exp Bot 56:389–393

Mullineaux CW, Tobin MJ, Jones GR (1997) Mobility of photosynthetic complexes in thylakoid membranes. Nature 390:421–424

Murata N (1969) Control of excitation transfer in photosynthesis. I. Light-induced change of chlorophyll a fluorescence in *Porphyridium cruentum*. Biochim Biophys Acta 172:242–251

Muzzopappa F, Wilson A, Yogarajah V, Cot S, Perreau F, Montigny C, Bourcier de Carbon C, Kirilovsky D (2017) Paralogs of the C-terminal domain of the Cyanobacterial Orange carotenoid protein are carotenoid donors to helical carotenoid proteins. Plant Physiol 175:1283–1303

Muzzopappa F, Wilson A, Kirilovsky D (2019) Interdomain interactions reveal the molecular evolution of the Orange carotenoid protein. Nat Plants 5:1076–1086

Nanba M, Katoh S (1985) Restoration by tetramethyl-p-phenylenediamine of photosynthesis in dibromothymoquinone-inhibited cells of the cyanobacterium *Synechococcus* sp. Biochim Biophys Acta 809:74–80

Niedzwiedzki DM, Liu H, Blankenship RE (2014) Excited state properties of 3′-hydroxyechinenone in solvents and in the orange carotenoid protein from Synechocystis sp. PCC 6803. J Phys Chem 118:6141–6149

Ogawa T, Sonoike K (2015) Dissection of respiration and photosynthesis in the cyanobacterium Synechocystis sp. PCC6803 by the analysis of chlorophyll fluorescence. J Photochem Photobiol 144:61–67

Olive J, Mbina I, Vernotte C, Astier C, Wollman FA (1986) Randomization of the Ef particles in thylakoid membranes of *Synechocystis* 6714 upon transition from state-I to state-II. FEBS Lett 208:308–312

Olive J, Ajlani G, Astier C, Recouvreur M, Vernotte C (1997) Ultrastructure and light adaptation of phycobilisome mutants of *Synechocystis* PCC 6803. Biochim Biophys Acta 1319:275–282

Polivka T, Kerfeld CA, Pascher T, Sundström V (2005) Spectroscopic properties of the carotenoid 3′-hydroxyechinenone in the orange carotenoid protein from the cyanobacterium *Arthrospira maxima*. Biochemistry 44:3994–4003

Polivka T, Chabera P, Kerfeld CA (2013) Carotenoid-protein interaction alters the S(1) energy of hydroxyechinenone in the orange carotenoid protein. Biochim Biophys Acta 1827:248–254

Punginelli C, Wilson A, Routaboul JM, Kirilovsky D (2009) Influence of zeaxanthin and echinenone binding on the activity of the orange carotenoid protein. Biochim Biophys Acta 1787:280–288

Rakhimberdieva MG, Boichenko VA, Karapetyan NV, Stadnichuk IN (2001) Interaction of phycobilisomes with photosystem II dimers and photosystem I monomers and trimers in the cyanobacterium *Spirulina platensis*. Biochemistry 40:15780–15788

Rakhimberdieva MG, Stadnichuk IN, Elanskaya IV, Karapetyan NV (2004) Carotenoid-induced quenching of the phycobilisome fluorescence in photosystem II-deficient mutant of *Synechocystis* sp. FEBS Lett 574:85–88

Rakhimberdieva MG, Elanskaya IV, Vermaas WFJ, Karapetyan NV (2010) Carotenoid-triggered energy dissipation in phycobilisomes of *Synechocystis* sp. PCC 6803 diverts excitation away from reaction centers of both photosystems. Biochim Biophys Acta 1797:241–249

Ranjbar Choubeh R, Wientjes E, Struik PC, Kirilovsky D, van Amerongen H (2018) State transitions in the cyanobacterium Synechococcus elongatus 7942 involve reversible quenching of the photosystem II core. Biochim Biophys Acta 1859:1059–1066

Redlinger T, Gantt E (1982) A M(r) 95,000 polypeptide in *Porphyridium cruentum* phycobilisomes and thylakoids: possible function in linkage of phycobilisomes to thylakoids and in energy transfer. Proc Natl Acad Sci U S A 79:5542–5546

Reuter W, Wiegand G, Huber R, Than ME (1999) Structural analysis at 2.2 angstrom of orthorhombic crystals presents the asymmetry of the allophycocyanin-linker complex, AP center dot L-C(7.8), from phycobilisomes of Mastigocladus laminosus. Proc Natl Acad Sci U S A 96:1363–1368

Sakurai I, Mizusawa N, Ohashi S, Kobayashi M, Wada H (2007a) Effects of the lack of phosphatidylglycerol on the donor side of photosystem II. Plant Physiol 144:1336–1346

Sakurai I, Mizusawa N, Wada H, Sato N (2007b) Digalactosyldiacylglycerol is required for stabilization of the oxygen-evolving complex in photosystem II. Plant Physiol 145:1361–1370

Sarcina M, Mullineaux CW (2004) Mobility of the IsiA chlorophyll-binding protein in cyanobacterial thylakoid membranes. J Biol Chem 279:36514–36518

Sarcina M, Tobin MJ, Mullineaux CW (2001) Diffusion of phycobilisomes on the thylakoid membranes of the cyanobacterium *Synechococcus* 7942. Effects of phycobilisome size, temperature, and membrane lipid composition. J Biol Chem 276:46830–46834

Schluchter WM, Shen GH, Zhao JD, Bryant DA (1996) Characterization of *psaI* and *psaL* mutants of *Synechococcus* sp strain PCC 7002: a new model for state transitions in cyanobacteria. Photochem Photobiol 64:53–66

Scott M, McCollum C, Vasil'ev S, Crozier C, Espie GS, Krol M, Huner NP, Bruce D (2006) Mechanism of the down regulation of photosynthesis by blue light in the Cyanobacterium *Synechocystis* sp. PCC 6803. Biochemistry 45:8952–8958

Shen G, Boussiba S, Vermaas WF (1993) *Synechocystis* sp PCC 6803 strains lacking photosystem I and phycobilisome function. Plant Cell 5:1853–1863

Singh AK, Bhattacharyya-Pakrasi M, Elvitigala T, Ghosh B, Aurora R, Pakrasi HB (2009) A systems-level analysis of the effects of light quality on the metabolism of a cyanobacterium. Plant Physiol 151:1596–1608

Slonimskiy YB, Maksimov EG, Lukashev EP, Moldenhauer M, Jeffries CM, Svergun DI, Friedrich T, Sluchanko NN (2018) Functional interaction of low-homology FRPs from different cyanobacteria with Synechocystis OCP. Biochim Biophys Acta 1859:382–393

Slouf V, Kuznetsova V, Fuciman M, de Carbon CB, Wilson A, Kirilovsky D, Polivka T (2017) Ultrafast spectroscopy tracks carotenoid configurations in the orange and red carotenoid proteins from cyanobacteria. Photosynth Res 131:105–117

Sluchanko NN, Klementiev KE, Shirshin EA, Tsoraev GV, Friedrich T, Maksimov EG (2017a) The purple Trp288Ala mutant of Synechocystis OCP persistently quenches phycobilisome fluorescence and tightly interacts with FRP. Biochim Biophys Acta 1858:1–11

Sluchanko NN, Slonimskiy YB, Moldenhauer M, Friedrich T, Maksimov EG (2017b) Deletion of the short N-terminal extension in OCP reveals the main site for FRP binding. FEBS Lett 591:1667–1676

Sluchanko NN, Slonimskiy YB, Shirshin EA, Moldenhauer M, Friedrich T, Maksimov EG (2018) OCP-FRP protein complex topologies suggest a mechanism for controlling high light tolerance in cyanobacteria. Nat Commun 9:3869

Spat P, Macek B, Forchhammer K (2015) Phosphoproteome of the cyanobacterium *Synechocystis* sp. PCC 6803 and its dynamics during nitrogen starvation. Front Microbiol 6:248

Stadnichuk IN, Yanyushin MF, Maksimov EG, Lukashev EP, Zharmukhamedov SK, Elanskaya IV, Paschenko VZ (2012) Site of non-photochemical quenching of the phycobilisome by orange carotenoid protein in the cyanobacterium Synechocystis sp. PCC 6803. Biochim Biophys Acta 1917:1436–1445

Steinbach G, Schubert F, Kana R (2015) Cryo-imaging of photosystems and phycobilisomes in Anabaena sp. PCC 7120 cells. J Photochem Photobiol 152 (395–399

Stoitchkova K, Zsiros O, Javorfi T, Pali T, Andreeva A, Gombos Z, Garab G (2007) Heat- and light-induced reorganizations in the phycobilisome antenna of Synechocystis sp. PCC 6803. Thermo-optic effect. Biochim Biophys Acta 1767:750–756

Straub C, Quillardet P, Vergalli J, de Marsac NT, Humbert JF (2011) A day in the life of microcystis aeruginosa strain PCC 7806 as revealed by a transcriptomic analysis. PLoS One 6:e16208

Stroebel D, Choquet Y, Popot JL, Picot D (2003) An atypical haem in the cytochrome b(6)f complex. Nature 426:413–418

Sutter M, Wilson A, Leverenz RL, Lopez-Igual R, Thurotte A, Salmeen AE, Kirilovsky D, Kerfeld CA (2013) Crystal structure of the FRP and identification of the active site for modulation of OCP-mediated photoprotection in cyanobacteria. Proc Natl Acad Sci U S A 110:10022–10027

Tandeau de Marsac N (2003) Phycobiliproteins and phycobilisomes: the early observations. Photosynth Res 76:197–205

Thurotte A, Lopez-Igual R, Wilson A, Comolet L, Bourcier de Carbon C, Xiao F, Kirilovsky D (2015) Regulation of Orange carotenoid protein activity in cyanobacterial photoprotection. Plant Physiol 169:737–747

Thurotte A, Bourcier de Carbon C, Wilson A, Talbot L, Cot S, Lopez-Igual R, Kirilovsky D (2017) The cyanobacterial fluorescence recovery protein has two distinct activities: orange carotenoid protein amino acids involved in FRP interaction. Biochim Biophys Acta Bioenerg 1858:308–317

Tian L, van Stokkum IH, Koehorst RB, Jongerius A, Kirilovsky D, van Amerongen H (2011) Site, rate, and mechanism of photoprotective quenching in cyanobacteria. J Am Chem Soc 133:18304–18311

Tian L, Gwizdala M, van Stokkum IH, Koehorst RB, Kirilovsky D, van Amerongen H (2012) Picosecond kinetics of light harvesting and photoprotective quenching in wild-type and mutant phycobilisomes isolated from the cyanobacterium Synechocystis PCC 6803. Biophys J 102:1692–1700

Umena Y, Kawakami K, Shen JR, Kamiya N (2011) Crystal structure of oxygen-evolving photosystem II at a resolution of 1.9 A. Nature 473:55–60

Veerman J, Bentley FK, Eaton-Rye JJ, Mullineaux CW, Vasil'ev S, Bruce D (2005) The PsbU subunit of photosystem II stabilizes energy transfer and primary photochemistry in the phycobilisome-photosystem II assembly of Synechocystis sp. PCC 6803. Biochemistry 44:16939–16948

Vener AV, Van Kan PJ, Gal A, Andersson B, Ohad I (1995) Activation/deactivation cycle of redox-controlled thylakoid protein phosphorylation. Role of plastoquinol bound to the reduced cytochrome bf complex. J Biol Chem 270:25225–25232

Vener AV, van Kan PJ, Rich PR, Ohad I, Andersson B (1997) Plastoquinol at the quinol oxidation site of reduced cytochrome bf mediates signal transduction between light and protein phosphorylation: thylakoid protein kinase deactivation by a single-turnover flash. Proc Natl Acad Sci U S A 94:1585–1590

Vernotte C, Picaud M, Kirilovsky D, Olive J, Ajlani G, Astier C (1992) Changes in the photosynthetic apparatus in the cyanobacterium *Synechocystis* sp PCC 6714 following light-to-dark and dark-to-light transitions. Photosynth Res 32:45–57

Vladkova R (2016) Chlorophyll a is the crucial redox sensor and transmembrane signal transmitter in the cytochrome b6f complex. Components and mechanisms of state transitions from the hydrophobic mismatch viewpoint. J Biomol Struct Dyn 34:824–854

Wang Q, Moerner WE (2015) Dissecting pigment architecture of individual photosynthetic antenna complexes in solution. Proc Natl Acad Sci U S A 112:13880–13885

Watanabe M, Ikeuchi M (2013) Phycobilisome: architecture of a light-harvesting supercomplex. Photosynth Res 116:265–276

Watanabe M, Semchonok DA, Webber-Birungi MT, Ehira S, Kondo K, Narikawa R, Ohmori M, Boekema EJ, Ikeuchi M (2014) Attachment of phycobilisomes in an antenna-photosystem I supercomplex of cyanobacteria. Proc Natl Acad Sci U S A 111:2512–2517

Williams RC, Gingrich JC, Glazer AN (1980) Cyanobacterial phycobilisomes. Particles from Synechocystis 6701 and two pigment mutants. J Cell Biol 85:558–566

Wilson A, Ajlani G, Verbavatz JM, Vass I, Kerfeld CA, Kirilovsky D (2006) A soluble carotenoid protein involved in phycobilisome-related energy dissipation in cyanobacteria. Plant Cell 18:992–1007

Wilson A, Boulay C, Wilde A, Kerfeld CA, Kirilovsky D (2007) Light-induced energy dissipation in iron-starved cyanobacteria: roles of OCP and IsiA proteins. Plant Cell 19:656–672

Wilson A, Punginelli C, Gall A, Bonetti C, Alexandre M, Routaboul JM, Kerfeld CA, van Grondelle R, Robert B, Kennis JT, Kirilovsky D (2008) A photoactive carotenoid protein acting as light intensity sensor. Proc Natl Acad Sci U S A 105:12075–12080

Wilson A, Kinney JN, Zwart PH, Punginelli C, D'Haene S, Perreau F, Klein MG, Kirilovsky D, Kerfeld CA (2010) Structural determinants underlying photoprotection in the photoactive orange carotenoid protein of cyanobacteria. J Biol Chem 285:18364–18375

Wilson A, Punginelli C, Couturier M, Perrau F, Kirilovsky D (2011) Essential role of two tyrosines and two tryptophans on photoprotection activity of the orange carotenoid protein. Biochim Biophys Acta 1807:293–301

Wilson A, Gwizdala M, Mezzetti A, Alexandre M, Kerfeld CA, Kirilovsky D (2012) The essential role of the N-terminal domain of the orange carotenoid protein in cyanobacterial photoprotection: importance of a positive charge for phycobilisome binding. Plant Cell 24:1972–1983

Wollman FA, Lemaire C (1988) Studies on kinase-controlled state transitions in photosystem II and b_6f mutants from *Chlamydomonas reinhardtii* which lack quinone-binding proteins. Biochim Biophys Acta 933:85–94

Wu YP, Krogmann DW (1997) The orange carotenoid protein of *Synechocystis* PCC 6803. Biochim Biophys Acta 1322:1–7

Yamanaka G, Glazer AN, Williams RC (1978) Cyanobacterial phycobilisomes. Characterization of the phycobilisomes of Synechococcus sp. 6301. J Biol Chem 253:8303–8310

Yang S, Su Z, Li H, Feng J, Xie J, Xia A, Gong Y, Zhao J (2007) Demonstration of phycobilisome mobility by the time- and space-correlated fluorescence imaging of a cyanobacterial cell. Biochim Biophys Acta 1767:15–21

Yang S, Zhang R, Hu C, Xie J, Zhao J (2009) The dynamic behavior of phycobilisome movement during light state transitions in cyanobacterium Synechocystis PCC6803. Photosynth Res 99:99–106

Yang MK, Qiao ZX, Zhang WY, Xiong Q, Zhang J, Li T, Ge F, Zhao JD (2013) Global phosphoproteomic analysis reveals diverse functions of serine/threonine/tyrosine phosphorylation in the model cyanobacterium Synechococcus sp. strain PCC 7002. J Proteome Res 12:1909–1923

Yu MH, Glazer AN (1982) Cyanobacterial phycobilisomes. Role of the linker polypeptides in the assembly of phycocyanin. J Biol Chem 257:3429–3433

Zhang Z, Huang L, Shulmeister VM, Chi YI, Kim KK, Hung LW, Crofts AR, Berry EA, Kim SH (1998) Electron transfer by domain movement in cytochrome bc1. Nature 392:677–684

Zhang H, Liu H, Niedzwiedzki DM, Prado M, Jiang J, Gross ML, Blankenship RE (2013) Molecular mechanism of photoactivation and structural location of the cyanobacterial orange carotenoid protein. Biochemistry 53:13–19

Zhao JD, Zhou JH, Bryant DA (1992) Energy transfer processes in phycobilisomes as deduced from mutational analyses. Photosynth Res 34:83–83

Zito F, Finazzi G, Delosme R, Nitschke W, Picot D, Wollman FA (1999) The Qo site of cytochrome b6f complexes controls the activation of the LHCII kinase. EMBO J 18:2961–2969

Chapter 15

Coherent Processes in Photosynthetic Energy Transport and Transduction

Harry W. Rathbone* and Paul M. G. Curmi*
School of Physics, The University of New South Wales, Sydney, NSW, Australia

and

Jeffrey A. Davis
Centre for Quantum and Optical Science, Faculty of Science, Engineering and Technology, Swinburne University of Technology, Hawthorn, VIC, Australia

*Author for correspondence, e-mail: h.rathbone@unsw.edu.au; p.curmi@unsw.edu.au

A. W. D. Larkum et al. (eds.), *Photosynthesis in Algae: Biochemical and Physiological Mechanisms*, Advances in Photosynthesis and Respiration 45, https://doi.org/10.1007/978-3-030-33397-3_15

I. Introduction

A large international collaborative effort has been underway over the last decade to understand interference patterns, or coherence, seen in spectroscopic analyses of light harvesting systems. Although the nature of the quantum interferences (or 'beats') has been widely explored, many ambiguities remain. This is largely because of the difficulty in accurately teasing apart vibrational and electronic quantum coherent mechanisms when energies are (near) resonant. Most researchers have suggested that in light harvesting systems exhibiting ambiguous quantum beats, the transfer of excitation energy between excited electronic states harbours coherent entangled states comprising a mixture of both electronic and vibrational degrees of freedom called vibronic states.

Quantum mechanics is the fundamental description of matter and biological systems are hence, at least trivially, quantum mechanical. Non-trivial quantum mechanical effects such as entanglement, however, are very delicate and are lost quickly in hot, wet environments like living cells. A current point of interest questions how far quantum mechanical effects and correlations can extend in time and space, and biological systems are an excellent playground in which to search.

In many light harvesting systems, quantum beats have been observed, which are stable over a time scale that is commensurate with the relevant energy transfer times. Gaining an understanding of the engineering principles behind the possible maintenance of this delicate quantum concert is paramount to many applications. Many theoretical studies highlight that having a tuned amount of quantum coherence in disordered light-harvesting systems can enhance energy transfer efficiency and robustness far more than would be the case for energy incoherently hopping between chromophores (the Förster limit). Making light harvesting processes as efficient and robust as possible would be a key evolutionary advantage, especially for organisms dwelling in deep aquatic environments where photon flux is minimal. Determining if and how coherence is used and selected for by photosynthetic organisms, is an open question as quantum phenomena are inherent in chromophores that are tightly packed. This is the most challenging problem faced in these studies, with the possibility that it is not feasible to determine definitively whether quantum coherence is under evolutionary selection.

A. General Description of Biological Light Harvesting

The input energy for photosynthesis comes from sunlight. The output is the generation of a stable chemical energy source, e.g. ATP or fixed carbon. The key photosynthetic complex in energy transduction is the reaction centre, which in eukaryotes lies in the greater photosystem. The reaction centre accepts the energy input from light and uses it to drive charge separation, which then powers the downstream processes ultimately generating ATP. In all stages, the photosynthetic complexes consist of a set of light-active organic molecules called chromophores that are embedded in a protein or protein complex. The protein itself does not interact directly with light or the electronic excitation produced by light in the chromophore molecules. Instead, the protein acts as a scaffold, setting the conformation of the chromophores, limiting their potential motion, tuning chromophore excitation energy and arranging the chromophores into specific separations and orientations, presumably to control and direct energy transfer processes between the chromophores.

A simple photosynthetic organism could just use a single reaction centre to both capture solar energy and separate charges. However, such an apparatus would be a poor light harvester because reaction centres absorb few photons (low absorption cross-section) in a limited range of frequencies. To live in low light environments, organisms have evolved elaborate light harvesting systems and antennae that solve both of these problems

(Chaps. 3, 4, 10, 11, 12, 14 & 16). They increase the capture cross-section and increase the spectral coverage resulting in high photon conversion efficiency by the organism as a whole (i.e. nearly all photons incident on the organism result in a charge separation in the reaction centre). With the evolution of light harvesting proteins and antenna complexes comes the caveat that energy needs to be efficiently transferred between the chromophores in a way that nearly all excitations result in a charge separation event at the reaction centre (i.e. high photon efficiency). Understanding the mechanisms by which this is achieved is the key concern of this review.

B. *Timescales and Length Scales*

Solar energy is comprised of a stream of spectrally incoherent photons with coherence volumes much larger than the cell and a flux such that only one photon will impinge on the cell during a single excitation event. From a quantum mechanical perspective, the photon will initially excite all resonant chromophores within the coherence volume (all chromophores within the cell) in a superposition of all possible states, however, this collective excitation will decay on a femtosecond time scale resulting in the excitation being localised to a single protein system. Rapid localisation of the excitation occurs as the phase relationships between chromophores, imparted by the oscillating electric field of the photon, are almost instantaneously lost. This is because weakly interacting chromophores in the coherence volume lose track of each other due to environmental perturbations (vibrations) slightly altering the energy of the excitation on the chromophore; the further apart the chromophores are, the greater the effect. Within the excited protein system (typically 3–10 nm length scale), the excitation is transferred from the initial chromophore to some final acceptor on a timescale of roughly 1–10 picoseconds (Fig. 15.1a). Usually, there will be several transfer steps between light harvesting proteins that are likely to be in physical contact with each other; thus, the excitation will travel across a region on the order of tens of nanometres until it finally reaches a reaction centre (10–100 ps). Charge separation within the reaction centre takes place on a timescale of 0.1–10 ns. Throughout light harvesting, the chromophores can lose energy via fluorescence, which typically has a lifetime of 1–10 ns. Thus, to prevent energy loss via fluorescence, the passage from initial photon capture to charge separation in the reaction centre must occur within this timeframe.

C. *Quantum Processes in Light Harvesting Proteins and Energy Transfer*

From a quantum mechanical perspective, the chromophores embedded in a protein may not act as independent systems. Simply, two chromophores that are strongly coupled will act as a single light absorbing unit. Coupling produces two possible excited states, one with lower energy and one with higher energy than that of the single, isolated chromophore (Fig. 15.1b). This coupling broadens the excitation spectrum of the single isolated chromophore, increasing the spectral range of the light harvesting system. Light harvesting proteins also use additional strategies for increasing their spectral range. The simplest approach is to incorporate a series of different chromophores, each with a distinct absorption spectrum (Fig. 15.1c).

A second area where quantum mechanical phenomena are likely to be important in light harvesting is in the process of energy transfer. Within a light harvesting complex, the excitation must be transferred to the final acceptor in a fast, efficient and robust way to ensure that the energy is not lost to the environment. Two extreme models for energy transfer involve either quantum coherent random walks (quantum searches) or a semi-classical Förster resonance energy transfer (FRET) mechanism. The latter has the excitation moving irreversibly from donor chro-

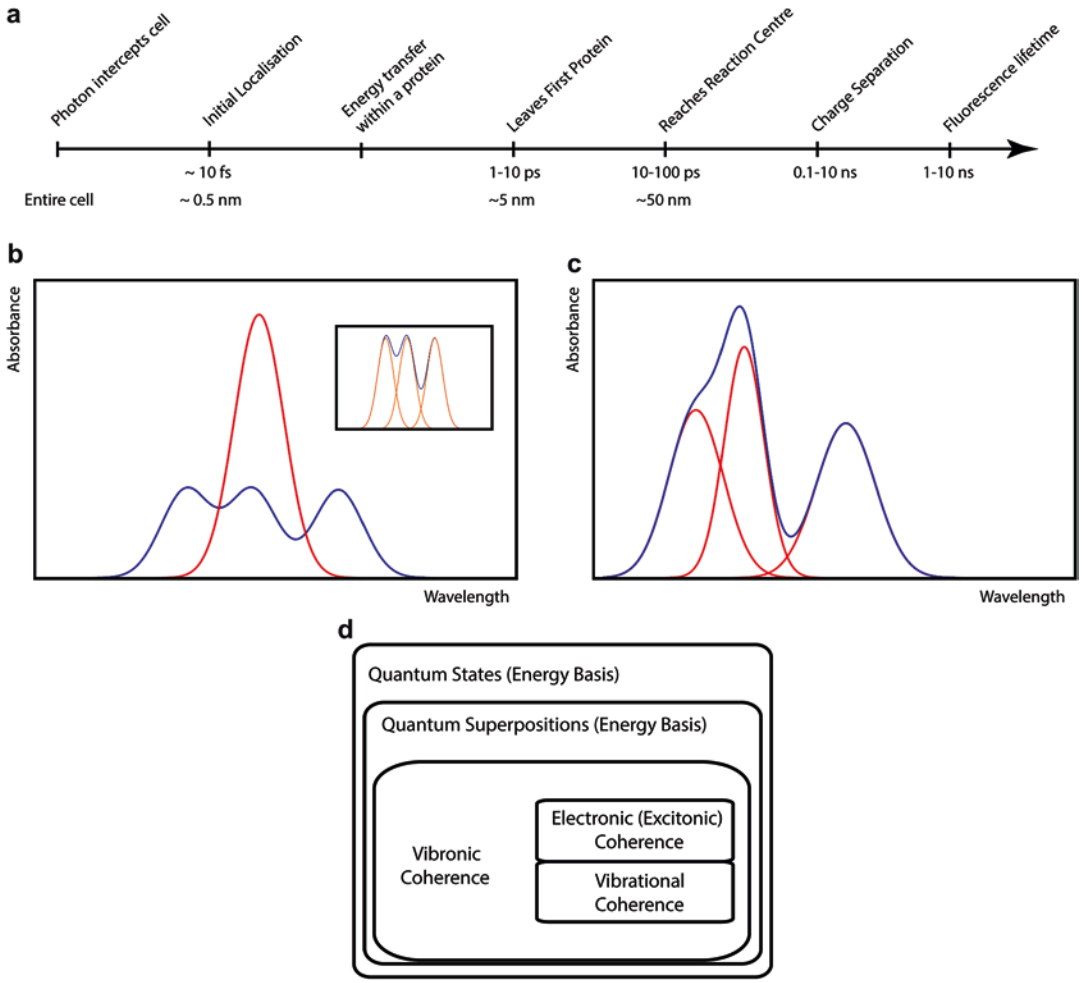

Fig. 15.1. **Quantum States and Quantum Coherences**— (**a**) Typical timeline and length scales for photosynthetic energy transfer. (**b**) The net effect (blue) of having energetically identical chromophores (red) that are strongly interacting in a toy system of three chromophores. The inset highlights that the new absorption spectrum of the three chromophores is produced by a new set of now energetically different states (orange). (**c**) The net effect (blue) of packing multiple different non-interacting chromophores (red) into a toy light harvesting system containing three chromophores. (**d**) Nesting of types of quantum states and processes. Electronic and vibrational coherences are a subset of the broader class of vibronic coherence

mophore to acceptor chromophore while in the former, the excitation resides simultaneously on multiple chromophores before decohering and localising on some final acceptor. The current debate centres on the extent to which energy transfer processes involve quantum coherent phenomena versus the FRET model or perhaps an intermediate model between these two extremes.

II. Quantum Behaviour, Coherence and Spectroscopy

At the most fundamental level, the universe behaves in way that is counter to our macroscopic intuitions. The interest in quantum phenomena in light harvesting arises from the apparent ability of these systems to sustain non-trivial quantum superpositions on

large scales (long coherence times $\gtrsim$100 fs and greater spatial extent $\gtrsim$1 nm). Quantum mechanics predicts physical correlations that are larger than those allowed by classical logic and probability. Within the context of classical probability, a given system has a set of states along with a set of probabilities, which may be made deterministic by some unknown parameters. Take the example of the coin toss. In this system, we can ascribe a probability to the outcome of heads or tails; however, the outcome can be completely determined at any time if all the parameters of the system are known (such as velocities of air molecules and the force imparted by the tossing hand). In quantum mechanics, we deal with a different kind of probability where systems can intrinsically be in many states at once with wavelike underlying dynamics and only when measured does the system collapse to a single state. At first glance, this does not appear as though it would make any measurable difference to the outcome of an experiment, however, this leads to some striking quirks in correlations and behaviours of systems and to the conclusion that the "quantum coin" must be both heads and tails at the same time prior to a measurement taking place.

A. *Quantum Measurement, Superposition & Entanglement*

One of the key features of quantum mechanics is quantum superposition. Particles are capable of being in many states at once or going through many processes at the same time. It is not merely that part of the system is in a specific state, it is that the whole system is in many states concurrently. To illustrate this, consider the example of a particle in a box. Classically, if we peeked inside the box we can find out the position and momentum of the particle and from then on we could predict the motion of the particle deterministically. Conversely, if we had a quantum particle and we peeked inside the box, we could never predict the evolution of the particle deterministically. The state we saw was merely one realisation of the superposition of the position and momentum states of the particle up to some uncertainty. Correlating repeated measurements of these parameters would not necessarily show a consistent trajectory. As an example, an electron in its orbital around an atom or molecule is in a superposition of all possible position states around the nucleus with the same energy.

The states of interest in this discourse are superpositions of electronic states. Orbitals are one example of *energy eigenstates* of a quantum system. Eigenstates are stationary in time and represent states corresponding to specific amounts of energy. Generally, a system evolving in time will pass through superpositions of its various energy eigenstates. Once a system is in a superposition it can produce many wavelike features. An energy eigenstate will have a oscillatory phase proportional to the energy of the state, which is unobservable in almost all cases. When a system is in a superposition of energy eigenstates, the system will accrue a phase proportional to the energy difference of the constituent states. What this means is that the system will oscillate between its constituent states according to that phase, which is observable as an oscillation in the probability for each state. This quantum interference is a hallmark of a quantum process and highlights the wave nature of matter.

When considering systems with more than one subsystem (such as a collection of chromophores with their various excitation states) even further correlations (i.e entanglement) can be introduced. Entanglement can be understood by considering two people, who are given a "quantum ball" each. They know that there can only be one red quantum ball and one blue quantum ball. If one person looks at the quantum ball they have (which in this instance appears red), then the second person immediately knows they have a blue quantum ball without looking at it. In the case where the systems are uncoupled, the second quantum

ball could be either blue or red. The subtlety here is that when the people received the quantum ball, the balls themselves did not have a specific colour until the first one was observed (as opposed to a classical ball, which must have an originally assigned colour).

Entanglement is just non-separable superposition of multiple subsystems. Information about the state of the subsystem is non-separable as it depends on the information within the whole system. The corollary of this is that when two subsystems interact they share information about each other and, hence, entanglement is generated. The quantum states involved in light harvesting processes are the excited states of the chromophores. In general, these excited states interact as the excitation is moving between chromophores and as such, superpositions are generated. These states are referred to as the exciton states. There are some further subtleties to exciton states that will be discussed in more depth in the context of biological systems. Furthermore, various degrees of freedom can be entangled. There is no real reason to suggest that the nuclear degrees of freedom (vibrations) are separable from the electronic degrees of freedom (the electronic excited states). Generally, an assumption is made that these degrees of freedom are more-or-less separable to ease mathematical difficulties, however, it is often the case that correlations between degrees of freedom are induced when energy scales are resonant. These can be on single chromophores or across many. These notions will become less opaque as the chapter progresses.

B. Quantum States—The Density Matrix

In order to analyse quantum systems, we need a language in which we can talk about their states. The first step in building a framework for analysing quantum dynamics is to note that quantum systems have a special type of probability that contains interference. In classical probability, a vector is assigned to the probabilities corresponding to the states of a system. In quantum mechanics, a *density matrix,* ρ, can be constructed where the diagonal elements of the matrix are the "classical" probabilities or *populations* and the off-diagonal elements or *coherences* contain the interference information between the corresponding states. Composite systems can also be described by considering all combinations of states within this framework. Hence, the density matrix for a light harvesting system can contain the complete set of combinations of all electronic and vibrational states in principle.

We are interested in the dynamics of quantum systems, which we can track by observing how the density matrix evolves in time. We describe quantum systems using a matrix equation called a *master equation*. This equation describes how states of the system evolve coherently (and non-locally) under a *Hamiltonian* (which encodes energetic information about the states of the system and their couplings) and incoherently (and locally) under a *Lindbladian* (which encodes how energy and correlations within the system are removed/reinjected via the environment/protein/solvent). The *Hamiltonian*, thus, can entrain coherent superpositions and wavelike behaviour in the system (depending on the initial state) and the *Lindbladian* can decohere these superpositions and localise the system to a single state. States that don't change under the action of the *Hamiltonian* are the energy eigenstates and hence do not change in time. The *Lindbladian* is a special case of a broader class of non-conservative mathemtical objects where we assume that the environment has no memory of its previous states (*Markovian*—which is often not valid) on the timescale of interest, however, more general formalisms do exist. The *Lindbladian* appears incoherent as we have no knowledge of the environment states and as such forms a decay and renewal between states of the system. In essence, we could include all of the states of the environment in our density matrix as well and the now larger system would just interact coherently, however, given the massive number of degrees of freedom in the environment this would become intractable. We stress here that there is a certain level of artifice in defin-

ing the boundary between system (the chromophores) and environment (the protein and solvent medium) and this is a long-standing issue in quantum mechanics.

C. Coherence

Coherence is a property of waves. Two waves (or two points on the same wave) are coherent if the phase difference between them is constant. The phase of a wave is important as certain spatio-temporal features, such as momentum and energy, define it (or indeed are defined by it). When two waves are coherent, their properties have non-local correlations and information is shared between them. Furthermore, when waves are coherent they are able to produce stable interference phenomena. As the system is perturbed by the environment, energy is gained/lost—the phase will change in time in a local way. Systems that are extended in space under the influence of a random external perturbation will have the non-local correlations in their properties decay in space and time as the phase will be different at different points—the further away, the larger the effect. The scale over which the waves share a degree of correlation is the coherence time/length. These scales are important measures in the study of quantum processes in light harvesting as they highlight the scales over which quantum interference phenomena can persist.

In quantum systems, the type of coherence that is produced is dependent on the basis set of states that harbour the coherence/superposition between them (Fig. 15.1d). Coherences can be over any state—electronic, vibrational or entangled states of the two (vibronic).

1. Coherence in the site/chromophore excited state basis refers to exciton states—often delocalised states over several chromophores that are stationary in time. Site coherences are ubiquitous in light harvesting systems and are generally produced when strong coupling between chromophores is present, resulting in the chromophores acting as one system.
2. Coherences in the exciton basis are states that are superpositions in the energy eigenbasis (basis of stationary states). These coherences are what can be observed through quantum beats in spectroscopic experiments as they represent oscillations between two states with different energies excited by a discrete packet of energy by a laser.
3. Processes where the system evolves through an energetic landscape while in a superposition (when dephasing from the environment is smaller than the interaction energy of the said process) harbour process coherence. This is the case where non-local effects dominate energy transfer.

All of these types of coherence can be represented as off-diagonal elements of a density matrix in some basis. If we were to represent the density matrix of the system in the site (chromophore) basis, off diagonal elements would reference coherences between sites (excitons). If the density matrix were represented in the energy basis (exciton states), off diagonal elements would represent coherences between excitons, and so on.

D. Decoherence

Broadly speaking, coherence refers to the persistence of quantum behaviour at the scales of interest, namely the preservation of superpositions of states which lead to quantum interference. Quantum processes under the influence of a random external perturbation decohere over time leading to a loss of quantum correlations over a given time or length scale, just as with classical waves. By interaction with the environment the system decoheres into a state that is stochastically selected by the perturbation. The environment can be thought of as making a measurement which *collapses the superposition* to a single state. It should be stressed that it is not by some virtue of consciousness that the system collapses to a single state by a measurement, any non-coherent interaction will do. The term measurement is a technical term referring to any interaction like this. Once entangled with the environment (or

other parts of the system), any originally superposed sub-states are lost as the information shared between them is irreversibly altered—a process tending to increase entropy. When the energy scale of the *Hamiltonian* (system-system coupling) is larger than that of the *Lindbladian* (system-environment coupling), the system will tend toward being coherent for a longer time and vice versa.

Environmental interactions with the chromophore system come in two flavours—both of which cause fluctuations and heterogeneity in the electronic structure of the chromophores and have implications for the scales of coherence.

1. The first effect is dynamic disorder where the environment alters phase relationships already present between excitons by independently changing the energy of each distinct chromophore in the superposition (generally via vibrations). Hence, phase relationships between states are lost much faster than the transfer time limiting the effect of coherence on energy transfer. If the energy scales of chromophore-environment interactions are larger than the energy scales of chromophore-chromophore interactions, the delocalised exciton state will become localised to a smaller number of chromophores which have mutually similar local environments.
2. The second effect is static disorder which arises from heterogeneity of chromophore excitation energies. This localisation effect takes place when the difference between chromophore excitation energies is larger than the coupling strength—when the electronic state transition energy is away from resonance. As such, chromophores with different energies tend not to mix whereas chromophores that have the same energy are resonant and hence will have a larger degree of mixing (superposition) providing the interaction energy is larger than the environmental perturbations. Differences in chromophore excitation energies can either be due to having different chromophores in the system or due to identical chromophores with different electrostatic environments from the protein. The electrostatic environment around each chromophore can also change very slowly (on the picosecond timescale—estimating the speed of sound in a protein as ~2 nm/ps (Nogly et al. 2018)), thereby shifting the chromophore excitation energy over time.

In energetically disordered systems (such as light harvesting antennae), a fluctuating environment that induces a robustly tuned level of dephasing can be beneficial. Perfectly coherent transport produces rapid localization due to the lack of order and correlations in energies of the system (known as Anderson localisation) and an infinitely incoherent system produces what's called the quantum Zeno effect (where the excitation state cannot travel anywhere as it is constantly being measured/localized by the environment) (Rebentrost et al. 2009). The fluctuating environment can also be thought of as transiently bringing chromophore excitation energies into resonance (de-trapping). Furthermore, partial spatial and energetic order can enhance transport by providing structure that allows for transport of excitations to converge on some key acceptor chromophore.

There is considerable debate concerning how quantum coherence can aid the efficiency of exciton transport. In subsets of chromophores in many light harvesting systems, the environmental interaction energy is of the same order as the electronic coupling implying that transport may not be purely semi-classical (FRET) and may harbour some quantum exotica. However, the argument that a light harvesting system will sample many pathways simultaneously and select the most energy efficient one (given the state of the environment) may not need to be invoked. Instead, starting at a high-energy state away from a local energetic minimum, a system may stochastically select the global energetic minimum in an incoherent manner instead of being trapped in a local minimum and fluorescing. Of course, having a coherent superposition of a local trap and non-trap state would mean that the system has a probability of moving away from the local trap instead of the 'classical' case where it is stuck until it fluoresces. The role of quantum

coherence in increasing efficiency remains one of the greatest open questions.

E. Experimental Probes

The term spectroscopy shares the same origin as the word *spectre*, which is rather fitting for modern optical studies. By using spectroscopic techniques, we are looking for short lived "ghosts" in optically active systems that give us hints of the mechanisms behind energy transfer. Linear spectroscopies (such as absorption and fluorescence) highlight only the initial and final states of energy transfer through light-activated molecules and obscure the myriad internal dynamics of these systems. Within light harvesting chromophores, optical photons are responsible for the excitation of electronic states (moving an electron from one orbital to a higher orbital) and the subsequent fluorescence of the molecule being the emission of optical photon as the electron falls to a lower lying state. Vibrational modes of chromophores can be excited by infrared photons which generate a resonance between nuclei, driving them into an oscillatory behaviour. Furthermore, vibrational modes can be excited in optical experiments via Raman scattering where the photon's energy excess upon electronic excitation is released as a vibration.

Clever spectroscopic techniques have been developed to probe deeper into the quantum mechanisms in complex molecules to understand the internal dynamics and pathways between the initial and final states. Our goal using these spectroscopic techniques is to search for coherences (non-classical off-diagonal elements of our system's density matrix) and excitation energy transfer between populations (diagonal elements) and how these evolve in time and mix with one another. The two main spectroscopic techniques used to probe the internal dynamics of light harvesting systems are transient absorption (TA) and two-dimensional electronic spectroscopy (2DES—an example of which is shown in Fig. 15.2), together with many variations that broadly fall into the category of *pump-probe* techniques (Jonas 2003; Cheng and Fleming 2008; Berera et al. 2009). These techniques facilitate the independent visualisation of different excitation energy transfer pathways with high temporal resolution.

All pump-probe techniques have some shared features. Most rely on femtosecond pulsed laser light and some require a defined phase relationship between the incoming light pulses. A typical transient absorption experiment begins with the excitation of a sample with a broad-spectrum pulse (a broad spectrum offering high time resolution). The system is then left to evolve according to its Hamiltonian plus perturbations from the environment. Subsequent pulses—generated from the same source—interact with the system and an absorption spectrum is measured. This is repeated, building up time slices of absorption spectra at different pulse waiting times. These absorption spectra are compared to the equilibrium absorption spectrum, with changes to the spectra occurring due to the evolving state of the system. This may involve a decreased absorption at some energy because the electronic state at that energy is already excited. By following changes to the absorption spectra over time, a picture of the energy transfer pathways and dynamics can be built up. The presence of coherences (vibrational, vibronic, or electronic) can lead to oscillations in the amplitude of the transient absorption spectra as the delay between pump and probe is varied. The frequencies of the oscillations can then be measured and the energy associated with the oscillation (coherence) can be observed and matched to exciton energy gaps and vibrational frequencies to assign coherent features to a plausible origin. The associated decay of the oscillation provides the decoherence time of the specific coherence. Furthermore, the associated phase and amplitude changes of signal oscillations across the detection wavelength can also help determine the origin of coherent oscillations.

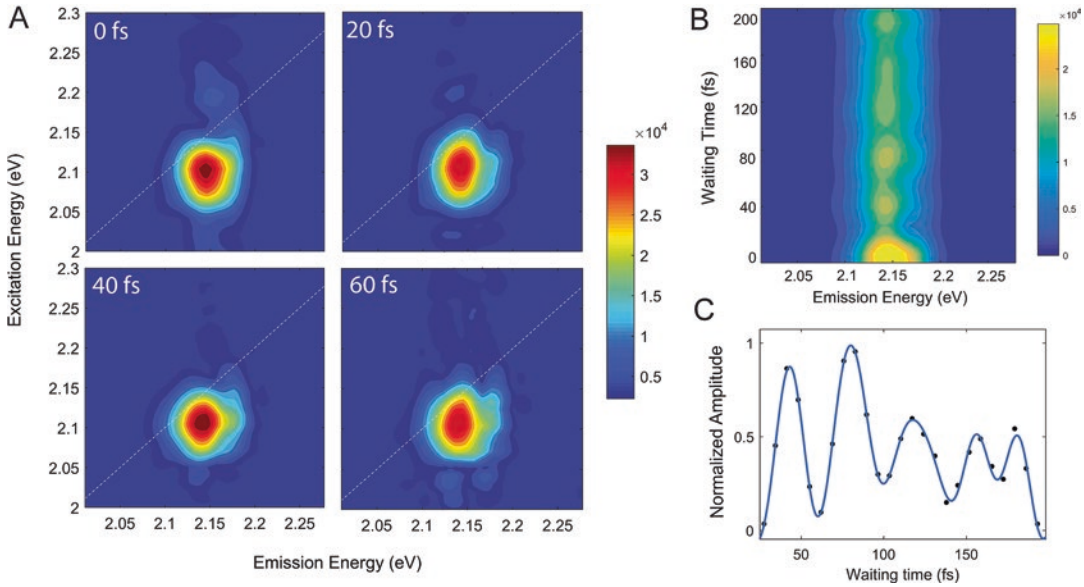

Fig. 15.2. **Spectra from Broadband 2DES Measurements on the Cryptophyte Phycobiliprotein PC645** — (**a**) A series of absolute value 2D spectra taken at different waiting (population) times highlighting the evolution of a specific spectral region. The dotted line designates the diagonal in the map. (**b**) A slice taken at an excitation energy of 2.072 eV showing the evolution of the amplitude in emission energy and waiting time. Here we can clearly see the emergence of an amplitude oscillation. (**c**) Taking a further slice at an emission energy of 2.15 eV, subtracting out the exponential decay of signal and plotting the residuals against waiting time we can even more clearly see and oscillator pattern in them. The residuals are then fit to a sum of sine functions, however experimenters will often take a Fourier transform to extract frequency data. Thank you to Ashkan Roozbeh for providing the data analysis and images used in this figure

By using multiple pulses, we can build an n^{th} order correlation map of different quantum states and their evolution through time. Cross correlations arise from energy transfer and oscillations can be observed through one of the waiting times between the pulses. Specifically, in 2DES, we have three pulses and are probing the third order susceptibility (dielectric response) of the system. The pulses in a typical 2DES set-up progress as follows: the first pulse excites the system into a coherence between the ground and excited state (oscillating between them at a frequency proportional to their energy); after the *coherence time* τ, a second pulse is incident on the sample which excites the system into a population state (not a coherence); after the *population time* T a third pulse excites the system again; a signal is emitted after the *rephasing time* t and the signal amplitude and phase information is subsequently detected. The coherence and rephasing time axes can be Fourier transformed to produce what is essentially an excitation-emission correlation spectra with slices through population time (Fig. 15.2a). Peaks in the spectra tell of the existence of certain populations (peaks on the diagonal) and couplings (cross peaks off the diagonal). Between the arrivals of each pulse, the system can evolve and undergo energy transfer while still retaining phase information about its previous states, thus leading to observed oscillations in the correlations between states (peaks in the spectra).

Complex, light activated quantum systems have many pathways through them from excitation to emission (*Liouville path-*

ways) and while 2DES allows observation of these pathways, they are overlayed in the spectra making it hard to separate out different contributions. A few tricks, however, have been developed to tease apart different contributions. Firstly, the spectra can be broken into rephasing (R) spectra and non-rephasing (NR) spectra which corresponds mathematically to changing the ordering of the pulses. Secondly, different pulse polarizations can excite specific pathways and coherences by selecting certain combinations of dipole moment orientations. Lastly, using different colours (frequencies/energies) for each pulse, we can excite specific coherences in the system when looking for properties of a certain pathway. Unfortunately, the inverse problem of deriving system dynamics from spectroscopic data is near impossible to solve and thus studies are often accompanied by a model of the system's Liouville pathways and where specific pathways will show up in the data with which it is compared. Thankfully, certain Liouville pathways are often favoured by different geometries or by different pulse polarizations. Namely, electronic coherences are suggested to appear as oscillations on the NR diagonal peaks and R cross peaks with a $\pi/2$ phase flip between diagonal and off diagonal peaks indicating energy transfer. Vibrational coherences, however, have no preferred position but are supressed when the pulses are polarized orthogonally. This leads lastly to a distinction for vibronic coherences, which have a mixed character which would otherwise be paradoxical.

Most spectroscopic studies will observe ensembles of particles and, hence, an ensemble average of the system is produced which obscures variations in properties of the individual complexes. Some members of the ensemble may be more or less delocalised than others and, hence, averaging will obscure the effects this produces. Notably, coherences can last much longer than seen in the density matrix due to this averaging. Even further still, all realisations of the different transfer pathways are present in the ensemble which may destroy coherent effects via destructive interference or at least obscure coherence in any experiment. One can extract the distribution of coherence times by performing single molecule variants of pump probe technique, however, many of these experimental methods are still being developed. One further issue is that of coherent light. All of the above spectroscopic methods require illumination by a coherent light source. Excitation by a coherent light source (laser light) will generate defined phase relationships between chromophores and a coherent superposition of energy eigenstates states, whereas illumination by sunlight will give rise to a statistically independent mixture of electronic excited states with different energies and adornments of vibrational states. If excitations generated by separate events are non-interacting, then the coherence between sites generated by excitonic splitting may not be destructively influenced by random phase of incoherent illumination. However, laser pulses are spectrally coherent, which means that the phases of the photons at different energies are correlated, whereas the phases of sunlight are completely uncorrelated. Hence, there is an obligate phase relationship imposed *a priori* on the system by the laser excitation as the phases of each excited chromophore state are correlated. Finally, most of the spectroscopic analyses done on light harvesting complexes are done at cryogenic temperatures to remove thermal fluctuations that cause inhomogeneous broadening. Lowering the temperature changes the chromophore-environment correlation time and thus increases the coherence time of the system. Hence, values given at cryogenic temperatures for coherence times should represent an upper limit for the capability of coherence for light harvesting systems.

III. Diversity of Biological Light Harvesting

For the purpose of this discourse, we break photosynthetic organisms into two main groups. The first group directly uses light-driven proton pumps to generate a proton gradient (bacteriorhodopsins, proteorhodopsins and archaerhodopsins) while the second group uses a reaction centre to drive charge separation, moving an electron to eventually generate a proton gradient indirectly. The second group generally comes with an antenna of some description which captures solar photons and funnels them to the reaction centre.

Bacteriorhodopsin

The first class of organisms are composed of various archaeal taxa and have taken a different evolutionary route than the second group. In the archaeon *Halobacterium salinarum*, this mechanism of energy production is switched on when oxygen levels decrease below the level needed for effective respiration (Oesterhelt and Stoeckenius 1973). Bacteriorhodopsin is a membrane embedded homo-trimer with each monomer having with a single retinal chromophore embedded in the centre. The photo-process that drives this proton pump initiates with all-trans retinal excited to a higher electronic orbital upon excitation from a photon. The retinal relaxes through a conical intersection (an intersection between ground and excited state vibrational manifolds) via intermediate states and eventually moving into a 13-cis conformational state. The new local dielectric environment and pH around the retinal causes the deprotonation of the Schiff base of the retinal which releases a proton into the extracellular space. The retinal then rotationally relaxes and is reprotonated from the cytoplasmic space. The process of retinal isomerisation takes approximately 1 ps to complete (Kraack et al. 2011). Following isomerisation, a complex and concerted series of conformational changes in the protein along with solvent reorganisation, is generated to drive the charge transfer event and to offer alternating access between the cytoplasmic and extracellular space (Nango et al. 2016; Nogly et al. 2018). Within the context of coherence, interest lies with whether the isomerisation event is vibrationally/vibronically coherent and how this affects the overall efficiency, if at all.

Reaction Centre

It has been posited that all photosynthetic organisms that make use of a reaction centre for charge separation derive from a single ancestral bacterium (Cardona 2014). Many suggest an ancestral bacterium (possibly an *Heliobacteriaceae organism*) had a single gene or set of genes for a bacterial reaction centre, which upon gene duplication produced what would become photosystem I and II (Fig. 15.3a). Some posit that a light switch existed between the two photosystems which was later lost and other photosynthetic bacteria lost genes for either the type I or type II reaction centre (Allen and Martin 2007). Others suggest that gene duplication along with lateral gene transfer diversified photosynthetic organisms (Raymond et al. 2002). Regardless, seven bacterial clades (delineated by their constituent light harvesting chromophores and reaction centers) appeared, the most studied in this field being purple bacteria, green sulphur bacteria and cyanobacteria. Through a series of endosymbiotic events involving cyanobacteria, photosynthetic eukaryotes (protists, red algae, green algae and higher plants) evolved incorporating the cyanobacterial light harvesting system and altering it in innumerable ways (Neilson and Durnford 2010; Chaps. 2 & 10). Interestingly, no photosynthetic eukaryotes appear to have evolved from the endosymbiosis of other photosynthetic bacteria while cyanobacteria appear to have been involved in at least two distinct endosymbiotic events (the generation of a proto-red alga + green alga + glaucophyte and, more recently, *Paulinella sp.* (Delaye et al. 2016; see Chaps. 2 & 10)). The two reaction centre proteins share structural similarity

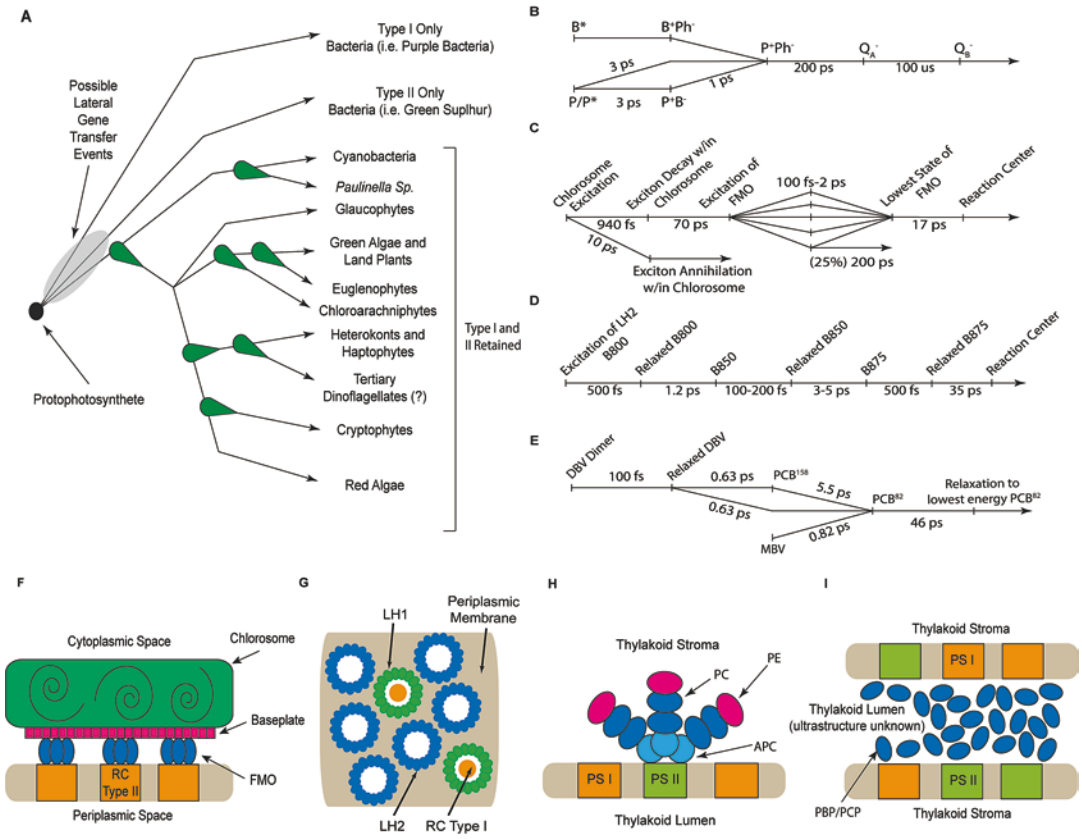

Fig. 15.3. **Ultrastructure and Energy Transfer**—*(***a***)* Possible phylogenic schematic of the evolution of modern photosynthetic organisms, tracing the chloroplast. Green arrows represent endosymbiotic events with the daughter organism in the direction of the arrow. Type I and Type II refer to the nature of the reaction centre or photosystem. (**b**, **c**, **d**, **e**) Provides energy transfer/charge transfer time scales for the reaction centre, green bacteria, purple bacteria and cryptophyte phycobiliprotein respectively. (**f**, **g**, **h**, **i**) Are the photosynthetic apparatus of green sulphur bacteria, purple bacteria, cyanobacteria/red algae/glaucophytes and cryptophytes/dinoflagellates, respectively. For green non-sulphur (filamentous) bacteria, remove FMO and replace RC II with RC I. Other proteins involved are not shown for simplicity. For further details see Chaps. 2 & 10

and are termed type I or type II based on their presence in their nominal photosystem. The two divergent bacterial groups contain, for example: type I only—green sulphur bacteria and heliobacteria; type II only—purple bacteria and green filamentous bacteria.

The role of the reaction centre is to develop a usable charge separation (voltage) that can ultimately be used to produce a proton gradient across the thylakoid membrane which then drives the ATPase to transform ADP to ATP, and reduced NADPH, thus storing chemical energy. Typically, a charge separation event is initiated by the excitation of two central chromophores in close contact (the special pair) which results in an electron being passed along a chain of other chromophores until it reaches a quinone and then on to the electron transport chain (Fig. 15.4a). However, this is not always the case as some other pathways are present where charge separation is initiated on chromophores other than the special pair with the special pair acting as the terminal electron donor. Reaction centres have a quasi-two-fold symmetry in their chromophore arrangement (A and B

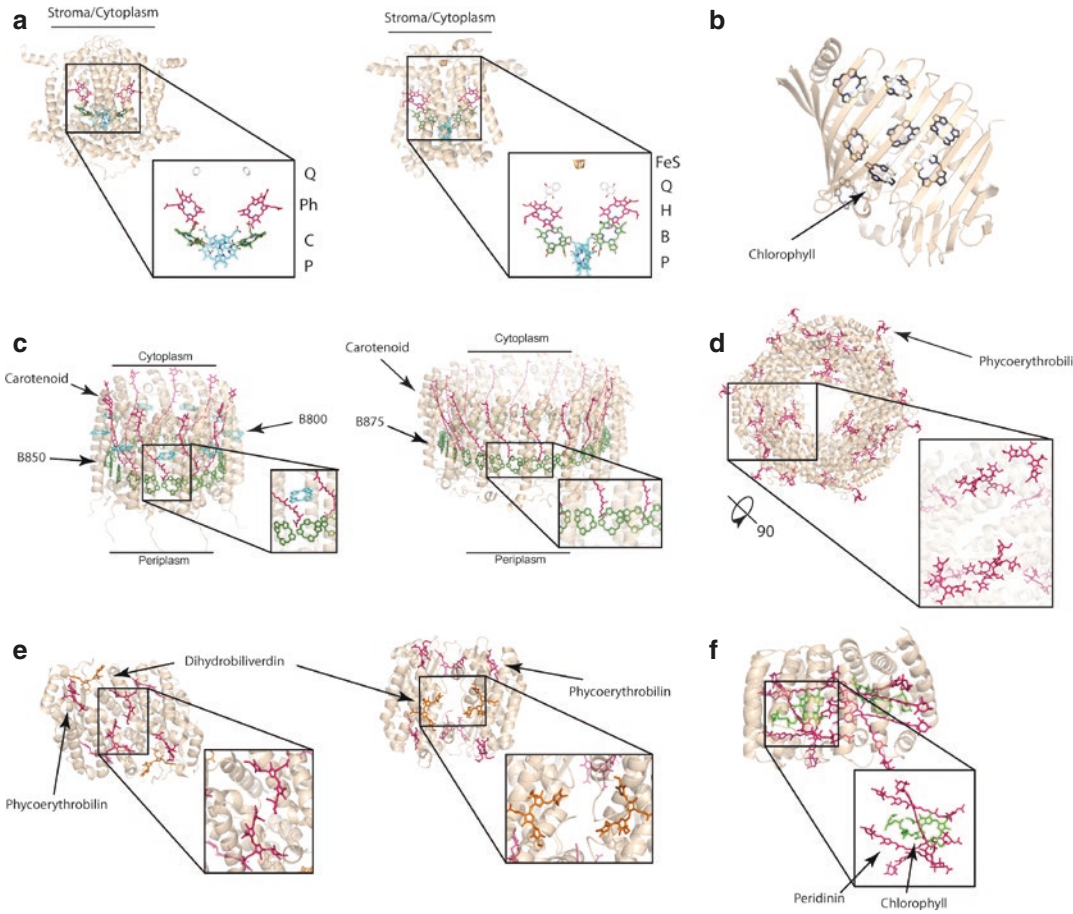

Fig. 15.4. **Proteins**—(**a**) Type II (left PDB: 3ZKI) and Type I (right PDB: 1JB0) reaction centres with chromophore arrangements and nomenclature. (**b**) The Fenna-Matthews-Olson complex (PDB: 3ENI) (**c**) Light harvesting complexes of purple bacteria LHII (left PDB: 2FKW) and LHI (right PDB: 3WMM) with inset highlighting the orientation of the chlorophylls. (**d**) Phycobilisome R-phycoerythrin hexamer $((\alpha\beta)_3)_2$ with inset highlighting a side view of chromophore packing (PDB: 1B8D). (**e**) Cryptophyte closed PE545 (left PDB: 1XG0) and open PE555 (right PDB: 4LMX) state phycobiliproteins with insets highlighting the separation of the central chromophores. (**f**) Dinoflagellate peridinin-chlorophyll protein (PCP) with inset showing carotenoid chlorophyll arrangement (PDB: 1PPR). Rendered in Pymol and chlorophyll tails are removed for clarity

branches – see Fig. 15.4a) with only slight asymmetry in the special pair which directs the excitation down one branch (the A branch) of the quasi-symmetric dimer. Note that the A/B branch notation changes for either eukaryotes or prokaryotes but will be used as standard throughout. The excitation and charge transfer kinetics for both type I and II reaction centres are very similar, with small changes to chromophores and also changes to nomenclature between eukaryotes and prokaryotes. There are two possible pathways described in the literature (Fig. 15.3b). The first begins with the photoexcitation of one of the excited states of the special pair (P and P∗), possibly via FRET from an antenna or from the greater light harvesting complex (for cyanobacteria and eukaryotes). The interplay between the exciton state and the protein electrostatic envi-

ronment generates a charge separation where an electron from the special pair is transferred directly to an A-branch (bacterio) pheophytin (denoted H_A for bacteria and Ph_A for eukaryotes) or via an intermediate A-branch (bacterio)chlorophyll (B_A for bacteria and C_A for eukaryotes). Charge separated states are generally denoted $Donor_A^+Acceptor_A^-$ the minus sign denoting the position of the electron). The electron is then transferred to a quinone (Q_A), onto the quinone on the opposite branch (Q_B) and then possibly to a metal cluster along the electron transport chain. The second pathway is the direct charge separation between the (bacterio)chlorophyll and (bacterio) pheophytin followed by the electron hole moving across to the special pair (Fig. 15.3b).

Light Harvesting Antennae

The light harvesting antenna is usually the first point of excitation for photosynthetic systems and is responsible for the efficient and robust transport of excitation energy to the reaction centre. Organisms that live in environments with very low photon flux have large and elaborate light harvesting antennae as every captured photon is precious. Furthermore, the excitation produced by each one of those photons must be efficiently and robustly carried to the reaction centre to prevent energy loss via fluorescence emission (the time scale of which is roughly nanoseconds). This highlights a key evolutionary trade-off for these organisms: they must have a large region with a high density of chromophores from which they can capture photons but they also must be able to transport the excitations to the closest reaction centre in under 5 ns. A further element of this trade-off is energy input in making antennae and reaction centres. If an organism makes a plethora of reaction centres, then energy is being wasted as many won't be used. Hence, there is a need for increases in efficiency of transport in the antennae themselves. Yet another complexity comes from the environment where perturbations can cause alterations to the energetic landscape and decay, potentially leading to reduced efficiency. There is hence a need for robustness against environmental effects which many organisms seem to exhibit in their transfer processes possibly due to coherence.

A. Green Bacteria

The predominant antenna of green bacteria is the chlorosome—a large, highly ordered aggregate of bacteriochlorophyll (BChl) molecules enclosed in a lipid/protein membrane. In green non-sulphur (filamentous) bacteria the chlorosome is coupled directly to the reaction centre via the bacteriochlorophyll/carotenoid-containing protein baseplate. In green sulphur bacteria, an additional coupling protein is added between the baseplate and the reaction centre known as the Fenna-Matthews-Olson complex (FMO; Fig. 15.3f). The FMO is a trimeric protein, where the monomer is almost entirely composed of β-sheet secondary structural elements that encapsulate seven closely-packed bacteriochlorophyll molecules in addition to one peripheral bacteriochlorophyll molecule that appears to be weakly coupled to the other seven (Fig. 15.4b). Energy transfer within the green sulphur bacterium *Chlorobium tepidum* is as follows (Dostál et al. 2016). Firstly, excitons relax within the chlorosome to the red edge of its absorption band with some excitons decaying due to exciton annihilation (when two excitons interact to destroy themselves and emit their energy which only takes place with a high density of excitons). Excitons in the chlorosome are transferred through the baseplate to the FMO with some transfer pathways within the FMO taking shorter or longer routes due to trapping. Excitons are then transferred from the FMO to the reaction centre (Fig. 15.3c).

B. Purple Bacteria

The two predominant light harvesting antennae of purple bacteria are comprised of integral membrane proteins containing chlorophyll and carotenoid molecules ordered in symmetric ring structures. Light harvesting complex 2 (LH2) is a peripheral antenna that funnels excitations to light harvesting complex 1 (LH1) which surrounds the reaction centre (Fig. 15.3g). The number of subunits in each ring structure varies from species to species, and even within a single organism. There are also variations on this symmetric ring structure including a lemniscate ("figure eight") structure that occurs upon interaction with an accessory protein. Some species have additional light harvesting antennae which have subtle differences in the energies of their constituent chromophores (Chmeliov et al. 2013). It should be noted that LH1 and LH2 are in no way related to LHCI and LHCII of higher plants despite a naming similarity. LH2 is comprised of two sets of concentric bacteriochlorophyll rings (B800 and another which is species dependent called B850; Fig. 15.4c, left panel). The B800 ring is comprised of monomeric bacteriochlorophyll molecules with their transition dipoles roughly in the plane and tangential to the ring with the same orientation (handedness) around (Fig. 15.4c, right panel). The B850 ring is comprised of dimeric bacteriochlorophyll molecules with their transition dipoles roughly tangent and in the plane of the ring but alternating in direction within the pair. LH1 is comprised of a single B875 (or B820) ring formed by pairs of bacteriochlorophylls in alternating orientation as in the B850 ring of LH2. However, there is often a break in the ring disrupting the symmetry. Carotenoids in both LH1 and LH2 are ignored in the following analysis and offer photoprotective properties and alterations to the electrostatic environment. During photoexcitation, excitons resident on the LH2 B800 ring relax to the lowest exciton level and are transferred to the B850 ring of the LH2. Excitons further relax on the B850 ring and are then transferred to the B875 ring of LH1, followed by relaxation and transfer to the reaction centre (Book et al. 2000; Cohen Stuart et al. 2011 – Fig. 15.3d).

C. Cyanobacteria

Cyanobacteria are the progenitors of all eukaryotic photosynthetic life—a complex story of theft and piracy (Fig. 15.3a) (for further details refer to Chaps. 2 & 10). Hence, there are many shared features in chromophore composition and antenna structures. One of the key light harvesting antenna of cyanobacteria is the phycobilisome which is a large assembly of rings of proteins including the chromophore-containing phycobiliproteins and linker proteins (Fig. 15.3h). Upon the primary endosymbiotic event driving the evolution of early eukaryotic photosynthesis, a cyanobacterium was harnessed and its descendants remain today as the modern plastids (chloroplasts). The first endosymbiotic event created what would become modern red algae (Fig. 15.3a). Within the chloroplast of modern red algae, the phycobilisome structure still exists with minimal alteration. At a later evolutionary time, a primitive red alga was engulfed to produce many of today's photosynthetic and non-photosynthetic protists which includes cryptophytes, heterokonts and alveolates (Green 2011). Within this supergroup of organisms, all have abandoned the phycobilisome, pilfering many of the proteins involved to produce derivative light harvesting proteins. Lastly, a group of dinoflagellates are purportedly tertiary endosymbionts and hence have captured the light harvesting apparatus of a protist and have evolved new light harvesting proteins (Fig. 15.3a).

The phycobilisome (PBS) is a large protein complex comprising around 600 polypeptides arranged in large rod-like stacks directed outward asteriform from photosystem II in the thylakoid of cyanobacteria, red algae and

glaucophytes (Fig. 15.3h). It should be noted that there are many different phycobilisome ultrastructural arrangments for different organisms. The main chromophorylated proteins are the phycobiliproteins which are αβ heterodimers arranged into trimer rings $(\alpha\beta)_3$ and/or hexamer double rings $((\alpha\beta)_3)_2$ with covalently attached linear tetrapyrrole chromophores as the light harvesting pigment (Fig. 15.4d). The phycobiliproteins that comprise each stack have been sorted into three main categories. At the end distal to the photosystem are the bluest absorbing complexes—the phycoerythrins. Further down the stack the absorption and emission becomes redder through phycocyanin and allophycocyanin, respectively, until the photosystem is reached (Zhang et al. 2017). A certain degree of ingenuity should be noted in this complex, where by having a synchronised energetic and spatial gradient, excitations are efficiently funnelled by virtue of the uni-directionality of the system. In other systems, such as the chlorosome, the energetic gradient through space is non-existent and despite the lack of funnelling, efficiency is maintained and must be derived from other means.

The light harvesting antennae of the cryptophytes are derived from the phycobilisome of an ancestral red alga—a product of secondary endosymbiosis. The soluble cryptophyte phycobiliproteins (PBPs) usually comprise an asymmetric heterodimer of dimers (usually $(\alpha_1\beta)(\alpha_2\beta)$), where the β subunit has evolved from the red algal β subunit, while the usually different α subunits (α_1 and α_2) are novel peptides (Fig. 15.4e). Linear tetrapyrrole chromophores are covalently-linked to the protein with one on each α subunit and three on each β subunit. These protein assemblies are transported across the thylakoid membrane and reside within the lumen as opposed to the stroma for the phycobilisome (Fig. 15.3i) (Gould et al. 2007). The β subunit is encoded by a single plastid gene while the genome of cryptophyte *Guillardia theta* shows multiple, nuclear-encoded α subunit genes suggesting multiple expressed PBPs (Curtis et al. 2012). It is unknown if these cryptophyte phycobiliproteins are arranged in an ordered assembly within the thylakoid lumen or reside as a concentrated solution (or glass) of proteins, however, electron dense material is observed in the lumen (Gantt 1971). Crystallographic studies have shown that two distinct quaternary forms exist within the cryptophyte phycobiliprotein family that have been called the *closed* and *open* forms and have been generated by a single residue insertion in the α subunit (Fig. 15.4e, left and right panels, respectively) (Harrop et al. 2014). The closed form exhibits a central pair of chromophores that are in van der Waals contact across the dimer interface (Fig. 15.4e left panel) (Wilk et al. 1999), while the open form has a central, water filled channel which has dramatic effects on the presence of quantum beats and is confined to the *Hemiselmis* genus (Harrop et al. 2014). The time scales of energy transfer between proteins and to the photosystem reaction centre remains an open question, with some preliminary work completed (van der Weij-De Wit et al. 2006). However, within each protein, time scales have been found for transfer events (Fig. 15.3e) between excitons (0.1 ps–40 ps), relaxation between exciton states (sub picosecond) and the fluorescence lifetime of 2.5 ns (Doust et al. 2004; Marin et al. 2011). Five phycobiliproteins have been extensively characterised by laser spectroscopy: PC645 (closed) from *Chroomonas sp.* CCMP270; PE545 (closed) from *Rhodomonas* sp. CS24; PC577 (open) from *Hemiselmis pacifica* and PC612 (open) from *Hemiselmis virescens*—which have a similar chromophore composition to PC645; and PE555 (open) from *Hemiselmis andersenii*—that has the same chromophore composition as the closed form PE545.

Dinoflagellates comprise a large group of disparate organisms. Some of the photosynthetic dinoflagellates are the product of yet another series of endosymbiotic events deriving their chloroplast from different sources (Morden and Sherwood 2002; Bodył

and Moszczyński 2006). The tertiary dinoflagellates that utilise peridinin as their main light harvesting carotenoid form a group of organisms. They contain a membrane-bound system similar to the LHC of plants and a water-soluble protein containing peridinin and chlorophyll a (peridinin chlorophyll binding protein—PCP; Fig. 15.3i). PCP resides in the lumen and each PCP contains 8 peridinins and 2 chlorophylls in a quasi-two-fold symmetric arrangement that is encapsulated in an α-helix rich protein shell (Fig. 15.4f) (Hofmann et al. 1996). Each chlorophyll is surrounded by four peridinin chromophores close-packed within the centre of the peripheral protein cage (Fig. 15.4f). There is a certain similarity in design to the FMO complex in that PCP creates a hollow protein shell enclosing close-packed chromophores, however, the dynamics of both differ greatly.

As has now been highlighted, there is a great diversity of light harvesting systems in nature—each using different chromophores and structural arrangements. In the following section, we will see how quantum mechanical effects manifest themselves in these different environments and how/if efficiency and robustness are proffered.

IV. Deeper Exploration of Energy Transport in Biological Systems

Now that we have established a language to describe quantum states of molecules, we can more deeply consider the possible interactions between them. Firstly, the case where excitations are strongly localised to single chromophores is considered. Solar photons are captured by light harvesting chromophores via absorption, exciting electronic, vibrational or vibronic (entangled electronic and vibrational) states. A way to think about this interaction is that the oscillating electric field of the photon interacts with the molecule upon absorption and an electron in the molecule oscillates from the ground to the excited state. The excitation is then transferred between chromophores via Coulombic coupling between the electric fields produced by one molecule and the electronic distribution of another in a similar manner to photon absorption. The electric fields induce excitation by interacting with the electronic states involved in the transition of the molecule exchanging the excitation. At long enough distances, the fields involved are dipolar and the interaction energy is low compared with the interactions with the environment, which decohere any superposition.

The picture described in the preceding paragraph is the Förster transfer limit, which has the further proviso that vibrations are at equilibrium with the environment, which is often broken by the persistence of chromophore motions throughout energy transfer. For general light activated systems, we also move away from the notion of transition dipoles and the like in favour of the average interaction energy of the excitation transfer. We tend not to use the dipole strength (à-la FRET) as, for closely packed chromophores, the interaction deviates dramatically from being dipolar as the electric fields from one chromophore will be felt differently across another chromophore as each chromophore is extended in space and not a point like object. Furthermore, this scheme is preferred as the molecules are by and large static and variations to the excitation energy can be treated as random perturbations from the environment (i.e surrounding protein and solvent medium). The energetic constraint that both chromophores must be at least *near* resonant (i.e. they have the same transition energy) is also important for energy to be transferred. Some energy can escape or be absorbed via the generation or absorption of phonons (vibrational wave packets). Generally, quantum mechanical processes require energy resonance so as to satisfy energy conservation. For any interaction to take place, it must be coherent at

least on a time scale which is proportional to the inverse of the energy of the interaction, even in Förster transfer. A rough calculation of this timescale using Heisenberg's uncertainty principle, places the coherence time for interactions between chromophores and light to be on the order of 1 fs. In the Förster regime, excitations merely *hop* from one chromophore to another until the reaction centre is reached and it is assumed that any phase information and electronic or vibrational coherence has decayed by dephasing and relaxation on a timescale far shorter than the time scale of exchange of excitation (the "hops"). The excited states in photosynthetic light harvesters have very short lifetimes on the order of nanoseconds before they fluoresce, which limits the timescale by which the excitation must reach its target, and, thus, predictions of Förster theory may not suffice.

For any sufficiently strong interaction (where the energy of the interacting systems is stronger than the energetic perturbation from the environment) coherence will be generated over some characteristic time scale. Hence, small subsystems may be internally coherent and transfer incoherently to other subsystems. The excitation is transferred between the excitons via Coulombic coupling whereby excitons hop between coherent clusters of chromophores (the excitons) in an incoherent or semi-coherent fashion. This is the essence of both supertransfer and generalised Förster theory. Many of the assumptions of Förster theory break down due to delocalisation, coherence of vibrations and the dipole approximation. The region where the break down occurs is in the intermediate regime, where the energy scales of the system and the environment are commensurate. This is the case for a great proportion of the light harvesting systems in nature. Förster theory is also complicated by the presence of vibronic states and vibronic coherence due to diabaticity, conical intersections, the Condon approximation and the general non-separability of vibrational and electronic states. A few recent reviews (Scholes et al. 2012; Mirkovic et al. 2016) provide valuable information that is not given here.

Of brief noteworthiness is the ability for photosynthetic organisms to alter their light harvesting properties based on the availability of photons. The risk of oxidative damage is significantly increased when photosynthesis goes into overproduction and when triplet excited states are produced. Photosynthetic organisms have myriad ways to decrease photosynthetic light harvesting by altering charge transfer. This often involves: a protein light switch and accessory proteins that decrease the efficiency of light harvest via quenching (Roach and Krieger-Liszkay 2012; Ballottari et al. 2013), tuned carotenoid-chlorophyll interactions (Di Valentin and Carbonera 2017), or possibly the use of the triplet excited states which phosphoresce after long lifetimes and are often unable to be transported (Kim et al. 2007). Photoprotection may be as important as the need for efficient energy transfer and hence energy transfer and photoprotective pathways may often compete.

Below is a pensive stroll through some of the studies that attempt to unravel the nature of quantum beats in observed spectra of many light harvesting systems. As understanding of the methodology has developed, understanding of the origin of coherences has shifted. Generally, all light harvesting systems are observed to have vibrational coherences. However, over the last decade of study, with the discovery of possibly electronic coherences, a to-and-fro between vibrational and electronic origin has occurred. Largely, in systems where this debate was prominent, the consensus seems to be settling on the origins of coherence as coherence between mixed vibrational/electronic states (vibronic states). The works presented here are a mere sample of the corpus of literature within the field and the sample presented is used to highlight some specific ideas that have been detailed.

A. *Exciton States*

The quantum object moving between chromophores created by the absorption of a photon cannot really be thought of as an electron. It is the excitation itself that is transferred between chromophores. Broadly speaking, these excitations are referred to as *excitons* and are part of a broader class of objects called *quasiparticles*. Quasiparticles are not fundamental particles but are some quantum state that behaves as though it is a particle because of interactions in the system. This may sound like an odd and unnecessary distinction to make, however, it is an important one. Further subtlety arises from quantum systems containing multiple, strongly coupled components (chromophores). Within a collection of chromophores, there are electronic couplings between them which results in a new set of delocalised states that extend over the strongly-coupled chromophores. This new set of delocalised states are the excitons that will be generated by excitation from a discrete packet of energy that is confluent with the energy of the state—the excitons are stationary in time (the eigenstates). Also note that if a system has uncoupled chromophores, then the excitons will just be excitations of specific (uncoupled) chromophore sites and not superpositions among them. Without a decohering environment, the system would remain in the exciton state in it's non-local superposition.

One other remarkable thing happens from the superposition of two (or more) chromophore states to produce stationary states: the energy spectrum of the joint system of two coupled chromophores is far different from that of the two lone chromophores (Fig. 15.1b). For example, uncoupled chlorophyll molecules embedded in a protein matrix all have very similar near resonant energy levels for their excited states. Thus, the absorption spectrum would contain a single peak in the absence of coupling (Fig. 15.1b, red absorption spectrum). However, due to coupling between the individual chromophores, the energies of the resonant excited states split into a set of states with energies higher and lower than the isolated chromophores (Fig. 15.1b, blue absorption spectrum). The degree to which the energy levels split is proportional to the coupling strength, thus, the stronger the coupling, the broader the spectrum. In the weak coupling limit, the exciton energies would be approximately the chromophore excitation energies given the weak to non-existent mixing between states. Hence, it must be stressed that the excitation energies seen in spectroscopic analysis of these systems are not necessarily the energies related to each individual chromophore, but rather the energies of the set of delocalised excitons in the system. The broad absorption spectra that result from coupling may be an evolutionary reason for the near-ubiquitous presence of strongly-coupled chromophore dimers and multimers in light harvesting systems. Generally, light harvesting systems exhibit excitons that are on the order of 2–4 chromophores, with the exception of the chlorosome which has excitons covering a much larger number of chromophores. The excitation is transferred between the excitons via Coulombic coupling whereby excitons hop between coherent clusters of chromophores in an incoherent or semi-coherent fashion.

In an evolutionary search for an efficient antenna, the chlorosome is an excellent example. Its construction is such that chromophores have large interaction energies (and hence a large degree of delocalisation) merely by the thousands of bacteriochlorophyll molecules being in spatial contact with each other and in having highly ordered domains. These domains take the shape of concentric rods, sheets and spirals. Estimates of exciton delocalisation from spectroscopic studies, however, vary wildly. Because of weak long range interactions, static crystal defects and the influence of the vibrational environment pervading the chlorosome structure, excitons are not extended across

the entire chlorosome but are partially localised into fluctuating regions, referred to as the *coherent domains*. These coherent domains will diffuse around until energy is dissipated to the FMO/reaction centre absorption band. Early estimates based on dipole couplings (possibly an erroneous approximation given the close proximity of chlorophylls) place the size of the delocalised exciton state as 2–3 chromophores in *Chlorobium* and 10–12 chromophores in *Chloroflexus* (Prokhorenko et al. 2000). Later work, however, suggests that the size of the coherent domains will be largely indiscernible as small differences in the phase of coherent oscillations within different coherent domains will greatly reduce the apparent dephasing time of electronic coherence upon averaging in spectroscopic studies (Jun et al. 2014). Given the energetic disorder present in the chlorosome, only randomised instances of exciton states are presents, making them hard to observe. Furthermore, the large number of interacting chromophores in the chlorosome produces a similarly large number of excitons and hence a broad continuous absorption spectrum making observations of quantum beats in 2DES almost impossible. Finally, there is an interesting evolutionary trade off at play within the chlorosome—the absorption probability of a photon by a lone chlorophyll is low and hence the capture cross section is maximised by the enormity of the chlorosome structure. However, as excitons have a characteristic diffusion length, given the speed of propagation and the fluorescence time, there is an upper limit to its size after which efficiency decreases (i.e. if the chlorosome were too large, the exciton would be lost to fluorescence before it reached the reaction centre).

The Fenna-Matthews-Olson complex (FMO) also has a close packed arrangement of chlorophyll molecules, with disordered dipole moment orientations packed within a protein shell (Fig. 15.4b). Close packing again gives rise to large interaction energies and hence delocalised exciton states. Protein electrostatics induce differences in site energies which are coupled to one another producing the excitons resulting in a very different absorption spectrum to that of bacteriochlorophyll in solution. It should be noted that the site energies and delocalisation patterns in many theoretical calculations are only estimates and still a matter of debate. This is because they are unobservable and the only observation we can make is of the energies of the exciton states as we are, in a sense, probing the states generated by the energy matrix (the Hamiltonian—after the influence of disorder). The calculated exciton states are shown in Fig. 15.5a as shadings across the chromophores representing the probability distribution of the excitation. The spectrum of the FMO trimer contains features for only seven excitons and not the full twenty-four expected if all chromophores were strongly coupled within the FMO trimer (Thyrhaug et al. 2016). Hence, intermonomer quantum coherent effects can be ruled out with coherence confined to the seven strongly coupled chromophores in each FMO monomer. In 2DES correlation spectra, all major diagonal peaks are connected by cross peaks indicating transfer between excitons. There are many possible pathways for energy transfer to the lowest energy exciton state, although specific pathways will be preferred. The fastest, and thus most prevalent energy transfer steps, tend to involve transfer between exciton states with some overlap in their chromophore composition. It may be suggested that overlaps of excitons across the chromophore sites may provide an efficient means of funnelling energy through space, not just down an energetic ladder.

The peridinin-chlorophyll protein (PCP) has a very similar design to the FMO, with the exception that PCP has a mixture of chlorophyll and carotenoid molecules that make up the chromophores encased in the protein shell (Fig. 15.4f). Energy transfer processes are initially mediated by a mixed chlorophyll-peridinin exciton state upon excitation.

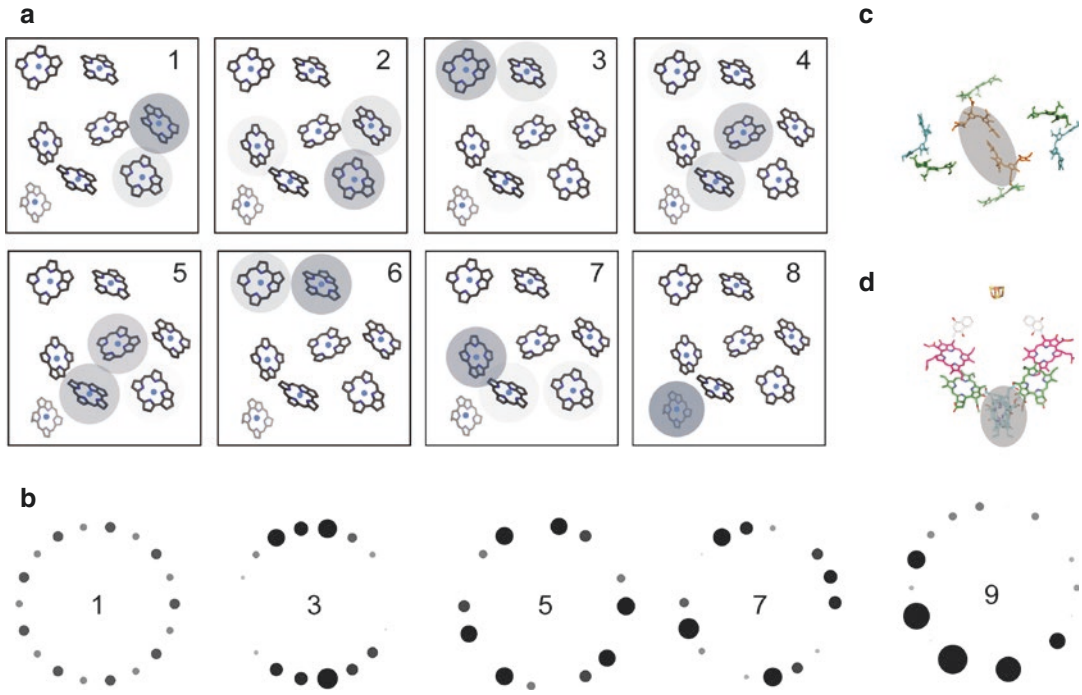

Fig. 15.5. **Comparison of Exciton States**—(**a**) Excitons of the FMO calculated from the Hamiltonian (Adolphs and Renger 2006) in Mathematica. As can be seen, many excitons have overlap across chromophore sites (for example the chromophore complement of states 3 and 6) making funnelling between them possible. (**b**) A selection of exciton states of the B850 ring calculated from the Hamiltonian (Strümpfer and Schulten 2009)**.** All other states up to 18 are symmetry partners. Exciton 3 (and its isoenergetic partner exciton 2) are the only states with a non-negligible dipole moment. The ground state is exciton 1. (**c** and **d**) Partially delocalised exciton states of closed form cryptophyte phycobiliproteins and reaction centres, respectively. Shading in all states indicates probability density

Excitonic coherence across the entire quasi-two-fold symmetric chromophore arrangement have been suggested on theoretical and experimental grounds to explain the strong circular dichroism signals that are observed (Bricker and Lo 2015). The dynamics of how the superpositions between the chromophores in the initial excitation dephase are complex owing to non-radiative processes in the excited state distorting the peridinins by torsional modes. In other words, the initial delocalised excitonic state passes through a conical intersection and peridinins decay to a different energy level leaving the excitation on the chlorophyll. The Hamiltonian for the excited state is thus altered and produces dynamic disorder, localising the exciton state. Electronic coherence effects are confined to 50 fs in *Amphidinium carterae* (Roscioli et al. 2017). Strong coupling increases the delocalisation of excitation while strained conformations of the molecules allows controlled dynamic localisation of the state.

The structural symmetry of purple bacterial light harvesting complexes (LH1 and LH2) permit some interesting pathways for energy transfer due to superpositions of electronic states interfering and altering the transition dipole moments of the system. The symmetry of the assembled protein complex leads to sets of exciton states in rings that form a ladder of pairs of degenerate (isoenergetic) states along with a ground and highest

excited state that are non-degenerate (Fig. 15.5b). Two states from each set (the lowest two excited states) have a large dipole moment (Fig. 15.5b, state 3); the rest have dipole moments that are an order of magnitude smaller (Fig. 15.5b, states 5–9) including the ground state (which is almost optically dark; Fig. 15.5b, state 1). The dipole moments of each exciton state are the weighted sums of the dipoles of each chromophore. The inclusion of disorder disrupts this excitonic structure and leads to different, slightly randomised delocalisation patterns of excitons. The randomized excitons, after environmental interactions, often have larger dipole moments, however, these dipole moments are still negligible compared with the lowest excited exciton states and are hence still optically dark. Many estimates of the average extent of delocalisation of the excitation on LH2 have been made ranging between 2–13 chromophore molecules on the B850 ring (Chachisvilis and Sundström 1996; Chachisvilis et al. 1997; Book et al. 2000; Dahlberg et al. 2015). Given environmental dephasing, it is apparent that the extent of the delocalisation of the exciton on the different rings is time dependent and relaxes to a smaller number of chromophores over 50–100 fs. At room temperature, it is observed that B800 experiences a larger degree of dephasing than the B850 ring and hence the members of the B850 ring are more strongly coupled to each other (and less strongly coupled to the environment) than the B800 ring. Differences in coupling are also evident in the redshift of B850 relative to B800 (50 nm); more strongly coupled chromophores have a broader absorption spectrum due to exciton splitting and hence the lowest excited state will be redder with more strongly coupled chromophores.

Most other light harvesting systems appear to have far more localised states than those mentioned above. All are inferred from circular dichroism signals and transient absorption polarization anisotropy which suggest the rotation of the dipole moment due to exciton relaxation. In the phycobilisome (PBS), the density of chromophores is far lower, with no chromophores in physical contact with each other. The most significant quantum effect in the PBS is that some individual pairs of chromophores are strongly coupled to form delocalised excitonic states resulting in energy splitting, and hence, broader spectral absorption and overlap between the chromophores of different phycobiliproteins. In the allophycocyanin (APC) trimer, delocalised excitonic effects have been observed by circular dichroism spectroscopy where three electronic transitions exist as opposed to one electronic transition in individual subunits (Zhang et al. 2001). Furthermore, two-colour pump-probe polarization anisotropy highlights the existence of delocalised excitonic states from large initial anisotropy (Womick and Moran 2009). The initial polarization anisotropy of individual C-phycocyanin (C-PC) monomers is minimal, suggesting exciton effects are not present until they are arranged into a quaternary structure (Edington et al. 1995). In R-phycoerythrin (R-PE), phycourobilin chromophores act as primary acceptors and their excitations are localised whereas the innermost pair of PEB chromophores is strongly coupled with the excitons possibly delocalised across them. The evolutionary successor of the PBS—the cryptophyte phycobiliproteins (PBPs)— have two forms: a closed form with two central chromophores in physical contact (Fig. 15.4e, left, and Fig. 15.5c) and an open form where they are separated (Fig. 15.4e, right). In closed forms PC645 and PE545, there is a noted presence of energy level splitting in circular dichroism spectroscopy due to the close proximity of the central linear tetrapyrroles generating delocalization (MacColl et al. 1999). This is not seen in the open form PC612. Small coupling suggests that excitons are highly localised in most cases (delocalised across two chromophores, if at all).

The reaction centre charge separation is most commonly initiated by a strongly cou-

pled pair of chromophores referred to as the special pair (Figs. 15.4a and 15.5d). The pair gives rise to two excitons, possibly coupled to a vibration, that allow for down conversion of energy for the rest of the electron transport (Raszewski et al. 2008). Given the packing of chromophores within the greater light harvesting complexes that surround many reaction centers, it is likely that these photosystems give rise to highly delocalised exciton states also. However, the photosystem is very energetically complex with many various carotenoid-chlorophyll states and electron transfer states which may obfuscate analysis.

The theme that emerges here is that closely packed chromophores give rise to large interaction energies and if the chromophore excitation energies are near resonant, a large degree of delocalisation will take place. In the examples of the chlorosome and the LH rings it becomes apparent that even in strongly interacting systems, the delocalisation of the exciton state can be reduced by the influence of the environment. Over large distances, the non-local coherent effects of the Hamiltonian become negligible when compared with the local effects of the Lindbladian, meaning that the decoherence is stronger. Fluctuations can be thought of as randomizing the Hamiltonian (the excitation and interaction energies) also which alters the exciton distribution significantly causing fluctuations in the exciton probability distribution. Fluctuations can alter downstream transfer pathways from changes in localisation patterns. Exciton states in molecules can only really be inferred from data given the splitting of identical states (with the exception of circular dichroic signatures and some others). Excitons are the quantum object that is being transported during photosynthetic light harvesting and have a range of delocalisation patterns ranging from large numbers of strongly coupled chromophores to single chromophore molecules. Some suggest that delocalised exciton states should not be referred to as coherent, however, they represent a quantum effect that is classically unexpected and could not be produced without coherence between chromophores.

B. Vibrational Coherence

The vibrational states of molecules are of importance in describing the quantum state of the system and energy transfer properties. Vibrational coherence can involve a singly excited vibrational mode in the ground or excited electronic state and it may involve different vibrational modes on the same molecule. Vibrations on different chromophores can also occur in tandem and can hence be coupled with phase locked (coherent) vibrations existing across many chromophores. The role of vibrations and vibrational coherence is made more complex by the superposition of different vibrational modes across different electronic states of the molecule and between molecules. These vibrational coherences can be observed spectroscopically through Raman transitions and can be difficult to discern from electronic coherence between states separated by similar energy values. These vibrational coherences can be particularly important in electronic energy transfer when their energy matches the energy gaps between excitons. In this case, the additional vibrational energy brings excited chromophore states into resonance that would not be otherwise and coherence may provide a period of time where electronic transfer is increased and excited state lifetime can be borrowed. In fact, almost every paper referenced here finds a slew of vibrational coherences. This is perhaps an artefact of coherent spectroscopic methods arising from stimulated impulsive Raman scattering. Vibrational coherences appear to be ubiquitous features of light harvesting systems, however, in most cases are inconsequential with respect to the rate/efficiency of energy given that electronic and vibrational states operate on very different energy scales.

There are, however, instances where nuclear coherence (vibrations and rotations) plays an important role. Vibrational and rotational states and their coherence feature in the movement between retinal isomers in bacteriorhodopsin and the dynamics in the isomerised state generating efficient and robust deprotonation. By tuning the excitation pulse to either be resonant or detuned to the red or blue in relation to the absorption maximum, details about the origin of coherent motions (either from the ground or excited state) can be ascertained. Red detuned excitation (lower energy than the absorbance maximum) highlights ground state vibrational coherences which lie in the high frequency regime and vice versa (Kraack et al. 2011). When excited by high energy light, energy is redistributed by vibrational relaxation and deposited into low frequency vibrational modes promoting nuclear motions. The generation of these modes is likely due to impulsive Raman scattering or the reorganisation of higher frequency modes from the ground state. Vibrational coherence of low frequency modes in the excited state decoheres over 300 fs—one third of the time reported scale of retinal isomerisation. Under incoherent illumination, the efficiency of retinal charge separation (photon in—proton out) is approximately 65%, however, using laser pulse shaping the efficiency can be optimised or anti-optimised by 24% (Prokhorenko et al. 2006). Optimal illumination consists of periodic electric field amplitude modulations of specific frequency whereas anti-optimal pulse shapes are highly aperiodic. The period of amplitude modulations in the optimal illumination case is slightly off resonant with a torsional mode in the retinal which drives isomerisation in the excited state. Creation of a specific vibrational coherence appears to drive efficient retinal isomerisation and, hence, proton translocation. This is in contrast to the anti-optimal pulse whose excitation does not decrease the excited state population, but whose essentially random phase destroys any coherent vibrational motions.

Prior to charge separation, exciton states are observed in type I and II reaction centres and excitation energy transfer to the special pair can come from (bacterio)chlorophylls or (bacterio)pheophytins. In pump-probe experiments performed on type I reaction centres, quantum beats are observed in the excited states of the special pair across a number of frequencies and do not fully dephase after charge separation. Further quantum beats are seen in the bacteriochlorophyll region of the spectra concurrent with a redshift of the absorption peak upon charge separation (Vos et al. 1991, 1994, 1998). Observed ultra-low frequency quantum beats are perhaps related to inter-chromophore or local concerted protein dynamics that are not thermally relaxed on the timescale of charge separation (over 500 fs). Low frequency vibrational movements alter the charge distribution, oscillating over the special pair leading to a distribution where electron tunnelling and charge separation can occur (and thus the $P^{+}B^{-}$ state) (Spörlein et al. 1998). This oscillation is also observed with many of the same features in reaction centres lacking a bacteriochlorophyll band, hence justifying the oscillations origin as the special pair (Streltsov et al. 1998). Furthermore, in mutant reaction centres with alterations in the local protein environment, a reduced amplitude of this mode is observed and correlates with a reduced charge transport rate.

In type II reaction centers, quantum beats in the excited states are observed that outlive the timescale over which excitations are resident on the chromophores which presents a causal problem. A possible explanation is that vibrational coherences, although derived from the excited state of a chromophore, continue to oscillate in the ground state, which assumes the ground and excited states have similar vibrational structures (Paleček et al. 2017). Excitation generates a coherence that is purely vibrational on the chlorophyll or has a mixed vibronic character over the chlorophyll and the pheophytin and, upon energy transfer to the special pair, this quantum beat is shifted to the ground state of the

chlorophyll or the pheophytin. This would result in a π phase shift of the beating pattern which has been observed during the characteristic time of transfer to the special pair and hence it may not be necessary to invoke wavelike transfer in the reaction centre (Paleček et al. 2017). Thus, the chlorophyll may act as a sink of energy accelerating transfer by retaining vibrational energy following exciton transfer.

There is a fundamental difference in the mechanism by which bacteriorhodopsin creates a charge separation compared to the photosystems and reaction centres. Bacteriorhodopsin utilises a structural change in retinal that includes the relocation of nuclei, whereas the reaction centres relocate electrons via charge transfer states. However, vibrational coherence appears to play some role in both where vibrations that are not thermally relaxed coherently move the system to a state where charges can be passed through the system. Although vibrational coherences have been observed almost ubiquitously in light harvesting systems, it remains unclear whether vibrational coherence aids or is even present in light harvesting processes *in vivo* (i.e. under incoherent solar illumination). There are some mechanisms that appear to find use in vibrational coherences, possibly increasing donor and acceptor energy resonance or movement of a system across a conical intersection between two excited states, however, further research is required.

C. *Excitonic Coherence*

A more subtle effect can take place when the donor and acceptor excitons are coherent. When the states of the system retain phase information about each other, the cluster can then sample multiple energy transfer pathways simultaneously and, later, an end state can be selected from the superposition based on the environment at the time. This excitation energy transfer mechanism is wavelike and hence different pathways can constructively and destructively interfere. Quantum coherence between the exciton states *may* allow the excitation to funnel efficiently and robustly to the global minimum (the final acceptor chromophore) instead of getting stuck in local energetic minima (trap states), however, there are caveats to this. An overlap between different excitons over the set of chromophore sites exists, thus population transfer can then be funnelled by this overlap downhill with respect to energy—even incoherent exciton dynamics are more efficient than chromophore to chromophore transfer. Excitonic coherence may also not need to be invoked as, if the system starts in a high lying state, it may simply funnel to the lowest energy state stochastically. Excitonic coherence ties into the possibility of process coherence which is detailed below, however, excitonic coherences deserve a spotlight given the possibility that vibronically mixed coherences are masquerading as electronic coherences.

The Fenna-Matthews-Olson complex (FMO) has been studied as a theoretical and experimental prototype for quantum biology and since the initial discovery of quantum beats in the FMO there has been considerable debate surrounding their origin. Two dominant coherent oscillations are observed on the cross peaks between excitons one and two (160 cm^{-1}) and excitons one and three (200 cm^{-1}) with coherence times ranging from 100 fs to 1.1 ps (around 300 fs at room temperature) depending on the method and author (Engel et al. 2007; Hayes et al. 2010; Panitchayangkoon et al. 2010, 2011; Thyrhaug et al. 2016, 2018; Duan et al. 2017). Oscillatory features are observed in peak widths and quantum beats are seen to grow in amplitude at early times possibly indicating transfer of coherence from higher energy excitonic states relaxing to lower lying ones. Coherence transfer would then support the sampling of multiple relaxation pathways to the sink exciton (process coherence) however the evocation of wavelike phenomena may not be necessary to under-

stand efficiency. The transfer of coherence via quantum transport is also supported by the changes in oscillatory phase between populations and coherences (π phase flip). However, it has remained unclear whether coherence arises from vibrations or electronic superpositions and evidence for each has been proposed.

In the light harvesting rings of purple bacteria, many excitons do not contribute given the symmetries of the states, which narrows the number of possible excitonic coherences considerably. In LH2, which contains two different rings with distinct absorption maxima, the B800 ring only decays to two states of the B850 ring with any great probability. Dephasing from the B800 ring follows a 177 fs time scale and the optically active states of B850 are observed to have persistent, coupled oscillations to each other and B800 that last for 30–500 fs with a 90% probability of being localised to either ring. (Cohen Stuart et al. 2011; Harel and Engel 2012; Fidler et al. 2013). A π/2 phase change between the spectral regions corresponding to the B800 and B850 states is observed and could be indicative of interference with another, optically dark state. In single molecule transient absorption experiments, coherence between excitons in the B800 and B850 rings coupled to an optically dark state of B850 is further supported (Hildner et al. 2013). Furthermore, in B820 of LH1, observed anisotropy in pump-probe population decay is characteristic of changes in the dipole moment during energy transfer and suggests selection of an exciton from an initial superposition of different exciton states (Diffey et al. 1998).

Cryptophyte phycobiliproteins provide an excellent tool for examining the possible existence of excitonic coherence given the two separate forms (open and closed)—proffering states with and without a strongly coupled chromophore dimer. Within the central dimer of PC645, internal conversion processes producing a decay of coherence between exciton states are evidenced by a rotation in the dipole moment (Marin et al. 2011). Oscillatory features are observed between the two dihydrobiliverdin (DBV) dimer states and also between states of the DBV dimer and the excited state of mesobiliverdin (MBV) over 400 fs (Collini et al. 2010). The oscillations of the upper DBV dimer state with the excited MBV state have a frequency confluent with the energy difference between the states indicative of electronic coherence (Turner et al. 2011). Initial two-colour laser spectroscopy studies (used to excite specific coherences) assigned a ladder of coherences to separable vibrational and electronic states of the DBV dimer, decohering at 900 fs and 300 fs, respectively (Richards et al. 2014). This suggests that electronic coherences may be sustained over the time scale of energy transfer in PC645. In PE545, exciton splitting in the central dimeric phycoerythrobilin (PEB) pair is observed as with the PCB pair in PC645 (MacColl et al. 1999). An oscillation between the central pair and peripheral PEBs dephases over 130 fs and the phase and amplitude of the 2DES cross peaks in PE545 show characteristics of electronic coherence. A control phycobilisome protein with a single PEB attached does not show such quantum beats (Wong et al. 2012). Given the delocalization of the excited state across the dimer pair, it is suggested that quantum coherence would aid in the eventual selection of the trap state at the red-most PEB (Doust et al. 2004).

Despite the presence of a water filled hole in the open form cryptophyte phycobiliprotein PE555 (suggesting little exciton splitting and no coherence between these states), quantum beats are still observed and persist over 100 fs (Collini 2012; Harrop et al. 2014). This was determined by examining shape and amplitude correlations of 2DES peaks and is hence an indirect measure of coherence in energy transfer. Conversely, in other open state phycobiliproteins (PC612 and PC577), no signs of exciton splitting are observed and quantum beats appear to be of vibrational origin, which is also coupled

with a slower transfer rate than PC645 in PC612 (MacColl et al. 1999; McClure et al. 2014; Harrop et al. 2014).

In type II reaction centres with an oxidised special pair (which disallows charge separation), quantum beats are observed to be persist for 400 fs on the bacteriopheophytin (H) and the bacteriochlorophyll (B) (Lee et al. 2007). Generally, spectroscopic methods cannot distinguish features from either the A or B branches in the reaction centre due to their isoenergetic nature and hence may arise from either branch. Quantum beats present between H and B match their energy difference and hence may be due to electronic coherence (Westenhoff et al. 2012). This is accompanied by many other quantum beats possibly due to vibrational coherences, other electronic coherences and the electrostatic response of the protein. Many of the quantum beats observed in type I reaction centres are also resonant with the energy gap involving special pair exciton states with similar frequency to that of type II reaction centres (Fuller et al. 2014) suggesting the possibility of electronic coherence within reaction centre chromophores.

D. Vibronic Coherence

Part of the initial source of confusion in assigning the origin of quantum beats was the inability to distinguish vibrational from electronic coherences in 2DES. Spectra appeared to have vibrational characteristics (given lifetime and positions) and electronic characteristics (given their strengths and oscillatory phases). After thorough modelling, it appeared that states with these mixed characteristics can be explained by vibronic states. Taking the nuclear and electronic degrees of freedom to be separable is a good approximation for a lot of systems but only works up to the point when the energy scales become inseparable. The reason is that the electronic and vibrational states are not the real eigenstates of the molecular system, the vibronic or even ro-vibronic states are. Calculating the vibronic eigenstates is computationally intractable and hence we can think of these states as superpositions of electronic states non-separably dressed with vibrational states and possibly across different molecules depending on the coupling. This still is an approximation, but is a much better one for modelling these systems. All molecular states are vibronic—however some have more electronic or more vibrational characteristics—and in 2DES we are generally observing superpositions of these. Vibronic states appear often at conical intersections where the nuclear potential energy surfaces of two electronic states overlap. Vibronic states are thus involved in internal conversion processes at these intersections, where a molecule (or collection of molecules) will non-radiatively decay. At these intersections the energy levels of the molecule (or collection of molecules) are degenerate (isoenergetic), which is disallowed unless there is another degree of freedom that is different between the states at this point. Hence a different set of states at that energy form. This is why vibronic states occur when the excitonic energy gap and vibrational energy are confluent. Conical intersections are sometimes referred to as avoided crossings; the potential energy surfaces are not allowed to cross and hence they mix. An illustration of vibronic states can be seen in Fig. 15.6. With significant vibronic coupling and hence a significant mixing of electronic and vibrational degrees of freedom comes some interesting effects on light harvesting. Firstly, the electronic states can borrow coherence lifetime from the vibrational states with which they are entangled, leading to vibronic coherences (that is, a coherent superposition between vibronic states), which can remain coherent longer than purely electronic coherences. Secondly, vibronic states can effectively enhance spectral overlap between electronic (excitonic) states and enhance resonant energy transfer.

Vibronic coherences have already been hinted at in the above sections. Retinal isom-

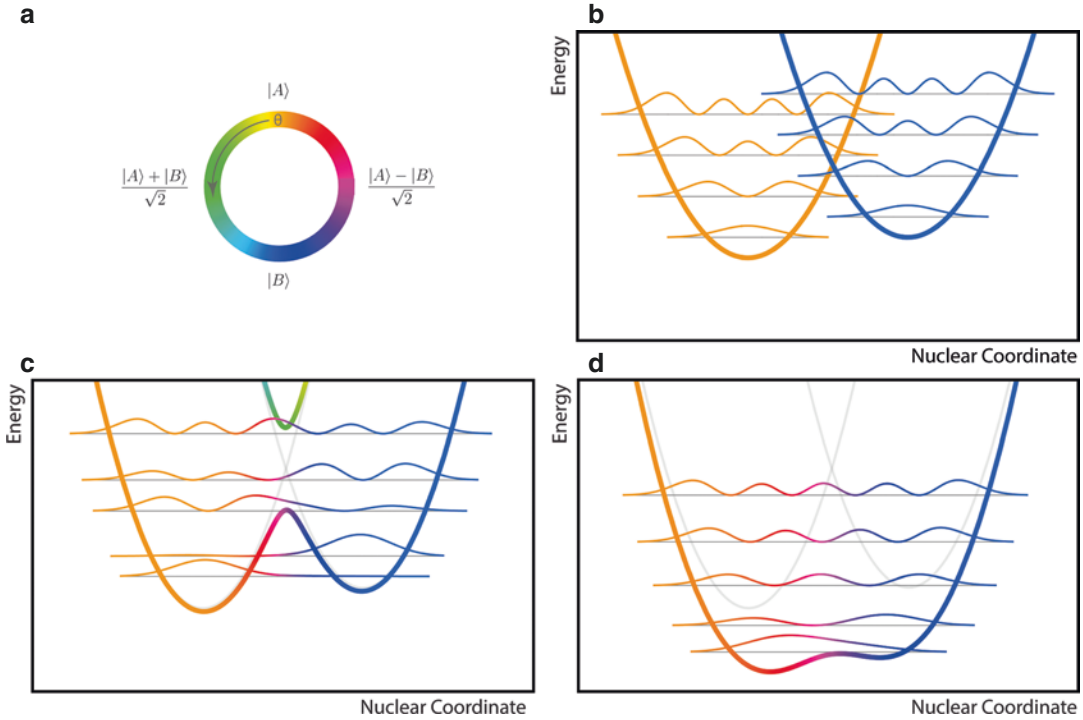

Fig. 15.6. **Vibronic States**—A selection of the lowest energy quantum states of a toy molecule with different regimes of coupling is provided. The system comprises two states, the A chromophore state (or |A>) and B state (or |B>), where the coupling between them is varied. (**a**) Guide to the extent of delocalisation of the states as represented by rotations on the Bloch sphere, where colour indicates the degree and form of mixing. In (**b**), (**c**) and (**d**), the potential energy for a given nuclear separation is shown as the bold lines, the quantum state probability density for a selection of states in each potential is shown as thin coloured lines with the y axis shifted to the relative energy of that state (grey thin lines). The original potentials are also shown as grey curves. (**b**) Two uncoupled molecules or states of the same molecule with a shared nuclear coordinate. The states of each molecule are purely vibrational and are separable and distinct—we can *index* the state of the system by two separate numbers (electronic and vibrational). (**c**) When we increase the coupling strength from zero we gain an avoided crossing. In the quantum chemistry sense, we have a derivative coupling between the potential energy surfaces, or, in another sense, we have an electronic coupling generating the excitons. The closer the two potential energy surfaces are in energy, the larger the alteration to the potential. We note two branches of this potential—an upper and a lower. We further note greater mixing of the electronic states (as shown by the colour with reference to the Bloch sphere in (**a**)) where the new potential deviates from the uncoupled potential. Take for example the third lowest state—the probability is composed of three peaks which describe the state of the system. The leftmost peak has small nuclear separation and is entirely in the A chromophore state (orange colour), the rightmost peak has less amplitude and means that the system at greater nuclear separation is mostly in the B state (blue colour) and the central peak has a mixed electronic state at intermediate nuclear separation (varying colour). Note that the lower energy states are more localised than the higher energy states. With an increased coupling strength, we cannot *index* the states like we can in (**b**) and hence they are inseparable (entangled), however, we can index the lower energy levels to some degree. This becomes even more dramatic as we increase the coupling strength even further as in (**d**)

erisation within bacteriorhodopsin follows a pathway in which an excited state with a more electronic character is internally converted to an excited state with a more vibrational character (torsion of the retinal). As the pathway includes movement across a conical intersection between electronic excited states, non-separable mixtures of vibrational and electronic states are present at that point given the energy constraints

between them. There is not necessarily vibronic *coherence* in retinal as the coherence is not between vibronic states comprising the internal conversion process. Vibronic states have also been observed in a sister protein—xanthorhodopsin—which harbours a retinal and a carotenoid molecule (Fujimoto and Balashov 2017). Vibronic states are also of importance in understanding energy transfer in peridinin-chlorophyll protein. Following excitation and development of a delocalised exciton state, the peridinin state moves across a conical intersection where the peridinin excited state internally converts to a state with a more vibrational character distorting the peridinins by torsional modes thereby transforming the structure of the ordered chromophore cluster and localising the excitation. The localised state results in a longer lived higher excited state due to mechanically unavailable relaxation pathways. Electronic coherence effects are confined to 50 fs in *Amphidinium carterae* and off-diagonal peaks in 2DES measurements between peridinins and between chlorophyll and peridinin decay rapidly (dephasing time of 20 fs). The rate of energy transfer to the lowest energy state is estimated to be around 2 orders of magnitude faster than what is predicted by Förster transfer and the initial quantum coherent process may account for 50–70% of the very high efficiency (90%) for energy transfer from peridinin to chlorophyll (Roscioli et al. 2017).

Within the complex energetic landscape and vibrational environment of the chlorosome, a set of long-lived oscillatory modes appear with low frequency which dephase over 1 ps in *Chloroflexus* and 1.5–2 ps in *Chlorobium* and are independent of spectral lineshape evolution (Savikhin et al. 1994, 1995a, b). These modes have been ascribed to either interfering ground state vibrations following resonant impulsive Raman scattering or intra/inter-molecular vibronic modes which may enhance electronic coherences by intensity borrowing from vibronic coupling (Ma et al. 1999; Prokhorenko et al. 2000; Dostál et al. 2014). Vibrational coherences would dephase too quickly to aid in transferring coherence between coherent domains given that the time scale of the random energy diffusion process between coherent domains is 4–5 ps between rods, however, they may aid in intra-domain relaxation (Prokhorenko et al. 2000; Dostál et al. 2014). Electronic or vibronic coherence dephasing over 60 fs can potentially allow the coherent domain to complete a sampling of the possible energy transfer pathways.

Growing evidence suggests that it may not be possible to separate vibrational and electronic dynamics of the FMO system either. In many cases the gaps in exciton energy and the energies of vibrations resident on chlorophylls from Raman studies are resonant, and hence, could result in strong vibronic coupling with persistent quantum beats corresponding to vibronic coherences. Part of this result came from trying to understand the problem of biological relevance and robustness of coherences to perturbations from the environment. The results suggested that the efficiency and coherence dynamics of FMO appear to be robust to alterations of the system's vibrational reservoir and chromophore excitation energies. Firstly, the presence of coherence may not be the result of evolutionary optimization of system-environment couplings but merely the result of optimizing the excitonic structure of the FMO (Hayes et al. 2011). Quantum beating frequencies and lifetimes of the strongest coherences between excitons in 2DES remain unchanged (1.1–1.4 ps) in FMO complexes that have: a random incorporation of different chlorophyll species with increased rigidity of their tails; 30% deuteration; or complete incorporation of carbon-13. Thus, at least some of the observed coherences do not arise from nuclear motions alone, which is particularly apparent in partially deuterated samples which suffer inhomogeneous broadening and dephasing as different chromophores now have different constituent vibrational

modes. Furthermore, coherences are also robust to changes in the excitonic structure, not just the thermal reservoir (Maiuri et al. 2018). Alterations to the excitonic Hamiltonian (and thus the exciton states) of the system can be made by site-directed mutagenesis thereby altering the site energies of specific chromophores by interaction with altered neighbouring amino acid residues. The changes in the exciton structure are observed via changes in the absorption spectra, however, the crystal structures of the mutants are unpublished. Again, the frequencies and dephasing times of the strongest quantum beats are resilient to alterations in excitonic structure. Both of these observations of robustness to changes in the vibrational environment and exciton structure suggests that quantum beats may arise from vibronic coherence. One puzzling feature of these results is that the dephasing rates have not shown any change, especially where the vibrational states are changed as electronic dephasing times are expected to be at least an order of magnitude smaller. Furthermore, by applying a vibronic model where vibrational modes are localised to single chromophores that comprise the exciton states, simulated long-lived coherences are in good agreement with the data (Christensson et al. 2012). The degree to which a system harbours vibronic states is dependent on the resonance in energy—the larger the detuning, the smaller the vibronic effects rendering the states practically separable—hence, the detuning of energy gaps may not have been enough to vibronically decouple the states completely. This remains an open question.

Vibronic states also make an appearance in light harvesting rings of purple bacteria. Quantum beats are observed for different polarization schemes in 2DES, with their lifetimes suggesting some specific quantum beats do not arise from purely electronic or vibrational coherences. It has thus been suggested that the B850 ring harbours coupled dark vibrational states and higher excited states (Singh et al. 2015). Furthermore, quantum beats are still observed between states of the B800 and B850 rings in organisms grown in 30% D_2O, with phase changes across the spectrum similar to that of the native scenario (Dahlberg et al. 2015). Possible vibronic coherence between states of LH2, while lasting less than 100 fs, has a similar lifetime to that of the energy transfer between them, however, its biological relevance is unclear assuming the upper state plays an intermediate role. Just as with states of LH2, vibronic resonances are potentially manifest in the B820 ring of LH1 which decay over 600 fs (Ferretti et al. 2014). Hence, vibronic coherences are potentially able to sustain electronic coherence on energy transfer time scales. Given the energies of exciton states and the frequencies of the quantum beats, it is suggested that a maximum averaged mixing ratio of vibrational and electronic states of 0.63 is present which drives coherent oscillations. In the LH1 of *T. tepidum,* calcium and barium metal ions can bind to the chlorophylls which alters the excitonic structure of the rings raising or lowering the absorption energy. A difference in the energy level structure that is produced by these variants does not appear to yield appreciable difference in population transfer or dephasing rates (estimated to be 57 fs via changes in the lineshape), however, phase changes in the spectra may be evidence for different pathways during energy transfer to the reaction centre (Ma et al. 2017). Oscillations are apparent for 1 ps and have two dominant modes, one of which is resonant with the energy difference of the first two excited states and the ground state and relaxation may progress in a vibronic manner which is accomplished by linking higher and lower states with vibrational coherences, independent of temperature.

A selection of open and closed state cryptophyte phycobiliproteins have been analysed and it appears that vibronic models best describe the dynamics in both systems (Jumper et al. 2018b). Within the evolution-

ary predecessor (the phycobilisome), vibronic mixing is also reported in allophycocyanin with coherence decaying within 35 fs, which increases the rate of internal conversion and subsequent relaxation to the lowest excited exciton state (Womick and Moran 2009). Both open and closed cryptophyte phycobiliproteins show significant coherence amplitudes for a specific vibrational mode. This vibrational mode has phase and amplitude changes across the spectrum which signify possible vibronic coupling for the closed state only (Arpin et al. 2015). Energy transfer rates and damping rates both scale with the intensity of coherence—which is a measure of vibronic intensity borrowing—and closed states cryptophyte phyocbiliproteins (owing to the delocalised exciton states) have an energy transfer rate that is double that of open (Jumper et al. 2018b). A follow-up study to the two-colour experiments performed on the cryptophyte phycobiliprotein PC645 was able to discern the vibronic nature of the quantum states by examining the two-colour spectra as a function of intensity (Novelli et al. 2015). With increasing intensity, one particular mode shows saturation (as opposed to a cubic increase as expected and observed for other modes). The only models that can accurately predict this behaviour are vibronic where the central DBV dimer is coupled to vibrational modes with this vibronic coherence decaying over 280 fs. In the DBV-PCB cross peaks of PC645 in 2DES, a quantum beat is observed which endures for 350 fs, showing indications of electronic coherence while being close in energy to vibrational states (Dean et al. 2016). Coherence between exciton states of DBV and PCB would be remarkable given the large detuning away from energetic resonance with each other. Hence, coherence may either be due to intensity borrowing from vibrations on each chromophore or, more likely given the energy gap involved, due to vibronic states resident across multiple chromophores from vibrations distorting the electronic state. For energy transfer purposes, it is proposed (Dean et al. 2016) that 3–4% of the excitation is transferred from the DBV pair to PCB chromophores in the vibronic state each vibrational period which acts as a mechanism of directing energy flow across very large gaps out of resonance at 3.5 times the rate predicted by FRET.

Reaction centres have a complex charge separation mechanism which is possibly aided by vibrations which move the electron to a position where it can tunnel to a neighbouring chromophore. The type-I reaction centre component of cyanobacteria through to higher plants is strongly coupled to low frequency chromophore and protein modes as in type-II reaction centres (Sarkisov et al. 2006). Many of the quantum beats are resonant with the energy gap involving special pair exciton states with similar frequency to that of type II reaction centres (Fuller et al. 2014). A vibronic model is in good agreement with the data suggesting the existence of coherence in excited states pre-charge separation. This resonance appears in simulation to speed up energy relaxation, energy transport and charge separation, which comes in bursts of charge separated state population (probability) increases in simulations.

At this point we need to recognise that limited research has been done to understand the nature of energy transport in the antennae of the larger light harvesting complexes (LHCI and LHCII) that surround the reaction centres in cyanobacteria and its descendants (Schlau-Cohen et al. 2012; Müh and Renger 2012; Wells et al. 2014; Duan et al. 2015; Lewis et al. 2016; Ramanan et al. 2017). Some research has provided numbers for bulk dephasing rates but less on specific vibrational and excitonic coherences, however, some specific oscillations are observed in 2DES. The reason for this is that the LHC's are very energetically complex, with large numbers of chromophores and it is difficult to tease apart specific coherences and energy transfer steps. It is possible that due to the

complex energetic landscape of LHC's may contain vibronic effects, especially given the mixture of chlorophyll and carotenoid that they often harbour.

Vibronic states are the true eigenstates of molecular systems—it is only when energy scales are separable enough that nuclear and electronic degrees of freedom are unentangled. As such, vibrational and excitonic coherence are the two extremes of coherences between vibronic states—either more excitonic or more vibrational. Given coupling between excited states of different chromophores, vibronic states may become delocalised across multiple chromophores and superpositions between these states may occur. Furthermore, it appears that a great number of biologically relevant energy transfer mechanisms/states lie in a regime where nuclear and electronic degrees of freedom cannot be approximated as separable. Vibronic states themselves give rise to mechanisms producing an energy transfer speed-up as a form of generalised Förster transfer (Jumper et al. 2018a). In this case, the overlap between donor and acceptor spectra is increased by the presence of vibronic states. This in itself is a possible evolutionary path where site energies and vibrational environments have been robustly tuned such that conical interactions and vibronically mixed states occur. Lastly, it is unclear if the loses from transferring electronic excited state energy into vibrational energy are balanced by the gains in transfer rate and furthermore it is unclear as to what tuning vibronic coupling and coherence is optimising with respect to biological light harvesting.

E. Process Coherence

Process coherence is a very particular case of quantum coherence where an initial coherent superposition of states engages in successive interactions (processes) and coherence between states is retained as the process progresses. It is possibly manifest during down-hill energy transfer steps where the state of the environment impinges on the success of the energy/charge transfer process. This means that a given process has potentially many possible splintering routes the system can sojourn through, allowing the superposition to spread to a great many states and select a finial state that is most viable given the environment at some later point in time. A possible manifestation of process coherence is within the reaction centre prior to charge separation. In the space of possible system states, *charge transfer* states need to be included which represent the system when an electron is stripped from the electron donor and the electron itself is transferred between chromophores. The various charge transfer states can also remain in a superposition of the reaction centre exciton states for a similar length of time and are influenced by all the same conditions as excitation energy transfer.

In type-II reaction centres, coherences in the electrochromic shift (a colour change due to local electric fields and redox reactions—namely charge separation) of the bacteriochlorophyll absorption band suggest the possibility of coherent electron transfer to the $P^{+}H_{A}^{-}$ state. One of the ultra low frequency quantum beats perhaps modulates the electrochromic shift (not just the P to P∗ transition) and given spectral dependence of this low frequency mode is coupled to the formation of the B_{A}^{-} state (Vos et al. 1998). There is also the possibility of another channel through which charge transfer can occur, initiated by the formation of an exciton chlorophyll state which decays to a $P^{+}B^{-}$ state with a time scale of 0.2–0.5 ps (Ma et al. 2018). The coherences are likely vibronic in nature given the resonance between vibrational energies, energy differences between the donor and acceptor states and the coherence energy with lifetimes of 54 fs, highlighted by the anti-diagonal broadening in 2DES. The two routes of electron transfer in type-I reaction centres are shown in Fig. 15.3b and proceed via the special pair-chlorophyll charge separated state coupled to

the special pair exciton state (pathway I) or via a mixed exciton/charge separated chlorophyll-pheophytin state (pathway II) (Romero et al. 2014, 2017). The three states initiating the two transfer pathways have varying degrees of delocalisation and exciton/charge transfer character. Two separate quantum beats have been observed that suggest vibronic coupling firstly between the states of pathway I and secondly between all three states. Vibronic states again emerge due to the confluence of the exciton energy gap and the energy of one vibrational quanta. Coherences present across the states initiating charge separation suggest a mechanism of coherent charge transfer showing long-lived coherences over 500 ps. Considering these states initiate both pathways, it is possible that this allows sampling of the energy landscape before selecting the most viable path given the present state of the environment. It is not necessarily that the electron and hole (a quasiparticle referring to the absence of electron) are coherent—it is more that the electron states, independent of the hole, are coherent.

It has also been suggested that wavelike transfer is present in the FMO complex, as the excitation samples the space of excitons as it move to the lowest energy state (which has been explained in the section on excitonic coherences). There are many possible pathways for excitation transfer through the system as seen in 2DES spectra, with the most prevalent being those with chromophore overlap between excitons. Coherence between excitons can thus produce process coherence and wavelike energy transfer throughout the complex down to the trap site which funnels to the reaction centre. These claims are often refuted by the fact that energy transfer may merely be modulated by vibronic coupling given the appearance of coherence in the spectra (Engel et al. 2007; Hayes et al. 2010; Panitchayangkoon et al. 2010, 2011; Thyrhaug et al. 2016, 2018; Duan et al. 2017).

Some mention of process coherence in LH2 is alluded to in the above sections, however, using single molecule tools single instances of energy transfer can be observed (not just an ensemble average) which can provide details on specific processes (Hildner et al. 2013). Quantum beats are observed and persist for at least 400 fs across all LH2 complexes, each with a distinct period, leading to a broad distribution indicating energy transfer is robust to static disorder (randomising the exciton states in the ensemble, their energies and transfer pathways). It is suggested that these persistent oscillations correspond to coherence between excitons in B800 and B850 to an optically dark state of B850, with coherence surviving long enough to average over local inhomogeneities of the excited state and allow for funnelling to the lowest energy state. A π phase jump in quantum beats is noted in the first 10 fs which may result from a change in accumulated phase during relaxation which may imply a modification of the energy transfer pathways towards a different low energy optically accessible state of B850 and hence long-lived coherences may play a role in allowing flexibility in transfer pathways.

Process coherence is the most debatable quantum behaviour in light harvesting systems. It is the most non-trivial effect as it suggests wave-like, non-local transport throughout the system and hence a larger degree of correlation than possibly allowed by the environment. Given the recent data presenting the case for coherent vibronic coupling instead of wavelike quantum transport, it is possibly unlikely that process coherence is present is most systems studied. There is some compelling evidence in that process coherence allows reaction centres to sample their initiating states for charge separation providing robustness—yet for many other systems robustness may come from other mechanisms. There has been a lot of debate around whether or not there is a quantum speed-up in light harvesting and an increase in quantum efficiency due to pro-

cess coherence or *quantum random walks* which is central to discussion on non-trivial quantum coherent effects in biology. Most other coherent phenomena mentioned are not under such scrutiny—such as the existence of excitons, vibrational coherence and vibronic states.

F. Protein and Solvent Effects

While the light-active molecules that support the excitons are the chromophores, the effects of the environment surrounding the chromophores are important in governing their behaviour. The environment, in this case, is composed of the surrounding protein and the solvent which can induce alterations to chromophore energy transfer and coherence. The most trivial effect the protein has on the chromophores is to "straight jacket" the chromophores by providing a scaffold that is quasi-rigid on the energy transfer timescale. As such, it will tune the chromophores via both setting their conformations and determining their electrostatic environments, impacting their electronic energy levels and thus supporting resonances and hence coherence. One non-trivial effect is that the environment may not be purely Markovian; that is, the time scale over which the environment relaxes to thermal equilibrium and loses memory (environment correlation time) is longer than the energy transfer time. In this case, the environment can remove phase information from one chromophore via discrete vibrational wave packets and then reinject the phase information and energy at a later time, possibly to a different chromophore, reinvigorating coherence. Furthermore, when chromophores are embedded in the same protein matrix their local environments are now correlated meaning that vibrations in the environment may influence the chromophores in the same or similar manner. For chromophores separated by distances comparable to even a fraction of a protein, this effect would be negligible, because the time over which mechanical perturbations propagate is long compared with interaction times—the prediction of the speed with which a disturbance propagates through a protein is reported to be on the order of 5 nm/ps (Young et al. 2013) and direct measurements of the speed of protein disturbances using time-resolved crystallography via X-ray free electron laser (in bacteriorhodopsin) is on the order of 2 nm/ps (Nogly et al. 2018). Locally, protein disturbances may influence energy transfer via specific vibrations but it is unlikely that any globally concerted dynamics will occur, especially due to dissipation and perturbation from the solvent. Hence, global vibrational coherences between molecules may not be transferred mechanically via the protein and must propagate electromagnetically.

Owing to the nature of the persistence of coherences in FMO under perturbation of the vibrational environment and excitonic Hamiltonian (described above), it has been postulated that correlated motions in the protein environment around the chromophores may play a critical role in supporting robust coherences. A correlated, fluctuating electrostatic environment provided by the protein may protect quantum coherences if they exist on the appropriate timescales enabling oscillatory population dynamics (Panitchayangkoon et al. 2010). If system-environment coupling is strong enough, fluctuations may cause entanglement with the environment in a non-trivial way and energy/information may be exchanged between system and environment on a femtosecond time scale (Panitchayangkoon et al. 2011). By looking at the movement of peaks in the spectra corresponding to each exciton in FMO, excitons appear to experience correlated oscillations with frequencies agreeing with that of excited state vibrations (Rolczynski et al. 2018). This correlation lasts for much of the first picosecond of the spectral evolution. Correlations may be explained by the residence of vibrations on individual chlorophylls that comprise each

different exciton—local motions on one chromophore affect multiple excitons and the global exciton energy. Excitons may also possibly be inheriting vibrational phase information from each other which enhances quantum beating lifetimes. Coupling of vibrational modes in different chromophores at distant ends of the protein can not be a mechanical effect as the speed of sound in a protein is too slow. Thus, electromagnetic interactions may correlate vibrations in distinct chromophores separated by protein, possibly by exciton overlap. Synchronised oscillations may stem from embedding multiple identical chromophores with the same internal vibrational modes in close proximity within an organized protein matrix and the response of the chromophores ensures that the spectral motions in the excited state will be correlated.

In open form cryptophyte phycobiliproteins, the central pair of chromophores is separated by a large water filled hole. In PC577 (McClure et al. 2014), oscillatory dynamics decaying over 62 fs and 46 fs are observed which may correspond to reorganisation of the solvent in the water filled hole. This may generate a "solvent quake" which is observed as a redshift in emission energy. This mechanism may be involved in the functioning of the central pair of open form PBPs that is now separated and their interaction mediated by the solvent. However, the organisation of the solvation shell may be irrelevant to energy transfer. Due to the residence of the cryptophyte phycobiliproteins in the thylakoid lumen, energy transfer must be robust to alterations in pH regardless of the origin of coherence (or if not, must provide some alteration to energy transfer to avoid oxidative stress). For pH values between 5.7 and 7.4, oscillatory dynamics appear to be robust for PC645 (Turner et al. 2012). At all pH values, modes decay on timescales of 170–300 fs. Hence, the protein appears to protect quantum beats against pH quenching.

It is unknown if the protein and solvent play any non-trivial role in photosynthetic light harvesting or whether they contribute to coherence—apart from straightjacketting the chromophores as to limit quenching and tuning the site energies and vibrational environment. Protein motions appear to be too slow to provide transduction of energy or phase information on a meaningful timescale, however, locally, this may not be the case. Any correlation set-up between vibrational states is more than likely to be electromagnetic and not mechanical and the prospect of solvent reorganisation as a signal transduction mechanism still requires elucidation.

V. Summary and Conclusions

Structural studies, particularly x-ray crystallography, have shown that light harvesting and photosynthetic proteins organise and arrange light-active chromophore molecules in order to capture light energy, funnel it to a target, and, in the case of reaction centres, facilitate the creation of a charge separated state to power photosynthesis. In many of these proteins, chromophores are arranged so that they are at high density, tightly-packed and in physical contact. Indeed, the green photosynthetic bacterial chlorosome has jettisoned the protein and stacked chromophores into organised structures within a lipid compartment, gaining maximal chromophore density.

The tight packing of chromophores is usually associated with strong coupling. This coupling means that the chromophores do not act independently when interacting with electromagnetic fields, instead they form delocalised excitons. In the multi-chromophore exciton, the energy levels are split, producing transitions with higher and lower energy when compared to isolated chromophores. Thus, the tight packing of chromophores has two consequences for light harvesting: it increases the physical capture

area of the antenna; and it broadens the absorption spectrum. Each of these consequences could be seen as an enhancement of the properties of the antenna complex and hence, may be selected for by evolution. In the extreme cases, chromophore packing is extended around circular arrays (LH1 and LH2) or linear arrays (chlorosome). In these cases, the exciton structure is dynamically delocalised. The exciton states can migrate through the system via diffusion. The challenge in these systems is understanding how the excitation can leave the system, ultimately progressing to the photosystem or reaction centre with high probability.

The advent of ultrafast, femtosecond laser technology has facilitated the development of spectroscopic techniques that probe energy transfer pathways through light harvesting and photosynthetic systems and proteins. These measurements have observed quantum beats in most biological light harvesting systems/proteins, with beat lifetimes ranging from ~10 fs through to ps. The presence of beats is a signature for underlying coherent phenomena. The difficulty is determining the nature of these coherences and whether they play a role in photosynthesis and/or light harvesting. When chromophore complexes form excitons delocalised across the chromophore array, beats often arise from superpositions of exciton states. Although interpretation is still mired in controversy, the beat frequencies and decoherence times are usually commensurate with vibrational and vibronic states. Purely vibrational coherences are not likely to play key roles in light harvesting, however, we note that they may be important in the function of bacteriorhodopsin, which directly converts a photon to an energy gradient via pumping a proton across a membrane. It is also apparent that time scales of coherence and time scales of energy transfer are commensurate as are the energy scales of couplings and environmental effects in most light harvesting systems. As such, energy transfer lies in an intermediate region that is not strictly classical nor is it quantum mechanical. It is an unresolved issue whether or not this enhances or diminishes transfer, however, theoretical studies indicate that energy transfer in this regime enhances transfer rates beyond that of classical hopping and purely quantum transport—as per the section '*Decoherence'* (Yin et al. 2008; Rebentrost et al. 2009).

There is growing consensus that most observed quantum beat signals that are relevant to energy transport are of a mixed, vibronic nature. Vibronic states result from mixing of vibrational states with electronic states in a non-separable manner. Vibronic coherences are likely to be important in energy transport within pigment/protein complexes when the vibrational energy is isoenergetic with the exciton energy gaps. Taken together, there is considerable evidence for non-trivial quantum effects within individual light harvesting and photosynthetic proteins. The presence of strongly-coupled chromophores leads to exciton states, with broader spectral coverage and possibly coherent dynamics. Vibronic coherences may play a role in excitation transfer through the protein's chromophore system, depositing the excitation in some final acceptor or trap state.

In contrast, there is very little evidence for quantum effects being involved in energy transfer between individual proteins. Thus, the pathway from the initially excited protein to the final destination in the reaction centre/photosystem is likely to proceed via a series of mostly incoherent transfers a-la FRET. Coherent superpositions of chromophores within a protein effectively enhance the rate of transfer to other proteins by increasing the dipole moment leading to super-transfer. For soluble protein systems such as the cryptophytes or the dinoflagellates, little is known about the ultrastructural organisation of these soluble luminal proteins, hence, the pathway to the photosystem remains a mystery. The phycobilisome, however, appears to be a prime example of a very

successful light harvesting system that does not utilise coherent phenomena. To date, there is no experimental evidence of any large scale quantum effects in the assembly. There is, however, evidence for delocalised excitonic states within the individual phycobiliprotein trimers and hexamers, extending their spectral properties. The phycobilisome appears to have optimised light harvesting photon efficiency by constructing an antenna with coordinated energy and spatial gradients from the high-energy rod tips to the lowest energy chromophores near the junction of the PBS with the photosystem.

Finally, there is debatable evidence for process coherence in light harvesting systems. Namely, coherences that occur between different pathways of a reaction. Specifically, these coherences are observed in reaction centres where several initiating states are coherent before a pathway is selected. Some evidence suggests this occurs during transport through the FMO. In purple bacteria, coherences between the exciton states of the B800 ring appear to have quantum control via a phase shift when transported down to the B850 ring. This phase shift would suggest a selection of pathway from an initial superposition based on the state of the environment. This potentially manifests as a means of increasing robustness in energy transfer.

This review only contains a brief overview of observations and analysis of quantum beats in biological light harvesting systems. Some systems have been omitted for the sake of brevity and many more studies exist for most of the systems discussed. While being worthy of discussion, we have omitted some analyses due to their complexity, however, these can be found within the references. New systems are being discovered and more precise methods are being developed to tease apart the nature and origin of quantum beats in light harvesting systems, and more generally, light-activated biological systems.

VI. New Horizons

The development of new techniques is needed to further dissect energy transfer pathways. Spectroscopic techniques that shows promise in extracting the nature of coherences and the mixing of vibrational and excitonic coherences are higher-dimensional (3D and above) pump probe techniques (Fidler et al. 2010; Zhang et al. 2013; Oliver et al. 2014; Loukianov et al. 2017; Goodknight and Aspuru-Guzik 2017; Harel 2018; Hutson et al. 2018). In these techniques, different parts of the spectrum (optical and infrared) are excited to generate a fifth order (or higher) correlation map of vibrational and excitonic coherences and can also be coupled to different optical phenomena (such as the Stark effect and circular dichroism).

Current experimental techniques require the use of femtosecond laser pulses to prepare the initial state of the system. An open question that needs to be addressed is the initial correlation between chromophore excitations as prepared by the laser. As all the frequencies of the laser pulse are coherent with one another (unlike sunlight), initial correlations can be prepared by the laser between energetically different exciton states. Furthermore, if an excitation is localised to a single chromophore in a coupled system, it is in a superposition of exciton states. Hence, beats would be present in a localised system when excited in the energy basis.

One further issue with most spectroscopic measurements is that all system measurements suffer averaging. That is to say that different members of the ensemble are performing different processes at once and upon averaging much of the coherent nature is coarse grained away. Using single molecule techniques, it is possible to forage for individual pathways, their probability and the distribution of time scales for coherence in these systems.

VII. The Wrong Question: "Does Evolution Select for Non-trivial Quantum Effects?"

The existence of quantum coherent mechanisms takes different forms and plays different roles in different organisms. Namely, quantum coherence can be used for: coupling of chromophores via excitons as a bridge between states; efficient funnelling of energy from a higher to a lower exciton state via vibronic coherence; and wavelike transport through clusters and superpositions of states that allow for robustness in choice of energy transfer pathways. The word *used* is possibly a bad turn of phrase as it implies that quantum mechanisms can be switched on and off, which really gets to the key point about quantum coherence in nature: quantum mechanics is ubiquitous. In many biological processes the quantum mechanisms are obvious, however, the presence or role of more wavelike transport properties is still debated.

The question of whether or not quantum coherence is selected for may not be the right one to ask. Nature is inherently quantum mechanical and, as such, any interaction must have some obligate quantumness that cannot be switched off. Teasing apart whether efficiency in ordered chromophore assemblies, for example, is driven by coherence or by large interaction energies is an unanswerable question. Analysis of similar light harvesting systems with different coherence times due to temperature or chromophore separation (as in cryptophytes) may be of some benefit in understanding the nature of quantum processes in light harvesting. Regardless, with large interaction energies comes quantum effects which means one cannot fully discern whether or not coherence is a spandrel or a property that is selected for during evolution.

Acknowledgments

We would like to thank the efforts of Ivan Kassal and Roger Hiller for their detailed critiques and illuminating insights into the many facets of this project. Thank you to Ashkan Roozbeh for providing the data analysis and images used in Fig. 15.2. We would also like to thank Neil Robertson, Katharine Michie and Sophia Goodchild for not only contributing to the review from which this chapter was birthed (Rathbone et al. 2018a, b), but for helping us learn how to unveil quantum mechanics to the biochemist.

References

Adolphs J, Renger T (2006) How proteins trigger excitation energy transfer in the FMO complex of green sulfur bacteria. Biophys J 91:2778–2797

Allen JF, Martin W (2007) Evolutionary biology: out of thin air. Nature 445:610–612

Arpin PC, Turner DB, McClure SD et al (2015) Spectroscopic studies of cryptophyte light harvesting proteins: vibrations and coherent oscillations. J Phys Chem B 119:10025–10034

Ballottari M, Mozzo M, Girardon J et al (2013) Chlorophyll triplet quenching and photoprotection in the higher plant monomeric antenna protein Lhcb5. J Phys Chem B 117:11337–11348

Berera R, van Grondelle R, Kennis JTM (2009) Ultrafast transient absorption spectroscopy: principles and application to photosynthetic systems. Photosynth Res 101:105–118

Bodył A, Moszczyński K (2006) Did the peridinin plastid evolve through tertiary endosymbiosis? A hypothesis. Eur J Phycol 41:435–448

Book LD, Ostafin AE, Ponomarenko N et al (2000) Exciton delocalization and initial dephasing dynamics of purple bacterial LH2. J Phys Chem B 104:8295–8307

Bricker W, Lo C (2015) Efficient pathways of excitation energy transfer from delocalized excitons in the peridinin–chlorophyll –protein complex. J Phys Chem B 119(18):5755–5764

Cardona T (2014) A fresh look at the evolution and diversification of photochemical reaction centers. Photosynth Res 126:111–134

Chachisvilis M, Sundström V (1996) Femtosecond vibrational dynamics and relaxation in the core light-harvesting complex of photosynthetic purple bacteria. Chem Phys Lett 261:165–174

Chachisvilis M, Kühn O, Pullerits T, Sundström V (1997) Excitons in photosynthetic purple bacteria: wavelike motion or incoherent hopping? J Phys Chem B 101:7275–7283

Cheng Y-C, Fleming GR (2008) Coherence quantum beats in two-dimensional electronic spectroscopy. J Phys Chem A 112:4254–4260

Chmeliov J, Songaila E, Rancova O et al (2013) Excitons in the LH3 complexes from purple bacteria. J Phys Chem B 117:11058–11068

Christensson N, Kauffmann HF, Pullerits T, Mančal T (2012) Origin of long-lived coherences in light-harvesting complexes. J Phys Chem B 116:7449–7454

Cohen Stuart TA, Vengris M, Novoderezhkin VI et al (2011) Direct visualization of exciton reequilibration in the LH1 and LH2 complexes of Rhodobacter sphaeroides by multipulse spectroscopy. Biophys J 100:2226–2233

Collini E (2012) Differences among coherent dynamics in evolutionary related light-harvesting complexes: evidence for subtle quantum-mechanical strategies for energy transfer optimization. In: Quantum optics II. SPIE, Bellingham

Collini E, Wong CY, Wilk KE et al (2010) Coherently wired light-harvesting in photosynthetic marine algae at ambient temperature. Nature 463:644–647

Curtis BA, Tanifuji G, Burki F et al (2012) Algal genomes reveal evolutionary mosaicism and the fate of nucleomorphs. Nature 492:59–65

Dahlberg PD, Norris GJ, Wang C et al (2015) Communication: coherences observed in vivo in photosynthetic bacteria using two-dimensional electronic spectroscopy. J Chem Phys 143:101101

Dean JC, Mirkovic T, Toa ZSD et al (2016) Vibronic enhancement of algae light harvesting. Chem 1:858–872

Delaye L, Valadez-Cano C, Pérez-Zamorano B (2016) How really ancient is Paulinella Chromatophora? PLoS Curr 8. https://doi.org/10.1371/currents.tol.e68a099364bb1a1e129a17b4e06b0c6b

Di Valentin M, Carbonera D (2017) The fine tuning of carotenoid–chlorophyll interactions in light-harvesting complexes: an important requisite to guarantee efficient photoprotection via triplet–triplet energy transfer in the complex balance of the energy transfer processes. J Phys B Atomic Mol Phys 50:162001

Diffey WM, Homoelle BJ, Edington MD, Beck WF (1998) Excited-state vibrational coherence and anisotropy decay in the Bacteriochlorophyll a Dimer protein B820. J Phys Chem B 102:2776–2786

Dostál J, Mančal T, Vácha F et al (2014) Unraveling the nature of coherent beatings in chlorosomes. J Chem Phys 140:115103

Dostál J, Pšenčík J, Zigmantas D (2016) In situ mapping of the energy flow through the entire photosynthetic apparatus. Nat Chem 8:705–710

Doust AB, Marai CNJ, Harrop SJ et al (2004) Developing a structure–function model for the Cryptophyte Phycoerythrin 545 using ultrahigh resolution crystallography and ultrafast laser spectroscopy. J Mol Biol 344:135–153

Duan H-G, Stevens AL, Nalbach P et al (2015) Two-dimensional electronic spectroscopy of light-harvesting complex II at ambient temperature: a joint experimental and theoretical study. J Phys Chem B 119:12017–12027

Duan H-G, Prokhorenko VI, Cogdell RJ et al (2017) Nature does not rely on long-lived electronic quantum coherence for photosynthetic energy transfer. Proc Natl Acad Sci 114:8493–8498

Edington MD, Riter RE, Beck WF (1995) Evidence for coherent energy transfer in Allophycocyanin Trimers. J Phys Chem 99:15699–15704

Engel GS, Calhoun TR, Read EL et al (2007) Evidence for wavelike energy transfer through quantum coherence in photosynthetic systems. Nature 446:782–786

Ferretti M, Novoderezhkin VI, Romero E et al (2014) The nature of coherences in the B820 bacteriochlorophyll dimer revealed by two-dimensional electronic spectroscopy. Phys Chem Chem Phys 16:9930–9939

Fidler AF, Harel E, Engel GS (2010) Dissecting hidden couplings using fifth-order three-dimensional electronic spectroscopy. J Phys Chem Lett 1:2876–2880

Fidler AF, Singh VP, Long PD et al (2013) Time scales of coherent dynamics in the light-harvesting complex 2 (LH2) of Rhodobacter sphaeroides. J Phys Chem Lett 4:1404–1409

Fujimoto KJ, Balashov SP (2017) Vibronic coupling effect on circular dichroism spectrum: carotenoid–retinal interaction in xanthorhodopsin. J Chem Phys 146:095101

Fuller FD, Pan J, Gelzinis A et al (2014) Vibronic coherence in oxygenic photosynthesis. Nat Chem 6:706–711

Gantt E (1971) Chloroplast structure of the cryptophyceae: evidence for phycobiliproteins within intrathylakoidal spaces. J Cell Biol 48:280–290

Goodknight J, Aspuru-Guzik A (2017) Taking six-dimensional spectra in finite time. Science 356:1333

Gould SB, Fan E, Hempel F et al (2007) Translocation of a phycoerythrin α subunit across five biological membranes. J Biol Chem 282:30295–30302

Green BR (2011) Chloroplast genomes of photosynthetic eukaryotes. Plant J 66:34–44

Harel E (2018) Zooming in on vibronic structure by lowest-value projection reconstructed 4D coherent spectroscopy. J Chem Phys 148:194201

Harel E, Engel GS (2012) Quantum coherence spectroscopy reveals complex dynamics in bacterial light-harvesting complex 2 (LH2). Proc Natl Acad Sci U S A 109:706–711

Harrop SJ, Wilk KE, Dinshaw R et al (2014) Single-residue insertion switches the quaternary structure and exciton states of cryptophyte light-harvesting proteins. Proc Natl Acad Sci U S A 111:E2666–E2675

Hayes D, Panitchayangkoon G, Fransted KA et al (2010) Dynamics of electronic dephasing in the Fenna–Matthews–Olson complex. New J Phys 12:065042

Hayes D, Wen J, Panitchayangkoon G et al (2011) Robustness of electronic coherence in the Fenna–Matthews–Olson complex to vibronic and structural modifications. Faraday Discuss 150:459

Hildner R, Brinks D, Nieder JB et al (2013) Quantum coherent energy transfer over varying pathways in single light-harvesting complexes. Science 340:1448–1451

Hofmann E, Wrench PM, Sharples FP et al (1996) Structural basis of light harvesting by carotenoids: peridinin-chlorophyll-protein from Amphidinium carterae. Science 272:1788–1791

Hutson WO, Spencer AP, Harel E (2018) Ultrafast four-dimensional coherent spectroscopy by projection reconstruction. J Phys Chem Lett 9:1034–1040

Jonas DM (2003) Two-dimensional femtosecond spectroscopy. Annu Rev Phys Chem 54:425–463

Jumper CC, Rafiq S, Wang S, Scholes GD (2018a) From coherent to vibronic light harvesting in photosynthesis. Curr Opin Chem Biol 47:39–46

Jumper CC, van Stokkum IHM, Mirkovic T, Scholes GD (2018b) Vibronic wavepackets and energy transfer in cryptophyte light-harvesting complexes. J Phys Chem B 122:6328–6340

Jun S, Yang C, Isaji M et al (2014) Coherent oscillations in chlorosome elucidated by two-dimensional electronic spectroscopy. J Phys Chem Lett 5:1386–1392

Kim H, Li H, Maresca JA et al (2007) Triplet exciton formation as a novel photoprotection mechanism in chlorosomes of Chlorobium tepidum. Biophys J 93:192–201

Kraack JP, Buckup T, Hampp N, Motzkus M (2011) Ground- and excited-state vibrational coherence dynamics in Bacteriorhodopsin probed with degenerate four-wave-mixing experiments. ChemPhysChem 12:1851–1859

Lee H, Cheng Y-C, Fleming GR (2007) Coherence dynamics in photosynthesis: protein protection of excitonic coherence. Science 316:1462–1465

Lewis NHC, Gruenke NL, Oliver TAA et al (2016) Observation of electronic excitation transfer through light harvesting complex II using two-dimensional electronic-vibrational spectroscopy. J Phys Chem Lett. https://doi.org/10.1021/acs.jpclett.6b02280

Loukianov A, Niedringhaus A, Berg B et al (2017) Two-dimensional electronic stark spectroscopy. J Phys Chem Lett 8:679–683

Ma Y-Z, Aschenbrücker J, Miller M, Gillbro T (1999) Ground-state vibrational coherence in chlorosomes of the green sulfur photosynthetic bacterium Chlorobium phaeobacteroides. Chem Phys Lett 300:465–472

Ma F, Yu L-J, Hendrikx R et al (2017) Excitonic and vibrational coherence in the excitation relaxation process of two LH1 complexes as revealed by two-dimensional electronic spectroscopy. J Phys Chem Lett 8:2751–2756

Ma F, Romero E, Jones MR et al (2018) Vibronic coherence in the charge separation process of the Rhodobacter sphaeroides reaction center. J Phys Chem Lett 9:1827–1832

MacColl R, Eisele LE, Marrone J (1999) Fluorescence polarization studies on four biliproteins and a Bilin model for phycoerythrin 545. Biochim Biophys Acta Bioenerg 1412:230–239

Maiuri M, Ostroumov EE, Saer RG et al (2018) Coherent wavepackets in the Fenna-Matthews-Olson complex are robust to excitonic-structure perturbations caused by mutagenesis. Nat Chem 10:177–183

Marin A, Doust AB, Scholes GD et al (2011) Flow of excitation energy in the cryptophyte light-harvesting antenna phycocyanin 645. Biophys J 101:1004–1013

McClure SD, Turner DB, Arpin PC et al (2014) Coherent oscillations in the PC577 Cryptophyte antenna occur in the excited electronic state. J Phys Chem B 118:1296–1308

Mirkovic T, Ostroumov EE, Anna JM et al (2016) Light absorption and energy transfer in the antenna complexes of photosynthetic organisms. Chem Rev 117:249–293

Morden CW, Sherwood AR (2002) Continued evolutionary surprises among dinoflagellates. Proc Natl Acad Sci U S A 99:11558–11560

Müh F, Renger T (2012) Refined structure-based simulation of plant light-harvesting complex II: linear optical spectra of trimers and aggregates. Biochim Biophys Acta 1817:1446–1460

Nango E, Royant A, Kubo M et al (2016) A three-dimensional movie of structural changes in bacteriorhodopsin. Science 354:1552–1557

Neilson JAD, Durnford DG (2010) Structural and functional diversification of the light-harvesting

complexes in photosynthetic eukaryotes. Photosynth Res 106:57–71

Nogly P, Weinert T, James D et al (2018) Retinal isomerization in bacteriorhodopsin captured by a femtosecond x-ray laser. Science 361. https://doi.org/10.1126/science.aat0094

Novelli F, Nazir A, Richards GH et al (2015) Vibronic resonances facilitate excited-state coherence in light-harvesting proteins at room temperature. J Phys Chem Lett 6:4573–4580

Oesterhelt D, Stoeckenius W (1973) Functions of a new photoreceptor membrane. Proc Natl Acad Sci 70:2853–2857

Oliver TAA, Lewis NHC, Fleming GR (2014) Correlating the motion of electrons and nuclei with two-dimensional electronic-vibrational spectroscopy. Proc Natl Acad Sci U S A 111:10061–10066

Paleček D, Edlund P, Westenhoff S, Zigmantas D (2017) Quantum coherence as a witness of vibronically hot energy transfer in bacterial reaction center. Sci Adv 3:e1603141

Panitchayangkoon G, Hayes D, Fransted KA et al (2010) Long-lived quantum coherence in photosynthetic complexes at physiological temperature. Proc Natl Acad Sci U S A 107:12766–12770

Panitchayangkoon G, Voronine DV, Abramavicius D et al (2011) Direct evidence of quantum transport in photosynthetic light-harvesting complexes. Proc Natl Acad Sci U S A 108:20908–20912

Prokhorenko VI, Steensgaard DB, Holzwarth AR (2000) Exciton dynamics in the chlorosomal antennae of the green bacteria Chloroflexus aurantiacus and Chlorobium tepidum. Biophys J 79:2105–2120

Prokhorenko VI, Nagy AM, Waschuk SA et al (2006) Coherent control of retinal isomerization in bacteriorhodopsin. Science 313:1257–1261

Ramanan C, Ferretti M, van Roon H et al (2017) Evidence for coherent mixing of excited and charge-transfer states in the major plant light-harvesting antenna, LHCII. Phys Chem Chem Phys 19:22877–22886

Raszewski G, Diner BA, Schlodder E, Renger T (2008) Spectroscopic properties of reaction center pigments in photosystem II core complexes: revision of the multimer model. Biophys J 95:105–119

Rathbone H, Davis J, Michie K, Goodchild S, Robertson N, Curmi P (2018a) Coherent phenomena in photosynthetic light harvesting: part one–theory and spectroscopy. Biophys Rev 10:1427–1441

Rathbone H, Davis J, Michie K, Goodchild S, Robertson N, Curmi P (2018b) Coherent phenomena in photosynthetic light harvesting: part two–observations in biological systems. Biophys Rev 10(5):1443–1463

Raymond J, Zhaxybayeva O, Gogarten JP et al (2002) Whole-genome analysis of photosynthetic prokaryotes. Science 298:1616–1620

Rebentrost P, Mohseni M, Kassal I et al (2009) Environment-assisted quantum transport. New J Phys 11:033003

Richards GH, Wilk KE, Curmi PMG, Davis JA (2014) Disentangling electronic and vibrational coherence in the Phycocyanin-645 light-harvesting complex. J Phys Chem Lett 5:43–49

Roach T, Krieger-Liszkay A (2012) The role of the PsbS protein in the protection of photosystems I and II against high light in Arabidopsis thaliana. Biochim Biophys Acta 1817:2158–2165

Rolczynski BS, Zheng H, Singh VP et al (2018) Correlated protein environments drive quantum coherence lifetimes in photosynthetic pigment-protein complexes. Chem 4:138–149

Romero E, Augulis R, Novoderezhkin VI et al (2014) Quantum coherence in photosynthesis for efficient solar-energy conversion. Nat Phys 10:676–682

Romero E, Prior J, Chin AW et al (2017) Quantum – coherent dynamics in photosynthetic charge separation revealed by wavelet analysis. Sci Rep 7. https://doi.org/10.1038/s41598-017-02906-7

Roscioli JD, Ghosh S, LaFountain AM et al (2017) Quantum coherent excitation energy transfer by carotenoids in photosynthetic light harvesting. J Phys Chem Lett 8:5141–5147

Sarkisov OM, Gostev FE, Shelaev IV et al (2006) Long-lived coherent oscillations of the femtosecond transients in cyanobacterial photosystem I. Phys Chem Chem Phys 8:5671–5678

Savikhin S, Zhu Y, Lin S et al (1994) Femtosecond spectroscopy of Chlorosome antennas from the Green photosynthetic bacterium Chloroflexus aurantiacus. J Phys Chem 98:10322–10334

Savikhin S, van Noort PI, Blankenship RE, Struve WS (1995a) Femtosecond probe of structural analogies between chlorosomes and bacteriochlorophyll c aggregates. Biophys J 69:1100–1104

Savikhin S, van Noort PI, Zhu Y et al (1995b) Ultrafast energy transfer in light-harvesting chlorosomes from the green sulfur bacterium Chlorobium tepidum. Chem Phys 194:245–258

Schlau-Cohen GS, Ishizaki A, Calhoun TR et al (2012) Elucidation of the timescales and origins of quantum electronic coherence in LHCII. Nat Chem 4:389–395

Scholes GD, Mirkovic T, Turner DB et al (2012) Solar light harvesting by energy transfer: from ecology to coherence. Energy Environ Sci 5:9374

Singh VP, Westberg M, Wang C et al (2015) Towards quantification of vibronic coupling in photosynthetic antenna complexes. J Chem Phys 142:212446

Spörlein S, Zinth W, Wachtveitl J (1998) Vibrational coherence in photosynthetic reaction centers observed in the Bacteriochlorophyll anion band. J Phys Chem B 102:7492–7496

Streltsov AM, Vulto SIE Y, Shkuropatov A et al (1998) BAand BBAbsorbance perturbations induced by coherent nuclear motions in reaction centers from Rhodobacter sphaeroidesupon 30-fs excitation of the primary donor. J Phys Chem B 102:7293–7298

Strümpfer J, Schulten K (2009) Light harvesting complex II B850 excitation dynamics. J Chem Phys 131:225101

Thyrhaug E, Žídek K, Dostál J et al (2016) Exciton structure and energy transfer in the Fenna–Matthews–Olson complex. J Phys Chem Lett 7:1653–1660

Thyrhaug E, Tempelaar R, Alcocer MJP et al (2018) Identification and characterization of diverse coherences in the Fenna–Matthews–Olson complex. Nat Chem. https://doi.org/10.1038/s41557-018-0060-5

Turner DB, Wilk KE, Curmi PMG, Scholes GD (2011) Comparison of electronic and vibrational coherence measured by two-dimensional electronic spectroscopy. J Phys Chem Lett 2:1904–1911

Turner DB, Dinshaw R, Lee K-K et al (2012) Quantitative investigations of quantum coherence for a light-harvesting protein at conditions simulating photosynthesis. Phys Chem Chem Phys 14:4857–4874

van der Weij-De Wit CD, Doust AB, van Stokkum IHM et al (2006) How energy funnels from the phycoerythrin antenna complex to photosystem I and photosystem II in cryptophyte Rhodomonas CS24 cells. J Phys Chem B 110:25066–25073

Vos MH, Lambry JC, Robles SJ et al (1991) Direct observation of vibrational coherence in bacterial reaction centers using femtosecond absorption spectroscopy. Proc Natl Acad Sci U S A 88:8885–8889

Vos MH, Jones MR, Hunter CN et al (1994) Coherent dynamics during the primary electron-transfer reaction in membrane-bound reaction centers of Rhodobacter sphaeroides. Biochemistry 33:6750–6757

Vos MH, Jones MR, Martin J-L (1998) Vibrational coherence in bacterial reaction centers: spectroscopic characterisation of motions active during primary electron transfer. Chem Phys 233:179–190

Wells KL, Lambrev PH, Zhang Z et al (2014) Pathways of energy transfer in LHCII revealed by room-temperature 2D electronic spectroscopy. Phys Chem Chem Phys 16:11640–11646

Westenhoff S, Paleček D, Edlund P et al (2012) Coherent picosecond Exciton dynamics in a photosynthetic reaction center. J Am Chem Soc 134:16484–16487

Wilk KE, Harrop SJ, Jankova L et al (1999) Evolution of a light-harvesting protein by addition of new subunits and rearrangement of conserved elements: crystal structure of a cryptophyte phycoerythrin at 1.63-a resolution. Proc Natl Acad Sci U S A 96:8901–8906

Womick JM, Moran AM (2009) Exciton coherence and energy transport in the light-harvesting dimers of allophycocyanin. J Phys Chem B 113:15747–15759

Wong CY, Alvey RM, Turner DB et al (2012) Electronic coherence lineshapes reveal hidden excitonic correlations in photosynthetic light harvesting. Nat Chem 4:396–404

Yin Y, Katsanos DE, Evangelou SN (2008) Quantum walks on a random environment. Phys Rev A 77. https://doi.org/10.1103/physreva.77.022302

Young HT, Edwards SA, Gräter F (2013) How fast does a signal propagate through proteins? PLoS One 8:e64746

Zhang JM, Shiu YJ, Hayashi M et al (2001) Investigations of ultrafast Exciton dynamics in Allophycocyanin Trimer†. J Phys Chem A 105:8878–8891

Zhang Z, Wells KL, Seidel MT, Tan H-S (2013) Fifth-order three-dimensional electronic spectroscopy using a pump-probe configuration. J Phys Chem B 117:15369–15385

Zhang J, Ma J, Liu D et al (2017) Structure of phycobilisome from the red alga Griffithsia pacifica. Nature 551:57–63

Chapter 16

Light-Harvesting Complexes of Diatoms: Fucoxanthin-Chlorophyll Proteins

Claudia Büchel*
Institute of Molecular Sciences, Goethe University, Frankfurt am Main, Germany

Abbreviations

Chl	*chlorophyll*
Dd	*diadinoxanthin*
Dt	*diatoxanthin*
FCP	*fucoxanthin chlorophyll protein*
Fx	*fucoxanthin*
HL	*high light*
LHC	*light-harvesting complex*
NPQ	*non-photochemical quenching*
PS	*photosystem*

I. Introduction

Diatoms are unicellular, eukaryotic organisms that belong to the Stramenopiles (together with e.g. brown algae, Xanthophytes and Chrysophytes) and are characterized by an ornamental silica shell. They derived from a so-called secondary endosymbiosis, whereby a eukaryotic host engulfed a predecessor of red algae, which was reduced to become the future chloroplast (Cavalier-Smith 2013; Keeling 2013; Chap. 2). Thus, the chloroplast is surrounded by four membranes and the thylakoids run in parallel throughout the whole plastid in bands of three thylakoids each (six thylakoid membranes surrounding three separate lumina - see Fig. 16.2). Since eukaryotic oxygenic photosynthesis relies on the same basic mechanisms, i.e., charge separation in both photosystem I and II that are connected by the electron transport chain, the splitting of water to provide electrons for eventually reducing ferredoxin and $NADP^+$, and the

*Author for correspondence, e-mail: C.Buechel@bio.uni-frankfurt.de

A. W. D. Larkum et al. (eds.), *Photosynthesis in Algae: Biochemical and Physiological Mechanisms*, Advances in Photosynthesis and Respiration 45, https://doi.org/10.1007/978-3-030-33397-3_16

chemiosmotic production of ATP driven by the pH gradient, most of the light reactions and the complexes involved are similar in diatoms compared to e.g. higher plants. However, the light-harvesting systems differ. In contrast to their red algal ancestors, diatoms possess only membrane intrinsic light-harvesting systems belonging to the large LHC protein family. Since they bind fucoxanthin as main light-harvesting pigment besides chlorophylls, they are also referred to as fucoxanthin-chlorophyll-proteins (FCPs). This review deals with the different polypeptides, their arrangement into complexes and their location in the thylakoid membrane, the specific pigments bound to the antenna proteins and the excitation energy transfer between them, as well as with the regulation of FCP expression.

II. Genes Coding for FCP Polypeptides

In higher plants, three major groups of LHC proteins serve as antenna for the photosystems that consist of three membrane helices and a small, membrane parallel helix. One group is bound to PSI (Lhca), the other two groups serve PSII as monomeric, minor antenna closest to the PSII core (Lhc4-6) or constitute the major, trimeric LHCII (Lhcb1-3, see other chapters). In addition, PsbS, a four helix protein of the LHC family, is involved in non-photochemical quenching (Li et al. 2000). All these proteins were characterised biochemically and except for PsbS, their location proven. Until now, distinction of different FCP proteins in diatoms was done mostly by analysis and annotation of the sequenced genomes (Armbrust et al. 2004; Bowler et al. 2008) or of EST data of diatoms (Mock et al. 2006; Park et al. 2010). Originally three groups were distinguished: Lhcf, Lhcr and Lhcx. Lhcf are the dominant proteins, found in the main FCP fraction that can be isolated by e.g. sucrose density centrifugation (Lepetit et al. 2007; Gundermann and Büchel 2008; Gundermann et al. 2013), and share high homologies with antenna proteins from related groups, e.g. brown algae. Lhcr were termed according to their sequence homology with red algal Lhca. The remaining group, Lhcx, shows homologies to the LhcSR (former LI818) proteins of green algae and other eukaryotic algae (see Chap. 10) as recognised already in 1998 by Eppard and Rhiel. They have a prospective role in photoprotection, thus functionally replacing PsbS in diatoms and other eukaryotic algae. Since especially the Lhcf group is rather diverse, other (sub)groups were postulated lately as well (Lhcz: Dittami et al. (2010); Neilson and Durnford (2010), Lhcy: Nymark et al. (2013), for review see Büchel (2015)). Each of the groups contains many members, e.g. in *Thalassiosira pseudonana* 6 *Lhcx*, 11 *Lhcf* and 14 *Lhcr* genes are annotated, coding for 5 different Lhcx, 9 different Lhcf and 14 different Lhcr proteins, due to the identity of Lhcx1/2, Lhcf1/2 and Lhcf8/9. *Phaeodactylum tricornutum* contains 4 *Lhcx* genes and proteins, 14 *Lhcr* and proteins, and 17 *Lhcf* genes coding for 15 different Lhcf proteins due to the identity of Lhcf3/4 and Lhcf6/7. In both organisms all these proteins were detected by mass spectrometry, and in *P. tricornutum* mRNAs for all genes were analysed and showed slightly different dependencies on pre-illumination conditions (Nymark et al. 2009), excluding the possibility of pseudogenes. In cases were genes are almost identical this holds even for major parts of their 5' and 3' untranslated regions, and they are most likely the result of recent gene duplication. In some species like the psychrophilic diatom *Fragilariopsis cylindrus* (Mock et al. 2017) numbers of LHC related genes are even higher, including some duplications as well. In summary, the number of different FCP polypeptides is smaller than the actual number of genes, but the number of proteins is still high compared to those present in higher plants.

III. Supramolecular Organisation of FCP Complexes

Many of the major antenna complexes of diatoms were reported to be trimeric like those of higher plants, and they share the same overall features (Röding et al. 2018). Diatoms can be divided in two subgroups, the pennate and centric diatoms. Concerning their FCP repertoire, differences were proven. Pennate diatoms like e.g. *P. tricornutum* contain various trimeric FCPs, composed of different Lhcf polypeptides (Lepetit et al. 2007; Grouneva et al. 2011; Gundermann et al. 2013). No higher oligomers of specific polypeptide composition were demonstrated so far, although trimers seem to associate to higher oligomers as well (Lepetit et al. 2007). Recently, a molecular structure of an FCP complex from *P. tricornutum* became available, whereby the Lhcf4 polypeptides were arranged in dimers (Wang et al. 2019). Centric diatoms like *C. meneghiniana*, *T. pseudonana* and *C. gracilis* also possess trimers, but additionally tetramers were found in the PSII supercomplex of *C. gracilis* (Pi et al. 2019; Nagao et al. 2019), and higher oligomers of a specific Lhcf composition can be isolated (Beer et al. 2006; Grouneva et al. 2011; Gundermann et al. 2013; Nagao et al. 2013a), whereby the Lhcf polypeptides that constitute the higher oligomers are only found in centrics (Gundermann et al. 2013). These higher oligomeric states most probably resemble nonamers (Röding et al. 2018). The trimeric FCP complex of *C. meneghiniana* was termed FCPa, in contrast to the higher oligomers called FCPb (Beer et al. 2006). FCPa is composed of Lhcf polypeptides, but in addition contains a Lhcx protein (named Fcp6 in *C. meneghiniana*), whereby the amount is correlated with the light intensity during growth (Beer et al. 2006; Gundermann and Büchel 2008), supporting the attribution of Lhcx proteins to light protection. In *T. pseudonana*, several Lhcx proteins were found in the trimeric FCP complexes, including Lhcx1, the orthologue of Fcp6. On the other hand, no Lhcx proteins could be found in the trimeric complexes of pennate diatoms so far, although Lhcx are found in the major FCP fraction that can be isolated via sucrose gradient centrifugation after mild solubilisation (Lepetit et al. 2010; Schaller-Laudel et al. 2015). Thus, Lhcx in pennates seems to be rather loosely attached to the major trimeric FCP fraction, whereas in centrics it is more tightly associated with the FCPa trimers.

In contrast to centric diatoms, the pennate *P. tricornutum* is characterised by a long wavelength fluorescence emission at room temperature of around 710 nm, which is especially prominent when cells are cultured under red light (Fujita and Ohki 2004). This fluorescence was attributed to a PSII-FCP complex at the time, but biochemical data were scarce. Kotabová et al. (2014) were the first to report such an antenna in *Chromera velia*, a species belonging to the Chromalveolates like dinoflagellates (see Chap. 2), and later Herbstová et al. (2015) could demonstrate the same for *P. tricornutum*. The main component is Lhcf15, a protein which is not closely related to the other main Lhcf proteins that constitute the trimers (Gundermann et al. 2013), and has no close homologue in centrics like *T. pseudonana*. This red-shifted antenna was interpreted as an evolutionary adaptation towards survival in shaded environments. On the other hand, the strength of the 710 nm fluorescence in different diatom strains correlates with the photoprotection capacity (Lavaud and Lepetit 2013).

Recently, the molecular structure of a PSII supercomplex consisting of the PSII core and its associated FCP became available for the centric diatom *Chaetoceros gracilis*. Although the core is almost identical and the overall arrangement of antenna proteins also resembles the built of complexes of higher plants, two decisive differences are present: monomers are arranged differently compared to the minor LHC of higher plants, and the FCPs complexes directly attached to PSII are tetramers, in contrast to what was reported

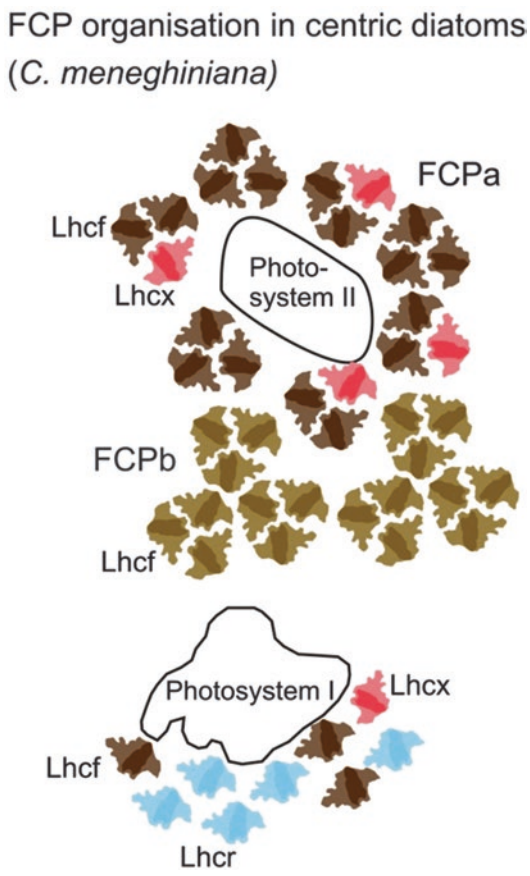

Fig. 16.1. Organisation of the peripheral FCPs in centric diatoms (here: *Cyclotella meneghiniana*). Trimeric FCPa complexes consist of Lhcf polypeptides (brown) and Lhcx (red), whereby the amount of the latter depends on the light intensity during growth (Beer et al. 2006). FCPb is built of different Lhcf proteins (light brown). No biochemical evidence for the arrangement of FCPa/FCPb and the photosystems exists, but excitation energy is predominantly transferred into PSII (Chukhutsina et al. 2013). PSI is a monomer (Veith and Büchel 2007) with Lhcr (blue) (Veith et al. 2009), Lhcf and Lhcx (Grouneva et al. 2011) attached. Note that in pennate diatoms FCPb is lacking and that Lhcx was not found in trimers, so its precise localisation is still unknown

for the pool of additional, more peripheral FCP complexes. The precise arrangement of those peripheral antenna complexes around PSII is still unknown (Fig. 16.1).

The situation is different for PSI (Fig. 16.1): in various species as well as with different methods PSI complexes containing FCP polypeptides could be prepared and characterised (Lepetit et al. 2007; Veith and Büchel 2007; Veith et al. 2009; Grouneva et al. 2011). Like in higher plants, PSI of diatoms is a monomer, with light-harvesting proteins attached (Veith and Büchel 2007; Veith et al. 2009). No structure is available but from preliminary analysis the overall structure seems to resemble the structure of PSI in *Chlamydomonas reinhardtii*, i.e., a monomeric PSI with several LHC attached (Kargul et al. 2003). From sequence similarities it was always assumed that Lhcr proteins serve as PSI antenna, which is indeed the case. However, also Lhcf and even Lhcx (Grouneva et al. 2011) are found in the antenna of PSI in both pennates and centrics, making Lhcr specific for PSI (like Lhca in higher plants), but not the sole antenna serving this photosystem. The antenna composition was shown to vary dependent on growth light intensity (Juhas and Büchel 2012). So far no changes in antenna composition depending on pre-illumination on a fast time scale comparable to those reported for green organisms were reported, but diatoms generally lack the phenomenon called state 1-state 2 transition (Owens 1986).

IV. Arrangement of Photosynthetic Complexes of Diatoms in the Thylakoid Membrane

Diatoms, like other Stramenopiles, display a characteristic arrangement of thylakoid membranes, whereby six membranes compose a band of three thylakoids that span the whole length of the plastids. Of old there is a debate whether this represents true ‘stacking’, i.e., whether there is a close appression of the inner membranes, or whether distances are not as small as in grana stacks. Neither in thin-sectioning transmission electron microscopy (Pyszniak and Gibbs 1992) nor in small angle neutron scattering (Nagy et al. 2011, 2012; Ünnep et al. 2014) is resolution good enough to unequivocally solve this question. Electron microscopy some-

times reveals distinct spacing between single thylakoids in a band arguing against close appression, whereas the distances measured by small angle neutron scattering are even significantly smaller than for grana (170 versus 210 Å). This uncertainty goes along with our lack of knowledge about i) complete or partial segregation of PSI and PSII complexes and ii) the forces which keep the inner membranes of one band together. Two models about the possible segregation are available in literature (Fig. 16.2): Immuno-labelling followed by electron microscopy showed a slight enrichment of PSI in the outer membranes (Pyszniak and Gibbs 1992; Flori et al. 2017) accompanied by an enrichment of PSII in the inner membranes (Flori et al. 2017). FCPs were more homogeneously distributed (Pyszniak and Gibbs 1992), but the antibody used recognised all different FCPs. In contrast, using antibodies specifically directed against Fcp4 (a Lhcr protein), Fcp2 (belonging to Lhcfs) or Fcp6 (Lhcx) of *C. meneghiniana*, no differences in distribution between the PSI antenna (Fcp4) and the main FCP complexes (Fcp2) could be detected using the same method and freeze-fracture immunolabelling (Westermann and Rhiel 2005). Based on the data by Pyszniak and Gibbs (1992), but also taking into account the consideration that electron transport seems impossible if PSI is only located in the outer membranes, Lepetit et al. (2012) proposed a model where PSI is enriched in the outer membranes, whereas PSII is found more often in the inner membranes. The more peripheral FCPs, i.e. those not directly bound to either photosystem, are predicted to be localised predominantly in the inner membrane. The segregation is hypothesised to be based on differences in the lipid composition of the outer and inner membranes, with the outer ones specifically enriched in sulfoquinovosyl diacylglyceride, whereas the inner membranes are speculated to contain more monogalactosyl diacylglyceride. Indeed, when isolating peripheral FCPs, a higher percentage of monogalactosyl diacylglyceride than in whole thylakoids was found (Lepetit et al. 2012). Differences in lipid composition were also discussed as reason for photosystem segregation by Büchel et al. (1992), albeit without having data about the lipid composition at the time. Using freeze-fracture electron microscopy to investigate the protein complex distribution in the thylakoids of a species of Xanthophytes, which are closely related to diatoms and display the same overall thylakoid arrangement, a patchwise enrichment in PSI complexes was found, whereas PSII was more homogeneously distributed. Note that both models can easily be combined by an enrichment of PSI patches on the outer membranes of a

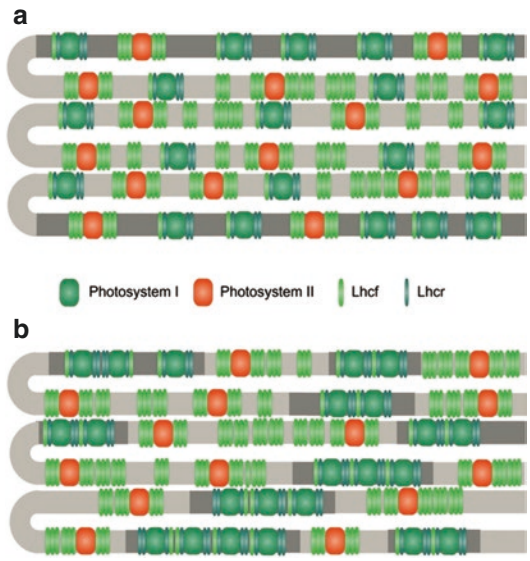

Fig. 16.2. Two different models of the distribution of photosystems and peripheral FCP complexes in diatoms. (**a**) was adopted from Lepetit et al. (2012), whereas (**b**) is an adaptation from the model for an alga from a group related to diatoms (*Pleurochloris meiringensis*, Xanthophyceae) by Büchel et al. (1992). For clarity, only photosystem II (red), photosystem I (green) and FCPs (either built of Lhcf, green, or Lhcr, dark green) are shown, whereas Lhcx proteins are omitted. In (**a**) the enrichment of the outer membranes in sulfoquinovosyl diacylglyceride is shown in dark grey, whereas the monogalactosyl diacylglyceride enriched inner membranes are depicted in light grey. In (**b**) the unknown lipids assumed to determine the areas enriched in PSI are shown in dark grey

band, and an enrichment of SQDG around PSI might be speculated as a reason, but no data exist so far about the real distribution of lipids across the six membranes. Two problems remain in all models so far: (i) ATPases can only be located in the peripheral membranes due to their bulkiness. Thus, only the two outer thylakoids would contribute to ATP production and this sink would be missing in the middle thylakoid. Since this is impossible, connections or anastomoses have to be present. These were indeed identified by classical transmission electron microscopy, albeit rarely (Bedoshvili et al. 2009). Recently, using more advanced methods, Flori et al. (2017) reported again connections, but unfortunately resolution is still too low to gain a precise 3D picture. (ii) the different FCP complexes are rather similar concerning their absorption capabilities (see below). When assuming close neighbourhood of PSI and PSII, spill-over, the transfer of energy from the higher energetic PSII to the lower lying PSI would become favoured, in the worst case leading to an under-excitation of PSII. The PSII/PSI stoichiometry is around one to three depending on growth conditions (Smith and Melis 1988; Strzepek and Harrison 2004), and thus not high enough to balance extremely uneven antenna or excitation energy distribution. The energetic separation of the two photosystems remains far from understood. In the related Dinoflagellates, a high percentage of PSII complexes involved in spill-over even under favourable light conditions was detected recently (Slavov et al. 2016). High spill-over rates might indeed occur also in the similarly built thylakoids of diatoms, but this has not been demonstrated yet. On the contrary, when studying excitation energy distribution between the photosystems in *C. meneghiniana*, a preferential excitation of PSII by FCPs but no substantial spill-over was reported (Chukhutsina et al. 2013). Studying electron transport, Flori et al. (2017) recently confirmed that spill over (see Chap. 10) is absent in diatoms.

V. Pigmentation of FCPs and Excitation Energy Transfer

As indicated by their name, FCPs bind Chl and fucoxanthin (Fx) as their main pigments (Fig. 16.3a), whereby the accessory Chl is Chl c. Estimates are in the range of maximal 8 Chl a/8 Fx/2 Chl c per monomer, a pigment ratio of 0.25 Chl *c*/1 Fx/1 Chl *a*, at least for FCPa and FCPb of *C. meneghiniana*. Variations are mainly due to different isolation protocols (Beer et al. 2006; Gundermann and Büchel 2008; Premvardhan et al. 2010). But there also seem to be differences depending on species, since for the oligomeric complex of *C. gracilis* 1 Chl *c* and 1.6 Fx per 1 Chl *a* are reported, whereas the trimer is even more heavily enriched in Fx as compared to C. *meneghiniana* FCPs with 0.6 Chl *c* and 1.9 Fx per Chl *a* (Nagao et al. 2013b). No absolute values per monomer were determined, but since the numbers reported for *C. meneghiniana* are already as high as in plant LHCII, and since the FCP trimer is smaller than LHCII (Röding et al. 2018) and thus does not allow for much more pigments, the amount of Chl a per monomer is likely reduced in the *C. gracilis* complexes at the expense of Chl *c* and Fx. For the pennate *P. tricornutum*, the Fx to Chl *a* values reported are usually slightly higher than for *C. meneghiniana*, although not as high as in *C. gracilis*. Values around 1.2 Fx/Chl *a* are consistently determined (Lavaud et al. 2003; Lepetit et al. 2007; Joshi-Deo et al. 2010; Gundermann et al. 2013) and in the structure 7 Chl *a*, 2 Chl *c*, 7 Fx and one diadinoxanthin were identified (Wang et al. 2019). On the other hand, the Chl *c* per Chl *a* ratio is also variable between different trimers, depending on the Lhcf proteins they consist of: whereas the main trimers composed of mainly Lhcf5 contain around 0.4 Chl *c* per Chl *a*, this value is only 0.35 in Lhcf4/Lhcf10 trimers (Gundermann et al. 2013).

The light-harvesting pigments Chl *a*, Chl *c* and Fx are accompanied by diadinoxanthin (Dd) and diatoxanthin (Dt), the main xantho-

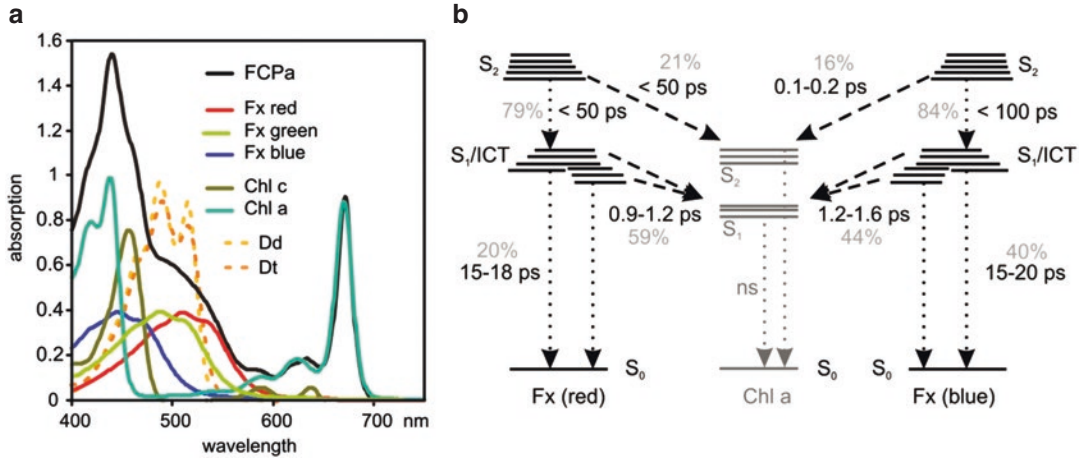

Fig. 16.3. (**a**) Typical absorption spectrum of a FCP complex (FCPa from *C. meneghiniana*, black line) and its pigments: Chl *a* (blue-green line), Chl *c* (olive-green line), and fucoxanthin bound in three different ways so that the absorption is more to the blue (Fx blue, blue line), intermediate (Fx green, green line) or to the red (Fx red, red line). Depending on light conditions during growth, different amounts of diadinoxanthin (yellow dotted line) and/or diatoxanthin (orange dotted line) are bound, which are not present in the FCPa spectrum shown here. Adopted from Premvardhan et al. (2009). (**b**) Energy transfer channels from Fx red and Fx blue to Chl a. Note that no transfer from Fx to Chl *c* was ever shown. The dotted arrows refer to internal conversion (relaxation by heat emission) and dashed lines demonstrate excitation energy transfer pathways. (Adopted from Gildenhoff et al. (2010a) and Gelzinis et al. (2015))

phyll cycle pigments of diatoms. The overall pool size of these two pigments and the epoxidation status (Dt/(Dt + Dd)) in cells as well as in FCPs depends on the culture conditions, predominantly the light intensity, and on the immediate pre-illumination of the cells (Lavaud et al. 2003; Gundermann and Büchel 2008; Lepetit et al. 2010; Gundermann et al. 2013). However, not every Dd and Dt molecule in cells is recovered when isolating FCPs. Part of it is bound to (the FCPs of) the photosystems, especially PSI (Veith and Büchel 2007; Veith et al. 2009; Lepetit et al. 2012), and some is argued to be found in the lipid phase (Lepetit et al. 2010), although Resonance Raman experiments have demonstrated that the Dd newly synthesised under high light is strongly influenced by a protein environment (Alexandre et al. 2014), pointing to at least close association with the proteins in their surrounding lipid shell. However, Dd as well as Dt do not participate in the excitation energy transfer inside the complexes (Papagiannakis et al. 2005; Gildenhoff et al. 2010a).

Fx is very efficient in excitation energy transfer to Chl *a* (Fig. 16.3b). This is mainly due to its additional so-called intramolecular charge transfer (ICT) state that is mixed with the first excited state (ICT/S1), leading to better energy transfer into the S1 state of Chl a than for carotenoids without a keto group in the conjugated system (Papagiannakis et al. 2005; Gildenhoff et al. 2010a, b; Nagao et al. 2013b). Fx is highly polarisable and one of the carotenoids exhibiting the largest shifts in absorption maxima upon binding to the proteins, leading to absorption up to 565 nm in the FCP complexes (Premvardhan et al. 2008). Since Fx is the only carotenoid contributing, a broad absorption between 490 and 565 nm, where neither Chl *a* nor Chl *c* can absorb, is only possible by Fx molecules bound in different ways (different polarity of the protein environment), leading to more blue shifted or red shifted absorption

features. Indeed, using Resonance Raman this was detected for FCP complexes of *C. meneghiniana* (Premvardhan et al. 2009) and also shown for *P. tricornutum* using electrochromic shift methods (Szabó et al. 2010).

Whereas energy transfer from Fx to Chl *a* is already fast with rates in the hundreds of fs to ps (Gildenhoff et al. 2010a; Gelzinis et al. 2015), transfer from Chl *c* to Chl *a* is even faster with 60 fs (Papagiannakis et al. 2005; Songaila et al. 2013; Butkus et al. 2015). However, the channels from Chl *c* and Fx into Chl *a* work independently, since Fx to Chl *c* transfer, although energetically possible, was never measured in any FCP complex.

In higher plant LHCII, strong excitonic coupling of Chl *a* molecules is enhancing robustness of light harvesting despite a protein environment always showing a certain degree of disorder. Strong excitionic interactions were never seen in circular dichroism spectra of diatom FCPs (Ghazaryan et al. 2016; Joshi-Deo et al. 2010). Recent single molecule spectroscopy data revealed that in FCPs the pigment energies are more susceptible to protein structural changes, but the complexes seem to use these fluctuations to switch frequently into low-energy states with improved light-harvesting properties (Krüger et al. 2017).

According to the structure of the FCP dimer of *P. tricornutum* (Wang et al. 2019), Fx replaces the luteins found in the centre of LHCII complexes (Wilhelm et al. 2006; Premvardhan et al. 2010) and acts as Chl triplet quencher as well (Di Valentin et al. 2013). These Fx molecules are assumed to be the more blue-shifted ones, whereas the red forms are located more peripherally. The Chl molecules close to the inner two helices (Chl a610, 612, 602 and 603 around helix 1 and 3, nomenclature according to Liu et al. (2004)) are conserved, but Chl a612 and Chl a603 are replaced by Chl *c*. Also Chl a604 and Chl a613 are conserved, whereas the other Chls have slightly different locations. The place left by the remaining Chls in LHC is filled by the additional carotenoid molecules, since much more carotenoids per Chl are found in FCP compared to LHCII (Premvardhan et al. 2010).

Due to the lack of grana and thus the lack of methods for easy separation of membranes enriched in either PSI or PSII complexes, our knowledge about binding of the peripheral FCP complexes to photosystems is scarce. In addition, the absorption characteristics of FCPs are rather similar, hampering spectroscopic differentiation. Still, by using different excitation and detection wavelengths in kinetic studies, separation is possible. Using this, Chukhutsina et al. (2013) could demonstrate that most FCP complexes transfer their energy into PSII, and that the more red-shifted Fx molecules are mostly found in those FCPs as already seen by steady state spectroscopy (Szabó et al. 2010). Since FCPb is slightly more enriched in the red forms of Fx (Premvardhan et al. 2009), FCPb might be predominantly serving PSII, although biochemical hints for its connection to PSI exist as well (Veith et al. 2009).

VI. FCPs in Photoprotection

FCPa, the trimeric complex of *C. meneghiniana*, also contains Lhcx proteins, more specifically Fcp6 that is most closely related to Lhcx1 of *T. pseudonana* and *P. tricornutum*. The participation of Lhcx1-4 in photoprotection of *P. tricornutum* (Bailleul et al. 2010; Taddei et al. 2016; Lepetit et al. 2016) and of Lhcx proteins in *T. pseudonana* (Zhu and Green 2010; Dong et al. 2015) was proven recently, but their role is still not entirely clear. Most molecular data concerning the mechanism of Lhcx action were acquired for FCPs from centric diatoms and are summarised first: as a constituent of the trimeric FCPa in *C. meneghiniana*, Fcp6(Lhcx1) might be pigmented as well, in contrast to PsbS but in agreement with LhcSR, the analogue protein in green algae and mosses

(Alboresi et al. 2008; Bonente et al. 2008, 2011; Peers et al. 2009), but proof is lacking so far. FCPa was shown to change fluorescence yield in dependence on pH (Gundermann and Büchel 2012). A strong decrease of the lumenal pH *in vivo* is only achieved by high light intensities, and the concomitant lowering of the fluorescence yield thus fits to the energy (ΔpH) dependent part of the phenomenon called non-photochemical quenching (NPQ), where heat emission is increased at the expense of fluorescence in order to protect the photosystems against a surplus of light. FCPa was shown to decrease its fluorescence when the distance between complexes becomes reduced, i.e. by aggregation of the complexes inside the membrane (Gundermann and Büchel 2008, 2012). This is accompanied by the occurrence of a red-shifted fluorescence emission band that has an extremely low yield but a strong charge transfer character (Wahadoszamen et al. 2013). In addition, a second quenching channel inside FCPa in the aggregated state was detected with virtually no difference in spectral shape to the unquenched chlorophylls, but faster than the red-shifted one (Ramanan et al. 2014). The reduction of fluorescence yield of FCPa is enhanced when higher amounts of Dt are bound (Gundermann and Büchel 2008, 2012), in accordance with *in vivo* data. In whole cells, two quenching mechanisms, dependent on Dt or independent of it, were distinguished (Grouneva et al. 2008; Miloslavina et al. 2009), and mechanisms further elaborated by Chukhutsina et al. (2014). Under a surplus of light, FCP complexes first aggregate, thereby lowering their fluorescence yield (fast, Dt independent quench). Later, Dt is synthesised and fluorescence yield of FCP complexes still bound to PSII is further diminished by the binding of Dt. Some stay closely attached to PSII, whereas a small pool becomes detached (slow, Dt dependent quench). The Dt-dependent and Dt–independent but pH dependent lowering of fluorescence is only present in FCPa, but not in FCPb *in vitro*, and is therefore most likely connected to the presence of Lhcx proteins in these complexes. So how is Lhcx1 (Fcp6) acting? As stated above no data about the single protein concerning even its pigmentation exist. Zhu and Green (2010) analysed the different Lhcx proteins in the related species *T. pseudonana* on gene and protein levels and correlated their abundance with NPQ. They concluded that Lhcx6 might play a role in direct Dt binding, whereas Lhcx1 was argued to have a more structural role. The structural role of Lhcx1 was supported lately by data from Ghazaryan et al. (2016) using knock-down strains with reduced Fcp6(Lhcx1) levels. In those cells NPQ was diminished and changes in the interaction of pigments inside thylakoids due to the reduced amount of Lhcx1 could be observed, but surprisingly pigment interactions inside FCPa were not changed. This argues for Lhcx1 being able to change the supramolecular organisation in favour of NPQ, but not for its direct participation in quenching. Whereas Fcp6(Lhcx1) is found in higher amounts in FCPa under high light in *C. meneghiniana* (Beer et al. 2006), Lhcx6 was recently shown to be the only Lhcx protein in the centric diatom *T. pseudonana* that is found in higher amounts after light treatment (Dong et al. 2015) and that is strongly regulated under fluctuating light (Grouneva et al. 2016). However, astonishingly enough it was not found in the trimeric FCP in cells grown under high light (Grouneva et al. 2011). This absence argues for an additional role ‘outside’ the main trimeric FCPs, comparable to the situation in pennate diatoms. Unfortunately, no comparable detailed analyses are available for the involvement of the antenna system of pennates in NPQ, but Lhcx1 was proven to be necessary for NPQ (Bailleul et al. 2010) and Lhcx2-4 were shown to at least enhance maximal NPQ capacity (Taddei et al. 2016). Whereas Lhcx1-3 are up-regulated under high light conditions, Lhcx4 expression is suppressed in the light, making it hard to explain why it

enhances NPQ when constitutively overexpressed (Taddei et al. 2016). However, analysis with different light regimes (Lepetit et al. 2016) or lack of nutrients (Taddei et al. 2016) point to different contributions of Lhcx1-4 to NPQ under different conditions, but none of the proteins was ever found in purified trimeric FCP complexes. In principle, fast fluorescence kinetics are comparable between centrics and pennates (Miloslavina et al. 2009). Accordingly, isolated, Dt-containing FCPs showed the typical spectra of aggregated FCPs when incubated at low pH (Schaller-Laudel et al. 2015) and Lhcx proteins have protonable amino acid residues to sense the lumenal pH. However, the molecular mechanism of the action of Lhcx in pennates remains enigmatic.

VII. Regulation of FCP Expression

Diatoms are algae that do not possess flagellae or other means to efficiently move in a water column, only some pennates can move along the substrate by extruding substances to glide on along their raphe. This implies that e.g. diatoms living in tidal mud flats change their vertical position in and out of the sheltering mud to protect themselves against photoinhibition (Perkins et al. 2010), but planktonic organisms are mainly drifted by currents, tidal waves and so on. In addition, the spectral characteristics of open and tidal waters differ tremendously, and freshwater environments like lakes are characterised by the succession of different taxa blooming, also leading to changes in the light environment. All these differences imply that diatoms have to be able to adapt to changes in light climates on different time scales, whereby the requirements are species dependent according to the ecological niche they occupy. Both short term regulation (as e.g. the quenching mechanism discussed above) and long term acclimation adapt the photosynthetic apparatus of diatoms to an optimal function.

Perhaps the best studied field is the acclimation to high light (HL) intensities of white light. When diatoms adapt to long term high light conditions, changes in the whole chloroplast structure take place: the number of thylakoids is reduced, albeit without changing the characteristic banding pattern of three thylakoids each (Rosen and Lowe 1984; Janssen et al. 2001; Kudo et al. 2000; Davey and Geider 2001; Beer et al. 2011). On a molecular level, the expression of *Fcp* genes is light dependent, whereby *Lhcf* genes are down-regulated and *Lhcx* genes as well as proteins are up-regulated under HL conditions (Oeltjen et al. 2002, 2004; Becker and Rhiel 2006; Beer et al. 2006; Nymark et al. 2009). Promoter motifs were found in *Lhcx1, 2* and *4* of *P. tricornutum* (Taddei et al. 2016) that were originally identified as responsive to CO_2 limitation (Ohno et al. 2012) and later shown to enable a signal crosstalk between the CO_2 and light signals (Tanaka et al. 2016). Protective mechanisms like the enrichment in xanthophyll cycle pigments can also be observed under HL conditions (Goss et al. 2006; Schumann et al. 2007; Grouneva et al. 2008), and higher amounts of Diadinoxanthin and Diatoxanthin can be found in the FCP complexes (Gundermann and Büchel 2008).

As pointed out above, not only the light intensity but also the light quality might differ depending on environment, and can undergo changes. Early work by Oeltjen et al. (2002) already identified changes in the transcription of some *Fcp(Lhc)* genes under blue, green and red light in *C. meneghiniana* using dot-blots. A comprehensive microarray study of *P. tricornutum* by Valle et al. (2014) revealed that green and red light induced the expression of most *Lhcf* and *Lhcr* genes more strongly than white light, whereas blue light had an opposite effect. Not surprisingly *Lhcf15*, the gene for the constituent of the 'red antenna' in *P. tricornutum* (Herbstová et al. 2015), reacted most strongly to longer red light application. The opposite was true for the *Lhcx* genes that

were analysed (*Lhcx2-4*). Thus, *Lhc* expression, amongst a whole array of other genes, is strongly dependent on the light colour as well.

To sense changes in light conditions, diatoms rely on a set of photoreceptors, where the whole complement as predicted from genomic sequences has not been studied as yet. From the sequenced genomes the following (groups of) photoreceptors are predicted (for a review see Depauw et al. (2012), Oliveri et al. (2014), Wilhelm et al. (2014)): members of the cryptochrome/photolyase family, aureochromes and phytochromes. Whereas the two former are blue light receptors, the latter are sensors for the ratio of red to far red light. The cryptochrome/photolyase family comprises members that are true photoreceptors (cryptochromes) and enzymes working in DNA repair (photolyases) (Chaves et al. 2011). This strict division was challenged not only in diatoms, where bi-functional proteins were detected; CPF1 in *P. tricornutum* was demonstrated to exhibit a double function (Coesel et al. 2009), acting as a 6-4 photolyase and influencing the expression levels of several genes, *Lhcs* being amongst those; also CryP (Juhas et al. 2014; Büchel et al. 2017), the cryptochrome with the highest sequence similarity to plant cryptochromes found in *P. tricornutum*, is involved in the regulation of *Lhc* expression. Whereas CPF1 reduces the amounts of *Lhcx1-3* transcripts and has no influence on *Lhcx4* and *Lhcf2* (Coesel et al. 2009), CryP shows different effects: a reduction of CryP levels in *P. tricornutum* led to a decrease in Lhcx protein levels and an increase of Lhcf proteins (Juhas et al. 2014). Although protein and mRNA data cannot be directly compared, this demonstrates an antagonistic regulation by two photoreceptors of the same family, i.e. with the same chromophore (FAD). This might be explained by the different diurnal expression pattern of the two photoreceptors. In the case of CryP, mRNA levels have their maximum towards the end of the night, whereas CPF1 is only expressed after the onset of light (Oliveri et al. 2014). On the other hand, differences in absorption maxima and redox states of the relaxed photosensor were reported, most probably due to different binding of the chromophore to the apoproteins (Coesel et al. 2009; Juhas et al. 2014). Thus, CryP is also absorbing in the yellow and near red spectral region, due to binding of FAD as neutral radical. The down-stream mechanism of CryP was not studied yet, but for CPF1, inhibition of Clock: BMAL-mediated transcription was reported, and only CPF1 seems to be involved in the circadian clock (comparable to some plant and animal cryptochromes) (Coesel et al. 2009). Lhc expression in diatoms shows at least diurnal, in some cases circadian changes. Lhcf mRNA levels display a midday peak, whereas Lhcx are expressed mostly in the first hours of the day (Oeltjen et al. 2002, 2004; Siaut et al. 2007). However, the involvement of clock components has to be established still.

The second type of blue light sensors is presented by the aureochromes, which are only found in heterokont algae and contain FMN as chromophore, organised in a so-called LOV (Light-Oxygen-Voltage) domain. These photoreceptors are transcription factors that directly influence gene expression (Takahashi et al. 2007). Aureochrome 1a is assumed to bind directly to the promotor sequence of *Lhcx1* for up-regulation under blue light, although in general it acts as a transcriptional repressor as demonstrated using aureochrome 1a deficient mutants (Schellenberger Costa et al. 2013a, b).

Whereas the need for blue light sensing is almost self-evident for aquatic organisms, the use of red light sensing is more enigmatic. As pointed out above, phytochrome sequences can be found in the genomes of diatoms, and recently their expression and the function of the protein in far-red light sensing was demonstrated (Fortunato et al. 2016). In the water column far-red light from the sun is only detectable at the surface and slightly below, but fluorescence and raman scattering might generate far-

red light at greater depth as well. It may well be that the ubiquitous presence of diatoms in algal mats and stromatolites where NIR is present can account for this situation in some diatoms from the earliest times. Nevertheless, the use of phytochrome-mediated sensing must remain enigmatic (Fortunato et al. 2016). Shorter wavelengths, i.e. around 660 nm, were demonstrated to regulate mainly indirectly through fluxes generated by the light reactions of photosynthesis, whereby the redox state of the PQ pool is discussed as retrograde signal (Lepetit et al. 2013; Lepetit and Dietzel 2015). Since CryP has its FAD in the neutral radical state in the dark, exhibiting an absorption maximum at 638 nm (Juhas et al. 2014), it might also sense red light and be responsible for Lhc gene expression changes induced by this wavelength range (Valle et al. 2014). But involvement of cryptochromes and/or phytochromes in the expression of the many different *Lhcs* by red light still has to be examined in detail, especially for the red light induced antenna of *P. tricornutum*.

VIII. Open Questions

Although huge progress has been made during the last decades concerning the antenna structure and function in diatoms, some basic questions have remained unsolved so far. Why do diatoms contain so many different FCP polypeptides? Why do only centrics harbour special oligomeric FCP complexes, whereas pennates seem to rely solely on trimers that are, however, also able to form higher oligmers? What is the molecular mechanism of the contribution of the different Lhcx proteins in photoprotection, and how do they interact with the main FCP complexes? How is the excitation energy transfer to PSII versus PSI regulated and how are the photosystems distributed along the thylakoid membranes? And last but not least: how are fucoxanthin and Chl *c* synthesised? Diatoms account for about 25% of the yearly carbon assimilation on the Earth and are thus ecologically extremely important. In addition, diatoms are often used as model organisms for the larger group of Chl *c* (Fx)-containing algae (see Chaps. 2 & 10). Only answering the questions raised above will help in understanding their huge ecological success.

References

Alboresi A, Caffarri S, Nogue F, Bassi R, Morosinotto T (2008) In silico and biochemical analysis of *Physcomitrella patens* photosynthetic antenna: identification of subunits which evolved upon land adaptation. PLoS ONE 3(4):e2033

Alexandre MTA, Gundermann K, Pascal AA, van Grondelle R, Büchel C, Robert B (2014) Probing the carotenoid content of intact *Cyclotella* cells by resonance Raman spectroscopy. Photosynth Res 119(3):273–281

Armbrust EV, Berges JA, Bowler C, Green BR, Martinez D, Putnam NH, Zhou S, Allen AE, Apt KE, Bechner M, Brzezinski MA, Chaal BK, Chiovitti A, Davis AK, Demarest MS, Detter JC, Glavina T, Goodstein D, Hadi MZ, Hellsten U, Hildebrand M, Jenkins BD, Jurka J, Kapitonov VV, Kröger N, Lau WWY, Lane TW, Larimer FW, Lippmeier JC, Lucas S, Medina M, Montsant A, Obornik M, Schnitzler Parker M, Palenik B, Pazour GJ, Richardson PM, Rynearson TA, Saito MA, Schwartz DC, Thamatrakoln K, Valentin K, Vardi A, Wilkerson FP, Rokhsar DS (2004) The genome of the diatom *Thalassiosira pseudonana*: ecology, evolution, and metabolism. Science 306(5693):79–86

Bailleul B, Rogato A, de Martino A, Coesel S, Cardol P, Bowler C, Falciatore A, Finazzi G (2010) An atypical member of the light-harvesting complex stress-related protein family modulates diatom responses to light. Proc Natl Acad Sci U S A 107(42):18214–18219

Becker F, Rhiel E (2006) Immuno-electron microscopic quantification of the fucoxanthin chlorophyll a/c binding polypeptides Fcp2, Fcp4, and Fcp6 of *Cyclotella cryptica* grown under low- and high-light intensities. Int Microbiol 9(1):29–36

Bedoshvili YD, Popkova TP, Likhoshway YV (2009) Chloroplast structure of diatoms of different classes. Cell Tissue Biol 3(3):297–310

Beer A, Gundermann K, Beckmann J, Büchel C (2006) Subunit composition and pigmentation of fucoxanthin-chlorophyll proteins in diatoms: evidence for a subunit involved in diadinoxanthin and diatoxanthin binding. Biochemistry 45(43):13046–13053

Beer A, Juhas M, Büchel C (2011) Influence of different light intensities and different iron nutrition on the photosynthetic apparatus in the diatom *Cyclotella meneghiniana* (Bacillariophyceae). J Phycol 47(6):1266–1273

Bonente G, Passarini F, Cazzaniga S, Mancone C, Buia MC, Tripodi M, Bassi R, Caffarri S (2008) The occurrence of the psbS gene product in *Chlamydomonas reinhardtii* and in other photosynthetic organisms and its correlation with energy quenching. Photochem Photobiol 84(6):1359–1370

Bonente G, Ballottari M, Truong TB, Morosinotto T, Ahn TK, Fleming GR, Niyogi KK, Bassi R (2011) Analysis of LhcSR3, a protein essential for feedback de-excitation in the green alga *Chlamydomonas reinhardtii*. PLoS Biol 9(1):e1000577

Bowler C, Allen AE, Badger JH, Grimwood J, Jabbari K, Kuo A, Maheswari U, Martens C, Maumus F, Otillar RP, Rayko E, Salamov A, Vandepoele K, Beszteri B, Gruber A, Heijde M, Katinka M, Mock T, Valentin K, Verret F, Berges JA, Brownlee C, Cadoret J, Chiovitti A, Choi CJ, Coesel S, de Martino A, Detter JC, Durkin C, Falciatore A, Fournet J, Haruta M, Huysman MJJ, Jenkins BD, Jiroutova K, Jorgensen RE, Joubert Y, Kaplan A, Kröger N, Kroth PG, La Roche J, Lindquist E, Lommer M, Martin-Jézéquel V, Lopez PJ, Lucas S, Mangogna M, McGinnis K, Medlin LK, Montsant A, Oudot-Le Secq M, Napoli C, Obornik M, Parker MS, Petit J, Porcel BM, Poulsen N, Robison M, Rychlewski L, Rynearson TA, Schmutz J, Shapiro H, Siaut M, Stanley M, Sussman MR, Taylor AR, Vardi A, von Dassow P, Vyverman W, Willis A, Wyrwicz LS, Rokhsar DS, Weissenbach J, Armbrust EV, Green BR, Van de Peer Y, Grigoriev IV (2008) The *Phaeodactylum* genome reveals the evolutionary history of diatom genomes. Nature 456(7219):239–244

Büchel C (2015) Evolution and function of light harvesting proteins. J Plant Physiol 172(19):62–75

Büchel C, Wilhelm C, Hauswirth N, Wild A (1992) Evidence for a lateral heterogeneity by patch-work like areas enriched in photosystem I complexes in the three thylakoid lamellae of *Pleurochloris meiringensis* (Xanthophyceae). Cryptogam Bot 2:375–386

Büchel C, Wilhelm C, Wagner V, Mittag M (2017) Functional proteomics of light-harvesting complex proteins under varying light-conditions in diatoms. J Plant Physiol 217:38–43

Butkus V, Gelzinis A, Augulis R, Gall A, Büchel C, Robert B, Zigmantas D, Valkunas L, Abramavicius D (2015) Coherence and population dynamics of chlorophyll excitations in FCP complex: two-dimensional spectroscopy study. J Chem Phys 142(21):212414

Cavalier-Smith T (2013) Symbiogenesis: mechanisms, evolutionary consequences, and systematic implications. Annu Rev Ecol Evol Syst 44(1):145–172

Chaves I, Pokorny R, Byrdin M, Hoang N, Ritz T, Brettel K, Essen L, van der Horst GTJ, Batschauer A, Ahmad M (2011) The cryptochromes: blue light photoreceptors in plants and animals. Annu Rev Plant Biol 62(1):335–364

Chukhutsina VU, Büchel C, van Amerongen H (2013) Variations in the first steps of photosynthesis for the diatom *Cyclotella meneghiniana* grown under different light conditions. Biochim Biophys Acta 1827(1):10–18

Chukhutsina VU, Büchel C, van Amerongen H (2014) Disentangling two non-photochemical quenching processes in *Cyclotella meneghiniana* by spectrally-resolved picosecond fluorescence at 77 K. Biochim Biophys Acta 1837(6):899–907

Coesel S, Mangogna M, Ishikawa T, Heijde M, Rogato A, Finazzi G, Todo T, Bowler C, Falciatore A (2009) Diatom PtCPF1 is a new cryptochrome/photolyase family member with DNA repair and transcription regulation activity. EMBO Rep 10(6):655–661

Davey M, Geider RJ (2001) Impact of iron limitation on the photosynthetic apparatus of the diatom *Chaetoceros muelleri* (Bacillariophyceae). J Phycol 37(6):987–1000

Depauw FA, Rogato A, Ribera d'Alcalá M, Falciatore A (2012) Exploring the molecular basis of responses to light in marine diatoms. J Exp Bot 63(4):1575–1591

Di Valentin M, Meneghin E, Orian L, Polimeno A, Büchel C, Salvadori E, Kay CWM, Carbonera D (2013) Triplet–triplet energy transfer in fucoxanthin-chlorophyll protein from diatom *Cyclotella meneghiniana*: insights into the structure of the complex. Biochim Biophys Acta 1827(10):1226–1234

Dittami SM, Michel G, Collén J, Boyen C, Tonon T (2010) Chlorophyll-binding proteins revisited – a multigenic family of light-harvesting and stress proteins from a brown algal perspective. BMC Evol Biol 10:365

Dong Y-L, Jiang T, Xia W, Dong H-P, Lu S-H, Cui L (2015) Light harvesting proteins regulate non-photochemical fluorescence quenching in the marine diatom *Thalassiosira pseudonana*. Algal Res 12:300–330

Eppard M, Rhiel E (1998) The genes encoding light-harvesting subunits of *Cyclotella cryptica* (Bacillariophyceae) constitute a complex and heterogeneous family. Mol Gen Genet 260(4):335–345

Flori S, Jouneau P-H, Bailleul B, Gallet B, Estrozi LF, Moriscot C, Bastien O, Eicke S, Schober A, Bártulos CR, Maréchal E, Kroth PG, Petroutsos D, Zeeman S, Breyton C, Schoehn G, Falconet D, Finazzi G

(2017) Plastid thylakoid architecture optimizes photosynthesis in diatoms. Nat Commun 8:15885

Fortunato AE, Jaubert M, Enomoto G, Bouly J, Raniello R, Thaler M, Malviya S, Bernardes JS, Rappaport F, Gentili B, Huysman MJJ, Carbone A, Bowler C, d'Alcalà MR, Ikeuchi M, Falciatore A (2016) Diatom phytochromes reveal the existence of far-red-light-based sensing in the ocean. Plant Cell 28(3):616–628

Fujita Y, Ohki K (2004) On the 710 nm fluorescence emitted by the diatom *Phaeodactylum tricornutum* at room temperature. Plant Cell Physiol 45(4):392–397

Gelzinis A, Butkus V, Songaila E, Augulis R, Gall A, Büchel C, Robert B, Abramavicius D, Zigmantas D, Valkunas L (2015) Mapping energy transfer channels in fucoxanthin-chlorophyll protein complex. Biochim Biophys Acta 1847(2):241–247

Ghazaryan A, Akhtar P, Garab G, Lambrev PH, Büchel C (2016) Involvement of the Lhcx protein Fcp6 of the diatom *Cyclotella meneghiniana* in the macro-organization and structural flexibility of thylakoid membranes. Biochim Biophys Acta 1857(9):1373–1379

Gildenhoff N, Amarie S, Gundermann K, Beer A, Büchel C, Wachtveitl J (2010a) Oligomerization and pigmentation dependent excitation energy transfer in fucoxanthin-chlorophyll proteins. Biochim Biophys Acta 1797(5):543–549

Gildenhoff N, Herz J, Gundermann K, Büchel C, Wachtveitl J (2010b) The excitation energy transfer in the trimeric fucoxanthin-chlorophyll protein from *Cyclotella meneghiniana* analyzed by polarized transient absorption spectroscopy. Chem Phys 373(1–2):104–109

Goss R, Pinto EA, Wilhelm C, Richter M (2006) The importance of a highly active and Δ-pH-regulated diatoxanthin epoxidase for the regulation of the PS II antenna function in diadinoxanthin cycle containing algae. J Plant Physiol 163(10):1008–1021

Grouneva I, Jakob T, Wilhelm C, Goss R (2008) A new multicomponent NPQ mechanism in the diatom *Cyclotella meneghiniana*. Plant Cell Physiol 49(8):1217–1225

Grouneva I, Rokka A, Aro E (2011) The thylakoid membrane proteome of two marine diatoms outlines both diatom-specific and species-specific features of the photosynthetic machinery. J Proteome Res 10(12):5338–5353

Grouneva I, Muth-Pawlak D, Battchikova N, Aro E-M (2016) Changes in relative Thylakoid protein abundance induced by fluctuating light in the diatom *Thalassiosira pseudonana*. J Proteome Res 15(5):1649–1658

Gundermann K, Büchel C (2008) The fluorescence yield of the trimeric fucoxanthin-chlorophyll-protein FCPa in the diatom *Cyclotella meneghiniana* is dependent on the amount of bound diatoxanthin. Photosynth Res 95(2–3):229–235

Gundermann K, Büchel C (2012) Factors determining the fluorescence yield of fucoxanthin-chlorophyll complexes (FCP) involved in non-photochemical quenching in diatoms. Biochim Biophys Acta 1817(7):1044–1052

Gundermann K, Schmidt M, Weisheit W, Mittag M, Büchel C (2013) Identification of several subpopulations in the pool of light harvesting proteins in the pennate diatom *Phaeodactylum tricornutum*. Biochim Biophys Acta 1827(3):303–310

Herbstová M, Bína D, Koník P, Gardian Z, Vácha F, Litvín R (2015) Molecular basis of chromatic adaptation in pennate diatom *Phaeodactylum tricornutum*. Biochim Biophys Acta 1847(6–7):534–543

Janssen M, Bathke L, Marquardt J, Krumbein WE, Rhiel E (2001) Changes in the photosynthetic apparatus of diatoms in response to low and high light intensities. Int Microbiol 4(1):27–33

Joshi-Deo J, Schmidt M, Gruber A, Weisheit W, Mittag M, Kroth PG, Büchel C (2010) Characterization of a trimeric light-harvesting complex in the diatom *Phaeodactylum tricornutum* built of FcpA and FcpE proteins. J Exp Bot 61(11):3079–3087

Juhas M, Büchel C (2012) Properties of photosystem I antenna protein complexes of the diatom *Cyclotella meneghiniana*. J Exp Bot 63(10):3673–3681

Juhas M, von Zadow A, Spexard M, Schmidt M, Kottke T, Büchel C (2014) A novel cryptochrome in the diatom *Phaeodactylum tricornutum* influences the regulation of light-harvesting protein levels. FEBS J 281(9):2299–2311

Kargul J, Nield J, Barber J (2003) Three-dimensional reconstruction of a light-harvesting complex I-photosystem I (LHCI-PSI) supercomplex from the green alga *Chlamydomonas reinhardtii*. J Biol Chem 278(18):16135–16141

Keeling PJ (2013) The number, speed, and impact of plastid endosymbioses in eukaryotic evolution. Annu Rev Plant Biol 64(1):583–607

Kotabová E, Jarešová J, Kaňa R, Sobotka R, Bína D, Prášil O (2014) Novel type of red-shifted chlorophyll a antenna complex from *Chromera velia*. I. Physiological relevance and functional connection to photosystems. Biochim Biophys Acta 1837(6):734–743

Krüger TPJ, Malý P, Alexandre MTA, Mančal T, Büchel C, van Grondelle R (2017) How reduced excitonic coupling enhances light harvesting in the

main photosynthetic antennae of diatoms. Proc Natl Acad Sci U S A 114(52):E11063–E11071

Kudo I, Miyamoto M, Noiri Y, Maita Y (2000) Combined effects of temperature and iron on the growth and physiology of the marine diatom *Phaeodactylum tricornutum* (Bacillariophyceae). J Phycol 36(6):1096–1102

Lavaud J, Lepetit B (2013) An explanation for the inter-species variability of the photoprotective non-photochemical chlorophyll fluorescence quenching in diatoms. Biochim Biophys Acta 1827(3):294–302

Lavaud J, Rousseau B, Etienne A (2003) Enrichment of the light-harvesting complex in diadinoxanthin and implications for the nonphotochemical fluorescence quenching in diatoms. Biochemistry 42(19):5802–5808

Lepetit B, Dietzel L (2015) Light signaling in photosynthetic eukaryotes with 'green' and 'red' chloroplasts. Environ Exp Bot 114:30–47

Lepetit B, Volke D, Szabó M, Hoffmann R, Garab G, Wilhelm C, Goss R (2007) Spectroscopic and molecular characterization of the oligomeric antenna of the diatom *Phaeodactylum tricornutum*. Biochemistry 46(34):9813–9822

Lepetit B, Volke D, Gilbert M, Wilhelm C, Goss R (2010) Evidence for the existence of one antenna-associated lipid-dissolved and two protein-bound pools of diadinoxanthin cycle pigments in diatoms. Plant Physiol 154(4):1905–1920

Lepetit B, Goss R, Jakob T, Wilhelm C (2012) Molecular dynamics of the diatom thylakoid membrane under different light conditions. Photosynth Res 111(1–2):245–257

Lepetit B, Sturm S, Rogato A, Gruber A, Sachse M, Falciatore A, Kroth PG, Lavaud J (2013) High light acclimation in the secondary plastids containing diatom *Phaeodactylum tricornutum* is triggered by the redox state of the plastoquinone pool. Plant Physiol 161(2):853–865

Lepetit B, Gélin G, Lepetit M, Sturm S, Vugrinec S, Rogato A, Kroth PG, Falciatore A, Lavaud J (2016) The diatom *Phaeodactylum tricornutum* adjusts nonphotochemical fluorescence quenching capacity in response to dynamic light via fine-tuned Lhcx and xanthophyll cycle pigment synthesis. New Phytol 214:205–218

Li X-P, Björkman O, Shih C, Grossman AR, Rosenquist M, Jansson S, Niyogi KK (2000) A pigment-binding protein essential for regulation of photosynthetic light-harvesting. Nature 403(6768):391–395

Liu Z, Yan H, Wang K, Kuang T, Zhang J, Gui L, An X, Chang W (2004) Crystal structure of spinach major light-harvesting complex at 2.72 Å resolution. Nature 428(6980):287–292

Miloslavina Y, Grouneva I, Lambrev PH, Lepetit B, Goss R, Wilhelm C, Holzwarth AR (2009) Ultrafast fluorescence study on the location and mechanism of non-photochemical quenching in diatoms. Biochim Biophys Acta 1787(10):1189–1197

Mock T, Krell A, Glockner G, Kolukisaoglu U, Valentin K (2006) Analysis of expressed sequence tags (ESTS) from the polar diatom *Fragilariopsis cylindrus*. J Phycol 42(1):78–85

Mock T, Otillar RP, Strauss J, McMullan M, Paajanen P, Schmutz J, Salamov A, Sanges R, Toseland A, Ward BJ, Allen AE, Dupont CL, Frickenhaus S, Maumus F, Veluchamy A, Wu T, Barry KW, Falciatore A, Ferrante MI, Fortunato AE, Glöckner G, Gruber A, Hipkin R, Janech MG, Kroth PG, Leese F, Lindquist EA, Lyon BR, Martin J, Mayer C, Parker M, Quesneville H, Raymond JA, Uhlig C, Valas RE, Valentin KU, Worden AZ, Armbrust EV, Clark MD, Bowler C, Green BR, Moulton V, van Oosterhout C, Grigoriev IV (2017) Evolutionary genomics of the cold-adapted diatom *Fragilariopsis cylindrus*. Nature 541(7638):536–540

Nagao R, Takahashi S, Suzuki T, Dohmae N, Nakazato K, Tomo T (2013a) Comparison of oligomeric states and polypeptide compositions of fucoxanthin chlorophyll a/c-binding protein complexes among various diatom species. Photosynth Res 117(1–3):281–288

Nagao R, Yokono M, Akimoto S, Tomo T (2013b) High excitation energy quenching in fucoxanthin chlorophyll *a/c*-binding protein complexes from the diatom *Chaetoceros gracilis*. J Phys Chem B 117(23):6888–6895

Nagao R, Kato K, Suzuki T, Ifuku K, Uchiyama I, Kashino Y, Dohmae N, Akimoto S, Shen J-R, Miyazaki N, Akita F (2019) Structural basis for energy harvesting and dissipation in a diatom PSII–FCPII supercomplex. Nature Plants 5(8):890–901

Nagy G, Posselt D, Kovács L, Holm JK, Szabó M, Ughy B, Rosta L, Peters J, Timmins P, Garab G (2011) Reversible membrane reorganizations during photosynthesis *in vivo*: revealed by small-angle neutron scattering. Biochem J 436(2):225–230

Nagy G, Szabó M, Ünnep R, Káli G, Miloslavina Y, Lambrev PH, Zsiros O, Porcar L, Timmins P, Rosta L, Garab G (2012) Modulation of the multilamellar membrane organization and of the chiral macrodomains in the diatom *Phaeodactylum tricornutum* revealed by small-angle neutron scattering and circular dichroism spectroscopy. Photosynth Res 111(1–2):71–79

Neilson JAD, Durnford DG (2010) Structural and functional diversification of the light-harvesting complexes in photosynthetic eukaryotes. Photosynth Res 106(1–2):57–71

Nymark M, Valle KC, Brembu T, Hancke K, Winge PW, Andresen K, Johnsen G, Bones AM (2009) An integrated analysis of molecular acclimation to high light in the marine diatom *Phaeodactylum tricornutum*. PLoS ONE 4(11):e7743

Nymark M, Valle KC, Hancke K, Winge P, Andresen K, Johnsen G, Bones AM, Brembu T, Subramanyam R (2013) Molecular and photosynthetic responses to prolonged darkness and subsequent acclimation to re-illumination in the diatom *Phaeodactylum tricornutum*. PLoS ONE 8(3):e58722

Oeltjen A, Krumbein WE, Rhiel E (2002) Investigations on transcript sizes, steady state mRNA concentrations and diurnal expression of genes encoding fucoxanthin chlorophyll a/c light harvesting polypeptides in the centric diatom *Cyclotella cryptica*. Plant Biol 4(2):250–257

Oeltjen A, Marquardt J, Rhiel E (2004) Differential circadian expression of genes fcp2 and fcp6 in *Cyclotella cryptica*. Int Microbiol 7(2):127–131

Ohno N, Inoue T, Yamashiki R, Nakajima K, Kitahara Y, Ishibashi M, Matsuda Y (2012) CO2-cAMP-responsive cis-elements targeted by a transcription factor with CREB/ATF-like basic zipper domain in the marine diatom *Phaeodactylum tricornutum*. Plant Physiol 158(1):499–513

Oliveri P, Fortunato AE, Petrone L, Ishikawa-Fujiwara T, Kobayashi Y, Todo T, Antonova O, Arboleda E, Zantke J, Tessmar-Raible K, Falciatore A (2014) The cryptochrome/photolyase family in aquatic organisms. Mar Genomics 14:23–37

Owens TG (1986) Light-harvesting function in the diatom *Phaeodactylum tricornutum* – II. Distribution of excitation energy between the photosystems. Plant Physiol 80(3):739–746

Papagiannakis E, van Stokkum IHM, Fey H, Büchel C, van Grondelle R (2005) Spectroscopic characterization of the excitation energy transfer in the fucoxanthin-chlorophyll protein of diatoms. Photosynth Res 86(1–2):241–250

Park S, Jung G, Hwang Y-S, Jin ES (2010) Dynamic response of the transcriptome of a psychrophilic diatom, *Chaetoceros neogracile*, to high irradiance. Planta 231(2):349–360

Peers G, Truong TB, Ostendorf E, Busch A, Elrad D, Grossman AR, Hippler M, Niyogi KK (2009) An ancient light-harvesting protein is critical for the regulation of algal photosynthesis. Nature 462(7272):518–521

Perkins RG, Lavaud J, Serôdio J, Mouget JL, Cartaxana P, Rosa P, Barille L, Brotas V, Jesus BM (2010) Vertical cell movement is a primary response of intertidal benthic biofilms to increasing light dose. Mar Ecol-Prog Ser 416:93–103

Pi X, Zhao S, Wang W, Liu D, Xu C, Han G, Kuang T, Sui S-F, Shen J-R (2019) The pigment-protein network of a diatom photosystem II–light-harvesting antenna supercomplex. Science 365(6452):eaax4406

Premvardhan L, Sandberg DJ, Fey H, Birge RR, Büchel C, van Grondelle R (2008) The charge-transfer properties of the S_2 state of fucoxanthin in solution and in fucoxanthin chlorophyll-a/c_2 protein (FCP) based on Stark spectroscopy and molecular-orbital theory. J Phys Chem B 112(37):11838–11853

Premvardhan L, Bordes L, Beer A, Büchel C, Robert B (2009) Carotenoid structures and environments in trimeric and oligomeric fucoxanthin chlorophyll a/c_2 proteins from resonance Raman spectroscopy. J Phys Chem B 113(37):12565–12574

Premvardhan L, Robert B, Beer A, Büchel C (2010) Pigment organization in fucoxanthin chlorophyll a/c_2 proteins (FCP) based on resonance Raman spectroscopy and sequence analysis. Biochim Biophys Acta 1797(9):1647–1656

Pyszniak AM, Gibbs SP (1992) Immunocytochemical localization of photosystem I and the fucoxanthin-chlorophyll a/c light-harvesting complex in the diatom *Phaeodactylum tricornutum*. Protoplasma 166(3–4):208–217

Ramanan C, Berera R, Gundermann K, van Stokkum IHM, Büchel C, van Grondelle R (2014) Exploring the mechanism(s) of energy dissipation in the light harvesting complex of the photosynthetic algae *Cyclotella meneghiniana*. Biochim Biophys Acta 1837(9):1507–1513

Röding A, Boekema E, Büchel C (2018) The structure of FCPb, a light-harvesting complex in the diatom *Cyclotella meneghiniana*. Photosynth Res 135(1):203–211

Rosen BH, Lowe RL (1984) Physiological and ultrastructural responses of *Cyclotella meneghiniana (*Bacillariophyta) to light intensity and nutrient limitation. J Phycol 20(2):173–183

Schaller-Laudel S, Volke D, Redlich M, Kansy M, Hoffmann R, Wilhelm C, Goss R (2015) The diadinoxanthin diatoxanthin cycle induces structural rearrangements of the isolated FCP antenna complexes of the pennate diatom *Phaeodactylum tricornutum*. Plant Physiol Bioch 96:364–376

Schellenberger Costa B, Jungandreas A, Jakob T, Weisheit W, Mittag M, Wilhelm C (2013a) Blue light is essential for high light acclimation and photoprotection in the diatom *Phaeodactylum tricornutum*. J Exp Bot 64(2):483–493

Schellenberger Costa B, Sachse M, Jungandreas A, Bartulos CR, Gruber A, Jakob T, Kroth PG, Wilhelm C, Campbell DA (2013b) Aureochrome 1a is involved in the photoacclimation of the dia-

tom *Phaeodactylum tricornutum*. PLoS ONE 8(9):e74451

Schumann A, Goss R, Jakob T, Wilhelm C (2007) Investigation of the quenching efficiency of diatoxanthin in cells of *Phaeodactylum tricornutum* (Bacillariophyceae) with different pool sizes of xanthophyll cycle pigments. Phycologia 46(1):113–117

Siaut M, Heijde M, Mangogna M, Montsant A, Coesel S, Allen A, Manfredonia A, Falciatore A, Bowler C (2007) Molecular toolbox for studying diatom biology in *Phaeodactylum tricornutum*. Gene 406(1–2):23–35

Slavov C, Schrameyer V, Reus M, Ralph PJ, Hill R, Büchel C, Larkum AWD, Holzwarth AR (2016) "Super-quenching" state protects *Symbiodinium* from thermal stress – Implications for coral bleaching. Biochim Biophys Acta 1857(6):840–847

Smith BM, Melis A (1988) Photochemical apparatus organization in the diatom *Cylindrotheca fusiformis*: photosystem stoichiometry and excitation distribution in cells grown under high and low irradiance. Plant Cell Physiol 29(5):761–769

Songaila E, Augulis R, Gelzinis A, Butkus V, Gall A, Büchel C, Robert B, Zigmantas D, Abramavicius D, Valkunas L (2013) Ultrafast energy transfer from chlorophyll c_2 to chlorophyll *a* in fucoxanthin-chlorophyll protein complex. J Phys Chem Lett 4:3590–3595

Strzepek RF, Harrison PJ (2004) Photosynthetic architecture differs in coastal and oceanic diatoms. Nature 431(7009):689–692

Szabó M, Premvardhan L, Lepetit B, Goss R, Wilhelm C, Garab G (2010) Functional heterogeneity of the fucoxanthins and fucoxanthin-chlorophyll proteins in diatom cells revealed by their electrochromic response and fluorescence and linear dichroism spectra. Chem Phys 373(1–2):110–114

Taddei L, Stella GR, Rogato A, Bailleul B, Fortunato AE, Annunziata R, Sanges R, Thaler M, Lepetit B, Lavaud J, Jaubert M, Finazzi G, Bouly J-P, Falciatore A (2016) Multisignal control of expression of the LHCX protein family in the marine diatom *Phaeodactylum tricornutum*. J Exp Bot 67(13):3939–3951

Takahashi F, Yamagata D, Ishikawa M, Fukamatsu Y, Ogura Y, Kasahara M, Kiyosue T, Kikuyama M, Wada M, Kataoka H (2007) Aureochrome, a photoreceptor required for photomorphogenesis in stramenopiles. Proc Natl Acad Sci U S A 104(49):19625–19630

Tanaka A, Ohno N, Nakajima K, Matsuda Y (2016) Light and CO_2/cAMP signal cross talk on the promoter elements of chloroplastic β-carbonic anhydrase genes in the marine diatom *Phaeodactylum tricornutum*. Plant Physiol 170(2):1105–1116

Ünnep R, Zsiros O, Solymosi K, Kovács L, Lambrev PH, Tóth T, Schweins R, Posselt D, Székely NK, Rosta L, Nagy G, Garab G (2014) The ultrastructure and flexibility of thylakoid membranes in leaves and isolated chloroplasts as revealed by small-angle neutron scattering. Biochim Biophys Acta 1837(9):1572–1580

Valle KC, Nymark M, Aamot I, Hancke K, Winge P, Andresen K, Johnsen G, Brembu T, Bones AM (2014) System responses to equal doses of photosynthetically usable radiation of blue, green, and red light in the marine diatom *Phaeodactylum tricornutum*. PLoS ONE 9(12):e114211

Veith T, Büchel C (2007) The monomeric photosystem I-complex of the diatom *Phaeodactylum tricornutum* binds specific fucoxanthin chlorophyll proteins (FCPs) as light-harvesting complexes. Biochim Biophys Acta 1767(12):1428–1435

Veith T, Brauns J, Weisheit W, Mittag M, Büchel C (2009) Identification of a specific fucoxanthin-chlorophyll protein in the light harvesting complex of photosystem I in the diatom *Cyclotella meneghiniana*. Biochim Biophys Acta 1787(7):905–912

Wahadoszamen M, Ghazaryan A, Cingil HE, Ara AM, Büchel C, van Grondelle R, Berera R (2013) Stark fluorescence spectroscopy reveals two emitting sites in the dissipative state of FCP antennas. Biochim Biophys Acta 1837(1):193–200

Wang W, Yu L-J, Xu C, Tomizaki T, Zhao S, Umena Y, Chen X, Qin X, Xin Y, Suga M, Han G, Kuang T, Shen J-R (2019) Structural basis for blue-green light harvesting and energy dissipation in diatoms. Science 363(6427):eaav0365

Westermann M, Rhiel E (2005) Localisation of fucoxanthin chlorophyll *a/c*-binding polypeptides of the centric diatom *Cyclotella cryptica* by immuno-electron microscopy. Protoplasma 225(3–4):217–223

Wilhelm C, Büchel C, Fisahn J, Goss R, Jakob T, LaRoche J, Lavaud J, Lohr M, Riebesell U, Stehfest K, Valentin K, Kroth PG (2006) The regulation of carbon and nutrient assimilation in diatoms is significantly different from green algae. Protist 157(2):91–124

Wilhelm C, Jungandreas A, Jakob T, Goss R (2014) Light acclimation in diatoms: from phenomenology to mechanisms. Mar Genomics 16:5–15

Zhu S-H, Green BR (2010) Photoprotection in the diatom *Thalassiosira pseudonana*: role of LI818-like proteins in response to high light stress. Biochim Biophys Acta 1797(8):1449–1457

Chapter 17

A Review: The Role of Reactive Oxygen Species in Mass Coral Bleaching

Milán Szabó*
Institute of Plant Biology, Biological Research Centre, Hungarian Academy of Sciences, Szeged, Hungary

Climate Change Cluster, University of Technology Sydney, Ultimo, Australia

Anthony W. D. Larkum
Climate Change Cluster, University of Technology Sydney, Ultimo, NSW, Australia

and

Imre Vass
Institute of Plant Biology, Biological Research Centre, Hungarian Academy of Sciences, Szeged, Hungary

*Author for correspondence, e-mail: szabo.milan@brc.hu

A. W. D. Larkum et al. (eds.), *Photosynthesis in Algae: Biochemical and Physiological Mechanisms*, Advances in Photosynthesis and Respiration 45, https://doi.org/10.1007/978-3-030-33397-3_17

I. Introduction

Mass coral bleaching has devastated coral reefs all around the world (Hughes et al. 2018a). In Australia, for example, the whole of the Great Barrier Reef, over 1000 km long, has been affected over the three last consecutive years (Hughes et al. 2018b, c) and the extent of recovery is still not known. There have also been severe impacts in the Indian Ocean, the Western Pacific, including Polynesia, and in the Caribbean (Hughes et al. 2003). The major primary cause of bleaching is the rise in summer sea surface temperatures (SSST); and the proximate cause of this is the rise in greenhouse gases in the atmosphere (Hoegh-Guldberg 2009). With current predictions for further rise in greenhouse gases, no matter what policy changes are put into effect over emissions, the coral reefs of the world are expected to undergo annual bleaching by 2050 (www.iucn.org/resources/issues-briefs/coral-reefs-and-climate-change).

Mass coral bleaching first gained attention in the late 1980s (Hoegh-Guldberg and Smith 1989a, b). Mass coral bleaching is characterised by the severe loss of colouration of a coral, which has generally been attributed to the significant loss of the algal symbiont (commonly also referred to as zooxanthellae), a dinoflagellate in the genus *Symbiodinium* (Symbiodiniaceae) from the host coral. Several possible mechanisms of bleaching have been reported in corals and sea anemones. These include (e.g. Bieri et al. 2016, see also Fig. 17.1):

1. exocytosis of algal cells
2. *in situ* degradation of algal cells,
3. detachment of host cells containing algae, and
4. death of host cells containing algae (by either apoptosis or necrosis)

Of these the loss of *Symbiodinium* cells (from here on the term Symbiodiniaceae for currently recognized species and genera will be used, see LaJeunesse et al. 2018) to the ambient environment, largely by release of symbiont cells to the enteron (gastric cavity) and then loss through the coral mouth to the surrounding seawater is the most common explanation.

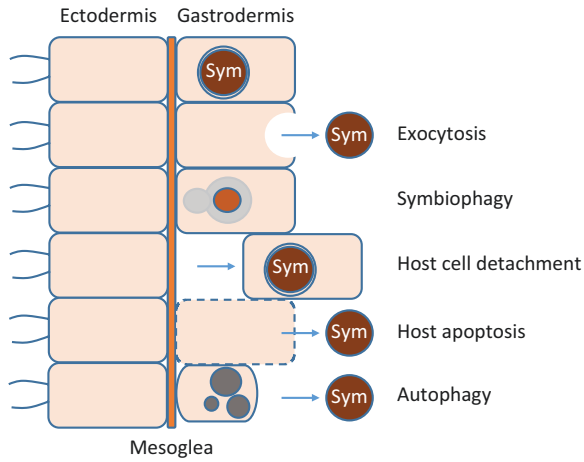

Fig. 17.1. A diagram showing the possible ways that coral bleaching, i.e. the loss of zooxanthellae, can take place. Exocytosis involves the release of zooxanthellae from endodermal cells to the gastric cavity; symbiophagy involves the digestion of zooxanthellae by host cells; host cell detachment is the release of host cells containing zooxanthellae to the gastric cavity; apoptosis is the breakdown of the host cell and the release of zooxanthellae to the gastric cavity; autophagy involves the disintegration of the host cell due to cellular breakdown which may also include the zooxanthellae. Much modified scheme of original diagram put forward by Gates et al. (1992)

The causes of this loss (exocytosis) are much debated but photosynthesis is implicated in most studies and these are dealt with first (hypotheses involving causes other than photosynthesis such as infections by bacteria or viruses are dealt with further on; see Sect. D, below).

A. Photosystem II

Of those studies suggesting an effect of bleaching via photosynthesis, Photosystem II (PSII) has often been suggested as the primary site of action. Since PSII is the site of the oxygen evolving complex and of photoinhibition, this suggestion might seem reasonable. Furthermore, it is plausible that the production of reactive oxygen species (ROS) by PSII might be a primary cause of damage. It is known that due to the high oxidation / reduction potential (E_m ~ 1.2 V) needed to split water it is not possible to place carotenoids close to the P680 reaction centre Chl of PSII, and as a result the production of singlet oxygen, a very damaging form of ROS, cannot be avoided. Indeed, for this reason the D1 protein of PSII is the most highly turned-over protein in nature (Aro et al. 2005). It has been shown that exposure of *Symbiodinium* (Symbiodiniaceae) cells to ROS causes impairment of PSII (Wang et al. 2011).

A number of investigations have put forward evidence to the effect that PSII is the site of damage resulting in coral bleaching (Warner et al. 1999; Jones et al. 2000; Ragni et al. 2010). All these investigations (and many more not cited) used Pulse Amplitude Modulation (PAM) fluorescence techniques to follow photosynthesis, which relies on assessing the activity of PSII. However, this could be manifested as a secondary effect if electron transport through Photosystem I were impaired and so cannot be taken as definitive evidence without other evidence. Another possibility has been put forward: an effect on the repair mechanism of D1 caused by heat stress, thereby accelerating photoinhibition (Takahashi et al. 2009). However, no mechanism of a heat effect on the repair mechanism over the few degrees of temperature change required for coral bleaching has been put forward. Therefore, the involvement of Photosystem II in coral bleaching except as a secondary effect remains debatable.

B. Mehler Ascorbate Peroxidase (MAP) Pathway and Photosystem I

Photosystem I (PSI) is an important regulatory component in electron transport (ET) chain, as is PSII, but the involvement of PSI in coral bleaching is much less characterized, mainly because it is a much more intricate complex to investigate and involves a number of intersecting electron transfer pathways (Fig. 17.2). The intersecting pathways are: cyclic electron flow (CEF), linear ET to the Calvin-Benson cycle, flavodiiron reduction, sulphur reduction, hydrogen formation, the Mehler reaction (Mehler Ascorbate Peroxidase Pathway), and, furthermore, interactions with respiratory pathways, light stimulated respiration and other ET pathways (Munekage et al. 2004; Cardol et al. 2011; Shikanai 2014; Larkum et al. 2017).

In general, under heat stress, PSI has been found to be more stable than PSII (Hoogenboom et al. 2012; Ivanov et al. 2017). Heat stress was even found to increase PSI-mediated electron transport activity, which might ensure the balanced energy distribution and the activation of alternative electron transport mechanisms (Ivanov et al. 2017). In *Symbiodinium* (Symbiodiniaceae), the activity of CEF has been found to be low as compared to the Mehler (MAP pathway) reaction (Roberty et al. 2014, 2015, 2016). Any effect on CEF is more likely the result of heat-induced damage rather than a photoprotective mechanism (Aihara et al. 2016). Coding genes for the CEF components NDH and PGR5/PGRL1 have been found in *Symbiodinium* (Symbiodiniaceae); however, the functioning of these proteins in physiological pathways has not been characterized.

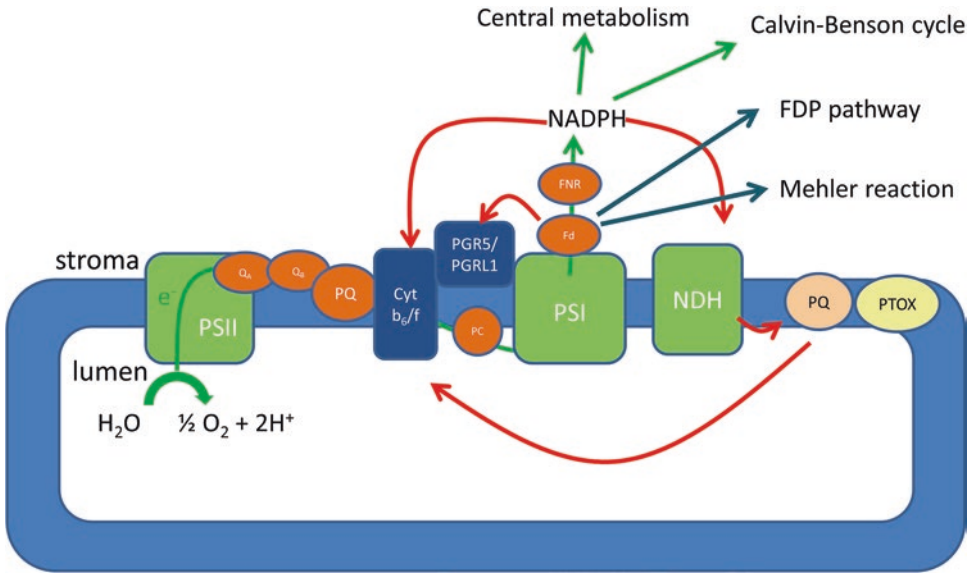

Fig. 17.2. Electron transfer pathways in *Symbiodinium* sp. (Symbiodiniaceae). Abbreviations: *Cyt b6f* cytochrome b_6f complex, *Fd* ferredoxin, *FDP* flavodiiron proteins, *FNR* ferredoxin-NADP reductase, *NDH* NAD(P)H dehydrogenase, *PC* plastocyanin, *PGR5* Proton Gradient Regulation 5, *PGRL1* PGR5-Like Photosynthetic Phenotype 1, *PQ* plastoquinone pool, *PSI* photosystem I, *PSII* photosystem II, *PTOX* plastid terminal oxidase

The genes of flavodiiron proteins have also been identified in *Symbiodinium* (Symbiodiniaceae) (Roberty et al. 2014), but their involvement in ET pathways also remains unknown.

Liñán-Cabello et al. 2010 carried out a very thorough comparison of superoxide radicals, lipid peroxidation and antioxidant activities in *Pocillopora capitata* communities in winter and summer on the Pacific coast of Mexico. Superoxide radicals were seven-fold higher in summer, and lipid peroxidation, catalase activity, glutathione-S-transferase and mycosporine pigments were all higher in summer. However, superoxide dismutase was somewhat higher in winter, although there is the possibility that this was caused by an artefactual effect of higher light in summer. Nevertheless, this work supports in great detail the fact that the production of ROS around PSI is responsible for a major effect of summer elevated temperatures and high light conditions. In another detailed study, Krueger et al. 2015b, no significant increased levels were found under coral bleaching conditions apart from an increase in catalase, which runs counter to all the above. This and a sister paper in 2015 (Hawkins et al. 2015), led these authors to doubt the pivotal role of ROS around PSI in coral bleaching and clearly needs some explanation. However, the latter conclusions are based on the supposition that steady state levels of antioxidants and antioxidant enzymes must reflect the likelihood of mass coral bleaching. In fact, coral bleaching is likely to be a reaction to a transient imbalance in ROS production, which triggers a rapid and largely irreversible exocytosis of zooxanthellae.

As mentioned in detail below the production of superoxide by photosystem I leads to the formation of hydrogen peroxide (H_2O_2) through the action of superoxide dismutase (SOD) in the MAP pathway. In *Arabidopsis thaliana* and *Chlamydomonas reinhardtii*, H_2O_2 has been identified as a key component of second messenger systems (Noctor et al.

Table 17.1. Investigations of hydrogen peroxide (H_2O_2) in corals, zooxanthellae and isolated Symbiodiniaceae

Organism	Conc.	Method	Notes	Authority
Coral				
Goniastrea	0–30 μM	Externally added	In ambient medium	Higuchi et al. (2009a)
Galaxea	0–3 μM	Externally added	In ambient medium	Higuchi et al. (2009b)
Corals in Gulf of Aquaba	100–250 nM	POHPPA method	Release to ambient medium	Shaked and Armoza-Zvuloni (2013)
Stylophora	~1 μM	POHPPA method	Release to ambient medium	Armoza-Zvuloni et al. (2014)
Stylophora	850 nM	POHPPA method	Release to ambient medium	Armoza-Zvuloni et al. (2016)
Symbiodinium				
Symbiodinium clades A1, B1 B2, D, E1, F2	1.2–10.2 pmol/cell/h	DCFH-DA	H_2O_2 Equiv.	McGinty et al. (2012)
Symbiodinium clades A1 & B1	1–2 pmol/cell/h	Amplex red method	Inside cell	Suggett et al. (2008)
Symbiodinium clades A3,B1, B2, D1–5	0.25–0.9 pmol/cell/h	Amplex red method	Inside cell	Goyen et al. (2017)
Symbiodinium clades	10 pmol/cell/h at 33 °C	Amplex red method	Inside cell	Roberty et al. (2015)

2017 and see below). H_2O_2 has been identified as a factor in coral bleaching in a number of studies; and these are set out in Table 17.1.

C. Rubisco

Symbiodinium spp. (Symbiodiniaceae) contain a Type II Ribulose 1,5-bisphosphate carboxylase oxygenase (Rubisco) (Whitney et al. 1995); this form of the CO_2-fixing enzyme of the Calvin-Benson cycle has two subunits as opposed to the 8 large and 8 small subunits of Type I Rubisco, the commonest form of Rubisco in algae and higher plants. Type II is widespread in anaerobic photosynthetic bacteria, but amongst eukaryotes only occurs in dinoflagellate algae. Just how and why it was transferred to dinoflagellates, presumably by lateral gene transfer, is unknown. Type II Rubisco of dinoflagellates has been found to be more sensitive to heat stress than Type I Rubisco (Leggat et al. 2004, Lilley et al. 2010). Lilley et al. 2010 found that the transition to the impaired state coincided well with the temperature range at which coral bleaching occurs (viz. 31–35 °C). Therefore, it is plausible to assume that damage of Rubisco may play a role in the initiation of coral bleaching (Bhagooli 2013; Hill et al. 2014; Oakley et al. 2014); for example, cyanide and glycolaldehyde inhibit CO_2 fixation (and oxygen evolution), and have effects consistent with coral bleaching. Cyanide probably acts by inhibiting Rubisco activase (see e.g. Crafts-Brandner and Law 2000). Glycolaldehyde inhibits phosphoribulokinase, which adds the second phosphate to ribulose-5-phosphate in the Calvin-Benson cycle. However, side effects of glycoaldehyde make the situation less than clear-cut (Hill et al. 2014). In practice it has been shown that inhibition of Rubisco leads to a highly reduced P700 and reduced PQ pool, which thus leads to inhibition of intersystem PSII-PSI electron transport (Szabó et al. 2017); however, while the inhibitor of Rubisco activase, cyanide, leads to symbiont expulsion, the inhibitor of the Calvin-Benson cycle, glycolaldehyde does not. This effect may be due to side effects of glycolaldehyde, so clearly more evidence is needed to make the situation fully compelling.

D. *Non-photosynthetic Proposals for Coral Bleaching*

Despite the main topic of this review it should be pointed out that non-photosynthetic mechanisms of coral bleaching have also been put forward and for completeness these are listed below:

1. Viruses
   Viruses have been implicated in coral bleaching because it is known that there are certain viruses in which replication is stimulated at enhanced temperatures (Davy et al. 2006; Levin et al. 2017).
2. Bacteria
   A number of examples occur in the literature in which bacteria cause coral infections. In the anenome *Exaiptasia*, *Vibrio* spp. have been shown to be important (Zaragoza et al. 2014).
3. Sedimentation
   Excessive sedimentation has been shown to cause detrimental effects on the structure and function of coral ecosystems, extreme increase in turbidity also resulted in bleaching (reviewed in Rogers 1990).
4. Other studies found that coral bleaching is independent of photosynthetic activity when investigated in the dark during heat stress, ruling out the possibility of involvement of ROS (Tolleter et al. 2013; Petrou et al. 2018).

II. Review of the Experimental Evidence for Reactive Oxygen Species in Corals and *Symbiodinium* (Symbiodiniaceae)

In microalgae there are two major ways of generating reactive oxygen species (ROS), (i) the generation of superoxide (O_2^-) by over-reduction of P700 (Endo and Asada 2008) and the action of ferredoxin (Bowyer and Camilleri 1985) and (ii) the generation of singlet oxygen, mainly in Photosystem II (PSII) and in the Chl containing light harvesting antenna complexes (Vass 2012). Clearly, both of these damaging processes have occurred over evolutionary history because microalgae have evolved processes to compensate for potential photoinhibition. In addition to these common forms of oxygen, radicals must be added: hydroxyl radical ($OH^{\cdot}$), which is formed by the interaction of H_2O_2 with ferrous ion ($H_2O_2 + Fe_2^+ \rightarrow Fe_3^+ + OH^- + OH^{\cdot}$) and the production of the reactive nitrogen species NO., NO_2. and ONOOH (Moldogazieva et al. 2018). Both these signal transduction mechanisms are gaining increased recognition in higher plants, but little is known about them in the coral symbiosis (but see possible effect of NO below).

The Mehler Ascorbate Peroxidase (MAP) pathway, which is connected to PSI via soluble electron carriers (ferredoxin, Fd), has evolved to detoxify the superoxide, O_2^- by the action of superoxide dismutase (SOD) on the hydrogenated O_2^- ($2\,O_2^- + 2\,H^+ \rightarrow O_2 + H_2O_2$) (Endo and Asada 2008; Miyake and Asada 2003). There are several forms of superoxide dismutase in algae, including Symbiodiniaceae (Miyake and Asada 2003; and see below). In Symbiodiniaceae there are at least 3 MnSOD isoforms and at least one FeSOD isoform (Krueger et al. 2015a). The H_2O_2 is then dismutated by ascorbate peroxidase, thioredoxin (Miyake and Asada 2003), monodehydroascorbate reductase (MDHAR) (Roberty et al. 2014) or by catalase to water and oxygen. Since the photosynthetic electron transport chain extends from the water-splitting, oxygen-evolving centre of PSII to the water-forming reaction of the MAP process, this is known as the water-water cycle and the net oxygen exchange for this cycle is zero (see also Chap. 8).

The production of hydrogen peroxide around PSI, and its dissimulation, has been well documented (Miyake and Asada 2003); but see the results of (Krueger et al. 2015b). However, another system to deal with over-reduction of PSI has been recently described: the flavodiiron system (Ilík et al. 2017).

Flavodiiron is a protein, on the outside of the thylakoid membrane, which reduces oxygen to water without ROS production and is a safety valve system to ward against over-reduction of P700 and ferredoxin, which otherwise can lead to photoinhibition of PSI (Tikkanen et al. 2014; Gerotto et al. 2016). However, the flavodiiron pool is limited and so this system is at best a limited safety valve (Chaux et al. 2015), which is augmented by the MAP pathway for further protection and by CEF (Chaux et al. 2015). As mentioned above, *Symbiodinium* (and likely all Symbiodiniaceae) has Flv genes (Flv1 and Flv3) and presumably expresses these proteins. An examination of flavodiiron proteins from cyanobacteria, through algae and up to gymnosperms, concluded that they played an important role as a safety valve in these organisms from fast changes in light at high light intensities (Ilík et al. 2017). Another aspect that must be discussed is the activity of cyclic electron flow (CEF) around PSI (Larkum et al. 2017). CEF augments the amount of ATP available to the Calvin-Benson cycle by recycling electrons back across the thylakoid membrane and generating extra ATP. It is therefore a potential component in considerations of P700 oxidation-reduction and can be measured in various ways, some of which are discussed below.

The production of singlet oxygen in *Symbiodinium* (Symbiodiniaceae) and corals has been well documented and will be described in detail below.

A. *The Evidence for Harmful Reactions Due to Over-Reduction of PSI in Symbiodinium (Symbiodiniaceae) and Corals*

In studying the effect of linear electron transport from PSII to PSI and beyond, chlorophyll fluorescence has been instrumental in investigating the photochemical efficiency of PSII and the electron transport kinetics from Q_A/Q_B (see Fig. 17.2) and to the plastoquinone pool using fast repetition rate (FRR) fluorometry and flash-induced chlorophyll fluorescence decay. The kinetics of PSI can be investigated using absorbance changes in the near infrared region (based on P700 characteristics, e.g. Klughammer and Schreiber 1994; Baker et al. 2007; Alric 2010). Another method, pioneered by Wah Soon Chow, is to chart the oxidation-reduction status of P700 and to quantitatively assess the contribution of linear ET from PSII (Chow et al. 2012; Jia et al. 2014). In corals, a simple method to reveal the redox state of P700 and intersystem electron transfer between PSII and PSI under heat stress has been developed by Szabó et al. 2017. Measurement of P700 kinetics is a powerful technique as it allows investigation of both PSII and PSI activity as well as donor and acceptor side limitations to the reaction centre of PSI in intact corals (Hoogenboom et al. 2012; Szabó et al. 2017). This method can also be coupled directly with chlorophyll fluorescence kinetics, e.g. via combining P700 absorbance change and FRR fluorometry in the same fibre-optics system (Szabó et al. 2017). In this manner, the quantum yield of PSII, the functional absorption cross-section of PSII, the fast and slow component of electron transfer (from Q_A to Q_B and from Q_B to the plastoquinone pool), the relative amount of oxidized PQ pool as well as the steady-state redox level of P700, the oxidation-reduction kinetics of $P700^+$, and the quantum yield of PSI can be investigated on the same sample, under the same optical and environmental conditions. On this basis, it was concluded that the technique of using fast repetition rate fluorometry and P700 kinetics could accurately define the photosynthetic properties of the coral used (*Pavona decussata*) (Szabó et al. 2017). They concluded that under a short-term (20 min) heat treatment (33 °C) the quantum yield of PSII (F_V/F_M) and the absorption cross-section of PSII (σPSII) remained unchanged; thus demonstrating the lack of effect of acute heat stress on the inherent properties of charge separation in PSII.

It is also possible to record light response curves, and thereby the electron transport rates of Photosystem II (ETR(II)) and Photosystem I (ETR(I)) can also be revealed. Using appropriate inhibitors, like DCMU, the linear electron flow can be blocked, when, upon switching off actinic light, the re-reduction kinetics of $P700^+$ may reflect largely cyclic electron flow (e.g. Aihara et al. 2016). In symbiotic systems such as corals and *Exaiptasia*, this provides information about the potential photoprotective role of cyclic electron flow under heat stress. Reynolds et al. 2008 and Aihara et al. 2016 concluded that different clades of *Symbiodinium* (Symbiodiniaceae) exhibited different activities of CEF. A clade with higher susceptibility to photoinhibition exhibited higher CEF, therefore it is possible that in certain clades of *Symbiodinium* (Symbiodiniaceae), CEF is a stress response rather than a preventive photoprotective mechanism. However, further investigations are needed to obtain more information about the role of CEF in zooxanthellae of different corals and *Symbiodinium* clades (Symbiodiniaceae) under different environmental conditions. Crucial to any such studies are the concomitant effects of the MAP pathway and flavodiiron proteins on the generation of H_2O_2 (c.f. Chaux et al. 2015).

B. Calvin-Benson Cycle Activity

The impact of acute heat stress on $P700^+$ kinetics in corals or *Symbiodinium* (Symbiodiniaceae) can also be related to the heat-induced damage on the Calvin-Benson cycle (Bhagooli 2013; Hill et al. 2014). The heat sensitivity of Type II Rubisco of *Symbiodinium* (Symbiodiniaceae) has been investigated extensively (Whitney et al. 1995; Leggat et al. 2004; Lilley et al. 2010; Hill et al. 2014), and it can be assumed that the heat induced damage of Rubisco exerts a direct effect on PS ET via several steps and that these influence the redox state of PQ pool and the delta pH across the thylakoid membrane. The impact of impaired Rubisco activity has also been tested using inhibitors; glycolaldehyde under light and heat stress led to bleaching in some, but not all coral species (Ragni et al. 2010; Bhagooli 2013; Hill et al. 2014). Overall the conclusion must be that impairment of Rubisco or Rubisco activase *does* occur at bleaching temperatures and that the reduction in CO_2 fixation feeds back to the PS ETC, however, other studies have found that under short term heat stress carbon concentrating mechanisms (CCM) became more efficient (Oakley et al. 2014).

C. Over-Reduction of PSI and Back Reactions

Irrespective of whether Rubisco inactivation occurs via administration of chemical inhibitors or heat stress, inhibition of the Calvin-Benson cycle necessarily leads to increased NADPH levels (due to the decreased consumption of NADPH by the damaged carbon fixation mechanisms), which in turn increases the equilibrium level of reduced ferredoxin (Fd^-). The higher level of reduced ferredoxin blocks the acceptor side of PSI and thus impairs charge separation of P700/$ChlA_o$, which can be observed by a decline in the level of photo-oxidized P700 following a saturation pulse (Szabó et al. 2017).

Back reactions from the elevated NADPH level also lead to a highly reduced PQ pool, either via a partially blocked linear electron flow (inhibited acceptor side of PSI), or via the cyclic electron flow, which can be modulated by several components, the NAD(P)H dehydrogenase complex (NDH-1 or NDH-2) or the Fd-mediated PGR5-PGRL1 pathway (Fig. 17.2). The *Symbiodinium* (Symbiodiniaceae) genome contains not only a type II NDH, (NDH-2) but also the PGR5-PGRL1 genes. However, so far, no physiological evidence has been provided for the operation of either of these CEF components. Their operation in algae is widespread and is discussed in Larkum et al. 2017; most

work has been done in *Chlamydomonas reinhardtii,* where there is clear evidence that PGR5-PGRL1 are involved in CEF (Larkum et al. 2017).

D. P700 Oxidation Reduction

The techniques for assessing redox changes of P700 provide indications for the CEF mechanisms, however, as the heat-stress-induced changes involve several components of the photosynthetic electron transport chain, spectroscopic methods that are able to deconvolute the kinetics of ferredoxin, plastocyanin and P700 are needed. In this regard new instruments (e.g. Schreiber and Klughammer 2016; Klughammer and Schreiber 2016) could potentially open new avenues in coral research to investigate electron flow around photosystem I in unprecedented detail.

E. The Mehler Reaction and the MAP Pathway

Notwithstanding that CEF may be an important mechanism in mediating heat-induced photoprotective responses, other alternative electron flow processes may be more important. For example, it has been suggested that the Mehler reaction (MAP pathway – see above) is the main alternative electron flow process in *Symbiodinium* (Symbiodiniaceae) (Roberty et al. 2014); and as mentioned above the Mehler reaction is responsible for the photoreduction of oxygen by PSI under high light. This is brought about by the upregulation of several enzymes which first act on superoxide and then convert the resultant H_2O_2 to water and oxygen (see above). Both superoxide and H_2O_2 are injurious ROS components, and their dissimulation has been a key evolutionary development from cyanobacteria onwards (for a general review of cyanobacterial and algal system see Schmitt et al. 2014). There is strong evidence that at least H_2O_2 is a causative factor in coral bleaching (Roberty et al. 2014, 2015; see Sect. II) and it is likely that H_2O_2 acts synergistically with singlet oxygen, produced by PSII, to trigger the expulsion of zooxanthellae (Roberty et al. 2016) and thus be a major cause of coral bleaching. Thus a major line of investigation in coral bleaching has been consideration of the levels of the enzymes of the Mehler reaction and their response to elevated temperatures and high light. If, as has been suggested, the level of H_2O_2 is the critical component in triggering bleaching, then the upregulation of associated enzymes in different clades of *Symbiodinium* (Symbiodiniaceae) is a critical feature and may explain the resistance of some corals with certain clades to bleaching.

Thus, under combined high light and temperature stress, it has been observed in the model *Symbiodinium* sp. (Clade A), that the high light treatment at 26 °C resulted in the upregulation of superoxide dismutase, ascorbate peroxidase, and glutathione reductase and was accompanied by an increased production of H_2O_2 with no significant change in O_2–dependent electron transport. Under high light and at 33 °C, O_2-dependent electron transport was significantly increased relative to total electron transport, and was accompanied by a twofold increase in H_2O_2 generation compared with the treatment at 26 °C, while Mehler enzymes appeared to be largely inactivated (Roberty et al. 2015). These results indicated that with elevated temperatures and high light stresses the antioxidant enzyme capacities of the Mehler reaction were overwhelmed under these conditions. This latter study also indicated that corals may be more prone to bleach if they harbor *Symbiodinium* (Symbiodiniaceae) cells with a highly active Mehler-type electron transport (water-water cycle), unless they are able to quickly upregulate their antioxidant capacities. Furthermore, the ability of *in hospite* Symbiodiniaceae to use alternative electron flow components, such as flavodiiron to reduce ROS generation could be a determinant factor in bleaching tolerance at the given habitat (Roberty et al. 2015, 2016).

In their study of Calvin-Benson cycle inhibitors, Hill et al. 2014 did not investigate ROS, but nevertheless came to the conclusion that an inhibition of Calvin-Benson activity alone could not explain all their results and that a stimulation of ROS levels as a result of cyanide exposure could explain some of the bleaching responses (but this raised the question as to whether cyanide inhibited ascorbate peroxidase and so led to the enhanced H_2O_2).

F. Flavodiirons

It is clear from the above that much more detailed work is needed before the hypothesis that ROS is a major trigger for coral bleaching can be upheld. More work is needed at the basic level of MAP pathway enzymes and the role of ROS components. Further work will undoubtedly come by a combination of biophysical methods; for example, mass spectrometry (e.g. membrane inlet mass spectrometry, MIMS) could uncover further details on the regulation of alternative electron flow pathways that involve oxygen uptake under stress conditions and this could be combined with the Dual-PAM and P700 work to map in detail the ET pathways around PSI and the involvement of oxygen uptake by the Mehler reaction and flavodiirons.

III. Molecular Physiology and Bioinformatics

Another important field to consider in the investigation of responses of *Symbiodinium* (Symbiodiniaceae) *in hospite* to bleaching stress is molecular physiology and bioinformatics. Integrative studies that apply physiological characterizations using e.g. chlorophyll fluorescence kinetics and transcriptomic analyses to investigate the expression of genes coding antioxidant enzymes could reveal the functional diversity of genetically different *Symbiodinium* clades (Symbiodiniaceae) (Goyen et al. 2017). Transcriptomic analyses thus could reveal the expression of stress and metabolism related genes. A particular interest for the current chapter is the global response of photosynthesis genes; it has been found that under moderate heat stress seven transcripts encoding photosystem I (Psa) subunit genes were significantly changed, moreover significant changes in the transcription of ferredoxin-$NADP^+$ reductase (petH), ferredoxin (petF), Rubisco (rbcL), violaxanthin de-epoxidase (vde) and chlorophyll *a*-chlorophyll c_2-peridinin protein complex (acpPC) coding genes were also observed, indicating a global response of photosynthesis related genes under heat stress (Gierz et al. 2017). The connection of photosynthetic electron flow to other metabolic pathways and morphological characteristics that may be prevalent under bleaching conditions could be assessed by applying multi-trait approaches; assessing photosynthesis and respiration along with ROS antioxidant enzyme systems and metabolites (such as DMSP) could provide a complete picture on the cascade events that lead to coral bleaching (Gardner et al. 2017; see below).

Transcriptomics (Rodriguez-Lanetty et al. 2006) and proteomics (Oakley et al. 2016) have been used to look at the effect of the Symbiodiniaceae symbionts on the host/symbiont interaction. In the earlier transcriptomic study, the somewhat counter-intuitive result was found that in the host cells the ROS enzymes were down-regulated. Oakley et al. 2016 found that oxidative stress-response pathways upregulated in aposymbiotic *Aiptasia* was generated by the host, which is seemingly contradictory to the conventional model of algal symbionts contributing to the host during thermal stress. Clearly more work is needed in the future to clarify whether symbiont may aid their host in protection from ROS.

IV. The Detection and Role of Singlet Oxygen

The most common source of singlet oxygen ($^1O_2$) in photosynthesis is its production by P680 of PSII (Krieger-Liszkay 2005; Krieger-Liszkay et al. 2008). Detection of singlet oxygen in photosynthetic systems is possible by using various methods. Different versions of electron paramagnetic resonance (EPR) spin trapping have been successfully used in isolated thylakoid membrane preparations, including purified PSII membrane particles and core complexes of PSII. The principle behind the method is the application of a suitable spin trap detection system, which is diamagnetic, i.e. EPR silent, in its basic form, but becomes paramagnetic, i.e. EPR detectable, after interaction with $^1O_2$. The most widely used $^1O_2$ spin trap compounds in photosynthetic systems are TEMP, and TEMPD, which are converted into EPR detectable TEMPO, and TEMPDO after capturing $^1O_2$ (Hideg et al. 2011). These compounds have been successfully used to detect light induced $^1O_2$ formation in isolated thylakoids and PSII membranes (Hideg et al. 1994; Fufezan et al. 2002). Unfortunately, none of the EPR spin traps are suitable for detection of $^1O_2$ production inside microalgal cells, due the relatively low sensitivity of the spin traps, combined with the limited penetration of spin trap detection compounds through the cell wall of microalgae.

Interaction with $^1O_2$ oxygen can change the yield of fluorescence emission of the so-called fluorescent spin trap compounds, and this makes it possible for the detection of $^1O_2$ production by simple fluorescence yield measurements. Such effects have been demonstrated by using DanePy, and singlet oxygen sensor green (SOSG), which decreases or increases its fluorescence yield, respectively, after capturing $^1O_2$. DanePy has been used in isolated thylakoid membrane particles (Kálai et al. 1998), and intact broad bean leaves (Kálai et al. 1998; Hideg and Schreiber 2007), while SOSG has been applied in in plant systems (Flors et al. 2006). Unfortunately, neither of these fluorescent spin traps are able to penetrate inside the cells of commonly used microalgae as shown for DanePy (personal communication by E. Hideg) and SOSG in case of *Synechocystis* sp. PCC6803 (Rehman et al. 2013) and *Symbiodinium* (Symbiodiniaceae) (Rehman et al. 2016; Wietheger et al. 2018).

The most direct way of $^1O_2$ detection is the use of the near infrared (1270 nm) luminescence emission, which arises from the radiative deactivation of excited $^1O_2$ molecules (Telfer et al. 1999). Unfortunately, this approach can be applied only in highly purified PSII core particles since the method is hampered by the influence of background Chl fluorescence in more intact systems (Li et al. 2012).

Despite all of the above methods, there exists another very simple method for $^1O_2$ detection, which is based on uptake of dissolved oxygen in aqueous environment by chemical trapping of $^1O_2$ by suitable chemicals, which have high and specific reactivity towards $^1O_2$ such as histidine (Verlhac et al. 1984) (Figs. 17.3, 17.4, 17.5 and 17.6). Surprisingly, this simple method has proven applicable and very useful in single celled microalgae, including the cyanobacterium *Synechocystis* 6803 (Rehman et al. 2013; Hakkila et al. 2014; Sedoud et al. 2014), and the dinoflagellate symbiotic alga *Symbiodinium* (Symbiodiniaceae) (Hill et al. 2014).

Application of His-mediated chemical trapping of $^1O_2$ has revealed that cultured *Symbiodinium* (Symbiodiniaceae) produces light-dependent $^1O_2$ production inside the cells (Rehman et al. 2016) (Fig. 17.3). This effect appears to be responsible for light-induced pigment bleaching since addition of His partly prevented this effect (Rehman et al. 2016). In addition to *Symbiodinium* (Symbiodiniaceae) cell cultures the His-mediated O_2 uptake was detected also in intact corals (*Pocillopora damicornis*) showing that $^1O_2$ production occurs also under natural conditions (Fig. 17.4).

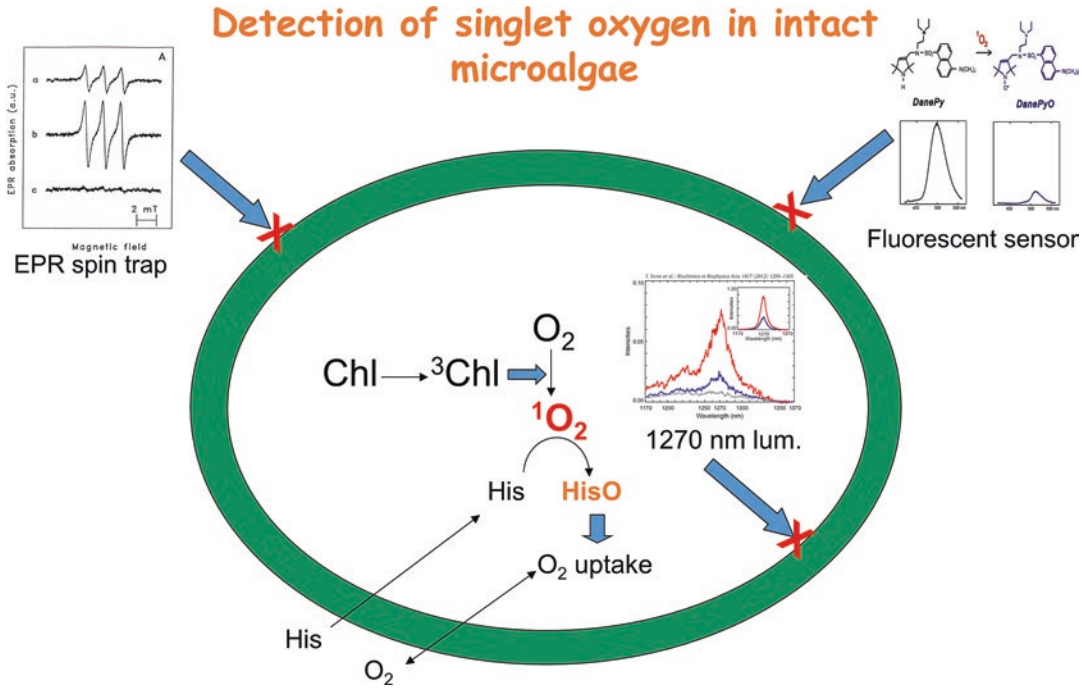

Fig. 17.3. Diagram illustrating how singlet oxygen ($^1O_2$) can be detected in microalgae
Traditional methods of $^1O_2$ detection, such as EPR fluorescent spin traps, and 1270 nm luminescence are hampered by the inability of the spin traps to penetrate inside the microalgal cells, and by the interference of chlorophyll fluorescence with the weak luminescence. Histidine, however, enters inside the cells and induces oxygen uptake, due its oxidation by singlet oxygen, which is produced from the interaction of excited chlorophylls with molecular oxygen. Oxygen inside the algal cells rapidly equilibrates with oxygen dissolved in the medium leading to oxygen consumption, which effect can be easily measured by sensitive O_2 sensors (Rehman et al. BBA (2013) 1827: 689–698)

A very interesting outcome of $^1O_2$ detection in the *Symbiodinium* (Symbiodiniaceae) system was that although the fluorescent $^1O_2$ sensor SOSG was not able to penetrate inside the *Symbiodinium* (Symbiodiniaceae) cell, it reported very clear $^1O_2$ production outside the cells (Fig. 17.6) and also in cell free culture medium after *Symbiodinium* (Symbiodiniaceae) cells had been in it (Rehman et al. 2016). The extracellular $^1O_2$ production was confirmed by using His-mediated O_2 uptake as well, which was accompanied with the appearance of a specific absorption band in the cell-free medium (Rehman et al. 2016). These data together demonstrate that *Symbiodinium* (Symbiodiniaceae) cells are able to excrete what are so far unidentified metabolite(s), which mediate(s) efficient $^1O_2$ production outside the cells. It has also been shown that the extracellular $^1O_2$ production is enhanced under conditions, which induce coral bleaching, i.e. elevated temperatures and increased light intensities. These data point to the possibility that excretion of $^1O_2$ sensitizer(s) from the *Symbiodinium* (Symbiodiniaceae) cells may serve as a trigger for the expulsion of zooxanthellae from the coral host tissue leading eventually to coral bleaching.

What these studies tell us is that under the right conditions a strong effect of singlet oxygen production can be shown in *Symbiodinium* (Symbiodiniaceae) cells, and in intact corals, and also that singlet oxygen scavenging provides partial protection against pigment bleaching in *Symbiodinium* (Symbiodiniaceae) cells. What is not clear is how much of an effect this has on coral

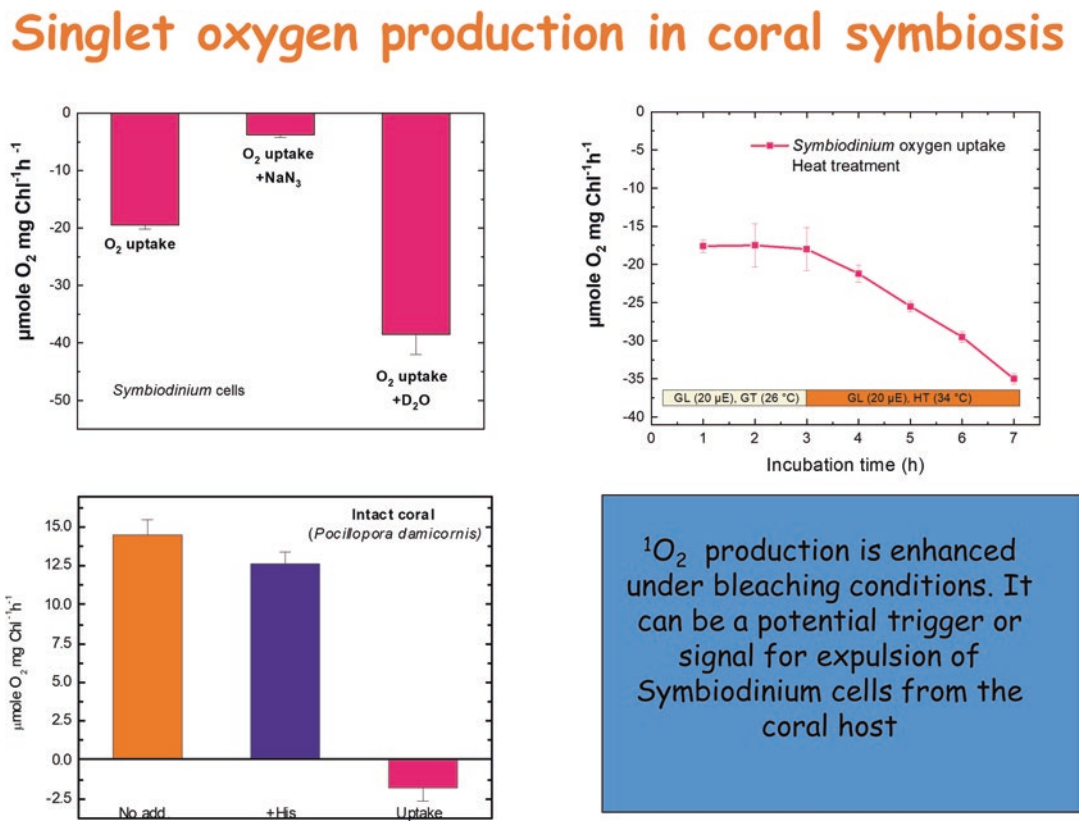

Fig. 17.4. Quantitative evidence for the involvement of singlet oxygen production in *Symbiodinium* (Symbiodiniaceae) involved in coral bleaching. Singlet oxygen production was measured in intact coral (*Pocillopora damicornis*) by the rate of His mediated O_2 uptake. Coral nubbins were placed into a closed chamber and the rate of light induced change in the level of dissolved O_2 in the medium surrounding the nubbin was measured by a PreSens oxygen sensor either without addition, or in the presence of 5 mM His. The rate of singlet oxygen production was obtained from the difference in the absence and presence of His

bleaching. There are studies that show an effect of elevated temperature and high light on photoinhibition in PSII of *Symbiodinium* (Symbiodiniaceae) phylotypes (Warner et al. 1999; Brown et al. 2000; Karim et al. 2015).

V. Symbiosis and Exocytosis in Corals

The symbiosis between dinoflagellate algae in the genus *Symbiodinium* (Symbiodiniaceae) and a coral host is a very ancient one: it probably predates the evolution of modern scleractinian corals since there is evidence that their forbears, the rugose corals, were also symbiotic (Stanley and van de Schootbrugge 2009; but see (Wood 1999)). Rugose corals existed from the Middle Ordovician to the Late Permian (450–251 Mya). In fact, there seems to be a history of *Symbiodinium* (or related symbiosis, i.e. members of the Symbiodiniaceae (LaJeunesse et al. 2018); going back to the early Cambrian (Stanley and van de Schootbrugge 2009), and today Symbiodiniaceae are widespread as symbionts in anthozoans and scyphozoans (scler-

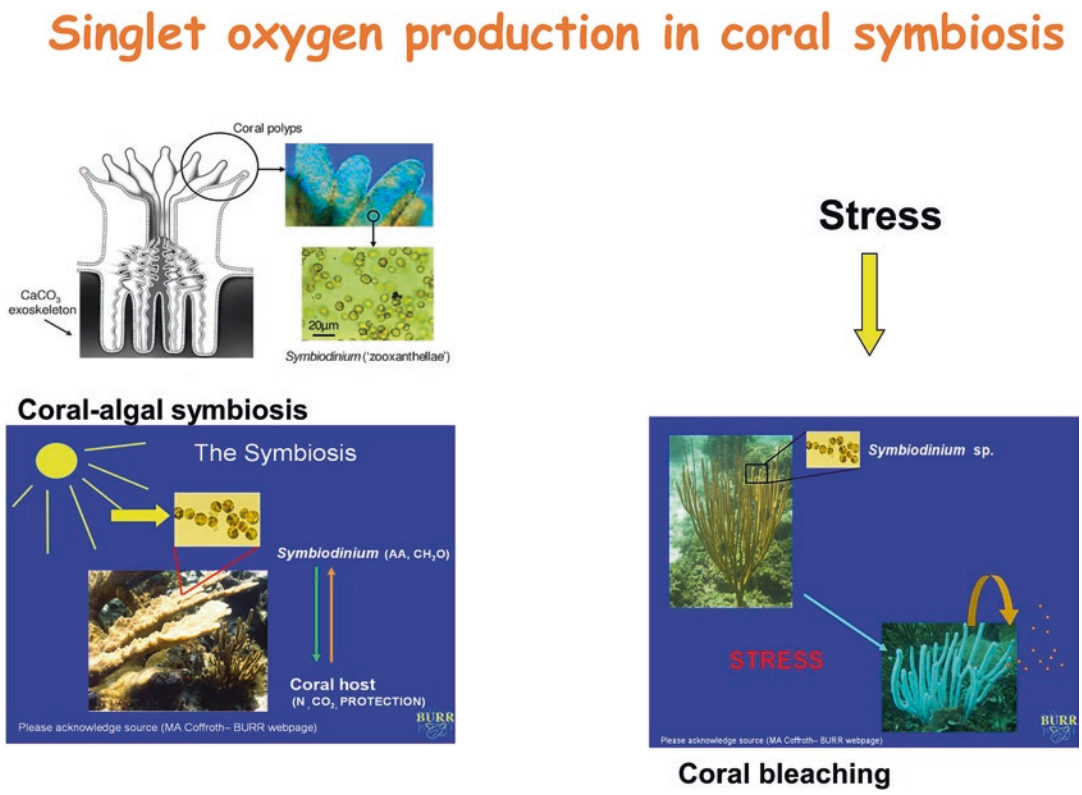

Fig. 17.5. Diagram illustrating the main features of singlet oxygen production in corals

actinian corals, anemones and jelly-fish), sponges, tridacnid molluscs, flatworms, foraminifera and some ciliates (LaJeunesse et al. 2018).

Free-living dinoflagellates are biflagellated unicellular phytoplankton with a cell wall of cellulose plates. Symbiodiniaceae organisms follow this rule, and indeed many of them do not enter into symbiosis, but those that do lose their flagella and cell wall and become what are familiarly known as zooxanthellae. In scleractinian corals zooxanthellae occur in the inner tissue cells (endoderm) and tentacles. Each zooxanthella is contained within a host membrane and the whole structure is known as a symbiosome; the host membrane is known as the symbiosome membrane and is derived from the endoplasmic reticulum of the host cell (Kazandjian et al. 2008) (Fig. 17.7). The process of uptake of free-living Symbiodiniaceae (endocytosis) and expulsion (exocytosis) has not been well researched in scleractinian corals because of the difficulty of observation in a calcified multicellular animal. However, much more is known about this process from studies of the processes in anemones, particularly *Aiptasia* (which is referred to below as *Exaiptasia*). Examination of symbiosomes has also been carried out in the anemone, *Zoanthus robustus* (Kazandjian et al. 2008) and it is from this study that we have the most detailed knowledge of symbiosome structure (Fig. 17.7).

Most corals harbor more than one type of zooxanthella in the Symbiodiniaceae. These types (clades) are inherited either vertically, i.e. by inheritance from the gametes or embryos, or horizontally, i.e. by uptake from the ambient seawater. A number of studies

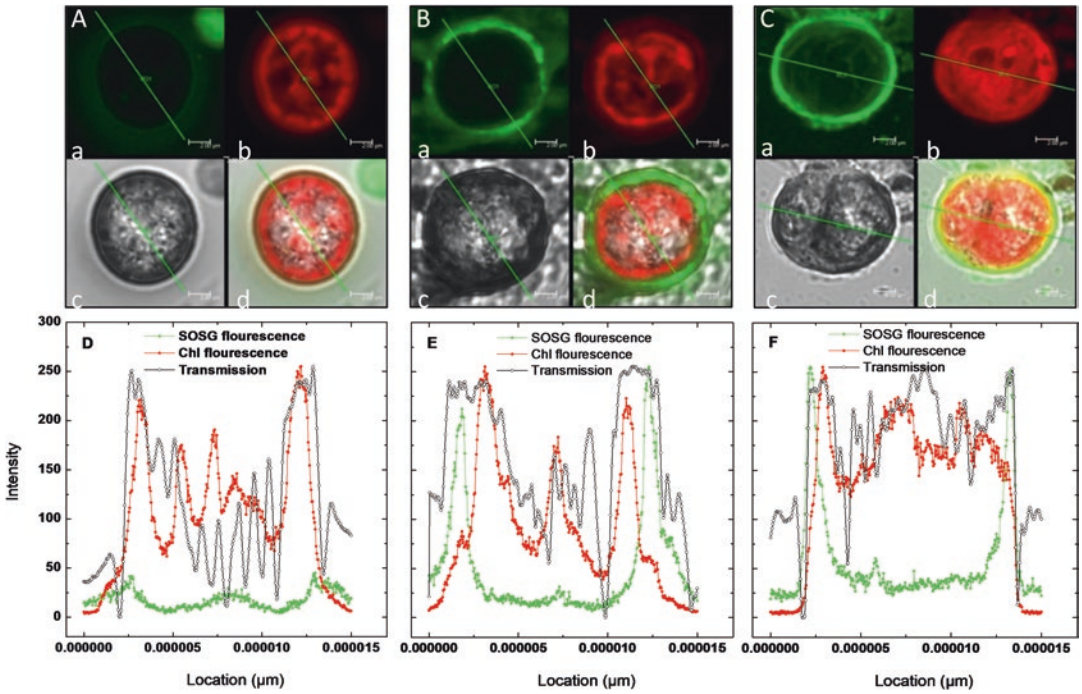

Fig. 17.6. The use of the compound singlet oxygen sensor green (SOSG) in the detection of singlet oxygen and the demonstration that singlet oxygen produced inside *Symbiodinium* (Symbiodiniaceae) cells can move out from these cells. (Data from Rehman et al. (2016) New Phytologist 212: 472–484; with permission)

have now shown that horizontal uptake is a frequent event (Abrego et al. 2009; Nitschke et al. 2016; Quigley et al. 2017). As mentioned in Sects. E and F, the clades, species, genotypes of Symbiodiniaceae help to explain how evolution may have responded to the need to adapt to the ever present hazard of thermal intolerance by changing the enzyme levels of Mehler enzymes, etc. to match trending changes in summer sea surface temperatures. In fact, the adaptive bleaching hypothesis (Buddemeier and Fautin 1993) has been put forward as a mechanism by which small scale changes in zooxanthellar composition could be a mechanism to adjust the proportion of different Symbiodiniaceae in any one coral, the better to match its ecological niche in a gradually changing climate. In the event it can be seen that global climate change has caused much greater changes than have ever been experienced on the Earth before and under these circumstances catastrophic mass coral bleaching events have become the norm as explained in Section I.

VI. The Possible Mechanisms of Coral Bleaching

Coming back to the possible mechanisms that cause mass coral bleaching there are several definitions of coral bleaching, ranging from (i) the loss of symbionts (with no loss of photosynthetic activity), (ii) loss of symbionts (with loss of photosynthetic activity), (iii) the degradation *in situ* of symbionts and (iv) the loss of pigmentation of symbionts, (v) degradation or apoptosis of *in situ* zooxanthellae or their host cells. It is not hard to see that the same set of toxic reactions could cause these changes *in seriatim*.

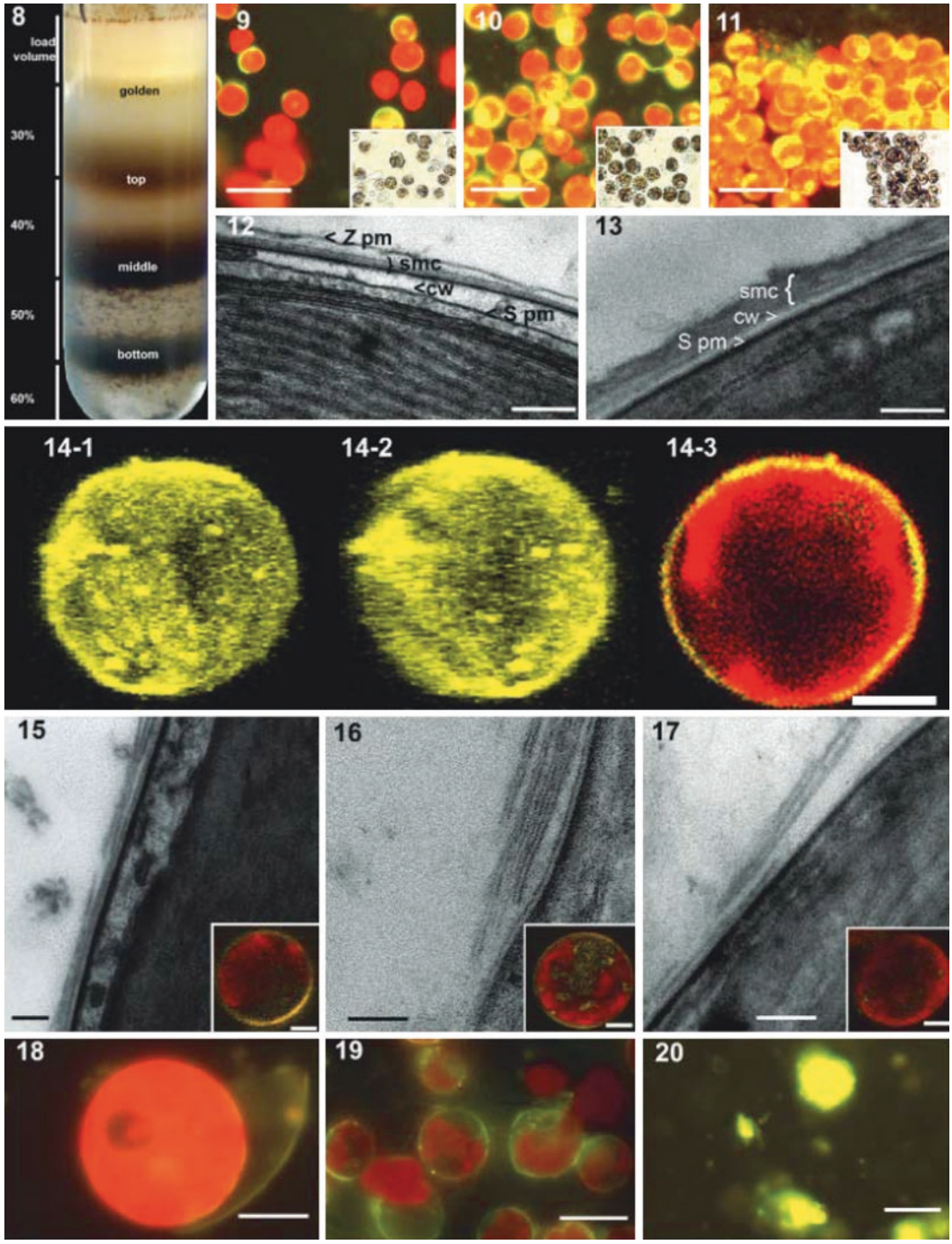

Fig. 17.7. The isolation of intact symbiosomes from *Zoanthus robustus* and the preparation of symbiosome membranes

8. Symbiosomes from *Zoanthus robustus* purified using a discontinuous sucrose density gradient (30–60%). Illustrated in 10–12).; 9. Symbiosomes isolated from the top (40%) band and stained with FM 1–43 (30 mM) and examined under epifluoresence microscopy. Scale bar, 20 μm; 10. Symbiosomes isolated from the middle (50%) band (insert: bright-field micrograph of the same field of view). Scale bar, 20 μm; 11. Symbiosomes isolated

For example, under the right conditions a rather mild set of trigger stimuli could set in action a cascade process of second messengers that would cause the exocytosis of a significant number of zooxanthellae, without significantly inhibiting the photosynthetic activity of the expelled cells. However, under slightly changed conditions one can imagine that higher level of ROS would have a chance to damage the photosynthetic mechanisms of the expelled cells, and thus the expelled cells would show impaired photosynthetic activity. Moving further along the stress spectrum one can imagine a condition where the level of ROS and other associated stress factors would cause the degeneration of zooxanthellae *in situ*. Further this might be accompanied by the degradation of zooxanthellar pigments before the breakdown of zooxanthellae or the demise of host cells by dislodgement or apoptosis. Thus mass coral bleaching is likely to be a continuum phenomenon and it is probably unreasonable to seek different explanations for each type of bleaching phenomenon.

Let us then seek to understand the most accepted view of the phenomenon of coral bleaching, where a certain compounds triggers a chain reaction, which leads to the mass expulsion of relatively undamaged zooxanthellae. If this possibility is sustained, then the more severe forms of mass bleaching can be reasonably accommodated along a spectrum of increasing stress.

A. Possible Cascade Processes Leading to Exocytosis

Understanding the role of ROS in higher plants has experienced great strides forward over the last decade (see e.g. Noctor et al. 2017, Fig. 17.8), but in corals we know much less about any specific mechanism that may be related to exocytosis and coral bleaching (the situation in anemones, e.g. *Exaiptasia*, is getting a little better and this subject is treated separately below).

The problem with ROS and signaling in plastids is that there is too much of it under high light. Thus if we are looking for a sig-

Fig. 17.7. (continued) from the bottom (60%) band examined under epifluoresence microscopy (insert: bright-field micrograph of the same field of view). Scale bar, 20 μm; 12. Verification of *Zoanthus robustus* symbiosome isolation protocol. TEM of periphery of isolated gastrodermal cell. Z pm = zoanthid gastrodermal plasma membrane, smc = symbiosome multilayered membrane complex, cw = algal cell wall, S pm = Symbiodinium plasma membrane. Scale bar, 0.2 μm; 13. TEM of periphery of a symbiosome middle band. Z pm = zoanthid gastrodermal plasma membrane, smc = symbiosome multilayered membrane complex, cw = algal cell wall, S pm = *Symbiodinium* plasma membrane. Scale bar, 0.2 μm; 14. Confocal microscopy of symbiosome from the middle band; 14–1 and 14–2 are composites of several images and demonstrate a degree of heterogeneity of the symbiosome membrane; Scale bar, 2 μm; 15. Isolation of the symbiosome membrane complex using detergent solubilisation. TEM of Triton X solubilisation of *Zoanthus robustus* symbiosome membrane complex treated with detergent for 1 min. Scale bar, 10 μm. (Insert: confocal image of FM1–43-stained symbiosomes treated in the same way. Scale bar, 2 μm); 16. Isolation of the symbiosome membrane complex using detergent solubilisation. TEM of Triton X solubilisation of *Zoanthus robustus* symbiosome membrane complex treated with detergent for 15 min. Scale bar, 10 μm. (Insert: confocal image of FM 1–43-stained symbiosomes treated in the same way. Scale bar, 2 μm); 17. Isolation of the symbiosome membrane complex using detergent solubilisation. TEM of Triton X solubilisation of symbiosome membrane complex. Scale bar, 10 μm. (Insert: confocal image of FM 1–43-stained symbiosomes treated in the same way. Scale bar, 2 μm); 18. FM 1–43-stained symbiosome that had been osmotically shocked: high-power epifluorescent microscopy. Scale bar, 5 μm; 19. FM 1–43-stained symbiosomes that have been osmotically shocked examined under epifluorescent microscopy. Scale bar, 10 μm; 20. FM 1–43-stained symbiosome membrane complex fragments isolated using the optimised method and examined under epifluorescent microscopy. Scale bar, 10 μm. (Taken from Kazandjian et al. (2008) Phycologia 47: 294–306; with permission)

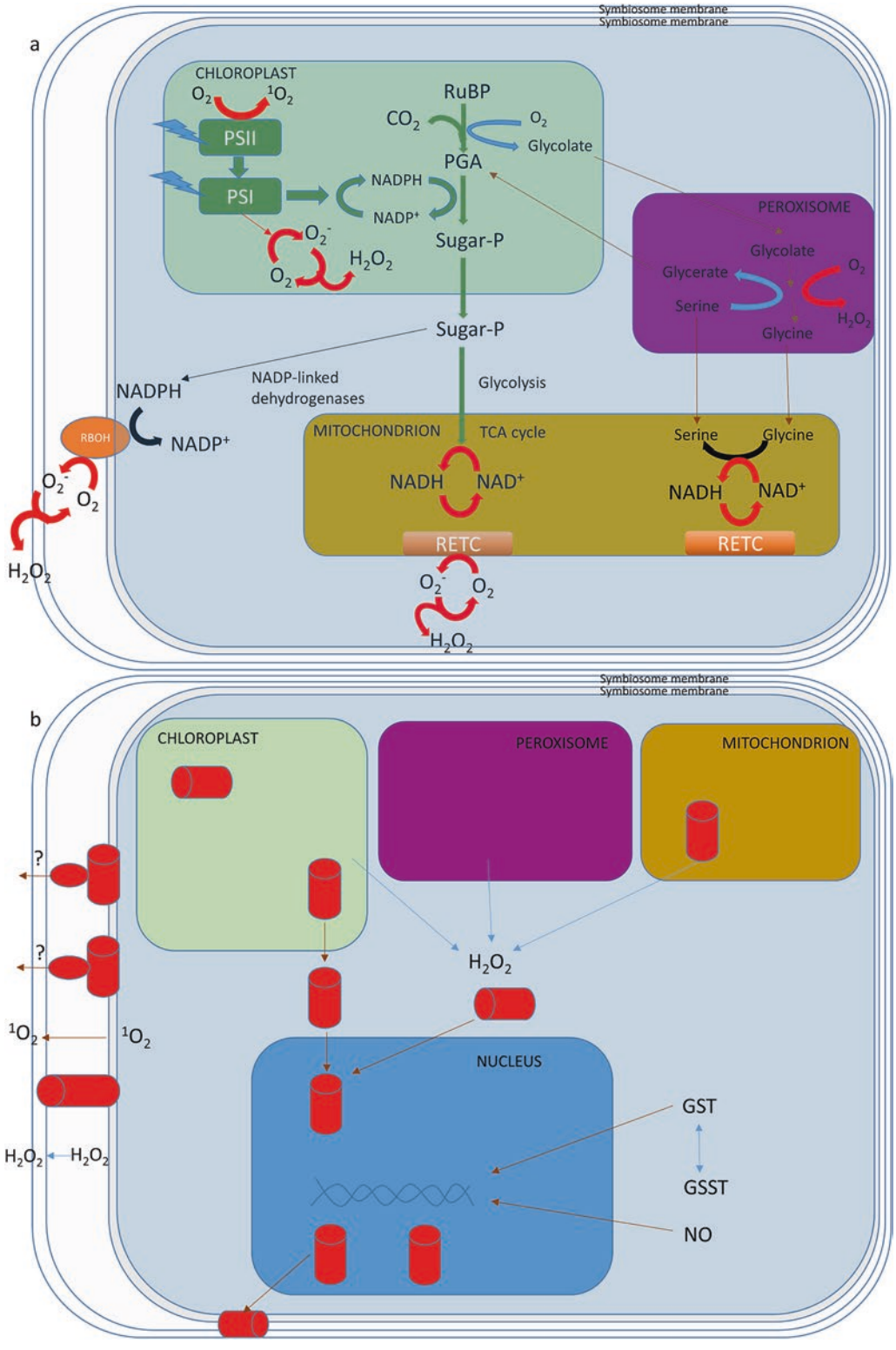

Fig. 17.8. Second messenger system of ROS signaling in *Symbiodinium* (Symbiodiniaceae). (**a**) Showing the major effects of elevated temperature on the production of key metabolites; and (**b**) the likely second messenger systems that are triggered under elevated temperatures. (Based on diagram of Noctor et al. 2017, with permission)

naling process, we have to look through the haze of powerful oxidants that will perform damage to a large array of cell constituents as well as acting as signals; and this has been recognized by the major workers in the field, e.g. Noctor et al. 2017. The major components of ROS could have dual roles. (1) At high concentrations they can cause damage to cell components such as proteins and lipids. These damaged components could in themselves cause photoinhibition, which could be a trigger for exocytosis, here seen as the most likely cause of bleaching; or they could cause degradation of zooxanthellae or destruction of pigments, a less likely cause of bleaching. In addition, the oxidized components, such as lipid peroxides, could act as triggering molecules for second messenger systems (Fig. 17.8), which could trigger exocytosis. (2) At low concentrations it is known that H_2O_2 and $^1O_2$ can act as signals for second messenger systems. In higher plants much is now known about the roles of these chemicals in control of plant function. However, in corals and cultured Symbiodiniaceae almost nothing is known. Table 17.1 sets out the limited information available. As pointed out by Noctor et al. (2017) H_2O_2 is not only produced by plastids but is also generated in mitochondria and in peroxisomes, so its presence and role in triggering cell responses is likely to be complex (Fig. 17.8). H_2O_2 can also be generated at the cell membrane of cells by a respiratory burst oxidase homologue (RBOH).

H_2O_2 is rather less reactive than $^1O_2$, has a longer lifetime and therefore can travel longer distances. Therefore, H_2O_2 is likely to reach the cell membrane of photosynthetic cells and to permeate beyond, i.e. in zooxanthellae, to reach the cytoplasm of host coral cells. In principle, this could be a signaling pathway. Numerous reports confirm the presence of H_2O_2 in zooxanthellae and its increased production in cells at elevated temperatures (Table 17.1, see also Downs et al. 2002; Smith et al. 2005; Suggett et al. 2008; Goyen et al. 2017; Lesser 1997, 2006, 2011; Roberty et al. 2014, 2015, 2016); and of course H_2O_2 can be generated in mitochondria and the cytoplasm of host cells themselves. Gustafsson et al. 2014 carried out a simulation model of bleaching in corals using the levels of H_2O_2 found by Suggett et al. 2008 and found that the general parameters could be modeled closely, but they assumed that H_2O_2 would initiate exocytosis by generating harmful levels, whereas it is more likely that it is caused by a specific second messenger cascade process involving a much more sophisticated mechanism of exocytosis. The role of H_2O_2 in triggering second messenger systems in higher plant chloroplast/cell systems has recently been established under high light (Exposito-Rodriguez et al. 2017). As above, singlet oxygen, a much more reactive molecule, can also mediate secondary signaling pathways leading to cell death in higher plants (Laloi et al. 2004), and mediate signaling between the chloroplast and the nucleus (Fischer et al. 2007), and can also permeate algal symbiont cells and reach the host cytoplasm, where a second messenger system could be triggered.

A key question in the role of H_2O_2 in triggering second messenger systems in corals or anemones is the level of enzyme antioxidants such as catalase, ascorbate peroxidase and GST. In addition to these it is now known that the fluorescent pigments of corals also stimulate the breakdown of H_2O_2. However, as pointed out in Sect. A, the critical question is where the second messenger system is triggered and how the ambient levels of H_2O_2 and antioxidants, in for instance, the zooxanthellae cytoplasm or the host cytoplasm relates to the triggering of second messengers. Interestingly there is only one study of the production of superoxide in corals (*Stylophora pistillata*) and *Symbiodinium sp.* (formerly Clade A) and *Cladocopium goreaui* LaJeunesse & H.J.Jeong gen. Nov., (formerly Clade C); here it was found that superoxide was generated at levels of 0.46 nmol. min^{-1}. mg^{-1} protein in the dark and 0.69 nmol. min^{-1}. mg^{-1} protein in bleaching corals in the light (Saragosti et al. 2010).

The signal transduction (cascade) processes are characterized in high details in higher plants and *Chlamydomonas reinhardtii* (e.g. Noctor et al. 2017). The following section also summarizes the currently known signal transduction pathways in algal-cnidarian symbiosis:

1. MAPK Protein Signaling

This is perhaps the most cited signal transduction pathway in coral bleaching research, although no firm evidence at the signal transduction level has been advanced. MAPK is a mitogen-activated protein kinase (MAPK or MAP kinase): a protein kinase that is specific to the amino acids serine and threonine. In plants and *Chlamydomonas*, MAPKs are involved in directing cellular responses to a diverse array of stimuli, such as mitogens, osmotic stress, heat shock and proinflammatory cytokines. They regulate cell functions including proliferation, gene expression, differentiation, mitosis, cell survival, apoptosis and exocytosis (Coxon et al. 2003). It is therefore possible that in corals MAPK may be involved in exocytosis and also in apoptosis. Its role in coral bleaching has been advanced by a number of authors dating back over the last 20 years, of which recent advocates are: Smith et al. 2005; Seneca et al. 2010; Bhagooli 2013; Palumbi et al. 2014.

2. Glutathione (GSH) Signaling

GSH has been recognized as a key metabolite in signal transduction networks (Noctor et al. 2017). In corals and zooxanthellae, a number of reports confirm the upregulation of GSH and associated enzymes under coral bleaching conditions (Lesser 2006, 2010; Weston et al. 2012; Krueger et al. 2015a, b; Rosic et al. 2015; Hillyer et al. 2016, 2017a, b).

3. Calcium Activated Signaling (CAS)

This is an important signal transduction process and occurs in the regulation of chloroplast proteins. Kaniewska et al. 2015 reported changes in CAS under bleaching conditions in corals.

4. WRKY Transcription Factors

As reported by Chen et al. 2012 WRKY gene family plays important roles in the regulation of transcriptional reprogramming associated with plant stress responses. A network of interactions of WRKY genes and/or changes in their activity contribute to various signaling pathways and regulatory networks. Interestingly, a single WRKY gene often responds to several stress factors, and modified proteins may participate in the regulation of several seemingly disparate processes in negative or positive ways. Thus WRKY proteins also undergo protein–protein interaction and autoregulation and cross-regulation is extensively recorded among WRKY genes. The possibility of WRKY genes in coral bleaching has been invoked but not proven (Weston et al. 2012; Pasaribu et al. 2015).

5. NAC (SNAC) Proteins

NAC (SNAC) proteins exhibit stress related properties (Nakashima et al. 2012). These proteins have a well-defined NAC domain of ~100 amino acids which bind DNA and while the C-terminal end can link to transcription factors. They are associated with stress response conditions.

6. Plant Heat Stress Factor (Hsf) Transcription Factors

Plant Heat Stress Factor (Hsf) transcription factors have been studied inter alia by Scharf et al. (2012).

In addition to these ROS related signal transduction systems, there is also:

7. Nitric Oxide Signaling

The nitric oxide (NO) signaling network is known to take part in many processes in a similar way to ROS signaling; in fact, there

is much evidence that the two signal pathways interact intimately (Trapido-Rosenthal et al. 2005; Perez and Weis 2006; Palavan-Unsal and Arisan 2009). In corals, NO has been implicated in a number of investigations by Hawkins and coworkers (Hawkins and Davy 2013; Hawkins et al. 2013, 2014, 2015). These authors suggest that bleaching may represent a host innate immune-like response to symbiont dysfunction that involves synthesis of the signaling compound NO and the induction of host apoptotic-like cell death. This may well be; and could explain some of the observed differences with a range of corals and the bleaching regimes; and does not necessarily speak against the overwhelming evidence for ROS and signal transduction cascades involving oxygen radicals as triggers for exocytosis.

VII. Bleaching in Anemones

In anemones (class Anthozoa, with corals) there is good experimental evidence on the processes of algal uptake into symbiosis and the loss of symbionts by a variety of means. Two experimental systems have been popular in the past: (i) *Hydra viridissima* with the green alga *Chlorella*, and (ii) various marine anemones with the dinoflagellate *Symbiodinium* (now taxonomically separated into various Symbiodiniaceae), of which the most information recently has come from *Exaiptasia* (Bieri et al. 2016; Matthews et al. 2017).

Recent work on the *Hydra-Chlorella* symbiosis have revealed a strong evolution of specialized genes and the important role of photosynthetic metabolites (Bosch 2012; Kawaida et al. 2013; Ishikawa et al. 2016; Hamada et al. 2018). Ishikawa et al. 2016 indicated that oxidative stress-related genes have played an important role in the ongoing process of symbiosis/endosymbiosis evolution in the *Chlorella* symbiosis.

Using *Exaiptasia* it has been shown that there are a number of responses to elevated temperature. Hillyer et al. 2016 show that the strongest response was in the increase in polyunsaturated fatty acids (PUFAs); and this is in line with the action of ROS on lipids. In addition, pools of the antioxidant glutathione were elevated. In a subsequent paper these authors noted a greater breakdown of lipid stores and an increase in the level of the antioxidant α-tocopherol, which eliminates mostly singlet oxygen (Hillyer et al. 2017a). Oakley et al. 2017 showed that *Aiptasia* maintained homeostasis without significant changes in the proteome under gradually elevated temperature, whereas short term heat shock caused widespread induction of physiological responses in the endoplasmic reticulum, protein folding, redox homeostasis and central metabolism. The initial mechanism of thermal disruption could not be identified, however the involvement of host-derived ROS was likely. Mitochondria could be a major source of ROS generation under heat shock; it was found that the amount of NADH-ubiquinone oxidoreductase subunit 1 (NDUFS1) increased under heat shock. Heat shock-induced increase in NDUFS1 may lead to elevated respiration rate and therefore production of ROS, which may leak from mitochondria and play a signaling role (Oakley et al. 2017).

With *Exaiptasia* the recent reviews by Bieri and Pringle 2015 and Matthews et al. 2017 have shown that there are a number of possible interactions with second messenger systems. Matthews et al. 2017 found that bleaching was **not** correlated with

(i) apoptosis, as measured by caspase activity,
(ii) *In situ* degradation, from evidence of electron microscopic sections: any degradation observed was not correlated with bleaching condition and bleaching onset (except for cold shock – see below),
(iii) Cell detachment: as evidenced by material collected after bleaching; detached cells were minimally present.

The results support exocytosis as the major mechanism of bleaching. The only exception to these results was from cold treatment (4 °C in the dark for 4 h) where considerable cell detachment was observed (and cell degradation was observed; this effect was also observed in cultured *Symbiodinium* (Symbiodiniaceae) cells subjected to cold shock). Interestingly, none of the second messenger systems mentioned above for the exocytosis of coral zooxanthellae was indicated, rather another system, the G Protein receptor signaling system was found to be activated (Matthews et al. 2017).

The work of Hillyer et al. 2017b made a number of observations in connection with signal transduction, although their investigation was not specifically designed to pinpoint second messengers. As mentioned before, increases in PUFAs and α-tocopherol could possibly be linked to signal transduction. Increased levels of gentobiose were found, which could be linked to the ascorbate (Asc)–glutathione (GSH) cycle and the production of sulphur-containing amino acids (methionine and cysteine), with the possible upregulation of associated genes. In addition, accumulations of the sugar alcohol, inositol, were detected in thermally stressed host pools, with corresponding declines in the turnover of inositol phosphates and phosphatidylinositol-based signalling pathways (inositol derivatives are present in both the dinoflagellate symbiont and the cnidarian host, see Klueter et al. 2015). In addition to functions as compatible solutes, inositol derivatives have highly conserved roles in cellular recognition, signalling and development, and the study by Rosic et al. 2015 in corals supported a role for inositol phosphates as participating in signal transduction in response to the effect of ROS on coral bleaching (see above). In a sister paper, Hillyer et al. 2017a used ^{13}C to follow metabolite changes associated with bleaching. More recently, changes in inositol abundance in *Aiptasia* hosting different symbiont genotypes have also been characterized (Matthews et al. 2018).

VIII. Conclusions

The subject of mass coral bleaching has acquired a vast array of observations since it was first investigated in the late 1980s. This is not surprising because the phenomenon of mass coral bleaching has been investigated in many different ways and with an array of techniques. Therefore, currently in the field the opinion is prevalent that it is a subject much too difficult to come to any firm conclusion or "road map" for future research.

However, we have taken a different stance. We have come to the opinion that the most likely explanation to the commonest form of mass coral bleaching involves the production of reactive oxygen species associated with Photosystem I of photosynthesis (and to some extent Photosystem II): namely superoxide (O_2^-), hydrogen peroxide (H_2O_2) and singlet oxygen. It is suggested that these then trigger second messenger (signal transduction) systems which induce the major form of mass coral bleaching, viz. exocytosis of zooxanthellae (i.e. exocytosis of *in hospite* cells of various members of the genera of Symbiodiniaceae).

The hypothesis for the over-production of O_2^- and H_2O_2 and the triggering of mass coral bleaching is as follows. Under normal (non-bleaching) conditions, corals exert a close control over the level of these powerful oxidants and put in place a number of antioxidants and antioxidant-removal enzymatic systems. These are the Mehler-Ascorbate-Peroxidase (MAP) pathway, glutathione (GSH) pathways, FLVs and other electron transfer pathways across the thylakoid membrane and also involving networks with mitochondrial redox systems. An important but unresolved issue at present is the FLV, Flavodiiron system; without clear evidence to date one can speculate as follows: under normal conditions the flavodiirons act as a buffer under fluctuating light, whereby under sudden increase in high light these membrane-bound enzymes operate to mop up excess reducing equivalents. Over longer terms, tens of minutes to hours, the other

antioxidant systems come into operation, along with alternative reduction systems using ferredoxin, such as sulphur reduction. Now as elevated temperatures are incurred and mid-day high light conditions come around, the Calvin-Benson cycle is impaired and cannot accept the reducing equivalents, which causes over-reduction of the electron transport chain. The result is a large over-accumulation of reducing equivalents on the reducing side of PSI. The limited pool of flavodiirons is unable to deal with this level of over-reduction and there is then an accumulation of O_2^- and H_2O_2 (and later singlet oxygen). Then the normal antioxidant systems are overwhelmed leading to i) back reactions to PSII with the increased formation of singlet oxygen and accompanying long-term damage to PSII, and ii) the triggering of signal transduction pathways. At present we do not know enough about the processes that are likely to be involved, but it seems possible that a signal transduction pathway is initiated. Whether this occurs in the zooxanthellae or in the host cells is undetermined, but note that the signal transduction pathways are triggered by very low concentrations of their active compounds so that the small amounts of O_2^- and H_2O_2 and singlet oxygen, which almost certainly reach the host cells, could act as a trigger. Once initiated, the exocytosis of zooxanthellae begins. It is also important to note that the H_2O_2, and singlet oxygen-dependent signaling pathways interact in higher plants (Laloi et al. 2007), which may also occur in *Symbiodinium* (Symbiodiniaceae). On earlier instances of coral bleaching it seems that limited bleaching with recovery was possible, so it appears that the signal transduction pathway can be modulated in some way. More recently, catastrophic bleaching has been recorded, for example, up and down the Great Barrier Reef, so it seems likely that the greater stresses associated with higher temperatures over longer time periods lead to much more prolonged exocytosis, and hence heavier bleaching episodes.

The side reactions of over-reduction of PSI, especially with singlet oxygen in PSII and its harmful effect on PSII, may well play a part in the observations of the other forms of bleaching. That is, the prolonged damaging effects of over-reduction of PSI may cause damage to cells, cell dislodgement, damage to pigments and apoptosis. Thus it is not surprising that various authors have observed these other forms of coral bleaching, notwithstanding firm conclusions that on the whole the evidence points to exocytosis as by far the most important mechanism of bleaching. Certainly, more work has to be done to understand the interplay of the host and symbiont in the whole signalling network mediated by ROS, particularly under stress scenarios that are prevalent in nature, which is difficult to simulate under laboratory conditions.

It is a sad reflection on the field of mass coral bleaching that these are largely hypotheticals. Putting legs on these hypotheses is quite possible and within the scope of modern science, but it would involve the deployment of a significant body of scientists, with backgrounds in the areas needed – plant physiology, plant biochemistry, ROS and second messenger systems and modern "omics" approaches. Even if we are misled and the answer to coral bleaching lies in other areas, any concerted effort must reveal basic truths and lead to rapid progress to understanding mass coral bleaching as a mechanism. Until we have such an understanding any *ex cathedra* explanation of bleaching will always run the risk of failing just through that lack of understanding.

Acknowledgements

We acknowledge the help in the laboratory and in the field at Heron Island, Great Barrier Reef of many people who contributed to this work in so many ways. The research was supported by the Hungarian Academy of Sciences, MTA Premium Postdoctoral

Research Program (PREMIUM-2017-38, M.S.), and by the grants of the National Research, Development and Innovation Office NKFIH FK-128977 (M.S.) and NKFIH K-116016 (I.V.).

References

Abrego D, van Oppen MJH, Willis BL (2009) Onset of algal endosymbiont specificity varies among closely related species of Acropora corals during early ontogeny. Mol Ecol 18:3532–3543

Aihara Y, Takahashi S, Minagawa J (2016) Heat induction of cyclic electron flow around photosystem I in the symbiotic dinoflagellate Symbiodinium. Plant Physiol 171(1):522–529

Alric J (2010) Cyclic electron flow around photosystem I in unicellular green algae. Photosynth Res 106(1–2):47–56

Aro E-M, Suorsa M, Rokka A, Allahverdiyeva Y, Paakkarinen V, Saleem A, Battchikova N, Rintamäki E (2005) Dynamics of photosystem II: a proteomic approach to thylakoid protein complexes. J Exp Bot 56:347–356

Armoza-Zvuloni R, Shaked Y (2014) Release of hydrogen peroxide and antioxidants by the coral to its external milieu. Biogeosciences 11(17):4587–4598

Armoza-Zvuloni R, Schneider A, Sher D, Shaked Y (2016) Rapid hydrogen peroxide release from the coral Stylophora pistillata during feeding and in response to chemical and physical stimuli. Sci Rep 6:21000

Baker NR, Harbinson J, Kramer DM (2007) Determining the limitations and regulation of photosynthetic energy transduction in leaves. Plant Cell Environ 30(9):1107–1125

Bhagooli R (2013) Inhibition of Calvin–Benson cycle suppresses the repair of photosystem II in Symbiodinium: implications for coral bleaching. Hydrobiologia 714(1):183–190

Bieri T, Pringle J (2015) Cellular mechanisms of cnidarian bleaching. In: Integrative and comparative biology. Oxford University Press, Oxford, pp E15–E15

Bieri T, Onishi M, Xiang T, Grossman AR, Pringle JR (2016) Relative contributions of various cellular mechanisms to loss of algae during cnidarian bleaching. PLoS One 11(4):e0152693

Bosch TC (2012) What Hydra has to say about the role and origin of symbiotic interactions. Biol Bull 223(1):78–84

Bowyer JR, Camilleri P (1985) Spin-trap study of the reactions of ferredoxin with reduced oxygen species in pea chloroplasts. Biochim Biophys Acta Bioenerg 808:235–242

Brown B, Dunne R, Warner M, Ambarsari I, Fitt W, Gibb S, Cummings D (2000) Damage and recovery of Photosystem II during a manipulative field experiment on solar bleaching in the coral Goniastrea aspera. Mar Ecol Prog Ser 195:117–124

Buddemeier RW, Fautin DG (1993) Coral bleaching as an adaptive mechanism. Bioscience 43(5):320–326

Cardol P, Forti G, Finazzi G (2011) Regulation of electron transport in microalgae. Biochim Biophys Acta Bioenerg 1807(8):912–918

Chaux F, Peltier G, Johnson X (2015) A security network in PSI photoprotection: regulation of photosynthetic control, NPQ and O-2 photoreduction by cyclic electron flow. Front Plant Sci 6:875. https://doi.org/10.3389/fpls.2015.00875

Chen L, Song Y, Li S, Zhang L, Zou C, Yu D (2012) The role of WRKY transcription factors in plant abiotic stresses. Biochim Biophys Acta, Gene Regul Mech 1819(2):120–128

Chow WS, Fan D-Y, Oguchi R, Jia H, Losciale P, Park Y-I, He J, Öquist G, Shen Y-G, Anderson JM (2012) Quantifying and monitoring functional photosystem II and the stoichiometry of the two photosystems in leaf segments: approaches and approximations. Photosynth Res 113(1–3, Sp. Iss. SI):63–74. https://doi.org/10.1007/s11120-012-9740-y

Coxon PY, Rane MJ, Uriarte S, Powell DW, Singh S, Butt W, Chen Q, McLeish K (2003) MAPK-activated protein kinase-2 participates in p38 MAPK-dependent and ERK-dependent functions in human neutrophils. Cell Signal 15:993–1001

Crafts-Brandner SJ, Law RD (2000) Effect of heat stress on inhibition and recovery of ribulose-1,5-bisphosphate carbox-ylase/oxygenase activation state. Planta 212:67–74

Davy SK, Burchett SG, Dale AL, Davies P, Davy JE, Muncke C, Hoegh-Guldberg O, Wilson WH (2006) Viruses: agents of coral disease? Dis Aquat Org 69(1):101–110

Downs CA, Fauth JE, Halas JC, Dustan P, Bemiss J, Woodley CM (2002) Oxidative stress and seasonal coral bleaching. Free Radical Bio Med 33(4):533–543

Endo T, Asada K (2008) Photosystem I and Photoprotection: Cyclic Electron Flow and Water-Water Cycle. In: Demmig-Adams B, Adams WW, Mattoo AK (eds) Photoprotection, Photoinhibition, Gene Regulation, and Environment. Advances in Photosynthesis and Respiration, vol 21. Springer, Dordrecht, pp 205–221

Exposito-Rodriguez M, Laissue PP, Yvon-Durocher G, Smirnoff N, Mullineaux PM (2017) Photosynthesis-dependent H 2 O 2 transfer from chloroplasts to

nuclei provides a high-light signalling mechanism. Nat Commun 8(1):49

Fischer BB, Krieger-Liszkay A, Hideg É, Šnyrychová I, Wiesendanger M, Eggen RI (2007) Role of singlet oxygen in chloroplast to nucleus retrograde signaling in Chlamydomonas reinhardtii. FEBS Lett 581(29):5555–5560

Flors C, Fryer MJ, Waring J, Reeder B, Bechtold U, Mullineaux PM, Nonell S, Wilson MT, Baker NR (2006) Imaging the production of singlet oxygen *in vivo* using a new fluorescent sensor, singlet oxygen sensor green®. J Exp Bot 57:1725–1734

Fufezan C, Rutherford AW, Krieger-Liszkay A (2002) Singlet oxygen production in herbicide-treated photosystem II. FEBS Lett 532:407–410

Gardner SG, Raina J-B, Nitschke MR, Nielsen DA, Stat M, Motti CA, Ralph PJ, Petrou K (2017) A multi-trait systems approach reveals a response cascade to bleaching in corals. BMC Biol 15(1):117

Gates RD, Baghdasarian G, Muscatine L (1992) Temperature stress causes host cell detachment in symbiotic cnidarians: implications for coral bleaching. Biol Bull 182:324–332

Gerotto C, Alboresi A, Meneghesso A, Jokel M, Suorsa M, Aro E-M, Morosinotto T (2016) Flavodiiron proteins act as safety valve for electrons in Physcomitrella patens. Proc Natl Acad Sci 113(43):12322–12327

Gierz SL, Forêt S, Leggat W (2017) Transcriptomic analysis of thermally stressed Symbiodinium reveals differential expression of stress and metabolism genes. Front Plant Sci 8:271

Goyen S, Pernice M, Szabó M, Warner ME, Ralph PJ, Suggett DJ (2017) A molecular physiology basis for functional diversity of hydrogen peroxide production amongst Symbiodinium spp.(Dinophyceae). Mar Biol 164(3):46

Gustafsson MSM, Baird ME, Ralph PJ (2014) Modeling photoinhibition-driven bleaching in Scleractinian coral as a function of light, temperature, and heterotrophy. Limnol Oceanogr 59(2):603–622

Hakkila K, Antal T, Rehman AU, Kurkela J, Wada H, Vass I, Tyystjärvi E, Tyystjärvi T (2014) Oxidative stress and photoinhibition can be separated in the cyanobacterium *Synechocystis* sp. PCC 6803. Biochim Biophys Acta 1837:217–225

Hamada M, Schröder K, Bathia J, Kürn U, Fraune S, Khalturina M, Khalturin K, Shinzato C, Satoh N, Bosch TC (2018) Metabolic co-dependence drives the evolutionarily ancient Hydra–Chlorella symbiosis. eLife 7:e35122

Hawkins TD, Davy SK (2013) Nitric oxide and coral bleaching: is peroxynitrite generation required for symbiosis collapse? J Exp Biol 216:3185–3188. https://doi.org/10.1242/jeb.087510

Hawkins TD, Bradley BJ, Davy SK (2013) Nitric oxide mediates coral bleaching through an apoptotic-like cell death pathway: evidence from a model sea anemone-dinoflagellate symbiosis. FASEB J 27(12):4790–4798

Hawkins TD, Krueger T, Becker S, Fisher PL, Davy SK (2014) Differential nitric oxide synthesis and host apoptotic events correlate with bleaching susceptibility in reef corals. Coral Reefs 33(1):141–153

Hawkins TD, Krueger T, Wilkinson SP, Fisher PL, Davy SK (2015) Antioxidant responses to heat and light stress differ with habitat in a common reef coral. Coral Reefs 34(4):1229–1241

Hideg É, Schreiber U (2007) Parallel assessment of ROS formation and photosynthesis in leaves by fluorescence imaging. Photosynth Res 92(1):103–108. https://doi.org/10.1007/s11120-007-9146-4

Hideg É, Spetea C, Vass I (1994) Singlet oxygen production in thylakoid membranes during photoinhibition as detected by EPR spectroscopy. Photosynth Res 39:191–199

Hideg É, Deák Z, Hakala-Yatkin M, Karonen M, Rutherford AW, Tyystjärvi E, Vass I, Krieger-Liszkay A (2011) Pure forms of the singlet oxygen sensors TEMP and TEMPD do not inhibit photosystem II. Biochim Biophys Acta, Bioenerg 1807(12):1658–1661. https://doi.org/10.1016/j.bbabio.2011.09.009

Higuchi T, Fujimura H, Ikota H, Arakaki T, Oomori T (2009a) The effects of hydrogen peroxide on metabolism in the coral Goniastrea aspera. J Exp Mar Biol Ecol 370(1–2):48–55

Higuchi T, Fujimura H, Arakaki T, Oomori T (2009b) The synergistic effects of hydrogen peroxide and elevated seawater temperature on the metabolic activity of the coral Galaxea fascicularis. Mar Biol 156(4):589–596

Hill R, Szabó M, Rehman AU, Vass I, Ralph PJ, Larkum AW (2014) Inhibition of photosynthetic CO_2 fixation in the coral Pocillopora damicornis and its relationship to thermal bleaching. J Exp Biol 217(12):2150–2162

Hillyer KE, Tumanov S, Villas-Bôas S, Davy SK (2016) Metabolite profiling of symbiont and host during thermal stress and bleaching in a model cnidarian–dinoflagellate symbiosis. J Exp Biol 219(4):516–527

Hillyer KE, Dias DA, Lutz A, Roessner U, Davy SK (2017a) Mapping carbon fate during bleaching in a model cnidarian symbiosis: the application of 13C metabolomics. New Phytol 214(4):1551–1562

Hillyer KE, Dias DA, Lutz A, Wilkinson SP, Roessner U, Davy SK (2017b) Metabolite profiling of symbiont and host during thermal stress and bleaching in the coral Acropora aspera. Coral Reefs 36(1):105–118

Hoegh-Guldberg O (2009) Climate change and coral reefs: Trojan horse or false prophecy? Coral Reefs 28(3):569–575. https://doi.org/10.1007/s00338-009-0508-6

Hoegh-Guldberg O, Smith GJ (1989a) The effect of sudden changes in temperature, light and salinity on the population density and export of zooxanthellae from the reef corals Stylophora pistillata Esper and Seriatopora hystrix Dana. J Exp Mar Biol Ecol 129(3):279–303

Hoegh-Guldberg O, Smith GJ (1989b) Influence of the population density of zooxanthellae and supply of ammonium on the biomass and metabolic characteristics of the reef corals Seriatopora hystrix and Stylophora pistillata. Mar Ecol Prog Ser 57:173–186

Hoogenboom MO, Campbell DA, Beraud E, Dezeeuw K, Ferrier-Pages C (2012) Effects of light, food availability and temperature stress on the function of photosystem II and photosystem I of coral symbionts. PLoS One 7(1):e30167. https://doi.org/10.1371/journal.pone.0030167

Hughes TP, Baird AH, Bellwood DR, Card M, Connolly SR, Folke C, Grosberg R, Hoegh-Guldberg O, Jackson JB, Kleypas J, Lough JM, Marshall P, Nystrom M, Palumbi SR, Pandolfi JM, Rosen B, Roughgarden J (2003) Climate change, human impacts, and the resilience of coral reefs. Science 301(5635):929–933. https://doi.org/10.1126/science.1085046301/5635/929

Hughes TP, Anderson KD, Connolly SR, Heron SF, Kerry JT, Lough JM, Baird AH, Baum JK, Berumen ML, Bridge TC, Claar DC, Eakin CM, Gilmour JP, Graham NAJ, Harrison H, Hobbs J-PA, Hoey AS, Hoogenboom M, Lowe RJ, McCulloch MT, Pandolfi JM, Pratchett M, Schoepf V, Torda G, Wilson SK (2018a) Spatial and temporal patterns of mass bleaching of corals in the Anthropocene. Science (Washington DC) 359(6371):80–82. https://doi.org/10.1126/science.aan8048

Hughes TP, Kerry JT, Baird AH, Connolly SR, Dietzel A, Eakin CM, Heron SF, Hoey AS, Hoogenboom MO, Liu G, McWilliam MJ, Pears RJ, Pratchett MS, Skirving WJ, Stella JS, Torda G (2018b) Global warming transforms coral reef assemblages. Nature (London) 556(7702):492–496. https://doi.org/10.1038/s41586-018-0041-2

Hughes TP, Kerry JT, Simpson T (2018c) Large-scale bleaching of corals on the great barrier reef. Ecology (Washington DC) 99(2):501. https://doi.org/10.1002/ecy.2092

Ilík P, Pavlovič A, Kouřil R, Alboresi A, Morosinotto T, Allahverdiyeva Y, Aro E-M, Yamamoto H, Shikanai T (2017) Alternative electron transport mediated by flavodiiron proteins is operational in organisms from cyanobacteria up to gymnosperms. New Phytol 214(3, Sp. Iss. SI):967–972. https://doi.org/10.1111/nph.14536

Ishikawa M, Shimizu H, Nozawa M, Ikeo K, Gojobori T (2016) Two-step evolution of endosymbiosis between hydra and algae. Mol Phylogenet Evol 103:19–25

Ivanov AG, Velitchkova MY, Allakhverdiev SI, Huner NP (2017) Heat stress-induced effects of photosystem I: an overview of structural and functional responses. Photosynth Res 133(1–3):17–30

Jia H, Dwyer SA, Fan DY, Han Y, Badger MR, von Caemmerer S, Chow WS (2014) A novel P700 redox kinetics probe for rapid, non-intrusive and whole-tissue determination of photosystem II functionality, and the stoichiometry of the two photosystems in vivo. Physiol Plant 152(3):403–413

Jones RJ, Ward S, Amri AY, Hoegh-Guldberg O (2000) Changes in quantum efficiency of photosystem II of symbiotic dinoflagellates of corals after heat stress, and of bleached corals sampled after the 1998 great barrier reef mass bleaching event. Mar Freshw Res 51(1):63–71

Kálai T, Hideg É, Vass I, Hideg K (1998) Double (fluorescent and spin) sensors for detection of reactive oxygen species in the thylakoid membrane. Free Radic Biol Med 24:649–652

Kaniewska P, Chan C-KK, Kline D, Ling EYS, Rosic N, Edwards D, Hoegh-Guldberg O, Dove S (2015) Transcriptomic changes in coral Holobionts provide insights into physiological challenges of future climate and ocean change. PLoS One 10(10):e0139223. https://doi.org/10.1371/journal.pone.0139223

Karim W, Seidi A, Hill R, Chow WS, Minagawa J, Hidaka M, Takahashi S (2015) Novel characteristics of photodamage to PSII in a high-light-sensitive Symbiodinium phylotype. Plant Cell Physiol 56(6):1162–1171

Kawaida H, Ohba K, Koutake Y, Shimizu H, Tachida H, Kobayakawa Y (2013) Symbiosis between hydra and chlorella: molecular phylogenetic analysis and experimental study provide insight into its origin and evolution. Mol Phylogen Evol 66(3):906–914

Kazandjian A, Shepherd VA, Rodriguez-Lanetty M, Nordemeier W, Larkum AWD, Quinnell RG (2008) Isolation of symbiosomes and the symbiosome membrane complex from the zoanthid Zoanthus

robustus. Phycologia 47(3):294–306. https://doi.org/10.2216/07-23.1

Klueter A, Crandall JB, Archer FI, Teece MA, Coffroth MA (2015) Taxonomic and environmental variation of metabolite profiles in marine dinoflagellates of the genus symbiodinium. Metabolites 5(1):74–99

Klughammer C, Schreiber U (1994) An improved method, using saturating light pulses, for the determination of photosystem I quantum yield via P700+-absorbance changes at 830 nm. Planta 192:261–268

Klughammer C, Schreiber U (2016) Deconvolution of ferredoxin, plastocyanin, and P700 transmittance changes in intact leaves with a new type of kinetic LED array spectrophotometer. Photosynth Res 128(2):195–214

Krieger-Liszkay A (2005) Singlet oxygen production in photosynthesis. J Exp Bot 56:337–346

Krieger-Liszkay A, Fufezan C, Trebst A (2008) Singlet oxygen production in photosystem II and related protection mechanism. Photosynth Res 98:551–564

Krueger T, Fisher PL, Becker S, Pontasch S, Dove S, Hoegh-Guldberg O, Leggat W, Davy SK (2015a) Transcriptomic characterization of the enzymatic antioxidants FeSOD, MnSOD, APX and KatG in the dinoflagellate genus Symbiodinium. BMC Evol Biol 15(1):48

Krueger T, Hawkins TD, Becker S, Pontasch S, Dove S, Hoegh-Guldberg O, Leggat W, Fisher PL, Davy SK (2015b) Differential coral bleaching-contrasting the activity and response of enzymatic antioxidants in symbiotic partners under thermal stress. Comp Biochem Physiol A Mol Integr Physiol 190:15–25. https://doi.org/10.1016/j.cbpa.2015.08.012

LaJeunesse TC, Parkinson JE, Gabrielson PW, Jeong HJ, Reimer JD, Voolstra CR, Santos SR (2018) Systematic revision of symbiodiniaceae highlights the antiquity and diversity of coral endosymbionts. Curr Biol 28(16):2570–2580

Laloi C, Apel K, Danon A (2004) Reactive oxygen signalling: the latest news. Curr Opin Plant Biol 7(3):323–328

Laloi C, Stachowiak M, Pers-Kamczyc E, Warzych E, Murgia I, Apel K (2007) Cross-talk between singlet oxygen-and hydrogen peroxide-dependent signaling of stress responses in Arabidopsis thaliana. Proc Natl Acad Sci 104(2):672–677

Larkum AWD, Szabó M, Fitzpatrick D, Raven JA (2017) Cyclic electron flow in cyanobacteria and eukaryotic algae. In: Barber J, Ruban AV (eds) Photosynthesis and bioenergetics. World Scientific, Singapore, pp 305–343

Leggat W, Whitney S, Yellowlees D (2004) Is coral bleaching due to the instability of the zooxanthellae dark reactions? Symbiosis 37(1–3):137–153

Lesser MP (1997) Oxidative stress causes coral bleaching during exposure to elevated temperatures. Coral Reefs 16(3):187–192. https://doi.org/10.1007/s003380050073

Lesser MP (2006) Oxidative stress in marine environments: biochemistry and physiological ecology. Annu Rev Physiol 68:253–278. https://doi.org/10.1146/annurev.physiol.68.040104.110001

Lesser MP (2011) Coral bleaching: causes and mechanisms. In: Dubinsky Z, Stambler N (eds) Coral reefs: an ecosystem in transition. Springer, Dordrecht, pp 405–419

Lesser MP, Slattery M, Stat M, Ojimi M, Gates RD, Grottoli A (2010) Photoacclimatization by the coral Montastraea cavernosa in the mesophotic zone: light, food, and genetics. Ecology 91:990–1003

Levin RA, Voolstra CR, Weynberg KD, van Oppen MJH (2017) Evidence for a role of viruses in the thermal sensitivity of coral photosymbionts. ISME J 11(3):808–812

Li H, Melø TB, Arellano JB, Naqvi KR (2012) Temporal profile of the singlet oxygen emission endogenously produced by photosystem II reaction centre in an aqueous buffer. Photosynth Res 112(1):75–79

Lilley RM, Ralph PJ, Larkum AW (2010) The determination of activity of the enzyme Rubisco in cell extracts of the dinoflagellate alga Symbiodinium sp. by manganese chemiluminescence and its response to short-term thermal stress of the alga. Plant Cell Environ 33(6):995–1004. https://doi.org/10.1111/j.1365-3040.2010.02121.x

Liñán-Cabello MA, Flores-Ramírez LA, Zenteno-Savin T, Olguín-Monroy NO, Sosa-Avalos R, Patiño-Barragan M, Olivos-Ortiz A (2010) Seasonal changes of antioxidant and oxidative parameters in the coral Pocillopora capitata on the Pacific coast of Mexico. Mar Ecol 31(3):407–417

Matthews JL, Crowder CM, Oakley CA, Lutz A, Roessner U, Meyer E, Grossman AR, Weis VM, Davy SK (2017) Optimal nutrient exchange and immune responses operate in partner specificity in the cnidarian-dinoflagellate symbiosis. Proc Natl Acad Sci 114(50):13194–13199

Matthews JL, Oakley CA, Lutz A, Hillyer KE, Roessner U, Grossman AR, Weis VM, Davy SK (2018) Partner switching and metabolic flux in a model cnidarian–dinoflagellate symbiosis. Proc R Soc B 285(1892):20182336

McGinty ES, Pieczonka J, Mydlarz LD (2012) Variations in reactive oxygen release and antioxidant activity in multiple Symbiodinium types in response to elevated temperature. Microbial Ecol 64(4):1000–1007

Miyake C, Asada K (2003) The water-water cycle in algae. In: Larkum AWD, Douglas SE, Raven JA (eds) Photosynthesis in algae. Advances in Photosynthesis and Respiration. Springer, Dordrecht, pp 183–204

Moldogazieva N, Mokhosoev IM, Feldman NB, Lutsenko SV (2018) ROS and RNS signalling: adaptive redox switches through oxidative/nitrosative protein modifications. Free Radic Res 52(5):507–543

Munekage Y, Hashimoto M, Miyake C, Tomizawa K-I, Endo T, Tasaka M, Shikanai T (2004) Cyclic electron flow around photosystem I is essential for photosynthesis. Nature 429(6991):579–582

Nakashima K, Takasaki H, Mizoi J, Shinozaki K, Yamaguchi-Shinozaki K (2012) NAC transcription factors in plant abiotic stress responses. Biochim Biophys Acta, Gene Regul Mech 1819(2):97–103

Nitschke MR, Davy SK, Ward S (2016) Horizontal transmission of Symbiodinium cells between adult and juvenile corals is aided by benthic sediment. Coral Reefs 35(1):335–344

Noctor G, Reichheld J-P, Foyer CH (2017) ROS-related redox regulation and signaling in plants. Semin Cell Dev Biol 80:3–12

Oakley CA, Schmidt GW, Hopkinson BM (2014) Thermal responses of Symbiodinium photosynthetic carbon assimilation. Coral Reefs 33(2):501–512. https://doi.org/10.1007/s00338-014-1130-9

Oakley CA, Ameismeier MF, Peng L, Weis VM, Grossman AR, Davy SK (2016) Symbiosis induces widespread changes in the proteome of the model cnidarian Aiptasia. Cell Microbiol 18(7):1009–1023

Oakley CA, Durand E, Wilkinson SP, Peng L, Weis VM, Grossman AR, Davy SK (2017) Thermal shock induces host proteostasis disruption and endoplasmic reticulum stress in the model symbiotic cnidarian Aiptasia. J Proteome Res 16(6):2121–2134

Palavan-Unsal N, Arisan D (2009) Nitric oxide signalling in plants. Bot Rev 75(2):203–229

Palumbi SR, Barshis DJ, Traylor-Knowles N, Bay RA (2014) Mechanisms of reef coral resistance to future climate change. Science 344:895–898

Pasaribu B, Weng L-C, Lin I-P, Camargo E, Tzen JT, Tsai C-H, Ho S-L, Lin M-R, Wang L-H, Chen C-S, Jiang P-L (2015) Morphological variability and distinct protein profiles of cultured and endosymbiotic Symbiodinium cells isolated from Exaiptasia pulchella. Sci Rep 5:15353

Perez S, Weis V (2006) Nitric oxide and cnidarian bleaching: an eviction notice mediates breakdown of a symbiosis. J Exp Biol 209:2804–2810

Petrou K, Nielsen DA, Heraud P (2018) Single-cell biomolecular analysis of coral algal symbionts reveals opposing metabolic responses to heat stress and expulsion. Front Mar Sci 5:110

Quigley KM, Willis BL, Bay LK (2017) Heritability of the Symbiodinium community in vertically-and horizontally-transmitting broadcast spawning corals. Sci Rep 7(1):8219

Ragni M, Airs RL, Hennige SJ, Suggett DJ, Warner ME, Geider RJ (2010) PSII photoinhibition and photorepair in Symbiodinium (Pyrrhophyta) differs between thermally tolerant and sensitive phylotypes. Mar Ecol Prog Ser 406:57–70. https://doi.org/10.3354/Meps08571

Rehman AU, Cser K, Sass L, Vass I (2013) Characterization of singlet oxygen production and its involvement in photodamage of photosystem II in the cyanobacterium *Synechocystis* PCC 6803 by histidine-mediated chemical trapping. Biochim Biophys Acta 1827:689–698

Rehman AU, Szabó M, Deák Z, Sass L, Larkum A, Ralph P, Vass I (2016) Symbiodinium sp. cells produce light-induced intra-and extracellular singlet oxygen, which mediates photodamage of the photosynthetic apparatus and has the potential to interact with the animal host in coral symbiosis. New Phytol 212(2):472–484

Reynolds JM, Bruns BU, Fitt WK, Schmidt GW (2008) Enhanced photoprotection pathways in symbiotic dinoflagellates of shallow-water corals and other cnidarians. Proc Natl Acad Sci U S A 105(36):13674–13678. https://doi.org/10.1073/pnas.0805187105

Roberty S, Bailleul B, Berne N, Franck F, Cardol P (2014) PSI Mehler reaction is the main alternative photosynthetic electron pathway in *Symbiodinium* sp., symbiotic dinoflagellates of cnidarians. New Phytol 204(1):81–91. https://doi.org/10.1111/nph.12903

Roberty S, Fransolet D, Cardol P, Plumier J-C, Franck F (2015) Imbalance between oxygen photoreduction and antioxidant capacities in Symbiodinium cells exposed to combined heat and high light stress. Coral Reefs 34:1063–1073

Roberty S, Furla P, Plumier J-C (2016) Differential antioxidant response between two Symbiodinium species from contrasting environments. Plant Cell Environ 39(12):2713–2724

Rodriguez-Lanetty M, Phillips WS, Weis VM (2006) Transcriptome analysis of a cnidarian-dinoflagellate mutualism reveals complex modulation of host gene expression. BMC Genomics 7(23). https://doi.org/10.1186/1471-2164-7-23

Rogers CS (1990) Responses of coral reefs and reef organisms to sedimentation. Mar Ecol Prog Ser 62(1):185–202

Rosic N, Ling EYS, Chan C-KK, Lee HC, Kaniewska P, Edwards D, Dove S, Hoegh-Guldberg O (2015) Unfolding the secrets of coral–algal symbiosis. ISME J 9(4):844–856

Saragosti E, Tchernov D, Katsir A, Shaked Y (2010) Extracellular production and degradation of superoxide in the coral Stylophora pistillata and cultured Symbiodinium. PLoS One 5(9):e12508. https://doi.org/10.1371/journal.pone.0012508

Scharf K-D, Berberich T, Ebersberger I, Nover L (2012) The plant heat stress transcription factor (Hsf) family: structure, function and evolution. Biochim Biophys Acta, Gene Regul Mech 1819(2):104–119

Schmitt FJ, Renger G, Friedrich T, Kreslavski VD, Zharmukhamedov SK, Los DA, Kuznetsov VV, Allakhverdiev SI (2014) Reactive oxygen species: re-evaluation of generation, monitoring and role in stress-signaling in phototrophic organisms. Biochim Biophys Acta, Bioenerg 1837(6):835–848. https://doi.org/10.1016/j.bbabio.2014.02.005

Schreiber U, Klughammer C (2016) Analysis of photosystem I donor and acceptor sides with a new type of online-deconvoluting kinetic LED-array spectrophotometer. Plant Cell Physiol 57(7):1454–1467

Sedoud A, Lopez-Igual R, Rehman AU, Wilson A, Perreau F, Boulay C, Vass I, Krieger-Liszkay A, Kirilovsky D (2014) The cyanobacterial photoactive orange carotenoid protein is an excellent singlet oxygen quencher. Plant Cell 26(4):1781–1791

Seneca FO, Forêt S, Ball EE, Smith-Keune C, Miller DJ, van Oppen MJH (2010) Patterns of gene expression in a Scleractinian coral undergoing natural bleaching. Mar Biotechnol 12:594–604

Shaked Y, Armoza-Zvuloni R (2013) Dynamics of hydrogen peroxide in a coral reef: sources and sinks. J Geophys Res: Biogeosciences 118(4):1793–1801

Shikanai T (2014) Central role of cyclic electron transport around photosystem I in the regulation of photosynthesis. Curr Opin Biotechnol 26:25–30

Smith DJ, Suggett DJ, Baker NR (2005) Is photoinhibition of zooxanthellae photosynthesis the primary cause of thermal bleaching in corals? Glob Chang Biol 11(1):1–11. https://doi.org/10.1111/j.1365-2486.2004.00895.x

Stanley GD Jr, van de Schootbrugge B (2009) The evolution of the coral-algal symbiosis. In: van Oppen MJH, Lough JM (eds) Coral bleaching: patterns, processes, causes and consequences, Ecological studies, vol 205. Springer, Berlin/Heidelberg, pp 7–19

Suggett DJ, Warner ME, Smith DJ, Davey P, Hennige S, Baker NR (2008) Photosynthesis and production of hydrogen peroxide by Symbiodinium (Pyrrhophyta) phylotypes with different thermal tolerances. J Phycol 44(4):948–956. https://doi.org/10.1111/j.1529-8817.2008.00537.x

Szabó M, Larkum AW, Suggett DJ, Vass I, Sass L, Osmond B, Zavafer A, Ralph PJ, Chow WS (2017) Non-intrusive assessment of photosystem II and photosystem I in whole coral tissues. Front Mar Sci 4:269

Takahashi S, Whitney SM, Badger MR (2009) Different thermal sensitivity of the repair of photodamaged photosynthetic machinery in cultured Symbiodinium species. Proc Natl Acad Sci U S A 106(9):3237–3242. https://doi.org/10.1073/pnas.0808363106

Telfer A, Oldham TC, Phillips D, Barber J (1999) Singlet oxygen formation detected by near-infrared emission from isolated photosystem II reaction centres: direct correlation between P680 triplet decay and luminescence rise kinetics and its consequences for photoinhibition. J Photochem Photobiol B 48:89–96

Tikkanen M, Mekala NR, Aro E-M (2014) Photosystem II photoinhibition-repair cycle protects photosystem I from irreversible damage. Biochim Biophys Acta, Bioenerg 1837(1):210–215. https://doi.org/10.1016/j.bbabio.2013.10.001

Tolleter D, Seneca FO, DeNofrio JC, Krediet CJ, Palumbi SR, Pringle JR, Grossman AR (2013) Coral bleaching independent of photosynthetic activity. Curr Biol 23(18):1782–1786

Trapido-Rosenthal H, Zielke S, Owen R, Buxton L, Boeing B, Bhagooli R, Archer J (2005) Increased zooxanthellae nitric oxide synthase activity is associated with coral bleaching. Biol Bull 208:3–6

Vass I (2012) Molecular mechanisms of photodamage in the photosystem II complex. Biochim Biophys Acta Bioenerg 1817(1):209–217

Verlhac JB, Gaudemer A, Kraljic I (1984) Water-soluble porphyrins and metalloporphyrins as photosensitizers in aerated aqueous solutions. I. Detection and determination of quantum yield of formation of singlet oxygen. Nouv J Chim 8:401–406

Wang J-T, Meng P-J, Sampayo E, Tang S-L, Chen CA (2011) Photosystem II breakdown induced by reactive oxygen species in freshly-isolated Symbiodinium from Montipora (Scleractinia; Acroporidae). Mar Ecol Prog Ser 422:51–62

Warner ME, Fitt WK, Schmidt GW (1999) Damage to photosystem II in symbiotic dinoflagellates: a determinant of coral bleaching. Proc Natl Acad Sci U S A 96(14):8007–8012

Weston AJ, Dunlap WC, Shick JM, Klueter A, Iglic K, Vukelic A, Starcevic A, Ward M, Wells ML, Trick CG, Long PF (2012) A profile of an endosymbiont-

enriched fraction of the coral Stylophora pistillata reveals proteins relevant to microbial-host interactions. Mol Cell Proteomics 11(6). https://doi.org/10.1074/mcp.M111.015487

Whitney SM, Shaw DC, Yellowlees D (1995) Evidence that some Dinoflagellates contain a Ribulose-1, 5-bisphosphate carboxylase/oxygenase related to that of the $\ alpha $-proteobacteria. Proc R Soc Lond B Biol Sci 259(1356):271–275

Wietheger A, Starzak DE, Gould KS, Davy SK (2018) Differential ROS generation in response to stress in Symbiodinium spp. Biol Bull 234(1):11–21

Wood R (1999) Reef evolution. Oxford University Press on Demand, Oxford, pp 414

Zaragoza WJ, Krediet CJ, Meyer JL, Canas G, Ritchie KB, Teplitski M (2014) Outcomes of infections of sea anemone Aiptasia pallida with Vibrio spp. pathogenic to corals. Microb Ecol 68(2):388–396

Correction to: Photosynthesis in Algae: Biochemical and Physiological Mechanisms

Anthony W. D. Larkum, Arthur R. Grossman, and John A. Raven

Correction to:
A. W. D. Larkum et al. (eds.), *Photosynthesis in Algae: Biochemical and Physiological Mechanisms*,
Advances in Photosynthesis and Respiration 45,
https://doi.org/10.1007/978-3-030-33397-3

This book was inadvertently published with a spell error in the name of the editor as Arthur R. Grossmann. This has now been corrected as Arthur R. Grossman on the Cover of the book and on the front matter pages iv, v, and xxvi.

The updated version of the book can be found at
https://doi.org/10.1007/978-3-030-33397-3

A. W. D. Larkum et al. (eds.), *Photosynthesis in Algae: Biochemical and Physiological Mechanisms*,
Advances in Photosynthesis and Respiration 45, https://doi.org/10.1007/978-3-030-33397-3_18

Subject Index

A. W. D. Larkum et al. (eds.), *Photosynthesis in Algae: Biochemical and Physiological Mechanisms*,
Advances in Photosynthesis and Respiration 45, https://doi.org/10.1007/978-3-030-33397-3